

Centre Armand-Frappier Santé Biotechnologie

Institut national de la recherche scientifique

MIMES MONO- ET OLIGOSACCHARIDIQUES BACTÉRIENS : SYNTHÈSE TOTALE ET APPLICATIONS

Par

Maude Cloutier

Thèse présentée pour l'obtention du grade de

Philosophiae Doctor (Ph.D.)

en biologie

Jury d'évaluation

Présidente du jury et
examinatrice interne

Pre Annie Castonguay
Centre Armand-Frappier Santé Biotechnologie
Institut national de la recherche scientifique

Examineur externe

Pr Denis Giguère
Département de chimie
Université Laval

Examineur externe

Pr Alexandre Gagnon
Département de chimie
Université du Québec à Montréal

Directeur de recherche

Pr Charles Gauthier
Centre Armand-Frappier Santé Biotechnologie
Institut national de la recherche scientifique

Per ardua ad astra

REMERCIEMENTS

Bien que celle-ci fût une incroyable aventure, la réalisation d'une thèse est tout sauf un long fleuve tranquille. À l'issue du long périple que celle-ci a été et qui marque la fin de mon parcours d'étudiante, je tiens à profondément remercier les gens qui m'ont accompagnée, aidée, et épaulée au travers les tempêtes et accalmies qui ont marqué les cinq dernières années.

À Charles, d'abord et avant tout. Au terme de ces cinq années, il m'apparaît évident que je n'aurais pu tomber sur un meilleur superviseur. Je te serai éternellement reconnaissante de m'avoir permis de m'épanouir et me développer en tant que scientifique et de m'avoir partagé ta passion inébranlable pour la chimie, sous toutes ses formes. Merci pour ta confiance, ton support, et ton enthousiasme contagieux. Je ne serais pas la scientifique que je suis aujourd'hui sans toi.

À mes collègues de laboratoire, présents et passés : Emmanilo, Kevin, Oscar, Nitish, Gokul, Floriane, Mathilde, Nazar, Arasakumar, Sujit, Sheida, Kumar, Sabrina, Marie-Joëlle, Anne-Sophie, Océanne, Samar, Gérard, Armand, Paul, et Justin. Merci de m'avoir accompagnée durant ces innombrables réactions et purifications, ainsi qu'au travers les hauts et les bas de la recherche. Merci pour votre écoute et vos précieux conseils, sans lesquels la présente thèse n'aurait pas pu être.

Aux nombreuses personnes qui ont croisé mon chemin lors de mon passage à l'INRS : Marianne, Hala, Van, Mustapha, Livie, David, Saba, Fares; aux membres du comité organisateur du Congrès Armand-Frappier 2018; aux membres du comité consultatif étudiant en matière d'équité, diversité et inclusion; aux membres de l'association étudiante; à Melany, Isabelle, Géraldine, Laurence et Léa Maude. Votre présence a fait de mon parcours aux cycles supérieurs une expérience particulièrement enrichissante, tant au niveau professionnel que personnel. Merci pour les nombreuses occasions où vous m'avez fait rire, réfléchir, et grandir.

À mes incroyables ami·es, qui m'ont soutenue tout au long de ce périple. Jodrey, Jérémie, Simon, merci pour votre présence, malgré la distance qui nous sépare, et vos encouragements. Geneviève et Isabelle, les mots me manquent pour vous exprimer la reconnaissance que je ressens face à votre existence. Faute d'avoir de meilleurs mots, je vous remercie pour l'impact colossal que vous avez eu dans ma vie depuis notre première rencontre il y a cinq ans. Mes ami·es, vous m'êtes une source

d'inspiration infinie. Merci pour les innombrables fous rires qui ont apaisé les inquiétudes que peuvent susciter les études supérieures.

À mon amoureuse, Roxane. Tu as été mon havre de paix au cours des derniers miles de mon doctorat. Merci pour ta compréhension, pour ton ouverture, tes encouragements. Merci d'avoir accueilli mes soucis à bras ouverts et d'avoir offert une oreille attentive à mes histoires de laboratoire sans fins. Merci pour toutes ces discussions qui me poussent à réfléchir, à me questionner, à me remettre en question, et *in fine* à faire de moi une meilleure personne. Merci de faire partie de ma vie, mon amour. Merci aussi à ton cher Gaston, le meilleur *study buddy* que je n'aurais pu avoir.

À ma famille : maman, papa, Mymi, Bern, Jess, Mohde, mes chers grands-parents. Vous êtes la meilleure famille à laquelle j'aurais pu rêver. Merci de m'avoir accompagnée aveuglément dans cette aventure un peu folle et de m'encourager à poursuivre mes passions, aussi variées et inattendues soient-elles. Merci pour votre enthousiasme—ma foi impressionnant—envers ma recherche et mes « momo-lécules ». Merci pour ces innumérables appels, repas, sorties, et moments apaisants qui embellissent ma vie. Mention spéciale à mon acolyte Matroskin, qui a bonifié ma dernière année de thèse à grands coups de miaulements incessants et de *zoomies*.

Enfin, à Justine. Je n'ai pas de mots pour t'exprimer la gratitude que je ressens pour tout ce que tu as fait pour moi. Même si la dernière année a été marquée par ton absence, je sais que tu m'as soutenue jusqu'à la toute fin, ton âme ayant imprégné l'univers dans lequel j'existe. Je suis une meilleure personne et scientifique grâce à toi. Merci de m'avoir partagé ta curiosité intellectuelle infinie et ton désir de contribuer à un monde meilleur. Merci d'avoir illuminé mes études supérieures en les ponctuant de *kata*, de commentaires sarcastiques, et de smoothies aux épinards. Merci d'avoir été.

À Justine.

RÉSUMÉ

Les glucides sont ubiquitaires chez les organismes vivants et occupent un rôle crucial dans de nombreux processus biologiques. Cette classe de composés présente donc un fort potentiel pour le développement de nouvelles avenues thérapeutiques, prophylactiques, ou diagnostiques. Différents composés glycosidiques sont d'ailleurs déjà utilisés en tant qu'agents thérapeutiques et prophylactiques, notamment en tant que vaccins glycoconjugués, agents anticancéreux, ou antibiotiques, pour ne nommer que quelques exemples. Dans ce contexte, la chimie de synthèse constitue un outil de taille pour l'accès à des composés saccharidiques bioactifs de structure optimisée et sous forme pure et homogène. Les travaux rapportés dans la présente thèse s'inscrivent ainsi dans un programme de recherche visant à développer des voies de synthèse donnant accès à des composés glycosidiques comme agents thérapeutiques ou prophylactiques potentiels.

Dans un premier temps, nous rapportons la synthèse du glucolipide ananatoside B et de son analogue 6-O-macrolactonisé ananatoside A, naturellement produits par la bactérie *Pantoea ananatis*, ainsi que de dérivés rhamnolipidiques macrolactonisés non-naturels. Inspirés du potentiel thérapeutique de macrolides glycosidiques et des rhamnolipides, ainsi que de l'activité tensioactive de ces derniers, nous avons postulé que ces composés synthétiques pourraient être bioactifs et tensioactifs. Nos travaux montrent que l'ananatoside B possède des propriétés tensioactives similaires aux rhamnolipides, et que les macrolactones sont cytotoxiques et hémolytiques, suggérant un mécanisme impliquant la formation de pores dans la membrane cellulaire. Nous montrons également que nos composés synthétiques sont reconnus par le système immunitaire de plants *Solanum lycopersicum*, suggérant que ce type de composés pourrait trouver application dans le domaine agroalimentaire.

La seconde partie de cette thèse porte quant à elle au développement de vaccins synthétiques contre *Burkholderia pseudomallei* et *Burkholderia mallei*, deux bactéries à Gram négatif causant la mélioïdose et la morve, respectivement, et considérées comme de potentielles armes bioterroristes. L'antigène-O du lipopolysaccharide de ces bactéries est un antigène prometteur pour le développement de vaccins. Nous rapportons la synthèse totale de tétrasaccharides formés d'unités 6-désoxy-L-talose et D-glucose mimant les épitopes majoritaires de cet antigène-O *via* une approche de glycosylations itératives. Les tests d'antigénicité réalisés montrent que ces tétrasaccharides synthétiques miment étroitement l'antigénicité du lipopolysaccharide natif de *B. pseudomallei*, suggérant que ces composés constituent des candidats prometteurs pour le développement de vaccins et/ou d'outils diagnostiques contre ces bactéries.

La troisième partie de cette thèse porte sur le développement de composés prophylactiques contre la bactérie encapsulée *Campylobacter jejuni* à l'origine de la campylobactériose. Compte tenu de sa grandissante résistance aux antibiotiques et de son association au syndrome de Guillain-Barré, beaucoup d'efforts sont investis envers le développement de vaccins contre cette bactérie,

notamment à base de son polysaccharide capsulaire. Notre objectif principal consistait ainsi en la synthèse de mimes disaccharidiques du polysaccharide capsulaire de *C. jejuni* HS:4c, la souche à l'origine de la majorité des infections à *C. jejuni*. L'unité répétitive de son polysaccharide capsulaire est un disaccharide de structure [\rightarrow 3)-6-désoxy- β -D-*ido*-heptopyranoside-(1 \rightarrow 4)-2-désoxy-2-acétamido- β -D-glucopyranoside-(1 \rightarrow)] non-stœchiométriquement substitué de groupements méthyl phosphoramidate. L'accès à des sucres de configuration *ido* étant non-triviale, nous nous sommes d'abord intéressés à leur synthèse. Dans un premier temps, nous rapportons ainsi nos travaux portant sur l'optimisation d'une méthode de synthèse de sucres de configuration D-*ido*. Dans un second temps, nous nous sommes intéressés à la synthèse de 1,2-*cis*- β -idosides, tels que présents au sein du polysaccharide capsulaire de *C. jejuni* HS:4c. Or, au cours de nos travaux visant à développer une méthode de β -idosylation, nous avons découvert un phénomène d'épimérisation d'acétals de benzyldène (*S*) \rightarrow (*R*) concomitant à un changement conformationnel ${}^4C_1 \rightarrow {}^1C_4$ spécifique aux β -D-idopyranosides 3-O-acylés. Nous rapportons ainsi une étude de glycosylation combinée à des expériences de résonance magnétique nucléaire et à de la modélisation moléculaire mettant en évidence différents aspects mécanistiques derrière ce phénomène unique aux β -D-idosides. Nous montrons également que nos conditions d'idosylation sont β -stéréosélectives en présence d'accepteurs aliphatiques, mais plutôt α -stéréosélectives lorsque des accepteurs glycosidiques sont employés. À la suite de cette étude, nous avons ainsi poursuivi notre investigation des réactions de β -idosylation afin d'accéder à des disaccharides mimant le polysaccharide capsulaire de *C. jejuni* HS:4c. Nous rapportons donc une étude de glycosylation extensive montrant que des idosylations β -stéréosélectives sont à portée de main via des approches intra- et intermoléculaires. Nous montrons également que la configuration 6-désoxy-*ido*-hepto spécifique à *C. jejuni* HS:4c peut être accédée via une homologation C6 \rightarrow C7 médiée par une réaction de type MOM-Wittig. Ces travaux frayent le chemin à la synthèse totale de mimes du polysaccharide capsulaire de *C. jejuni* HS:4c et pourraient devenir la première validation de principe d'un vaccin synthétique à base de sucre contre ce pathogène bactérien.

Dans l'ensemble, nos travaux mettent en évidence le potentiel de la chimie de synthèse pour le développement de composés glycosidiques dotés d'activités thérapeutiques et prophylactiques et ouvrent la voie à la découverte de nouvelles molécules bioactives.

Mots-clés : glucides, oligosaccharides, synthèse, glycosylation, agents thérapeutiques, agents prophylactiques

ABSTRACT

Carbohydrates are found ubiquitously in living organisms and play a crucial role in many biological processes. This class of compounds therefore has great potential for the development of new therapeutic, prophylactic or diagnostic avenues. Various glycosidic compounds are already used as therapeutic and prophylactic agents, such as glycoconjugate vaccines, anticancer agents, or antibiotics, to name a few examples. In this context, synthetic chemistry is a major tool to access bioactive saccharide compounds with an optimized structure and in pure and homogeneous forms. The work reported in this thesis is thus part of a research program aimed at developing synthetic routes giving access to glycosidic compounds as potential therapeutic or prophylactic agents.

First, we report the synthesis of the glucolipid ananatoside B and its 6-O-macrolactonized analog ananatoside A, naturally produced by the bacterium *Pantoea ananatis*, as well as non-natural macrolactonized rhamnolipid derivatives. Inspired by the therapeutic potential of glycosidic macrolides and rhamnolipids, as well as the surfactant activity of these latter, we hypothesized that these synthetic compounds could be bioactive and tensioactive. Our work shows that ananatoside B has surfactant properties similar to rhamnolipids, and that macrolactones are cytotoxic and hemolytic, suggesting a mechanism involving the formation of pores in the cell membrane. We also show that our synthetic compounds are recognized by the immune system of *Solanum lycopersicum*, suggesting that this type of compound could find application in the agri-food industry.

The second part of this thesis focuses on the development of synthetic vaccines against *Burkholderia pseudomallei* et *Burkholderia mallei*, two Gram-negative bacteria causing melioidosis and glanders, respectively, and considered as potential bioterrorist weapons. As the lipopolysaccharide O-antigen of these bacteria is a promising antigen for vaccine development, we report the total synthesis of tetrasaccharides formed of 6-deoxy-L-talose and D-glucose units mimicking the major epitopes of this O-antigen *via* an iterative glycosylation approach. Antigenicity assays show that these synthetic tetrasaccharides closely mimic the antigenicity of *B. pseudomallei* native lipopolysaccharide, suggesting that these compounds constitute potential candidates for the development of vaccines and/or diagnostic tools against both bacteria.

The third part of this thesis focuses on the development of prophylactic compounds against the encapsulated bacterium *Campylobacter jejuni*, which causes campylobacteriosis. Considering its growing resistance to antibiotics and its association with Guillain-Barré syndrome, efforts are invested in the development of vaccines against this bacterium, particularly vaccines based on its capsular polysaccharide. Our main goal therefore consisted in the synthesis of disaccharide mimics of *C. jejuni* HS:4c capsular polysaccharide, which is the strain at the origin of most of *C. jejuni* infections. The repeating unit of its capsular polysaccharide is a disaccharide of structure $[\rightarrow 3)\text{-6-deoxy-}\beta\text{-D-ido-heptopyranoside-(1}\rightarrow 4)\text{-2-deoxy-2-acetamido-}\beta\text{-D-glucopyranoside-(1}\rightarrow]$ non-

stoichiometrically modified with methyl phosphoramidate groups. Access to *ido*-configured sugars being non-trivial, we were first interested in their synthesis. We thus first report our work on the optimization of a synthetic method enabling access to D-idosides. We were then interested in the synthesis of 1,2-*cis*- β -idosides, as found in the capsular polysaccharide of *C. jejuni* HS:4c. However, throughout our work aimed at developing a method of β -idosylation, we discovered a phenomenon of (*S*) \rightarrow (*R*) epimerization of benzylidene acetals concomitant with a ${}^4C_1\rightarrow{}^1C_4$ conformational change specific to 3-*O*-acetylated β -D-idosides. We thus report a glycosylation study combined with nuclear magnetic resonance experiments and molecular modeling, highlighting different mechanistic aspects behind this unique phenomenon specific to 3-*O*-acetylated β -D-idosides. We also show that our idosylation conditions are β -stereoselective in the presence of aliphatic acceptors but are instead α -stereoselective when glycosidic acceptors are employed. Following this study, we pursued our investigation of β -idosylation reactions as to access disaccharides mimicking the capsular polysaccharide of *C. jejuni* HS:4c. We therefore report an extensive glycosylation study showing that β -stereoselective idosylations are within reach *via* intra- and intermolecular approaches. We also show that the 6-deoxy-*ido*-hepto configuration specific to *C. jejuni* HS:4c can be accessed via a C6 \rightarrow C7 homologation mediated by a MOM-Wittig-type reaction. Overall, this work paves the way for the total synthesis of *C. jejuni* HS:4c capsular polysaccharide mimics and could become the first proof-of-concept of a synthetic sugar-based vaccine against this pathogen.

Overall, our work highlights the potential of synthetic chemistry for the development of glycosidic compounds with therapeutic and prophylactic activities and paves the way for the discovery of novel bioactive molecules.

Keywords: carbohydrate, oligosaccharides, synthesis, glycosylation, therapeutic agents, prophylactic agents

TABLE DES MATIÈRES

REMERCIEMENTS.....	v
RÉSUMÉ	ix
ABSTRACT.....	xi
TABLE DES MATIÈRES	xiii
LISTE DES FIGURES	xix
LISTE DES SCHÉMAS	xxiii
LISTE DES TABLEAUX.....	xxvii
LISTE DES ABRÉVIATIONS.....	xxix
CHAPITRE 1 : INTRODUCTION.....	1
1.1 Introduction.....	3
1.2 Sucres en tant qu'agents thérapeutiques.....	4
1.3 Sucres en tant qu'agents prophylactiques	6
1.3.1 Vaccins antibactériens	6
1.3.2 Autres types de vaccins	11
1.4 Autres applications des glucides	14
1.4.1 Les sucres en tant qu'outils diagnostiques	14
1.4.2 Les sucres en tant que biosurfactants	15
1.5 Synthèse de mono- et oligosaccharides.....	17
1.5.1 Réactions de glycosylation	18
1.5.1.1 Glycosylations stéréosélectives	20
1.6 Contenu de la thèse	23
CHAPITRE 2 : TOTAL SYNTHESIS, ISOLATION, SURFACTANT PROPERTIES, AND BIOLOGICAL EVALUATION OF ANANATOSIDES AND RELATED MACRODILACTONE-CONTAINING RHAMNOLIPIDS	27
2.1 Résumé.....	29
2.2 Abstract	29
2.3 Introduction	30
2.4 Results and discussion.....	33
2.4.1 Isolation of ananatoside A (1) and ananatoside B (2)	33
2.4.2 Total synthesis of ananatoside A (1) and ananatoside B (2)	34

2.4.2.1 Retrosynthetic analysis	34
2.4.2.2 Synthesis of building blocks	37
2.4.2.3 Synthesis of anatoside B	38
2.4.2.4 Synthesis of anatoside A by intramolecular glycosylation	39
2.4.2.5 Synthesis of anatoside A by chemical macrolactonization.....	41
2.4.2.6 Synthesis of anatoside A by enzymatic macrolactonization	43
2.4.3 Synthesis of RhaC ₁₀ C ₁₀ (3) and macrolactonized rhamnolipids 4-6	44
2.4.3.1 Retrosynthetic analysis	44
2.4.3.2 Synthesis of building blocks	45
2.4.3.3 Synthesis of rhamnolipid C ₁₀ C ₁₀	46
2.4.3.4 Macrolactonization of rhamnolipids	47
2.4.4 Molecular modeling of macrolactonized rhamnolipids.....	49
2.4.5 Surfactant properties of natural glycolipids.....	50
2.4.6 Antimicrobial activity, cytotoxicity, and hemolytic activity of natural and synthetic glycolipids	52
2.4.7 Interaction of natural and synthetic glycolipids with the plant immune system	54
2.5 Conclusions	57
2.6 Acknowledgements	58
2.7 Experimental section	59
2.7.1 General methods	59
2.7.2 Experimental procedures for isolation and synthesis	60
2.7.3 Experimental procedures for biological evaluation and surfactant properties	99
2.7.4 Molecular modeling.....	102
CHAPITRE 3 : SYNTHESIS OF OLIGOSACCHARIDES RELATED TO POTENTIAL BIOTERRORIST PATHOGENS	105
3.1 Résumé	107
3.2 Abstract	107
3.3 Introduction	108
3.4 <i>Bacillus anthracis</i>	109
3.5 <i>Burkholderia pseudomallei</i> and <i>Burkholderia mallei</i>	149
3.5.1 Capsular polysaccharides	149
3.5.2 Lipopolysaccharides	154
3.5.3 Exopolysaccharides	159
3.6 <i>Francisella tularensis</i>	161

3.7 <i>Yersinia pestis</i>	166
3.8 <i>Brucella spp.</i>	174
3.8 Conclusion.....	182
CHAPITRE 4 : MELIOIDOSIS PATIENT SERUM-REACTIVE SYNTHETIC TETRASACCHARIDES BEARING THE PREDOMINANT EPITOPES OF <i>BURKHOLDERIA</i> <i>PSEUDOMALLEI</i> AND <i>BURKHOLDERIA MALLEI</i> O-ANTIGENS	185
4.1 Résumé.....	187
4.2 Abstract	187
4.3 Introduction	188
4.4 Results and Discussion.....	190
4.4.1 Retrosynthetic approach	190
4.4.2 First generation synthesis of tetrasaccharides	192
4.4.3 Second generation synthesis of tetrasaccharides	195
4.4.4 Third generation synthesis of tetrasaccharides.....	197
4.4.5 Global deprotection of tetrasaccharides	199
4.4.6 Reactivity of the synthetic oligosaccharides with <i>Bm</i> LPS-specific mAbs.....	202
4.4.7 Reactivity of the synthetic oligosaccharides with melioidosis patient serum.	204
4.5 Conclusions	207
4.6 Acknowledgments.....	207
4.7 Conflicts of interest	207
4.8 Experimental section	208
4.8.1 General methods	208
4.8.2 ELISAs	209
4.8.3 Experimental procedures for synthesis.....	210
CHAPITRE 5 : PROGRESS TOWARDS THE DEVELOPMENT OF GLYCAN-BASED VACCINES AGAINST CAMPYLOBACTERIOSIS.....	245
5.1 Résumé.....	247
5.2 Abstract	247
5.3 Campylobacteriosis	248
5.4 Challenges of campylobacteriosis vaccines	250
5.5 Capsular polysaccharides	251
5.5.1 Chemical structures	251
5.6 Glycoconjugate vaccines.....	254
5.6.1 Role of carrier proteins.....	254

5.6.2 CPS-based vaccines	255
5.7 Synthesis of oligosaccharide mimics	256
5.7.1 Incorporation of MeOPN moieties	257
5.7.2 <i>C. jejuni</i> HS:4c	260
5.7.3 <i>C. jejuni</i> HS:23/36	262
5.7.4 <i>C. jejuni</i> HS:2	267
5.7.5 <i>C. jejuni</i> HS:53c	270
5.8 Conclusions	274
5.9 Acknowledgments	276
CHAPITRE 6 : SYNTHESIS OF α -D-IDOSE PENTAACETATE FROM β -D-GLUCOSE PENTAACETATE VIA PAULSEN ACETOXONIUM REARRANGEMENT	277
6.1 Résumé	279
6.2 Abstract	279
6.3 Results	279
6.4 Experimental	283
6.5 Acknowledgments	285
CHAPITRE 7 : C7 EPIMERIZATION OF BENZYLIDENE-PROTECTED β -D- IDOPYRANOSIDES BRINGS STRUCTURAL INSIGHTS INTO IDOSE CONFORMATIONAL FLEXIBILITY	289
7.1 Résumé	291
7.2 Abstract	291
7.3 Introduction	291
7.4 Results and discussion	295
7.4.1 Synthetic approach	295
7.4.2 Synthesis of idopyranosyl donors	296
7.4.3 Glycosylation study, characterization, and molecular modeling	299
7.5 Conclusions	312
7.6 Acknowledgments	313
7.7 Experimental section	314
CHAPITRE 8 : TOWARDS THE SYNTHESIS OF AN IDOSE-CONTAINING DISACCHARIDE MIMIC OF <i>CAMPYLOBACTER JEJUNI</i> HS:4C CAPSULAR POLYSACCHARIDE	353
8.1 Résumé	355
8.2 Abstract	355
8.3 Introduction	356

8.4 Results and Discussion.....	359
8.4.1 Intramolecular aglycon delivery approach	359
8.5 Next steps	372
8.6 Conclusions	374
8.7 Acknowledgments.....	375
8.8 Experimental section.....	375
CHAPITRE 9 : CONCLUSIONS ET PERSPECTIVES.....	405
LISTE DES RÉALISATIONS	417
Articles et chapitres de livres	417
Brevet	418
Présentations orales et par affiches	418
ANNEXE DU CHAPITRE 2.....	421
ANNEXE DU CHAPITRE 4.....	489
ANNEXE DU CHAPITRE 7.....	527
ANNEXE DU CHAPITRE 8.....	603
Bibliographie.....	639

LISTE DES FIGURES

Figure 1.1. Exemples sélectionnés de composés thérapeutiques à base de sucres	5
Figure 1.2. Mécanisme d'activation immunitaire par des polysaccharides et glycoconjugués	8
Figure 1.3. Structure du vaccin Quimi-Hib et du vaccin en étude clinique contre <i>Shigella flexneri</i> 2a.....	10
Figure 1.4. Structure des glycoconjugués Qβ-5 contre le VIH et Globo H-KLH contre le cancer	12
Figure 1.5. Structure de QS21 et domaines (A–D) faisant l'objet d'études structurales	14
Figure 1.6. Biopuces à glycanes	15
Figure 1.7. Exemples de glycolipides utilisés comme biosurfactants	17
Figure 1.8. Défis rencontrés en chimie des sucres.....	18
Figure 1.9. Mécanisme de glycosylation à l'interface S _N 1/S _N 2.....	19
Figure 1.10. Terminologie α/β vs 1,2- <i>cis</i> /1,2- <i>trans</i>	21
Figure 1.11. Glycosylations stéréosélectives	22
Figure 1.12. Exemples de composés naturels contenant des liens glycosidiques 1,2- <i>cis</i>	22
Figure 1.13. Exemples d'approches permettant la formation de liens glycosidiques 1,2- <i>cis</i> - β	23
Figure 1.14. Résumé du contenu de la présente thèse	25
Figure 2.1. (A) Exemples of macrolactone-containing <i>glucolipids</i> produced by microbes; (B) Structure of target ananatoside A (1) and ananatoside B (2) produced by <i>Pantoea ananatis</i> along with the related RhaC ₁₀ C ₁₀ (3); (C) Structures of target macrodilactone-containing rhamnolipids 4-6	32
Figure 2.2. Retrosynthetic disconnection strategy for the total synthesis of ananatoside A (1) and ananatoside B (2) according to three different pathways: chemical macrolactonization, enzymatic macrolactonization, and inter- or intramolecular glycosylation	36
Figure 2.3. Retrosynthetic analysis of rhamnolipid 3 and macrodilactone-containing rhamnolipids 4-6	45
Figure 2.4. 3D structure of the macrolactonized rhamnolipids models 48-50	50
Figure 2.5. Extracellular reactive oxygen species (ROS) production following treatment of tomato leaf disks with ananatoside A (1), ananatoside B (2), RhaC ₁₀ C ₁₀ (3), and related macrodilactone-containing rhamnolipids (4-6).....	56
Figure 3.1. Major cell wall repeating unit hexasaccharide from <i>Bacillus anthracis</i> vegetative cells bearing two different linkers for carrier protein conjugation prepared by Seeberger and Boons	140
Figure 3.2. <i>B. anthracis</i> vegetative cell wall polysaccharide derivatives prepared by Boons....	146

Figure 3.3. Inner core oligosaccharide of <i>F. tularensis</i> LPS bearing an aminolinker for carrier protein conjugation	162
Figure 3.4. <i>Y. pestis</i> LPS inner core oligosaccharide fragment	167
Figure 3.5. A and M antigens of <i>Brucella</i> spp. OPS structure	176
Figure 4.1. Structures of <i>B. pseudomallei</i> and <i>B. mallei</i> LPS O-antigens showing the predominant terminal and intra-chain epitopes.....	189
Figure 4.2. (A) Structures of previously synthesized di- and trisaccharides (1–7); and (B) target synthetic tetrasaccharides 8 and 9 related to <i>Bp</i> and <i>Bm</i> LPS OAGs, respectively.....	190
Figure 4.3. Retrosynthetic analysis of target tetrasaccharides 8 and 9	191
Figure 4.4. Interactions of <i>Bm</i> LPS-specific mAbs with <i>Bp</i> LPS antigens and synthetic oligosaccharides	204
Figure 4.5. Reactivity of human serum samples with <i>Bp</i> LPS and synthetic oligosaccharides .	206
Figure 5.1. Comparison between <i>C. jejuni</i> serotypes HS:19 and HS:4 LOS core structure (A) and human gangliosides GM1a and GD1a (B).....	249
Figure 5.2. Repeating units of characterized <i>C. jejuni</i> serotypes CPS including the MeOPN moieties and other non-stoichiometric structural modifications (in pink).....	253
Figure 6.1. Experimental set-up for the adapted cannula filtration and representative TLC (1:2 hexanes-EtOAc) of the reaction sequence on silica gel 60 F ₂₅₄ 0.25 mm pre-coated glass plate..	282
Figure 7.1. (A) Conformational equilibrium of D-idopyranosides as compared to other D-aldohexoses; (B) Examples of naturally occurring glycosides and oligosaccharides containing L- (blue) and D- (red) <i>ido</i> -configured sugars.....	293
Figure 7.2. (A) Ling and (B) Li's indirect approaches towards the preparation of 1,2- <i>cis</i> - β -linked idopyranosides; (C) This work: direct β -glycosylation of thioidopyranosyl donors and spontaneous acid-mediated <i>in situ</i> C7-epimerization with concomitant chair flip.....	304
Figure 7.3. (A) Comparison between theoretical and experimental NMR data; (B) Most relevant NOE correlations and comparison between theoretical and experimental distances	304
Figure 7.4. X-ray crystallographic structure of β -glycoside 20a	305
Figure 7.5. Proposed mechanism for the ring flipping with concomitant benzylidene epimerization	312
Figure 8.1. Structure of <i>C. jejuni</i> HS:4c CPS repeating unit	357
Figure 8.2. Ling's (A), Li's (B) and our (C) approaches to access 1,2- <i>cis</i> - β -linked idosides	358
Figure 8.3. NAP-mediated IAD procedure	359
Figure 8.4. (A) Retrosynthetic analysis of disaccharides 1 and 2 ; (B) Target model idoside donors	361
Figure 8.5. Significant NMR coupling constants of disaccharide 26a	372
Figure 9.1. (A) Structure des anatosides A et B, du rhamnolipide, et d'analogues rhamnolipides macrolactonisés; (B) Analyse rétrosynthétique de l'anatoside A dimérique	408

Figure 9.2. (A) Structure des tétrasaccharides synthétiques mimant l'antigène-O du LPS de *B. pseudomallei* et *B. mallei*; (B) Rétrosynthèse du nouveau tétrasaccharide cible 410

Figure 9.3. (A) Structure de l'unité répétitive du CPS de *C. jejuni* HS :4c; (B) Optimisation du réarrangement de Paulsen; (C) Étude de flexibilité conformation de β -D-idopyranosides; (D) Potentiels ligands diphosphonate pour catalyse asymétrique ; (E) Synthèse de mimes du CPS de *C. jejuni* HS:4c et conjugaison à CRM₁₉₇..... 412

LISTE DES SCHÉMAS

Scheme 2.1. Synthesis of β -hydroxydecanoic acid derivatives	37
Scheme 2.2. Synthesis of thioglucoside derivatives 9 and 11	38
Scheme 2.3 Total synthesis of ananatoside B	39
Scheme 2.4. Synthesis of alcohol 20 ready for intramolecular glycosylation	39
Scheme 2.5. Deprotection of macrolides 21 and 23 into ananatoside A (1).....	43
Scheme 2.6. Synthesis of thiorhamnoside building blocks 25 , 29 , 30 and 31	46
Scheme 2.7. Total synthesis of RhaC ₁₀ C ₁₀ (3).....	47
Scheme 2.8. Synthesis of (1→4), (1→2), and (1→3)-macrolactonized rhamnolipids 4-6	48
Scheme 3.1. Synthesis of anthrax tetrasaccharide by Seeberger	112
Scheme 3.2. Gram-scale synthesis of anthrax tetrasaccharide by Kováč	117
Scheme 3.3. Synthesis of trisaccharides related to anthrax tetrasaccharide by Boons	120
Scheme 3.4. Synthesis of anthrax tetrasaccharide by Crich	123
Scheme 3.5. Synthesis of an anthrose-containing disaccharide by Grandjean	127
Scheme 3.6. Synthesis of a non-methylated anthrose-containing disaccharide by Grandjean...	128
Scheme 3.7. Synthesis of anthrax tetrasaccharide by Grandjean.....	130
Scheme 3.8. Synthesis of anthrax tetrasaccharide by Wang.....	133
Scheme 3.9. <i>De novo</i> synthesis of anthrax tetrasaccharide building blocks by O’Doherty	135
Scheme 3.10. Anthrax-related tetrasaccharides synthesis by O’Doherty	136
Scheme 3.11. <i>De novo</i> synthesis of di- and trisaccharides related to anthrax tetrasaccharide by O’Doherty	138
Scheme 3.12. Seeberger’s group synthesis of the hexasaccharide repeating unit of the first proposed structure of <i>B. anthracis</i> cell wall polysaccharide	142
Scheme 3.13. Synthesis of trisaccharides related to the first proposed structure of <i>B. anthracis</i> cell wall polysaccharide.....	144
Scheme 3.14. Boons group synthesis of the hexasaccharide repeating unit of the first proposed structure of <i>B. anthracis</i> cell wall polysaccharide	148
Scheme 3.15. Intramolecular aglycon delivery allowing the synthesis of mono- and disaccharide mimics of <i>B. pseudomallei</i> and <i>B. mallei</i> CPS	151
Scheme 3.16. Synthesis of a hexasaccharide related to <i>B. pseudomallei</i> and <i>B. mallei</i> CPS.....	153
Scheme 3.17. Synthesis of non-acetylated di-, tetra, and hexasaccharides related to <i>B. pseudomallei</i> and <i>B. mallei</i> LPS OAg.....	156
Scheme 3.18. Synthesis of a trisaccharide related to the main intrachain substitution pattern of <i>B. pseudomallei</i> and <i>B. mallei</i> LPS OAg	158

Scheme 3.19. Synthesis of disaccharides mimicking the terminal end of <i>B. pseudomallei</i> and <i>B. mallei</i> LPS OAg.....	159
Scheme 3.20. Synthesis of the biological repeating unit of the β -Kdo-containing EPS produced by <i>B. pseudomallei</i>	161
Scheme 3.21. Synthesis of a pivotal disaccharide <i>en route</i> to the synthesis of <i>F. tularensis</i> inner core oligosaccharide.....	163
Scheme 3.22. Total synthesis of <i>F. tularensis</i> inner core oligosaccharide	165
Scheme 3.23. <i>De novo</i> synthesis of L-glycero-D-manno-heptose building blocks <i>en route</i> to the synthesis of <i>Y. pestis</i> inner core LPS	168
Scheme 3.24. Synthesis of building blocks <i>en route</i> to the preparation of a CRM197-trisaccharide conjugate.....	170
Scheme 3.25. Synthesis of a CRM197-trisaccharide conjugate for the serodiagnosis of plague	171
Scheme 3.26. Synthesis of L-glycero-D-manno-heptose-containing oligosaccharide related to the inner core of <i>Y. pestis</i> by Seeberger.....	173
Scheme 3.27. Synthesis of a nonasaccharide mimicking both A and M antigens of <i>Brucella</i> spp. sLPS	177
Scheme 3.28. Synthesis of a hexasaccharide mimicking the A antigen of <i>Brucella</i> spp. sLPS.	179
Scheme 3.29. Synthesis of a hexasaccharide mimicking the capping antigen of <i>Brucella</i> spp. sLPS	180
Scheme 4.1. (A) Synthesis of 2- <i>O</i> -AZMB-containing glucose derivative 15 ; and (B) failed attempts to cleave the TBS group in disaccharide 22	193
Scheme 4.2. Synthesis of disaccharide acceptor 12	194
Scheme 4.3. Attempt to synthesize tetrasaccharide 10 <i>via</i> a [2 + 2] glycosylation.....	195
Scheme 4.4. Synthesis of rhamnose-containing tetrasaccharide 10 <i>via</i> a [1 + 1 + 1 + 1] glycosylation sequence	196
Scheme 4.5. Synthesis of 6-deoxy-L-talopyranoside derivatives 34 and 35	197
Scheme 4.6. Final approach for the synthesis of protected tetrasaccharides 31 and 40	198
Scheme 4.7. Alternative pathways for the final deprotection of tetrasaccharides 31 and 40	202
Scheme 5.1. (A) Lowary and (B) Wang investigations of MeOPN moieties incorporation in carbohydrates and compatibility with various protecting groups	258
Scheme 5.2. Ling synthesis of 6-deoxy- β -D- <i>ido</i> -heptopyranoside 45 and disaccharide 51 related to <i>C. jejuni</i> HS:4c.....	262
Scheme 5.3. Monteiro synthesis of MeOPN-bearing galactosides 54-58 and glycoconjugate 59	263
Scheme 5.4. Nam Shin frame-shifted oligosaccharides (A) and Lowary synthesis of trisaccharides 73 , 74 , 78 , and 79 (B) mimicking <i>C. jejuni</i> HS:23/36 CPS repeating unit.....	265

Scheme 5.5. Lowary's synthesis of BSA-conjugated heptopyranoside 89 from D-galactose (A) and <i>de novo</i> approach towards thioglycoside β - 86 (B) associated with <i>C. jejuni</i> HS:2.....	268
Scheme 5.6. Crich's synthesis of phosphodiester-containing disaccharide 106 (A) and α - and β -stereoselective <i>manno</i> -heptopyranoside building blocks 115 and 113 (B) related to <i>C. jejuni</i> HS:53c CPS	271
Scheme 5.7. Yang <i>de novo</i> synthesis of trisaccharide 129 as a mimic of <i>C. jejuni</i> HS:53 CPS	274
Scheme 6.1 Synthesis of peracetylated idoside 4 via Paulsen acetoxonium rearrangement	279
Scheme 7.1. Synthesis of 3- <i>O</i> -acylated <i>ido</i> -configured thioglycoside donors 6–9	297
Scheme 7.2. Partial deprotection of glycosides 14a–14c	302
Scheme 7.3. Post-glycosylation epimerization experiments.....	306
Scheme 7.4. Synthesis of thiotaloside 28	309
Scheme 8.1. Synthesis of idoside donors 4a , 4b , and 5a–5d	362
Scheme 8.2. Homologation of alcohol 11	365
Scheme 8.3. Unsuccessful intramolecular aglycon delivery using heptoside 13	366
Scheme 8.4. Synthesis of 2- <i>O</i> -TBS (A) and 3- <i>O</i> -TBS (B) donors 15a–15d and 18	369
Scheme 8.5. Planned synthetic route to access target disaccharides 1 and 2	374

LISTE DES TABLEAUX

Table 2.1. NIS/triflate-promoted intramolecular glycosylation of precursor 20	41
Table 2.2. Chemical macrolactonization of precursor 22	42
Table 2.3. Enzymatic macrolactonization of ananatoside B (2) into ananatoside A (1)	44
Table 2.4. Critical Micelle Concentration (CMC), surface tension (γ_{CMC}), and hydrodynamic diameter (<i>Z</i> -average) of naturally occurring biosurfactants (1-3)	51
Table 2.5. Cytotoxicity and hemolytic activity of natural and synthetic glycolipids (1-6)	54
Table 4.1. Optimization of the Staudinger reaction for azide reduction.....	201
Table 7.1. Optimization of the regioselective silylation of diol 4a	299
Table 7.2. Glycosylation study of <i>ido</i> -configured thioglycosyl donors 6-9	301
Table 7.3. Synthesis of 3-O-benzylated thioidoside 24 via regioselective 3-O-benzylation.....	308
Table 7.4. Glycosylation study of <i>ido</i> - and <i>talo</i> -configured thioglycosyl donors 24 and 28	310
Table 7.5. Glycosylation study of <i>ido</i> -configured thioglycosyl donors 6a , 6b , and 24 with glycosidic acceptors	311
Table 8.1. Intramolecular aglycon delivery using idoside donors 4a , 4b , and 5a-5d	363
Table 8.2. Intermolecular glycosylation with model compounds.....	367
Table 8.3. Intermolecular glycosylation with 6-deoxy- <i>ido</i> -heptopyranosyl donors 13 and 22-24	371

LISTE DES ABRÉVIATIONS

2,2-DMP	2,2-Diméthoxypropane
9-BBN	9-Borabicyclo[3.3.1]nonane
Ac	Acétyle
ADMB	4-Acétoxy-2,2-diméthylbutanoyle
All	Allyle
Alloc	Allyloxy-carbonyle
At	Azabenzotriazole
AZMB	(2-Azidométhyle)benzoyle
BclA	<i>Bacillus collagen-like protein of anthracis</i>
<i>Bm</i>	<i>Burkholderia mallei</i>
Bn	Benzyle
Boc	<i>tert</i> -Butoxycarbonyle
<i>Bp</i>	<i>Burkholderia pseudomallei</i>
br	<i>Broad</i>
brsm	<i>Based on recovered starting material</i>
BSA	<i>Bovine serum albumin</i>
BSATs	<i>Biological select agents or toxins</i>
BSP	Benzènesulfinylpipéridine
Bt	Benzotriazole
Bu	Butyle
Bz	Benzoyle
CAD	<i>Charged aerosol detector</i>
CALB	<i>Candida antarctica</i> lipase B
CAN	Nitrate de cérium et d'ammonium
Cbz	Carboxybenzyle
CDC	<i>Centers for Disease Control and Prevention</i>
CLSM	<i>Confocal laser scanning microscopy</i>
CMC	<i>Critical micelle concentration</i>
COD	1,5-Cyclooctadiène
COSY	<i>Correlated spectroscopy</i>
CPS	Polysaccharide capsulaire
CRM197	<i>Cross reacting material</i>
CSA	Acide camphorsulfonique

d	Doublet
DABCO	1,4-Diazabicyclo[2.2.2]octane
DALY	<i>Disability-adjusted life-year</i>
DBU	1,8-Diazabicyclo[5.4.0]undéc-7-ène
DCC	Dicyclohexylcarbodiimide
DCE	1,2-Dichloroéthane
DCM	Dichlorométhane
DDQ	2,3-Dichloro-5,6-dicyano-1,4-benzoquinone
DEIPS	Diéthylisopropylsilyle
DFT	<i>Density functional theory</i>
DIBALH	Hydrure de diisobutylaluminium
DIPC	<i>N,N'</i> -Diisopropylcarbodiimide
DIPEA	<i>N,N</i> -Diisopropyléthylamine
DLS	<i>Dynamic light scattering</i>
DMAP	4-Diméthylaminopyridine
DMC	Chlorure de 2-chloro-1,3-diméthylimidazolium
DMF	Diméthylformamide
DMSO	Diméthylsulfoxyde
DMTST	Trifluorométhanesulfonate de diméthyl(méthylthio)sulfonium
dppb	1,4-bis(Diphénylphosphino)butane
DT	<i>Diphtheria toxoid</i> (anatoxine diphtérique)
DTBMP	2,6-Di- <i>tert</i> -butyle-4-méthylpyridine
DTBP	Di- <i>tert</i> -butylperoxyde
DTBS	Di- <i>tert</i> -butylsilylène
EDC	1-Éthyl-3-[3-diméthylaminopropyl]carbodiimide
EIA	<i>Enzymatic immunoassay</i>
ELISA	<i>Enzyme-linked immunosorbent assay</i>
EPS	Exopolysaccharide
ESI	<i>Electrospray ionisation</i>
Et	Éthyle
Et ₂ O	Éther diéthylique
EtOAc	Acétate d'éthyle
Fmoc	Fluorénylméthoxycarbonyle
GBS	Syndrôme de Guillain-Barré
GEMS	<i>Global Enteric Multicenter Study</i>

GNB	<i>Gram-negative bacteria</i>
GP	Groupe partant
HATU	Hexafluorophosphate d' <i>O</i> -(7-azabenzotriazol-1-yl)- <i>N,N,N',N'</i> -tétraméthyluronium
HBTU	Hexafluorophosphate d' <i>O</i> -(1 <i>H</i> -benzotriazole-1-yl)- <i>N,N,N',N'</i> -tétraméthyluronium
HC50	Concentration hémolytique médiane
HF-PS	<i>Hydrogen fluoride-polysaccharide</i>
HiD	<i>Haemophilus influenzae protein D</i>
HMBC	<i>Heteronuclear multiple-bond coherence</i>
HMDS	Hexaméthylidisilazane
HPLC	<i>High performance liquid chromatography</i>
HR	<i>High resolution</i>
HS	<i>Heat-stable</i>
HSQC	<i>Heteronuclear single quantum coherence</i>
Hz	Hertz
IAD	<i>Intramolecular aglycon delivery</i>
IC50	Concentration inhibitrice médiane
IFA	<i>Immunofluorescence assay</i>
IgG	Immunoglobuline G
IgM	Immunoglobuline M
Im	Imidazole
iPr ₂ NEt	<i>N,N</i> -Diisopropyléthylamine
Kdo	Acide 3-désoxy-D- <i>manno</i> -oct-2-ulosonique
KLH	<i>Keyhole Limpet Hemocyanin</i>
LDA	Diisopropylamide de lithium
Lev	Lévulinoyle
LOS	Lipooligosaccharide
LPS	Lipopolysaccharide
m	Multiplet
mAbs	<i>Monoclonal antibodies</i>
MAE	<i>Means of the absolute values of the errors</i>
MALDI	<i>Matrix-assisted laser desorption/ionization</i>
mCPBA	Acide <i>m</i> -chloroperoxybenzoïque
Me	Méthyle
MeOPN	Phosphoramidate de méthyle

MMFF	<i>Merck Molecular Force Field</i>
MS	<i>Mass spectrometry</i>
MS	<i>Molecular sieves</i>
Ms	Mésyle
NAP	2-Naphthylméthyle
NBS	<i>N-Bromosuccinimide</i>
NGP	<i>Neighboring group participation</i>
NHS	<i>N-Hydroxysuccinimide</i>
NHTCA	Trichloroacétamide
NIS	<i>N-Iodosuccinimide</i>
NMI	<i>N-Méthylimidazole</i>
NMO	<i>N-Oxyde de N-méthylmorpholine</i>
NMR	<i>Nuclear magnetic resonance</i>
NOE	<i>Nuclear overhauser effect</i>
NOESY	<i>Nuclear overhauser effect spectroscopy</i>
oABz	<i>o-Alkynylbenzoyle</i>
OAg	<i>O-Antigen</i>
OMPC	<i>Outer membrane protein complex</i>
OPS	<i>O-Polysaccharide</i>
OTf	Triflate
PBS	<i>Phosphate-buffered saline</i>
PDCP	Phényldichlorophosphate
Pent	Pentényle
Ph	Phényle
PIA	<i>Polysaccharide intercellular adhesin</i>
Piv	Pivaloyle
PMB	<i>p-Méthoxybenzyle</i>
PMP	<i>p-Methoxyphenyle</i>
ppm	Partie par million
PPTs	<i>p-Toluènesulfonate de pyridinium</i>
PTFA	<i>N-Phényltrifluoroacétimide</i>
PTSA	Acide <i>p</i> -toluènesulfonique
py	Pyridine
q	Quadruplet
Rf	Rapport frontal

RLU	<i>Relative luminescence units</i>
RMN	Résonance magnétique nucléaire
rmsd	<i>Root-mean-square deviation</i>
ROS	<i>Reactive oxygen species</i>
s	Singulet
SAMA-Opfp	2-(Acétylthio)acétate de perfluorophényle
SEM	<i>Standard error of the mean</i>
SEt	Thioéthyle
sLPS	<i>Smooth LPS</i>
SN1	Substitution nucléophile unimoléculaire
SN2	Substitution nucléophile bimoléculaire
SPR	<i>Surface plasmon resonance</i>
STD	<i>Saturation-transfer difference</i>
STol	Méthylphénylthio (ou thiotolyle)
t	Triplet
TACA	<i>Tumor-associated carbohydrate antigen</i>
TBA	Tétrabutylammonium
TBDPS	<i>tert</i> -Butyldiphénylsilyle
TBS	<i>tert</i> -Butyldiméthylsilyle
TCA	Trichloroacétimide
TDS	Thexyldiméthylsilyle
TetHc	<i>Tetanus toxin protein</i>
Tf ₂ O	Anhydride triflique
TFA	Acide trifluoroacétique
TFAA	Anhydride trifluoroacétique
THF	Tétrahydrofurane
TLC	<i>Thin layer chromatography</i>
TMS	Triméthylsilyle
TOF	<i>Time of flight</i>
tol	Toluène
Tr	Trityle
TREAT-HF	Trihydrofluorure de triéthylamine
Troc	Trichloroéthoxycarbonyle
Ts	Tosyle
TT	<i>Tetanus toxoid</i>

TTBP	Tri- <i>tert</i> -butylpyrimidine ou tri- <i>tert</i> -butylpyridine
VIH	Virus de l'immunodéficience humaine
WHO	<i>World Health Organization</i>
γ_{CMC}	Tension de surface

CHAPITRE 1 : INTRODUCTION

1.1 Introduction

Ubiquitaires dans la nature, les glucides sont depuis longtemps reconnus pour leur rôle clé dans le métabolisme et l'entreposage énergétique. Depuis plus récemment, ceux-ci sont également caractérisés au niveau de leur fonction dans une grande variété de processus biologiques. Grâce à leur grande hétérogénéité structurelle et à leur omniprésence au niveau intracellulaire, membranaire, et particulièrement extracellulaire, les composés glycosidiques sont notamment impliqués dans les processus de transduction de signaux, d'adhésion cellulaire, de reconnaissance moléculaire, de croissance cellulaire, et d'apoptose.¹ Couvrant virtuellement toute surface cellulaire, incluant celle des bactéries et virus, les glycanes possèdent un rôle clé dans un contexte d'infection, notamment au niveau de l'adhérence des pathogènes aux cellules de l'hôte et à l'invasion des tissus.² De nombreuses toxines bactériennes reconnaissent également des oligosaccharides sialylés et fucosylés situés à la surface de cellules de l'hôte.³ Par ailleurs, les composés glycosidiques sont critiques dans le contexte de certaines maladies chroniques. Par exemple, des motifs de glycosylation aberrants à la surface de cellules cancéreuses peut refléter le type et la progression de cancers,⁴ alors que l'induction d'auto-anticorps contre des motifs de glycosylation de glycolipides humains est associée à plusieurs maladies auto-immunes telles que le syndrome de Guillain-Barré.⁵

Considérant le rôle central qu'occupent les glucides quant à de nombreux processus biologiques et grâce à l'émergence de nouvelles technologies facilitant l'étude du glycome, il n'est pas étonnant que les dernières années aient été marquées par une croissance fulgurante de la découverte et du développement d'agents prophylactiques et thérapeutiques à base de sucres.⁶ Dans cette optique, bien que de nombreux composés thérapeutiques et prophylactiques soient d'origine naturelle, la chimie de synthèse s'avère un outil de taille pour permettre l'accès à des composés de structure optimisée, contrôlée et homogène, et facilite l'obtention de molécules exemptes de contaminants biologiques. Par ailleurs, la chimie de synthèse se veut particulièrement intéressante dans un contexte glycobiologique. En synthétisant des mimes synthétiques de glucides naturels, il est effectivement beaucoup plus facile d'étudier leur importance biologique, notamment via l'étude des interactions glucides-protéines.

CHAPITRE 1 - INTRODUCTION

Ainsi, les prochaines sections présenteront un survol de l'utilisation de composés glycosidiques en tant qu'agents thérapeutiques et en tant que vaccins, suivi de quelques exemples sélectionnés d'autres applications des glucides, avec une emphase sur les composés synthétiques. Enfin, les défis associés à la préparation de tels composés seront adressés.

1.2 Sucres en tant qu'agents thérapeutiques

Depuis l'isolation de la streptomycine (Fig. 1) en 1944 de la bactérie à Gram positif *Streptomyces griseus*,⁷ les recherches portant sur la découverte et la synthèse de composés thérapeutiques contenant des unités glycosidiques se sont exponentiellement multipliées. Outre l'importance biologique démontrée des glucides, certaines de leurs propriétés et caractéristiques intrinsèques en font des composés intéressants pour le développement de nouvelles molécules bioactives. La nature hydrophile des sucres due à la présence de nombreux groupements hydroxyles ou amines augmente la solubilité des drogues, permettant par le fait même de ne pas utiliser de co-solvants tels que le Tween 80.^{6, 8} Ces multiples groupements OH et NH₂ favorisent par ailleurs les interactions avec les cibles macromoléculaires,⁶ augmentant ainsi l'activité thérapeutique du composé, tout en offrant un éventail de possibilités de fonctionnalisation pour l'optimisation de son activité biologique. Enfin, étant ubiquitaires dans le corps, l'ajout d'unités glycosidiques à des composés thérapeutiques peut les rendre davantage biocompatibles.⁶

CHAPITRE 1 - INTRODUCTION

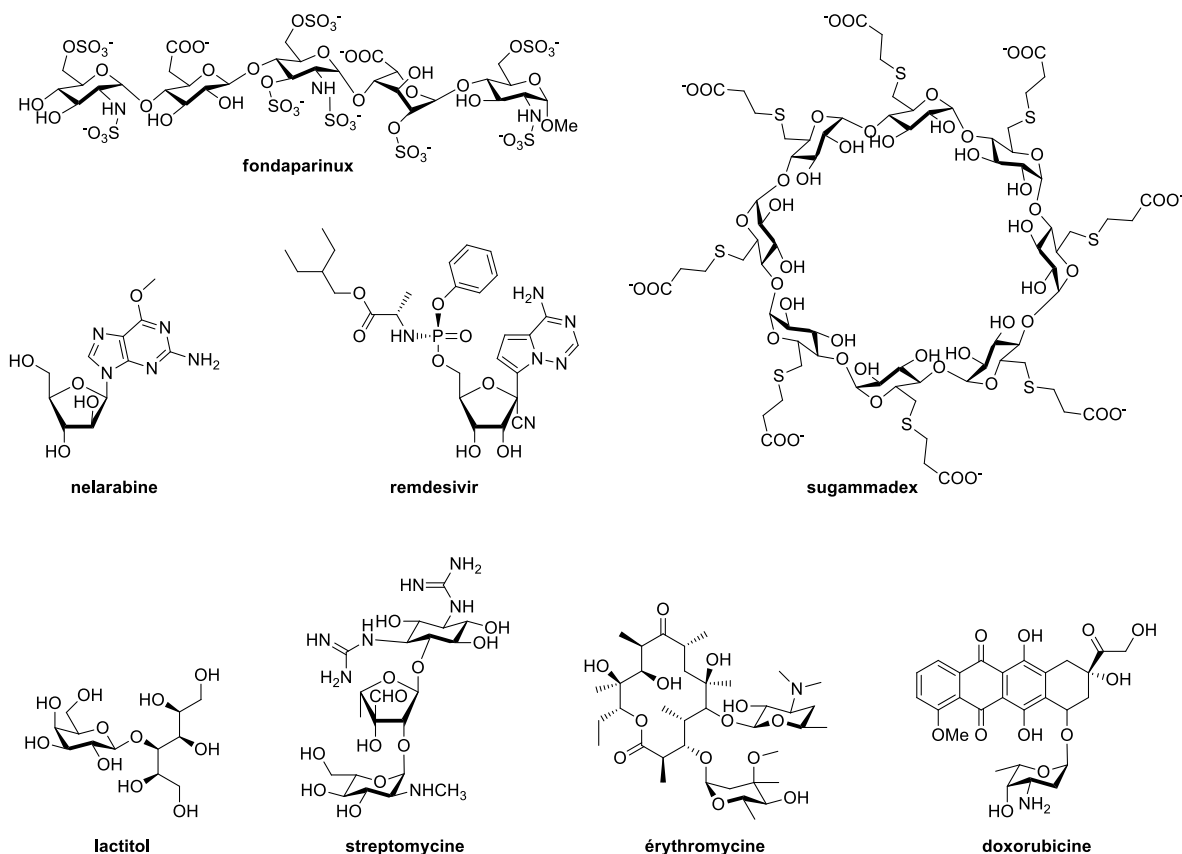


Figure 1.1. Exemples sélectionnés de composés thérapeutiques à base de sucres

Pour ces raisons, de nombreux composés glycosidiques ont été étudiés dans les dernières années quant à leur potentiel pour le traitement d'infections, de cancers, de maladies cardio-cérébrovasculaires, de maladies métaboliques, et bien plus encore.⁶ L'un des exemples les plus frappants quant à l'utilité d'oligosaccharides synthétiques dans un contexte thérapeutique est la découverte du fondaparinux (Fig. 1). S'apparentant à l'héparine, un glycosaminoglycane naturel isolé de sources bovines et porcines,⁹ ce composé consiste en un pentasaccharide synthétique employé cliniquement comme anticoagulant grâce à sa capacité à catalyser l'inactivation d'une enzyme impliquée dans la cascade de coagulation.^{10, 11} Comparativement à l'héparine et à d'autres analogues naturels de faible poids moléculaire, le fondaparinux est davantage biodisponible et prévisible et, grâce à sa nature synthétique, ne présente pas de risques de contamination biologique.^{12, 13} L'oligosaccharide cyclique sugammadex¹⁴ (Fig. 1), un analogue de la γ -cyclodextrine, constitue un autre exemple du succès de la chimie de synthèse et de l'utilité des glucides pour le développement de nouvelles thérapies. Ce composé est particulièrement novateur

CHAPITRE 1 - INTRODUCTION

en pharmacologie neuromusculaire,¹⁵ celui-ci pouvant chélater et ainsi mettre fin à l'action des relaxants musculaires rocuronium et vécuronium, tous deux employés lors de l'intubation de patients.^{14, 16-18} La nelarabine¹⁹ et le remdesivir,^{20, 21} des dérivés nucléosidiques synthétiques utilisés pour le traitement de lymphomes et de la COVID-19, respectivement, l'antibiotique macrolide érythromycine,^{6, 22, 23} l'anthracycline anticancer doxorubicine,^{24, 25} ainsi que le laxatif lactitol²⁶ sont d'autres exemples représentatifs de la versatilité thérapeutique des composés glycosidiques (Fig. 1).

En dépit de leur énorme potentiel comme agents thérapeutiques—prouvé à maintes reprises—et aux nombreuses études précliniques passées et en cours, les composés thérapeutiques à base de sucres demeurent grandement sous-représentés au niveau commercial. En effet, selon une récente revue de littérature, uniquement neuf des 200 médicaments à petites molécules (« *Small molecule drugs* ») approuvés par le *Food and Drug Administration* aux États-Unis entre 2015 et 2020 étaient à base de sucres.⁶ Si cette donnée ne corrèle pas à l'importance biologique des glucides et à leur présence ubiquitaire dans les organismes vivants, elle peut toutefois être rationalisée par les défis inhérents aux glucides, particulièrement aux difficultés reliées à leur synthèse (*vide infra*). Avec l'avènement de nouvelles technologies facilitant l'étude du glycome et des interactions sucres-protéines, de méthodes permettant la préparation automatisée d'oligosaccharides, le développement de nouvelles approches de synthèse régio- et stéréosélectives, et la préparation de glycomimétiques, il est cependant espéré que les prochaines années seront caractérisées par une augmentation du nombre d'agents thérapeutiques à base de sucres.²⁷

1.3 Sucres en tant qu'agents prophylactiques

1.3.1 Vaccins antibactériens

Omniprésents à la surface cellulaire, les glucides y sont souvent attachés à des unités lipidiques ou protéiques, formant ainsi des glycolipides et glycoprotéines. Chez les bactéries à Gram négatif, ceux-ci incluent notamment les lipopolysaccharides (LPS), les exopolysaccharides (EPS) et, chez les bactéries encapsulées, les polysaccharides capsulaires (CPS). La structure de ces polysaccharides se veut spécifique à chaque espèce bactérienne mais peut également varier de façon significative d'une souche bactérienne à l'autre.

CHAPITRE 1 - INTRODUCTION

Ces polysaccharides de surface bactériens sont connus pour être d'importants facteurs de virulence et de puissants antigènes en raison de leur rôle clé dans les processus d'interactions hôte-pathogène²⁸ et sont ainsi des candidats de choix pour le développement de vaccins. Malgré leur potentiel, ces polysaccharides ne peuvent qu'induire une réponse immunitaire de type « cellules T indépendantes ». Tel qu'illustré à la Figure 2, les polysaccharides libres peuvent activer les cellules B via « *cross-linking* ». Une telle activation mène à une réponse immunitaire caractérisée par sa courte durée, l'absence d'une mémoire immunitaire, et la production d'anticorps temporaires IgM.^{29, 30} Or, ce mécanisme n'est pas mature chez les enfants en bas âges et les vaccins polysaccharidiques ne sont donc pas efficaces chez ceux-ci, ni chez les patient·es splénectomisé·es ou immunodéprimé·es.³¹ Afin de contourner ce problème, les polysaccharides antigéniques peuvent être conjugués à une protéine de transport, ce qui leur permet d'induire une réponse immunitaire impliquant les cellules T. Lors d'une telle réponse, le glycoconjugué est d'abord traité par des cellules présentatrices d'antigènes, celles-ci générant alors un fragment glycane-peptides (Fig. 2). La fraction peptidique de ce fragment a pour rôle d'agir comme fonction d'ancrage lui permettant d'être présenté par le complexe majeur d'histocompatibilité de type II aux cellules T, ces dernières reconnaissant la fraction glycane. Cette reconnaissance induit alors l'activation des cellules T et celles-ci peuvent ensuite induire la maturation de cellules B activées en cellules effectrices et mémoires.³² Enfin, cette cascade mène également au changement de classe IgM vers IgG, offrant ainsi une protection à long terme contre le pathogène.³³

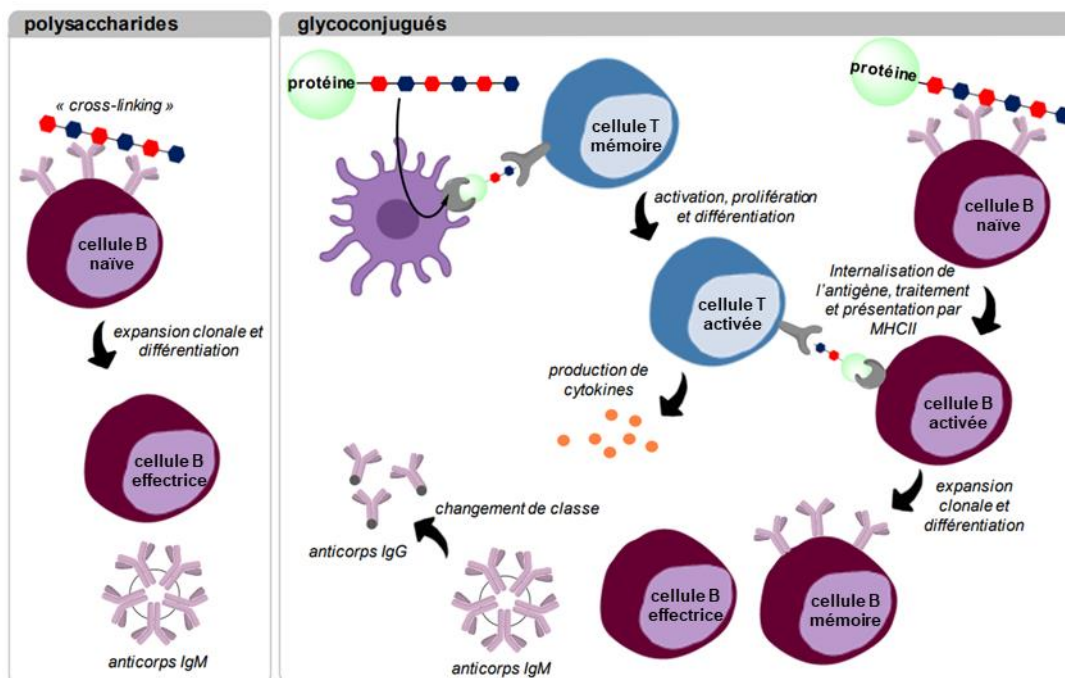


Figure 1.2. Mécanisme d'activation immunitaire par des polysaccharides et glycoconjugués

Bien que d'autres soient étudiées au niveau pré-clinique,³⁴ les protéines de transport actuellement employées pour la préparation de vaccins glycoconjugués sont l'anatoxine diphtérique (*diphtheria toxoid*, DT), le variant non-toxique de l'anatoxine diphtérique CRM₁₉₇, l'anatoxine tétanique (*tetanus toxoid*, TT), le complexe protéique de la membrane externe du méningocoque du sérotype B (*outer membrane protein complex*, OMPC), et la protéine D d'*Haemophilus influenzae* (*H. influenzae protein D*, HiD).^{35, 36} La conjugaison des oligosaccharides peut se faire de façon aléatoire via l'activation chimique des groupements hydroxyles, formant un glycoconjugué de type « treillis », ou de façon dirigée à l'extrémité réductrice ou non-réductrice de l'oligosaccharide, résultant en un glycoconjugué de type « soleil ».³⁷ Lorsque ce sont des oligosaccharides synthétiques qui sont employés, c'est cette dernière méthodologie qui est priorisée, celle-ci permettant d'accéder à des préparations homogènes. Par ailleurs, afin de réduire l'encombrement stérique engendré par la protéine de transport, des molécules de liaison peuvent être introduites entre l'oligosaccharide et la protéine.³⁷

Étudiée pour la première fois par Avery et Goebel en 1929 avec des polysaccharidiques pneumococciques,³⁸ l'efficacité clinique d'une telle approche a d'abord été démontrée par

CHAPITRE 1 - INTRODUCTION

l'introduction de vaccins glycoconjugués à base de CPS contre *H. influenzae* de type b en 1988.³⁹ Plusieurs vaccins glycoconjugués ont depuis été commercialisés, non seulement contre *H. influenzae* de type b mais également contre *Streptococcus pneumoniae*, *Neisseria meningitidis* et *Salmonella typhi*.^{40, 41}

Malgré le succès de ces vaccins glycoconjugués, l'utilisation d'oligosaccharides naturels n'est pas sans défis. L'hétérogénéité structurale des poly- et oligosaccharidiques isolés induit des variations d'un lot de vaccins à l'autre ainsi qu'au niveau de leur efficacité. Les difficultés associées au contrôle de la conjugaison peuvent la rendre non-reproductible et ainsi affecter la qualité de la réponse immunitaire induite par la vaccination. De plus, les potentiels contaminants biologiques présentent un risque important de toxicité et nécessitent que des étapes de purification extensives, complexes et dispendieuses soient effectuées. Enfin, la nécessité d'effectuer des cultures de pathogènes bactériens à grande échelle pour isoler une quantité suffisante de polysaccharides présente un risque réel pour la santé du personnel de laboratoire.⁴² Pour ces raisons, la préparation de vaccins glycoconjugués à base de polysaccharides synthétiques constitue une avenue de plus en plus prisée. La chimie organique permet effectivement la préparation de composés homogènes de façon reproductible et exempts de contamination biologique, et ce, à un coût potentiellement moindre que pour la production de vaccins à base de polysaccharides naturels.⁴³ Cette avenue se veut également avantageuse en ce qui concerne le contrôle et la reproductibilité de l'étape de conjugaison à une protéine de transport.²⁹

De nombreux vaccins glycoconjugués semi-synthétiques sont actuellement étudiés au niveau préclinique, notamment contre *Campylobacter jejuni*,⁴⁴ *Burkholderia pseudomallei* et *Burkholderia mallei* (*vide infra*),⁴⁵ pour ne nommer que ceux-ci. Cependant, un seul vaccin formé d'oligosaccharides synthétiques a jusqu'à maintenant été commercialisé, c'est-à-dire le vaccin QuimiHib contre *H. influenzae* de type b (Fig. 3).^{29, 46} Entamé en 1989 par des équipes de recherche cubaines et canadiennes, c'est en 2004 que ce vaccin semi-synthétique économiquement avantageux et constitué d'environ huit unités ribosylribitol phosphate a finalement été commercialisé à Cuba, après avoir montré un taux d'efficacité de 99.7% chez les enfants.⁴⁶

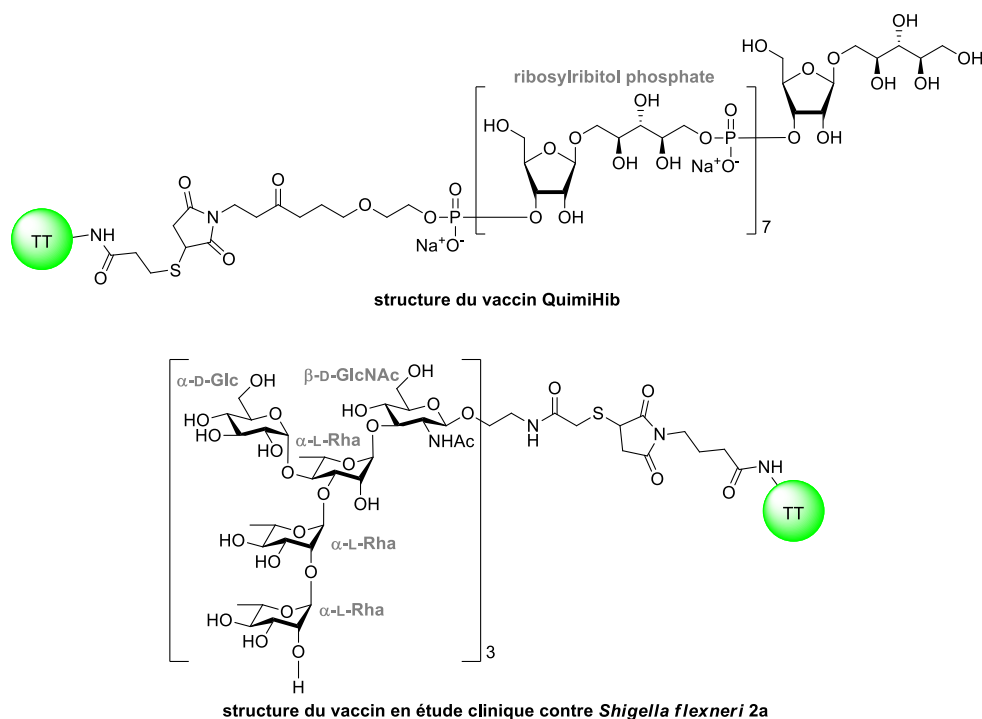


Figure 1.3. Structure du vaccin Quimi-Hib et du vaccin en étude clinique contre *Shigella flexneri* 2a

Le glycoconjugué contre *Shigella flexneri* 2a à base d'un oligosaccharide 15-mère synthétique développé par Mulard *et al.*⁴⁷ est un autre exemple de réussite de la chimie de synthèse pour la mise au point de vaccins contre des pathogènes bactériens (Fig. 3). Formé d'un pentasaccharide de structure $[\rightarrow 2)\text{-}\alpha\text{-L-Rhap-(1}\rightarrow 2)\text{-}\alpha\text{-L-Rhap-(1}\rightarrow 3)\text{-}[\alpha\text{-D-Glcp-(1}\rightarrow 4)]\text{-}\alpha\text{-L-Rhap-(1}\rightarrow 3)\text{-}\beta\text{-D-GlcpNAc-(1}\rightarrow]$ répété à trois reprises^{48, 49} et conjugué à la protéine TT via une molécule liante de type thiol-maléimide, ce glycoconjugué a fait l'objet d'un essai clinique de phase I après avoir démontré son antigénicité et son immunogénicité dans des modèles animaux. Cette étude a permis de mettre en évidence l'innocuité du glycoconjugué tout en montrant que celui-ci pouvait induire des titres élevés d'anticorps anti-LPS de *S. flexneri* 2a, démontrant son immunogénicité.⁵⁰ Suite à ces résultats, ce composé fait actuellement l'objet d'un essai clinique de phase II,⁴⁷ attestant ainsi du potentiel de la chimie de synthèse pour le développement de vaccins antibactériens.

1.3.2 Autres types de vaccins

En plus des vaccins antibactériens, les glucides sont de plus en plus étudiés pour le développement de vaccins contre d'autres maladies, telles que le virus de l'immunodéficience humaine (VIH) et le cancer. L'approche synthétique se veut d'autant plus pertinente dans de tels cas, où les antigènes oligosaccharidiques naturels sont difficiles d'accès ou ne peuvent pas être isolés.⁵¹

En 1996,⁵² il a été découvert qu'un anticorps neutralisant⁵³⁻⁵⁶ pouvant se lier à des oligomannoses⁵⁷ de l'enveloppe glycoprotéique de VIH-1 était capable de neutraliser un large éventail de souches de VIH-1 et protégeait des infections chez des modèles animaux.⁵⁸⁻⁶² Le groupe de Davis s'est ainsi inspiré de ces observations afin de développer un vaccin oligosaccharidique synthétique à base d'unités mannosés pouvant mimer l'épitope naturel reconnu par cet anticorps.⁵⁹ Cette équipe a réalisé la synthèse d'un glycoconjugué formé de trois résidus α -D-Man et d'une unité non-naturelle 6-méthyle- α -D-Man à l'extrémité réductrice (Fig. 4). Ce tétrasaccharide a été conjugué à la particule de type virus (*virus-like particle*) Q β , caractérisée par son immunogénicité et par sa grande densité de résidus lysine disponibles pour conjugaison.⁶³ Alors que ce glycoconjugué présentait une forte antigénicité et était capable de produire des anticorps reconnaissant l'oligosaccharide naturel, ces anticorps n'étaient malheureusement pas capables de neutraliser VIH-1.⁵⁹

CHAPITRE 1 - INTRODUCTION

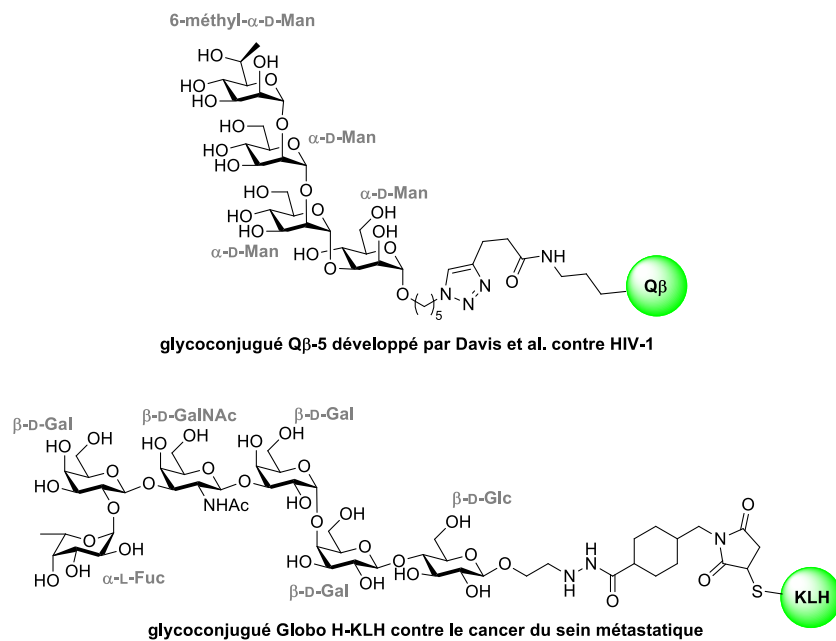


Figure 1.4. Structure des glycoconjugués Qβ-5 contre le VIH et Globo H-KLH contre le cancer

Tel que mentionné précédemment, la présence de motifs de glycosylation aberrants à la surface de cellules cancéreuses est un marqueur du type et de la progression de cancers.⁶⁴ Ces motifs peuvent agir en tant qu'antigènes glycosidiques associés aux tumeurs (*tumor-associated carbohydrate antigen*, TACA) et sont donc des cibles de choix pour le développement de nouvelles immunothérapies contre le cancer.⁶⁵ Parmi les TACA identifiés à ce jour, l'hexasaccharide Globo H, isolé pour la première fois à partir d'une lignée cellulaire de cancer du sein, est l'un des plus importants, celui-ci étant surexprimé dans de nombreux types de cancer.⁶⁶

Dans le cadre de leur programme de recherche ayant débuté en 1995 et visant à développer un vaccin contre le cancer, Danishefsky⁶⁷ et Wong ont rapporté^{68, 69} puis optimisé⁷⁰ la synthèse totale de l'hexasaccharide Globo H (Fig. 4).⁷¹ Plus récemment, les auteurs ont par ailleurs développé une approche enzymatique pour accéder à cet oligosaccharide dans l'optique de réduire les coûts de fabrication ainsi que les étapes de purification.⁷² Après avoir démontré sa capacité à induire la production d'anticorps capables de lyse cellulaire chez la souris,⁷³ le glycoconjugué Globo H-KLH a fait l'objet d'un essai clinique de phase I contre le cancer de la prostate et le cancer du sein, démontrant son innocuité et son immunogénicité,^{67, 74} et fait ainsi actuellement l'objet d'essais cliniques de phase II et III.^{71, 75, 76}

CHAPITRE 1 - INTRODUCTION

Toujours dans un contexte de vaccination, les composés glycosidiques se sont d'ailleurs démontrés être intéressants en tant qu'adjuvants, c'est-à-dire en tant que composés augmentant l'intensité et la durée de la réponse immunitaire induite par un vaccin. En comparaison aux agents à base d'aluminium actuellement utilisés, les glucides présentent plusieurs avantages, tels que leur innocuité, leur tolérabilité par les patients, leur capacité à être métabolisés et excrétés par l'organismes, et leur tendance à induire moins d'effets secondaires.⁷⁷ Le composé QS21, une saponine glycosidique isolée de *Quillaja saponaria* (QS), est l'un des adjuvants glycosidiques les plus étudiés (Fig. 5). Cet adjuvant consiste en fait en un mélange de deux composés, *i.e.*, QS21-apiose et QS21-xylose, et s'est montré efficace dans des formulations de vaccin contre l'herpès, le VIH, et le cancer, notamment.⁷⁷ Toutefois, l'hétérogénéité de cet adjuvant, combinée aux difficultés associées à son isolation, à son instabilité, et à sa toxicité, limite grandement son utilisation.^{78, 79} Pour cette raison, des efforts ont été investis dans la synthèse d'analogues de structure simplifiée et caractérisés par des activités adjuvantes optimisées. Notamment, le groupe de Gin s'est intéressé à la modification structurelle des quatre domaines (A–B, Fig. 5) de QS21 afin de réaliser une étude de relations structure-activité.⁸⁰ Leur étude a montré que le domaine trisaccharidique A n'était pas nécessaire à l'activité adjuvante de la saponine, alors que le domaine trisaccharidique C était requis. L'aldéhyde équatorial du domaine B n'est pas indispensable alors que le groupement hydroxyle axial est important pour l'activité biologique des composés. Enfin, Gin *et al.* ont montré que le domaine D tolérait certaines modifications, telles que l'introduction de fonctions amides remplaçant les fonctions esters ou la simplification de la chaîne acyle.⁸⁰ Au travers leurs travaux, cette équipe a ainsi non seulement mis en valeur la pertinence des glucides dans un contexte de développement d'adjuvants, mais également le rôle crucial qu'occupe la chimie de synthèse pour accéder à de tels composés.

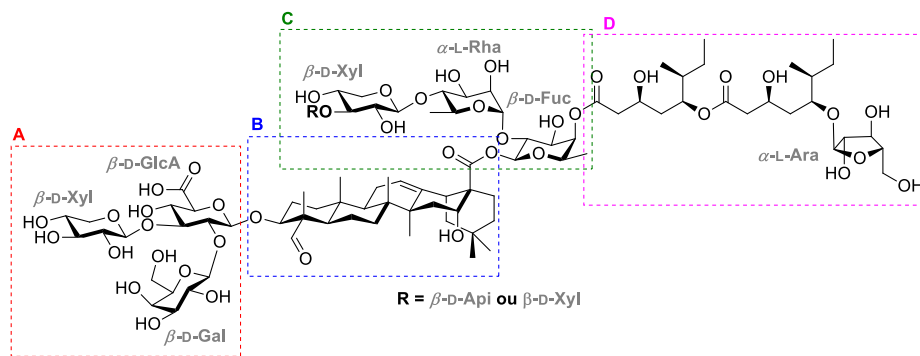


Figure 1.5. Structure de QS21 et domaines (A–D) faisant l’objet d’études structurales

Outre les saponines, d’autres adjuvants glycosidiques font l’objet de nombreuses recherches, notamment des composés analogues du glycolipide synthétique α -galactosylcéramide dérivé d’éponges marines et des analogues du lipide A des LPS.⁸¹

1.4 Autres applications des glucides

En plus de leur utilité en tant qu’agents thérapeutiques et prophylactiques, les glucides ont démontré à maintes reprises leur potentiel pour différentes applications, notamment en tant qu’outils diagnostiques ou biosurfactants.

1.4.1 Les sucres en tant qu’outils diagnostiques

Par leur ubiquité à la surface cellulaire, les poly- et oligosaccharides sont un outil particulièrement intéressant dans un contexte de diagnostic. Plus spécifiquement, ceux-ci sont utilisés pour la préparation de biopuces à glycanes (*glycan microarrays*) consistant en une surface à laquelle est attachée une variété d’oligosaccharides de structures connues (Fig. 6).⁸² Souvent de natures synthétiques, ces oligosaccharides sont liés à cette surface à l’aide d’une molécule liante. Une fois immobilisés, ces sucres peuvent être reconnus par des protéines (*e.g.*, des anticorps) ou même des cellules complètes ou des virus.⁸² En utilisant le sérum de personnes infectées par des pathogènes, ces biopuces à glycanes peuvent ainsi être mises à profit pour détecter des pathogènes et procéder à un diagnostic. Cette approche a d’ailleurs été employée pour détecter différentes infections, telles que la salmonelle⁸³ et la malaria.⁸⁴ De façon similaire, une biopuce à glycane basée sur l’hexasaccharide Globo H a permis la détection d’anticorps associés au cancer du sein, démontrant le potentiel de cette méthode pour le diagnostic de différents cancers.⁸⁵ Par ailleurs, puisque la

CHAPITRE 1 - INTRODUCTION

structure des oligosaccharides situés à la surface cellulaire de pathogènes se veut spécifique à chaque souche, il a été suggéré que les biopuces à glycanes pourraient être employées pour la surveillance d'événements épidémiques.⁸²

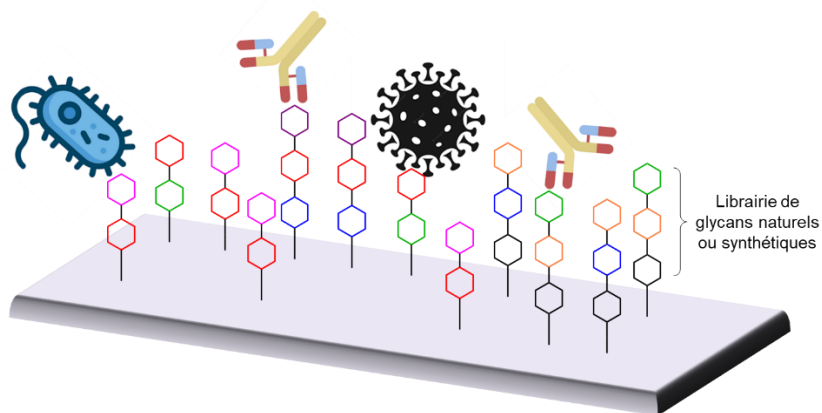


Figure 1.6. Biopuces à glycanes

Outre ces utilisations, il est important de mentionner qu'une telle technologie est également employée pour l'étude de processus de reconnaissances des glucides ou comme outil d'identification de nouveaux candidats prophylactiques. Le groupe de Seeberger a par exemple développé une biopuce à glycanes formée d'oligomannoses afin d'identifier de potentiels antigènes pour la mise au point de vaccins contre le VIH.⁸⁶ Enfin, cette technologie a également été mise à profit pour la découverte de nouveaux biomarqueurs pour le diagnostic de différentes maladies.⁸⁷

1.4.2 Les sucres en tant que biosurfactants

Les surfactants sont des molécules amphiphiles équipées de portions hydrophiles et hydrophobes. Grâce à cette dichotomie intrinsèque, ces composés ont l'habileté de réduire les tensions de surface à l'interface liquide/liquide, liquide/air ou liquide/solide. Ainsi, par la formation de micelles, de tels agents augmentent la solubilité de composés normalement insolubles dans l'eau, tel que l'huile. Pour cette raison, les surfactants trouvent application dans bon nombre de domaines, tel que la bioremédiation et la récupération de déversement d'huile, l'industrie pharmaceutique, l'industrie cosmétique, les détergents et agents nettoyants, et l'industrie agroalimentaire.⁸⁸ Or, la majorité des surfactants actuellement produits sont dérivés de sources pétrolières non-

CHAPITRE 1 - INTRODUCTION

renouvelables et se trouvent sous forme de sulfates ou sulfonates d'alcanes. À cause de leur origine, de tels agents sont souvent toxiques, difficilement biodégradables, et donc nocifs pour l'environnement, stimulant ainsi la recherche de surfactants pouvant substituer ceux-ci.⁸⁹

Afin d'adresser cette problématique environnementale, les biosurfactants, définis comme des surfactants d'origines biologiques, font l'objet d'extensives recherches. Parmi les différents types de biosurfactants, il est possible de compter sur les glycolipides, qui forment la plus importante classe. Ceux-ci sont composés d'un ou plusieurs sucres reliés à une longue chaîne lipidique et trouvent actuellement application dans le domaine des biotechnologies environnementales⁹⁰ et dans les industries cosmétiques⁹¹ et alimentaires.⁹² Par exemple, les sophorolipides (Fig. 7) sont notamment utilisés dans l'industrie cosmétique grâce à leur propriétés moussantes, solubilisantes et détergentes ainsi que leur bonne biocompatibilité.⁹¹ Les plus étudiés des biosurfactants glycolipidiques sont les rhamnolipides, généralement classifiés comme mono- ou dirhamnolipidiques, et dont l'unité lipidique consiste en un acide gras C10 hydroxylé en C3 (Fig. 7).⁸⁸ Ceux-ci sont principalement issus de la bactérie à Gram négatif *Pseudomonas aeruginosa*.⁹³ Or, comme il s'agit d'un agent pathogène opportuniste classé dans la catégorie de risques biologiques de niveau 2,⁹³ de nombreuses recherches sont effectuées afin de trouver une autre méthode de production de rhamnolipides à l'échelle industrielle,⁹⁴ notamment par synthèse chimique.⁹⁵⁻⁹⁷ Il est important de mentionner qu'outre leur potentiel dans les domaines mentionnés ci-dessus, les glycolipides sont également d'un très grand intérêt dans un contexte de développement d'agents thérapeutiques. En effet, leur nature amphiphile leur permet d'altérer les membranes cellulaires, leur conférant une activité antimicrobienne.⁹⁸ Les rhamnolipides ont par exemple montré posséder une activité antimicrobienne contre de nombreux pathogènes incluant *Escherichia coli*⁹⁹ et *Klebsiella pneumoniae*.¹⁰⁰ Dans un ordre d'idées similaires, les sophorolipides ont également été étudiés pour leur potentiel antimicrobien contre plusieurs bactéries à Gram positif.⁹⁸

CHAPITRE 1 - INTRODUCTION

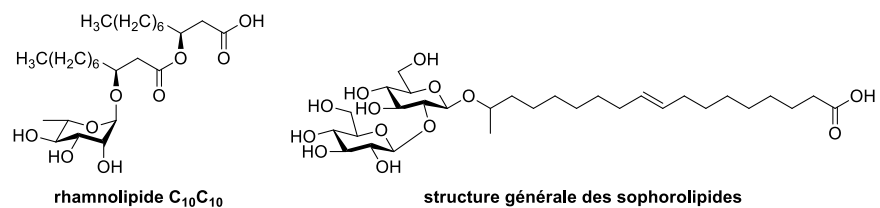


Figure 1.7. Exemples de glycolipides utilisés comme biosurfactants

1.5 Synthèse de mono- et oligosaccharides

Il apparaît ainsi évident que les glucides sont une vraie mine d'or pour le développement de nouveaux agents thérapeutiques et prophylactiques, de nouveaux outils diagnostiques, et de nouvelles biotechnologies. Les mono- et oligosaccharides synthétiques se veulent particulièrement attrayants, notamment grâce à la possibilité d'obtenir des composés homogènes de façon reproductible, de contrôler leur structure, ainsi que de fonctionnaliser les différents groupements OH et NH₂ des unités glycosidiques.

L'accès à de tels composés synthétiques n'est toutefois pas sans défis. En effet, en dépit des progrès significatifs dans le domaine de la chimie des sucres dans les dernières années, il n'existe toujours pas de voie générale permettant l'accès facile à des glycosides fonctionnalisés. Les caractéristiques intrinsèques des glucides, *i.e.*, leur nature polyfonctionnelle et la présence de plusieurs centres stéréogènes, en font des composés particulièrement difficiles à contrôler au niveau réactionnel. Pour la synthèse d'oligosaccharides, non seulement les glycosylations sont grandement imprévisibles en termes de réactivité, régiosélectivité et stéréosélectivité (α vs β), mais la nécessité de bloquer temporairement les groupements hydroxyles des donneurs et accepteurs de glycosyles par des groupements protecteurs orthogonaux pouvant par la suite être sélectivement clivés pour procéder à l'élongation de l'oligosaccharide représente un défi de taille. Ces protections et déprotections régiosélectives requièrent de nombreuses étapes de synthèse et sont spécifiques au sucre étudié. Elles demandent donc une grande connaissance des différents types de groupements protecteurs (silyl, éthers, esters, amides, *etc.*) et des réactivités respectives des hydroxyles du sucre étudié (glucose, mannose, rhamnose, idose, *etc.*). Par exemple, des groupements stériquement encombrants, *e.g.*, trityle (Tr) ou *tert*-butyldiméthylsilyle (TBS), vont préférentiellement réagir avec les hydroxyles primaires vs les hydroxyles secondaires. En ce qui concerne la réactivité des groupements hydroxyles secondaires, il a notamment été observé que dans la série *D-gluco*, la

CHAPITRE 1 - INTRODUCTION

position C2 se veut la plus réactive dans une réaction de benzylation.¹⁰¹ À l'inverse, la position secondaire la plus réactive dans la série D-manno est plutôt C3.^{101, 102} La régiosélectivité des hydroxyles variant d'un sucre à l'autre, leur protection régiosélective se veut donc très complexe. La Figure 8 résume les différents défis rencontrés en synthèse de glycosides.

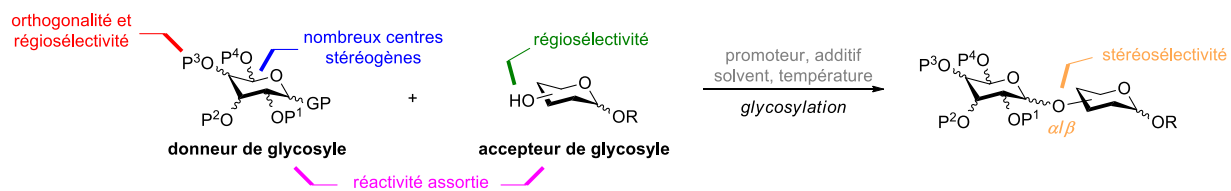


Figure 1.8. Défis rencontrés en chimie des sucres

1.5.1 Réactions de glycosylation

L'une des plus grandes difficultés en synthèse oligosaccharidique demeure cependant la formation de liens glycosidiques.¹⁰³ Dans une réaction de glycosylation typique, un donneur de glycosyle doté d'un groupement partant en position anomérique est activé par un promoteur, formant ainsi une espèce électrophile pouvant être attaquée par le nucléophile entrant, aussi appelé accepteur. Ce dernier peut être un sucre mais peut également être un composé non-glycosidique.

Il est aujourd'hui généralement accepté que les réactions de glycosylations se font à l'interface S_N1/S_N2 (Fig. 9).¹⁰⁴ Tel qu'illustré, entre ces extrêmes réactionnels s'insère un continuum d'intermédiaires pouvant être impliqués dans une réaction de glycosylation. L'importance de ceux-ci est contrôlée par différents facteurs tels que la température, la nature des groupements protecteurs, la réactivité de l'accepteur de glycosyle, le solvant, le système de promoteur, etc. Ainsi, l'activation du groupement partant (GP) d'un donneur de glycosyle (**A**) peut mener à la formation d'une variété d'électrophiles (**B-D**) pouvant réagir selon des mécanismes de s'apparentant aux types S_N1 ou S_N2 . Une espèce intermédiaire covalente **B-β**, e.g. un intermédiaire triflate, peut par exemple être sujet à une substitution nucléophile S_N2 par l'accepteur entrant, menant à la formation d'un glycoside **E-α** via un mécanisme bimoléculaire. L'intermédiaire **B-β** est également en équilibre avec la paire d'ions de contact (**C-β**), dont le contre ion X^- encombre la face supérieure du sucre et mène ainsi au glycoside **E-α** via une réaction s'apparentant au type S_N2 . Enfin, l'intermédiaire **C-β** se veut en équilibre avec la paire d'ions séparés par le

CHAPITRE 1 - INTRODUCTION

solvant (**D**), s'apparentant à un ion oxocarbenium. Ce dernier peut quant à lui être sujet à une réaction de glycosylation de type S_N1 , pouvant donc mener aux glycosides **E- α** et **E- β** .¹⁰⁴

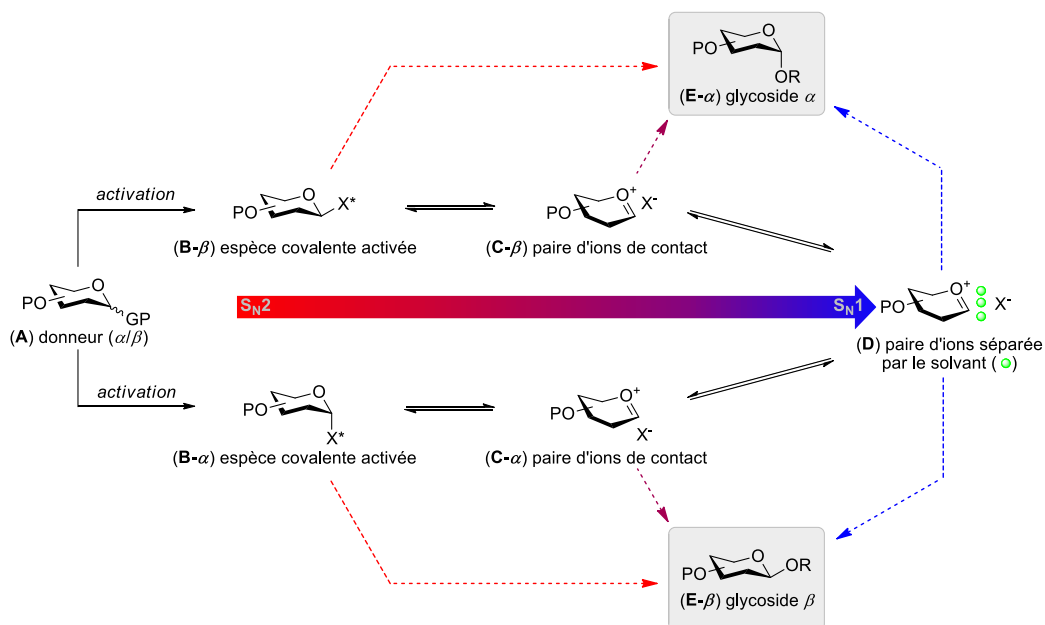


Figure 1.9. Mécanisme de glycosylation à l'interface S_N1/S_N2

Tel que mentionné, l'importance de chacun de ces intermédiaires, et par conséquent la stéréosélectivité de la réaction, est déterminée par de nombreux facteurs, dont la nature du solvant. L'utilisation de solvants pouvant stabiliser l'ion oxocarbenium (*i.e.*, paire d'ions séparés par le solvant) favorise les glycosylations de type S_N1 , alors que l'utilisation d'un solvant non polaire avantagera plutôt les mécanismes S_N2 .¹⁰⁴ Par ailleurs, les solvants étherés (Et_2O , THF) peuvent participer de façon équatoriale aux réactions de glycosylation,¹⁰⁵ menant préférentiellement au glycoside axial via un mécanisme de type S_N2 . Cet intermédiaire correspondrait au composé **B- β** dans la Figure 9, où $X = Et_2O$ ou THF. De façon analogue, les solvants de type nitrile participent via la formation d'un intermédiaire axial¹⁰⁶ et mènent à la formation préférentielle du glycoside équatorial.

Dans le même ordre d'idées, certains additifs et types de promoteurs peuvent être employés pour induire la formation contrôlée d'intermédiaires covalents (**B** dans Fig. 9). Un exemple représentatif est la formation des triflates,^{107, 108} pouvant notamment être induite par l'utilisation de TMSOTf lors de l'activation du donneur de glycosyle. Du fait de l'effet anomérique, la grande majorité des

CHAPITRE 1 - INTRODUCTION

intermédiaires triflates visualisés à ce jour sont de configuration axiale. Ceux-ci peuvent toutefois être en équilibre avec leur analogue équatorial généralement davantage réactif.¹⁰⁸ Ces intermédiaires triflates sont typiquement considérés comme étant impliqués dans des mécanismes de glycosylation de type S_N2 , de sorte qu'un α -triflate mènerait à un glycoside β , alors qu'un β -triflate (**B- β**) mènera au glycoside α (**E- α**). La stéréosélectivité de la réaction de glycosylation se veut ainsi dépendante de la stabilité respective des triflates, qui est quant à elle contrôlée par différents facteurs incluant l'orientation des groupements en C2 et C3. Ainsi, Asensio *et al.* ont mis de l'avant qu'un groupement axial en C3 déstabiliserait un triflate axial via des interactions 1,3-*syn*-diaxiales. À l'inverse, un triflate équatorial serait déstabilisé par un groupement axial en C2 par des effets stériques et électroniques, alors qu'un groupement axial en C3 le stabiliserait via la formation de liaisons hydrogènes non-canoniques avec l'hydrogène axial en C1.¹⁰⁹ Tel que mentionné précédemment, l'utilisation d'un solvant non-polaire tel que le toluène déstabiliserait quant à lui l'ion oxocarbénium, favorisant par le fait même la formation de l'intermédiaire triflate.¹¹⁰

La nature des groupements protecteurs du donneur de glycosyle influence elle aussi de façon significative la stéréosélectivité de la glycosylation. D'un côté, la présence de groupements électrodonneurs augmente la réactivité du donneur, alors que d'un autre côté, ceux-ci peuvent stabiliser la charge positive de l'ion oxocarbénium et favoriser des réactions de type S_N1 . À l'inverse, des groupements protecteurs électroattracteurs réduisent la réactivité du donneur de glycosyle, mais peuvent stabiliser les intermédiaires réactifs covalents (*e.g.*, triflates).^{104, 111} Les groupements protecteurs sur l'accepteur de glycosyle influencent eux aussi le résultat de la réaction de glycosylation en modulant sa nucléophilicité.¹¹² Enfin, la température est également un élément critique des réactions de glycosylation. Non seulement celle-ci influence la voie réactionnelle empruntée (S_N1 vs S_N2) ainsi que la stabilité des intermédiaires réactionnels, mais une plus basse température a également montré favoriser la formation des produits cinétiques β .¹¹³

1.5.1.1 Glycosylations stéréosélectives

Bien que le mécanisme réactionnel se situant à l'interface S_N1/S_N2 tout juste présenté est accepté dans la communauté glycochimique, l'énorme complexité des réactions de glycosylation implique qu'elles sont souvent abordées de façon simplifiée. Ainsi, sans oublier les intermédiaires

CHAPITRE 1 - INTRODUCTION

réactionnels présentés à la Figure 9, les sections suivantes seront basées sur une vision simplifiée des réactions de glycosylation impliquant la formation d'un intermédiaire ion oxocarbenium à la suite de l'activation du donneur de glycosyle lorsque la réaction est sous contrôle thermodynamique.

Tel que mentionné, à l'issu d'une réaction de glycosylation, deux stéréoisomères peuvent être formés, *i.e.*, les anomères α et β . Une autre façon d'aborder la stéréochimie des liens glycosidiques consiste à employer la terminologie 1,2-*cis* et 1,2-*trans* qui est basée sur l'orientation spatiale des groupements en position C1 et C2 des sucres. Cette terminologie se veut davantage générale : alors qu'un α -D-mannoside est caractérisé par un lien 1,2-*trans*, un α -D-glucoside est quant à lui caractérisé par un lien 1,2-*cis* (Fig. 10). Les prochains paragraphes emploieront donc la terminologie 1,2-*cis*/1,2-*trans* puisque celle-ci se veut davantage générale.

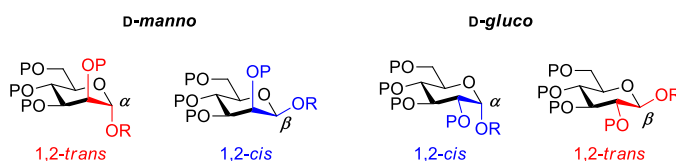


Figure 1.10. Terminologie α/β vs 1,2-*cis*/1,2-*trans*

Dans un contexte de synthèse totale, il est primordial de pouvoir contrôler la stéréosélectivité des réactions de glycosylation afin d'obtenir le composé cible anomériquement pur. L'une des méthodes les plus employées consiste en l'utilisation d'un groupement participant, *e.g.*, un ester, en position C2 du donneur de glycosyle. À la suite de l'activation du donneur de glycosyle et départ du groupement partant (GP), l'ion oxocarbenium résultant se retrouve en équilibre avec l'ion acyloxonium formé par participation anchimérique de l'ester en position C2 (Fig. 11A). Cet intermédiaire est ensuite impliqué dans un mécanisme de type S_N2 avec l'accepteur de glycosyle entrant, menant à la formation stéréosélective d'un lien 1,2-*trans*. À l'inverse, l'ion oxocarbenium formé pourrait mener à la formation des deux types de liens. Lorsque le groupement en position C2 du donneur de glycosyle n'est pas participant, *e.g.*, un éther, il est donc difficile de contrôler la stéréosélectivité de la réaction (Fig. 11B), d'autant plus que l'effet anomérique favorise la formation du lien glycosidique orienté axialement.

CHAPITRE 1 - INTRODUCTION

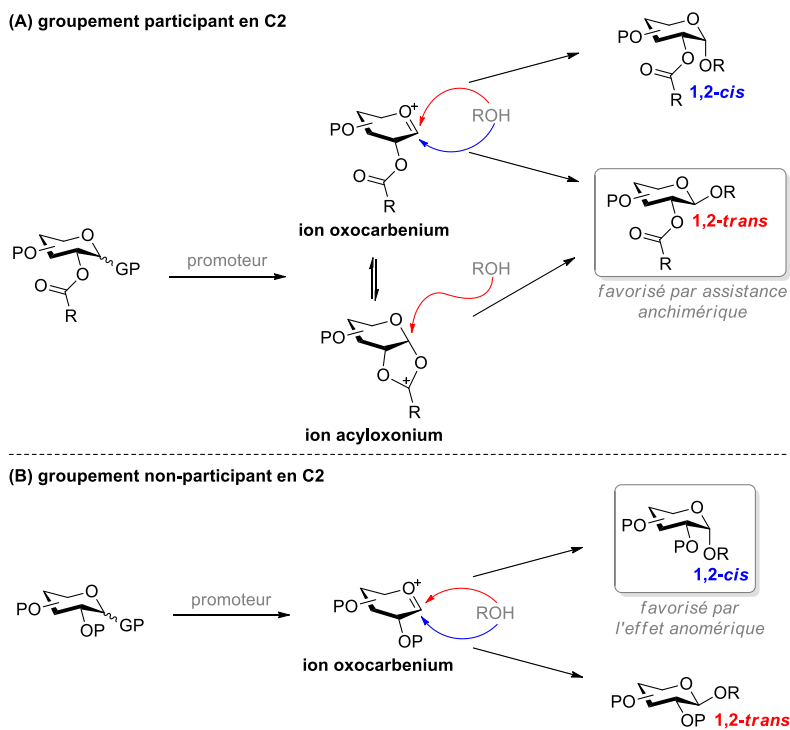


Figure 1.11. Glycosylations stéréosélectives

Alors que l'utilisation de groupements participants est très fiable pour former des liens 1,2-*trans*, notamment présents au sein de α -D-mannosides ou β -D-glucosides, la synthèse de leurs stéréoisomères 1,2-*cis* (β -D-mannosides, α -D-glucosides) se veut donc particulièrement fastidieuse et demande généralement une optimisation extensive des conditions de glycosylation.¹¹⁴ Or, les liens glycosidiques 1,2-*cis* constituent d'importantes cibles en synthèse chimique dû à leur présence ubiquitaire dans les glycanes biologiquement actifs, tels que l'EPS^{115, 116} et le CPS¹¹⁷⁻¹¹⁹ de *B. pseudomallei* et *B. mallei* et le CPS^{120, 121} de *C. jejuni* HS:4c (Fig. 12).

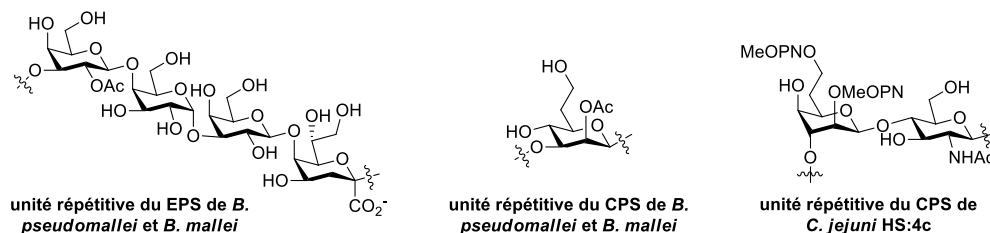


Figure 1.12. Exemples de composés naturels contenant des liens glycosidiques 1,2-*cis*

Pour adresser les défis que représentent la synthèse de tels types de liens glycosidiques, de nombreuses approches ont été développées, particulièrement pour la synthèse de liens 1,2-*cis*- β

CHAPITRE 1 - INTRODUCTION

tels que présents au sein des β -D-mannosides et β -D-idosides. La Figure 13 présente un survol de ces méthodes. Par exemple, Demchenko a montré que l'utilisation de groupements picolyle (ou picolinyle) en positions éloignées résultait en la formation stéréosélective de β -D-mannosides via formation de ponts hydrogène avec l'accepteur de glycosyle (**A**).^{122, 123} D'autres approches basées sur le déplacement de type S_N2 d'un intermédiaire α -nitrilium (**B**)¹²⁴ ou α -triflate (**C**),^{107, 125-129} sur l'utilisation d'un auxiliaire chiral en C2 (**D**),¹³⁰ sur l'inversion de configuration de la position C2 d'un glycoside de configuration 1,2-*trans*- β (**E**), ou sur la restriction conformationnelle du donneur de glycosyle (**F**),¹³⁰⁻¹³² se sont également montrées efficaces. Actuellement, l'une des méthodes les plus prometteuses¹³³ pour la préparation stéréosélective de liens 1,2-*cis*- β consiste en une glycosylation intramoléculaire par délivrance d'aglycone (**G**).¹³⁴ Cette méthode est basée sur l'introduction d'une fonction d'ancrage (2-naphthylméthyl [NAP], *p*-méthoxybenzyle [PMB], allyle, silyle, etc.) en position C2 du donneur de glycosyle menant à la formation d'un acétal mixte en présence de l'accepteur, ce dernier pouvant ensuite être « délivré » de façon complètement stéréosélective suivant l'activation de l'acétal mixte.

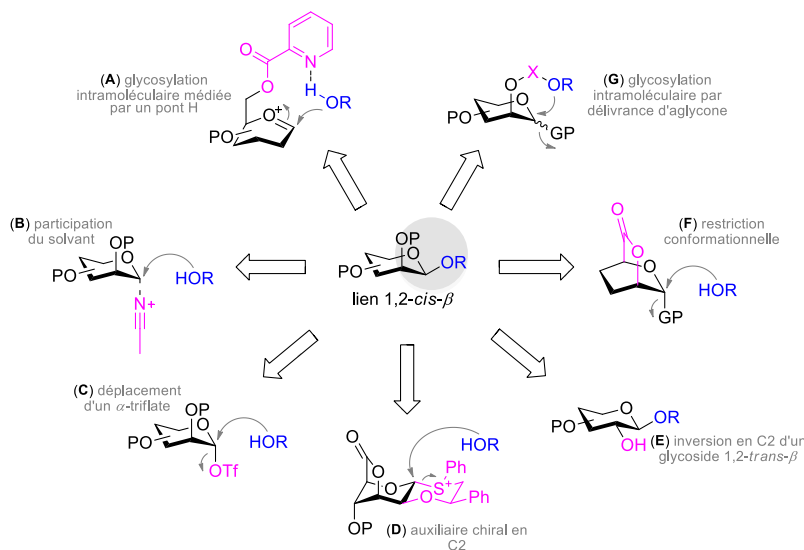


Figure 1.13. Exemples d'approches permettant la formation de liens glycosidiques 1,2-*cis*- β

1.6 Contenu de la thèse

La présente thèse s'inscrit dans un programme de recherche dont l'objectif principal vise à développer des voies de synthèse donnant accès à de potentiels agents thérapeutiques et prophylactiques. D'abord, le chapitre 2 s'articulera autour de la découverte de nouveaux agents

CHAPITRE 1 - INTRODUCTION

thérapeutiques et portera sur la synthèse totale et l'évaluation biologique des ananatosides A et B et de dérivés non-naturels (Fig. 14A; *Chem. Sci.* **2021**, *12*, 7533-7546). Ce même chapitre abordera par le fait même le potentiel tensioactif de ces composés synthétiques et leur capacité à activer le système immunitaire de certaines plantes. Les chapitres subséquents s'articuleront autour du thème des agents prophylactiques. Le chapitre 3 consistera en une revue de littérature sur la synthèse d'oligosaccharides de pathogènes à potentiel bioterroriste (*Recent Trends in Carbohydrate Chemistry*, **2020**, 143-206) et agira à titre d'introduction du chapitre 4, portant quant à lui sur la synthèse totale de tétrasaccharides en tant que potentiels vaccins contre *B. pseudomallei* et *B. mallei* (Fig. 14B; *Org. Biomol. Chem.* **2019**, *17*, 8878-8901). Le chapitre 5 offrira une vue d'ensemble sur la synthèse de mimes oligosaccharidiques du CPS de *C. jejuni* et leur potentielle activité prophylactique (*ACS Infect. Dis.* **2021**, *7*, 969-986) et introduira les chapitres subséquents qui seront orientés autour du CPS de *C. jejuni* HS:4c. Ainsi, le chapitre 6 consistera en l'optimisation d'une méthode de synthèse donnant accès aux sucres de configuration *D-ido* tel que présent dans l'unité répétitive du CPS de *C. jejuni* HS:4c (Fig. 14C, *Carbohydrate Chemistry : Proven Synthetic Methods*, **2022**, article accepté). Le chapitre 7 présentera une étude sur la formation de 1,2-*cis-β*-idosides et sur la flexibilité intrinsèque des sucres de configuration *ido* (Fig. 14D, *J. Org. Chem.* **2022**, *87*, 12932-12953). Suivra ensuite le chapitre 8 rapportant nos progrès réalisés pour effectuer la synthèse totale de l'unité répétitive disaccharidique du CPS de *C. jejuni* HS:4c (Fig. 14E, article en préparation). Enfin, le chapitre 9 offrira un résumé des travaux complétés dans le cadre de la présente thèse et conclura cette dernière.

CHAPITRE 1 - INTRODUCTION

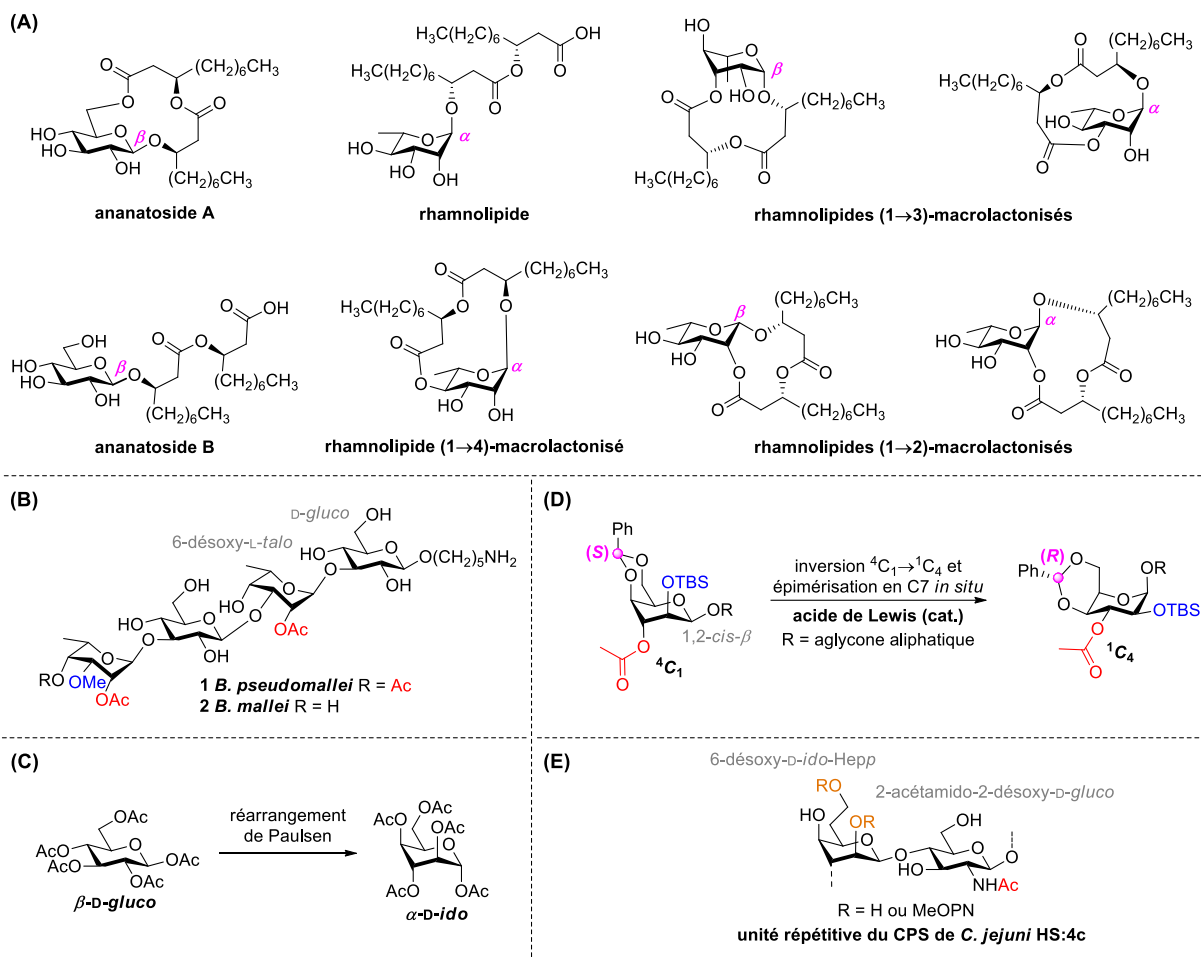


Figure 1.14. Résumé du contenu de la présente thèse

CHAPITRE 2 : TOTAL SYNTHESIS, ISOLATION, SURFACTANT PROPERTIES, AND BIOLOGICAL EVALUATION OF ANANATOSIDES AND RELATED MACRODILACTONE-CONTAINING RHAMNOLIPIDS

Maude Cloutier,^a Marie-Joëlle Prévost,^a Serge Lavoie,^b Thomas Feroldi,^b Marianne Piochon,^a Marie-Christine Groleau,^a Jean Legault,^b Sandra Villaume,^c Jérôme Crouzet,^c Stéphan Dorey,^c Mayri Alejandra Díaz de Rienzo,^{ad} Eric Déziel,^a et Charles Gauthier^a

^a*Centre Armand-Frappier Santé Biotechnologie, Institut national de la recherche scientifique (INRS), 531, boul. des Prairies, Laval (Québec), H7V 1B7, Canada*

^b*Laboratoire d'analyse et de séparation des essences végétales (LASEVE), Département des Sciences Fondamentales, Université du Québec à Chicoutimi, 555, Boulevard de l'Université, Chicoutimi (Québec), G7H 2B1, Canada*

^c*Université de Reims Champagne-Ardenne, INRAE, USC RIBP 1488, SFR Condorcet-FE CNRS 3417, 51100 Reims, France*

^d*School of Pharmacy and Biomolecular Sciences, Liverpool John Moores University, L3 3AF, Liverpool, UK*

Article publié dans *Chemical Sciences*, 2021, 12, 7533-7546, doi 10.1039/D1SC01146D

Titre français : Synthèse totale, isolation, propriétés tensioactives et évaluation biologique des ananatosides et d'analogues rhamnolipides contenant des fonctionnalités macrodilactone

Contribution des auteurs : Les synthèses chimiques ont été réalisées par Maude Cloutier et Marie-Joëlle Prévost (stagiaire de 1^{er} cycle sous la supervision de Maude Cloutier). Marianne Piochon, Serge Lavoie et Charles Gauthier ont réalisé l'isolation des ananatosides A et B ainsi que leur élucidation structurale. Les calculs de modélisation moléculaire ont été réalisés par Serge Lavoie et Thomas Feroldi. Les tests d'activité antimicrobienne et hémolytique ont été effectués par Marie-Christine Groleau, les tests de cytotoxicité par Jean Legault, les tests d'activité tensioactive par Mayri Alejandra Díaz de Rienzo, et les tests sur le système immunitaire des plantes par Sandra Villaume, Jérôme Crouzet et Stéphan Dorey. Maude Cloutier, Serge Lavoie, Marianne Piochon, Eric Déziel et Charles Gauthier ont rédigé l'article. Maude Cloutier a réalisé la caractérisation des composés synthétiques.

2.1 Résumé

Les rhamnolipides sont une classe spécifique de tensioactifs microbiens qui détiennent un grand potentiel biotechnologique et thérapeutique. Cependant, leur exploitation au niveau industriel est entravée car ils sont principalement produits par le pathogène opportuniste *Pseudomonas aeruginosa*. *Pantoea ananatis*, une bactérie non pathogène pour l'humain, est une productrice alternative de métabolites de type rhamnolipide contenant du glucose à la place des résidus rhamnose. Ici, nous présentons l'isolation, la caractérisation structurale et la synthèse totale de l'ananatoside A, un glucolipide contenant une macrolactone à 15 membres, et de l'ananatoside B, son congénère à chaîne ouverte, à partir d'extraits organiques de *P. ananatis*. L'ananatoside A a été synthétisé par trois voies alternatives impliquant une glycosylation intramoléculaire, une macrolactonisation chimique ou une transformation enzymatique directe de l'ananatoside B. Une série de rhamnolipides macrolactonisés en (1→2), (1→3), and (1→4) ont également été synthétisés par glycosylation intramoléculaire et leur configuration anomérique ainsi que leur conformation cyclique ont été résolues par modélisation moléculaire combinée à des études de résonance magnétique nucléaire. Nous montrons que l'ananatoside B est un tensioactif plus puissant que son homologue macrolide. Nous présentons des résultats suggérant que la macrolactonisation des rhamnolipides améliore leur potentiel cytotoxique et hémolytique, pointant vers un mécanisme impliquant la formation de pores dans la membrane cellulaire lipidique. Enfin, nous démontrons que l'ananatoside A et l'ananatoside B ainsi que les rhamnolipides macrolactonisés synthétiques peuvent être perçus par le système immunitaire des plantes, et que cette détection est plus prononcée pour un macrolide présentant une unité rhamnose dans sa conformation native 1C_4 . Dans l'ensemble, nos résultats suggèrent que la macrolactonisation des glycolipides peut considérablement interférer avec leurs propriétés tensioactives et leur activité biologique.

2.2 Abstract

Rhamnolipids are a specific class of microbial surfactants, which hold great biotechnological and therapeutic potential. However, their exploitation at the industrial level is hampered because they are mainly produced by the opportunistic pathogen *Pseudomonas aeruginosa*. The non-human

CHAPITRE 2 – TOTAL SYNTHESIS, ISOLATION, SURFACTANT PROPERTIES, AND BIOLOGICAL EVALUATION OF ANANATOSIDES AND RELATED MACRODILACTONE-CONTAINING RHAMNOLIPIDS

pathogenic bacterium *Pantoea ananatis* is an alternative producer of rhamnolipid-like metabolites containing glucose instead of rhamnose residues. Herein, we present the isolation, structural characterization, and total synthesis of ananatoside A, a 15-membered macrodilactone-containing glucolipid, and ananatoside B, its open-chain congener, from organic extracts of *P. ananatis*. Ananatoside A was synthesized through three alternative pathways involving either an intramolecular glycosylation, a chemical macrolactonization or a direct enzymatic transformation from ananatoside B. A series of diastereoisomerically pure (1→2), (1→3), and (1→4)-macrolactonized rhamnolipids were also synthesized through intramolecular glycosylation and their anomeric configurations as well as ring conformations were solved using molecular modeling in tandem with NMR studies. We show that ananatoside B is a more potent surfactant than its macrolide counterpart. We present evidence that macrolactonization of rhamnolipids enhances their cytotoxic and hemolytic potential, pointing towards a mechanism involving the formation of pores into the lipidic cell membrane. Lastly, we demonstrate that ananatoside A and ananatoside B as well as synthetic macrolactonized rhamnolipids can be perceived by the plant immune system, and that this sensing is more pronounced for a macrolide featuring a rhamnose moiety in its native ${}^1\text{C}_4$ conformation. Altogether our results suggest that macrolactonization of glycolipids can dramatically interfere with their surfactant properties and biological activity.

2.3 Introduction

Bacteria represent a rich reservoir of structurally diverse glycosylated metabolites.¹³⁵ Among these compounds, microbial glycolipids show considerable potential for biomedical and biotechnological applications.¹³⁶ Microbial glycolipids are surfactants, *i.e.*, amphiphilic surface-active compounds, which are made by the combination of a lipidic chain covalently linked to a carbohydrate moiety. Because of their ability to form pores and destabilize biological membranes, microbial glycolipids have attracted increased attention as therapeutic agents.¹³⁷ Glycolipids exhibit a wide range of pharmaceutical activities, including antibacterial,¹³⁸ antifungal,¹³⁹ antiviral,¹⁴⁰ hemolytic,¹⁴¹ anticancer,¹⁴² and adjuvant¹⁴³ activities. In addition, surfactants of microbial origin are increasingly considered for use in diverse biotechnological applications such as in the food and cosmetic industries as well as in bioremediation technologies.¹³⁶

CHAPITRE 2 – TOTAL SYNTHESIS, ISOLATION, SURFACTANT PROPERTIES, AND BIOLOGICAL EVALUATION OF ANANATOSIDES AND RELATED MACRODILACTONE-CONTAINING RHAMNOLIPIDS

Rhamnolipids are a specific class of microbial biosurfactants that have been intensively investigated in recent years.¹⁴⁴ Structurally, rhamnolipids are α -configured mono- or di-L-rhamnose residue(s) *O*-linked to an (*R*)- β -hydroxyalkanoic acid dilipidic chain of C₆ to C₁₄ carbon length (see RhaC₁₀C₁₀ **3** in Fig. 1). As compared to the commercially available petroleum-derived synthetic surfactants, the biodegradability, low critical micelle concentrations (CMCs), and high tension surface activity make rhamnolipids exquisite environmental alternatives for industrial applications.¹⁴⁵ Rhamnolipids are also of interest because they exhibit a plethora of intriguing pharmacological activities. They inhibit the formation of microbial biofilms,¹⁴⁶⁻¹⁴⁸ which play crucial role in infections caused by many pathogenic bacteria. They exhibit antimicrobial activities against both Gram-positive and Gram-negative bacteria as well as against plant pathogenic fungi.¹⁴⁵ Because of their ability to interact with biological membranes, rhamnolipids can trigger the death of cancer cells¹⁴⁹ and induce hemolysis of red blood cells.^{150, 151} Furthermore, as invasion pattern molecules (also known as elicitors),¹⁵² rhamnolipids can stimulate the plant immune system resulting in the strengthening of plant cell walls along with the production of antimicrobial compounds.¹⁵³⁻¹⁵⁶

CHAPITRE 2 – TOTAL SYNTHESIS, ISOLATION, SURFACTANT PROPERTIES, AND BIOLOGICAL EVALUATION OF ANANATOSIDES AND RELATED MACRODILACTONE-CONTAINING RHAMNOLIPIDS

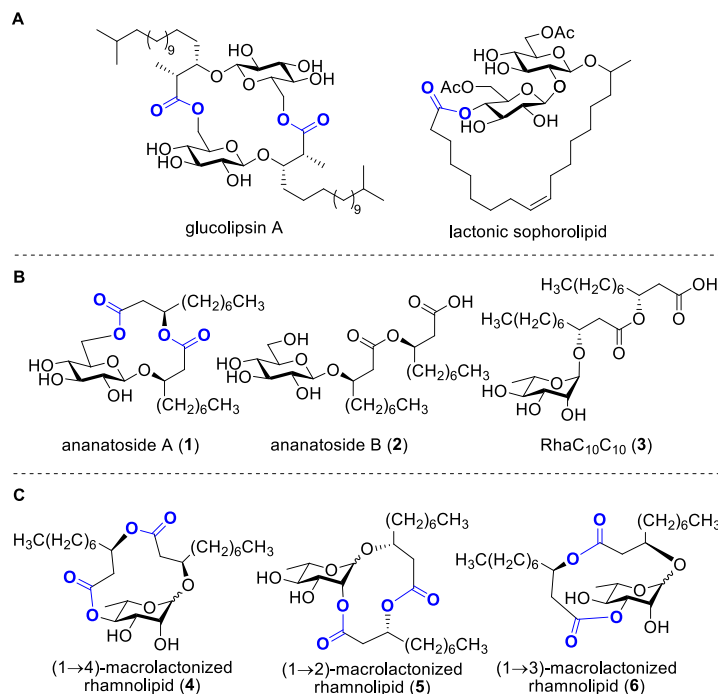


Figure 2.1. (A) Examples of macrolactone-containing *glucolipids* produced by microbes; (B) Structure of target ananatoside A (1) and ananatoside B (2) produced by *Pantoea ananatis* along with the related RhaC₁₀C₁₀ (3); (C) Structures of target macrodilactone-containing rhamnolipids 4-6

Rhamnolipids are mainly produced by pathogenic Gram-negative bacteria belonging to the *Pseudomonas* and *Burkholderia* genera,^{144, 157} which hampers their exploitation at the industrial level since several are human pathogens. As such, there is an increased interest to identify non-pathogenic bacteria that can produce high concentrations of rhamnolipids and structurally-related biosurfactants. Our group has recently identified the bacterium *Pantoea ananatis* BRT175 as an alternative non-pathogenic producer of biosurfactants.^{158, 159} The biosynthesis of rhamnolipids involves the successive function of three enzymes: RhIA, which directs the biosynthesis of the lipidic precursor, along with RhIB and RhIC, which are two rhamnosyltransferases.^{160, 161} Although the production of biosurfactants in *P. ananatis* was also catalyzed by RhIA and RhIB homologues, we unexpectedly identified a *gluco-* rather than a *rhamnolipid* from *P. ananatis* ethyl acetate extracts.¹⁵⁸ The isolated compound, that we called ananatoside A (1, Fig. 1), features an unprecedented 15-membered macrodilactone ring comprising a β -D-glucose residue linked to a C₁₀C₁₀ dilipid chain through both C1 and C6 positions.¹⁵⁹ Biologically active glucolipids containing

CHAPITRE 2 – TOTAL SYNTHESIS, ISOLATION, SURFACTANT PROPERTIES, AND BIOLOGICAL EVALUATION OF ANANATOSIDES AND RELATED MACRODILACTONE-CONTAINING RHAMNOLIPIDS

mono-, di-, and trilactones of different macrocycle sizes have been identified from other microorganisms¹⁶²⁻¹⁶⁴ including, to name a few examples, lactonic sophorolipids (Fig. 1), glucolipins (Fig. 1), cycloviracins, fattiviracins, macroviracins, and anthrobacilins. By restricting the rotation of the substituents and stabilizing the active conformation of the glycolipid, the presence of the macrocycle is a prerequisite to the bioactivity of these constrained saccharides.^{163, 165}

The identification of ananatoside A (**1**) as a novel microbial macrolide prompted us to investigate *P. ananatis* extracts with the aim of identifying structurally similar biosurfactants. As part of our research program on the synthesis of microbial glycans,¹⁶⁶⁻¹⁶⁹ we were interested in developing synthetic routes that would allow an alternative and straightforward access to these macrodilactone-containing glycolipids, and enable the assessment of their tensioactive properties and biological activities. Within this framework, we herein present the total synthesis of ananatoside A (**1**), its newly identified open-chain congener ananatoside B (**2**), the related RhaC₁₀C₁₀ (**3**) as well as five unprecedented, anomerically pure (1→2)-, (1→3)-, and (1→4)-macrodilactone-containing rhamnolipids (**4–6**) (Fig. 1). We show that ananatoside A (**1**) can be efficiently obtained via three different pathways implying either a chemo- or enzymatic macrolactonization, or an intramolecular glycosylation as the key step of these synthetic sequences. DFT calculations were used to decipher the ring conformations and anomeric configurations of synthetic macrolactonized rhamnolipids **4–6**, which were readily obtained through intramolecular glycosylation. Their surfactant properties and biological activity, *i.e.*, antimicrobial activity, cytotoxicity, hemolytic activity, as well as their interaction with the plant immune system, were also investigated, providing meaningful fundamental insights into the impact of the presence of the macrodilactonic ring on the physical and biological properties of this relevant class of microbial glycolipids.

2.4 Results and discussion

2.4.1 Isolation of ananatoside A (**1**) and ananatoside B (**2**)

The non-pathogenic bacterium *P. ananatis* BRT175 was found to be a producer of surface-active glycolipids based on its genetic homologies with rhamnolipid biosynthetic genes. The microbial biosurfactants were extracted with EtOAc from the supernatant of a liquid culture of BRT175, which

CHAPITRE 2 – TOTAL SYNTHESIS, ISOLATION, SURFACTANT PROPERTIES, AND BIOLOGICAL EVALUATION OF ANANATOSIDES AND RELATED MACRODILACTONE-CONTAINING RHAMNOLIPIDS

was acidified to pH ~ 3 prior the extraction. Purification of the crude extract was performed using a semi-preparative reversed-phase HPLC system equipped with a charged aerosol detector (CAD).¹⁷⁰ The use of the CAD detector was particularly appealing over traditional UV/visible detectors as it allows the detection of molecules lacking chromophore groups such as glycolipids (see Fig. S1). Through this optimized procedure, ananatoside A (**1**) was isolated as a yellow oil and its physical and analytical data (R_f , specific rotation, HRMS, and 1D and 2D NMR) were in perfect agreement with those recently published by our group.¹⁵⁹ A more polar and major congener (see Fig. S1), that we have named ananatoside B (**2**), was also isolated from the EtOAc extract as a white amorphous powder. This compound was analyzed by HR-ESI-TOF-MS in the positive mode, yielding pseudomolecular ion peaks at m/z 538.3587 $[M + NH_4]^+$ and m/z 543.3142 $[M + Na]^+$, pointing towards the presence of a glycolipid featuring a hexose residue linked to two hydroxydecanoic acid chains. Comparison of the 1D and 2D NMR data of ananatoside B (**2**, see Fig. S2 for main COSY and HMBC correlations) with our previously reported data for ananatoside A (**1**) suggested the presence of an open-chain β -linked glucolipid congener without the macrolide ring (no HMBC cross-peak between H6 and C1’’). The absolute configuration of both the glucose and β -hydroxydecanoid acid chains were determined following acid hydrolysis and measurement of specific rotation in comparison with an authentic D-glucose sample and literature data for the lipid chain, as we previously described.¹⁵⁹ Based on these chemical and spectroscopic evidences, we established the complete structure of ananatoside B (**2**) as shown in Fig. 1. The structural determination of ananatoside A (**1**) and ananatoside B (**2**) were further proved through their total synthesis as described in the next section.

2.4.2 Total synthesis of ananatoside A (**1**) and ananatoside B (**2**)

2.4.2.1 Retrosynthetic analysis

The total synthesis of macrolactone-containing natural products has usually been accomplished *via* late-stage ring-closing metathesis or macrolactonization as key steps of the synthetic routes.^{162, 163, 171} Notwithstanding the success of these pioneering approaches, they present some drawbacks such as the use of highly diluted reaction mixtures and the possible di- or oligomerization of the acyclic

CHAPITRE 2 – TOTAL SYNTHESIS, ISOLATION, SURFACTANT PROPERTIES, AND BIOLOGICAL EVALUATION OF ANANATOSIDES AND RELATED MACRODILACTONE-CONTAINING RHAMNOLIPIDS

precursors.¹⁶² Owing to their thermal stabilities together with their optimal regio- and enantioselectivities, commercially available lipases stand as a tantalizing synthetic tool for the formation of macrolactone rings from unprotected substrates.¹⁷²⁻¹⁷⁴ Alternatively, capitalizing on glycosylation chemistry,^{175, 176} carbohydrate-embedded macrolactones can be built upon stereoselective intramolecular glycosylation using the ester-linked β -hydroxy lipid as a stereodirecting tether.¹⁷⁷ Importantly, the latter approach has only been implemented in rare occasions for the total synthesis of macrolactone-containing natural products.¹⁶²

Along these lines and as depicted in our retrosynthetic analysis strategy (Fig. 2), we envisioned to build the macrolide skeleton of ananatoside A (**1**) *via* three parallel synthetic pathways (routes A–C) as to maximize the chances of efficiently reaching our target. We first hypothesized that ananatoside A (**1**) would be formed through the intramolecular glycosylation of derivative **7** following chemoselective cleavage of the C6-*O*-TBS group (route A). Notably, precursor **7**, activated in the form of an STol glycoside,¹⁷⁸ would be equipped with a (2-azidomethyl)benzoyl (AZMB)¹⁷⁹ group at C2 that would act as a neighboring participating group enabling the formation of the 1,2-*trans*-glucosidic linkage. The β -selectivity would also be favored by the steric constraint exerted by the resulting macrolide.¹⁷⁷ The propensity of the AZMB group to be orthogonally cleaved by means of, for instance, Staudinger reduction^{169, 180} without affecting the macrolide functionality represents a further advantage of using this protecting group at this specific position. Precursor **7** would be readily synthesized by Steglich esterification¹⁸¹ between thioglucoside **9** and dilipid **10**.

CHAPITRE 2 – TOTAL SYNTHESIS, ISOLATION, SURFACTANT PROPERTIES, AND BIOLOGICAL EVALUATION OF ANANATOSIDES AND RELATED MACROLACTONE-CONTAINING RHAMNOLIPIDS

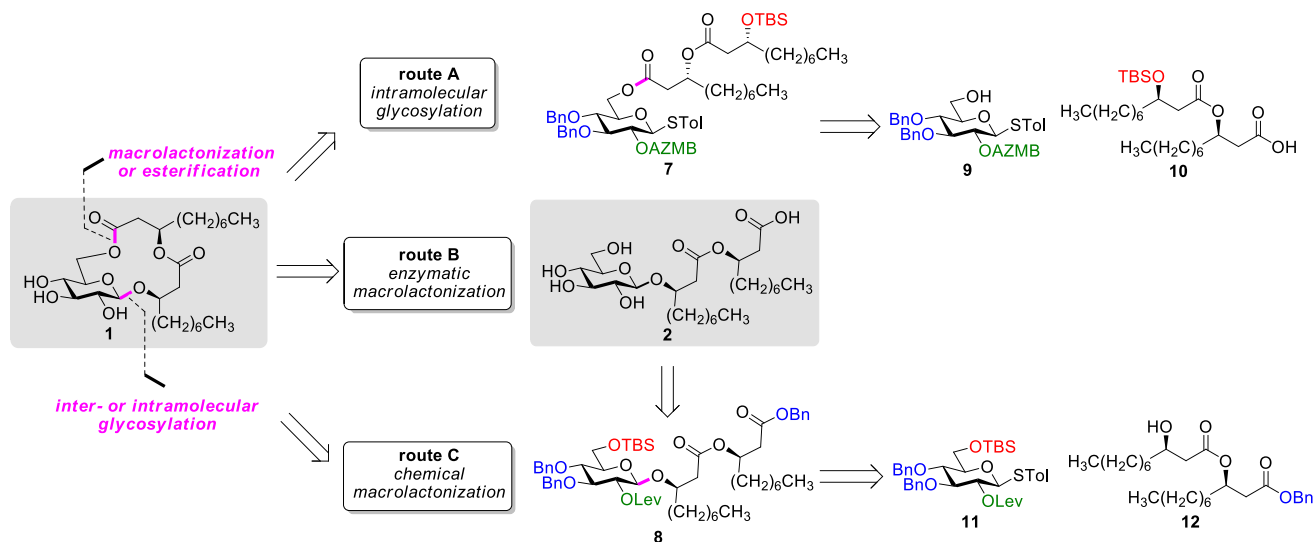


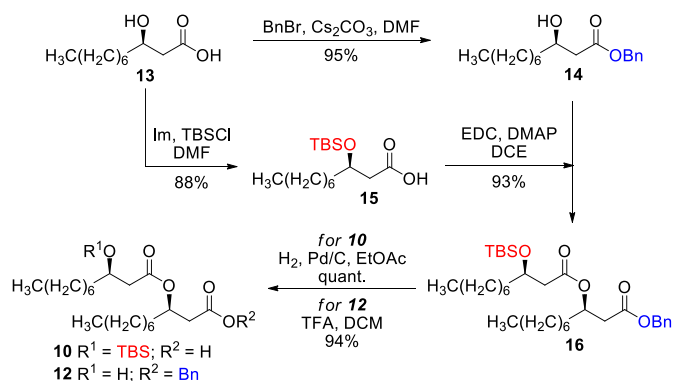
Figure 2.2. Retrosynthetic disconnection strategy for the total synthesis of ananatoside A (1) and ananatoside B (2) according to three different pathways: chemical macrolactonization, enzymatic macrolactonization, and inter- or intramolecular glycosylation

Inspired by the success story of the total synthesis of several macrolide-containing natural products^{162, 171, 182-185} and by way of comparison with the intramolecular glycosylation strategy, we have also wanted to construct the 15-membered ring of ananatoside A (1) through both enzymatic and chemical macrolactonizations (Fig. 2). Regarding the chemical macrolactonization (route C), glucolipid **8** would act as an exquisite acyclic precursor for this intramolecular transformation following unmasking of the seco acid functionality. Moreover, global deprotection of this compound (**8**) would complete the total synthesis of ananatoside B (2). Glucolipid **8** would be prepared through the stereocontrolled glycosylation of thioglucoside **11** with benzylated dilipid **12**. Here again, the use of a neighboring participating group, *i.e.*, levulinoyl (Lev),^{169, 180, 186} that could be selectively cleaved in the presence of an ester functionality would insure a successful outcome for the final steps of the synthetic route. Finally, we hypothesized that ananatoside A (1) could be enzymatically synthesized from unprotected ananatoside B (2) using commercially available solid-supported lipase such as Novozyme 435 (route B).¹⁷⁴ If successful, this enzymatic process would allow the direct and straightforward conversion of ananatoside B (2) into ananatoside A (1) from the isolated natural product or the synthetic compound.

CHAPITRE 2 – TOTAL SYNTHESIS, ISOLATION, SURFACTANT PROPERTIES, AND BIOLOGICAL EVALUATION OF ANANATOSIDES AND RELATED MACRODILACTONE-CONTAINING RHAMNOLIPIDS

2.4.2.2 Synthesis of building blocks

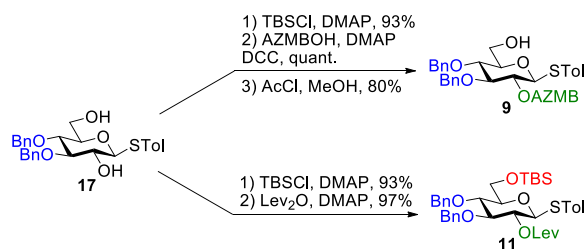
Our synthetic journey commenced with the assembly of the dilipidic side chain derivatives. To do so, (*R*)- β -hydroxydecanoic acid **13** had to be synthesized first. According to the literature, monolipid **13** had previously been prepared via either a cross-metathesis/Mitsunobu sequence,¹⁸⁷ the Reformatsky reaction⁹⁵ or from Meldrum's acid.¹⁸⁸⁻¹⁹¹ We decided to follow the latter approach as it allowed the straightforward formation of target monolipid **13** in high overall yield and enantiomeric purity. Therefore, as depicted in Scheme S1, (*R*)- β -hydroxydecanoic acid **13**¹⁸⁹ was prepared in a four-step sequence. The configuration and enantiomeric purity (*R*, 99% *ee*) of methyl ester **S4** was confirmed through the preparation of Mosher's ester **S5**¹⁸⁸ and comparison with literature data (see Fig. S3). Thereafter, β -hydroxydecanoic acid **13** was subjected to regioselective benzylation at the carboxylic acid moiety yielding benzyl ester **14** in a nearly quantitative yield (Scheme 1). In parallel, derivative **13** was protected with a TBS group at the C3 position affording silylated derivative **15**.¹⁸⁹ These two compounds were condensed together under the activation of EDC/DMAP. Resulting protected dilipid derivative **16** was then either subjected to Pd-catalyzed hydrogenolysis of the benzyl ester or to TFA-mediated cleavage of the TBS group leading to the formation of acid **10** or alcohol **12**, respectively, ready for coupling with the carbohydrate derivatives. Optimization of this synthetic sequence allowed us to prepare gram amounts of these chiral lipidic intermediates.



Scheme 2.1. Synthesis of β -hydroxydecanoic acid derivatives

CHAPITRE 2 – TOTAL SYNTHESIS, ISOLATION, SURFACTANT PROPERTIES, AND BIOLOGICAL EVALUATION OF ANANATOSIDES AND RELATED MACRODILACTONE-CONTAINING RHAMNOLIPIDS

Having completed the synthesis of the dilipid derivatives, we then focused our attention on the synthesis of thioglucosides **9** and **11**, which were either used for subsequent Steglich esterification or glycosylation reactions, respectively. These two compounds were prepared from diol **17**,¹⁹² which was obtained in a three-step, one-pot sequence from the corresponding *per*trimethylsilylated thioglucoside. As revealed in Scheme 2, regioselective silylation at the C6 position of diol **17** followed by esterification with AZMBOH and subsequent desilylation under the action of *in situ* generated HCl led to derivative **9** bearing a free OH at C6 in 74% yield over three steps. Alternatively, a levulinoyl group was installed at C2 by treatment of the C6-*O*-TBS-protected derivative with levulinic anhydride to provide fully protected thioglucoside **11** in 90% yield over two steps.

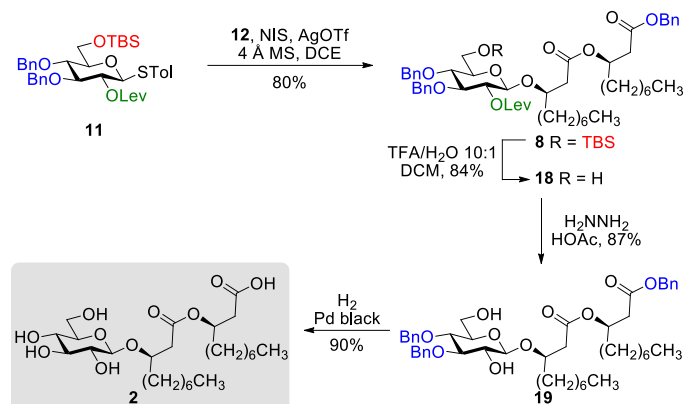


Scheme 2.2. Synthesis of thioglucoside derivatives **9** and **11**

2.4.2.3 Synthesis of ananatoside B

Our next challenge was to proceed with the total synthesis of ananatoside B (**2**). Fully protected thioglucoside **11** was glycosylated with alcohol acceptor **12** under the promotion of NIS/AgOTf activating system,¹⁹³ providing anomerically pure β -glucolipid **8** in 80% yield (Scheme 3). The stereoselectivity of the reaction was confirmed by ¹H NMR (H-1, d, ³J_{H1,H2} = 8.0 Hz for Glcp in ⁴C₁ conformation). Then, TFA-mediated cleavage of the TBS group, delevulinoylation under the action of hydrazine acetate, and Pd-catalyzed hydrogenolysis cleanly led to ananatoside B (**2**) in 66% yield over three steps. Physical and analytical data (*R*_f, specific rotation, HRMS, and NMR) of synthetic ananatoside B (**2**) were in perfect agreement with the isolated natural product (see Supporting Information for details).

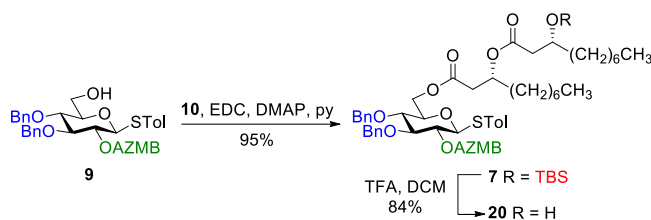
CHAPITRE 2 – TOTAL SYNTHESIS, ISOLATION, SURFACTANT PROPERTIES, AND BIOLOGICAL EVALUATION OF ANANATOSIDES AND RELATED MACRODILACTONE-CONTAINING RHAMNOLIPIDS



Scheme 2.3. Total synthesis of ananatoside B

2.4.2.4 Synthesis of ananatoside A by intramolecular glycosylation

The total synthesis of ananatoside A (**1**) was our next task. We commenced by studying the intramolecular glycosylation pathway. To do this, we needed to prepare the acyclic precursor **20**. Dilipid **10** was condensed at the C6 position of thioglucoside **9** through activation with EDC/DMAP (Scheme 4). Resulting derivative **7** was treated with TFA in DCM to cleave the TBS group giving ω -hydroxy thioglucoside **20** in 84% yield ready for intramolecular glycosylation.



Scheme 2.4. Synthesis of alcohol **20** ready for intramolecular glycosylation

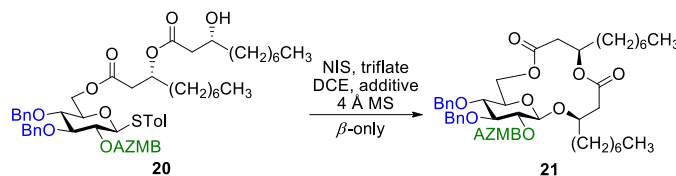
As shown in Table 1, different conditions were screened for the intramolecular glycosylation of acyclic precursor **20**, *i.e.*, promoter, molar volume, and additive. Initially, the concentration was set to 0.01 M (corresponding molar volume of 100 mL \cdot mmol $^{-1}$) to minimize intermolecular interactions and thus preventing the formation of di- and oligomeric byproducts. At this concentration, AgOTf and TMSOTf were first evaluated as catalysts in combination with NIS (entries 1 and 2).¹⁹³ In both

CHAPITRE 2 – TOTAL SYNTHESIS, ISOLATION, SURFACTANT PROPERTIES, AND BIOLOGICAL EVALUATION OF ANANATOSIDES AND RELATED MACRODILACTONE-CONTAINING RHAMNOLIPIDS

conditions, target macrolide **21** was isolated in good yields with full β -stereoselectivity while no traces of diolide or higher oligomers were detected. Encouraged by these results, the impact of the concentration of precursor **20** on the reaction outcome was investigated by conducting the intramolecular glycosylation at 0.001 and 0.1 M (entries 3 and 4). We were pleased to find that macrolide **21** was formed quantitatively when the concentration of the acyclic precursor was set to 0.001 M. Moreover, even at a concentration of 0.1 M, which could have favored intermolecular interactions, only monomer **21** was isolated although the yield was significantly lower (47%). The use of excess amounts of TMSOTf (entry 5) or other triflates such as Yb(OTf)₃ and Zn(OTf)₂ (entries 6 and 7, respectively) also resulted in the exclusive formation of target macrolide **21**. Inspired by Fürstner and co-workers¹⁸³ who completed the total synthesis of cycloviracin B₁ through metal-templated macrolactonization, we then sought to evaluate the impact of an excess of metallic ions on the outcome of the glycosylation and to observe if oligomeric macrolides could be generated. As it is known that potassium and sodium are effective ions for such templated reactions,¹⁸³ KOTf and NaOTf were employed as additives in the presence of catalytic amounts of TMSOTf (entries 11-13). Once again, the intramolecular reaction was highly favored as no other products than macrolide **21** were isolated from the reaction mixture.

CHAPITRE 2 – TOTAL SYNTHESIS, ISOLATION, SURFACTANT PROPERTIES, AND BIOLOGICAL EVALUATION OF ANANATOSIDES AND RELATED MACRODILACTONE-CONTAINING RHAMNOLIPIDS

Table 2.1. NIS/triflate-promoted intramolecular glycosylation of precursor **20**.



entry	triflate (equiv)	molar volume (mL·mmol ⁻¹)	additive	yield (%) ^a
1	AgOTf (0.4)	100	-	70
2	TMSOTf (0.2)	100	-	83
3	TMSOTf (0.2)	1000	-	quant.
4	TMSOTf (0.2)	10	-	47
5	TMSOTf (2.1)	100	-	85
6	Yb(OTf) ₃ (1.6)	100	-	21
7	Zn(OTf) ₂ (1.6)	100	-	75
8	TMSOTf (0.2)	100	NaOTf	78
9	TMSOTf (0.2)	100	KOTf	63
10	TMSOTf (0.2)	50	KOTf	61

^aIsolated yield.

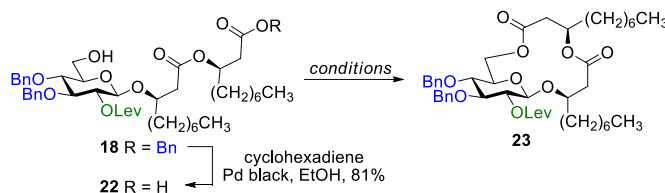
2.4.2.5 Synthesis of ananatoside A by chemical macrolactonization

As previously mentioned, the second pathway that we chose to investigate for the preparation of ananatoside A (**1**) was based on a chemical macrolactonization¹⁸² as the key step. As depicted in Table 2, glucolipid derivative **18** was used as an advanced intermediate for this approach. The benzyl ester moiety of the latter compound was thus selectively cleaved by catalytic hydrogenation transfer, using cyclohexadiene as the hydrogen transfer source.^{194, 195} Intramolecular cyclization of the resulting secoacid **22** was then studied through Keck (DCC, DMAP, PPTs)¹⁹⁶ and Fujisawa [2-chloro-1,3-dimethylimidazolium chloride (DMC), DMAP]¹⁹⁷ macrolactonizations. These intramolecular esterifications were performed at different concentrations and temperatures, with and without the slow addition of seco acid **22**, and by using two different coupling systems (Table 2, entries 1-4). Pleasingly, target macrolide **23** was formed in 71% yield when using DMC-mediated macrolactonization under concentrated conditions (entry 4) and, as for the intramolecular

CHAPITRE 2 – TOTAL SYNTHESIS, ISOLATION, SURFACTANT PROPERTIES, AND BIOLOGICAL EVALUATION OF ANANATOSIDES AND RELATED MACROLACTONE-CONTAINING RHAMNOLIPIDS

glycosylation, only monomer **23** was detected. Cs₂CO₃ or KOTf were then added in the reaction mixture as to favor oligomerization but only traces of dimer were detected by HRMS (entries 5-7). Interestingly, it was possible to improve the yield up to 80% for the formation of target macrolide **23** when KOTf was used as an additive (entry 6).

Table 2.2. Chemical macrolactonization of precursor **22**



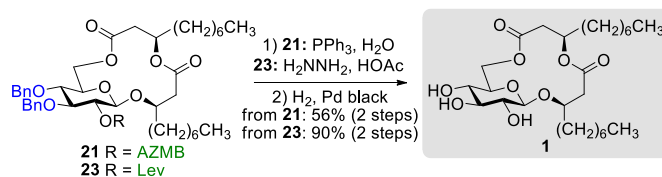
entry	reagents	molar volume (mL•mmol ⁻¹)	yield (%) ^a
1	DCC, DMAP, PPTS	860	64
2	DCC, DMAP, PPTS	60	40
3	DMC, DMAP	60	67
4	DMC, DMAP	15	71
5	DMC, DMAP, Cs ₂ CO ₃	60	47 ^b
6	DMC, DMAP, KOTf	60	80 ^b
7	DMC, DMAP, KOTf	15	73

^aIsolated yield; ^bTraces of dimer were detected.

With protected macrolides **21** and **23** in hand, we were able to complete the total synthesis of ananatoside A (**1**) (Scheme 5). Therefore, the AZMB group of macrolide **21** and the Lev group of macrolide **23** were orthogonally removed through Staudinger reduction or treatment with hydrazine acetate, respectively. Pd-catalyzed hydrogenolysis of the resulting alcohols cleanly led to the formation of ananatoside A (**1**) in 56 or 90% yield over two steps from macrolide **21** or **23**, respectively. Physical and analytical data (*R_f*, specific rotation, HRMS, and NMR) of synthetic ananatoside A (**1**) were in perfect agreement with the isolated natural product¹⁵⁹ (see Supporting Information for details). The overall yields and number of steps for both synthetic sequences were

CHAPITRE 2 – TOTAL SYNTHESIS, ISOLATION, SURFACTANT PROPERTIES, AND BIOLOGICAL EVALUATION OF ANANATOSIDES AND RELATED MACRODILACTONE-CONTAINING RHAMNOLIPIDS

very similar, *i.e.*, 33 and 35% over eight steps from known diol **17** for the intramolecular glycosylation and macrolactonization pathways, respectively.



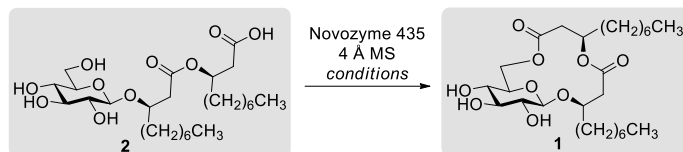
Scheme 2.5. Deprotection of macrolides **21** and **23** into ananatoside A (**1**)

2.4.2.6 Synthesis of ananatoside A by enzymatic macrolactonization

We were also interested in the direct conversion of ananatoside B (**2**) into ananatoside A (**1**) by taking advantage of enzyme-catalyzed macrolactonization. Although efficient in terms of overall yields, both previously described synthetic approaches required protecting groups manipulation. Contrarywise, enzymatic reactions offer the advantages of being renewable and specific, and of minimizing side product formation and purification steps.¹⁷⁴ Immobilized *Candida antarctica* lipase B (CALB), commercially available under the brand name of “Novozyme 435”, was therefore selected for this synthetic study as it has showed high substrate versatility and efficiency for macrolactonization reactions.¹⁷² As revealed in Table 3, the reaction was conducted in the presence of molecular sieves (4 Å) as to insure strictly anhydrous conditions throughout the enzymatic process. As hydrophobic solvents are known to favor such type of enzymatic reactions,¹⁷² toluene was first employed at 75 °C (entry 1). However, after a seven day-period, only 30% of conversion was observed (as estimated by ¹H NMR). When switching to hexanes, an even lower conversion was obtained (entry 2), and only traces of ananatoside A (**1**) were detected when the more polar THF was employed as the reaction medium (entry 3). We were pleased to find that switching back to toluene and conducting this enzyme-catalyzed reaction under microwave irradiations for three hours at 75 °C allowed the isolation of ananatoside A (**1**) in a satisfying 64% yield. To the best of our knowledge, this is the first report of using CALB for the enzymatic conversion of a monoglycolipid into a macrolide.

CHAPITRE 2 – TOTAL SYNTHESIS, ISOLATION, SURFACTANT PROPERTIES, AND BIOLOGICAL EVALUATION OF ANANATOSIDES AND RELATED MACRODILACTONE-CONTAINING RHAMNOLIPIDS

Table 2.3. Enzymatic macrolactonization of ananatoside B (2) into ananatoside A (1)



entry	solvent	temp. (°C)	time (h)	yield ^a (%)
1	toluene	75	168	30
2	hexanes ^b	55	114	10
3	THF ^b	55	112	traces
4	toluene ^b	75 ^c	3	64 ^d

^aConversion (estimated by NMR); ^bReaction in sealed tube;

^cMicrowave heating; ^dIsolated yield.

2.4.3 Synthesis of RhaC₁₀C₁₀ (3) and macrolactonized rhamnolipids 4-6

2.4.3.1 Retrosynthetic analysis

The preparation of microbial rhamnolipids has only been reported in few occasions in the literature.^{95, 96, 188, 190, 191, 198} We thought it would be worth reinvestigating the synthesis of RhaC₁₀C₁₀ (3) as to obtain pure a synthetic sample that could be evaluated for its physical properties and biological activity in direct comparison with ananatosides. Furthermore, using an orthogonally protected donor such as thiorhamnoside 25 in which each hydroxyl groups (C2, C3, and C4) could be selectively unmasked (Fig. 3), we hypothesized that a series of unprecedented macrolactonized rhamnolipids (4–6) could be produced via an intramolecular glycosylation strategy. As a parallel to ananatoside A (1) and B (2) acid/lactone pair, these macrolides would serve as model compounds to study the impact of macrolactonization on the physical properties and biological activity of rhamnolipids. Therefore, as depicted in Fig. 3, rhamnolipid 3 would be obtained from the intermolecular glycosylation of rhamnoside 25 with dilipid 12 followed by global deprotection. As for macrolactones 4–6, they would become accessible *via* the intramolecular glycosylation of ester-linked rhamnolipid acyclic precursors 26–38, which would be formed by Steglich condensation of dilipid 10 with their corresponding unmasked alcohols (29, 30, and 31). We anticipated that the

CHAPITRE 2 – TOTAL SYNTHESIS, ISOLATION, SURFACTANT PROPERTIES, AND BIOLOGICAL EVALUATION OF ANANATOSIDES AND RELATED MACRODILACTONE-CONTAINING RHAMNOLIPIDS

presence of a macrolactone functionality in target rhamnolipids **4–6** would induce substantial conformational changes of the rhamnopyranose ring, which is typically found in the 1C_4 conformation, hence making non-trivial the determination of anomeric configurations in resulting macrolides. As such, DTF calculations would be used as a theoretical tool in conjunction with NMR spectroscopy to determine the exact anomeric configurations and ring conformations of rhamnolactones **4–6**.

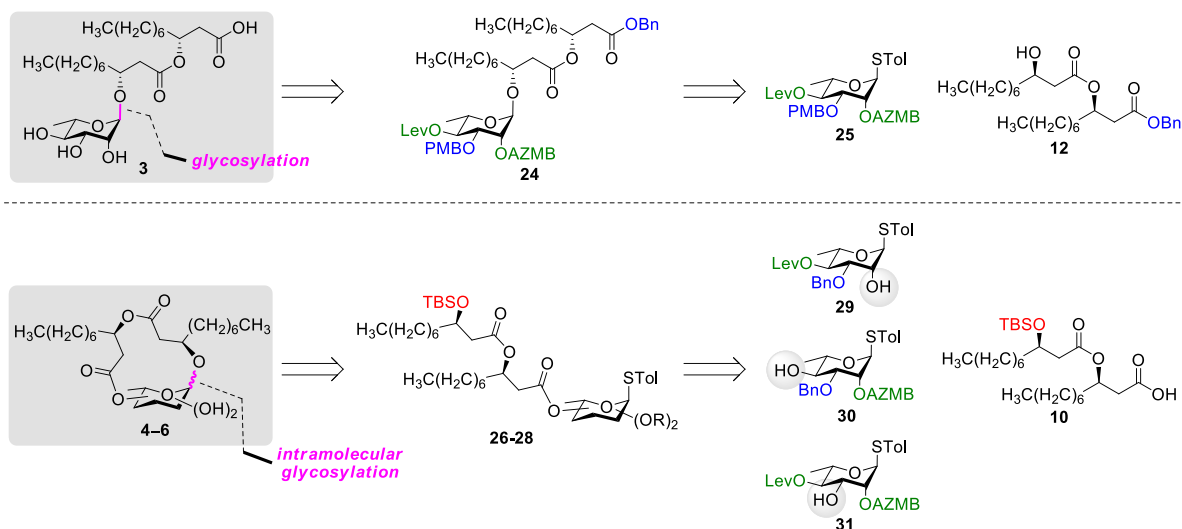


Figure 2.3. Retrosynthetic analysis of rhamnolipid **3** and macrodilactone-containing rhamnolipids **4–6**¹

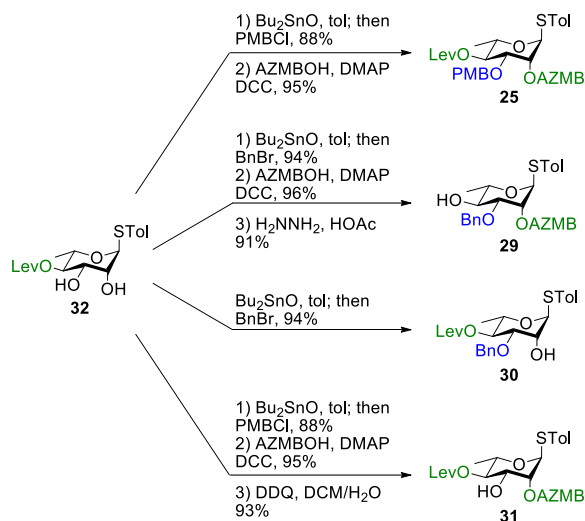
2.4.3.2 Synthesis of building blocks

The synthesis of the thiorhamnoside building blocks was straightforward (Scheme 6). Our approach mainly relied on the stannylene acetal-mediated¹⁹⁹ regioselective introduction of either PMB or Bn groups at C3 from known diol **32**.¹⁶⁹ Then, installation of the AZMB group at C2 followed by orthogonal cleavage at either C3 or C4 positions provided functionalized thiorhamnosides **25**, **29**,

¹ Blue: permanent protecting groups (Bn and PMB); red: temporary protecting groups (TBS); green: esters used as temporary protecting groups enabling neighboring group participation when branched at C2 (AZMB and Lev)

CHAPITRE 2 – TOTAL SYNTHESIS, ISOLATION, SURFACTANT PROPERTIES, AND BIOLOGICAL EVALUATION OF ANANATOSIDES AND RELATED MACRODILACTONE-CONTAINING RHAMNOLIPIDS

30, and **31**. These optimized procedures allowed us to prepare gram amounts of each building blocks in pure anomeric forms.

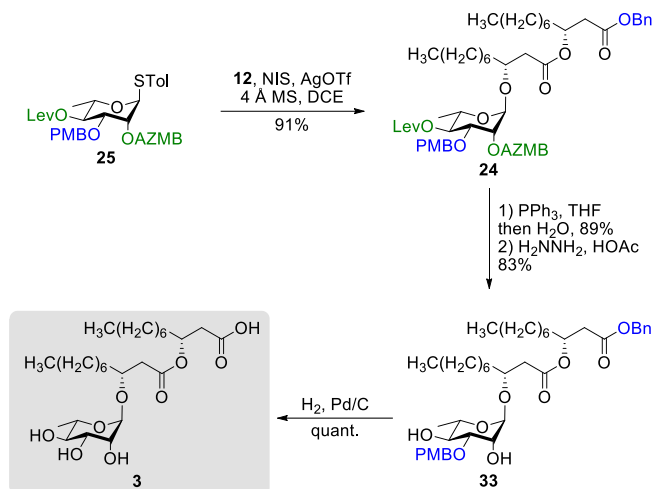


Scheme 2.6. Synthesis of thiorhamnoside building blocks **25**, **29**, **30** and **31**.

2.4.3.3 Synthesis of rhamnolipid $\text{C}_{10}\text{C}_{10}$

With our newly developed fully functionalized thiorhamnoside **25** in hand, we were ready to conduct the synthesis of $\text{RhaC}_{10}\text{C}_{10}$ (**3**).¹⁹¹ As depicted in Scheme 7, coupling of rhamnosyl donor **25** with dilipid acceptor **12** under the promotion of NIS/AgOTf cleanly provided protected rhamnolipid **24** in 91% yield with full control of 1,2-*trans* stereoselectivity owing to the neighboring group participation of the AZMB group at C2. Then, global deprotection of derivative **24** was accomplished uneventfully following a three-step sequence including Staudinger reduction, chemoselective cleavage of the Lev ester, and Pd-catalyzed hydrogenolysis of both benzyl ester and PMB ether functionalities. The overall yield for the synthesis of $\text{RhaC}_{10}\text{C}_{10}$ (**3**) was 56% over six steps starting from diol **32**. We have also completed the total synthesis of rhamnolipid **3** from thiorhamnoside **S6**²⁰⁰ bearing the commonly used 3,4-*O*-butanediactal^{96, 188} as protecting group (see Scheme S2). The latter route was less efficient in terms of overall yield as compared to the former one.

CHAPITRE 2 – TOTAL SYNTHESIS, ISOLATION, SURFACTANT PROPERTIES, AND BIOLOGICAL EVALUATION OF ANANATOSIDES AND RELATED MACROLACTONE-CONTAINING RHAMNOLIPIDS



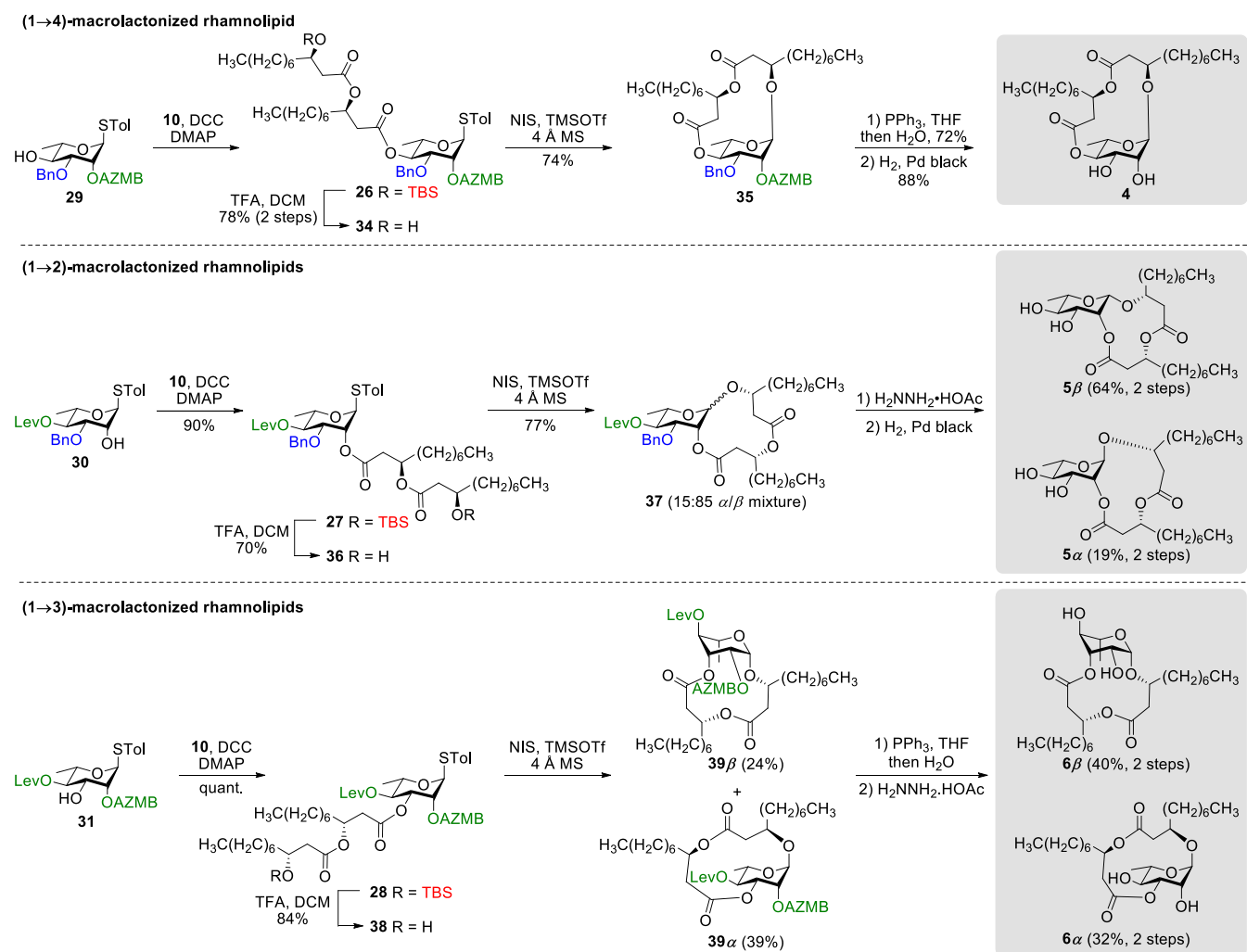
Scheme 2.7. Total synthesis of RhaC₁₀C₁₀ (**3**)

2.4.3.4 Macrolactonization of rhamnolipids

Our last synthetic challenge consisted in the preparation of (1→2)-, (1→3)- and (1→4)-macrolactonized rhamnolipids (**4–6**). These three types of macrolactones were obtained following a similar synthetic route (Scheme 8). Our approach entailed esterification of thiorhamnosides **29**, **30**, or **31** with dilipid **10** by means of DCC/DMAP coupling reactions to afford derivatives **26**, **27**, and **28**, respectively, in excellent yields. Subsequent chemoselective cleavage of the C3'' TBS group in the presence of TFA led to acyclic precursors **34**, **36**, and **38**, respectively, which were ready to be macrolactonized. Intramolecular glycosylation of precursor **34** under the activation of NIS/TMSOTf furnished protected (1→4)-macrolide **35** in 74% yield with full control of α -selectivity. Then, Staudinger reduction followed by Pd black-mediated hydrogenolysis provided target (1→4)-macrolide **4**. Because of the presence of the dilipid chain at C2 imposing steric constraints on the pyranose conformation, intramolecular glycosylation of precursor **36** under previously mentioned conditions led to the formation of an inseparable α/β anomeric mixture of protected (1→2)-macrolide **37** with the β -anomer found as the major compound ($\alpha/\beta = 15:85$). Following cleavage of both the Lev and Bn groups, α - and β -(1→2)-macrolides, *i.e.*, compounds **5a** and **5b**, respectively, were isolated in pure forms in a combined yield of 83%. Intramolecular glycosylation of precursor **38** also generated a mixture of anomers although this time they were

CHAPITRE 2 – TOTAL SYNTHESIS, ISOLATION, SURFACTANT PROPERTIES, AND BIOLOGICAL EVALUATION OF ANANATOSIDES AND RELATED MACROLACTONE-CONTAINING RHAMNOLIPIDS

easily separable by silica gel chromatography under their protected forms (**39 β** , 24%, β -anomer; and **39 α** , 39%, α -anomer). Orthogonal cleavage of both the AZMB and Lev groups completed the total synthesis of target (1 \rightarrow 3)-macrolide **6** in pure α - and β -anomeric forms. The determination of the anomeric configurations in macrolides **4**, **5 β** , **5 α** , **6 β** , and **6 α** was accomplished by NMR with the help of DFT calculations as described in the next section.



Scheme 2.8. Synthesis of (1 \rightarrow 4), (1 \rightarrow 2), and (1 \rightarrow 3)-macrolactonized rhamnolipids 4-6.

2.4.4 Molecular modeling of macrolactonized rhamnolipids

To determine the anomeric configuration of a monosaccharide, the $^3J_{\text{H1-H2}}$ coupling constant is commonly measured by ^1H NMR.²⁰¹ In the case of rhamnopyranosides, the J values for the two anomers are too low to be a suitable selection criterion. Therefore, the δ_{C} at C-5 (70.0 ppm for α -Rhap or 73.2 ppm for β -Rhap)²⁰² or the $^1J_{\text{C1-H1}}$ coupling constant (167.2–172.3 Hz for α -Rhap or 152.3–159.8 Hz for β -Rhap) are preferred for rhamnopyranosides.²⁰³ These methods are valid only because rhamnopyranosides usually adopt a typical 1C_4 conformation. However, in the case of macrolactonized rhamnolipids **4–6**, other conformations are likely to appear due to the steric constraints imposed by the bicyclic nature of these compounds, rendering useless these empirical rules for identifying the proper anomer. To overcome this problem, *in silico* models of synthetic rhamnolipids were prepared with truncated alkyl chains as to minimize the number of conformers to be considered (Fig. S4). The conformational space of these models was explored in depth (Fig. S5) using the improved RDKit algorithm, which is based on the geometry of distances and empirical preferences for certain angles of torsion (ETKDGv2).²⁰⁴ The geometry of the unique conformers was optimized by molecular mechanics (MMFF94) followed by quantum molecular modeling using density functional theory (mPW1PW91) and the basis set 6-31G(d, p). The thermochemical parameters were calculated to deduce the abundance of conformers in solution using the Boltzmann equation, thus eliminating marginal conformers (<1%). The retained conformers were inspected so that no imaginary vibrational frequency could be found. Examination of the sugar conformation of the conserved structures confirmed the irregular nature of these glycosides. Indeed, three different skew boat (1S_3 for **4**, 2S_0 for **5 α** , and 5S_1 for **6 β**) along with two chair conformations (4C_1 for **6 α** and 1C_4 for **5 β**) were found for the main conformers of the modeled compounds (Fig. 4). The shielding tensors were calculated with the same level of theory and then converted to chemical shifts using the multiple reference method.^{205, 206} First, the means of the absolute values of the errors (MAE) were calculated between each synthetic molecules **4–6** and the corresponding *in silico* anomer pairs **40–42** (Table S1). In most cases, it was possible to assign the α - and β -anomers to a single model, but the case of compound **5 β** was found to be ambiguous at B97-2/pVTZ level of theory. Indeed, when only the ^1H NMR data were considered, we found that **5 α** and **5 β** would both

CHAPITRE 2 – TOTAL SYNTHESIS, ISOLATION, SURFACTANT PROPERTIES, AND BIOLOGICAL EVALUATION OF ANANATOSIDES AND RELATED MACROLACTONE-CONTAINING RHAMNOLIPIDS

be of α -configuration. To ensure the validity of these assignments, the pooled comparison method proposed by Lauro *et al.*²⁰⁷ was performed for the $5\alpha/5\beta$ and $6\alpha/6\beta$ anomeric pairs (Table S1). In this way, the anomeric configuration of each synthetic macrolactone was unambiguously assigned as depicted in Scheme 8.

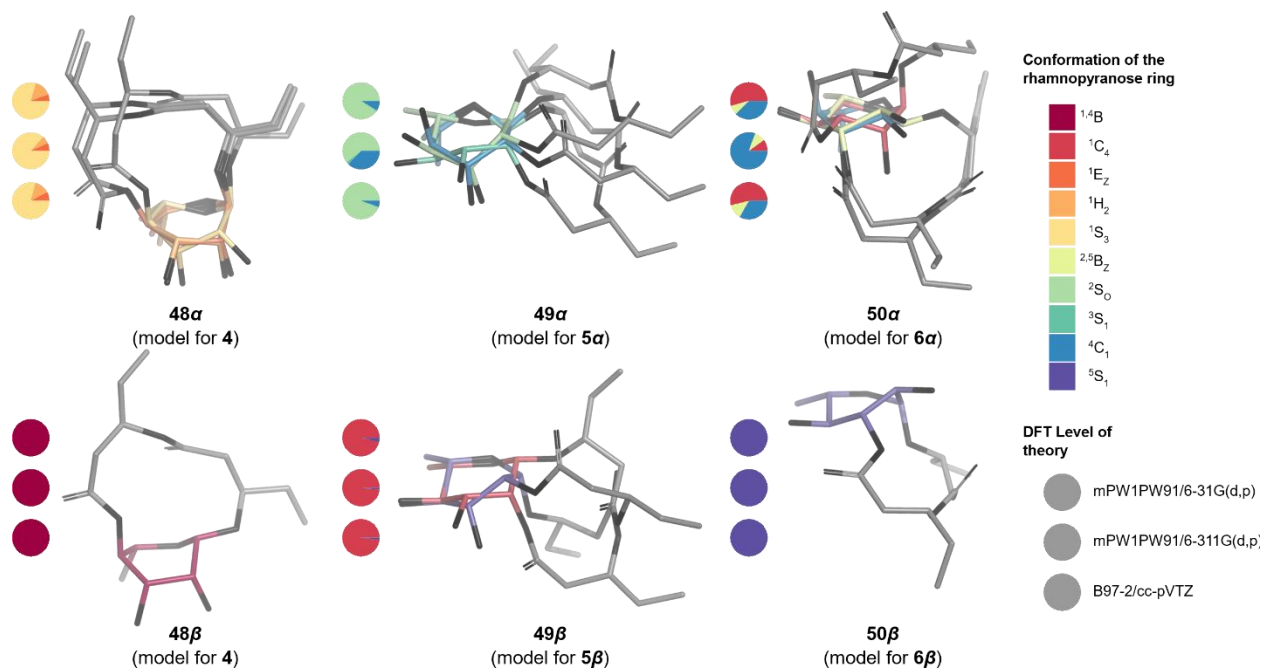


Figure 2.4. 3D structure of the macrolactonized rhamnolipids models 48-50^{208,2}

2.4.5 Surfactant properties of natural glycolipids

Biosurfactants are molecules that can associate with each other leading to the formation of micelles. They can also interact with surfaces between phases of different polarity such as the air/water or oil/water interface.²⁰⁹ To gain quantitative insights into the surfactant properties of microbial glycolipids, the surface tensions (γ_{CMC}) of ananatoside A (**1**) and ananatoside B (**2**) were measured using a Fisher tensiometer by means of the du Noüy ring method. The CMC, referring to the

² Only the most stable structure of each conformer is depicted. Pie chart gives Boltzmann population for standard six-membered ring for the three level of theory used in this study (from top to bottom: mPW1PW91/6-31G(d,p), mPW1PW91/6-311G(d,p) and B97-2/pVTZ).

CHAPITRE 2 – TOTAL SYNTHESIS, ISOLATION, SURFACTANT PROPERTIES, AND BIOLOGICAL EVALUATION OF ANANATOSIDES AND RELATED MACRODILACTONE-CONTAINING RHAMNOLIPIDS

concentration of surfactant at which micelles start to form, was determined from a plot of surface tension against each concentration. These data were compared to those obtained for synthetic RhaC₁₀C₁₀ (**3**). Due to the presence of a free carboxylic acid moiety in biosurfactants **2** and **3**, the surface tensions were measured at neutral pH, which corresponds to the presence of their anionic forms in solution based on an estimated p*K*_a of 5.5 for RhaC₁₀C₁₀ (**3**).²¹⁰ As shown in Table 4, the CMC value for ananatoside B (**2**) was similar to the one measured for rhamnolipid **3**, denoting that ananatoside B (**2**) can be considered as a potent biosurfactant. In the case of ananatoside A (**1**), the measured CMC value was even lower than for RhaC₁₀C₁₀ (**3**). However, the latter value must be taken with caution as the presence of the macrolactone functionality decreased considerably the water solubility of ananatoside A (**1**) as compared to its open-chain congener. Consequently, the surface tension measurements were performed quickly to avoid the precipitation of ananatoside A (**1**) into the aqueous medium. It is interesting to note that the surface tension values measured for biosurfactants **2** and **3** were on the same order of magnitude than those measured by Pemberton and co-workers¹⁹¹ for structurally similar synthetic rhamnolipids bearing C₁₀C₁₀ lipid chains.

Table 2.4. Critical Micelle Concentration (CMC), surface tension (γ_{CMC}), and hydrodynamic diameter (Z-average) of naturally occurring biosurfactants (1-3)

biosurfactant ^a	CMC (μM) ^b	γ_{CMC} (nM/m) ^b	Z-average (nm) ^{b,c}
ananatoside A (1)	43 ± 2	37 ± 1	>800 ^d
ananatoside B (2)	63 ± 2	28 ± 1	99.0
RhaC ₁₀ C ₁₀ (3)	58 ± 1	30 ± 1	92.1

^aSynthetic samples; ^bData taken at pH 7.0; ^cHydrodynamic diameter of micelles measured with a Zetasizer instrument at concentrations of 80 μM for ananatoside B (**2**) and RhaC₁₀C₁₀ (**3**), and 100 μM for ananatoside A (**1**); ^dSize distribution showed the formation of aggregated particles.

In parallel to these experiments, we took advantage of dynamic light scattering (DLS) to evaluate the hydrodynamic diameter of biosurfactant micelles formed at concentrations above the CMC (Table 4).²¹¹ DLS considers the intensity of light scattered by spherical particles, which prevents its application for highly polydisperse and non-spherical colloidal systems. Using a Zetasizer instrument, the results showed that the Z-average, *i.e.*, the mean diameter of the micelles, was in the same range for ananatoside B (**2**) and for rhamnolipid **3** (see Fig. S6). Once again, due to its

CHAPITRE 2 – TOTAL SYNTHESIS, ISOLATION, SURFACTANT PROPERTIES, AND BIOLOGICAL EVALUATION OF ANANATOSIDES AND RELATED MACRODILACTONE-CONTAINING RHAMNOLIPIDS

hydrophobicity, ananatoside A (**1**) was too polydisperse for conducting a proper distribution analysis, showing a Z-average value above 800 nm, which meant that the particles were aggregated in water at the tested concentration. Similar results were obtained for ananatoside A (**1**) when the DLS experiments were conducted in DMSO as the solvent. These results showed that ananatoside B (**2**), similarly to rhamnolipid **3**, formed monodisperse colloidal particles at concentrations above its CMC.

The propensity of surfactants to stabilize emulsions shows promising for biotechnological applications such as bioremediation of contaminated soils and water.²⁰⁹ Therefore, the emulsifying properties of microbial biosurfactants **1–3** were evaluated against light as well as heavy hydrocarbon contaminants such as cyclohexane and kerosene, respectively (see Fig. S7). The emulsifying activity results showed that ananatoside B (**2**) and RhaC₁₀C₁₀ (**3**) were equally able to generate emulsions in cyclohexane and kerosene while ananatoside A (**1**) was unable to form any emulsion, mainly because of its lack of affinity with water. Altogether, these results once again highlighted that ananatoside B (**2**), but not its macrolide counterpart **1**, exhibits potent surfactant properties that could be advantageously used for biotechnological applications.

2.4.6 Antimicrobial activity, cytotoxicity, and hemolytic activity of natural and synthetic glycolipids

As previously mentioned in the introduction section, numerous studies have reported the antimicrobial potential of rhamnolipids against several pathogenic bacteria and fungi.¹⁴⁵ However, as rhamnolipids were usually tested as mixtures of different congeners and not as pure synthetic compounds, there seems to be no clear consensus regarding the antimicrobial activity of one specific congener. Hence, as an initial investigation toward their biological functions in bacteria, the *in vitro* antimicrobial activity of ananatoside A (**1**), ananatoside B (**2**), RhaC₁₀C₁₀ (**3**), and macrolides **4–6** was evaluated against pathogenic Gram-negative, *i.e.*, *Pseudomonas aeruginosa* PA14, *Pseudomonas aeruginosa* LESD58, and *Escherichia coli* DH5 α , and Gram-positive bacteria, *i.e.*, *Staphylococcus aureus* MRSA, *Staphylococcus aureus* Newman, and *Bacillus subtilis* PY79, as well as against fungi, *i.e.*, *Candida albicans* ATCC 10231 and *Candida albicans* LSPQ 0199. At the

CHAPITRE 2 – TOTAL SYNTHESIS, ISOLATION, SURFACTANT PROPERTIES, AND BIOLOGICAL EVALUATION OF ANANATOSIDES AND RELATED MACRODILACTONE-CONTAINING RHAMNOLIPIDS

maximum tested concentration ($37.5\mu\text{g}\cdot\text{mL}^{-1}$), glycolipids **1–6** were unable to inhibit the growth of these microbes. These results seem to demonstrate that the biosynthetic production of ananatoside A (**1**) and ananatoside B (**2**) by the bacterium *P. ananatis* is not aimed for antimicrobial purposes.

As the anticancer potential of microbial rhamnolipids has previously been reported,¹⁴⁹ we next sought to evaluate the *in vitro* cytotoxicity of our synthetic and natural glycolipids **1–6** against cancerous cell lines, *i.e.*, human lung carcinoma (A549) and colorectal adenocarcinoma (DLD-1). The compounds were also tested against human normal skin fibroblasts (WS1) to estimate their selectivity towards cancer cells. As revealed in Table 5, very interesting conclusions can be derived from these cytotoxicity results. First, it appears that only macrolactones, as compared to their open forms, were able to inhibit the growth of human cell lines. Second, the cytotoxic activity of the active macrolides was not specific to cancer cell lines as comparable IC_{50} values were measured against healthy cells (WS1), pointing toward a mechanism involving the formation of pores in cell membrane.¹⁴⁹ Specifically, ananatoside A (**1**) was cytotoxic against human cell lines ($\text{IC}_{50} = 50\text{--}58\ \mu\text{M}$) while its open form counterpart ananatoside B (**2**) was inactive at the maximum tested concentration ($\text{IC}_{50} > 200\ \mu\text{M}$). Furthermore, macrolactonization of the inactive RhaC₁₀C₁₀ (**3**, $\text{IC}_{50} > 200\ \mu\text{M}$) generated cytotoxic macrolides **4**, **5 β** , and **6 β** ($\text{IC}_{50} = 50\text{--}112\ \mu\text{M}$). While (1→4)-macrolactonized rhamnolipid **4** was the most active congener, only the β -anomers of (1→2)- and (1→3)-macrolactonized rhamnolipid **5 β** and **6 β** , respectively, were found to inhibit the growth of human cell lines. These results showed that both the position of the macrolactone ring and the anomeric configuration of the glycosidic bonds can impact the cytotoxicity of the rhamnolipids.

CHAPITRE 2 – TOTAL SYNTHESIS, ISOLATION, SURFACTANT PROPERTIES, AND BIOLOGICAL EVALUATION OF ANANATOSIDES AND RELATED MACRODILACTONE-CONTAINING RHAMNOLIPIDS

Table 2.5. Cytotoxicity and hemolytic activity of natural and synthetic glycolipids (1-6)

Glycolipid ^a	Cytotoxicity (IC ₅₀ in μM) ^b			Hemolysis (HC ₅₀ in μM) ^c
	A549	DLD-1	WS1	erythrocytes
ananatoside A (1)	50 ± 7	58 ± 2	52 ± 4	12.3 ± 0.3
ananatoside B (2)	>200 ^d	>200 ^d	>200 ^d	>200 ^d
RhaC ₁₀ C ₁₀ (3)	>200 ^d	>200 ^d	>200 ^d	65 ± 6
α 1,4RhaC ₁₀ C ₁₀ (4)	56 ± 2	70 ± 10	57 ± 1	12.0 ± 0.7
β 1,2RhaC ₁₀ C ₁₀ (5 β)	103 ± 7	110 ± 2	105 ± 5	14 ± 2
α 1,2RhaC ₁₀ C ₁₀ (5 α)	>200 ^d	>200 ^d	>200 ^d	>200 ^d
β 1,3RhaC ₁₀ C ₁₀ (6 β)	112 ± 2	112 ± 3	110 ± 1	12.3 ± 0.5
α 1,3RhaC ₁₀ C ₁₀ (6 α)	>200 ^d	>200 ^d	>200 ^d	>200 ^d

^aSynthetic samples; ^bHalf maximal inhibitory concentration measured *via* the resazurin assay. Etoposide was used as a positive control²¹² showing IC₅₀ values of 1.2, 27, and 34 μM against A549, DLD-1, and WS1 cell lines, respectively; ^cHalf maximal inhibitory concentration measured on sheep blood erythrocytes. Triton X-100 was used as a positive control showing an HC₅₀ value of 52 ± 2 μM ; ^dNo inhibition or activity at the maximum tested concentration (IC₅₀ or HC₅₀>200 μM).

Owing to their surfactant properties, glycolipids can break the membrane of red blood cells causing hemolytic activity.¹⁵¹ To understand if the cytotoxicity of macrolactones **1**, **4**, **5 β** , and **6 β** was due to their surface tension activity, we evaluated the hemolytic potential of synthetic glycolipids **1–6** against sheep erythrocytes (Table 5). As anticipated, all the cytotoxic glycolipids were shown to exhibit hemolytic activities on red blood cells with HC₅₀ ranging from 12.0 to 14 μM . The non-cytotoxic rhamnolipid **3** was also found to exert a weak hemolytic activity (HC₅₀ = 65 ± 6 μM). Altogether, these data suggest a non-specific mechanism of cytotoxicity involving the intercalation of macrolactones **1**, **4**, **5 β** , and **6 β** into the lipid constituents of the cell membranes.

2.4.7 Interaction of natural and synthetic glycolipids with the plant immune system

Bacterial rhamnolipids, such as compound **3**, trigger the plant immune system, which can ultimately lead to plant protection against diseases caused by fungal and bacterial pathogens.¹⁵⁶ As ananatoside A (**1**) and ananatoside B (**2**) share structural similarities with rhamnolipid **3** and because they have been isolated from *P. ananatis*, an emerging plant pathogen causing important agricultural damage worldwide,²¹³ we wanted to investigate whether these bacterial glycolipids, along with our

CHAPITRE 2 – TOTAL SYNTHESIS, ISOLATION, SURFACTANT PROPERTIES, AND BIOLOGICAL EVALUATION OF ANANATOSIDES AND RELATED MACRODILACTONE-CONTAINING RHAMNOLIPIDS

unprecedented series of synthetic rhamnolactones, could be perceived by the plant immune system. We relied on measuring the extracellular content of reactive oxygen species (ROS) produced by tomato plants (*Solanum lycopersicum*) following treatment with the synthetic compounds, as an early and important marker of plant immunity.^{153, 155, 214} Tomato leaves were challenged with synthetic glycolipids **1–6** at concentrations of 100 μ M and the production of ROS was monitored over a 720-min time frame (Fig. 5). As expected, rhamnolipid **3**, used as a positive control in this study, triggered a long-lasting and strong production of ROS in tomato leaves.

CHAPITRE 2 – TOTAL SYNTHESIS, ISOLATION, SURFACTANT PROPERTIES, AND BIOLOGICAL EVALUATION OF ANANATOSIDES AND RELATED MACRODILACTONE-CONTAINING RHAMNOLIPIDS

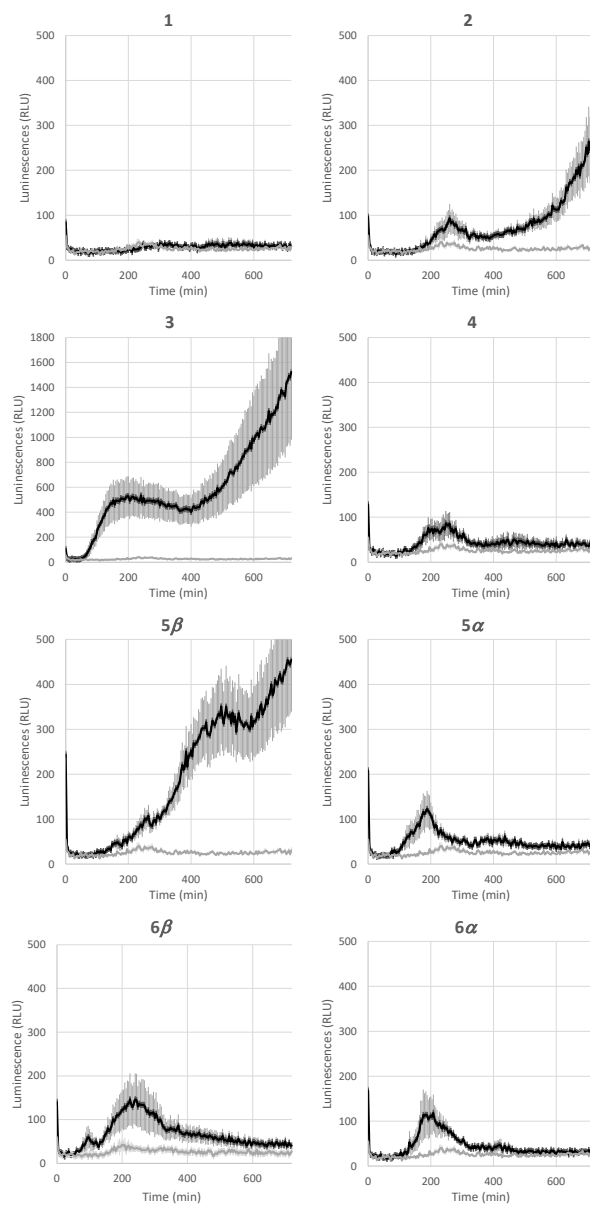


Figure 2.5. Extracellular reactive oxygen species (ROS) production following treatment of tomato leaf disks with anatanoside A (1), anatanoside B (2), RhaC₁₀C₁₀ (3), and related macrodilactone-containing rhamnolipids (4-6)³

³ Production of ROS was measured in tomato leaf disks following treatment at 100 μ M with synthetic glycolipids (1–6). MeOH (0.5%) was used as a control. ROS production was measured using the chemiluminescence of luminol and photon counts were expressed as relative luminescence units (RLUs). Data are mean \pm SEM ($n = 6$). Experiments were independently realized three times with similar results.

CHAPITRE 2 – TOTAL SYNTHESIS, ISOLATION, SURFACTANT PROPERTIES, AND BIOLOGICAL EVALUATION OF ANANATOSIDES AND RELATED MACRODILACTONE-CONTAINING RHAMNOLIPIDS

Although less strong in amplitude, a similar pattern of ROS production was measured for ananatoside B (**2**), but not for ananatoside A (**1**), its macrolactonic counterpart. These responses seem to be however plant-specific because, when tested in *Arabidopsis thaliana*, both natural glycolipids **1** and **2** were perceived by plants (see Fig. S8). As for rhamnolactones **4–6**, all of them were sensed by tomatoes: the luminescence curves showed a small burst at 200 min followed by a return to basal levels over the next 200 min. The only exception to this general trend was compound **5 β** . Indeed, (1 \rightarrow 2)-macrolactonized rhamnolipid **5 β** induced a strong and long-lasting production of ROS following the initial burst at 200 min. This response was stereospecific as corresponding α -anomer **5 α** did not show similar sensing patterns. Interestingly, our molecular modeling showed that macrolide **5 β** was the only one to be found in the native 1C_4 conformation for the rhamnose ring (see Fig. 4), which could be part of the explanation for these intriguing results. Taken together, these results highlight that (1), glycolipids sharing the same 3-hydroxyalkanoate dilipidic chain than rhamnolipids but bearing a glucose instead of a rhamnose moiety can be perceived by plants; and (2) macrolactonization of these glycolipids alter the sensing patterns according to the plant species as well as the conformation of the rhamnopyranose ring.

2.5 Conclusions

In summary, we have isolated and structurally characterized rhamnolipid-like ananatoside A (**1**) and ananatoside B (**2**) from an organic extract of *P. ananatis*, a non-human pathogenic producer of biosurfactants. We have accomplished, for the first time, the total synthesis of ananatoside A (**1**) and ananatoside B (**2**), confirming without any doubt the structure of these bacterial *glucolipids*. The macrodilactone-containing ananatoside A (**1**) was efficiently synthesized according to three alternative pathways: (1) *via* the stereoselective intramolecular glycosylation of a thioglucoside donor; (2) *via* the chemical macrolactonization of a seco acid precursor; and (3) *via* the direct enzymatic macrolactonization of its open form congener ananatoside B (**2**) using a solid-supported lipase. Capitalizing on the expeditious intramolecular glycosylation of orthogonally protected thiorhamnoside donors, we have accomplished the synthesis of diastereoisomerically pure (1 \rightarrow 2), (1 \rightarrow 3), and (1 \rightarrow 4)-macrolactonized rhamnolipids. We have determined the anomeric configuration

CHAPITRE 2 – TOTAL SYNTHESIS, ISOLATION, SURFACTANT PROPERTIES, AND BIOLOGICAL EVALUATION OF ANANATOSIDES AND RELATED MACRODILACTONE-CONTAINING RHAMNOLIPIDS

of these unprecedented macrolides through molecular modeling and found that the rhamnose ring adopts unusual conformations including skew boat and flipped chair conformations. Determination of the surfactant properties of bacterial glucolipids **1** and **2** in comparison with rhamnolipid **3** has revealed that ananatoside B (**2**), but not its macrolide counterpart **1**, represents a potent biosurfactant, as shown by its efficient emulsifying activity. Furthermore, we have shown that synthetic glycolipids **1–6** did not exhibit any antimicrobial activity against pathogenic Gram-negative and Gram-positive bacteria as well as against fungi. We have also highlighted that the presence of the macrodilactone functionality can convert non-cytotoxic glycolipids into cytotoxic ones according to the position and anomeric configuration of the macrolides. We have revealed a direct correlation between the cytotoxicity and the hemolytic activity of these macrolides pointing towards a mechanism involving the formation of pores into the lipidic cell membrane. Finally, we have demonstrated that natural glucolipids **1** and **2** as well as unnatural macrolides **4–6** can be perceived by the plant immune system, and that this sensing was long-lasting for macrolide **5 β** featuring a rhamnose moiety in its native 1C_4 conformation. Altogether our results proved that macrolactonization of glycolipids can dramatically interfere with their surfactant properties and biological activity. Our interdisciplinary study could serve as a foundation for the rational design of rhamnolipid-like biosurfactants with improved properties for biotechnological and/or therapeutic applications.

2.6 Acknowledgements

This article is dedicated to the memory of Pr. Éric Marsault, University of Sherbrooke, who passed away in early 2021. This work was supported by Discovery grants from the Natural Sciences and Engineering Research Council of Canada (NSERC) under award number RGPIN-2016-04950 (to C. G.) and RGPIN-2020-06771 (to E. D.). C. G. was supported by a Fonds de recherche du Québec – Santé (FRQS) Research Scholars Junior 2 Career Award. S. V., J. C., and S. D. thank the SFR Condorcet FR CNRS 3417 (project P3IA) and French MESRI for financial support. M. A. D. D. R. thank the Microbiology Society (Round 1 Research Visit Grant 2019) and Liverpool John Moores University (ECR Fellowships 2018-2019) for travel funds. M. C. thanks NSERC and Fonds de recherche du Québec – Nature et technologies (FRQNT) for M.Sc. and Ph.D. scholarships. M. J. P.

CHAPITRE 2 – TOTAL SYNTHESIS, ISOLATION, SURFACTANT PROPERTIES, AND BIOLOGICAL EVALUATION OF ANANATOSIDES AND RELATED MACRODILACTONE-CONTAINING RHAMNOLIPIDS

thanks NSERC for an undergraduate scholarship. We thank Sylvain Milot, INRS, for valuable discussions.

2.7 Experimental section

2.7.1 General methods

All starting materials and reagents were purchased from commercial sources and used as received without further purification. Air and water sensitive reactions were performed in oven-dried glassware under an Ar atmosphere. Moisture sensitive reagents were introduced *via* dried syringe. Anhydrous solvents were either prepared from commercial solvents and dried over heat-gun activated 4 Å molecular sieves (MS) or supplied over MS and used as received. Powdered 4 Å MS were activated before use by heating with a heat gun for approx. 15 min under high vacuum. Reactions were monitored by thin-layer chromatography (TLC) with silica gel 60 F₂₅₄ 0.25 mm pre-coated aluminum foil plates. Compounds were visualized by using UV₂₅₄ and/or orcinol (1 mg•mL⁻¹) in 10% aqueous H₂SO₄ solution with heating and/or CAM and/or KMnO₄ with heating. Normal-phase flash column chromatography was performed on silica gel 60 Å (15-40 μm). NMR spectra were recorded at 297 K in the indicated solvent (CDCl₃, py-*d*₅) with 400 or 600 MHz instruments, employing standard softwares given by the manufacturer. ¹H and ¹³C NMR spectra were referenced to tetramethylsilane (TMS, δ_H = δ_C = 0.00 ppm) as internal reference. Assignments were based on ¹H, ¹³C, COSY, HSQC, uncoupled HSQC, and HMBC experiments. High-resolution mass spectra (HRMS) were recorded on an ESI-Q-TOF mass spectrometer. Optical rotations [α]_D²⁰ were measured on an Anton Paar polarimeter. The retention factors (*R*_f) were calculated from silica gel F₂₅₄ 0.25 mm pre-coated glass TLC plates. Preparative TLC purification was accomplished using PLC silica gel F₂₅₄ 1 mm pre-coated 20 × 20 cm glass TLC plates.

CHAPITRE 2 – TOTAL SYNTHESIS, ISOLATION, SURFACTANT PROPERTIES, AND BIOLOGICAL EVALUATION OF ANANATOSIDES AND RELATED MACRODILACTONE-CONTAINING RHAMNOLIPIDS

2.7.2 Experimental procedures for isolation and synthesis

Bacterial Culture for Isolation.

Pre-culture tubes of *Pantoea ananatis* BRT175 (3 mL) were grown at 30 °C in LB medium with shaking (240 rpm) in a TC-7 roller drum (New Brunswick, Canada). Under exponential growth phase, LB medium pre-culture flasks (100 mL, each) were seeded with an initial $OD_{600} = 0.1$ and cultures were incubated overnight at 30 °C with shaking (150 rpm). Six two-liter flasks, each containing 500 mL Mineral Salts Medium (MSM), were inoculated at an initial $OD_{600} = 0.1$ and cultures were grown at 30 °C with shaking (150 rpm) for five days. The MSM contained ($g \cdot L^{-1}$): 0.9 Na_2HPO_4 , 0.7 KH_2PO_4 , 2.0 $NaNO_3$, 0.1 $CaCl_2 \cdot 2H_2O$, 0.4 $MgSO_4 \cdot 7H_2O$, and trace element solution ($2 mL \cdot L^{-1}$). The composition of trace element solution was ($g \cdot L^{-1}$): 2.0 $FeSO_4 \cdot 7H_2O$, 1.5 $MnSO_4 \cdot H_2O$ and 0.6 $(NH_4)_6Mo_7O_{24} \cdot 4H_2O$. Dextrose ($20 g \cdot L^{-1}$) was provided as a carbon source.

Isolation of Ananatoside A (1) and Ananatoside B (2).

At the end of the cultivation period, culture supernatant was recovered by centrifugation and concentrated HCl was added to reach a final $pH = 3$. Pooled supernatants (3 L total) were then extracted twice with equal volumes of EtOAc. The organic fractions were then pooled, dried over anhydrous $MgSO_4$, and concentrated under reduced pressure. The crude extract (0.2 g) was suspended in CH_3CN/H_2O (1:1) and used directly for purification. Semi-preparative HPLC purification was performed on a Thermo Fisher Scientific Ultimate 3000 HPLC-CAD system equipped with a Dionex LPG-3400SD pump, a WPS-3000SL autosampler, a TCC-3000SD column oven, and a charged aerosol detector (CAD) Corona Veo. The power function value was set at 1.0, the filter at 1 s, the data collection rate at 10 Hz, and the evaporator temperature at 35 °C. Nitrogen (57.2 psi) was used for nebulization. All data were analyzed using the Thermo Fischer Chromeleon 7.2.9 software. For the purification, a reverse phase column Hypersil Gold (250 × 10 mm) was used with a mobile phase consisting of CH_3CN/H_2O gradient containing 0.1% formic acid. Prior the injection, the column was equilibrated for 10 min with 50% of CH_3CN . The injection volume was set to 250 μL . The elution gradient started from 50 to 60% CH_3CN for 20 min, then to 100% CH_3CN

CHAPITRE 2 – TOTAL SYNTHESIS, ISOLATION, SURFACTANT PROPERTIES, AND BIOLOGICAL EVALUATION OF ANANATOSIDES AND RELATED MACRODILACTONE-CONTAINING RHAMNOLIPIDS

within the next 40 min and hold for 15 min. HPLC flow rate was set to $5.0 \text{ mL}\cdot\text{min}^{-1}$ and the oven temperature was set at $28 \text{ }^{\circ}\text{C}$. A flow splitter was used after the column to deliver only 5% of the mixture to the CAD detector and the remaining to the fraction collector. Fractions containing ananatoside A (**1**, 42.0 min) and ananatoside B (**2**, 23.6 min), respectively, were pooled and concentrated under reduced pressure to give ananatoside A (**1**, 37 mg) as a light yellow oil (physical and analytical data agreed with those published)¹⁵⁹ and ananatoside B (**2**, 30 mg) as a white amorphous powder. Data for ananatoside B (**2**): $[\alpha]_{\text{D}}^{20} +14.6$ (c 0.24; EtOAc); ^1H NMR (600 MHz, pyr- d_5) δ (ppm) 5.81-5.77 (m, 1H, H-3''), 4.99 (d, $J = 7.7$ Hz, 1H, H-1), 4.60-4.58 (m, 1H, H-3'), 4.52 (d, $J = 10.4$ Hz, 1H, H-6a), 4.39 (dd, $J = 11.6$ Hz, $J = 5.3$ Hz, 1H, H-6b), 4.26-4.21 (m, 2H, H-3, H-4), 4.03 (t, $J = 7.9$ Hz, 1H, H-2), 3.95-3.91 (m, 1H, H-5), 3.27 (dd, $J_{2a'-2b'} = 15.0$ Hz, $J_{2a'-3'} = 5.4$ Hz, 1H, H-2a'), 3.04 (dd, $J_{2a''-2b''} = 15.5$ Hz, $J_{2a''-3''} = 6.9$ Hz, H-2a''), 2.87 (dd, $J_{2b''-2a''} = 15.8$ Hz, $J_{2b''-3''} = 5.7$ Hz, 1H, H-2b''), 2.82 (dd, $J_{2b'-2a'} = 15.1$ Hz, $J_{2b'-3'} = 7.3$ Hz, 1H, H-2b'), 1.84-1.17 (m, 24H, $12 \times \text{CH}_2$), 0.85-0.80 (m, 6H, $2 \times \text{CH}_3$); ^{13}C NMR (150 MHz, pyr- d_5) δ (ppm) 173.8, 172.0 (2C, C-1', C-1''), 105.4 (C-1), 79.0, 78.7 (2C, C-5, C-3), 77.8 (C-3'), 75.8 (C-2'), 72.2, 72.0 (2C, C-3'', C-4), 63.5 (C-6), 42.6 (C-2'), 40.4 (C-2''), 35.8-23.3 (12C, $12 \times \text{CH}_2$), 14.7 (2C, $2 \times \text{CH}_3$); $[\alpha]_{\text{D}}^{20} +103$ (c 0.2, CHCl_3); HRMS (ESI-TOF) m/z $[\text{M} + \text{NH}_4]^+$ calcd for $\text{C}_{26}\text{H}_{52}\text{NO}_{10}$ 538.3586; found 538.3587; m/z $[\text{M} + \text{Na}]^+$ calcd for $\text{C}_{26}\text{H}_{48}\text{NaO}_{10}$ 543.3140; found 543.3142.

HPLC Analysis of Natural and Synthetic Compounds.

Analytical reversed phase HPLC analyses were performed using the same equipment as described above. For the separation, a reverse phase column Hypersil Gold (250×4.6 mm) was employed. The method was the same as described for the semi-preparative purification. The injection volume was set to $50 \mu\text{L}$, the flow rate was $0.8 \text{ mL}\cdot\text{min}^{-1}$, oven temperature was set to $28 \text{ }^{\circ}\text{C}$, and detection was accomplished using the CAD detector. The gradients consisted of: method A: 50 to 60% CH_3CN (20 min), 60 to 100% CH_3CN (30 min), and 100% CH_3CN (10 min); method B: 50 to 60% CH_3CN (10 min), 60 to 100% CH_3CN (25 min), and 100% CH_3CN (25 min); method C: 50 to 80% CH_3CN (50 min) and 80 to 90% CH_3CN (10 min); and method D: 50 to 60% CH_3CN (20 min) and 60 to 100% CH_3CN (40 min).

CHAPITRE 2 – TOTAL SYNTHESIS, ISOLATION, SURFACTANT PROPERTIES, AND BIOLOGICAL EVALUATION OF ANANATOSIDES AND RELATED MACRODILACTONE-CONTAINING RHAMNOLIPIDS

(R)-Benzyl 3-Hydroxydecanoate (14).

Acid **13**⁴ (143 mg, 0.761 mmol, 1.0 equiv) was solubilized in anhydrous DMF (3.8 mL) under Ar. BnBr (0.20 mL, 1.7 mmol, 2.2 equiv) and Cs₂CO₃ (347 mg, 1.07 mmol, 1.4 equiv) were successively added and the mixture was stirred for 21 h at rt under Ar. The suspension was diluted with DCM and washed with saturated aqueous NH₄Cl. The aqueous layer was extracted with DCM (2×). The combined organic layers were washed with brine, dried over anhydrous MgSO₄, filtered, and evaporated under reduced pressure. The residue was purified by silica gel flash chromatography (Hex/EtOAc 95:5 to 85:5) to give benzyl ester **14** (201 mg, quant.) as a colorless oil: *R_f* 0.24 (Hex/EtOAc 8:2); [α]_D²⁰ -15 (*c* 0.6, CHCl₃); ¹H NMR (600 MHz, CDCl₃) δ (ppm) 7.38–7.32 (m, 5H, 5 × CH_{Bn}), 5.15 (s, 2H, CH_{2Bn}), 4.04–4.01 (m, 1H, H-3), 2.85 (d, *J* = 3.5 Hz, 1H, OH), 2.56 (dd, *J*_{2a-2b} = 16.5 Hz, *J*_{2a-3} = 3.0 Hz, 1H, H-2a), 2.46 (dd, *J*_{2b-2a} = 16.5 Hz, *J*_{2b-3} = 9.1 Hz, 1H, H-2b), 1.54–1.26 (m, 12H, H-4, H-5, H-6, H-7, H-8, H-9), 0.88 (t, *J* = 7.0 Hz, 3H, H-10); ¹³C NMR (150 MHz, CDCl₃) δ (ppm) 173.0 (C-1), 135.7 (C_{Bn}), 128.8 (2C, 2 × CH_{Bn}), 128.5 (CH_{Bn}), 128.4 (2C, 2 × CH_{Bn}), 68.2 (C-3), 66.6 (CH_{2Bn}), 41.5 (C-2), 36.7–22.8 (6C, C-4, C-5, C-6, C-7, C-8, C-9), 14.2 (C-10); HRMS (ESI-TOF) *m/z* [M + Na]⁺ calcd for C₁₇H₂₆NaO₃ 301.1774; found 301.1764.

(R)-3-(tert-Butyldimethylsilyloxy)decanoic acid (15).

Imidazole (904 mg, 13.3 mmol, 10.0 equiv) was added to a solution of TBSCl (701 mg, 4.65 mmol, 3.5 equiv) in anhydrous DMF (2.3 mL) at 0 °C. The mixture was stirred at 0 °C for 15 min under an Ar atmosphere, after which a solution of acid **13** (252 mg, 1.33 mmol, 1.0 equiv) in anhydrous DMF (0.5 mL) was added. The solution was stirred at rt for 16 h under an Ar atmosphere, then transferred to a separatory funnel. Brine was added to the mixture and the latter was extracted with a Hex/Et₂O mixture (3:1 v/v). The organic layer was dried over anhydrous MgSO₄, filtered, and evaporated under reduced pressure. The residue was solubilized in a mixture of MeOH (36 mL) and THF (18 mL), to which a solution of K₂CO₃ (450 mg, 3.26 mmol, 2.45 equiv) in H₂O (6 mL) was added at 0

⁴ Se référer à l'annexe du Chapitre 2 pour la synthèse de ce composé.

CHAPITRE 2 – TOTAL SYNTHESIS, ISOLATION, SURFACTANT PROPERTIES, AND BIOLOGICAL EVALUATION OF ANANATOSIDES AND RELATED MACRODILACTONE-CONTAINING RHAMNOLIPIDS

°C. The mixture was stirred at 0 °C for 1 h after which brine (18 mL) was added. The solution was acidified with aqueous 1 M HCl until a pH of ~3 was reached. The solution was extracted with a Hex/Et₂O mixture (3:1 v/v), dried over anhydrous MgSO₄, filtered, and evaporated under reduced pressure. The residue was dried under high vacuum for 16 h (evaporation of the remaining solvents and TBS alcohol) to give acid **15** (402 mg, quant.) as a colorless oil. Physical and analytical data of compound **15** agreed with those published.¹⁸⁹

(R)-Benzyl 3-(((R)-3-((tert-Butyldimethylsilyl)oxy)decanoyl)oxy)decanoate (16).

Alcohol **14** (91 mg, 0.32 mmol, 1.0 equiv) and acid **15** (121 mg, 0.388 mmol, 1.2 equiv) were solubilized in anhydrous DCE (3.9 mL) under Ar. EDC (186 mg, 0.970 mmol, 3.0 equiv) and DMAP (12 mg, 0.10 mmol, 0.3 equiv) were successively added and the mixture was stirred at rt for 16 h under Ar. The solution was evaporated under reduced pressure and the residue was purified by silica gel flash chromatography (Hex/EtOAc 95:5) to give dilipid **16** (171 mg, 93%) as a colorless oil: *R_f* 0.57 (Hex/EtOAc 8:2); $[\alpha]_D^{20} +53$ (*c* 0.7, CHCl₃); ¹H NMR (600 MHz, CDCl₃) δ (ppm) 7.37–7.31 (m, 5H, 5 × CH_{Bn}), 5.24–5.20 (m, 1H, H-3'), 5.11 (s, 2H, CH_{2Bn}), 4.07 (p, *J* = 6.8 Hz, 1H, H-3), 2.65 (dd, *J*_{2a'-2b'} = 15.4 Hz, *J*_{2a'-3'} = 7.1 Hz, 1H, H-2a'), 2.57 (dd, *J*_{2b'-2a'} = 15.4 Hz, *J*_{2b'-3'} = 5.8 Hz, 1H, H-2b'), 2.41 (dd, *J*_{2a-2b} = 14.8 Hz, *J*_{2a-3} = 5.9 Hz, 1H, H-2a), 2.36 (dd, *J*_{2b-2a} = 14.8 Hz, *J*_{2b-3} = 6.7 Hz, 1H, H-2b), 1.63–1.24 (m, 24H, 12 × CH₂), 0.89–0.86 (m, 15H, H-10, H-10', C(CH₃)₃TBS), 0.06 (s, 3H, CH₃TBS), 0.04 (s, 3H, CH₃TBS); ¹³C NMR (150 MHz, CDCl₃) δ (ppm) 171.1, 170.3 (2C, C-1, C-1'), 135.9 (C_{Bn}), 128.7, 128.4 (5C, 5 × CH_{Bn}), 70.7 (C-3'), 69.4 (C-3), 66.6 (CH_{2Bn}), 42.9 (C-2), 39.3 (C-2'), 37.5–29.3 (8C, 8 × CH₂), 26.0 (3C, C(CH₃)₃TBS), 25.3–22.8 (4C, 4 × CH₂), 18.2 (C(CH₃)₃TBS), 14.3, 14.2 (2C, C-10, C-10'), –4.46 (2C, 2 × CH₃TBS); HRMS (ESI-TOF) *m/z* [M + Na]⁺ calcd for C₁₇H₂₆NaO₃ 585.3946; found 585.3928.

(R)-3-(((R)-3-((tert-Butyldimethylsilyl)oxy)decanoyl)oxy)decanoic acid (10).

Dilipid **16** (122 mg, 0.216 mmol, 1.0 equiv) was solubilized in EtOAc under an Ar atmosphere, and 10% Pd/C (12 mg, 1 mg•mg⁻¹ of dilipid) was added. The suspension was stirred at rt for 20 h under an H₂ atmosphere. The suspension was filtered over Celite and the solvents were evaporated under

CHAPITRE 2 – TOTAL SYNTHESIS, ISOLATION, SURFACTANT PROPERTIES, AND BIOLOGICAL EVALUATION OF ANANATOSIDES AND RELATED MACRODILACTONE-CONTAINING RHAMNOLIPIDS

reduced pressure yielding acid **10** (102 mg, quant.) as a colorless oil: R_f 0.43 (DCM/MeOH 96:4); $[\alpha]_D^{20} +19$ (c 0.7, CHCl₃); ¹H NMR (600 MHz, CDCl₃) δ (ppm) 5.20 (p, $J = 6.0$ Hz, 1H, H-3'), 4.09 (p, $J = 6.0$ Hz, 1H, H-3), 2.65 (dd, $J_{2a'-2b'} = 15.9$ Hz, $J_{2a'-3'} = 6.9$ Hz, 1H, H-2a'), 2.57 (dd, $J_{2b'-2a'} = 15.9$ Hz, $J_{2b'-3'} = 5.8$ Hz, 1H, H-2b'), 2.46 (dd, $J_{2a-2b} = 14.9$ Hz, $J_{2a-3} = 6.0$ Hz, 1H, H-2a), 2.41 (dd, $J_{2b-2a} = 14.9$ Hz, $J_{2b-3} = 6.5$ Hz, 1H, H-2b), 1.69-1.26 (m, 24H, 12 x CH₂), 0.89-0.85 (m, 15H, H-10, H-10'), C(CH₃)₃TBS), 0.06 (s, 3H, CH₃TBS), 0.05 (s, 3H, CH₃TBS); ¹³C NMR (150 MHz, CDCl₃) δ (ppm) 176.2, 171.2 (2C, C-1, C-1'), 70.4 (C-3'), 69.3 (C-3), 42.9 (C-2), 38.9 (C-2'), 37.5-29.3 (8C, 8 x CH₂), 26.0 (3C, C(CH₃)₃TBS), 25.3-22.8 (4C, 4 x CH₂), 18.2 (C(CH₃)₃TBS), 14.3, 14.2 (C-10, C-10'), -4.46 (CH₃TBS), -4.52 (CH₃TBS); HRMS (ESI-TOF) m/z [M + H]⁺ calcd for C₂₆H₅₃O₅Si 473.3657; found 473.3653; m/z [M + Na]⁺ calcd for C₂₆H₅₂NaO₅Si 495.3476; found 495.3465.

(R)-Benzyl 3-(((R)-3-Hydroxydecanoyl)oxy)decanoate (12).

A solution of dilipid **16** (192 mg, 0.340 mmol, 1.0 equiv) in DCM (0.7 mL) was added dropwise in TFA (1.4 mL) during a one-minute period, then the mixture was stirred for one additional minute. The reaction mixture was quenched with saturated aqueous NaHCO₃. The organic layer was dried over anhydrous MgSO₄, filtered, and evaporated under reduced pressure. The residue was purified by silica gel flash chromatography (Hex/EtOAc 9:1 to 8:2) to give alcohol **12** (143 mg, 94%) as a colorless oil: R_f 0.28 (Hex/EtOAc 8:2); $[\alpha]_D^{20} -13$ (c 0.4, CHCl₃); ¹H NMR (600 MHz, CDCl₃) δ (ppm) 7.38–7.32 (m, 5H, 5 x CH_{Bn}), 5.30-5.26 (m, 1H, H-3'), 5.11 (s, 2H, CH₂Bn), 3.98–3.94 (m, 1H, H-3), 2.95 (br s, 1H, OH), 2.63 (dd, $J_{2a'-2b'} = 14.2$ Hz, $J_{2a'-3'} = 6.2$ Hz, 1H, H-2a'), 2.60 (dd, $J_{2b'-2a'} = 14.2$ Hz, $J_{2b'-3'} = 4.1$ Hz, 1H, H-2b'), 2.42 (dd, $J_{2a-2b} = 15.8$ Hz, $J_{2a-3} = 2.9$ Hz, 1H, H-2a), 2.31 (dd, $J_{2b-2a} = 15.8$ Hz, $J_{2b-3} = 9.2$ Hz, 1H, H-2b), 1.64–1.25 (m, 24H, 12 x CH₂), 0.89–0.85 (m, 6H, H-10, H-10'); ¹³C NMR (150 MHz, CDCl₃) δ (ppm) 172.6, 170.6 (2C, C-1, C-1'), 135.7 (C_{Bn}), 128.7 (2C, 2 x CH_{Bn}), 128.6 (2C, 2 x CH_{Bn}), 128.5 (CH_{Bn}), 71.0 (C-3'), 68.4 (C-3), 66.8 (CH₂Bn), 41.9 (C-2), 39.3 (C-2'), 36.7–22.8 (12C, 12 x CH₂), 14.2 (2C, C-10, C-10'); HRMS (ESI-TOF) m/z [M + Na]⁺ calcd for C₂₇H₄₄NaO₅ 471.3081; found 471.3089; m/z [M + K]⁺ calcd for C₂₇H₄₄O₅K 487.2820; found 487.2824.

CHAPITRE 2 – TOTAL SYNTHESIS, ISOLATION, SURFACTANT PROPERTIES, AND BIOLOGICAL EVALUATION OF ANANATOSIDES AND RELATED MACRODILACTONE-CONTAINING RHAMNOLIPIDS

***para*-Methylphenyl 3,4-Di-*O*-benzyl-6-*O*-*tert*-butyldimethylsilyl-1-thio- β -D-glucopyranoside (18).**

TBSCl (866 mg, 5.54 mmol, 1.5 equiv) and DMAP (45 mg, 0.37 mmol, 0.1 equiv) were successively added to a solution of diol **17**¹⁹² (1.72 g, 3.69 mmol, 1.0 equiv) in anhydrous pyridine (5.6 mL). The mixture was stirred at rt under Ar for 3 h, then diluted in toluene (80 mL), washed with water (30 mL) and brine (30 mL). The organic layer was dried over MgSO₄, filtered, and evaporated under pressure. The residue was purified by silica gel flash chromatography (Hex/EtOAc 9:1) furnishing alcohol **18** (1994.6 mg, 93%) as a colorless oil: *R*_f 0.38 (Hex/EtOAc 8:2); [α]_D²⁰ -21 (*c* 1.4, CHCl₃); ¹H NMR (600 MHz, CDCl₃) δ (ppm) 7.47-7.45 (m, 2H, 2 \times CH-STol), 7.36-7.27 (m, 10H, 10 \times CH-Bn), 7.09-7.08 (m, 2H, 2 \times CH-STol), 4.89 (d, *J* = 11.1 Hz, 1H, CHH_{Bn}), 4.85-4.83 (m, 2H, CHH_{Bn}, CHH_{Bn}), 4.67 (d, *J* = 10.8 Hz, 1H, CHH_{Bn}), 4.40 (d, *J* = 9.6 Hz, 1H, H-1), 3.90 (dd, *J*_{6a-6b} = 11.4 Hz, *J*_{6a-5} = 1.8 Hz, 1H, H-6a), 3.87 (dd, *J*_{6b-6a} = 11.4 Hz, *J*_{6b-5} = 3.6 Hz, 1H, H-6b), 3.61 (t, *J* = 9.1 Hz, 1H, H-4), 3.58 (t, *J* = 8.6 Hz, 1H, H-3), 3.40 (t, *J* = 8.9 Hz, 1H, H-2), 3.34 (ddd, *J*₅₋₄ = 9.2 Hz, *J*_{5-6b} = 3.5 Hz, *J*_{5-6a} = 1.8 Hz, 1H, H-5), 2.37 (s, 1H, OH), 2.33 (s, 3H, CH₃STol), 0.92 (s, 9H, C(CH₃)₃TBS), 0.10 (s, 3H, CH₃TBS), 0.09 (s, 3H, CH₃TBS); ¹³C NMR (150 MHz, CDCl₃) δ (ppm) 138.6 (C-Ar), 138.50 (C-Ar), 138.48 (C-Ar), 133.8 (2C, 2 \times CH-STol), 129.8 (2C, 2 \times CH-STol), 128.6-127.6 (11C, 1 \times C-Ar, 10 \times CH-Bn), 88.1 (C-1), 86.1 (C-3), 80.5 (C-5), 77.1 (C-4), 75.5 (CH₂Bn), 75.2 (CH₂Bn), 72.5 (C-2), 62.2 (C-6), 26.1 (3C, C(CH₃)₃TBS), 21.3 (CH₃STol), 18.5 (C(CH₃)₃TBS), -5.0 (CH₃TBS), -5.2 (CH₃TBS); HRMS (ESI-TOF) *m/z* [M + NH₄]⁺ calcd for C₃₃H₄₈NO₅SSi 598.3017; found 598.3019; *m/z* [M + Na]⁺ calcd for C₃₃H₄₄NaO₅SSi 603.2571; found 603.2578.

***para*-Methylphenyl 3,4-Di-*O*-benzyl-6-*O*-*tert*-butyldimethylsilyl-2-*O*-levulinoyl-1-thio- β -D-glucopyranoside (11).**

Alcohol **18** (507 mg, 0.861 mmol, 1.0 equiv) was solubilized in anhydrous pyridine (5.6 mL) and DMAP (263 mg, 2.15 mmol, 2.5 equiv) was added to the solution. A solution of Lev₂O (1.42 g, 6.63 mmol, 7.7 equiv) in anhydrous pyridine (6.6 mL) was added dropwise to the mixture, which was then stirred at 50 °C for 1 h under an Ar atmosphere. The solvents were then evaporated under

CHAPITRE 2 – TOTAL SYNTHESIS, ISOLATION, SURFACTANT PROPERTIES, AND BIOLOGICAL EVALUATION OF ANANATOSIDES AND RELATED MACRODILACTONE-CONTAINING RHAMNOLIPIDS

reduced pressure and co-evaporated with toluene. The residue was purified by silica gel flash chromatography (Hex/EtOAc 9:1 to 8:2) to give fully protected **11** (567 mg, quant.) as a colorless oil: R_f 0.37 (Hex/EtOAc 7:3); $[\alpha]_D^{20} +54$ (c 0.9, CHCl_3); $^1\text{H NMR}$ (600 MHz, CDCl_3) δ (ppm) 7.40-7.39 (m, 2H, $2 \times \text{CH}_{\text{STol}}$), 7.34-7.25 (m, 10H, $10 \times \text{CH}_{\text{Bn}}$), 7.08-7.07 (m, 2H, $2 \times \text{CH}_{\text{STol}}$), 4.93-4.89 (m, 1H, H-2), 4.79 (d, $J = 11.3$ Hz, 1H, CHH_{Bn}), 4.78 (d, $J = 10.9$ Hz, 1H, CHH_{Bn}), 4.69 (d, $J = 11.3$ Hz, 1H, CHH_{Bn}), 4.67 (d, $J = 10.9$ Hz, 1H, CHH_{Bn}), 4.52 (d, $J = 10.0$ Hz, 1H, H-1), 3.88 (dd, $J_{6a-6b} = 11.4$ Hz, $J_{6a-5} = 1.6$ Hz, 1H, H-6a), 3.84 (dd, $J_{6b-6a} = 11.5$ Hz, $J_{6b-5} = 3.9$ Hz, 1H, H-6b), 3.69-3.65 (m, 2H, H-3, H-4), 3.34-3.31 (m, 1H, H-5), 2.73-2.71 (m, 2H, $\text{CH}_{2\text{Lev}}$), 2.57 (dt, $J_{\text{Ha-Hb}} = 17.2$ Hz, $J_{\text{Ha-CH}_2} = 6.6$ Hz, 1H, $\text{CH}^a\text{H}_{\text{Lev}}$), 2.48 (dt, $J_{\text{Hb-Ha}} = 17.2$ Hz, $J_{\text{Hb-CH}_2} = 7.0$ Hz, 1H, $\text{CHH}^b_{\text{Lev}}$), 2.32 (s, 3H, $\text{CH}_{3\text{STol}}$), 2.17 (s, 3H, $\text{CH}_{3\text{Lev}}$), 0.91 (s, 9H, $\text{C}(\text{CH}_3)_3\text{TBS}$), 0.10 (s, 3H, $\text{CH}_{3\text{TBS}}$), 0.07 (s, 3H, $\text{CH}_{3\text{TBS}}$); $^{13}\text{C NMR}$ (150 MHz, CDCl_3) δ (ppm) 206.4 (CO_{Lev}), 171.5 (COOR_{Lev}), 138.33 (C_{Ar}), 138.28 (C_{Ar}), 138.1 (C_{Ar}), 133.3-127.8 (15C, C_{Ar} , $14 \times \text{CH}_{\text{Ar}}$), 86.3 (C-1), 84.5 (C-3), 80.4 (C-5), 77.5 (C-4), 75.4 ($\text{CH}_{2\text{Bn}}$), 75.2 ($\text{CH}_{2\text{Bn}}$), 72.4 (C-2), 62.2 (C-6), 38.0 ($\text{CH}_{2\text{Lev}}$), 30.1 ($\text{CH}_{3\text{Lev}}$), 28.3 ($\text{CH}_{2\text{Lev}}$), 26.1 (3C, $\text{C}(\text{CH}_3)_3\text{TBS}$), 21.3 ($\text{CH}_{3\text{STol}}$), 18.5 ($\text{C}(\text{CH}_3)_3\text{TBS}$), -5.0 ($\text{CH}_{3\text{TBS}}$), -5.2 ($\text{CH}_{3\text{TBS}}$). HRMS (ESI-TOF) m/z $[\text{M} + \text{K}]^+$ calcd for $\text{C}_{38}\text{H}_{50}\text{KO}_7\text{SSi}$ 701.2939; found 701.2940; m/z $[\text{M} + \text{Na}]^+$ calcd for $\text{C}_{38}\text{H}_{50}\text{NaO}_7\text{SSi}$ 717.2678; found 717.2688.

Benzyl (R)-3-O-[(R)-(3'-O-Decyl)-3,4-di-O-benzyl-6-O-tert-butyltrimethylsilyl-2-O-levulinoyl- β -D-glucopyranosyl]decanoate (8).

Donor **11** (221 mg, 0.326 mmol, 1.2 equiv), acceptor **12** (122 mg, 0.272 mmol, 1.0 equiv), and NIS (98 mg, 0.44 mmol, 1.6 equiv) were dried under high vacuum for 1 h. Activated 4 Å MS (488 mg, 4 $\text{mg} \cdot \text{mg}^{-1}$ of acceptor **12**) and anhydrous DCE (5.4 mL) were added and the suspension was stirred under an Ar atmosphere for 1 h. The mixture was cooled to -10 °C and AgOTf (14 mg, 0.054 mmol, 0.2 equiv) was added while the reaction flask was protected from light with aluminum foil. The suspension was stirred from -10 to 0 °C for 30 min, quenched with Et_3N , and filtered over Celite. The solvents were evaporated under reduced pressure and the residue was purified by silica gel flash chromatography (Hex/EtOAc 95:5 to 9:1) to give glucolipid **8** (219 mg, 80%) as a yellowish oil: R_f 0.35 (Hex/EtOAc 8:2); $[\alpha]_D^{20} -3$ (c 0.5, CHCl_3); $^1\text{H NMR}$ (600 MHz, CDCl_3) δ (ppm) 7.37-7.28 (m,

CHAPITRE 2 – TOTAL SYNTHESIS, ISOLATION, SURFACTANT PROPERTIES, AND BIOLOGICAL EVALUATION OF ANANATOSIDES AND RELATED MACRODILACTONE-CONTAINING RHAMNOLIPIDS

15H, 15 x CH_{Bn}), 5.23-5.19 (m, 1H, H-3''), 5.10 (s, 2H, CH_2COOBn), 4.89 (dd, $J_{2-3} = 9.2$ Hz, $J_{2-1} = 8.2$ Hz, 1H, H-2), 4.80-4.78 (m, 2H, CHH_{Bn} , CHH_{Bn}), 4.70-4.67 (m, 2H, CHH_{Bn} , CHH_{Bn}), 4.41 (d, $J = 8.0$ Hz, 1H, H-1), 3.90-3.87 (m, 1H, H-3'), 3.85 (dd, $J_{6b-6a} = 11.5$ Hz, $J_{6b-5} = 3.5$ Hz, 1H, H-6b), 3.81 (dd, $J_{6a-6b} = 11.4$ Hz, $J_{6a-5} = 1.3$ Hz, 1H, H-6a), 3.70 (t, $J = 9.3$ Hz, 1H, H-4), 3.63 (t, $J = 9.3$ Hz, 1H, H-3), 3.28-3.26 (m, 1H, H-5), 2.89 (dd, $J_{2a'-2b'} = 15.4$ Hz, $J_{2a'-3'} = 4.1$ Hz, 1H, H-2a'), 2.71 (dt, $J_{Ha-Hb} = 18.1$ Hz, $J_{Ha-CH_2} = 7.1$ Hz, 1H, CHH_{Lev}), 2.66-2.59 (m, 2H, H-2a''), CHH_{Lev}), 2.56-2.51 (m, 1H, H-2b''), 2.51-2.44 (m, 2H, CH_{2Lev}), 2.42-2.37 (m, 1H, H-2b'), 2.15 (s, 3H, CH_{3Lev}), 0.89-0.85 (m, 15H, $C(CH_3)_3TBS$, H-10', H-10''), 0.05 (s, 3H, CH_{3TBS}), 0.03 (s, 3H, CH_{3TBS}); ^{13}C NMR (150 MHz, $CDCl_3$) δ (ppm) 206.2 (CO_{Lev}), 171.5, 170.8, 170.2 (3C, $COOR_{Lev}$, C-1', C-1''), 138.5 (C_{Bn}), 138.4 (C_{Bn}), 135.8 (C_{Bn}), 128.7-127.8 (15C, 15 x CH_{Bn}), 101.8 (C-1), 82.9 (C-3), 77.8, 77.6 (2C, C-4, C-3'), 76.0 (C-5), 75.22 (CH_{2Bn}), 75.16 (CH_{2Bn}), 74.0 (C-2), 70.7 (C-3''), 66.6 (CH_2COOBn), 62.1 (C-6), 41.4 (C-2'), 39.3 (C-2''), 38.0 (CH_{2Lev}), 34.8-22.8 (13C, CH_{3Lev} , 12 x CH_2), 28.1 (CH_{2Lev}), 26.1 (3C, $C(CH_3)_3TBS$), 18.5 ($C(CH_3)_3TBS$), 14.2 (2C, C-10', C-10''), -4.9 (CH_{3TBS}), -5.3 (CH_{3TBS}); HRMS (ESI-TOF) m/z [$M + NH_4$] $^+$ calcd for $C_{58}H_{90}NO_{12}Si$ 1020.6227; found 1020.6229; m/z [$M + Na$] $^+$ calcd for $C_{58}H_{86}NaO_{12}Si$ 1025.5781; found 1025.5783.

Benzyl (R)-3-O-[(R)-(3'-O-Decyl)-3,4-di-O-benzyl-2-O-levulinoyl- β -D-glucopyranosyl]decanoate (**20**).

To a solution of glucolipid **8** (172 mg, 0.172 mmol, 1.0 equiv) in DCM (0.4 mL) was added a TFA/H₂O solution (10:1 v/v, 0.09 mL). The reaction mixture was stirred at rt for 40 min and then quenched by adding saturated aqueous NaHCO₃. The organic layer was dried over MgSO₄, filtered, and the solvents were evaporated under reduced pressure. The residue was purified by silica gel flash chromatography (Hex/EtOAc 9:1 to 8:2) to give alcohol **20** (129 mg, 84%) as a white amorphous solid: R_f 0.28 (Hex/EtOAc 7:3); $[\alpha]_D^{20} -12$ (c 1.1, $CHCl_3$); 1H NMR (600 MHz, $CDCl_3$) δ (ppm) 7.37-7.25 (m, 15H, 15 x CH_{Bn}), 5.24-5.18 (m, 1H, H-3''), 5.13 (s, 2H, CH_2COOBn), 4.91 (dd, $J_{2-3} = 9.5$ Hz, $J_{2-1} = 8.1$ Hz, 1H, H-2), 4.77 (d, $J = 11.3$ Hz, 1H, CHH_{Bn}), 4.75 (d, $J = 10.8$ Hz, 1H, CHH_{Bn}), 4.69 (d, $J = 11.4$ Hz, 1H, CHH_{Bn}), 4.54 (d, $J = 10.9$ Hz, 1H, CHH_{Bn}), 4.41 (d, $J = 8.0$ Hz, 1H, H-1), 3.99-3.95 (m, 1H, H-3'), 3.84 (dd, $J_{6a-6b} = 11.5$ Hz, $J_{6a-5} = 3.5$ Hz, 1H, H-6a), 3.67-3.62

CHAPITRE 2 – TOTAL SYNTHESIS, ISOLATION, SURFACTANT PROPERTIES, AND BIOLOGICAL EVALUATION OF ANANATOSIDES AND RELATED MACRODILACTONE-CONTAINING RHAMNOLIPIDS

(m, 2H, H-3, H-6b), 3.50 (t, $J = 9.3$ Hz, 1H, H-4), 3.40-3.37 (m, 1H, H-5), 2.94 (br s, 1H, OH), 2.72-2.56 (m, 5H, CH_{2Lev} , H-2a'', H-2b'', H-2a'), 2.49-2.46 (m, 2H, CH_{2Lev}), 2.36 (dd, $J_{2b'-2a'} = 15.3$ Hz, $J_{2b'-3'} = 5.0$ Hz, 1H, H-2b'), 2.15 (s, 3H, CH_{3Lev}), 1.62-1.24 (m, 24H, $12 \times CH_2$), 0.89-0.86 (m, 6H, $2 \times CH_3$); ^{13}C NMR (150 MHz, $CDCl_3$) δ (ppm) 206.1 (CO_{Lev}), 171.5, 171.4, 170.4 (3C, $COOR_{Lev}$, C-1', C-1''), 138.4 (C_{Bn}), 137.9 (C_{Bn}), 135.9 (C_{Bn}), 128.7-127.8 (15C, $15 \times CH_{Bn}$), 101.1 (C-1), 83.0 (C-3), 78.4 (C-4), 77.8 (C-3'), 75.7 (C-5), 75.2 (2C, $2 \times CH_{2Bn}$), 73.9 (C-2), 71.1 (C-3''), 66.7 (CH_2COOBn), 62.3 (C-6), 41.4 (C-2'), 39.1 (C-2''), 37.0 (CH_{2Lev}), 35.6-22.8 (13C, $12 \times CH_2$, CH_{3Lev}), 28.0 (CH_{2Lev}), 14.2 (2C, $2 \times CH_3$); HRMS (ESI-TOF) m/z $[M + NH_4]^+$ calcd for $C_{52}H_{76}NO_{12}$ 906.5362; found 906.5365; m/z $[M + Na]^+$ calcd for $C_{52}H_{72}NaO_{12}$ 911.4916; found 911.4929.

Benzyl (R)-3-O-[(R)-(3'-O-Decyl)-3,4-di-O-benzyl- β -D-glucopyranosyl]decanoate (21).

Hydrazine monohydrate (32 μ L, 5.0 equiv) and HOAc (0.55 mL) were successively added to a solution of alcohol **20** (117 mg, 0.131 mmol, 1.0 equiv) in anhydrous pyridine (0.85 mL) at 0 °C. The mixture was stirred at rt for 16 h under an Ar atmosphere, then co-evaporated with toluene. The residue was purified by silica gel flash chromatography (Tol/EtOAc 95:5 to 9:1) to give diol **21** (91 mg, 87%) as a white amorphous solid: R_f 0.54 (Tol/EtOAc 8:2); $[\alpha]_D^{20} -9$ (c 0.6, $CHCl_3$); 1H NMR (600 MHz, $CDCl_3$) δ (ppm) 7.37-7.27 (m, 15H, $15 \times CH_{Bn}$), 5.25-5.20 (m, 1H, H-3''), 5.12 (d, $J = 4.7$ Hz, 2H, CH_2COOBn), 4.93 (d, $J = 11.2$ Hz, 1H, CHH_{Bn}), 4.83 (d, $J = 11.1$ Hz, 1H, CHH_{Bn}), 4.81 (d, $J = 10.7$ Hz, 1H, CHH_{Bn}), 4.56 (d, $J = 10.9$ Hz, 1H, CHH_{Bn}), 4.32 (d, $J = 7.8$ Hz, 1H, H-1), 4.08-4.04 (m, 1H, H-3'), 3.84 (dd, $J_{6a-6b} = 11.8$ Hz, $J_{6a-5} = 2.0$ Hz, 1H, H-6a), 3.63 (dd, $J_{6b-6a} = 11.9$ Hz, 1H, H-6b), 3.59 (t, $J = 8.9$ Hz, 1H, H-3), 3.47-3.42 (m, 2H, H-2, H-4), 3.40-3.37 (m, 1H, H-5), 2.67 (dd, $J_{2a''-2b''} = 15.5$ Hz, $J_{2a''-3''} = 7.0$ Hz, 1H, H-2a''), 2.61-2.56 (m, 2H, H-2b'', H-2a'), 2.43 (dd, $J_{2b'-2a'} = 15.1$ Hz, $J_{2b'-3'} = 4.9$ Hz, 1H, H-2b'), 1.56-1.24 (m, 24H, $12 \times CH_2$), 0.89-0.86 (m, 6H, $2 \times CH_3$); ^{13}C NMR (150 MHz, $CDCl_3$) δ (ppm) 171.4, 170.4 (2C, C-1', C-1''), 138.8 (C_{Bn}), 138.1 (C_{Bn}), 135.8 (C_{Bn}), 128.7-127.8 (15C, $15 \times CH_{Bn}$), 102.3 (C-1), 84.6 (C-3), 78.0 (C-4), 75.7 (C-3'), 75.3 (C-5), 75.2, 75.1 (3C, C-2, $2 \times CH_{2Bn}$), 71.1 (C-3''), 66.7 (CH_3COOBn), 62.4 (C-6), 41.3 (C-2'), 39.2 (C-2''), 35.3-22.8 (12C, $12 \times CH_2$), 14.2 (2C, $2 \times CH_3$); HRMS (ESI-TOF) m/z $[M + NH_4]^+$ calcd

CHAPITRE 2 – TOTAL SYNTHESIS, ISOLATION, SURFACTANT PROPERTIES, AND BIOLOGICAL EVALUATION OF ANANATOSIDES AND RELATED MACRODILACTONE-CONTAINING RHAMNOLIPIDS

for C₄₇H₇₀NO₁₀ 808.4994; found 808.4967; *m/z* [M + Na]⁺ calcd for C₄₇H₆₆NaO₁₀ 813.4548; found 813.4532.

Synthetic Ananatoside B (2).

Pd black (78 mg, 1 mg•mg⁻¹ of diol **21**) was added to a solution of diol **21** (78 mg, 0.099 mmol, 1.0 equiv) in DCE (1 mL) and MeOH (2 mL). The mixture was stirred under an H₂ atmosphere at 40 °C for 16 h, after which it was filtered over Celite and the solvents were evaporated under reduced pressure. The residue was purified by silica gel flash chromatography (DCM/MeOH 95:5 to 8:2) to give synthetic ananatoside B (**2**, 46 mg, 90%) as a white foam. *R_f* 0.50 (DCM/MeOH 8:2); [α]²⁰_D +103 (*c* 0.2, CHCl₃). Physical and analytical data of synthetic ananatoside B (**2**) agreed with those of the isolated compound. Analytical HPLC analysis was performed using method D (23.3 min.).

***para*-Methylphenyl 2-*O*-*ortho*-(Azidomethyl)benzoyl-3,4-*di-O*-benzyl-6-*O*-*tert*-butyldimethylsilyl-1-thio-β-D-glucopyranoside (19).**

To a solution of alcohol **18** (889 mg, 1.53 mmol, 1.0 equiv) in anhydrous DCM (15.3 mL) were added DMAP (187 mg, 1.53 mmol, 1.0 equiv), DCC (632 mg, 3.06 mmol, 2.0 equiv), and AZMBOH (407 mg, 2.30 mmol, 1.5 equiv). The mixture was refluxed for 4 h, after which the suspension was cooled at 0 °C and filtered over Celite. The solvents were evaporated under reduced pressure and the residue was purified by silica gel flash chromatography (Hex/EtOAc 95:5) to give fully protected **19** (1.14 g, quant.) as a colorless oil: *R_f* 0.46 (Hex/EtOAc 8:2); [α]²⁰_D +5 (*c* 0.8, CHCl₃); ¹H NMR (600 MHz, CDCl₃) δ (ppm) 7.94-7.92 (m, 1H, CH-AZMB), 7.59-7.57 (m, 1H, CH-AZMB), 7.54-7.53 (m, 1H, CH-Ar), 7.40-7.28 (m, 8H, 8 × CH-Ar), 7.13-7.11 (m, 5H, 5 × CH-Ar), 7.07-7.05 (m, 2H, 2 × CH-Ar), 5.16 (dd, *J* = 9.8 Hz, *J* = 9.0 Hz, 1H, H-2), 4.84-4.77 (m, 3H, CHH_{AZMB}, CH_{2Bn}), 4.72-4.66 (m, 3H, H-1, CHH_{AZMB}, CHH_{Bn}), 4.60 (d, *J* = 11.2 Hz, 1H, CHH_{Bn}), 3.93 (dd, *J*_{6a-6b} = 11.4 Hz, *J*_{6a-5} = 1.7 Hz, H-6a), 3.89 (dd, *J*_{6b-6a} = 11.4 Hz, *J*_{6b-5} = 3.8 Hz, 1H, H-6b), 3.81-3.76 (m, 2H, H-3, H-4), 3.41 (ddd, *J*₅₋₄ = 9.3 Hz, *J*_{5-6b} = 3.5 Hz, *J*_{5-6a} = 1.6 Hz, 1H, H-5), 2.32 (s, 3H, CH_{3STol}), 0.83 (s, 9H, C(CH₃)₃TBS), 0.13 (s, 3H, CH₃TBS), 0.10 (s, 3H, CH₃TBS); ¹³C NMR (150 MHz, CDCl₃) δ (ppm) 165.2 (COOR_{AZMB}), 138.29 (C-Ar), 138.25 (C-Ar), 138.0 (C-Ar), 137.9 (C-Ar), 133.5-127.8

CHAPITRE 2 – TOTAL SYNTHESIS, ISOLATION, SURFACTANT PROPERTIES, AND BIOLOGICAL EVALUATION OF ANANATOSIDES AND RELATED MACRODILACTONE-CONTAINING RHAMNOLIPIDS

(20C, 2 × C-Ar, 18 × CH-Ar), 86.3 (C-1), 84.5 (C-3), 80.6 (C-5), 77.7 (C-4), 75.5 (CH_{2Bn}), 75.2 (CH_{2Bn}), 72.5 (C-2), 62.2 (C-6), 53.0 (CH_{2AZMB}), 26.1 (3C, C(CH₃)₃TBS), 21.3 (CH₃STol), 18.5 (C(CH₃)₃TBS), -4.93 (CH₃TBS), -5.21 (CH₃TBS); HRMS (ESI-TOF) *m/z* [M + Na]⁺ calcd for C₄₁H₄₉NaN₃O₆SSi 762.3004; found 762.3001; *m/z* [M + K]⁺ calcd for C₄₁H₄₉N₃O₆KSSi 778.2743; found 778.2779.

***para*-Methylphenyl 2-*O*-*ortho*-(Azidomethyl)benzoyl-3,4-di-*O*-benzyl-1-thio-β-D-glucopyranoside (9).**

AcCl (1.5 μL, 0.021 mmol, 0.30 equiv) was added to a solution of derivative **19** (52 mg, 0.071 mmol, 1.0 equiv) in anhydrous MeOH (1.42 mL) and anhydrous DCM (0.5 mL) at 0 °C. The mixture was slowly heated to rt over 3.5 h under Ar, then diluted in DCM (2 mL) and washed with saturated aqueous NaHCO₃ (5 mL) and brine (5 mL). The organic layers were dried over MgSO₄, filtered, and evaporated under reduced pressure. The residue was purified by silica gel flash chromatography (Hex/EtOAc 8:2 to 7:3) to give alcohol **9** (35.4 mg, 80%) as a white amorphous solid: *R_f* 0.26 (Hex/EtOAc 7:3); [α]²⁰_D +26 (*c* 0.5, CHCl₃); ¹H NMR (600 MHz, CDCl₃) δ (ppm) 7.93-7.92 (m, 1H, CH-AZMB), 7.59-7.58 (m, 1H, CH-AZMB), 7.55-7.54 (m, 1H, CH-Ar), 7.40-7.37 (m, 1H, CH-Ar), 7.35-7.28 (m, 7H, 7 × CH-Ar), 7.15-7.12 (m, 5H, 5 × CH-Ar), 7.11-7.09 (m, 2H, 2 × CH-Ar), 5.20 (t, *J* = 9.6 Hz, 1H, H-2), 4.85-4.81 (m, 2H, CHH_{Bn}, CHH_{AZMB}), 4.78 (d, *J* = 9.6 Hz, 1H, CHH_{Bn}), 4.75 (d, *J* = 10.0 Hz, 1H, H-1), 4.70 (d, *J* = 14.9 Hz, 1H, CHH_{AZMB}), 4.66 (d, *J* = 11.0 Hz, 1H, CHH_{Bn}), 4.63 (d, *J* = 11.2 Hz, 1H, CHH_{Bn}), 3.92 (ddd, *J*_{6a-6b} = 11.9 Hz, *J* = 2.7 Hz, *J* = 2.3 Hz, 1H, H-6a), 3.83 (t, *J* = 9.1 Hz, 1H, H-3), 3.75-3.71 (m, 1H, H-6b), 3.68 (t, *J* = 9.4 Hz, 1H, H-4), 3.48 (ddd, *J*₅₋₄ = 9.7 Hz, *J*_{5-6a} = 4.6 Hz, *J*_{5-6b} = 2.6 Hz, 1H, H-5), 2.33 (s, 3H, CH₃STol), 1.91 (t, *J* = 6.5 Hz, 1H, OH); ¹³C NMR (150 MHz, CDCl₃) δ (ppm) 165.2 (COOR_{AZMB}), 138.7 (C-Ar), 138.0 (C-Ar), 137.8 (2C, 2 × C-Ar), 133.4-127.9 (20C, 2 × C-Ar, 18 × CH-Ar), 86.3 (C-1), 84.2 (C-3), 79.7 (C-5), 77.72 (C-4), 75.4 (CH_{2Bn}), 75.3 (CH_{2Bn}), 72.5 (C-2), 62.1 (C-6), 53.0 (CH_{2AZMB}), 21.3 (CH₃STol); HRMS (ESI-TOF) *m/z* [M + NH₄]⁺ calcd for C₃₅H₃₉N₄O₆S 643.2585; found 643.2592; *m/z* [M + Na]⁺ calcd for C₃₅H₃₅NaN₃O₆S 648.2139; found 648.2146.

CHAPITRE 2 – TOTAL SYNTHESIS, ISOLATION, SURFACTANT PROPERTIES, AND BIOLOGICAL EVALUATION OF ANANATOSIDES AND RELATED MACRODILACTONE-CONTAINING RHAMNOLIPIDS

***para*-Methylphenyl 2-*O*-*ortho*-(Azidomethyl)benzoyl-3,4-di-*O*-benzyl-6-*O*-(*R*)-3-(((*R*)-3-(((*tert*-butyldimethylsilyl)oxy)decanoyl)oxy)decanoyl-1-thio- β -D-glucopyranoside (7).**

To a solution of alcohol **9** (115 mg, 0.184 mmol, 1.0 equiv) and dilipid **10** (104 mg, 0.221 mmol, 1.2 equiv) in anhydrous DCE (2.2 mL) were successively added DMAP (7 mg, 0.06 mmol, 0.3 equiv) and EDC (106 mg, 0.551 mmol, 3.0 equiv). The mixture was stirred at rt for 16 h under Ar atmosphere. The solution was then evaporated under reduced pressure and the residue was purified by silica gel flash chromatography (Hex/EtOAc 95:5 to 90:10) to give compound **7** (188 mg, 95%) as a colorless oil: R_f 0.5 (Hex/EtOAc 8:2); $[\alpha]_D^{20} +8$ (c 0.4, CHCl₃); ¹H NMR (600 MHz, CDCl₃) δ (ppm) 7.94-7.93 (m, 1H, CH_{AZMB}), 7.60-7.58 (m, 1H, CH_{AZMB}), 7.55-7.54 (m, 1H, CH_{AZMB}), 7.41-7.38 (m, 1H, CH_{AZMB}), 7.35-7.27 (m, 7H, 5 \times CH_{Bn}, 2 \times CH_{STol}), 7.15-7.12 (m, 5H 5 \times CH_{Bn}), 7.09-7.08 (m, 2H, 2 \times CH_{STol}), 5.24-5.20 (m, 1H, H-3''), 5.19 (t, J = 9.4 Hz, 1H, H-2), 4.84-4.81 (m, 2H, CHH_{AZMB}, CHH_{Bn}), 4.76 (d, J = 11.1 Hz, 1H, CHH_{Bn}), 4.70-4.68 (m, 2H, H-1, CHH_{AZMB}), 4.62 (d, J = 11.4 Hz, CHH_{Bn}), 4.60 (d, J = 11.3 Hz, 1H, CHH_{Bn}), 4.47 (d, J = 11.6 Hz, 1H, H-6a), 4.23-4.21 (m, 1H, H-6b), 4.08 (p, J = 6.1 Hz, 1H, H-3'), 3.83-3.80 (m, 1H, H-3), 3.63-3.59 (m, 2H, H-4, H-5), 2.66 (dd, $J_{2a''-2b''}$ = 15.7 Hz, $J_{2a''-3''}$ = 7.0 Hz, 1H, H-2a''), 2.52 (dd, $J_{2b''-2a''}$ = 15.7 Hz, $J_{2b''-3''}$ = 6.0 Hz, 1H, H-2b''), 2.45 (dd, $J_{2a'-2b'}$ = 14.8 Hz, $J_{2a'-3'}$ = 5.9 Hz, 1H, H-2a'), 2.41 (dd, $J_{2b'-2a'}$ = 14.9 Hz, $J_{2b'-3'}$ = 6.7 Hz, 1H, H-2b'), 2.33 (s, 3H, CH_{3STol}), 1.64-1.22 (m, 24H, 24 \times CH₂), 0.88-0.85 (m, 15H, C(CH₃)_{3TBS}, 2 \times CH₃), 0.06 (s, 3H, CH_{3TBS}), 0.05 (s, 3H, CH_{3TBS}); ¹³C NMR (150 MHz, CDCl₃) δ (ppm) 171.1, 170.1 (2C, C-1', C-1''), 165.1 (COOR_{AZMB}), 138.5-128.0 (24C, 6 \times C_{Ar}, 18 \times CH_{Ar}), 86.2 (C-1), 84.5 (C-3), 77.8, 77.2 (2C, C-4, C-5), 75.5 (CH_{2Bn}), 75.3 (CH_{2Bn}), 72.3 (C-2), 70.5 (C-3''), 69.4 (C-3'), 63.2 (C-6), 53.0 (CH_{2AZMB}), 42.9 (C-2'), 39.0 (C-2''), 37.5-22.8 (15C, 12 \times CH₂, C(CH₃)_{3TBS}), 21.3 (CH_{3STol}), 18.2 (C(CH₃)_{3TBS}), 14.25 (CH₃), 14.23 (CH₃), -4.42 (CH_{3TBS}), -4.45 (CH_{3TBS}); HRMS (ESI-TOF) m/z [M + NH₄]⁺ calcd for C₆₁H₈₉N₄O₁₀SSi 1097.6063; found 1097.6038; m/z [M + Na]⁺ calcd for C₆₁H₈₅NaN₃O₁₀SSi 1102.5616; found 1102.5600.

CHAPITRE 2 – TOTAL SYNTHESIS, ISOLATION, SURFACTANT PROPERTIES, AND BIOLOGICAL EVALUATION OF ANANATOSIDES AND RELATED MACRODILACTONE-CONTAINING RHAMNOLIPIDS

***para*-Methylphenyl 2-*O*-*ortho*-(Azidomethyl)benzoyl-3,4-di-*O*-benzyl-6-*O*-(*R*)-3-(((*R*)-3-(hydroxydecanoyl)oxy)decanoyl-1-thio- β -D-glucopyranoside (22).**

A solution of compound **7** (450 mg, 0.416 mmol, 1.0 equiv) in DCM (0.9 mL) was added dropwise to TFA (1.8 mL) over a one-minute period. The mixture was stirred for one additional minute and quenched with saturated aqueous NaHCO₃. The organic layer was dried over MgSO₄, filtered, and the solvents were evaporated under reduced pressure. The residue was purified by silica gel flash chromatography (Hex/EtOAc 9:1 to 8:2) to give alcohol **22** (338 mg, 84%) as a white amorphous solid: *R*_f 0.37 (Hex/EtOAc 7:3); [α]_D²⁰ +9 (*c* 0.4, CHCl₃); ¹H NMR (600 MHz, CDCl₃) δ (ppm) 7.94-7.93 (m, 1H, 1 CH_{AZMB}), 7.60-7.58 (m, 1H, CH_{AZMB}), 7.55-7.54 (m, 1H, CH_{AZMB}), 7.40-7.38 (m, 1H, CH_{AZMB}), 7.35-7.26 (m, 7H, 5 \times CH_{Bn}, 2 \times CH_{STol}), 7.15-7.11 (m, 5H, 5 \times CH_{Bn}), 7.09-7.08 (m, 2H, 2 \times CH_{STol}), 5.31-5.27 (m, 1H, H-3''), 5.19 (t, *J* = 9.6 Hz, 1H, H-2), 4.84-4.81 (m, 2H, CHH_{AZMB}, CHH_{Bn}), 4.76 (d, *J* = 11.1 Hz, 1H, CHH_{Bn}), 4.71 (d, *J* = 8.4 Hz, 1H, H-1), 4.69 (d, *J* = 13.1 Hz, 1H, CHH_{AZMB}), 4.62 (d, *J* = 9.2 Hz, 1H, CHH_{Bn}), 4.60 (d, *J* = 8.9 Hz, 1H, CHH_{Bn}), 4.47 (d, *J*_{6a-6b} = 11.5 Hz, 1H, H-6a), 4.21 (dd, *J*_{6b-6a} = 11.7 Hz, *J*_{6b-5} = 4.1 Hz, 1H, H-6b), 3.97 (br s, 1H, H-3'), 3.84-3.81 (m, 1H, H-3), 3.64-3.61 (m, 2H, H-4, H-5), 2.93 (s, 1H, OH), 2.62 (dd, *J*_{2a''-2b''} = 15.5 Hz, *J*_{2a''-3''} = 8.1 Hz, 1H, H-2a''), 2.55 (dd, *J*_{2b''-2a''} = 15.6 Hz, *J*_{2b''-3''} = 4.6 Hz, 1H, H-2b''), 2.45 (dd, *J*_{2a'-2b'} = 15.8 Hz, *J*_{2a'-3'} = 3.0 Hz, 1H, H-2a'), 2.37 (dd, *J*_{2b'-2a'} = 15.8 Hz, *J*_{2b'-3'} = 9.2 Hz, 1H, H-2b'), 2.33 (s, 3H, CH_{3STol}), 1.67-1.22 (m, 24H, 12 \times CH₂), 0.88-0.86 (m, 6H, 2 \times CH₃); ¹³C NMR (150 MHz, CDCl₃) δ (ppm) 172.6, 170.4 (2C, C-1', C-1''), 165.1 (COOR_{AZMB}), 138.6-128.0 (24C, 6 \times C_{Ar}, 18 \times CH_{Ar}), 86.2 (C-1), 84.5 (C-3), 77.4 (2C, C-4, C-5), 75.6 (CH_{2Bn}), 75.3 (CH_{2Bn}), 72.3 (C-2), 70.8 (C-3''), 68.5 (C-3'), 63.3 (C-6), 53.0 (CH_{2AZMB}), 42.0 (C-2'), 39.1 (C-2''), 36.8-22.8 (12C, 12 \times CH₂), 21.3 (CH_{3STol}), 14.2 (2C, 2 \times CH₃); HRMS (ESI-TOF) *m/z* [M + NH₄]⁺ calcd for C₅₅H₇₅N₄O₁₀S 983.5198; found 983.5237; *m/z* [M + Na]⁺ calcd for C₅₅H₇₁NaN₃O₁₀S 988.4752; found 988.4781.

CHAPITRE 2 – TOTAL SYNTHESIS, ISOLATION, SURFACTANT PROPERTIES, AND BIOLOGICAL EVALUATION OF ANANATOSIDES AND RELATED MACRODILACTONE-CONTAINING RHAMNOLIPIDS

Macrolide 23.

Compound **22** (71 mg, 0.073 mmol, 1.0 equiv) and NIS (28 mg, 0.12 mmol, 1.6 equiv) were dried together under high vacuum for 1 h. Activated 4 Å MS (300 mg, 4 mg•mg⁻¹ of substrate) and anhydrous DCE (7.8 mL) were subsequently added to the reaction flask and the mixture was stirred at rt for 1 h under an Ar atmosphere, after which TMSOTf (3 µL, 0.003 mmol, 0.2 equiv) was added at 0 °C. The reaction was stirred for an additional 30 min at 0 °C, then quenched with Et₃N. The suspension was filtered over Celite and the solvents were evaporated under reduce pressure. The residue was purified by silica gel flash chromatography (Hex/EtOAc 95:5 to 9:1) to give macrolactone **23** (54 mg, 86%) as a white amorphous solid: *R_f* 0.43 (Hex/EtOAc 8:2); $[\alpha]_D^{20} +21$ (*c* 0.2, CHCl₃); ¹H NMR (600 MHz, CDCl₃) δ (ppm) 7.96-7.95 (m, 1H, CH_{AZMB}), 7.59-7.54 (m, 2H, 2 × CH_{Ar}), 7.39-7.27 (m, 6H, 6 × CH_{Ar}), 7.12-7.10 (m, 5H, 5 × CH_{Ar}), 5.55-5.50 (m, 1H, H-3''), 5.16 (dd, *J*₂₋₃ = 9.6 Hz, *J*₂₋₁ = 8.4 Hz, 1H, H-2), 4.87 (d, *J* = 11.2 Hz, 1H, CHH_{Bn}), 4.81 (d, *J* = 15.2 Hz, 1H, CHH_{AZMB}), 4.77-4.73 (m, 3H, H-1, CHH_{Bn}, CHH_{AZMB}), 4.62-4.56 (m, 2H, CHH_{Bn}, CHH_{Bn}), 4.34 (t, *J* = 10.8 Hz, 1H, H-6a), 4.14 (td, *J* = 9.4 Hz, *J* = 3.6 Hz, 1H, H-3'), 4.08 (dd, *J*_{6b-6a} = 11.3 Hz, *J*_{6b-5} = 1.7 Hz, 1H, H-6b), 3.80 (t, *J* = 9.2 Hz, 1H, H-3), 3.60 (td, *J*₅₋₄ = 10.0 Hz, *J*_{5-6b} = 1.7 Hz, 1H, H-5), 3.38 (t, *J* = 9.6 Hz, 1H, H-4), 2.67 (dd, *J*_{2a'-2b'} = 18.5 Hz, *J*_{2a'-3'} = 8.7 Hz, 1H, H-2a'), 2.60-2.56 (m, 2H, H-2''), 2.30 (d, *J*_{2b'-2a'} = 18.4 Hz, 1H, H-2b'), 1.53-0.94 (m, 24H, 12 × CH₂), 0.87 (t, *J* = 7.0 Hz, 3H, CH₃), 0.77 (t, *J* = 7.3 Hz, 3H, CH₃); ¹³C NMR (150 MHz, CDCl₃) δ (ppm) 171.6, 169.6 (C-1', C-1''), 164.9 (COOR_{AZMB}), 138.5 (C_{Ar}), 137.7 (C_{Ar}), 137.6 (C_{Ar}), 133.1-127.9 (15C, C_{Ar}, 14 × CH_{Ar}), 101.8 (C-1), 82.8 (C-3), 79.0 (C-4), 77.9 (C-3'), 75.3 (CH_{2Bn}), 75.1 (CH_{2Bn}), 73.8 (C-2), 72.6 (C-5), 69.7 (C-3''), 63.9 (C-6), 53.2 (CH_{2AZMB}), 41.7 (C-2'), 40.5 (C-2''), 36.5-22.7 (12C, 12 × CH₂), 14.2, 14.1 (2C, C-10', C-10''); HRMS (ESI-TOF) *m/z* [M + NH₄]⁺ calcd for C₄₈H₆₇N₄O₁₀ 859.4852; found 859.4877; *m/z* [M + Na]⁺ calcd for C₄₈H₆₃NaN₃O₁₀ 864.4406; found 864.4434.

CHAPITRE 2 – TOTAL SYNTHESIS, ISOLATION, SURFACTANT PROPERTIES, AND BIOLOGICAL EVALUATION OF ANANATOSIDES AND RELATED MACRODILACTONE-CONTAINING RHAMNOLIPIDS

(R)-3-O-[(R)-(3'-O-Decyl)-3,4-di-O-benzyl-2-O-levulinoyl- β -D-glucopyranosyl] Decanoic acid (25).

Glucolipid **20** (153 mg, 0.172 mmol, 1.0 equiv) was solubilized in absolute EtOH (3.4 mL) and one drop of anhydrous DCM was added. To this solution were added 1,4-cyclohexadiene (0.14 mL, 1.7 mmol, 10 equiv) and Pd black (153 mg, 1 mg•mg⁻¹ of glucolipid **20**), and the mixture was stirred at rt for 4 h under an Ar atmosphere. The mixture was filtered over Celite and the solvents were evaporated under reduced pressure. The residue was purified by silica gel flash chromatography (DCM/MeOH 98:2 to 9:1) to give acid **25** (112 mg, 81%) as a white amorphous solid: *R_f* 0.36 (DCM/MeOH 95:5); [α]_D²⁰ -16 (*c* 0.6, CHCl₃); ¹H NMR (600 MHz, CDCl₃) δ (ppm) 7.34-7.26 (m, 10H, 10 \times CH_{Bn}), 5.25-5.21 (m, 1H, H-3''), 4.96 (t, *J* = 8.5 Hz, 1H, H-2), 4.79 (d, *J* = 11.0 Hz, 1H, CHH_{Bn}), 4.78 (d, *J* = 11.4 Hz, 1H, CHH_{Bn}), 4.69 (d, *J* = 11.5 Hz, 1H, CHH_{Bn}), 4.63 (d, *J* = 10.9 Hz, 1H, CHH_{Bn}), 4.42 (d, *J* = 7.9 Hz, 1H, H-1), 4.04-4.00 (m, 1H, H-3'), 3.89 (dd, *J*_{6a-6b} = 12.1 Hz, *J*_{6a-5} = 1.9 Hz, 1H, H-6a), 3.71 (dd, *J*_{6b-6a} = 11.8 Hz, *J*_{6b-5} = 5.1 Hz, 1H, H-6b), 3.68-3.63 (m, 2H, H-3, H-4), 3.40-3.36 (m, 1H, H-5), 2.72-2.61 (m, 2H, CH_{2Lev}), 2.59-2.49 (m, 3H, H-2a', H-2a'', H-2b''), 2.48-2.46 (m, 2H, CH_{2Lev}), 2.41 (dd, 1H, *J*_{2b'-2a'} = 15.3 Hz, *J*_{2b'-3'} = 4.3 Hz, 1H, H-2b'), 2.15 (s, 3H, CH_{3Lev}), 1.62-1.21 (m, 24H, 12 \times CH₂), 0.89-0.86 (m, 6H, 2 \times CH₃); ¹³C NMR (150 MHz, CDCl₃) δ (ppm) 206.2 (CO_{Lev}), 172.1, 171.8 (3C, COOR_{Lev}, C-1', C-1''), 138.3 (C_{Bn}), 138.0 (C_{Bn}), 128.6-127.9 (10C, 10 \times CH_{Bn}), 100.2 (C-1), 82.8 (C-3), 78.0 (C-4), 77.7 (C-3'), 75.6 (C-5), 75.2 (CH_{2Bn}), 75.1 (CH_{2Bn}), 73.9 (C-2), 71.7 (C-3''), 61.8 (C-6), 41.0 (2C, C-2' C-2''), 37.9 (CH_{2Lev}), 35.2-22.8 (14C, CH_{2Lev}, CH_{3Lev}, 12 \times CH₂), 14.2 (2C, 2 \times CH₃); HRMS (ESI-TOF) *m/z* [M + NH₄]⁺ calcd for C₄₅H₇₀NO₁₂ 816.4893; found 816.4907; *m/z* [M + Na]⁺ calcd for C₄₅H₆₆NaO₁₂ 821.4447; found 821.4468.

Macrolide 26.

A mixture of DCC (39 mg, 0.19 mmol, 10 equiv), DMAP (234 mg, 1.92 mmol, 102 equiv), and PPTS (47 mg, 0.19 mmol, 10 equiv) in anhydrous DCE (10.7 mL) was stirred under reflux. To the mixture was added dropwise a solution of acid **25** (15 mg, 0.019 mmol, 1.0 equiv) in anhydrous

CHAPITRE 2 – TOTAL SYNTHESIS, ISOLATION, SURFACTANT PROPERTIES, AND BIOLOGICAL EVALUATION OF ANANATOSIDES AND RELATED MACRODILACTONE-CONTAINING RHAMNOLIPIDS

DCE (5.4 mL) by using a syringe pump over 2 h. The reaction mixture was stirred for an additional 1 h, then cooled at 0 °C, filtered over Celite, and the solvents were evaporated under reduced pressure. The residue was purified by silica gel flash chromatography (Hex/EtOAc 95:5 to 8:2) to give macrolactone **26** (9.4 mg, 64%) as a white amorphous solid: R_f 0.59 (Hex/EtOAc 7:3); $[\alpha]_D^{20} +11$ (c 0.5, CHCl₃); ¹H NMR (600 MHz, CDCl₃) δ (ppm) 7.34-7.26 (m, 8H, 8 × CH_{Bn}), 7.25-7.24 (m, 2H, 2 × CH_{Bn}), 5.52-5.47 (m, 1H, H-3''), 4.91 (dd, $J_{2-3} = 9.6$ Hz, $J_{2-1} = 8.3$ Hz, 1H, H-2), 4.83 (d, $J = 11.1$ Hz, 1H, CHH_{Bn}), 4.75 (d, $J = 11.3$ Hz, CHH_{Bn}), 4.70 (d, $J = 11.3$ Hz, 1H, CHH_{Bn}), 4.57 (d, $J = 8.2$ Hz, 1H, H-1), 4.51 (d, $J = 11.2$ Hz, 1H, CHH_{Bn}), 4.29 (dd, $J_{6a-6b} = 11.2$ Hz, $J_{6a-5} = 10.2$ Hz, 1H, H-6a), 4.15-4.11 (m, 1H, H-3'), 4.05 (dd, $J_{6b-6a} = 11.4$ Hz, $J_{6b-5} = 1.8$ Hz, 1H, H-6b), 3.67 (t, $J = 9.2$ Hz, 1H, H-3), 3.53 (td, $J_{5-4, 5-6a} = 10.0$ Hz, $J_{5-6b} = 1.8$ Hz, 1H, H-5), 3.29 (t, $J = 9.3$ Hz, 1H, H-4), 2.75-2.69 (m, 1H, CHH_{Lev}), 2.67-2.58 (m, 2H, H-2a', CHH_{Lev}), 2.57-2.45 (m, 4H, CH_{2Lev}, H-2a'', H-2b''), 2.32 (d, $J_{2b'-2a'} = 18.5$ Hz, 1H, H-2b'), 2.15 (s, 3H, CH_{3Lev}), 1.54-1.23 (m, 24H, 12 × CH₂), 0.89-0.86 (m, 6H, 2 × CH₃); ¹³C NMR (150 MHz, CDCl₃) δ (ppm) 206.1 (CO_{Lev}), 171.5, 171.4, 169.6 (3C, COOR_{Lev}, C-1', C-1''), 138.1 (C_{Bn}), 137.6 (C_{Bn}), 126.7-128.0 (10C, 10 × CH_{Bn}), 101.7 (C-1), 83.0 (C-3), 78.8 (C-4), 77.7 (C-3'), 75.3 (CH_{2Bn}), 75.1 (CH_{2Bn}), 73.7 (C-2), 72.5 (C-5), 69.6 (C-3''), 64.0 (C-6), 41.6 (C-2'), 40.5 (C-2''), 37.9 (CH_{2Lev}), 36.4-22.8 (14C, CH_{2Lev}, CH_{3Lev}, 12 × CH₂), 14.2 (2C, 2 × CH₃); HRMS (ESI-TOF) m/z [M + Na]⁺ calcd for C₄₅H₆₄NaO₁₁ 803.4341; found 803.4337; m/z [M + K]⁺ calcd for C₄₅H₆₄KO₁₁ 819.4080; found 819.4077. HRMS data for the corresponding dimer: HRMS (ESI-TOF) m/z [M + Na]⁺ calcd for C₉₀H₁₂₈NaO₂₂ 1583.8789; found 1583.8749.

3,4-Di-*O*-benzylated Macrolide **24**.

Route A: PPh₃ (24 mg, 0.090 mmol, 1.6 equiv) was added to a solution of macrolactone **23** (48 mg, 0.056 mmol, 1.0 equiv) in anhydrous THF (1.7 mL). The mixture was stirred under an Ar atmosphere at 60 °C for 2 h, after which H₂O (0.2 mL) was added. The solution was stirred at 60 °C for an additional 4 h. The solvents were then evaporated under reduced pressure and co-evaporated with toluene. The residue was purified by silica gel flash chromatography (Tol/EtOAc 98:2 to 95:5) to give alcohol **24** (24 mg, 62%) as a white amorphous solid.

CHAPITRE 2 – TOTAL SYNTHESIS, ISOLATION, SURFACTANT PROPERTIES, AND BIOLOGICAL EVALUATION OF ANANATOSIDES AND RELATED MACRODILACTONE-CONTAINING RHAMNOLIPIDS

Route B: To a solution of macrolide **26** (20 mg, 0.026 mmol, 1.0 equiv) in anhydrous THF/MeOH (10:1 v/v, 1.8 mL) was slowly added a solution of H₂NNH₂·H₂O (18 μL, 0.37 mmol, 14 equiv) and HOAc (45 μL) in anhydrous THF/MeOH (5:1 v/v, 0.4 mL). The solution was stirred under an Ar atmosphere for 30 min until a white solid was formed. The suspension was co-evaporated with toluene and the residue was purified by silica gel flash chromatography (Hex/EtOAc 95:5 to 9:1) to give alcohol **24** (17 mg, quant.) as a white amorphous solid. *R_f* 0.67 (Tol/EtOAc 8:2); [α]²⁰_D +4 (c 0.4, CHCl₃); ¹H NMR (600 MHz, CDCl₃) δ (ppm) 7.37-7.24 (m, 10H, 10 × CH_{Bn}), 5.54-5.49 (m, 1H, H-3''), 4.96 (d, *J* = 11.1 Hz, 1H, CHH_{Bn}), 4.89 (d, *J* = 11.1 Hz, 1H, CHH_{Bn}), 4.80 (d, *J* = 11.1 Hz, 1H, CHH_{Bn}), 4.52 (d, *J* = 11.2 Hz, 1H, CHH_{Bn}), 3.36 (d, *J* = 8.0 Hz, 1H, H-1), 4.37 (dd, *J*_{6a-6b} = 11.3 Hz, *J*_{6a-5} = 10.1 Hz, 1H, H-6a), 4.27-4.23 (m, 1H, H-3'), 4.03 (dd, *J*_{6b-6a} = 11.3 Hz, *J*_{6b-5} = 1.9 Hz, 1H, H-6b), 3.61 (t, *J* = 8.9 Hz, 1H, H-3), 3.54 (td, *J*_{5-6a, 5-4} = 10.0 Hz, *J*_{5-6b} = 1.9 Hz, 1H, H-5), 3.48-3.45 (m, 1H, H-2), 3.23 (dd, *J*₄₋₅ = 10.0 Hz, *J*₄₋₃ = 8.7 Hz, 1H, H-4), 2.65 (dd, *J*_{2a'-2b'} = 18.5 Hz, *J*_{2a'-3'} = 8.8 Hz, 1H, H-2a'), 2.60-2.52 (m, 2H, H-2''), 2.36 (d, *J*_{2b'-2a'} = 18.3 Hz, 1H, H-2b'), 2.21 (d, *J* = 1.8 Hz, 1H, OH), 1.67-1.25 (m, 24H, 12 × CH₂); ¹³C NMR (150 MHz, CDCl₃) δ (ppm) 171.3, 169.6 (2C, C-1', C-1''), 138.6 (C_{Bn}), 137.9 (C_{Bn}), 128.6-127.9 (10C, 10 × CH_{Bn}), 103.5 (C-1), 84.4 (C-3), 78.4 (C-4), 77.8 (C-3'), 75.3, 75.1 (3C, CH_{2Bn}, CH_{2Bn}, C-2), 72.8 (C-5), 69.7 (C-3''), 64.1 (C-6), 41.5 (C-2'), 40.5 (C-2''), 36.4-22.8 (12C, 12 × CH₂), 14.2 (2C, C-10', C-10''); HRMS (ESI-TOF) *m/z* [M + Na]⁺ calcd for C₄₀H₅₈NaO₉ 705.3973; found 705.3988; *m/z* [M + NH₄]⁺ calcd for C₄₀H₆₂NO₁₀ 700.4419; found 700.4435.

Synthetic Ananatoside A (1).

Route A: Protected macrolide **23** (21 mg, 0.031 mmol, 1.0 equiv) was solubilized in MeOH (0.6 mL) and DCE (0.3 mL) under an Ar atmosphere. Pd black (21 mg, 1 mg•mg⁻¹) of substrate was added, and the mixture was stirred at 40 °C for 16 h under an H₂ atmosphere. The suspension was filtered over Celite and evaporated under reduced pressure. The residue was purified by silica gel flash chromatography (DCM/MeOH 99:1 to 95:5) to give ananatoside A (**1**, 14 mg, 90%) as a white amorphous solid. Analytical HPLC analysis was performed using method D (41.5 min.).

CHAPITRE 2 – TOTAL SYNTHESIS, ISOLATION, SURFACTANT PROPERTIES, AND BIOLOGICAL EVALUATION OF ANANATOSIDES AND RELATED MACRODILACTONE-CONTAINING RHAMNOLIPIDS

Route B: Novozyme 435 (2.4 mg) was dried over activated 4 Å MS (90 mg) in a desiccator under vacuum containing calcium sulfate at 63 °C for 3 days. The enzyme and the molecular sieves were then added to a suspension of ananatoside B (**2**, 4.7 mg, 9.0 μmol, 1.0 equiv) and 4 Å MS (90 mg) in anhydrous toluene (0.9 mL). The suspension was stirred at 75 °C under microwave radiations for 3 h then filtered over a pad of MgSO₄ and silica (DCM/MeOH 8:2) to give ananatoside A (**1**, 3 mg, 64%) as a white amorphous solid. *R_f* 0.43 (DCM/MeOH 9:1); $[\alpha]_D^{20} +19$ (*c* 0.7, CHCl₃). Physical and analytical data of synthetic ananatoside A (**1**) agreed with our previously published data.¹⁵⁹

***para*-Methylphenyl 4-*O*-Levulinoyl-3-*O*-*para*-methoxybenzyl-1-thio- α -L-rhamnopyranoside (**32**).**

Bu₂SnO (1.54 g, 6.17 mmol, 1.1 equiv.) was added to a solution of diol **31**¹⁶⁹ (2.07 g, 5.61 mmol, 1.0 equiv.) in toluene (67 mL) and the mixture was refluxed using a Dean–Stark trap for 2 h. The solution was cooled to rt and CsF (895 mg, 5.89 mmol, 1.05 equiv.), TBAI (2.18 g, 5.89 mmol, 1.05 equiv.), and PMBCl (0.91 mL, 5.9 mmol, 1.2 equiv.) were successively added. The mixture was stirred under an Ar atmosphere at 40 °C for 16 h. The suspension was cooled at 0 °C, filtered over Celite, and rinsed with DCM. The solvents were evaporated under reduced pressure. The residue was purified by silica gel flash chromatography (Hex/EtOAc 9:1 to 7:3) to give compound **32** (2.41 g, 88%) as a yellow oil: *R_f* 0.6 (Hex/EtOAc 4 : 6); $[\alpha]_D^{20} -140$ (*c* 1.2, CHCl₃); ¹H NMR (600 MHz, CDCl₃) δ (ppm) 7.33–7.32 (m, 2H, 2 × CH_{STol}), 7.27–7.26 (m, 2H, 2 × CH_{PMB}), 7.12–7.10 (m, 2H, 2 × CH_{STol}), 6.91–6.89 (m, 2H, 2 × CH_{PMB}), 5.46 (d, *J* = 1.2 Hz, 1H, H-1), 5.08 (t, *J* = 9.6 Hz, 1H, H-4), 4.59 (d, *J* = 11.7 Hz, 1H, CHH_{PMB}), 4.53 (d, *J* = 11.8 Hz, 1H, CHH_{PMB}), 4.22 (dq, *J*₅₋₄ = 9.9 Hz, *J*₅₋₆ = 6.2 Hz, 1H, H-5), 4.18 (dd, *J*₂₋₃ = 3.0 Hz, *J*₂₋₁ = 1.5 Hz, 1H, H-2), 3.81 (s, 3H, CH_{3PMB}), 3.75 (dd, *J*₃₋₄ = 9.4 Hz, *J*₃₋₂ = 3.3 Hz, 1H, H-3), 2.77–2.72 (m, 2H, CH_{2Lev}), 2.59–2.49 (m, 2H, CH_{2Lev}), 2.32 (s, 3H, CH_{3STol}), 2.19 (s, 3H, CH_{3Lev}), 1.18 (d, *J* = 6.3 Hz, 3H, H-6); ¹³C NMR (150 MHz, CDCl₃) δ (ppm) 206.5 (CO_{Lev}), 172.1 (COOR_{Lev}), 159.6 (C_{Ar}), 137.8 (C_{Ar}), 132.1 (2C, 2 × CH_{STol}), 130.0, 129.7 (5C, C_{Ar}, 2 × CH_{STol}, 2 × CH_{PMB}), 129.6 (C_{Ar}), 114.1 (2C, 2 × CH_{PMB}), 87.3 (C-1), 76.7 (C-3), 73.0 (C-4), 71.7 (CH_{2PMB}), 69.9 (C-2), 67.6 (C-5), 55.4 (CH_{3PMB}), 37.9 (CH_{2Lev}), 30.0 (CH_{3Lev}), 28.1 (CH_{2Lev}), 21.2 (CH_{3STol}), 17.4 (C-6); HRMS (ESI-TOF) *m/z* [M + NH₄]⁺ calcd

CHAPITRE 2 – TOTAL SYNTHESIS, ISOLATION, SURFACTANT PROPERTIES, AND BIOLOGICAL EVALUATION OF ANANATOSIDES AND RELATED MACRODILACTONE-CONTAINING RHAMNOLIPIDS

for C₂₆H₃₆NO₇S 506.2207; found 506.2204; *m/z* [M + Na]⁺ calcd for C₂₆H₃₂NaO₇S 511.1761; found 511.1756.

***para*-Methylphenyl 2-*O*-*ortho*-(Azidomethyl)benzoyl-4-*O*-levulinoyl-3-*O*-*para*-methoxybenzyl-1-thio- α -L-rhamnopyranoside (33).**

AZMBOH (229 mg, 1.29 mmol, 1.6 equiv), EDC (497 mg, 2.59 mmol, 3.3 equiv), and DMAP (201 mg, 0.863 mmol, 1.1 equiv) were successively added to a solution of alcohol **32** (387 mg, 0.793 mmol, 1.0 equiv) in anhydrous DCM (8.6 mL). The mixture was refluxed under an Ar atmosphere for 4 h, then cooled at rt, and the solvents were evaporated under reduced pressure. The residue was purified by silica gel flash chromatography (Hex/EtOAc 95:5 to 7:3) to give fully protected **33** (490 mg, 95%) as a colorless oil: *R_f* 0.63 (Hex/EtOAc 1:1); [α]_D²⁰ -24 (*c* 0.8, CHCl₃); ¹H NMR (600 MHz, CDCl₃) δ (ppm) 8.04-8.03 (m, 1H, CH_{AZMB}), 7.57-7.54 (m, 1H, CH_{AZMB}), 7.49-7.48 (m, 1H, CH_{AZMB}), 7.41-7.39 (m, 1H, CH_{AZMB}), 7.37-7.36 (m, 2H, 2 \times CH_{STol}), 7.24-7.22 (m, 2H, 2 \times CH_{PMB}), 7.14-7.12 (m, 2H, 2 \times CH_{STol}), 6.87-6.85 (m, 2H, 2 \times CH_{PMB}), 5.77 (dd, *J*₂₋₃ = 3.2 Hz, *J*₂₋₁ = 1.7 Hz, 1H, H-2), 5.49 (d, *J* = 1.5 Hz, 1H, H-1), 5.18 (t, *J* = 9.7 Hz, 1H, H-4), 4.78 (d, *J* = 14.6 Hz, 1H, CHH_{AZMB}), 4.74 (d, *J* = 14.6 Hz, 1H, CHH_{AZMB}), 4.63 (d, *J* = 11.8 Hz, 1H, CHH_{Bn}), 4.47 (d, *J* = 11.8 Hz, 1H, CHH_{Bn}), 4.33 (dq, *J*₅₋₄ = 9.8 Hz, *J*₅₋₆ = 6.2 Hz, 1H, H-5), 3.90 (dd, *J*₃₋₄ = 9.7 Hz, *J*₃₋₂ = 3.2 Hz, 1H, H-3), 3.80 (s, 3H, CH_{3PMB}), 2.79 (ddd, *J* = 18.3 Hz, *J* = 8.0 Hz, *J* = 5.8 Hz, 1H, CHH_{Lev}), 2.68 (dt, *J* = 18.3 Hz, *J* = 6.0 Hz, 1H, CHH_{Lev}), 2.63-2.58 (m, 1H, CHH_{Lev}), 2.50 (dt, *J* = 17.2 Hz, *J* = 6.1 Hz, 1H, CHH_{Lev}), 2.33 (s, 3H, CH_{3STol}), 2.18 (s, 3H, CH_{3Lev}), 1.25 (d, *J* = 6.2 Hz, 3H, H-6); ¹³C NMR (150 MHz, CDCl₃) δ (ppm) 206.5 (CO_{Lev}), 172.1 (COOR_{Lev}), 165.9 (COOR_{AZMB}), 159.5 (C_{Ar}), 138.3 (C_{Ar}), 137.5-128.4 (14C, 4 \times C_{Ar}, 10 \times CH_{Ar}), 113.9 (2C, 2 \times CH_{PMB}), 86.5 (C-1), 74.4 (C-3), 73.1 (C-4), 71.21, 71.17 (2C, CH_{2PMB}, C-2), 68.0 (C-5), 55.4 (CH_{3PMB}), 53.2 (CH_{2AZMB}), 38.0 (CH_{2Lev}), 30.0 (CH_{3Lev}), 28.1 (CH_{2Lev}), 21.3 (CH_{3STol}), 17.5 (C-6); HRMS (ESI-TOF) *m/z* [M + NH₄]⁺ calcd for C₃₄H₄₁N₄O₈S 665.2640; found 665.2623; *m/z* [M + Na]⁺ calcd for C₃₄H₃₇NaN₃O₈S 670.2194; found 670.2223.

Benzyl (R)-3-*O*-[(R)-(3'-*O*-Decyl)-2-*O*-*ortho*-(azidomethyl)benzoyl-4-*O*-levulinoyl-3-*O*-*para*-methoxybenzyl- α -L-rhamnopyranosyl]decanoate (27).

CHAPITRE 2 – TOTAL SYNTHESIS, ISOLATION, SURFACTANT PROPERTIES, AND BIOLOGICAL EVALUATION OF ANANATOSIDES AND RELATED MACRODILACTONE-CONTAINING RHAMNOLIPIDS

Donor **33** (210 mg, 0.324 mmol, 1.2 equiv), acceptor **12** (121 mg, 0.270 mmol, 1.0 equiv) and NIS (97 mg, 0.43 mmol, 1.6 equiv) were dried under high vacuum for 1 h. Activated 4 Å MS (484 mg, 4 mg•mg⁻¹ of acceptor **12**) and anhydrous DCE (5.4 mL) were added and the suspension was stirred under an Ar atmosphere for 1 h. The mixture was cooled to -10 °C and AgOTf (14 mg, 0.054 mmol, 0.2 equiv) was added while the reaction flask was protected from light with aluminum foil. The suspension was stirred from -10 to 0 °C for 1.5 h, quenched with Et₃N, and filtered over Celite. The solvents were evaporated under reduced pressure and the residue was purified by silica gel flash chromatography (Hex/EtOAc 95:5 to 8:2) to give rhamnolipid **27** (238 mg, 91%) as a yellow oil: *R_f* 0.30 (Hex/EtOAc 7:3); [α]_D²⁰ +8 (*c* 0.6, CHCl₃); ¹H NMR (600 MHz, CDCl₃) δ (ppm) 8.05-8.03 (m, 1H, CH_{AZMB}), 7.57-7.54 (m, 1H, CH_{AZMB}), 7.49-7.48 (m, 1H, CH_{AZMB}), 7.42-7.39 (m, 1H, CH_{AZMB}), 7.36-7.30 (m, 5H, 5 × CH_{COOBn}), 7.18-7.16 (m, 2H, 2 × CH_{PMB}), 6.82-6.80 (m, 2H, 2 × CH_{PMB}), 5.45 (dd, *J*₂₋₃ = 3.2 Hz, *J*₂₋₁ = 1.9 Hz, 1H, H-2), 5.26-5.21 (m, 1H, H-3''), 5.12-5.10 (m, 3H, CH_{2COOBn}, H-4), 5.00 (d, *J* = 1.7 Hz, 1H, H-1), 4.79 (d, *J* = 14.7 Hz, 1H, CHH_{AZMB}), 4.73 (d, *J* = 14.7 Hz, 1H, CHH_{AZMB}), 4.59 (d, *J* = 11.7 Hz, 1H, CHH_{PMB}), 4.41 (d, *J* = 11.7 Hz, 1H, CHH_{PMB}), 4.08-4.04 (m, 1H, H-3'), 3.93-3.89 (m, 2H, H-3, H-5), 3.77 (s, 3H, CH_{3PMB}), 2.75 (ddd, *J* = 18.3 Hz, *J* = 7.8 Hz, *J* = 6.1 Hz, 1H, CHH_{Lev}), 2.68-2.63 (m, 2H, CHH_{Lev}, H-2a''), 2.61-2.52 (m, 3H, CHH_{Lev}, H-2a', H-2b''), 2.47-2.42 (m, 2H, CHH_{Lev}, H-2b'), 2.16 (s, 3H, CH_{3Lev}), 1.58-1.24 (m, 24H, 12 × CH₂), 1.21 (d, *J* = 6.3 Hz, 3H, H-6), 0.90-0.85 (m, 6H, 2 × CH₃); ¹³C NMR (150 MHz, CDCl₃) δ (ppm) 206.5 (CO_{Lev}), 172.2, 170.6, 170.3 (3C, COOR_{Lev}, C-1', C-1''), 166.1 (COOR_{AZMB}), 159.3 (C_{Ar}), 137.5 (C_{Ar}), 135.9 (C_{Ar}), 133.0-128.4 (13C, 2 × C_{Ar}, 11 × CH_{Ar}), 113.8 (2C, 2 × CH_{PMB}), 96.8 (C-1), 75.3 (C-3'), 74.5 (C-3), 73.1 (C-4), 71.2, 71.0 (2C, CH_{2PMB}, C-3''), 70.1 (C-2), 67.1 (C-5), 66.6 (CH_{2COOBn}), 55.4 (CH_{3PMB}), 53.2 (CH_{2AZMB}), 40.4 (C-2'), 39.2 (C-2''), 38.0 (CH_{2Lev}), 34.0-22.8 (14C, 12 × CH₂, CH_{3Lev}, CH_{2Lev}), 17.6 (C-6), 14.2 (2C, 2 × CH₃); HRMS (ESI-TOF) *m/z* [M + NH₄]⁺ calcd for C₅₄H₇₇N₄O₁₃ 989.5482; found 989.5479; *m/z* [M + Na]⁺ calcd for C₅₄H₇₃NaN₃O₁₃ 994.5036; found 994.5053.

CHAPITRE 2 – TOTAL SYNTHESIS, ISOLATION, SURFACTANT PROPERTIES, AND BIOLOGICAL EVALUATION OF ANANATOSIDES AND RELATED MACRODILACTONE-CONTAINING RHAMNOLIPIDS

Benzyl (R)-3-O-[(R)-(3'-O-Decyl)-4-O-levulinoyl-3-O-para-methoxybenzyl- α -L-rhamnopyranosyl]decanoate (34).

To a solution of rhamnolipid **27** (360 mg, 0.371 mmol, 1.0 equiv) in anhydrous THF (11 mL) was added PPh₃ (156 mg, 0.593 mmol, 1.6 equiv). The mixture was stirred at 60 °C under an Ar atmosphere for 2 h, after which water (1.5 mL) was added. The mixture was heated at 60 °C for 4 h, then co-evaporated with toluene. The residue was purified by silica gel flash chromatography (Hex/EtOAc 9:1 to 65:35) to give alcohol **34** (269 mg, 89%) as a yellowish oil: *R*_f 0.37 (Hex/EtOAc 6:4); [α]_D²⁰ -17 (*c* 0.6, CHCl₃); ¹H NMR (600 MHz, CDCl₃) δ (ppm) 7.36-7.30 (m, 5H, 5 \times CH_{COOBn}), 7.23-7.21 (m, 2H, 2 \times CH_{PMB}), 6.87-6.86 (m, 2H, 2 \times CH_{PMB}), 5.25-5.21 (m, 1H, H-3''), 5.11 (s, 2H, CH₂COOBn), 5.01 (t, *J* = 9.7 Hz, 1H, H-4), 4.92 (d, *J* = 1.3 Hz, 1H, H-1), 4.55 (d, *J* = 11.7 Hz, 1H, CHH_{PMB}), 4.49 (d, *J* = 11.6 Hz, 1H, CHH_{PMB}), 4.05-4.01 (m, 1H, H-3'), 3.92 (br s, 1H, H-2), 3.86-3.82 (m, 1H, H-5), 3.79 (s, 3H, CH₃PMB), 3.71 (dd, *J*₃₋₄ = 9.5 Hz, *J*₃₋₂ = 3.3 Hz, 1H, H-3), 2.71-2.62 (m, 3H, CH₂Lev, H-2a''), 2.59-2.54 (m, 2H, H-2b'', H-2a'), 2.50-2.46 (m, 2H, CH₂Lev), 2.42 (dd, *J* = 15.2 Hz, *J* = 6.0 Hz, 1H, H-2b'), 2.16 (s, 3H, CH₃Lev), 1.62-1.22 (24H, 12 \times CH₂), 1.16 (d, *J* = 6.3 Hz, 3H, H-6), 0.90-0.86 (m, 6H, 2 \times CH₃); ¹³C NMR (150 MHz, CDCl₃) δ (ppm) 206.4 (CO_{Lev}), 172.1, 170.6, 170.2 (3C, COOR_{Lev}, C-1', C-1''), 159.5 (C_{Ar}), 135.8 (C_{Ar}), 130.0-128.4 (8C, C_{Ar}, 7 \times CH_{Ar}), 113.9 (2C, 2 \times CH_{PMB}), 98.0 (C-1), 76.7 (C-3), 74.6 (C-3'), 72.9 (C-4), 71.7 (CH₂PMB), 70.9 (C-3''), 68.9 (C-2), 66.5 (2C, CH₂COOBn, C-5), 55.3 (CH₃PMB), 40.3 (C-2'), 39.1 (C-2''), 37.9 (CH₂Lev), 33.9-22.7 (14C, CH₂Lev, CH₃Lev, 12 \times CH₂), 17.3 (C-6), 14.19 (CH₃), 14.17 (CH₃); HRMS (ESI-TOF) *m/z* [M + NH₄]⁺ calcd for C₄₆H₇₂NO₁₂ 830.5049 found 830.5056; *m/z* [M + Na]⁺ calcd for C₄₆H₆₈NaO₁₂ 835.4603; found 835.4616.

Benzyl (R)-3-O-[(R)-(3'-O-Decyl)-3-O-para-methoxybenzyl- α -L-rhamnopyranosyl]decanoate (35).

To a solution of compound **34** (212 mg, 0.261 mmol, 1.0 equiv) in anhydrous THF/MeOH (10:1 v/v, 18.3 mL) was slowly added a solution of H₂NNH₂·H₂O (177 μ L, 3.66 mmol, 14 equiv) and HOAc (444 μ L) in anhydrous THF/MeOH (5:1 v/v, 3 mL). The solution was stirred under an Ar

CHAPITRE 2 – TOTAL SYNTHESIS, ISOLATION, SURFACTANT PROPERTIES, AND BIOLOGICAL EVALUATION OF ANANATOSIDES AND RELATED MACRODILACTONE-CONTAINING RHAMNOLIPIDS

atmosphere for 45 min until a white solid was formed. The suspension was co-evaporated with toluene and the residue was purified by silica gel flash chromatography (Hex/EtOAc 9:1 to 7:3) to give diol **35** (155 mg, 83%) as a colorless oil: R_f 0.52 (Hex/EtOAc 1:1); $[\alpha]_D^{20}$ -19 (c 0.6, CHCl₃); ¹H NMR (600 MHz, CDCl₃) δ (ppm) 7.36-7.31 (m, 5H, 5 \times CH_{COOBn}), 7.27-7.26 (m, 2H, 2 \times CH_{PMB}), 6.88-6.86 (m, 2H, 2 \times CH_{PMB}), 5.25-5.21 (m, 1H, H-3''), 5.10 (d, J = 1.1 Hz, 2H, CH₂COOBn), 4.91 (d, J = 1.4 Hz, 1H, H-1), 4.60 (d, J = 11.2 Hz, 1H, CHH_{PMB}), 4.53 (d, J = 11.2 Hz, 1H, CHH_{PMB}), 4.11-4.07 (m, 1H, H-3'), 3.94 (dd, $J_{2,3}$ = 3.1 Hz, $J_{2,1}$ = 1.6 Hz, 1H, H-2), 3.79 (s, 3H, CH₃PMB), 3.74 (dq, J_{5-4} = 9.6 Hz, J_{5-6} = 6.5 Hz, 1H, H-5), 3.60 (dd, J_{3-4} = 9.2 Hz, J_{3-2} = 3.3 Hz, 1H, H-3), 3.50 (t, J = 9.4 Hz, 1H, H-4), 2.65 (dd, J = 15.6 Hz, J = 7.6 Hz, 1H, H-2a''), 2.60-2.53 (m, 2H, H-2b'', H-2a'), 2.41 (dd, J = 15.3 Hz, J = 5.6 Hz, 1H, H-2b'), 1.62-1.26 (m, 27H, H-6, 12 \times CH₂), 0.90-0.86 (m, 6H, 2 \times CH₃); ¹³C NMR (150 MHz, CDCl₃) δ (ppm) 170.8, 170.6 (2C, C-1', C-1''), 159.6 (C_{Ar}), 135.7 (C_{Ar}), 130.1-128.4 (8C, C_{Ar}, 7 \times CH_{Ar}), 114.2 (2C, 2 \times CH_{PMB}), 97.9 (C-1), 79.7 (C-3), 73.9 (C-3'), 72.0 (C-4), 71.6 (CH₂PMB), 70.9 (C-3''), 68.5 (C-2), 68.2 (C-5), 66.7 (CH₂COOBn), 55.4 (CH₃PMB), 40.2 (C-2'), 39.2 (C-2''), 34.1-22.8 (12C, 12 \times CH₂), 17.7 (C-6), 14.23 (CH₃), 14.21 (CH₃); HRMS (ESI-TOF) m/z [M + Na]⁺ calcd for C₄₁H₆₂NaO₁₀ 737.4235; found 737.4245; m/z [M + Na]⁺ calcd for C₄₁H₆₂KO₁₀ 753.3975; found 753.3982.

Rhamnolipid 3.

Pd black (12 mg, 1 mg•mg⁻¹ of diol **35**) was added to a solution of diol **35** (12 mg, 17 μ mol, 1.0 equiv) in MeOH (0.34 mL) and DCE (0.17 mL). The suspension was stirred under an H₂ atmosphere at 40 °C for 16 h. The mixture was then filtered over Celite and the solvents were evaporated under reduced pressure. The residue was purified by silica gel flash chromatography (DCM/MeOH 95:5 to 8:2) to give C₁₀-C₁₀ rhamnolipid **3** (7.9 mg, quant.) as a colorless oil. R_f 0.61 (DCM/MeOH 8:2); $[\alpha]_D^{20}$ -45 (c 0.7, CHCl₃); HRMS (ESI-TOF) m/z [M + NH₄]⁺ calcd for C₂₆H₅₂NO₉ 522.3637; found 522.3639; m/z [M + Na]⁺ calcd for C₂₆H₄₈NaO₉ 527.3191; found 527.3189. Physical and analytical data of C₁₀-C₁₀ rhamnolipid (**3**) agreed with those published.¹⁹¹ Analytical HPLC analysis was performed using method C (36.3 min.).

CHAPITRE 2 – TOTAL SYNTHESIS, ISOLATION, SURFACTANT PROPERTIES, AND BIOLOGICAL EVALUATION OF ANANATOSIDES AND RELATED MACRODILACTONE-CONTAINING RHAMNOLIPIDS

***para*-Methylphenyl 3-*O*-Benzyl-4-*O*-levulinoyl-1-thio- α -L-rhamnopyranoside (36).**

Bu₂SnO (128 mg, 0.514 mmol, 1.1 equiv) was added to a solution of diol **31**¹⁶⁹ (172 mg, 0.467 mmol, 1.0 equiv) in anhydrous toluene (5.6 mL). The suspension was refluxed with a Dean-Stark apparatus for 2 h and cooled to rt. CsF (75 mg, 0.49 mmol, 1.05 equiv), TBAI (181 mg, 0.491 mmol, 1.05 equiv), and BnBr (67 μ L, 0.56 mmol, 1.2 equiv) were then added to the mixture and the latter was stirred at 40 °C for 16 h under an Ar atmosphere. The suspension was cooled at 0 °C, filtered over Celite, and the solvents were evaporated under reduced pressure. The residue was purified by silica gel flash chromatography (Hex/EtOAc 9:1 to 6:4) to give alcohol **36** (201 mg, 94%) as a white amorphous solid: *R*_f 0.48 (Hex/EtOAc 1:1); $[\alpha]_D^{20}$ -149 (*c* 0.9, CHCl₃); ¹H NMR (600 MHz, CDCl₃) δ (ppm) 7.39-7.36 (m, 2H, 2 \times CH_{Bn}), 7.34-7.31 (m, 5H, 2 \times CH_{STol}, 3 \times CH_{Bn}), 7.12-7.11 (m, 2H, 2 \times CH_{STol}), 5.47 (d, *J* = 1.5 Hz, 1H, H-1), 5.11 (t, *J* = 9.6 Hz, 1H, H-4), 4.67 (d, *J* = 12.0 Hz, 1H, CHH_{Bn}), 4.60 (d, *J* = 12.0 Hz, 1H, CHH_{Bn}), 4.26-4.21 (m, 2H, H-2, H-5), 3.77 (dd, *J*₃₋₄ = 9.4 Hz, *J*₃₋₂ = 3.3 Hz, 1H, H-3), 2.79-2.68 (m, 2H, CH_{2Lev}), 2.59-2.48 (m, 2H, CH_{2Lev}), 2.33 (s, 3H, CH_{3STol}), 2.18 (s, 3H, CH_{3Lev}), 1.19 (d, *J* = 6.3 Hz, 3H, H-6); ¹³C NMR (150 MHz, CDCl₃) δ (ppm) 206.5 (CO_{Lev}), 172.2 (COOR_{Lev}), 137.9 (C_{Ar}), 137.6 (C_{Ar}), 132.1-128.1 (10C, C_{Ar}, 9 \times CH_{Ar}), 87.3 (C-1), 77.0 (C-3), 73.0 (C-4), 72.1 (CH_{2Bn}), 69.9 (C-2), 67.6 (C-5), 38.0 (CH_{2Lev}), 30.0 (CH_{3Lev}), 28.1 (CH_{2Lev}), 21.2 (CH_{3STol}), 17.4 (C-6); HRMS (ESI-TOF) *m/z* [M + NH₄]⁺ calcd for C₂₅H₃₄NO₆S 476.2101; found 476.2115; *m/z* [M + Na]⁺ calcd for C₂₅H₃₀NaO₆S 481.1655; found 481.1670.

***para*-Methylphenyl 2-*O*-*ortho*-(Azidomethyl)benzoyl-3-*O*-benzyl-4-*O*-levulinoyl-1-thio- α -L-rhamnopyranoside (37).**

To a solution of alcohol **36** (380 mg, 0.828 mmol, 1.0 equiv) in anhydrous DCM (8.3 mL) were added DMAP (101 mg, 0.828 mmol, 1.0 equiv), DCC (342 mg, 1.66 mmol, 2.0 equiv), and AZMBOH (220 mg, 1.24 mmol, 1.5 equiv). The solution was refluxed under an Ar atmosphere for 4 h, then cooled at 0 °C, filtered over Celite, and the solvents were evaporated under reduced pressure. The residue was purified by silica gel flash chromatography (Hex/EtOAc 9:1 to 8:2) to give compound **37** (493 mg, 96%) as a colorless oil: *R*_f 0.51 (Hex/EtOAc 6:4); $[\alpha]_D^{20}$ -22 (*c* 2.2,

CHAPITRE 2 – TOTAL SYNTHESIS, ISOLATION, SURFACTANT PROPERTIES, AND BIOLOGICAL EVALUATION OF ANANATOSIDES AND RELATED MACRODILACTONE-CONTAINING RHAMNOLIPIDS

CHCl₃); ¹H NMR (600 MHz, CDCl₃) δ (ppm) 8.05-8.03 (m, 1H, CH_{AZMB}), 7.56-7.54 (m, 1H, CH_{AZMB}), 7.49-7.47 (m, 1H, CH_{AZMB}), 7.42-7.39 (m, 1H, CH_{AZMB}), 7.37-7.36 (m, 2H, 2 × CH_{STol}), 7.34-7.37 (m, 5H, 5 × CH_{Bn}), 7.14-7.12 (m, 2H, 2 × CH_{STol}), 5.79 (dd, J₂₋₃ = 3.2 Hz, J₂₋₁ = 1.7 Hz, 1H, H-2), 5.50 (d, J = 1.5 Hz, 1H, H-1), 5.21 (t, J = 9.7 Hz, 1H, H-4), 4.77 (d, J = 14.6 Hz, 1H, CHH_{AZMB}), 4.74-4.70 (m, 2H, CHH_{AZMB}, CHH_{Bn}), 4.54 (d, J = 12.1 Hz, 1H, CHH_{Bn}), 4.34 (dq, J₅₋₄ = 9.9 Hz, J₅₋₆ = 6.2 Hz, 1H, H-5), 3.92 (dd, J₃₋₄ = 9.7 Hz, J₃₋₂ = 3.2 Hz, 1H, H-3), 2.80 (ddd, J = 18.1 Hz, J = 8.0 Hz, J = 5.7 Hz, 1H, CHH_{Lev}), 2.69-2.58 (m, 2H, CHH_{Lev}, CHH_{Lev}), 2.49 (dt, J = 17.2 Hz, J = 6.0 Hz, 1H, CHH_{Lev}), 2.33 (s, 3H, CH_{3STol}), 2.17 (s, 3H, CH_{3Lev}), 1.26 (d, J = 6.2 Hz, 3H, H-6); ¹³C NMR (150 MHz, CDCl₃) δ (ppm) 206.5 (CO_{Lev}), 172.1 (COOR_{Lev}), 165.9 (COOR_{AZMB}), 138.3 (C_{Ar}), 137.6 (C_{Ar}), 137.5 (C_{Ar}), 133.1-128.0 (15C, 2 × C_{Ar}, 12 × CH_{Ar}), 86.4 (C-1), 75.0 (C-3), 73.1 (C-4), 71.6 (CH_{2Bn}), 71.1 (C-2), 68.0 (C-5), 53.1 (CH_{2AZMB}), 38.0 (CH_{2Lev}), 29.9 (CH_{3Lev}), 28.1 (CH_{2Lev}), 21.3 (CH_{3STol}), 17.5 (C-6); HRMS (ESI-TOF) m/z [M + NH₄]⁺ calcd for C₃₃H₃₉N₄O₇S 635.2534; found 635.2540.

***para*-Methylphenyl 2-*O*-*ortho*-(Azidomethyl)benzoyl-3-*O*-benzyl-1-thio- α -L-rhamnopyranoside (38).**

AcOH (2.4 mL) and hydrazine monohydrate (139 μ L, 2.87 mmol, 5.0 equiv) were successively added to a solution of compound **37** (409 mg, 0.662 mmol, 1.0 equiv) in anhydrous pyridine (3.7 mL) at 0 °C. The mixture was stirred at rt for 16 h under an Ar atmosphere then co-evaporated with toluene. The residue was purified by silica gel flash chromatography (Hex/EtOAc 9:1 to 8:2) to give alcohol **38** (313 mg, 91%) as a yellow oil: R_f 0.67 (Hex/EtOAc 6:4); [α]_D²⁰ -23 (c 1.1, CHCl₃); ¹H NMR (600 MHz, CDCl₃) δ (ppm) 8.02-8.01 (m, 1H, CH_{AZMB}), 7.57-7.55 (m, 1H, CH_{AZMB}), 7.59-7.48 (m, 1H, CH_{AZMB}), 7.41-7.38 (m, 3H, CH_{AZMB}, 2 × CH_{STol}), 7.32-7.29 (m, 5H, 5 × CH_{Bn}), 7.14-7.12 (m, 2H, 2 × CH_{STol}), 5.82 (dd, J₂₋₃ = 2.7 Hz, J₂₋₁ = 1.6 Hz, 1H, H-2), 5.50 (br s, 1H, H-1), 4.79 (d, J = 11.3 Hz, 1H, CHH_{Bn}), 4.74 (s, 2H, CH_{2AZMB}), 4.54 (d, J = 11.3 Hz, 1H, CHH_{Bn}), 4.27 (dq, J₅₋₄ = 9.3 Hz, J₅₋₆ = 6.2 Hz, 1H, H-5), 3.83 (dd, J₃₋₄ = 9.4 Hz, J₃₋₂ = 3.1 Hz, 1H, H-3), 3.74 (t, J = 9.4 Hz, 1H, H-4), 2.33 (s, 3H, CH_{3STol}), 1.38 (d, J = 6.2 Hz, 3H, H-6); ¹³C NMR (150 MHz, CDCl₃) δ (ppm) 165.8 (COOR_{AZMB}), 138.2 (C_{Ar}), 137.5 (C_{Ar}), 137.4 (C_{Ar}), 133.2-128.3 (14C, C_{Ar}, 13 ×

CHAPITRE 2 – TOTAL SYNTHESIS, ISOLATION, SURFACTANT PROPERTIES, AND BIOLOGICAL EVALUATION OF ANANATOSIDES AND RELATED MACRODILACTONE-CONTAINING RHAMNOLIPIDS

CH_{Ar}), 86.7 (C-1), 78.1 (C-3), 72.4 (C-4), 71.7 (CH_{2Bn}), 70.7 (C-2), 69.4 (C-5), 53.1 (CH_{2AZMB}), 21.3 (CH_{3STol}), 17.9 (C-6); HRMS (ESI-TOF) *m/z* [M + Na]⁺ calcd for C₂₈H₂₉NaN₃O₅S 542.1720; found 542.1731; *m/z* [M + K]⁺ calcd for C₂₈H₂₉KN₃O₅S 558.1460; found 558.1470.

***para*-Methylphenyl 2-*O*-*ortho*-(Azidomethyl)benzoyl-3-*O*-benzyl-4-*O*-(*R*)-3-(((*R*)-3-hydroxydecanoyl)oxy)decanoyl-1-thio- α -L-rhamnopyranoside (39).**

Alcohol **38** (195 mg, 0.375 mmol, 1.0 equiv) and acid **10** (248 mg, 0.525 mmol, 1.4 equiv) were solubilized in anhydrous DCE (4.5 mL). To this solution were successively added DMAP (5 mg, 0.04 mmol, 0.1 equiv) and DCC (232 mg, 1.13 mmol, 3.0 equiv). The mixture was refluxed for 1 h under an Ar atmosphere, then cooled at 0 °C, filtered over Celite, and the solvents were evaporated under reduced pressure. The residue was filtered over silica gel to remove most of the impurities, then solubilized in DCM (3.7 mL). TFA (3.6 mL) was added to the latter solution and the reaction mixture was stirred at rt for 10 min after which it was quenched with saturated aqueous NaHCO₃. The organic layer was dried over MgSO₄, filtered, and evaporated under reduced pressure. The residue was purified by silica gel flash chromatography (Hex:EtOAc 9:1 to 8:2) to give alcohol **39** (245 mg, over 2 steps) as a colorless oil: *R_f* 0.63 (Hex/EtOAc 7:3); [α]²⁰_D -20 (*c* 0.7, CHCl₃); ¹H NMR (600 MHz, CDCl₃) δ (ppm) 8.05-8.03 (m, 1H, CH_{AZMB}), 7.57-7.55 (m, 1H, CH_{AZMB}), 7.49-7.48 (m, 1H, CH_{AZMB}), 7.44-7.41 (m, 1H, CH_{AZMB}), 7.37-7.36 (m, 2H, 2 \times CH_{STol}), 7.32-7.26 (m, 5H, 5 \times CH_{Bn}), 7.14-7.12 (m, 2H, 2 \times CH_{STol}), 5.79 (dd, *J*₂₋₃ = 3.2 Hz, *J*₂₋₁ = 1.8 Hz, 1H, H-2), 5.51 (d, *J* = 1.6 Hz, 1H, H-1), 5.27-5.20 (m, 2H, H-4, H-3''), 4.77-4.69 (m, 3H, CH_{2AZMB}, CHH_{Bn}), 4.52 (d, *J* = 12.1 Hz, 1H, CHH_{Bn}), 4.33 (dq, *J*₅₋₄ = 9.8 Hz, *J*₅₋₆ = 6.2 Hz, 1H, H-5), 4.00-3.96 (m, 1H, H-3'), 3.93 (dd, *J*₃₋₄ = 9.7 Hz, *J*₃₋₂ = 3.2 Hz, 1H, H-3), 2.61 (dd, *J*_{2a''-2b''} = 16.0 Hz, *J*_{2a''-3''} = 7.2 Hz, 1H, H-2a''), 2.51 (dd, *J*_{2b''-2a''} = 16.0 Hz, *J*_{2b''-3''} = 5.4 Hz, 1H, H-2b''), 2.45 (dd, *J*_{2a'-2b'} = 16.1 Hz, *J*_{2a'-3'} = 2.9 Hz, 1H, H-2a'), 2.36-2.32 (m, 4H, H-2b', CH_{3STol}), 1.62-1.24 (m, 27H, H-6, 12 \times CH₂), 0.89-0.86 (m, 6H, 2 \times CH₃); ¹³C NMR (150 MHz, CDCl₃) δ (ppm) 172.5, 169.7 (2C, C-1', C-1''), 165.9 (COOR_{AZMB}), 138.4 (C_{Ar}), 137.6 (C_{Ar}), 137.5 (C_{Ar}), 133.2-127.8 (15C, 2 \times C_{Ar}, 13 \times CH_{Ar}), 86.4 (C-1), 75.2 (C-3), 73.2 (C-4), 71.5 (CH_{2Bn}), 71.0, 70.9 (2C, C-2, C-3''), 68.3 (C-3'), 67.8 (C-5), 53.1 (CH_{2AZMB}), 41.8 (C-2'), 38.9 (C-2''), 36.7-22.8 (12C, 12 \times CH₂), 21.3 (CH_{3STol}), 17.7 (C-

CHAPITRE 2 – TOTAL SYNTHESIS, ISOLATION, SURFACTANT PROPERTIES, AND BIOLOGICAL EVALUATION OF ANANATOSIDES AND RELATED MACRODILACTONE-CONTAINING RHAMNOLIPIDS

6), 14.2 (2C, 2 × CH₃); HRMS (ESI-TOF) *m/z* [M + NH₄]⁺ calcd for C₄₈H₆₉N₄O₉S 877.4780; found 877.4756; *m/z* [M + Na]⁺ calcd for C₄₈H₆₅NaN₃O₉S 882.4334; found 882.4313.

Macrolide 40.

Alcohol **39** (101 mg, 0.116 mmol, 1.0 equiv) and NIS (42 mg, 0.19 mmol, 1.6 equiv) were dried under high vacuum for 1 h. Activated 4 Å MS (400 mg, 4 mg•mg⁻¹ of alcohol **39**) and anhydrous DCE (11.6 mL) were added and the suspension was stirred under an Ar atmosphere for 1 h. The mixture was cooled to 0 °C and TMSOTf (8 μL, 0.05 mmol, 0.4 equiv) was added. The suspension was stirred at 0 °C for 1 h, quenched with Et₃N, and filtered over Celite. The solvents were evaporated under reduced pressure and the residue was purified by silica gel flash chromatography (Hex/EtOAc 9:1) to give macrolactone **40** (63 mg, 74%) as a colorless oil: *R_f* 0.70 (Hex/EtOAc 7:3); [α]_D²⁰ -50 (*c* 0.6, CHCl₃); ¹H NMR (600 MHz, CDCl₃) δ (ppm) 8.11-8.10 (m, 1H, CH_{AZMB}), 7.60-7.57 (m, 1H, CH_{AZMB}), 7.51-7.50 (m, 1H, CH_{AZMB}), 7.40-7.37 (m, 1H, CH_{AZMB}), 7.21-7.19 (m, 3H, 3 × CH_{Bn}), 7.16-7.13 (m, 2H, 2 × CH_{Bn}), 5.43-5.39 (m, 1H, H-3''), 5.20 (s, 1H, H-1), 5.15 (d, *J* = 5.7 Hz, 1H, H-2), 4.81 (d, *J* = 4.0 Hz, 1H, H-4), 4.75 (d, *J* = 14.6 Hz, 1H, CHH_{AZMB}), 4.70 (d, *J* = 14.6 Hz, 1H, CHH_{AZMB}), 4.63 (d, *J* = 11.8 Hz, 1H, CHH_{Bn}), 4.49 (d, *J* = 11.8 Hz, 1H, CHH_{Bn}), 4.29 (br t, *J* = 4.9 Hz, 1H, H-3), 4.25-4.21 (m, 1H, H-3'), 3.96 (q, *J* = 6.8 Hz, 1H, H-5), 2.57 (dd, *J*_{2a''-2b''} = 12.7 Hz, *J*_{2a''-3''} = 11.1 Hz, 1H, H-2a''), 2.50-2.41 (m, 3H, H-2b'', H-2a', H-2b'), 1.69-1.53 (m, 4H, 2 × CH₂), 1.47 (d, *J* = 6.8 Hz, 3H, H-6), 1.31-1.21 (m, 20H, 10 × CH₂), 0.88 (t, *J* = 7.0 Hz, 3H, CH₃), 0.83 (t, *J* = 7.0 Hz, 3H, CH₃); ¹³C NMR (150 MHz, CDCl₃) δ (ppm) 172.8, 170.9 (2C, C-1', C-1''), 165.6 (COOR_{AZMB}), 137.9-128.1 (12C, 3 × C_{Ar}, 9 × CH_{Ar}), 94.3 (C-1, ¹*J*_{Cl-H1} = 173 Hz), 73.5 (CH_{2Bn}), 73.2 (C-2), 72.2 (C-3), 71.5, 71.4, 71.1 (3C, C-3', C-3'', C-4), 68.4 (C-5), 53.1 (CH_{2AZMB}), 41.4 (C-2''), 40.3 (C-2'), 35.5-22.7 (12C, 12 × CH₂), 20.9 (C-6), 14.22 (CH₃), 14.17 (CH₃); HRMS (ESI-TOF) *m/z* [M + Na]⁺ calcd for C₄₁H₅₇NaN₃O₉ 758.3987; found 758.4010; *m/z* [M + K]⁺ calcd for C₄₁H₅₇KN₃O₉ 774.3726; found 774.3742.

CHAPITRE 2 – TOTAL SYNTHESIS, ISOLATION, SURFACTANT PROPERTIES, AND BIOLOGICAL EVALUATION OF ANANATOSIDES AND RELATED MACRODILACTONE-CONTAINING RHAMNOLIPIDS

Macrolide S10.

PPh₃ (30 mg, 0.12 mmol, 1.6 equiv) was added to a solution of compound **40** (53 mg, 0.072 mmol, 1.0 equiv) in anhydrous THF (2.2 mL). The mixture was stirred at 60 °C for 2 h under an Ar atmosphere, after which H₂O (0.3 mL) was added. The solution was stirred at 60 °C for 4 h and co-evaporated with toluene. The residue was purified by silica gel flash chromatography (Hex/EtOAc 95:5 to 9:1) to give compound **S10** (30 mg, 72%) as a colorless oil: *R_f* 0.61 (Hex/EtOAc 7:3); [α]_D²⁰ -90 (*c* 0.2, CHCl₃); ¹H NMR (600 MHz, CDCl₃) δ (ppm) 7.38-7.31 (m, 5H, 5 × CH_{Bn}), 5.40-5.36 (m, 1H, H-3''), 4.94 (s, 1H, H-1), 4.82 (d, *J* = 3.8 Hz, 1H, H-4), 4.77 (d, *J* = 11.4 Hz, 1H, CHH_{Bn}), 4.55 (d, *J* = 11.4 Hz, 1H, CHH_{Bn}), 4.19-4.14 (m, 2H, H-3'), 3.93 (dd, *J* = 6.0 Hz, 3.9 Hz, 1H, H-3), 3.87-3.81 (m, 2H, H-2, H-5), 3.17 (d, *J* = 10.9 Hz, 1H, OH), 2.52 (dd, *J*_{2a''-2b''} = 12.8 Hz, *J*_{2a''-3''} = 11.0 Hz, 1H, H-2a''), 2.47 (dd, *J*_{2a'-2b'} = 13.0 Hz, *J*_{2a'-3'} = 3.2 Hz, 1H, H-2a'), 2.43-2.40 (m, 2H, H-2b', H-2b''), 1.71-1.44 (m, 4H, 2 × CH₂), 1.40 (d, *J* = 6.8 Hz, 3H, H-6), 1.30-1.26 (m, 20H, 10 × CH₂), 0.88 (t, *J* = 6.7 Hz, 6H, 2 × CH₃); ¹³C NMR (150 MHz, CDCl₃) δ (ppm) 172.8, 170.9 (2C, C-1', C-1''), 136.8 (C_{Bn}), 128.9 (2C, 2 × CH_{Bn}), 128.5 (C_{Bn}), 128.3 (2C, 2 × CH_{Bn}), 97.8 (C-1), 73.8 (C-3), 73.6 (CH_{2Bn}), 71.4, 71.0, 70.8 (3C, C-3', C-3'', C-4), 68.4 (C-2), 67.5 (C-5), 41.4 (C-2''), 40.4 (C-2'), 35.4-22.8 (12C, 12 × CH₂), 20.9 (C-6), 14.2 (2C, 2 × CH₃); HRMS (ESI-TOF) *m/z* [M + Na]⁺ calcd for C₃₃H₅₂NaO₈ 599.3554; found 599.3564; *m/z* [M + K]⁺ calcd for C₃₃H₅₂KO₈ 615.3294; found 615.3302.

(1→4)-Macrolactonized Rhamnolipid (4).

Pd black (41 mg, 1 mg•mg⁻¹ of alcohol **S10**) was added to a solution of alcohol **S10** (41 mg, 0.072 mmol, 1.0 equiv) in DCE (0.7 mL) and MeOH (1.4 mL). The suspension was stirred under H₂ atmosphere at 40 °C for 16 h, filtered over Celite, and evaporated under reduced pressure. The residue was purified by silica gel flash chromatography (Hex/EtOAc 9:1 to 6:4) to give diol **4** (31 mg, 88%) as a colorless oil: *R_f* 0.28 (Hex/EtOAc 6:4); [α]_D²⁰ -71 (*c* 0.5, CHCl₃); ¹H NMR (600 MHz, CDCl₃) δ (ppm) 5.43-5.39 (m, 1H, H-3''), 4.97 (s, 1H, H-1), 4.73 (d, *J* = 4.1 Hz, 1H, H-4), 4.17-4.13 (m, 1H, H-3'), 3.88-3.84 (m, 2H, H-2, H-5), 2.80 (d, *J* = 8.4 Hz, 1H, OH), 2.54-2.41 (m,

CHAPITRE 2 – TOTAL SYNTHESIS, ISOLATION, SURFACTANT PROPERTIES, AND BIOLOGICAL EVALUATION OF ANANATOSIDES AND RELATED MACRODILACTONE-CONTAINING RHAMNOLIPIDS

5H, OH, H-2a'', H-2b'', H-2a', H-2b'), 1.73-1.47 (m, 4H, 2 × CH₂), 1.43 (d, *J* = 6.9 Hz, 3H, H-6), 1.30-1.26 (m, 20H, 10 × CH₂), 0.89-0.86 (m, 6H, 2 × CH₃); ¹³C NMR (150 MHz, CDCl₃) δ (ppm) 172.7, 170.8 (2C, C-1', C-1''), 97.8 (C-1), 73.9 (C-4), 71.6 (C-3''), 71.2 (C-3'), 69.0, 68.2, 67.8 (3C, C-2, C-3, C-5), 41.3, 40.4 (2C, C-2', C-2''), 35.4-22.8 (12C, 12 × CH₂), 21.4 (C-6), 14.2 (2C, 2 × CH₃); HRMS (ESI-TOF) *m/z* [M + NH₄]⁺ calcd for C₂₆H₅₀NO₈ 504.3531; found 504.3525; *m/z* [M + Na]⁺ calcd for C₂₆H₄₆NaO₈ 509.3085; found 509.3078. Analytical HPLC analysis was performed using method A (39.4 min.).

***para*-Methylphenyl**

3-*O*-Benzyl-2-*O*-(*R*)-3-(((*R*)-3-((*tert*-

butyldimethylsilyl)oxy)decanoyl)oxy)decanoyl-4-*O*-levulinoyl-1-thio- α -L-rhamnopyranoside (29).

DMAP (5 mg, 0.04 mmol, 0.1 equiv) and DCC (244 mg, 1.18 mmol, 3.0 equiv) were added to a solution of alcohol **36** (181 mg, 0.394 mmol, 1.0 equiv) and acid **10** (261 mg, 0.551 mmol, 1.4 equiv) in anhydrous DCE (4.7 mL). The suspension was refluxed for 1 h under an Ar atmosphere then cooled at 0 °C, filtered over Celite, and the solvents were evaporated under reduced pressure. The residue was purified by silica gel flash chromatography (Hex/EtOAc 97:3 to 92:8) to give compound **29** (323 mg, 90%) as a colorless oil: *R_f* 0.46 (Hex/EtOAc 8:2); [α]_D²⁰ -20 (*c* 0.6, CHCl₃); ¹H NMR (600 MHz, CDCl₃) δ (ppm) 7.35-7.32 (m, 4H, 2 × CH_{STol}, 2 × CH_{Bn}), 7.30-7.28 (m, 3H, 3 × CH_{Bn}), 7.12-7.11 (m, 2H, 2 × CH_{STol}), 5.60 (dd, *J*₂₋₃ = 3.2 Hz, *J*₂₋₁ = 1.7 Hz, 1H, H-2), 5.33 (d, *J* = 1.5 Hz, 1H, H-1), 5.18-5.14 (m, 1H, H-3''), 5.04 (t, *J* = 9.7 Hz, 1H, H-4), 4.64 (d, *J* = 12.0 Hz, 1H, CHH_{Bn}), 4.43 (d, *J* = 12.0 Hz, 1H, CHH_{Bn}), 4.26 (dq, *J*₅₋₄ = 9.6 Hz, *J*₅₋₆ = 6.1 Hz, 1H, H-5), 4.07-4.03 (m, 1H, H-'), 3.79 (dd, *J*₃₋₄ = 9.7 Hz, *J*₃₋₂ = 3.3 Hz, 1H, H-3), 2.81-2.76 (m, 1H, CHH_{Lev}), 2.71-2.56 (m, 4H, H-2a'', H-2b'', CHH_{Lev}, CHH_{Lev}), 2.50-2.44 (m, 1H, CHH_{Lev}), 2.42 (dd, *J*_{2a'-2b'} = 14.8 Hz, *J*_{2a'-3'} = 5.9 Hz, 1H, H-2a'), 2.37 (dd, *J*_{2b'-2a'} = 14.8 Hz, *J*_{2b'-3'} = 6.8 Hz, 1H, H-2b'), 2.32 (s, 3H, CH_{3STol}), 2.17 (s, 3H, CH_{3Lev}), 1.59-1.21 (m, 27H, 12 × CH₂, H-6), 0.90-0.82 (m, 15H, 2 × CH₃, C(CH₃)_{3TBS}), 0.03 (s, 3H, CH_{3TBS}), 0.02 (s, 3H, CH_{3TBS}); ¹³C NMR (150 MHz, CDCl₃) δ (ppm) 206.5 (CO_{Lev}), 172.0, 171.1, 169.8 (3C, C-1', C-1'', COOR_{Lev}), 138.2 (C_{Ar}), 137.7 (C_{Ar}), 132.4-128.0 (10C, C_{Ar}, 9 × CH_{Ar}), 86.4 (C-1), 75.0 (C-3), 72.9 (C-4), 71.6 (CH_{2Bn}), 70.5, 70.3 (2C, C-3'', C-2), 69.4 (C-3'),

CHAPITRE 2 – TOTAL SYNTHESIS, ISOLATION, SURFACTANT PROPERTIES, AND BIOLOGICAL EVALUATION OF ANANATOSIDES AND RELATED MACRODILACTONE-CONTAINING RHAMNOLIPIDS

67.9 (C-5), 42.9 (C-2'), 38.9 (C-2''), 38.0 (CH_{2Lev}), 37.4-22.8 (17C, 12 × CH₂, CH_{2Lev}, CH_{3Lev}, C(CH₃)_{3TBS}), 18.2 (C(CH₃)_{3TBS}), 17.5 (C-6), 14.2 (2C, 2 × CH₃), -4.5 (2C, 2 × CH_{3TBS}); HRMS (ESI-TOF) *m/z* [M + NH₄]⁺ calcd for C₅₁H₈₄NO₁₀SSi 930.5580; found 930.5605; *m/z* [M + Na]⁺ calcd for C₅₁H₈₀NaO₁₀SSi 935.5134; found 935.5159.

***para*-Methylphenyl 3-*O*-Benzyl-2-*O*-(*R*)-3-((*R*)-3-(hydroxydecanoyl)oxy)decanoyl-4-*O*-levulinoyl-1-thio- α -L-rhamnopyranoside (42).**

TFA (2.7 mL) was added to a solution of compound **29** (256 mg, 0.280 mmol, 1.0 equiv) in DCM (2.8 mL). The mixture was stirred at rt for 10 min and quenched with saturated aqueous NaHCO₃. The organic layer was dried over MgSO₄, filtered, and the solvents were evaporated under reduced pressure. The residue was purified by silica gel flash chromatography (Hex/EtOAc 9:1 to 8:2) to give alcohol **42** (158 mg, 70%) as a colorless oil: *R_f* 0.39 (Hex/EtOAc 7:3); [α]_D²⁰ -26 (*c* 0.9, CHCl₃); ¹H NMR (600 MHz, CDCl₃) δ (ppm) 7.36-7.32 (m, 4H, 2 × CH_{Bn}, 2 × CH_{STol}), 7.30-7.28 (m, 3H, 3 × CH_{Bn}), 7.12-7.11 (m, 2H, 2 × CH_{STol}), 5.60 (dd, *J*₂₋₃ = 3.2 Hz, *J*₂₋₁ = 1.7 Hz, 1H, H-2), 5.35 (d, *J* = 1.4 Hz, 1H, H-1), 5.25-5.21 (m, 1H, H-3''), 5.04 (t, *J* = 9.8 Hz, 1H, H-4), 4.64 (d, *J* = 12.0 Hz, 1H, CHH_{Bn}), 4.43 (d, *J* = 12.0 Hz, 1H, CHH_{Bn}), 4.26 (dq, *J*₅₋₄ = 9.9 Hz, *J*₅₋₆ = 6.2 Hz, 1H, H-5), 3.95-3.91 (m, 1H, H-3'), 3.79 (dd, *J*₃₋₄ = 9.7 Hz, *J*₃₋₂ = 3.3 Hz, 1H, H-3), 2.79 (ddd, *J* = 18.3 Hz, *J* = 8.0 Hz, *J* = 5.8 Hz, 1H, CHH_{Lev}), 2.69-2.64 (m, 3H, CHH_{Lev}, H-2a'', H-2b''), 2.58 (ddd, *J* = 17.2 Hz, *J* = 8.0 Hz, *J* = 5.5 Hz, 1H, CHH_{Lev}), 2.48 (dt, *J* = 17.2 Hz, *J* = 6.2 Hz, 1H, CHH_{Lev}), 2.37 (dd, *J*_{2a'-2b'} = 15.9 Hz, *J*_{2a'-3'} = 3.3 Hz, 1H, H-2a'), 2.34-2.29 (m, 4H, CH_{3STol}, H-2b'), 2.18 (s, 3H, CH_{3Lev}), 1.59-1.21 (m, 27H, H-6, 12 × CH₂), 0.89-0.86 (m, 6H, 2 × CH₃); ¹³C NMR (150 MHz, CDCl₃) δ (ppm) 206.5 (CO_{Lev}), 172.6, 172.0, 170.0 (3C, COOR_{Lev}, C-1', C-1''), 138.2 (C_{Ar}), 137.6 (C_{Ar}), 132.4-128.0 (10C, C_{Ar}, 9 × CH_{Ar}), 86.3 (C-1), 74.9 (C-3), 72.9 (C-4), 71.6 (CH_{2Bn}), 70.9 (C-3''), 70.4 (C-2), 68.3 (C-3'), 67.9 (C-5), 41.8 (C-2'), 39.1 (C-2''), 38.0 (CH_{2Lev}), 36.7-22.7 (14C, 12 × CH₂, CH_{2Lev}, CH_{3Lev}), 17.4 (C-6), 14.2 (2C, 2 × CH₃); HRMS (ESI-TOF) *m/z* [M + Na]⁺ calcd for C₄₅H₆₆NaO₁₀S 821.4269; found 821.4270.

CHAPITRE 2 – TOTAL SYNTHESIS, ISOLATION, SURFACTANT PROPERTIES, AND BIOLOGICAL EVALUATION OF ANANATOSIDES AND RELATED MACRODILACTONE-CONTAINING RHAMNOLIPIDS

Macrolide 43.

Alcohol **29** (120 mg, 0.150 mmol, 1.0 equiv) and NIS (54 mg, 0.24 mmol, 1.6 equiv) were dried under high vacuum for 1 h. Activated 4 Å MS (480 mg, 4 mg•mg⁻¹ of alcohol **29**) and anhydrous DCE (15 mL) were added and the suspension was stirred under an Ar atmosphere for 1 h. The mixture was cooled to -10 °C and TMSOTf (11 µL, 0.06 mmol, 0.4 equiv) was added. The suspension was stirred at -10 °C for 35 min, quenched with Et₃N, and filtered over Celite. The solvents were evaporated under reduced pressure and the residue was purified by silica gel flash chromatography (Hex/EtOAc 9:1 to 8:2) to give macrolactone **43** (78 mg, 77%) as a 15:85 α/β mixture as a colorless oil: *R_f* 0.20 (Hex/EtOAc 7:3); ¹H NMR (600 MHz, CDCl₃) δ (ppm) (data for major β-anomer) 7.37-7.27 (m, 5H, 5 × CH_{Bn}), 5.55-5.49 (m, 1H, H-3''), 5.42 (dd, *J*₂₋₃ = 3.7 Hz, *J*₂₋₁ = 1.9 Hz, 1H, H-2), 4.97 (t, *J* = 9.0 Hz, 1H, H-4), 4.78 (d, *J* = 12.2 Hz, 1H, CHH_{Bn}), 4.67 (d, *J* = 1.9 Hz, 1H, H-1), 4.50 (d, *J* = 12.2 Hz, 1H, CHH_{Bn}), 3.92-3.88 (m, 1H, H-3'), 3.58 (dd, *J*₃₋₄ = 9.2 Hz, *J*₃₋₂ = 3.7 Hz, 1H, H-3), 3.49 (dq, *J*₅₋₄ = 8.7 Hz, *J*₅₋₆ = 6.3 Hz, 1H, H-5), 2.80-2.75 (m, 1H, CHH_{Lev}), 2.72-2.66 (m, 2H, CHH_{Lev}, H-2a''), 2.60-2.49 (m, 4H, CH_{2Lev}, H-2b'', H-2a'), 2.38 (dd, *J*_{2b'-2a'} = 12.3 Hz, *J*_{2b'-3'} = 2.2 Hz, 1H, H-2b'), 2.17 (s, 3H, CH_{3Lev}), 1.73-1.26 (m, 27H, 12 × CH₂, H-6), 0.88 (t, *J* = 4.9 Hz, 6H, 2 × CH₃); ¹³C NMR (150 MHz, CDCl₃) δ (ppm) (data for major β-anomer) 206.5 (CO_{Lev}), 172.1, 171.9, 171.8 (3C, C-1', C-1'', COOR_{Lev}), 137.8 (C_{Bn}), 128.5 (2C, 2 × CH_{Bn}), 128.1 (2C, 2 × CH_{Bn}), 127.9 (C_{Bn}), 96.1 (C-1, ¹*J*_{Cl-H1} = 162 Hz), 76.6 (C-3'), 75.8 (C-3), 72.32, 72.30 (2C, C-3'', C-4), 71.4 (CH_{2Bn}), 70.9 (C-5), 68.7 (C-2), 41.5, 41.3 (2C, C-2', C-2''), 38.0 (CH_{2Lev}), 34.7-22.7 (14C, 12 × CH₂, CH_{2Lev}, CH_{3Lev}), 18.1 (C-6), 14.2 (2 × CH₃); HRMS (ESI-TOF) *m/z* [M + NH₄]⁺ calcd for C₃₈H₆₂NO₁₀ 692.4368; found 692.4374; *m/z* [M + Na]⁺ calcd for C₃₈H₅₈NaO₁₀ 697.3922; found 697.3928.

Macrolides S11β and S11α.

To a solution of compound **43** (66 mg, 0.098 mmol, 1.0 equiv) in anhydrous THF/MeOH (10:1 v/v, 6.9 mL) was slowly added a solution of hydrazine monohydrate (67 µL, 1.4 mmol, 14 equiv) and HOAc (167 µL) in anhydrous THF/MeOH (5:1 v/v, 1.4 mL). The solution was stirred under an Ar

CHAPITRE 2 – TOTAL SYNTHESIS, ISOLATION, SURFACTANT PROPERTIES, AND BIOLOGICAL EVALUATION OF ANANATOSIDES AND RELATED MACRODILACTONE-CONTAINING RHAMNOLIPIDS

atmosphere for 1 h until a white solid was formed and TLC showed complete conversion. The suspension was co-evaporated with toluene and the anomers were rapidly purified by silica gel flash chromatography (Tol/EtOAc 95:5 to 9:1) to give macrolides **S11 β** (β -anomer, 42 mg, 74%) and **S11 α** (α -anomer, 11.6 mg, 21%, contaminated with 15% of compound **43**) as colorless oils.

Data for compound **S11 β** : R_f 0.50 (Tol/EtOAc 8:2); $[\alpha]_D^{20} +10$ (c 0.6, CHCl₃); ¹H NMR (600 MHz, CDCl₃) δ (ppm) 7.35-7.30 (m, 5H, 5 \times CH_{Bn}), 5.56-5.52 (m, 1H, H-3''), 5.43 (dd, $J_{2-3} = 3.1$ Hz, $J_{2-1} = 1.4$ Hz, 1H, H-2), 4.93 (d, $J = 11.0$ Hz, 1H, CHH_{Bn}), 4.65 (d, $J = 1.3$ Hz, 1H, H-1), 4.43 (d, $J = 11.0$ Hz, 1H, CHH_{Bn}), 3.89-3.85 (m, 1H, H-3'), 3.50 (t, $J = 9.3$ Hz, 1H, H-4), 3.42 (dd, $J_{3-4} = 9.5$ Hz, $J_{3-2} = 3.5$ Hz, 1H, H-3), 3.36 (dq, $J_{5-4} = 9.0$ Hz, $J_{5-6} = 6.1$ Hz, 1H, H-5), 2.69 (dd, $J_{2a''-2b''} = 13.2$ Hz, $J_{2a''-3''} = 12.1$ Hz, 1H, H-2a''), 2.56-2.52 (m, 2H, H-2b'', H-2a'), 2.38 (dd, $J_{2a'-2b'} = 12.1$ Hz, $J_{2a'-3'} = 2.1$ Hz, 1H, H-2b'), 2.32 (s, 1H, OH), 1.54-1.21 (m, 4H, 2 \times CH₂), 1.37 (d, $J = 6.1$ Hz, 3H, H-6), 1.31-1.26 (m, 20H, 10 \times CH₂), 0.89-0.87 (m, 6H, 2 \times CH₃); ¹³C NMR (150 MHz, CDCl₃) δ (ppm) 172.2, 172.1 (2C, C-1', C-1''), 137.3 (C_{Bn}), 128.8 (2C, 2 \times CH_{Bn}), 128.6 (2C, 2 \times CH_{Bn}), 128.3 (CH_{Bn}), 96.0 (C-1, ¹ $J_{C1-H1} = 156$ Hz), 79.3 (C-3), 76.0 (C-3'), 72.5, 72.4 (2C, C-5, C-3''), 71.6 (CH_{2Bn}), 71.0 (C-4), 68.6 (C-2), 41.4, 41.2 (2C, C-2', C-2''), 34.7-22.8 (12C, 12 \times CH₂), 18.0 (C-6), 14.2 (2C, 2 \times CH₃); HRMS (ESI-TOF) m/z [M + NH₄]⁺ calcd for C₃₃H₅₆NO₈ 594.4000; found 594.4013; m/z [M + Na]⁺ calcd for C₃₃H₅₂NaO₈ 599.3554; found 599.3569.

Partial data for compound **S11 α** (contaminated with 15% of compound **43**): R_f 0.34 (Tol/EtOAc 8:2); HRMS (ESI-TOF) m/z [M + NH₄]⁺ calcd for C₃₃H₅₆NO₈ 594.4000; found 594.3999; m/z [M + Na]⁺ calcd for C₃₃H₅₂NaO₈ 599.3554; found 599.3556.

(1 \rightarrow 2)-Macrolactonized Rhamnolipid 5 β .

To a solution of **S11 β** (12.3 mg, 0.0260 mmol, 1.0 equiv) in MeOH (0.5 mL) and DCE (0.3 mL) was added Pd black (12.3 mg, 1 mg \cdot mg⁻¹ of alcohol **S11 β**). The suspension was stirred at 40 °C under an atmosphere of H₂ for 16 h then filtered over Celite. The solvents were evaporated under reduced pressure and the residue was purified by silica gel flash chromatography (Hex/EtOAc 8:2 to 1:1) to give macrolactone **5 β** (9 mg, 86%) as a colorless oil: R_f 0.38 (DCM/MeOH 95:5); $[\alpha]_D^{20}$

CHAPITRE 2 – TOTAL SYNTHESIS, ISOLATION, SURFACTANT PROPERTIES, AND BIOLOGICAL EVALUATION OF ANANATOSIDES AND RELATED MACRODILACTONE-CONTAINING RHAMNOLIPIDS

–22 (*c* 1.3, CHCl₃); ¹H NMR (600 MHz, CDCl₃) δ (ppm) 5.37-5.33 (m, 1H, H-3''), 4.96 (dd, *J* = 1.5 Hz, 3.3 Hz, 1H, H-2), 4.68 (d, *J* = 1.0 Hz, 1H, H-1), 3.92-3.89 (m, 1H, H-3'), 3.71-3.69 (m, 1H, H-3), 3.45-3.41 (m, 2H, H-4, H-5), 2.68 (t, *J* = 11.7 Hz, 1H, H-2a''), 2.52 (t, *J* = 12.6 Hz, 1H, H-2a'), 2.47 (dd, *J*_{2b''-2a''} = 12.1 Hz, *J*_{2b''-3''} = 1.7 Hz, 1H, H-2b''), 2.38 (dd, *J*_{2b'-2a'} = 12.9 Hz, *J*_{2b'-3'} = 1.9 Hz, 1H, H-2b'), 1.72-1.54 (m, 4H, 2 × CH₂), 1.39 (d, *J* = 5.1 Hz, 3H, H-6), 1.30-1.26 (m, 20H, 10 × CH₂), 0.89-0.87 (m, 6H, 2 × CH₃); ¹³C NMR (150 MHz, CDCl₃) δ (ppm) 174.3, 172.9 (2C, C-1', C-1''), 97.2 (C-1), 76.5 (C-3'), 73.8 (C-2), 73.1, 73.0, 72.8 (3C, C-3, C-4, C-5), 72.3 (C-3''), 41.13, 41.12 (2C, C-2', C-2''), 35.0-22.7 (12C, 12 × CH₂), 18.1 (C-6), 14.2 (2C, 2 × CH₃); HRMS (ESI-TOF) *m/z* [M + NH₄]⁺ calcd for C₂₆H₅₀NO₈ 504.3531; found 504.3534; *m/z* [M + Na]⁺ calcd for C₂₆H₄₆NaO₈ 509.3085; found 509.3087. Analytical HPLC analysis was performed using method B (32.1 min.).

(1→2)-Macrolactonized Rhamnolipid 5a.

To a solution of **S11a** (8.8 mg, 0.015 mmol, 1.0 equiv) in MeOH (0.3 mL) and DCE (0.2 mL) was added Pd black (8.8 mg, 1 mg•mg⁻¹ of alcohol **S11a**). The suspension was stirred at 40 °C under an atmosphere of H₂ for 16 h then filtered over Celite. The solvents were evaporated under reduced pressure and the residue was purified by silica gel flash chromatography (Hex/EtOAc 8:2 to 6:4) to give macrolactone **5a** (6.3 mg, 85%) as a colorless oil: *R_f* 0.36 (DCM/MeOH 95:5); [α]_D²⁰ –54 (*c* 0.5, CHCl₃); ¹H NMR (600 MHz, CDCl₃) δ (ppm) 5.37-5.35 (m, 1H, H-3''), 5.15 (dd, *J*₂₋₁ = 6.8 Hz, *J*₂₋₃ = 2.6 Hz, 1H, H-2), 5.04 (d, *J* = 6.8 Hz, 1H, H-1), 4.26-4.24 (m, 1H, H-3'), 3.88 (br s, 1H, H-5), 3.83 (p, *J* = 6.5 Hz, 1H, H-5), 3.56 (d, *J* = 6.8 Hz, 1H, H-4), 2.57-2.52 (m, 2H, H-2a'', H-2a'), 2.44 (dd, *J*_{2b''-2a''} = 11.8 Hz, *J*_{2b''-3''} = 2.7 Hz, 1H, H-2b''), 2.33 (dd, *J*_{2b'-2a'} = 14.5 Hz, *J*_{2b'-3'} = 3.0 Hz, H-2b'), 1.79-1.33 (m, 6H, 3 × CH₂), 1.30 (d, *J* = 6.4 Hz, 3H, H-6), 1.22-1.19 (m, 18H, 9 × CH₂), 0.81 (t, *J* = 6.9 Hz, 6H, 2 × CH₃); ¹³C NMR (150 MHz, CDCl₃) δ (ppm) 170.9, 170.2 (2C, C-1', C-1''), 91.9 (C-1), 76.8 (C-4), 76.3 (C-3'), 73.8 (C-3), 72.7 (C-2), 71.4 (C-3''), 71.0 (C-5), 41.1 (C-2''), 38.8 (C-2'), 35.2-22.8 (12C, 12 × CH₂), 19.1 (C-6), 14.2 (2 × CH₃); HRMS (ESI-TOF) *m/z* [M + NH₄]⁺ calcd for C₂₆H₅₀NO₈ 504.3531; found 504.3532; *m/z* [M + Na]⁺ calcd for

CHAPITRE 2 – TOTAL SYNTHESIS, ISOLATION, SURFACTANT PROPERTIES, AND BIOLOGICAL EVALUATION OF ANANATOSIDES AND RELATED MACRODILACTONE-CONTAINING RHAMNOLIPIDS

C₂₆H₄₆NaO₈ 509.3085; found 509.3086. Analytical HPLC analysis was performed using method B (47.3 min.).

***para*-Methylphenyl 2-*O*-*ortho*-(Azidomethyl)benzoyl-4-*O*-levulinoyl-1-thio- α -L-rhamnopyranoside (45).**

To a solution of rhamnoside **34** (248 mg, 0.383 mmol, 1.0 equiv) in DCM/H₂O (10:1, 8.4 mL) was added DDQ (174 mg, 0.766 mmol, 2.0 equiv). The reaction mixture was stirred at rt for 4 h then quenched with saturated aqueous NaHCO₃. The aqueous phase was extracted with DCM (3 \times) and the combined organic layers were washed with saturated aqueous NaHCO₃ and brine. The organic phase was dried over MgSO₄, filtered, and the solvents were evaporated under reduced pressure. The residue was purified by silica gel flash chromatography (Hex:EtOAc 9:1 to 65:35) to give alcohol **45** (187 mg, 93%) as a colorless oil: *R*_f 0.42 (Hex/EtOAc 1:1); [α]_D²⁰ -99 (*c* 0.3, CHCl₃); ¹H NMR (600 MHz, CDCl₃) δ (ppm) 8.06-8.04 (m, 1H, CH_{AZMB}), 7.58-7.55 (m, 1H, CH_{AZMB}), 7.47-7.46 (m, 1H, CH_{AZMB}), 7.44-7.42 (m, 1H, CH_{AZMB}), 7.39-7.38 (m, 2H, 2 \times CH_{STol}), 7.14-7.12 (m, 2H, 2 \times CH_{STol}), 5.62 (dd, *J*₂₋₃ = 3.4 Hz, *J*₂₋₁ = 1.5 Hz, 1H, H-2), 5.54 (d, *J* = 1.3 Hz, 1H, H-1), 5.08 (t, *J* = 9.8 Hz, 1H, H-4), 4.83 (d, *J* = 14.4 Hz, 1H, CHH_{AZMB}), 4.70 (d, *J* = 14.4 Hz, 1H, CHH_{AZMB}), 4.40 (dq, *J*₅₋₄ = 9.8 Hz, *J*₅₋₆ = 6.2 Hz, 1H, H-5), 4.18 (dd, *J*₃₋₄ = 9.8 Hz, *J*₃₋₂ = 3.3 Hz, 1H, H-3), 3.22 (br s, 1H, OH), 2.89-2.78 (m, 2H, CH_{2Lev}), 2.67-2.61 (m, 2H, CH_{2Lev}), 2.33 (s, 3H, CH_{3STol}), 2.20 (s, 3H, CH_{3Lev}), 1.28 (d, *J* = 6.2 Hz, 3H, H-6); ¹³C NMR (150 MHz, CDCl₃) δ (ppm) 207.3 (CO_{Lev}), 173.2 (COOR_{Lev}), 166.2 (COOR_{AZMB}), 138.3 (C_{Ar}), 137.1 (C_{Ar}), 133.3-128.5 (10C, 2 \times C_{Ar}, 8 \times CH_{Ar}), 86.2 (C-1), 75.4-75.2 (C-2, C-4), 69.3 (C-3), 67.4 (C-5), 53.6 (CH_{2AZMB}), 38.3 (CH_{2Lev}), 29.9 (CH_{3Lev}), 28.3 (CH_{2Lev}), 21.3 (CH_{3STol}), 17.5 (C-6); HRMS (ESI-TOF) *m/z* [M + NH₄]⁺ calcd for C₂₆H₃₃N₄O₇S 545.2065; found 545.2070; *m/z* [M + Na]⁺ calcd for C₂₆H₂₉NaN₃O₇S 550.1618; found 550.1619.

CHAPITRE 2 – TOTAL SYNTHESIS, ISOLATION, SURFACTANT PROPERTIES, AND BIOLOGICAL EVALUATION OF ANANATOSIDES AND RELATED MACRODILACTONE-CONTAINING RHAMNOLIPIDS

para-Methylphenyl 2-*O*-*ortho*-(Azidomethyl)benzoyl-3-*O*-(*R*)-3-(((*R*)-3-((*tert*-butyldimethylsilyl)oxy)decanoyl)oxy)decanoyl-4-*O*-levulinoyl-1-thio- α -L-rhamnopyranoside (30).

DMAP (4 mg, 0.03 mmol, 0.1 equiv) and DCC (206 mg, 0.996 mmol, 3.0 equiv) were successively added to a solution of alcohol **45** (175 mg, 0.332 mmol, 1.0 equiv) and acid **22** (220 mg, 0.465 mmol, 1.4 equiv) in anhydrous DCE (4 mL). The reaction mixture was refluxed for 2 h under an Ar atmosphere then cooled at 0 °C, filtered over Celite, and the solvents were evaporated under reduced pressure. The residue was purified by silica gel flash chromatography (Hex/EtOAc 97:3 to 87:13) to give compound **30** (326 mg, quant.) as a colorless oil: R_f 0.44 (Hex/EtOAc 8:2); $[\alpha]_D^{20} -3$ (c 0.4, CHCl₃); ¹H NMR (600 MHz, CDCl₃) δ (ppm) 8.06-8.05 (m, 1H, CH_{AZMB}), 7.60-7.57 (m, 1H, CH_{AZMB}), 7.52-7.51 (m, 1H, CH_{AZMB}), 7.45-7.42 (m, 1H, CH_{AZMB}), 7.39-7.38 (m, 2H, 2 \times CH_{STol}), 7.14-7.13 (m, 2H, 2 \times CH_{STol}), 5.71 (dd, $J_{2-3} = 3.3$ Hz, $J_{2-1} = 1.6$ Hz, 1H, H-2), 5.48 (d, $J = 1.3$ Hz, 1H, H-1), 5.40 (dd, $J_{3-4} = 10.1$ Hz, $J_{3-2} = 3.3$ Hz, 1H, H-3), 5.28 (t, $J = 9.9$ Hz, 1H, H-4), 5.14-5.10 (m, 1H, H-3''), 4.82 (d, $J = 14.7$ Hz, 1H, CHH_{AZMB}), 4.79 (d, $J = 14.7$ Hz, 1H, CHH_{AZMB}), 4.46 (dq, $J_{5-4} = 12.4$ Hz, $J_{5-6} = 6.2$ Hz, 1H, H-5), 4.08-4.04 (m, 1H, H-3'), 2.82-2.71 (m, 2H, CH_{2Lev}), 2.57-2.55 (m, 4H, CH_{2Lev}, H-2a'', H-2b''), 2.45 (dd, $J_{2a'-2b'} = 14.8$ Hz, $J_{2a'-3'} = 5.8$ Hz, 1H, H-2a'), 2.37 (d, $J_{2b'-2a'} = 14.8$ Hz, $J_{2b'-3'} = 6.9$ Hz, 1H, H-2b'), 2.33 (s, 3H, CH_{3STol}), 2.18 (s, 3H, CH_{3Lev}), 1.56-1.19 (m, 27H, 12 \times CH₂, H-6), 0.88-0.85 (m, 15H, 2 \times CH₃, C(CH₃)₃TBS), 0.06 (s, 3H, CH₃TBS), 0.04 (s, 3H, CH₃TBS); ¹³C NMR (150 MHz, CDCl₃) δ (ppm) 206.3 (CO_{Lev}), 172.0, 171.1, 169.6 (3C, C-1', C-1'', COOR_{Lev}), 165.5 (COOR_{AZMB}), 138.4 (C_{Ar}), 137.7 (C_{Ar}), 133.4-128.0 (10C, 2 \times C_{Ar}, 8 \times CH_{Ar}), 86.1 (C-1), 72.5 (C-2), 71.5 (C-4), 70.2 (C-3''), 69.7, 69.4 (2C, C-3, C-3'), 67.9 (C-5), 53.2 (CH₂AZMB), 42.9 (C-2'), 38.8 (C-2''), 37.9 (CH₂Lev), 37.4-22.8 (16C, 12 \times CH₂, CH₃Lev, C(CH₃)₃TBS), 21.3 (CH₃STol), 18.2 (C(CH₃)₃TBS), 17.5 (C-6), 14.3 (CH₃), 14.2 (CH₃), -4.5 (2C, 2 \times CH₃TBS); HRMS (ESI-TOF) m/z [M + H]⁺ calcd for C₅₂H₈₀N₃O₁₁SSi 982.5277; found 982.5286; m/z [M + Na]⁺ calcd for C₅₂H₇₉NaN₃O₁₁SSi 1004.5097; found 1004.5111.

CHAPITRE 2 – TOTAL SYNTHESIS, ISOLATION, SURFACTANT PROPERTIES, AND BIOLOGICAL EVALUATION OF ANANATOSIDES AND RELATED MACRODILACTONE-CONTAINING RHAMNOLIPIDS

para-Methylphenyl 2-*O*-*ortho*-(Azidomethyl)benzoyl-3-*O*-(*R*)-3-((*R*)-3-(hydroxy decanoyl)oxy)decanoyl-4-*O*-levulinoyl-1-thio- α -L-rhamnopyranoside (**46**).

TFA (3 mL) was slowly added to a solution of compound **30** (307 mg, 0.313 mmol, 1.0 equiv) in DCM (3.1 mL). The reaction mixture was stirred at rt for 10 min then quenched with saturated aqueous NaHCO₃. The organic layer was dried over MgSO₄, filtered, and the solvents were evaporated under reduced pressure. The residue was purified by silica gel flash chromatography (Hex/EtOAc 9:1 to 7:3) to give alcohol **46** (227 mg, 84%) as a colorless oil: *R*_f 0.51 (Hex/EtOAc 6:4); [α]_D²⁰ -28 (*c* 0.7, CHCl₃); ¹H NMR (600 MHz, CDCl₃) δ (ppm) 8.06-8.05 (m, 1H, CH_{AZMB}), 7.61-7.58 (m, 1H, CH_{AZMB}), 7.52-7.51 (m, 1H, CH_{AZMB}), 7.46-7.43 (m, 1H, CH_{AZMB}), 7.40-7.38 (m, 2H, 2 \times CH_{STol}), 7.14-7.13 (m, 2H, 2 \times CH_{STol}), 5.73 (dd, *J*₂₋₃ = 3.3 Hz, *J*₂₋₁ = 1.6 Hz, 1H, H-2), 5.47 (d, *J* = 1.4 Hz, 1H, H-1), 5.41 (dd, *J*₃₋₄ = 10.1 Hz, *J*₃₋₂ = 3.3 Hz, 1H, H-3), 5.27 (t, *J* = 9.9 Hz, 1H, H-4), 5.22-5.18 (m, 1H, H-3''), 4.82 (d, *J* = 14.6 Hz, 1H, CHH_{AZMB}), 4.77 (d, *J* = 14.6 Hz, 1H, CHH_{AZMB}), 4.46 (dq, *J*₅₋₄ = 9.9 Hz, *J*₅₋₆ = 6.1 Hz, 1H, H-5), 3.99-3.95 (m, 1H, H-3'), 2.77-2.75 (m, 2H, CH_{2Lev}), 2.64-2.52 (m, 4H, CH_{2Lev}, H-2a'', H-2b''), 2.45 (dd, *J*_{2a'-2b'} = 15.8 Hz, *J*_{2a'-3'} = 3.2 Hz, 1H, H-2a'), 2.39 (dd, *J*_{2b'-2a'} = 15.8 Hz, *J*_{2b'-3'} = 8.9 Hz, 1H, H-2b'), 2.33 (s, 3H, CH_{3STol}), 2.18 (s, 3H, CH_{3Lev}), 1.60-1.21 (m, 27H, H-6, 12 \times CH₂), 0.88-0.85 (m, 6H, 2 \times CH₃); ¹³C NMR (150 MHz, CDCl₃) δ (ppm) 206.3 (CO_{Lev}), 172.6, 172.1, 170.0 (3C, COOR_{Lev}, C-1', C-1''), 165.6 (COOR_{AZMB}), 138.4 (C_{Ar}), 137.7 (C_{Ar}), 133.4-128.0 (10C, 2 \times C_{Ar}, 8 \times CH_{Ar}), 86.1 (C-1), 72.4 (C-2), 71.5 (C-4), 70.6 (C-3''), 69.8 (C-3), 68.4 (C-3'), 67.9 (C-5), 53.2 (CH_{2AZMB}), 41.9 (C-2'), 38.8 (C-2''), 37.8 (CH_{2Lev}), 36.8-22.7 (14C, 12 \times CH₂, CH_{2Lev}, CH_{3Lev}), 21.3 (CH_{3STol}), 17.5 (C-6), 14.23 (CH₃), 14.20 (CH₃); HRMS (ESI-TOF) *m/z* [M + NH₄]⁺ calcd for C₄₆H₆₉N₄O₁₁S 885.4678; found 885.4691; *m/z* [M + Na]⁺ calcd for C₄₆H₆₅NaN₃O₁₁S 890.4232; found 890.4252.

Macrolides 47 β and 47 α .

Alcohol **46** (209 mg, 0.241 mmol, 1.0 equiv) and NIS (87 mg, 0.39 mmol, 1.6 equiv) were dried under high vacuum for 1 h. Activated 4 Å MS (836 mg, 4 mg \cdot mg⁻¹ of alcohol **46**) and anhydrous DCE (24 mL) were added and the suspension was stirred under an Ar atmosphere for 1 h. The

CHAPITRE 2 – TOTAL SYNTHESIS, ISOLATION, SURFACTANT PROPERTIES, AND BIOLOGICAL EVALUATION OF ANANATOSIDES AND RELATED MACRODILACTONE-CONTAINING RHAMNOLIPIDS

mixture was cooled to $-10\text{ }^{\circ}\text{C}$ and TMSOTf ($17\text{ }\mu\text{L}$, $96\text{ }\mu\text{mol}$, 0.4 equiv) was added. The suspension was stirred at -10 to $0\text{ }^{\circ}\text{C}$ for 45 min, quenched with Et_3N , and filtered over Celite. The solvents were evaporated under reduced pressure and the residue was purified by silica gel flash chromatography (Hex/EtOAc 9:1 to 7:3) to give macrolactone **47 β** (β -anomer, 43 mg, 24%) and macrolactone **47 α** (α -anomer, 71 mg, 39%) as yellow oils.

Data for compound **47 β** : R_f 0.60 (Hex/EtOAc 6:4); $[\alpha]_{\text{D}}^{20}$ -38 (c 0.7, CHCl_3); ^1H NMR (600 MHz, CDCl_3) δ (ppm) 8.13-8.11 (m, 1H, CH_{AZMB}), 7.59-7.56 (m, 1H, CH_{AZMB}), 7.50-7.47 (m, 2H, $2 \times \text{CH}_{\text{AZMB}}$), 5.44 (br t, $J = 3.6$ Hz, 1H, H-3), 5.31 (t, $J = 3.7$ Hz, 1H, H-2), 5.18-5.14 (m, 1H, H-3''), 5.08 (d, $J = 3.3$ Hz, 1H, H-1), 5.05 (t, $J = 3.2$ Hz, 1H, H-4), 4.93 (d, $J = 14.6$ Hz, 1H, CHH_{AZMB}), 4.77 (d, $J = 14.6$ Hz, 1H, CHH_{AZMB}), 4.09-4.05 (m, 1H, H-5), 3.92-3.87 (m, 1H, H-3'), 2.87-2.61 (m, 5H, $2 \times \text{CH}_{2\text{Lev}}$, H-2a''), 2.48 (dd, $J_{2a'-2b'} = 12.0$ Hz, $J_{2a'-3'} = 3.3$ Hz, 1H, H-2a'), 2.41-2.34 (m, 2H, H-2b', H-2b''), 2.21 (s, 3H, $\text{CH}_{3\text{Lev}}$), 1.90-1.86 (m, 1H, CHH), 1.62 (d, $J = 7.3$ Hz, 3H, H-6), 1.52-1.24 (m, 23H, $11 \times \text{CH}_2$, CHH), 0.88 (t, $J = 6.9$ Hz, 6H, $2 \times \text{CH}_3$); ^{13}C NMR (150 MHz, CDCl_3) δ (ppm) 206.4 (CO_{Lev}), 171.7, 171.5, 170.5 (3C, C-1', C-1'', COOR_{Lev}), 166.0 ($\text{COOR}_{\text{AZMB}}$), 138.0 (C_{AZMB}), 133.2-127.6 (5C, C_{AZMB} , $4 \times \text{CH}_{\text{AZMB}}$), 95.4 (C-1, $^1J_{\text{C1-H1}} = 168$ Hz), 79.3 (C-3'), 73.1 (C-4), 71.4, 71.2 (2C, C-5, C-3''), 67.9, 67.8 (2C, C-3, C-2), 53.3 ($\text{CH}_{2\text{AZMB}}$), 41.4 (C-2'), 40.6 (C-2''), 38.1 ($\text{CH}_{2\text{Lev}}$), 36.0-22.8 (14C, $\text{CH}_{2\text{Lev}}$, $\text{CH}_{3\text{Lev}}$, $12 \times \text{CH}_2$), 20.9 (C-6), 14.2 (2C, $2 \times \text{CH}_3$); HRMS (ESI-TOF) m/z $[\text{M} + \text{NH}_4]^+$ calcd for $\text{C}_{39}\text{H}_{61}\text{N}_4\text{O}_{11}$ 761.4331; found 761.4339; m/z $[\text{M} + \text{Na}]^+$ calcd for $\text{C}_{39}\text{H}_{57}\text{NaN}_3\text{O}_{11}$ 766.3885; found 766.3891.

Data for compound **47 α** : R_f 0.51 (Hex/EtOAc 6:4); $[\alpha]_{\text{D}}^{20}$ -8 (c 0.3, CHCl_3); ^1H NMR (600 MHz, CDCl_3) δ (ppm) 8.12-8.10 (m, 1H, CH_{AZMB}), 7.61-7.58 (m, 1H, CH_{AZMB}), 7.54-7.53 (m, 1H, CH_{AZMB}), 7.47-7.44 (m, 1H, CH_{AZMB}), 5.64 (dd, $J_{3-4} = 10.0$ Hz, $J_{3-2} = 3.6$ Hz, 1H, H-3), 5.40 (dd, $J_{2-3} = 3.7$ Hz, $J_{2-1} = 1.4$ Hz, 1H, H-2), 5.22-5.17 (m, 2H, H-3'', H-4), 5.03 (br s, 1H, H-1), 4.87 (d, $J = 14.7$ Hz, 1H, CHH_{AZMB}), 4.84 (d, $J = 14.7$ Hz, 1H, CHH_{AZMB}), 4.29 (dq, $J_{5-4} = 12.4$ Hz, $J_{5-6} = 6.2$ Hz, 1H, H-5), 4.26-4.22 (m, 1H, H-3'), 2.76-2.74 (m, 2H, CHH_{Lev} , CHH_{Lev}), 2.65-2.60 (m, 2H, H-2a'', H-2a'), 2.58-2.56 (m, 2H, CHH_{Lev} , CHH_{Lev}), 2.45 (dd, $J_{2b''-2a''} = 6.6$ Hz, $J_{2b''-3''} = 4.1$ Hz, 1H, H-2b''*), 2.43 (dd, $J_{2b'-2a'} = 6.5$ Hz, $J_{2b'-3'} = 4.1$ Hz, 1H, H-2b'*), 2.17 (s, 3H, $\text{CH}_{3\text{Lev}}$), 1.65-

CHAPITRE 2 – TOTAL SYNTHESIS, ISOLATION, SURFACTANT PROPERTIES, AND BIOLOGICAL EVALUATION OF ANANATOSIDES AND RELATED MACRODILACTONE-CONTAINING RHAMNOLIPIDS

1.20 (m, 27H, 12 × CH₂, H-6), 0.87-0.85 (m, 6H, 2 × CH₃); ¹³C NMR (150 MHz, CDCl₃) δ (ppm) 206.5 (CO_{Lev}), 172.4, 171.2, 168.8 (3C, C-1', C-1'', COOR_{Lev}), 165.8 (COOR_{AZMB}), 137.6-128.5 (6C, 2 × C_{AZMB}, 4 × CH_{AZMB}), 94.2 (C-1, ¹J_{Cl-H1} = 170 Hz), 72.24, 72.15, 71.8 (3C, C-2, C-4, C-3'), 70.7 (C-3''), 66.5 (C-5), 53.2 (CH_{2AZMB}), 38.8, 38.4, 37.9 (3C, C-2', C-2'', CH_{2Lev}), 34.2-22.8 (14C, CH_{2Lev}, CH_{3Lev}, 12 × CH₂), 17.3 (C-6), 14.2 (2C, 2 × CH₃); HRMS (ESI-TOF) *m/z* [M + H]⁺ calcd for C₃₉H₅₈N₃O₁₁ 744.4066; found 744.4068; *m/z* [M + NH₄]⁺ calcd for C₃₉H₆₁N₄O₁₁ 761.4331; found 761.4338.

Macrolide S12β.

PPh₃ (16 mg, 0.060 mmol, 1.2 equiv) was added to a solution of compound **47β** (38 mg, 50 μmol, 1.0 equiv) in anhydrous THF (1.5 mL). The mixture was stirred at 60 °C for 2 h under an Ar atmosphere, after which H₂O (0.2 mL) was added. The solution was stirred at 60 °C for 4 h and co-evaporated with toluene. The residue was purified by silica gel flash chromatography (Hex/EtOAc 9:1 to 75:25) to give the corresponding *O*-2 alcohol **S12β** (15 mg, 50%) as a colorless oil. *R_f* 0.35 (Hex/EtOAc 6:4); [α]²⁰_D +61 (*c* 0.3, CHCl₃); ¹H NMR (600 MHz, CDCl₃) δ (ppm) 5.54-5.48 (m, 1H, H-3''), 5.18 (t, *J* = 3.9 Hz, 1H, H-3), 4.97 (t, *J* = 3.8 Hz, 1H, H-4), 4.89 (d, *J* = 2.5 Hz, 1H, H-1), 4.10-4.06 (m, 1H, H-3'), 3.99 (dt, *J*_{2-OH} = 12.6 Hz, *J*_{2-1, 2-3} = 3.6 Hz, 1H, H-2), 3.93-3.87 (m, 1H, H-5), 3.40 (d, *J* = 12.6 Hz, 1H, OH), 2.82-2.46 (m, 8H, 2 × CH_{2Lev}, H-2a'', H-2b'', H-2a', H-2b'), 2.18 (s, 3H, CH_{3Lev}), 1.80-1.52 (m, 4H, 2 × CH₂), 1.40 (d, *J* = 7.0 Hz, 3H, H-6), 1.30-1.26 (m, 20H, 10 × CH₂), 0.90-0.87 (m, 6H, 2 × CH₃); ¹³C NMR (150 MHz, CDCl₃) δ (ppm) 206.3 (CO_{Lev}), 175.1, 171.6, 170.1 (3C, C-1', C-1'', COOR_{Lev}), 98.2 (C-1), 78.5 (C-3'), 73.4 (C-4), 71.2 (C-3), 70.8 (C-3''), 70.1 (C-5), 66.9 (C-2), 41.3, 40.9 (2C, C-2', C-2''), 38.0 (CH_{2Lev}), 35.7-22.8 (14C, CH_{2Lev}, CH_{3Lev}, 12 × CH₂), 20.5 (C-6), 14.2 (2C, 2 × CH₃); HRMS (ESI-TOF) *m/z* [M + NH₄]⁺ calcd for C₃₁H₅₆NO₁₀ 602.3899; found 602.3904; *m/z* [M + Na]⁺ calcd for C₃₁H₅₂NaO₁₀ 607.3453; found 607.3454.

CHAPITRE 2 – TOTAL SYNTHESIS, ISOLATION, SURFACTANT PROPERTIES, AND BIOLOGICAL EVALUATION OF ANANATOSIDES AND RELATED MACRODILACTONE-CONTAINING RHAMNOLIPIDS

(1→3)-Macrolactonized Rhamnolipid 6 β .

To a solution of alcohol **S12 β** (13 mg, 22 μ mol, 1.0 equiv) in anhydrous THF/MeOH (10:1 *v/v*, 1.5 mL) was added a solution of hydrazine monohydrate (15 μ L, 0.30 mmol, 14 equiv) and HOAc (37 μ L) in anhydrous THF/MeOH (5:1 *v/v*, 0.3 mL). The solution was stirred at rt under an Ar atmosphere for 30 min until a white precipitate was formed. The suspension was co-evaporated with toluene and the residue was purified by silica gel flash chromatography (Hex/EtOAc 8:2) to give macrolactone **6 β** (β -anomer, 8.3 mg, 79%) as a colorless oil: R_f 0.47 (Hex/EtOAc 6 :4); $[\alpha]_D^{20}$ -47 (*c* 0.6, CHCl₃); ¹H NMR (600 MHz, CDCl₃) δ (ppm) 5.59-5.55 (m, 1H, H-3''), 4.80 (d, J = 0.9 Hz, 1H, H-1), 4.68 (dd, J_{3-2} = 5.6 Hz, J_{3-4} = 3.9 Hz, 1H, H-3), 4.10-4.04 (m, 3H, H-2, H-3', OH), 3.71-3.65 (m, 2H, H-4, H-5), 3.36 (d, J = 12.8 Hz, 1H, OH), 2.80 (dd, $J_{2a''-2b''}$ = 18.3 Hz, $J_{2a''-3''}$ = 11.3 Hz, 1H, H-2a''), 2.66 (dd, $J_{2b''-2a''}$ = 18.3 Hz, $J_{2b''-3''}$ = 1.4 Hz, 1H, H-2b''), 2.55 (dd, $J_{2a'-2b'}$ = 13.4 Hz, $J_{2a'-3'}$ = 3.8 Hz, 1H, H-2a'), 2.44 (dd, $J_{2b'-2a'}$ = 13.4 Hz, $J_{2b'-3'}$ = 11.4 Hz, 1H, H-2b'), 1.73-1.26 (m, 27H, 12 \times CH₂, H-6), 0.89-0.83 (m, 6H, 2 \times CH₃); 175.0, 171.8 (2C, C-1', C-1''), 99.6 (C-1), 79.5, 79.2 (2C, C-3, C-3'), 74.9 (C-4), 69.3, 69.1 (2C, C-3'', C-5), 66.9 (C-2), 40.9 (C-2'), 39.6 (C-2''), 35.0-22.8 (12C, 12 \times CH₂), 19.9 (C-6), 14.2 (2C, 2 \times CH₃); HRMS (ESI-TOF) m/z [M + NH₄]⁺ calcd for C₂₆H₅₀NO₈ 504.3531; found 504.3537; m/z [M + Na]⁺ calcd for C₂₆H₄₆NaO₈ 509.3085; found 509.3094. Analytical HPLC analysis was performed using method B (45.4 min.).

Macrolide S12 α .

PPh₃ (30 mg, 0.12 mmol, 1.2 equiv) was added to a solution of macrolactone **47 α** (71 mg, 95 μ mol, 1.0 equiv) in anhydrous THF (2.9 mL). The mixture was stirred at 60 °C for 2 h under an Ar atmosphere, after which H₂O (0.4 mL) was added. The solution was stirred at 60 °C for 4 h and co-evaporated with toluene. The residue was purified by silica gel flash chromatography (Tol/EtOAc 95:5 to 85:15) to give *O*-2 alcohol **S12 α** (28 mg, 50%) as a colorless oil: R_f 0.32 (Tol/EtOAc 8:2); $[\alpha]_D^{20}$ -60 (*c* 0.9, CHCl₃); ¹H NMR (600 MHz, CDCl₃) δ (ppm) 5.45 (dd, J_{3-4} = 9.9 Hz, J_{3-2} = 3.6 Hz, 1H, H-3), 5.31-5.28 (m, 1H, H-3''), 5.08 (t, J = 10.0 Hz, 1H, H-4), 4.90 (s, 1H, H-1), 4.25-4.23 (m, 1H, H-3'), 4.10-4.05 (m, 2H, H-2, H-5), 2.75-2.70 (m, 3H, CH_{2Lev}, H-2a''), 2.60-2.54 (m, 3H,

CHAPITRE 2 – TOTAL SYNTHESIS, ISOLATION, SURFACTANT PROPERTIES, AND BIOLOGICAL EVALUATION OF ANANATOSIDES AND RELATED MACRODILACTONE-CONTAINING RHAMNOLIPIDS

CH_{2Lev} , H-2b''), 2.47-2.43 (m, 2H, H-2a', H-2b'), 2.29 (d, $J = 2.6$ Hz, 1H, OH), 2.17 (s, 3H, CH_{3Lev}), 1.65-1.21 (m, 27H, $12 \times CH_2$, H-6), 0.89-0.86 (m, 6H, $2 \times CH_3$); ^{13}C NMR (150 MHz, $CDCl_3$) δ (ppm) 206.5 (CO_{Lev}), 172.3, 170.8, 169.0 (3C, C-1', C-1'', $COOR_{Lev}$), 95.5 (C-1), 71.83, 71.75, 71.5 (3C, C-3, C-4, C-3''), 70.3 (C-3'), 69.7 (C-5), 66.3 (C-2), 39.4, 38.8 (C-2', C-2''), 37.9 (CH_{2Lev}), 34.4-22.8 (14C, CH_{2Lev} , CH_{3Lev} , $12 \times CH_2$), 18.3 (C-6), 14.24 (CH_3), 14.23 (CH_3); HRMS (ESI-TOF) m/z $[M + NH_4]^+$ calcd for $C_{31}H_{56}NO_{10}$ 602.3899; found 602.3907; m/z $[M + Na]^+$ calcd for $C_{31}H_{52}NaO_{10}$ 607.3453; found 607.3459.

(1→3)-Macrolactonized Rhamnolipid 6a.

To a solution of alcohol **S12a** (25 mg, 42 μ mol, 1.0 equiv) in anhydrous THF/MeOH (10:1 v/v, 3 mL) was added a solution of hydrazine monohydrate (29 μ L, 0.59 mmol, 14 equiv) and HOAc (72 μ L) in anhydrous THF/MeOH (5:1 v/v, 0.6 mL). The solution was stirred at rt under an Ar atmosphere for 30 min until a white precipitate was formed. The suspension was co-evaporated with toluene and the residue was purified by preparative TLC (DCM/MeOH 94:6) to give macrolactone **6a** (α -anomer, 13 mg, 63%) as a colorless oil: R_f 0.45 (DCM/MeOH 95 :5); $[\alpha]_D^{20} -16$ (c 0.8, $CHCl_3$); 1H NMR (600 MHz, $CDCl_3$) δ (ppm) 5.26 (dd, $J_{3-4} = 9.6$ Hz, $J_{3-2} = 3.4$ Hz, 1H, H-3), 5.17-5.12 (m, 1H, H-3''), 4.86 (s, 1H, H-1), 4.28-4.26 (m, 1H, H-3'), 3.92-3.87 (m, 2H, H-2, H-5), 3.44 (t, $J = 9.7$ Hz, 1H, H-4), 2.74 (dd, $J_{2a''-2b''} = 16.0$ Hz, $J_{2a''-3''} = 2.6$ Hz, 1H, H-2a''), 2.66 (dd, $J_{2b''-2a''} = 16.0$ Hz, $J_{2b''-3''} = 10.7$ Hz, 1H, H-2b''), 2.46 (dd, $J_{2a'-2b'} = 15.8$ Hz, $J_{2a'-3'} = 2.3$ Hz, 1H, H-2a'), 2.40 (dd, $J_{2b'-2a'} = 15.9$ Hz, $J_{2b'-3'} = 10.1$ Hz, 1H, H-2b'), 1.72-1.46 (m, 4H, $2 \times CH_2$), 1.33 (d, $J = 6.2$ Hz, 3H, H-6), 1.28-1.26 (m, 20H, $10 \times CH_2$), 0.88 (t, $J = 6.8$ Hz, 6H, $2 \times CH_3$); ^{13}C NMR (150 MHz, $CDCl_3$) δ (ppm) 171.4, 170.5 (2C, C-1', C-1''), 96.7 (C-1), 74.7 (C-3), 73.0 (C-3'), 72.6 (C-4), 71.3 (C-3''), 70.7, 68.4 (2C, C-2, C-5), 39.3 (C-2'), 39.1 (C-2''), 34.2-22.8 (12C, $12 \times CH_2$), 17.2 (C-6), 14.2 (2C, $2 \times CH_3$); HRMS (ESI-TOF) m/z $[M + H]^+$ calcd for $C_{26}H_{47}O_8$ 487.3265; found 487.3976. Analytical HPLC analysis was performed using method B (32.8 min.).

CHAPITRE 2 – TOTAL SYNTHESIS, ISOLATION, SURFACTANT PROPERTIES, AND BIOLOGICAL EVALUATION OF ANANATOSIDES AND RELATED MACRODILACTONE-CONTAINING RHAMNOLIPIDS

2.7.3 Experimental procedures for biological evaluation and surfactant properties

Antimicrobial Activity and Synergy Testing.

Minimum inhibitory concentration (MIC) determinations and synergy testing were performed for *Pseudomonas aeruginosa* ED14, *Pseudomonas aeruginosa* ED639, *Staphylococcus aureus* MRSA ED711, *Staphylococcus aureus* ED94, *Escherichia coli* DH5 α , *Bacillus subtilis* PY79, *Candida albicans* ATCC 10231, and *Candida albicans* LSPQ 0199 by the checkerboard method in 96 well plates with Mueller-Hinton broth. Kanamycin and tetracyclin (antibiotics used as controls) were tested at concentrations ranging from 3.125 to 37.5 $\mu\text{g}\cdot\text{mL}^{-1}$, and ananatoside A (**1**), ananatoside B (**2**), and RhaC₁₀C₁₀ (**3**) were tested at concentrations ranging from 1.5625 to 37.5 $\mu\text{g}\cdot\text{mL}^{-1}$. The biosurfactants were serially diluted along the ordinate, while the antibiotics were diluted along the abscissa. Overnight cultures of each microorganism were diluted by 1000-fold in Mueller-Hinton broth, and added to each well with the corresponding combination of compounds. The plates were incubated aerobically overnight at 30 °C and 200 rpm. Control wells were included with each run. Fractional inhibitory concentrations (ΣFICs) were calculated as follows: $\Sigma\text{FIC} = \text{FIC A} + \text{FIC B}$, where FIC A is the MIC of compound A in the combination/MIC of compound A alone, and FIC B is the MIC of compound B in the combination/MIC of compound B alone. The combination is considered synergistic when the ΣFIC is ≤ 0.5 , indifferent when the ΣFIC is >0.5 to <2 , and antagonistic when the ΣFIC is ≥ 2 .²¹⁵

Cell Culture.

Human lung carcinoma (A549), human colorectal adenocarcinoma (DLD-1), and human normal skin fibroblasts (WS1) cell lines were obtained from the American Type Culture Collection (ATCC). All cell lines were cultured in minimum essential medium containing Earle's salts and L-glutamine (Mediatech Cellgro, VA), to which were added 10% foetal bovine serum (Hyclone), vitamins (1 \times), penicillin (100 IU $\cdot\text{mL}^{-1}$), streptomycin (100 $\mu\text{g}\cdot\text{mL}^{-1}$), essential amino acids (1 \times), and sodium pyruvate (1 \times) (Mediatech Cellgro, VA). Cells were kept at 37 °C in a humidified environment containing 5% CO₂.

CHAPITRE 2 – TOTAL SYNTHESIS, ISOLATION, SURFACTANT PROPERTIES, AND BIOLOGICAL EVALUATION OF ANANATOSIDES AND RELATED MACRODILACTONE-CONTAINING RHAMNOLIPIDS

Cytotoxicity Assay.

Exponentially growing A549, DLD-1 or WS1 cells were plated in 96-well microplates (Costar, Corning Inc.) at a density of 5×10^3 cells per well in 100 μL of culture medium and were allowed to adhere for 16 h prior treatment. Increasing concentrations of each compound in biotech DMSO (Sigma-Aldrich) were then added (100 μL per well) and the cells were incubated for 48 h. The final concentration of DMSO in the culture medium was maintained at 0.5% (v/v) to avoid solvent toxicity. Cytotoxicity was assessed using resazurin²¹⁶ on an automated 96-well Fluoroskan Ascent F1™ plate reader (Labsystems) using excitation and emission wavelengths of 530 and 590 nm, respectively. Fluorescence was proportional to the cellular metabolic activity in each well. Survival percentage was defined as the fluorescence in experimental wells as compared to that in control wells after subtraction of blank values. Each experiment was carried out three times in triplicate. IC₅₀ results were expressed as means \pm standard deviation.

Hemolytic Activity.

The hemolytic activity of the synthetic surfactants was evaluated as previously described with small modifications.²¹⁷ Defibrinated sheep blood (Oxoid) was centrifuged at $1000 \times g$ for 5 min. The pellet containing erythrocytes was washed once and suspended in 1X PBS to obtain a 1% erythrocytes suspension. All samples were suspended in DMSO/PBS (5:1 v/v) and serially diluted in a 96-well plate to obtain a range of concentrations from 1 mM to 7.8 μM . The erythrocytes suspension (160 μL) was added to 40 μL of samples to obtain final concentrations ranging between 200 μM and 1.56 μM . Triton X-100 was used as a positive hemolysis control. The plate was then incubated at 37 °C with agitation at 150 rpm for 1 h and centrifuged at $1500 \times g$ for 5 min. The supernatant was transferred in an empty plate and absorbance was measured at 540 nm using a Cytation3 microplate reader (Biotek). HC₅₀ was calculated in comparison with the positive control. The experiment was performed in triplicate and repeated three times.

CHAPITRE 2 – TOTAL SYNTHESIS, ISOLATION, SURFACTANT PROPERTIES, AND BIOLOGICAL EVALUATION OF ANANATOSIDES AND RELATED MACRODILACTONE-CONTAINING RHAMNOLIPIDS

Plant Material and Growth Conditions.

Tomato plants (*Solanum lycopersicum* L var. Ailsa craig, Scotland) were grown on soil in growth chamber with white fluorescent light [$200 \mu\text{mol}\cdot(\text{m}^{-2} \text{s}^{-1})$], under 16 h/8 h light/dark regime, 60% relative humidity, and a temperature of 24/20 °C during four weeks prior treatment. *Arabidopsis thaliana* plants (ecotype Col-0) were grown on soil in growth chambers with white fluorescent light ($150 \mu\text{mol m}^{-2} \text{s}^{-1}$), under 12 h/12 h light/dark regime, 60% relative humidity, and a temperature of 20/20 °C during six weeks prior treatment.

Reactive Oxygen Species (ROS) Production.

ROS assays were performed on four-week old tomato plants or six-week old *Arabidopsis* plants. Briefly, tomato leaf disks of 6 mm diameter or *Arabidopsis* petiole sections of 5 mm long were cut and placed in a 96-well plate (Optiplate TM-96 white, PerkinElmer) containing 150 μL of distilled H_2O and then incubated at rt for 24 h to reduce the wounding response.¹⁵³ The elicitation solution containing 0.2 $\mu\text{g}\cdot\text{mL}^{-1}$ luminol (A4685-5 g, Sigma), 20 μM horseradish peroxidase (P6782, Sigma) and the tested glycolipids (**1**, **2**, **3**, **4**, **5 α** , **5 β** , **6 α** or **6 β**) at 100 μM was prepared. Methanol (0.5%) was used as negative control. Prior elicitation, the incubating distilled H_2O was carefully removed from each well, avoiding any tissue damage or desiccation. Then, the elicitation solution (150 μL) was quickly added to each well containing a leaf disk or a petiole. Luminescence (relative light units, RLU) was measured every 4 min during 720 min with a luminometer (Tecan SPARK 10M). Data are mean \pm SEM ($n = 6$) and experiments were realized three times.

Surface Tension of Biosurfactants.

The surface tensions of ananatoside A (**1**), ananatoside B (**2**), and RhaC₁₀C₁₀ (**3**) were measured in 20 mL aliquots by the du Noüy ring method using a Fisher tensiometer model 20 (Fisher Scientific, Pittsburgh, PA). The instrument was calibrated against water and measurements were performed in triplicate at rt. The critical micelle concentration (CMC) was determined from a plot of surface tension against each concentration, where the CMC value corresponds to the intersection between

CHAPITRE 2 – TOTAL SYNTHESIS, ISOLATION, SURFACTANT PROPERTIES, AND BIOLOGICAL EVALUATION OF ANANATOSIDES AND RELATED MACRODILACTONE-CONTAINING RHAMNOLIPIDS

the regression straight line of the linearly dependent region and the straight line passing through the plateau.¹⁵⁸

Emulsification Analysis.

The emulsification activity of culture extracts was tested against kerosene, *n*-hexadecane, and cyclohexane. Aliquots (5 mg) of ananatoside A (**1**), ananatoside B (**2**), and RhaC₁₀C₁₀ (**3**) were mixed with 5 mL of each solvent and vortexed at high speed for 2 min. After 24 h, the height of the stable emulsion layer was measured. The emulsification activity (E_{24}) is calculated as the ratio of the height of the emulsion layer and the total height of liquid after 24 h.²¹⁸

Particles Size Analysis.

Size measurements were performed in triplicate for ananatoside A (**1**), ananatoside B (**2**), and RhaC₁₀C₁₀ (**3**) in pure water using dynamic light scattering (DLS) on a Malvern Zetasizer Nano-ZS (Malvern Instruments, Malvern, UK). Samples were irradiated with red light (HeNe laser, wavelength $\lambda = 632.8$ nm) and the intensity fluctuations of the scattered light (using an angle of 173°) analysed to obtain an autocorrelation function. The Z-Ave value was reported as the mean diameter of nanoparticles where the cumulant method was adopted for data analysis, data was acquired in automatic mode, the software incorporated a data quality report that indicated good quality for all data obtained.²¹⁹

2.7.4 Molecular modeling

Model compounds of macrolactonized rhamnolipids **4** to **6** were generated with ethyl groups instead of heptyl side chains (**48** to **50**) because we supposed that they would only increase the degree of liberty without improving the precision of the prediction for the chemical shifts. Both anomers were built in Avogadro²²⁰ and files were exported in MDL mol file.²²¹ The RDKit ETKDGV2 algorithm^{204, 222} was invoked in python to generate 1 000 conformers which were pruned with a RMSD threshold of 0.25 Å. The conformers were minimized using the MMFF94s force field and filtered with an energy windows of 80 kJ/mol followed by a RMSD threshold of 0.25 Å. Following this step, the

CHAPITRE 2 – TOTAL SYNTHESIS, ISOLATION, SURFACTANT PROPERTIES, AND BIOLOGICAL EVALUATION OF ANANATOSIDES AND RELATED MACRODILACTONE-CONTAINING RHAMNOLIPIDS

conformers of each isomer were aligned and inspected visually to ensure that the conformational space was thoroughly covered (Fig. S5). The conformers were further optimized at the mPW1PW91/6-31G(d,p) level of theory²²³ using Gaussian 16 (rev. C.01)²²⁴ after which a last filtration was accomplished using a 10 kJ•mol⁻¹ window. All the DFT calculations were performed with the polarizable continuum model using the integral equation formalism variant (IEFPCM) to consider the solvent effect (chloroform) and an ultrafine grid for the integrals. The number of conformers retained after each step is presented in Table S2.

The retained geometries were optimized at two additional levels of theory, mPW1PW91/6-311+G(d,p) and B97-2/cc-pVTZ,^{225, 226} after which the vibrational frequencies and thermochemical parameters were computed at each corresponding level of theory. NMR shielding tensors were computed using the gauge-independent atomic orbital (GIAO) method²²⁷ and averaged using a Boltzmann-weighting function based on the thermal free energies at 25 °C of each conformer.²²⁸ Shielding tensors for acetone and TMS were calculated at the same levels of theory and then used to compute NMR chemical shifts based on a multi-standard approach.^{205, 206} A regression analysis between experimental and referenced values was also performed to reduce systematic errors,²²⁸ but it led to the same conclusion.

The experimental and calculated chemical shifts were compared following two schemes, a classical one in which each experimental NMR dataset was separately compared against both *in silico* anomers, and the combination scheme as developed by Lauro,²⁰⁷ in which one pair of isolated anomers (ex. **5 α /5 β**) was compared against their *in silico* analogs (e.g., **49 α /49 β** or **49 β /49 α**). The comparison criterium was the maximum absolute error (MAE) in both schemes, and the ¹H and ¹³C chemical shifts were treated separately.

The conformers were categorized in conventional cyclohexane conformations assessed based on the six torsional angles of the sugar ring.²⁰⁸ The relative abundances of these conformations were evaluated for each model compounds at each level of theory. 3D representations of the most abundant conformer in each category were rendered with PyMol, while the pie charts were crafted using the ggplot2 module in R.

CHAPITRE 3 : SYNTHESIS OF OLIGOSACCHARIDES RELATED TO POTENTIAL BIOTERRORIST PATHOGENS

Maude Cloutier,^a Kevin Muru,^a Charles Gauthier^a

^aCentre Armand-Frappier Santé Biotechnologie, Institut national de la recherche scientifique (INRS), 531, boul. des Prairies, Laval (Québec), H7V 1B7, Canada

Chapitre publié dans *Recent Trends in Carbohydrate Chemistry: Synthesis and Biomedical Applications of Glycans and Glycoconjugates*, 1st edition, Ed.: Rauter, A., Christensen, B., Somsak, L., Kosma, P., Adamo, R.; 2020 Elsevier, 532 pp, doi: 10.1016/B978-0-12-820954-7.00005-0.

Titre français : Synthèse d'oligosaccharides liés à de potentiels pathogènes bioterroristes

Contribution des auteurs : Maude Cloutier et Charles Gauthier ont réalisé la revue de littérature. Maude Cloutier a rédigé la totalité du chapitre et fait les figures et schémas. Kevin Muru et Charles Gauthier ont révisé le chapitre.

3.1 Résumé

Le bioterrorisme est considéré comme une menace sérieuse dans le monde d'aujourd'hui. Certains agents pathogènes bactériens ont été répertoriés comme potentiels agents bioterroristes en raison de leurs faibles doses infectieuses, de leur capacité à être aérosolisés, de leur taux de transmission élevé et de leur tolérance à un large éventail de conditions environnementales. Cette liste comprend les agents sélectionnés de niveau 1 du CDC *Bacillus anthracis*, *Yersinia pestis*, *Francisella tularensis*, *Burkholderia pseudomallei*, et *Burkholderia mallei*. Les bactéries à Gram négatif du genre *Brucella*, même si elles ne figurent pas sur cette liste, sont également intéressantes car la brucellose est considérée comme l'une des zoonoses les plus négligées. Ces bactéries produisent à leur surface des polysaccharides hautement immunogènes, qui agissent comme des antigènes exquis pour le développement de vaccins et d'outils de diagnostic. Au cours des dernières années, un certain nombre d'oligosaccharides liés à ces potentiels agents bioterroristes ont été synthétisés. Ce chapitre de livre vise à couvrir les développements récents dans ce domaine important du point de vue du chimiste des glucides.

3.2 Abstract

Bioterrorism is seen as a serious threat in today's world. Some bacterial pathogens have been listed as potential bioterrorism agents due to their low infectious doses, ability to be aerosolized, high transmission rate, and tolerance to a wide range of environmental conditions. This list includes the CDC Tier 1 Select Agents *Bacillus anthracis*, *Yersinia pestis*, *Francisella tularensis*, *Burkholderia pseudomallei*, and *Burkholderia mallei*. Gram-negative pathogenic *Brucella* spp., even if not on this list, are also of interest as brucellosis is considered to be one of the most neglected zoonoses. These bacteria are producing highly immunogenic polysaccharides at their surface, which act as exquisite antigens for the development of vaccines and diagnostic tools. In past years, a number of oligosaccharides related to these potential bioterrorist pathogens have been synthesized. This book chapter aims at covering the recent developments in this important field from the perspective of the carbohydrate chemist.

3.3 Introduction

Bioterrorism is seen as a serious threat in today's society. Bioterrorism can be defined as the unlawful use of biological agents to infect humans in the pursuit of social and/or political aims. This threat comes from the fact that biological weapons are difficult to detect, they are easily delivered, and they are excessively cheap while being highly dangerous.²²⁹ Indeed, the cost of inflicting death or diseases on civilians per square kilometers is 2000 times smaller for biological weapons than for standard weapons.²³⁰ The risks that poses bioterrorism are also exacerbated by the availability of materials, technologies, and expertise needed for the production of biological weapons.²²⁹ The unsuccessful biological strikes attempted by the Japanese cult Aum Shinrikyo,²³¹ ²³² the *Salmonella typhimurium* intentional contamination of salad bars in Oregon by a religious commune,²³³ and the 2001 United States postal service attack with *Bacillus anthracis*²³⁴ are only few examples of the deliberate use of biological agents for wrongful reasons.

The Centers for Disease Control and Prevention (CDC) have created categories in which biological agents are classified based on the threat they pose. Categories A, B, and C represent three different levels of lethality, where category A is the highest priority. The United States Department of Health and Human Services and the United States Department of Agriculture also chose agents, called biological select agents or toxins (BSATs), which constitute the highest threat to public, animal, and plant health, based on CDC's categories. Among these agents, some have additionally been classified as "Tier 1" BSATs. These are considered to be the most important to understand for medical responders due to the high risk of being wrongfully used, their potential deadliness, and the catastrophic outcome they could have on society. "Tier 1" select agents include Gram-negative pathogenic bacteria *Yersinia pestis*, *Francisella tularensis*, *Burkholderia pseudomallei*, and *Burkholderia mallei*, as well as Gram-positive bacteria *Bacillus anthracis* (see <https://www.selectagents.gov>).

Gram-negative bacteria (GNB) produce multiple cell-surface exposed carbohydrates, such as capsular polysaccharides (CPS), lipopolysaccharides (LPS), and exopolysaccharides (EPS). These polysaccharides, which are often species-specific, are known to be virulence factors due to their key role in host-pathogen interactions and also act as targets for protective antibodies.²³⁵

Polysaccharide vaccines have proven to be useful against infectious diseases caused by virulent pathogens. To this day, a few glycoconjugate vaccines have been licensed for use, such as the Quimi-Hib vaccine, which is a semi-synthetic *Haemophilus influenzae* type b vaccine.⁴⁶ Since polysaccharides are T cell independent, meaning they can only elicit B cells responses, they are not effective in infants and young children. Conjugation of polysaccharides to carrier proteins enables them to stimulate T cells to produce protective antibodies, and the immune response is therefore more complete, no matter the age.²³⁶

In the current global context, particular attention must be paid to potential bioterrorism weapons and prophylactic measures such as vaccination must be envisaged. Glycoconjugate vaccines are attractive targets against biological weapons²³⁷ but, there are however some difficulties inherent in using native polysaccharides. Among others, it is necessary to obtain pure compounds free from bacterial contaminants and the heterogeneity of polysaccharides may jeopardize the reproducibility of their immunogenicity and protective efficacy.²³⁸ Moreover, conjugation of native polysaccharides to carrier proteins can induce structural modifications affecting the immunogenic response.²³⁹ Thanks to organic synthesis, the vast majority of these hurdles can be overcome.²⁴⁰ In addition, the synthetic oligosaccharides can also be designed in such a way to decipher the mechanisms underlying antibodies production and recognition.²⁴¹

Throughout the recent years, attention has been paid to the synthesis of pathogen-related oligosaccharides for use as vaccines and diagnostic tools. Herein, we present an account of the syntheses of *Y. pestis*, *F. tularensis*, *B. anthracis*, *B. pseudomallei*, *B. mallei*, and *Brucella* spp. related oligosaccharides. The biophysical and immunological assays, *i.e.*, antigenicity, immunogenicity, protective efficacy, and detection systems, conducted with these synthetic oligosaccharides are reviewed as well.

3.4 *Bacillus anthracis*

Bacillus anthracis is a Gram-positive, spore-forming bacterium part of the *B. cereus* group and is the causative agent of anthrax. Humans can contract it, although it is primarily an herbivore disease. Infections can present themselves in multiple ways, such as in cutaneous, gastrointestinal,

and inhalational forms, and each of them can lead to fatal systemic anthrax. If the inoculation is achieved through the gastrointestinal or inhalational pathway, diagnosis can be difficult and the disease can develop quickly into a systemic form.²⁴² Among other incidents involving *B. anthracis*, the 2001 United States mail attacks are evident reminders of the risks surrounding this bacterium as a biological weapon.

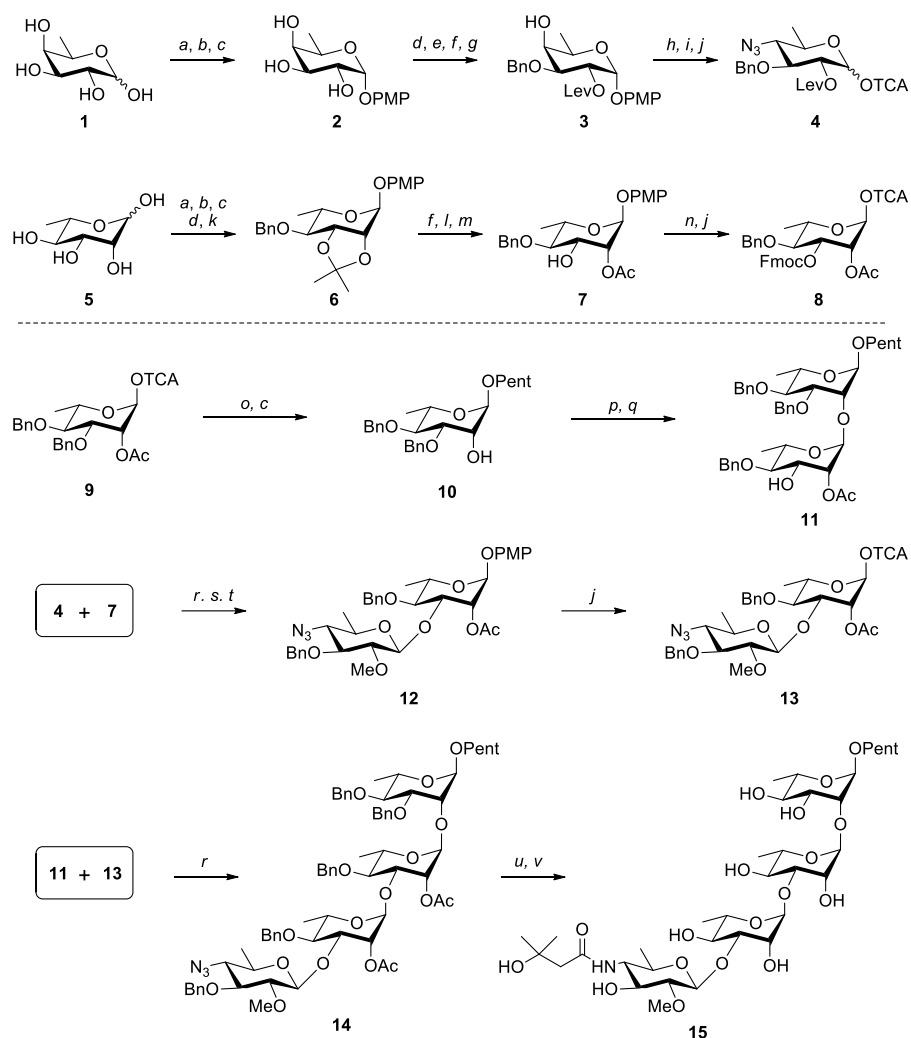
When *B. anthracis* vegetative cells lack nutrients, they produce highly resistant spores.²⁴³ It is believed that the exosporium present at the surface of the spore plays a role in pathogenesis due to its interaction with environmental factors.²⁴⁴ Rather recently, exosporium glycoprotein *Bacillus* collagen-like protein of anthracis (BclA) was characterized by Turnbough and co-workers, and they determined that its repeating oligosaccharidic portion was a tetrasaccharide of structure β -Ant-(1 \rightarrow 3)- α -L-Rha-(1 \rightarrow 3)- α -L-Rha-(1 \rightarrow 2)- α -L-Rha. The singularity of this tetrasaccharide lies in the presence of the anthrose moiety at the non-reducing end, which appears to be specific to *B. anthracis*.²⁴⁵ This makes anthrax tetrasaccharide a potential vaccine candidate and could be helpful for the development of specific diagnostic tools, motivating many teams to study its synthesis. Reported syntheses to study the role of this oligosaccharide on the immune system were also recently reviewed by Milhomme and Grandjean.²⁴⁶

As depicted in Scheme 1, Seeberger and co-workers developed a convergent [2 + 2] synthetic method to obtain tetrasaccharide **15**.²⁴⁷ This method could also enable the synthesis of analogues and shorter oligosaccharides. Their synthesis started with peracetylation of D-fucose, allowing the introduction of a *para*-methoxyphenyl (PMP) moiety at the anomeric position, and intermediate **2** was obtained following deacetylation. Hydroxyl functions at C-2 and C-3 were respectively levulinoylated and benzylated in four steps, which included protection of C-3 and C-4 hydroxyl groups as an acetal, levulinoylation at C-2, acetal removal under acidic conditions, and benzylation using dibutyltin oxide, resulting in alcohol **3**. The levulinoyl (Lev) group was introduced at the desired position because it would be useful for further installation of the β -(1 \rightarrow 3) linkage during glycosylation and could be cleaved orthogonally. The remaining hydroxyl function was converted into a triflate, which was displaced under the action of sodium azide in a S_N2-like fashion, resulting in the inversion of configuration. The PMP group was then cleaved employing cerium ammonium

CHAPITRE 3 – SYNTHESIS OF OLIGOSACCHARIDES RELATED TO POTENTIAL BIOTERRORIST PATHOGENS

nitrate (CAN), and the resulting alcohol was converted into anthrose trichloroacetimidate (TCA) **4** using standard conditions. Intermediate **6** was prepared from rhamnose **5** through general functional rearrangement steps. Treatment with HCl in methanol followed by reaction with 1,1,1-triethoxyethane and a catalytic amount of *para*-toluenesulfonic acid allowed the conversion of the acetal into an orthoester. Ring opening of the latter in a mixture of acetic acid and water provided alcohol **7** bearing the kinetically favored axial acetyl at C-2. Since α -selectivity was required to synthesize the target tetrasaccharide, the acetyl group was inserted to act as a neighboring participating group. Finally, a fluorenylmethoxycarbonyl (Fmoc) protecting group was added on the remaining alcohol function using FmocCl in pyridine and the anomeric PMP was replaced by a TCA under standard conditions, giving rise to target synthon **8**.

CHAPITRE 3 – SYNTHESIS OF OLIGOSACCHARIDES RELATED TO POTENTIAL BIOTERRORIST PATHOGENS



Scheme 3.1. Synthesis of anthrax tetrasaccharide by Seeberger⁵

Derivative **9** as well as compounds **4**, **7**, and **8** were then used in multiple glycosylations to afford tetrasaccharide **15**. First, glycosyl donor **9** was coupled with 4-pentenol under the promotion of TMSOTf, then deacetylated, giving rise to alcohol **10**. The pentenyl moiety at the anomeric

⁵ a) Ac₂O, py (**2** and **6**: quant.); b) PMPOH, BF₃·OEt₂, acetone, 0 to 25 °C (**2**: 71%; **6**: 80%); c) NaOMe, MeOH (**2**: quant.; **6**: 96%; **10**: 96%); d) 2,2-dimethoxypropane, BF₃·OEt₂, acetone, 0 to 25 °C, (**3**: 96%; **6**: 84%); e) LevOH, DMAP, DIPC, CH₂Cl₂, 0 °C, 92%; f) HCl (pH 3), MeOH, 50 °C, (**3**: 85%; **7**: 89%); g) *i.* *n*Bu₂SnO, tol, reflux; *ii.* BnBr, TBAL, tol, reflux, 95% (2 steps); h) Tf₂O, py, 0 °C; i) NaN₃, DMF, 25 °C, 80% (2 steps); j) *i.* CAN, H₂O/CH₃CN, 25 °C (**8**: 76%) then *ii.* Cl₃CCN, NaH, CH₂Cl₂, 25 °C (**4**: 78%; **8**: 94%; **13**: 95%, 2 steps); k) NaH, BnBr, DMF, 0 to 25 °C, quant.; l) 1,1,1-triethoxyethane, *p*-TsOH, DMF, 50 °C, 98% (2 steps); m) AcOH/H₂O 4:1, 10 °C, 98% (2 steps); n) FmocCl, py, 25 °C, 88%; o) 4-pentenol, TMSOTf, CH₂Cl₂, -20 °C, 79%; p) **8**, TMSOTf, CH₂Cl₂, 91%; q) piperidine, DMF, 25 °C, 89%; r) TMSOTf, CH₂Cl₂, 0 °C, (**12**: 90%; **14**: 73%); s) H₂NNH₂·HOAc, CH₂Cl₂, MeOH, 25 °C, quant.; t) MeI, Ag₂O, THF, Me₂S, 25 °C, 73%; u) Na/NH₃ (l), THF, -78 °C, 60%; v) 3-hydroxy-3-methylbutanoic acid, HATU, DIPEA, DMF, 25 °C, 75%.

CHAPITRE 3 – SYNTHESIS OF OLIGOSACCHARIDES RELATED TO POTENTIAL BIOTERRORIST PATHOGENS

position would allow further conjugation of the oligosaccharide with carrier proteins to conduct biological assays. Coupling of alcohol **10** with TCA **8** was then achieved and the resulting intermediate was converted into disaccharide glycosyl acceptor **11** by cleavage of the Fmoc protecting group employing piperidine in DMF. During the deprotection, approximately 10% of the disaccharide underwent acetyl migration from C-2 to C-3, but the undesirable compound was successfully removed by column chromatography. Meanwhile, protected disaccharide **12** was assembled by the reaction of anthroside **4** and alcohol **7** and conversion of the Lev ester into a methyl ether. Cleavage of the anomeric PMP and installation of the TCA moiety afforded disaccharide building block **13**. The latter was glycosylated with disaccharide **11** and deprotected using sodium and liquid ammonia in THF, which also reduced the azido moiety into an amine. Target tetrasaccharide **15** was finally obtained after forming the amide on the anthrose residue using hexafluorophosphate azabenzotriazole tetramethyl uronium (HATU), *N,N*-diisopropylethylamine (DIPEA), and DMF as the activating mixture and 3-hydroxy-3-methylbutanoic acid. Immunological studies through conjugation of compound **15** to keyhole limpet hemocyanin (KLH) carrier protein were conducted. Immunoglobulin G (IgG) antibodies were produced following immunization of mice. Moreover, tetrasaccharide **15** specific monoclonal IgG antibodies artificially induced in mice spleen cells did not cross-react with endospores of species related to *B. anthracis*, highlighting the sensitivity and specificity of these antibodies.²⁴⁸

Based on their previous work, Seeberger and co-workers reported a few years later the synthesis of a pentasaccharide composed of tetrasaccharide **15** α -linked to a *N*-acetylated galactosamine residue at its reducing end.²⁴⁹ The galactosamine moiety links the tetrasaccharide to BclA.²⁴⁵ Their [3 + 2] methodology proved to be challenging due to the need to differentiate the amino groups: this was achieved by masking the amine of the anthrose residue as an azide, whereas trichloroacetyl was used to mask the amine of galactosamine. To avoid undesired rearrangements such as acetyl migration while maintaining α -selectivity, a benzoyl protecting group was used rather than an acetyl group in glycosyl donor **8**, but transesterification still occurred. Following assembly of the building blocks into a protected pentasaccharide, the authors proceeded to the deprotection of the trichloroacetylated amine using a radical-initiated reaction involving tributyltin hydride in toluene

at high temperatures, and complete deprotection was achieved using standard conditions. However, the pentasaccharide composed of an α/β mixture at the anomeric carbon of the reducing end could not be separated.

Tetrasaccharide **15** was subjected to extensive immunological studies carried out by Tamborrini's group.²⁵⁰ An anthrose-rhamnose disaccharide and an anthrose monosaccharide, synthesized based on the previously reported methods, were studied as well. All three antigens were found to be immunogenic, and immunoblotting assays were also conducted to evaluate the cross-reactivity of antibodies produced by synthetic tetrasaccharide-immunized mice with the natural oligosaccharide produced by *B. anthracis*. Multiple bacterial strains were employed, showing that the generated antibodies cross-reacted with a large range of *B. anthracis* species as well as with some strains of *B. cereus*. However, the anti-tetrasaccharide and anti-disaccharide monoclonal antibodies (mAbs) did not recognize spores from the closely related strain *B. thuringiensis*. These findings were further confirmed by enzyme-linked immunosorbent assay (ELISA) and specific bead-based Luminex assays.²⁵¹ Even though the anthrose unit appeared to be not strictly specific to *B. anthracis* species, these experiments still support the possibility of using the synthetic anthrax oligosaccharides for the development of spore detection systems. Indeed, the highly sensitive Luminex assay developed in the course of this study could be a potential tool for the recognition of *B. anthracis*.

Thorough analyses of the previously described di- and tetrasaccharide, as well as of other anthrax tetrasaccharide derivatives, were also carried out to identify the minimal units required for antibody recognition.²⁵² Seeberger and co-workers showed that a combination of microarray screening, surface plasmon resonance (SPR) analysis, and saturation-transfer difference (STD)-NMR spectroscopy were useful for that matter. Indeed, these techniques indicated that the anthrose moiety was necessary for antibody-binding, and that mono-, di- and trirhamnosides were not recognized. To strongly bind to anti-tetrasaccharide mAbs, the oligosaccharide must minimally be composed of an anthrose moiety linked to a dirhamnoside. It was moreover found by SPR analysis that the strongest and fastest interaction was between the tetrasaccharide and its specific mAbs, and STD-NMR spectroscopy showed that all four sugars tightly bound to the antibody, but the

CHAPITRE 3 – SYNTHESIS OF OLIGOSACCHARIDES RELATED TO POTENTIAL BIOTERRORIST PATHOGENS

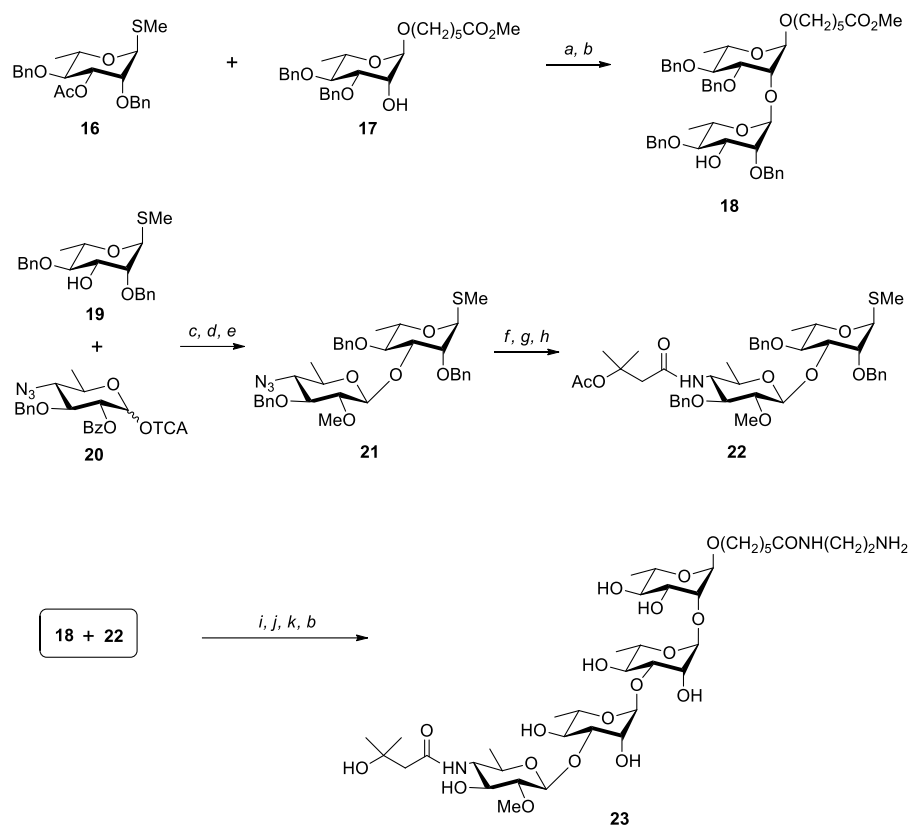
strongest effect was on the anthrose unit. The C-4 side chain of the latter showed significant STD effect, whereas the C-2 methyl ether had minor effect. These findings and the combination of these techniques could be of great interest to gain more knowledge about the complex carbohydrates-antibodies interactions.

Kováč and co-workers also extensively worked towards the synthesis of *B. anthracis* BclA tetrasaccharide. With the aim of conducting studies of inhibition and binding with anthrax tetrasaccharide specific antibodies, Kováč reported the synthesis of α - and β -5-methoxycarbonylpentenyl glycosides of the tetrasaccharide through a [1 + 1 + 1 + 1] methodology as well as fragments thereof.²⁵³⁻²⁵⁶ His group also prepared anthrose in large-scale.²⁵⁷ In another work, the tetrasaccharide and the anthrose monosaccharide were further immobilized on epoxide modified glass to create a carbohydrate microarray platform. The latter allowed the successful differentiation of *B. pseudomallei*, *F. tularensis*, and *B. anthracis* antibodies and could therefore find value in the identification of bacterial biothreat agents.²⁵⁸ Furthermore, photogenerated glycan arrays prepared from fragments and derivatives of anthrax tetrasaccharide were used to assess their biological potential.²⁵⁹ These glycan arrays were tested against anti-*B. anthracis* spore antibodies, which proved to recognize the synthetic oligosaccharides, revealing the immunogenicity of the BclA tetrasaccharide.

Following these encouraging results, Kováč *et al.* presented in 2009 an alternative, optimized strategy for the gram-scale synthesis of anthrax tetrasaccharide, involving a one-pot deprotection method (Scheme 2).²⁶⁰ Unlike the previously presented methods, they used the fully assembled anthrose as a building block instead of completing its synthesis after the construction of the tetrasaccharide. The proposed synthesis commenced with building blocks **16** and **17**, which were glycosylated employing *N*-iodosuccinimide (NIS) and AgOTf as the promoting system. The resulting disaccharide was then deacetylated to yield glycosyl acceptor **18**, containing a protected spacer arm needed for the conjugation of the tetrasaccharide to a carrier protein. The employed conditions allowed the selective formation of an α -linkage. In parallel, thioglycoside **19**, obtained following deacetylation of glycosyl donor **16**, was reacted with TCA **20** at low temperatures using TMSOTf, whose synthesis from inexpensive galactopyranoside had already been reported by

Kováč.²⁶¹ These conditions minimized the formation of an aglycon transfer by-product, whereas $\text{BF}_3 \cdot \text{OEt}_2$ exacerbated it. The benzoyl protecting group, which ensured β -selectivity during the glycosylation, was cleaved under Zemplén conditions and replaced by a methyl group following treatment with MeI in presence of KOH. The azide in resulting disaccharide **21** was converted into an amine using H_2S , allowing the introduction of the 3-hydroxy-*N*-3-dimethylbutanamide moiety employing HATU and Hünig's base in CH_2Cl_2 . The hydroxyl function of the resulting intermediate was then protected with an acetyl group, yielding disaccharide **22** containing the fully assembled anthrose moiety. [2 + 2] Glycosylation of disaccharides **18** and **22** was then achieved using NIS and AgOTf, and conducting the reaction at $-50\text{ }^\circ\text{C}$ improved the yield. Hydrogenolysis allowed the cleavage of the benzyl ether, and one-pot conversion of the anomeric methyl ester into an amine followed by deacetylation were successfully achieved in 85% yield. Since deacetylation was not complete during the conversion of the anomeric spacer arm, Zemplén deacetylation was employed to perform the reaction in a one-pot process.

CHAPITRE 3 – SYNTHESIS OF OLIGOSACCHARIDES RELATED TO POTENTIAL BIOTERRORIST PATHOGENS



Scheme 3.2. Gram-scale synthesis of anthrax tetrasaccharide by Kováč⁶

As previously mentioned, towards the immunological evaluation of anthrax tetrasaccharide, Tamborrini and co-workers produced antibodies that recognized *B. anthracis* but also cross-reacted with some *B. cereus* strains. With the aim of discriminating *B. anthracis* spores from other *Bacillus* species, Grunow studied the development of *B. anthracis* specific antibodies for its detection in complex matrices.²⁶² To achieve this, the authors immunized diverse animal models with peracetic acid- and paraformaldehyde-inactivated spores in the presence of synthetic tetrasaccharide **23**. The generated antibodies appeared to be specific to *B. anthracis* against other GNB, as revealed by ELISA, immunofluorescence assay (IFA), and capture ELISA. Even if the produced pc115 polyclonal anthrose antibody cross-reacted with one *B. cereus* strain during the

⁶ a) NIS, AgOTf, 4 Å MS, CH₂Cl₂, 91%; b) NaOMe, MeOH, (**18**: 94%; **23**: 85%, 2 steps); c) 4 Å MS, TMSOTf, CH₂Cl₂, -78 °C, 89%; d) NaOMe, MeOH, CH₂Cl₂, 50 °C, 94%; e) KOH, MeI, DMSO, 83%; f) H₂S, H₂O·py, 83%; g) HATU, Hünig's base, 3-hydroxy-3-methoxybutanoic acid, CH₂Cl₂, 85%; h) Ac₂O, DMAP, CH₂Cl₂, 93%; i) NIS, AgOTf, 4 Å MS, CH₂Cl₂, -50 °C, 71%; j) H₂, Pd/C, MeOH-EtOAc, 85%; k) H₂N(CH₂)₂NH₂, 50 °C, overnight.

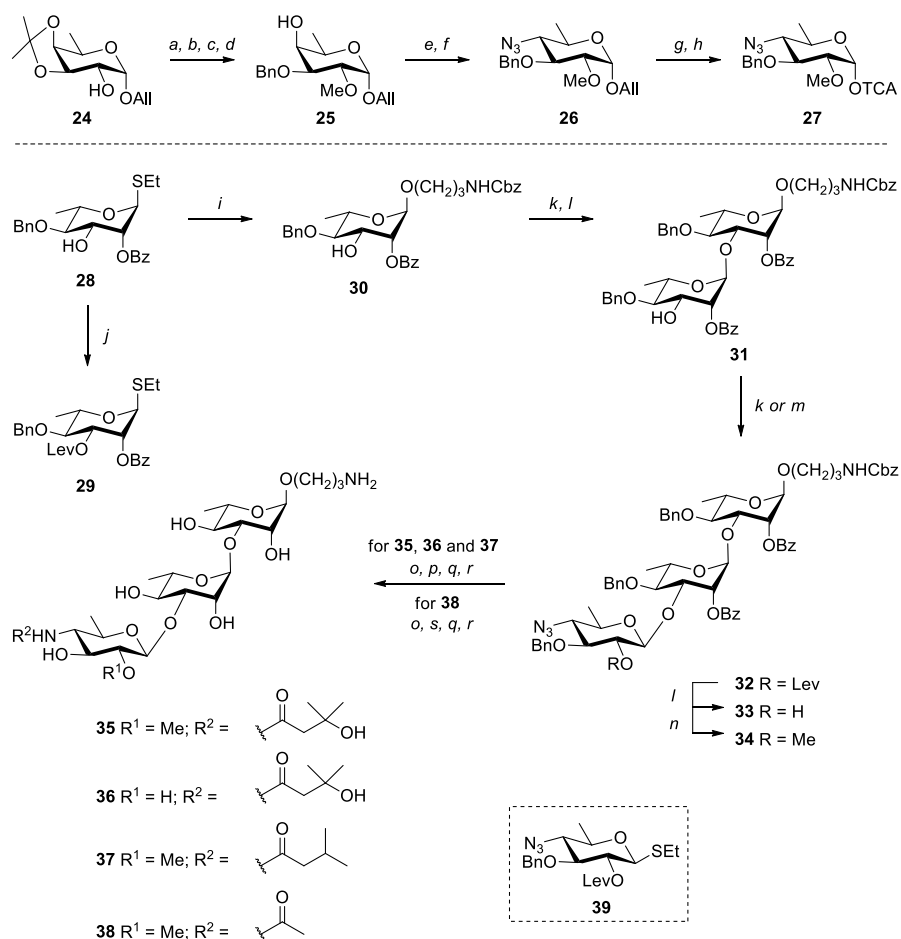
CHAPITRE 3 – SYNTHESIS OF OLIGOSACCHARIDES RELATED TO POTENTIAL BIOTERRORIST PATHOGENS

ELISA and IFA experiments, no recognition was visible following the capture ELISA assay, indicating that this strain either produced less anthrose or its spores surface oligosaccharides were not identical to those of *B. anthracis*. Therefore, the antibodies produced by Grunow's group, combined with the capture ELISA, could be employed to detect *B. anthracis* spores with high sensitivity.

Boons and co-workers studied the antigenic nature of *B. anthracis* tetrasaccharide by synthesizing four related anthrose-containing trisaccharides.²⁶³ To this end, synthon **27** was first assembled from allyl-6-deoxygalactoside **24** as shown in Scheme 3. The C-2 hydroxyl was methylated using MeI and sodium hydride. The acetal was cleaved under the action of aqueous acetic acid and the resulting alcohol was selectively benzylated using tin chemistry, providing intermediate **25**. Inversion of the configuration of the axial substituent at C-4 was achieved through the formation of a triflate and resulting allyl anthroside **26** was converted into TCA building block **27** under standard conditions. Rhamnoside **29** was obtained following levulinoylation of known intermediate **28**. In parallel, the latter was also glycosylated with *N*-carboxybenzylaminopropanol, yielding rhamnoside **30** only as the α -anomer due to the neighboring group participation (NGP) of the benzoyl moiety. Even though thiorhamnoside **28** possesses a free hydroxyl function, no self-condensation occurred since the employed glycosyl acceptor presented a much higher reactivity. Alcohol **30** was then coupled with glycosyl donor **29** and the Lev group was cleaved using hydrazinium acetate. Glycosylation of resulting disaccharide **31** was first carried out with *O*-methylated glycosyl acceptor **27** under the promotion of $\text{BF}_3 \cdot \text{OEt}_2$ in acetonitrile and at low temperatures. As a result of the formation of a nitrilium ion intermediate, protected trisaccharide **34** was generated in an 86% yield as a 1:4 mixture of α/β -anomers. In an attempt to reach a higher yield, glycosylation of dirhamnoside **31** was also performed with levulinoylated thioglycoside **39**. It was hypothesized that using a glycosyl donor bearing a participating group at C-2, such as a Lev ester, would ensure better β -selectivity. Indeed, trisaccharide **32** was obtained exclusively in its β -form in 76% yield. Cleavage of the Lev ester and methylation provided methylated trisaccharide **34** in low yield, indicating that it was much more advantageous to use the methylated building block for the glycosylation instead of thioglycoside **39**. Trisaccharides **35-38**, differing only from the nature of the amide moiety of the anthrose residue, were then synthesized. Trisaccharides **35**,

37, and **38** were obtained from methylated trisaccharide **34**, whereas trisaccharide **36** was synthesized from alcohol **33**. In each case, 1,3-propanedithiol and triethylamine in pyridine and H₂O were used for the conversion of the azide into an amine. For compounds **35** and **36**, the amide moiety was synthesized by reacting the amine with 3-hydroxy-3-methylbutanoic acid using 1-hydroxy-7-azabenzotriazole (HOAt), HATU, and DIPEA as the activating agents, whereas 3-methylbutanoic acid was employed for trisaccharide **37**. Ac₂O and 4-dimethylaminopyridine (DMAP) in pyridine were used to construct the *N*-acetylated trisaccharide **38**. For all compounds, deprotection was achieved by a two-step sequence, entailing deacylation and hydrogenolysis, resulting in the fully deprotected analogous target trisaccharides.

CHAPITRE 3 – SYNTHESIS OF OLIGOSACCHARIDES RELATED TO POTENTIAL BIOTERRORIST PATHOGENS



Scheme 3.3. Synthesis of trisaccharides related to anthrax tetrasaccharide by Boons⁷

For immunological studies, trisaccharide **35** was reacted with *S*-acetylthioglycolic acid pentafluorophenyl ester and the resulting thioacetate derivative was de-*S*-acetylated to afford a thiolated trisaccharide. The latter was incubated with bromoacetyl activated KLH, yielding glycoconjugate KLH-BrAc-**35**. Rabbits were immunized with live or irradiated spores of *B. anthracis* Sterne 34F₂, an attenuated strain, and ELISA assays were conducted, revealing the

⁷ a) MeI, NaH, DMF, rt, 99%; b) 60% aq. AcOH, H₂O, 90 °C; c) Bu₂SnO, MeOH, reflux; d) CsF, BnBr, DMF, rt, 96% (3 steps); e) Tf₂O, py, CH₂Cl₂, 0 °C; f) NaN₃, DMF, 40 °C, 80% (2 steps); g) PdCl₂, NaOAc, 90% aq. HOAc/H₂O, rt; h) Cl₃CCN, DBU, CH₂Cl₂, rt, 85% (2 steps); i) *N*-carboxybenzyl-3-aminopropan-1-ol, NIS, TfOH, CH₂Cl₂, 0 °C, 72%; j) LevOH, DCC, DMAP, CH₂Cl₂, rt, 86%; k) **29** or **39**, NIS, TfOH, CH₂Cl₂, 0 °C, (**31**: 78%; **32**: 76%); l) H₂NNH₂·HOAc, MeOH, CH₂Cl₂, rt, (**31** and **32**: 93%); m) **27**, BF₃·OEt₂, MeCN, -40 °C, 86%, α/β 1:4; n) MeI, Ag₂O, Me₂S, THF, rt, 51%; o) **33** or **34**, 1,3-propanedithiol, Et₃N, py, H₂O; p) HOAt, HATU, DIPEA, DMF, rt, for **35** and **36**: β-hydroxyisovaleric acid; for **37**: isovaleric acid (**35**: 63%; **36**: 78%; **37**: 61%); q) NaOMe, MeOH, rt; r) Pd/C, H₂, *t*BuOH/H₂O/AcOH 40:1:1, rt (**35**: 98%; **36**: 96%; **37**: 94%; **38**: 92%; 2 steps); s) Ac₂O, py, DMAP, rt, 66%.

antigenic nature of trisaccharide **35**. Indeed, binding was observed between the antisera and the glycoconjugate, but not between the antisera and the native KLH moiety. Competitive inhibition ELISA also showed that the interaction between the antibodies and trisaccharide **35** was specific. In addition, trisaccharides **35-38** were linked to maleimide activated bovine serum albumin (BSA) to evaluate their ability to inhibit the binding between the antisera and glycoconjugate KLH-BrAc-**35**. The results highlighted that the 3-methylbutyryl moiety on the anthrose residue is important for anti-spore antibody binding, whereas the methyl ether at C-2 is not critical.

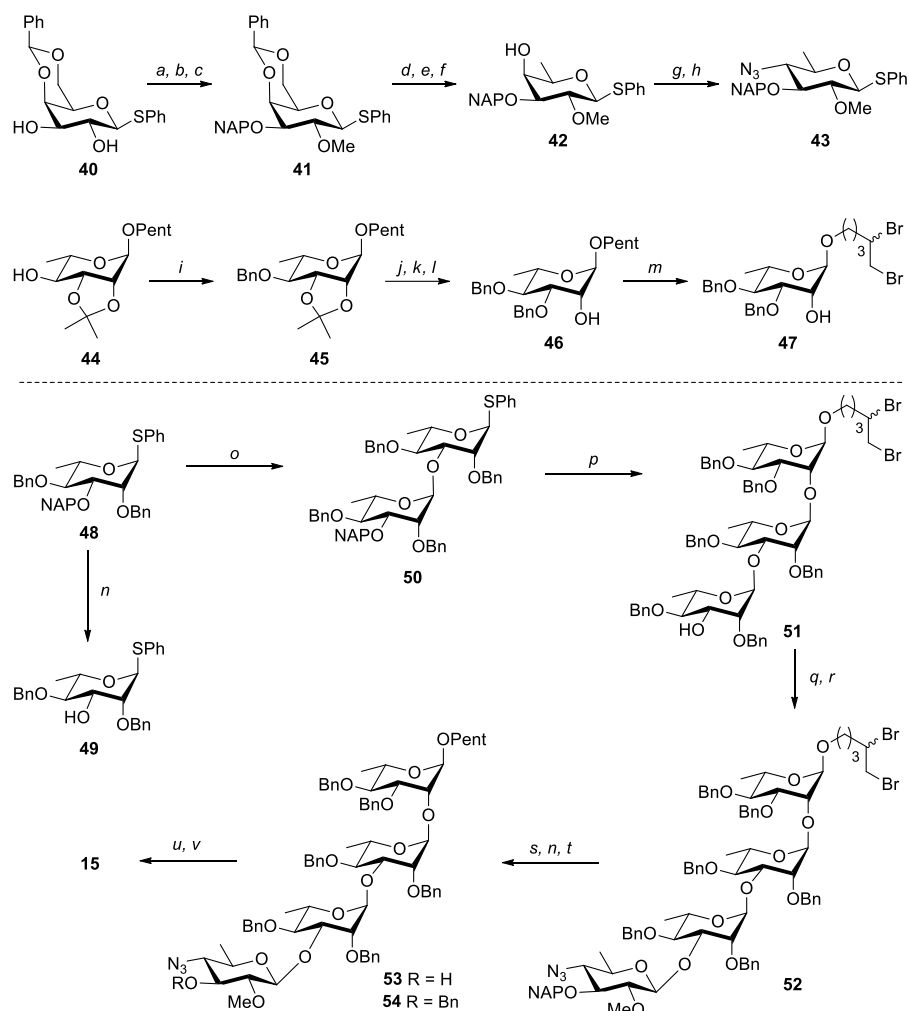
Subsequently to these findings, trisaccharide **35** was studied as a marker of nonfatal inhalation infection of *B. anthracis* in rhesus macaques.²⁶⁴ For that matter, the animals were exposed to aerosolized virulent *B. anthracis* Ames spores and their sera were tested against trisaccharide KLH-**35** glycoconjugate using ELISA. Results showed that the anti-trisaccharide **35** IgG response was specific to the anthrose moiety. Inhibition ELISA using trisaccharide BSA-**35** and trisaccharide BSA-**38** conjugates supported this finding. Moreover, the anti-trisaccharide **35** antibodies production was observable even in rhesus macaques administered with ciprofloxacin. These results demonstrated that anti-trisaccharide **35** antibodies could be used as a serologic marker for the identification of subjects exposed to aerosolized *B. anthracis* spores. As spore growth and production of toxins are required for actual detection methods and that antibiotic treatment can prevent these to occur, these findings are especially relevant because the markers appeared to be independent of these factors.

Following the syntheses developed by Seeberger, Kováč, and Boons, Crich and co-workers devised a [3 + 1] glycosylation methodology, involving the use of D-galactose as the starting material, allowing the preparation of anthrax tetrasaccharide.²⁶⁵ Previous methods exploited NGP in order to achieve configuration selectivity among the glycosidic linkages. They also either required considerable manipulations of the protecting groups or the use of expensive starting compounds. By taking advantage of α -nitrilium-mediated β -selective glycosylation and iterative glycosylation strategies, Crich *et al.* attempted to get around these problems.

As depicted in Scheme 4, they initiated the preparation of the anthrose moiety with galactose derivative **40**, which was converted into fully protected thioglycoside **41** following introduction of the 2-naphthylmethyl (NAP) group and methylation. The benzylidene group was cleaved under

acidic conditions, and the resulting hydroxyl group at C-6 was regioselectively substituted with a phenylseleno group. Tributyltin hydride induced the reduction of the intermediate into 6-deoxygalactose derivative **42**. Triflate-mediated inversion of the configuration and substitution of the C-4 hydroxyl by an azide furnished building block **43**. The second building block was synthesized from known derivative **44**. Functional group manipulations afforded alcohol **46**. CuBr₂ and LiBr were then employed for the dibromination of the *n*-pentenyl moiety, providing building block **47**. This step was realized in order to prevent the activation of the *n*-pentenyl moiety during glycosylations. Indeed, the *n*-pentenyl group has to be intact at the end of the synthesis, since it was needed for coupling tetrasaccharide **15** to a carrier protein. Alcohol **49** was synthesized from glycosyl donor **48** using 2,3-dichloro-5,6-dicyano-1,4-benzoquinone (DDQ) in a mixture of MeOH and CH₂Cl₂ to cleave the NAP ether.

CHAPITRE 3 – SYNTHESIS OF OLIGOSACCHARIDES RELATED TO POTENTIAL BIOTERRORIST PATHOGENS



Scheme 3.4. Synthesis of anthrax tetrasaccharide by Crich⁸

Disaccharide **50** was synthesized following preactivation of thiorhamnoside **48** employing diphenylsulfoxide, tri-*tert*-butylpyrimidine (TTBP), and triflic anhydride at low temperatures, subsequent glycosidation with glycosyl acceptor **49**, and quenching using triethylphosphite. The reaction furnished a separable mixture of α and β anomers, where the former was the major

⁸ a) Bu₂SnO, toluene, reflux; b) NAPBr, CsF, TBAI, DMF, reflux, 60% (2 steps); c) NaH, MeI, DMF, 80%; d) *p*-TsOH·H₂O, MeOH, reflux, 95%; e) PhSe₂Ph, Bu₃P, toluene, reflux, 77%; f) Bu₃SnH, AIBN, benzene, reflux, 85%; g) Tf₂O, pyridine, CH₂Cl₂; h) NaN₃, DMF, 87% (2 steps); i) NaH, BnBr, DMF, 90%; j) 80% aqueous AcOH, 90 °C; k) Bu₂SnO, benzene, reflux; l) BnBr, CsF, DMF, 74% (3 steps); m) CuBr₂, LiBr, THF/CH₃CN, 89%; n) DDQ, MeOH/CH₂Cl₂, (**49** : 74%; **53** : 67%); o) i. Ph₂SO, TTBP, Tf₂O, CH₂Cl₂, 3 Å MS, -60 °C then **49**, CH₂Cl₂, -60 °C; ii. P(OEt)₃, 49%; p) i. Ph₂SO, TTBP, Tf₂O, CH₂Cl₂, 3 Å MS, -60 °C; then **47**, CH₂Cl₂, -60 °C; ii. DDQ, MeOH/CH₂Cl₂, 45% (2 steps); q) **43**, NIS, TiOH, C₂H₅CN, 3 Å MS, -60 °C; r) Et₃N, 71% (2 steps); s) NaI, 2-butanone, reflux; t) for the mixture of debenzylated byproducts: BnBr, NaH, DMF (**54**: 22%); u) Na, NH₃, THF, -78 °C; v) 3-hydroxy-3-methylbutyric acid, HATU, (*i*-Pr)₂EtN, DMF, 54% (2 steps).

constituent. Iteration of the first two steps with disaccharide **50** and building block **48** and cleavage of the NAP ether furnished trisaccharide glycosyl acceptor **51**. The latter was then coupled with anthrose derivative **43** under the promotion of NIS and TfOH in propionitrile, resulting in a separable 3:1 β/α -anomeric mixture of tetrasaccharide **52**. Glycosylation tests revealed that employing NIS/TfOH as the promoter system and conducting the reaction in propionitrile enhanced the overall yield and the stereoselectivity toward the β -form due to the formation of an α -nitrilium intermediate. In contrast, benzenesulfonylpiperidine (BSP)/TTBP/Tf₂O in CH₂Cl₂ did not provide β -selectivity, whereas BSP/TTBP/Tf₂O in propionitrile gave a 1/1 β/α -anomeric mixture. The anomeric linker of β -tetrasaccharide **52** was debrominated using NaI and 2-butanone at high temperatures, and the NAP protecting group on the anthroside residue was cleaved. This resulted in the formation of a mixture of alcohol **53** and debenzylated byproducts due to the competition between benzyl and NAP ethers during DDQ-promoted deprotections. The two compounds were separated by chromatography, and the isolated byproducts were benzylated, resulting in tetrasaccharide **54**. Alcohol **53** was synthesized from the perspective that it could be further transformed at the level of the anthrose residue. Tetrasaccharides **53** and **54** were finally deprotected through the action of sodium and ammonia, which also reduced the azide moiety into an amine. The latter was reacted with 3-hydroxy-3-methylbutanoic acid using peptide-coupling conditions, yielding target tetrasaccharide **15**.

B. anthracis tetrasaccharide was also studied by Djedaïni-Pilard and co-workers. Their main objective was to investigate the production of antibodies specific to fragments of this oligosaccharide for further development of an anthrax detection tool. In 2008, they reported the synthesis of an anthrose derivative for evaluation of its immunogenic potential.²⁶⁶ The anthrose derivative, equipped with an aminolinker for attachment to KLH, was synthesized in 18 steps from D-galactose. Their methodology relied on the iodination of the C-6 carbon followed by hydrogenation, which allowed the conversion of the primary hydroxyl group into the target deoxy functionality. They also used this technique for the synthesis of an anthrose-containing trisaccharide.²⁶⁷ The latter as well as the previously prepared anthrose derivative were conjugated to KLH through covalent coupling using glutaraldehyde. Both conjugates were used to immunize rabbits, and the antibody titers were measured employing enzymatic immunoassay (EIA). By using

different natural sugars and synthetic intermediates as competitors during the biological assays, the authors showed that the C-6 methyl ether, the C-4 butamido group, and the hydroxyl at C-3 of the anthrose moiety were required for antibody recognition. In agreement with Boons results, Djedaïni-Pilard was able to show that the C-2 methyl ether did not seem to have a role in the immunogenicity of the tested compounds. Results also revealed that the rhamnoside units were less involved in the immunogenic response, which corroborates previous findings.

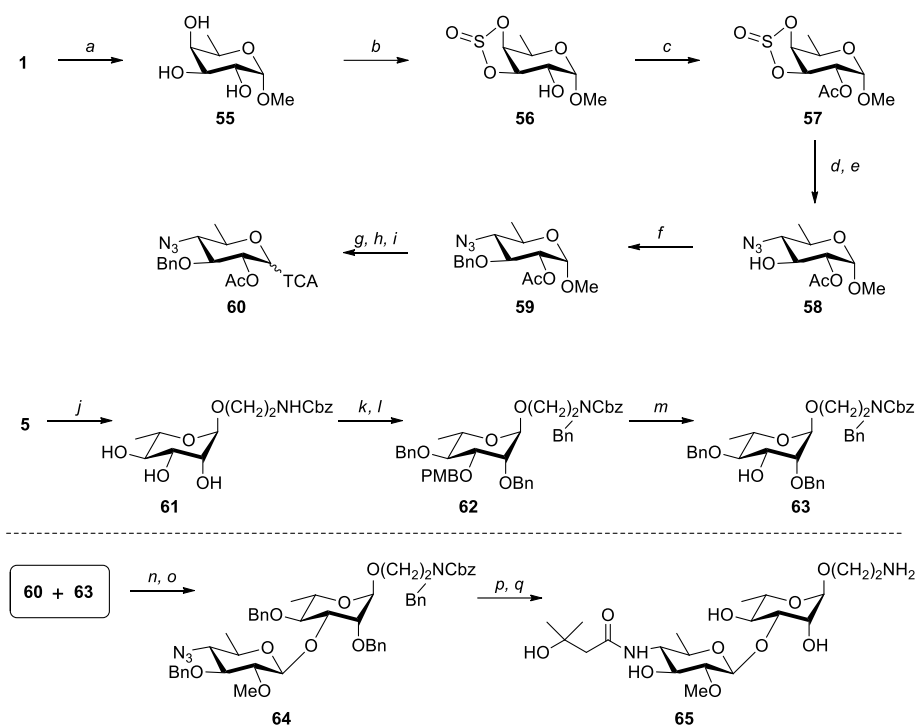
With the aim of studying the ability of anthrose-related compounds to induce a memory immune response for the development of glycoconjugate vaccines, Grandjean and co-workers studied the synthesis of an anthrose-containing disaccharide. Previously, all of the methods employed by other research groups involved the use of multiple protecting groups and an S_N2 -like reaction to install the amide chain at C-4. Grandjean proposed an alternative method based on the manipulation of cyclic sulfites/sulfates that could act as 3,4-diol protecting groups as well as leaving groups.²⁶⁸ This kind of bis-functional group would allow the selective protection of hydroxyl functions and the introduction of the azido group in a stereo- and regioselective manner. This method was advantageous as it offers a shorter alternative to previously reported synthetic pathways.

The selectivity of the reactions was first assessed according to the steric hindrance of the starting compound. Cyclic sulfites/sulfates ring-opening reactions were tested on β -pyranosides, and results showed that this configuration favored the attack of the azide at the C-3 position, rather than at C-4 as desired. However, when using α -pyranosides, the attack resulting in the ring-opening was selective to the C-4 position, due to the steric hindrance caused by the anomeric substituent. It was also shown that cyclic sulfites prepared from D-fucose were not reactive, and the authors hypothesized that it could be attributed to the axial C-1 and equatorial C-5 substituents, which cause steric hindrance. Therefore, oxidation of the cyclic sulfites into sulfates was required to achieve good reactivity.

Having established that better results were obtained using α -pyranosides, building blocks **60** and **63** were synthesized (Scheme 5). D-Fucose was used as the starting compound for the synthesis of anthroside **60**. The anomeric hydroxyl group was first methylated, yielding triol **55** in a 4:1 α/β

anomeric mixture. This group was used as it is stable toward oxidative experimental conditions, unlike *O*-pentenyl, and it can readily be converted into a TCA moiety. The 3,4-diol was protected as a cyclic sulfite, followed by the selective acetylation of the C-2 hydroxyl group. Resulting intermediate **57** was oxidized into a cyclic sulfate under Sharpless' conditions.^{269, 270} Ring-opening was achieved using sodium azide and the resulting acyclic sulfate at C-3 was hydrolyzed under acidic conditions, furnishing alcohol **58** in the desired *gluco* conformation. The latter was protected as a benzyl ether using BnTCA and triflic acid, giving rise to fully protected intermediate **59**. Finally, acetolysis of derivative **59**, deacetylation using BnNH₂ in THF, and conversion of resulting alcohol into a TCA resulted in building block **60**. Coupling of rhamnose **5** with *N*-carboxybenzyl-aminoethanol under the promotion of TsOH in toluene gave triol **61**. Regioselective stannylene-mediated alkylation of this alcohol allowed the selective protection of the C-3 hydroxyl so that the hydroxyl groups at C-2 and C-4, as well as the carbamate, could further be benzylated into intermediate **62**. Cleavage of the *para*-methoxybenzyl (PMB) group through the use of DDQ afforded glycosyl acceptor **63**. It is worth mentioning that the present method was also successfully employed for the synthesis of analogues containing different protecting groups, such as esters and ethers, showing that the method allows the synthesis of multiple anthrose-like compounds. Glycosidation of building blocks **60** and **63**, deacetylation and methylation of the anthrose-like moiety, reduction of the azide into an amine and reaction of the latter with 3-hydroxy-3-methylbutanoic acid preactivated with hydroxybenzotriazole (HOBt) and HATU followed by hydrogenolysis furnished unprotected anthrose-containing disaccharide **65** in its β -configuration.

CHAPITRE 3 – SYNTHESIS OF OLIGOSACCHARIDES RELATED TO POTENTIAL BIOTERRORIST PATHOGENS

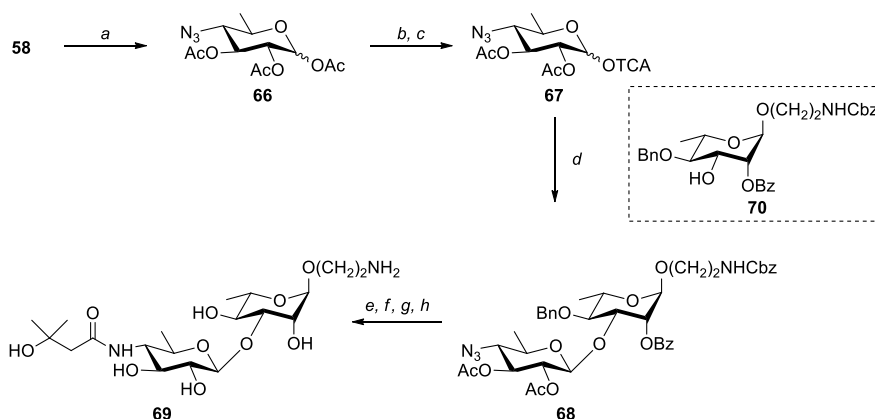


Scheme 3.5. Synthesis of an anthrose-containing disaccharide by Grandjean⁹

Grandjean and co-workers used their synthetic method based on the introduction of cyclic sulfites and sulfates into glycosides in order to synthesize another disaccharide akin to anthrax tetrasaccharide. As Boons and Djedaïni-Pilard showed, the hydroxyl at C-2 on the anthrose residue does not need to be methylated to cross-react with *B. anthracis* spores. Moreover, Kubler-Kielb revealed that mice serum induced by *Shewanella* CPS, which contains residues similar to anthrose where the hydroxyl at C-2 is not methylated,²⁷¹ cross-reacts with *B. anthracis* spores.²⁷² Keeping that in mind, Grandjean reported the synthesis of non-methylated anthrose related disaccharide **69** (Scheme 6).²⁷³ This was advantageous as the introduction of the methoxy moiety usually requires extensive protecting group manipulations, which were then avoided in the present case.

⁹ a) AcCl, MeOH, -20 °C to rt, 78% (α/β 4:1); b) i. Bu₂SnO, MeOH, reflux; ii. SOCl₂, 0 °C, 86%; c) Ac₂O, Et₃N, DMAP, CH₂Cl₂, 0 °C to rt, 90%; d) NaIO₄, RuCl₃·H₂O, CCl₄/CH₃CN/H₂O, 0 °C; e) i. NaN₃, 50 °C, DMF; ii. H₂SO₄, H₂O, THF, rt, 74% (3 steps); f) BnTCA, TFOH, cyclohexane/CH₂Cl₂ 2:1, rt, 70%; g) Ac₂O, AcOH, H₂SO₄, rt, 78%; h) BnNH₂, THF, rt, 70%; i) Cl₃CCN, DBU, CH₂Cl₂, 0 °C to rt, 78%; j) *N*-carboxybenzyl-2-aminoethan-1-ol, TsOH, tol, reflux, 64% (α/β 5:1); k) i. Bu₂SnO, MeOH, reflux; ii. PMBCl, DMF, rt, 54%; l) NaH, BnBr, DMF, rt, 2 h, 64%; m) DDQ, CH₂Cl₂/H₂O 14:1, 0 °C, 69%; n) TMSOTf, CH₂Cl₂, -40 °C, 68%; o) i. MeONa, MeOH, rt, 75%; ii. NaH, MeI, DMF, 62%; p) i. NaBH₄, NiCl₂·6H₂O, EtOH/CH₂Cl₂ 4:1, rt; ii. 3-hydroxy-3-methylbutanoic acid, HOBT, HATU, DIPEA, DMF, rt, 55%; q) H₂ (10 bars), Pd(OH)₂, EtOH/H₂O 3:1, 50 °C, 91%.

CHAPITRE 3 – SYNTHESIS OF OLIGOSACCHARIDES RELATED TO POTENTIAL BIOTERRORIST PATHOGENS



Scheme 3.6. Synthesis of a non-methylated anthrose-containing disaccharide by Grandjean¹⁰

Intermediate **58** was subjected to acetolysis, allowing the replacement of the anomeric methyl group for an acetyl to give **66**. The latter was selectively deprotected using benzylamine, and the resulting alcohol was converted into TCA **67** under standard conditions. TCA anthrose **67** and rhamnoside **70** were coupled in the presence of TMSOTf, providing disaccharide **68**. Target non-methylated disaccharide **69** was obtained through a previously described procedure.

For biological evaluation, disaccharides **65** and **69** were covalently linked to BSA carrier protein through their free amine. Both disaccharides were conjugated using glutaraldehyde, resulting in a carbohydrate/protein ratio of 19:1 and 18:1, respectively, whereas disaccharide **69** was also conjugated to BSA in a carbohydrate/protein ratio of 6:1 using thiomaleimide chemistry. BALB/c mice were immunized with the three glycoconjugates and anti-tetrasaccharide antibody titers were measured by ELISA, in which synthetic biotinylated anthrax tetrasaccharide was immobilized on the microtiter plates. Results showed that the glycoconjugates are able to induce the formation of anti-tetrasaccharide IgM and IgG antibodies. They also suggested that conjugates of **65** and **69** could elicit a T-dependent immune response towards *B. anthracis* tetrasaccharide. However, the impact of the conjugation method on the immune response was not assessed. The sera obtained following immunization also cross-reacted with *B. anthracis* spores. These findings validate the

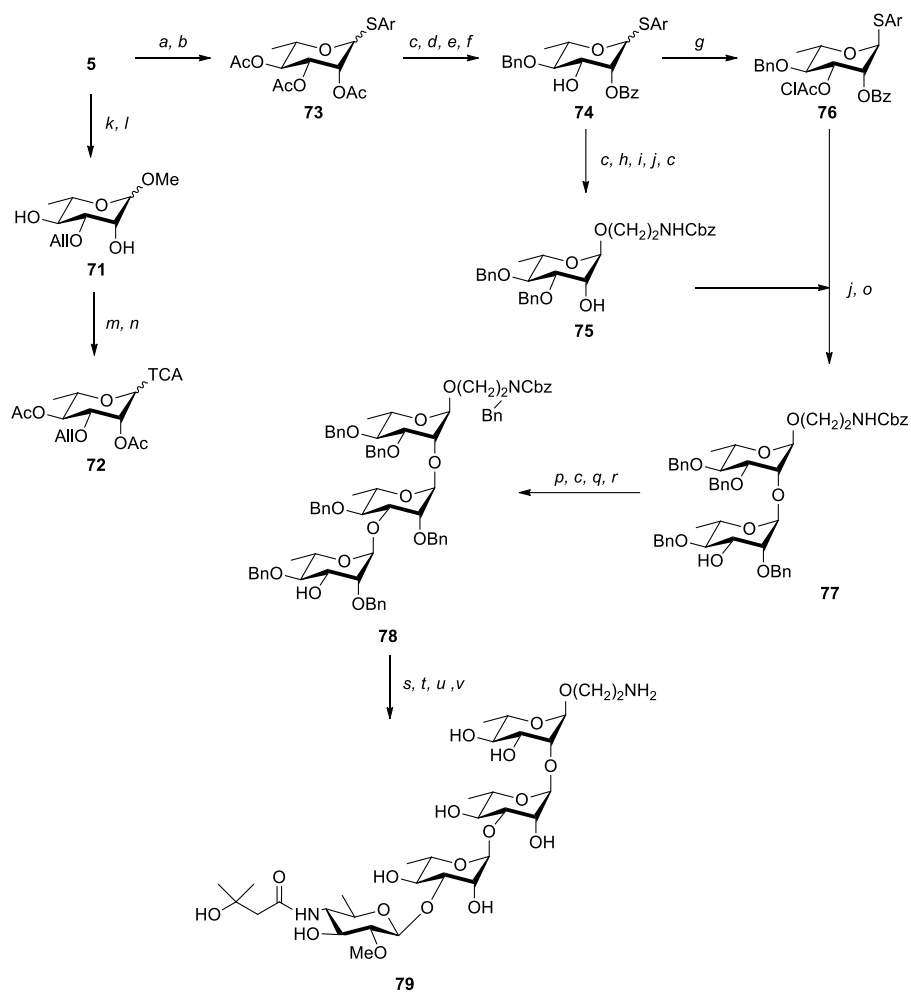
¹⁰ a) Ac₂O, AcOH, H₂SO₄, rt; b) BnNH₂, THF, rt; c) Cl₃CCN, DBU, CH₂Cl₂, 0 °C to rt, 66% (3 steps); d) **70**, TMSOTf, 4 Å MS, CH₂Cl₂, -20 °C, 80%; e) NaBH₄, NiCl₂·6H₂O, EtOH/CH₂Cl₂, rt; f) 3-hydroxy-3-methylbutanoic acid, HATU, DIPEA, CH₂Cl₂, rt, 55% (two steps); g) MeONa, MeOH, rt, h) H₂ (10 bars), Pd(OH)₂/C, 50 °C, 82% (two steps).

CHAPITRE 3 – SYNTHESIS OF OLIGOSACCHARIDES RELATED TO POTENTIAL BIOTERRORIST PATHOGENS

fact that the 2-methoxy moiety on the anthrose residue is indeed not essential to induce an immunogenic response.

In a subsequent work, the Grandjean's group reported the synthesis of anthrax tetrasaccharide derivative **79**, as presented in Scheme 7.²⁷⁴ Their synthesis relied on the use of anthrose derivative **60**, which was prepared *via* cyclic sulfite/sulfate intermediates. Prior to synthesizing the tetrasaccharide, methylation and deacetylation tests were conducted with various anthrose-containing disaccharides. This was achieved in an attempt to compare the feasibility of the [1 + 3] and [2 + 2] glycosylation approaches. Results showed that the [1 + 3] approach was efficient as the presence of the 2-*O*-acetyl in anthrose derivative **60**, which is required for its synthesis, prevented the use of the [2 + 2] approach.

CHAPITRE 3 – SYNTHESIS OF OLIGOSACCHARIDES RELATED TO POTENTIAL BIOTERRORIST PATHOGENS



Scheme 3.7. Synthesis of anthrax tetrasaccharide by Grandjean¹¹

Retrosynthetic analysis of tetrasaccharide **79** revealed that the trirhamnoside building blocks could all be obtained from L-rhamnose. Methylation of the anomeric position and selective protection of the 3-OH as an allyl ether through the formation of a stannylene acetal furnished diol **71**, which was peracetylated and converted into TCA **72**. In parallel, introduction of an arylthiol moiety at

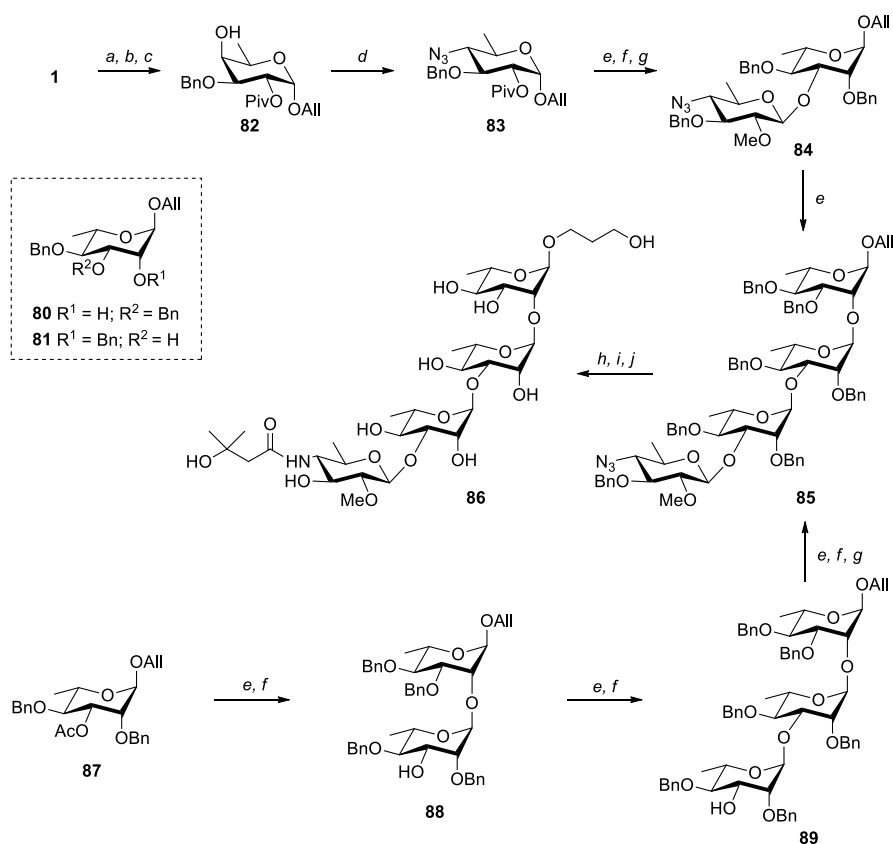
¹¹ a) Ac₂O, py; b) 3-methyl-5-*tert*-butylthiophenol, CH₂Cl₂, BF₃·OEt₂, -40 to 0 °C, 91% (2 steps); c) MeONa, MeOH (**75**: quant.; **78**: 70%); d) triethylorthobenzoate, CSA, DMF; e) NaH, BnBr, DMF, 0 °C to rt; f) 2 M aq. HCl, 46% (4 steps); g) (ClAc)₂O, DMAP, Et₃N, CH₂Cl₂, 0 °C to rt, 95%; h) *i.* Bu₂SnO, MeOH, reflux; *ii.* BnBr, DMF, 71%; i) BzCl, py, 0 °C to rt, quant.; j) *N*-carboxybenzyl-2-aminoethan-1-ol or **75**, NIS, AgOTf, 4 Å MS, CH₂Cl₂, (**75**: quant.; **77**: 79%) k) AcCl, MeOH, -20 °C to rt, 70%; l) *i.* Bu₂SnO, MeOH, reflux; *ii.* AllBr, DMF, 70 °C, 40%; m) Ac₂O, AcOH, H₂SO₄, 67%; n) *i.* BnNH₂, THF, 75%; *ii.* Cl₃CCN, DBU, CH₂Cl₂, 0 °C to rt, 80%; o) thiourea, NaHCO₃, Bu₄NI, THF, 55 °C; p) **72**, TMSOTf, 4 Å MS, CH₂Cl₂, 0 °C, 99%; q) BnBr, NaH, DMF, 0 °C to rt, 87%; r) *i.* (Ph₃P)₃RhCl, DABCO, EtOH/tol/H₂O, reflux; *ii.* HgCl₂, HgO, acetone/H₂O, 88%; s) **60**, TMSOTf, 4 Å MS, CH₂Cl₂, -40 °C, 56%; t) *i.* MeONa, MeOH, 85%; *ii.* MeI, NaH, DMF, 0 °C to rt, 96%; u) *i.* NaBH₄, NiCl₂·6H₂O, EtOH/CH₂Cl₂; *ii.* 3-hydroxy-3-methylbutanoic acid, HATU, DIPEA, DMF, 40%; v) H₂, 10 bars, Pd/C, MeOH/AcOH, 50 °C, 88%.

the anomeric position of L-rhamnose following its peracetylation yielded rhamnopyranoside **73**. The latter was deacetylated under Zemplén conditions, and a one-pot three-step sequence was conducted to afford alcohol **74**. This sequence, developed by Field and co-workers, consisted in the formation of a 2,3-orthoester, benzylation of the hydroxyl group at C-4, and selective benzylation of the C-2 hydroxyl through the regioselective opening of the orthoester in acidic media. Alcohol **74** was used for the synthesis of glycosyl donor **76** following chloroacetylation, and glycosyl acceptor **75** in five steps including debenzoylation, stannyl-mediated benzylation of the resulting hydroxyl group at C-3, benzylation of the free OH, NIS/AgOTf-mediated glycosylation with *N*-Cbz-ethanolamine, and cleavage of the benzoyl ester. Arylthiol **76** and alcohol **75** were coupled under the promotion of NIS and AgOTf and the chloroacetyl protecting group was cleaved by treatment with thiourea. Resulting disaccharide **77** was glycosylated with TCA **72**, yielding a trisaccharide exclusively as the α -anomer. The esters were cleaved using sodium methoxide, the resulting alcohol was perbenzylated, and the allyl protecting group was cleaved through double bond isomerization and hydrolysis. This allowed resulting trisaccharide **78** to be further glycosylated with anthrose derivative **60**, followed by deacetylation and methylation of the C-2 hydroxyl function at the non-reducing end. Conversion of the protected tetrasaccharide into anthrax tetrasaccharide derivative **79** was finally accomplished by the introduction of the amide moiety on the anthrose residue and deprotection by hydrogenolysis.

Wang *et al.* designed a short and simplified method allowing the synthesis of anthrax tetrasaccharide.²⁷⁵ The authors based their synthetic pathway on the use of allyl glycosides as building blocks, which can easily be isomerized into prop-1-enyl donors. Moreover, bearing an allyl group at the anomeric position, the tetrasaccharide could further be functionalized through different reactions for conjugation. By following this synthetic route, tetrasaccharide **86** could be obtained in 17 steps from commercially available L-rhamnose and D-fucose. As depicted in Scheme 8, an iterative and a [2 + 2] glycosylation approach were proposed using building blocks **80**, **81**, **83**, and **87**. Intermediates **80** and **87** were synthesized from L-rhamnose in six steps whereas compound **81** was obtained from intermediate **87** by deacetylation. Building block **83** was prepared from D-fucose by allylation of the anomeric hydroxyl group, selective benzylation through the formation of a stannylene acetal intermediate, installation of the pivaloyl (Piv) group at the C-2

position and epimerization of the C-4 substituent *via* a triflate intermediate. All glycosylations proceeded following the same route, that is, isomerization of the allyl glycosides into prop-1-enyl donors using $[\text{Ir}(\text{COD})(\text{PMePh}_2)_2]\text{PF}_6$ in THF, followed by glycosylation with the appropriate acceptor under the promotion of NIS/TMSOTf. Thus, protected tetrasaccharide was either synthesized by iteration of these steps from building block **87** and appropriate donors or by glycosylation of disaccharides **84** and **88** using the same conditions. To obtain target compound **86** from common tetrasaccharide **85**, hydroboration was used to convert the anomeric allyl group into an alcohol, available for further functionalization. Hydrogenolysis resulted in the removal of the benzyl protecting groups and reduction of the azide moiety into an amine, and the latter was finally converted into an amide.

CHAPITRE 3 – SYNTHESIS OF OLIGOSACCHARIDES RELATED TO POTENTIAL BIOTERRORIST PATHOGENS



Scheme 3.8. Synthesis of anthrax tetrasaccharide by Wang¹²

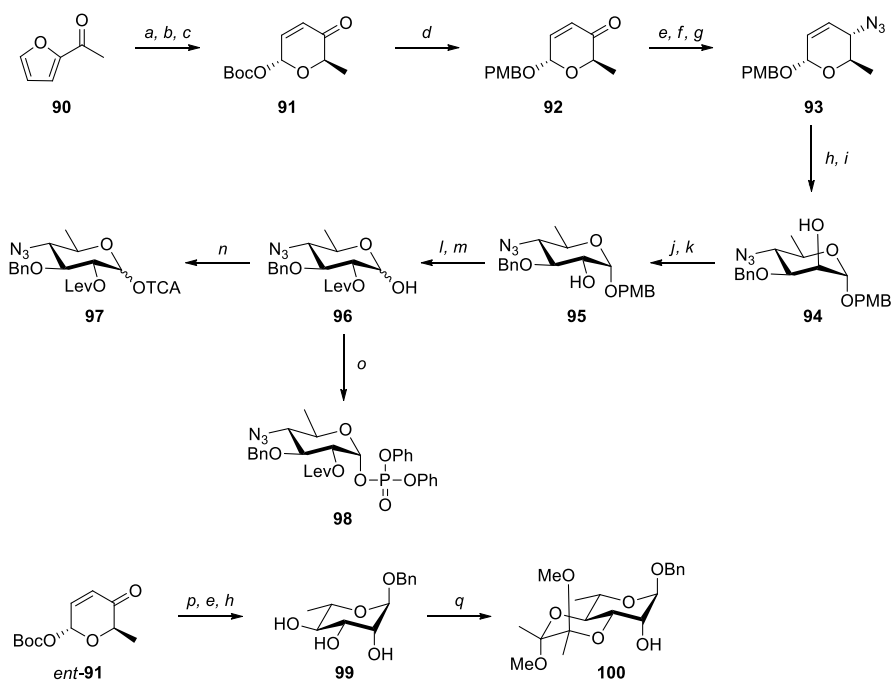
O'Doherty studied anthrax tetrasaccharide synthesis through a highly stereocontrolled pathway using cheap and achiral acetylfuran as starting material,^{276, 277} unlike other previously reported methods that were based on the use of free sugars. The approach involved the use of their palladium-catalyzed glycosylation conditions,²⁷⁸ Noyori reduction, and Luche reduction, among others, and they employed a convergent [3 + 1] method to achieve the glycosylations.

The *de novo* asymmetric synthesis of anthrax-related tetrasaccharides **109** and **111** by O'Doherty (Schemes 9 and 10) commenced with Noyori asymmetric hydrogenation of ketone **90**. This step allowed the introduction of the D-stereochemistry needed in target anthroside building blocks **97**

¹² a) AcCl, allyl alcohol, 92%; b) *i.* Bu₂SnO, toluene, reflux; *ii.* BnBr, CsF, DMF, 84%; c) PivCl, py, 89%; d) *i.* Tf₂O, py, CH₂Cl₂; *ii.* NaN₃, 91%; e) *i.* [Ir(COD)(PMePh₂)₂]PF₆, THF; *ii.* **80**, **81**, **83**, **87**, or **88** NIS, TfOH, CH₃CN (**85**: 59% from **84**); f) MeONa, MeOH (**88**: 82%, 2 steps; **89**: 84% α/β 7:1, 2 steps; **85**: 85% from **89**, 2 steps); g) NaH, MeI, DMF, (**84**: 66%, 3 steps; **85**: 92%); h) 9-BBN, NaOH, H₂O₂, THF, 87%; i) Pd/C, H₂, MeOH/THF; j) 3-hydroxy-3-methylbutanoic acid, HATU, DIPEA, DMF, 72% (2 steps).

and **98**. This was followed by Achmatowicz oxidative rearrangement using *N*-bromosuccinimide and Boc protection of the alcohol in a diastereoselective manner, resulting in pyranone **91** in an α/β ratio of 3:1. Single diastereomer **92** was then formed following reaction of pyranone **91** with PMBOH using palladium-catalyzed glycosylation conditions. Luche reduction, which involves the use of CeCl_3 and NaBH_4 , formation of a methyl carbonate and regio- and stereoselective replacement of the latter with an azide group furnished allylic azide **93**. This last step was achieved through a palladium-mediated allylation using TMSN_3 , $[\text{Pd}(\text{allyl})\text{Cl}]_2$ and 1,4-bis(diphenylphosphino)butane. Upjohn conditions were then employed to achieve dihydroxylation of alkene **93**. Subsequent stannylene-mediated selective benzylation yielded alcohol **94**. Conversion of the latter to target *gluco* conformation was realized through the formation of a triflate intermediate, followed by a $\text{S}_{\text{N}}2$ displacement, and resulted in the formation of intermediate **95**. Levulinoylation and deprotection of the PMB group furnished anomeric alcohol **96**, which was converted into anthroside donors **97** and **98**. The authors also attempted to prepare an anthroside intermediate bearing an anomeric fluoride using Nicolaou procedure but it was not successful. Preparation of a monosaccharide having an unprotected hydroxyl group at the C-2 position to act as the first glycosyl acceptor was then achieved. Compound *ent*-**91** was used as starting material, and was synthesized as previously described but with Noyori-(*S,S*) reagent instead of Noyori-(*R,R*) for acetylfuran **90** reduction. Benzylation of the anomeric position through palladium-catalyzed glycosylation, Luche reduction and diastereoselective dihydroxylation allowed the formation of triol **99**. Finally, Ley spiroketal procedure was employed for the protection of C-3 and C-4 hydroxyl functions, affording alcohol building block **100**.

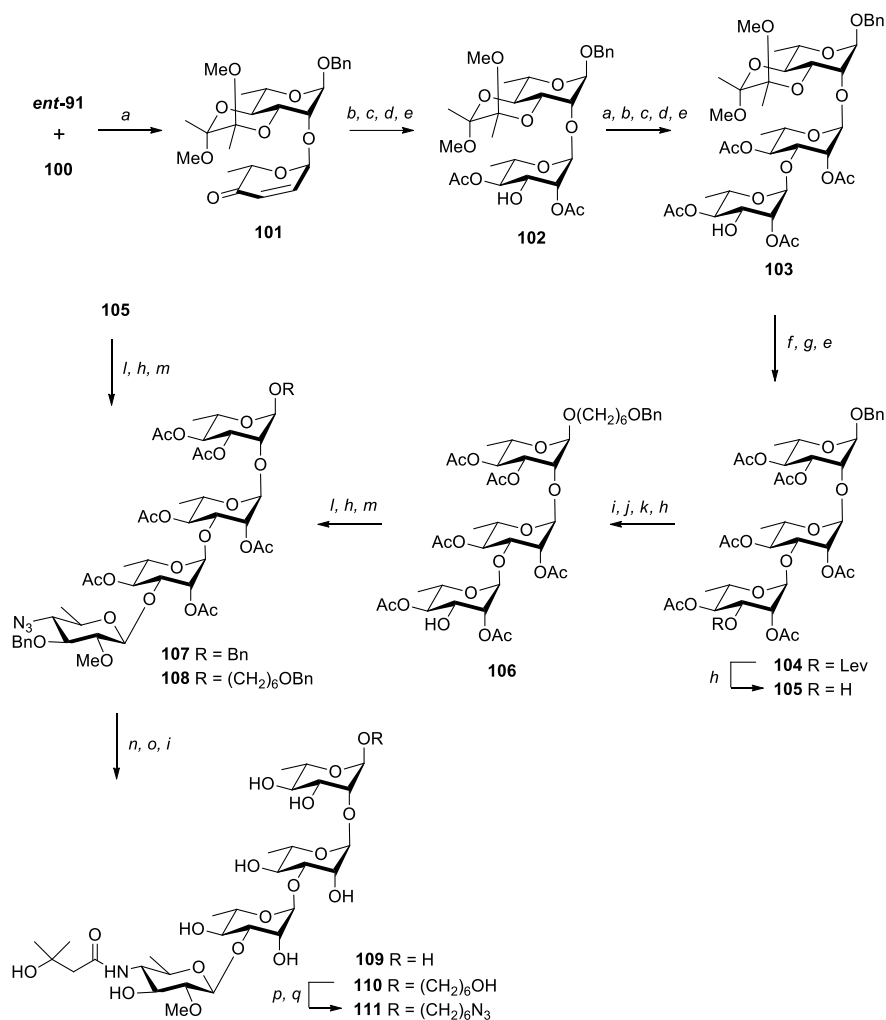
CHAPITRE 3 – SYNTHESIS OF OLIGOSACCHARIDES RELATED TO POTENTIAL BIOTERRORIST PATHOGENS



Scheme 3.9. *De novo* synthesis of anthrax tetrasaccharide building blocks by O'Doherty¹³

¹³ a) Noyori-(*R,R*), formic acid, Et₃N, CH₂Cl₂; b) NaHCO₃, NBS, THF/H₂O 3:1, 0 °C; c) (Boc)₂O, DMAP, CH₂Cl₂, -78 to 30 °C, 60% (3 steps); d) PMBOH, Pd₂(DBA)₃·CHCl₃, PPh₃, CH₂Cl₂, 96%; e) CeCl₃, MeOH, NaBH₄, CH₂Cl₂, -78 °C (**93**: 93%; **99**: 89%) f) methylchloroformate, DMAP, py, CH₂Cl₂, 0 °C, 99%; g) [Pd(allyl)Cl]₂, dppb, TMSN₃, THF, 93%; h) NMO/OsO₄, *t*-butanol/acetone 1:1, (**94**: 98%; **99**: 94%); i) *i*. *n*Bu₂SnO, toluene, reflux; *ii*. CsF, TBAI, BnBr, reflux, 99%; j) Tf₂O, py, CH₂Cl₂, 99%; k) NaNO₂, DMF, 45 °C, 56%; l) LevOH, DMAP, CH₂Cl₂, DCC, 0 °C to rt, 94%; m) DDQ, CH₂Cl₂/H₂O 10:1, 95%; n) Cl₃CCN, NaH, CH₂Cl₂, 0 °C, 83%; o) (PhO)₂POCl, DMAP, CH₂Cl₂, 89%; p) BnOH, Pd₂(DBA)₃·CHCl₃, PPh₃, 0 °C, 90%; q) trimethylorthoacetate, TsOH, 2,3-butanedione, MeOH, 70 °C to reflux, 88%.

CHAPITRE 3 – SYNTHESIS OF OLIGOSACCHARIDES RELATED TO POTENTIAL BIOTERRORIST PATHOGENS



Scheme 3.10. Anthrax-related tetrasaccharides synthesis by O'Doherty¹⁴

With the building blocks in hand, glycosylations were conducted (Scheme 10). First, compounds *ent*-91 and 100 were coupled using a palladium catalyst, yielding intermediate 101. Luche reduction, dihydroxylation, formation of a cyclic orthoester intermediate using trimethyl orthoacetate, selective acetylation of the C-4 hydroxyl, and opening of the cyclic orthoester

¹⁴ a) Pd₂(DBA)₃·CHCl₃, PPh₃, CH₂Cl₂, 0 °C to rt (**101**: 86%; **103**: 94%); b) CeCl₃, MeOH, NaBH₄, CH₂Cl₂, -78 °C; c) NMO/OsO₄, *t*-butanol/acetone 1:1, 0 °C to rt (**102**: 83%, 2 steps; **103**: 80%, 2 steps); d) trimethylorthoacetate, CH₃CN, TsOH·H₂O; e) Ac₂O, DMAP, py (**102**: 97%, 2 steps; **103**: 97%, 2 steps); f) LevOH, DMAP, CH₂Cl₂, DCC, 0 °C to rt; g) TFA/H₂O 10 : 1, CH₂Cl₂, 97% (2 steps); h) H₂NNH₂·AcOH, MeOH, CH₂Cl₂ (**105** : 94%, 2 steps; **106**: 95%); i) H₂, Pd/C, MeOH (**106**: 96%; **109**: 96% (α & β); **110**: 97%); j) Cl₃CCN, NaH, CH₂Cl₂, 0 °C, 83%; k) 6-benzyloxyhexanol, TMSOTf, CH₂Cl₂, 0 °C, 82%; l) TMSOTf, CH₂Cl₂, 0 °C (for **107**: **105** + **97**, 90%; **105** + **98**, 85%; for **108**: **106** + **97**, 82%); m) Ag₂O, MeI, 55 °C (**107**: 90%, 2 steps; **108**: 87%, 2 steps); n) PEt₃, LiOH, MeOH/THF/H₂O 10:10:1; o) HBTU, 3-hydroxy-3-methylbutanoic acid, Et₃N, THF (**109** and **110**: 86%, 2 steps); p) MsCl, py, CH₂Cl₂, 58%; q) NaN₃, DMF, 87%.

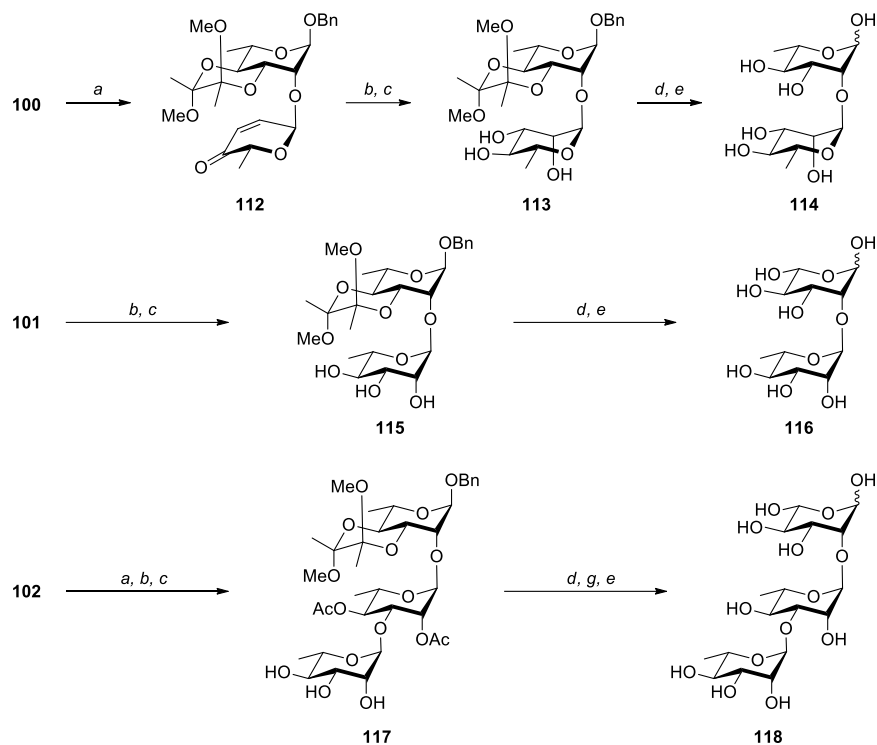
CHAPITRE 3 – SYNTHESIS OF OLIGOSACCHARIDES RELATED TO POTENTIAL BIOTERRORIST PATHOGENS

through hydrolysis furnished disaccharide **102** having an unprotected hydroxyl group at C-3. Glycosylation of disaccharide **102** and ketone *ent*-**91** was realized in an analogous manner. Subsequent glycosylation of resulting trisaccharide with either TCA **97** or phosphate **98** were unsuccessful, as only hydrolysis of the spiroketal could be observed. It was hypothesized that converting the trisaccharide into a more acid-stable compound, such as trisaccharide **104**, could overcome these glycosylation problems. Indeed, tetrasaccharides **109** and **111** were successfully synthesized from trisaccharides **105** and **106**, respectively, through two different pathways. Compound **108**, precursor of tetrasaccharide **111**, was synthesized from levulinoylated trisaccharide **104** in a multi-step fashion. Hydrogenolysis was conducted to cleave the benzyl ether at the anomeric position, resulting alcohol was converted into a TCA intermediate, which was glycosidated with 6-benzyloxyhexanol under the promotion of TMSOTf, and the Lev group was removed using hydrazinium acetate. Coupling of resulting trisaccharide **106** with anthroside **97** under the promotion of TMSOTf followed by delevulinoylation and methylation afforded tetrasaccharide **108**. It is worth mentioning that the methylation could only be achieved using methyl iodide as reagent/solvent and silver(I) oxide as the promoter. As of protected compound **107**, it was prepared from delevulinoylated trisaccharide **105** and either TCA **97** or phosphate **98**. One-pot acetate cleavage and azide reduction were achieved by employing PEt_3 and LiOH in a mixture of MeOH , THF and H_2O . Tetrasaccharides **109** and **110** were then prepared following standard deprotection procedures. NMR analysis of tetrasaccharide **109** revealed that its spectroscopic data were identical to those of the isolated natural anthrax tetrasaccharide. Finally, selective mesylation of primary alcohol **110** and displacement of the mesylate with NaN_3 through an $\text{S}_{\text{N}}2$ -like reaction afforded anthrax-related tetrasaccharide **111** ready for subsequent conjugation to carrier proteins.

The O'Doherty's group also prepared di- and trisaccharides related to anthrax tetrasaccharide²⁷⁹ acting as control compounds to attest that the previously reported detection methods^{248, 251, 264} targeted the anthrose moiety rather than the trirhamnose. Control compounds **114**, **116** and **118** were synthesized using the author's *de novo* approach (Scheme 11). L/D-Disaccharide **114**, L-disaccharide **116** and L-trisaccharide **118** were prepared, respectively, from compounds **91**, **101**, and *ent*-**91** by taking once again advantage of Luche reduction and palladium-catalyzed

CHAPITRE 3 – SYNTHESIS OF OLIGOSACCHARIDES RELATED TO POTENTIAL BIOTERRORIST PATHOGENS

glycosylation. Deprotection of disaccharides **113** and **115** was achieved following treatment with aqueous TFA and hydrogenolysis. Due to concomitant partial acetyl hydrolysis and migration during deprotection of trisaccharide **117**, treatment with basic methanol had to be realized prior to hydrogenolysis.



Scheme 3.11. *De novo* synthesis of di- and trisaccharides related to anthrax tetrasaccharide by O'Doherty¹⁵

It is thought that a GalNAc residue connects the tetrasaccharide from *B. anthracis* exosporium, but the stereochemistry of this linkage is lost during isolation of the compound of interest.²⁴⁵ Therefore, Adamo and co-workers recently reported the synthesis of different glycoconjugates related to anthrax tetrasaccharide to assess the role of the configuration of this linkage on immunogenicity.²⁸⁰ Two tetrasaccharides equipped with a methyl ester linker in either α - or β -configuration, two trirhamnosides anomers and a non-methylated α -tetrasaccharide were prepared

¹⁵ a) **91** or *ent*-**91**, Pd₂(DBA)₃·CHCl₃, PPh₃, CH₂Cl₂, 0 °C (**112**: 85%; **117**: 94%); b) CeCl₃, NaBH₄, MeOH, CH₂Cl₂, -78 °C (**113**: 90%); c) OsO₄, NMO/H₂O, *t*-butanol/acetone 1:1 (**113**: 93%; **115**: 83%, 2 steps; **117**: 80%, 2 steps); d) TFA/H₂O 10:1, CH₂Cl₂; e) H₂, Pd/C, MeOH (**114**: 88%, 2 steps; **116**: 85%, 2 steps; **118**: 81%, 3 steps); f) LiOH, MeOH.

CHAPITRE 3 – SYNTHESIS OF OLIGOSACCHARIDES RELATED TO POTENTIAL BIOTERRORIST PATHOGENS

and conjugated to carrier proteins for biological assays. BALB/c mice were immunized with the α - or β -tetrasaccharide conjugate and their sera were tested against both tetrasaccharides. Result showed that notwithstanding the stereochemistry of the downstream rhamnose, similar IgG levels were measured. The absence of the methyl group on the anthrose moiety appeared to have no effect on the result, as already reported. However, when the sera were tested against the trirhamnosides, the stereochemistry of the downstream rhamnoside appeared to have significance, highlighting the immunological importance of the anthrose moiety. The immunological potential of both the α - and β -tetrasaccharide was also underlined by the fact that the sera of mice immunized with these oligosaccharides reacted with Sterne spores. Mutant Δ BclA spores that did not express BclA exosporium were also recognized, suggesting that the studied tetrasaccharide could also be expressed elsewhere by *B. anthracis*.

Even if it was reported that the anthrose moiety is a unique component of *B. anthracis* BclA exosporium, other bacteria produce similar saccharides. Indeed, as previously stated, *Shewanella* spp. MR-4 possesses a CPS containing a terminal residue related to anthrose, but lacking the C-2 methyl ether.²⁷¹ A variant of this CPS is substituted with 3-hydroxybutyrate rather than 3-hydroxy-3-methylbutyrate. *Pseudomonas syringae* flagellae also possess an oligosaccharide composed of a structure similar to anthrose but substituted with 3-hydroxybutyrate.²⁸¹ Kubler-Kielb recently conducted assays that indicated that the C-2 methyl ether as well as the C-3 methyl substituent on the 3-hydroxybutyrate moiety were not essential for antibody recognition,²⁷² as did other studies on *B. anthracis*. Anti-*B. anthracis* spore sera cross-reacted with *Shewanella* CPSs and *Pseudomonas syringae* flagellae, and anti-*Shewanella* and anti-*Pseudomonas syringae* sera recognized *B. anthracis* spores, highlighting the potential of *Shewanella* CPS as a possible constituent of anthrax vaccines.

Apart from BclA oligosaccharide, *B. anthracis* produces another polysaccharide of interest. More particularly, vegetative cells possess a secondary cell wall polysaccharide, whose structure has recently been elucidated.²⁸² It consists in a backbone of structure $\rightarrow 6)-\alpha\text{-GlcNAc-(1}\rightarrow 4)-\beta\text{-ManNAc-(1}\rightarrow 4)-\beta\text{-GlcNAc-(1}\rightarrow$. The $\alpha\text{-GlcNAc}$ residue is substituted at C-3 and C-4 with $\alpha\text{-Gal}$ and $\beta\text{-Gal}$ residues, respectively, whereas the $\beta\text{-GlcNAc}$ is substituted at C-3 with an $\alpha\text{-Gal}$ moiety

CHAPITRE 3 – SYNTHESIS OF OLIGOSACCHARIDES RELATED TO POTENTIAL BIOTERRORIST PATHOGENS

(Figure 1). However, these substitutions are non-stoichiometric, leading to microheterogeneity in *B. anthracis* cell wall polysaccharides population.²⁸² Being species-specific, this hexasaccharide could be of substantial help for the development of diagnostic tools and/or vaccines. Therefore, synthesis of this hexasaccharide and analogues was investigated by different research teams.

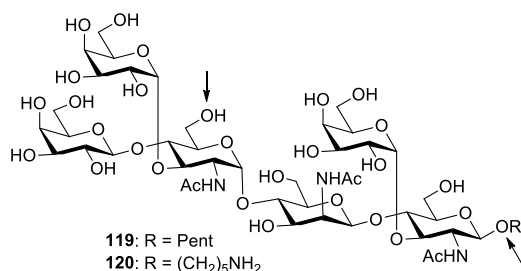
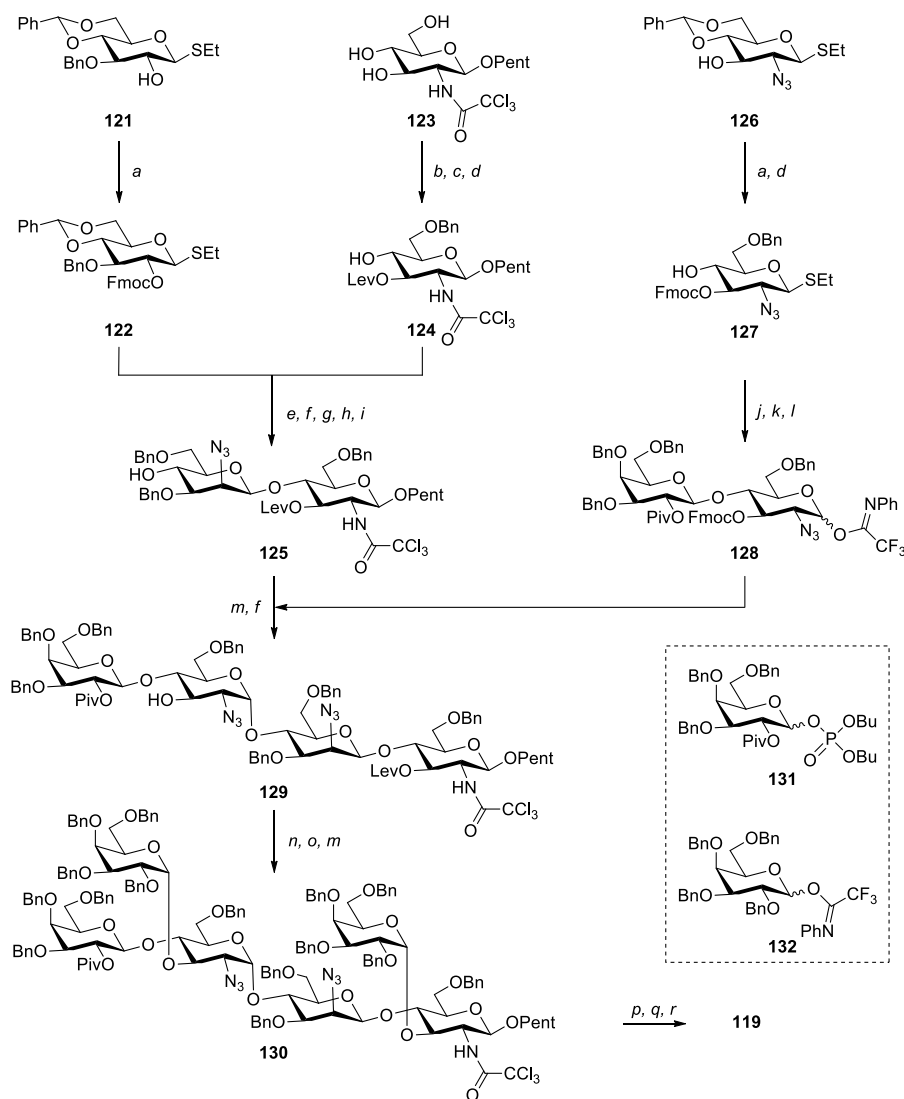


Figure 3.1 Major cell wall repeating unit hexasaccharide from *Bacillus anthracis* vegetative cells bearing two different linkers for carrier protein conjugation prepared by Seeberger and Boons

An analogue of *B. anthracis* major cell wall hexasaccharide repeating unit, hexasaccharide **119**, was assembled by Seeberger and co-workers (Scheme 12).²⁸³ Their synthesis pathway enabled the formation of characteristic α - and β -linkages, which are challenging to obtain. Intermediates **121**, **123**, and **126** were used as starting material for the preparation of building blocks **122**, **124**, and **127**, respectively, which were prepared through various standard protecting groups manipulations. As for the hexasaccharide construction, it was realized using a convergent [2 + 2] approach. Thioglucoside **122** and glycosyl acceptor **124** were coupled under the promotion of MeOTf, and the *trans*-linkage was created due to the NGP of the Fmoc group. The non-reductive glucose unit was then converted into a mannosazide residue following cleavage of the Fmoc protecting group, and inversion of the configuration through the displacement of a triflate by tetrabutylammonium azide. These steps allowed the successful introduction of the challenging β -mannosamine linkage. It is worth mentioning that the benzylidene protecting group at C-4 and C-6 of the glucoside moiety appeared to be required for the inversion. Finally, disaccharide **125** was obtained following benzylidene ring opening. In parallel, glycosylation of building blocks **127** and **131**, the latter being known to be useful for the preparation of β -galactose units, was achieved. The Piv protecting group at the C-2 position of galactose phosphate **131** was needed for the introduction of target β -glycosidic linkage. Coupling of the resulting disaccharide with disaccharide acceptor **125** was

attempted but appeared to be fruitless. The thiodisaccharide was then converted into *N*-phenyltrifluoroacetimidate **128**. This derivative was successfully glycosidated with disaccharide **125** through an α -glucosamine linkage using TMSOTf as the promoter and a mixture of CH₂Cl₂ and Et₂O, and the Fmoc group was cleaved using triethylamine, furnishing tetrasaccharide **129**. The latter underwent an α -galactosylation using building block **132**, a delevulinoylation, and a second α -galactosylation to afford fully assembled, protected hexasaccharide **130**. The α -galactosidic linkages were introduced using a mixture of CH₂Cl₂ and Et₂O as the reaction medium. Finally, target *B. anthracis*-related hexasaccharide **119** bearing an *n*-pentenyl linker at the reducing end was obtained following global deprotection under Birch conditions. Extensive spectroscopic analyses were conducted and confirmed that the characteristic α -linkages were indeed present in the synthetic compound.

CHAPITRE 3 – SYNTHESIS OF OLIGOSACCHARIDES RELATED TO POTENTIAL BIOTERRORIST PATHOGENS



Scheme 3.12. Seeberger's group synthesis of the hexasaccharide repeating unit of the first proposed structure of *B. anthracis* cell wall polysaccharide¹⁶

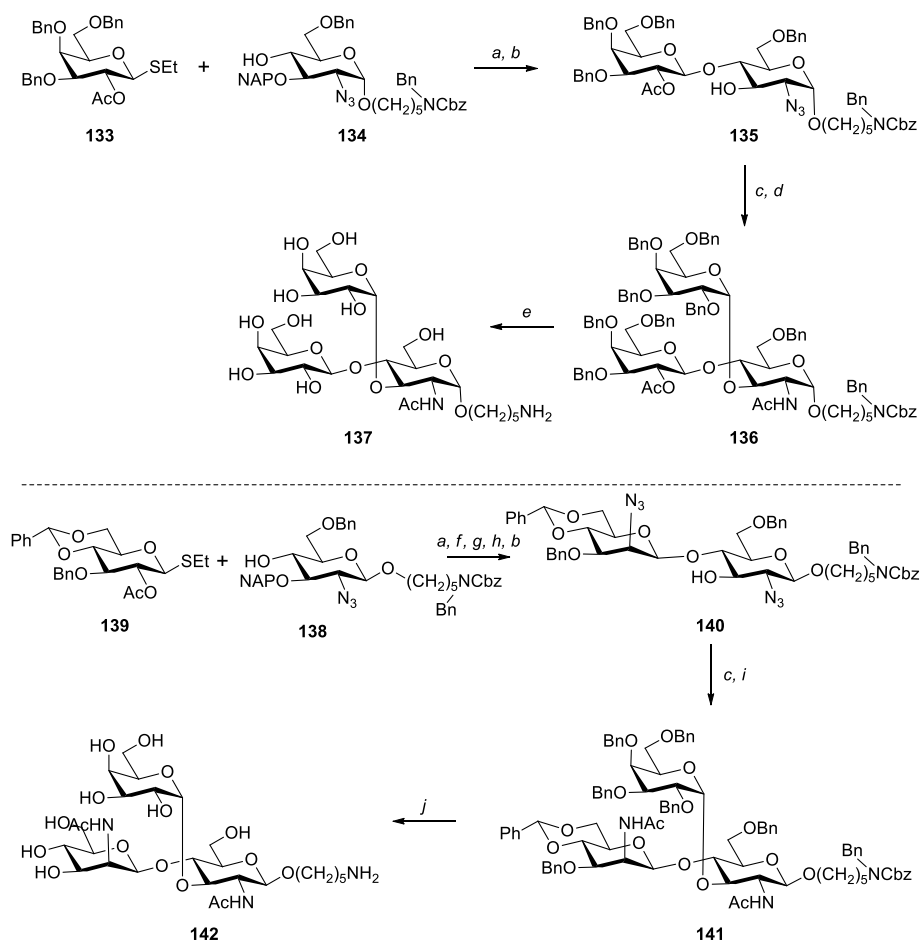
Trisaccharides **137** and **142**, derived from *B. anthracis* cell wall hexasaccharide repeating unit, were synthesized by Boons for the determination of the antigenic determinants of the hexasaccharide (Scheme 13).²⁸⁴ Building blocks **132**, **133**, **134**, **138**, and **139** were used to

¹⁶ a) FmocCl, py (**122**: 91%; **126**: 96%); b) PhCH(OMe)₂, TsOH·H₂O, CH₃CN, 90%; c) LevOH, DIPC, DMAP, CH₂Cl₂, 96%; d) TFA, Et₃SiH, CH₂Cl₂ (**124**: 92%; **127**: 83%); e) MeOTf, CH₂Cl₂, 0 °C to rt, 82%; f) Et₃N, CH₂Cl₂ (**125**: 93%; **129**: 73%); g) Tf₂O, DMAP, py, CH₂Cl₂; h) (*n*Bu)₄NN₃, DMF, 87% (2 steps); i) BF₃·OEt₂, Et₃SiH, CH₂Cl₂, 60%; j) **131**, TMSOTf, CH₂Cl₂, -30 to -20 °C, 92%; k) NBS, acetone/H₂O, 84%; l) CF₃C(NPh)Cl, Cs₂CO₃, CH₂Cl₂, 85%; m) **128** or **132**, TMSOTf, CH₂Cl₂/Et₂O, 1:4, -50 to 0 °C, (**129**: 80%; **130**: 70%); n) **132**, TMSOTf, CH₂Cl₂/Et₂O 1:4, -45 to 0 °C, 84%; o) H₂NNH₂·H₂O, AcOH, py, CH₂Cl₂, 94%; p) Na, NH₃(l), THF, *t*-BuOH, -78 °C; q) Ac₂O, py, DMAP, 57% (2 steps); r) NaOMe, MeOH, 85%.

CHAPITRE 3 – SYNTHESIS OF OLIGOSACCHARIDES RELATED TO POTENTIAL BIOTERRORIST PATHOGENS

commence the syntheses. Similar strategies as those previously mentioned were employed to ensure glycosylation selectivity. Coupling of thioglycoside **133** and alcohol **134** was achieved under the promotion of NIS and TMSOTf and was followed by oxidative removal of the NAP ether, yielding disaccharide acceptor **135** selectively in its β -form. A lower yield was obtained when the protected linker of alcohol **134** was a carboxybenzyl-3-aminopropyl function. Disaccharide acceptor **135** was glycosylated with *N*-phenyltrifluoroacetimidate **138** employing TMSOTf in a mixture of CH₂Cl₂ and Et₂O and the azide function was converted into target acetamido moiety following treatment with Zn/CuSO₄ and acetylation. Anomerically pure trisaccharide **136** was thus successfully formed. Target trisaccharide **137** was finally prepared after saponification and hydrogenolysis of protected compound **136**.

CHAPITRE 3 – SYNTHESIS OF OLIGOSACCHARIDES RELATED TO POTENTIAL BIOTERRORIST PATHOGENS



Scheme 3.13. Synthesis of trisaccharides related to the first proposed structure of *B. anthracis* cell wall polysaccharide¹⁷

Coupling of compounds **139** and **138** followed by deacetylation, inversion of the C-2 stereocenter and removal of the NAP protecting group afforded β -disaccharide **140**. The glycosylation conditions and the inversion of the C-2 stereocenter allowed the installation of the challenging β -mannosamine moiety. It is worth mentioning that both the acetyl ester and the NAP ether were used as protecting groups in intermediates **139** and **138** since they are orthogonal to each others. Therefore, they make possible the installation of the azido moiety and allow the α -galactosylation to be performed in a selective manner. Glycosylation of mannoside acceptor **140** and glycosyl

¹⁷ a) NIS, TMSOTf, CH₂Cl₂, 0 °C (**135**: 87%; **140**: 88%); b) DDQ, CH₂Cl₂, H₂O (**135**: 94%; **140**: 94%); c) **132**, TMSOTf, CH₂Cl₂, Et₂O, 50 °C (**136**: 86%; **141**: 83%); d) Zn/CuSO₄, AcOH, Ac₂O, THF, 63%; e) i. NaOMe, MeOH; ii. Pd(OH)₂/C, H₂, AcOH, *t*BuOH, H₂O, 56% (2 steps); f) NaOMe, MeOH, 90%; g) Tf₂O, py, CH₂Cl₂, 0 °C; h) NaN₃, DMF, 50 °C, 90% (2 steps); i) i. PMe₃, THF, H₂O; ii. Ac₂O, py, 58%; j) Pd(OH)₂/C, H₂, AcOH, *t*BuOH, H₂O, 73%.

CHAPITRE 3 – SYNTHESIS OF OLIGOSACCHARIDES RELATED TO POTENTIAL BIOTERRORIST PATHOGENS

donor **132** was then achieved using previously mentioned conditions in order to introduce an α -galactoside linkage. The azide was then reduced under the action of trimethylphosphine in THF in the presence of water, and the resulting amine was acetylated, furnishing trisaccharide **141**. Catalytic hydrogenation over Pd was finally used to cleave the benzyl ethers and the benzyloxycarbamate, yielding target trisaccharide **142**.

Immunological assays were conducted on *B. anthracis* polysaccharide as well as trisaccharides **137** and **142** to assess their biological potential. These trisaccharides were conjugated to maleimide activated BSA after being thiolated. Meanwhile, *B. anthracis* polysaccharide was conjugated to BSA and KLH. Hence, rabbits were inoculated with either polysaccharide-KLH conjugate, live- or irradiated spores, and ELISA was used to analyze the sera. Results showed that antibodies were elicited by the polysaccharide-KLH conjugate, and that IgG antibodies produced following inoculation with live- and irradiated-spores of *B. anthracis* recognized the polysaccharide. Moreover, **137**-BSA and **142**-BSA conjugates proved to be recognized by IgG antibodies elicited by KLH-polysaccharide conjugate and live and irradiated-spores. Competitive ELISA also revealed that BSA-polysaccharide conjugate was able to offer a complete inhibition of antibodies binding, while **137**-BSA and **142**-BSA were only partial inhibitors, suggesting that the antibodies produced were heterogeneous. These results highlight the fact that the hexasaccharide is probably not only produced by vegetative cells, but also by *B. anthracis* spores, and could therefore provide protection against vegetative cells and spores.

This *B. anthracis* secondary cell wall polysaccharide was investigated for its antigenicity in a work reported by Leoff *et al.*²⁸⁵ This polysaccharide was detached from the cell wall by aqueous hydrogen fluoride (HF-PS) and rabbits were immunized with *B. anthracis* live or killed spores. It should be mentioned that HF treatment also lead to cleavage of the 4,5-pyruvyl unit at the terminal β -ManNAc residue. Their sera proved to contain anti-HF-PS IgG antibodies, revealing the antigenicity of the polysaccharide. Biological assays also highlighted that *B. anthracis* and *B. cereus* cell wall polysaccharides share epitopes linked to the pathogenicity of both bacteria. Moreover, following exposure of rhesus macaques to aerosolized *B. anthracis*, anti-HF-PS

CHAPITRE 3 – SYNTHESIS OF OLIGOSACCHARIDES RELATED TO POTENTIAL BIOTERRORIST PATHOGENS

antibodies were detected in their sera, underlining the potential use of HF-PS glycoconjugates for the detection of *B. anthracis* infection or for the development of vaccines.

An alternative to specific antibodies for rapid detection of bacilli can be the use of endolysins.²⁸⁶ These enzymes are produced by bacteriophages – viruses infecting bacteria – and are known to be highly specific for their hosts due to coevolution. Endolysins proceed to cleave glycosidic or peptide bonds at a late stage of the infection, resulting in cell lysis and thus liberation of bacteriophages. Interest in endolysins comes from the binding specificity of their cell wall binding domain.²⁸⁷ Indeed, *B. anthracis* lysins PlyG and PlyL target essential polysaccharides such as *B. anthracis* cell wall hexasaccharide.²⁸⁸ However, molecular mechanisms underlying *B. anthracis* lysins are still unknown. Boons and co-workers addressed this issue by synthesizing hexasaccharide **120** and derivatives **143-148**, as shown in Figures 1 and 2, and studying their binding affinities with PlyL and PlyG.²⁸⁸ Hexasaccharide **120** is a derivative of *B. anthracis* cell wall polysaccharide containing an aminopentyl linker for further biological studies. Trisaccharide **143** possesses the hexasaccharide backbone structure, whereas tetrasaccharides **144-146** differentiate themselves by the position of the additional galactosyl moiety. Disaccharide **147** is derived from trisaccharide **143**, but lacks the GlcNAc residue, and trisaccharide **148** possesses an *N*-acetyl-galactosamine moiety instead of GlcNAc. The difference between the compounds will be helpful to identify the residues that can be accommodated by PlyG and PlyL.

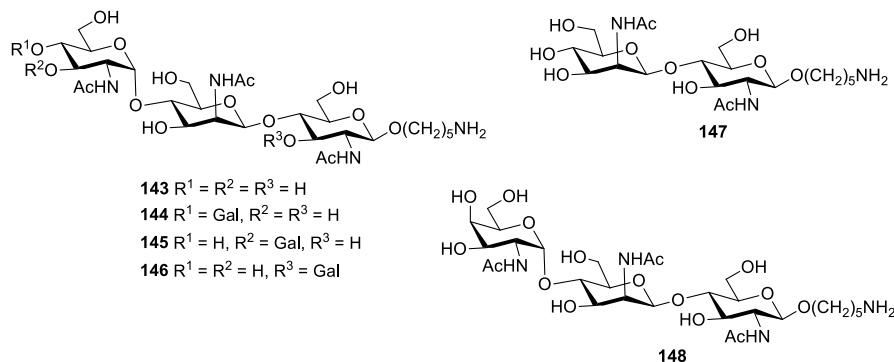
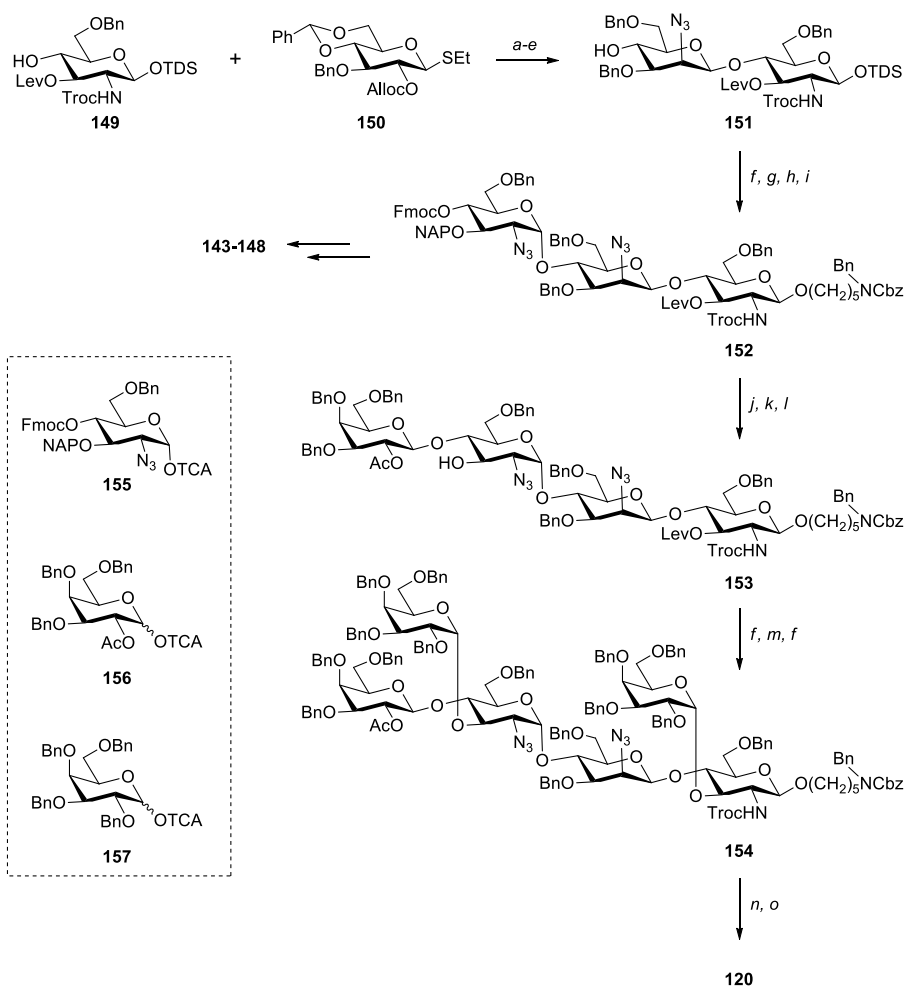


Figure 3.2. *B. anthracis* vegetative cell wall polysaccharide derivatives prepared by Boons

Boons and co-workers approach was based on the use of orthogonal protecting groups such as Fmoc, NAP, Lev, and thexyldimethylsilyl (TDS), which would provide chemical flexibility by

allowing selective modifications of the intermediate compounds. They commenced their synthesis by coupling thioglucoside **149** and glucoside **150** under the promotion of NIS and TMSOTf (Scheme 14). The NGP of allyloxycarbonyl (Alloc) enabled the formation of the β -glycosidic linkage. This protecting group was removed following treatment with Pd(PPh₃)₄ and the introduction of the β -mannoside was completed through displacement of a triflate intermediate. Reductive cleavage of the benzylidene protecting group at C-4 and C-6 furnished disaccharide acceptor **151**. The latter was glycosylated with TCA building block **155**, and the use of Et₂O and CH₂Cl₂ as the reaction media allowed the formation of a trisaccharide in an α/β ratio of 8:1. The TDS group was cleaved to allow the introduction of the *N*-benzyl-*N*-carboxybenzylpentenyl linker by employing standard conditions. Removal of the Fmoc carbamate of resulting trisaccharide **152** using triethylamine was followed by glycosylation with intermediate **156**. The NAP protecting group was cleaved under oxidative conditions, furnishing tetrasaccharide **153**. The latter subsequently underwent glycosylation with perbenzylated TCA **157**, delevulinoylation and another glycosylation with compound **157**. These steps afforded hexasaccharide **154**, which was converted into target hexasaccharide **120** upon transformation of the azido and 2,2,2-trichloroethoxycarbonyl (Troc) groups into acetamido moieties and complete deprotection. For the sake of brevity, syntheses of compounds **143-148** are not included in Scheme 14. Trisaccharide **143** was prepared by standard deprotection of intermediate **152**. Tetrasaccharides **144-146** were synthesized upon removal of the Fmoc, NAP or Lev protecting groups, α -galactosylation, and global deprotection. As for disaccharide **147** and trisaccharide **148**, they were obtained in an analogous manner.

CHAPITRE 3 – SYNTHESIS OF OLIGOSACCHARIDES RELATED TO POTENTIAL BIOTERRORIST PATHOGENS



Scheme 3.14. Boons group synthesis of the hexasaccharide repeating unit of the first proposed structure of *B. anthracis* cell wall polysaccharide¹⁸

Binding of synthesized derivatives **120** and **143-148** with the cell wall binding domain of PlyL and PlyG was evaluated through SPR experiments. Since the results for PlyL and PlyG were quite similar, these endolysins seem to recognize similar galactosylation patterns. Results also showed that tetrasaccharide **144** bound strongest, suggesting that the β -galactoside moiety at C-4 contributes to the binding. In contrast, the α -galactoside at C-3 of the terminal GlcNAc seems to

¹⁸ a) NIS, TMSOTf, CH₂Cl₂, -20 °C, 86%; b) Pd(PPh₃)₄, THF/H₂O, 91%; c) Tf₂O, DMAP, py, CH₂Cl₂, 0 °C; d) NaN₃, DMF, 55 °C, 86% (2 steps); e) Et₃SiH, TfOH, CH₂Cl₂, -78 to -35 °C, 65%; f) **155** or **157**, TMSOTf, Et₂O/CH₂Cl₂, -55 to 0 °C (**152**: 54%; **154**: 72% and 65% $\alpha/\beta > 20:1$); g) HF·py, THF, 92%; h) Cl₃CCN, K₂CO₃, CH₂Cl₂, 91%; i) *N*-benzyl-*N*-carboxybenzyl-5-aminopentan-1-ol, TMSOTf, -30 to -20 °C, 87%; j) Et₃N, CH₂Cl₂, 98%; k) **156**, TMSOTf, CH₂Cl₂, -35 to -25 °C, 88%; l) DDQ, CH₂Cl₂/H₂O, 78%; m) H₂NNH₂·AcOH, MeOH, CH₂Cl₂, 93%; n) Zn, Ac₂O/AcOH/THF, CuSO₄, 72%; o) i. NaOMe, MeOH, CH₂Cl₂; ii. Pd(OH)₂/C, H₂, *t*BuOH, AcOH, H₂O, 69%.

preclude interaction with the binding domains. Results additionally showed that the α -galactoside at the reducing end, although accommodated by endolysins, did not enhance the binding affinity as tetrasaccharide **146** and trisaccharide **143** displayed similar binding affinity.

3.5 *Burkholderia pseudomallei* and *Burkholderia mallei*

Endemic of tropical and subtropical regions, melioidosis and glanders are diseases caused by the GNB *B. pseudomallei* and *B. mallei*, respectively. Expression of these diseases is polymorph, as infections can manifest themselves as localized skin lesions, pneumonia, and even septicemia. *B. mallei* is pathogenic for humans, as is *B. pseudomallei*, but mainly infects animals such as horses. Inoculation can occur through inhalation, both bacteria are intrinsically resistant to routinely used antibiotics, their infectious dose is particularly low, mortality rates are up to 50% in endemic regions,²⁸⁹ and no vaccines are currently licensed for use, rendering them potential bioterrorism weapons. Moreover, *B. mallei* was reportedly used during World Wars I and II.²⁹⁰ *B. pseudomallei* and *B. mallei* produce diverse cell surface-exposed polysaccharides, including CPS, LPS, and EPS. These are known as virulence factors and cause the production of specific and protective antibodies in humans, making them interesting targets for the development of vaccines or diagnostic tools.²⁹¹

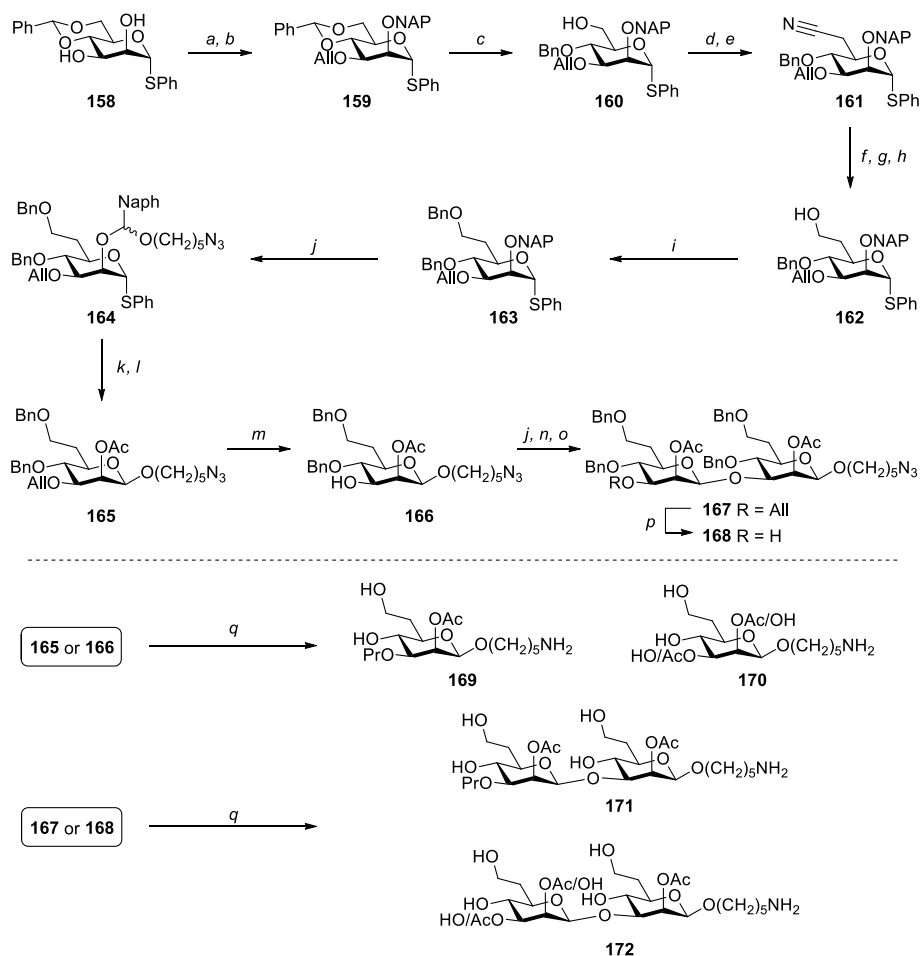
3.5.1 Capsular polysaccharides

Elucidation of the chemical structure of *B. pseudomallei* and *B. mallei* 6-deoxyheptan CPS showed that it is constituted of a heteropolymer composed of (1→3)-linked 2-*O*-acetyl-6-deoxy- β -D-*manno*-heptopyranose residues as the repeating unit.²⁹² In 2014, the Gauthier's group prepared mono- and disaccharide mimics of this CPS.²⁹³ Their methodology relied on the use of intramolecular aglycon delivery (IAD), allowing the introduction of the challenging 1,2-*cis* glycosidic linkages without the need of rigid 4,6-*O*-benzylidene protecting groups, which are precluded due to the presence of the one-carbon extension at C-6, nor the rigorously stereoselective formation of the intermediate acetal.

Therefore, thiomannoside **158** was used as the starting material (Scheme 15). A thiophenyl moiety was chosen for the anomeric position as it can be activated with soft electrophiles without having

an impact on the other protecting groups. Diol **158** was converted into intermediate **159** following allylation through the formation of a stannylene acetal and introduction of the NAP ether. The latter was chosen for the IAD rather than PMB since it usually provides higher yields during both the mixed acetal formation and the glycosylation steps.²⁹⁴ Regioselective opening of the 4,6-*O*-benzylidene group was achieved using a mixture of DIBALH and toluene, furnishing C-6 alcohol **160** as the major product. The latter underwent tosylation to allow the preparation of nitrile **161** through a bimolecular nucleophilic substitution with KCN in the presence of 18-crown-6, resulting in the introduction of an additional carbon. A three-step protocol was then employed to convert the nitrile group into alcohol **162**, involving its reduction into an imine, hydrolysis of the latter into an aldehyde, and subsequent reduction. The primary alcohol was then benzylated, resulting in thioglycoside donor **163**. The latter was converted into mixed acetals **164**, ready for IAD, by oxidative treatment with DDQ in the presence of 5-azido-1-pentanol. Dimethyl(methylthio)sulfonium trifluoromethanesulfonate (DMTST) and 2,6-di-*tert*-butyl-4-methylpyridine (DTBMP) in diluted DCE were then employed to conduct the intramolecular glycosylation and yielded anomerically pure compound **165** following acetylation. The allyl group was cleaved using PdCl₂ and resulting alcohol **166** was glycosylated with thioheptoside **163** through the developed IAD conditions and acetylated, furnishing disaccharide **167**. The latter was converted into alcohol **168** upon cleavage of the allyl group. Finally, hydrogenolysis of compounds **165-168** afforded deprotected mono- and disaccharides **169-172**. Acetyl migration from *O*-2 to *O*-3 occurred for compounds **170** and **172**. Therefore, compounds **169** and **171**, containing a propyl group at C-3, were prepared to avoid acetyl migration. The propyl group could potentially mimic the elongation or termination at C3.

CHAPITRE 3 – SYNTHESIS OF OLIGOSACCHARIDES RELATED TO POTENTIAL BIOTERRORIST PATHOGENS



Scheme 3.15. Intramolecular aglycon delivery allowing the synthesis of mono- and disaccharide mimics of *B. pseudomallei* and *B. mallei* CPS¹⁹

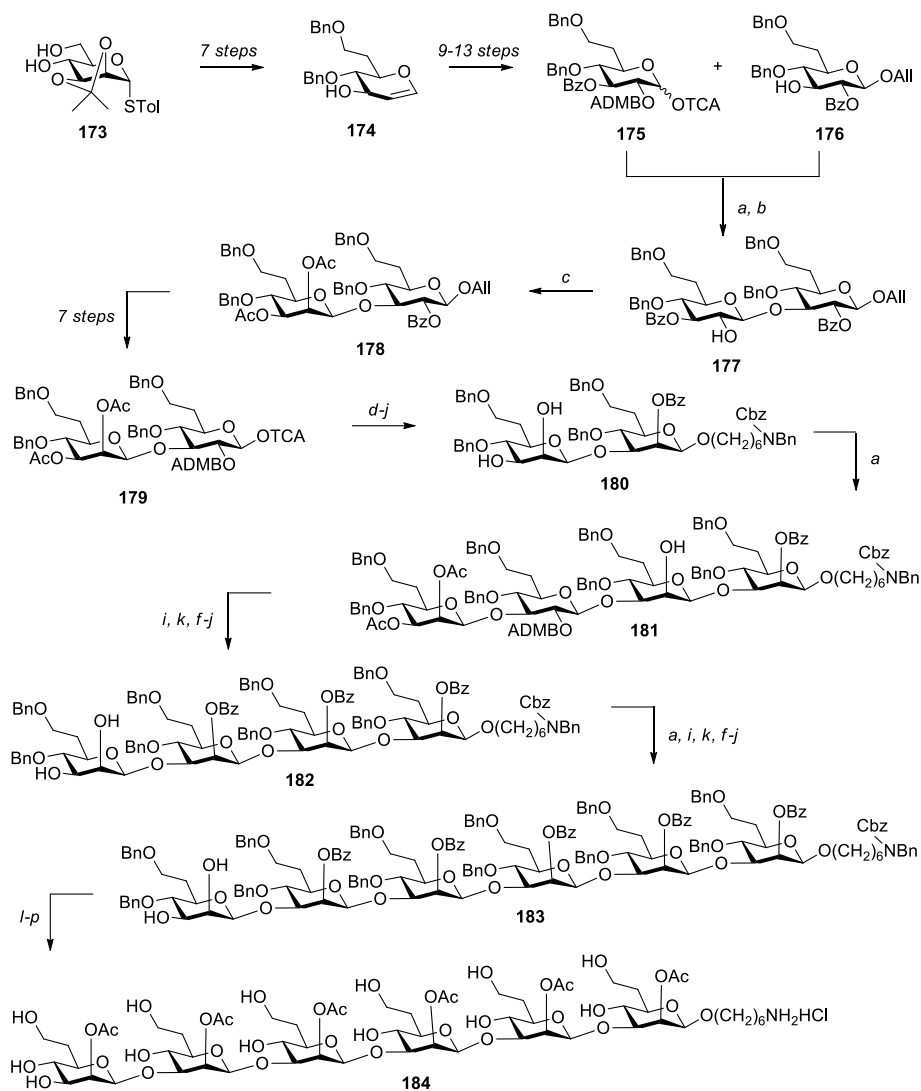
Following these syntheses, mono- and disaccharides **169** and **171** were studied to investigate their interaction between anti-CPS mAb 4C4.²⁹⁵ Various NMR analysis methods revealed that the acetyl groups at C-2 are essential for recognition by mAb 4C4, and that protons H-4, H-5, H-6, and H-7 of disaccharide **171** were strongly recognized. Moreover, it was shown that, upon binding of disaccharide **171** to mAb 4C4, no conformational changes occurred. These findings put forward

¹⁹ a) *i.* Bu₂SnO, toluene, reflux; *ii.* CsF, TBAI, AlIBr; b) NAPBr, NaH, DMF, 85% (2 steps); c) DIBALH/toluene, 73%; d) TsCl, DMAP, pyridine; e) KCN, 18-crown-6, 59% (2 steps); f) DIBALH/toluene, -78 °C; g) THF/HCl 9:1; h) NaBH₄, MeOH/CH₂Cl₂, 87% (3 steps); i) BnBr, NaH, TBAI, DMF, quant.; j) HO(CH₂)₅N₃ or **163**, DDQ, CH₂Cl₂, 4 Å MS, ROH; k) DTBMP, DMTST, DCE, 5 Å MS, 40 °C, 60% (2 steps); l) Ac₂O, pyridine, DMAP, 92%; m) PdCl₂, MeOH, rt, 55%; n) DTBMP, DMTST, DCE, 5 Å MS, 58% (2 steps); o) Ac₂O, pyridine, DMAP, 96%; p) PdCl₂, MeOH/CH₂Cl₂, rt, 69%; q) Pd black, H₂, MeOH, HCl, 40 °C (**169-172**: quant.).

the potential use of the synthesized CPS fragments for vaccines design and development of diagnostic tools against melioidosis and glanders.

Scott and co-workers developed an iterative method for the preparation of a hexasaccharide mimicking *B. pseudomallei* and *B. mallei* 6-deoxyheptan CPS based on the use of a disaccharide building block containing a 4-acetoxy-2,2-dimethylbutanoyl (ADMB) participating group at C-2, ensuring the formation of 1,2-*trans*-glycosidic linkages, and obtained from common precursor **173**.²⁹⁶ As depicted in Scheme 16, acetonide **173** was transformed into glucoheptoside glycal **174** in seven steps. Multi-step modification of the latter furnished glycosyl acceptor **175** and TCA **176**, which were glycosylated by employing TMSOTf as the promoter, and selective removal of the ADMB protection group under the action of AcCl and methanol in CH₂Cl₂ yielded disaccharide **177**. This last step enabled the epimerization of the *O*-2 position into the *manno* configuration through the displacement of a triflate intermediate by Bu₄NOAc. Functionalization of disaccharide **178** afforded target disaccharide building block **179** in a 54% yield in seven steps. The latter was glycosidated with a protected aminolinker and further converted into diol **180** following saponification, protection of the 2,3-diol with an isopropylidene group, epimerization of the *gluco* *O*-2 position through an oxidation/reduction sequence using Dess-Martin periodinane and NaBH₄, benzylation, and removal of the isopropylidene. These steps allowed the formation of a disaccharide having the desired *β*-*manno*-*β*-*manno* configuration. Assembly of the hexasaccharide commenced with the [2 + 2] coupling of disaccharides **179** and **180**, furnishing tetrasaccharide **181**. This compound was converted into tetramannoside **182** in a seven-step sequence similar to the one described before, and iteration of the previous glycosylation and epimerization steps furnished hexamannoside **183**. In order to differentiate the two hydroxyl groups at the non-reducing end of the oligosaccharide to allow the regioselective acetylation at C-2, a 2,3-orthoester was prepared using trimethyl orthobenzoate. Its opening introduced a benzoyl group at C-2 and the resulting free alcohol was benzylated employing benzyl TCA under the catalysis of Yb(OTf)₃. All the hydroxyl groups being differentiated, Zemplén deacetylation was used to cleave the benzoyl groups and the resulting alcohols were acetylated. Subsequent hydrogenolysis finally furnished hexasaccharide **184** without detection of acetyl migration.

CHAPITRE 3 – SYNTHESIS OF OLIGOSACCHARIDES RELATED TO POTENTIAL BIOTERRORIST PATHOGENS



Scheme 3.16. Synthesis of a hexasaccharide related to *B. pseudomallei* and *B. mallei* CPS²⁰

Conjugation of oligosaccharide **184** to tetanus toxin protein (TetH_c) carrier protein was then achieved using a glutaric acid linker. It was found that the glycoconjugate was moderately immunogenic and the immunized BALB/c mice produced IgM and IgG that recognized the native

²⁰ a) (for **181** and **183**: **179**) TMSOTf, CH₂Cl₂, rt (**177**: 95%; **181**: 86%); b) AcCl, MeOH, CH₂Cl₂, 0 °C, 89%; c) i. Tf₂O, py, CH₂Cl₂, 0 °C; ii. Bu₄NOAc, tol, rt, 77% (2 steps); d) *N*-benzyl-*N*-carboxybenzyl-6-aminohexan-1-ol, TMSOTf, CH₂Cl₂, rt; e) NaOMe, MeOH, THF, rt; f) PTSA, acetone, 2,2-DMP, rt; g) Dess-Martin periodinane, CH₂Cl₂, rt; h) NaBH₄, CH₂Cl₂/MeOH, 0 °C; i) BzCl, py, DMAP, rt; j) 80% aq. HOAc, 50 °C, (**180**: 55%, 6 steps; **182**: 43%, 7 steps; **183**: 26%, 8 steps); k) Mg(OMe)₂, MeOH/THF, rt; l) PhC(OMe)₃, CH₂Cl₂, CH₃CN, CSA, rt, then H₂O; m) Yb(OTf)₃, BnTCA, tol, rt; n) NaOMe, MeOH/THF, rt; o) Ac₂O, py, DMAP, CH₂Cl₂, rt; p) 10% Pd/C, H₂, MeOH, H₂O, HCl, rt, 26% (5 steps).

CPS. The mice also showed to be protected against high doses of *B. pseudomallei* strain K96243 following immunization with the glycoconjugate.

Field and co-workers also investigated *B. pseudomallei* and *B. mallei* CPS.²⁹⁷ More particularly, they identified that the CPS structure of *B. thailandensis* E555, a strain closely related to *B. pseudomallei* and *B. mallei*, is identical to that of *B. pseudomallei*. Protection of a mouse model of melioidosis with *B. thailandensis* acetylated and deacetylated CPS conjugates revealed that the immune response is dependent on the acetylation. Moreover, *B. thailandensis* appeared to be antigenic. This finding is all the more relevant as *B. thailandensis* is non-pathogenic to humans, therefore rendering its CPS extraction easier.

3.5.2 Lipopolysaccharides

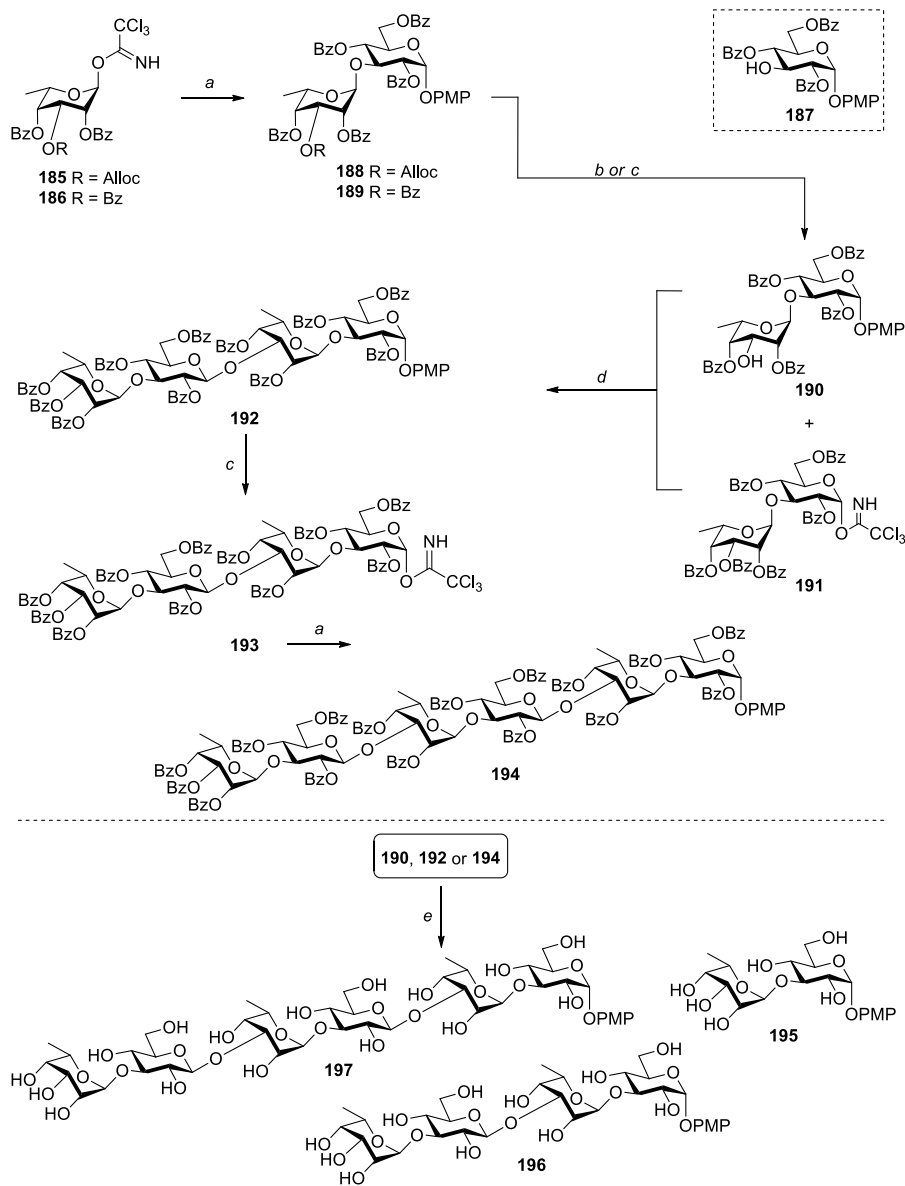
Apart from the previously described 6-deoxyheptan CPS, *B. pseudomallei* and *B. mallei* also produce LPS of similar structures. The *O*-antigen (OAg) is composed of a repetition of [\rightarrow 3)- β -D-Glcp-(1 \rightarrow 3)-6d- α -L-Talp-(1 \rightarrow)] disaccharide residues.²⁹² Investigation of the acetylation/methylation substitution pattern of the talose residues revealed that at least seven different arrangements were distinguishable.^{118, 292, 298} For both *B. pseudomallei* and *B. mallei*, the major intrachain epitope is composed of a talose residue acetylated at C-2. Meanwhile, the talose residue of *B. pseudomallei* terminal epitope is 2,4-*O*-diacetylated and 3-*O*-methylated, whereas *B. mallei* terminal epitope is also 3-*O*-methylated but only bears an acetyl group at C-2.^{298, 299}

Zhang and co-workers reported the synthesis of di-, tetra-, and hexasaccharides **195-197**, mimicking *B. pseudomallei* and *B. mallei* LPS OAg in its unacetylated form, using a convergent approach, as depicted in Scheme 17.^{300, 301} Building blocks **185** and **186** were obtained from L-rhamnose in 11 and 10 steps, respectively, whereas tribenzoylated glucoside **187** was readily prepared from D-glucose in eight steps. The latter possessed a PMP group at the anomeric position for further conjugation to a carrier protein. Rhamnosides donors **185** and **186** were both glycosidated with glucoside **187** under the promotion of TMSOTf, furnishing disaccharides **188** and **189**, respectively. Disaccharide glycosyl acceptor **190** was synthesized upon selective removal of Alloc group in disaccharide **188** using ammonium acetate, Pd[P(Ph)₃]₄ and NaBH₄ in a mixture

CHAPITRE 3 – SYNTHESIS OF OLIGOSACCHARIDES RELATED TO POTENTIAL BIOTERRORIST PATHOGENS

of MeOH and THF at low temperatures. In parallel, disaccharide **189** was converted into TCA **191** through standard protecting group manipulations, and further glycosidated with disaccharide glycosyl acceptor **190**. Resulting tetrasaccharide **192** was transformed into TCA **193** upon cleavage of the PMP group and coupled with disaccharide **190**. Finally, oligosaccharides **190**, **192**, and **194** were saponified employing saturated ammonia in MeOH, yielding target compounds **195-197**.

CHAPITRE 3 – SYNTHESIS OF OLIGOSACCHARIDES RELATED TO POTENTIAL BIOTERRORIST PATHOGENS



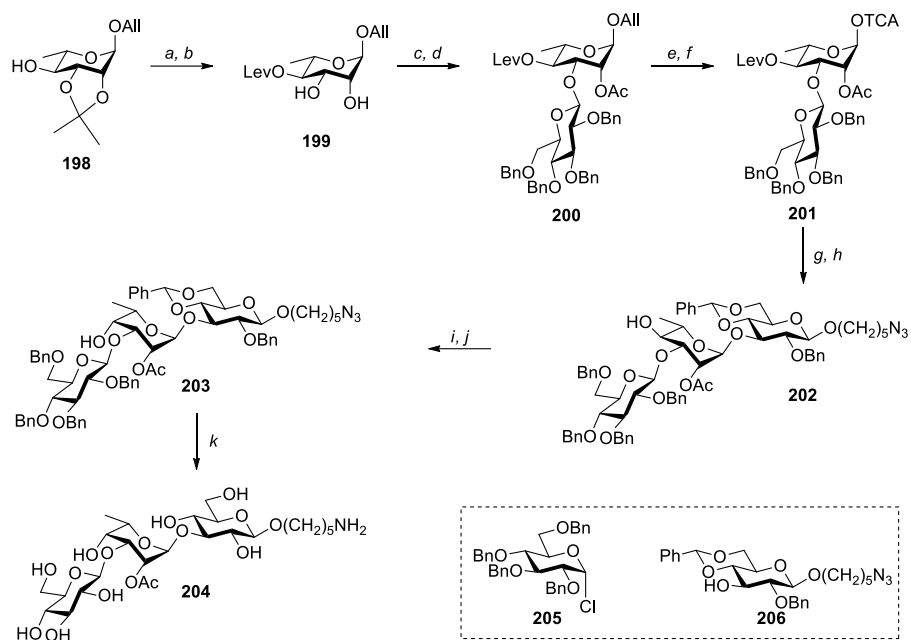
Scheme 3.17. Synthesis of non-acetylated di-, tetra-, and hexasaccharides related to *B. pseudomallei* and *B. mallei* LPS OAg²¹

Gauthier and co-workers reported the synthesis of oligosaccharidic fragments composed of the terminal and intrachain epitopes of *B. pseudomallei* and *B. mallei* OAg LPS.²⁴¹ Their synthesis

²¹ a) **187** or **190**, TMSOTf, CH₂Cl₂, -10 °C to rt (**188**: 82%; **189**: 89%; **194**: 65%); b) CH₃CO₂NH₄, Pd[P(Ph)₃]₄, NaBH₄, MeOH/THF, -10 °C, 85%; c) i. CH₃CN/H₂O, CAN, 30 °C, then ii. CCl₃CN, DBU, CH₂Cl₂, rt, (**191**: 75%; **193**: 70%; 2 steps); d) TMSOTf, CH₂Cl₂, -10 °C to rt, 77%; e) satd NH₃ in MeOH, rt, 83-88%.

was developed in order to avoid the migration of the acetyl groups at C-2, which were hypothesized to have an impact on the immunological action of the compounds. Scheme 18 depicts the synthesis of the main intrachain substitution, although Gauthier and co-workers also prepared trisaccharides presenting the less abundant substitutions. The preparation of the target compounds commenced with common intermediate allyl rhamnoside **198**, which was converted into diol **199** following levulinoylation and cleavage of the isopropylidene group under acidic conditions. For the synthesis of the trisaccharides containing the intrachain acetylation pattern, diol **199** was selectively glucosylated at C-3 with perbenzylated glucoside chloride **205** under the catalytic action of 2-aminoethyl diphenylborinate in the presence of silver(I) oxide. Following acetylation, resulting disaccharide **200** was converted into TCA **201** *via* standard transformations. Coupling of the latter with glycosyl acceptor **206** and removal of the Lev ester furnished trisaccharide **202** having an azido linker at the reducing end. Conversion of the intrachain rhamnose residue into its talose configuration was achieved through a Pfitzner-Moffatt oxidation/stereocontrolled reduction sequence. Finally, Pd black-catalyzed hydrogenolysis of trisaccharide **203** quantitatively afforded unprotected target compound **204** whose talose moiety was acetylated at C-2.

CHAPITRE 3 – SYNTHESIS OF OLIGOSACCHARIDES RELATED TO POTENTIAL BIOTERRORIST PATHOGENS

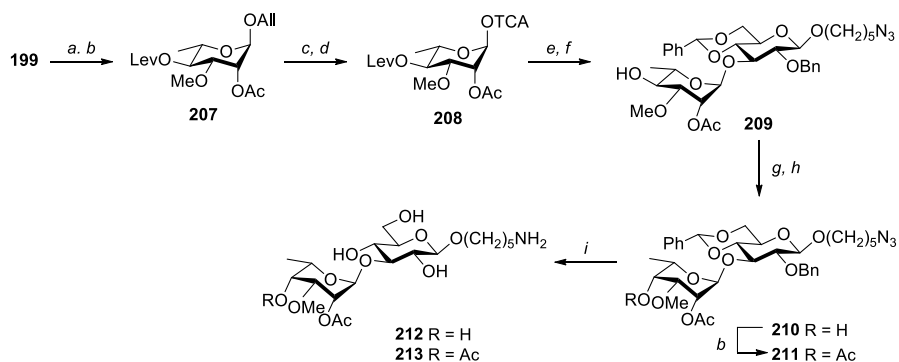


Scheme 3.18. Synthesis of a trisaccharide related to the main intrachain substitution pattern of *B. pseudomallei* and *B. mallei* LPS OAg²²

Disaccharides mimicking the terminal end substitution pattern of *B. pseudomallei* and *B. mallei* LPS OAg were also prepared in a similar approach (Scheme 19). Diol intermediate **199** was used as starting compound and tin chemistry was taken advantage of to selectively methylate the *O*-2 position. Acetylation of the free hydroxyl group enabled the formation of protected allyl rhamnoside **207**, which was converted into glycosyl donor **208** in two steps. The latter was glycosidated with glucoside acceptor **206** and delevulinoylated to afford alcohol **209**. Oxidation by PDCP and DMSO and subsequent reduction by the action of NaBH₄ converted the rhamnose residue into a talose, yielding disaccharide **210**. Diacetylated oligosaccharide **211** was prepared by acetylation of the free C-4 hydroxyl group, and both disaccharides underwent hydrogenolysis through previously mentioned conditions to respectively yield target disaccharides **212** and **213**, containing the terminal epitope of both *B. pseudomallei* and *B. mallei* LPS OAg.

²² a) Lev₂O, py, DMAP, 50 °C, quant.; b) 80% aq. HOAc, 60 °C, 82%; c) **205**, (Ph₂)BO(CH₂)₂NH₂, Ag₂O, CH₃CN, 60 °C, 74%; d) Ac₂O, py, DMAP, rt, 98%; e) [Ir(COD)(PMePh₂)₂]⁺PF₆⁻, H₂, THF, rt, then I₂, THF/H₂O, rt; f) CCl₃CN, Cs₂CO₃, CH₂Cl₂, acetone, rt, 81% (3 steps); g) **206**, TMSOTf, Et₂O/DCE, -10 °C; h) H₂NNH₂·H₂O, py, HOAc, 0 °C to rt, 77% (2 steps); i) PDCP, DMSO, Et₃N, CH₂Cl₂, -10 °C; j) NaBH₄, MeOH/CH₂Cl₂, -10 °C to rt, 85% (2 steps); k) Pd black, H₂, HCl, 40 °C, MeOH/DCE, quant.

CHAPITRE 3 – SYNTHESIS OF OLIGOSACCHARIDES RELATED TO POTENTIAL BIOTERRORIST PATHOGENS



Scheme 3.19. Synthesis of disaccharides mimicking the terminal end of *B. pseudomallei* and *B. mallei* LPS OAg²³

ELISA experiments on the synthesized compounds showed that disaccharides **212** and **213** were recognized by *B. pseudomallei* and *B. mallei* LPS-specific mAbs, revealing that these antibodies did not interact with the intrachain epitope mimicked by trisaccharide **204**. These observations were confirmed by SPR analysis, which also showed that disaccharide **212** bound strongly to *B. mallei* LPS-specific mAbs (mAb 4C7) whereas disaccharide **213** interacted less. L-Talose protons H-1, H-2, and H-4 as well as the *O*-2 acetyl group of disaccharide **212** appeared to have the highest importance in antibody binding, as revealed by STD-NMR. The prevalent role of the talose residue in the binding process with mAb 4C7 was therefore underlined by these observations, which could be profitable for future development of vaccine candidates or diagnostic tools against melioidosis and glanders.

3.5.3 Exopolysaccharides

The high molecular weight EPS produced by *B. pseudomallei* is an acidic 3-deoxy-D-manno-2-octulosonic acid (Kdo)-containing EPS, and consists in a linear heteropolymer whose repeating unit is a tetrasaccharide composed of three galactose residues and a 2-*O*-acetylated Kdo unit.³⁰²

³⁰³ This polysaccharide being reactive with melioidosis patient serum,³⁰⁴ Gauthier and co-workers

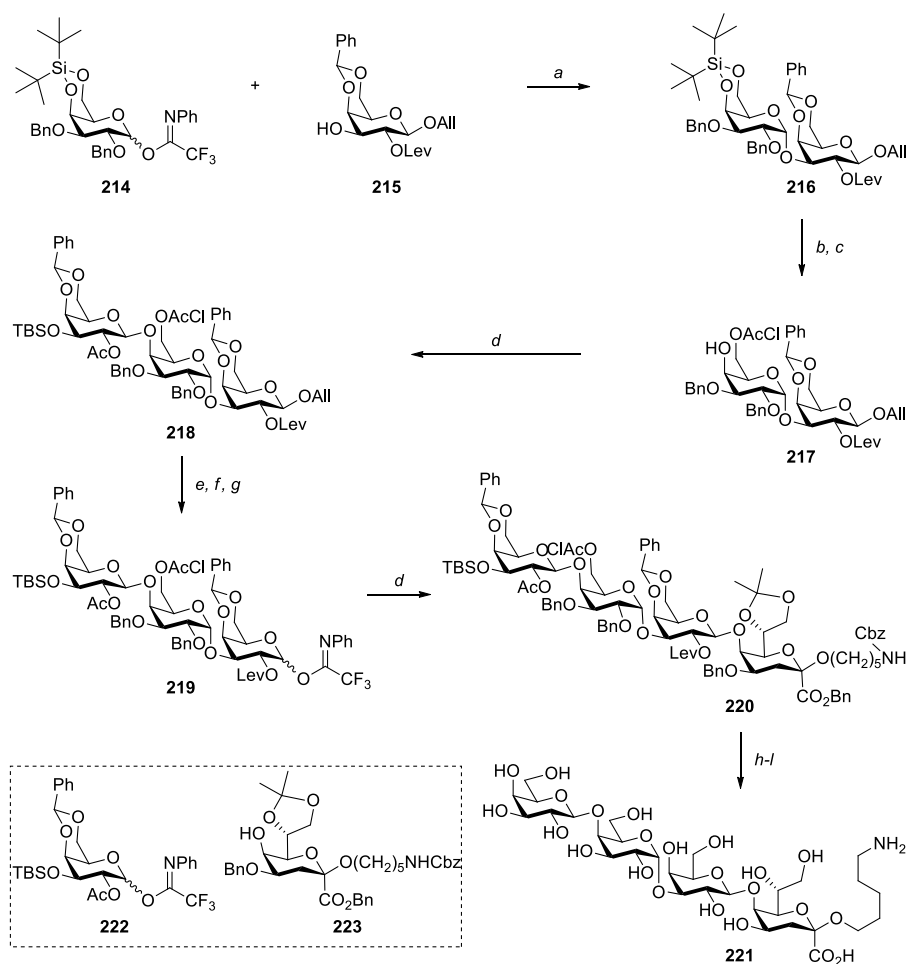
²³ a) *i.* Bu₂SnO, toluene, reflux; *ii.* MeI, CsF, 80 °C, 96% (2 steps); b) Ac₂O, py, DMAP, rt (**207**: 88%; **211**: 65%) c) [Ir(COD)(PMePh₂)₂]⁺PF₆⁻, H₂, THF, rt, then I₂, THF/H₂O, rt; d) CCl₃CN, Cs₂CO₃, CH₂Cl₂, acetone, rt, 87% (3 steps); e) **206**, TMSOTf, Et₂O/DCE, -10 °C to rt, 92%; f) H₂NNH₂·H₂O, py, HOAc, 0 °C to rt, quant.; g) PDCCP, DMSO, Et₃N, CH₂Cl₂, -10 °C; h) NaBH₄, MeOH/CH₂Cl₂, -10 °C to rt, 66% (2 steps); i) Pd black, H₂, HCl, 40 °C, MeOH/CH₂Cl₂, quant.

CHAPITRE 3 – SYNTHESIS OF OLIGOSACCHARIDES RELATED TO POTENTIAL BIOTERRORIST PATHOGENS

were interested in the synthesis of its tetrasaccharide biological repeating unit for further studies as a potential vaccine candidate or diagnostic tool against *B. pseudomallei*.³⁰⁵

As depicted in Scheme 20, the synthetic pathway developed by Gauthier initiated with the coupling of *N*-phenyltrifluoroacetimidate donor **214** bearing a 4,6-*O*-di-*tert*-butylsilylene (DTBS) group and galactose acceptor **215**. Using TMSOTf as the promoter, this reaction gave rise to disaccharide **216** in its α -form due to the steric hindrance of the DTBS group. Et₃N·3HF was used to cleave the latter, and the resulting primary alcohol was chloroacetylated using Yamamoto regioselective acylation, involving the use of *sym*-collidine. To avoid migration of the chloroacetyl group from *O*-6 to *O*-4, resulting alcohol **217** was not purified and directly glycosylated with glycosyl donor **222** to mainly provide β,α,β -trigalactoside **218**. The anomeric allyl group was converted into an *N*-phenyltrifluoroacetimidate moiety to allow its coupling with Kdo acceptor **223**, prepared in seven steps from ammonium Kdo. Resulting tetrasaccharide was deprotected in five steps consisting of: (1) deprotection of the chloroacetyl group employing thiourea; (2) delevulinoylation; (3) removal of the *tert*-butyldimethylsilyl (TBS) group; (4) cleavage of the isopropylidene group under acidic conditions and; (5) hydrogenolysis under microfluidic conditions (H-Cube). Due to the needed presence of two equivalents of HCl during the last step, the acetyl group was cleaved, resulting in fully deprotected tetrasaccharide **221**.

CHAPITRE 3 – SYNTHESIS OF OLIGOSACCHARIDES RELATED TO POTENTIAL BIOTERRORIST PATHOGENS



Scheme 3.20. Synthesis of the biological repeating unit of the β -Kdo-containing EPS produced by *B. pseudomallei*²⁴

3.6 *Francisella tularensis*

F. tularensis, a Gram-negative bacillus and intracellular pathogen, is the etiological agent of zoonotic disease tularemia. It can be transmitted to humans directly from infected animals or through vectors such as ticks, by inhalation, or by ingestion of contaminated food or water.³⁰⁶ Severity of symptoms greatly varies depending on the inoculation route, but the pneumonic form, which can be developed irrespectively of the entry route, is the most severe form and is associated

²⁴ a) TMSOTf, DCE, 4 Å MS, -10 °C, 87% (α -only); b) TREAT-HF, THF, 83%; c) *sym*-coll, chloroacetyl chloride, DCE, -10 °C; d) **222** or **223**, TMSOTf, DCE, 4 Å MS, -10 °C (**218**: 50%, 2 steps; **220**: 45%); e) [Ir(COD)(PMePh₂)₂]⁺PF₆⁻, H₂, THF, rt; f) I₂, THF/H₂O, rt; g) PTFACl, Cs₂CO₃, acetone, rt, 58% (3 steps); h) thiourea, py, MeOH, 60 °C; i) H₂NNH₂·HOAc, CH₂Cl₂, MeOH, rt; j) TREAT-HF, THF, reflux; k) 80% aq. HOAc, rt, 49% (4 steps); l) H-Cube, 20% Pd(OH)₂/C, MeOH/H₂O, HCl, 10 bars, 45 °C, 67%.

CHAPITRE 3 – SYNTHESIS OF OLIGOSACCHARIDES RELATED TO POTENTIAL BIOTERRORIST PATHOGENS

with the highest mortality rates.³⁰⁷ Although a live strain vaccine was developed in the 1950s and was shown to protect humans against *F. tularensis*,³⁰⁸ no vaccine is currently licensed for use in humans. However, studies have recently shown that LPS are able to protect mice against virulent strains of the pathogen.³⁰⁹⁻³¹¹ Therefore, Boons *et al.* developed a synthetic pathway to the inner core oligosaccharide of *F. tularensis* LPS that could find usefulness in the development of vaccines, immunotherapeutic agents, and diagnostic tools against tularemia.^{312, 313}

The inner core oligosaccharide of *F. tularensis* LPS is a hexasaccharide composed of two mannosyl residues (**B** and **C**), substituted with an α -glucoside (**A**), a 2-deoxy- α -galactosamine (**E**), a β -glucoside (**F**), and an α -Kdo moiety (**D**) that is in turn linked to the lipid A of the LPS³¹⁴ (Figure 3).

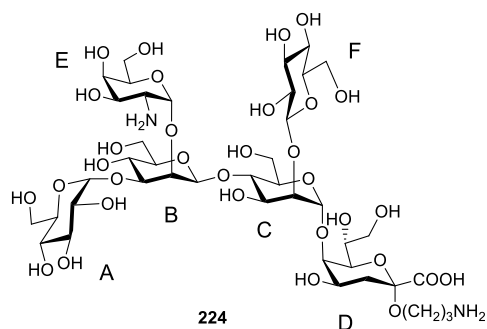
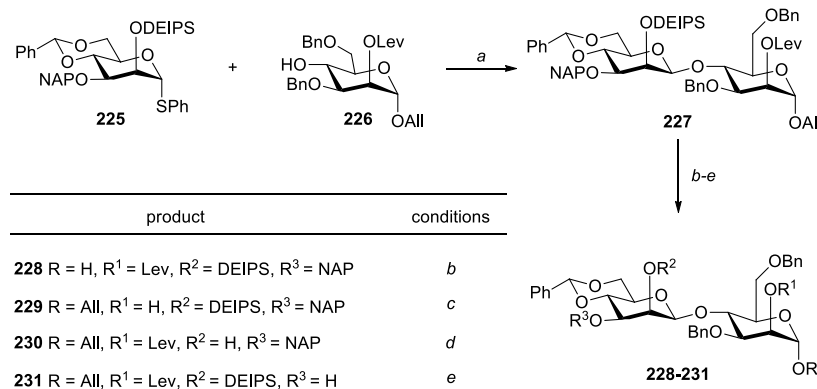


Figure 3.3. Inner core oligosaccharide of *F. tularensis* LPS bearing an aminolinker for carrier protein conjugation

In order to synthesize this complex and highly branched oligosaccharide, Boons *et al.* developed a new set of orthogonal protecting groups, composed of diethylisopropyl silyl (DEIPS), NAP, and allyl (All) ethers as well as a Lev ester.³¹³ This set allowed the preparation of a functionalized β -D-Man-(1 \rightarrow 4)- α -D-Man disaccharide (Scheme 21) that could be used as the backbone for the construction of *F. tularensis* inner core oligosaccharide. The synthesis of this disaccharide was particularly relevant as β -mannosides are known to be difficult to obtain due to the axial substituent at C-2 that sterically blocks the β -face of the glycosyl donor. This difficulty is also enhanced by the Δ -anomeric effect, which stabilizes the α -anomer.

CHAPITRE 3 – SYNTHESIS OF OLIGOSACCHARIDES RELATED TO POTENTIAL BIOTERRORIST PATHOGENS



Scheme 3.21. Synthesis of a pivotal disaccharide *en route* to the synthesis of *F. tularensis* inner core oligosaccharide²⁵

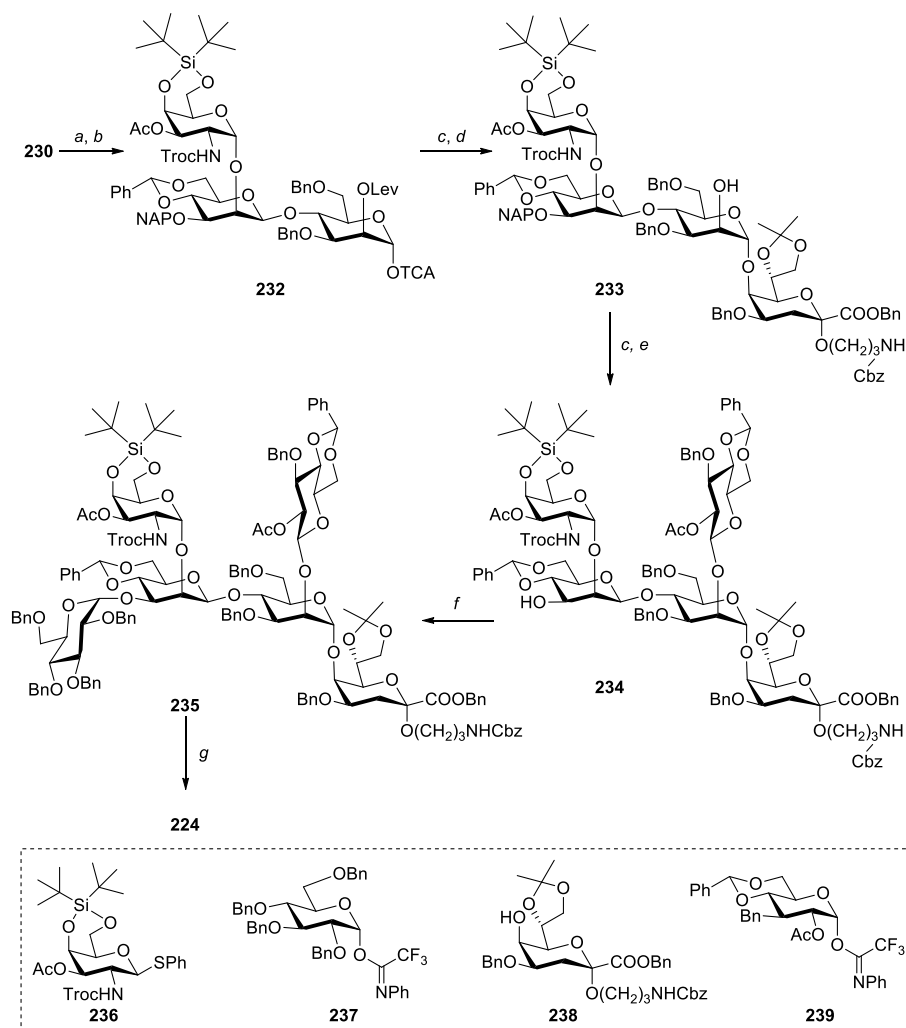
IAD is a useful method to achieve absolute β -anomeric selectivity. In the case of target disaccharide **227**, IAD was tried but proved to be low yielding. Therefore, the authors used a different approach in which an α -anomeric triflate undergoes a S_N2 -like displacement by the glycosyl acceptor, giving rise to the β -mannoside. Derivative **225** was used as the glycosyl donor due to the presence of the 4,6-*O*-benzylidene acetal permanent protecting group, which was needed for the formation of β -mannosides. It has been hypothesized that this acetal causes torsional strains that oppose the formation of the oxocarbenium intermediate. This strain, together with the destabilizing electronic effect when the *O*-6 dipole is antiparallel to the oxocarbenium ion, enabled the selective formation of β -mannosides.³¹⁵ Glycosyl donor **225** was thereby reacted with *p*-nitrobenzenesulfonyl chloride and AgOTf to form the α -triflate *in situ*, followed by the addition of glycosyl acceptor **226** to give target disaccharide **227** in a satisfying yield and in a β/α ratio greater than 20/1. The temporary protecting groups were orthogonally cleaved using standard conditions, allowing the selective introduction of the glycoside substituents at C-1, C-2, C-2', and/or C-3'.

In a subsequent work, Boons and co-workers developed a synthetic pathway to obtain *F. tularensis* inner core oligosaccharide, using their previously described β -D-Man-(1 \rightarrow 4)- α -D-Man disaccharide **227** as the foundation, as depicted in Scheme 22.³¹² To allow the installation of 2-deoxy- α -galactosamine moiety **236** at the C-2' position, disaccharide **230** was used as the starting

²⁵ a) **225**, *p*-NO₂C₆H₄SOCl, AgOTf, DTBMP, 5 min, -78 °C, then **226**, 3 h, -78 to -35 °C, 73%; b) PdCl₂, NaOAc, AcOH, H₂O, 16 h, rt 72%; c) H₂NNH₂·AcOH, Tol/EtOH, 3 h, rt, 99%; d) TBAF, AcOH, THF, 16 h, rt, 98%; e) DDQ, CH₂Cl₂, H₂O, 4 h, rt, 93%.

material. Its glycosylation with glycosyl donor **236** was realized using NIS and TfOH as the promoter system and gave rise to a trisaccharide in its α -form, which was converted into TCA **232** in a two-step sequence: (1) deprotection of the anomeric allyl ether by treatment with Pd(PPh₃)₄ in the presence of AcOH; and (2) introduction of the TCA moiety under standard conditions. The presence of the DTBS group in donor **236** sterically hindered the β -face, hence favoring the exclusive formation of the α -anomer. This glycosylation was carried out first since it was discovered that the 1,2,3-*cis* configuration of the β -mannoside renders glycosylation at C-2' difficult when positions C-1' and C-3' were already glycosylated. Then, the presence of the TCA enabled the glycosidation of **232** with Kdo moiety **238** under the promotion of TfOH, resulting in the formation of a tetrasaccharide solely in its α -anomer form. The selective removal of the levulinoyl protecting group was achieved employing hydrazinium acetate in a mixture of toluene and ethanol, furnishing alcohol **233**. The latter was then coupled with glycosyl donor **239** using TfOH in CH₂Cl₂ and the NAP ether was removed by treatment with DDQ in a mixture of CH₂Cl₂ to afford pentasaccharide **234** in the β -form. Introduction of glucoside moiety **237** was performed using TfOH in Et₂O. Since donor **237** carries a nonparticipating benzyl ether at C-2, the glycosylation had to take place in Et₂O, a solvent able to stabilize the oxacarbenium intermediate to control the α -anomeric selectivity. Resulting hexasaccharide **235**, obtained in an α/β ratio greater than 20/1, was finally deprotected to give target compound **224** in a five-step sequence: (1) removal of the isopropylidene and benzylidene acetals; (2) deprotection of the DTBS group; (3) cleavage of the Troc carbamate followed by purification by size exclusion chromatography; (4) removal of the acetyl esters by saponification; and (5) hydrogenolysis of the amide and the benzyl ether.

CHAPITRE 3 – SYNTHESIS OF OLIGOSACCHARIDES RELATED TO POTENTIAL BIOTERRORIST PATHOGENS



Scheme 3.22. Total synthesis of *F. tularensis* inner core oligosaccharide²⁶

To conduct biological assays, the synthesized oligosaccharide was linked to a biotin moiety via the aminopropyl linker. This was achieved by employing *N*-hydroxysuccinimido biotin in PBS buffer at pH 7.4. The conjugation with the aminolinker was successful due to its greater reactivity compared to the amine of the 2-deoxy- α -galactosamine moiety. The biotin made it possible to carry out an ELISA experiment to measure the antigenic responses against the inner core

²⁶ a) **236**, NIS, TfOH, CH₂Cl₂, 10 min, 0 °C, 77%; b) *i.* Pd(PPh₃)₄, AcOH, CH₂Cl₂, 3 h, rt, then *ii.* CCl₃CN, DBU, CH₂Cl₂, 1 h, rt, 75%; c) **238** or **239**, TfOH, CH₂Cl₂, 10 min, 0 °C (**223**: 61%; **234**: 82%); d) H₂NNH₂·AcOH, EtOH, tol, 30 min, rt, 78%; e) DDQ, CH₂Cl₂, H₂O, 3 h, rt, 76%; f) **237**, TfOH, Et₃O, 10 min, -35 °C, 73%; g) *i.* TFA, CH₂Cl₂, H₂O, 1 h, rt, *ii.* HF·pyridine, THF, 30 min, rt; *iii.* Zn, AcOH, CH₂Cl₂, 3 h, rt, 89% (3 steps); *iv.* NaOMe, MeOH, H₂O, THF, 1 h, rt, 55% and *v.* Pd(OH)₂, H₂, *t*-BuOH, H₂O, 16 h, rt, 85%.

oligosaccharide of *F. tularensis* LPS induced by an attenuated live vaccine and by hexasaccharide **224**. Significant levels of IgG antibodies were observed only in the serum of mice immunized with the latter. These results suggested that this compound is antigenic in certain conditions but might not be usable as a diagnostic tool. Hexasaccharide **224** was also successfully linked to carrier protein KLH for future immunization assays. The synthesized hexasaccharide was first reacted with perfluorophenyl 2-(acetylthio)acetate (SAMA-Opfp) and DIPEA in DMF, resulting in a thioacetyl that was cleaved using ammonia in DMF, releasing a thiol end. The latter was reacted with maleimide-activated KLH to give a **224**-KLH glycoconjugate, and high-pH anion-exchange chromatography showed that an average of 339 oligosaccharides was linked to each KLH, corresponding to a 65% conversion rate.

3.7 *Yersinia pestis*

Plague is a zoonotic disease transmitted to humans from rodents by fleas, and is caused by the Gram-negative, facultative intracellular pathogen *Yersinia pestis*.³¹⁶ This disease is endemic in the south-western United States as well as in Africa, Asia, and South America.³¹⁷ The most common form of plague is bubonic plague, whereas septicemic plague and pneumonic plague are secondary forms. However, it is thought that in the case of a bioterrorist attack, plague would present itself as an epidemic pneumonia,³¹⁶ which is generally fatal if not treated rapidly.³¹⁸ Since *Y. pestis* is part of the *Enterobacteriaceae* family, this pathogen is able to exchange genetic material with different organisms within this family. This suggests that multi-drug resistant *Y. pestis* could see the day following natural selection or bioengineering,³¹⁹ and highlights the relevance of working toward the development of prophylactic treatment such as vaccines.

Between different GNB, the LPS inner core is highly conserved.^{320, 321} Among the various conserved residues, L-glycero-D-manno-heptose (Hep) is frequently detected in the LPS inner core.³²² In *Y. pestis* LPS inner core, three Hep are α -linked, and resulting trisaccharide is attached to a Kdo residue (Figure 4). The necessity of employing enantioselective reactions, the presence of α -linkages, and the sterically hindered nature of *Y. pestis* inner core oligosaccharide make its synthesis challenging.

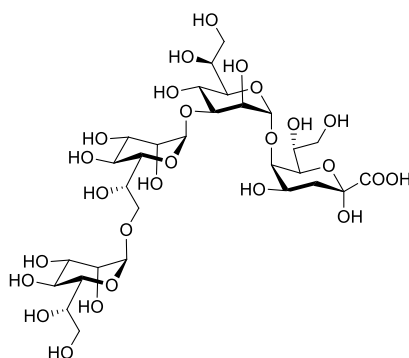
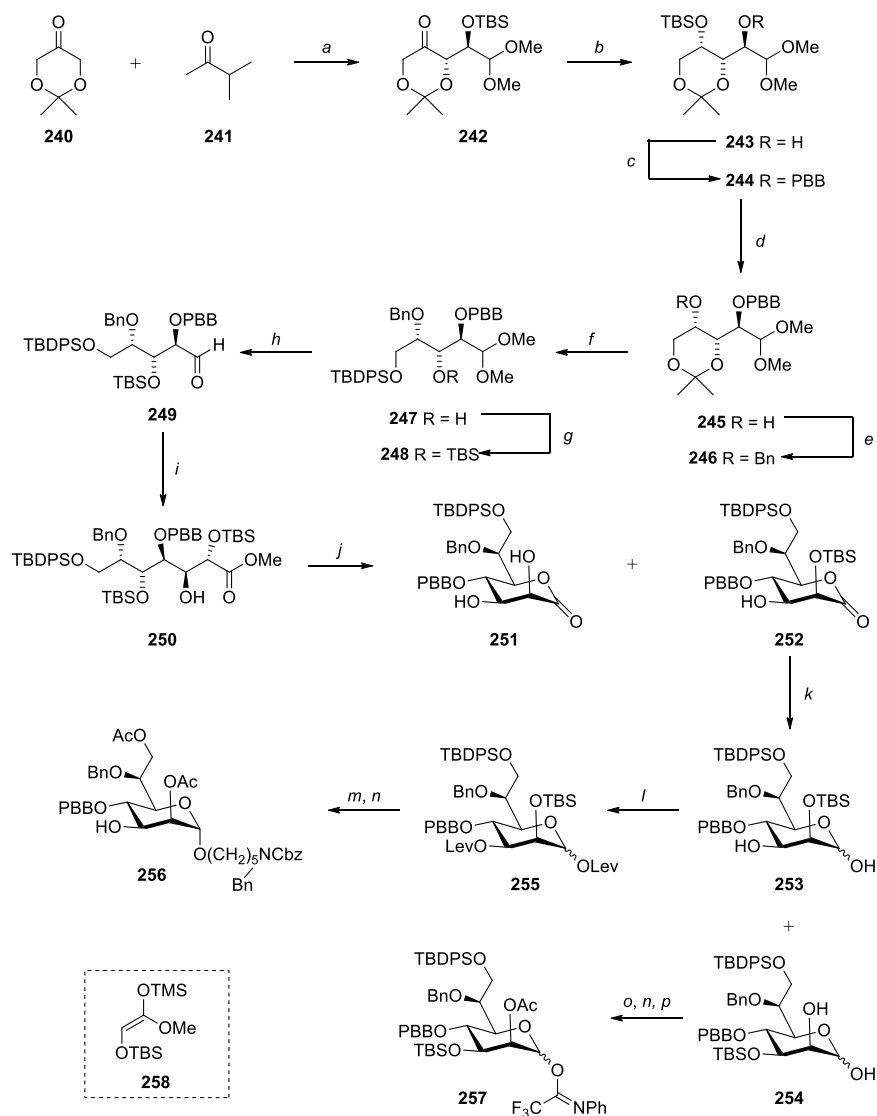


Figure 3.4. *Y. pestis* LPS inner core oligosaccharide fragment

With the intention of enabling the synthesis of *Y. pestis* LPS inner core, Seeberger and co-workers developed an enantioselective *de novo* synthesis of L-glycero-D-manno-heptose building blocks. Their developed synthetic pathway, described in Scheme 23, relies on the use of aldol reactions as well as orthogonal protecting groups.³²³ Synthesis of building blocks **256** and **257** commenced with an L-proline catalyzed aldol reaction between **240** and **241**, followed by TBS protection of the aldol product. Reduction of ketone **242** using L-selectride resulted in the migration of TBS, yielding alcohol **243**. Several steps of functional modifications, including protection and deprotection sequences and hydrolysis of the dimethylacetal, gave rise to aldehyde **249** in seven steps. The latter underwent an aldol reaction with silyl enol ether **258** in a mixture of MgBr·Et₂O, which was acting as a chelating activator to enable the reaction. Resulting derivative **250** was obtained with excellent configuration selectivity, although the yield was moderate. Cleavage of TBS next to the ester by trifluoroacetic acid allowed the lactonization of compound **250**. Lactone **252** was the major product, but deprotection of both TBS groups also occurred (**251**). Derivative **252** was reduced using LiAlH(OtBu)₃, resulting in alcohols **253** and **254** due to the partial migration of the silyl group from C-2 to C-3. Synthesis of building block **256** was achieved using alcohol **253**. The latter was dilevulinoylated and the Lev group at the anomeric position was replaced by a protected amino linker using BF₃·OEt₂. The silyl groups were then cleaved, the resulting free hydroxyl groups were acetylated, and the Lev group at C-3 was removed, which yielded glycosyl acceptor **256**. As for building block **257**, it was prepared following acetylation, selective removal of the anomeric acetyl group using hydrazine acetate, and addition of an *N*-

CHAPITRE 3 – SYNTHESIS OF OLIGOSACCHARIDES RELATED TO POTENTIAL BIOTERRORIST PATHOGENS

phenyltrifluoroacetimidate group at the anomeric position of diol **254**. The authors also achieved the glycosylation of building blocks **256** and **257** to demonstrate their synthetic utility.



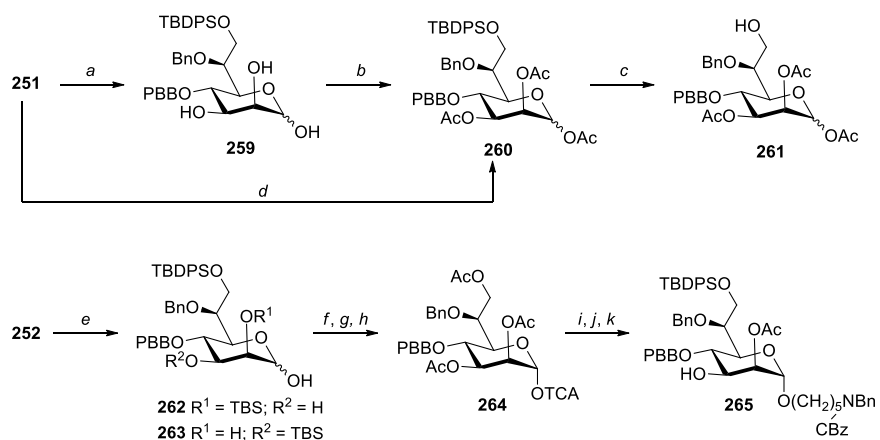
Scheme 3.23. De novo synthesis of L-glycero-D-manno-heptose building blocks en route to the synthesis of *Y. pestis* inner core LPS²⁷

²⁷ a) *i.* L-proline; *ii.* TBSCl, imidazole; b) L-selectride, 79%; c) *p*-BrBnBr, NaH; d) TBAF, 82% (2 steps); e) BnBr, NaH, 95%; f) *i.* CSA, MeOH; *ii.* TBDPSCl, imidazole, DMAP, CH₂Cl₂, 93%; g) TBSOTf, 2,6-lutidine, 97%; h) *p*-TsOH, H₂O, acetone, 97%; i) **258**, MgBr·Et₂O, 61%; j) TFA, CH₂Cl₂ (**251**: 20%; **252**: 36%); k) LiAlH(O*t*Bu)₃ (**253**: 38%; **254**: 47%); l) LevOH, DIPC, DMAP, 88%; m) *i.* *N*-benzyl-*N*-carboxybenzyl-5-aminopentan-1-ol, BF₃·Et₂O; *ii.* HF·py; *iii.* Ac₂O, py, 76%; n) H₂NNH₂·AcOH (**256**: 85%; **257**: 89%); o) Ac₂O, py, quant.; p) CF₃C(=NPh)Cl, Cs₂CO₃, 96%.

CHAPITRE 3 – SYNTHESIS OF OLIGOSACCHARIDES RELATED TO POTENTIAL BIOTERRORIST PATHOGENS

Intermediates **251** and **252** of the previous synthetic route were taken advantage of in a following work realized by Seeberger, whose objective was to synthesize plague-specific oligosaccharide antigens.³²⁴ More particularly, they reported the synthesis of *Y. pestis* LPS inner core heptose trisaccharide. Retrosynthetic analysis revealed that heptosides **261**, **264**, and **265** could allow the synthesis of target trisaccharide **268**, as shown in Schemes 24 and 25. To achieve this, lactone **251** was first converted into an orthoacetate intermediate, reduced by $\text{LiAlH}(\text{O}t\text{Bu})_3$, treated with aqueous acetic acid, then acetylated using acetic anhydride in THF, giving rise to intermediate **260** in 70% yield over four steps. In contrast, direct reduction of lactone **251** by $\text{LiAlH}(\text{O}t\text{Bu})_3$ was not satisfying, as the reaction was incomplete even after two days. Building block **261** was obtained following cleavage of the silyl protecting group. Regarding glycosyl donor **264** and glycosyl acceptor **265**, they were both synthesized from derivative **252**. The latter was first reduced with $\text{LiAlH}(\text{O}t\text{Bu})_3$ to give a mixture of hemiacetals **262** and **263** due to the migration of TBS from C-2 to C-3 under basic conditions. Both hemiacetals were desilylated using TBAF and acetylated, followed by selective deacetylation of the anomeric position using ammonia in methanol. Resulting hemiacetal was converted into target TCA **264** using acetonitrile and DBU. From TCA **264**, glycosyl acceptor **265** was obtained in four steps, that are, (1) installation of a protected amine linker at the anomeric position for further conjugation to a carrier protein; (2) deacetylation of positions C-2, C-3, and C-7; (3) protection of the C-7 position with a *tert*-butyldiphenylsilyl (TBDPS) group; and (4) formation of an orthoacetate intermediate followed by its opening under aqueous acidic conditions.

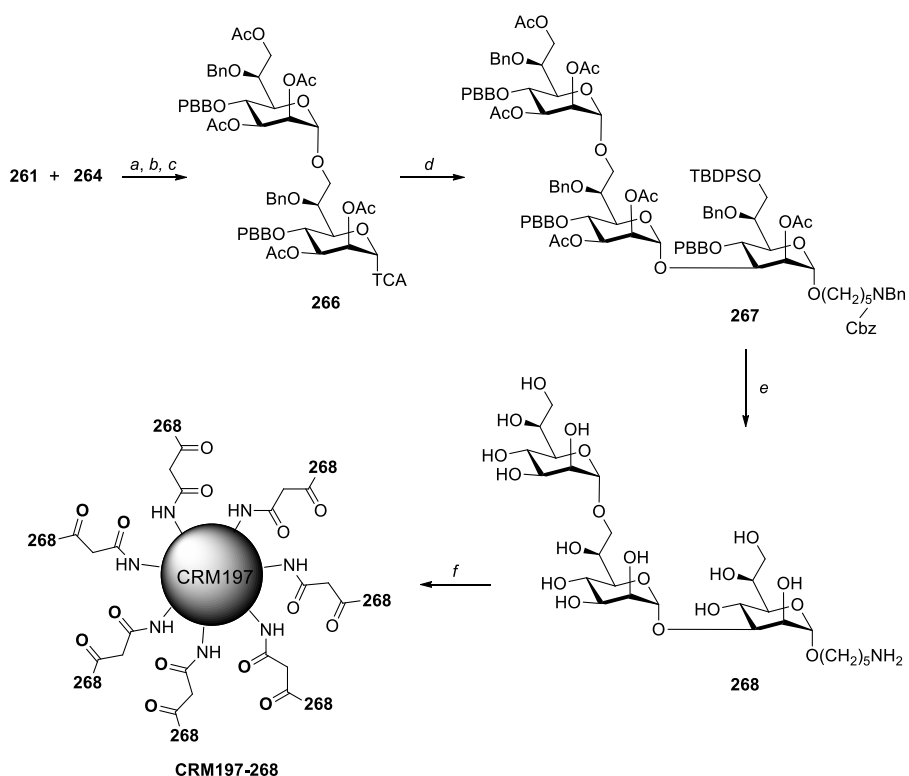
CHAPITRE 3 – SYNTHESIS OF OLIGOSACCHARIDES RELATED TO POTENTIAL BIOTERRORIST PATHOGENS



Scheme 3.24. Synthesis of building blocks en route to the preparation of a CRM197-trisaccharide conjugate²⁸

²⁸ a) $\text{LiAlH}(\text{O}t\text{Bu})_3$, THF, rt, 40%; b) Ac_2O , py, quant.; c) HF·py, THF, quant; d) *i.* triethyl orthoacetate, PTSA, tol; *ii.* $\text{LiAlH}(\text{O}t\text{Bu})_3$, THF, -20 to -15 °C; *iii.* 80% aq. AcOH, THF; *iv.* Ac_2O , py, 70% (4 steps); e) $\text{LiAlH}(\text{O}t\text{Bu})_3$, THF, -20 to -15 °C (**262**: 30%; **263**: 38%); f) *i.* TBAF, THF; *ii.* Ac_2O , py, quant.; g) NH_3 , MeOH, quant.; h) Cl_2CCN , DBU, CH_2Cl_2 , 70% to quant.; i) *i.* *N*-benzyl-*N*-carboxybenzyl-5-aminopentan-1-ol, TMSOTf, CH_2Cl_2 , -30 °C; *ii.* NaOMe, MeOH, 35%; j) TBDPSCl, imidazole, DMAP, CH_2Cl_2 , 76%; k) *i.* triethyl orthoacetate, PTSA, tol; *ii.* 80% aq. AcOH, THF, 70 to 78%.

CHAPITRE 3 – SYNTHESIS OF OLIGOSACCHARIDES RELATED TO POTENTIAL BIOTERRORIST PATHOGENS



Scheme 3.25. Synthesis of a CRM197-trisaccharide conjugate for the serodiagnosis of plague²⁹

Building blocks **261**, **264**, and **265** were further used to synthesize target trisaccharide **268** (Scheme 25). Glycosyl donor **261** and glycosyl acceptor **264** were first reacted under the promotion of TMSOTf, followed by deacetylation of the resulting disaccharide anomeric position. The isolated disaccharide was converted into TCA **266** using previously reported conditions. Disaccharide glycosyl donor **266** was coupled with building block **265** using TMSOTf as the promoter, and desilylation, deacetylation, and hydrogenolysis furnished target trisaccharide **268**. The latter was finally coupled to carrier protein CRM197 by taking advantage of NHS ester chemistry, resulting in CRM197-**268** conjugate in an average ratio of 1:7 as determined by MALDI-TOF-MS analysis. The coupling of *Y. pestis* LPS inner core trisaccharide to a carrier protein was required to elicit a T cell dependent immune response.

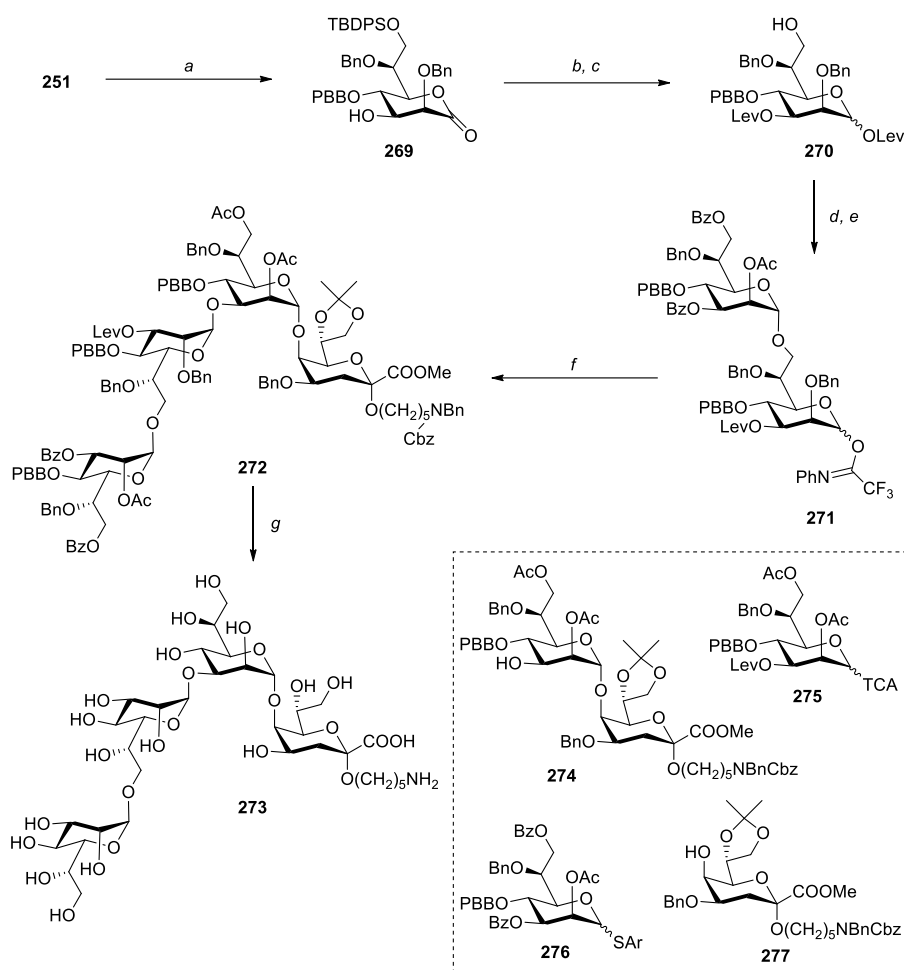
²⁹ a) TMSOTf, CH₂Cl₂, -35 to -10 °C, 65 to 86%; b) H₂NNH₂·AcOH, DMF, 74% or NH₃, MeOH, 87%; c) Cl₃CCN, DBU, CH₂Cl₂, 80%; d) **265**, TMSOTf, CH₂Cl₂, -40 to -30°C, 68%; e) i. NaOMe, MeOH; ii. TBAF, THF, quant.; iii. 10% Pd/C, H₂, MeOH/H₂O/AcOH 10:10:1, 60 to 95%; f) i. Et₃N, disuccinimido adipate, DMSO, 37 °C; ii. CRM197 carrier protein, PBS buffer solution (pH 7.4), 37 °C.

CHAPITRE 3 – SYNTHESIS OF OLIGOSACCHARIDES RELATED TO POTENTIAL BIOTERRORIST PATHOGENS

Biological assays were further conducted to attest the potential of trisaccharide **268** as an immunological agent for bacterial detection. Immunogenicity was first evaluated by glycan microarray analysis following immunization of C57BL/6 mice with glycoconjugate CRM197-**268**. Results showed that antibodies that specifically bound the trisaccharide were produced. Immunofluorescence and confocal laser scanning microscopy (CLSM) also showed that monoclonal anti-**268** antibodies recognize *Y. pestis* LPS. These results highlighted the potential of the synthesized trisaccharide for the specific detection of *Y. pestis*.

In a subsequent work, Seeberger presented the synthesis of the LPS inner core oligosaccharide of a variety of GNB, including *Y. pestis*.³²⁵ Intermediate **251** was once again taken advantage of with the aim of synthesizing the inner core tetrasaccharide of *Y. pestis*, composed of trisaccharide **268** linked to a Kdo moiety. This synthesis is depicted in Scheme 26. To obtain this compound, disaccharide **274** was first synthesized following coupling of Kdo moiety **277** and glycosyl donor **275** and subsequent delevulinoylation. In parallel, intermediate **251** was selectively benzylated at the C-2 position using BnBr and silver(I) oxide to give ketone **269**. The latter was reduced by LiAlH(O*t*Bu)₃ and hydroxyl groups at C-1 and C-3 were levulinoylated. Cleavage of TBDPS protecting group at C-7 using HF in pyridine allowed the coupling of resulting alcohol with glycosyl donor **276**. Ammonia in methanol was then used to selectively delevulinoylate the anomeric position, which allowed the formation of *N*-phenyltrifluoroacetimidate glycosyl donor **271**. [2 + 2] Glycosylation of the latter with previously synthesized disaccharide **274** under the promotion of TMSOTf furnished fully protected tetrasaccharide **272**. Its deprotection was achieved *via* a three-step sequence: (1) acidic cleavage of the isopropylidene acetal; (2) saponification; and (3) hydrogenolysis, giving rise to target tetrasaccharide **273**. Moreover, the ¹H NMR spectrum of the latter was almost identical to the one reported for isolated LPS fragments, showing the accuracy of the tetrasaccharide structure. It is also worth mentioning that the synthetic pathway developed by the authors is flexible so that other oligosaccharides consisting of Hep and Kdo residues could be readily accessible. Indeed, their methodology allowed the LPS inner core oligosaccharides of *H. influenzae* and *Proteus*, as well as *Y. pestis*, to be synthesized, since all three involved the use of common intermediates (cf. chapter 12).

CHAPITRE 3 – SYNTHESIS OF OLIGOSACCHARIDES RELATED TO POTENTIAL BIOTERRORIST PATHOGENS



Scheme 3.26. Synthesis of *L-glycero-D-manno-heptose*-containing oligosaccharide related to the inner core of *Y. pestis* by Seeberger³⁰

Besides its LPS, *Y. pestis* also expresses EPS, which is another essential component in its biofilm matrix. More particularly, *Y. pestis* produces a partially *N*-deacetylated β -(1→6)-D-*N*-acetylglucosamine homopolymer, called polysaccharide intercellular adhesin (PIA),³²⁶ that is common to other biofilm forming bacterial strains. Several studies have revealed the potential of poly *N*-acetylglucosamine as vaccine candidates since this oligosaccharide, when conjugated to

³⁰ a) BnBr, Ag₂O, CH₂Cl₂, 0 °C to rt, 70%; b) i. LiAlH(O*t*Bu)₃, THF, -15 °C; ii. LevOH, DIPC, DMAP, CH₂Cl₂, rt, 53% (2 steps); c) HF·py, THF, rt, 83%; d) **276**, NIS, TMSOTf, 4 Å MS, CH₂Cl₂, 0 °C to rt, 79%; e) i. NH₃, THF, MeOH, 0 °C, 78%; ii. PTFACl, K₂CO₃, acetone, rt, 70%; f) **274**, TMSOTf, 4 Å MS, CH₂Cl₂, Et₂O, 0 °C to rt, 67%; g) i. HOAc, H₂O, 70 °C; ii. NaOH, dioxane, MeOH, H₂O, rt; iii. H₂, Pd/C, MeOH, H₂O, HOAc, rt, 71% (3 steps).

CHAPITRE 3 – SYNTHESIS OF OLIGOSACCHARIDES RELATED TO POTENTIAL BIOTERRORIST PATHOGENS

carrier proteins, appeared to be immunogenic in mice and rabbits, even when partially *N*-deacetylated.³²⁷

In an effort to contribute to the development of glyconjugate vaccines against bacterial strains producing PIA such as *Y. pestis*, the Nitz's group described a method for the synthesis of PIA oligosaccharides.³²⁸ Their methodology relied on an acid reversion reaction, which could be achieved using 70% HF·pyridine and ensured the stereo- and regiospecific formation of β -(1→6)-linkages between the *N*-acetylglucosamine residues. Indeed, optimization of the conditions allowed the predominant formation of the β -anomer in approximately a 95% yield. The oligosaccharides, purified by size exclusion chromatography, were further functionalized with an *N*-methyl-*O*-alkylhydroxylamine linker through a condensation reaction. The linker also bore a disulfide group that, upon reduction, was used for the conjugation of the oligosaccharides to BSA to eventually conduct ELISAs. Alkaline hydrolysis was also employed to *N*-deacetylate the oligosaccharides that could therefore offer more antibodies recognition details upon biological assays.

3.8 *Brucella* spp.

Gram-negative and intracellular pathogens *Brucella* spp. are the causative agents of brucellosis,³²⁹ a bacterial disease that is considered as a neglected zoonose by the World Health Organization (see http://www.who.int/neglected_diseases/zoonoses). This disease is primarily contracted by animals but is the most common bacterial disease to be transmitted to humans: this can occur through the ingestion of unsterilized milk or meat from infected animals.³²⁹ Although non-fatal in humans, this widespread disease can be debilitating. In bovines, brucellosis is mostly induced by *B. abortus*, but can also be caused by *B. melitensis* or *B. suis*.³³⁰

As of now, diagnostic of *Brucella* spp. infections is achieved through the detection of antibodies specific to the bacterial cell wall O-polysaccharide (OPS) of the smooth LPS (sLPS).³³¹ Since the actual most protective vaccine against brucellosis – which can be harmful to both humans and animals – is based on the use of OPS, vaccination compromises diagnostic, rendering the efforts to combat the disease fruitless.³³² Fortunately, *Brucella* spp. antigens received scientists' attention

CHAPITRE 3 – SYNTHESIS OF OLIGOSACCHARIDES RELATED TO POTENTIAL BIOTERRORIST PATHOGENS

for many years and chemical synthesis has proven to be useful to produce oligosaccharides that could be specifically used for either serodiagnosis or vaccination.

In the 1930s,³³³ it was found that *Brucella* spp. could be classified into three categories based on their OPS antigenic phenotypes: A-dominant (A⁺M⁻), M-dominant (A⁻M⁺) and A⁺M⁺. Early on, it was discovered that both A and M antigens of *B. abortus* were exclusively formed of the monosaccharide 4-formamido-4,6-dideoxy- α -D-mannopyranose (D-Rha4NFo).³³⁴ The nature of the linkages present in both the A and M antigens were however the subject of inaccurate conclusions. It was first thought that the D-Rha4NFo residues were exclusively α -1,2-linked in the A antigen,³³⁴ whereas the M antigen contained one 1,3-linked residue for every three 1,2-linked.³³⁵ Later, studies revealed that the A⁺M⁻ strains, although being A-dominant, were composed of at least 2% 1,3-linkages, which are present in a rate of 21% in the A⁻M⁺ strain. These are the extremes and every *Brucella* strain lies in between, excepted for *B. suis* biovar 2.³³⁶⁻³³⁸

It is only in 2013 that the structure of *Brucella* OPS was definitely elucidated³³⁹ and results showed that it was much more complicated than previously reported. In fact, the OPS can now be described as a copolymer whose repeating units are the A and M antigens. The A epitope is indeed a linear sequence of α -1,2-linked D-Rha4NFo residues. The M epitopes caps the A epitope and is constituted of a tetrasaccharide of structure α -Rha4NFo-2 α -Rha4NFo-3 α -Rha4NFo-2 α -Rha4NFo, repeated *n* times (Figure 5).

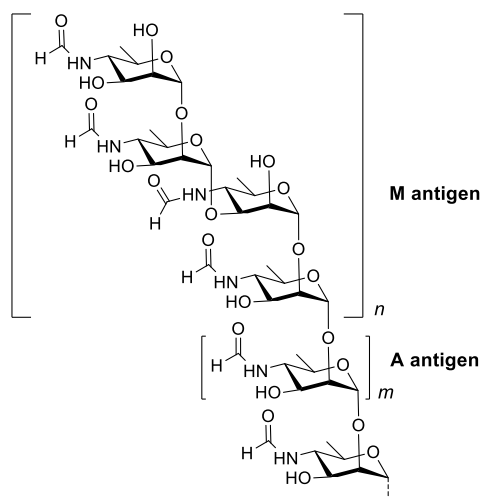
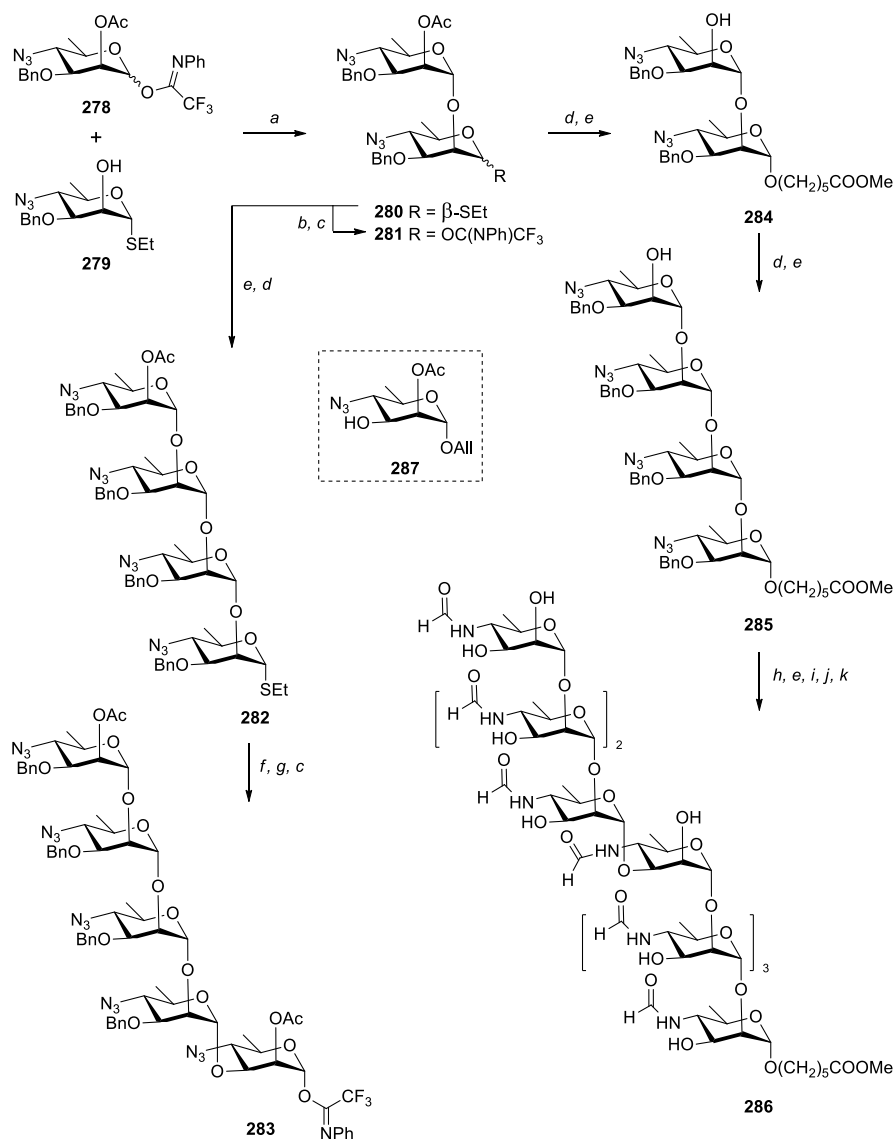


Figure 3.5. A and M antigens of *Brucella* spp. OPS structure

Bundle *et al.* initiated their work on the synthesis of *Brucella* spp. OPS-like oligosaccharides prior to the definitive elucidation of the A and M antigens structure,³⁴⁰⁻³⁴⁵ as presented in the overview of their work published in 2017.³⁴⁶ Based on their previous work, they identified nonasaccharide **286** (Scheme 27) that contained the first reported structures of A and M antigens and that could be useful as a diagnostic tool. To produce this oligosaccharide, they developed a synthetic pathway that enabled the formation of internal 1,3-linkages.³⁴⁷

CHAPITRE 3 – SYNTHESIS OF OLIGOSACCHARIDES RELATED TO POTENTIAL BIOTERRORIST PATHOGENS



Scheme 3.27. Synthesis of a nonasaccharide mimicking both A and M antigens of *Brucella* spp. sLPS³¹

Monosaccharides **278**, **279**, and **287** were used as starting materials for the synthesis of nonasaccharide **286**. Bundle and co-workers synthesis commenced with the glycosylation of glycosyl donor **278** and glycosyl acceptor **279**, yielding thioglycoside **280**. An *N*-

³¹ a) TMSOTf, CH₂Cl₂, 94%; b) NIS, H₂O, acetone, 76%; c) CF₃C(NPh)Cl, Cs₂CO₃, CH₂Cl₂ (**281**: 90%; **283**: 79%); d) HO(CH₂)₅COOMe, **281**, or **280**, TMSOTf, toluene, 100 °C (**284**: 53%; **282**: 81%; **285**: 77%); e) MeONa, MeOH (**282**: 81%; **284**: quant.; **285**: 84%; **286**: 78%); f) **287**, NIS, TfOH, CH₂Cl₂, 68%; g) PdCl₂, AcONa, AcOH, H₂O, 62%; h) **283**, TMSOTf, CH₂Cl₂, 30%; i) H₂S, py/Et₃N 1:1; j) Ac₂O/HCOOH 2:1, MeOH, 62% (2 steps); k) H₂, Pd/C, AcOH, 48%.

CHAPITRE 3 – SYNTHESIS OF OLIGOSACCHARIDES RELATED TO POTENTIAL BIOTERRORIST PATHOGENS

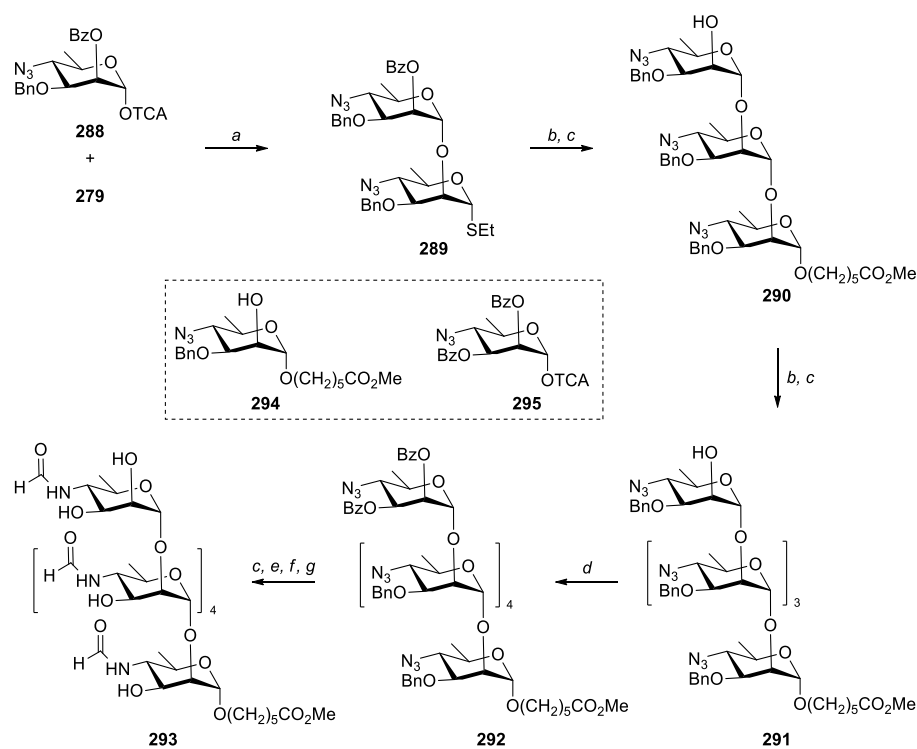
phenyltrifluoroacetimidate was used rather than a TCA since the latter was shown to be less effective for glycosylation reactions with 6-deoxy sugar donors. Hydrolysis of disaccharide **280** allowed its conversion into corresponding *N*-phenyltrichloroacetimidate **281**. The latter could then be glycosylated with a methyl 6-hydroxyhexanoate linker using TMSOTf in toluene at high temperature and deacetylated to furnish disaccharide glycosyl acceptor **284**. The methyl 6-hydroxyhexanoate was used as the linker for further conjugation to a protein because it is compatible with the reactions involving the protecting groups. Thioglycoside **280** was also used as a glycosyl acceptor upon its deacetylation for the synthesis of tetrasaccharide glycosyl donor **282**, which was subsequently glycosidated with derivative **287** under the promotion of NIS and TfOH. The allyl ether was converted into an *N*-phenyltrifluoroacetimidate through standard procedures. These steps furnished pentasaccharide building block **283** that could be further used for the synthesis of the nonasaccharide. This was achieved following its glycosylation with linear tetrasaccharide **285**, obtained after coupling glycosyl acceptor **284** with glycosyl donor **281**. This yielded a nonasaccharide in a moderate yield of 30% due to the low reactivity of the glycosyl acceptor, and the authors had insufficient reactants to optimize this glycosylation. The resulting compound was converted into target nonasaccharide **286** after undergoing a four-step sequence: (1) deacetylation; (2) reduction of the azides using H₂S in pyridine and Et₃N; (3) introduction of the formamido groups employing Ac₂O and HCOOH in methanol; and (4) hydrogenolysis.

For biological purposes, the linker moiety was converted into an amide by ethylenediamine and conjugated with BSA in an oligosaccharide:BSA ratio of 16:1. This glycoconjugate was tested against mAbs YsT9-1 and Bm10, respectively specific to *Brucella* A and M antigens, by conducting ELISA experiments and results showed that nonasaccharide **286** binds to both mAbs with equivalent potency.

With the aim of developing diagnostic tools against brucellosis, Bundle and co-workers also reported the synthesis of six oligosaccharides related to the OPS of *Brucella* spp.³⁴⁸ Among others, they prepared hexasaccharide **293**, exemplifying an A epitope (Scheme 28), and hexasaccharide **300** representing the capping tetrasaccharide sequence linked to two 1,2-linked D-Rha4FNo

CHAPITRE 3 – SYNTHESIS OF OLIGOSACCHARIDES RELATED TO POTENTIAL BIOTERRORIST PATHOGENS

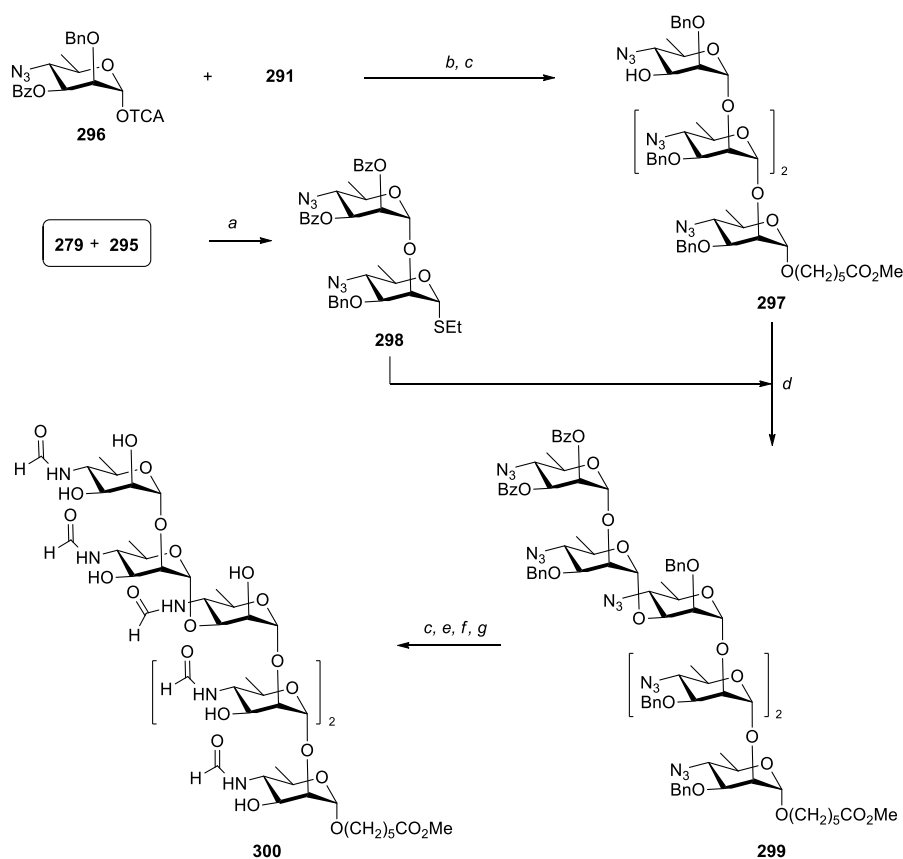
residues (Scheme 29). The other four oligosaccharides represented constituent structures of the *Brucella* M antigen.



Scheme 3.28. Synthesis of a hexasaccharide mimicking the A antigen of *Brucella* spp. sLPS³²

³² a) TMSOTf, 3 Å MS, CH₂Cl₂, 85%; b) **294** or **289**, MeOTf, 3 Å MS, CH₂Cl₂, rt (**290**: 85%; **291**: 86%); c) NaOMe, MeOH, rt (**290**: 94%; **291**: 94%; **293**: 87%); d) **295**, TMSOTf, 3 Å MS, CH₂Cl₂, 90%; e) H₂S, py/H₂O, 40 °C; f) (HCO)₂O, MeOH, -20 °C; g) H₂, Pd(OH)₂, MeOH/H₂O, rt, 55% (3 steps).

CHAPITRE 3 – SYNTHESIS OF OLIGOSACCHARIDES RELATED TO POTENTIAL BIOTERRORIST PATHOGENS



Scheme 3.29. Synthesis of a hexasaccharide mimicking the capping antigen of *Brucella* spp. sLPS³³

Pure A epitope hexasaccharide **293** was prepared from monosaccharide building blocks **288**, **279**, **294**, and **295** which underwent iterative glycosylations. The synthesis commenced with the coupling of derivatives **288** and **279** using TMSOTf as the promoter and the α -configuration of resulting disaccharide **289** was obtained due to the presence of the axial benzoyl group at C-2 of glycosyl donor **288**. It is worth mentioning that the authors used benzoyl esters rather than acetate esters as previously described since it allowed the use of simple benzoylated TCA donors. Disaccharide glycosyl donor **289** was coupled with building block **294** employing MeOTf and resulting trisaccharide was debenzoylated into glycosyl acceptor **290**. MeOTf was used for glycosylation activation since it selectively formed the α -anomers. Coupling of the latter with

³³ a) TMSOTf, 3 Å MS, CH₂Cl₂, 90%; b) TMSOTf, 3 Å MS, toluene, 95 °C, 87%; c) NaOMe, MeOH, rt (**297**: 89%; **300**: 91%); d) MeOTf, 3 Å MS, CH₂Cl₂, rt, 92%; e) H₂S, py/H₂O, 40 °C; f) (HCO)₂O, MeOH, -20 °C; g) H₂, Pd(OH)₂, MeOH/H₂O, rt, 60% (3 steps).

CHAPITRE 3 – SYNTHESIS OF OLIGOSACCHARIDES RELATED TO POTENTIAL BIOTERRORIST PATHOGENS

disaccharide **289**, debenzoylation, and subsequent glycosylation with monosaccharide **295** yielded fully protected hexasaccharide **292**. Finally, target hexasaccharide **293** was obtained following debenzoylation of intermediate **292**, reduction of the azides, installation of the formamido groups, and hydrogenolysis. In contrast to their previously reported method for the installation of the formamido groups, Bundle and co-workers herein used (HCO)₂O in MeOH at low temperatures, since the use of Ac₂O in formic acid resulted in the formation of traces amounts of *N*-acetylated byproducts.

Hexasaccharide **300**, mimicking the capping antigen of *Brucella* sLPS, was synthesized using a [4 + 2] pathway. Previously synthesized trisaccharide **290** was first coupled to monosaccharide building block **296** employing MeOTf in toluene at high temperatures. These thermodynamic controlled conditions led to the formation of an α -1,2-glycosidic linkage. Debenzoylation of the resulting tetrasaccharide afforded glycosyl acceptor **297**, which was glycosylated with disaccharide **298** at room temperature, yielding protected hexasaccharide **299**. Target oligosaccharide **300** was finally obtained following the same deprotection procedure as the one employed for pure A antigen hexasaccharide **293**.

A major issue in the combat against brucellosis is the difficulty to differentiate infected animals from vaccinated animals. The diagnostic of brucellosis is based on the detection of antibodies specific to antigens A and M of *Brucella* spp. sLPS. However, animal brucellosis vaccines are composed of oligosaccharides containing these epitopes, hence the differentiation problem. With the aim of developing a new diagnostic tool, biological assays were conducted. Hexasaccharides **293** and **300** and the four other synthesized oligosaccharides were conjugated to BSA following their derivatization into squarate half esters at room temperature to avoid *N*-deformylation. Immunogenic evaluation of the oligosaccharide glycoconjugates revealed that the M antigen-related disaccharide composed of two 1,3-linked D-Rha4FNo residues was immunodominant since it was able to detect antibodies in the sera of subjects infected with A⁺M⁻ strains. This result highlighted the fact that this disaccharide could be used as a diagnostic tool against brucellosis. By using this M antigen-related oligosaccharide with pure A antigen hexasaccharide **293** for diagnosis, false positives could be avoided since cross reactive bacteria would only bind to

hexasaccharide **293** but not to the disaccharide. Indeed, false positives are frequent during infections detection since some bacteria have O-antigen purely 1,2-linked, and therefore react as *Brucella* A antigen. Discrimination could be accomplished using additional M antigen-related disaccharide. Immunization of mice with a hexasaccharide **293** conjugate showed that the induced antibodies reacted with LPS antigens of two *Brucella* strains. Using hexasaccharide **293** as a vaccine component could confer protection to the subjects, and differentiation from infected animals could be accomplished using the M antigen-related disaccharide during diagnostic. The diagnostic potential of the *Brucella* M antigen was supported by another study.³⁴⁹ Subsequently to these first steps towards the development of a novel diagnostic tools based on the A and M epitopes of *Brucella* spp. sLPS, a follow-up investigation was conducted.³³² Results showed that by conjugating the natural polysaccharide to tetanus toxoid at its nonreducing end through a periodate oxidation, the terminal M epitope could be destroyed, therefore releasing a longer pure-A antigen. The latter induced high titers of A-specific antibodies that did not react with the M epitope, again highlighting the fact that vaccines based on the A-antigen and a diagnostic tool using the M antigens could enable the differentiation of infected and vaccinated animals. Binding studies reported in 2017 gave supplementary insights on the binding specificities of A and M antigens that could help develop diagnostic tools and vaccines.³⁵⁰

3.8 Conclusion

As the threat posing bioterrorism increases, it is fundamental to keep on working toward the development of prophylactic treatments against dangerous diseases such as *B. anthracis*, *B. pseudomallei*, *B. mallei*, *F. tularensis*, *Y. pestis*, and *Brucella* spp. However, development of vaccines and diagnostic tools is difficult due to the lack of knowledge regarding carbohydrate-antibody interactions. Chemical synthesis is a leading tool to acquire this information, as oligosaccharides of different lengths and substitution patterns can be prepared and tested for their antigenicity and immunogenicity, while demystifying the antibodies recognition mechanisms.

In the present chapter, recent developments regarding the chemical syntheses of oligosaccharide mimics of biologically active compounds were reviewed. Various methods employed to bypass the synthetic challenges related to these oligosaccharides were reported, underlining the structural

CHAPITRE 3 – SYNTHESIS OF OLIGOSACCHARIDES RELATED TO POTENTIAL BIOTERRORIST PATHOGENS

complexity of these compounds. The results of biological assays also highlighted the relevance of carbohydrate chemistry for the development of glycoconjugate vaccines and diagnostic tools. These data will assuredly contribute to future researches towards the development of prophylactic measures against potential bioterrorism agents.

CHAPITRE 4 : MELIOIDOSIS PATIENT SERUM-REACTIVE SYNTHETIC TETRASACCHARIDES BEARING THE PREDOMINANT EPITOPES OF *BURKHOLDERIA PSEUDOMALLEI* AND *BURKHOLDERIA MALLEI* O-ANTIGENS

Maude Cloutier,^a Emmanilo Delar,^a Kevin Muru,^a Seynabou Ndong,^a Robert R. Hoyeck,^a Taniya Kaewarpai,^b Narisara Chantratita,^{bc} Mary N. Burtnick,^d Paul J. Brett,^d Charles Gauthier^a

^a*Centre Armand-Frappier Santé Biotechnologie, Institut national de la recherche scientifique (INRS), 531, boul. des Prairies, Laval (Québec), H7V 1B7, Canada*

^b*Department of Microbiology and Immunology, Faculty of Tropical Medicine, Mahidol University, 420/6 Rajvithi Road, Bangkok 10400, Thailand*

^c*Mahidol-Oxford Tropical Medicine Research Unit, Faculty of Tropical Medicine, Mahidol University, 420/6 Rajvithi Road, Bangkok 10400, Thailand*

^d*Department of Microbiology and Immunology, University of Nevada, Reno School of Medicine, 1664, N. Virginia Street, Reno, Nevada, 89557, United States of America*

Article publié dans *Organic & Biomolecular Chemistry*, 2019, 17, 8878-8901, doi 10.1039/C9OB01711A (contribution invitée à l'édition web thématique « [Glycosylation: New methodologies and applications](#) »)

Titre français: Des tétrasaccharides synthétiques dotés des épitopes prédominants des antigènes-O de *Burkholderia pseudomallei* et *Burkholderia mallei* sont réactifs au sérum de patients atteints de la mélioïdose

Contribution des auteurs: Maude Cloutier (60%), Emmanilo Delar (25%), Kevin Muru (5%), Seynabou Ndong (5%) et Robert R. Hoyeck (5%) ont réalisé la synthèse chimique. Maude Cloutier a réalisé la caractérisation des composés synthétiques. Taniya Kaewarpai, Narisara Chantratita, Mary N. Burtnick et Paul J. Brett ont effectué les tests d'antigénicité. Maude Cloutier, Charles Gauthier, Mary N. Burtnick et Paul J. Brett ont rédigé l'article.

4.1 Résumé

La mélioïdose et la morve, respectivement causées par les bactéries à Gram négatif *Burkholderia pseudomallei* (*Bp*) et *Burkholderia mallei* (*Bm*), sont considérées comme des problèmes de santé publique urgents dans les pays en voie de développement et comme des agents potentiels de bioterrorisme. Les lipopolysaccharides (LPS) de *Bp* et *Bm* ont été identifiés comme des candidats attrayants pour le développement de mesures prophylactiques contre la mélioïdose et la morve. *Bp* et *Bm* expriment des LPS structurellement similaires dans lesquels la partie antigène-O (OAg) consiste en un hétéropolymère dont l'unité répétitive est un disaccharide composé de résidus D-glucose et 6-désoxy-L-talose, ce dernier étant diversement acétylé et méthylé. Nous rapportons ici la synthèse de deux tétrasaccharides imitant les principaux épitopes de substitution des OAg du LPS de *Bp* et *Bm*. L'assemblage des tétrasaccharides a été réalisé en utilisant une stratégie de glycosylation itérative tout en s'appuyant sur l'épimérisation tardive du rhamnose interne en un résidu 6-désoxy-L-talose. Nous montrons que ces composés synthétiques réagissent fortement avec le sérum de patients atteints de la mélioïdose et imitent étroitement l'antigénicité du LPS natif de *Bp*. Nos résultats suggèrent que ces tétrasaccharides pourraient être des candidats prometteurs pour le développement de vaccins et/ou d'outils diagnostiques contre la mélioïdose et la morve.

4.2 Abstract

Melioidosis and glanders, respectively caused by the Gram-negative bacteria *Burkholderia pseudomallei* (*Bp*) and *Burkholderia mallei* (*Bm*), are considered as urgent public health issues in developing countries and potential bioterrorism agents. *Bp* and *Bm* lipopolysaccharides (LPS) have been identified as attractive vaccine candidates for the development of prophylactic measures against melioidosis and glanders. *Bp* and *Bm* express structurally similar LPSs wherein the O-antigen (OAg) portion consists of a heteropolymer whose repeating unit is a disaccharide composed of D-glucose and 6-deoxy-L-talose residues, the latter being diversely acetylated and methylated. Herein we report the synthesis of two tetrasaccharides mimicking the main substitution epitopes of *Bp* and *Bm* LPS OAg. The assembly of the tetrasaccharides was achieved using a sequential glycosylation strategy while relying on the late-stage epimerization of the inner

CHAPITRE 4 – MELIOIDOSIS PATIENT SERUM-REACTIVE SYNTHETIC TETRASACCHARIDES BEARING THE PREDOMINANT EPITOPES OF BURKHOLDERIA PSEUDOMALLEI AND BURKHOLDERIA MALLEI O-ANTIGENS

rhamnose into a 6-deoxy-L-talose residue. We show that these synthetic compounds strongly react with culture-confirmed Thai melioidosis patient serum and closely mimic the antigenicity of native *Bp* OAg. Our results suggest that these tetrasaccharides could be suitable candidates for the development of vaccines and/or diagnostic tools against melioidosis and glanders.

4.3 Introduction

Burkholderia pseudomallei (*Bp*) and *Burkholderia mallei* (*Bm*), two closely related facultative intracellular Gram-negative bacteria (GNB), are the respective etiologic agents of melioidosis and glanders. Endemic in tropical and sub-tropical regions and sporadically found worldwide,^{351, 352} these two neglected bacteria are highly virulent and, if left untreated, are fatal in up to 50% of infected patients.³⁵³⁻³⁵⁵ Notably, the urgent public health issues that these diseases represent is highlighted by the fact that melioidosis is considered the third most common cause of infectious diseases-related deaths in Northeast Thailand.³⁵⁶ The protean manifestations of melioidosis and glanders can hinder diagnosis, and treatment of infected patients is challenging due to the intracellular nature of these pathogens as well as their intrinsic resistance to commonly used antibiotics such as aminoglycosides, polymyxins, and β -lactams.³⁵⁷ Importantly, in addition to the public health threat that they represent, *Bp* and *Bm* are considered potential biological weapons by the U. S. Centers for Disease Control and Prevention, as they have been classified as “Tier 1” biological select agents.³⁵⁸

Notwithstanding the efforts put towards the development of prophylactic measures against melioidosis and glanders, there are currently no licensed vaccines against these diseases. In light of the many attempts to develop protective vaccines,³⁵⁹ recent studies underlined the potential of using lipopolysaccharides (LPS) as subunit vaccines owing to their stimulating effect on the adaptive immune system.³⁶⁰ LPSs are surface-exposed antigenic and virulence-associated polysaccharides anchored in the outer membrane of GNB such as *Bp* and *Bm*.³⁶¹ It was shown that LPS-specific monoclonal antibodies (mAbs) have the ability to passively protect animal models from infection,³⁶²⁻³⁶⁷ and that immunization of mice with LPS conjugates induces significant protection against lethal challenges of *Bp*.^{360, 368}

CHAPITRE 4 – MELIOIDOSIS PATIENT SERUM-REACTIVE SYNTHETIC TETRASACCHARIDES BEARING THE PREDOMINANT EPITOPES OF BURKHOLDERIA PSEUDOMALLEI AND BURKHOLDERIA MALLEI O-ANTIGENS

The predominant serotype A (97%) O-antigens (OAg) of *Bp* and *Bm* LPSs³⁶⁹ are of similar composition and consist of linear heteropolymers whose repeating unit is a disaccharide of the following structure: [\rightarrow 3)-6-deoxy- α -L-talopyranosyl-(1 \rightarrow 3)- β -D-glucopyranosyl-(1 \rightarrow] (Figure 1). One atypical characteristic of these OAg lies in the non-stoichiometric methylation and acetylation patterns of the 6-deoxy-L-talose residues, which slightly vary between species. It has been revealed that the predominant inner disaccharide unit of both *Bp* and *Bm* is acetylated at O-2. In addition, the terminal residue of *Bm* is 3-O-methylated and 2-O-acetylated whereas *Bp*'s is also acetylated at O-4.³⁷⁰⁻³⁷⁵

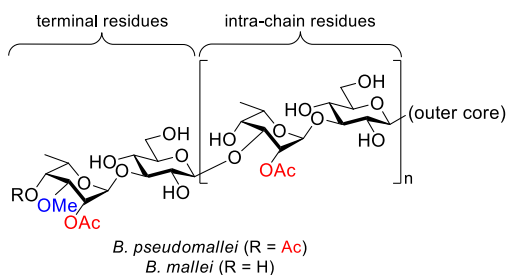


Figure 4.1. Structures of *B. pseudomallei* and *B. mallei* LPS O-antigens showing the predominant terminal and intra-chain epitopes

We recently described the synthesis of seven di- and trisaccharides (**1–7**) as the minimal structures mimicking all of the reported substitution patterns of *Bp* and *Bm* OAg (Figure 2A).¹⁶⁸ Enzyme-linked immunosorbent assay, saturation transfer difference-nuclear magnetic resonance, and surface plasmon resonance assays were jointly used to assess the molecular interactions of the synthetic oligosaccharides with LPS-specific mAbs. These biophysical studies revealed the crucial role of the capping 3-O-methylated-6-deoxy-L-talose residues in the binding process. Moreover, we showed that high-titer antibody responses can be raised in mice injected with a CRM197:*Bm*-like disaccharide **6** construct and that these responses were cross-reactive with *Bm*-like LPS. In contrast, a CRM197:*Bp*-like disaccharide **7** construct was not able to induce a strong antibody response in both BALB/c and C57BL/6 mice suggesting a gap in the mice B cell repertoire against the OAg motif bearing an additional 4-O-acetyl group. We also showed that Thai melioidosis patient serum samples can react with *Bp*-like disaccharide **7**, which indicates that, unlike mice, humans can generate antibody responses against this unique OAg epitope.

CHAPITRE 4 – MELIOIDOSIS PATIENT SERUM-REACTIVE SYNTHETIC TETRASACCHARIDES BEARING THE PREDOMINANT EPITOPES OF BURKHOLDERIA PSEUDOMALLEI AND BURKHOLDERIA MALLEI O-ANTIGENS

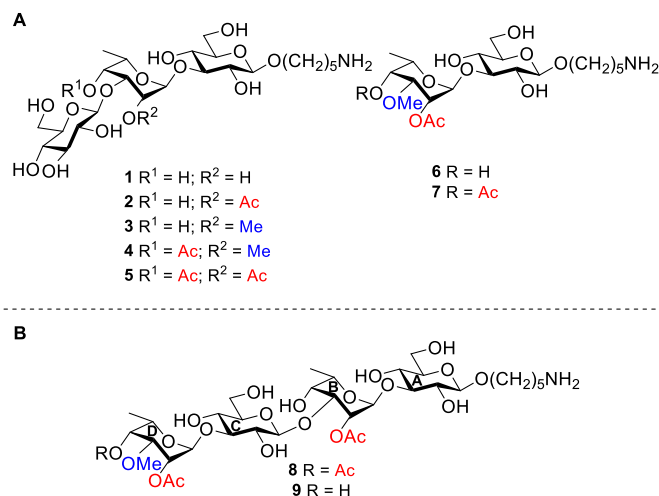


Figure 4.2. (A) Structures of previously synthesized di- and trisaccharides (1–7); and (B) target synthetic tetrasaccharides **8** and **9** related to *Bp* and *Bm* LPS OAgS, respectively

We now show that longer oligosaccharidic fragments, such as tetrasaccharides **8** and **9** (Figure 2B), bearing both internal and terminal epitopes of *Bp* and *Bm* OAgS are suitable candidates for the development of diagnostics and subunit vaccines against melioidosis and glanders. We herein describe a synthetic approach enabling the preparation of tetrasaccharides related to *Bp* and *Bm* LPS OAg featuring the main intrachain and terminal acetylation and methylation patterns. The reactivity profiles of synthetic oligosaccharides **1–9** were assessed against Thai melioidosis patient serum samples highlighting that tetrasaccharides **8** and **9** act as exquisite mimics of the whole *Bp* and *Bm* LPS OAgS.

4.4 Results and Discussion

4.4.1 Retrosynthetic approach

The presence of acetyl groups in target tetrasaccharides **8** and **9** posed a substantial challenge in the development of the synthetic route, which had to be designed so that their migration or cleavage would be avoided. Retrosynthetic analysis of these oligosaccharides, as depicted in Figure 3, led to the identification of synthons **13**, **14**,¹⁶⁸ **15**, and **16**¹⁶⁸ as the most readily accessible functionalized monosaccharides that could enable their assembly. Our synthetic approach would be based on a convergent [2 + 2] glycosylation strategy in which disaccharides **11** and **12**,

CHAPITRE 4 – MELIOIDOSIS PATIENT SERUM-REACTIVE SYNTHETIC TETRASACCHARIDES BEARING THE PREDOMINANT EPITOPES OF BURKHOLDERIA PSEUDOMALLEI AND BURKHOLDERIA MALLEI O-ANTIGENS

assembled from building blocks **13–16**, would be coupled into fully protected tetrasaccharide **3**, the latter being a precursor of both *Bp*- and *Bm*-like oligosaccharides **8** and **9**, respectively. We plan to introduce *O*-acetyl and *O*-methyl groups in synthons **13** and **14** prior to the synthesis of the tetrasaccharides. These building blocks would have to be designed in order to preserve orthogonality among the temporary protecting groups and acetates. The acetyl groups at *O*-2 on rhamnosides **13** and **14** as well as the (2-azidomethyl)benzoyl (AZMB)³⁷⁶ group of glucoside **15** would act as neighbouring participating groups (NPG) to ensure the stereoselective formation of 1,2-*trans* glycosidic linkages in the target compounds.³⁷⁷ Moreover, assisted cleavage of the AZMB group, which involves the reduction of the primary azide into the corresponding amine followed by *in situ* intramolecular cyclization into an isoindolinone, thereby releasing the C2 hydroxyl group,³⁷⁶⁻³⁷⁸ would be achieved during the final hydrogenolysis step. The anomeric position of monosaccharides **13** and **14** would be activated with a trichloroacetimidate (TCA) leaving group in an attempt to achieve high-yielding couplings, as previously reported for structurally similar L-rhamnose donors.³⁷⁹ In contrast, glucoside **15** would be thiolated at the anomeric position to ensure its orthogonal glycosylation with respect to donor **14**. The methylphenylthio (STol) group is known to be highly stable under a broad variety of conditions while being readily accessible from peracetylated sugars,³⁸⁰ and thioglucoside **15** would be converted into other donors in the event that the coupling proves ineffective.

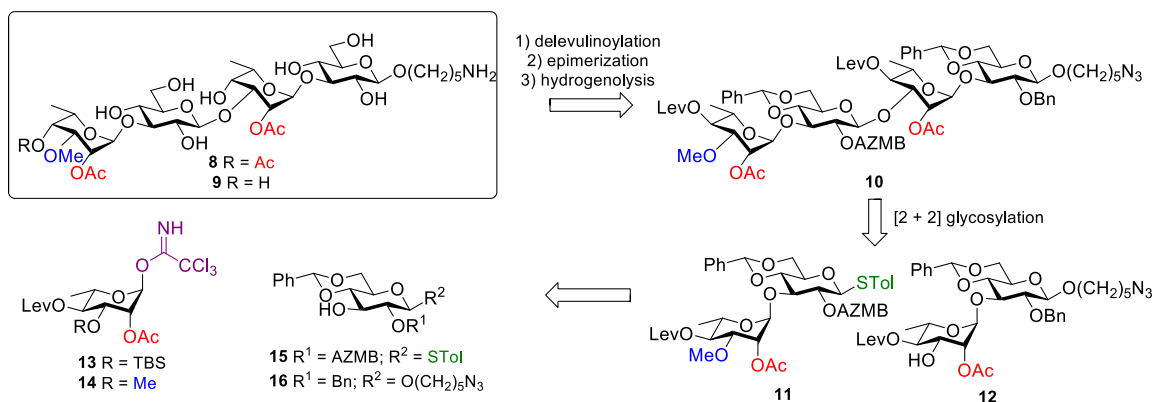


Figure 4.3. Retrosynthetic analysis of target tetrasaccharides **8** and **9**

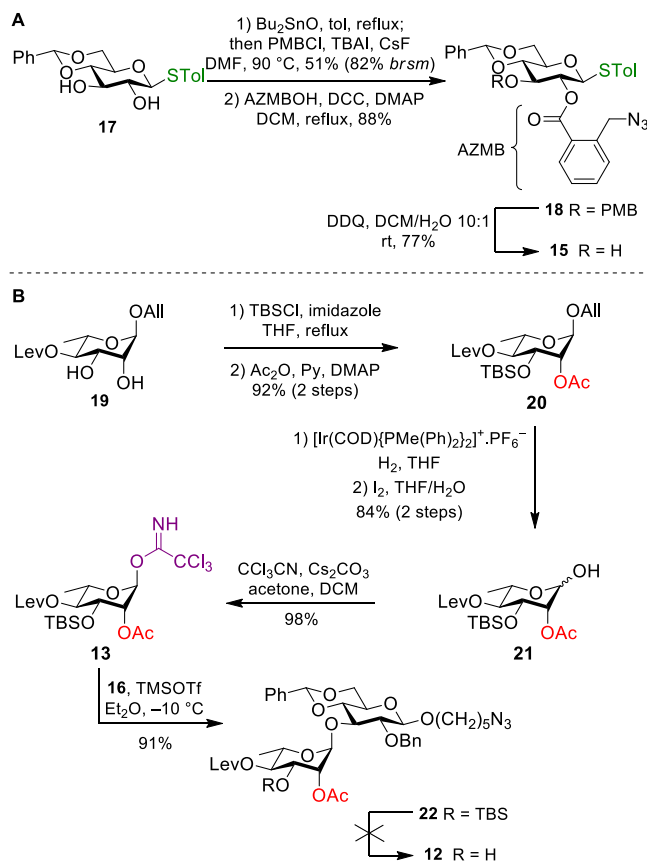
CHAPITRE 4 – MELIOIDOSIS PATIENT SERUM-REACTIVE SYNTHETIC TETRASACCHARIDES BEARING THE PREDOMINANT EPITOPES OF BURKHOLDERIA PSEUDOMALLEI AND BURKHOLDERIA MALLEI O-ANTIGENS

As 6-deoxy-L-talose derivatives are not commercially available, rhamnosides **13** and **14** would instead be employed. We envisioned to conduct both C4 epimerization simultaneously at a later stage of the synthetic route *via* a two-step oxidation/reduction sequence.³⁸¹ To reach *Bp*-like tetrasaccharide **8**, we intended to take advantage of the steric hindrance surrounding the inner 6-deoxy-L-talose residue to acetylate regioselectivity the *O*-4 position of the non-reducing end residue. Finally, acceptor **16** would be equipped with an azidolinker at C1, which upon reduction would allow the coupling of the fully assembled, unprotected oligosaccharides to activated ELISA plates enabling antigenicity assays with serum samples and/or covalent coupling with carrier proteins.

4.4.2 First generation synthesis of tetrasaccharides

As depicted in Scheme 1, the synthesis of glucoside acceptor **15** was performed in three steps from known diol **17**.³⁸² A *para*-methoxybenzyl (PMB) group was selectively introduced at *O*-3 through the formation of a stannylene acetal.¹⁹⁹ This step was followed by esterification of the resulting alcohol³⁸³ with 2-(azidomethyl)benzoic acid (AZMBOH), which was prepared using Steglich conditions.^{379,384} The PMB group finally underwent oxidative cleavage using 2,3-dichloro-5,6-dicyano-1,4-benzoquinone (DDQ), furnishing acceptor **15**.

CHAPITRE 4 – MELIOIDOSIS PATIENT SERUM-REACTIVE SYNTHETIC TETRASACCHARIDES BEARING THE PREDOMINANT EPITOPES OF BURKHOLDERIA PSEUDOMALLEI AND BURKHOLDERIA MALLEI O-ANTIGENS



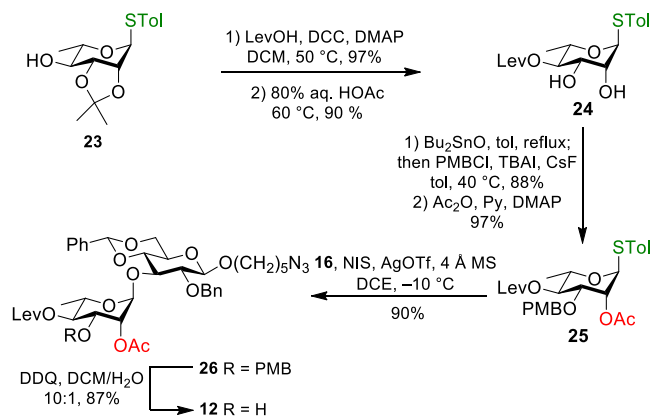
Scheme 4.1. (A) Synthesis of 2-O-AZMB-containing glucose derivative **15**; and (B) failed attempts to cleave the TBS group in disaccharide **22**

Allyl rhamnoside **19**¹⁶⁸ was used as starting material for the preparation of TCA **13**. Imidazole was used as catalyst for the selective protection of the C3 hydroxyl with a *tert*-butyldimethylsilyl (TBS) group and the remaining free OH was acetylated under standard conditions, yielding rhamnoside **20** in 92% yield over two steps. Allyl isomerization into the corresponding 1-propenyl ether was accomplished using an iridium-based catalyst^{385, 386} and was followed by its hydrolysis promoted by iodine³⁸⁷ in a mixture of THF and water. Resulting hemiacetal **21** was successfully converted into TCA **13** (~9:1 α/β mixture) through a standard procedure³⁸⁸ involving the use of trichloroacetonitrile and cesium carbonate. The latter was coupled with acceptor **16** under the promotion of trimethylsilyl trifluoromethanesulfonate (TMSOTf),³⁸⁹⁻³⁹² providing disaccharide **22** in an excellent 91% yield as the sole α -anomer. In order to lengthen the disaccharide, deprotection of the TBS group was attempted using Et₃N·3HF, but acetyl cleavage was unfortunately observed.

CHAPITRE 4 – MELIOIDOSIS PATIENT SERUM-REACTIVE SYNTHETIC TETRASACCHARIDES BEARING THE PREDOMINANT EPITOPES OF BURKHOLDERIA PSEUDOMALLEI AND BURKHOLDERIA MALLEI O-ANTIGENS

Tetra-*n*-butylammonium fluoride (TBAF)-mediated cleavage, with and without acetic acid buffer, also led to acetyl deprotection.

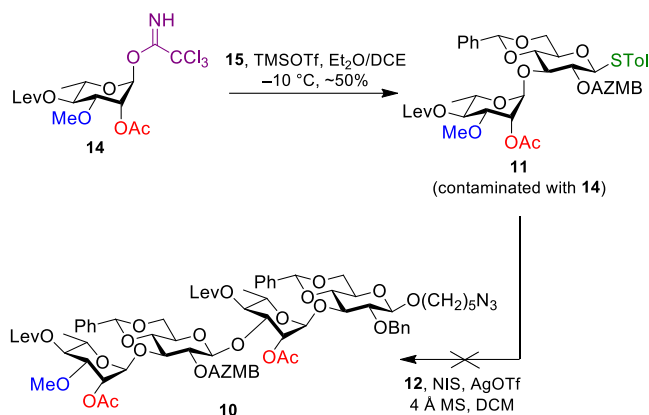
Due to the poor selectivity of the silyl ether deprotection, we prepared thiorhamnoside **25**, bearing an orthogonal PMB group at *O*-3 instead of a TBS group as previously reported by us (Scheme 2).¹⁶⁸ Alcohol **23**³⁹³ was therefore levulinoylated under the action of dicyclohexylcarbodiimide (DCC) and catalytic DMAP and the isopropylidene group was cleaved in acidic media, furnishing diol **24** in excellent yield. Tin acetal chemistry was taken advantage of for the selective alkylation of the *O*-3 position and the remaining hydroxyl group was acetylated into donor **25**. *N*-Iodosuccinimide (NIS)/silver triflate (AgOTf)-promoted glycosidation^{394, 395} of the latter with acceptor **16** at $-10\text{ }^{\circ}\text{C}$ in DCE provided disaccharide **26** in 90% yield. Satisfyingly, only the α -anomer was formed, which was then successfully transformed into acceptor **12** following PMB deprotection without noticeable acetyl migration.



Scheme 4.2. Synthesis of disaccharide acceptor **12**

Planning on employing a [2 + 2] glycosylation strategy (Scheme 3), disaccharide **11** was then prepared through TMSOTf-promoted glycosylation of TCA **7**¹⁶⁸ and acceptor **15**. However, complete conversion could not be achieved and disaccharide **11** was contaminated with donor **14** even upon extensive column chromatography purifications. Synthesis of fully protected tetrasaccharide **10** was nonetheless attempted using NIS/AgOTf but proved unsuccessful, as NMR and HRMS analyses showed no sign of the expected glycosidic bond.

CHAPITRE 4 – MELIOIDOSIS PATIENT SERUM-REACTIVE SYNTHETIC TETRASACCHARIDES BEARING THE PREDOMINANT EPITOPES OF BURKHOLDERIA PSEUDOMALLEI AND BURKHOLDERIA MALLEI O-ANTIGENS

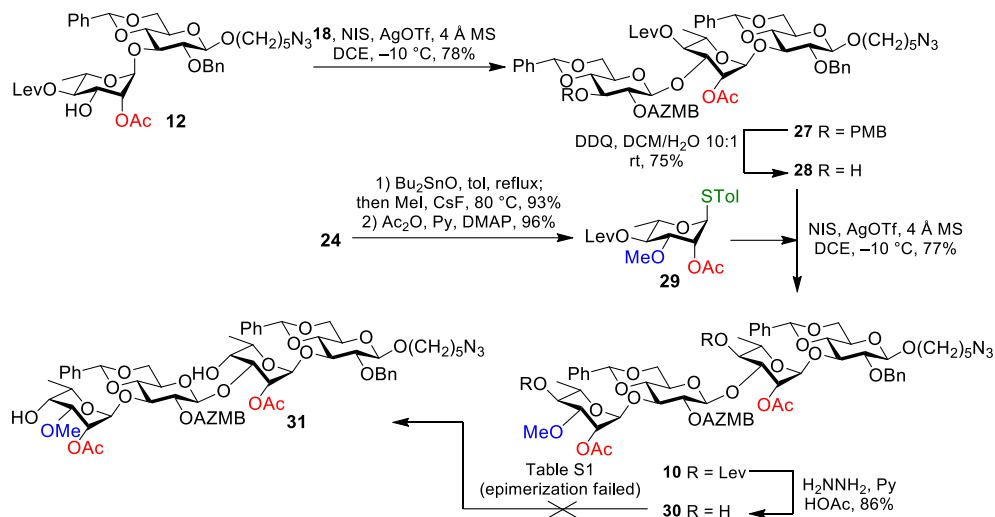


Scheme 4.3. Attempt to synthesize tetrasaccharide **10** via a [2 + 2] glycosylation

4.4.3 Second generation synthesis of tetrasaccharides

As our previously envisioned methodology appeared ineffective, we chose to focus our attention on an alternative sequential [1 + 1 + 1 + 1] glycosylation pathway (Scheme 4). First, disaccharide acceptor **12** was glycosylated with donor **18** using the aforementioned conditions, yielding trisaccharide **27**. The AZMB group appeared to be an efficient NPG, as the β -anomer was exclusively formed. DDQ-mediated dealkylation of trisaccharide **27** enabled its coupling with thiorhamnoside **29**, which was prepared from intermediate **24** through a methodology similar as the one used for donor **25**. In the course of this reaction sequence, O-methylation of diol **24** partially occurred at *O*-2, resulting in a mixture of regioisomers. Upon glycosylation, tetrasaccharide **10** was produced in a 65% yield, along with an inseparable unknown impurity. To achieve the desired 6dTal ρ configuration, the levulinoyl groups in compound **10** were selectively cleaved under the action of hydrazine and epimerization of both free hydroxyl groups in resulting tetrasaccharide **30** was attempted.

CHAPITRE 4 – MELIOIDOSIS PATIENT SERUM-REACTIVE SYNTHETIC TETRASACCHARIDES BEARING THE PREDOMINANT EPITOPES OF BURKHOLDERIA PSEUDOMALLEI AND BURKHOLDERIA MALLEI O-ANTIGENS



Scheme 4.4. Synthesis of rhamnose-containing tetrasaccharide 10 via a [1 + 1 + 1 + 1] glycosylation sequence

Several approaches have been developed for the epimerization of rhamnose glycosides. For instance, Kováč reported the synthesis of the C-2 rhamnose epimer L-quinovose through the formation of 1,2-*O*-stannylene acetals.³⁹⁶ Chloral/DCC-induced inversion, which requires the presence of a 2,3,4-triol, resulted in C-3 epimerization of rhamnose.³⁹⁷ The Mitsunobu reaction^{398,399} has been shown to lead to an elimination reaction in rhamnosides due to the axial H-5.³⁸¹ Intramolecular displacement of an *O*-4 triflate has also been reported for the synthesis of 6-deoxy-taloside from rhamnose.^{400,401} However, this approach has been shown to be less reliable compared to the oxidation-reduction sequence in which the stereochemical outcome can be consistently predicted using the Cram chelate model.^{381, 402-404}

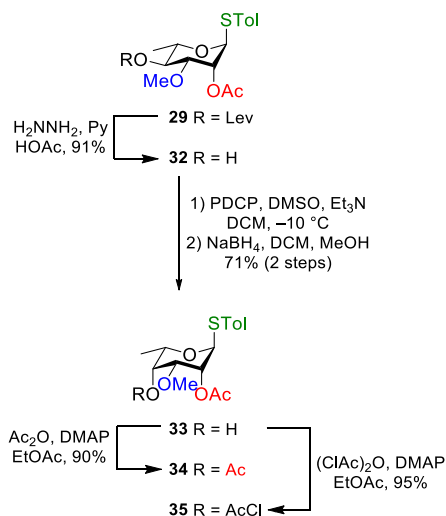
Therefore, our strategy was based on an oxidation step (see Table S1) followed by a stereoselective reduction using NaBH₄ in a mixture of MeOH and DCM. Pfitzner-Moffatt oxidation⁴⁰⁵ (entry 1) was first tried as we previously showed that this condition was high-yielding for similar substrates,¹⁶⁸ nevertheless complete degradation of the starting material was observed. The same reaction was conducted at -78°C (entry 2) with the hope of stabilizing the reactive intermediate formed between phenyl dichlorophosphate (PDCP) and DMSO, but without success. Substituting the PDCP reagent with oxalyl chloride³⁸¹ also gave no conversion (entry 3). Other oxidation

CHAPITRE 4 – MELIOIDOSIS PATIENT SERUM-REACTIVE SYNTHETIC TETRASACCHARIDES BEARING THE PREDOMINANT EPITOPES OF BURKHOLDERIA PSEUDOMALLEI AND BURKHOLDERIA MALLEI O-ANTIGENS

reactions were carried out using DMSO and Ac₂O at room temperature⁴⁰⁶ (entry 4) or Dess-Martin periodinane in refluxing DCE¹⁶⁸ (entry 5), but both failed to provide clean oxidation products.

4.4.4 Third generation synthesis of tetrasaccharides

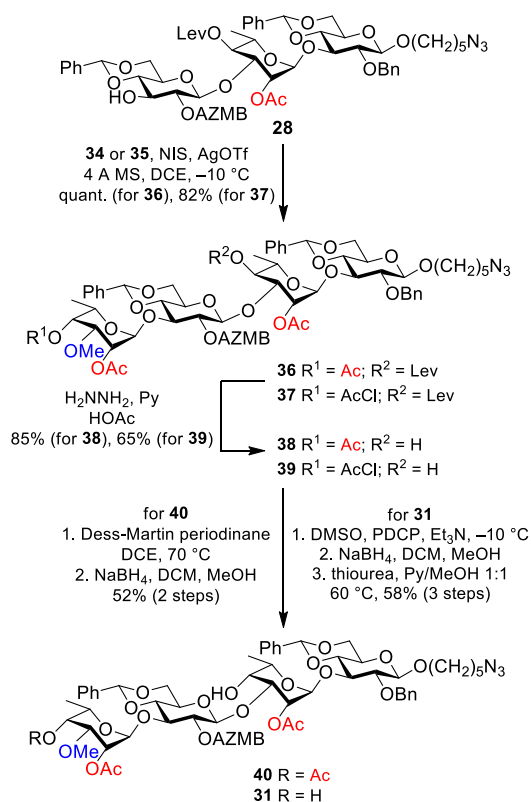
As the previous double epimerization step could not be carried out successfully, we hypothesized that the simultaneous presence of two hydroxyl groups could lead to macromolecular interactions preventing the oxidation step to occur. Therefore, we envisioned that the introduction of a terminal 6-deoxy-talose residue would restrict these interactions and consequently enable the epimerization of the inner rhamnose unit. As depicted in Scheme 5, derivatives **34** and **35** were prepared from building block **29**. Delevulinoylation of the latter was performed using standard conditions. Pfitzner-Moffatt oxidation followed by reduction of the crude ketone with NaBH₄ furnished thiotalosite **33** in 65% yield over three steps. Acetylation of the remaining hydroxyl group using Ac₂O and catalytic DMAP in refluxing EtOAc led to building block **34**, which mimics *Bp* LPS OAg terminal residue. As for *Bm*-like LPS OAg terminal residue, a chloroacetyl group was used as a temporary protecting group, which could be further transformed into an acetyl group following its orthogonal deprotection. This reaction was performed using chloroacetic anhydride and catalytic DMAP in refluxing EtOAc providing building block **35** in an almost quantitative yield.



Scheme 4.5. Synthesis of 6-deoxy-L-talopyranoside derivatives **34** and **35**

CHAPITRE 4 – MELIOIDOSIS PATIENT SERUM-REACTIVE SYNTHETIC TETRASACCHARIDES BEARING THE PREDOMINANT EPITOPES OF BURKHOLDERIA PSEUDOMALLEI AND BURKHOLDERIA MALLEI O-ANTIGENS

To prepare *Bp* and *Bm* LPS OAg-like tetrasaccharides, trisaccharide acceptor **28** was coupled with thiotaloside **34** and **35**, respectively, under previously mentioned conditions, affording tetrasaccharides **36** and **37** exclusively as the α -anomers (Scheme 6). Upon delevulinoylation of these latter, either Dess-Martin periodinane reagent or Pfitzner-Moffatt conditions were successfully used for their oxidations. In both cases, the resulting ketone was filtered over silica gel and then reduced with complete stereoselectivity into its talose configuration under the action of NaBH₄. This two-step sequence enabled the isolation of tetrasaccharide **40** in a moderate 52% yield due to its partial degradation during the oxidation step. Derivative **31** was ultimately reached in a 58% yield over three steps following chloroacetyl cleavage using thiourea in a mixture of pyridine and methanol.



Scheme 4.6. Final approach for the synthesis of protected tetrasaccharides **31** and **40**

4.4.5 Global deprotection of tetrasaccharides

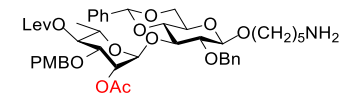
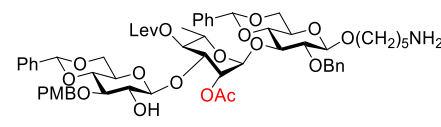
Two alternative pathways were studied for the global deprotection of tetrasaccharides **40** and **31** in order to reach target compounds **8** and **9**, respectively. The first pathway (route A) consisted in the selective reduction of both azides followed by hydrogenolysis of the remaining benzyl and benzyldiene groups, whereas the second route (route B) only involved the hydrogenolysis step. We therefore investigated a series of conditions for the selective reduction of both azides *via* the Staudinger reaction, which would result in the assisted cleavage of the AZMB group. We first planned to use trisaccharide **27** as a model compound, as we hypothesized that if difficulties had to arise during AZMB deprotection, it would be due to the electrophilic acetyl group at the inner talose residue. Intramolecular rearrangement of iminophosphorane intermediates during the Staudinger reduction can indeed occur in compounds containing a neighbouring ester.³⁷⁷ Preliminary reduction tests were first conducted with trisaccharide **27**, but we noticed that the reduction of the azidolinker reduction required harsher conditions than the AZMB group itself. Our hypothesis was that the formation of the isoindolinone by-product acted as the driving force for the AZMB cleavage. Our attention therefore shifted toward disaccharide **26** and conditions were optimized for the sole reduction of the azidolinker (Table 1). Triphenylphosphine was first used in a mixture of THF/H₂O in the presence of SiO₂ (entry 1).³⁷⁹ After 20 h, the starting material was totally consumed but, as shown by TLC, the intermediates were not fully hydrolysed. Following work-up with aqueous NaHCO₃ and purification, target amine **41** was isolated in low yield (21%). We then attempted to conduct the reaction through a two-step procedure, *i.e.*, 1) formation of the iminophosphorane and 2) its hydrolysis, while heating the reaction mixture to 60 °C, but a lower yield of amine **41** was obtained (entry 2). Switching the solvent for DMF and avoiding the work-up procedure allowed to improve the yield to 38% (entry 3). Satisfyingly, using the same reaction conditions than in entry 3 while avoiding the work-up provided amine **41** in excellent yield (88%, entry 4). Tris(4-methoxyphenyl)phosphine [P(PMP)₃] was also tested but without yield improvement (entry 5). The optimized reduction conditions were then applied to trisaccharide **27** bearing both the azidolinker and the AZMB group, providing alcohol **42** in good yield (76%, entry 6). These conditions finally successfully furnished tetrasaccharide **43** from diol

CHAPITRE 4 – MELIOIDOSIS PATIENT SERUM-REACTIVE SYNTHETIC TETRASACCHARIDES BEARING THE PREDOMINANT EPITOPES OF BURKHOLDERIA PSEUDOMALLEI AND BURKHOLDERIA MALLEI O-ANTIGENS

31 (63%, entry 7), which was then deprotected into target compound **9** through a Pd-catalyzed hydrogenolysis, as shown in Scheme 7.

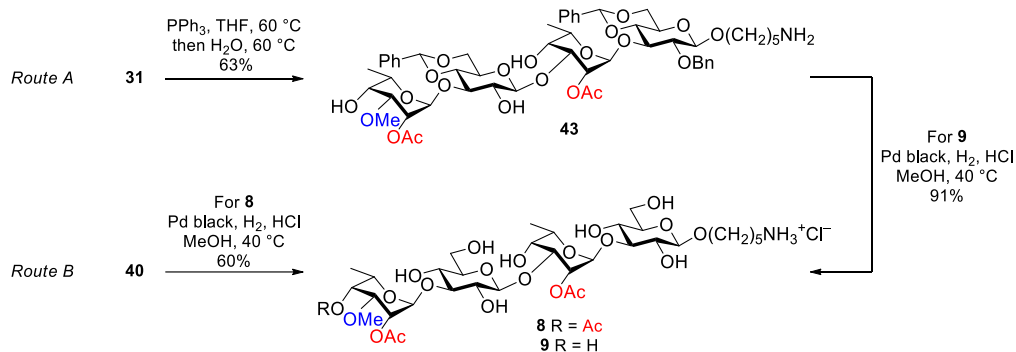
CHAPITRE 4 – MELIOIDOSIS PATIENT SERUM-REACTIVE SYNTHETIC TETRASACCHARIDES BEARING THE PREDOMINANT EPITOPES OF BURKHOLDERIA PSEUDOMALLEI AND BURKHOLDERIA MALLEI O-ANTIGENS

Table 4.1. Optimization of the Staudinger reaction for azide reduction

entry	substrate	conditions	work-up	product	yield (%) ^a
1	26	PPh ₃ , SiO ₂ THF/H ₂ O, rt 20 h	NaHCO ₃ H ₂ O, DCM	 <p>41</p>	21
2	26	PPh ₃ , THF 60 °C, 2 h, then H ₂ O, 60 °C, 4 h	NaHCO ₃ H ₂ O, DCM	41	13
3	26	PPh ₃ , DMF, 0 °C to rt 2 h, then H ₂ O, rt, 26 h	toluene co- concentration	41	38
4	26	PPh ₃ , THF, 60 °C 2 h then H ₂ O 60 °C, 4 h	concentration	41	88
5	26	P(PMP) ₃ , THF 60 °C, 2 h, then H ₂ O, 60 °C, 4 h	concentration	41	63
6	27	PPh ₃ , THF, 60 °C 2 h, then H ₂ O 60 °C, 4 h	concentration	 <p>42</p>	76
7	31	PPh ₃ , THF, 60 °C 2 h then H ₂ O, 60 °C, 4 h	concentration	43	63

^aIsolated yield.

CHAPITRE 4 – MELIOIDOSIS PATIENT SERUM-REACTIVE SYNTHETIC TETRASACCHARIDES BEARING THE PREDOMINANT EPITOPES OF BURKHOLDERIA PSEUDOMALLEI AND BURKHOLDERIA MALLEI O-ANTIGENS



Scheme 4.7. Alternative pathways for the final deprotection of tetrasaccharides 31 and 40

Alternatively, reduction of the azides into the corresponding amines and cleavage of the permanent protecting groups were carried out *via* a one-step hydrogenolysis procedure, enabling the conversion of compound 40 into *Bp*-like tetrasaccharide 8. Noteworthy, the presence of the azidolinker required the addition of concentrated HCl (1.0 equiv) in the reaction mixture in order to protonate the amine formed upon its reduction, as primary amines are known to poison transition metal catalysts.¹⁶⁸ Partial protonation of the 2-(aminomethyl)benzoyl group therefore also occurred prior to completion of the intramolecular cyclization, preventing the complete release of the corresponding hydroxyl group. The partial cleavage of the AZMB group not only diminished the isolated yield, but also complicated the purification of the target compound. First, exclusion size chromatography using LH-20 resin was employed to purify the tetrasaccharides from the isoindolinone, which was released following AZMB cleavage. Then, reverse phase chromatography was required to isolate tetrasaccharide 8 from the derivative still bearing the protonated 2-(aminomethyl)benzoyl group. Despite this, direct hydrogenolysis of compound 40 enabled the isolation of pure tetrasaccharide 8 in good yield (60%), as shown in Scheme 7.

4.4.6 Reactivity of the synthetic oligosaccharides with *Bm* LPS-specific mAbs.

Studies from our laboratories and others have shown that LPS-specific mAbs differentially recognize *Bm* and *Bp* OAgS as well as disaccharides 6 and 7.^{168, 373, 407} To determine whether tetrasaccharides 8 and 9 synthesized in this study (oligosaccharides 8 and 9) were recognized by *Bm* LPS-specific mAbs 3D11 and 9C1-2, ELISAs were conducted using oligosaccharides 6-9

CHAPITRE 4 – MELIOIDOSIS PATIENT SERUM-REACTIVE SYNTHETIC TETRASACCHARIDES BEARING THE PREDOMINANT EPITOPES OF BURKHOLDERIA PSEUDOMALLEI AND BURKHOLDERIA MALLEI O-ANTIGENS

along with *Bp* LPS controls. As shown in Figure 4, mAbs 3D11 and 9C1-2 reacted strongly with RR4744 LPS (4-*O*-acetyl mutant), oligosaccharides **6** and **9**, but only weakly with RR2808 LPS (wild type), and oligosaccharides **7** and **8**. These findings are consistent with our previous work and also show that mAb 3D11 appears to recognize the newly synthesized tetrasaccharide (oligosaccharide **9**), which represents both intrachain and terminal residues associated with *Bm* OAg, more strongly than the previously synthesized disaccharide (oligosaccharide **6**). The reactivity levels of mAb 9C1-2 with RR2808 LPS and oligosaccharides **6** and **9** were similar to one another. Taken together, these results suggest that the epitopes on *Bm* OAg that are recognized by these two mAbs are slightly different from one another. Importantly, since 9C1-2 has been shown to be passively protective in a mouse model of glanders,³⁶⁵ these data support the potential use of oligosaccharide **9** in the development of novel glanders vaccine candidates.

CHAPITRE 4 – MELIOIDOSIS PATIENT SERUM-REACTIVE SYNTHETIC TETRASACCHARIDES BEARING THE PREDOMINANT EPITOPES OF BURKHOLDERIA PSEUDOMALLEI AND BURKHOLDERIA MALLEI O-ANTIGENS

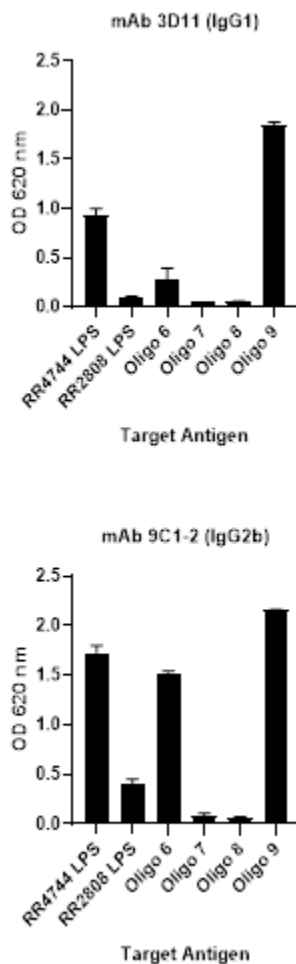


Figure 4.4. Interactions of *Bm* LPS-specific mAbs with *Bp* LPS antigens and synthetic oligosaccharides³⁴

4.4.7 Reactivity of the synthetic oligosaccharides with melioidosis patient serum.

We have previously demonstrated that both *Bp* OAg and oligosaccharide **7** are recognized more strongly by serum from culture-confirmed Thai melioidosis patients compared to serum from healthy donors.¹⁶⁸ Extending upon these findings, ELISAs⁴⁰⁷ were used to assess the reactivity of an expanded set of culture-confirmed Thai melioidosis patient and Thai healthy donor serum

³⁴ Reactivity profiles of mAbs 3D11 and 9C1-2 with LPS antigens purified from *Bp* strains RR2808 (wild type) and RR4744 (4-*O*-acetyl mutant) and synthetic oligosaccharides **6-9** as determined by ELISA. Values represent the means \pm SD of assays conducted in triplicate

CHAPITRE 4 – MELIOIDOSIS PATIENT SERUM-REACTIVE SYNTHETIC TETRASACCHARIDES BEARING THE PREDOMINANT EPITOPES OF BURKHOLDERIA PSEUDOMALLEI AND BURKHOLDERIA MALLEI O-ANTIGENS

samples with oligosaccharides **1-9** along with a *Bp* LPS control. Results demonstrated strong reactivity of immune serum samples with *Bp* LPS, oligosaccharides **8** and **9**, moderate reactivity with oligosaccharide **2**, and low to moderate reactivity with oligosaccharides **1, 3, 4, 5, 6** and **7** (based upon mean reactivities; Figure 5). In contrast, the healthy donor serum samples showed relatively low reactivity with all of the tested target antigens (based upon mean reactivities; Figure 5). These results agree with our previous studies and indicate that oligosaccharides **8** and **9**, which consist of a combination of epitopes associated with oligosaccharides [**2** + **7**] and [**2** + **6**], respectively, closely mimic the antigenicity of native *Bp* OAg. Additionally, these results demonstrate that the lack of the C4 *O*-acetyl group in *Bm*-like tetrasaccharide **9** does not significantly impact its recognition by melioidosis patient serum. This is not entirely surprising since human immune responses against OAg following infection with *Bp* would be expected to be polyclonal and thus recognize multiple epitopes at the non-reducing end of the polysaccharide. Based on these observations, we anticipate that glycoconjugates synthesized using either oligosaccharide **8** or **9** will be able to stimulate the production of carbohydrate-specific polyclonal responses capable of recognizing both native *Bp* and *Bm* OAg. Collectively, our findings suggest that oligosaccharides **8** and **9** may be valuable tools for developing countermeasures to combat diseases caused by *Bm* and *Bp*.

CHAPITRE 4 – MELIOIDOSIS PATIENT SERUM-REACTIVE SYNTHETIC TETRASACCHARIDES BEARING THE PREDOMINANT EPITOPES OF BURKHOLDERIA PSEUDOMALLEI AND BURKHOLDERIA MALLEI O-ANTIGENS

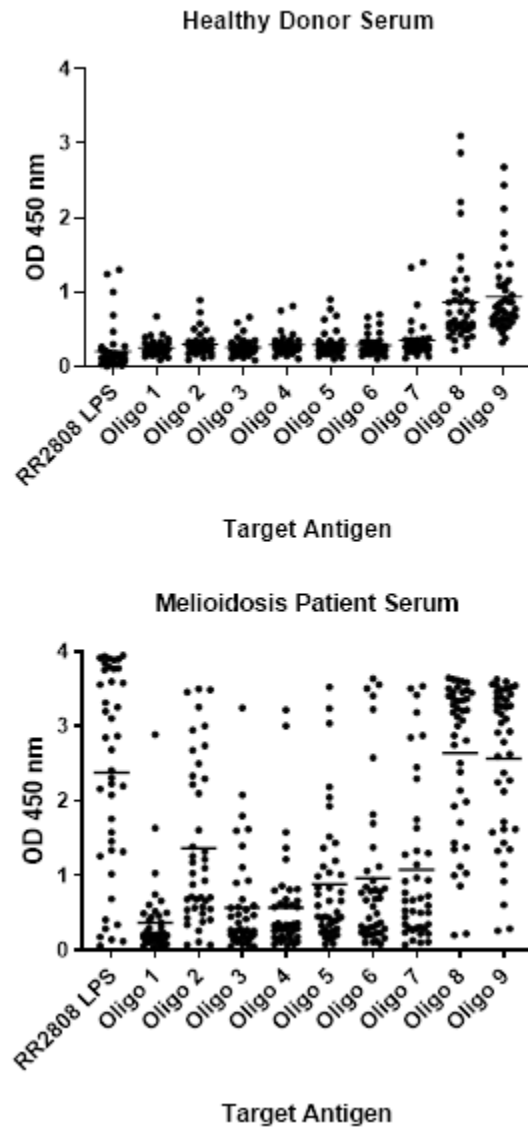


Figure 4.5. Reactivity of human serum samples with *Bp* LPS and synthetic oligosaccharides³⁵

³⁵ Serum samples from culture confirmed Thai melioidosis patients (n = 42) and Thai healthy donors (n = 42) were assayed for reactivity with *Bp* RR2808 LPS and synthetic oligosaccharides 1-9 using single-dilution ELISAs (1:2,000). Black dots represent the means of assays conducted in duplicate for individual samples. Black bars represent mean reactivity for each target antigen.

4.5 Conclusions

In summary, we have reported the synthesis of two tetrasaccharides mimicking the predominant epitopes of *Bp* and *Bm* LPS OAg. We have shown that these compounds can be efficiently prepared using a sequential [1 + 1 + 1 + 1] glycosylation strategy. Oligosaccharide **9**, which mimics *Bm* LPS OAg, is strongly recognized by *Bm* LPS specific mAbs, highlighting the potential of using this compound as a vaccine candidate against glanders. Additionally, *Bp*- and *Bm*-related tetrasaccharides **8** and **9** exhibit high reactivity towards the serum of culture-confirmed Thai melioidosis patients. Therefore, we have shown that by including both the terminal and the major intra-chain epitopes of *Bp* and *Bm* LPS OAg within the same compounds, their antigenicity is similar to that of native *Bp* OAg. These results suggest that synthetic oligosaccharides **8** and **9** represent exquisite mimics of the whole OAg epitope, which bodes well for their use as functional antigens in glycoconjugate vaccine preparations against melioidosis and glanders.

4.6 Acknowledgments

This work was supported by a Discovery grant from the Natural Sciences and Engineering Research Council of Canada (NSERC) under award number RGPIN-2016-04950 (to C.G.). C.G. holds a Fonds de recherche du Québec – Santé (FRQS) Research Scholars Junior 2 Career Award. M. C. thanks NSERC and Fonds de recherche du Québec – Nature et technologies (FRQNT) for M.Sc. scholarships. R. R. H. thanks NSERC for an undergraduate student research award. We thank David DeShazer for providing mAb 9C1-2.

4.7 Conflicts of interest

A related provisional patent has been filed with the title “Tetrasaccharides for diagnosis, prevention, and treatment of melioidosis and glanders” by C. G., M. C. and the Institut national de la recherche scientifique (USPTO 62/857,346). The remaining authors have no conflicts of interest to declare.

4.8 Experimental section

4.8.1 General methods

All starting materials and reagents were purchased from commercial sources and used as received without further purification. Air and water sensitive reactions were performed in oven-dried glassware under Ar atmosphere. Moisture sensitive reagents were introduced *via* a dry syringe. Anhydrous solvents were either prepared from commercial solvents and dried over heat-gun activated 4 Å molecular sieves or supplied over molecular sieves and used as received. Powdered 4 Å molecular sieves were activated before use by heating with a heat gun for ~5 min under high vacuum. Reactions were monitored by thin-layer chromatography (TLC) with silica gel 60 F₂₅₄ 0.25 mm pre-coated aluminium foil plates. Compounds were visualized by using UV₂₅₄ and/or orcinol (1 mg·mL⁻¹) in 10% aq H₂SO₄ solution with heating. Normal-phase flash column chromatography was performed on silica gel 60 Å (15-40 μm). Reversed-phase flash column chromatography was performed on C₁₈ silica gel (fully capped, 25-40 μm). Size exclusion chromatography was performed on GE Healthcare Sephadex LH-20 resin (70 μm). NMR spectra were recorded at 297 K in the indicated solvent (CDCl₃, py-*d*₅ or D₂O) with a 600 MHz instrument, employing standard softwares given by the manufacturer. ¹H and ¹³C NMR spectra were referenced to tetramethylsilane (TMS, δ_H = δ_C = 0.00 ppm) as internal reference for spectra in CDCl₃ and py-*d*₅, or to internal acetone (δ_H = 2.218 ppm; δ_C = 30.9 ppm) for spectra in D₂O. Assignments were based on ¹H, ¹³C, COSY, HSQC and uncoupled HSQC experiments. Interchangeable assignments are marked with an asterisk (*). Sugar moieties are identified from the reducing end (sugar A) to the non-reducing end (sugar D). High-resolution mass spectra (HRMS) were recorded on an ESI-Q-TOF mass spectrometer. Optical rotations [α]²⁰_D were measured on an Anton Paar polarimeter. The retention factors (*R*_f) were calculated from silica gel 60 F₂₅₄ 0.25 mm pre-coated glass TLC plates. Di- and trisaccharides **1-7** have been synthesized according to our previous work.¹⁶⁸

4.8.2 ELISAs

Reactivity with Bm LPS-specific mAbs.

Reactivity of the *Bm* LPS-specific mAbs (3D11 and 9C1-2) with synthetic oligosaccharides **6-9** and *Bp* LPS antigens was assessed by ELISA essentially as previously described.¹⁶⁸ In brief, maleic anhydride 96-well plates (Pierce) were coated overnight at 4 °C with oligosaccharides **6-9** (5 µg/mL) or purified LPS antigens (10 µg/mL) solubilized in carbonate buffer (pH 9.6). The LPS antigens used in this study were purified from *Bp* strains RR2808 ($\Delta wcbB$; *Bp* LPS) and RR4744 ($\Delta wcbB\Delta oacA$; *Bm*-like LPS) as previously described.⁴⁰⁸ The coated plates were blocked at room temperature for 30 min with StartingBlock T20 (TBS) Blocking Buffer (SB; Pierce), washed with Tris-buffered saline + 0.05% Tween 20 (TBS-T), incubated for 1 h at 37 °C with the mAbs diluted 1/2000 in TBS-T + 10% SB, washed with TBS-T, and then incubated for 1 h at 37 °C with a 1/2000 dilution of goat anti-mouse IgG-horse radish peroxidase (HRP) conjugate (Southern Biotech). Following a final wash with TBS-T, the plates were developed with TMB substrate (KPL) and read at 620 nm. The data were plotted and analyzed using GraphPad Prism 8 (GraphPad Software Inc.).

Reactivity with serum samples from Thai melioidosis patients and Thai healthy donors.

Reactivity of serum samples from culture-confirmed Thai melioidosis patients ($n = 42$) and Thai healthy donors ($n = 42$) with oligosaccharides **1-9** and *Bp* LPS was assessed by ELISA. Plates were coated with the oligosaccharides and LPS as described above and ELISAs were performed essentially as previously described.⁴⁰⁷ In brief, the coated plates were blocked at 37 °C for 2 h with TBS-T + 5% skim milk, washed with TBS-T, incubated for 30 min at 37 °C with human serum samples diluted 1/2000 in TBS-T + 1% bovine serum albumin (BSA), washed with TBS-T, and then incubated for 30 min at 37 °C with a 1/2000 dilution of rabbit anti-human IgG- HRP conjugate (Dako). Following a final wash with TBS-T, the plates were developed with TMB substrate (Invitrogen), after 15 min 1 N aq HCl was added to stop the reaction and plates were read at 450 nm. The study was approved by the Ethics Committee of Faculty of Tropical Medicine,

CHAPITRE 4 – MELIOIDOSIS PATIENT SERUM-REACTIVE SYNTHETIC TETRASACCHARIDES BEARING THE PREDOMINANT EPITOPES OF BURKHOLDERIA PSEUDOMALLEI AND BURKHOLDERIA MALLEI O-ANTIGENS

Mahidol University (approval number MUTM 2014-079-02). Written informed consent was obtained from all subjects.

4.8.3 Experimental procedures for synthesis

***para*-Methylphenyl 2-*O*-*ortho*-(azidomethyl)benzoyl-4,6-*O*-benzylidene-3-*O*-*para*-methoxybenzyl-1-thio- β -D-glucopyranoside (**18**).**

Bu₂SnO (1902 mg, 7.640 mmol, 1.1 equiv) was added to a solution of diol **17**³⁸² (2411 mg, 6.946 mmol, 1.0 equiv) in toluene (83 mL). The mixture was refluxed with a Dean-Stark trap for 3 h, after which the solvents were evaporated under reduced pressure. The residue was solubilized in anhydrous DMF (83 mL) and CsF (1076 mg, 7.085 mmol, 1.02 equiv), TBAI (2617 mg, 7.085 mmol, 1.02 equiv), and PMBCl (1.13 mL, 8.34 mmol, 1.2 equiv) were successively added. The mixture was stirred at 90 °C for 16 h and the resulting suspension was cooled at 0 °C and filtered over Celite. The solution was co-evaporated with toluene and the residue was purified by silica gel flash chromatography (Hex/EtOAc 9:1 to 3:7) to give *para*-methylphenyl 4,6-*O*-benzylidene-3-*O*-*para*-methoxybenzyl-1-thio- β -D-glucopyranoside³⁸³ (1738 mg, 51%, 82% brsm) as a white amorphous solid. DMAP (144 mg, 1.18 mmol, 1.0 equiv), DCC (486 mg, 2.36 mmol, 2.0 equiv), and AZMBOH (313 mg, 1.77 mmol, 1.5 equiv) were successively added to a solution of the previously prepared alcohol (582 mg, 1.18 mmol, 1.0 equiv) in anhydrous DCM (12 mL). The mixture was refluxed for 4 h under Ar and the resulting suspension was filtered over Celite. The solvent was evaporated under reduced pressure and the residue was purified by silica gel flash chromatography (Hex/EtOAc 9:1 to 2:8), furnishing glucoside **18** (751 mg, 98%) as a white amorphous solid: *R*_f 0.6 (Hex/EtOAc 7:3); [α]_D²⁰ +36 (*c* 0.7, CHCl₃); ¹H NMR (600 MHz, CDCl₃) δ (ppm) 7.87–7.86 (m, 1H, CH_{AZMB}), 7.61–7.59 (m, 1H, CH_{Ar}), 7.56–7.55 (m, 1H, CH_{Ar}), 7.50–7.49 (m, 2H, 2 \times CH_{Ar}), 7.41–7.37 (m, 4H, 4 \times CH_{Ar}), 7.35–7.33 (m, 2H, 2 \times CH_{STol}), 7.10–7.09 (m, 2H, 2 \times CH_{STol}), 7.05–7.03 (m, 2H, 2 \times CH_{PMB}), 6.60–6.59 (m, 2H, 2 \times CH_{PMB}), 5.60 (s, 1H, H-7), 5.20 (dd, *J* = 9.9 Hz, *J* = 9.0 Hz, 1H, H-2), 4.81–4.72 (m, 4H, H-1, CH_{2AZMB}, CHH_{PMB}), 4.57 (d, *J* = 11.6 Hz, 1H, CHH_{PMB}), 4.41 (dd, *J*_{6a-6b} = 10.5 Hz, *J*_{6a-5} = 5.0 Hz, 1H, H-6a), 3.87–3.82 (m, 2H, H-3 and H-6b), 3.77 (t, *J* = 9.3 Hz, 1H, H-4), 3.69 (s, 3H, CH_{3PMB}), 3.55 (td, *J*₅₋₄ = 9.8 Hz, *J*₅₋

CHAPITRE 4 – MELIOIDOSIS PATIENT SERUM-REACTIVE SYNTHETIC TETRASACCHARIDES BEARING THE PREDOMINANT EPITOPES OF BURKHOLDERIA PSEUDOMALLEI AND BURKHOLDERIA MALLEI O-ANTIGENS

δ_{6a} = 5.0 Hz, 1H, H-5), 2.33 (s, 3H, CH_{3STol}); ^{13}C NMR (150 MHz, $CDCl_3$) δ (ppm) 165.0 ($COOR_{AZMB}$), 159.3 (C_{Ar}), 138.8 (C_{Ar}), 137.8 (C_{Ar}), 137.3 (C_{Ar}), 133.8 (2C, $2 \times CH_{STol}$), 133.0 (CH_{Ar}), 131.2 (CH_{AZMB}), 130.0 (C_{Ar}), 129.9, 129.8 (4C, $2 \times CH_{STol}$, $2 \times CH_{PMB}$), 129.5 (CH_{Ar}), 129.2 (C_{Ar}), 128.6 (CH_{Ar}), 128.4 (3C, $3 \times CH_{Ar}$), 128.0 (C_{Ar}), 126.1 (2C, $2 \times CH_{Ar}$), 113.7 (2C, $2 \times CH_{PMB}$), 101.4 (C-7), 87.1 (C-1), 81.7 (C-4), 79.2 (C-3), 74.1 (CH_{2PMB}), 72.1 (C-2), 70.7 (C-5), 68.7 (C-6), 55.2 (CH_{3PMB}), 53.0 (CH_{2AZMB}), 21.3 (CH_{3STol}); HRMS (ESI-TOF) m/z $[M + Na]^+$ calcd for $C_{36}H_{35}N_3NaO_7S$ 676.2088; found 676.2067.

***para*-Methylphenyl 2-*O*-*ortho*-(azidomethyl)benzoyl-4,6-*O*-benzylidene-1-thio- β -D-glucopyranoside (15).**

DDQ (378 mg, 1.66 mmol, 2.0 equiv) was added to a solution of glucoside **18** (544 mg, 0.832 mmol, 1.0 equiv) in DCM (18 mL) and H_2O (1.7 mL) and the mixture was stirred at rt for 2 h. Saturated $NaHCO_3(aq)$ (20 mL) was added to quench the solution, which was then diluted in EtOAc (30 mL) and transferred into a separatory funnel. The organic layer was washed with saturated $NaHCO_3(aq)$ (30 mL) and brine (30 mL), dried over anhydrous $MgSO_4$, and evaporated under reduced pressure. The residue was purified by silica gel flash chromatography (Hex/EtOAc 90:10 to 85:15) to give alcohol **15** (343 mg, 77%) as a white amorphous solid: R_f 0.5 (Hex/EtOAc 7:3); $[\alpha]_D^{20}$ -26 (c 0.7, $CHCl_3$); 1H NMR (600 MHz, $CDCl_3$) δ (ppm) 8.05–8.04 (m, 1H, CH_{AZMB}), 7.60–7.58 (m, 1H, CH_{Ar}), 7.52–7.51 (m, 1H, CH_{Ar}), 7.49–7.47 (m, 2H, $2 \times CH_{Ar}$), 7.46–7.43 (m, 1H, CH_{Ar}), 7.37–7.36 (m, 5H, $2 \times CH_{STol}$, $3 \times CH_{Ar}$), 7.12–7.11 (m, 2H, $2 \times CH_{STol}$), 5.56 (s, 1H, H-7), 5.15 (dd, $J_{2-1} = 9.9$ Hz, $J_{2-3} = 8.9$ Hz, 1H, H-2), 4.85–4.76 (m, 3H, H-1, CH_{2AZMB}), 4.41 (dd, $J_{6a-6b} = 10.5$ Hz, $J_{6a-5} = 4.9$ Hz, 1H, H-6a), 4.05 (t, $J = 9.0$ Hz, 1H, H-3), 3.82 (t, $J = 10.2$ Hz, 1H, H-6b), 3.61 (t, $J = 9.3$ Hz, 1H, H-4), 3.55 (ddd, $J_{5-6b} = 9.7$ Hz, $J_{5-4} = 9.2$ Hz, $J_{5-6a} = 4.9$ Hz, 1H, H-5), 2.35 (s, 3H, CH_{3STol}); ^{13}C NMR (150 MHz, $CDCl_3$) : δ (ppm) 166.0 ($COOR_{AZMB}$), 138.9 (C_{Ar}), 137.3 (C_{Ar}), 136.9 (C_{Ar}), 133.7 (2C, $2 \times CH_{STol}$), 133.1 (CH_{Ar}), 131.3 (CH_{AZMB}), 130.0–126.4 (11C, $2 \times C_{Ar}$, $9 \times CH_{Ar}$), 102.1 (C-7), 86.7 (C-1), 80.6 (C-4), 73.7 (C-3), 73.4 (C-2), 70.6 (C-5), 68.6 (C-6), 53.3 (CH_{2AZMB}), 21.3 (CH_{3STol}); HRMS (ESI-TOF) m/z $[M + Na]^+$ calcd for

CHAPITRE 4 – MELIOIDOSIS PATIENT SERUM-REACTIVE SYNTHETIC TETRASACCHARIDES BEARING THE PREDOMINANT EPITOPES OF BURKHOLDERIA PSEUDOMALLEI AND BURKHOLDERIA MALLEI O-ANTIGENS

C₂₈H₂₇N₃NaO₆S 556.15128; found 556.15109; *m/z* [M+NH₄]⁺ calcd for C₂₈H₃₁N₄O₆S 551.19588; found 551.19581.

Allyl 2-*O*-acetyl-3-*O*-*tert*-butyldimethylsilyl-4-*O*-levulinoyl- α -L-rhamnopyranoside (20).

TBSCl (1989 mg, 13.23 mmol, 4.0 equiv), imidazole (674 mg, 9.92 mmol, 3.0 equiv), and DMAP (81 mg, 0.7 mmol, 0.2 equiv) were successively added to a solution of diol **19**¹⁶⁸ (1000 mg, 3.307 mmol, 1.0 equiv) in anhydrous THF (80 mL). The mixture was refluxed for 16 h under Ar. The suspension was filtered over Celite, rinsed, and evaporated under reduced pressure. The residue was purified by silica gel flash chromatography (Hex/EtOAc) to give allyl 3-*O*-*tert*-butyldimethylsilyl-4-*O*-levulinoyl- α -L-rhamnopyranoside (1375 mg, quantitative) as a yellow oil: *R_f* 0.4 (Hex/EtOAc 7:3); [α]_D²⁰ -40 (*c* 1.1, CHCl₃); ¹H NMR (700 MHz, CDCl₃) δ (ppm) 5.91 (dddd, *J*_{2-3a} = 17.2 Hz, *J*_{2-3b} = 10.4 Hz, *J*_{2-1a} = 6.1 Hz, *J*_{2-1b} = 5.1 Hz, 1H, H-2_{Allyl}), 5.29 (ddt, *J* = 17.2 Hz, 5.4 Hz, 1.6 Hz, 1H, H-3a_{Allyl}), 5.21 (ddt, *J* = 10.4 Hz, 4.8 Hz, 1.3 Hz, 1H, H-3b_{Allyl}), 4.97 (t, *J* = 9.6 Hz, 1H, H-4), 4.87 (d, *J* = 1.4 Hz, 1H, H-1), 4.17 (ddt, *J* = 13.1 Hz, 5.1 Hz, 1.5 Hz, 1H, H-1a_{Allyl}), 4.04–3.98 (m, 2H, H-3, H-1b_{Allyl}), 3.83 (dd, *J*₂₋₃ = 3.6 Hz, *J*₂₋₁ = 1.5 Hz, 1H, H-2), 3.76 (dq, *J*₅₋₄ = 9.8 Hz, *J*₅₋₆ = 6.3 Hz, 1H, H-5), 2.89–2.81 (m, 1H, CHH_{Lev}), 2.74–2.67 (m, 1H, CHH_{Lev}), 2.64 (m, 1H, CHH_{Lev}), 2.54–2.47 (m, 1H, CHH_{Lev}), 2.20 (s, 3H, CH_{3Lev}), 1.19 (d, *J* = 6.3 Hz, 3H, H-6), 0.88 (s, 9H, C(CH₃)₃TBS), 0.11 (s, 3H, CH₃TBS), 0.08 (s, 3H, CH₃TBS); ¹³C NMR (176 MHz, CDCl₃) δ (ppm) 206.5 (CO_{Lev}), 172.1 (COOR_{Lev}), 133.9 (C-2_{Allyl}), 117.6 (C-3_{Allyl}), 98.0 (C-1), 74.3 (C-4), 71.8 (C-2), 70.6 (C-3), 68.2 (C-1_{Allyl}), 66.3 (C-5), 38.0 (CH_{2Lev}), 30.0 (CH_{3Lev}), 28.2 (CH_{2Lev}), 25.7 (3C, C(CH₃)₃TBS), 18.0 (C(CH₃)₃TBS), 17.5 (C-6), -4.5 (CH₃TBS), -4.7 (CH₃TBS); HRMS (ESI-TOF) *m/z* [M + Na]⁺ calcd for C₂₀H₃₆NaO₇Si 439.21225; found 439.21102. The latter alcohol (1000 mg, 2.400 mmol, 1.0 equiv) was dissolved in anhydrous pyridine (40 mL), and Ac₂O (40 mL) and DMAP (59 mg, 0.48 mmol, 0.2 equiv) were added. The mixture was stirred at rt for 16 h under Ar. The solution was diluted in toluene and evaporated under reduced pressure. The residue was purified by silica gel flash chromatography (Hex/EtOAc) to give glycoside **20** (1013 mg, 92%) as a colorless oil: *R_f* 0.6 (Hex/EtOAc 7:3); [α]_D²⁰ -23 (*c* 1.0, CHCl₃); ¹H NMR (600 MHz, CDCl₃) δ (ppm) 5.90 (dddd, *J*_{2-3a} = 16.6 Hz, *J*_{2-3b} = 10.5 Hz, *J*_{2-1a} = 6.0 Hz, *J*_{2-1b} = 5.3 Hz, 1H, H-2_{Allyl}), 5.29 (ddt, *J* = 17.1 Hz, 3.6 Hz, 1.5 Hz, 1H, H-3a_{Allyl}), 5.22 (ddt, *J* = 10.4 Hz, 3.2 Hz,

CHAPITRE 4 – MELIOIDOSIS PATIENT SERUM-REACTIVE SYNTHETIC TETRASACCHARIDES BEARING THE PREDOMINANT EPITOPES OF BURKHOLDERIA PSEUDOMALLEI AND BURKHOLDERIA MALLEI O-ANTIGENS

1.3 Hz, 1H, H-3b_{Allyl}), 5.10 (dd, $J_{2-3} = 3.6$ Hz, $J_{2-1} = 1.8$ Hz, 1H, H-2), 4.98 (t, $J = 9.7$ Hz, 1H, H-4), 4.73 (d, $J = 1.6$ Hz, 1H, H-1), 4.16 (ddt, $J = 13.0$ Hz, 5.2 Hz, 1.4 Hz, 1H, H-1a_{Allyl}), 4.08 (dd, $J_{3-4} = 9.5$ Hz, $J_{3-2} = 3.6$ Hz, 1H, H-3), 3.99 (ddt, $J = 13.0$ Hz, 6.1 Hz, 1.3 Hz, 1H, H-1b_{Allyl}), 3.78 (dq, $J_{5-4} = 9.9$ Hz, $J_{5-6} = 6.4$ Hz, 1H, H-5), 2.88–2.82 (m, 1H, CHH_{Lev}), 2.70–2.62 (m, 2H, CHH_{Lev}, CHH_{Lev}), 2.52–2.47 (m, 1H, CHH_{Lev}), 2.20 (s, 3H, CH_{3Lev}), 2.11 (s, 3H, CH_{3Ac}), 1.20 (d, $J = 6.3$ Hz, 3H, H-6), 0.82 (s, 9H, C(CH₃)_{3TBS}), 0.07 (s, 3H, CH_{3TBS}), 0.05 (s, 3H, CH_{3TBS}); ¹³C NMR (150 MHz, CDCl₃) δ (ppm) 206.5 (CO_{Lev}), 172.0 (COOR_{Lev}), 170.5 (COOR_{Ac}), 133.7 (C-2_{Allyl}), 117.8 (C-3_{Allyl}), 96.9 (C-1), 74.5 (C-4), 72.3 (C-2), 68.4, 68.3 (2C, C-1_{Allyl}, C-3), 66.7 (C-5), 38.0 (CH_{2Lev}), 30.0 (CH_{3Lev}), 28.2 (CH_{2Lev}), 25.6 (3C, C(CH₃)_{3TBS}), 21.1 (CH_{3Ac}), 17.9, 17.6 (2C, C-6, C(CH₃)_{3TBS}), -4.7 (CH_{3TBS}), -4.9 (CH_{3TBS}); HRMS (ESI-TOF) m/z [M + NH₄]⁺ calcd for C₂₂H₄₂NO₈Si 476.26742; found 476.26647; m/z [M + Na]⁺ calcd for C₂₂H₃₈NaO₈Si 481.22282; found 481.22179.

2-O-Acetyl-3-O-tert-butyldimethylsilyl-4-O-levulinoyl-L-rhamnopyranose (21).

1,5-Cyclooctadiene-bis(methyldiphenylphosphine)-iridium(I) hexafluorophosphate (132 mg, 0.156 mmol, 0.05 equiv) was dissolved in anhydrous THF (15 mL) and the red solution was degassed under Ar. Hydrogen was bubbled through the solution for 5 min and the resulting yellow solution was once again degassed under argon. A solution of rhamnoside **20** (1435 mg, 3.129 mmol, 1.0 equiv) in anhydrous THF (15 mL) was added and the reaction mixture was stirred for 2 h at rt under Ar. Then, a solution of iodine (1588 mg, 6.258 mmol, 2.0 equiv) in THF/H₂O (4:1, 18 mL) was added to the mixture, which was stirred for 1 h at rt. The excess of iodine was quenched by adding a freshly prepared 10% Na₂S₂O₃(aq) solution and stirred until the color turned bright yellow. THF was evaporated under reduced pressure and the resulting aqueous phase was extracted using EtOAc (3 × 25 mL). The combined organic layers were washed with saturated NaHCO₃(aq) (50 mL) and brine (50 mL). The organic phase was dried over anhydrous MgSO₄ and evaporated under reduced pressure. The residue was purified by silica gel flash chromatography (Hex/EtOAc) to give hemiacetal **21** (1100 mg, 84%, ratio $\alpha/\beta \sim 85:15$) as a brown oil: R_f 0.6 (Tol/EtOAc 1:1); $[\alpha]_D^{20} -14$ (c 1.1, CHCl₃); ¹H NMR (600 MHz, CDCl₃, α -anomer) δ (ppm) 5.11 (m, 2H, H-1, H-2), 4.98 (t, $J = 9.6$ Hz, 1H, H-4), 4.14 (dd, $J_{3-4} = 9.4$ Hz, $J_{3-2} = 3.0$ Hz, 1H, H-3), 4.01 (dq, $J_{5-4} =$

CHAPITRE 4 – MELIOIDOSIS PATIENT SERUM-REACTIVE SYNTHETIC TETRASACCHARIDES BEARING THE PREDOMINANT EPITOPES OF BURKHOLDERIA PSEUDOMALLEI AND BURKHOLDERIA MALLEI O-ANTIGENS

9.7 Hz, $J_{5-6} = 6.3$ Hz, 1H, H-5), 3.14 (br s, 1H, OH), 2.88–2.82 (m, 1H, CHH_{Lev}), 2.69–2.64 (m, 2H, CHH_{Lev} , CHH_{Lev}), 2.54–2.49 (m, 1H, CHH_{Lev}), 2.20 (s, 3H, CH_{3Lev}), 2.12 (s, 3H, CH_{3Ac}), 1.20 (d, $J = 6.3$ Hz, 3H, H-6), 0.83 (s, 9H, $(C(CH_3)_3TBS)$), 0.08 (s, 3H, CH_{3TBS}), 0.06 (s, 3H, CH_{3TBS}); ^{13}C NMR (150 MHz, $CDCl_3$) δ (ppm) 206.6 (CO_{Lev}), 172.1 ($COOR_{Lev}$), 170.7 ($COOR_{Ac}$), 92.4 (C-1), 74.5 (C-4), 72.6 (C-2), 67.9 (C-3), 66.9 (C-5), 38.0 (CH_{2Lev}), 30.0 (CH_{3Lev}), 28.2 (CH_{2Lev}), 25.6 (3C, $C(CH_3)_3TBS$), 21.1 (CH_{3Ac}), 17.9, 17.7 (2C, C-6, $C(CH_3)_3TBS$), –4.7 (CH_{3TBS}), –4.9 (CH_{3TBS}); HRMS (ESI-TOF) m/z $[M + NH_4]^+$ calcd for $C_{19}H_{38}NO_8Si$ 436.23612; found 436.2351; m/z $[M + Na]^+$ calcd for $C_{19}H_{34}NaO_8Si$ 441.19152; found 441.19063.

2-O-Acetyl-3-O-tert-butyldimethylsilyl-4-O-levulinoyl- α -L-rhamnopyranosyl 2,2,2-trichloroacetimidate (13).

To a cooled (0 °C) solution of hemiacetal **21** (383 mg, 0.915 mmol, 1.0 equiv) in acetone (2.3 mL) and DCM (11.5 mL) were added Cs_2CO_3 (59 mg, 0.18 mmol, 0.2 equiv) and CCl_3CN (0.46 mL, 4.6 mmol, 5.0 equiv). The mixture was stirred for 1 h at rt, then the suspension was filtered over Celite and rinsed with DCM. The solvents were evaporated under reduced pressure. The residue was purified by silica gel flash chromatography (Tol/EtOAc + 1% Et_3N 95:5 to 9:1) to give trichloroacetimidate **13** (504 mg, 98%, $\alpha/\beta \sim 9:1$) as a yellow oil: R_f 0.3 (Tol/EtOAc 9:1 + 1% Et_3N); R_f 0.5 (Tol/AcOEt 8:2 + 1% Et_3N); 1H NMR (600 MHz, $py-d_5$, α -anomer) δ (ppm) 6.71 (br s, 1H, H-1), 5.75 (br s, 1H, H-2), 5.58 (t, $J = 9.7$ Hz, 1H, H-4), 4.60 (dd, $J_{3-4} = 9.6$ Hz, $J_{3-2} = 3.5$ Hz, 1H, H-3), 4.40 (dq, $J_{5-4} = 12.2$ Hz, $J_{5-6} = 6.0$ Hz, 1H, H-5), 2.96–2.73 (m, 4H, $2 \times CH_{2Lev}$), 2.08 (s, 3H, CH_{3Lev}), 2.03 (s, 3H, CH_{3Ac}), 1.48 (d, $J = 6.2$ Hz, 3H, H-6), 0.96 (s, 9H, $C(CH_3)_3TBS$), 0.26 (s, 3H, CH_{3TBS}), 0.24 (s, 3H, CH_{3TBS}); ^{13}C NMR (150 MHz, $py-d_5$) δ (ppm) 206.7 (CO_{Lev}), 172.9 ($COOR_{Lev}$), 170.4 ($COOR_{Ac}$), 159.3 (OCN), 95.8 (C-1), 91.8 (CCl_3), 74.3 (C-4), 71.5 (C-2), 70.7 (C-5), 69.5 (C-3), 38.4 (CH_{2Lev}), 30.0 (CH_{3Lev}), 29.1 (CH_{2Lev}), 26.2 (3C, $C(CH_3)_3TBS$), 21.0 (CH_{3Ac}), 18.6, 18.4 (C-6, $C(CH_3)_3TBS$), –4.3 (CH_{3TBS}), –4.4 (CH_{3TBS}); HRMS (ESI-TOF) m/z $[M + Na]^+$ calcd for $C_{21}H_{34}NaO_8Si$ 584.10115; found 584.10006.

CHAPITRE 4 – MELIOIDOSIS PATIENT SERUM-REACTIVE SYNTHETIC TETRASACCHARIDES BEARING THE PREDOMINANT EPITOPES OF BURKHOLDERIA PSEUDOMALLEI AND BURKHOLDERIA MALLEI O-ANTIGENS

(5-Azido-1-pentyl) 2-O-acetyl-3-O-tert-butyltrimethylsilyl-4-O-levulinoyl- α -L-rhamnopyranosyl-(1 \rightarrow 3)-2-O-benzyl-4,6-O-benzylidene- β -D-glucopyranoside (22).

To solution of trichloroacetimidate **13** (449 mg, 0.798 mmol, 1.5 equiv) in anhydrous Et₂O (7 mL) cooled at -10 °C were successively added glucoside **16** (250 mg, 0.532 mmol, 1.0 equiv) and TMSOTf (1.9 μ L, 11 μ mol, 0.02 equiv). The mixture was stirred under Ar at -10 °C for 15 min after which the solution was quenched with Et₃N (0.07 mL, 0.5 mmol, 1.0 equiv). The solvents were evaporated under reduced pressure and co-evaporated with toluene. The residue was purified by silica gel flash chromatography (Tol/EtOAc 95:5 to 80:20) to give disaccharide **22** (421 mg, 91%) as a white amorphous solid: *R*_f 0.7 (Tol/EtOAc 7:3); [α]_D²⁰ -51 (*c* 0.6, CHCl₃); ¹H NMR (600 MHz, CDCl₃) δ (ppm) 7.48–7.46 (m, 2H, 2 \times CH_{Ar}), 7.38–7.34 (m, 3H, 3 \times CH_{Ar}), 7.32–7.30 (m, 4H, 4 \times CH_{Ar}), 7.28–7.27 (m, 1H, CH_{Ar}), 5.56 (s, 1H, H-7A), 5.20 (dd, *J*₂₋₃ = 3.6 Hz, *J*₂₋₁ = 1.6 Hz, 1H, H-2B), 5.13 (d, *J* = 1.3 Hz, 1H, H-1B), 4.87–4.84 (m, 2H, CHH_{Bn}, H-4B), 4.72 (d, *J* = 10.8 Hz, 1H, CHH_{Bn}), 4.49 (d, *J* = 7.8 Hz, 1H, H-1A), 4.36 (dd, *J*_{6a-6b} = 10.5 Hz, *J*_{6a-5} = 5.0 Hz, 1H, H_{6a}A), 4.04 (dq, *J*₅₋₄ = 9.7 Hz, *J*₅₋₆ = 6.2 Hz, 1H, H-5B), 3.99 (dd, *J*₃₋₄ = 9.5 Hz, *J*₃₋₂ = 3.6 Hz, 1H, H-3B), 3.94–3.89 (m, 2H, H-1_{linker}, H-3A), 3.78 (t, *J* = 10.3 Hz, 1H, H-6bA), 3.59–3.54 (m, 2H, H-1_{linker}, H-4A), 3.46 (dd, *J* = 8.7 Hz, *J* = 7.9 Hz, 1H, H-2A), 3.42 (dt, *J* = 9.8 Hz, *J* = 5.0 Hz, 1H, H-5A), 3.22 (t, *J* = 6.9 Hz, 2H, H-5_{linker}), 2.78–2.73 (m, 1H, CHH_{Lev}), 2.64–2.59 (m, 1H, CHH_{Lev}), 2.54–2.49 (m, 1H, CHH_{Lev}), 2.47–2.42 (m, 1H, CHH_{Lev}), 2.18 (s, 3H, CH₃Lev), 2.04 (s, 3H, CH₃Ac), 1.69–1.63 (m, 2H, H-2_{linker}), 1.62–1.59 (m, 2H, H-4_{linker}), 1.50–1.41 (m, 2H, H-3_{linker}), 0.81 (s, 9H, C(CH₃)₃TBS), 0.78 (d, *J* = 6.3 Hz, 3H, H-6B), 0.08 (s, 3H, CH₃TBS), 0.04 (s, 3H, CH₃TBS); ¹³C NMR (150 MHz, CDCl₃) δ (ppm) 206.3 (CO_{Lev}), 171.9 (COOR_{Lev}), 170.1 (COOR_{Ac}), 138.0 (C_{Ar}), 137.3 (C_{Ar}), 129.3–126.3 (10C, 10 \times CH_{Ar}), 104.3 (C-1A), 101.8 (C-7A), 98.2 (C-1B), 82.6 (C-2A), 79.3 (C-4A), 76.2 (C-3A), 74.9 (CH₂Bn), 74.5 (C-4B), 72.0 (C-2B), 70.2 (C-1_{linker}), 69.0 (C-6A), 68.3 (C-3B), 66.43, 66.37 (2C, C-5A, C-5B), 51.4 (C-5_{linker}), 37.9 (CH₂Lev), 30.1 (CH₃Lev), 29.5 (C-2_{linker}), 28.8 (C-4_{linker}), 28.2 (CH₂Lev), 25.6 (3C, C(CH₃)₃TBS), 23.5 (C-3_{linker}), 21.0 (CH₃Ac), 17.9 (C(CH₃)₃TBS), 17.0 (C-6B), -4.6 (CH₃TBS), -4.9 (CH₃TBS); HRMS (ESI-TOF) *m/z* [M + NH₄]⁺ calcd for C₄₄H₆₇N₄O₁₃Si 887.44684; found 887.44683; *m/z* [M + Na]⁺ calcd for C₄₄H₆₃NaO₁₃Si 892.4022; found 892.4035.

CHAPITRE 4 – MELIOIDOSIS PATIENT SERUM-REACTIVE SYNTHETIC TETRASACCHARIDES BEARING THE PREDOMINANT EPITOPES OF BURKHOLDERIA PSEUDOMALLEI AND BURKHOLDERIA MALLEI O-ANTIGENS

***para*-Methylphenyl 4-*O*-levulinoyl-1-thio- α -L-rhamnopyranoside (24).**

Levulinic acid (1.0 mL, 9.5 mmol, 1.15 equiv), DCC (1952 mg, 9.462 mmol, 1.15 equiv), and DMAP (101 mg, 0.823 mmol, 0.1 equiv) were added in a solution of alcohol **23**³⁹³ (2554 mg, 8.228 mmol, 1 equiv) in anhydrous DCM (100 mL). The mixture was stirred under Ar at 50 °C for 2 h. The suspension was cooled to 0 °C, filtered over Celite, and rinsed with cold DCM. The solvents were evaporated under reduced pressure and co-evaporated with toluene. The residue was purified by silica gel flash chromatography (Tol/EtOAc 8:2) to give *para*-methylphenyl 4-*O*-levulinoyl-2,3-*O*-isopropylidene-1-thio- α -L-rhamnopyranoside (3254 mg, 97%) as a white amorphous solid: R_f 0.5 (Tol/EtOAc 7:3); $[\alpha]_D^{20}$ -158 (c 0.6, CHCl₃); ¹H NMR (600 MHz, CDCl₃) δ (ppm) 7.37–7.35 (m, 2H, 2 \times CH_{STol}), 7.14–7.12 (m, 2H, 2 \times CH_{STol}), 5.68 (s, 1H, H-1), 4.92 (dd, J = 9.9 Hz, J = 7.9 Hz, 1H, H-4), 4.35 (d, J = 5.3 Hz, 1H, H-2), 4.24–4.18 (m, 2H, H-3, H-5), 2.90–2.85 (m, 1H, CHH_{Lev}), 2.72–2.69 (m, 1H, CHH_{Lev}), 2.68–2.66 (m, 1H, CHH_{Lev}), 2.61–2.56 (m, 1H, CHH_{Lev}), 2.33 (s, 3H, CH_{3STol}), 2.19 (s, 3H, CH_{3Lev}), 1.55 (s, 3H, CH_{3iso}), 1.35 (s, 3H, CH_{3iso}), 1.15 (d, J = 6.3 Hz, 3H, H-6); ¹³C NMR (150 MHz, CDCl₃) δ (ppm) 206.5 (CO_{Lev}), 172.1 (COOR_{Lev}), 138.2 (C_{STol}), 132.7 (2C, 2 \times CH_{STol}), 130.0 (2C, 2 \times CH_{STol}), 129.4 (C_{STol}), 110.1 (C_{iso}), 84.1 (C-1), 76.6 (C-2), 75.6 (C-3), 75.1 (C-4), 65.6 (C-5), 38.0 (CH_{2Lev}), 29.9 (CH_{3Lev}), 28.1 (CH_{2Lev}), 27.8 (CH_{3iso}), 26.7 (CH_{3iso}), 21.3 (CH_{3STol}), 16.9 (C-6); HRMS (ESI-TOF) m/z [M + NH₄]⁺ calcd for C₂₁H₃₂NO₆S 426.1945; found 426.1957; m/z [M + Na]⁺ calcd for C₂₁H₂₈NaO₆S 431.1499; found 431.1512. The latter thiorhamnoside (3239 mg, 7.930 mmol, 1.0 equiv) was dissolved in 80% AcOH(aq) (99 mL) and the solution was stirred at 60 °C for 2 h. The solvents were evaporated under reduced pressure and co-evaporated with toluene. The residue was purified by silica gel flash chromatography (Hex/EtOAc 1:1 to 2:8) to give diol **24** (2615 mg, 90%) as a white amorphous solid: R_f 0.5 (DCM/MeOH 95:5); $[\alpha]_D^{20}$ -230 (c 0.7, CHCl₃); ¹H NMR (600 MHz, CDCl₃) δ (ppm) 7.36–7.34 (m, 2H, 2 \times CH_{STol}), 7.13–7.11 (m, 2H, 2 \times CH_{STol}), 5.46 (d, J = 0.6 Hz, 1H, H-1), 4.95 (t, J = 9.6 Hz, 1H, H-4), 4.29 (dq, J_{5-4} = 9.8 Hz, J_{5-6} = 6.2 Hz, 1H, H-5), 4.22 (br s, 1H, H-2), 3.95–3.94 (m, 1H, H-3), 3.48 (d, J = 4.4 Hz, 1H, OH_{C-3}), 3.06 (br s, 1H, OH_{C-2}), 2.88–2.79 (m, 2H, CH_{2Lev}), 2.65–2.56 (m, 2H, CH_{2Lev}), 2.33 (s, 3H, CH_{3STol}), 2.20 (s, 3H, CH_{3Lev}), 1.22 (d, J = 6.3 Hz, 3H, H-6); ¹³C NMR (150 MHz, CDCl₃) δ (ppm) 207.7 (CO_{Lev}), 173.6

CHAPITRE 4 – MELIOIDOSIS PATIENT SERUM-REACTIVE SYNTHETIC TETRASACCHARIDES BEARING THE PREDOMINANT EPITOPES OF BURKHOLDERIA PSEUDOMALLEI AND BURKHOLDERIA MALLEI O-ANTIGENS

(COOR_{Lev}), 137.9 (C_{STol}), 132.1 (2C, 2 × CH_{STol}), 130.2 (C_{STol}), 130.0 (2C, 2 × CH_{STol}), 87.8 (C-1), 75.8 (C-4), 72.4 (C-2), 70.7 (C-3), 67.0 (C-5), 38.5 (CH_{2Lev}), 29.9 (CH_{3Lev}), 28.4 (CH_{2Lev}), 21.3 (CH_{3STol}), 17.4 (C-6); HRMS (ESI-TOF) m/z [M + NH₄]⁺ calcd for C₁₈H₂₈NO₆S 386.1632; found 386.1641; m/z [M + Na]⁺ calcd for C₁₈H₂₄NaO₆S 391.1186; found 391.1197.

***para*-Methylphenyl 2-*O*-acetyl-4-*O*-levulinoyl-3-*O*-*para*-methoxybenzyl-1-thio- α -L-rhamnopyranoside (25).**

Bu₂SnO (1536 mg, 6.170 mmol, 1.1 equiv) was added to a solution of compound **24** (2067 mg, 5.609 mmol, 1.0 equiv) in toluene (67 mL) and the mixture was refluxed with a Dean-Stark trap for 2 h. The solution was cooled to rt and CsF (895 mg, 5.89 mmol, 1.05 equiv), TBAI (2175 mg, 5.889 mmol, 1.05 equiv), and PMBCl (0.91 mL, 5.9 mmol, 1.2 equiv) were successively added. The mixture was stirred under Ar at 40 °C for 16 h. The suspension was cooled at 0 °C, filtered over Celite, and rinsed with DCM. The solvents were evaporated under reduced pressure. The residue was purified by silica gel flash chromatography (Hex/EtOAc 9:1 to 7:3) to give *para*-methylphenyl 4-*O*-levulinoyl-3-*O*-*para*-methoxybenzyl-1-thio- α -L-rhamnopyranoside (2412 mg, 88%) as a yellow oil: R_f 0.6 (Hex/EtOAc 4:6); $[\alpha]_D^{20}$ -140 (c 1.2, CHCl₃); ¹H NMR (600 MHz, CDCl₃) δ (ppm) 7.33–7.32 (m, 2H, 2 × CH_{STol}), 7.27–7.26 (m, 2H, 2 × CH_{PMB}), 7.12–7.10 (m, 2H, 2 × CH_{STol}), 6.91–6.89 (m, 2H, 2 × CH_{PMB}), 5.46 (d, J = 1.2 Hz, 1H, H-1), 5.08 (t, J = 9.6 Hz, 1H, H-4), 4.59 (d, J = 11.7 Hz, 1H, CHH_{PMB}), 4.53 (d, J = 11.8 Hz, 1H, CHH_{PMB}), 4.22 (dq, J_{5-4} = 9.9 Hz, J_{5-6} = 6.2 Hz, 1H, H-5), 4.18 (dd, J_{2-3} = 3.0 Hz, J_{2-1} = 1.5 Hz, 1H, H-2), 3.81 (s, 3H, CH_{3PMB}), 3.75 (dd, J_{3-4} = 9.4 Hz, J_{3-2} = 3.3 Hz, 1H, H-3), 2.77–2.72 (m, 2H, CH_{2Lev}), 2.59–2.49 (m, 2H, CH_{2Lev}), 2.32 (s, 3H, CH_{3STol}), 2.19 (s, 3H, CH_{3Lev}), 1.18 (d, J = 6.3 Hz, 3H, H-6); ¹³C NMR (150 MHz, CDCl₃) δ (ppm) 206.5 (CO_{Lev}), 172.1 (COOR_{Lev}), 159.6 (C_{Ar}), 137.8 (C_{Ar}), 132.1 (2C, 2 × CH_{STol}), 130.0, 129.7 (5C, C_{Ar}, 2 × CH_{STol}, 2 × CH_{PMB}), 129.6 (C_{Ar}), 114.1 (2C, 2 × CH_{PMB}), 87.3 (C-1), 76.7 (C-3), 73.0 (C-4), 71.7 (CH_{2PMB}), 69.9 (C-2), 67.6 (C-5), 55.4 (CH_{3PMB}), 37.9 (CH_{2Lev}), 30.0 (CH_{3Lev}), 28.1 (CH_{2Lev}), 21.2 (CH_{3STol}), 17.4 (C-6); HRMS (ESI-TOF) m/z [M + NH₄]⁺ calcd for C₂₆H₃₆NO₇S 506.2207; found 506.22041; m/z [M + Na]⁺ calcd for C₂₆H₃₂NaO₇S 511.1761; found 511.17561. The latter alcohol (2249 mg, 4.603 mmol, 1.0 equiv) was dissolved in anhydrous

CHAPITRE 4 – MELIOIDOSIS PATIENT SERUM-REACTIVE SYNTHETIC TETRASACCHARIDES BEARING THE PREDOMINANT EPITOPES OF BURKHOLDERIA PSEUDOMALLEI AND BURKHOLDERIA MALLEI O-ANTIGENS

pyridine (23 mL) and Ac₂O (23 mL), and DMAP (6 mg, 0.05 mmol, 0.01 equiv) was added. The solution was stirred under Ar at rt for 16 h, then the solvents were evaporated under reduced pressure and co-evaporated with toluene. The residue was purified by silica gel flash chromatography (Hex/EtOAc 9:1 to 7:3) to give compound **25** (2378 mg, 97%) as a white amorphous solid: *R_f* 0.6 (Hex/EtOAc 1:1); [α]_D²⁰ -37 (*c* 1.1, CHCl₃); ¹H NMR (600 MHz, CDCl₃) δ (ppm) 7.33–7.32 (m, 2H, 2 \times CH_{STol}), 7.24–7.23 (m, 2H, 2 \times CH_{PMB}), 7.12–7.11 (m, 2H, 2 \times CH_{STol}), 6.90–6.88 (m, 2H, 2 \times CH_{PMB}), 5.56 (dd, *J*₂₋₃ = 3.2 Hz, *J*₂₋₁ = 1.6 Hz, 1H, H-2), 5.34 (d, *J* = 1.4 Hz, 1H, H-1), 5.05 (t, *J* = 9.8 Hz, 1H, H-4), 4.58 (d, *J* = 11.9 Hz, 1H, CHH_{PMB}), 4.38 (d, *J* = 11.9 Hz, 1H, CHH_{PMB}), 4.24 (dq, *J*₅₋₄ = 9.9 Hz, *J*₅₋₆ = 6.2 Hz, 1H, H-5), 3.81 (s, 3H, CH_{3PMB}), 3.77 (dd, *J*₃₋₄ = 9.7 Hz, *J*₃₋₂ = 3.2 Hz, 1H, H-3), 2.80–2.75 (m, 1H, CHH_{Lev}), 2.70–2.65 (m, 1H, CHH_{Lev}), 2.60–2.55 (m, 1H, CHH_{Lev}), 2.52–2.47 (m, 1H, CHH_{Lev}), 2.33 (s, 3H, CH_{3STol}), 2.18 (s, 3H, CH_{3Lev}), 2.12 (s, 3H, CH_{3Ac}), 1.21 (d, *J* = 6.3 Hz, 1H, H-6); ¹³C NMR (150 MHz, CDCl₃) δ (ppm) 206.5 (CO_{Lev}), 172.1 (COOR_{Lev}), 170.4 (COOR_{Ac}), 159.5 (C_{Ar}), 138.2 (C_{Ar}), 132.4 (2C, 2 \times CH_{STol}), 130.1, 129.8 (5C, C_{Ar}, 2 \times CH_{STol}, 2 \times CH_{PMB}), 129.7 (C_{Ar}), 113.9 (2C, 2 \times CH_{PMB}), 86.6 (C-1), 74.2 (C-3), 72.9 (C-4), 71.1 (CH_{2PMB}), 70.2 (C-2), 68.0 (C-5), 55.4 (CH_{3PMB}), 38.0 (CH_{2Lev}), 30.0 (CH_{3Lev}), 28.1 (CH_{2Lev}), 21.3 (CH₃), 21.2 (CH₃), 17.5 (C-6); HRMS (ESI-TOF) *m/z* [M + NH₄]⁺ calcd for C₂₈H₃₈NO₈S 548.23216; found 548.23176; *m/z* [M + Na]⁺ calcd for C₂₈H₃₄NaO₈S 553.18666; found 553.1874.

(5-Azido-1-pentyl) 2-O-acetyl-4-O-levulinoyl-3-O-para-methoxybenzyl- α -L-rhamnopyranosyl-(1 \rightarrow 3)-2-O-benzyl-4,6-O-benzylidene- β -D-glucopyranoside (26).

Alcohol **16**¹⁶⁸ (702 mg, 1.50 mmol, 1.0 equiv), donor **25** (952 mg, 1.79 mmol, 1.2 equiv), and NIS (505 mg, 2.24 mmol, 1.5 equiv) were dried together under high vacuum for 1 h. Activated ground molecular sieves (4 Å, 2808 mg) and anhydrous DCM (30 mL) were successively added and the mixture was stirred under Ar for 1 h. The reaction flask was cooled to -10 °C and protected from light using aluminum foil. AgOTf (38 mg, 0.15 mmol, 0.1 equiv) was added and the mixture was stirred under Ar for 1 h while being gradually warmed to 0 °C. Et₃N (0.21 mL, 1.5 mmol, 1.0 equiv) was added, the yellow suspension was filtered over Celite, and the solvents were evaporated

CHAPITRE 4 – MELIOIDOSIS PATIENT SERUM-REACTIVE SYNTHETIC TETRASACCHARIDES BEARING THE PREDOMINANT EPITOPES OF BURKHOLDERIA PSEUDOMALLEI AND BURKHOLDERIA MALLEI O-ANTIGENS

under reduced pressure. The residue was purified by silica gel flash chromatography (Hex/EtOAc 8:2 to 6:4) to give disaccharide **26** (1177 mg, 90%) as a white amorphous solid: R_f 0.6 (Hex/EtOAc 1:1); $[\alpha]_D^{20}$ -31 (c 0.6, CHCl_3); ^1H NMR (600 MHz, CDCl_3) δ (ppm) 7.45–7.43 (m, 2H, $2 \times \text{CH}_{\text{Ar}}$), 7.35–7.28 (m, 8H, $8 \times \text{CH}_{\text{Ar}}$), 7.19–7.18 (m, 2H, $2 \times \text{CH}_{\text{PMB}}$), 6.85–6.83 (m, 2H, $2 \times \text{CH}_{\text{PMB}}$), 5.52 (s, 1H, H-7A), 5.43 (dd, $J_{2,3} = 3.2$ Hz, $J_{2,1} = 1.6$ Hz, 1H, H-2B), 5.17 (d, $J = 1.0$ Hz, 1H, H-1B), 4.90–4.85 (m, 2H, H-4B, CHH_{Ph}), 4.69 (d, $J = 10.8$ Hz, 1H, CHH_{Ph}), 4.58 (d, $J = 11.5$ Hz, 1H, CHH_{Ph}), 4.50 (d, $J = 7.8$ Hz, 1H, H-1A), 4.35 (dd, $J_{6a-6b} = 10.5$ Hz, $J_{6a-5} = 5.0$ Hz, 1H, H-6aA), 4.33 (d, $J = 11.6$ Hz, 1H, CHH_{Ph}), 4.09–4.04 (m, 1H, H-5B), 3.96–3.92 (m, 1H, H-1a_{linker}), 3.90 (t, $J = 9.2$ Hz, 1H, H-3A), 3.79–3.75 (m, 5H, H-3B, H-6bA, CH_3_{PMB}), 3.59–3.56 (m, 1H, H-1b_{linker}), 3.53 (t, $J = 9.5$ Hz, 1H, H-4A), 3.46 (t, $J = 8.1$ Hz, 1H, H-2A), 3.44–3.39 (m, 1H, H-5A), 3.23 (t, $J = 6.9$ Hz, 2H, H-5_{linker}), 2.71–2.66 (m, 1H, CHH_{Lev}), 2.62–2.57 (m, 1H, CHH_{Lev}), 2.48–2.43 (m, 1H, CHH_{Lev}), 2.42–2.38 (m, 1H, CHH_{Lev}), 2.15 (s, 3H, CH_3_{Lev}), 2.05 (s, 3H, CH_3_{Ac}), 1.70–1.65 (m, 2H, H-2_{linker}), 1.64–1.59 (m, 2H, H-4_{linker}), 1.50–1.44 (m, 2H, H-3_{linker}), 0.78 (d, $J = 6.2$ Hz, 3H, H-6B); ^{13}C NMR (150 MHz, CDCl_3) δ (ppm) 206.4 (CO_{Lev}), 172.0 (COOR_{Lev}), 170.2 (COOR_{Ac}), 159.3 (C_{Ar}), 137.9 (C_{Ar}), 137.2 (C_{Ar}), 130.4 (C_{Ar}), 129.5–126.3 (12C, $12 \times \text{CH}_{\text{Ar}}$), 113.8 (2C, $2 \times \text{CH}_{\text{PMB}}$), 104.3 (C-1A), 101.8 (C-7A), 98.4 (C-1B), 82.8 (C-2A), 79.3 (C-4A), 76.3 (C-3A), 75.0 (CH_2_{Ph}), 74.6 (C-3B), 72.9 (C-4B), 71.1 (CH_2_{Ph}), 70.2 (C-1_{linker}), 68.9 (C-6A), 68.5 (C-2B), 66.5 (2C, C-5A, C-5B), 55.4 (CH_3_{PMB}), 51.4 (C-5_{linker}), 37.9 (CH_2_{Lev}), 30.0 (CH_3_{Lev}), 29.5 (C-2_{linker}), 28.8 (C-4_{linker}), 28.1 (CH_2_{Lev}), 23.5 (C-3_{linker}), 21.1 (CH_3_{Ac}), 17.0 (C-6B); HRMS (ESI-TOF) m/z $[\text{M} + \text{Na}]^+$ calcd for $\text{C}_{46}\text{H}_{57}\text{N}_3\text{NaO}_{14}$ 898.3733; found 898.3756; m/z $[\text{M} + \text{NH}_4]^+$ calcd for $\text{C}_{46}\text{H}_{61}\text{N}_4\text{O}_{14}$ 893.4179; found 893.4196.

(5-Azido-1-pentyl) 2-O-acetyl-4-O-levulinoyl- α -L-rhamnopyranosyl-(1→3)-2-O-benzyl-4,6-O-benzylidene- β -D-glucopyranoside (12).

DDQ (609 mg, 2.68 mmol, 2.0 equiv) was added to a solution of disaccharide **26** (1175 mg, 1.342 mmol, 1.0 equiv) in DCM (27 mL) and H_2O (2.7 mL), and the mixture was stirred at rt for 2 h. Saturated $\text{NaHCO}_3(\text{aq})$ (40 mL) was added to quench the solution, which was then diluted in EtOAc (30 mL) and transferred into a separatory funnel. The organic layer was washed with

CHAPITRE 4 – MELIOIDOSIS PATIENT SERUM-REACTIVE SYNTHETIC TETRASACCHARIDES BEARING THE PREDOMINANT EPITOPES OF BURKHOLDERIA PSEUDOMALLEI AND BURKHOLDERIA MALLEI O-ANTIGENS

saturated NaHCO₃(aq) (40 mL) and brine (40 mL), dried over anhydrous MgSO₄, and evaporated under reduced pressure. The residue was purified by silica gel flash chromatography (Hex/EtOAc 9:1 to 1:1) to give alcohol **12** (878 mg, 87%) as a white amorphous solid: *R_f* 0.3 (Hex/EtOAc 4:6); [α]_D²⁰ -43 (*c* 0.7, CHCl₃); ¹H NMR (600 MHz, CDCl₃) δ (ppm) 7.47–7.46 (m, 2H, 2 \times CH_{Ar}), 7.35–7.34 (m, 3H, 3 \times CH_{Ar}), 7.32–7.31 (m, 4H, 4 \times CH_{Ar}), 7.28–7.27 (m, 1H, CH_{Ar}), 5.52 (s, 1H, H-7A), 5.22–5.21 (m, 2H, H-1B, H-2B), 4.87 (d, *J* = 10.8 Hz, 1H, CHH_{Bn}), 4.79–4.73 (m, 2H, H-4B, CHH_{Bn}), 4.49 (d, *J* = 7.8 Hz, 1H, H-1A), 4.35 (dd, *J*_{6a-6b} = 10.5 Hz, *J*_{6a-5} = 5.0 Hz, 1H, H-6aA), 4.13 (dq, *J*₅₋₄ = 10.1 Hz, *J*₅₋₆ = 6.2 Hz, 1H, H-5B), 4.04 (dd, *J*₃₋₄ = 9.8 Hz, *J*₃₋₂ = 3.2 Hz, 1H, H-3B), 3.95–3.90 (m, 2H, H-3A, H-1a_{linker}), 3.77 (t, *J*_{6b-6a} = 10.3 Hz, 1H, H-6bA), 3.57–3.53 (m, 2H, H-4A, H-1b_{linker}), 3.47–3.40 (m, 2H, H-2A, H-5A), 3.22 (t, *J* = 6.9 Hz, 2H, H-5_{linker}), 2.77–2.69 (m, 2H, CH_{2Lev}), 2.51–2.49 (m, 2H, CH_{2Lev}), 2.16 (s, 3H, CH_{3Lev}), 2.07 (s, 3H, CH_{3Ac}), 1.68–1.63 (m, 2H, H-2_{linker}), 1.62–1.58 (m, 2H, H-4_{linker}), 1.48–1.41 (m, 2H, H-3_{linker}), 0.82 (d, *J* = 6.2 Hz, 3H, H-6B); ¹³C NMR (150 MHz, CDCl₃) δ (ppm) 207.0 (CO_{Lev}), 173.2 (COOR_{Lev}), 170.5 (COOR_{Ac}), 138.1 (C_{Ar}), 137.3 (C_{Ar}), 129.2 (CH_{Ar}), 128.4 (2C, 2 \times CH_{Ar}), 128.3 (2C, 2 \times CH_{Ar}), 128.3 (2C, 2 \times CH_{Ar}), 127.9 (CH_{Ar}), 126.4 (2C, 2 \times CH_{Ar}), 104.3 (C-1A), 101.8 (C-7A), 97.8 (C-1B), 82.9 (C-2A), 79.3 (C-4A), 76.1 (C-3A), 75.2, 75.0 (2C, C-4B, CH_{2Bn}), 72.3 (C-2B), 70.2 (C-1_{linker}), 68.9 (C-6A), 68.6 (C-3B), 66.4 (C-5A), 65.8 (C-5B), 51.4 (C-5_{linker}), 38.2 (CH_{2Lev}), 29.9 (CH_{3Lev}), 29.4 (C-2_{linker}), 28.7 (C-4_{linker}), 28.2 (CH_{2Lev}), 23.5 (C-3_{linker}), 21.1 (CH_{3Ac}), 16.9 (C-6B); HRMS (ESI-TOF) *m/z* [M + Na]⁺ calcd for C₃₈H₄₉N₃NaO₁₃ 778.3158; found 778.3159; *m/z* [M + K]⁺ calcd for C₃₈H₄₉KN₃O₁₃ 794.2897; found 794.292.

(5-Azido-1-pentyl) 2-O-ortho-(azidomethyl)benzoyl-4,6-O-benzylidene-3-O-paramethoxybenzyl- β -D-glucopyranosyl-(1 \rightarrow 3)-2-O-acetyl-4-O-levulinoyl- α -L-rhamnopyranosyl-(1 \rightarrow 3)-2-O-benzyl-4,6-O-benzylidene- β -D-glucopyranoside (27).

Disaccharide **12** (583 mg, 0.772 mmol, 1.0 equiv), thioglucoside **18** (757 mg, 1.16 mmol, 1.5 equiv), and NIS (260 mg, 1.16 mmol, 1.5 equiv) were dried together under high vacuum for 1 h. Activated ground molecular sieves (4 Å, 2333 mg) and anhydrous DCM (15 mL) were successively added and the mixture was stirred under Ar for 1 h. The reaction flask was cooled to

CHAPITRE 4 – MELIOIDOSIS PATIENT SERUM-REACTIVE SYNTHETIC TETRASACCHARIDES BEARING THE PREDOMINANT EPITOPES OF BURKHOLDERIA PSEUDOMALLEI AND BURKHOLDERIA MALLEI O-ANTIGENS

–10 °C and protected from light using aluminum foil. AgOTf (20 mg, 0.077 mmol, 0.1 equiv) was added and the mixture was stirred under Ar for 2 h while being gradually warmed to 0 °C. Et₃N (0.11 mL, 0.77 mmol, 1.0 equiv) was added, the yellow suspension was filtered over Celite, and the solvents were evaporated under reduced pressure. The residue was purified by silica gel flash chromatography (Hex/EtOAc 8:2 to 7:3) to give trisaccharide **27** (773 mg, 78%) as a white solid foam along with an inseparable unknown impurity (10%): *R_f* 0.7 (Hex/EtOAc 6:4); [α]_D²⁰ –28 (*c* 0.6, CHCl₃); ¹H NMR (600 MHz, CDCl₃) δ (ppm) 7.71–7.69 (m, 1H, CH_{AZMB}), 7.56–7.55 (m, 1H, CH_{Ar}), 7.51–7.50 (m, 2H, 2 × CH_{Ar}), 7.41–7.25 (m, 15H, 15 × CH_{Ar}), 7.07–7.05 (m, 2H, 2 × CH_{PMB}), 6.63–6.61 (m, 2H, 2 × CH_{PMB}), 5.60 (s, 1H, H-7C), 5.51 (s, 1H, H-7A), 5.35 (dd, *J*₂₋₃ = 3.4 Hz, *J*₂₋₁ = 1.5 Hz, 1H, H-2B), 5.19 (d, *J* = 1.3 Hz, 1H, H-1B), 5.13 (dd, *J*₂₋₃ = 8.5 Hz, *J*₂₋₁ = 7.6 Hz, 1H, H-2C), 4.89 (t, *J* = 10.0 Hz, 1H, H-4B), 4.86 (d, *J* = 10.7 Hz, 1H, CHH_{Bn}), 4.78–4.75 (m, 2H, CHH_{Bn}, CHH_{PMB}), 4.72 (d, *J* = 15.1 Hz, 1H, CHH_{AZMB}), 4.71 (d, *J* = 7.5 Hz, 1H, H-1C), 4.63 (d, *J* = 15.1 Hz, 1H, CHH_{AZMB}), 4.59 (d, *J* = 11.7 Hz, 1H, CHH_{PMB}), 4.49 (d, *J* = 7.8 Hz, 1H, H-1A), 4.37 (dd, *J*_{6a-6b} = 10.5 Hz, *J*_{6a-5} = 5.0 Hz, 1H, H-6aC), 4.34 (dd, *J*_{6b-6a} = 10.5 Hz, *J*_{6b-5} = 4.9 Hz, 1H, H-6aA), 4.06 (dq, *J*₅₋₄ = 10.0 Hz, *J*₅₋₆ = 6.1 Hz, 1H, H-5B), 4.02 (dd, *J*₃₋₄ = 9.8 Hz, *J*₃₋₂ = 3.5 Hz, 1H, H-3B), 3.93–3.90 (m, 2H, H-3A, H-1a_{linker}), 3.83–3.81 (m, 2H, H-3C, H-4C), 3.80–3.75 (m, 2H, H-6bA, H-6bC), 3.70 (s, 3H, CH_{3PMB}), 3.58–3.53 (m, 2H, H-1b_{linker}, H-4A), 3.51–3.46 (m, 2H, H-2A, H-5C), 3.40 (ddd, *J*_{5-4, 5-6b} = 9.6 Hz, *J*_{5-6a} = 5.0 Hz, 1H, H-5A), 3.21 (t, *J* = 6.9 Hz, 2H, H-5_{linker}), 2.30–2.24 (m, 1H, CHH_{Lev}), 2.13–2.09 (m, 1H, CHH_{Lev}), 2.07 (s, 3H, CH_{3Ac}), 2.04–2.02 (m, 1H, CHH_{Lev}), 2.01 (s, 3H, CH_{3Lev}), 1.82–1.77 (m, 1H, CHH_{Lev}), 1.67–1.63 (m, 2H, H-2_{linker}), 1.62–1.57 (m, 2H, H-4_{linker}), 1.49–1.41 (m, 2H, H-3_{linker}), 0.75 (d, *J* = 6.2 Hz, 3H, H-6B); ¹³C NMR (150 MHz, CDCl₃) δ (ppm) 206.1 (CO_{Lev}), 171.4 (COOR_{Lev}), 170.0 (COOR_{Ac}), 164.7 (COOR_{AZMB}), 159.2 (C_{Ar}), 138.2 (C_{Ar}), 138.0 (C_{Ar}), 137.3 (C_{Ar}), 137.1 (C_{Ar}), 132.7 (CH_{AZMB}), 130.7 (CH_{Ar}), 130.1 (C_{Ar}), 129.7 (2C, 2 × CH_{PMB}), 129.2 (CH_{Ar}), 129.1–126.1 (17C, C_{Ar}, 16 × CH_{Ar}), 113.6 (2C, 2 × CH_{PMB}), 104.2 (C-1A), 101.7 (C-7A), 101.3 (C-7C), 101.1 (C-1C), 97.8 (C-1B), 82.7 (C-2A), 81.6 (C-4C), 79.2 (C-4A), 77.6 (C-3C), 76.0 (C-3A), 74.9 (2C, C-3B, CH_{2Bn}), 73.6, 73.5 (2C, C-2C, CH_{2PMB}), 72.5 (C-4B), 71.0 (C-2B), 70.2 (C-1_{linker}), 68.9, 68.7 (2C, C-6A, C-6C), 66.3, 66.17, 66.15 (3C, C-5A, C-5B, C-5C), 55.2 (CH_{3PMB}), 52.9 (CH_{2AZMB}), 51.3 (C-

CHAPITRE 4 – MELIOIDOSIS PATIENT SERUM-REACTIVE SYNTHETIC TETRASACCHARIDES BEARING THE PREDOMINANT EPITOPES OF BURKHOLDERIA PSEUDOMALLEI AND BURKHOLDERIA MALLEI O-ANTIGENS

5linker), 37.5 (CH₂Lev), 29.7 (CH₃Lev), 29.4 (C-2linker), 28.7 (C-4linker), 27.4 (CH₂Lev), 23.5 (C-3linker), 21.0 (CH₃Ac), 16.7 (C-6B); HRMS (ESI-TOF) m/z [M + NH₄]⁺ calcd for C₆₇H₈₀N₇O₂₀ 1302.5453; found 1302.5453; m/z [M + Na]⁺ calcd for C₆₇H₇₆N₆NaO₂₀ 1307.5007; found 1307.5003.

(5-Azido-1-pentyl) 2-O-ortho-(azidomethyl)benzoyl-4,6-O-benzylidene-β-D-glucopyranosyl-(1→3)-2-O-acetyl-4-O-levulinoyl-α-L-rhamnopyranosyl-(1→3)-2-O-benzyl-4,6-O-benzylidene-β-D-glucopyranoside (28).

Trisaccharide **27** (99 mg, 0.077 mmol, 1.0 equiv) was dissolved in DCM (1.6 mL) and H₂O (0.2 mL) and DDQ (35 mg, 0.16 mmol, 2.0 equiv) was added. The mixture was stirred at rt for 2 h, then quenched with saturated NaHCO₃(aq) (2 mL). The solution was transferred into a separatory funnel, DCM (10 mL) was added, and the organic and aqueous layers were separated. The aqueous phase was extracted with DCM (2 × 10 mL). The combined organic phases were washed with saturated NaHCO₃(aq) (20 mL) and brine (20 mL), dried over anhydrous MgSO₄, and evaporated under reduced pressure. The residue was purified by silica gel flash chromatography (Hex/EtOAc 8:2 to 4:6) to give alcohol **28** (68 mg, 75%) as a white solid foam: R_f 0.6 (Hex/EtOAc 1:1); $[\alpha]_D^{20}$ -62 (c 0.6, CHCl₃); ¹H NMR (600 MHz, CDCl₃) δ (ppm) 7.89–7.88 (m, 1H, CH_{AZMB}), 7.56–7.54 (m, 1H, CH_{Ar}), 7.51–7.49 (m, 3H, 3 × CH_{Ar}), 7.44–7.43 (m, 2H, 2 × CH_{Ar}), 7.39–7.28 (m, 12H, 12 × CH_{Ar}), 5.54 (s, 1H, H-7C), 5.53 (s, 1H, H-7A), 5.36 (dd, $J_{2-3} = 1.9$ Hz, $J_{2-1} = 1.0$ Hz, 1H, H-2B), 5.20 (br s, 1H, H-1B), 5.08 (dd, $J_{2-3} = 8.6$ Hz, $J_{2-1} = 7.8$ Hz, 1H, H-2C), 4.92 (t, $J = 9.9$ Hz, 1H, H-4B), 4.86 (d, $J = 10.7$ Hz, 1H, CHH_{Bn}), 4.77 (d, $J = 10.7$ Hz, 1H, CHH_{Bn}), 4.75 (d, $J = 14.8$ Hz, 1H, CHH_{AZMB}), 4.74 (d, $J = 7.4$ Hz, 1H, H-1C), 4.69 (d, $J = 14.7$ Hz, 1H, CHH_{AZMB}), 4.48 (d, $J = 7.7$ Hz, 1H, H-1A), 4.37–4.33 (m, 2H, H-6aA, H-6aC), 4.09 (dq, $J_{5-4} = 10.1$ Hz, $J_{5-6} = 5.8$ Hz, 1H, H-5B), 4.05 (dd, $J_{3-4} = 9.8$ Hz, $J_{3-2} = 3.5$ Hz, 1H, H-3B), 3.99 (t, $J = 9.0$ Hz, 1H, H-3C), 3.94–3.89 (m, 2H, H-1a_{linker}, H-3A), 3.76 (t, $J = 10.2$ Hz, 2H, H-6bA, H-6bC), 3.62 (t, $J = 9.3$ Hz, 1H, H-4C), 3.58–3.53 (m, 2H, H-1b_{linker}, H-4A), 3.51–3.46 (m, 2H, H-2A, H-5C), 3.40 (td, $J_{5-4, 5-6b} = 9.7$ Hz, $J_{5-6a} = 5.0$ Hz, 1H, H-5A), 3.21 (t, $J = 6.9$ Hz, 2H, H-5_{linker}), 2.87 (br s, 1H, OH), 2.28–2.22 (m, 1H, CHH_{Lev}), 2.17–2.12 (m, 1H, CHH_{Lev}), 2.09 (s, 3H, CH₃Ac), 2.07–2.03 (m, 1H, CHH_{Lev}), 2.01 (s, 3H, CH₃Lev), 1.88–1.84 (m, 1H, CHH_{Lev}), 1.65 (quint, $J = 7.1$ Hz, 2H, H-2_{linker}), 1.59 (quint, $J = 7.3$ Hz, 2H, H-4_{linker}), 1.48–1.41 (m, 2H, H-3_{linker}), 0.78 (d, $J = 6.2$ Hz, 3H, H-6B);

CHAPITRE 4 – MELIOIDOSIS PATIENT SERUM-REACTIVE SYNTHETIC TETRASACCHARIDES BEARING THE PREDOMINANT EPITOPES OF BURKHOLDERIA PSEUDOMALLEI AND BURKHOLDERIA MALLEI O-ANTIGENS

^{13}C NMR (150 MHz, CDCl_3) δ (ppm) 206.2 (CO_{Lev}), 171.5 (COOR_{Lev}), 170.0 (COOR_{Ac}), 165.6 ($\text{COOR}_{\text{AZMB}}$), 138.0 (C_{Ar}), 137.5 (C_{Ar}), 137.1 (C_{Ar}), 137.0 (C_{Ar}), 132.7–126.2 (20C, C_{Ar} , $19 \times \text{CH}_{\text{Ar}}$), 104.2 (C-1A), 101.9, 101.7 (2C, C-7A, C-7C), 101.0 (C-1C), 97.7 (C-1B), 82.6 (C-2A), 80.7 (C-4C), 79.2 (C-4A), 76.1 (C-3A), 75.0, 74.9, 74.8 (3C, CH_2_{Bn} , C-3B, C-2C), 72.7 (C-4B), 72.2 (C-3C), 71.1 (C-2B), 70.2 (C-1_{linker}), 68.9, 68.6 (2C, C-6A, C-6C), 66.3, 66.2 (3C, C-5A, C-5B, C-5C), 53.0 ($\text{CH}_2_{\text{AZMB}}$), 51.3 (C-5_{linker}), 37.4 (CH_2_{Lev}), 29.7 (CH_3_{Lev}), 29.4 (C-2_{linker}), 28.7 (C-4_{linker}), 27.5 (CH_2_{Lev}), 23.4 (C-3_{linker}), 21.0 (CH_3_{Ac}), 16.8 (C-6B); HRMS (ESI-TOF) m/z [$\text{M} + \text{Na}$] $^+$ calcd for $\text{C}_{59}\text{H}_{68}\text{N}_6\text{NaO}_{19}$ 1187.4431; found 1187.4412.

***para*-Methylphenyl 2-*O*-acetyl-4-*O*-levulinoyl-3-*O*-methyl-1-thio- α -L-rhamnopyranoside (29).**

Bu_2SnO (1557 mg, 6.254 mmol, 1.1 equiv) was added to a solution of diol **24** (2095 mg, 5.686 mmol, 1.0 equiv) in toluene (23 mL) and the mixture was refluxed with a Dean-Stark trap for 5 h. The solution was cooled to rt, and CsF (881 mg, 5.80 mmol, 1.02 equiv) and MeI (17.7 mL, 284 mmol, 50.0 equiv) were successively added. The mixture was stirred under Ar at 80 °C for 16 h. The suspension was cooled at 0 °C, filtered over Celite, and rinsed with DCM. The solvents were evaporated under reduced pressure. The residue was purified by silica gel flash chromatography (Hex/EtOAc 1:1) to give *para*-methylphenyl 4-*O*-levulinoyl-3-*O*-methyl-1-thio- α -L-rhamnopyranoside (2019 mg, 93%, ~83:17 mixture with its inseparable 2-*O*-methyl anomer) as a colorless oil: R_f 0.3 (Hex/EtOAc 4:6); ^1H NMR (600 MHz, CDCl_3) δ (ppm) 7.36–7.35 (m, 2H, $2 \times \text{CH}_{\text{STol}}$), 7.13–7.11 (m, 2H, $2 \times \text{CH}_{\text{STol}}$), 5.49 (d, $J = 1.4$ Hz, 1H, H-1), 5.05 (t, $J = 9.5$ Hz, 1H, H-4), 4.31 (dd, $J_{2-3} = 3.2$ Hz, $J_{2-1} = 1.6$ Hz, 1H, H-2), 4.27 (dq, $J_{5-4} = 9.8$ Hz, $J_{5-6} = 6.2$ Hz, 1H, H-5), 3.53 (dd, $J_{3-4} = 9.4$ Hz, $J_{3-2} = 3.3$ Hz, 1H, H-3), 3.45 (s, 3H, CH_3_{OMe}), 2.82–2.77 (m, 2H, CH_2_{Lev}), 2.63–2.60 (m, 2H, CH_2_{Lev}), 2.33 (s, 3H, $\text{CH}_3_{\text{STol}}$), 2.20 (s, 3H, CH_3_{Lev}), 1.20 (d, $J = 6.3$ Hz, 3H, H-6); ^{13}C NMR (150 MHz, CDCl_3) δ (ppm) 206.6 (CO_{Lev}), 172.2 (COOR_{Lev}), 137.8 (C_{STol}), 132.1 (2C, $2 \times \text{CH}_{\text{STol}}$), 130.02 (C_{STol}), 129.97 (2C, $2 \times \text{CH}_{\text{STol}}$), 87.4 (C-1), 79.2 (C-3), 73.0 (C-4), 69.2 (C-2), 67.4 (C-5), 57.8 (CH_3_{OMe}), 38.0 (CH_2_{Lev}), 29.9 (CH_3_{Lev}), 28.1 (CH_2_{Lev}), 21.2 ($\text{CH}_3_{\text{STol}}$), 17.3 (C-6); HRMS (ESI-TOF) m/z [$\text{M} + \text{NH}_4$] $^+$ calcd for $\text{C}_{19}\text{H}_{30}\text{NO}_6\text{S}$ 400.1788; found 400.1806; m/z [$\text{M} + \text{Na}$] $^+$ calcd for $\text{C}_{19}\text{H}_{26}\text{NaO}_6\text{S}$ 405.1342; found 405.1362. The latter alcohol (1678 mg, 4.387

CHAPITRE 4 – MELIOIDOSIS PATIENT SERUM-REACTIVE SYNTHETIC TETRASACCHARIDES BEARING THE PREDOMINANT EPITOPES OF BURKHOLDERIA PSEUDOMALLEI AND BURKHOLDERIA MALLEI O-ANTIGENS

mmol, 1.0 equiv) was dissolved in anhydrous pyridine (22 mL) and Ac₂O (22 mL), and DMAP (5 mg, 0.04 mmol, 0.01 equiv) were added. The reaction mixture was stirred at rt for 16 h under Ar. The solution was evaporated under reduced pressure and co-evaporated with toluene (3×). The residue was purified by silica gel flash chromatography (Hex/EtOAc 5:5 to 4:6) to give thiorhamnoside **29** (1786 mg, 96%, ~9:1 mixture with its inseparable 3-*O*-acetyl-2-*O*-methyl isomer) as a white amorphous solid: *R*_f 0.6 (Hex/EtOAc 4:6); ¹H NMR (600 MHz, CDCl₃) δ (ppm) 7.36–7.35 (m, 2H, 2 × CH_{STol}), 7.13–7.12 (m, 2H, 2 × CH_{STol}), 5.57 (dd, *J*₂₋₃ = 3.2 Hz, *J*₂₋₁ = 1.6 Hz, 1H, H-2), 5.36 (d, *J*₁₋₂ = 1.3 Hz, 1H, H-1), 5.04 (t, *J* = 9.8 Hz, 1H, H-4), 4.30 (dq, *J*₅₋₄ = 9.8 Hz, *J*₅₋₆ = 6.2 Hz, 1H, H-5), 3.59 (dd, *J*₃₋₄ = 9.8 Hz, *J*₃₋₂ = 3.3 Hz, 1H, H-3), 3.37 (s, 3H, CH_{3OMe}), 2.87–2.84 (m, 1H, CHH_{Lev}), 2.76–2.71 (m, 1H, CHH_{Lev}), 2.69–2.63 (m, 1H, CHH_{Lev}), 2.61–2.57 (m, 1H, CHH_{Lev}), 2.33 (s, 3H, CH_{3STol}), 2.20 (s, 3H, CH_{3Lev}), 2.11 (s, 3H, CH_{3Ac}), 1.23 (d, *J* = 6.3 Hz, 3H, H-6); ¹³C NMR (150 MHz, CDCl₃) δ (ppm) 206.5 (CO_{Lev}), 172.2 (COOR_{Lev}), 170.4 (COOR_{Ac}), 138.2 (C_{STol}), 132.4 (2C, 2 × CH_{STol}), 130.1 (2C, 2 × CH_{STol}), 129.9 (C_{STol}), 86.6 (C-1), 77.6 (C-3), 73.0 (C-4), 69.7 (C-2), 67.8 (C-5), 57.9 (CH_{3OMe}), 38.0 (CH_{2Lev}), 30.0 (CH_{3Lev}), 28.1 (CH_{2Lev}), 21.2 (CH₃), 21.1 (CH₃), 17.4 (C-6); HRMS (ESI-TOF) *m/z* [M + NH₄]⁺ calcd for C₂₁H₃₂NO₇S 442.1894; found 442.19005; *m/z* [M + Na]⁺ calcd for C₂₁H₂₈NaO₇S 447.1448; found 447.1453.

(5-Azido-1-pentyl) 2-*O*-acetyl-4-*O*-levulinoyl-3-*O*-methyl- α -L-rhamnopyranosyl-(1→3)-2-*O*-ortho-(azidomethyl)benzoyl-4,6-*O*-benzylidene- β -D-glucopyranosyl-(1→3)-2-*O*-acetyl-4-*O*-levulinoyl- α -L-rhamnopyranosyl-(1→3)-2-*O*-benzyl-4,6-*O*-benzylidene- β -D-glucopyranoside (10).

Trisaccharide **28** (300 mg, 0.257 mmol, 1.0 equiv), thiorhamnoside **29** (164 mg, 0.386 mmol, 1.5 equiv) and NIS (87 mg, 0.39 mmol, 1.5 equiv) were dried together under high vacuum for 1 h. 4 Å activated ground molecular sieves (1200 mg) and anhydrous DCM (5 mL) were successively added and the mixture was stirred under Ar for 1 h. The reaction flask was cooled at –10 °C and protected from light using aluminum foil. AgOTf (7 mg, 0.03 mmol, 0.1 equiv) was added and the mixture was stirred under Ar for 2 h while being gradually warmed to 0 °C. Et₃N (0.04 mL, 0.3

CHAPITRE 4 – MELIOIDOSIS PATIENT SERUM-REACTIVE SYNTHETIC TETRASACCHARIDES BEARING THE PREDOMINANT EPITOPES OF BURKHOLDERIA PSEUDOMALLEI AND BURKHOLDERIA MALLEI O-ANTIGENS

mmol, 1.0 equiv) was added, the yellow suspension was filtered over Celite, and the solvents were evaporated under reduced pressure. The residue was purified by silica gel flash chromatography (Hex/EtOAc 6:4 to 5:5) to give tetrasaccharide **10** (246 mg, 65%) as a white amorphous solid along with an inseparable unknown impurity (12%): R_f 0.5 (Hex/EtOAc 4:6); $[\alpha]_D^{20}$ -62 (c 0.4, CHCl_3); ^1H NMR (600 MHz, CDCl_3) δ (ppm) 7.87–7.84 (m, 1H, CH_{AZMB}), 7.59–7.55 (m, 2H, $2 \times \text{CH}_{\text{Ar}}$), 7.50–7.47 (m, 2H, $2 \times \text{CH}_{\text{Ar}}$), 7.43–7.42 (m, 2H, $2 \times \text{CH}_{\text{Ar}}$), 7.38–7.29 (m, 12H, $12 \times \text{CH}_{\text{Ar}}$), 5.57 (s, 1H, H-7C), 5.53 (s, 1H, H-7A), 5.36 (d, $J = 1.7$ Hz, 1H, H-2B), 5.21–5.19 (m, 2H, H-1B, H-2C), 5.07 (d, $J = 1.1$ Hz, H-2D), 4.91–4.87 (m, 2H, CHH_{Bn} , H-4B), 4.85–4.76 (m, 6H, CHH_{Bn} , H-1C, H-1D, $\text{CH}_{2\text{AZMB}}$, H-4D), 4.49 (d, $J = 7.7$ Hz, 1H, H-1A), 4.39 (dd, $J_{6a-6b} = 10.5$ Hz, $J_{6a-5} = 4.9$ Hz, 1H, H-6aC), 4.35 (dd, $J_{6a-6b} = 10.2$ Hz, $J_{6a-5} = 4.9$ Hz, 1H, H-6aA), 4.10–4.03 (m, 3H, H-3B, H-3C, H-5B), 4.01 (dq, $J_{5-4} = 10.0$ Hz, $J_{5-6} = 5.6$ Hz, 1H, H-5D), 3.94–3.90 (m, 2H, H-1a_{linker}, H-3A), 3.82–3.75 (m, 2H, H-6bA, H-6bC), 3.72 (t, $J = 9.4$ Hz, 1H, H-4C), 3.59–3.52 (m, 3H, H-1b_{linker}, H-4A, H-5C), 3.50–3.47 (m, 2H, H-2A, H-3D), 3.41 (td, $J_{5-4} = 9.6$ Hz, $J_{5-6} = 4.9$ Hz, 1H, H-5A), 3.22 (t, $J = 14.2$ Hz, 2H, H-5_{linker}), 3.21 (s, 3H, $\text{CH}_{3\text{OMe}}$), 2.78–2.73 (m, 1H, CHH_{Lev}), 2.67–2.62 (m, 1H, CHH_{Lev}), 2.56–2.47 (m, 2H, $\text{CH}_{2\text{Lev}}$), 2.32–2.29 (m, 1H, CHH_{Lev}), 2.16 (s, 3H, $\text{CH}_{3\text{Lev}}$), 2.13–2.11 (m, 2H, $\text{CH}_{2\text{Lev}}$), 2.08 (s, 3H, $\text{CH}_{3\text{Ac}}$), 2.04 (s, 3H, $\text{CH}_{3\text{Lev}}$), 1.87–1.80 (m, 4H, $\text{CH}_{3\text{Ac}}$, CHH_{Lev}), 1.68–1.63 (m, 2H, H-2_{linker}), 1.62–1.58 (m, 2H, H-4_{linker}), 1.48–1.42 (m, 2H, H-3_{linker}), 0.77–0.76 (m, 6H, H-6B, H-6D); ^{13}C NMR (150 MHz, CDCl_3) δ (ppm) 206.4 (CO_{Lev}), 206.1 (CO_{Lev}), 172.0 (COOR_{Lev}), 171.4 (COOR_{Lev}), 170.0 (COOR_{Ac}), 169.5 (COOR_{Ac}), 164.4 ($\text{COOR}_{\text{AZMB}}$), 139.2 (C_{Ar}), 138.0 (C_{Ar}), 137.1 (C_{Ar}), 137.0 (C_{Ar}), 133.1–126.2 (20C, C_{Ar} , $19 \times \text{CH}_{\text{Ar}}$), 104.2 (C-1A), 101.8, 101.7 (2C, C-7A, C-7C), 100.9 (C-1C), 98.2 (C-1D), 97.7 (C-1B), 82.7 (C-2A), 79.2 (C-4A), 79.0 (C-4C), 76.7 (C-3D), 76.6 (C-3C), 76.1 (C-3A), 74.9, 74.7, 74.5 (3C, C-3B, $\text{CH}_{2\text{Bn}}$, C-2C), 72.6 (2C, C-4B, C-4D), 71.0 (C-2B), 70.2 (C-1_{linker}), 68.9, 68.7 (2C, C-6A, C-6C), 67.74 (C-2D), 66.71, 66.4, 66.3, 66.1 (4C, C-5A, C-5B, C-5C, C-5D), 57.6 ($\text{CH}_{3\text{OMe}}$), 53.0 ($\text{CH}_{2\text{AZMB}}$), 51.3 (C-5_{linker}), 37.9 ($\text{CH}_{2\text{Lev}}$), 37.4 ($\text{CH}_{2\text{Lev}}$), 29.9 ($\text{CH}_{3\text{Lev}}$), 29.7 ($\text{CH}_{3\text{Lev}}$), 29.4 (C-2_{linker}), 28.7 (C-4_{linker}), 28.0 ($\text{CH}_{2\text{Lev}}$), 27.4 ($\text{CH}_{2\text{Lev}}$), 23.4 (C-3_{linker}), 21.0, 20.6 (2C, $2 \times \text{CH}_{3\text{Ac}}$), 16.8, 16.7 (2C, C-6B, C-6D); HRMS (ESI-TOF) m/z $[\text{M} + \text{NH}_4]^+$ calcd for $\text{C}_{73}\text{H}_{92}\text{N}_7\text{O}_{26}$ 1482.6087; found 1482.6047; m/z $[\text{M} + \text{Na}]^+$ calcd for $\text{C}_{73}\text{H}_{88}\text{N}_6\text{NaO}_{26}$ 1487.564; found 1487.5617.

CHAPITRE 4 – MELIOIDOSIS PATIENT SERUM-REACTIVE SYNTHETIC TETRASACCHARIDES BEARING THE PREDOMINANT EPITOPES OF BURKHOLDERIA PSEUDOMALLEI AND BURKHOLDERIA MALLEI O-ANTIGENS

(5-Azido-1-pentyl) 2-O-acetyl-3-O-methyl- α -L-rhamnopyranosyl-(1 \rightarrow 3)-2-O-ortho-(azidomethyl)benzoyl-4,6-O-benzylidene- β -D-glucopyranosyl-(1 \rightarrow 3)-2-O-acetyl- α -L-rhamnopyranosyl-(1 \rightarrow 3)-2-O-benzyl-4,6-O-benzylidene- β -D-glucopyranoside (30).

A solution of tetrasaccharide **10** (214 mg, 0.146 mmol, 1.0 equiv) in anhydrous pyridine (1 mL) was cooled at 0 °C. Acetic acid (0.6 mL) and hydrazine monohydrate (0.07 mL, 1 mmol, 10.0 equiv) were successively slowly added. The mixture was stirred for 16 h under Ar while gradually being warmed to rt. The solution was evaporated under reduced pressure and co-evaporated with toluene (3 \times). The residue was purified by silica gel flash chromatography (Tol/EtOAc 9:1 to 7:3) to give diol **30** (160 mg, 86%) as a white amorphous solid: R_f 0.5 (Tol/EtOAc 1:1); $[\alpha]_D^{20}$ -40 (c 1.0, AcOEt); $^1\text{H NMR}$ (600 MHz, CDCl_3) δ (ppm) 7.97–7.95 (m, 1H, CH_{AZMB}), 7.55–7.52 (m, 1H, CH_{Ar}), 7.50–7.47 (m, 3H, 3 \times CH_{Ar}), 7.40–7.39 (m, 2H, 2 \times CH_{Ar}), 7.36–7.31 (m, 8H, 8 \times CH_{Ar}), 7.29–7.27 (m, 2H, 2 \times CH_{Ar}), 7.25–7.23 (m, 2H, 2 \times CH_{Ar}), 5.55 (s, 1H, H-7A), 5.49 (s, 1H, H-7C), 5.32 (dd, $J_{2-3} = 3.5$ Hz, $J_{2-1} = 1.6$ Hz, 1H, H-2B), 5.28 (dd, $J_{2-3} = 8.6$ Hz, $J_{2-1} = 7.8$ Hz, 1H, H-2C), 5.14 (d, $J = 1.2$ Hz, 1H, H-1B), 5.08 (dd, $J_{2-3} = 3.2$ Hz, $J_{2-1} = 1.7$ Hz, 1H, H-2D), 4.91 (d, $J = 14.7$ Hz, 1H, CHH_{AZMB}), 4.86 (d, $J = 10.7$ Hz, 1H, CHH_{Bn}), 4.85 (d, $J = 7.6$ Hz, 1H, H-1C), 4.82 (d, $J = 1.3$ Hz, 1H, H-1D), 4.79 (d, $J = 10.7$ Hz, 1H, CHH_{Bn}), 4.76 (d, $J = 14.7$ Hz, 1H, CHH_{AZMB}), 4.48 (d, $J = 7.8$ Hz, 1H, H-1A), 4.37 (dd, $J_{6a-6b} = 10.6$ Hz, $J_{6a-5} = 4.9$ Hz, 1H, H-6aC), 4.33 (dd, $J_{6a-6b} = 10.4$ Hz, $J_{6a-5} = 4.9$ Hz, 1H, H-6aA), 4.07 (t, $J = 9.0$ Hz, 1H, H-3C), 3.97–3.89 (m, 4H, H-1a_{linker}, H-5B, H-5D, H-3A), 3.87 (dd, $J_{3-4} = 9.4$ Hz, $J_{3-2} = 3.6$ Hz, 1H, H-3B), 3.77–3.69 (m, 3H, H-6bA, H-6bC, H-4C), 3.57–3.51 (m, 3H, H-1b_{linker}, H-5C, H-4A), 3.48–3.44 (m, 2H, H-2A, H-4B), 3.40–3.38 (m, 2H, H-3D, H-5A), 3.35–3.31 (m, 1H, H-4D), 3.29 (s, 3H, $\text{CH}_{3\text{OMe}}$), 3.20 (t, $J = 6.9$ Hz, 2H, H-5_{linker}), 2.41 (s, 1H, OH), 2.25 (br s, 1H, OH), 2.04 (s, 3H, $\text{CH}_{3\text{Ac}}$), 1.80 (s, 3H, $\text{CH}_{3\text{Ac}}$), 1.66–1.61 (m, 2H, H-2_{linker}), 1.61–1.56 (m, 2H, H-4_{linker}), 1.47–1.40 (m, 2H, H-3_{linker}), 0.90 (d, $J = 6.2$ Hz, 3H, H-6B*), 0.86 (d, $J = 6.2$ Hz, 3H, H-6D*); $^{13}\text{C NMR}$ (150 MHz, CDCl_3) δ (ppm) 169.9 (COOR_{Ac}), 169.6 (COOR_{Ac}), 165.2 ($\text{COOR}_{\text{AZMB}}$), 138.6 (C_{Ar}), 138.2 (C_{Ar}), 137.1 (C_{Ar}), 137.0 (C_{Ar}), 133.3–126.2 (20C, C_{Ar} , 19 \times CH_{Ar}), 104.2 (C-1A), 101.8, 101.5 (2C, C-7A, C-7C), 101.4 (C-1C), 98.5 (C-1D), 98.1 (C-B), 82.8 (C-2A), 79.3, 79.2 (2C, C-4A, C-3D), 78.2 (2C, C-3B, C-4C), 76.6, 76.5 (2C, C-3A, C-3C), 75.1, 74.9 (2C, $\text{CH}_{2\text{Bn}}$, C-2C),

CHAPITRE 4 – MELIOIDOSIS PATIENT SERUM-REACTIVE SYNTHETIC TETRASACCHARIDES BEARING THE PREDOMINANT EPITOPES OF BURKHOLDERIA PSEUDOMALLEI AND BURKHOLDERIA MALLEI O-ANTIGENS

71.7, 71.5 (2C, C-4B, C-4D), 70.7 (C-2B), 70.2 (C-1_{linker}), 68.8, 68.6 (2C, C-6A, C-6C), 68.5, 67.8 (2C, C-5B, C-5D), 67.3 (C-2D), 66.5 (C-5C), 66.3 (C-5A), 57.3 (CH₃OMe), 53.3 (CH₂AZMB), 51.3 (C-5_{linker}), 29.4 (C-2_{linker}), 28.7 (C-4_{linker}), 23.4 (C-3_{linker}), 21.0 (CH₃Ac), 20.6 (CH₃Ac), 17.14, 17.07 (2C, C-6B, C-6D); HRMS (ESI-TOF) m/z [M + NH₄]⁺ calcd for C₆₃H₈₀N₇O₂₂ 1286.5351; found 1286.5342; m/z [M + Na]⁺ calcd for C₆₃H₇₆N₆NaO₂₂ 1291.4905; found 1291.4892.

***para*-Methylphenyl 2-*O*-acetyl-3-*O*-methyl-1-thio- α -L-rhamnopyranoside (32).**

A solution of thiorhamnoside **29** (876 mg, 2.06 mmol, 1.0 equiv) in anhydrous pyridine (13 mL) was cooled at 0 °C. Acetic acid (8.5 mL) and hydrazine monohydrate (0.5 mL, 10 mmol, 5.0 equiv) were successively added dropwise. The mixture was stirred for 16 h under Ar while gradually being warmed to rt. The solution was evaporated under reduced pressure and co-evaporated with toluene (3 \times). The residue was purified by silica gel flash chromatography (Hex/EtOAc 7:3 to 6:4) to give alcohol **32** (616 mg, 91%, ~83:17 mixture with its inseparable 3-*O*-acetyl-2-*O*-methyl isomer) as a colorless oil: R_f 0.5 (Hex/EtOAc 4:6); ¹H NMR (600 MHz, CDCl₃) δ (ppm) 7.36–7.35 (m, 2H, 2 \times CH_{STol}), 7.13–7.12 (m, 2H, 2 \times CH_{STol}), 5.56 (dd, J_{2-3} = 3.1 Hz, J_{2-1} = 1.5 Hz, 1H, H-2), 5.35 (d, J = 1.2 Hz, 1H, H-1), 4.21 (dq, J_{5-4} = 9.3 Hz, J_{5-6} = 6.2 Hz, 1H, H-5), 3.58 (td, $J_{4-3,4-5}$ = 9.4 Hz, J_{4-OH} = 2.0 Hz, 1H, H-4), 3.47 (dd, J_{3-4} = 9.4 Hz, J_{3-2} = 3.1 Hz, 1H, H-3), 3.43 (s, 3H, CH₃OMe), 2.50 (d, J = 2.2 Hz, 1H, OH), 2.33 (s, 3H, CH₃STol), 2.11 (s, 3H, CH₃Ac), 1.36 (d, J = 6.2 Hz, 3H, H-6); ¹³C NMR (150 MHz, CDCl₃) δ (ppm) 170.3 (COOR_{Ac}), 138.1 (C_{STol}), 132.4 (2C, 2 \times CH_{STol}), 130.1 (C_{STol}), 130.0 (2C, 2 \times CH_{STol}), 86.8 (C-1), 80.1 (C-3), 72.1 (C-4), 69.4, 69.3 (2C, C-2, C-5), 57.5 (CH₃OMe), 21.3 (CH₃), 21.1 (CH₃), 17.7 (C-6); HRMS (ESI-TOF) m/z [M + Na]⁺ calcd for C₁₆H₂₂NaO₅S 349.1080; found 349.1078.

***para*-Methylphenyl 2-*O*-acetyl-6-deoxy-3-*O*-methyl-1-thio- α -L-talopyranoside (33).**

A solution of anhydrous DMSO (0.57 mL, 8.0 mmol, 5.0 equiv) and anhydrous DCM (16 mL) was cooled to –10 °C and PDCl₄ (0.72 mL, 4.8 mmol, 3.0 equiv) and Et₃N (1.11 mL, 7.98 mmol, 5.0 equiv) were successively added. A solution of alcohol **32** (521 mg, 1.60 mmol, 1.0 equiv) in anhydrous DCM (8 mL) was added dropwise during 1 h. The mixture was stirred at –10 °C for 10 min under Ar, and for an additional 30 min while gradually being warmed to rt. Water (50 mL)

CHAPITRE 4 – MELIOIDOSIS PATIENT SERUM-REACTIVE SYNTHETIC TETRASACCHARIDES BEARING THE PREDOMINANT EPITOPES OF BURKHOLDERIA PSEUDOMALLEI AND BURKHOLDERIA MALLEI O-ANTIGENS

was added to the solution, which was then transferred into a separatory funnel. The organic and aqueous layers were separated, and the aqueous phase was extracted with DCM (3 × 30 mL). The combined organic layers were washed with brine (50 mL), then dried over anhydrous MgSO₄, and evaporated under reduced pressure. The resulting ketone was solubilized in MeOH (16 mL) and cooled at -10 °C. NaBH₄ (109 mg, 2.87 mmol, 1.8 equiv) was slowly added and the mixture was stirred for 1 h while gradually being warmed to 0 °C. The solution was diluted with DCM (50 mL), transferred into a separatory funnel, and washed with water (30 mL). The aqueous phase was extracted with DCM (3 × 30 mL), the combined organic phases were washed with brine (60 mL) and dried over anhydrous MgSO₄. The solution was evaporated under reduced pressure and the residue was purified by silica gel flash chromatography (Tol/EtOAc 95:5 to 85:15) to give taloside **33** (371 mg, 71%, 2 steps) as a colorless oil: *R_f* 0.4 (Tol/EtOAc 1:1); [α]_D²⁰ +268 (*c* 0.4, CHCl₃); ¹H NMR (600 MHz, CDCl₃) δ (ppm) 7.37–7.35 (m, 2H, 2 × CH_{STol}), 7.14–7.12 (m, 2H, 2 × CH_{STol}), 5.46 (m, 1H, H-2), 5.41 (d, *J* = 1.1 Hz, 1H, H-1), 4.40 (qd, *J*₅₋₆ = 6.5 Hz, *J*₅₋₄ = 0.7 Hz, 1H, H-5), 3.83 (br dd, *J*_{4-OH} = 9.1 Hz, *J*₄₋₃ = 3.2 Hz, 1H, H-4), 3.55 (t, *J* = 3.5 Hz, 1H, H-3), 3.46 (s, 3H, CH_{3OMe}), 2.46 (d, *J* = 9.3 Hz, 1H, OH), 2.33 (s, 3H, CH_{3STol}), 2.14 (s, 3H, CH_{3Ac}), 1.36 (d, *J* = 6.5 Hz, 3H, H-6); ¹³C NMR (150 MHz, CDCl₃) δ (ppm) 169.6 (COOR_{Ac}), 138.3 (C_{STol}), 132.5 (2C, 2 × CH_{STol}), 130.1 (2C, 2 × CH_{STol}), 129.8 (C_{STol}), 86.9 (C-1), 75.0 (C-3), 70.2 (C-2), 69.7 (C-4), 68.4 (C-5), 56.5 (CH_{3OMe}), 21.3 (2C, 2 × CH₃), 16.5 (C-6); HRMS (ESI-TOF) *m/z* [M + Na]⁺ calcd for C₁₆H₂₂NaO₅S 349.10802; found 349.10839.

***para*-Methylphenyl 2,4-di-*O*-acetyl-6-deoxy-3-*O*-methyl-1-thio- α -L-talopyranoside (**34**).**

Alcohol **33** (197 mg, 0.613 mmol, 1.0 equiv) was solubilized in EtOAc (6 mL) and Ac₂O (0.58 mL, 6.1 mmol, 10.0 equiv) and DMAP (8 mg, 0.06 mmol, 0.1 equiv) were added. The mixture was refluxed for 3 h under Ar. The solvents were evaporated under reduced pressure and co-evaporated with toluene (3×). The residue was purified by silica gel flash chromatography (Hex/EtOAc 9:1 to 7:3) to give compound **34** (200 mg, 90%) as a white amorphous solid: *R_f* 0.6 (Hex/EtOAc 1:1); [α]_D²⁰ -137 (*c* 0.7, CHCl₃); ¹H NMR (600 MHz, CDCl₃) δ (ppm) 7.35–7.34 (m, 2H, 2 × CH_{STol}), 7.13–7.11 (m, 2H, 2 × CH_{STol}), 5.48 (s, 1H, H-1), 5.40 (d, *J* = 3.7 Hz, 1H, H-2),

CHAPITRE 4 – MELIOIDOSIS PATIENT SERUM-REACTIVE SYNTHETIC TETRASACCHARIDES BEARING THE PREDOMINANT EPITOPES OF BURKHOLDERIA PSEUDOMALLEI AND BURKHOLDERIA MALLEI O-ANTIGENS

5.31 (br d, $J = 3.4$ Hz, 1H, H-4), 4.52 (qd, $J_{5-6} = 6.3$ Hz, $J_{5-4} = 0.8$ Hz, 1H, H-5), 3.59 (t, $J = 3.6$ Hz, 1H, H-3), 3.40 (s, 3H, CH_{3OMe}), 2.33 (s, 3H, CH_{3STol}), 2.16 (s, 3H, CH_{3Ac}), 2.13 (s, 3H, CH_{3Ac}), 1.21 (d, $J = 6.5$ Hz, 3H, H-6); ^{13}C NMR (150 MHz, $CDCl_3$) δ (ppm) 170.8 ($COOR_{Ac}$), 170.4 ($COOR_{Ac}$), 138.0 (C_{STol}), 132.0 (2C, $2 \times CH_{STol}$), 130.0 (2C, $2 \times CH_{STol}$), 129.8 (C_{STol}), 86.9 (C-1), 74.5 (C-3), 68.6, 68.5 (2C, C-2, C-4), 66.5 (C-5), 57.4 (CH_{3OMe}), 21.3, 21.2 (2C, $2 \times CH_3$), 21.0 (CH_3), 16.4 (C-6); HRMS (ESI-TOF) m/z $[M + Na]^+$ calcd for $C_{18}H_{24}NaO_6S$ 391.11858; found 391.11991.

***para*-Methylphenyl 2-*O*-acetyl-4-*O*-chloroacetyl-6-deoxy-3-*O*-methyl-1-thio- α -L-talopyranoside (35).**

Chloroacetic anhydride (268 mg, 1.57 mmol, 5.0 equiv) and DMAP (4 mg, 0.03 mmol, 0.1 equiv) were added to a solution of alcohol **33** (102 mg, 0.313 mmol, 1.0 equiv) in EtOAc (3 mL). The mixture was refluxed for 1 h under Ar, then diluted with EtOAc (3 mL). The solution was poured into a separatory funnel, washed with saturated $NaHCO_3(aq)$ (3×5 mL) and brine (5 mL), and dried over anhydrous $MgSO_4$. The solvents were evaporated under reduced pressure. The residue was purified by silica gel flash chromatography (Hex/EtOAc 8:2 to 7:3) to give compound **35** (120 mg, 95%) as a yellow oil: R_f 0.4 (Hex/EtOAc 7:3); $[\alpha]_D^{20} -107$ (c 1.0, $CHCl_3$); 1H NMR (600 MHz, $CDCl_3$) δ (ppm) 7.35–7.33 (m, 2H, $2 \times CH_{STol}$), 7.13–7.12 (m, 2H, $2 \times CH_{STol}$), 5.48 (d, $J = 1.0$ Hz, 1H, H-1), 5.41–5.38 (m, 1H, H-2), 5.37 (br d, $J = 3.5$ Hz, 1H, H-4), 4.56 (qd, $J_{5-6} = 6.5$ Hz, $J_{5-4} = 1.1$ Hz, 1H, H-5), 4.19 (d, $J = 14.9$ Hz, 1H, CHH_{AcCl}), 4.14 (d, $J = 14.9$ Hz, 1H, CHH_{AcCl}), 3.62 (t, $J = 3.6$ Hz, 1H, H-3), 3.40 (s, 3H, CH_{3OMe}), 2.33 (s, 3H, CH_{3STol}), 2.13 (s, 3H, CH_{3Ac}), 1.23 (d, $J = 6.5$ Hz, 3H, H-6); ^{13}C NMR (150 MHz, $CDCl_3$) δ (ppm) 170.4 ($COOR_{Ac}$), 167.3 ($COOR_{AcCl}$), 138.2 (C_{Ar}), 132.2 (2C, $2 \times CH_{STol}$), 130.1 (2C, $2 \times CH_{STol}$), 129.6 (C_{Ar}), 86.8 (C-1), 74.2 (C-3), 70.5 (C-4), 68.3 (C-2), 66.2 (C-5), 57.4 (CH_{3OMe}), 40.9 (CH_{2AcCl}), 21.3, 21.2 (2C, $2 \times CH_3$), 16.3 (C-6); HRMS (ESI-TOF) m/z $[M + Na]^+$ calcd for $C_{18}H_{23}ClNaO_6S$ 425.07961; found 425.07992.

CHAPITRE 4 – MELIOIDOSIS PATIENT SERUM-REACTIVE SYNTHETIC TETRASACCHARIDES BEARING THE PREDOMINANT EPITOPES OF BURKHOLDERIA PSEUDOMALLEI AND BURKHOLDERIA MALLEI O-ANTIGENS

(5-Azido-1-pentyl) 2,4-di-O-acetyl-6-deoxy-3-O-methyl- α -L-talopyranosyl-(1 \rightarrow 3)-2-O-ortho-(azidomethyl)benzoyl-4,6-O-benzylidene- β -D-glucopyranosyl-(1 \rightarrow 3)-2-O-acetyl-4-O-levulinoyl- α -L-rhamnopyranosyl-(1 \rightarrow 3)-2-O-benzyl-4,6-O-benzylidene- β -D-glucopyranoside (36).

Trisaccharide **29** (87 mg, 0.074 mmol, 1.0 equiv), thiotaloside **34** (41 mg, 0.11 mmol, 1.5 equiv) and NIS (25 mg, 0.11 mmol, 1.5 equiv) were dried together under high vacuum for 1 h. Activated ground molecular sieves (4 Å, 346 mg) and anhydrous DCM (1.5 mL) were successively added and the mixture was stirred under Ar for 1 h. The reaction flask was cooled to -10 °C and protected from light using aluminum foil. AgOTf (2 mg, 0.007 mmol, 0.1 equiv) was added and the mixture was stirred under Ar for 2 h while being gradually warmed to 0 °C. Et₃N (0.01 mL, 0.09 mmol, 1.0 equiv) was added, the yellow suspension was filtered over Celite, and the solvents were evaporated under reduced pressure. The residue was purified by silica gel flash chromatography (Hex/EtOAc 8:2 to 5:5) to give tetrasaccharide **36** (105 mg, quant.) as a white amorphous solid: R_f 0.5 (Hex/EtOAc 4:6); $[\alpha]_D^{20}$ -54 (c 0.6, CHCl₃); ¹H NMR (600 MHz, CDCl₃) δ (ppm) 7.86–7.85 (m, 1H, CH_{Ar}), 7.61–7.59 (m, 1H, CH_{Ar}), 7.57–7.54 (m, 1H, CH_{Ar}), 7.45–7.41 (m, 4H, 4 \times CH_{Ar}), 7.36–7.33 (m, 7H, 7 \times CH_{Ar}), 7.32–7.27 (m, 5H, 5 \times CH_{Ar}), 5.53 (s, 1H, H-7C), 5.52 (s, 1H, H-7A), 5.35 (dd, $J_{2-3} = 3.5$ Hz, $J_{2-1} = 1.6$ Hz, 1H, H-2B), 5.21 (dd, $J_{2-3} = 8.7$ Hz, $J_{2-1} = 7.8$ Hz, 1H, H-2C), 5.18 (br s, 1H, H-1B), 5.02 (d, $J = 3.1$ Hz, 1H, H-2D), 4.96 (br d, $J = 3.9$ Hz, 1H, H-4D), 4.91–4.82 (m, 5H, CH_{2AZMB}, CHH_{Bn}, H-4B, H-1D), 4.77 (d, $J = 10.6$ Hz, 1H, CHH_{Bn}), 4.76 (d, $J = 7.5$ Hz, 1H, H-1C), 4.49 (d, $J = 7.7$ Hz, 1H, H-1A), 4.38 (dd, $J_{6a-6b} = 10.7$ Hz, $J_{6a-5} = 5.0$ Hz, 1H, H-6aC), 4.35 (dd, $J_{6a-6b} = 11.1$ Hz, $J_{6a-5} = 5.6$ Hz, 1H, H-6aA), 4.17 (qd, $J_{5-6} = 6.5$ Hz, $J_{5-4} = 1.3$ Hz, 1H, H-5D), 4.09 (t, $J = 9.2$ Hz, 1H, H-3C), 4.10–4.04 (m, 2H, H-3B, H-5B), 3.94–3.90 (m, 2H, H-1a_{linker}, H-3A), 3.79–3.75 (m, 2H, H-6bA, H-6bC), 3.67 (t, $J = 9.4$ Hz, 1H, H-4C), 3.59–3.52 (m, 3H, H-1b_{linker}, H-5C, H-4A), 3.50–3.45 (m, 2H, H-2A, H-3D), 3.41 (td, $J_{5-4, 5-6b} = 9.7$ Hz, $J_{5-6a} = 5.0$ Hz, H-5A), 3.24 (s, 3H, CH_{3OMe}), 3.22 (t, $J = 6.9$ Hz, 2H, H-5_{linker}), 2.36–2.30 (m, 1H, CHH_{Lev}), 2.17–2.10 (m, 2H, CHH_{Lev}, CHH_{Lev}), 2.08 (s, 3H, CH_{3Ac}), 2.05 (s, 3H, CH_{3Lev}), 2.04 (s, 3H, CH_{3Ac}), 1.81–1.77 (m, 1H, CHH_{Lev}), 1.77 (s, 3H, CH_{3Ac}), 1.67–1.64 (m, 2H, H-2_{linker}) 1.60–1.59 (m, 2H, H-4_{linker}), 1.49–1.41 (m, 2H, H-3_{linker}), 0.76 (d, $J = 6.2$ Hz, 3H, H-6B), 0.70 (d, $J =$

CHAPITRE 4 – MELIOIDOSIS PATIENT SERUM-REACTIVE SYNTHETIC TETRASACCHARIDES BEARING THE PREDOMINANT EPITOPES OF BURKHOLDERIA PSEUDOMALLEI AND BURKHOLDERIA MALLEI O-ANTIGENS

6.5 Hz, 3H, H-6D); ^{13}C NMR (150 MHz, CDCl_3) δ (ppm) 206.2 (CO_{Lev}), 171.4 (COOR_{Lev}), 170.8 (COOR_{Ac}), 170.0 (COOR_{Ac}), 169.5 (COOR_{Ac}), 164.2 ($\text{COOR}_{\text{AZMB}}$), 138.7 (C_{Ar}), 138.0 (C_{Ar}), 137.14 (C_{Ar}), 137.07 (C_{Ar}), 133.1–126.2 (20C, C_{Ar} , $19 \times \text{CH}_{\text{Ar}}$), 104.2 (C-1A), 102.1, 101.7 (2C, C-7A, C-7C), 100.9 (C-1C), 99.1 (C-1D), 97.8 (C-1B), 82.7 (C-2A), 79.3 (C-4A), 79.0 (C-4C), 76.2, 76.1 (2C, C-3A, C-3C), 75.0, 74.9 (2C, C-3B, CH_2_{Bn}), 74.6 (C-2C), 73.4 (C-3D), 72.6 (C-4B), 70.9 (C-2B), 70.3 (C-1_{linker}), 68.9, 68.7, 68.5 (3C, C-6A, C-6C, C-2D), 66.5, 66.3, 66.2 (4C, C-5A, C-5B, C-5C, C-4D), 65.5 (C-5D), 57.2 (CH_3_{OMe}), 53.1 ($\text{CH}_2_{\text{AZMB}}$), 51.4 (C-5_{linker}), 37.5 (CH_2_{Lev}), 29.8 (CH_3_{Lev}), 29.4 (C-2_{linker}), 28.8 (C-4_{linker}), 27.5 (CH_2_{Lev}), 23.5 (C-3_{linker}), 21.1 (CH_3_{Ac}), 21.0 (CH_3_{Ac}), 20.8 (CH_3_{Ac}), 16.8 (C-6B), 15.8 (C-6D); HRMS (ESI-TOF) m/z [$\text{M} + \text{NH}_4$] $^+$ calcd for $\text{C}_{70}\text{H}_{88}\text{N}_7\text{O}_{25}$ 1426.58244; found 1426.58819; m/z [$\text{M} + \text{Na}$] $^+$ calcd for $\text{C}_{70}\text{H}_{84}\text{N}_6\text{NaO}_{25}$ 1431.53873; found 1431.54367.

(5-Azido-1-pentyl) 2-O-acetyl-4-O-chloroacetyl-6-deoxy-3-O-methyl- α -L-talopyranosyl-(1 \rightarrow 3)-2-O-ortho-(azidomethyl)benzoyl-4,6-O-benzylidene- β -D-glucopyranosyl-(1 \rightarrow 3)-2-O-acetyl-4-O-levulinoyl- α -L-rhamnopyranosyl-(1 \rightarrow 3)-2-O-benzyl-4,6-O-benzylidene- β -D-glucopyranoside (37).

Trisaccharide **29** (109 mg, 0.0933 mmol, 1.0 equiv), thiotaloside **35** (56 mg, 0.14 mmol, 1.5 equiv), and NIS (32 mg, 0.14 mmol, 1.5 equiv) were dried together under high vacuum for 1 h. Activated ground molecular sieves (4 Å, 435 mg) and anhydrous DCM (1.9 mL) were successively added and the mixture was stirred under Ar for 1 h. The reaction flask was cooled to -10 °C and protected from light using aluminum foil. AgOTf (2 mg, 0.009 mmol, 0.1 equiv) was added and the mixture was stirred under Ar for 2 h while being gradually warmed to 0 °C. Et_3N (0.01 mL, 0.09 mmol, 1.0 equiv) was added, the yellow suspension was filtered over Celite, and the solvents were evaporated under reduced pressure. The residue was purified by silica gel flash chromatography (Hex/EtOAc 8:2 to 5:5) to give tetrasaccharide **37** (110 mg, 82%) as a white amorphous solid: R_f 0.4 (Tol/EtOAc 7:3); $[\alpha]_{\text{D}}^{20}$ -68 (c 0.6, CHCl_3); ^1H NMR (600 MHz, CDCl_3) δ (ppm) 7.86–7.85 (m, 1H, CH_{AZMB}), 7.61–7.59 (m, 1H, CH_{Ar}), 7.57–7.55 (m, 1H, CH_{Ar}), 7.45–7.44 (m, 2H, $2 \times \text{CH}_{\text{Ar}}$), 7.42–7.41 (m, 2H, $2 \times \text{CH}_{\text{Ar}}$), 7.37–7.33 (m, 7H, $7 \times \text{CH}_{\text{Ar}}$), 7.31–7.28 (m, 5H, $5 \times \text{CH}_{\text{Ar}}$),

CHAPITRE 4 – MELIOIDOSIS PATIENT SERUM-REACTIVE SYNTHETIC TETRASACCHARIDES BEARING THE PREDOMINANT EPITOPES OF BURKHOLDERIA PSEUDOMALLEI AND BURKHOLDERIA MALLEI O-ANTIGENS

5.53 (s, 1H, H-7C), 5.52 (s, 1H, H-7A), 5.35 (dd, $J_{2-3} = 3.5$ Hz, $J_{2-1} = 1.7$ Hz, 1H, H-2B), 5.19 (dd, $J_{2-3} = 8.7$ Hz, $J_{2-1} = 7.8$ Hz, 1H, H-2C), 5.18 (d, $J = 1.6$ Hz, 1H, H-1B), 5.07 (d, $J = 3.3$ Hz, 1H, H-2D), 4.94 (br d, $J = 3.9$ Hz, 1H, H-4D), 4.90–4.81 (m, 5H, CH_{2AZMB} , CHH_{Bn} , H-1D, H-4B), 4.77 (d, $J = 7.4$ Hz, 1H, H-1C), 4.76 (d, $J = 11.0$ Hz, 1H, CHH_{Bn}), 4.49 (d, $J = 7.7$ Hz, 1H, H-1A), 4.38 (dd, $J_{6a-6b} = 10.6$ Hz, $J_{6a-5} = 4.9$ Hz, 1H, H-6aC), 4.35 (dd, $J_{6a-6b} = 10.4$ Hz, $J_{6a-5} = 4.9$ Hz, 1H, H-6aA), 4.20 (qd, $J_{5-6} = 6.2$ Hz, $J_{5-4} = 1.1$ Hz, 1H, H-5D), 4.10–4.05 (m, 3H, H-3B, H-5B, H-3C), 4.03 (d, $J = 14.8$ Hz, 1H, CHH_{AcCl}), 4.01 (d, $J = 14.8$ Hz, 1H, CHH_{AcCl}), 3.94–3.90 (m, 2H, H-1a_{linker}, H-3A), 3.77 (m, 2H, H-6bA, H-6bC), 3.67 (t, $J = 9.4$ Hz, 1H, H-4C), 3.59–3.52 (m, 3H, H-1b_{linker}, H-5C, H-4A), 3.49–3.47 (m, 2H, H-2A, H-3D), 3.41 (td, $J_{5-4, 5-6b} = 9.8$ Hz, $J_{5-6a} = 5.0$ Hz, 1H, H-5A), 3.24 (s, 3H, CH_{3OMe}), 3.22 (t, $J = 6.9$ Hz, 2H, H-5_{linker}), 2.36–2.30 (m, 1H, CHH_{Lev}), 2.14–2.07 (m, 2H, CHH_{Lev} , CHH_{Lev}), 2.07 (s, 3H, CH_{3Ac}), 2.05 (s, 3H, CH_{3Lev}), 1.82–1.80 (m, 1H, CHH_{Lev}), 1.77 (s, 3H, CH_{3Ac}), 1.69–1.63 (m, 2H, H-2_{linker}), 1.61–1.60 (m, 2H, H-4_{linker}), 1.48–1.42 (m, 2H, H-3_{linker}), 0.76 (d, $J = 6.2$ Hz, 3H, H-6B), 0.70 (d, $J = 6.5$ Hz, 3H, H-6D); ^{13}C NMR (150 MHz, $CDCl_3$) δ (ppm) 206.2 (CO_{Lev}), 171.4 ($COOR_{Lev}$), 170.0 ($COOR_{Ac}$), 169.4 ($COOR_{Ac}$), 167.3 ($COOR_{AcCl}$), 164.2 ($COOR_{AZMB}$), 139.7 (C_{Ar}), 138.0 (C_{Ar}), 137.2 (2C, 2 \times C_{Ar}), 137.1–126.2 (20C, C_{Ar} , 19 \times CH_{Ar}), 104.3 (C-1A), 102.2, 101.7 (2C, C-7A, C-7C), 100.9 (C-1C), 99.0 (C-1D), 97.8 (C-1B), 82.7 (C-2A), 79.3 (C-4A), 79.0 (C-4C), 76.4, 76.1 (2C, C-3A, C-3C), 75.0, 74.9 (2C, C-3B, CH_{2Bn}), 74.6 (C-2C), 73.1 (C-3D), 72.6 (C-4B), 71.0 (C-2B), 70.6 (C-2D), 70.3 (C-1_{linker}), 68.9, 68.7 (2C, C-6A, C-6C), 66.5, 66.3, 66.2, 66.1 (4C, C-5A, C-5B, C-5C, C-4D), 65.2 (C-5D), 57.3 (CH_{3OMe}), 53.1 (CH_{2AZMB}), 51.4 (C-5_{linker}), 40.9 (CH_{2AcCl}), 37.5 (CH_{2Lev}), 29.8 (CH_{3Lev}), 29.5 (C-2_{linker}), 28.8 (C-4_{linker}), 27.5 (CH_{2Lev}), 23.5 (C-3_{linker}), 21.1 (CH_{3Ac}), 20.8 (CH_{3Ac}), 16.8 (C-6B), 15.7 (C-6D); HRMS (ESI-TOF) m/z $[M + NH_4]^+$ calcd for $C_{70}H_{87}ClN_7O_{25}$ 1460.54347; found 1460.54641.

(5-Azido-1-pentyl) 2,4-di-O-acetyl-6-deoxy-3-O-methyl- α -L-talopyranosyl-(1 \rightarrow 3)-2-O-ortho-(azidomethyl)benzoyl-4,6-O-benzylidene- β -D-glucopyranosyl-(1 \rightarrow 3)-2-O-acetyl- α -L-rhamnopyranosyl-(1 \rightarrow 3)-2-O-benzyl-4,6-O-benzylidene- β -D-glucopyranoside (38).

A solution of tetrasaccharide **36** (98 mg, 0.070 mmol, 1.0 equiv) in anhydrous pyridine (0.45 mL) was cooled to 0 °C. Acetic acid (0.3 mL) and hydrazine monohydrate (0.02 mL, 0.4 mmol, 5.0

CHAPITRE 4 – MELIOIDOSIS PATIENT SERUM-REACTIVE SYNTHETIC TETRASACCHARIDES BEARING THE PREDOMINANT EPITOPES OF BURKHOLDERIA PSEUDOMALLEI AND BURKHOLDERIA MALLEI O-ANTIGENS

equiv) were successively added dropwise. The mixture was stirred for 16 h under Ar while gradually being warmed to rt. The solution was evaporated under reduced pressure and co-evaporated with toluene (3×). The residue was purified by silica gel flash chromatography (Tol/EtOAc 9:1 to 7:3) to give alcohol **38** (78 mg, 85%) as a white amorphous solid: R_f 0.5 (Tol/EtOAc 6:4); $[\alpha]_D^{20}$ -59 (c 0.8, CHCl_3); $^1\text{H NMR}$ (600 MHz, CDCl_3) δ (ppm) 7.95 (m, 1H, CH_{AZMB}), 7.55–7.50 (m, 2H, $2 \times \text{CH}_{\text{Ar}}$), 7.45–7.43 (m, 2H, $2 \times \text{CH}_{\text{Ar}}$), 7.39–7.27 (m, 12H, $12 \times \text{CH}_{\text{Ar}}$), 7.24–7.22 (m, 2H, $2 \times \text{CH}_{\text{Ar}}$), 5.52 (s, 1H, H-7C), 5.48 (s, 1H, H-7A), 5.31 (dd, $J_{2-3} = 3.5$ Hz, $J_{2-1} = 1.5$ Hz, 1H, H-2B), 5.29 (dd, $J = 8.7$ Hz, $J = 8.0$ Hz, 1H, H-2C), 5.14 (s, 1H, H-1B), 5.03 (d, $J = 3.1$ Hz, 1H, H-2D), 4.98 (br d, $J = 3.9$ Hz, 1H, H-4D), 4.94 (d, $J = 14.9$ Hz, 1H, CHH_{AZMB}), 4.91 (s, 1H, H-1D), 4.86 (d, $J = 10.7$ Hz, 1H, CHH_{Bn}), 4.83 (d, $J = 7.7$ Hz, 1H, H-1C), 4.79–4.77 (m, 2H, CHH_{Bn} , CHH_{AZMB}), 4.48 (d, $J = 7.7$ Hz, 1H, H-1A), 4.36 (dd, $J_{6a-6b} = 10.6$ Hz, $J_{6a-5} = 4.9$ Hz, 1H, H-6aC), 4.34 (dd, $J_{6a-6b} = 10.4$ Hz, $J_{6a-5} = 4.9$ Hz, 1H, H-6aA), 4.18 (br q, $J = 6.5$ Hz, 1H, H-5D), 4.08 (t, $J = 9.2$ Hz, 1H, H-3C), 3.96–3.89 (m, 3H, H-1a_{linker}, H-5B, H-3A), 3.85 (dd, $J_{3-4} = 9.4$ Hz, $J_{3-2} = 3.6$ Hz, 1H, H-3B), 3.77–3.72 (m, 2H, H-6bA, H-6bC), 3.66 (t, $J = 9.4$ Hz, 1H, H-4C), 3.56–3.52 (m, 2H, H-1b_{linker}, H-4A), 3.50 (m, 1H, H-5C), 3.48–3.44 (m, 3H, H-3D, H-2A, H-4B), 3.39 (td, $J = 9.7$ Hz, $J = 4.7$ Hz, 1H, H-5A), 3.26 (s, 3H, CH_3OMe), 3.20 (t, $J = 6.9$ Hz, 2H, H-5_{linker}), 2.11 (br s, 1H, OH), 2.05 (s, 3H, CH_3Ac), 2.04 (s, 3H, CH_3Ac), 1.76 (s, 3H, CH_3Ac), 1.66–1.63 (m, 2H, H-2_{linker}), 1.60–1.56 (m, 2H, H-4_{linker}), 1.46–1.40 (m, 2H, H-3_{linker}), 0.85 (d, $J = 6.2$ Hz, 3H, H-6B), 0.72 (d, $J = 6.5$ Hz, 3H, H-6D); $^{13}\text{C NMR}$ (150 MHz, CDCl_3) δ (ppm) 170.8 (COOR_{Ac}), 169.9 (COOR_{Ac}), 169.6 (COOR_{Ac}), 165.0 ($\text{COOR}_{\text{AZMB}}$), 139.0 (C_{Ar}), 138.2 (C_{Ar}), 137.1 (2C, $2 \times \text{C}_{\text{Ar}}$), 133.4–126.2 (20C, C_{Ar} , $19 \times \text{CH}_{\text{Ar}}$), 104.2 (C-1A), 102.1 (C-7C), 101.5 (2C, C-7A, C-1C), 99.0 (C-1D), 98.1 (C-1B), 82.8 (C-2A), 79.3, 79.1, 78.9 (3C, C-4A, C-4C, C-3B), 76.5 (C-3A), 75.9 (C-3C), 75.1, 75.0 (2C, C-2C, CH_2Bn), 73.4 (C-3D), 71.7 (C-4B), 70.5 (C-2B), 70.2 (C-1_{linker}), 68.9, 68.7, 68.5 (3C, C-6A, C-6C, C-2D), 67.8 (C-5B), 66.6, 66.4 (3C, C-4D, C-5A, C-5C), 65.5 (C-5D), 57.2 (CH_3OMe), 53.4 (CH_2AZMB), 51.4 (C-5_{linker}), 29.4 (C-2_{linker}), 28.7 (C-4_{linker}), 23.5 (C-3_{linker}), 21.1 (CH_3Ac), 21.0 (CH_3Ac), 20.8 (CH_3Ac), 17.1 (C-6B), 15.8 (C-6D); HRMS (ESI-TOF) m/z $[\text{M} + \text{NH}_4]^+$ calcd for $\text{C}_{65}\text{H}_{82}\text{N}_7\text{O}_{23}$ 1328.54566; found 1328.5449; m/z $[\text{M} + \text{Na}]^+$ calcd for $\text{C}_{65}\text{H}_{78}\text{N}_6\text{NaO}_{23}$ 1333.50105; found 1333.50103.

CHAPITRE 4 – MELIOIDOSIS PATIENT SERUM-REACTIVE SYNTHETIC TETRASACCHARIDES BEARING THE PREDOMINANT EPITOPES OF BURKHOLDERIA PSEUDOMALLEI AND BURKHOLDERIA MALLEI O-ANTIGENS

(5-Azido-1-pentyl) 2-O-acetyl-4-O-chloroacetyl-6-deoxy-3-O-methyl- α -L-talopyranosyl-(1 \rightarrow 3)-2-O-ortho-(azidomethyl)benzoyl-4,6-O-benzylidene- β -D-glucopyranosyl-(1 \rightarrow 3)-2-O-acetyl- α -L-rhamnopyranosyl-(1 \rightarrow 3)-2-O-benzyl-4,6-O-benzylidene- β -D-glucopyranoside (39).

A solution of tetrasaccharide **37** (476 mg, 0.330 mmol, 1.0 equiv) in anhydrous pyridine (2 mL) was cooled at 0 °C. Acetic acid (1.4 mL) and hydrazine monohydrate (0.08 mL, 2 mmol, 5.0 equiv) were successively added dropwise. The mixture was stirred for 3 h under Ar while gradually being warmed to rt. The solution was evaporated under reduced pressure and co-evaporated with toluene (3 \times). The residue was purified by silica gel flash chromatography (Tol/EtOAc 9:1 to 7:3) to give alcohol **39** (290 mg, 65%) as a white amorphous solid: R_f 0.7 (Tol/EtOAc 7:3); $[\alpha]_D^{20}$ -52 (c 0.6, CHCl₃); ¹H NMR (600 MHz, CDCl₃) δ (ppm) 7.95–7.93 (m, 1H, CH_{AZMB}), 7.55–7.51 (m, 2H, 2 \times CH_{Ar}), 7.45–7.43 (m, 2H, 2 \times CH_{Ar}), 7.39–7.27 (m, 12H, 12 \times CH_{Ar}), 7.24–7.22 (m, 2H, 2 \times CH_{Ar}), 5.52 (s, 1H, H-7C), 5.49 (s, 1H, H-7A), 5.31 (dd, $J_{2-3} = 3.5$ Hz, $J_{2-1} = 1.6$ Hz, 1H, H-2B), 5.28 (dd, $J = 8.8$ Hz, $J = 7.8$ Hz, 1H, H-2C), 5.14 (d, $J = 1.2$ Hz, H-1B), 5.08 (br s, 1H, H-2D), 4.97 (br d, $J = 3.9$ Hz, 1H, H-4D), 4.94 (d, $J = 14.9$ Hz, 1H, CHH_{AZMB}), 4.90 (br s, 1H, H-1D), 4.86 (d, $J = 10.7$ Hz, 1H, CHH_{Bn}), 4.83 (d, $J = 7.7$ Hz, 1H, H-1C), 4.79–4.76 (m, 2H, CHH_{AZMB}, CHH_{Bn}), 4.48 (d, $J = 7.7$ Hz, 1H, H-1A), 4.36 (dd, $J_{6a-6b} = 10.8$ Hz, $J_{6a-5} = 5.1$ Hz, 1H, H-6aC), 4.34 (dd, $J_{6a-6b} = 10.6$ Hz, $J_{6a-5} = 5.1$ Hz, 1H, H-6aA), 4.20 (br q, $J = 6.6$ Hz, 1H, H-5D), 4.08–4.00 (m, 3H, CH_{2AcCl}, H-3C), 3.95–3.89 (m, 3H, H-1a_{linker}, H-5B, H-3A), 3.85 (dd, $J_{3-4} = 9.4$ Hz, $J_{3-2} = 3.6$ Hz, 1H, H-3B), 3.76 (br d, $J = 10.4$ Hz, 1H, H-6bA) 3.73 (br d, $J = 10.5$ Hz, 1H, H-6bC), 3.67 (t, $J = 9.4$ Hz, 1H, H-4C), 3.56–3.50 (m, 4H, H-1b_{linker}, H-3D, H-4A, H-5C), 3.48–3.43 (m, 2H, H-2A, H-4B), 3.39 (td, $J = 9.7$ Hz, $J = 5.0$ Hz, 1H, H-5A), 3.26 (s, 3H, CH_{3OMe}), 3.20 (t, $J = 6.9$ Hz, 2H, H-5_{linker}), 2.08 (br s, 1H, OH), 2.03 (s, 3H, CH_{3Ac}), 1.76 (s, 3H, CH_{3Ac}), 1.66–1.62 (m, 2H, H-2_{linker}), 1.61–1.56 (m, 2H, H-4_{linker}), 1.47–1.40 (m, 2H, H-3_{linker}), 0.85 (d, $J = 6.2$ Hz, 3H, H-6B), 0.72 (d, $J = 6.2$ Hz, 3H, H-6D); ¹³C NMR (150 MHz, CDCl₃) δ (ppm) 169.9 (COOR_{Ac}), 169.5 (COOR_{Ac}), 167.3 (COOR_{AcCl}), 165.0 (COOR_{AZMB}), 139.0 (C_{Ar}), 138.2 (C_{Ar}), 137.1 (C_{Ar}), 137.0 (C_{Ar}), 133.4–126.2 (20C, C_{Ar}, 19 \times CH_{Ar}), 104.2 (C-1A), 102.2, 101.59, 101.56 (3C, C-1C, C-7A, C-7C), 98.9 (C-1D), 98.1 (C-1B), 82.8 (C-2A), 79.4, 79.1, 78.9 (3C, C-4A, C-4C, C-3B), 76.5 (C-3A), 76.1

CHAPITRE 4 – MELIOIDOSIS PATIENT SERUM-REACTIVE SYNTHETIC TETRASACCHARIDES BEARING THE PREDOMINANT EPITOPES OF BURKHOLDERIA PSEUDOMALLEI AND BURKHOLDERIA MALLEI O-ANTIGENS

(C-3C), 75.1, 75.0 (2C, CH₂Bn, C-2C), 73.1 (C-3D), 71.8 (C-4B), 70.6, 70.5 (2C, C-2B, C-2D), 70.2 (C-1_{linker}), 68.9, 68.7 (2C, C-6A, C-6C), 67.8 (C-5B), 66.5 (C-5A), 66.4 (C-5C), 66.2 (C-4D), 65.2 (C-5D), 57.3 (CH₃OMe), 53.4 (CH₂AZMB), 51.4 (C-5_{linker}), 40.9 (CH₂AcCl), 29.4 (C-2_{linker}), 28.8 (C-4_{linker}), 23.5 (C-3_{linker}), 21.1 (CH₃Ac), 20.8 (CH₃Ac), 17.1 (C-6B), 15.8 (C-6D); HRMS (ESI-TOF) m/z [M + NH₄]⁺ calcd for C₆₅H₈₁N₇O₂₃ 1362.50669; found 1362.51071; m/z [M + Na]⁺ calcd for C₆₅H₇₇ClN₆NaO₂₃ 1367.46208; found 1367.46835.

(5-Azido-1-pentyl) 2,4-di-O-acetyl-6-deoxy-3-O-methyl- α -L-talopyranosyl-(1→3)-2-O-ortho-(azidomethyl)benzoyl-4,6-O-benzylidene- β -D-glucopyranosyl-(1→3)-2-O-acetyl-6-deoxy- α -L-talopyranosyl-(1→3)-2-O-benzyl-4,6-O-benzylidene- β -D-glucopyranoside (40).

Dess-Martin periodinane (10 mg, 0.023 mmol, 2.2 equiv) was added to a solution of alcohol **38** (14 mg, 0.011 mmol, 1.0 equiv) in anhydrous DCE (0.16 mL). The mixture was refluxed under Ar for 1 h, then cooled to rt. The solution was diluted with DCM (1 mL) and quenched with 10% Na₂S₂O₃(aq) (1 mL). The solution was transferred into a separatory funnel and the organic and aqueous layers were separated. The organic phase was washed with brine (1 mL), dried over anhydrous MgSO₄, and evaporated under reduced pressure. The residue was purified by silica gel flash chromatography (Hex/EtOAc 9:1 to 6:4) to give the corresponding ketone as a white solid. The latter was dissolved in anhydrous DCM/MeOH (0.2 mL, 1:3) and the solution was cooled to -10 °C. NaBH₄ (2 mg, 0.04 mmol, 4.0 equiv) was slowly added and the mixture was stirred under Ar for 1 h while gradually being warmed to 0 °C. The solution was diluted with DCM (1 mL) and washed with water (1 mL). The aqueous layer was extracted with DCM (3 × 1 mL). The combined organic layers were washed with brine (4 mL), dried over anhydrous MgSO₄, and evaporated under reduced pressure. The residue was purified by silica gel flash chromatography (Tol/EtOAc 9:1 to 7:3) to give alcohol **40** (7 mg, 52%) as a white amorphous solid: R_f 0.3 (Tol/EtOAc 7:3); $[\alpha]_D^{20}$ -96 (c 0.1, CHCl₃); ¹H NMR (600 MHz, CDCl₃) δ (ppm) 8.00-7.98 (m, 1H, CH_{AZMB}), 7.56-7.52 (m, 2H, 2 × CH_{Ar}), 7.45-7.42 (m, 4H, 4 × CH_{Ar}), 7.38-7.34 (m, 6H, 6 × CH_{Ar}), 7.31-7.27 (m, 5H, 5 × CH_{Ar}), 7.25-7.24 (m, 1H, CH_{Ar}), 5.54 (s, 1H, H-7C), 5.50 (s, 1H, H-7A), 5.31 (dd, J_{2-3} = 8.9 Hz, J_{2-1} = 7.9 Hz, 1H, H-2C), 5.22 (br d, J = 3.7 Hz, 1H, H-2B), 5.20 (s, 1H, H-1B), 5.03 (br d, J

CHAPITRE 4 – MELIOIDOSIS PATIENT SERUM-REACTIVE SYNTHETIC TETRASACCHARIDES BEARING THE PREDOMINANT EPITOPES OF BURKHOLDERIA PSEUDOMALLEI AND BURKHOLDERIA MALLEI O-ANTIGENS

= 3.1 Hz, 1H, H-2D), 4.98 (br d, $J = 3.9$ Hz, 1H, H-4D), 4.93 (d, $J = 7.7$ Hz, 1H, H-1C), 4.89-4.84 (m, 4H, CH_{2AZMB} , CHH_{Bn} , H-1D), 4.71 (d, $J = 10.8$ Hz, 1H, CHH_{Bn}), 4.48 (d, $J = 7.8$ Hz, 1H, H-1A), 4.36 (dd, $J_{6a-6b} = 10.8$ Hz, $J_{6a-5} = 5.1$ Hz, 1H, H-6aC), 4.33 (dd, $J_{6a-6b} = 11.0$ Hz, $J_{6a-5} = 5.4$ Hz, 1H, H-6aA), 4.17 (br q, $J = 5.4$ Hz, 1H, H-5D), 4.12-4.08 (m, 2H, H-5B, H-3C), 4.07 (t, $J = 3.6$ Hz, 1H, H-3B), 3.94 (t, $J = 8.2$ Hz, 1H, H-3A), 3.93-3.88 (m, 1H, H-1a_{linker}), 3.80-3.74 (m, 2H, H-6bA, H-6bC), 3.69 (t, $J = 9.4$ Hz, 1H, H-4C), 3.57-3.50 (m, 4H, H-1b_{linker}, H-4A, H-4B, H-5C), 3.48 (t, $J = 3.7$ Hz, 1H, H-3D), 3.46-3.38 (m, 2H, H-2A, H-5A), 3.27 (s, 3H, CH_{3OMe}), 3.19 (t, $J = 6.9$ Hz, 2H, H-5_{linker}), 2.24 (br d, $J = 9.7$ Hz, 1H, OH), 2.04 (s, 3H, CH_{3Ac}), 1.76 (s, 3H, CH_{3Ac}), 1.67-1.61 (m, 2H, H-2_{linker}), 1.61 (s, 3H, CH_{3Ac}), 1.60-1.53 (m, 2H, H-4_{linker}), 1.46-1.39 (m, 2H, H-3_{linker}), 0.93 (d, $J = 6.5$ Hz, 3H, H-6B), 0.72 (d, $J = 6.5$ Hz, 3H, H-6D); ^{13}C NMR (150 MHz, $CDCl_3$) δ (ppm) 170.9 ($COOR_{Ac}$), 169.6 ($COOR_{Ac}$), 168.8 ($COOR_{Ac}$), 164.5 ($COOR_{AZMB}$), 139.4 (C_{Ar}), 138.2 (C_{Ar}), 137.4 (C_{Ar}), 137.0 (C_{Ar}), 133.2-126.28 (20C, C_{Ar} , $19 \times CH_{Ar}$), 104.3 (C-1A), 102.2, 101.8 (2C, C-7A, C-7C), 99.0 (C-1D), 98.4 (C-1B), 97.2 (C-1C), 83.1 (C-2A), 79.23, 79.16 (2C, C-4A, C-4C), 76.1 (C-3A), 75.7 (C-3C), 74.9 (CH_{2Bn}), 74.5 (C-2C), 73.4 (C-3D), 70.4 (C-3B), 70.3 (C-1_{linker}), 69.4, 69.0, 68.8, 68.5, 68.0 (5C, C-2B, C-2D, C-6A, C-6C, C-4B), 66.9, 66.41, 66.39, 66.37 (4C, C-5A, C-5B, C-5C, C-4D), 65.4 (C-5D), 57.2 (CH_{3OMe}), 53.1 (CH_{2AZMB}), 51.4 (C-5_{linker}), 29.4 (C-2_{linker}), 28.7 (C-4_{linker}), 23.5 (C-3_{linker}), 21.0 (CH_{3Ac}), 20.8 (CH_{3Ac}), 20.3 (CH_{3Ac}), 16.1 (C-6B), 15.9 (C-6D); HRMS (ESI-TOF) m/z $[M + NH_4]^+$ calcd for $C_{65}H_{82}N_7O_{23}$ 1328.54566; found 1328.54556; m/z $[M + Na]^+$ calcd for $C_{65}H_{78}N_6NaO_{23}$ 1333.50105; found 1333.50256.

(5-Azido-1-pentyl) 2-O-acetyl-4-O-chloroacetyl-6-deoxy-3-O-methyl- α -L-talopyranosyl-(1 \rightarrow 3)-2-O-ortho-(azidomethyl)benzoyl-4,6-O-benzylidene- β -D-glucopyranosyl-(1 \rightarrow 3)-2-O-acetyl-6-deoxy- α -L-talopyranosyl-(1 \rightarrow 3)-2-O-benzyl-4,6-O-benzylidene- β -D-glucopyranoside (31).

A solution of anhydrous DMSO (0.06 mL, 0.8 mmol, 10.0 equiv) in anhydrous DCM (1.4 mL) was cooled at -10 °C and PDCP (0.07 mL, 0.5 mmol, 6.0 equiv) and Et_3N (0.11 mL, 0.80 mmol, 10.0 equiv) were successively added. A solution of alcohol **39** (108 mg, 0.0803 mmol, 1.0 equiv) in anhydrous DCM (0.4 mL) was added dropwise for 30 min. The mixture was stirred at -10 °C for 10 min under Ar, and for an additional 30 min while gradually being warmed to rt. Water (5

CHAPITRE 4 – MELIOIDOSIS PATIENT SERUM-REACTIVE SYNTHETIC TETRASACCHARIDES BEARING THE PREDOMINANT EPITOPES OF BURKHOLDERIA PSEUDOMALLEI AND BURKHOLDERIA MALLEI O-ANTIGENS

mL) was added to the solution, which was then transferred into a separatory funnel. The organic and aqueous layers were separated, and the aqueous phase was extracted with DCM (3×5 mL). The combined organic layers were washed with brine (10 mL), then dried over anhydrous MgSO_4 , and evaporated under reduced pressure. The residue was purified by silica gel flash chromatography (Tol/EtOAc 9:1 to 8:2) to give the ketone as a white amorphous solid. The latter was solubilized in MeOH (1.1 mL) and DCM (0.4 mL) and cooled to -10 °C. NaBH_4 (12 mg, 0.32 mmol, 4.0 equiv) was slowly added and the mixture was stirred 1 h while gradually being warmed to 0 °C. The solution was diluted with DCM (5 mL), transferred in a separatory funnel, and washed with water (5 mL). The aqueous phase was extracted with DCM (3×5 mL), the combined organic phases were washed with brine (10 mL) and dried over anhydrous MgSO_4 . The solution was evaporated under reduced pressure. The resulting crude alcohol (80.8 mg) was dissolved in anhydrous MeOH (2.3 mL) and anhydrous pyridine (2.3 mL). Thiourea (183 mg, 2.40 mmol, 30 eq.) was added and the solution was stirred under Ar for 3 h at 60 °C. The solvents were evaporated under reduced pressure and co-evaporated with toluene. The resulting white solid was dissolved in a 2:1 mixture of DCM/MeOH (10 mL) and washed with 1 N HCl(aq) (10 mL). The aqueous phase was extracted with DCM (3×10 mL) and the combined organic layers were washed with saturated NaHCO_3 (aq) (30 mL) and brine (30 mL). The organic phase was dried over anhydrous MgSO_4 and evaporated under reduced pressure. The residue was purified by silica gel flash chromatography (Tol/EtOAc 9:1 to 7:3) to give alcohol **31** (58.9 mg, 58% over 3 steps) as a white amorphous solid: R_f 0.5 (Tol/EtOAc 1:1); $[\alpha]_D^{20} -79$ (c 0.9, CHCl_3); $^1\text{H NMR}$ (600 MHz, CDCl_3) δ (ppm) 8.02–8.00 (m, 1H, CH_{AZMB}), 7.56–7.52 (m, 2H, $2 \times \text{CH}_{\text{Ar}}$), 7.47–7.45 (m, 2H, $2 \times \text{CH}_{\text{Ar}}$), 7.43–7.42 (m, 2H, $2 \times \text{CH}_{\text{Ar}}$), 7.37–7.28 (m, 11H, $11 \times \text{CH}_{\text{Ar}}$), 7.26–7.22 (m, 1H, CH_{Ar}), 5.54 (s, 1H, H-7C), 5.50 (s, 1H, H-7A), 5.30 (dd, $J_{2-3} = 9.0$ Hz, $J_{2-1} = 7.8$ Hz, 1H, H-2C), 5.22 (br d, $J = 3.8$ Hz, 1H, H-2B), 5.20 (br s, 1H, H-1B), 5.02 (br d, $J = 3.7$ Hz, 1H, H-2D), 4.92 (d, $J = 7.8$ Hz, 1H, H-1C), 4.88–4.85 (m, 4H, CHH_{Bn} , $\text{CH}_2_{\text{AZMB}}$, H-1D), 4.71 (d, $J = 10.8$ Hz, 1H, CHH_{Bn}), 4.48 (d, $J = 7.8$ Hz, 1H, H-1A), 4.36 (dd, $J_{6a-6b} = 10.6$ Hz, $J_{6a-5} = 4.9$ Hz, 1H, H-6aC), 4.33 (dd, $J_{6a-6b} = 10.6$ Hz, $J_{6a-5} = 5.0$ Hz, 1H, H-6aA), 4.13 (t, $J = 9.2$ Hz, 1H, H-3C), 4.11–4.05 (m, 3H, H-3B, H-5B, H-5D), 3.94 (t, $J = 9.2$ Hz, 1H, H-3A), 3.91–3.89 (m, 1H, H-1a_{linker}), 3.78 (t, $J = 10.2$ Hz, 1H,

CHAPITRE 4 – MELIOIDOSIS PATIENT SERUM-REACTIVE SYNTHETIC TETRASACCHARIDES BEARING THE PREDOMINANT EPITOPES OF BURKHOLDERIA PSEUDOMALLEI AND BURKHOLDERIA MALLEI O-ANTIGENS

H-6bA*), 3.76 (t, $J = 10.3$ Hz, 1H, H-6bC*), 3.68 (t, $J = 9.4$ Hz, 1H, H-4C), 3.58–3.50 (m, 5H, H-1b_{linker}, H-5C, H-4B, H-4D, H-4A), 3.45–3.39 (m, 3H, H-5A, H-2A, H-3D), 3.32 (s, 3H, CH_{3OMe}), 3.19 (t, $J = 6.9$ Hz, 2H, H-5_{linker}), 2.22 (d, $J = 9.8$ Hz, 1H, OH), 2.20 (d, $J = 8.5$ Hz, 1H, OH), 1.78 (s, 3H, CH_{3Ac}), 1.66–1.62 (m, 2H, H-2_{linker}), 1.60 (s, 3H, CH_{3Ac}), 1.59–1.56 (m, 2H, H-4_{linker}), 1.45–1.40 (m, 2H, H-3_{linker}), 0.93 (d, $J = 6.5$ Hz, 3H, H-6B*), 0.90 (d, $J = 6.5$ Hz, 3H, H-6D*); ¹³C NMR (150 MHz, CDCl₃) δ (ppm) 168.9 (COOR_{Ac}), 168.8 (COOR_{Ac}), 164.6 (COOR_{AZMB}), 139.3 (C_{Ar}), 138.1 (C_{Ar}), 137.3 (C_{Ar}), 137.0 (C_{Ar}), 133.2–126.3 (20C, C_{Ar}, 19 \times CH_{Ar}), 104.2 (C-1A), 102.1, 101.8 (2C, C-7A, C-7C), 98.6, 98.4 (2C, C-1B, C-1D), 97.2 (C-1C), 83.0 (C-2A), 79.2 (2C, C-4A, C-4C), 76.1 (C-3A), 75.8 (C-3C), 74.9 (CH_{2Bn}), 74.5 (C-2C), 73.9 (C-3D), 70.4 (C-3B), 70.2 (C-1_{linker}), 69.34, 69.26, 68.9, 68.8 (4C, C-6A, C-6C, C-2B, C-4D), 68.0, 67.7, 67.2 (3C, C-4B, C-2D, C-5D), 66.8 (C-5C), 66.4 (2C, C-5A, C-5B), 56.3 (CH_{3OMe}), 53.1 (CH_{2AZMB}), 51.4 (C-5_{linker}), 29.4 (C-2_{linker}), 28.7 (C-4_{linker}), 23.5 (C-3_{linker}), 20.7 (CH_{3Ac}), 20.3 (CH_{3Ac}), 16.1, 16.0 (2C, C-6B, C-6D); HRMS (ESI-TOF) m/z [M + NH₄]⁺ calcd for C₆₃H₈₀N₇O₂₂ 1286.53509; found 1286.53314; m/z [M + Na]⁺ calcd for C₆₃H₇₆N₆NaO₂₂ 1291.49049; found 1291;48805.

(5-Amino-1-pentyl) 2-O-acetyl-4-O-levulinoyl-3-O-para-methoxybenzyl- α -L-rhamnopyranosyl-(1 \rightarrow 3)-2-O-benzyl-4,6-O-benzylidene- β -D-glucopyranoside (41).

PPh₃ (3 mg, 0.01 mmol, 2.0 equiv) was added to a solution of disaccharide **26** (5 mg, 0.006 mmol, 1.0 equiv) in anhydrous THF (0.17 mL). The mixture was stirred at 60 °C under argon for 2 h, after which water (0.02 mL) was added. The solution was stirred for an additional 4 h at 60 °C and the solvents were evaporated under reduced pressure. The residue was purified by silica gel flash chromatography (DCM/MeOH 95:5 to 8:2) to give disaccharide **41** (4 mg, 88%) as a white amorphous solid; R_f 0.5 (DCM/MeOH 8:2); $[\alpha]_D^{20}$ -41 (c 0.4, CHCl₃); ¹H NMR (600 MHz, CDCl₃) δ (ppm) 7.44–7.43 (m, 2H, 2 \times CH-Ar), 7.35–7.30 (m, 8H, 8 \times CH-Ar), 7.19 (m, 2H, 2 \times CH_{PMB}), 6.85 (m, 2H, 2 \times CH_{PMB}), 5.51 (s, 1H, H-7A), 5.43 (dd, $J_{2-3} = 3.2$ Hz, $J_{2-1} = 1.7$ Hz, 1H, H-2B), 5.17 (br s, 1H, H-1B), 4.89–4.83 (m, 2H, H-4B, CHHPh), 4.69 (d, $J = 10.8$ Hz, 1H, CHHPh), 4.58 (d, $J = 10.6$ Hz, 1H, CHHPh), 4.49 (d, $J = 7.8$ Hz, 1H, H-1A), 4.35 (dd, $J_{6a-6b} = 10.6$ Hz, $J_{6a-5} = 5.0$ Hz, 1H, H-6aA), 4.32 (d, $J = 11.6$ Hz, 1H, CHHPh), 4.06 (dq, $J_{5-4} = 10.0$ Hz, $J_{5-6} = 6.2$ Hz, 1H, H-5B), 3.94–3.88 (m, 2H, H-1a_{linker}, H-3A), 3.80–3.78 (m, 1H, H-3B), 3.77 (s, 3H, CH_{3PMB}),

CHAPITRE 4 – MELIOIDOSIS PATIENT SERUM-REACTIVE SYNTHETIC TETRASACCHARIDES BEARING THE PREDOMINANT EPITOPES OF BURKHOLDERIA PSEUDOMALLEI AND BURKHOLDERIA MALLEI O-ANTIGENS

3.75 (m, 1H, H-6bA), 3.58–3.51 (m, 2H, H-1b_{linker}, H-4A), 3.45–3.39 (m, 2H, H-2A, H-5A), 2.80 (br s, 2H, H-5_{linker}), 2.71–2.66 (m, 1H, CHH_{Lev}), 2.62–2.57 (m, 1H, CHH_{Lev}), 2.48–2.38 (m, 2H, CH_{2Lev}), 2.14 (s, 3H, CH_{3Lev}), 2.05 (s, 3H, CH_{3Ac}), 1.69–1.64 (m, 4H, H-2_{linker}, H-4_{linker}), 1.45–1.41 (m, 2H, H-3_{linker}), 0.78 (d, $J = 6.2$ Hz, 3H, H-6B). ¹³C NMR (600 MHz, CDCl₃) δ (ppm) 206.4 (CO_{Lev}), 172.0 (COOR_{Lev}), 170.2 (COOR_{Ac}), 159.3 (C-Ar), 137.9 (C-Ar), 137.2 (C-Ar), 130.4 (C-Ar), 129.5–126.3 (12C, 12 \times CH-Ar), 113.8 (2C, 2 \times CH_{PMB}), 104.3 (C-1A), 101.8 (C-7A), 98.4 (C-1B), 82.7 (C-2A), 79.3 (C-4A), 76.3 (C-3A), 75.0 (CH₂Ph), 74.6 (C-3B), 72.9 (C-4B), 71.1 (CH₂Ph), 70.2 (C-1_{linker}), 68.9 (C-6A), 68.5 (C-2B), 66.5 (2C, C-5A, C-5B), 55.4 (CH_{3PMB}), 40.5 (C-5_{linker}), 38.0 (CH_{2Lev}), 30.0 (CH_{3Lev}), 29.9 (C-2_{linker}), 29.5 (C-4_{linker}), 28.1 (CH_{2Lev}), 23.4 (C-3_{linker}), 21.1 (CH_{3Ac}), 17.0 (C-6B); HRMS (ESI-TOF) m/z [M + H]⁺ calcd for C₄₆H₆₀NO₁₄ 850.40083; found 850.40044; m/z [M + Na]⁺ calcd for C₄₆H₅₉NNaO₁₄ 872.3828; found 872.3821.

(5-Amino-1-pentyl) 4,6-O-benzylidene-3-O-para-methoxybenzyl- β -D-glucopyranosyl-(1 \rightarrow 3)-2-O-acetyl-4-O-levulinoyl- α -L-rhamnopyranosyl-(1 \rightarrow 3)-2-O-benzyl-4,6-O-benzylidene- β -D-glucopyranoside (42).

PPh₃ (8 mg, 0.03 mmol, 4.0 equiv) was added to a solution of trisaccharide **27** (10 mg, 0.0078 mmol, 1.0 equiv) in anhydrous THF (0.23 mL). The mixture was stirred at 60 °C under argon for 2 h, after which water (0.02 mL) was added. The solution was stirred for an additional 4 h at 60 °C and the solvents were evaporated under reduced pressure. The residue was purified by silica gel flash chromatography (DCM/MeOH 95:5 to 8:2) to give trisaccharide **42** (7 mg, 76%) as a white amorphous solid: R_f 0.4 (DCM/MeOH 8:2); $[\alpha]_D^{20}$ -42 (c 0.5, CHCl₃); ¹H NMR (600 MHz, CDCl₃) δ (ppm) 7.48–7.46 (m, 4H, 4 \times CH-Ar), 7.37–7.30 (m, 13H, 13 \times CH-Ar), 6.83–6.81 (m, 2H, 2 \times CH-Ar), 5.54 (s, 1H, H-7C), 5.52 (s, 1H, H-7A), 5.30 (br d, $J = 3.7$, 1H, H-2B), 5.21 (br s, 1H, H-1B), 4.97 (t, $J = 9.9$ Hz, 1H, H-4B), 4.85–4.76 (m, 4H, CH_{2Bn}, CH_{2PMB}), 4.46 (d, $J = 7.7$ Hz, 1H, H-1A), 4.41 (d, $J = 7.5$ Hz, 1H, H-1C), 4.34 (dd, $J_{6a-6b} = 10.4$ Hz, $J_{6a-5} = 4.7$ Hz, 1H, H-6aC), 4.31 (dd, $J_{6a-6b} = 10.5$ Hz, $J_{6a-5} = 4.9$ Hz, 1H, H-6aA), 4.16 (dq, $J_{5-4} = 10.0$ Hz, $J_{5-6} = 6.1$ Hz, 1H, H-5B), 4.04 (dd, $J_{3-4} = 9.8$ Hz, $J_{3-2} = 3.5$ Hz, 1H, H-3B), 3.93 (t, $J = 9.2$ Hz, 1H, H-3A), 3.88-

CHAPITRE 4 – MELIOIDOSIS PATIENT SERUM-REACTIVE SYNTHETIC TETRASACCHARIDES BEARING THE PREDOMINANT EPITOPES OF BURKHOLDERIA PSEUDOMALLEI AND BURKHOLDERIA MALLEI O-ANTIGENS

3.85 (m, 1H, H-1_alinker), 3.80–3.75 (m, 4H, CH₃PMB, H-6bC), 3.70–3.66 (m, 1H, H-6bA), 3.59–3.51 (m, 5H, H-1_blinker, H-2C, H-3C, H-4C, H-4A), 3.47 (t, *J* = 8.3 Hz, 1H, H-2A), 3.41 (t, *J* = 9.8 Hz, 1H, H-4A*), 3.40 (t, *J* = 9.6 Hz, 1H, H-5C*), 2.85–2.82 (m, 2H, H-5_{linker}), 2.81–2.78 (m, 1H, CHH_{Lev}), 2.65–2.53 (m, 2H, CHH_{Lev}, CHH_{Lev}), 2.38–2.34 (m, 1H, CHH_{Lev}), 2.18 (s, 3H, CH₃Lev), 2.04 (s, 3H, CH₃Ac), 1.70–1.68 (m, 2H, H-2_{linker}), 1.62–1.60 (m, 2H, H-4_{linker}), 1.40–1.36 (m, 2H, H-3_{linker}), 0.82 (d, *J* = 6.1 Hz, 3H, H-6B); ¹³C NMR (150 MHz, CDCl₃) δ (ppm) 207.7 (CO_{Lev}), 172.4 (COOR_{Lev}), 170.0 (COOR_{Ac}), 159.3 (C-Ar), 138.1 (C-Ar), 137.6 (C-Ar), 137.3 (C-Ar), 131.0–126.2 (18C, C-Ar, 17 x CH-Ar), 113.8 (2C, 2 x CH_{PMB}), 104.6, 104.2 (2C, C-1A, C-1C), 101.8, 101.3 (2C, C-7A, C-7C), 97.7 (C-1B), 82.7 (C-2A), 81.0, 79.3 (2C, C-4A, C-4C), 76.5, 76.0 (C-3A, C-3C*), 74.9 (2C, C-3B, CH₂Bn), 74.4, 74.3 (2C, CH₂PMB, C-2C*), 72.8 (C-4B), 71.4 (C-2B), 70.0 (C-1_{linker}), 68.9, 68.8 (2C, C-6A, C-6C), 66.44, 66.35, 65.9 (3C, C-5A, C-5B, C-5C), 55.4 (CH₃PMB), 39.9 (C-5_{linker}), 37.9 (CH₂Lev), 30.1 (CH₃Lev), 29.9 (C-2_{linker}), 29.2 (C-4_{linker}), 27.4 (CH₂Lev), 23.1 (C-3_{linker}), 21.2 (CH₃Ac), 16.9 (C-6B); HRMS (ESI-TOF) *m/z* [M + H]⁺ calcd for C₅₉H₇₄NO₁₉ 1100.48496; found 1100.48469; *m/z* [M + Na]⁺ calcd for C₅₉H₇₃NNaO₁₉ 1122.4669; found 1122.4666.

(5-Amino-1-pentyl) 2-O-acetyl-4-O-chloroacetyl-6-deoxy-3-O-methyl-α-L-talopyranosyl-(1→3)-4,6-O-benzylidene-β-D-glucopyranosyl-(1→3)-2-O-acetyl-6-deoxy-α-L-talopyranosyl-(1→3)-2-O-benzyl-4,6-O-benzylidene-β-D-glucopyranoside (43).

PPh₃ (3 mg, 0.01 mmol, 4.0 equiv) was added to a solution of tetrasaccharide **31** (4 mg, 0.003 mmol, 1.0 equiv) in anhydrous THF (0.1 mL). The mixture was stirred at 60 °C under argon for 2 h, after which water (0.01 mL) was added. The solution was stirred for an additional 4 h at 60 °C, and the solvents were evaporated under reduced pressure. The residue was purified by silica gel flash chromatography (DCM/MeOH 95:5 to 8:2) to give tetrasaccharide **43** (2.1 mg, 63%) as a white amorphous solid: *R_f* 0.5 (DCM/MeOH 8:2); [α]_D²⁰ –75 (*c* 0.2, CHCl₃); ¹H NMR (600 MHz, CDCl₃) δ (ppm) 7.44–7.43 (m, 4H, 4 x CH-Ar), 7.37–7.29 (m, 11H, 11 x CH-Ar), 5.49 (2 x s, 2H, H-7A, H-7C), 5.31 (br s, 1H, H-1B*), 5.30 (br d, *J* = 2.7 Hz, 1H, H-2D), 5.28 (br d, *J* = 3.4 Hz, 1H, H-2B), 5.26 (s, 1H, H-1D*), 4.84 (d, *J* = 10.9 Hz, 1H, CHH_{Bn}), 4.76 (d, *J* = 10.9 Hz, 1H, CHH_{Bn}), 4.49 (d, *J* = 7.8 Hz, 1H, H-1A*), 4.48 (d, *J* = 7.7 Hz, 1H, H-1C*), 4.34 (dd, *J*_{6a-6b} = 10.2

CHAPITRE 4 – MELIOIDOSIS PATIENT SERUM-REACTIVE SYNTHETIC TETRASACCHARIDES BEARING THE PREDOMINANT EPITOPES OF BURKHOLDERIA PSEUDOMALLEI AND BURKHOLDERIA MALLEI O-ANTIGENS

Hz, $J_{6a-5} = 4.9$ Hz, 1H, H-6aA*), 4.32 (dd, $J_{6a-6b} = 10.2$ Hz, $J_{6a-5} = 4.7$ Hz, 1H, H-6aC*), 4.19–4.14 (m, 2H, H-5B, H-5D), 4.03 (t, $J = 3.5$ Hz, 1H, H-3B), 3.95 (t, $J = 9.2$ Hz, 1H, H-3A), 3.91–3.86 (m, 2H, H-1a_{linker}, H-3C), 3.75 (t, $J = 10.2$ Hz, 2H, H-6bA, H-6bC), 3.60–3.58 (m, 2H, H-2C, H-4D), 3.54–3.50 (m, 5H, H-3D, H-4A, H-4B, H-4C, H-1b_{linker}), 3.46–3.42 (m, 3H, H-2A, H-5A, H-5C), 3.40 (s, 3H, CH₃Me), 2.85 (br s, 2H, H-5_{linker}), 2.11 (s, 3H, CH₃Ac), 2.05 (s, 3H, CH₃Ac), 1.72–1.70 (m, 2H, H-2_{linker}), 1.63–1.60 (m, 2H, H-4_{linker}), 1.41–1.38 (m, 2H, H-3_{linker}), 1.03 (d, $J = 6.5$ Hz, 3H, H-6B*), 0.92 (d, $J = 6.4$ Hz, 3H, H-6D*); ¹³C NMR (150 MHz, CDCl₃) δ (ppm) 169.8 (COOR_{Ac}), 168.9 (COOR_{Ac}), 138.2 (C-Ar), 137.2 (2C, 2 \times C-Ar), 129.6–126.2 (15C, 15 \times CH-Ar), 104.2 (C-1A*), 102.0, 101.8 (2C, C-7A, C-7C), 101.4 (C-1C*), 98.4, 98.2 (2C, C-1B, C-1D), 83.0 (C-2A), 79.2, 78.8 (2C, C-4A, C-4C), 76.4, 76.3 (C-3A, C-3C), 75.8 (C-2C), 74.9 (CH₂Bn), 74.3 (C-3D), 72.2 (C-3B), 70.0 (C-1_{linker}), 69.7–66.2 (10C, C-2B, C-2D, C-4B, C-4D, C-5A, C-5B, C-5C, C-5D, C-6A, C-6C), 56.4 (CH₃Me), 40.0 (C-5_{linker}), 29.2 (C-4_{linker}), 27.8 (C-2_{linker}), 23.2 (C-3_{linker}), 21.3 (CH₃Ac), 21.2 (CH₃Ac), 16.2, 16.0 (2C, C-6B, C-6D); HRMS (ESI-TOF) m/z [M + H]⁺ calcd for C₅₅H₇₄NO₂₁ 1084.47478; found 1084.47259; m/z [M + Na]⁺ calcd for C₅₅H₇₃NNaO₂₁ 1106.45673; found 1106.45461.

(5-Amino-1-pentyl) 2,4-di-O-acetyl-6-deoxy-3-O-methyl- α -L-talopyranosyl-(1 \rightarrow 3)- β -D-glucopyranosyl-(1 \rightarrow 3)-2-O-acetyl-6-deoxy- α -L-talopyranosyl-(1 \rightarrow 3)- β -D-glucopyranoside hydrochloride (8).

Alcohol **40** (37 mg, 0.028 mmol, 1.0 equiv) was dissolved in DCE (0.3 mL) and MeOH (7.2 mL). The solution was degassed with Ar and Pd black (37 mg, 1 mg/mg of alcohol **40**) and 12 N HCl(aq) (2.3 μ L, 0.028 mmol, 1.0 equiv) were successively added. The suspension was stirred under an atmosphere of H₂ at 40 °C for 16 h. The mixture was filtered over Celite to remove the catalyst and the cake was rinsed with MeOH. The solution was evaporated under reduced pressure. The residue was purified by LH-20 resin (MeOH) followed by reverse phase chromatography (100% H₂O to 1:1 H₂O/MeOH) to give tetrasaccharide **8** (15 mg, 60%) as a white amorphous solid: R_f 0.3 (CHCl₃/MeOH/H₂O 10:10:3); $[\alpha]_D^{20} -34$ (c 0.8, MeOH); ¹H NMR (600 MHz, D₂O) δ (ppm) 5.37 (d, $J = 3.1$ Hz, 1H, H-4D), 5.28 (br s, 2H, H-1B*, H-2D), 5.22–5.21 (m, 2H, H-1D*, H-2B), 4.63 (d, $J = 8.0$ Hz, 1H, H-1C*), 4.52 (br q, $J = 6.4$ Hz, 1H, H-5D), 4.45 (d, $J = 8.1$ Hz, 1H, H-1A),

CHAPITRE 4 – MELIOIDOSIS PATIENT SERUM-REACTIVE SYNTHETIC TETRASACCHARIDES BEARING THE PREDOMINANT EPITOPES OF BURKHOLDERIA PSEUDOMALLEI AND BURKHOLDERIA MALLEI O-ANTIGENS

4.36 (br q, $J = 6.6$ Hz, 1H, H-5B), 4.24 (t, $J = 3.6$ Hz, 1H, H-3B), 3.98 (t, $J = 3.4$ Hz, 1H, H-3D), 3.96–3.90 (m, 3H, H-1a_{linker}, H-6aA*, H-4B), 3.85 (dd, $J = 12.3$ Hz, $J = 2.0$ Hz, 1H, H-6aC*), 3.75–3.66 (m, 3H, H-1b_{linker}, H-6bA, H-6bC), 3.63–3.57 (m, 2H, H-3A, H-3C), 3.52–3.43 (m, 5H, H-2C*, H-4A, H-4C, H-5A, H-5C), 3.40 (s, 3H, CH₃Me), 3.37 (dd, $J = 9.0$ Hz, $J = 8.3$ Hz, 1H, H-2A*), 3.00 (t, $J = 7.2$ Hz, 2H, H-5_{linker}), 2.21 (s, 3H, CH₃Ac), 2.17 (s, 3H, CH₃Ac), 2.16 (s, 3H, CH₃Ac), 1.71–1.64 (m, 4H, H-2_{linker}, H-4_{linker}), 1.48–1.43 (m, 2H, H-3_{linker}), 1.24 (d, $J = 6.6$ Hz, 3H, H-6B), 1.14 (d, $J = 6.6$ Hz, 3H, H-6D); ¹³C NMR (150 MHz, D₂O) δ (ppm) 174.4 (COOR_{Ac}), 174.1 (COOR_{Ac}), 173.7 (COOR_{Ac}), 102.6, 102.4 (2C, ¹J_{C-H} = 163.9 Hz, ¹J_{C-H} = 162.1 Hz, C-1A, C-1C), 99.4, 99.3 (2C, ¹J_{C-H} = 173.4 Hz, ¹J_{C-H} = 176.5 Hz, C-1B, C-1D), 82.8, 82.6 (2C, C-3A, C-3C), 76.5, 76.4 (2C, C-5A, C-5C), 74.2, 74.1 (2C, C-2A, C-2C), 73.9, 73.6 (2C, C-3B, C-3D), 70.8, 70.7 (2C, C-1_{linker}, C-2B), 70.1, 69.2, 68.8, 68.3, 68.1, 67.8 (6C, C-2D, C-4B, C-4D, C-4A, C-5B, C-4C), 66.3 (C-5D), 61.4, 61.1 (2C, C-6A, C-6C), 57.3 (CH₃Me), 40.0 (C-5_{linker}), 28.8 (C-4_{linker}), 27.1 (C-2_{linker}), 22.7 (C-3_{linker}), 21.3 (CH₃Ac), 21.1 (CH₃Ac), 21.0 (CH₃Ac), 16.0, 15.8 (2C, C-6B, C-6D); HRMS (ESI-TOF) m/z [M + H]⁺ calcd for C₃₆H₆₂NO₂₂ 860.3758; found 860.3776.

(5-Amino-1-pentyl) 2-O-acetyl-6-deoxy-3-O-methyl- α -L-talopyranosyl-(1→3)- β -D-glucopyranosyl-(1→3)-2-O-acetyl-6-deoxy- α -L-talopyranosyl-(1→3)- β -D-glucopyranoside hydrochloride (9).

Tetrasaccharide **43** (2 mg, 0.002 mmol, 1.0 equiv) was dissolved in DCE (0.02 mL) and MeOH (0.5 mL). The solution was degassed with Ar and Pd black (2 mg, 1 mg/mg of tetrasaccharide **43**) and 12 N HCl(aq) (0.2 μ L, 0.002 mmol, 1.0 equiv) were successively added. The suspension was stirred under an atmosphere of H₂ at 40 °C for 16 h. The mixture was filtered over Celite to remove the catalyst and the cake was rinsed with MeOH. The solution was evaporated under reduced pressure. The residue was purified on reverse phase chromatography (100% H₂O to 1:1 H₂O/MeOH) to give tetrasaccharide **9** (1.5 mg, 91%) as a white amorphous solid; R_f 0.2 (CHCl₃/MeOH/H₂O 10:10:3); $[\alpha]_D^{20}$ –25 (c 0.2, MeOH); ¹H NMR (600 MHz, D₂O) δ (ppm) 5.25 (br d, $J = 3.8$ Hz, 1H, H-2D), 5.24 (br s, 1H, H-1B*), 5.22–5.21 (m, 2H, H-1D*, H-2B), 4.63 (d, $J = 8.1$ Hz, 1H, H-1A*), 4.45 (d, $J = 8.2$ Hz, 1H, H-1C*), 4.38–4.33 (m, 2H, H-5B, H-5D), 4.24 (t, $J = 3.6$ Hz, 1H, H-3B), 3.96–3.95 (m, 2H, H-4B, H-4D), 3.94–3.90 (m, 2H, H-1a_{linker}, H-6aA*),

CHAPITRE 4 – MELIOIDOSIS PATIENT SERUM-REACTIVE SYNTHETIC TETRASACCHARIDES BEARING THE PREDOMINANT EPITOPES OF BURKHOLDERIA PSEUDOMALLEI AND BURKHOLDERIA MALLEI O-ANTIGENS

3.85 (dd, $J = 12.3$ Hz, $J = 2.1$ Hz, 1H, H-6aC*), 3.79 (t, $J = 3.6$ Hz, 1H, H-3D), 3.75–3.66 (m, 3H, H-1b_{linker}, H-6bA, H-6bC), 3.61–3.57 (m, 2H, H-3A, H-3C), 3.50–3.43 (m, 5H, H-2A*, H-4A, H-4C, H-5A, H-5C), 3.41 (s, 3H, CH₃Me), 3.38 (dd, $J = 9.1$ Hz, $J = 8.4$ Hz, 1H, H-2C*), 2.99 (t, $J = 7.4$ Hz, 2H, H-5_{linker}), 2.16 (s, 3H, CH₃Ac), 2.14 (s, 3H, CH₃Ac), 1.71–1.64 (m, 4H, H-2_{linker}, H-4_{linker}), 1.48–1.43 (m, 2H, H-3_{linker}), 1.24 (d, $J = 6.6$ Hz, 6H, H-6B, H-6D); ¹³C NMR (150 MHz, D₂O) δ (ppm) 174.1 (COOR_{Ac}), 173.9 (COOR_{Ac}), 102.6, 102.4 (2C, C-1A, C-1C), 99.4, 99.3 (2C, C-1B, C-1D), 82.8, 82.4 (2C, C-3A, C-3C), 76.5, 76.4 (2C, C-5A, C-5C), 74.3, 74.2 (2C, C-2A, C-2C), 74.1, 73.9 (2C, C-3B, C-3D), 70.8, 70.7 (2C, C-1_{linker}, C-2B), 69.2, 68.8, 68.6, 68.3, 68.2, (5C, C-2D, C-4B, C-4D, C-4A, C-4C), 67.8, 67.7 (2C, C-5B, C-5D), 61.4, 61.1 (2C, C-6A, C-6C), 56.2 (CH₃Me), 40.0 (C-5_{linker}), 28.8 (C-4_{linker}), 27.1 (C-2_{linker}), 22.7 (C-3_{linker}), 21.3 (CH₃Ac), 21.2 (CH₃Ac), 16.04, 15.99 (2C, C-6B, C-6D); HRMS (ESI-TOF) m/z [M + H]⁺ calcd for C₃₄H₆₀NO₂₁ 818.36523; found 818.36495.

CHAPITRE 5 : PROGRESS TOWARDS THE DEVELOPMENT OF GLYCAN-BASED VACCINES AGAINST CAMPYLOBACTERIOSIS

Maude Cloutier,^a Charles Gauthier^a

^a*Centre Armand-Frappier Santé Biotechnologie, Institut national de la recherche scientifique (INRS), 531, boul. des Prairies, Laval (Québec), H7V 1B7, Canada*

Article publié dans ACS Infectious Diseases, 2020, 7, 969-986, doi: 10.1021/acsinfecdis.0c00332 (contribution invitée à l'édition thématique « [Gut pathogens](#) »)

Titre français : Progrès vers le développement de vaccins à base de glycanes contre la campylobactériose

Contribution des auteurs : Maude Cloutier a réalisé la revue de littérature et rédigé la totalité de l'article. Charles Gauthier a révisé l'article.

5.1 Résumé

En tant que l'une des principales causes de diarrhée bactérienne et un facteur de risque majeur du syndrome de Guillain-Barré, la campylobactériose, causée par les infections à *Campylobacter*, représente un problème majeur de santé publique dans le monde. Il existe donc un besoin pressant de développer un vaccin efficace et à large couverture contre la campylobactériose. *Campylobacter jejuni*, une bactérie à Gram négatif encapsulée et multirésistante, exprime des polysaccharides capsulaires (CPS) associés à la virulence qui constituent des cibles privilégiées pour la conception de vaccins glycoconjugués. Dans ce contexte, la chimie des glucides synthétique agit comme une technologie cruciale pour la préparation de composés homogènes tout en permettant la détermination des épitopes antigéniques et leur étude au niveau moléculaire. Cette revue de littérature vise à couvrir les récents développements dans la mise au point de vaccins contre la campylobactériose à base de CPS ainsi que dans les synthèses totales de mimes d'oligosaccharides liés à *C. jejuni*.

5.2 Abstract

As one of the main causes of bacterial diarrhea and a major risk factor for triggering Guillain-Barré autoimmune syndrome, campylobacteriosis, *i.e.*, *Campylobacter* spp. infections, represents a major health issue worldwide. There is thus a pressing need for developing an effective and broad-coverage campylobacteriosis vaccine. *Campylobacter jejuni*, an encapsulated, multi-drug resistant Gram-negative bacterium, expresses virulence-associated capsular polysaccharides (CPSs), which constitute exquisite targets for the design of glycoconjugate vaccines. In that context, synthetic carbohydrate chemistry acts as a crucial enabling technology for the preparation of homogenous constructs while allowing antigenic epitopes to be deciphered and probed at the molecular level. This review aims at covering recent developments in CPS-based campylobacteriosis vaccines as well as in the total syntheses of *C. jejuni*-related oligosaccharide mimics.

5.3 Campylobacteriosis

Diarrheal diseases constitute an important public health issue, ranking second in causes of death in children under five years and sixth in global disability-adjusted life-year (DALY) burden.^{409,410} In 2016, reanalysis of the Global Enteric Multicenter Study (GEMS) case-control study,⁴¹¹ which aimed at identifying the principal causative agents of moderate-to-severe diarrhea in young children in Africa and Asia, showed that six pathogens accounted for 78% of all attributable diarrhea, one of them being *Campylobacter* spp.⁴¹² These results were supported by a previous cohort study from The Etiology, Risk Factors, and Interactions of Enteric Infections and Malnutrition and the Consequences for Child Health and Development Project (MAL-ED),⁴¹³ as both highlighted the weight of *Campylobacter* spp. as major diarrheal pathogens. The 2010 Global Burden of Disease study additionally reported that *Campylobacter* infections account for 7.5 million DALYs.⁴¹⁴

Campylobacter spp. are estimated to cause up to 400 million campylobacteriosis cases each year,⁴¹⁵ of which 90% are attributed to the enteric Gram-negative bacterium (GNB) *C. jejuni*, making campylobacteriosis endemic and hyperendemic in developed and developing countries, respectively.^{416,417} In developing countries, campylobacteriosis is mainly a pediatric disease with incidence rates reaching up to 60% in children under the age of five, whereas repeated childhood exposures lead to reduced incidence rates in adults.⁴¹⁶ Following colonization of the lower digestive tract, infections are typically characterized by abdominal pain, fever, and bloody diarrhea,⁴¹⁸ and are generally ascribed to the consumption of contaminated water, chicken or non-pasteurized milk.⁴¹⁹ Antibiotic treatment is difficult because of the growing incidence of multi-resistant strains.⁴²⁰⁻⁴²² Because of this antimicrobial resistance, *Campylobacter* spp. are classified as high priority pathogens for the research and development of new antibiotics by the World Health Organization (WHO)⁴²³ and as serious threats in the 2019 Antibiotic Resistance Threats Report of the Centers for Disease Control and Prevention (CDC),⁴²⁴ emphasizing the need for novel prevention tools against *Campylobacter* infections. Although campylobacteriosis is considered self-limiting, it has been linked to a variety of post-infection chronic sequelae, including Guillain-Barré autoimmune syndrome (GBS) with an estimated prevalence of 1/1000 cases of *C. jejuni*

CHAPITRE 5 – PROGRESS TOWARDS THE DEVELOPMENT OF GLYCAN-BASED VACCINES AGAINST CAMPYLOBACTERIOSIS

infection.⁴²⁵ Indeed, *C. jejuni* lipooligosaccharides (LOSs)—a truncated form of lipopolysaccharides (LPSs)—contain α -*N*-acetyl-D-neuraminic acid (α -Neu5Ac) moieties mimicking gangliosides,^{426, 427} which are glycosphingolipids particularly abundant in the human peripheral nervous system. For instance, as depicted in Figure 1, *C. jejuni* serostrains HS:19 and HS:4 produce LOSs that heterogeneously contain tetra- and pentasaccharides of structure $\pm[\alpha$ -Neu5Ac-(2 \rightarrow 3)]- β -D-Galp-(1 \rightarrow 3)- β -D-GalpNAc-(1 \rightarrow 4)-[α -Neu5Ac-(2 \rightarrow 3)]- β -D-Galp, which respectively mimic the glycosidic portion of gangliosides GM1a and GD1a.⁴²⁷⁻⁴³¹ Noteworthy, this molecular mimicry is not limited to these specific *C. jejuni* strains and gangliosides, as expertly reviewed by Moran and co-workers, and their LOSs core structure mainly differs in the substitution pattern of the Neu5Ac moieties as well as other small modifications.⁴³¹ Antibodies directed towards these LOSs can, in some cases, induce an autoimmune response triggering GBS. Other post-infections sequelae such as reactive arthritis and irritable colon syndrome have also been associated with *C. jejuni* infections.⁴³²

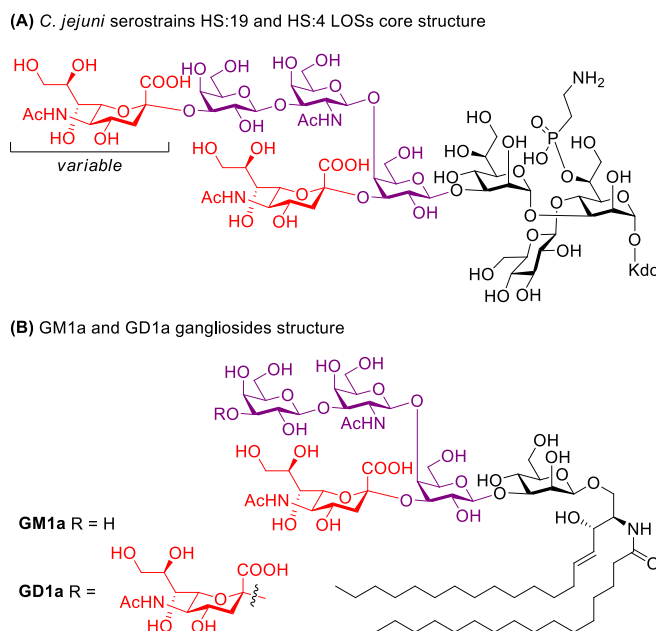


Figure 5.1. Comparison between *C. jejuni* serotypes HS:19 and HS:4 LOS core structure (A) and human gangliosides GM1a and GD1a (B)

5.4 Challenges of campylobacteriosis vaccines

Considering the burden of *Campylobacter*-associated illnesses and the increasing number of infections with *C. jejuni* resistant strains, there is an urgent need for prophylactic measures against this enteric GNB. Not only would it reduce diarrhea-associated deaths, it would also alleviate the socio-economic burden of campylobacteriosis. One of the best approaches for reducing human infections would be to reduce colonization of the main host, *i.e.*, broiler chickens, which are usually colonized in their first weeks of life.⁴¹⁷ As such, a multidisciplinary project conducted between 2001 and 2004 in The Netherlands revealed that increasing hygienic levels during poultry processing and phage therapy would constitute effective and economically viable strategies.^{433, 434} Alternatively, poultry vaccination appears to be a promising approach for reducing their colonization by *C. jejuni* and consequently decreasing human infections. Live attenuated, killed whole-cell vaccines as well as subunit vaccines have been investigated over the past years, as comprehensively reviewed by de Zoete *et al.* in 2007,⁴³⁵ but these approaches have been only partially successful. Among the many challenges surrounding the design of a vaccine in poultry, it is possible to count on the identification of universal *C. jejuni* protective antigens, the need for effective novel adjuvants and vaccination methods, and the short life of broiler chickens.⁴¹⁸

One of the currently preferred strategy for minimizing *C. jejuni* infections is the design of vaccines intended for human use. This approach could be particularly useful for preventing infections of travelers, soldiers, and children in developing countries, who are the most at risk populations.⁴³⁶ Its feasibility is supported by the observation of a decrease in incidence rates in parallel with the increase in patients' age, suggesting that protection against *C. jejuni* is acquired with time and repeated exposures.^{437, 438} Production of LOSs mimicking human gangliosides by this enteric GNB is however a major hurdle for the development of such immunoprophylactic tools due to the risk of triggering GBS. Live attenuated and killed whole-cell vaccines are therefore proscribed whereas subunit vaccines constitute a safer alternative. More specifically, glycoconjugate vaccines based on capsular polysaccharides (CPSs) expressed by *C. jejuni* represent the most promising approach to date. Although details are lacking surrounding *C. jejuni* pathogenesis, these CPSs are known as key mediators for host-pathogen interactions as well as virulence factors that appear critical for

colonization, invasion of epithelial cells, and serum resistance.⁴³⁹⁻⁴⁴² Non-encapsulated mutants of various *C. jejuni* strains exhibited reduced virulence, suggesting that anti-CPS antibodies could protect against infections.⁴⁴³

Nonetheless, the necessity to obtain pure polysaccharides free from bacterial contaminants, the heterogeneity of isolated polysaccharides, and the potential structural modifications induced by conjugation to carrier proteins affecting immunogenic responses are important challenges inherent to the use of native polysaccharides.^{238, 444} Relying on synthetic carbohydrate chemistry, most of these hurdles can be overcome, more knowledge can be gained into the structural requirements for potent antigenic/immunogenic responses, and glycosyltransferases involved in CPS biosynthesis can be effectively probed.^{239, 240} For these reasons, many research groups have recently been involved in the synthesis of *C. jejuni* CPS mimics.

In the past years, advances towards the development of vaccines against campylobacteriosis have been comprehensively reviewed a few times with focus on *Campylobacter* pathogenesis and glycoconjugate approaches.^{416, 445-447} Herein, we rather wish to offer an overview of recent works on the development of *C. jejuni* CPS-based vaccines, specifically enabled by the total synthesis of oligosaccharide mimics.

5.5 Capsular polysaccharides

In the 1990s, it had been proposed by Aspinall *et al.* that the polysaccharides expressed by *C. jejuni* consisted in the *O*-antigenic region of surface-exposed LPSs.⁴⁴⁸⁻⁴⁵⁰ Structural analysis of *C. lari* surface polysaccharides later linked them to CPSs,^{451, 452} which was subsequently confirmed by genomic analysis.⁴⁵³ Unlike most enteric GNB, *C. jejuni* produces CPSs anchored in its outer membrane along with LOSs rather than LPSs. As mentioned earlier, these CPSs play key roles in the mediation of host-pathogen interactions while being crucial virulence factors.⁴³⁹⁻⁴⁴²

5.5.1 Chemical structures

The structure of *C. jejuni* CPSs greatly varies between strains and these polysaccharides constitute the major determinants of the Penner serotyping scheme (or heat-stable, HS), a passive

CHAPITRE 5 – PROGRESS TOWARDS THE DEVELOPMENT OF GLYCAN-BASED VACCINES AGAINST CAMPYLOBACTERIOSIS

hemagglutination test developed in 1980 by Penner and Hennessy that distinguishes 47 serotypes based on their CPS composition although other structures such as LOSs also contribute to the serotype specificity.^{454, 455} On the basis of similarities between their CPS structures, these 47 serotypes can be further organized into 35 pairs or complexes of serotypes.⁴⁴⁶ Until now, the structures of 11 CPSs have been elucidated, *i.e.*, HS:2,⁴⁵⁶⁻⁴⁵⁹ HS:4c,^{120, 460} HS23/36,^{448, 459, 461, 462} HS:3,^{463, 464} HS:41,^{459, 465} HS:53,⁴⁶⁶ HS:15,⁴⁶⁷ HS:19,^{428, 459, 468, 469} HS:1/44,^{459, 464, 470, 471} HS:10,^{464, 472} and HS:5.⁴⁶⁴ As depicted in Figure 2, these CPSs are atypical in that they are composed of L- and D-*glycero*-heptoses and 6-deoxy-heptoses of rare configurations (*i.e. gulo, altro, and ido*). Because of slipped-strand mispairing caused by homopolymeric tracts of cytosine nucleotides,⁴⁶⁰ phase-variable structural modifications further exacerbate CPSs diversity by introducing heterogeneity within the same serotype, such as methylation, acylation, dehydration, and the presence of additional branched sugars. However, the most remarkable structural modification is the non-stoichiometric incorporation of *O*-methyl phosphoramidate (MeOPN) moieties at different positions in these polysaccharides. These chemical substituents are found in up to 70% of *C. jejuni* isolates, whereas to date they have never been observed in other living organisms.⁴⁷³ It has, moreover, been hypothesized that these MeOPN moieties are involved in the colonization process of the host and in resistance to serum, as demonstrated by a *C. jejuni* HS:23/36 mutant not expressing this modification and exhibiting reduced serum resistance.^{443, 474} Importantly, not only do *C. jejuni* CPSs structures undergo phase variation, but the expression of these polysaccharides itself appears to be regulated transcriptionally,⁴³⁹ suggesting that the advantages this structure provides to *C. jejuni* virulence might be context-dependent.⁴³⁶

CHAPITRE 5 – PROGRESS TOWARDS THE DEVELOPMENT OF GLYCAN-BASED VACCINES AGAINST CAMPYLOBACTERIOSIS

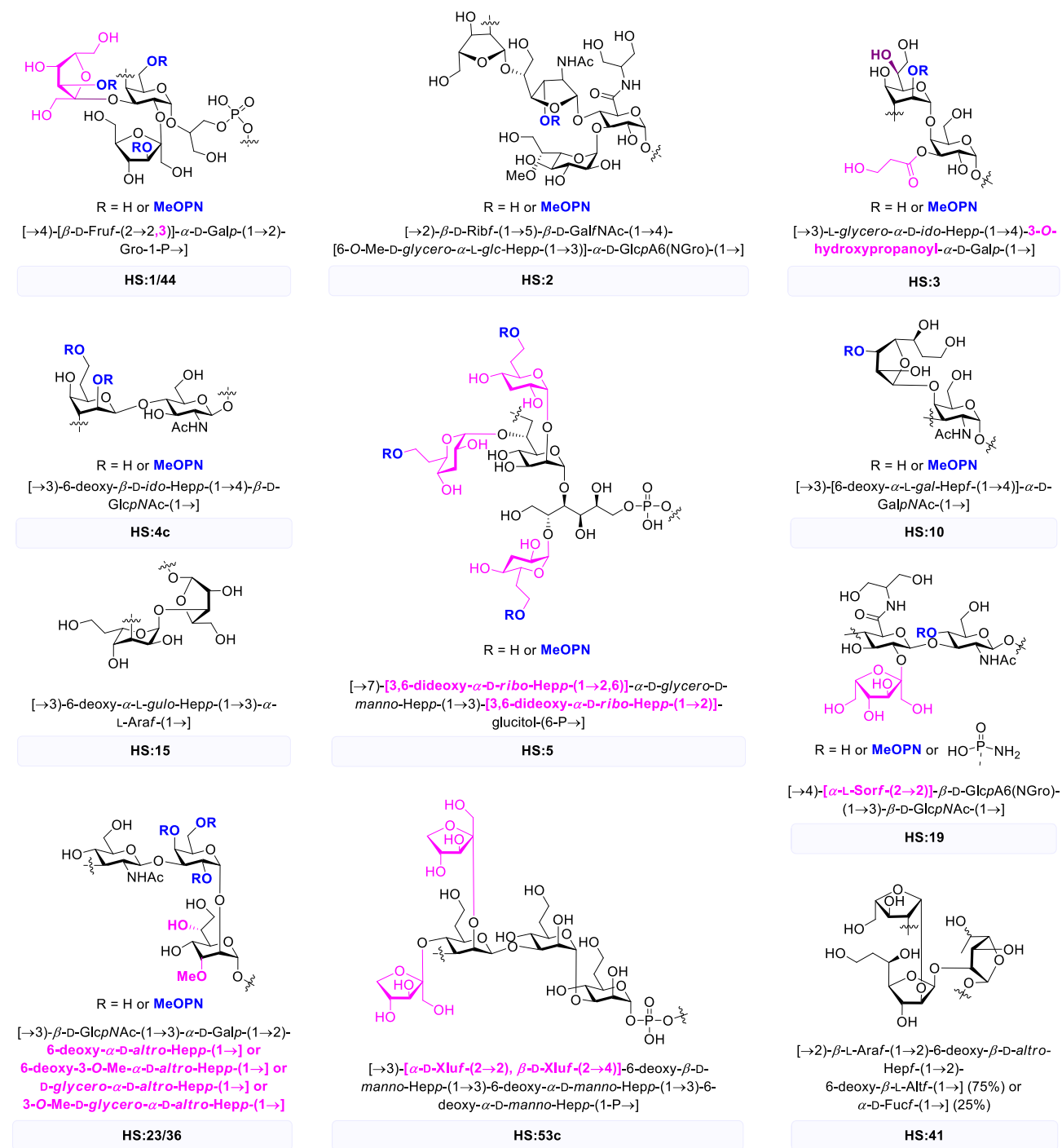


Figure 5.2. Repeating units of characterized *C. jejuni* serotypes CPS including the MeOPN moieties and other non-stoichiometric structural modifications (in pink)

In 2013, Pike and co-workers reported a systematic review on the frequency and distribution of campylobacteriosis based on Penner serotypes, covering infections that occurred between 1978 and 2008.⁴⁷⁵ Available epidemiological data revealed that more than 50% of isolates at the origin of approximately 21 000 sporadic *C. jejuni* infections were associated with only eight pairs or complexes of serotypes, namely (in descending order) HS:4c, HS:2, HS:1/44, HS:11, HS:5/31, HS:8/17, HS:6/7, and HS:3. Additionally, it was observed that serotypes HS:4c, HS:2, and HS:1/44 are prevalent both inter-regionally and globally, highlighting the attention that must be paid to these serotypes in the context of the development of a broad-coverage vaccine. This study however mainly covered cases from developed countries, while there is a blatant lack of data surrounding *C. jejuni* infections in developing countries where the incidence is higher and a vaccine would be most beneficial. To make up for this data deficiency, isolates from Africa, Middle East, Southeast Asia, and South America were analyzed with a PCR typing method employing 35 capsule primer sets.^{460,464,476,477} Results showed that serotypes HS:4c, HS:2, HS:3, HS:55/31, HS:8, HS:1, HS:15, HS:23/36, HS:10, and HS:53c accounted for up to 70% of all *C. jejuni* infections.⁴⁶⁴ This suggests that a multivalent vaccine against *C. jejuni* including the CPS of these 10 prevalent serotypes would protect against the majority of *C. jejuni* infections in the endemic regions covered in these latter studies,⁴⁶⁴ although more information on *C. jejuni* serotypes distribution is still needed to better understand the valency requirements for a truly effective CPS-based vaccine. The feasibility of such an approach based only on the most prevalent serotypes is further demonstrated by current anti-pneumococcal glycoconjugate vaccine, which only includes 13 of the more than 90 *S. pneumoniae* serotypes.⁴⁷⁸

5.6 Glycoconjugate vaccines

5.6.1 Role of carrier proteins

Surface-exposed polysaccharides from bacterial pathogens are known as potent antigens and therefore constitute exquisite candidates for the development of vaccines.⁴⁷⁹ However, these polysaccharides have the major drawback of inducing the so-called T cell-independent responses, in which only B cells are stimulated through the cross-linking of B cell receptors by the polysaccharides.⁴⁸⁰ Such activated pathway is characterized by the production of short-lived, low-

affinity type M immunoglobulins (IgM).^{481, 482} As this mechanism is not mature in young children, polysaccharide-based vaccines are ineffective for this population.³¹ Conversely, when these polysaccharides are covalently linked to a carrier protein, the immune response is rather T cell-dependent. Once administered, the glycoconjugate is processed by antigen-presenting cells to generate glycan-peptide fragments. The peptide portion acts as an anchor enabling presentation of these antigenic glycans to T cells by a class II major histocompatibility complex (MHCII). Recognition of the glycan fragment by T cells induces B cells maturation into effector and high-avidity memory B cells³² as well as antibodies class-switching from IgM to IgG, thus offering long-term protection.⁴⁸³ In the past years, several glycoconjugate vaccines have been clinically approved against various invasive mucosal pathogens such as encapsulated strains of *Haemophilus influenzae* type B, *Streptococcus pneumoniae*, and *Neisseria meningitidis*.^{40, 41} Furthermore, synthetic chemistry was taken advantage of to create the QuimiHib[®] vaccine against *H. influenzae* type b administered in Cuba, the first semi-synthetic vaccine to be marketed.⁴⁶

5.6.2 CPS-based vaccines

Despite numerous on-going investigations, there is only a limited number of licensed vaccines against enteric pathogens,⁴⁸⁴ and no conjugate vaccines are available. The need for a gut-effective immunity constitutes a major hurdle in the development of such prophylactic measures against this type of pathogens.⁴⁸⁵ Although there is no CPS-based vaccines available against enteric GNB—as they generally do not express such a capsule, with the main exception of *C. jejuni*—the efficacy of LPSs for the development of *Shigella* vaccines has already been demonstrated.^{486, 487} Since *Shigella* invasion is similar to that of *C. jejuni*,⁴⁴⁵ these results support the current hypothesis proposing that a glycoconjugate vaccine could successfully prevent *C. jejuni* infections. The use of synthetic carbohydrates for vaccines against *Shigella* also shows promise, as highlighted by a synthetic glycan related to *S. flexneri* 2a O-antigen that recently completed a phase 1 clinical trial (ClinicalTrials.gov NCT02797236)⁴⁸⁸ and that is currently moving forward to a phase 2b clinical trial (ClinicalTrials.gov NCT04078022), yet again supporting the role of synthetic chemistry to reduce the burden of campylobacteriosis.⁴⁸⁹⁻⁴⁹² The most striking example of the feasibility of CPS-based vaccines against *C. jejuni* was however achieved by Guerry and co-workers in 2009.

In their study, the authors prepared two glycoconjugates, *i.e.*, CRM₁₉₇-CPS₈₁₋₁₇₆ (serotype HS:23/36) and CRM₁₉₇-CPS_{CG8486} (serotype HS:4c), which were administered subcutaneously to mice.⁴⁹³ Not only did they both elicit significant protection following intranasal challenge with the homologous *C. jejuni* strains, but conjugate CRM₁₉₇-CPS₈₁₋₁₇₆ also provided complete protection against diarrheal disease in the New World monkey *Aotus nancymaae* model after orogastric challenge with *C. jejuni* strain 81-176. The production of CPS-specific IgG was moreover found to be dose-dependent. The relevance of this non-human primate model is supported by the observation that, following intragastric challenge with *C. jejuni* 81-176, it developed diarrheal disease mirroring aspects of human illness.⁴⁹⁴ This glycoconjugate was subsequently the subject of a phase 1 clinical trial in 2014 (ClinicalTrials.gov NCT02067676), but unfortunately did not induce significant immune responses in the majority of subjects. This lack of strong immune responses was attributed to the lack of MeOPN moieties on the isolated CPS⁴¹⁶ and the administration of only two doses (pre-clinical studies in the monkey model used three doses). An upcoming trial will use a glycoconjugate with the full MeOPN modifications in the CPS component.⁴⁹⁵

5.7 Synthesis of oligosaccharide mimics

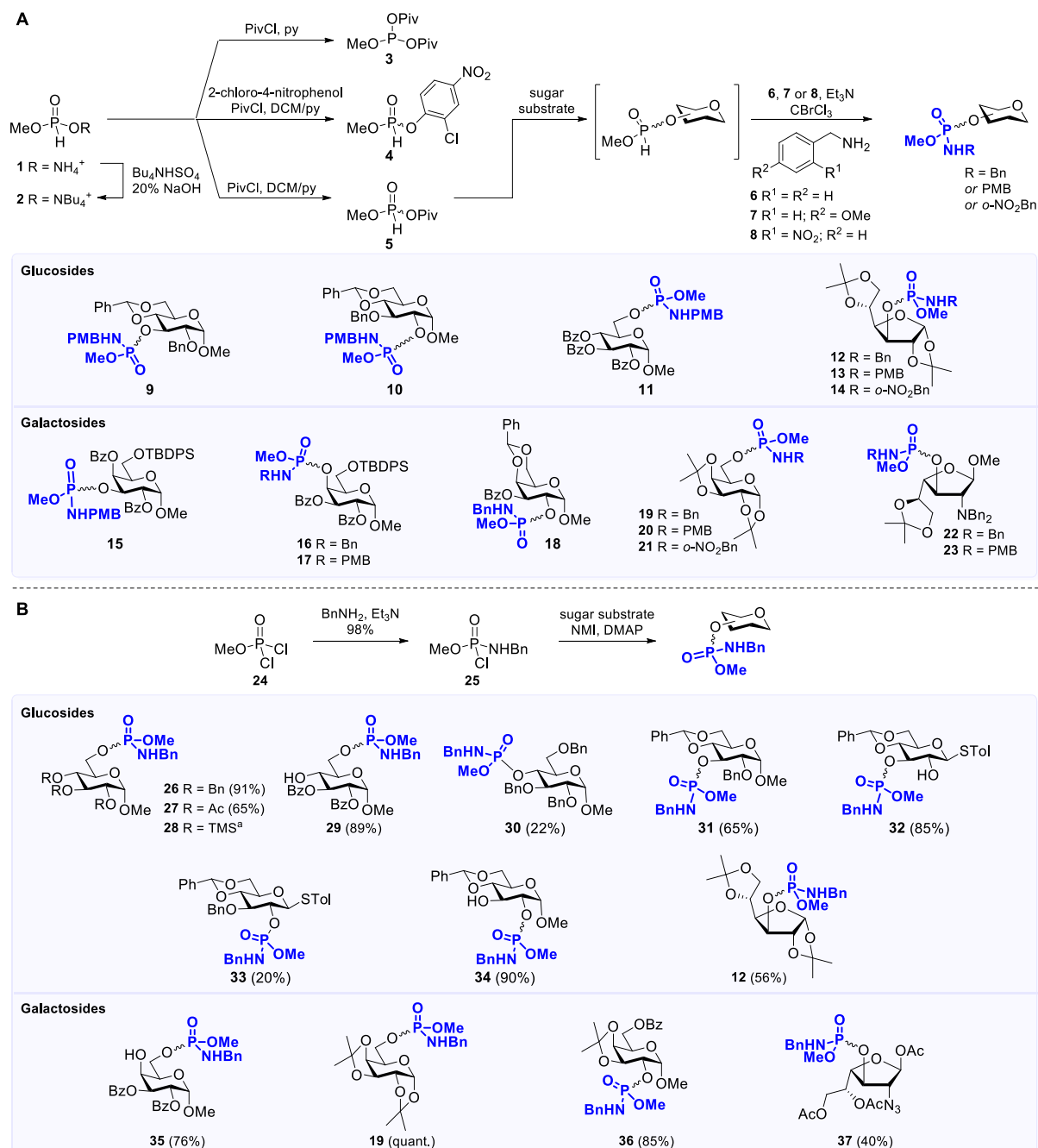
Considering the current absence of vaccines against *C. jejuni*, the proven potential of CPSs for the development of subunit vaccines and the lack of knowledge on the pathogenesis of this bacterium, synthetic chemistry constitutes an exquisite tool to decipher the structural requirements of the epitopes for a potent immunogenic activity and to probe enzymes involved in CPS biosynthesis. Numerous research groups therefore focused their interest on the synthesis of mono- and oligosaccharide mimics of *C. jejuni* CPSs, syntheses that are challenging due to the existence of heptoses in unusual configurations as well as acid- and base-labile MeOPN groups. The following sections will first specifically address the methods developed for the incorporation of MeOPN moieties in carbohydrates and will be followed by the synthesis of *C. jejuni* HS:4c-, HS:23/36-, HS:2- and HS:53c-related oligosaccharide mimics.

5.7.1 Incorporation of MeOPN moieties

As previously mentioned, the MeOPN modification is found in up to 70% of *C. jejuni* CPSs and has never been observed in other living organisms. Although little is known on the precise biological role of this moiety, it was suggested to be involved in host colonization and serum resistance.^{443, 474} MeOPN-containing carbohydrates thus constitute crucial synthetic targets, as such constructs could be effective tools for deciphering its biosynthetic assembly pathway and its immunological importance. Chemical synthesis of these compounds could also help unravel the exact stereochemistry of the MeOPN moieties. As of 2014, no effective synthetic methods were however available for the incorporation of these moieties bearing a free amine group. Lowary and co-workers therefore undertook an extensive study on the preparation of carbohydrates bearing the MeOPN modification.⁴⁹⁶

Following rather unsuccessful attempts at incorporating MeOPN moieties through the use of phosphoryl chloride, diphenyl phosphite, 2-cyanoethyl *N,N*-diisopropylchlorophosphoramidite as well as methyl dichlorophosphate as phosphorylating reagents, the Lowary group investigated the conversion of *H*-phosphonate into activated reagents. As depicted in Scheme 1A, methyl *H*-phosphonate tetra-*N*-butylammonium salt **2** could be pivaloylated using pyridine or DCM/pyridine as solvents, respectively yielding compounds **3** and **5**. Conversely, when 2-chloro-4-nitrophenol was added in the reaction mixture containing pivaloyl chloride in DCM/pyridine, active compound **4** was obtained. These compounds were employed *in situ* for the formation of a methyl sugar *H*-phosphonate intermediate. Via an Atherton-Todd reaction, which consists in the substitution of the hydrogen atom by a protected amine, the *H*-phosphonate intermediate was readily converted into the corresponding *N*-protected MeOPN-containing monosaccharide. Because reagent **5** proved to be the most efficient for the incorporation of the MeOPN moiety, the authors highlighted its versatility through the synthesis of various galactose and glucose derivatives. Noteworthy, it was shown that benzylamine, *p*-methoxybenzylamine, and *o*-nitrobenzylamine were all convenient for the incorporation of the protected-amine group during Atherton-Todd reaction.⁴⁹⁶

CHAPITRE 5 – PROGRESS TOWARDS THE DEVELOPMENT OF GLYCAN-BASED VACCINES AGAINST CAMPYLOBACTERIOSIS



Scheme 5.1. (A) Lowary and (B) Wang investigations of MeOPN moieties incorporation in carbohydrates and compatibility with various protecting groups³⁶

³⁶ a = isolated as the triacetylated form following derivatization (75%)

Feeling the need of a more efficient, versatile, and regioselective method for the preparation of MeOPN-containing carbohydrates, Wang *et al.* subsequently developed a one-step protocol for the incorporation of this moiety.⁴⁹⁷ As shown in Scheme 1B, their approach was based on the use of methyl benzylphosphoramidochloridate **25**, readily prepared from methyl dichlorophosphate **24**, as the phosphorylating reagent. Similarly to Lowary and co-workers, the authors studied the scope of their approach through the preparation of various glucose and galactose derivatives bearing the *N*-benzylated MeOPN modification. In both cases, it can be observed that benzoyl, acetyl, silyl, isopropylidene, benzyl, and benzylidene groups were tolerated during the MeOPN installation process. In Wang's approach, azide groups could also be employed, as illustrated with compound **37**. The latter approach additionally showed that when diols were employed as starting material, the regioselectivity was based on the steric hindrance at the reaction sites. When a bulky β -STol group was present at the anomeric position of a 4,6-*O*-benzylidene protected glucoside, the *N*-protected MeOPN group preferred the C3 alcohol rather than C2 with complete selectivity (**32**). Contrarywise, when a similar substrate bearing a less hindered α -OMe anomeric group is employed, phosphorylation regioselectively occurs at *O*-2 (**34**).

Because of the acid- and base-labile nature of MeOPN groups, both Lowary and Wang's groups chose to investigate the cleavage of various protecting groups when in presence of such a moiety. Whereas Lowary observed that the *N*-benzylated MeOPN functionality could not be deprotected using Pd/C as a catalyst, Wang conversely showed that its cleavage could be achieved when switching to Pd(OH)₂/C. Both groups also showed that this *N*-benzyl group could be deprotected oxidatively using NaBrO₃/Na₂S₂O₄, while Lowary demonstrated that the *N*-*para*-methoxybenzyl (PMB) and *N*-*ortho*-nitrobenzyl (*O*-NO₂Bn) groups could be respectively removed with CAN and UV-light irradiation. Benzoyl and acetyl esters can be efficiently cleaved using a carefully prepared mixture of MeOH/H₂O/Et₃N or MeOH/H₂O/K₂CO₃. Although Monteiro's group recently showed that MeOPN groups can withstand the use of 0.01 M NaOMe in MeOH, the solution pH must be closely monitored otherwise MeOPN cleavage and/or NH₂ replacement with a hydroxyl group was observed.⁴⁹⁸ Benzyl ethers and benzylidene acetals can either be deprotected concomitantly with the *N*-benzylated MeOPN group using H₂ and Pd(OH)₂/C, or can be cleaved separately with Raney Ni. Treatment with hydrogen fluoride in pyridine allowed the removal of

silyl groups, whereas isopropylidene protecting groups can be readily cleaved using 7.5% I₂ in MeOH. Finally, allyl groups can be deprotected when employing PdCl₂ in MeOH, as shown by Monteiro *et al.* during their synthesis of MeOPN-bearing monosaccharides, as later discussed.⁴⁹⁹

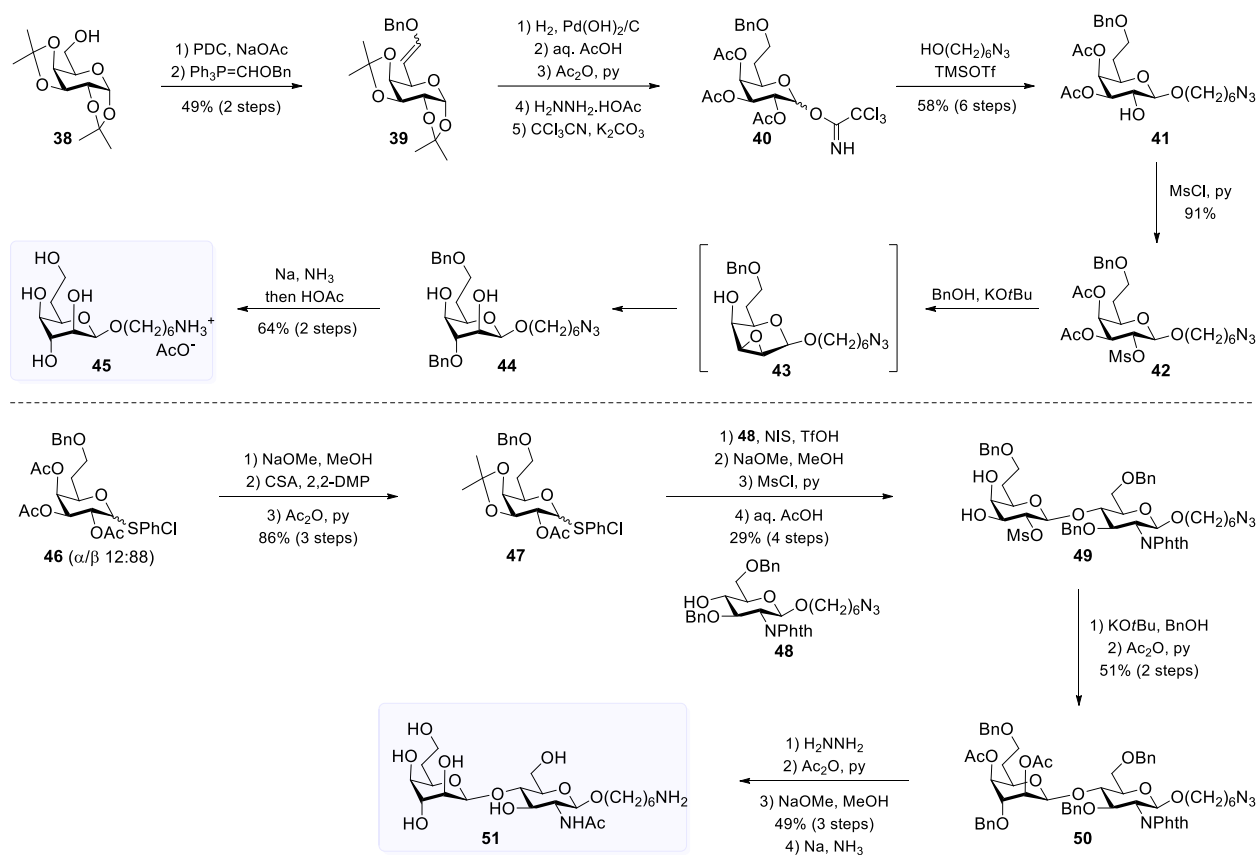
5.7.2 *C. jejuni* HS:4c

In 2012, the Ling group designed synthetic routes towards mono- and disaccharide mimics of *C. jejuni* HS:4c CPS, as this serotypes complex is the cause of the majority of *C. jejuni* infections reported worldwide. However, synthesis of such mimics is particularly challenging due to the presence of an *ido*-configured 6-deoxy-heptopyranoside moiety as well as a 1,2-*cis*- β glycosidic bond. Noteworthy, only little interest towards the synthesis of *ido*-configured sugars in the D-series has been shown over the years due to their scarcity in naturally occurring compounds. Asymmetric tandem biocatalytic aldolization reactions,⁵⁰⁰ addition to nitromethane to D-xylose followed by a modified Nef reaction,⁵⁰¹ Paulsen's rearrangement using peracetylated D-glucose as starting material⁵⁰² as well as the C2/C3 double-inversion of galactose⁵⁰³ are the few methods that were shown convenient for the preparation of D-idose and derivatives. Ling's optimized methodology relied on the latter approach to achieve the rare *ido* configuration and was based on the regioselective opening of 2,3-anhydro- β -D-talopyranosides intermediates, formed from an activated β -D-galactopyranoside precursor with a 2,3-dimesylation or ditosylation; a potassium alkoxide-mediated transesterification regioselectively activated the *O*-3-sulfonyl ester, cleaving the S-O bond to form an *O*-3 oxide anion.⁵⁰⁴⁻⁵⁰⁶ Investigation of their synthetic pathway mechanistic features suggested that this anion adopted ⁴S₂ and ¹C₄ conformations and intramolecularly displaced an *O*-2 mesylate group, resulting in the formation of an epoxide intermediate. *In situ* opening of the latter by an alkoxide then resulted in the inversion of the C2 and C3 substituents thus affording the *ido* configuration with complete regio- and stereoselectivities. Although this method successfully enabled the preparation of a β -D-idopyranose-containing disaccharide, their construct lacked the seventh carbon to achieve the 6-deoxy-D-*ido*-heptopyranoside skeleton characteristic of *C. jejuni* HS:4c CPS. Ling's subsequent work therefore focused on this structural requirement.

Because of the ubiquitous nature of 6-deoxy-D-manno-heptosides,⁵⁰⁷ their preparation has been extensively studied, as opposed to 6-deoxy-D-ido-heptopyranosides. Main approaches for the homologation of mannosides are either based on a Wittig reaction of a C6 aldehyde followed by anti-Markovnikov hydroboration-oxidation of the resulting terminal alkene⁵⁰⁸ or on the nucleophilic substitution of a leaving group with a cyanide anion followed by its conversion into a primary alcohol.^{293, 509, 510} Both approaches unfortunately proved fruitless for the preparation of 6-deoxy- β -D-ido-heptopyranosides, as shown by Ling *et al.*⁵¹¹ The authors observed that the 6,7-dideoxy-hept-6-enopyranoside intermediate obtained through Wittig olefination predominantly existed in the ¹C₄ chair conformer, which caused the vinyl group to be in the more sterically hindered axial position and prevented the hydroboration-oxidation step to take place.

Facing these problems, Ling and co-workers elaborated an alternative synthetic pathway towards 6-deoxy- β -D-ido-heptopyranosides using D-galactose as the homologation substrate, as depicted in Scheme 2.⁵¹² The authors first oxidized diisopropylidene galactoside **38** and incorporated the seventh carbon *via* Wittig olefination using phosphine Ph₃P=CHOBn. Resulting *galacto*-heptopyranoside **39** underwent a series of standard protecting groups manipulations to afford trichloroacetimidate **40**. The latter was coupled with 6-azido-1-hexanol, furnishing compound **41** as the sole anomer because of the participating-group nature of the C2 acetate. Their previously developed methodology based on the regio- and stereoselective opening of an epoxide intermediate with an alkoxide was then taken advantage of to achieve compound **44** in the required *ido* configuration. Noteworthy, this synthetic step also resulted in the formation of a 1,2-*cis*- β -glycosidic linkage, which is otherwise difficult to obtain because of the steric hindrance caused by the axial C2 substituent and the anomeric effect stabilizing the α -anomer. Target compound **45**, isolated as the acetic acid salt, was finally achieved through Birch reduction of intermediate **44**. The same approach was subsequently employed for the preparation of disaccharide **51** mimicking the repeating unit of *C. jejuni* HS:4c CPS.^{512, 513}

CHAPITRE 5 – PROGRESS TOWARDS THE DEVELOPMENT OF GLYCAN-BASED VACCINES AGAINST CAMPYLOBACTERIOSIS

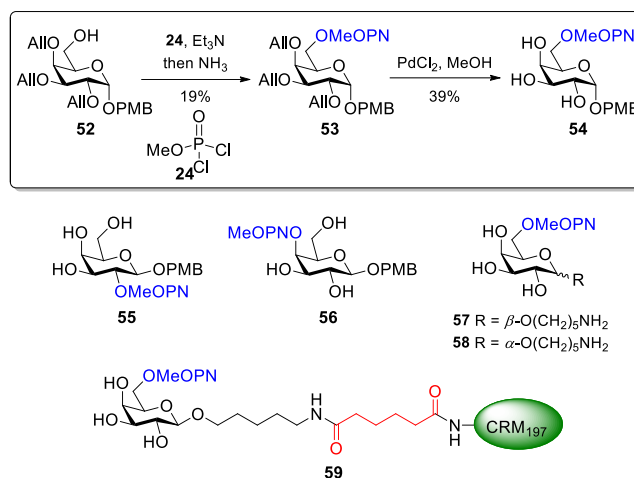


Scheme 5.2. Ling synthesis of 6-deoxy- β -D-ido-heptopyranoside **45** and disaccharide **51** related to *C. jejuni* HS:4c

5.7.3 *C. jejuni* HS:23/36

After having demonstrated the potent immunogenicity of a CRM₁₉₇-CPS₈₁₋₁₇₆ glycoconjugate in a non-human primate model and having revealed the crucial immunogenic role of the MeOPN moieties in a following clinical trial, Monteiro's group reported in 2015 the synthesis of MeOPN-bearing galactoside **54** associated with *C. jejuni* HS:23/36 CPS (Scheme 3).⁴⁹⁹ To introduce the 6-*O*-MeOPN group, as opposed to the previously described methodologies developed by Wang and Lowary, compound **52** was treated with methyl dichlorophosphate **24** in the presence of Et₃N followed by ammonolysis to introduce the amine group. This reaction yielded compound **53** in the form of a 1:1 unseparable diastereoisomeric mixture. Several side products were also formed during this reaction including a compound bearing two amine groups, explaining the particularly low yield. Triol **54** was ultimately reached—again as a mixture of diastereoisomers—by removing the allyl groups with PdCl₂ in methanol. With this compound in hand, the authors undertook its

antigenicity study using antisera raised against the CPS of *C. jejuni* HS:23/36, HS:1/44, HS:3, and HS:4c. Monosaccharide **54** was showed to react strongly with serotypes HS:23/36 and HS:4 antisera and moderately with HS:1, but not with HS:3 antiserum. Considering that *C. jejuni* HS:4c and HS:1 CPSs possess MeOPN moieties at primary positions (*O*-7 and *O*-6, respectively), as does HS:23/36 CPS (*O*-6), these results support the existence of primary MeOPN antibodies and emphasize the attention that must be put towards the inclusion of these moieties in glycoconjugate vaccine candidates. This importance is further enhanced by the observation that a galactoside lacking the MeOPN moiety did not react with *C. jejuni* HS:23/36 CPS antiserum. It is also relevant to mention that the significant antigenicity of MeOPN-bearing monosaccharide **54** was observed despite that it consisted in a diastereoisomeric mixture.



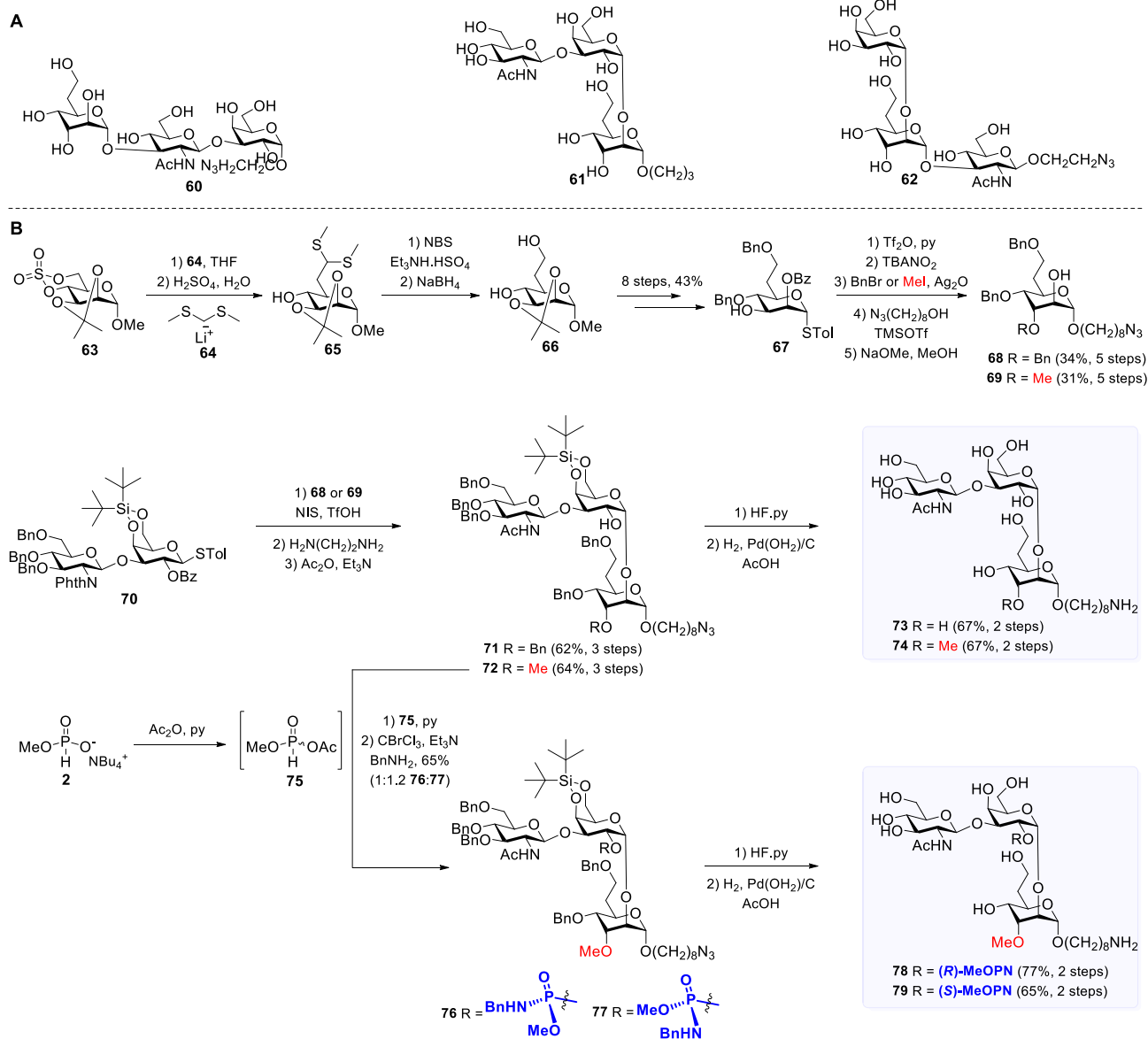
Scheme 5.3. Monteiro synthesis of MeOPN-bearing galactosides **54-58** and glycoconjugate **59**

While working under Monteiro's supervision, Jiao reported in his PhD thesis the synthesis of 2-*O*- (**55**), 4-*O*- (**56**), and 6-*O*-MeOPN galactosides (**57** and **58**) depicted in Scheme 3 using a similar strategy as for monosaccharide **54**.⁴⁹⁸ Compound **55** was shown to react with antisera raised against a wild-type 81-176 strain (serotype HS:23/36) containing MeOPN moieties at both C2 and C6. However, antisera of a conjugate only bearing 6-*O*-MeOPN groups did not detect this monosaccharide, once again demonstrating the antibody specificity towards primary and secondary MeOPN moieties. β -Galactoside **57** was immuno-recognized to the same extent as α -galactoside **54** by antisera specific to HS:23/36, HS:4c, and HS:1, revealing that the anomeric

configuration does not have an impact on the antigenicity of the constructs. Similar results were obtained with β -glycoconjugate **59**, which was isolated in a 1:8 protein/sugar ratio. Finally, flow cytometry analysis showed that antisera raised against this semi-synthetic glycoconjugate recognized *C. jejuni* HS:23/36 cells, although to a lesser extent than antiserum raised against a native HS:23/36 CPS conjugate, highlighting the potential of 6-*O*-MeOPN galactosides-containing oligosaccharides as vaccine candidates.

With the aim of gaining more insight into the importance of the reading frame for the induction of immunological responses as well as elucidating the role of *altro*-heptose residues, Nam Shin *et al.* prepared various oligosaccharides consisting of 6-deoxy- α -D-*altro*-Hepp, β -D-GlcNAc, and α -D-Gal moieties as *C. jejuni* HS:23/36 CPS mimics.⁵¹⁴⁻⁵¹⁶ The structure of these synthetic oligosaccharides with varying reading frames are depicted in Scheme 4A. To achieve the rare *altro*-Hepp configuration, the authors conducted an oxidation/reduction-mediated C3 inversion of an α -D-*manno*-Hepp glycoside, which was prepared beforehand *via* the displacement of a 6-*O*-mesylate at a mannoside derivative by KCN. No antigenic and immunological studies have been reported using these compounds.

CHAPITRE 5 – PROGRESS TOWARDS THE DEVELOPMENT OF GLYCAN-BASED VACCINES AGAINST CAMPYLOBACTERIOSIS



Scheme 5.4. Nam Shin frame-shifted oligosaccharides (A) and Lowary synthesis of trisaccharides **73**, **74**, **78**, and **79** (B) mimicking *C. jejuni* HS:23/36 CPS repeating unit

Because Nam Shin's group failed to incorporate *C. jejuni* HS:23/36 CPS characteristic substitution motifs (MeOPN and *O*-Me), Lowary undertook the synthesis of three variants of this CPS repeating unit, as shown in Scheme 4B.⁵¹⁷ Among the four variants of the α -D-*altro*-Hepp, they targeted the 6-deoxy (**73**) and 6-deoxy-*O*-Me (**74**) motifs. In one of the trisaccharides bearing the latter substitution pattern, the authors additionally incorporated the 2-*O*-MeOPN modification of the galactoside moiety (**78** and **79**).

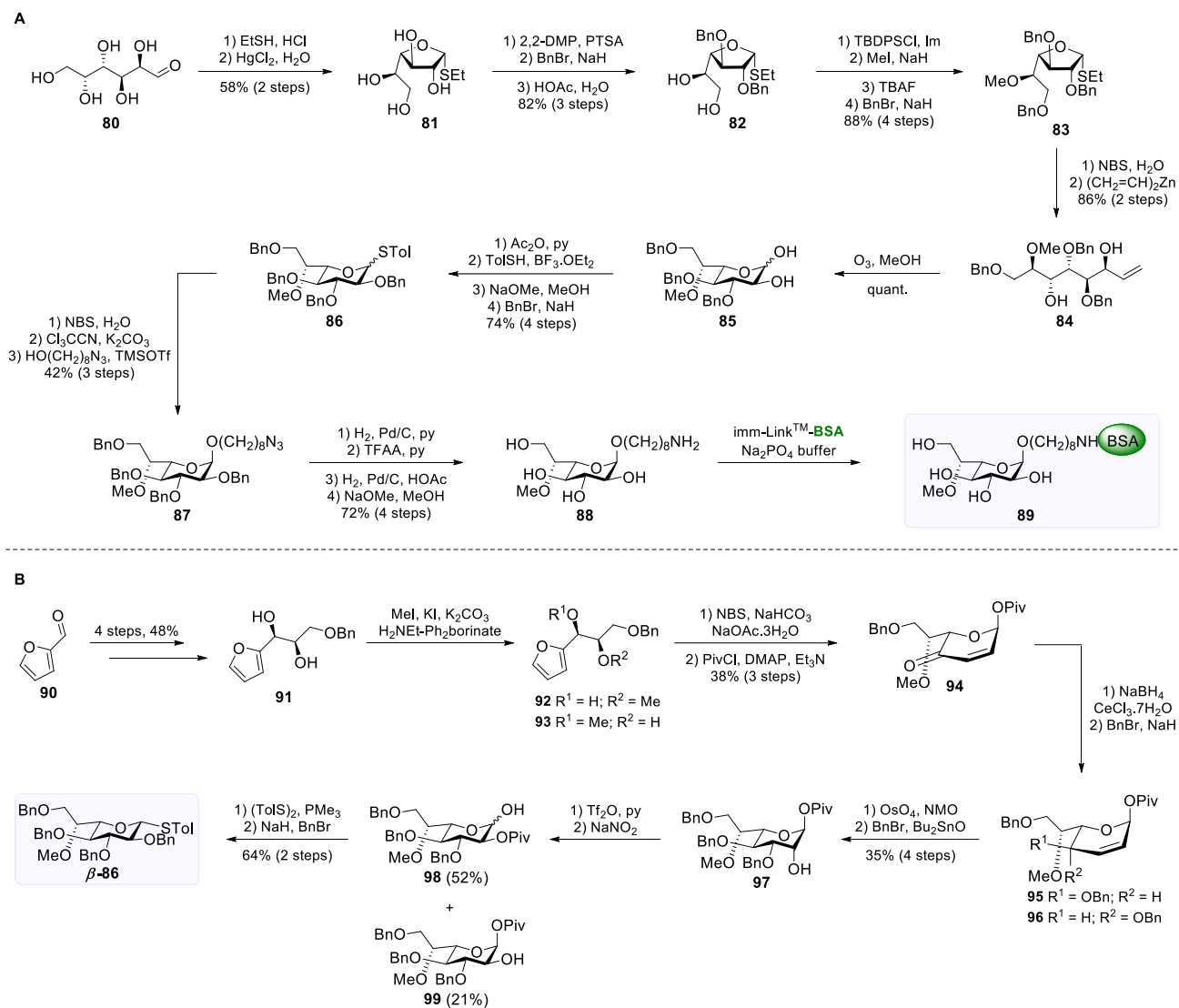
Lowary's synthesis of compounds **73**, **74**, **78**, and **79** commenced with the preparation of 6-deoxy- α -D-*altro*-heptopyranosides **68** and **69** bearing azido-functionalized alkyl linkers at the anomeric position. Using mannoside **63** as starting material, the seventh carbon was incorporated through the regioselective opening of the cyclic sulfate with lithiated dithianyl **64**, which acted as a masked aldehyde functionality, as previously described by van Boom.⁵¹⁸ Unmasking of the latter was achieved through the action of NBS and the resulting aldehyde was reduced into primary alcohol **66**. Protecting group manipulations then furnished thioheptomannoside **67**. To reach the *altro* stereochemistry, the free 3-*OH* underwent inversion *via* formation of a triflate. The resulting intermediate was either benzylated or methylated, each compound was coupled with 8-azido-1-octanol under the action of trimethylsilyl triflate (TMSOTf), and the benzoyl groups were saponified to yield alcohols **68** and **69**. With these compounds in hands, the authors moved on to the assembly of the target trisaccharides. Besides the need for a building block in the D-*altro* stereochemistry, another challenge surrounding the synthesis of these oligosaccharides was the existence of a 1,2-*cis*- α glycosidic bond linking the galactose unit to the 6-deoxy-*altro*-Hepp moiety. The presence of a di-*tert*-butyl silyl acetal at O-4 and O-6 of the galactose moiety of disaccharide **70** allowed the stereoselective formation of this glycosidic bond with either **68** or **69** by hindering the top face of the sugar. The benzoyl and phthalimide groups were cleaved by treatment with ethylenediamine and the resulting free amine was acetylated to afford trisaccharides **71** and **72**. These latter were deprotected into target trisaccharides **73** and **74**, respectively, *via* desilylation with hydrogen fluoride in pyridine and hydrogenolysis. Alternatively, 3-*O*-methylated trisaccharide **72** was coupled with activated phosphonate **75** in the presence of pyridine and the resulting intermediate underwent Atherton-Todd's reaction with benzylamine to afford *N*-benzyl-MeOPN diastereoisomers **76** (*R*) and **77** (*S*). The authors successfully chromatographically separated these isomers and were able to obtain an X-ray structure of compound **76**, which allowed to assign the proper stereochemistry of the MeOPN groups. Both diastereoisomers were then deprotected as previously described. By comparing the NMR spectra of synthetic compounds **78** and **79** with the spectrum of the native CPS of *C. jejuni* strain 81-176 (HS:23/36), it was concluded that the stereochemistry of the MeOPN groups in the latter is *R*. As the assembly of this group is

performed enzymatically, it can be assumed that this stereochemistry is the same for all *C. jejuni* CPS bearing this modification.

5.7.4 *C. jejuni* HS:2

In 2011, the Lowary group described the synthesis of the unusual 6-*O*-Me-D-*glycero-α*-L-*gluco*-heptopyranose monosaccharide unit included in the tetrasaccharide repeating unit of *C. jejuni* NCTC11168 (serotype HS:2, see Figure 1).⁵¹⁹ As described in Scheme 5A, their approach was based on the use of six-carbon sugar D-galactose as starting material, which would be homologated into the corresponding heptose through the extension of the C1 aldehyde functionality. If most heptoses are usually synthesized *via* the chain elongation of a C6 aldehyde through Grignard or Wittig reactions, as mentioned earlier, Lowary's method was advantageous as it only required the use of D-galactose instead of the more expensive L-glucose, which would have been needed to reach the *gulo* configuration.

CHAPITRE 5 – PROGRESS TOWARDS THE DEVELOPMENT OF GLYCAN-BASED VACCINES AGAINST CAMPYLOBACTERIOSIS



Scheme 5.5. Lowary's synthesis of BSA-conjugated heptopyranoside **89** from D-galactose (A) and *de novo* approach towards thiogalactoside β -**86** (B) associated with *C. jejuni* HS:2

The authors thus first prepared thiogalactofuranoside **81** through the formation of a diethyl dithioacetal from the opened-form of D-galactose and subsequent HgCl₂-mediated cyclization. Intermediate **81** was converted into compound **83** ready for the key homology step through standard protecting group manipulations. Hydrolysis of thioglycoside **83** under the action of *N*-bromosuccinimide (NBS) in the presence of water afforded a hemiacetal which, upon treatment with divinyl zinc, stereoselectively yielded alkene **84**. Ozonolysis of the latter then furnished glycoside **85** *via* hemiacetalization of the resulting aldehyde. Acetylation, installation of a tolyl

CHAPITRE 5 – PROGRESS TOWARDS THE DEVELOPMENT OF GLYCAN-BASED VACCINES AGAINST CAMPYLOBACTERIOSIS

group at the anomeric position, saponification, and benzylation subsequently afforded thioglycoside **86**. Noteworthy, a crystalline tetra-*para*-nitrobenzoyl derivative of the latter was prepared and confirmed the stereochemistry of the heptose ring substituents. Compound **86** was converted into the corresponding trichloroacetimidate and was coupled with 8-azido-1-octanol, which would later act as a spacer arm for conjugation to a carrier protein. This reaction afforded a 4:1 mixture of α/β anomers that could be separated chromatographically. Deprotection of α -anomer **87** into target 6-*O*-Me-D-*glycero*- α -L-*gluco*-heptopyranoside **88** was effectively achieved in a four-step sequence. Finally, coupling of compound **88** with bovine serum albumin (BSA) allowed the preparation of glycoconjugate **89** in a 4:1 sugar/protein ratio, which would be useful for the generation of antibodies as well as for probing enzymes involved in *C. jejuni* CPSs assembly.

Following this work, Lowary *et al.* took inspiration from Ogasawara⁵²⁰ and O'Doherty's^{278, 521-523} furfural-based pathways towards hexopyranosides for the design of a novel *de novo* approach requiring less chromatographic purification steps than their previous approach based on D-galactose as starting material.⁵²⁴ As depicted in Scheme 5B, diol **91** was prepared in good yield through a four-step sequence from furfural **90**. Methylation of compound **91** under the catalysis of 2-aminoethyl diphenylborinic acid yielded a 1:1 regioisomeric mixture of **92** and **93**. Dihydropyran **94** was prepared through the Achmatowicz rearrangement of the latter mixture and subsequent α -selective pivaloylation. Luche reduction was then carried out followed by benzylation to afford diastereoisomers **95** and **96** with a preference for the former. The pseudoaxial orientation of the groups at C1 and C4 of compound **96** presumably prevented its dihydroxylation, which consequently allowed the chemoselective preparation of intermediate **97** after tin-catalyzed benzylation of the C3 hydroxyl group. To achieve the target L-*gluco* configuration, the free 2-*OH* group underwent inversion through the formation of a triflate. Despite extensive investigation of alternative inversion conditions, pivaloyl migration could not be prevented and compound **98** (52% yield) was obtained as the major product but could not be separated from the expected product **99** (21% yield). The mixture was therefore treated with *p*-tolyl disulfide in presence of trimethylphosphine followed by benzyl bromide. Importantly, the final benzylation step allowed the separation of target thioheptopyraoside β -**86** from unreacted intermediate **99**. By reducing the

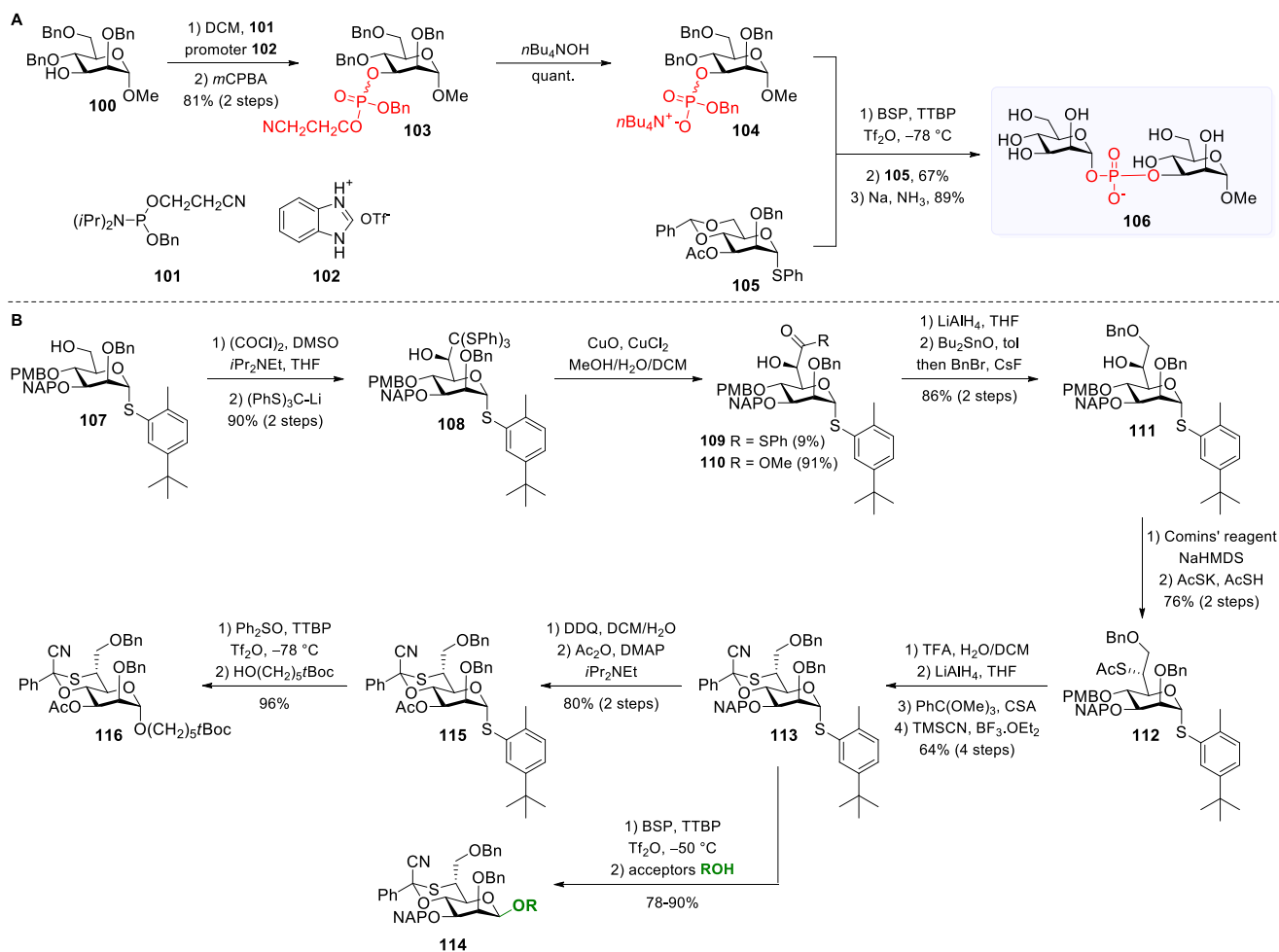
number of purification steps to six compared to 15 for their approach using D-galactose as starting material, this alternative synthetic method towards a 6-*O*-Me-D-glycero- α -L-gluco-heptopyranoside derivative will prove useful for the large-scale synthesis of the latter.

5.7.5 *C. jejuni* HS:53c

The trisaccharide repeating unit of *C. jejuni* HS:53c CPS constitutes a challenging target in synthetic chemistry for many reasons. First, its backbone is composed of 6-deoxy-D-manno-heptopyranoside units, which require extensive protecting groups manipulations for the incorporation of the seventh carbon. Additionally, these moieties are linked through both α - and β -linkages. If the α -glycosidic bonds can be readily formed by neighboring group participation, β -mannosidic linkages preparation is less trivial because of the steric hindrance of the C2 axial substituent and the anomeric effect, which stabilizes the α -anomer, as previously mentioned. Finally, two of these three *manno*-heptopyranoside units are linked through a phosphodiester linkage (see Figure 2).

In 2009, Crich's group reported the synthesis of phosphodiester-containing α -disaccharide **106** related to *C. jejuni* HS:53c CPS as well as other analogous mannopyranosyl phosphosugars not depicted here (Scheme 6A).⁵²⁵ Using benzylated mannopyranoside **100** as starting material, the authors introduced the phosphodiester moiety by coupling the latter with benzyl 2-cyanoethyl *N,N*-diisopropylphosphoramidite **101** under the promotion of benzimidazolium trifluoromethanesulfonate **102**. *In situ* oxidation of the resulting intermediate then furnished diester **103** as a 1:1 mixture of diastereoisomers. Treatment with tetrabutylammonium hydroxide allowed the cleavage of the 2-cyanoethyl group and thus furnished salt **104**, which was readily coupled with thioglycoside **105** using 1-benzenesulfinyl piperidine (BSP) and triflic anhydride (Tf₂O) as the promoting system. Noteworthy, due to the presence of the stereodirecting 3-*O*-acetyl group and the 4,6-benzylidene acetal,⁵²⁶ the reaction exhibited complete α -stereoselectivity. Phosphodiester-linked disaccharide **106**, mimicking part of *C. jejuni* HS:53c CPS, was finally reached *via* Birch's reduction.

CHAPITRE 5 – PROGRESS TOWARDS THE DEVELOPMENT OF GLYCAN-BASED VACCINES AGAINST CAMPYLOBACTERIOSIS



Scheme 5.6. Crich's synthesis of phosphodiester-containing disaccharide **106** (A) and α - and β -stereoselective *manno*-heptopyranoside building blocks **115** and **113** (B) related to *C. jejuni* HS:53c CPS

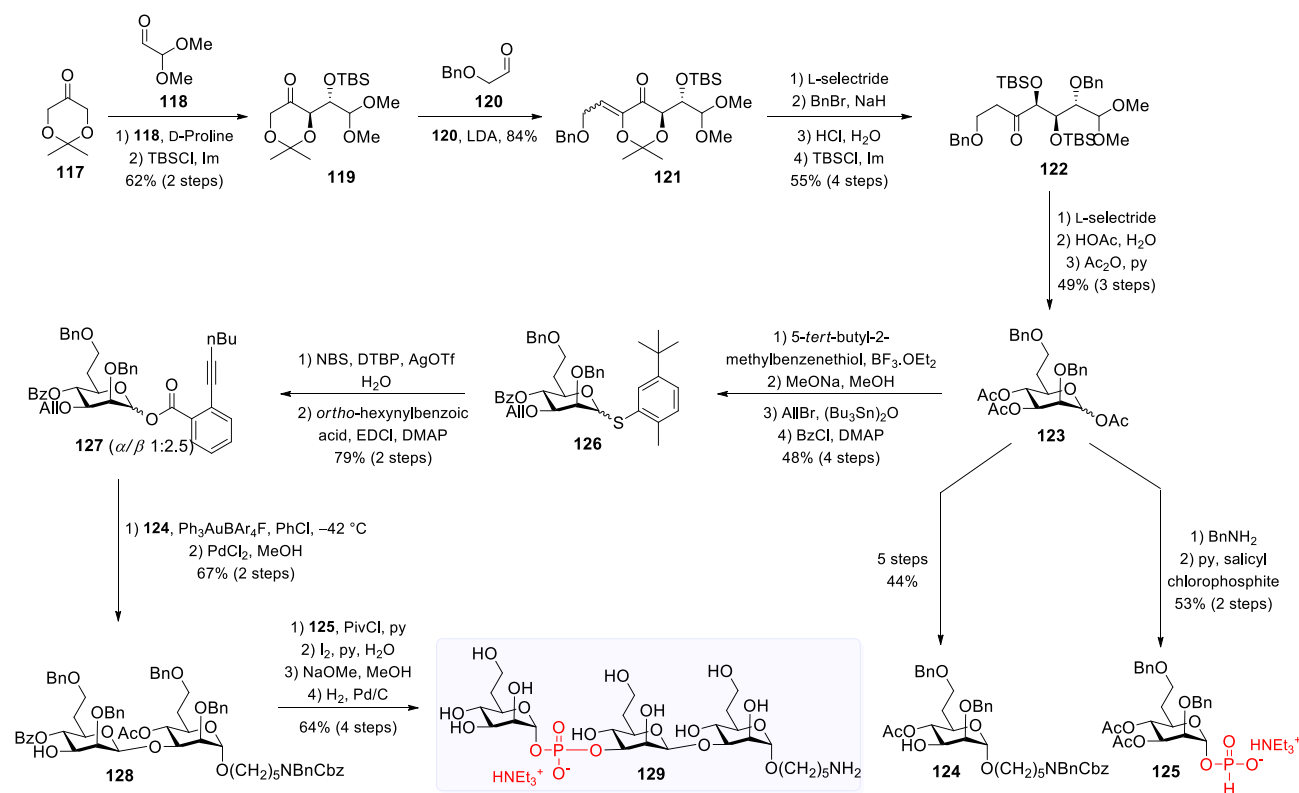
Having established an efficient way to incorporate the phosphodiester linkage characteristic of *C. jejuni* HS:53c, Crich and co-workers were later interested in the design of *manno*-heptopyranoside building blocks that could either display β - and α -stereoselectivities.⁵²⁷ As depicted in Scheme 6B, 4-*O*-6-*S*- α -cyanobenzylidene thio-*D*-*manno*-heptopyranosides **113** and **115**, differing only by the 3-*O*-substituent, respectively exhibited complete β - and α -stereoselectivities. For the preparation of these compounds, mannoside **107** was first oxidized *via* Swern's conditions and the resulting aldehyde was treated with the hindered reagent tris(phenylthio)methyl lithium. The latter reaction exclusively afforded (L,D)-isomer **108**. A mixture of thiophenyl ester **109** and methyl ester **110** was formed upon treatment with CuO and CuCl₂, and both were reduced into a primary alcohol,

which was subsequently regioselectively benzylated through the formation of a tin acetal. Resulting alcohol **111** was isomerized through a two-step protocol involving triflation with Comin's reagent and displacement with a mixture of potassium thioacetate and thioacetic acid, affording compound **112** in good yield. Conversely, other isomerization protocols such as thio-Mitsunobu inversion, triflic anhydride (Tf₂O)-mediated triflation/displacement with NH₄SCN or AcSH/*i*Pr₂NEt, as well as triflation with Comins' reagent/ AsSK-mediated inversion, gave unsatisfying results. Then, a four-step sequence involving PMB protecting group removal, thioacetal reduction, orthoester exchange, and cyanation allowed the introduction of the 4-*O*-6-*S*- α -cyanobenzylidene system and thus afforded key compound **113**. Because of the cyanobenzylidene structure, coupling of the latter donor with different glycosyl acceptors under the promotion of BSP and Tf₂O at low temperature resulted in the stereoselective formation of β -glycosides in good yields. Removal of the 2-naphthylmethyl (NAP) group and acetylation of the resulting hydroxyl group alternatively furnished compound **115** which, because of the 3-*O*-ester group, rather exhibited complete α -stereoselectivity when coupled with *tert*-butyl 6-hydroxyhexanoate. The stereodirecting nature of compound **113** can thus be carefully modulated by modifying the 3-*O*-substituent and this compound therefore constitutes an elegant building block for the assembly of *C. jejuni* HS:53c CPS mimics.

Following Crich's work, Yang *et al.* reported the first total synthesis of *C. jejuni* HS:53c CPS trisaccharide repeating unit.⁵²⁸ To efficiently reach the 6-deoxy-*D*-manno-heptopyranoside backbone, the authors chose to employ a *de novo* approach involving two successive aldol reactions, as shown in Scheme 7. Ketone **117** and 2,2-dimethoxyacetaldehyde **118** were first aldolized under the catalysis of *D*-proline providing a 2,3-*anti*- β -hydroxyketone intermediate, which was silylated into compound **119**. The latter underwent the second aldol reaction with benzyloxyacetaldehyde **120** under the promotion of LDA at low temperature. This step solely furnished ketone **121** with a seven-carbon skeleton, whose double bond stereochemistry could unfortunately not be determined. Compound **122** was then reached *via* a four-step protocol involving (1) L-selectride-mediated reduction of ketone **121** with excellent 2,3-*anti*-3,4-*syn* selectivity and almost complete concomitant migration of the *tert*-butyldimethylsilyl (TBS) group from *O*-2 to *O*-4; (2) benzylation of the resulting C2 hydroxyl group; (3) biphasic deprotection of

the isopropylidene group; and (4) TBS-protection of the C3 alcohol. Cyclization of compound **122** into 6-deoxy-D-manno-heptopyranoside **123** was achieved by reducing the ketone functionality and removing the TBS groups under acidic conditions, and the resulting hemiacetal was finally acetylated. Heptose **123** acted as a key intermediate in Yang's sequence by being the entry point of the three building blocks (**124**, **125**, and **127**) required for the assembly of target trisaccharide **129**. Thus, *via* standard protecting groups manipulations, reducing-end building block **124**, obtained as the sole anomer, was prepared in five steps and bore a protected amino-functionalized alkyl linker at the anomeric position. Alternatively, selective deacetylation of the anomeric position using benzylamine allowed the α -stereoselective introduction of the phosphodiester group in **125** through treatment with salicyl chlorophosphite and pyridine. To reach the third building block **127**, intermediate **126** was first prepared by treating compound **123** with 5-*tert*-butyl-2-methylbenzene thiol in presence of Lewis acid $\text{BF}_3 \cdot \text{OEt}_2$, cleaving the acetyl groups, selectively installing an allyl group at *O*-3 through the formation of a tin-acetal, and protecting the remaining C4 alcohol with a benzoyl group. Thioglycoside **126** was then hydrolyzed and the anomeric position was esterified with *ortho*-hexynylbenzoic acid, furnishing glycoside **127** as a 1.0:2.5 α/β anomeric mixture. This mixture of anomer was employed for the coupling with previously prepared acceptor **124**. Satisfyingly, when conducting the glycosylation under the promotion of $\text{PPh}_3\text{AuBAR}_4^{\text{F}}$ at -42°C in chlorobenzene, a β -disaccharide could be obtained as the major product ($\alpha/\beta = 1.0:3.5$) and in excellent yield, probably because the reaction proceeded in an $\text{S}_{\text{N}}1$ manner *via* a contact ion pair. The authors indeed showed that when β -**127** and α -**127** were separately used for the glycosylation reaction, the β -disaccharide was always the preferred anomer. The β -anomer of the resulting disaccharide was thus isolated and the allyl group was cleaved under the action of PdCl_2 , yielding disaccharide acceptor **128**. Its coupling with *H*-phosphonate ester **125** was achieved successfully using pivaloyl chloride in pyridine. The resulting intermediate was oxidized with iodine in a mixture of pyridine and water to form the required phosphodiester linkage. Lastly, the benzoyl and acetyl groups were removed by transesterification and the remaining benzyl ethers were hydrogenolyzed, which simultaneously liberated the amine group of the spacing arm, therefore being available for protein conjugation.

CHAPITRE 5 – PROGRESS TOWARDS THE DEVELOPMENT OF GLYCAN-BASED VACCINES AGAINST CAMPYLOBACTERIOSIS



Scheme 5.7. Yang *de novo* synthesis of trisaccharide 129 as a mimic of *C. jejuni* HS:53 CPS

5.8 Conclusions

Considering the socio-economical and public health burden that is campylobacteriosis, there is an urgent need for prophylactic measures to reduce *C. jejuni* infections. As opposed to other enteric pathogens, this bacterium produces serospecific CPSs that act as exquisite targets for vaccine development, as demonstrated by the immunization of New World Monkeys with a CRM₁₉₇-CPS_{HS:23/36} glycoconjugate that offered complete protection against diarrheal disease following orogastric infection with the corresponding *C. jejuni* strain. These CPSs are characterized by the presence of heptoses and 6-deoxy-heptoses in unusual configurations as well as acid- and base-labile MeOPN moieties that are highly specific to *C. jejuni*. Because of the role of these polysaccharides in virulence and immunogenicity as well as the synthetic challenges that they represent, the preparation of mono- and oligosaccharide mimics has been the subject of intensive research efforts. Such research works proved useful in that they revealed the absolute configuration of the MeOPN moieties in strain 81-176 of serotype HS:23/36—which was shown to be *R*—and

CHAPITRE 5 – PROGRESS TOWARDS THE DEVELOPMENT OF GLYCAN-BASED VACCINES AGAINST CAMPYLOBACTERIOSIS

demonstrated the existence of primary MeOPN-specific antibodies. Keeping the crucial immunogenicity of the MeOPN groups in mind, novel methods for their efficient introduction in various carbohydrates have been established. Preparation of sugars in rare configuration has also been addressed and these approaches could be useful for the synthesis of other *C. jejuni* serotypes mimics.

Unfortunately, because research surrounding synthetic carbohydrates as vaccine candidates against campylobacteriosis is still at an early stage, little is known about the structure-immunogenicity relationship of the reported constructs—aside from Monteiro’s demonstration of the existence of MeOPN-specific antibodies. The fact that *C. jejuni* CPSs are made of rare sugars made it necessary for glycochemists to first develop the appropriate synthetic tools to achieve the required glycosides, as reviewed herein, which are now available for subsequent investigations. To guide future synthetic work, one could for instance take inspiration from the work on *S. pneumoniae*—an invasive mucosal pathogen—synthetic vaccines regarding the oligosaccharides structural features and number of repeating units required for optimal antibodies production.⁵²⁹⁻⁵³⁴ The investigation of Berti and co-workers surrounding the impact of oligosaccharides conjugation at defined sites of the carrier protein on the immunogenic response against *Candida* could also guide eventual work on anti-*Campylobacter* vaccines.⁵³⁵ In this context, one-pot glycosylation or automated glycan assembly strategies could prove useful to efficiently provide oligosaccharides of varying constitution. These latter could then be employed for the development of synthetic glycan microarrays to screen for potential protective epitopes that would be able to elicit IgA and IgG, as they have been shown to protect against pathogens at mucosal surfaces.^{536, 537}

Altogether, these data and future work towards the evaluation of the antigenicity and immunogenicity of these synthetic constructs will doubtlessly contribute to the unraveling of the structural requirements for *C. jejuni* and to the development of such prophylactic measures or CPS-based diagnostic tools.

5.9 Acknowledgments

This work was supported by a Discovery grant from the Natural Sciences and Engineering Research Council of Canada (NSERC) under award number RGPIN-2016-04950 (to C. G.). C. G. holds a Fonds de recherche du Québec – Santé (FRQS) Research Scholars Junior 2 Career Award. M. C. thanks NSERC for a Vanier Canada Graduate Scholarship and Fonds de recherche du Québec – Nature et technologies (FRQNT) for Ph.D. fellowships.

CHAPITRE 6 : SYNTHESIS OF α -D-IDOSE PENTAACETATE FROM β -D-GLUCOSE PENTAACETATE VIA PAULSEN ACETOXONIUM REARRANGEMENT

Nitish Verma,^{a‡} Maude Cloutier,^{a‡} David Clément,^{†b} Charles Gauthier^{a*}

^a*Unité Mixte de Recherche INRS-UQAC, Centre Armand-Frappier Santé Biotechnologie, Institut national de la recherche scientifique (INRS), 531, boul. des Prairies, Laval (Québec), H7V 1B7, Canada*

^b*Institut Pasteur, Université Paris Cité, CNRS UMR3523, Unité de Chimie des Biomolécules, 28 rue du Dr Roux, 75 724 Paris Cedex 15, France*

[‡]*Both authors contributed equally to this work.*

[†]*Checker; under supervision of Laurence A. Mulard.*

Chapitre accepté dans Carbohydrate Chemistry : Proven Synthetic Methods, Volume 6, Ed.: Giguère, D., Vincent, S. P.; 2023, CRC Press, accepted (invited contribution).

Titre français : Synthèse de l' α -D-idose pentaacétate à partir du β -D-glucose pentaacétate *via* le réarrangement d'acétoxonium de Paulsen

Contribution des auteurs : Maude Cloutier (60%) et Nitish Verma (40%) ont réalisé l'optimisation de la méthode de synthèse. David Clément a validé la méthode proposée. Maude Cloutier a réalisé la caractérisation des composés et rédigé le chapitre. Charles Gauthier, Nitish Verma, David Clément et Laurence A. Mulard ont révisé le chapitre.

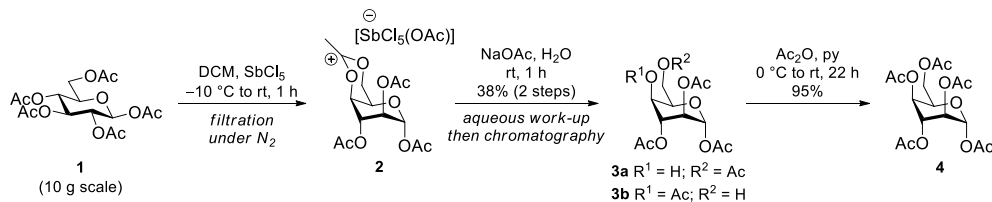
6.1 Résumé

Le D-idose est un sucre rare mais biologiquement important qui n'est pas disponible commercialement. Parmi les différentes méthodes de synthèse rapportées pour accéder à ce sucre, le réarrangement de Paulsen est l'approche la plus directe et présente l'avantage d'employer du β -D-glucose peracétylé comme produit de départ. Nous avons toutefois observé que le protocole standard n'est pas reproductible lorsque les conditions de laboratoire sont particulièrement humides et mène plutôt à une décomposition significative du produit. Nous rapportons ici un protocole amélioré pour le réarrangement de Paulsen basé sur une étape de filtration en conditions anhydres permettant la synthèse reproductible d' α -D-idose peracétylé à l'échelle du gramme.

6.2 Abstract

D-Idose is a rare albeit biologically important sugar that is not commercially available. Among the different synthetic methods reported to access this sugar, the Paulsen acetoxonium rearrangement is the most straightforward one and possesses the advantage of using cheap β -D-glucose pentaacetate as starting material. We have however observed that the standard work-up protocol is not reproducible when in humid weather and instead leads to significant decomposition. We herein report an improved protocol for the Paulsen acetoxonium rearrangement based on a filtration step under anhydrous conditions that allows the reproducible gram-scale synthesis of α -D-idose pentaacetate.

6.3 Results



Scheme 6.1. Synthesis of peracetylated idoside 4 via Paulsen acetoxonium rearrangement

D-Idose is a commercially unavailable, yet important sugar that has been employed for the synthesis of biologically relevant compounds such as lupane-type saponins,⁵³⁸ functionalized gold

CHAPITRE 6 – SYNTHESIS OF α -D-IDOSE PENTAACETATE FROM β -D-GLUCOSE PENTAACETATE VIA PAULSEN ACETOXONIUM REARRANGEMENT

nanoparticles,⁵³⁹ and *Campylobacter jejuni*-related oligosaccharides.⁴⁴ Despite the attractiveness of D-idose building blocks, only few methods have been developed for their challenging synthesis. As such, late-stage conversion of functionalized D-galactoside,^{503, 504} C-allyl α -D-glucoside,⁵⁴⁰ or *gluco*-heptonic acid,⁵⁴¹ all available through multi-step syntheses, enabled the preparation of D-idose analogues. Alternatively, Dromowicz and Köll reported the synthesis of D-idose via a two-step protocol involving the addition of nitromethane to D-xylose followed by a modified Nef reaction,⁵⁰¹ while Szekrenyi and co-workers accomplished its synthesis biocatalytically.⁵⁴² However, these methods show limited synthetic applicability due to the need for highly modified precursors, large excess of reagents, potentially explosive chemicals, or specialized equipment.

Using inexpensive β -D-glucose pentaacetate (**1**), Paulsen acetoxonium rearrangement provides a straightforward and effective method for the early-stage preparation of D-idoses that can be readily functionalized.⁵⁰² This elegant protocol, first reported in 1967⁵⁰² and reinvestigated in 2013 by Kopitzki and Thiem,⁵³⁹ relies on the activation of the anomeric acetate of **1** through the action of antimony pentachloride. This is followed by a cascade reaction involving the successive nucleophilic displacement of the C1, C2, C3, and C4 acetates, yielding the insoluble 4,6-*O*-acetoxonium-1,2,3-tri-*O*-acetyl- α -D-idopyranosyl acetoxopentachloroantimonate (**2**). Hydrolysis of the latter (yielding intermediates **3a** and **3b**), and subsequent acetylation then enable the formation of α -D-idose pentaacetate (**4**).

However, when conducting the Paulsen rearrangement during warm and humid weather conditions, we observed serious reproducibility issues. It resulted in poor yields (< 2%) for the first two steps along with significant decomposition of the antimonate salt **2**. After careful investigation, we managed to overcome these issues by taking additional precautions improving the work-up and the protocol. As such, performing the filtration of salt **2** under inert atmosphere using an adapted cannula filtration technique – as opposed to a standard Büchner filtration – prevented decomposition and minimized product losses (see Fig. 1). This step was rapidly followed by hydrolysis of the resulting salt with aqueous sodium acetate, providing a mixture of alcohols **3a** and **3b** in 38% yield over two steps. To avoid the formation of HCl arising from hydrolysis of SbCl₅ under moisture conditions (which would decompose salt **2**), the reaction and

CHAPITRE 6 – SYNTHESIS OF α -D-IDOSE PENTAACETATE FROM β -D-GLUCOSE PENTAACETATE VIA PAULSEN ACETOXONIUM REARRANGEMENT

filtration were performed under anhydrous conditions. Moreover, the rapid addition of a 2.4 M aqueous solution of sodium acetate during the second step prevented the reaction mixture from becoming strongly acidic and provided suitable conditions for the hydrolysis of salt **2** into compounds **3a** and **3b**, without decomposition. During work-up, additional washings of the organic layer with saturated aqueous NaHCO₃ quenched the remaining traces of SbCl₅ and minimized further decomposition. Silica gel column chromatography was performed to remove the unreacted starting material **1** that would otherwise be difficult to separate from α -D-idose pentaacetate (**4**). Acetylation of alcohols **3a** and **3b** finally furnished target compound **4** in 95% yield (see Fig. 1 for TLC).

The all-axial arrangement of the protons H1, H2, H3 and H4, characterized by small coupling constants ($^3J = 2\text{-}4$ Hz), allowed the straightforward confirmation of the *ido* configuration of compound **4** by ¹H NMR analysis. This optimized three-step procedure, which can be easily performed within two days, enabled the reproducible gram-scale synthesis of α -D-idose pentaacetate **4**.

CHAPITRE 6 – SYNTHESIS OF α -D-IDOSE PENTAACETATE FROM β -D-GLUCOSE PENTAACETATE VIA PAULSEN ACETOXONIUM REARRANGEMENT

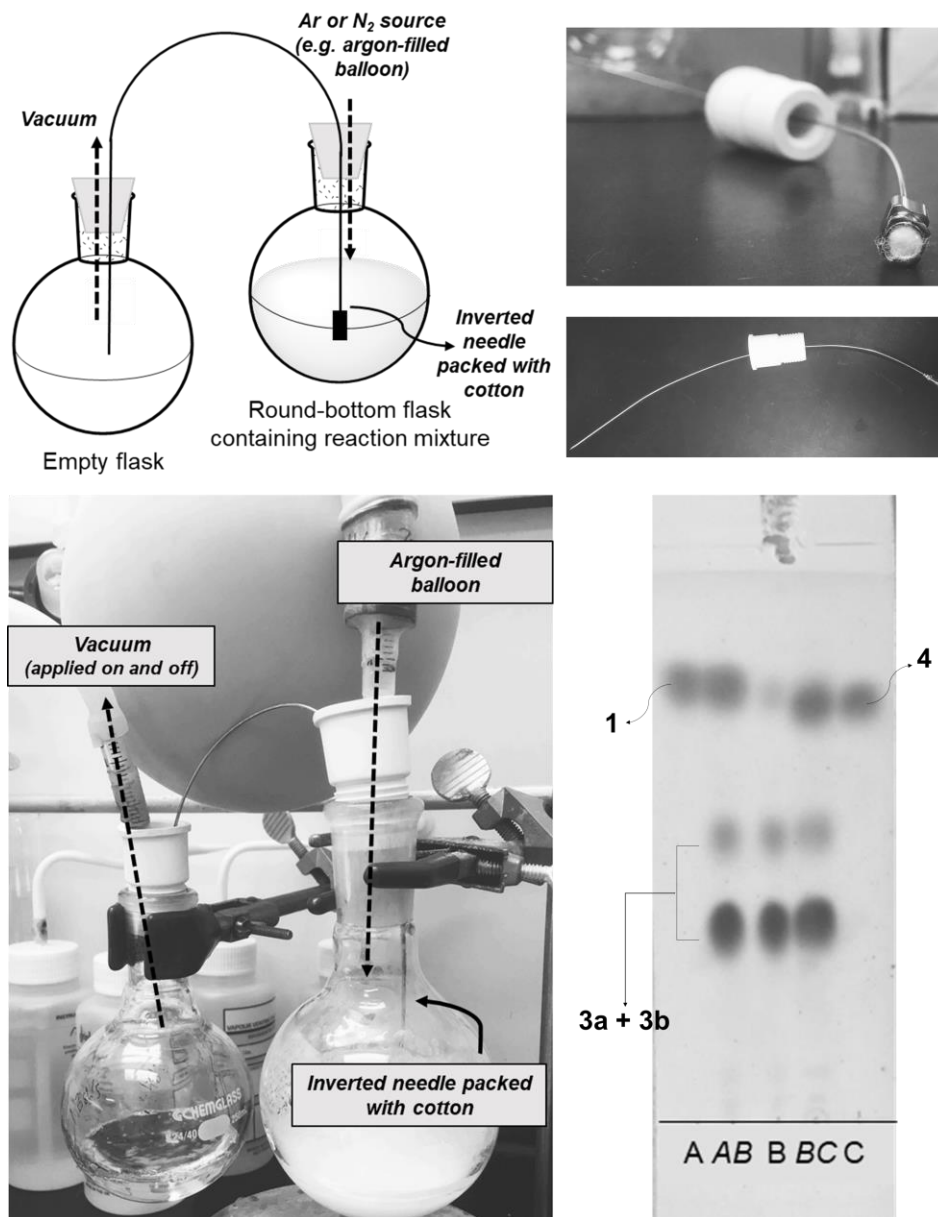


Figure 6.1. Experimental set-up for the adapted cannula filtration and representative TLC (1:2 hexanes-EtOAc) of the reaction sequence on silica gel 60 F₂₅₄ 0.25 mm pre-coated glass plate³⁷

³⁷ A: peracetylated β -D-glucose **1**; AB: A + B co-spot; B: crude mixture of hydrolysis step; BC: B + C co-spot; C: crude peracetylated α -D-idose (**4**).

6.4 Experimental

General methods.

Reagents were purchased from Sigma-Aldrich and used as received. Peracetylated β -D-glucose was prepared (100 g scale) from D-glucose according to a known procedure or bought from a commercial source.⁵⁴³ Anhydrous solvents were prepared by storing commercial solvents (ACS grade) over activated 4 Å molecular sieves for at least three days. Reactions were monitored by thin-layer chromatography (TLC) on silica gel 60 F₂₅₄ 0.25 mm pre-coated aluminum foil plates (Silicycle). Spots were visualized by spraying with orcinol (1 mg.mL⁻¹) in 10% aqueous H₂SO₄ and heating. Flash column chromatography was performed on silica gel 60 Å (15-40 µm). Nuclear magnetic resonance (NMR) spectra were recorded at 297 K in the solvent indicated with a 600 MHz instrument equipped with a cryoprobe, employing software supplied by the manufacturer. ¹H NMR spectra were referenced to internal tetramethylsilane (TMS, $\delta_{\text{H}} = 0.00$ ppm), while ¹³C NMR spectra were referenced to CDCl₃ residual peaks ($\delta_{\text{C}} = 77.16$ ppm). Assignments were based on ¹H, ¹³C, COSY, and HSQC experiments. High-resolution mass spectra (HRMS) were recorded on an ESI-Q-TOF mass spectrometer. Optical rotations $[\alpha]_{\text{D}}^{20}$ were measured with an Anton Paar polarimeter using a 1 mL quartz cell and a path length of 1 dm. Concentrations (*c*) are given in g.100 mL⁻¹. Elemental analyses were performed by Ján Veizer Stable Isotope Laboratory at University of Ottawa. Unless stated otherwise, solutions in organic solvents were dried with anhydrous MgSO₄ and concentrated under reduced pressure at 40 °C.

1,2,3,4,6-Penta-*O*-acetyl- α -D-idopyranose (4).

Step I. β -D-Glucose pentaacetate **1**³⁸⁵⁴³ (10.0 g, 25.6 mmol, 1.0 equiv) was dried under high vacuum for 8 h in a 250 mL round-bottom flask. Anhydrous CH₂Cl₂ (59 mL) was added under argon and the solution was cooled to -10 °C using an ice-acetone bath. A solution of antimony pentachloride (SbCl₅,³⁹ 4.22 mL, 33.3 mmol, 1.3 equiv) in anhydrous CH₂Cl₂ (10 mL) was added

³⁸Only the β -anomer can be used for the Paulsen rearrangement described herein.

³⁹SbCl₅ is highly corrosive, toxic, hazardous, and should be handled carefully.

CHAPITRE 6 – SYNTHESIS OF α -D-IDOSE PENTAACETATE FROM β -D-GLUCOSE PENTAACETATE VIA PAULSEN ACETOXONIUM REARRANGEMENT

using a glass syringe.^A The ice-acetone bath was removed, and the solution was allowed to slowly warm up. After 15 to 20 min, a precipitate started to appear, corresponding to antimonate salt **2**. The suspension was stirred for an additional 40 to 45 min (total stirring time = 1 h) at rt. The solvents were removed under inert atmosphere through an adapted cannula filtration technique by applying a negative pressure with the fume hood vacuum line (pressure = 240 mbar, refer to Fig. 1 for experimental set-up). While maintaining an inert atmosphere, the white solid (antimonate salt **2**) was washed once with Et₂O (30 mL) and the solvent was again sucked off through cannula filtration.⁴⁰

Step II. Directly after the previous washing step, an aqueous NaOAc solution (2.4 M, 156 mL) was added to the white solid (antimonate salt **2**) at rt. The mixture was stirred at rt for 1 h, after which it was extracted with CH₂Cl₂ (3 × 20 mL). The combined organic layers were washed with H₂O (1 × 50 mL), a saturated aq. solution of NaHCO₃ (2 × 50 mL), and H₂O (1 × 50 mL), filtered, dried and concentrated. The residue was chromatographed (3:1 → 1:2 hexanes-EtOAc) to remove any remaining β -D-glucose pentaacetate **1** (372 mg, 4%), yielding a mixture of alcohols **3a** and **3b** (0.16:1.0) as a colorless oil (3.40 g, 38% in two steps): R_f (**3a**) = 0.4 (1:4 hexanes-EtOAc); R_f (**3b**) = 0.3 (1:4 hexanes-EtOAc); ¹H NMR (600 MHz, CDCl₃): δ (ppm) 6.05 (d, 1 H, J 1.2 Hz, H-1^{3b}), 6.03 (s, 0.16 H, H-1^{3a}), 5.08 (t, 1 H, J 3.9 Hz, H-3^{3b}), 4.99-4.98 (m, 1.16 H, H-4^{3b}, H-3^{3a}), 4.92-4.90 (m, 0.16 H, H-2^{3a}), 4.90 (dd, 1 H, J 3.9 Hz, 2.7 Hz, H-2^{3b}), 4.35-4.30 (m, 1.48 H, H-5^{3b}, H-5^{3a}, H-6a^{3a}, H-6b^{3a}), 3.78-3.73 (m, 1.16 H, H-6a^{3b}, H-4^{3a}), 3.59-3.56 (m, 1 H, H-6b^{3b}), 2.74 (d, 1 H, J 10.2 Hz, OH^{3a}), 2.45 (br s, 1 H, OH^{3b}), 2.15 (s, 0.48 H, CH₃^{3a}), 2.14 (s, 3 H, CH₃^{3b}), 2.13-2.12 (4 × s, 9.96 H, CH₃^{3b}, CH₃^{3b}, CH₃^{3b}, CH₃^{3a}), 2.13 (s, 3 H, CH₃^{3a}); ¹³C NMR (150 MHz, CDCl₃): δ (ppm) 170.5-168.5 (4 × CO^{3b}, 4 × CO^{3a}), 90.9 (C-1^{3a}), 90.7 (C-1^{3b}), 69.2 (C-5^{3b}), 68.9 (C-3^{3a}), 67.8 (C-5^{3a}), 67.2-66.7 (C-3^{3b}, C-4^{3b}, C-2^{3a}, C-2^{3b}), 65.9 (C-4^{3a}), 62.9 (C-6^{3a}), 60.7 (C-6^{3b}), 21.0-20.8 (4 × CH₃^{3b}, 4 × CH₃^{3a}); HRMS (ESI-TOF) m/z : calcd for C₁₄H₂₀O₁₀Na [M + Na]⁺, 371.0948; found, 371.0944.

^AUpon addition of SbCl₅, the needle should be quickly rinsed with CH₂Cl₂ to prevent corrosion.

⁴⁰A new syringe packed with cotton should be used for the washing step, to prevent clogging of the cotton by salt **2**.

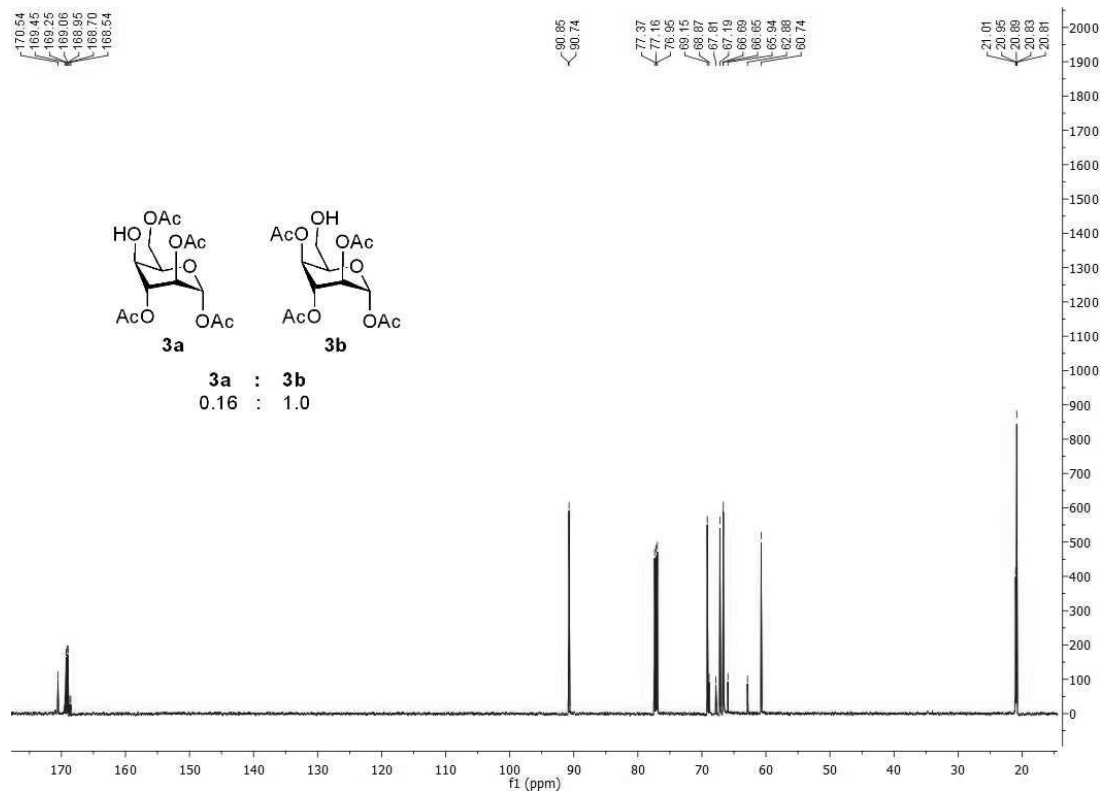
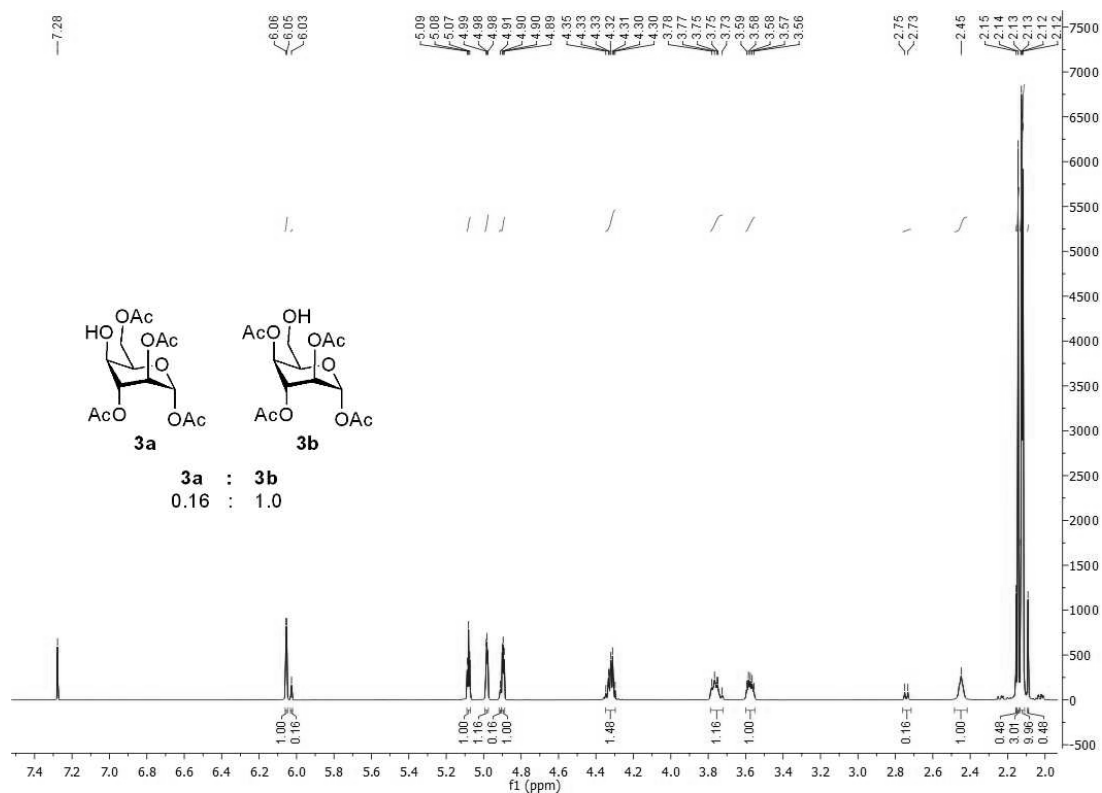
CHAPITRE 6 – SYNTHESIS OF α -D-IDOSE PENTAACETATE FROM β -D-GLUCOSE PENTAACETATE VIA PAULSEN ACETOXONIUM REARRANGEMENT

Step III. A solution of the crude mixture of alcohols **3a** and **3b** (3.28 g, 9.42 mmol, 1.0 equiv) in anhydrous pyridine (21 mL) was cooled to 0 °C (ice-water bath) and Ac₂O (64 mL) was added slowly using a glass syringe. The cooling bath was removed, and the mixture was stirred at rt overnight. When TLC (1:4 hexanes-EtOAc) showed that the reaction was complete, CH₂Cl₂ (40 mL) was added, and the mixture was transferred to a 250 mL conical flask. Ice water (15 mL) was added with slow stirring, followed by slow addition of 1 M aq. HCl (40 mL). The organic layer was washed again with 1 M aq. HCl (1 x 50 mL) and then with a saturated aq. solution of NaHCO₃ (2 x 50 mL). The organic layers were dried, filtered, concentrated, and co-evaporated with toluene (3x). The residue was chromatographed (1:0 → 1:1 hexanes-EtOAc) to give 1,2,3,4,6-penta-*O*-acetyl- α -D-idopyranose (**4**) as a white amorphous solid (3.50 g, 95%). Crystallization from a minimal amount of EtOH (~10 mL) gave compound **4** (3.05 g): mp 93.0–96.4 °C, lit. 92 °C;⁵³⁹ $[\alpha]_{\text{D}}^{20} +72.5$ (*c* 1, CHCl₃), lit. $[\alpha]_{\text{D}}^{20} +69.7$ (*c* 1, CHCl₃);⁵³⁹ $R_f = 0.6$ (1:4 hexane-EtOAc); ¹H NMR (600 MHz, CDCl₃): δ (ppm) 6.07 (d, 1 H, *J* 1.9 Hz, H-1), 5.08 (t, 1 H, *J* 3.9 Hz, H-3), 4.95 (t, 1 H, *J* 3.0 Hz, H-4), 4.90–4.87 (m, 1 H, H-2), 4.48 (td, 1 H, *J* 6.4 Hz, 2.4 Hz, H-5), 4.23–4.16 (m, 2 H, H-6a, H-6b), 2.13 (s, 3 H, CH₃), 2.12 (s, 3 H, CH₃), 2.12 (s, 3 H, CH₃), 2.11 (s, 3 H, CH₃), 2.07 (s, 3 H, CH₃); ¹³C NMR (150 MHz, CDCl₃) δ (ppm) 170.6 (CO), 169.8 (CO), 169.2 (CO), 168.9 (CO), 168.5 (CO), 90.7 (C-1), 66.8, 66.4, 66.34, 66.26 (C-2, C-3, C-4, C-5), 61.9 (C-6), 21.0 (CH₃), 20.83 (CH₃), 20.79 (CH₃), 20.75 (CH₃); HRMS (ESI-TOF) *m/z*: calcd for C₁₆H₂₂O₁₁Na [M + Na]⁺, 413.1054; found, 413.1069. Anal. Calcd for C₁₆H₂₂O₁₁ C, 49.23; H, 5.68. Found: C, 49.58; H, 5.21.

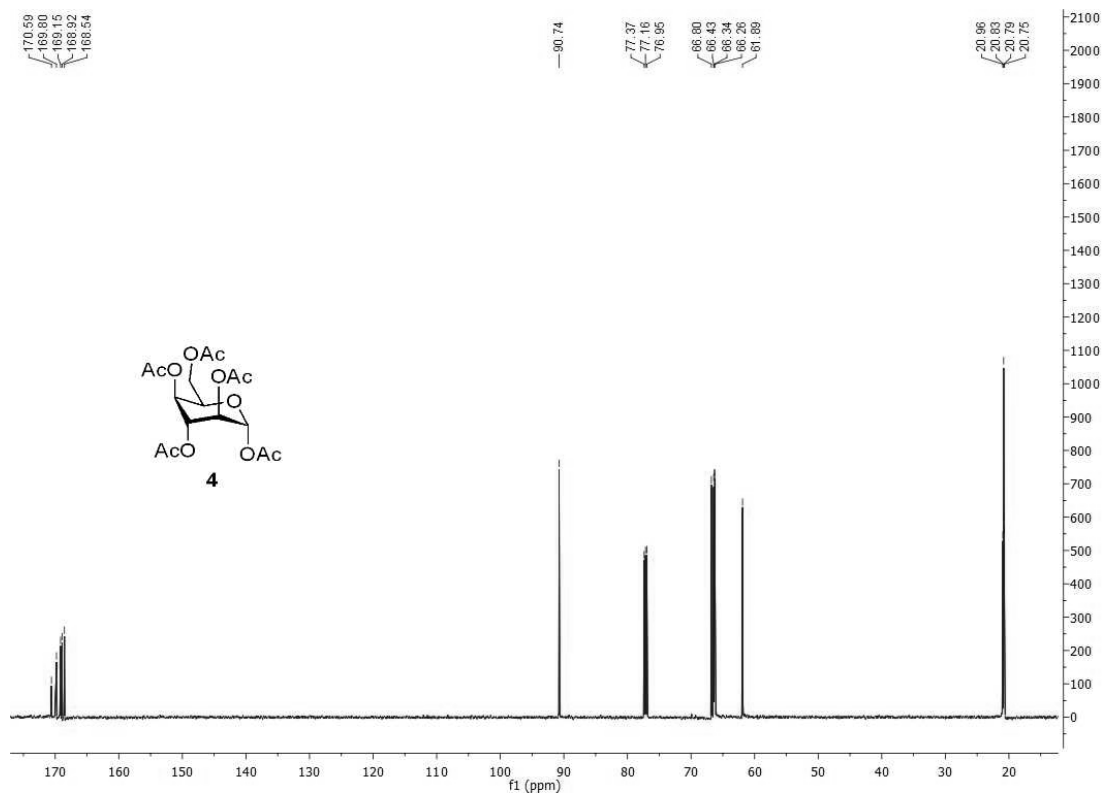
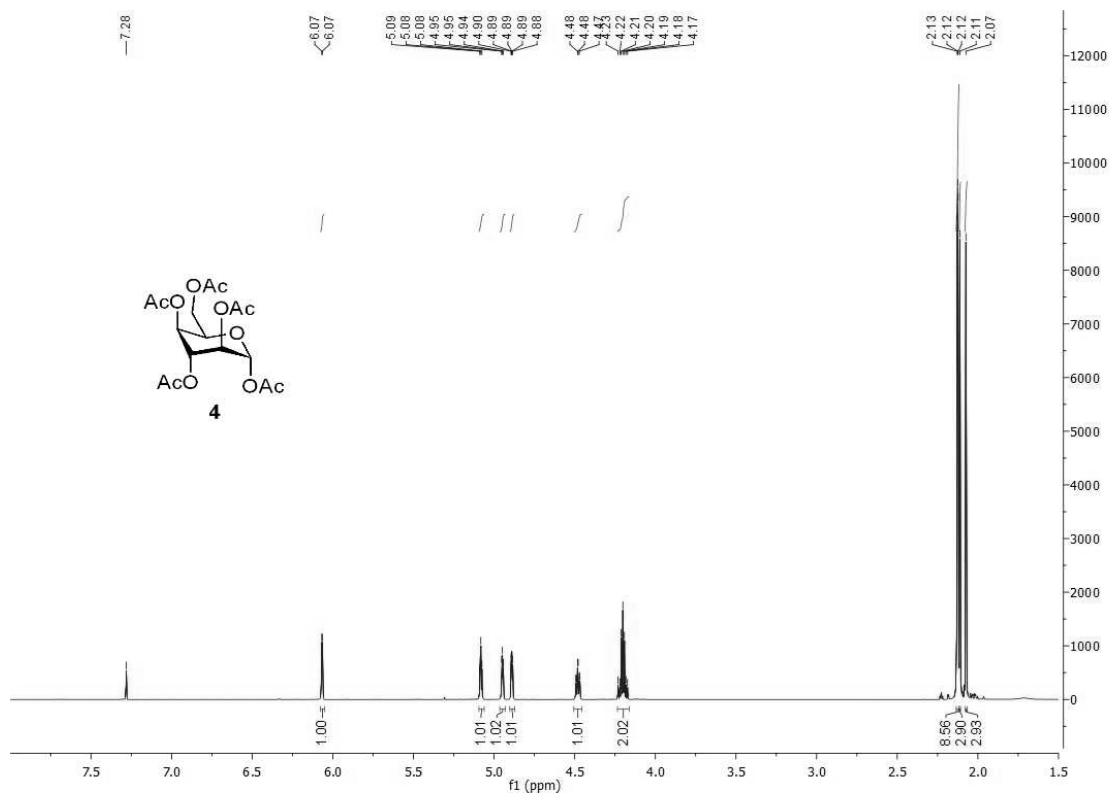
6.5 Acknowledgments

This work was supported by a Discovery grant from the Natural Sciences and Engineering Research Council of Canada (NSERC) under award number RGPIN-2016-04950. This work was also supported by a PTR (Programmes Transversaux de Recherche) grant (PTR 380-20) from Institut Pasteur Paris. M. C. thanks NSERC Vanier and Fonds de recherche du Québec – Nature et technologies (FRQNT) for Ph.D. scholarships.

CHAPITRE 6 – SYNTHESIS OF α -D-IDOSE PENTAACETATE FROM β -D-GLUCOSE PENTAACETATE VIA PAULSEN ACETOXONIUM REARRANGEMENT



CHAPITRE 6 – SYNTHESIS OF α -D-IDOSE PENTAACETATE FROM β -D-GLUCOSE PENTAACETATE VIA PAULSEN ACETOXONIUM REARRANGEMENT



CHAPITRE 7 : C7 EPIMERIZATION OF BENZYLIDENE-PROTECTED β -D-IDOPYRANOSIDES BRINGS STRUCTURAL INSIGHTS INTO IDOSE CONFORMATIONAL FLEXIBILITY

Maude Cloutier,^a Serge Lavoie^b, and Charles Gauthier^{a,b}

^a*Unité Mixte de Recherche INRS-UQAC, Centre Armand-Frappier Santé Biotechnologie, Institut national de la recherche scientifique (INRS), 531, boul. des Prairies, Laval (Québec), H7V 1B7, Canada*

^b*Laboratoire LASEVE, Département des Sciences Fondamentales, Université du Québec à Chicoutimi (UQAC), 555, boulevard de l'Université, Chicoutimi (Québec), Canada, G7H 2B1.*

Article publié dans Journal of Organic Chemistry, 2022, 87, 12932-12953, doi : 10.1021/acs.joc.2c01504

Titre français : L'épimérisation en C7 des β -D-idopyranosides protégés par un benzylidène apporte des informations structurelles quant à la flexibilité conformationnelle de l'idose.

Contribution des auteurs : Maude Cloutier a réalisé la synthèse des composés et l'étude de glycosylation. Maude Cloutier a réalisé la modélisation moléculaire sous la supervision de Serge Lavoie. Serge Lavoie a réalisé les analyses RMN poussées. Maude Cloutier a rédigé l'article, et Serge Lavoie et Charles Gauthier l'ont révisé.

7.1 Résumé

L'idose est unique parmi les autres aldohexoses en raison de sa grande flexibilité conformationnelle en solution. Nous montrons ici que les 3-*O*-acyl- β -D-idopyranosides protégés par un 4,6-*O*-benzylidène subissent une épimérisation en C7 catalysée par un acide de Lewis avec une inversion concomitante de la conformation du sucre 4C_1 vers 1C_4 . Les conditions réactionnelles ainsi que les paramètres structuraux requis pour que cette transformation se produise ont été étudiés en profondeur grâce à une étude de glycosylation combinée à des analyses RMN, à de la diffraction des rayons X, et à de la modélisation moléculaire. En plus de rapporter une approche directe d'idosylation β -stéréosélective, notre travail rapporte des informations structurelles fondamentales quant à la flexibilité conformationnelle de l'idose.

7.2 Abstract

Idose is unique among other aldohexoses because of its high conformational flexibility in solution. We herein show that benzylidene acetal-protected 3-*O*-acyl- β -D-idopyranosides undergo Lewis acid-catalyzed C7 epimerization with concomitant 4C_1 to 1C_4 ring inversion. The reaction conditions and structural parameters for this transformation to occur have been thoroughly investigated through an extensive glycosylation study combined with NMR analyses, X-ray diffraction, and quantum molecular modeling. In addition to reporting a direct, β -stereoselective idosylation approach, our work brings fundamental structural insights into the conformational flexibility of idose.

7.3 Introduction

Idose is a rare, albeit biologically important naturally occurring hexose that stands out from its counterparts by its remarkable ring flexibility in solution. The presence of several axially-oriented substituents induces significant 1,3-*syn*-diaxial interactions that lowers the energy barrier between the 4C_1 and 1C_4 chairs, increasing the conformational freedom of idose.^{544, 545} In α -D-idopyranosides, these destabilizing interactions are balanced by the equatorial orientation of the large C5 substituent as well as the anomeric effect. This unique flexibility is denoted by the fact

CHAPITRE 7 – C7 EPIMERIZATION OF BENZYLIDENE-PROTECTED β-D-IDOPYRANOSIDES BRINGS STRUCTURAL INSIGHTS INTO IDOSE CONFORMATIONAL FLEXIBILITY

that while D-aldohexoses typically adopt the 4C_1 conformation in solution, D-idose exists as a mixture of 4C_1 and 1C_4 chairs,⁵⁴⁵ whose ratio is directly related to the solvent and substitution pattern of its hydroxyl groups (Fig. 1A).⁵⁴⁶ Furthermore, Angyal and Kondo reported that intramolecular hydrogen bonds between OH-2/O-4 and OH-3/O-1 stabilize the 4C_1 conformation of 4,6-*O*-benzylidene α -D-idopyranosides in solvents with no hydrogen bonding properties, whereas these compounds predominantly adopt a skew-boat (0S_2) conformation when dissolved in DMSO and D₂O.⁵⁴⁷ Similarly, Nifantiev and co-workers recently reported that the 3-*O*-substituents in such compounds have a significant influence on the ${}^4C_1/{}^0S_2$ equilibrium.⁵⁴⁸

CHAPITRE 7 – C7 EPIMERIZATION OF BENZYLIDENE-PROTECTED β -D-IDOPYRANOSIDES BRINGS STRUCTURAL INSIGHTS INTO IDOSE CONFORMATIONAL FLEXIBILITY

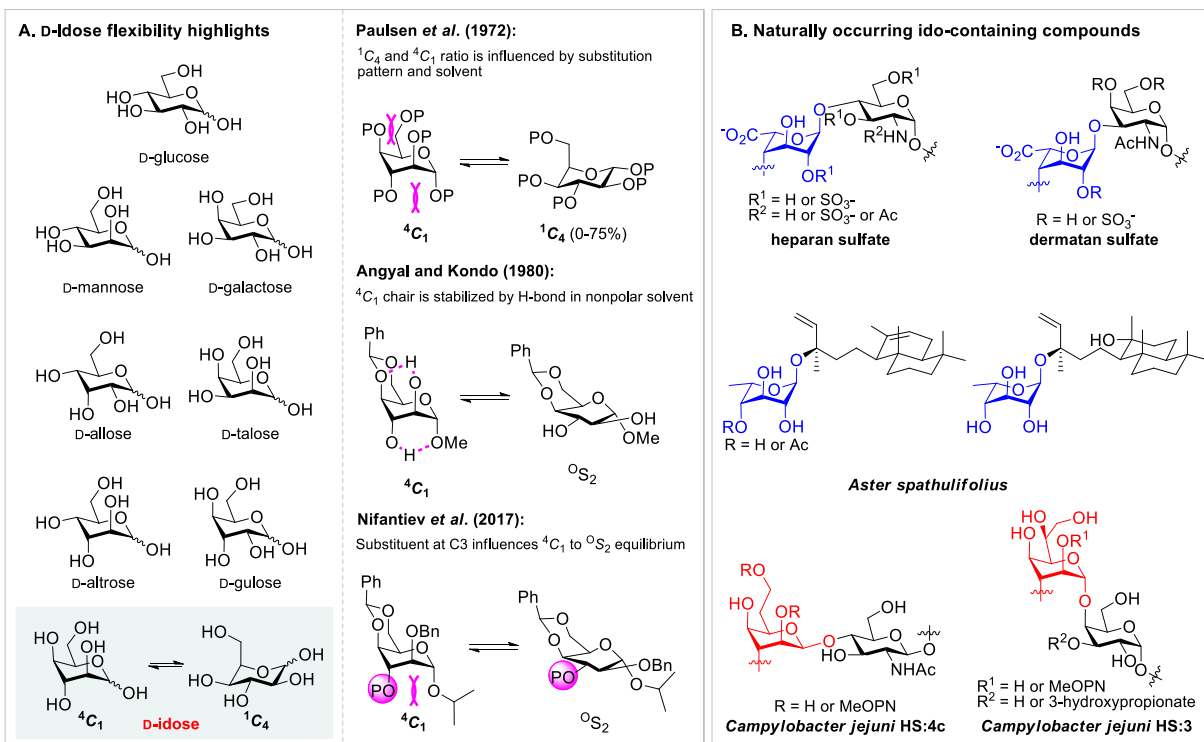


Figure 7.1. (A) Conformational equilibrium of D-idopyranosides as compared to other D-aldohexoses; (B) Examples of naturally occurring glycosides and oligosaccharides containing L- (blue) and D- (red) *ido*-configured sugars

These unique conformational properties make *ido*-configured carbohydrates biologically valuable. For instance, L-iduronic acid residues significantly modulate the flexibility of glycosaminoglycans (Fig. 1B), which in turn impacts their ability to interact with biomacromolecules.⁵⁴⁹ The biological relevance of idosides is further highlighted by the identification of 6-deoxy-L-idose in labdane-type diterpenes produced by *Aster spathulifolius*.⁵⁵⁰ L-idose was also studied for its inhibitory effect against the growth of *Caenorhabditis elegans*,⁵⁵¹ whereas D-idose was shown to exert an antiproliferative activity against leukemia cell lines.⁵⁵² Moreover, L-glycero-D-*ido*-heptoses and 6-deoxy-D-*ido*-heptoses are found in the capsular polysaccharide (CPS) of *Campylobacter jejuni* HS:3^{463, 464} and HS:4c,^{120, 121} respectively.

Because of the biological importance of *ido*-configured glycosides, along with their unique conformational flexibility, there has been an increased interest in the development of synthetic

CHAPITRE 7 – C7 EPIMERIZATION OF BENZYLIDENE-PROTECTED β -D-IDOPYRANOSIDES BRINGS STRUCTURAL INSIGHTS INTO IDOSE CONFORMATIONAL FLEXIBILITY

pathways that would enable access to idose-containing oligosaccharides. More specifically, different research groups have been involved in the preparation of 1,2-*cis*- β -linked idopyranosides, as found in *C. jejuni* HS:4c CPS. Preparation of such compounds represents an interesting synthetic challenge: not only does the expensiveness of D-idose implies it must be prepared synthetically (*vide infra*), but access to such 1,2-*cis*- β -glycosidic bonds stands as a nontrivial task. To address these challenges, Ling and co-workers optimized an approach based on the C2/C3 inversion of β -D-galactosides through the regioselective opening of 2,3-anhydro- β -D-talopyranoside intermediates (Fig. 2A).^{503, 504, 512} Alternatively, Li's group recently reported the preparation of a 6-deoxy- β -D-*ido*-heptopyranoside-containing oligosaccharide via the C2 epimerization of a 6-deoxy- β -D-*gulo*-heptopyranoside (Fig. 2B).⁵⁴⁰ Both approaches thus depended on the formation of a 1,2-*trans*- β -glycosidic linkage through neighboring group participation (NGP) of C2 esters, prior to performing the mono (C2) or double (C2/C3) epimerization. β -Glycosylation of D-*ido*-configured donors therefore remains an underexplored area of carbohydrate chemistry and an efficient stereoselective method has yet to be disclosed. In this regard, we have been interested to develop a β -stereoselective glycosylation method using benzylidene-protected thiodosyl donors. In the course of this work, we have uncovered an unexpected *in situ* epimerization of benzylidene acetals with concomitant 4C_1 to 1C_4 ring flipping, which is specific to β -D-idopyranosides bearing C3 acyl groups (Fig. 2C). We herein report the thorough investigation of this transformation through a glycosylation study combined with NMR experiments and quantum molecular modeling. These experiments have allowed us to identify the reaction conditions and structural requirements needed for the epimerization to occur, thus shedding light on the unusual conformational flexibility of β -D-idopyranosides.

CHAPITRE 7 – C7 EPIMERIZATION OF BENZYLIDENE-PROTECTED β -D-IDOPYRANOSIDES BRINGS STRUCTURAL INSIGHTS INTO IDOSE CONFORMATIONAL FLEXIBILITY

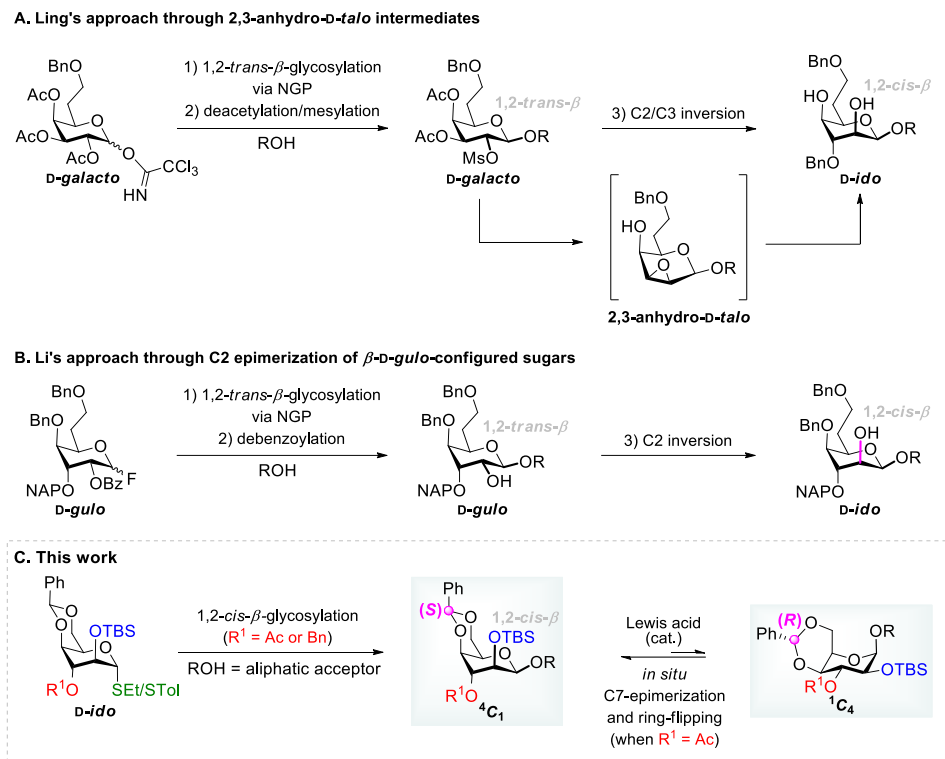


Figure 7.2. (A) Ling and (B) Li's indirect approaches towards the preparation of 1,2-*cis*- β -linked idopyranosides; (C) this work: direct β -glycosylation of thiodopyranosyl donors and spontaneous acid-mediated *in situ* C7-epimerization with concomitant chair flip⁴¹

7.4 Results and discussion

7.4.1 Synthetic approach

As previously mentioned, whereas the 1,2-*trans* glycosidic linkages can be readily assembled with the help of a participating group at C2, the preparation of 1,2-*cis* bonds is nontrivial. Various synthetic approaches have been developed to circumvent this difficulty, including but not limited to hydrogen bond-mediated aglycon delivery,^{122, 123} intramolecular aglycon delivery,⁵⁵³ participation of chiral auxiliaries at C2,⁵⁵⁴ and solvent participation.⁵⁵⁵ The anchimeric assistance by remote carbonyl groups has also been shown to stand as an exquisite approach to achieve high 1,2-*cis*-stereoselectivity in glycosylation reactions.⁵⁵⁶ Of relevance, the potential of axially-

⁴¹ NGP: neighboring group participation.

CHAPITRE 7 – C7 EPIMERIZATION OF BENZYLIDENE-PROTECTED β -D-IDOPYRANOSIDES BRINGS STRUCTURAL INSIGHTS INTO IDOSE CONFORMATIONAL FLEXIBILITY

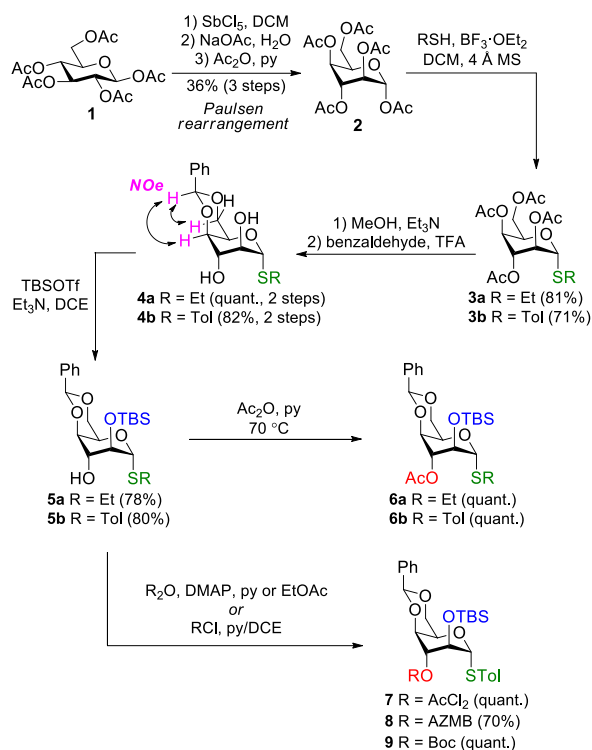
oriented C3 carbonyl groups to act as long distance participating groups has been highlighted by the isolation of a 1,3-cyclic carbamate by Wiesner *et al.*⁵⁵⁷ Similarly, Crich and co-workers demonstrated the remote anchimeric assistance of axial 3-*O*-esters in glycosylation reactions through the trapping of a 1,3-*O*-cyclic carbonate.⁵²⁶ These results prompted us to hypothesize that 3-*O*-acylation of benzylidene-protected idosyl donors could enable their β -stereoselective glycosylation. Triflates¹⁰⁴ could also be important reactive intermediates in idosylation reactions. In a recent report by Asensio and colleagues,¹⁰⁹ the influence of the orientation of C2 and C3 substituents on the stability of α - and β -triflates was put forward. Quantum mechanic calculations highlighted that in D-mannosides, axially-oriented substituents at C2 increase the weight of the anomeric effect, thus stabilizing α -triflates and consequently reducing their reactivity. In contrast, in the case of D-*allo*-configured sugars, the energy gap between both anomers is diminished due to 1,3-*syn*-diaxial repulsive interactions that destabilize the α -triflate, and oppositely noncanonical hydrogen bonding between H-1_{ax} and *O*-3 that stabilizes the β -triflate. In D-idosides, the presence of axial substituents at both C2 and C3 implies that all these effects should have an impact on the population of the respective anomers, their reactivity, and their rate of anomerization, which would in turn affect the glycosylation stereoselectivity.

7.4.2 Synthesis of idopyranosyl donors

Our first task therefore consisted in the synthesis of orthogonally protected α -D-thioidopyranosyl donors. Despite the attractiveness of D-*ido*-configured sugars, limited efforts have been directed towards their synthesis. Dromowicz and Köll reported a two-step protocol involving addition of nitromethane to D-xylose followed by a modified Nef reaction for the synthesis of D-idose.⁵⁰¹ Szekrenyi *et al.* alternatively performed its preparation using biocatalytic conditions.⁵⁴² Methods involving the late-stage conversion of functionalized D-galactosides,^{503,504} *gluco*-heptonic acid,⁵⁴¹ and more recently *C*-allyl α -D-glucosides⁵⁴⁰ have additionally been reported. Notwithstanding the success of these approaches, they present some drawbacks such as the need for highly functionalized precursors, large excess of reagents, potentially explosive chemicals, or specialized equipment. As such, these methods show limited synthetic applicability. On the other hand, Paulsen acetoxonium rearrangement provides a straightforward method for the preparation of α -

CHAPITRE 7 – C7 EPIMERIZATION OF BENZYLIDENE-PROTECTED β -D-IDOPYRANOSIDES BRINGS STRUCTURAL INSIGHTS INTO IDOSE CONFORMATIONAL FLEXIBILITY

D-idose pentaacetate **2** from inexpensive peracetylated β -D-glucose **1**⁵⁴³ through a Lewis acid-mediated C1 to C4 epimerization cascade.^{502, 539} This three-step approach was successfully employed for the gram-scale synthesis of idoside **2** (Scheme 1) through our optimized protocol. The latter compound was then readily converted into thioidosides **3a** and **3b** under the action of $\text{BF}_3 \cdot \text{OEt}_2$.



Scheme 7.1. Synthesis of 3-O-acylated *ido*-configured thioglycoside donors 6–9

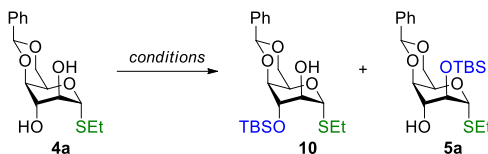
Functionalization of *D-ido*-configured compounds remain a significant challenge because of the presence of three axially-oriented substituents. Furthermore, to the best of our knowledge, methods for the regioselective protection of 1,2-*trans*-diols in carbohydrates are scarce and usually focus on *gluco*-configured compounds.⁵⁵⁸ To address this challenge, we first performed the deacetylation of thioidosides **3a** and **3b** followed by their 4,6-O-benzylideneation. The expected (*S*)-stereochemistry⁵⁴⁷ of resulting intermediates **4a** and **4b** was confirmed with the help of NOESY NMR, which highlighted the through-space coupling between the benzylic proton and H-6_{axial} and H-4.

CHAPITRE 7 – C7 EPIMERIZATION OF BENZYLIDENE-PROTECTED β -D-IDOPYRANOSIDES BRINGS STRUCTURAL INSIGHTS INTO IDOSE CONFORMATIONAL FLEXIBILITY

We then set out to silylate diol **4a** regioselectively at C2 (Table 1). TBS was chosen as an ideal protecting group because of its enhanced stability compared to other silyl-based groups, its straightforward orthogonal cleavage, and its ability to increase the reactivity of glycosyl donors.⁵⁵⁹ We envisioned that, due to the poor nucleophilicity of 3-OH in idosides,⁵⁴⁰ silylation would preferentially occur at C2. However, because of the low reactivity of the axial 2-OH, we observed that using TBSCl as a silylating agent was unsuccessful (entries 1 and 2). Disilylation under the action of TBSOTf and subsequent regioselective monodesilylation using tetra-*n*-butylammonium fluoride (TBAF) was also fruitless (entry 3). On the other hand, lowering the number of equivalents of TBSOTf and performing the reaction in 1,2-dichloroethane (DCE) allowed isolation of 2-O-silylated idoside **5a** in 29% yield (entry 5). Switching from DCE to tetrahydrofuran (THF) increased the yield of compound **5a**, but significant 3-O-silylation (**10**) nonetheless occurred (entry 6). Using pyridine as base and solvent (entry 7) or a mixture of pyridine and DCE (entry 8) gave similar results, while performing the reaction in DCE with 1.5 equivalents of pyridine significantly enhanced the regioselectivity of the reaction (entry 9). Pleasingly, using a combination of TBSOTf and Et₃N in DCE and fine-tuning the number of equivalents (entries 10-12) drastically minimized the 3-O-silylation and enabled isolation of target compound **5a** in a 78% yield (entry 12). On the other hand, lower amounts of TBSOTf and Et₃N (entry 10) led to uncomplete conversion of the starting material, whereas increasing the number of equivalents of both reagents (entry 11) led to significant decomposition. We attributed the latter result to the acidity of the silyl triflate, which could additionally be converted into triflic acid in the presence of moisture in the reaction mixture. The regioselectivity was similar when conducted with thiotolyl **4b**. Finally, an acetyl group was introduced at C3, which could potentially act as a long-distance participating group, thus furnishing orthogonally protected α -D-thioidopyranosides **6a** and **6b**.

CHAPITRE 7 – C7 EPIMERIZATION OF BENZYLIDENE-PROTECTED β -D-IDOPYRANOSIDES BRINGS STRUCTURAL INSIGHTS INTO IDOSE CONFORMATIONAL FLEXIBILITY

Table 7.1. Optimization of the regioselective silylation of diol **4a**



entry	conditions	yield (%) ^a	
		10	5a
1	TBSCl, Im, DMAP, DMF, 60 °C ^b	-	-
2	TBSCl, Im, I ₂ , DCE, rt	- ^c	- ^c
3	TBSOTf, Et ₃ N, DCE, 60 °C; then TBAF, THF, 0 °C to rt ^b	-	-
4	TBSOTf, 2,6-lutidine, DMF, 100 °C	-	-
5	TBSOTf (1.0 equiv), 2,6-lutidine (2.4 equiv), DCE, 0 °C to rt	- ^c	22
6	TBSOTf (1.3 equiv), Et ₃ N (1.5 equiv), THF, 0 °C to rt	29	43
7	TBSOTf (1.3 equiv), py, 0 °C	31	49
8	TBSOTf (1.3 equiv), py/DCE 1:1, 0 °C	28	42
9	TBSOTf (1.3 equiv), py (1.5 equiv), DCE, 0 °C to rt	4	61
10	TBSOTf (1.3 equiv), Et ₃ N (1.5 equiv), DCE, 0 °C to rt	- ^c	51
11	TBSOTf (2.5 equiv), Et ₃ N (3.0 equiv), DCE, 0 °C	7	19
12	TBSOTf (1.5 equiv), Et ₃ N (1.8 equiv), DCE, 0 °C	4	78

^aIsolated yields; ^bDiol **4a** was recovered; ^cTraces of compounds were detected by thin-layer chromatography (TLC).

7.4.3 Glycosylation study, characterization, and molecular modeling

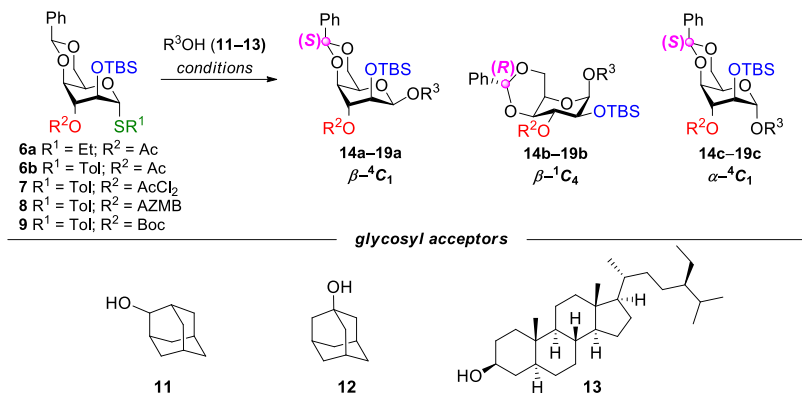
Having compounds **6a** and **6b** in hand, we then set out to investigate their behavior under glycosylation conditions. As previously mentioned, we hypothesized that the 3-*O*-acetyl group might provide long distance anchimeric assistance, leading to the stereoselective formation of β -glycosidic linkages. Simultaneously, destabilization of the plausible α -triflate intermediate mediated by 1,3-*syn*-diaxial repulsion could enhance its reactivity towards the acceptors, thus favoring the formation of the β -glycosidic linkage. As shown in Table 2, coupling of thiodosyl donor **6a** and 2-adamantanol (**11**) under the promotion of *N*-iodosuccinimide (NIS) and trimethylsilyl trifluoromethanesulfonate (TMSOTf) in DCE was indeed β -stereoselective (β/α 6.6:1.0, entry 1). NMR identification of β - and α -anomers **14a** and **14c**, respectively, was performed on the basis of the small coupling constants between protons H1, H2, H3, and H4, characteristic of their all-axial arrangement, and the $^1J_{C1,H1}$ (156 Hz for β , 171 Hz for α).⁵⁶⁰

CHAPITRE 7 – C7 EPIMERIZATION OF BENZYLIDENE-PROTECTED β -D-IDOPYRANOSIDES BRINGS STRUCTURAL INSIGHTS INTO IDOSE CONFORMATIONAL FLEXIBILITY

Unexpectedly, a third chromatographically distinct compound (**14b**) was additionally isolated and characterized by a large $^3J_{H2,H3}$ (10 Hz) value, which is typical of a D-idoside in the 1C_4 chair conformation. The β -configuration of this compound was revealed through the small coupling constant between H1 and H2 ($^3J = 3.7$ Hz) as well as the $^1J_{C1,H1}$ (171 Hz), which was distinctive of an equatorially-oriented anomeric proton.⁵⁶⁰ High-resolution mass spectrometry (HRMS) analysis revealed a molecular ion at m/z 581.29228 ($[M + Na]^+$), correlating with the expected chemical formula $C_{31}H_{46}O_7Si$. In addition, as depicted in Scheme 2, both β -glycosides remained distinguishable upon removal of the TBS and acetyl groups while the 1C_4 conformer converted back to the 4C_1 form following benzylidene acetal cleavage.

CHAPITRE 7 – C7 EPIMERIZATION OF BENZYLIDENE-PROTECTED β -D-IDOPYRANOSIDES BRINGS STRUCTURAL INSIGHTS INTO IDOSE CONFORMATIONAL FLEXIBILITY

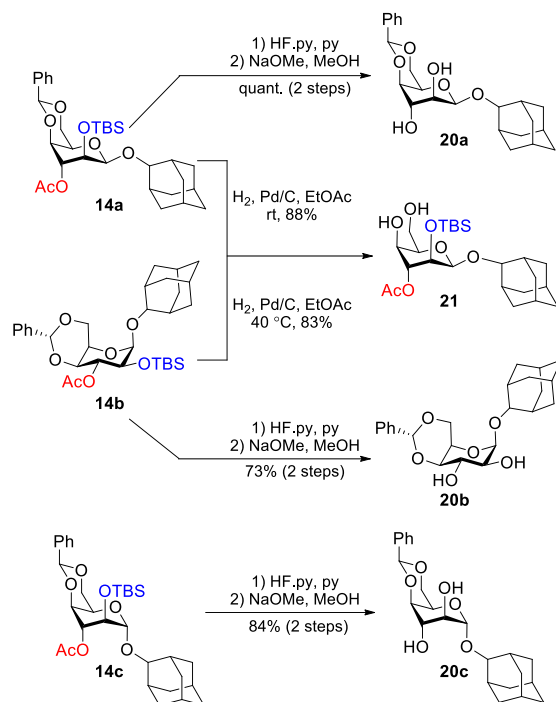
Table 7.2. Glycosylation study of *ido*-configured thioglycosyl donors 6–9



entry	donor	R ³ OH	promotor	solvent ^a	T (°C)	NMR ratio			β/α ratio	NMR conversion (%)	products
						β - ⁴ C ₁	β - ¹ C ₄	α - ⁴ C ₁			
1	6a	11	NIS/TMSOTf	DCE	-10	3.8	2.8	1.0	6.6:1.0	>95	14a-c
2	6a	11	NIS/TMSOTf	THF	-10	1.0	-	1.5	1.0:1.5	75	14a-c
3	6a	11	NIS/TMSOTf	Et ₂ O	-10	6.0	1.0	1.0	7.0:1.0	85	14a-c
4	6a	11	NIS/TMSOTf	Tol	-10	11.4	4.0	1.0	15.4:1.0	>95	14a-c
5	6b	11	DMTST	DCE	rt	4.8	1.1	1.0	5.9:1.0	56	14a-c
6	6b	11	NIS/Yb(OTf) ₃	DCE	-10	8.0	1.0	2.2	4.1:1.0	>95	14a-c
7	6b	11	NIS/AgBF ₄	DCE	-10	4.3	1.0	1.1	4.8:1.0	>95	14a-c
8	6a	11	CuBr ₂ /Bu ₄ NBr	DCE	rt	15.7	1.0	11.0	1.5:1.0	62	14a-c
9	6b	12	NIS/TMSOTf	DCE	-10	12.0	1.0	3.2	4.1:1.0	>95	15a-c
10	6b	13	NIS/TMSOTf	DCE	-10	5.0	1.0	1.0	6.0:1.0	>95	16a-c
11	7	11	NIS/TMSOTf	DCE	-10	1.6	1.2	1.0	2.8:1.0	>95	17a-c
12	8	11	NIS/TMSOTf	DCE	-10	2.5	1.0	1.0	3.5:1.0	>95	18a-c
13	9	11	NIS/TMSOTf	DCE	-10	4.4	1.0	1.0	5.4:1.0	>95	19a-c

^aMolar concentration was 0.05 M; donor (1.2 equiv), acceptor (1.0 equiv). DMTST: dimethyl(methylthio)sulfonium trifluoromethanesulfonate.

CHAPITRE 7 – C7 EPIMERIZATION OF BENZYLIDENE-PROTECTED β -D-IDOPYRANOSIDES BRINGS STRUCTURAL INSIGHTS INTO IDOSE CONFORMATIONAL FLEXIBILITY



Scheme 7.2 Partial deprotection of glycosides 14a–14c

Interestingly, formation of this unanticipated compound occurred systematically, independently of the solvent (entries 1-4), promoter (entries 5-8), and glycosyl acceptor (entries 9 and 10). Changing the nature of the ester at C3 (7–9, Scheme 1) also did not significantly affect the outcome of the reaction (entries 11-13). The exception to this observation is when THF was employed as the solvent. Not only was this third unanticipated compound not observed, but the reaction was also slightly α -stereoselective (entry 2; β/α 1.0:1.5). This was not entirely unexpected as ether-based solvents have been shown to participate in glycosylation reactions by equatorially binding transient oxocarbenium intermediates, thus leading to the preferential formation of α -anomers.⁵⁵⁵ With the exception of this latter entry, all reactions were performed with some β -stereoselectivity, which could be attributed to the remote participation of the 3-*O*-ester as well as to the formation of transient α -triflate intermediates. 1,3-*Syn*-diaxial repulsion induced by the axially-oriented 3-*O*-ester could increase the reactivity of this triflate towards the studied aliphatic acceptors, preferentially leading to β -glycosides.¹⁰⁹ Another significant observation can be made from the glycosylation reaction performed in toluene (entry 4): this solvent provided the higher β -

CHAPITRE 7 – C7 EPIMERIZATION OF BENZYLIDENE-PROTECTED β -D-IDOPYRANOSIDES BRINGS STRUCTURAL INSIGHTS INTO IDOSE CONFORMATIONAL FLEXIBILITY

stereoselectivity (β/α ratio 15.4:1.0). This could stem from the fact that in nonpolar solvents such as toluene, the destabilization of the oxocarbenium ion is exacerbated, thus favoring S_N2 -like reactions involving either the acetoxonium ion or the α -triflate.¹¹⁰ Noteworthy, butanol was also employed as a highly nucleophilic acceptor for this glycosylation study. Although similar results were achieved with this alcohol, the reaction was poorly reproducible and as such was not included in Table 2. Similarly, glycosylation reactions were attempted using methanol and *para*-methoxybenzyl alcohol as acceptors, but proved unsuccessful due to significant hydrolysis and decomposition of the donor.

Close examination of the 2D spectroscopic data of this third compound (**14b**) revealed strong NOE correlations between the benzylic proton and H-3, suggesting an (*R*)-configured benzylic acetal rather than the initially expected (*S*) configuration. Intrigued by this result, we carried out theoretical calculations to establish its definitive structure, as well as that of α - and β -glycosides **14a** and **14c**. As such, *in silico* diols **22a** [(*S*)- β -⁴C₁], (*S*)-**22b** [(*S*)- β -¹C₄], (*R*)-**22b** [(*R*)- β -¹C₄], and **22c** [(*S*)- α -⁴C₁] bearing a simplified methoxy group at the anomeric position were modeled (Fig. 3A). For each glycoside, a conformational search was performed on Spartan using molecular mechanics (MMFF) and each geometry was optimized on Gaussian using B3LYP/6-31+G(d,p) level of theory. Low abundance conformers were eliminated based on their calculated thermochemical parameters using the Boltzmann equation. ¹H and ¹³C NMR chemical shifts were predicted in chloroform through the calculation of the shielding tensors using the multi-standard approach with the density functional theory (DFT) functional mPW1PW91 and basis set 6-311+G(2d,p).^{561, 562} In parallel, theoretical ¹H-¹H coupling constants were determined by NMR single-point calculation. Using the previously optimized most abundant geometries, thermochemical parameters were additionally calculated using the higher DFT level of theory B3LYP/6-311++G(2d,2p) to determine their respective abundance, to which theoretical NMR data were correlated. The resulting values were compared with experimentally determined ¹³C and ¹H NMR chemical shifts and coupling constants of synthetic compounds **20a–c** prepared following cleavage of the TBS and acetyl groups (Scheme 2). Root-mean-square deviation (rmsd) values are reported in Fig. 3A (see Tables S6-S27 for complete data).

CHAPITRE 7 – C7 EPIMERIZATION OF BENZYLIDENE-PROTECTED β -D-IDOPYRANOSIDES BRINGS STRUCTURAL INSIGHTS INTO IDOSE CONFORMATIONAL FLEXIBILITY

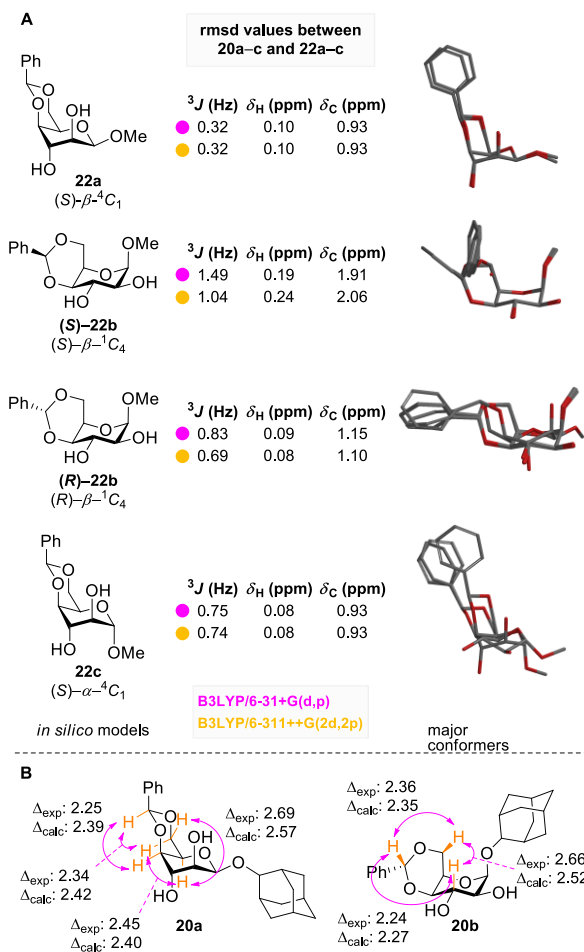


Figure 7.3. (A) Comparison between theoretical and experimental NMR data; (B) Most relevant NOE correlations and comparison between theoretical and experimental distances

We found that while theoretical data of *in silico* compounds **22a** and **22c** correlated well with experimental data of corresponding synthetic compounds **20a** and **20c**, respectively, this was not the case for model compound (S)-**22b**. Instead, rmsd values were significantly lower for its benzylidenic epimer (R)-**22b**, a result that is coherent with our previous observation that strong NOE correlations existed between H3 and the benzylidenic proton. Nonetheless, to further confirm that the third isolated compound indeed consisted in a 4,6-*O*-(R)-benzylidene- β -D-idopyranoside, relevant interproton distances of synthetic compound **20b** were measured experimentally by quantitative NOESY using the distance between H14 and H24B (refer to Fig. S1) as a reference and compared to extracted values from the optimized modeled structures (S)-**22b** and (R)-**22b**.

CHAPITRE 7 – C7 EPIMERIZATION OF BENZYLIDENE-PROTECTED β -D-IDOPYRANOSIDES BRINGS STRUCTURAL INSIGHTS INTO IDOSE CONFORMATIONAL FLEXIBILITY

Figure 3B reports the experimental interproton distances of compound **20b** (Δ_{exp}) for the three most significant NOE correlations, *i.e.*, H7/H6b, H7/H3, and H3/H6b, and the corresponding calculated distances of *in silico* model compound (**R**)-**22b**. The quantitative NOESY-derived distance between the benzylic proton and H3 (2.24 Å) was an excellent match with the calculated distance for *in silico* model compound (**R**)-**22b** (2.27 Å), as opposed to the one determined for the modeled (*S*)-epimer (**S**)-**22b** (4.06 Å, see Table S17). These results strengthened our hypothesis that following the glycosylation reaction between 3-O-acylated 4,6-*O*-benzylidene thiodopyranosyl donors and non-glycosidic acceptors, the third and unexpected compound consists in the benzylic C7-(*R*)-epimer. In parallel, the same comparisons were performed between diol **20a** and *in silico* model compound **22a** and we found that experimental interproton distances were in excellent agreement with theoretical values (Fig. 3B). Crystallization of β -glycoside **20a** allowed us to obtain an X-ray structure of the compound, which proved the (*S*)-stereochemistry of the benzylidene acetal as well as the 4C_1 conformation of the pyranose ring in the solid state (Fig. 4).

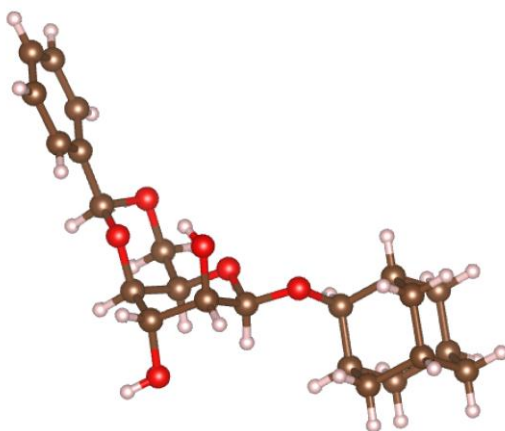
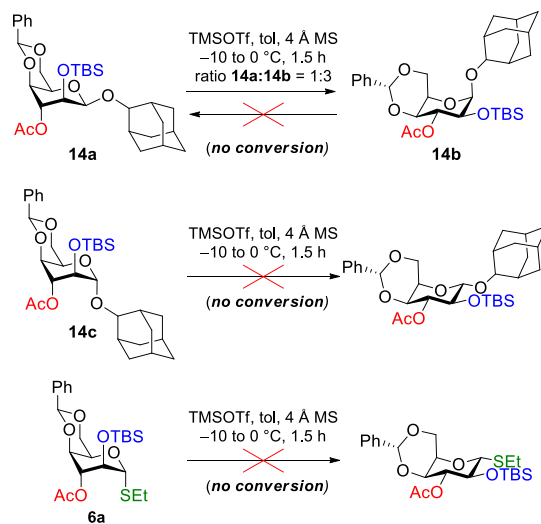


Figure 7.4. X-ray crystallographic structure of β -glycoside **20a**

Regioselective opening of benzylidene acetals are often performed under the catalysis of Lewis acids such as TMSOTf.⁵⁶³ On that account, we postulated that formation of the benzylic epimer **14b** could occur post-glycosylation through the acid-catalyzed opening of the benzylidene acetal. Both β - and α -glycosides were therefore subjected to glycosylation conditions (Scheme 3).

CHAPITRE 7 – C7 EPIMERIZATION OF BENZYLIDENE-PROTECTED β -D-IDOPYRANOSIDES BRINGS STRUCTURAL INSIGHTS INTO IDOSE CONFORMATIONAL FLEXIBILITY

As expected, we observed that under these conditions, β -glycoside **14a** was transformed into its corresponding C7-epimer **14b** in the 1C_4 conformation (final ${}^4C_1/{}^1C_4$ NMR ratio 1.0:2.9). On the other hand, when C7-epimer **14b** was subjected to these same conditions, the compound remained stable and no traces of (*S*)-benzylidenated β -glycoside **14a** were detected. Similarly, this ring-flipping/epimerization transformation did not occur when the experiment was performed on α -anomer **14c**. To rule out the possibility that epimerization might occur prior to the glycosylation reaction, the same experiment was performed on α -donor **6a**: apart from slight hydrolysis, no changes were observed, thus suggesting that this transformation indeed takes place post-glycosylation. This result is also coherent with the observation that the ring-flipping/epimerization transformation did not occur when the experiment was performed on α -configured glycoside **14c**. Additional experiments were also performed in which the ring-flipping/epimerization of β -glycoside **14a** was attempted using catalytic and stoichiometric amounts of aliphatic acceptors (*i.e.* MeOH, 2-adamantanol) instead of a Lewis acid. Again, no changes were observed, suggesting that this transformation was catalyzed by the Lewis acid employed for the glycosylation reaction.



Scheme 7.3. Post-glycosylation epimerization experiments

As previously mentioned, *D*-ido-configured compounds are recognized for their low energy barrier between the 4C_1 and 1C_4 conformation. This flexibility is ascribed to the existence of destabilizing 1,3-*syn*-diaxial interactions, which in the 4C_1 conformation are balanced by the equatorial

CHAPITRE 7 – C7 EPIMERIZATION OF BENZYLIDENE-PROTECTED β -D-IDOPYRANOSIDES BRINGS STRUCTURAL INSIGHTS INTO IDOSE CONFORMATIONAL FLEXIBILITY

orientation of the large C5 substituent and, in α -D-idosides, by the anomeric effect. We thus propose that the β -configuration of glycoside **14a** significantly decreases the stability of the 4C_1 conformer. Subsequently to the glycosylation reaction, the benzylidene acetal could undergo TMSOTf-catalyzed ring opening, leading to a more conformationally labile system. Isomerization into the 1C_4 conformation would then be favored because of the anomeric effect. In this thermodynamically favored conformation, ring closing would occur with concomitant (*S*) to (*R*) epimerization of the benzylidenic chiral center as to reduce the steric hindrance caused by the phenyl group. On the other hand, α -glycoside **14c** would not undergo this ring flipping with concomitant epimerization because the 4C_1 chair remains the thermodynamically preferred conformer due, in part, to the anomeric effect. Of note, observation of this ring flipping specific to 4C_1 β -glycosides is coherent with a recent report from Ling and co-workers who observed that upon reductive opening of a benzylidene-protected β -D-idopyranoside, the resulting compound bearing a 6-hydroxyl group preferentially existed in the 1C_4 conformation.⁵¹¹

Having highlighted that formation of this benzylidenic epimer occurred independently of the type of ester present at C3 and that it was specific to β -glycosides, we were subsequently interested in the impact of changing the configuration and nature of the substituent at this position. First, we focused our attention on the synthesis of a 3-O-benzylated analogue. Regioselective benzylation of diol **4b** was the main challenge to access this glycosidic donor. As shown in Table 3, standard benzylation conditions (entry 1; BnBr, NaH, dimethylformamide (DMF)) enabled the preparation of target intermediate **23**, albeit in low yield. In contrast, employing silver oxide as a base (entry 2) or attempting benzylation under acidic conditions using benzyl 2,2,2-trichloroacetimidate (BnTCA, entries 3-5) proved unsuccessful. Reductive etherification of the disilylated derivative of diol **4b** under the conditions reported by Hung *et al.*⁵⁶⁴ was also ineffective (entry 6). Finally, we were pleased to find that phase transfer conditions⁵⁶⁵ offered excellent regioselectivity and enabled the preparation of 3-O-benzylated idoside **23** in 75% yield (entry 7). 2-O-Silylation under our previously optimized conditions cleanly led to our target donor **24**.

CHAPITRE 7 – C7 EPIMERIZATION OF BENZYLIDENE-PROTECTED β -D-IDOPYRANOSIDES BRINGS STRUCTURAL INSIGHTS INTO IDOSE CONFORMATIONAL FLEXIBILITY

Table 7.3. Synthesis of 3-O-benzylated thioidoside **24** via regioselective 3-O-benylation

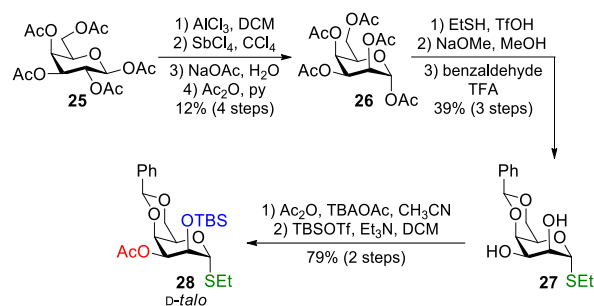
entry	conditions	yield ^a (%)
1	BnBr, NaH, DMF, 0 °C to rt	13
2	BnBr, Ag ₂ O, Hex/DCE, 4 Å MS, 60 °C	-
3	BnTCA, TMSOTf, DCE, 0 °C to rt	^b
4	BnTCA, TfOH, THF, 4 Å MS, rt	^b
5	BnTCA, TfOH, Tol/DCE, 4 Å MS	-
6	1) TBSOTf, Et ₃ N, DCE, 0 °C to rt 2) benzaldehyde, FeCl ₃ , Et ₃ SiH CH ₃ CN, 0 °C to rt	^b
7	BnBr, NaOH(aq), TBAHS, DCM, 40 °C	75

^aIsolated yields; ^bDiol **4b** was recovered.

We next tackled the preparation of D-talo derivative **28** bearing an equatorially-oriented acetate at C3 (Scheme 4). We reasoned that inverting this position could affect the formation of the corresponding benzylidenic epimer because destabilizing 1,3-*syn*-diaxial interactions are lessened in this configuration. Once again taking advantage of the Paulsen rearrangement,^{539, 566} we were able to prepare peracetylated α -D-talose **26** in four steps from β -D-galactose peracetate **25**.⁵⁶⁷ We then focused on the thioglycosylation of taloside **26**, which turned out to be surprisingly challenging. Bromination of the latter, as reported by Blanchard *et al.* on the same substrate,⁵⁶⁸ proceeded uneventfully but complete decomposition occurred when attempting to introduce the thioethyl moiety under phase transfer conditions.⁵⁶⁹ Thioglycosylation under the promotion of TMSOTf or BF₃·OEt₂ only led to small amounts of the target thioglycoside (<20%). Noteworthy, Bundle and co-workers reported similar difficulties when attempting the thioglycosylation of taloside **26** using BF₃·OEt₂.⁵⁷⁰ Pleasingly, TfOH-mediated thioalkylation under Demchenko's conditions⁵⁷¹ enabled the preparation of our target thiotaloside intermediate, which was subsequently deacetylated and benzylidenated. Acetylation under the catalysis of

CHAPITRE 7 – C7 EPIMERIZATION OF BENZYLIDENE-PROTECTED β -D-IDOPYRANOSIDES BRINGS STRUCTURAL INSIGHTS INTO IDOSE CONFORMATIONAL FLEXIBILITY

tetrabutylammonium acetate (TBAOAc)⁵⁷² furnished the expected 3-O-acetylated regioisomer with full selectivity, which was followed by 2-O-silylation to give target D-thiotaloside **28**.



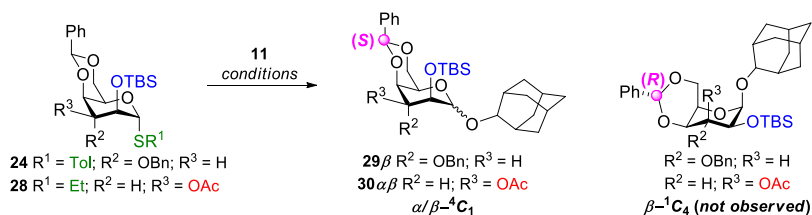
Scheme 7.4. Synthesis of thiotaloside **28**

With 3-O-benzylated D-idoside **24** and 3-O-acetylated D-taloside **28** in hand, both compounds were tested in various glycosylation conditions using 2-adamantanol (**11**) as the glycosyl acceptor (Table 4). In the case of the former compound, performing the reaction under the promotion of NIS/AgOTf in DCE led to a mixture of the corresponding β -glycoside and its desilylated derivative (entry 1). Switching to toluene (entry 2) or diethyl ether (entry 3) and using TMSOTf as triflate also exclusively furnished β -glycoside **29**. Similar results were achieved when using NIS/AgBF₄ (entry 4) or dimethyl(methylthio)sulfonium trifluoromethanesulfonate (DMTST) (entry 5) as promoters. Several factors could explain this complete β -stereoselectivity. First, it could be attributed to the steric bulkiness of the axial 3-O-Bn, shielding the bottom face of the sugar,^{573, 574} as well as to the potential oxocarbenium ion stabilization by the π -system of this remote aromatic ring, thus favoring the top-face attack of the acceptor.⁵⁷⁵ Moreover, if transient triflates intermediates are involved in these glycosylation reactions, the axially-oriented benzyl group at C3 could destabilize the α -triflate through 1,3-*syn*-diaxial interaction,¹⁰⁹ thus increasing its reactivity towards 2-adamantanol. Noteworthy, no traces of the (*R*)-4,6-*O*-benzylidene stereoisomer were detected and no epimerization/chair flip occurred when β -glycoside **29** was treated with TMSOTf, highlighting that this transformation did not occur when the 3-*O*-ester is replaced with a benzyl group. Additionally, as expected, no benzylidenic epimer in the ¹C₄ conformation was detected when the reaction was carried out with D-talosyl donor **28** (entry 6).

CHAPITRE 7 – C7 EPIMERIZATION OF BENZYLIDENE-PROTECTED β -D-IDOPYRANOSIDES BRINGS STRUCTURAL INSIGHTS INTO IDOSE CONFORMATIONAL FLEXIBILITY

This result is coherent with a greater stability of the 4C_1 chair due to the equatorial orientation of the C3 substituent which lessens 1,3-*syn*-diaxial repulsion.

Table 7.4. Glycosylation study of *ido*- and *talo*-configured thioglycosyl donors **24** and **28**



entry	donor	promotor	solvent	T (°C)	isolated ratio			yield (%) ^a
					β - 4C_1	β - 1C_4	α - 4C_1	
1	24	NIS/AgOTf	DCE	-10	1.0	-	-	41 ^b
2	24	NIS/TMSOTf	Tol	-10	1.0	-	-	39
3	24	NIS/TMSOTf	Et ₂ O	-10	1.0	-	-	51
4	24	NIS/AgBF ₄	DCE	-10	1.0	-	-	57
5	24	DMTST	DCE	rt	1.0	-	-	57
6	28	NIS/TMSOTf	DCE	-10	1.0	-	8.4	47 ^c

^aIsolated yields; ^bThe corresponding desilylated β -glycoside (**31**) was also isolated in a 40% yield; ^cThe corresponding desilylated α -glycoside (**32**) was also isolated in an 18% yield.

Having established a β -stereoselective glycosylation method with aliphatic acceptors and uncovered the C7-epimerization of 3-O-acylated β -idopyranosides, we were finally interested in the behavior of donors **6a**, **6b**, and **24** when coupled with various glycosidic acceptors (**33–36**, Table 5).⁵⁷⁶⁻⁵⁷⁸ These reactions were performed under the promotion of DMTST, as the latter condition enabled the stereoselective preparation of β -glycosidic linkages and also led to the formation of the benzylidenic epimer of the corresponding 3-O-acylated β -idosides. Of note, significant decomposition occurred when the following [1 + 1] glycosylations were attempted under the promotion of NIS and TMSOTf, further justifying the use of DMTST.

CHAPITRE 7 – C7 EPIMERIZATION OF BENZYLIDENE-PROTECTED β -D-IDOPYRANOSIDES BRINGS STRUCTURAL INSIGHTS INTO IDOSE CONFORMATIONAL FLEXIBILITY

Table 7.5. Glycosylation study of *ido*-configured thioglycosyl donors **6a**, **6b**, and **24** with glycosidic acceptors

6a R¹ = Et; R² = OAc
6b R¹ = Tol; R² = OAc
24 R¹ = Tol; R² = OBn

37–40 R² = OAc; R³ = 33–36
41 R² = OBn; R³ = 36

R² = OAc or OBn
 β -¹C₄ (not observed)

glycosyl acceptors

33 **34** **35** **36**

entry	donor	R ³ OH	isolated ratio			yield, % ^a (products)
			β - ⁴ C ₁	β - ¹ C ₄	α - ⁴ C ₁	
1	6a	33	1.0	-	1.3	37 (37β) 51 (37α)
2	6a	34	-	-	1.0	57 (38)
3	6a	35	-	-	(1→4): 1.0 (1→3): 3.8	8 (39a) 30 (39b)
4	6b	36	-	-	1.0	29 (40)
5	24	36	1.0	-	7.2	8 (41β) 58 (41α)

^aIsolated yields.

As opposed to our previous results with less hindered aliphatic acceptors having a high nucleophilic character, these [1 + 1] glycosylations tended to be α -stereoselective, independently of the nature of the substituent at C3. Only two instances led to the formation of the target β -disaccharides as the minor product (entries 1 and 5), whereas no benzylidenic epimer in the ¹C₄ conformation was observed. Because we previously highlighted that this ring-flipping/epimerization transformation was specific to β -configured glycosides, it is not surprising that the C7-(*R*)-epimer was not observed in entries 2–4. As for entries 1 and 5, we hypothesize that the presence of esters or amides in the glycoside acceptors could attenuate the promoters acidity and thus prevent the acid-mediated *in situ* epimerization. Additionally, the observed α -stereoselectivity is coherent with previous reports on benzylidene-protected pyranosyl donors. If triflates are indeed reactive intermediate in these reactions, the diminished nucleophilic character of these glycosyl acceptors would favor the α -glycosylation due to a preferred consumption of the

CHAPITRE 7 – C7 EPIMERIZATION OF BENZYLIDENE-PROTECTED β -D-IDOPYRANOSIDES BRINGS STRUCTURAL INSIGHTS INTO IDOSE CONFORMATIONAL FLEXIBILITY

slightly more reactive β -triflate.^{109, 579} Of note, glycosyl acceptors **33** and **36** that led to the formation of the corresponding β -disaccharides are characterized by an enhanced nucleophilic character owing to neighboring alkyl substituents.

In their work on the flexibility of 4,6-*O*-benzylidene idosides, Nifantiev and co-workers estimated that while their reported 3-*O*-acetylated β -D-idopyranosides mainly existed in the 4C_1 conformation in chloroform, the amount of 0S_2 fell between 0% and 19% due to the 1,3-*syn*-diaxial interactions between the substituents at C2 and C4.⁵⁴⁸ If β -glycoside **14a** adopts such a conformation, even if its population remains small, this would ideally orient the 3-*O*-ester carbonyl to form a chelate with the Lewis acid and the acetal oxygen at C4 (Fig. 5).⁵⁸⁰ This would then be followed by opening of the benzylidene ring, 4C_1 to 1C_4 isomerization, and ring closing with concomitant epimerization of the benzylidenic center. This could explain why this transformation does not occur with 3-*O*-benzylated β -glycoside **29**, as the latter does not have the ability to form a chelate with the oxygen at C4. Moreover, as mentioned above, the driving force for this conformational change would be the anomeric effect, explaining why this behavior is specific to β -glycosides, which would then adopt their thermodynamically favored 1C_4 conformation.

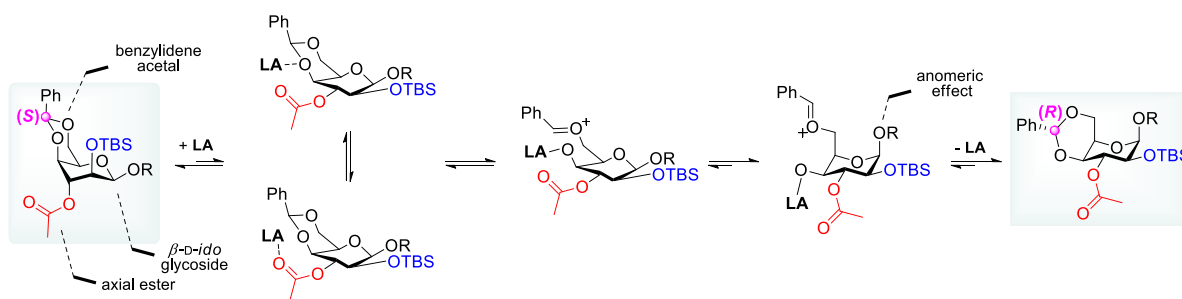


Figure 7.5. Proposed mechanism for the ring flipping with concomitant benzylidene epimerization

7.5 Conclusions

In summary, this work presents the glycosylation study of benzylidene-protected thioidosyl donors and describes a unique behavior of β -idosides related to their significant flexibility. Access to these thioidosyl donors was accomplished through the development of synthetic approaches enabling the regioselective silylation and benzylation of C2 and C3 hydroxyl groups, respectively. We have

CHAPITRE 7 – C7 EPIMERIZATION OF BENZYLIDENE-PROTECTED β -D-IDOPYRANOSIDES BRINGS STRUCTURAL INSIGHTS INTO IDOSE CONFORMATIONAL FLEXIBILITY

highlighted that with glycosyl acceptors having a high nucleophilic character, glycosylation reactions with 3-*O*-acylated 4,6-*O*-benzylidene thioidosyl donors were generally β -stereoselective to different extents (β/α ratio 1.5:1.0 to 15.4:1.0). On the other hand, replacing the 3-*O*-acyl group with a benzyl group led to complete β -stereoselectivity, whereas performing these reactions with less nucleophilic glycosidic acceptors favored formation of the α -disaccharides. We have uncovered and studied in detail an unusual behavior of *ido*-configured sugars that exemplifies their characteristic flexibility. Through the above-mentioned glycosylation study and with the help of NMR analyses and molecular modeling, we show that post-glycosylation acid-catalyzed benzylidene acetal opening with concomitant ring flipping and C7-epimerization occurs when the following conditions are met: (1) the glycosyl donor is D-*ido*-configured and esterified at C3; (2) the C4 and C6 positions are protected as a benzylidene acetal; (3) the alcohol acceptors are non-glycosidic; and (4) the resulting glycoside is β -configured. Our results suggest that the driving force for this transformation is the stabilization of the sugar conformation *via* the anomeric effect that outweighs the presence of axially-oriented substituents. Altogether, our study highlights the unique flexibility of D-idosides and their unusual behavior under glycosylation conditions.

7.6 Acknowledgments

This work was supported by Discovery grants from the Natural Sciences and Engineering Research Council of Canada (NSERC) under award number RGPIN-2016-04950 (to C. G.), RGPIN-2022-04515 (to C. G.), and RGPIN-2022-03982 (to S. L.). This work was also supported by a PTR (Programmes Transversaux de Recherche) grant (PTR 380-20) from Institut Pasteur Paris. M. C. thanks NSERC Vanier and Fonds de recherche du Québec – Nature et technologies (FRQNT) for Ph.D. scholarships. This research has been enabled by the use of computing resources provided by WestGrid and Compute Canada. We thank Thierry Maris (X-Ray Diffraction Laboratory, University of Montreal) for the X-ray analysis of diol **20a**.

7.7 Experimental section

General methods.

All starting materials and reagents were purchased from commercial sources and used as received without further purification. Air and water sensitive reactions were performed in oven-dried glassware under an Ar atmosphere. Moisture sensitive reagents were introduced *via* a dried syringe. Anhydrous solvents were either prepared from commercial solvents and dried over heat-gun activated 4 Å molecular sieves (MS) or supplied over MS and used as received. Powdered 4 Å MS were activated before use by heating with a heat gun for approx. 15 min under vacuum. Room temperature reactions were performed at 23 °C. Reactions were monitored by thin-layer chromatography (TLC) with silica gel 60 F₂₅₄ 0.25 mm pre-coated aluminum foil plates. Compounds were visualized by using UV₂₅₄ and/or orcinol (1 mg•mL⁻¹) in 10% aqueous H₂SO₄ solution with heating. Normal-phase flash column chromatographies were performed on silica gel 60 Å (15-40 μm). NMR spectra were recorded at 297 K in CDCl₃) with a 600 MHz instrument, employing standard softwares given by the manufacturer. ¹H and ¹³C NMR spectra were referenced to tetramethylsilane (TMS, $\delta_H = \delta_C = 0.00$ ppm) as an internal reference. Assignments were based on ¹H, ¹³C, COSY, HSQC, uncoupled HSQC, NOESY, and HMBC experiments. NMR spectra of compounds **20a**, **20b** and **20c** were recorded at 298 K with a 500 MHz instruments equipped with a N₂-cooled cryogenic broadband probe. 1D and 2D experiments were recorded using standard pulse program. For the NOESY quantitative experiment, relaxation and mixing time were set to 20 and 0.5 seconds, respectively. Terminal units in disaccharides are designated B, whereas sugars at the non-reducing end are designated A. High-resolution mass spectra (HRMS) were recorded on an ESI-Q-TOF mass spectrometer. Optical rotations $[\alpha]_D^{20}$ were measured on an Anton Paar polarimeter.

1,2,3,4,6-Penta-*O*-acetyl- α -D-idopyranose (**2**).

Compound **2** was synthesized according to our optimized approach. Briefly, β -D-glucose pentaacetate **1**⁵⁴³ (10.0 g, 25.6 mmol, 1.0 equiv) was solubilized in dry DCM (59 mL) under Ar. The solution was cooled to -10 °C and a solution of SbCl₅ (4.22 mL, 33.3 mmol, 1.3 equiv) in dry

CHAPITRE 7 – C7 EPIMERIZATION OF BENZYLIDENE-PROTECTED β -D-IDOPYRANOSIDES BRINGS STRUCTURAL INSIGHTS INTO IDOSE CONFORMATIONAL FLEXIBILITY

DCM (10 mL) was added dropwise. The solution was brought back to rt and was stirred for 1 h, during which a white precipitate formed. The solvents were removed under inert atmosphere through the cannula filtration technique while maintaining an inert atmosphere. The precipitate was washed once with Et₂O and the solvent was again removed by cannula filtration while maintaining the inert atmosphere. An aqueous solution of NaOAc (156 mL, 2.4 M) was added to the solid and the mixture was stirred at rt for 1 h, after which it was extracted three times with DCM. The combined organic layers were washed with H₂O, a saturated aqueous NaHCO₃ solution (2×), and H₂O, then dried over MgSO₄, filtered, and evaporated under reduced pressure. The residue was purified by silica gel flash chromatography (Hex/EtOAc 3:1 to 1:2) to give a mixture of 4-OH and 6-OH as a colorless oil (3.40 g, 38% in two steps). The latter mixture was solubilized in dry pyridine (21 mL) and cooled to 0 °C. Ac₂O (64 mL) was added, the solution was brought back to rt and was allowed to stir at this temperature for 16 h. The solution was diluted with DCM and ice-cold water was added, followed by the slow addition of a 1 N aqueous HCl solution while stirring. The organic layer was washed again with a 1 N aqueous HCl solution and twice with a saturated aqueous NaHCO₃ solution. The organic layers were dried over MgSO₄, filtered, evaporated under reduced pressure, and co-evaporated with toluene. The residue was purified by silica gel flash chromatography (Hex/EtOAc 1:0 to 1:1) to give peracetylated α -D-idopyranose **2** (3.5 g, 36%, 3 steps) as a white amorphous solid. Physical and analytical data agreed with those published.⁵³⁹

Ethyl 2,3,4,6-Tetra-O-acetyl-1-thio- α -D-idopyranoside (3a).

To a suspension of compound **2** (685 mg, 1.76 mmol, 1.0 equiv), activated 4 Å MS (446 mg) and EtSH (1.3 mL, 17 mmol, 10 equiv) in dry DCM (18 mL) at 0 °C was added dropwise BF₃·OEt₂ (0.32 mL, 2.6 mmol, 1.5 equiv). The suspension was stirred at rt for 3.5 h under Ar atmosphere. A saturated aqueous NaHCO₃ solution was added followed by I₂ (until the coloration persisted). A freshly prepared 10% aqueous Na₂S₂O₃ solution was added until the coloration disappeared and the aqueous phase was extracted with DCM (3×). The organic layer was then washed with brine, dried over MgSO₄, filtered over Celite and concentrated under reduced pressure. The residue was purified by silica gel flash chromatography (Tol/EtOAc 95:5 to 8:2) to give thioglycoside **3a** (556

CHAPITRE 7 – C7 EPIMERIZATION OF BENZYLIDENE-PROTECTED β-D-IDOPYRANOSIDES BRINGS STRUCTURAL INSIGHTS INTO IDOSE CONFORMATIONAL FLEXIBILITY

mg, 81%) as a colorless oil: R_f 0.5 (Tol/EtOAc 6:4); $[\alpha]_D^{20} +81$ (c 0.50, CHCl_3); $^1\text{H NMR}$ (600 MHz, CDCl_3): δ (ppm) 5.26 (br s, 1H, H-1), 5.01 (t, $J = 3.0$ Hz, 1H, H-3), 4.86 (m, 2H, H-2, H-4), 4.77 (td, $J = 6.2$ Hz, $J = 1.7$ Hz, 1H, H-5), 4.26–4.19 (m, 2H, H-6a, H-6b), 2.71–2.59 (m, 2H, $\text{CH}_{2\text{SEt}}$), 2.14 (s, 3H, $\text{CH}_{3\text{Ac}}$), 2.13 (s, 3H, $\text{CH}_{3\text{Ac}}$), 2.12 (s, 3H, $\text{CH}_{3\text{Ac}}$), 2.07 (s, 3H, $\text{CH}_{3\text{Ac}}$), 1.31 (t, $J = 7.4$ Hz, 3H, $\text{CH}_{3\text{SEt}}$); $^{13}\text{C}\{^1\text{H}\}$ NMR (150 MHz, CDCl_3): δ (ppm) 170.6 (COOR_{Ac}), 169.8 (COOR_{Ac}), 169.4 (COOR_{Ac}), 168.9 (COOR_{Ac}), 82.1 (C-1), 68.6, 66.61, 66.55 (3C, C-2, C-3, C-4), 65.0 (C-5), 62.3 (C-6), 26.4 ($\text{CH}_{2\text{SEt}}$), 21.0 ($\text{CH}_{3\text{Ac}}$), 20.9 ($\text{CH}_{3\text{Ac}}$), 20.84 ($\text{CH}_{3\text{Ac}}$), 20.80 ($\text{CH}_{3\text{Ac}}$), 15.0 ($\text{CH}_{3\text{SEt}}$); HRMS (ESI-TOF) m/z $[\text{M} + \text{NH}_4]^+$ calcd for $\text{C}_{16}\text{H}_{28}\text{NO}_9\text{S}$ 410.1479; found 410.1481; m/z $[\text{M} + \text{Na}]^+$ calcd for $\text{C}_{16}\text{H}_{24}\text{NaO}_9\text{S}$ 415.1033; found 415.1041.

***para*-Methylphenyl 2,3,4,6-Tetra-*O*-acetyl-1-thio- α -D-idopyranoside (3b).**

To a solution of peracetylated idopyranoside **2** (219 mg, 0.560 mmol, 1.0 equiv) in dry DCM (5.6 mL) were added activated 4 Å MS (142 mg) and HSTol (696 mg, 5.60 mmol, 10.0 equiv). The suspension was cooled to 0 °C and $\text{BF}_3 \cdot \text{OEt}_2$ (104 μL , 0.840 mmol, 1.5 equiv) was added dropwise. The mixture was stirred at rt for 4 h under Ar atmosphere. Then, the reaction was quenched with a saturated aqueous NaHCO_3 solution. I_2 was added until the color persisted, followed by a freshly prepared 10% aqueous $\text{Na}_2\text{S}_2\text{O}_3$ solution until the color disappeared. The aqueous layer was extracted with DCM (3 \times), and the combined organic layers were dried over MgSO_4 , filtered, and evaporated under reduced pressure. The residue was purified by silica gel flash chromatography (Hex/EtOAc 9:1 to 75:25) to give thioglycoside **3b** (180 mg, 71%) as a colorless oil: R_f 0.4 (Hex/EtOAc 1:1); $[\alpha]_D^{20} +127$ (c 2.40, CHCl_3); $^1\text{H NMR}$ (600 MHz, CDCl_3): δ (ppm) 7.42–7.41 (m, 2H, $2 \times \text{CH}_{\text{STol}}$), 7.12–7.11 (m, 2H, $2 \times \text{CH}_{\text{STol}}$), 5.39 (br s, 1H, H-1), 5.06–5.05 (m, 1H, H-3), 5.02–5.01 (m, 1H, H-2), 4.93 (ddd, $J = 7.3$ Hz, $J = 5.0$ Hz, $J = 2.0$ Hz, 1H, H-5), 4.90–4.89 (m, 1H, H-4), 4.26 (dd, $J = 11.6$ Hz, $J = 7.6$ Hz, 1H, H-6a), 4.22 (dd, $J = 11.6$ Hz, $J = 5.0$ Hz, 1H, H-6b), 2.33 (s, 3H, $\text{CH}_{3\text{STol}}$), 2.19 (s, 3H, $\text{CH}_{3\text{Ac}}$), 2.12 (s, 3H, $\text{CH}_{3\text{Ac}}$), 2.09 (s, 3H, $\text{CH}_{3\text{Ac}}$), 2.06 (s, 3H, $\text{CH}_{3\text{Ac}}$); $^{13}\text{C}\{^1\text{H}\}$ NMR (150 MHz, CDCl_3): δ (ppm) 170.7 (COOR_{Ac}), 169.9 (COOR_{Ac}), 169.3 (COOR_{Ac}), 168.8 (COOR_{Ac}), 138.2 (C_{STol}), 132.5 (2C, $2 \times \text{CH}_{\text{STol}}$), 131.0 (C_{STol}), 129.9 (2C, $2 \times \text{CH}_{\text{STol}}$), 86.0 (C-1), 68.4 (C-2), 66.5, 66.4 (2C, C-3, C-4), 65.4 (C-5), 62.5 (C-6), 21.3 ($\text{CH}_{3\text{STol}}$),

CHAPITRE 7 – C7 EPIMERIZATION OF BENZYLIDENE-PROTECTED β -D-IDOPYRANOSIDES BRINGS STRUCTURAL INSIGHTS INTO IDOSE CONFORMATIONAL FLEXIBILITY

20.99 (CH₃Ac), 20.98 (CH₃Ac), 20.9 (CH₃Ac), 20.8 (CH₃Ac); HRMS (ESI-TOF) m/z [M + NH₄]⁺ calcd for C₂₁H₃₀NO₉S 472.1636; found 472.1646.

Ethyl 4,6-*O*-Benzylidene-1-thio- α -D-idopyranoside (4a).

A neat solution of compound **3a** (50 mg, 0.22 mmol, 1.0 equiv), benzaldehyde (0.73 mL), and TFA (0.04 mL) was stirred at rt for 1 h under Ar atmosphere. The reaction flask was then cooled to 0 °C, slowly quenched with Et₃N, and evaporated under reduced pressure. The residue was purified by silica gel flash chromatography (Hex/EtOAc 9:1 to 6:4) to give compound **4a** (69 mg, quant.) as a colorless oil: R_f 0.25 (Hex/EtOAc 6:4); [α]_D²⁰ +111 (*c* 0.960, CHCl₃); ¹H NMR (600 MHz, CDCl₃): δ (ppm) 7.48–7.46 (m, 2H, 2 \times CH_{Ar}), 7.38–7.34 (m, 3H, 3 \times CH_{Ar}), 5.51 (s, 1H, CHPh), 5.40 (br s, 1H, H-1), 4.29 (dd, J = 12.6 Hz, 1.3 Hz, 1H, H-6a), 4.23 (br s, 1H, H-5), 4.10 (dd, J = 12.6 Hz, 1.6 Hz, 1H, H-6b), 4.03 (br s, 1H, H-4), 4.00 (br s, 1H, H-3), 3.73 (m, 1H, H-2), 2.70–2.59 (m, 2H, CH₂SEt), 1.30 (t, J = 7.4 Hz, 3H, CH₃SEt); ¹³C{¹H} NMR (150 MHz, CDCl₃): δ (ppm) 137.3 (C_{Ar}), 129.3 (CH_{Ar}), 128.4 (2C, 2 \times CH_{Ar}), 126.0 (2C, 2 \times CH_{Ar}), 101.5 (CHPh), 84.5 (C-1), 75.7 (C-4), 70.11, 70.06 (2C, C-6, C-2), 68.1 (C-3), 59.4 (C-5), 26.4 (CH₂SEt), 14.8 (CH₃SEt); HRMS (ESI-TOF) m/z [M + H]⁺ calcd for C₁₅H₂₁O₅S 313.1104; found 313.1096; m/z [M + Na]⁺ calcd for C₁₅H₂₀NaO₅S 335.0924; found 335.0915.

***para*-Methylphenyl 4,6-*O*-Benzylidene-1-thio- α -D-idopyranoside (4b).**

Et₃N (434 μ L, 3.11 mmol, 8.0 equiv) was added to a solution of compound **3b** (177 mg, 0.389 mmol, 1.0 equiv) in MeOH (3 mL). The mixture was stirred at rt for three days, after which the solvents were co-evaporated with toluene. The crude tetraol (125 mg, 0.437 mmol, 1.0 equiv) was solubilized in benzaldehyde (1.4 mL) and TFA (70 μ L) was added to the resulting solution. The mixture was stirred at rt for 1 h, cooled at 0 °C, and quenched with the slow addition of Et₃N. The solvents were co-evaporated with toluene and the residue was purified by silica gel flash chromatography to give diol **4b** (135 mg, 82%) as a white foam: R_f 0.3 (Hex/EtOAc 6:4); [α]_D²⁰ +217 (*c* 0.450, CHCl₃); ¹H NMR (600 MHz, CDCl₃): δ (ppm) 7.47–7.46 (m, 2H, 2 \times CH_{Ar}), 7.39–7.35 (m, 5H, 5 \times CH_{Ar}), 7.12–7.10 (m, 2H, 2 \times CH_{Ar}), 5.61 (br s, 1H, H-1), 5.54 (s, 1H, CHPh), 4.39 (br s, 1H, H-5), 4.32 (dd, J = 12.6 Hz, J = 1.3 Hz, 1H, H-6a), 4.13 (dd, J = 12.7 Hz,

CHAPITRE 7 – C7 EPIMERIZATION OF BENZYLIDENE-PROTECTED β -D-IDOPYRANOSIDES BRINGS STRUCTURAL INSIGHTS INTO IDOSE CONFORMATIONAL FLEXIBILITY

$J = 1.5$ Hz, 1H, H-6b), 4.11 (br s, 2H, H-2, H-4), 3.90 (br s, 1H, H-3), 3.81 (br s, 1H, OH), 2.56 (br s, 1H, OH), 2.32 (s, 3H, CH_{3STol}); $^{13}C\{^1H\}$ NMR (150 MHz, $CDCl_3$): δ (ppm) 137.5–126.1 (12C, $3 \times C_{Ar}$, $9 \times CH_{Ar}$), 101.7 (CHPh), 88.5 (C-1), 75.6 (C-4), 70.4, 70.1 (2C, C-6, C-3), 68.2 (C-2), 60.2 (C-5), 21.2 (CH_{3STol}); HRMS (ESI-TOF) m/z $[M + Na]^+$ calcd for $C_{20}H_{22}NaO_5S$ 397.1080; found 397.1074.

Ethyl 4,6-*O*-Benzylidene-2-*O*-*tert*-butyldimethylsilyl-1-thio- α -D-idopyranoside (5a) and Ethyl 4,6-*O*-Benzylidene-3-*O*-*tert*-butyldimethylsilyl-1-thio- α -D-idopyranoside (10).

Et_3N (0.76 mL, 5.5 mmol, 1.8 equiv) and TBSOTf (1.1 mL, 4.8 mmol, 1.5 equiv) were sequentially added to a solution of compound **4a** (948 mg, 3.03 mmol, 1.0 equiv) in anhydrous DCM (46 mL) at 0 °C. The solution was stirred at 0 °C for 10 min under Ar atmosphere then quenched with Et_3N and co-evaporated with toluene. The residue was purified by silica gel flash chromatography (Hex/EtOAc 95:5 to 7:3) to give compound **5a** (1014 mg, 78%) as a colorless oil and regioisomer **10** (52 mg, 4%) as a colorless oil.

Data for 2-*O*-silylated 5a: R_f 0.6 (Hex/EtOAc 6:4); $[\alpha]_D^{20} +87$ (c 0.83, $CHCl_3$); 1H NMR (600 MHz, $CDCl_3$): δ (ppm) 7.54–7.53 (m, 2H, $2 \times CH_{Ar}$), 7.34–7.32 (m, 3H, $3 \times CH_{Ar}$), 5.53 (s, 1H, CHPh), 5.23 (d, $J = 3.5$ Hz, 1H, H-1), 4.28 (d, $J = 12.6$ Hz, 1H, H-6a), 4.16 (dd, $J = 12.9$ Hz, 1.9 Hz, 1H, H-6b), 4.03–4.02 (m, 2H, H-4, H-5), 3.91–3.89 (m, 1H, H-3), 3.64 (dd, $J = 5.5$ Hz, 3.6 Hz, 1H, H-2), 2.71 (dq, $J = 14.6$ Hz, 7.3 Hz, 1H, CHH_{SEt}), 2.58 (dq, $J = 14.9$ Hz, 7.5 Hz, 1H, CHH_{SEt}), 2.43 (d, $J = 6.2$ Hz, 1H, OH-3), 1.31 (t, $J = 7.4$ Hz, 3H, CH_{3SEt}), 0.87 (s, 9H, $C(CH_3)_3TBS$), 0.14 (s, 3H, CH_{3TBS}), 0.09 (s, 3H, CH_{3TBS}); $^{13}C\{^1H\}$ NMR (150 MHz, $CDCl_3$): δ (ppm) 138.0 (C_{Ar}), 129.1 (CH_{Ar}), 128.2 (2C, $2 \times CH_{Ar}$), 126.7 (2C, $2 \times CH_{Ar}$), 100.9 (CHPh), 85.2 (C-1), 76.4 (C-4), 73.0 (C-3), 72.1 (C-2), 69.7 (C-6), 60.3 (C-5), 25.9 (3C, $C(CH_3)_3TBS$), 25.3 (CH_{2SEt}), 18.3 ($C(CH_3)_3TBS$), 14.9 (CH_{3SEt}), -4.4 (CH_{3TBS}), -4.6 (CH_{3TBS}); HRMS (ESI-TOF) m/z $[M+Na]^+$ calcd for $C_{21}H_{34}NaO_5SSi$ 449.1788; found 449.1800.

Data for 3-*O*-silylated 10: R_f 0.7 (Hex/EtOAc 6:4); $[\alpha]_D^{20} +50$ (c 0.31, $CHCl_3$); 1H NMR (600 MHz, $CDCl_3$): δ (ppm) 7.50–7.48 (m, 2H, $2 \times CH_{Ar}$), 7.38–7.36 (m, 3H, $3 \times CH_{Ar}$), 5.54 (s, 1H, CHPh), 5.33 (br s, 1H, H-1), 4.35 (br s, 1H, H-5), 4.30 (d, $J = 12.5$ Hz, 1H, H-6a), 4.13 (dd, $J =$

CHAPITRE 7 – C7 EPIMERIZATION OF BENZYLIDENE-PROTECTED β-D-IDOPYRANOSIDES BRINGS STRUCTURAL INSIGHTS INTO IDOSE CONFORMATIONAL FLEXIBILITY

12.5 Hz, 1.3 Hz, 1H, H-6b), 3.97 (t, $J = 2.4$ Hz, H-3), 3.85 (d, $J = 2.6$ Hz, 1H, H-4), 3.76 (d, $J = 12.0$ Hz, 1H, OH-2), 3.66 (dd, $J = 11.8$ Hz, $J = 1.1$ Hz, 1H, H-2), 2.67–2.58 (m, 2H, CH₂SEt), 1.30 (t, $J = 7.4$ Hz, 3H, CH₃SEt), 0.95 (s, 9H, C(CH₃)₃TBS), 0.14 (s, 3H, CH₃TBS), 0.13 (s, 3H, CH₃TBS); ¹³C{¹H} NMR (150 MHz, CDCl₃): δ (ppm) 137.5 (C_{Ar}), 129.4 (CH_{Ar}), 128.5 (2C, 2 × CH_{Ar}), 126.2 (2C, 2 × CH_{Ar}), 101.7 (CHPh), 86.2 (C-1), 76.6 (C-4), 71.1 (C-2), 70.6 (C-6), 68.4 (C-3), 59.6 (C-5), 27.4 (CH₂SEt), 25.9 (3C, C(CH₃)₃TBS), 18.2 (C(CH₃)₃TBS), 15.3 (CH₃SEt), -4.7 (CH₃TBS), -5.0 (CH₃TBS). HRMS (ESI-TOF) m/z [M+NH₄]⁺ calcd for C₂₁H₃₈NO₅SSi 444.2234; found 444.2253.

***para*-Methylphenyl 4,6-*O*-Benzylidene-2-*O*-*tert*-butyldimethylsilyl-1-thio- α -D-idopyranoside (5b).**

To a solution of diol **4b** (310 mg, 0.823 mmol, 1.0 equiv) in dry DCE (12.4 mL) at 0 °C was successively added Et₃N (208 μ L, 1.49 mmol, 1.8 equiv) and TBSOTf (288 μ L, 1.25 mmol, 1.5 equiv) dropwise. The solution was stirred at 0 °C for 10 min, quenched with Et₃N, and concentrated under reduced pressure. The residue was purified by silica gel flash chromatography (Hex/EtOAc 95:5 to 7:3) to give compound **5b** as a white amorphous solid (323 mg, 80%): R_f 0.55 (Hex/EtOAc 6:4); [α]_D²⁰ +76 (c 0.42, CHCl₃); ¹H NMR (600 MHz, CDCl₃): δ (ppm) 7.53–7.51 (m, 2H, 2 × CH_{Ar}), 7.40–7.39 (m, 2H, 2 × CH_{STol}), 7.34–7.32 (m, 3H, 3 × CH_{Ar}), 7.11–7.10 (m, 2H, 2 × CH_{STol}), 5.53 (s, 1H, CHPh), 5.37 (d, $J = 4.1$ Hz, 1H, H-1), 4.28 (dd, $J = 12.8$ Hz, $J = 0.9$ Hz, 1H, H-6a), 4.17 (dd, $J = 12.8$ Hz, $J = 2.5$ Hz, 1H, H-6b), 4.13 (br s, 1H, H-5), 4.07 (dd, $J = 3.3$ Hz, $J = 2.3$ Hz, 1H, H-4), 3.95 (br s, 1H, H-3), 3.78 (dd, $J = 6.1$ Hz, $J = 4.2$ Hz, 1H, H-2), 2.32 (s, 3H, CH₃STol), 2.30 (s, 1H, OH-3), 0.87 (s, 9H, C(CH₃)₃TBS), 0.16 (s, 3H, CH₃TBS), 0.11 (s, 3H, CH₃TBS); ¹³C{¹H} NMR (150 MHz, CDCl₃): δ (ppm) 138.0–126.6 (12C, 3 × C_{Ar}, 9 × CH_{Ar}), 100.8 (CHPh), 89.7 (C-1), 76.7 (C-4), 73.4 (C-3), 72.4 (C-2), 69.5 (C-6), 61.3 (C-5), 26.0 (3C, C(CH₃)₃TBS), 21.2 (CH₃STol), 18.3 (C(CH₃)₃TBS), -4.2 (CH₃TBS), -4.5 (CH₃TBS); HRMS (ESI-TOF) m/z [M + NH₄]⁺ calcd for C₂₆H₄₀NO₅SSi 506.2391; found 506.2405.

CHAPITRE 7 – C7 EPIMERIZATION OF BENZYLIDENE-PROTECTED β -D-IDOPYRANOSIDES BRINGS STRUCTURAL INSIGHTS INTO IDOSE CONFORMATIONAL FLEXIBILITY

Ethyl 3-O-Acetyl-4,6-O-benzylidene-2-O-tert-butyltrimethylsilyl-1-thio- α -D-idopyranoside (6a).

To a solution of alcohol **5a** (525 mg, 1.23 mmol, 1.0 equiv) in dry pyridine (17 mL) was added Ac₂O (17 mL). The solution was heated at 70 °C with an oil bath and stirred at this temperature for 16 h under Ar atmosphere. The solvents were co-evaporated with toluene and the residue was purified by silica gel flash chromatography (Hex/EtOAc 9:1 to 8:2) to give compound **6a** (562 mg, quant.) as a white amorphous solid: R_f 0.45 (Hex/EtOAc 7:3); $[\alpha]_D^{20} +128$ (c 0.800, CHCl₃); ¹H NMR (600 MHz, CDCl₃): δ (ppm) 7.54–7.53 (m, 2H, 2 \times CH_{Ar}), 7.33–7.31 (m, 3H, 3 \times CH_{Ar}), 5.51 (s, 1H, CHPh), 5.30 (s, 1H, H-1), 4.89 (t, J = 2.3 Hz, 1H, H-3), 4.31 (dd, J = 12.6 Hz, J = 1.2 Hz, 1H, H-6a), 4.20 (m, 1H, H-5), 4.14 (dd, J = 12.6 Hz, J = 2.0 Hz, 1H, H-6b), 3.92 (t, J = 2.1 Hz, 1H, H-4), 3.78–3.77 (m, 1H, H-2), 2.69 (dq, J = 13.2 Hz, J = 7.4 Hz, 1H, CHH_{SEt}), 2.60 (dq, J = 13.1 Hz, J = 7.4 Hz, 1H, CHH_{SEt}), 2.12 (s, 3H, CH_{3Ac}), 1.30 (t, J = 7.4 Hz, 3H, CH_{3SEt}), 0.85 (s, 9H, C(CH₃)₃TBS), 0.11 (s, 3H, CH₃TBS), 0.08 (s, 3H, CH₃TBS); ¹³C{¹H} NMR (150 MHz, CDCl₃): δ (ppm) 169.4 (COOR_{Ac}), 138.0 (C_{Ar}), 129.0 (CH_{Ar}), 128.0 (2C, 2 \times CH_{Ar}), 126.8 (2C, 2 \times CH_{Ar}), 101.5 (CHPh), 86.0 (C-1), 72.8 (C-4), 70.8 (C-3), 69.9 (C-6), 68.6 (C-2), 59.8 (C-5), 26.3 (CH₂SEt), 25.8 (3C, C(CH₃)₃TBS), 21.2 (CH_{3Ac}), 18.1 (C(CH₃)₃TBS), 15.2 (CH_{3SEt}), –4.75 (CH₃TBS), –4.84 (CH₃TBS); HRMS (ESI-TOF) m/z [M + NH₄]⁺ calcd for C₂₃H₄₀NO₆SSi 486.2340; found 486.2362.

***para*-Methylphenyl 3-O-Acetyl-4,6-O-benzylidene-2-O-tert-butyltrimethylsilyl-1-thio- α -D-idopyranoside (6b).**

To a solution of alcohol **5b** (38 mg, 0.078 mmol, 1.0 equiv) in dry pyridine (1.1 mL) was added Ac₂O (1.1 mL). The solution was heated at 70 °C with an oil bath and stirred at this temperature for 16 h under an Ar atmosphere. The solvents were co-evaporated with toluene and the residue was purified by silica gel flash chromatography (Hex/EtOAc 9:1) to give compound **6b** (41 mg, quant.) as a colorless oil: R_f 0.48 (Hex/EtOAc 7:3); $[\alpha]_D^{20} +99$ (c 0.87, CHCl₃); ¹H NMR (600 MHz, CDCl₃): δ (ppm) 7.54–7.52 (m, 2H, 2 \times CH_{Ar}), 7.39–7.38 (m, 2H, 2 \times CH_{Ar}), 7.32–7.31 (m, 3H, 3 \times CH_{Ar}), 7.12–7.10 (m, 2H, 2 \times CH_{Ar}), 5.52 (s, 1H, CHPh), 5.50 (br s, 1H, H-1), 4.94 (t, J

CHAPITRE 7 – C7 EPIMERIZATION OF BENZYLIDENE-PROTECTED β-D-IDOPYRANOSIDES BRINGS STRUCTURAL INSIGHTS INTO IDOSE CONFORMATIONAL FLEXIBILITY

= 2.5 Hz, 1H, H-3), 4.35–4.33 (m, 2H, H-6a, H-5), 4.16 (dd, $J = 12.9$ Hz, $J = 2.2$ Hz, 1H, H-6b), 3.97 (br s, 1H, H-4), 3.95 (t, $J = 1.3$ Hz, 1H, H-2), 2.32 (s, 3H, CH_{3STol}), 2.19 (s, 3H, CH_{3Ac}), 0.83 (s, 9H, $C(CH_3)_3TBS$), 0.10 (s, 3H, CH_{3TBS}), 0.09 (s, 3H, CH_{3TBS}); $^{13}C\{^1H\}$ NMR (150 MHz, $CDCl_3$): δ (ppm) 169.4 ($COOR_{Ac}$), 137.9–126.8 (12C, $3 \times C_{Ar}$, $9 \times CH_{Ar}$), 101.5 ($CHPh$), 89.6 (C-1), 72.7 (C-4), 70.6 (C-3), 69.8 (C-6), 68.7 (C-2), 60.4 (C-5), 25.8 (3C, $C(CH_3)_3TBS$), 21.3, 21.2 (2C, CH_{3STol} , CH_{3Ac}), 18.1 ($C(CH_3)_3TBS$), -4.7 (CH_{3TBS}), -4.8 (CH_{3TBS}); HRMS (ESI-TOF) m/z [$M + NH_4$] $^+$ calcd for $C_{28}H_{42}NO_6SSi$ 548.2497; found 548.2508.

***para*-Methylphenyl 4,6-*O*-Benzylidene-2-*O*-*tert*-butyldimethylsilyl-3-*O*-dichloroacetyl-1-thio- α -D-idopyranoside (7).**

To a solution of alcohol **5b** (30 mg, 0.061 mmol, 1.0 equiv) in dry DCE (0.6 mL) at 0 °C was added dry pyridine (30 μ L, 0.37 mmol, 6.0 equiv) followed by a solution of dichloroacetyl chloride (18 μ L, 0.18 mmol, 3.0 equiv) in dry DCE (0.25 mL). The reaction mixture was stirred at 0 °C for 1 h, then co-evaporated with toluene. The residue was purified by silica gel flash chromatography (Hex/EtOAc 95:5 to 85:15) to give compound **7** (37 mg, quant.) as a colorless oil: R_f 0.44 (Hex/EtOAc 8:2); $[\alpha]_D^{20} +83$ (c 1.3, $CHCl_3$); 1H NMR (600 MHz, $CDCl_3$): δ (ppm) 7.53–7.51 (m, 2H, $2 \times CH_{Ar}$), 7.39–7.37 (m, 2H, $2 \times CH_{Ar}$), 7.33–7.31 (m, 3H, $3 \times CH_{Ar}$), 7.12–7.11 (m, 2H, $2 \times CH_{Ar}$), 6.07 (s, 1H, $CHCl_2$), 5.55 (s, 1H, $CHPh$), 5.51 (br s, 1H, H-1), 5.02 (t, $J = 2.2$ Hz, 1H, H-3), 4.35–4.33 (m, 2H, H-5, H-6a), 4.18 (dd, $J = 13.0$ Hz, $J = 2.1$ Hz, 1H, H-6b), 4.04 (br s, 1H, H-4), 3.98 (br s, 1H, H-2), 2.33 (s, 3H, CH_{3STol}), 0.83 (s, 9H, $C(CH_3)_3TBS$), 0.11 (s, 3H, CH_{3TBS}), 0.09 (s, 3H, CH_{3TBS}); $^{13}C\{^1H\}$ NMR (150 MHz, $CDCl_3$): δ (ppm) 163.3 ($COOR_{AcCl_2}$), 137.7–126.7 (12C, $3 \times C_{Ar}$, $9 \times CH_{Ar}$), 101.5 ($CHPh$), 89.3 (C-1), 73.7 (C-3), 72.0 (C-4), 69.7 (C-6), 68.3 (C-2), 64.2 ($CHCl_2$), 60.2 (C-5), 25.8 (3C, $C(CH_3)_3TBS$), 21.2 (CH_{3STol}), 18.1 ($C(CH_3)_3TBS$), -4.8 (2C, $2 \times CH_{3TBS}$); HRMS (ESI-TOF) m/z [$M+NH_4$] $^+$ calcd for $C_{28}H_{40}Cl_2NO_6SSi$ 616.1717; found 616.1735.

CHAPITRE 7 – C7 EPIMERIZATION OF BENZYLIDENE-PROTECTED β -D-IDOPYRANOSIDES BRINGS STRUCTURAL INSIGHTS INTO IDOSE CONFORMATIONAL FLEXIBILITY

***para*-Methylphenyl 3-O-(2-Azidomethyl)benzoyl-4,6-O-benzylidene-2-O-*tert*-butyldimethylsilyl-1-thio- α -D-idopyranoside (8).**

To a solution of alcohol **5b** (15 mg, 0.031 mmol, 1.0 equiv) and DMAP (9 mg, 0.08 mmol, 2.5 equiv) in dry pyridine (107 μ L) was added a solution of AZMB₂O (39 mg, 0.12 mmol, 3.8 equiv) in dry pyridine (61 μ L). The mixture was heated at 50 °C with an oil bath and stirred at this temperature for 24 h under Ar, after which it was co-evaporated with toluene. The residue was purified by silica gel flash chromatography (Tol/Hex 95:5) to give ester **8** (14 mg, 70%) as a colorless oil: R_f 0.4 (Hex/EtOAc 8:2); $[\alpha]_D^{20}$ +70 (c 0.31, CHCl₃); ¹H NMR (600 MHz, CDCl₃): δ (ppm) 8.36–8.34 (m, 1H, CH_{AZMB}), 7.63–7.61 (m, 1H, CH_{AZMB}), 7.56–7.55 (m, 3H, 3 \times CH_{Ar}), 7.50–7.47 (m, 1H, CH_{AZMB}), 7.41–7.40 (m, 2H, 2 \times CH_{STol}), 7.33–7.32 (m, 3H, 3 \times CH_{Ar}), 7.12–7.11 (m, 2H, 2 \times CH_{STol}), 5.58 (br s, 1H, H-1), 5.56 (s, 1H, CHPh), 5.22 (br s, 1H, H-3), 4.93 (d, J = 14.7 Hz, 1H, CHH_{AZMB}), 4.90 (d, J = 14.7 Hz, 1H, CHH_{AZMB}), 4.44 (br d, J = 1.0 Hz, 1H, H-5), 4.37 (d, J = 12.7 Hz, 1H, H-6a), 4.19 (dd, J = 12.7 Hz, J = 1.8 Hz, 1H, H-6b), 4.10 (br s, 1H, H-4), 4.07 (m, 1H, H-2), 2.33 (s, 3H, CH_{3STol}), 0.85 (s, 9H, C(CH₃)_{3TBS}), 0.12 (s, 6H, 2 \times CH_{3TBS}); ¹³C{¹H} NMR (150 MHz, CDCl₃): δ (ppm) 164.7 (COOR_{AZMB}), 138.4–126.8 (18C, 5 \times C_{Ar}, 13 \times CH_{Ar}), 101.6 (CHPh), 89.5 (C-1), 72.4 (C-4), 70.9 (C-3), 69.8 (C-6), 68.9 (C-2), 60.5 (C-5), 53.3 (CH_{2AZMB}), 25.8 (3C, C(CH₃)_{3TBS}), 21.2 (CH_{3STol}), 18.1 (C(CH₃)_{3TBS}), –4.7 (CH_{3TBS}), –4.8 (CH_{3TBS}); HRMS (ESI-TOF) m/z [M+NH₄]⁺ calcd for C₃₄H₄₅N₄O₆SSi 665.2824; found 665.2835.

***para*-Methylphenyl 4,6-O-Benzylidene-2-O-*tert*-butyldimethylsilyl-3-O-*tert*-butoxycarbonyl-1-thio- α -D-idopyranoside (9).**

To a solution of alcohol **5b** (44 mg, 0.089 mmol, 1.0 equiv) in dry DCE (1.3 mL) were sequentially added Boc₂O (78 mg, 0.36 mmol, 4.0 equiv), Et₃N (16 μ L, 0.12 mmol, 1.3 equiv), and DMAP (1 mg, 0.009 mmol, 0.1 equiv). The mixture was stirred at rt for 40 h, after which it was diluted with EtOAc and washed with a saturated aqueous NaHCO₃ solution and brine. The organic layers were dried over MgSO₄, filtered, and concentrated under reduced pressure. The residue was purified by silica gel flash chromatography (Hex/EtOAc 9:1) to give compound **9** (53 mg, quant.) as a colorless oil: R_f 0.47 (Hex/EtOAc 8:2); $[\alpha]_D^{20}$ +89 (c 0.27, CHCl₃); ¹H NMR (600 MHz, CDCl₃):

CHAPITRE 7 – C7 EPIMERIZATION OF BENZYLIDENE-PROTECTED β -D-IDOPYRANOSIDES BRINGS STRUCTURAL INSIGHTS INTO IDOSE CONFORMATIONAL FLEXIBILITY

δ (ppm) 7.53–7.51 (m, 2H, $2 \times CH_{Ar}$), 7.40–7.39 (m, 2H, $2 \times CH_{Ar}$), 7.32–7.31 (m, 3H, $3 \times CH_{Ar}$), 7.11–7.09 (m, 2H, $2 \times CH_{Ar}$), 5.53 (s, 1H, CH_{Ph}), 5.48 (br s, 1H, H-1), 4.76 (t, $J = 2.8$ Hz, 1H, H-3), 4.32–4.30 (m, 2H, H-5, H-6a), 4.14 (dd, $J = 12.9$ Hz, $J = 2.3$ Hz, 1H, H-6b), 4.06 (br s, 1H, H-4), 4.00 (t, $J = 2.6$ Hz, 1H, H-2), 2.32 (s, 3H, CH_{3STol}), 1.53 (s, 9H, $C(CH_3)_3Boc$), 0.84 (s, 9H, $C(CH_3)_3TBS$), 0.12 (s, 3H, CH_{3TBS}), 0.10 (s, 3H, CH_{3TBS}); $^{13}C\{^1H\}$ NMR (150 MHz, $CDCl_3$): δ (ppm) 152.3 ($COOR_{Boc}$), 138.0–126.7 ($12C$, $3 \times C_{Ar}$, $9 \times CH_{Ar}$), 101.3 (CH_{Ph}), 89.5 (C-1), 83.2 ($C(CH_3)_3Boc$), 73.8 (C-3), 73.2 (C-4), 69.7 (C-6), 68.9 (C-2), 60.7 (C-5), 27.9 (3C, $C(CH_3)_3Boc$), 25.9 (3C, $C(CH_3)_3TBS$), 21.2 (CH_{3STol}), 18.1 ($C(CH_3)_3TBS$), -4.6 (CH_{3TBS}), -4.7 (CH_{3TBS}); HRMS (ESI-TOF) m/z $[M + NH_4]^+$ calcd for $C_{31}H_{48}NO_7SSi$ 606.2915; found 606.2932.

General Procedure for the NIS/TMSOTf-promoted Glycosylation.

The donor (1.2 equiv), acceptor (1.0 equiv), and NIS (1.5 equiv) were dried together under vacuum for 1 h. Then, activated 4 Å MS (4 mg/mg of donor) and dry solvent ($20 \text{ mL} \cdot \text{mmol}^{-1}$) were added, and the suspension was stirred at rt under Ar atmosphere for 1 h. The suspension was cooled at -10 °C and TMSOTf (0.1 equiv) was added. The mixture was stirred under Ar while being allowed to gradually warm to 0 °C for a period of 30 min to 1 h. The reaction was then quenched with Et_3N , filtered over Celite, and concentrated under reduced pressure. The residue was purified by silica gel flash chromatography.

(2-Adamantyl) 3-O-Acetyl-(S)-4,6-O-benzylidene-2-O-tert-butyldimethylsilyl- β -D-idopyranoside (14a), (2-Adamantyl) 3-O-Acetyl-(R)-4,6-O-benzylidene-2-O-tert-butyldimethylsilyl- β -D-idopyranoside (14b) and (2-Adamantyl) 3-O-Acetyl-(S)-4,6-O-benzylidene-2-O-tert-butyldimethylsilyl- α -D-idopyranoside (14c).

Donor **6a** (14.8 mg, 0.0315 mmol, 1.2 equiv) and 2-adamantanol (4.0 mg, 0.026 mmol, 1.0 equiv) were reacted according to the general procedure for NIS/TMSOTf-promoted glycosylation. Purification by silica gel flash chromatography (Hex/ $EtOAc$ 95:5 to 85:15) gave compounds **14a** (3.6 mg, 25%, colorless oil), **14b** (6.7 mg, 46%, white amorphous solid), and **14c** (0.8 mg, 5%, colorless oil).

CHAPITRE 7 – C7 EPIMERIZATION OF BENZYLIDENE-PROTECTED β -D-IDOPYRANOSIDES BRINGS STRUCTURAL INSIGHTS INTO IDOSE CONFORMATIONAL FLEXIBILITY

Data for β -glycoside 14a: R_f 0.3 (Hex/EtOAc 8:2); $[\alpha]_D^{20}$ -27 (c 0.60, CHCl_3); ^1H NMR (600 MHz, CDCl_3): δ (ppm) 7.55–7.53 (m, 2H, $2 \times \text{CH}_{\text{Ar}}$), 7.31–7.30 (m, 3H, $3 \times \text{CH}_{\text{Ar}}$), 5.46 (s, 1H, CHPh), 5.05 (t, $J = 2.5$ Hz, 1H, H-3), 4.68 (d, $J = 1.1$ Hz, 1H, H-1), 4.36 (d, $J = 12.5$ Hz, 1H, H-6a), 4.06 (dd, $J = 12.5$ Hz, 2.1 Hz, 1H, H-6b), 3.96 (t, $J = 2.9$ Hz, 1H, H-2_{ad}), 3.81 (br s, 1H, H-4), 3.66 (d, $J = 2.8$ Hz, 1H, H-2), 3.58 (m, 1H, H-5), 2.21–1.43 (m, 14H, $4 \times \text{CH}_{\text{ad}}$, $5 \times \text{CH}_{2\text{ad}}$), 2.11 (s, 3H, CH_3Ac), 0.85 (s, 9H, $\text{C}(\text{CH}_3)_3\text{TBS}$), 0.14 (s, 3H, CH_3TBS), 0.10 (s, 3H, CH_3TBS); $^{13}\text{C}\{^1\text{H}\}$ NMR (150 MHz, CDCl_3): δ (ppm) 169.2 (COOR_{Ac}), 138.0 (C_{Ar}), 128.9 (CH_{Ar}), 127.9 (2C, $2 \times \text{CH}_{\text{Ar}}$), 126.9 (2C, $2 \times \text{CH}_{\text{Ar}}$), 101.6 (CHPh), 96.8 (C-1, $^1J_{\text{C1,H1}} = 156$ Hz), 79.7 (C-2_{ad}), 73.6 (C-3), 73.0 (C-4), 69.8 (C-6), 68.3 (C-2), 67.1 (C-5), 37.8–27.6 (9C, $4 \times \text{CH}_{\text{ad}}$, $5 \times \text{CH}_{2\text{ad}}$), 25.9 (3C, $\text{C}(\text{CH}_3)_3\text{TBS}$), 21.3 (CH_3Ac), 18.5 ($\text{C}(\text{CH}_3)_3\text{TBS}$), -4.4 (CH_3TBS), -5.1 (CH_3TBS); HRMS (ESI-TOF) m/z $[\text{M} + \text{NH}_4]^+$ calcd for $\text{C}_{31}\text{H}_{50}\text{NO}_7\text{Si}$ 576.3351; found 576.3363; m/z $[\text{M} + \text{Na}]^+$ calcd for $\text{C}_{31}\text{H}_{46}\text{NaO}_7\text{Si}$ 581.2905; found 581.2918.

Data for β -glycoside 14b: R_f 0.53 (Hex/EtOAc 8:2); $[\alpha]_D^{20}$ -38 (c 0.28, CHCl_3); ^1H NMR (600 MHz, CDCl_3): δ (ppm) 7.45–7.44 (m, 2H, $2 \times \text{CH}_{\text{Ar}}$), 7.35–7.31 (m, 3H, $3 \times \text{CH}_{\text{Ar}}$), 6.01 (t, $J = 10.1$ Hz, 1H, H-3), 5.91 (s, 1H, CHPh), 4.86 (d, $J = 3.7$ Hz, 1H, H-1), 4.59 (t, $J = 11.3$ Hz, 1H, H-6a), 4.34 (dt, $J = 11.8$ Hz, $J = 5.9$ Hz, 1H, H-5), 4.14–4.09 (m, 2H, H-6b, H-4), 3.78 (t, $J = 3.0$ Hz, 1H, H-2_{ad}), 3.76 (dd, $J = 9.8$ Hz, $J = 3.7$ Hz, 1H, H-2), 2.20–1.42 (m, 14H, $4 \times \text{CH}_{\text{ad}}$, $5 \times \text{CH}_{2\text{ad}}$), 2.10 (s, 3H, CH_3Ac), 0.89 (s, 9H, $\text{C}(\text{CH}_3)_3\text{TBS}$), 0.11 (s, 3H, CH_3TBS), 0.07 (s, 3H, CH_3TBS); $^{13}\text{C}\{^1\text{H}\}$ NMR (150 MHz, CDCl_3): δ (ppm) 170.6 (COOR_{Ac}), 137.8 (C_{Ar}), 129.0 (CH_{Ar}), 128.4 (2C, $2 \times \text{CH}_{\text{Ar}}$), 126.4 (2C, $2 \times \text{CH}_{\text{Ar}}$), 97.5 (C-1, $^1J_{\text{C1,H1}} = 171$ Hz), 96.3 (CHPh), 80.4 (C-2_{ad}), 75.2 (C-4), 71.4 (C-2), 68.2 (C-6), 67.4 (C-5), 66.7 (C-3), 37.5–27.4 (9C, $4 \times \text{CH}_{\text{ad}}$, $5 \times \text{CH}_{2\text{ad}}$), 25.8 (3C, $\text{C}(\text{CH}_3)_3\text{TBS}$), 21.4 (CH_3Ac), 18.2 ($\text{C}(\text{CH}_3)_3\text{TBS}$), -4.0 (CH_3TBS), -4.8 (CH_3TBS); HRMS (ESI-TOF) m/z $[\text{M} + \text{NH}_4]^+$ calcd for $\text{C}_{31}\text{H}_{50}\text{NO}_7\text{Si}$ 576.3351; found 576.3365; m/z $[\text{M} + \text{Na}]^+$ calcd for $\text{C}_{31}\text{H}_{46}\text{NaO}_7\text{Si}$ 581.2905; found 581.2923.

Data for α -glycoside 14c (contaminated with traces of β -glycoside 14b): R_f 0.47 (Hex/EtOAc 8:2); $[\alpha]_D^{20}$ $+28$ (c 0.22, CHCl_3); ^1H NMR (600 MHz, CDCl_3): δ (ppm) 7.54–7.52 (m, 2H, $2 \times \text{CH}_{\text{Ar}}$), 7.33–7.31 (m, 3H, $3 \times \text{CH}_{\text{Ar}}$), 5.50 (s, 1H, CHPh), 4.97 (d, $J = 1.7$ Hz, 1H, H-1), 4.94 (t, $J = 3.5$ Hz, 1H, H-3), 4.28 (dd, $J = 12.5$ Hz, $J = 1.5$ Hz, 1H, H-6a), 4.11 (dd, $J = 12.6$ Hz, 2.0 Hz,

CHAPITRE 7 – C7 EPIMERIZATION OF BENZYLIDENE-PROTECTED β -D-IDOPYRANOSIDES BRINGS STRUCTURAL INSIGHTS INTO IDOSE CONFORMATIONAL FLEXIBILITY

1H, H-6b), 3.96 (t, $J = 2.4$ Hz, 1H, H-4), 3.92 (m, 1H, H-5), 3.78 (t, $J = 2.9$ Hz, 1H, H-2_{ad}), 3.75 (dd, $J = 4.2$ Hz, $J = 2.1$ Hz, 1H, H-2), 2.09 (s, 3H, CH_{3Ac}), 2.06–1.49 (m, 14H, 4 × CH_{ad}, 5 × CH_{2ad}), 0.85 (s, 9H, C(CH₃)_{3TBS}), 0.095 (s, 3H, CH_{3TBS}), 0.091 (s, 3H, CH_{3TBS}); ¹³C{¹H} NMR (150 MHz, CDCl₃): δ (ppm) 169.8 (COOR_{Ac}), 138.1 (C_{Ar}), 129.0 (CH_{Ar}), 128.1 (2C, 2 × CH_{Ar}), 126.8 (2C, 2 × CH_{Ar}), 101.3 (CHPh), 100.3 (C-1, ¹J_{C1,H1} = 171 Hz), 80.1 (C-2_{ad}), 73.9 (C-4), 72.2 (C-3), 69.7 (C-6), 68.1 (C-2), 60.1 (C-5), 37.7–27.3 (9C, 4 × CH_{ad}, 5 × CH_{2ad}), 25.8 (3C, C(CH₃)_{3TBS}), 21.3 (CH_{3Ac}), 18.1 (C(CH₃)_{3TBS}), –4.7 (CH_{3TBS}), –4.8 (CH_{3TBS}); HRMS (ESI-TOF) m/z [M + NH₄]⁺ calcd for C₃₁H₅₀NO₇Si 576.3351; found 576.3362; m/z [M + Na]⁺ calcd for C₃₁H₄₆NaO₇Si 581.2905; found 581.2925.

(1-Adamantyl) 3-O-Acetyl-(S)-4,6-O-benzylidene-2-O-tert-butyltrimethylsilyl- β -D-idopyranoside (15a), (1-Adamantyl) 3-O-Acetyl-(R)-4,6-O-benzylidene-2-O-tert-butyltrimethylsilyl- β -D-idopyranoside (15b) and (1-Adamantyl) 3-O-Acetyl-(S)-4,6-O-benzylidene-2-O-tert-butyltrimethylsilyl- α -D-idopyranoside (15c)

Donor **6a** (11.1 mg, 0.0236 mmol, 1.2 equiv) and 1-adamantanol (3.0 mg, 0.020 mmol, 1.0 equiv) were reacted according to the general procedure for NIS/TMSOTf-promoted glycosylation. Purification by silica gel flash chromatography (Hex/EtOAc 95:5 to 9:1) gave compounds **15a** (4.3 mg, 39%, colorless oil), **15b** (2.2 mg, 20%, colorless oil), and **15c** (1.3 mg, 12%, colorless oil).

Data for β -glycoside 15a: R_f 0.38 (Hex/EtOAc 8:2); $[\alpha]_D^{20}$ –20 (c 0.45, CHCl₃); ¹H NMR (600 MHz, CDCl₃): δ (ppm) 7.55–7.54 (m, 2H, 2 × CH_{Ar}), 7.30–7.29 (m, 3H, 3 × CH_{Ar}), 5.45 (s, 1H, CHPh), 5.02 (t, $J = 2.4$ Hz, 1H, H-3), 4.82 (br s, 1H, H-1), 4.33 (d, $J = 12.4$ Hz, 1H, H-6a), 4.05 (dd, $J = 12.5$ Hz, $J = 2.0$ Hz, 1H, H-6b), 3.77 (br s, 1H, H-4), 3.57 (br s, 1H, H-5), 3.49 (br s, 1H, H-2), 2.14 (br s, 3H, 3 × CH_{ad}), 2.13 (s, 3H, CH_{3Ac}), 1.90–1.61 (m, 12H, 6 × CH_{2ad}), 0.86 (s, 9H, C(CH₃)_{3TBS}), 0.15 (s, 3H, CH_{3TBS}), 0.08 (s, 3H, CH_{3TBS}); ¹³C{¹H} NMR (150 MHz, CDCl₃): δ (ppm) 169.2 (COOR_{Ac}), 138.1 (C_{Ar}), 128.9 (CH_{Ar}), 127.9 (2C, 2 × CH_{Ar}), 127.0 (2C, 2 × CH_{Ar}), 101.6 (CHPh), 92.4 (C-1, ¹J_{C1,H1} = 153 Hz), 74.8 (C-1_{ad}), 73.7 (C-3), 72.4 (C-4), 69.9 (C-6), 69.3 (C-2), 67.0 (C-5), 42.6 (3C, 3 × CH_{2ad}), 36.5 (3C, 3 × CH_{2ad}), 30.8 (3C, 3 × CH_{ad}), 26.0 (3C,

CHAPITRE 7 – C7 EPIMERIZATION OF BENZYLIDENE-PROTECTED β -D-IDOPYRANOSIDES BRINGS STRUCTURAL INSIGHTS INTO IDOSE CONFORMATIONAL FLEXIBILITY

C(CH₃)₃TBS), 21.3 (CH₃Ac), 18.6 (C(CH₃)₃TBS), -4.1 (CH₃TBS), -5.2 (CH₃TBS); HRMS (ESI-TOF) m/z [M + NH₄]⁺ calcd for C₃₁H₅₀NO₇Si 576.3351; found 576.3357.

Data for β -glycoside 15b: R_f 0.48 (Hex/EtOAc 8:2); $[\alpha]_D^{20}$ -39 (c 0.30, CHCl₃); ¹H NMR (600 MHz, CDCl₃): δ (ppm) 7.45–7.43 (m, 2H, 2 \times CH_{Ar}), 7.35–7.31 (m, 3H, 3 \times CH_{Ar}), 5.97 (t, J = 10.1 Hz, 1H, H-3), 5.90 (s, 1H, CHPh), 5.07 (d, J = 3.8 Hz, 1H, H-1), 4.70 (t, J = 11.4 Hz, 1H, H-6a), 4.32 (dt, J = 11.8 Hz, J = 6.0 Hz, 1H, H-5), 4.12–4.07 (m, 2H, H-6b, H-4), 3.69 (dd, J = 9.8 Hz, J = 3.8 Hz, 1H H-2), 2.16 (br s, 3H, 3 \times CH_{ad}), 2.09 (s, 3H, CH₃Ac), 1.85–1.60 (m, 12H, 6 \times CH_{2ad}), 0.90 (s, 9H, C(CH₃)₃TBS), 0.12 (s, 3H, CH₃TBS), 0.08 (s, 3H, CH₃TBS); ¹³C{¹H} NMR (150 MHz, CDCl₃): δ (ppm) 170.6 (COOR_{Ac}), 137.9 (C_{Ar}), 128.9 (CH_{Ar}), 128.4 (2C, 2 \times CH_{Ar}), 126.4 (2C, 2 \times CH_{Ar}), 96.2 (CHPh), 92.9 (C-1, ¹J_{C1,H1} = 171 Hz), 75.2 (C-4), 75.0 (C-1_{ad}), 71.1 (C-2), 68.7 (C-6), 67.5 (C-5), 66.9 (C-3), 42.9 (3C, 3 \times CH_{2ad}), 36.4 (3C, 3 \times CH_{2ad}), 30.8 (3C, 3 \times CH_{ad}), 25.8 (3C, C(CH₃)₃TBS), 21.4 (CH₃Ac), 18.2 (C(CH₃)₃TBS), -3.9 (CH₃TBS), -4.8 (CH₃TBS); HRMS (ESI-TOF) m/z [M + Na]⁺ calcd for C₃₁H₄₆NaO₇Si 581.2905; found 581.2898.

Data for α -glycoside 15c: R_f 0.34 (Hex/EtOAc 8:2); $[\alpha]_D^{20}$ +32 (c 0.25, CHCl₃); ¹H NMR (600 MHz, CDCl₃): δ (ppm) 7.54–7.52 (m, 2H, 2 \times CH_{Ar}), 7.32–7.31 (m, 3H, 3 \times CH_{Ar}), 5.49 (s, 1H, CHPh), 5.24 (d, J = 2.9 Hz, 1H, H-1), 4.95 (dd, J = 4.8 Hz, J = 3.2 Hz, 1H, H-3), 4.27 (dd, J = 12.5 Hz, J = 0.9 Hz, 1H, H-6a), 4.11 (dd, J = 12.6 Hz, J = 2.1 Hz, 1H, H-6b), 4.00–3.99 (m, 1H, H-5), 3.97 (m, 1H, H-4), 3.65 (dd, J = 4.9 Hz, J = 3.0 Hz, 1H, H-2), 2.13 (br s, 3H, 3 \times CH_{ad}), 2.08 (s, 3H, CH₃Ac), 1.83–1.59 (m, 12H, 6 \times CH_{2ad}), 0.86 (s, 9H, C(CH₃)₃TBS), 0.11 (s, 3H, CH₃TBS), 0.08 (s, 3H, CH₃TBS); ¹³C{¹H} NMR (150 MHz, CDCl₃): δ (ppm) 169.8 (COOR_{Ac}), 138.1 (C_{Ar}), 129.0 (CH_{Ar}), 128.1 (2C, 2 \times CH_{Ar}), 126.7 (2C, 2 \times CH_{Ar}), 101.0 (CHPh), 95.3 (C-1, ¹J_{C1,H1} = 168 Hz), 74.5 (C-4), 74.3 (C-1_{ad}), 73.0 (C-3), 69.8 (C-6), 69.3 (C-2), 60.3 (C-5), 42.7 (3C, 3 \times CH_{2ad}), 36.5 (3C, 3 \times CH_{2ad}), 30.8 (3C, 3 \times CH_{ad}), 25.9 (3C, C(CH₃)₃TBS), 21.4 (CH₃Ac), 18.1 (C(CH₃)₃TBS), -4.4 (CH₃TBS), -4.7 (CH₃TBS); HRMS (ESI-TOF) m/z [M + NH₄]⁺ calcd for C₃₁H₅₀NO₇Si 576.3351; found 576.3361.

CHAPITRE 7 – C7 EPIMERIZATION OF BENZYLIDENE-PROTECTED β -D-IDOPYRANOSIDES BRINGS STRUCTURAL INSIGHTS INTO IDOSE CONFORMATIONAL FLEXIBILITY

(3-Stigmastanyl) 3-*O*-Acetyl-(*S*)-4,6-*O*-benzylidene-2-*O*-*tert*-butyldimethylsilyl- β -D-idopyranoside (16a), (3-Stigmastanyl) 3-*O*-Acetyl-(*R*)-4,6-*O*-benzylidene-2-*O*-*tert*-butyldimethylsilyl- β -D-idopyranoside (16b) and (3-Stigmastanyl) 3-*O*-Acetyl-(*S*)-4,6-*O*-benzylidene-2-*O*-*tert*-butyldimethylsilyl- α -D-idopyranoside (16c).

Donor **6a** (9.4 mg, 0.020 mmol, 1.2 equiv) and stigmastanol (7.0 mg, 0.017 mmol, 1.0 equiv) were reacted according to the general procedure for NIS/TMSOTf-promoted glycosylation. Purification by silica gel flash chromatography (Hex/EtOAc 98:2 to 92:8) gave compounds **16a** (2.0 mg, 14%, colorless oil), **16b** (1.7 mg, 12%, white amorphous solid), and **16c** (0.5 mg, 4%, colorless oil).

Data for β -glycoside 16a (contaminated with traces of β -glycoside **16b**): R_f 0.37 (Hex/EtOAc 8:2); $[\alpha]_D^{20}$ -16 (c 0.20, CHCl₃); ¹H NMR (600 MHz, CDCl₃): δ (ppm) 7.55–7.53 (m, 2H, 2 \times CH_{Ar}), 7.30–7.29 (m, 3H, 3 \times CH_{Ar}), 5.46 (s, 1H, CHPh), 5.02 (t, J = 2.5 Hz, 1H, H-3), 4.69 (br s, 1H, H-1), 4.36 (d, J = 12.2 Hz, 1H, H-6a), 4.06 (dd, J = 12.5 Hz, J = 1.9 Hz, 1H, H-6b), 3.79 (br s, 1H, H-4), 3.75–3.70 (m, 1H, H-3_{stig}), 3.59 (d, J = 2.6 Hz, 1H, H-2), 3.57 (br s, 1H, H-5), 2.11 (s, 3H, CH_{3Ac}), 1.97–0.59 (m, 59H, C(CH₃)₃TBS, 12 \times CH₂stig, 8 \times CH_{stig}, 6 \times CH₃stig), 0.13 (s, 3H, CH₃TBS), 0.07 (s, 3H, CH₃TBS); ¹³C{¹H} NMR (150 MHz, CDCl₃): δ (ppm) 169.1 (COOR_{Ac}), 138.1 (C_{Ar}), 128.9 (CH_{Ar}), 128.0 (2C, 2 \times CH_{Ar}), 126.9 (2C, 2 \times CH_{Ar}), 101.6 (CHPh), 96.9 (C-1, ¹J_{C1,H1} = 155 Hz), 76.9 (C-3_{stig}), 73.5 (C-3), 72.6 (C-4), 69.8 (C-6), 68.3 (C-2), 67.0 (C-5), 56.7–12.1 (33C, C(CH₃)₃TBS, C(CH₃)₃TBS, CH_{3Ac}, 6 \times CH₃stig, 12 \times CH₂stig, 8 \times CH_{stig}, 2 \times C_{stig}), -4.2 (CH₃TBS), -5.2 (CH₃TBS); HRMS (ESI-TOF) m/z [M + NH₄]⁺ calcd for C₅₀H₈₆NO₇Si 840.6168; found 840.6171.

Data for β -glycoside 16b: R_f 0.57 (Hex/EtOAc 8:2); $[\alpha]_D^{20}$ -30 (c 0.23, CHCl₃); ¹H NMR (600 MHz, CDCl₃): δ (ppm) 7.44–7.43 (m, 2H, 2 \times CH_{Ar}), 7.33–7.32 (m, 3H, 3 \times CH_{Ar}), 5.95 (t, J = 10.1 Hz, 1H, H-3), 5.89 (s, 1H, CHPh), 4.85 (d, J = 3.9 Hz, 1H, H-1), 4.60 (t, J = 11.4 Hz, 1H, H-6a), 4.33 (dt, J = 11.9 Hz, J = 5.9 Hz, 1H, H-5), 4.12–4.06 (m, 2H, H-6b, H-4), 3.71 (dd, J = 9.8 Hz, 3.8 Hz, 1H, H-2), 3.56–3.50 (m, 1H, H-3_{stig}), 2.09 (s, 3H, CH_{3Ac}), 1.98–0.59 (m, 59H, C(CH₃)₃TBS, 12 \times CH₂stig, 8 \times CH_{stig}, 6 \times CH₃stig) 0.10 (s, 3H, CH₃TBS), 0.09 (s, 3H, CH₃TBS); ¹³C{¹H} NMR (150 MHz, CDCl₃): δ (ppm) 170.6 (COOR_{Ac}), 137.8 (C_{Ar}), 129.0 (CH_{Ar}), 128.4

CHAPITRE 7 – C7 EPIMERIZATION OF BENZYLIDENE-PROTECTED β -D-IDOPYRANOSIDES BRINGS STRUCTURAL INSIGHTS INTO IDOSE CONFORMATIONAL FLEXIBILITY

(2C, 2 \times CH_{Ar}), 126.4 (2C, 2 \times CH_{Ar}), 98.1 (C-1, $^1J_{C1,H1}$ = 170 Hz), 96.3 (CHPh), 78.2 (C-3_{stig}), 75.0 (C-4), 71.2 (C-2), 68.2 (C-6), 67.3 (C-5), 66.8 (C-3), 56.6–12.1 (33C, C(CH₃)₃TBS, C(CH₃)₃TBS, CH₃Ac, 6 \times CH₃stig, 12 \times CH₂stig, 8 \times CH_{stig}, 2 \times C_{stig}), -4.3 (CH₃TBS), -4.7 (CH₃TBS); HRMS (ESI-TOF) m/z [M + NH₄]⁺ calcd for C₅₀H₈₆NO₇Si 840.6168; found 840.6169.

Data for α -glycoside 16c (contaminated with traces of β -glycoside 16b): R_f 0.47 (Hex/EtOAc 8:2); $[\alpha]_D^{20}$ -49 (c 0.13, CHCl₃); 1H NMR (600 MHz, CDCl₃): δ (ppm) 7.53–7.51 (m, 2H, 2 \times CH_{Ar}), 7.33–7.31 (m, 3H, 3 \times CH_{Ar}), 5.49 (s, 1H, CHPh), 5.00 (dd, J = 5.7 Hz, J = 3.2 Hz, 1H, H-3), 4.97 (d, J = 3.0 Hz, 1H, H-1), 4.29 (d, J = 12.6 Hz, 1H, H-6a), 4.11 (dd, J = 12.6 Hz, J = 1.9 Hz, 1H, H-6b), 3.99 (m, 1H, H-4), 3.86 (br s, 1H, H-5), 3.69 (dd, J = 5.7 Hz, J = 3.1 Hz, 1H, H-2), 3.63–3.58 (m, 1H, H-3_{stig}), 2.08 (s, 3H, CH₃Ac), 1.97–0.60 (m, 59H, C(CH₃)₃TBS, 12 \times CH₂stig, 8 \times CH_{stig}, 6 \times CH₃stig), 0.09 (s, 3H, CH₃TBS), 0.07 (s, 3H, CH₃TBS); $^{13}C\{^1H\}$ NMR (150 MHz, CDCl₃): δ (ppm) 169.8 (COOR_{Ac}), 138.0 (C_{Ar}), 129.0 (CH_{Ar}), 128.1 (2C, 2 \times CH_{Ar}), 126.7 (2C, 2 \times CH_{Ar}), 100.9 (CHPh), 99.7 (C-1, $^1J_{C1,H1}$ = 171 Hz), 75.9 (C-3_{stigmastanol}), 75.0 (C-4), 73.2 (C-3), 69.6 (C-6), 69.1 (C-2), 60.7 (C-5), 56.6–12.1 (33C, C(CH₃)₃TBS, C(CH₃)₃TBS, CH₃Ac, 6 \times CH₃stig, 12 \times CH₂stig, 8 \times CH_{stig}, 2 \times C_{stig}), -4.5 (CH₃TBS), -4.7 (CH₃TBS); HRMS (ESI-TOF) m/z [M + NH₄]⁺ calcd for C₅₀H₈₆NO₇Si 840.6168; found 840.6176.

(2-Adamantyl) (S)-4,6-O-Benzylidene-2-O-tert-butyltrimethylsilyl-3-O-dichloroacetyl- β -D-idopyranoside (17a), (2-Adamantyl) (R)-4,6-O-Benzylidene-2-O-tert-butyltrimethylsilyl-3-O-dichloroacetyl- β -D-idopyranoside (17b) and (2-Adamantyl) (S)-4,6-O-Benzylidene-2-O-tert-butyltrimethylsilyl-3-O-dichloroacetyl- α -D-idopyranoside (17c).

Donor **7** (8.7 mg, 0.015 mmol, 1.2 equiv) and 2-adamantanol (2.0 mg, 0.013 mmol, 1.0 equiv) were reacted according to the general procedure for NIS/TMSOTf-promoted glycosylation. Purification by silica gel flash chromatography (Hex/EtOAc 95:5) gave compounds **17a** (3.5 mg, 42%, colorless oil), and **17b** and **17c** (2.1 mg, 25%, colorless oil, inseparable mixture **17b/17c** 1.0:0.3).

Data for β -glycoside 17a: R_f 0.37 (Hex/EtOAc 8:2); $[\alpha]_D^{20}$ -28 (c 0.45, CHCl₃); 1H NMR (600 MHz, CDCl₃): δ (ppm) 7.54–7.53 (m, 2H, 2 \times CH_{Ar}), 7.32–7.31 (m, 3H, 3 \times CH_{Ar}), 5.99 (s, 1H,

CHAPITRE 7 – C7 EPIMERIZATION OF BENZYLIDENE-PROTECTED β -D-IDOPYRANOSIDES BRINGS STRUCTURAL INSIGHTS INTO IDOSE CONFORMATIONAL FLEXIBILITY

CHCl_2), 5.49 (s, 1H, CHPh), 5.11 (t, $J = 2.6$ Hz, 1H, H-3), 4.72 (d, $J = 0.8$ Hz, 1H, H-1), 4.38 (d, $J = 12.5$ Hz, 1H, H-6a), 4.10 (dd, $J = 12.6$ Hz, $J = 2.0$ Hz, 1H, H-6b), 3.98 (t, $J = 3.1$ Hz, H-2_{ad}), 3.90 (br s, 1H, H-4), 3.72 (br d, $J = 2.9$ Hz, 1H, H-2), 3.64 (br d, $J = 1.2$ Hz, 1H, H-5), 2.19–1.44 (m, 14H, $5 \times \text{CH}_{2\text{ad}}$, $4 \times \text{CH}_{\text{ad}}$), 0.85 (s, 9H, $\text{C}(\text{CH}_3)_3\text{TBS}$), 0.15 (CH_3TBS), 0.11 (CH_3TBS); $^{13}\text{C}\{^1\text{H}\}$ NMR (150 MHz, CDCl_3): δ (ppm) 162.9 ($\text{COOR}_{\text{AcCl}_2}$), 137.8 (C_{Ar}), 129.1 (CH_{Ar}), 128.0 (2C, $2 \times \text{CH}_{\text{Ar}}$), 126.8 (2C, $2 \times \text{CH}_{\text{Ar}}$), 101.7 (CHPh), 96.4 (C-1, $^1J_{\text{C}_1, \text{H}_1} = 155$ Hz), 79.6 (C-2_{ad}), 76.2 (C-3), 72.4 (C-4), 69.7 (C-6), 67.6 (C-2), 67.0 (C-5), 64.2 (CHCl_2), 37.8–27.5 (9C, $5 \times \text{CH}_{2\text{ad}}$, $4 \times \text{CH}_{\text{ad}}$), 25.9 (3C, $\text{C}(\text{CH}_3)_3\text{TBS}$), 18.4 ($\text{C}(\text{CH}_3)_3\text{TBS}$), -4.4 (CH_3TBS), -5.2 (CH_3TBS); HRMS (ESI-TOF) m/z [$\text{M} + \text{NH}_4$]⁺ calcd for $\text{C}_{31}\text{H}_{48}\text{Cl}_2\text{NO}_7\text{Si}$ 644.2572; found 644.2573.

Data for β -glycoside 17b: R_f 0.5 (Hex/EtOAc 8:2); ^1H NMR (600 MHz, CDCl_3): δ (ppm) 7.45–7.43 (m, 2H, $2 \times \text{CH}_{\text{Ar}}$), 7.35–7.31 (m, 3H, $3 \times \text{CH}_{\text{Ar}}$), 6.09 (t, $J = 9.9$ Hz, 1H, H-3), 5.97 (s, 1H, CHCl_2), 5.86 (s, 1H, CHPh), 4.89 (d, $J = 3.7$ Hz, 1H, H-1), 4.57 (t, $J = 11.3$ Hz, 1H, H-6a), 4.36 (dt, $J = 11.8$ Hz, $J = 5.7$ Hz, 1H, H-5), 4.23 (dd, $J = 10.3$ Hz, $J = 6.6$ Hz, 1H, H-4), 4.15–4.13 (m, 1H, H-6b), 3.83 (dd, $J = 9.7$ Hz, $J = 3.7$ Hz, 1H, H-2), 3.80 (s, 1H, H-2_{ad}), 2.17–1.44 (14H, $5 \times \text{CH}_{2\text{ad}}$, $4 \times \text{CH}_{\text{ad}}$), 0.89 (s, 9H, $\text{C}(\text{CH}_3)_3\text{TBS}$), 0.14 (s, 3H, CH_3TBS), 0.08 (s, 3H, CH_3TBS); $^{13}\text{C}\{^1\text{H}\}$ NMR (150 MHz, CDCl_3): δ (ppm) 164.8 ($\text{COOR}_{\text{AcCl}_2}$), 137.3 (C_{Ar}), 129.0 (CH_{Ar}), 128.3 (2C, $2 \times \text{CH}_{\text{Ar}}$), 126.3 (2C, $2 \times \text{CH}_{\text{Ar}}$), 97.5 (C-1, $^1J_{\text{C}_1, \text{H}_1} = 170$ Hz), 96.1 (CHPh), 80.6 (C-2_{ad}), 74.7 (C-4), 71.1 (C-2), 70.6 (C-3), 68.1 (C-6), 67.2 (C-5), 64.3 (CHCl_2), 37.6–27.3 (9C, $5 \times \text{CH}_{2\text{ad}}$, $4 \times \text{CH}_{\text{ad}}$), 25.9 (3C, $\text{C}(\text{CH}_3)_3\text{TBS}$), 18.1 ($\text{C}(\text{CH}_3)_3\text{TBS}$), -4.8 (2C, $2 \times \text{CH}_3\text{TBS}$); HRMS (ESI-TOF) m/z [$\text{M} + \text{Na}$]⁺ calcd for $\text{C}_{31}\text{H}_{44}\text{Cl}_2\text{NaO}_7\text{Si}$ 649.2126; found 649.2121.

Data for α -glycoside 17c: R_f 0.5 (Hex/EtOAc 8:2); ^1H NMR (600 MHz, CDCl_3): δ (ppm) 7.53–7.52 (m, 0.6H, $2 \times \text{CH}_{\text{Ar}}$), 7.39–7.37 (m, 0.3H, CH_{Ar}), 7.15–7.10 (m, 0.6H, $2 \times \text{CH}_{\text{Ar}}$), 5.96 (s, 0.3H, CHCl_2), 5.53 (s, 0.3H, CHPh), 5.00–4.99 (m, 0.6H, H-1, H-3), 4.30 (dd, $J = 12.6$ Hz, $J = 1.1$ Hz, 0.3H, H-6a), 4.15–4.12 (m, 0.3H, H-6b), 4.01 (s, 0.3H, H-4), 3.94 (d, $J = 1.3$ Hz, 0.3H, H-5), 3.80 (s, 0.3H, H-2_{ad}), 3.78–3.77 (m, 0.3H, H-2), 2.17–1.44 (m, 4.2H, $5 \times \text{CH}_{2\text{ad}}$, $4 \times \text{CH}_{\text{ad}}$), 0.85 (s, 3H, $\text{C}(\text{CH}_3)_3\text{TBS}$), 0.14 (s, 1H CH_3TBS), 0.10 (s, 1H, CH_3TBS); $^{13}\text{C}\{^1\text{H}\}$ NMR (150 MHz, CDCl_3): δ (ppm) 164.8 ($\text{COOR}_{\text{AcCl}_2}$), 136.2 (C_{Ar}), 128.7 (CH_{Ar}), 128.1 (2C, $2 \times \text{CH}_{\text{Ar}}$), 126.7 (2C, $2 \times \text{CH}_{\text{Ar}}$), 101.4 (CHPh), 99.5 (C-1, $^1J_{\text{C}_1, \text{H}_1} = 170$ Hz), 80.0 (C-2_{ad}), 74.8 (C-3), 72.7 (C-4), 69.6

CHAPITRE 7 – C7 EPIMERIZATION OF BENZYLIDENE-PROTECTED β -D-IDOPYRANOSIDES BRINGS STRUCTURAL INSIGHTS INTO IDOSE CONFORMATIONAL FLEXIBILITY

(C-6), 67.5 (C-2), 64.3 (CHCl₂), 59.7 (C-5), 37.6–27.3 (9C, 5 × CH_{2ad}, 4 × CH_{ad}), 25.8 (3C, C(CH₃)_{3TBS}), 18.1 (C(CH₃)_{3TBS}), –3.8 (2C, 2 × CH_{3TBS}); HRMS (ESI-TOF) m/z [M + Na]⁺ calcd for C₃₁H₄₄Cl₂NaO₇Si 649.2126; found 649.2121.

(2-Adamantyl) 3-*O*-(2-Azidomethyl)benzoyl-(*S*)-4,6-*O*-Benzylidene-2-*O*-*tert*-butyldimethylsilyl- β -D-idopyranoside (**18a**), (2-Adamantyl) 3-*O*-(2-Azidomethyl)benzoyl-(*R*)-4,6-*O*-benzylidene-2-*O*-*tert*-butyldimethylsilyl- β -D-idopyranoside (**18b**) and (2-Adamantyl) 3-*O*-(2-Azidomethyl)benzoyl-(*S*)-4,6-*O*-benzylidene-2-*O*-*tert*-butyldimethylsilyl- α -D-idopyranoside (**18c**).

Donor **8** (7.8 mg, 0.013 mmol, 1.2 equiv) and 2-adamantanol (1.7 mg, 0.011 mmol, 1.0 equiv) were reacted according to the general procedure for NIS/TMSOTf-promoted glycosylation. Purification by silica gel flash chromatography (Hex/EtOAc 95:5 to 85:15) gave compounds **18a** (4.2 mg, 55%, colorless oil), and **18b** and **18c** (1.0 mg, 13%, colorless oil, inseparable mixture **18b/18c** 1.0:0.7).

Data for β -glycoside 18a: R_f 0.3 (Hex/EtOAc 8:2); $[\alpha]_D^{20}$ –19 (c 0.49, CHCl₃); ¹H NMR (600 MHz, CDCl₃): δ (ppm) 7.97–7.95 (m, 1H, CH_{AZMB}), 7.62–7.59 (m, 1H, CH_{AZMB}), 7.58–7.55 (m, 2H, 2 × CH_{Ar}), 7.53–7.52 (m, 1H, CH_{AZMB}), 7.47–7.44 (m, 1H, CH_{AZMB}), 7.33–7.31 (m, 3H, 3 × CH_{Ar}), 5.51 (s, 1H, CHPh), 5.31 (t, J = 2.6 Hz, 1H, H-3), 4.82 (d, J = 1.2 Hz, 1H, H-1), 4.81 (s, 2H, CH_{2AZMB}), 4.40 (dd, J = 12.5 Hz, J = 0.7 Hz, 1H, H-6a), 4.11 (dd, J = 12.5 Hz, J = 2.1 Hz, 1H, H-6b), 4.00 (br s, 1H, H-2_{ad}), 3.97 (br s, 1H, H-4), 3.82 (br d, J = 2.9 Hz, 1H, H-2), 3.70 (br d, J = 1.3 Hz, 1H, H-5), 2.22–1.45 (m, 14H, 5 × CH_{2ad}, 4 × CH_{ad}), 0.88 (s, 9H, C(CH₃)_{3TBS}), 0.17 (s, 3H, CH_{3TBS}), 0.13 (s, 3H, CH_{3TBS}); ¹³C{¹H} NMR (150 MHz, CDCl₃): δ (ppm) 164.8 (COOR_{AZMB}), 138.0–126.9 (12C, 3 × C_{Ar}, 9 × CH_{Ar}), 101.7 (CHPh), 97.0 (C-1, ¹J_{C1,H1} = 156 Hz), 79.8 (C-2_{ad}), 74.2 (C-3), 72.9 (C-4), 69.8 (C-6), 68.3 (C-2), 67.4 (C-5), 53.2 (CH_{2AZMB}), 37.8–27.6 (9C, 5 × CH_{2ad}, 4 × CH_{ad}), 26.0 (3C, C(CH₃)_{3TBS}), 18.5 (C(CH₃)_{3TBS}), –4.3 (CH_{3TBS}), –5.1 (CH_{3TBS}); HRMS (ESI-TOF) m/z [M + NH₄]⁺ calcd for C₃₇H₅₃N₄O₇Si 693.3678; found 693.3679.

Data for β -glycoside 18b: R_f 0.4 (Hex/EtOAc 8:2); ¹H NMR (600 MHz, CDCl₃): δ (ppm) 8.01 (d, J = 7.8 Hz, 1H, CH_{AZMB}), 7.58–7.27 (m, 8H, 8 × CH_{Ar}), 6.30 (t, J = 10.0 Hz, 1H, H-3), 5.99 (s,

CHAPITRE 7 – C7 EPIMERIZATION OF BENZYLIDENE-PROTECTED β -D-IDOPYRANOSIDES BRINGS STRUCTURAL INSIGHTS INTO IDOSE CONFORMATIONAL FLEXIBILITY

1H, *CHPh*), 4.93 (d, $J = 3.7$ Hz, 1H, H-1), 4.76 (d, $J = 14.9$ Hz, 1H, *CHH*_{AZMB}), 4.71 (d, $J = 14.8$ Hz, 1H, *CHH*_{AZMB}), 4.67 (t, $J = 11.3$ Hz, 1H, H-6a), 4.41 (dt, $J = 11.7$ Hz, $J = 5.9$ Hz, 1H, H-5), 4.34–4.30 (m, 1H, H-4), 4.17–4.12 (m, 1H, H-6b), 3.91 (dd, $J = 9.7$ Hz, $J = 3.7$ Hz, 1H, H-2), 3.82 (s, 1H, H-2_{ad}), 2.36–1.45 (m, 14H, $5 \times \text{CH}_{2\text{ad}}$, $4 \times \text{CH}_{\text{ad}}$), 0.76 (s, 9H, $\text{C}(\text{CH}_3)_3\text{TBS}$), 0.03 (s, 3H, *CH*_{3TBS}), -0.04 (s, 3H, *CH*_{3TBS}); ¹³C{¹H} NMR (150 MHz, CDCl₃): δ (ppm) 166.3 (*COOR*_{AZMB}), 137.7 (*C*_{Ar}), 137.6 (*C*_{Ar}), 133.2–126.4 (10C, $1 \times \text{C}_{\text{Ar}}$, $9 \times \text{CH}_{\text{Ar}}$), 97.6 (C-1, $^1J_{\text{C1,H1}} = 170$ Hz), 96.4 (*CHPh*), 80.5 (C-2_{ad}), 75.1 (C-4), 71.5 (C-2), 67.6, 67.4 (2C, C-3, C-5), 53.0 (*CH*_{2AZMB}), 37.6–27.4 (9C, $5 \times \text{CH}_{2\text{ad}}$, $4 \times \text{CH}_{\text{ad}}$), 25.6 (3C, $\text{C}(\text{CH}_3)_3\text{TBS}$), 18.0 ($\text{C}(\text{CH}_3)_3\text{TBS}$), -4.74 (*CH*_{3TBS}), -4.92 (*CH*_{3TBS}); HRMS (ESI-TOF) m/z [$\text{M} + \text{Na}$]⁺ calcd for C₃₇H₄₉N₃NaO₇Si 698.3232; found 698.3236.

Data for α -glycoside 18c: R_f 0.4 (Hex/EtOAc 8:2); 8.19 (d, $J = 7.7$ Hz, 0.7H, *CH*_{AZMB}), 7.58–7.27 (m, 5.6H, $5.6 \times \text{CH}_{\text{Ar}}$), 5.54 (s, 0.7H, *CHPh*), 5.19 (t, $J = 2.6$ Hz, 0.7H, H-3), 5.08 (s, 0.7H, H-1), 4.88 (d, $J = 15.5$ Hz, 0.7H, *CHH*_{AZMB}), 4.86 (d, $J = 15.2$ Hz, 0.7H, *CHH*_{AZMB}), 4.34–4.30 (m, 0.7H, H-6a), 4.17–4.12 (m, 0.7H, H-6b), 4.06 (s, 0.7H, H-4), 4.01 (s, 0.7H, H-5), 3.87 (s, 0.7H, H-2_{ad}), 3.82 (s, 0.7H, H-2), 2.36–1.45 (m, 9.8H, $5 \times \text{CH}_{2\text{ad}}$, $4 \times \text{CH}_{\text{ad}}$), 0.86 (s, 6.3H, $\text{C}(\text{CH}_3)_3\text{TBS}$), 0.10 (s, 2.1H, *CH*_{3TBS}), 0.10 (s, 2.1H, *CH*_{3TBS}); ¹³C{¹H} NMR (150 MHz, CDCl₃): δ (ppm) 166.3 (*COOR*_{AZMB}), 138.1 (*C*_{Ar}), 138.0 (*C*_{Ar}), 133.2–126.4 (10C, $1 \times \text{C}_{\text{Ar}}$, $9 \times \text{CH}_{\text{Ar}}$), 101.5 (*CHPh*), 99.2 (C-1, $^1J_{\text{C1,H1}} = 172$ Hz), 79.3 (C-2_{ad}), 72.7 (C-4), 71.6 (C-3), 68.3 (C-6), 67.9 (C-2), 59.7 (C-5), 53.2 (*CH*_{2AZMB}), 37.6–27.4 (9C, $5 \times \text{CH}_{2\text{ad}}$, $4 \times \text{CH}_{\text{ad}}$), 25.8 (3C, $\text{C}(\text{CH}_3)_3\text{TBS}$), 18.0 ($\text{C}(\text{CH}_3)_3\text{TBS}$), -4.88 (*CH*_{3TBS}), -4.92 (*CH*_{3TBS}); HRMS (ESI-TOF) m/z [$\text{M} + \text{Na}$]⁺ calcd for C₃₇H₄₉N₃NaO₇Si 698.3232; found 698.3236.

(2-Adamantyl) (S)-4,6-O-Benzylidene-2-O-tert-butyltrimethylsilyl-3-O-tert-butoxycarbonyl- β -D-idopyranoside (19a), (2-Adamantyl) (R)-4,6-O-Benzylidene-2-O-tert-butyltrimethylsilyl-3-O-tert-butoxycarbonyl- β -D-idopyranoside (19b) and (2-Adamantyl) (S)-4,6-O-Benzylidene-2-O-tert-butyltrimethylsilyl-3-O-tert-butoxycarbonyl- α -D-idopyranoside (19c).

Donor **9** (10.2 mg, 0.017 mmol, 1.2 equiv) and 2-adamantanol (2.2 mg, 0.015 mmol, 1.0 equiv) were reacted according to the general procedure for NIS/TMSOTf-promoted glycosylation. Purification by silica gel flash chromatography (Hex/EtOAc 97:3 to 9:1) gave compounds **19a** (5.4

CHAPITRE 7 – C7 EPIMERIZATION OF BENZYLIDENE-PROTECTED β-D-IDOPYRANOSIDES BRINGS STRUCTURAL INSIGHTS INTO IDOSE CONFORMATIONAL FLEXIBILITY

mg, 64%, colorless oil), and **19b** and **19c** (1.6 mg, 18%, colorless oil, inseparable mixture **19b/19c** 1.0:0.7).

Data for β-glycoside 19a: R_f 0.17 (Hex/EtOAc 9:1); $[\alpha]_D^{20}$ -23 (c 0.61, CHCl₃); ¹H NMR (600 MHz, CDCl₃): δ (ppm) 7.55–7.53 (m, 2H, 2 × CH_{Ar}), 7.31–7.29 (m, 3H, 3 × CH_{Ar}), 5.48 (s, 1H, CHPh), 4.85 (t, J = 2.5 Hz, 1H, H-3), 4.73 (d, J = 1.1 Hz, 1H, H-1), 4.35 (d, J = 12.5 Hz, 1H, H-6a), 4.06 (dd, J = 12.5 Hz, J = 2.1 Hz, 1H, H-6b), 3.95 (br s, 1H, H-2_{ad}), 3.88 (br s, 1H, H-4), 3.73 (d, J = 2.9 Hz, 1H, H-2), 3.62 (d, J = 1.4 Hz, 1H, H-5), 2.21–1.42 (m, 14H, 5 × CH_{2ad}, 4 × CH_{ad}), 1.51 (s, 9H, C(CH₃)_{3Boc}), 0.85 (s, 9H, C(CH₃)_{3TBS}), 0.14 (s, 3H, CH_{3TBS}), 0.10 (s, 3H, CH_{3TBS}); ¹³C{¹H} NMR (150 MHz, CDCl₃): δ (ppm) 152.2 (COOR_{Boc}), 138.1 (C_{Ar}), 128.9 (CH_{Ar}), 127.9 (2C, 2 × CH_{Ar}), 126.9 (2C, 2 × CH_{Ar}), 101.5 (CHPh), 96.8 (C-1, ¹J_{C1,H1} = 155 Hz), 83.2 (C(CH₃)_{3Boc}), 79.7 (C-2_{ad}), 76.1 (C-3), 73.1 (C-4), 69.8 (C-6), 68.4 (C-2), 66.9 (C-5), 37.8–27.6 (9C, 5 × CH_{2ad}, 4 × CH_{ad}), 27.9 (3C, C(CH₃)_{3Boc}), 26.0 (3C, C(CH₃)_{3TBS}), 18.4 (C(CH₃)_{3TBS}), -4.4 (CH_{3TBS}), -5.1 (CH_{3TBS}); HRMS (ESI-TOF) m/z [M + NH₄]⁺ calcd for C₃₄H₅₆NO₈Si 634.3770; found 634.3794.

Data for β-glycoside 19b: R_f 0.31 (Hex/EtOAc 9:1); ¹H NMR (600 MHz, CDCl₃): δ (ppm) 7.47–7.46 (m, 2H, 2 × CH_{Ar}), 7.32–7.29 (m, 3H, 3 × CH_{Ar}), 5.95 (s, 1H, CHPh), 5.76 (t, J = 10.1 Hz, 1H, H-3), 4.86 (d, J = 3.8 Hz, 1H, H-1), 4.59 (t, J = 11.3 Hz, 1H, H-6a), 4.36–4.32 (m, 1H, H-5), 4.17 (dd, J = 10.4 Hz, J = 6.5 Hz, 1H, H-4), 4.11 (dd, J = 9.7 Hz, J = 4.0 Hz, 1H, H-6b), 3.78 (br s, 1H, H-2_{ad}), 3.74 (dd, J = 9.8 Hz, J = 3.8 Hz, 1H, H-2), 2.20–1.55 (m, 14H, 5 × CH_{2ad}, 4 × CH_{ad}), 1.44 (s, 9H, C(CH₃)_{3Boc}), 0.89 (s, 9H, C(CH₃)_{3TBS}), 0.13 (s, 3H, CH_{3TBS}), 0.07 (s, 3H, CH_{3TBS}); ¹³C{¹H} NMR (150 MHz, CDCl₃): δ (ppm) 153.8 (COOR_{Boc}), 137.8 (C_{Ar}), 128.8 (CH_{Ar}), 128.1 (2C, 2 × CH_{Ar}), 126.4 (2C, 2 × CH_{Ar}), 97.7 (C-1, ¹J_{C1,H1} = 168 Hz), 96.1 (CHPh), 82.2 (C(CH₃)_{3Boc}), 80.5 (C-2_{ad}), 75.0 (C-4), 71.4 (C-2), 69.4 (C-3), 68.3 (C-6), 67.4 (C-5), 37.7–27.3 (9C, 5 × CH_{2ad}, 4 × CH_{ad}), 27.9 (3C, C(CH₃)_{3Boc}), 25.9 (3C, C(CH₃)_{3TBS}), 18.2 (C(CH₃)_{3TBS}), -4.2 (CH_{3TBS}), -4.9 (CH_{3TBS}); HRMS (ESI-TOF) m/z [M + NH₄]⁺ calcd for C₃₄H₅₆NO₈Si 634.3770; found 634.3781.

CHAPITRE 7 – C7 EPIMERIZATION OF BENZYLIDENE-PROTECTED β -D-IDOPYRANOSIDES BRINGS STRUCTURAL INSIGHTS INTO IDOSE CONFORMATIONAL FLEXIBILITY

Data for α -glycoside 19c: R_f 0.28 (Hex/EtOAc 9:1); ^1H NMR (600 MHz, CDCl_3): δ (ppm) 7.53–7.51 (m, 1.5H, $2 \times \text{CH}_{\text{Ar}}$), 7.32–7.29 (m, 2.25H, $3 \times \text{CH}_{\text{Ar}}$), 5.50 (s, 0.75H, CHPh), 4.95 (d, $J = 2.5$ Hz, 0.75H, H-1), 4.75 (dd, $J = 5.0$ Hz, $J = 3.2$ Hz, 0.75H, H-3), 4.26 (dd, $J = 12.6$ Hz, $J = 1.1$ Hz, 0.75H, H-6a), 4.09 (dd, $J = 12.6$ Hz, $J = 2.2$ Hz, 0.75H, H-6b), 4.06 (t, $J = 2.4$ Hz, 0.75H, H-4), 3.93 (d, $J = 1.6$ Hz, 0.75H, H-5), 3.83 (dd, $J = 5.1$ Hz, $J = 2.6$ Hz, 0.75H, H-2), 3.78 (br s, 0.75H, H-2_{ad}), 2.20–1.55 (m, 10.5H, $5 \times \text{CH}_{2\text{ad}}$, $4 \times \text{CH}_{\text{ad}}$), 1.48 (s, 6.75H, $\text{C}(\text{CH}_3)_3\text{Boc}$), 0.86 (s, 6.75H, $\text{C}(\text{CH}_3)_3\text{TBS}$), 0.10 (s, 4.5H, $2 \times \text{CH}_{3\text{TBS}}$); $^{13}\text{C}\{^1\text{H}\}$ NMR (150 MHz, CDCl_3): δ (ppm) 152.5 (COOR_{Boc}), 183.1 (C_{Ar}), 128.9 (CH_{Ar}), 128.1 (2C, $2 \times \text{CH}_{\text{Ar}}$), 126.7 (2C, $2 \times \text{CH}_{\text{Ar}}$), 101.0 (CHPh), 100.7 (C-1, $^1J_{\text{C1,H1}} = 172$ Hz), 82.4 ($\text{C}(\text{CH}_3)_3\text{Boc}$), 80.4 (C-2_{ad}), 75.1 (C-3), 74.5 (C-4), 69.5 (C-6), 68.5 (C-2), 60.5 (C-5), 37.7–27.3 (9C, $5 \times \text{CH}_{2\text{ad}}$, $4 \times \text{CH}_{\text{ad}}$), 27.9 (3C, $\text{C}(\text{CH}_3)_3\text{Boc}$), 25.9 (3C, $\text{C}(\text{CH}_3)_3\text{TBS}$), 18.1 ($\text{C}(\text{CH}_3)_3\text{TBS}$), –4.68 ($\text{CH}_{3\text{TBS}}$), –4.73 ($\text{CH}_{3\text{TBS}}$); HRMS (ESI-TOF) m/z [$\text{M} + \text{NH}_4$] $^+$ calcd for $\text{C}_{34}\text{H}_{56}\text{NO}_8\text{Si}$ 634.3770; found 634.3781.

(2-Adamantyl) (S)-4,6-O-Benzylidene- β -D-idopyranoside (20a).

To a solution of compound **14a** (3.9 mg, 0.0070 mmol, 1.0 equiv) in dry pyridine (390 μL) at 0 $^\circ\text{C}$ was slowly added HF.py (195 μL). The mixture was stirred at rt for 16 h, after which it was diluted in EtOAc, and quenched with a saturated aqueous NaHCO_3 solution. The organic layer was washed with brine, dried over MgSO_4 , filtered, and concentrated under reduced pressure. The resulting alcohol was solubilized in MeOH (100 μL) and THF (100 μL) and NaOMe (25% wt in MeOH, 1 μL) was added. The mixture was stirred at rt for 1 h, then neutralized by adding Dowex until $\text{pH} \approx 7$, filtered over Celite, and evaporated under reduced pressure. The residue was purified by silica gel flash chromatography (Hex/EtOAc 8:2 to 5:5) to give diol **20a** (3.0 mg, quant.) as a white amorphous solid: R_f 0.3 (Hex/EtOAc 1:1); $[\alpha]_{\text{D}}^{20} -70$ (c 0.37, CHCl_3); ^1H NMR (600 MHz, CDCl_3): δ (ppm) 7.49–7.47 (m, 2H, $2 \times \text{CH}_{\text{Ar}}$), 7.36–7.33 (m, 3H, $3 \times \text{CH}_{\text{Ar}}$), 5.49 (s, 1H, CHPh), 4.94 (s, 1H, H-1), 4.37 (dd, $J = 12.4$ Hz, $J_{6a-5} = 1.1$ Hz, 1H, H-6a), 4.21 (t, $J = 2.5$ Hz, 1H, H-3), 4.06 (d, $J = 12.5$ Hz, $J = 1.9$ Hz, 1H, H-6b), 3.96–3.95 (m, 1H, H-2_{ad}), 3.93–3.92 (m, 1H, H-4), 3.75 (d, $J = 1.2$ Hz, 1H, H-5), 3.62 (dd, $J = 10.8$ Hz, $J = 2.4$ Hz, 1H, H-2), 3.15 (d, $J = 10.9$ Hz, 1H, OH-2), 2.22–1.47 (m, 15H, OH-3, $5 \times \text{CH}_{2\text{ad}}$, $4 \times \text{CH}_{\text{ad}}$); $^{13}\text{C}\{^1\text{H}\}$ NMR (150 MHz, CDCl_3): δ (ppm) 137.6 (C_{Ar}), 129.3 (CH_{Ar}), 128.4 (2C, $2 \times \text{CH}_{\text{Ar}}$), 126.3 (2C, $2 \times \text{CH}_{\text{Ar}}$), 101.5 (CHPh),

CHAPITRE 7 – C7 EPIMERIZATION OF BENZYLIDENE-PROTECTED β-D-IDOPYRANOSIDES BRINGS STRUCTURAL INSIGHTS INTO IDOSE CONFORMATIONAL FLEXIBILITY

95.9 (C-1), 80.1 (C-2_{ad}), 75.6 (C-4), 70.44 (C-2*), 70.39 (C-3*), 70.0 (C-6), 66.6 (C-5), 37.7–27.5 (9C, 5 × CH_{2ad}, 4 × CH_{ad}); HRMS (ESI-TOF) *m/z* [M + NH₄]⁺ calcd for C₂₃H₃₄NO₆ 420.2381; found 420.2386.

(2-Adamantyl) (R)-4,6-O-Benzylidene-β-D-idopyranoside (20b).

To a solution of compound **14b** (186 mg, 0.332 mmol, 1.0 equiv) in dry pyridine (9.3 mL) at 0 °C was slowly added HF·py (3.5 mL). The mixture was stirred at rt for 16 h, after which it was diluted with EtOAc and quenched with a saturated aqueous NaHCO₃ solution. The organic layer was washed with brine, dried over MgSO₄, filtered, and concentrated under reduced pressure. The resulting alcohol was solubilized in MeOH (1.6 mL) and THF (1.1 mL), and NaOMe (25% wt in MeOH, 0.1 mL) was added. The mixture was stirred at rt for 1 h, then neutralized by adding Dowex resin until pH ≈ 7, filtered over Celite and the solvents were evaporated. The residue was purified by silica gel flash chromatography (Hex/EtOAc 8:2 to 5:5) to give diol **20b** (95 mg, 73% in two steps) as a white solid foam: *R_f* 0.17 (Hex/EtOAc 6:4); [α]_D²⁰ -5.8 (*c* 0.24, CHCl₃); ¹H NMR (600 MHz, CDCl₃): δ (ppm) 7.51–7.48 (m, 2H, 2 × CH_{Ar}), 7.39–7.34 (m, 2H, 2 × CH_{Ar}), 5.86 (s, 1H, CHPh), 4.96 (d, *J* = 5.0 Hz, 1H, H-1), 4.55 (t, *J* = 8.5 Hz, 1H, H-3), 4.30 (dd, *J* = 11.1 Hz, *J* = 9.7 Hz, 1H, H-6a), 4.20 (dt, *J* = 9.9 Hz, *J* = 5.2 Hz, 1H, H-5), 4.08–4.04 (m, 2H, H-6b, H-4), 3.87 (t, *J* = 3.4 Hz, 1H, H-2_{ad}), 3.57 (td, *J* = 8.7 Hz, *J* = 3.6 Hz, 1H, H-2), 2.79 (s, 1H, OH-3), 2.51 (d, *J* = 9.8 Hz, 1H, OH-2), 2.10–1.54 (m, 14H, 5 × CH_{2ad}, 4 × CH_{ad}); ¹³C{¹H} NMR (150 MHz, CDCl₃): δ (ppm) 137.2 (C_{Ar}), 129.2 (CH_{Ar}), 128.6 (2C, 2 × CH_{Ar}), 126.5 (2C, 2 × CH_{Ar}), 96.1 (C-1), 95.6 (CHPh), 80.0 (C-2_{ad}), 74.4 (C-4), 72.4 (C-2), 67.2 (C-6), 66.9 (C-5), 65.7 (C-3), 37.5–27.3 (9C, 5 × CH_{2ad}, 4 × CH_{ad}); HRMS (ESI-TOF) *m/z* [M + NH₄]⁺ calcd for C₂₃H₃₄NO₆ 420.2381; found 420.2389.

(2-Adamantyl) (S)-4,6-O-Benzylidene-α-D-idopyranoside (20c).

To a solution of compound **14c** (8.1 mg, 0.015 mmol, 1.0 eq) in dry pyridine (540 μL) at 0 °C was slowly added HF·py (270 μL). The mixture was stirred at rt 16 h, after which it was diluted with EtOAc and quenched with a saturated aqueous NaHCO₃ solution. The organic layer was washed with brine, dried over MgSO₄, filtered, and concentrated under reduced pressure. The resulting

CHAPITRE 7 – C7 EPIMERIZATION OF BENZYLIDENE-PROTECTED β-D-IDOPYRANOSIDES BRINGS STRUCTURAL INSIGHTS INTO IDOSE CONFORMATIONAL FLEXIBILITY

alcohol was solubilized in MeOH (97 μL) and THF (70 μL), and NaOMe (25% wt in MeOH, 5 μL) was added. The mixture was stirred at rt for 1 h, then quenched by adding Dowex resin until pH \approx 7, filtered over Celite and the solvents were evaporated. The residue was purified by silica gel flash chromatography (Hex/EtOAc 8:2 to 7:3) to give diol **20c** (4.9 mg, 84% in two steps) as a white amorphous solid: R_f 0.47 (Hex/EtOAc 6:4); $[\alpha]_D^{20}$ +47 (c 0.34, CHCl_3); ^1H NMR (600 MHz, CDCl_3): δ (ppm) 7.49–7.47 (m, 2H, $2 \times \text{CH}_{\text{Ar}}$), 7.39–7.36 (m, 3H, $3 \times \text{CH}_{\text{Ar}}$), 5.54 (s, 1H, CHPh), 5.20 (br s, 1H, H-1), 4.36 (dd, $J = 12.6$ Hz, $J = 1.3$ Hz, 1H, H-6a), 4.15 (d, $J = 2.7$ Hz, 1H, H-4), 4.13 (dd, $J = 12.6$ Hz, $J = 1.7$ Hz, 1H, H-6b), 4.07 (d, $J = 10.2$ Hz, 1H, OH-3), 4.01–4.00 (m, 2H, H-3, H-5), 3.92 (t, $J = 2.8$ Hz, 1H, H-2_{ad}), 3.71 (br d, $J = 11.9$ Hz, 1H, H-2), 3.65 (d, $J = 12.0$ Hz, 1H, OH-2), 2.08–1.54 (m, 14H, $5 \times \text{CH}_{2\text{ad}}$, $4 \times \text{CH}_{\text{ad}}$); $^{13}\text{C}\{^1\text{H}\}$ NMR (150 MHz, CDCl_3): δ (ppm) 137.4 (C_{Ar}), 129.4 (CH_{Ar}), 128.5 (2C, $2 \times \text{CH}_{\text{Ar}}$), 126.1 (2C, $2 \times \text{CH}_{\text{Ar}}$), 101.6 (CHPh), 99.2 (C-1), 80.4 (C-2_{ad}), 76.0 (C-4), 70.2 (C-6), 68.0 (C-3), 67.2 (C-2), 59.5 (C-5), 37.4–27.2 (9C, $5 \times \text{CH}_{2\text{ad}}$, $4 \times \text{CH}_{\text{ad}}$); HRMS (ESI-TOF) m/z $[\text{M} + \text{Na}]^+$ calcd for $\text{C}_{23}\text{H}_{30}\text{NaO}_6$ 425.1935; found 425.1917.

(2-Adamantyl) 3-O-Acetyl-2-O-tert-butyldimethylsilyl-β-D-idopyranoside (21).

Procedure from 14a: To a solution of compound **14a** (8.8 mg, 0.016 mmol 1.0 equiv) in EtOAc (0.19 mL) was added 10% Pd/C (8.8 mg). The mixture was stirred under H_2 at rt for 2 h, after which it was filtered over Celite and the solvents were evaporated under reduced pressure. The residue was purified by silica gel flash chromatography (Hex/EtOAc 8:2 to 6:4) to give diol **21** (6.5 mg, 88%) as a colorless oil.

Procedure from 14b: To a solution of compound **14b** (6.4 mg, 0.012 mmol, 1.0 equiv) in EtOAc (0.20 mL) was added 10% Pd/C (6.4 mg). The mixture was heated at 40 °C with an oil bath and stirred at this temperature under H_2 for 2 h, after which it was filtered over Celite and the solvents were evaporated under reduced pressure. The residue was purified by silica gel flash chromatography (Hex/EtOAc 8:2 to 6:4) to give diol **21** (4.5 mg, 83%) as a colorless oil: R_f 0.28 (Hex/EtOAc 1:1); $[\alpha]_D^{20}$ +33 (c 0.48, CHCl_3); ^1H NMR (600 MHz, CDCl_3): δ (ppm) 5.03 (t, $J = 3.4$ Hz, 1H, H-3), 4.71 (br s, 1H, H-1), 3.99 (dd, $J = 11.6$ Hz, $J = 7.6$ Hz, 1H, H-6a), 3.92 (t, $J =$

CHAPITRE 7 – C7 EPIMERIZATION OF BENZYLIDENE-PROTECTED β -D-IDOPYRANOSIDES BRINGS STRUCTURAL INSIGHTS INTO IDOSE CONFORMATIONAL FLEXIBILITY

3.0 Hz, 1H, H-2_{ad}), 3.83 (ddd, $J = 7.4$ Hz, $J = 4.2$ Hz, $J = 1.1$ Hz, 1H, H-5), 3.78–3.76 (m, 2H, H-2, H-6b), 3.69 (d, $J = 11.8$ Hz, 1H, 4-OH), 3.56–3.54 (m, 1H, H-4), 2.16–1.50 (m, 18H, 6-OH, CH_{3Ac}, 5 × CH_{2ad}, 4 × CH_{ad}), 0.94 (s, 9H, C(CH₃)_{3TBS}), 0.19 (s, 6H, 2 × CH_{3TBS}); ¹³C{¹H} NMR (150 MHz, CDCl₃): δ (ppm) 169.4 (COOR_{Ac}), 97.1 (C-1), 81.2 (C-2_{ad}), 75.8 (C-5), 72.0 (C-3), 70.0 (C-2), 67.3 (C-4), 62.8 (C-6), 37.7–27.4 (9C, 5 × CH_{2ad}, 4 × CH_{ad}), 25.9 (3C, C(CH₃)_{3TBS}), 21.2 (CH_{3Ac}), 18.4 (C(CH₃)_{3TBS}), -4.5 (CH_{3TBS}), -5.2 (CH_{3TBS}); HRMS (ESI-TOF) m/z [M + Na]⁺ calcd for C₂₄H₄₂NaO₇Si 493.2592; found 493.2615.

General method for the post-glycosylation epimerization experiments.

The glycoside (1.0 equiv) was dried under high vacuum for 1 h. Activated 4Å MS (4 mg/mg of glycoside) and dry toluene (20 mL·mmol⁻¹) were then added, and the suspension was stirred at rt under Ar atmosphere for 30 min. The mixture was cooled to -10 °C and TMSOTf (0.1 equiv) was added. The mixture was stirred under Ar while being allowed to gradually warm to 0 °C for a period of 1.5 h. The reaction was then quenched with Et₃N, filtered over Celite, and concentrated under reduced pressure. The crude residue was then directly analyzed by ¹H NMR in CDCl₃.

***para*-Methylphenyl 3-*O*-Benzyl-4,6-*O*-benzylidene-1-thio- α -D-idopyranoside (23).**

To a solution of compound **4b** (165 mg, 0.441 mmol, 1.0 equiv) in DCM (5.3 mL) were successively added NaOH 5% (1.8 mL), TBAHS (30 mg, 0.088 mmol, 0.2 equiv) and BnBr (79 μ L, 0.66 mmol, 1.0 equiv). The mixture was heated at 40 °C with an oil bath and stirred at this temperature for 18 h. The mixture was then extracted with DCM (×3), dried over MgSO₄, filtered, and concentrated under reduced pressure. The residue was purified by silica gel flash chromatography to give benzylated compound **23** (154 mg, 75%) as a white foam: R_f 0.5 (Hex/EtOAc 6:4); [α]_D²⁰ +132 (c 1.00, CHCl₃); ¹H NMR (600 MHz, CDCl₃): δ (ppm) 7.47–7.31 (m, 12H, 12 × CH_{Ar}), 7.11–7.10 (m, 2H, 2 × CH_{STol}), 5.60 (br s, 1H, H-1), 5.54 (s, 1H, CHPh), 4.85 (d, $J = 11.8$ Hz, 1H, CHH_{Bn}), 4.60 (d, $J = 11.8$ Hz, 1H, CHH_{Bn}), 4.46 (br s, 1H, H-5), 4.33 (dd, $J = 12.6$ Hz, $J = 1.4$ Hz, 1H, H-6a), 4.14–4.10 (m, 3H, H-6b, H-2, H-4), 3.83–3.81 (m, 2H, H-3, OH), 2.32 (s, 3H, CH_{3STol}); ¹³C{¹H} NMR (150 MHz, CDCl₃): δ (ppm) 137.5 (C_{Ar}), 137.4 (C_{Ar}), 137.0 (C_{Ar}), 133.6 (C_{Ar}), 130.9 (2C, 2 × CH_{Ar}), 129.8 (2C, 2 × CH_{Ar}), 129.4 (CH_{Ar}), 128.7

CHAPITRE 7 – C7 EPIMERIZATION OF BENZYLIDENE-PROTECTED β -D-IDOPYRANOSIDES BRINGS STRUCTURAL INSIGHTS INTO IDOSE CONFORMATIONAL FLEXIBILITY

(2C, 2 \times CH_{Ar}), 128.5 (2C, 2 \times CH_{Ar}), 128.2 (CH_{Ar}), 127.9 (2C, 2 \times CH_{Ar}), 126.1 (2C, 2 \times CH_{Ar}), 101.7 (CHPh), 89.6 (C-1), 74.6 (C-4*), 73.9 (C-3), 72.5 (CH_{2Bn}), 70.2 (C-6), 67.8 (C-2*), 60.7 (C-5), 21.2 (CH_{3STol}); HRMS (ESI-TOF) m/z [M + NH₄]⁺ calcd for C₂₇H₃₂NO₅S 482.1996; found 482.2004.

***para*-Methylphenyl 3-*O*-Benzyl-4,6-*O*-benzylidene-2-*O*-*tert*-butyldimethylsilyl-1-thio- α -D-idopyranoside (24).**

A solution of alcohol **23** (124 mg, 0.267 mmol, 1.0 equiv) in dry DCE (4 mL) was cooled to 0 °C, and Et₃N (67 μ L, 0.48 mmol, 1.8 equiv) and TBSOTf (93 μ L, 0.40 mmol, 1.5 equiv) were successively added dropwise. The mixture was stirred at 0 °C under Ar atmosphere for 10 min, then quenched with Et₃N. The solvents were co-evaporated with toluene and the residue was purified by silica gel flash chromatography (Hex/EtOAc 95:5) to give silylated compound **24** (116 mg, 75%) as a white amorphous solid: R_f 0.6 (Hex/EtOAc 7:3); $[\alpha]_D^{20}$ +89 (c 0.88, CHCl₃); ¹H NMR (600 MHz, CDCl₃): δ (ppm) 7.54–7.52 (m, 2H, 2 \times CH_{Ar}), 7.44–7.42 (m, 4H, 4 \times CH_{Ar}), 7.39–7.36 (m, 2H, 2 \times CH_{Ar}), 7.33–7.30 (m, 4H, 4 \times CH_{Ar}), 7.12–7.10 (m, 2H, 2 \times CH_{STol}), 5.53 (s, 1H, CHPh), 5.50 (d, J = 1.6 Hz, 1H, H-1), 4.75 (d, J = 12.0 Hz, 1H, CHH_{Bn}), 4.70 (d, J = 12.0 Hz, 1H, CHH_{Bn}), 4.33–4.31 (m, 2H, H-6a, H-5), 4.15 (dd, J = 13.1 Hz, J = 2.5 Hz, 1H, H-6b), 4.07 (br s, 1, H-4), 4.04 (dd, J = 3.3 Hz, J = 2.5 Hz, 1H, H-2), 3.66 (t, J = 2.9 Hz, 1H, H-3), 2.33 (s, 3H, CH_{3STol}), 0.84 (s, 9H, C(CH₃)₃TBS), 0.07 (s, 3H, CH₃TBS), -0.01 (s, 3H, CH₃TBS); ¹³C{¹H} NMR (150 MHz, CDCl₃): δ (ppm) 138.1 (C_{Ar}), 137.9 (C_{Ar}), 136.9 (C_{Ar}), 133.1 (C_{Ar}), 130.9 (2C, 2 \times CH_{Ar}), 129.8 (2C, 2 \times CH_{Ar}), 129.0 (CH_{Ar}), 128.6 (2C, 2 \times CH_{Ar}), 128.1 (2C, 2 \times CH_{Ar}), 128.0 (CH_{Ar}), 127.9 (2C, 2 \times CH_{Ar}), 126.8 (2C, 2 \times CH_{Ar}), 101.3 (CHPh), 90.0 (C-1), 77.5 (C-3), 74.2 (C-4), 72.5 (CH_{2Bn}), 70.0 (C-6), 69.5 (C-2), 60.8 (C-5), 25.9 (3C, C(CH₃)₃TBS), 21.2 (CH_{3STol}), 18.2 (C(CH₃)₃TBS), -4.7 (2C, 2 \times CH₃TBS); HRMS (ESI-TOF) m/z [M + NH₄]⁺ calcd for C₃₃H₄₆NO₅SSi 596.2861; found 596.2885.

1,2,3,4,6-Penta-*O*-acetyl- α -D-talopyranose (26).

Peracetylated β -D-galactopyranoside⁵⁶⁷ **25** (5000 mg, 12.81 mmol, 1.0 equiv) was solubilized in dry DCM (63 mL). AlCl₃ (1110 mg, 8.326 mmol, 0.7 equiv) was added and the mixture was stirred

CHAPITRE 7 – C7 EPIMERIZATION OF BENZYLIDENE-PROTECTED β -D-IDOPYRANOSIDES BRINGS STRUCTURAL INSIGHTS INTO IDOSE CONFORMATIONAL FLEXIBILITY

at rt for 2 h. Then, the solution was diluted with CHCl_3 and washed three times with ice-cold water. After evaporation of the solvents under reduced pressure, the crude material was solubilized in dry CCl_4 (125 mL). The solution was heated to 50 °C with an oil bath and a solution of SbCl_5 (1.9 mL, 15 mmol, 1.2 equiv) in dry CCl_4 (7 mL) was added dropwise. The mixture was stirred at rt for 15 min under argon, after which the resulting solid was retrieved by filtration, yielding the corresponding *talo*-configured antimony salt. The latter was solubilized in an aqueous solution of NaOAc (78 mL, 2.4 M). The mixture was stirred for 20 min at rt, then extracted three times with DCM. The organic layers were dried over MgSO_4 , filtered, and evaporated under reduced pressure. The resulting alcohol was solubilized in dry pyridine (29 mL). The solution was cooled to 0 °C, Ac_2O (87 mL) was slowly added, and the resulting mixture was brought back to rt and stirred at this temperature for 16 h. The solution was diluted with DCM, washed three times with a 1 N aqueous HCl solution, and washed with brine. The organic layers were dried over MgSO_4 , filtered, evaporated under reduced pressure, and co-evaporated with toluene. The residue was purified by silica gel flash chromatography to give peracetylated D-talopyranoside **26** (581 mg, 12%). Physical and analytical data agreed with those published.⁵³⁹

Ethyl 4,6-*O*-Benzylidene-1-thio- α -D-talopyranoside (27).

To a solution of peracetylated taloside **26** (50 mg, 0.13 mmol, 1.0 equiv) in dry DCM (0.5 mL) was added activated 4 Å MS (50 mg) and EtSH (19 μL , 0.26 mmol, 2.0 equiv). The suspension was cooled to 0 °C and TfOH (23 μL , 0.26 mmol, 2.0 equiv) was added dropwise. The mixture was allowed to gradually reach rt over a period of 1.5 h, after which the reaction was quenched by the addition of a saturated aqueous NaHCO_3 solution. I_2 was then added until the coloration persisted, followed by a 10% aqueous $\text{Na}_2\text{S}_2\text{O}_3$ solution until there were no more coloration. The aqueous layer was extracted with DCM ($\times 3$) and the combined organic layers were washed with brine, dried over MgSO_4 , filtered, and concentrated under reduced pressure. The residue was purified by silica gel flash chromatography (Hex/EtOAc 8:2 to 7:3) to give ethyl 2,3,4,6-tetra-*O*-acetyl-1-thio- α -D-talopyranoside (35 mg, 70%) as a colorless oil: R_f 0.3 (Hex/EtOAc 4:6); $[\alpha]_{\text{D}}^{20} +66$ (c 0.39, CHCl_3); $^1\text{H NMR}$ (600 MHz, CDCl_3): δ (ppm) 5.38 (s, 1H, H-1), 5.33–5.32 (m, 1H, H-4), 5.21 (t, $J = 3.7$ Hz, 1H, H-3), 5.18–5.17 (m, 1H, H-2), 4.63 (td, $J = 6.6$ Hz, $J = 1.4$ Hz, 1H,

CHAPITRE 7 – C7 EPIMERIZATION OF BENZYLIDENE-PROTECTED β -D-IDOPYRANOSIDES BRINGS STRUCTURAL INSIGHTS INTO IDOSE CONFORMATIONAL FLEXIBILITY

H-5), 4.21 (dd, $J = 9.1$ Hz, $J = 4.6$ Hz, 1H, H-6a), 4.18 (dd, $J = 9.2$ Hz, $J = 4.0$ Hz, 1H, H-6b), 2.71–2.59 (m, 2H, $\text{CH}_{2\text{SEt}}$), 2.15 (s, 3H, $\text{CH}_{3\text{Ac}}$), 2.14 (s, 3H, $\text{CH}_{3\text{Ac}}$), 2.05 (s, 3H, $\text{CH}_{3\text{Ac}}$), 1.99 (s, 3H, $\text{CH}_{3\text{Ac}}$), 1.32 (t, $J = 7.4$ Hz, 3H, $\text{CH}_{3\text{SEt}}$); $^{13}\text{C}\{^1\text{H}\}$ NMR (150 MHz, CDCl_3): δ (ppm) 170.6 (COOR_{Ac}), 170.3 (COOR_{Ac}), 170.1 (COOR_{Ac}), 169.6 (COOR_{Ac}), 82.6 (C-1), 69.1 (C-2), 67.4 (C-5), 66.31, 66.29 (2C, C-3, C-4), 62.2 (C-6), 25.3 ($\text{CH}_{2\text{SEt}}$), 21.1 ($\text{CH}_{3\text{Ac}}$), 20.8 (2C, $2 \times \text{CH}_{3\text{Ac}}$), 20.7 ($\text{CH}_{3\text{Ac}}$), 14.8 ($\text{CH}_{3\text{SEt}}$); HRMS (ESI-TOF) m/z calcd for $\text{C}_{16}\text{H}_{28}\text{NO}_9\text{S}$ 410.1473; found 410.1495. The latter compound (51 mg, 0.13 mmol, 1.0 equiv) was solubilized in dry MeOH (0.8), and NaOMe (25% wt in MeOH, 5.8 μL , 0.027 mmol, 0.2 equiv) was added. The mixture was stirred at rt for 30 min, then neutralized with Dowex resin until pH = 7. The suspension was filtered over Celite and the solvents were evaporated under reduced pressure. The resulting crude tetraol was solubilized in benzaldehyde (440 μL) and TFA (22 μL) was added to the solution. The mixture was stirred at rt for 40 min under Ar atmosphere, cooled to 0 °C, and quenched by the slow addition of Et_3N . The solvents were co-evaporated with toluene and the residue was purified by silica gel flash chromatography (Hex/EtOAc 9:1 to 7:3) to give diol **27** (23 mg, 55% in 2 steps) as a colorless oil: R_f 0.23 (Hex/EtOAc 6:4); $[\alpha]_{\text{D}}^{20} +101$ (c 0.190, CHCl_3); ^1H NMR (600 MHz, CDCl_3): δ (ppm) 7.48–7.47 (m, 2H, $2 \times \text{CH}_{\text{Ar}}$), 7.39–7.38 (m, 3H, $3 \times \text{CH}_{\text{Ar}}$), 5.52 (s, 1H, CHPh), 5.50 (br s, 1H, H-1), 4.32 (dd, $J = 12.9$ Hz, $J = 1.9$ Hz, 1H, H-6a), 4.29–4.28 (m, 1H, H-4), 4.14–4.11 (m, 2H, H-6b, H-5), 3.87–3.85 (m, 2H, H-2, H-3), 3.47 (d, $J = 11.9$ Hz, 1H, OH), 2.95 (d, $J = 9.7$ Hz, 1H, OH), 2.73–2.60 (m, 2H, $\text{CH}_{2\text{SEt}}$), 1.32 (t, $J = 7.4$ Hz, 3H, $\text{CH}_{3\text{SEt}}$); $^{13}\text{C}\{^1\text{H}\}$ NMR (150 MHz, CDCl_3): δ (ppm) 137.3 (C_{Ar}), 129.5 (CH_{Ar}), 128.6 (2C, $2 \times \text{CH}_{\text{Ar}}$), 126.1 (2C, $2 \times \text{CH}_{\text{Ar}}$), 101.9 (CHPh), 85.9 (C-1), 77.0 (C-4), 71.8 (C-2*), 69.9 (C-6), 66.4 (C-3*), 63.2 (C-5), 25.5 ($\text{CH}_{2\text{SEt}}$), 15.1 ($\text{CH}_{3\text{SEt}}$); HRMS (ESI-TOF) m/z $[\text{M} + \text{Na}]^+$ calcd for $\text{C}_{15}\text{H}_{20}\text{NaO}_5\text{S}$ 335.0924; found 335.0936.

Ethyl 3-O-Acetyl-4,6-O-benzylidene-2-O-tert-butyltrimethylsilyl-1-thio- α -D-talopyranoside (28).

Diol **27** (12 mg, 0.037 mmol, 1.0 equiv) was solubilized in dry acetonitrile (300 μL), and Ac_2O (3.9 μL , 0.041 mmol, 1.1 equiv) and TBAOAc (7 mg, 0.02 mmol, 0.6 equiv) were successively added. The mixture was heated at 40 °C with an oil bath and stirred at this temperature under Ar

CHAPITRE 7 – C7 EPIMERIZATION OF BENZYLIDENE-PROTECTED β-D-IDOPYRANOSIDES BRINGS STRUCTURAL INSIGHTS INTO IDOSE CONFORMATIONAL FLEXIBILITY

atmosphere for 6 h. Then, the solvents were co-evaporated with toluene and the residue was purified by silica gel flash chromatography (Hex/EtOAc 9:1 to 7:3) to give ethyl 3-*O*-acetyl-4,6-*O*-benzylidene-1-thio- α -D-talopyranoside (13 mg, quant.) as a colorless oil: R_f 0.47 (Hex/EtOAc 6:4); $[\alpha]_D^{20} +167$ (c 0.210, CHCl₃); ¹H NMR (600 MHz, CDCl₃): δ (ppm) 7.49–7.48 (m, 2H, 2 \times CH_{Ar}), 7.39–7.37 (m, 3H, 3 \times CH_{Ar}), 5.50 (s, 1H, CHPh), 5.49 (d, J = 1.3 Hz, 1H, H-1), 5.03 (t, J = 3.3 Hz, 1H, H-3), 4.46–4.45 (m, 1H, H-4), 4.32 (dd, J = 12.6 Hz, J = 1.5 Hz, 1H, H-6a), 4.16 (br s, 1H, H-5), 4.12 (dd, J = 12.6 Hz, J = 1.7 Hz, 1H, H-6b), 4.09 (d, J = 11.2 Hz, 1H, OH), 3.97–3.95 (m, 1H, H-2), 2.74–2.61 (m, 2H, CH₂SEt), 2.16 (s, 3H, CH₃Ac), 1.32 (t, J = 7.4 Hz, 3H, CH₃SEt); ¹³C{¹H} NMR (150 MHz, CDCl₃): δ (ppm) 170.7 (COOR_{Ac}), 137.2 (C_{Ar}), 129.5 (CH_{Ar}), 128.5 (2C, 2 \times CH_{Ar}), 126.2 (2C, 2 \times CH_{Ar}), 101.7 (CHPh), 86.5 (C-1), 74.8 (C-4), 70.1, 69.9 (2C, C-2, C-6), 68.8 (C-3), 63.1 (C-5), 25.6 (CH₂SEt), 21.3 (CH₃Ac), 15.1 (CH₃SEt); HRMS (ESI-TOF) m/z [M + Na]⁺ calcd for C₁₇H₂₂NaO₆S 377.1029; found 377.1041. To a solution of the latter alcohol (12 mg, 0.034 mmol, 1.0 equiv) in dry DCE (510 μ L) at 0 °C were successively slowly added Et₃N (8.5 μ L, 0.061 mmol, 1.8 equiv) and TBSOTf (14 μ L, 0.061 mmol, 1.8 equiv). The mixture was stirred at 0 °C under an Ar atmosphere for 15 min, quenched with Et₃N, and co-evaporated under reduced pressure. The residue was purified by silica gel flash chromatography (Hex/EtOAc 9:1 to 85:15) to give compound **28** (13 mg, 79%) as a colorless oil: R_f 0.36 (Hex/EtOAc 8:2); $[\alpha]_D^{20} +109$ (c 0.420, CHCl₃); ¹H NMR (600 MHz, CDCl₃): δ (ppm) 7.56–7.54 (m, 2H, 2 \times CH_{Ar}), 7.32–7.31 (m, 3H, 3 \times CH_{Ar}), 5.44 (s, 1H, CHPh), 5.40 (br s, 1H, H-1), 4.96 (t, J = 3.7 Hz, 1H, H-3), 4.31–4.28 (m, 2H, H-4, H-6a), 4.09 (dd, J = 12.5 Hz, J = 1.9 Hz, 1H, H-6b), 4.07 (br s, 1H, H-5), 3.99 (br d, J = 3.6 Hz, 1H, H-2), 2.71–2.56 (m, 2H, CH₂SEt), 2.10 (s, 3H, CH₃Ac), 1.31 (t, J = 7.4 Hz, 3H, CH₃SEt), 0.86 (s, 9H, C(CH₃)₃TBS), 0.06 (s, 3H, CH₃TBS), 0.02 (s, 3H, CH₃TBS); ¹³C{¹H} NMR (150 MHz, CDCl₃): δ (ppm) 170.6 (COOR_{Ac}), 138.3 (C_{Ar}), 128.9 (CH_{Ar}), 128.0 (2C, 2 \times CH_{Ar}), 126.9 (2C, 2 \times CH_{Ar}), 101.4 (CHPh), 86.5 (C-1), 72.5 (C-4), 70.0 (C-3), 69.8 (C-6), 69.4 (C-2), 62.8 (C-5), 25.8 (3C, C(CH₃)₃TBS), 25.2 (CH₂SEt), 21.3 (CH₃Ac), 18.4 (C(CH₃)₃TBS), 15.0 (CH₃SEt), -4.8 (2C, 2 \times CH₃TBS); HRMS (ESI-TOF) m/z [M + Na]⁺ calcd for C₂₃H₃₆NaO₆SSi 491.1894; found 491.1895.

CHAPITRE 7 – C7 EPIMERIZATION OF BENZYLIDENE-PROTECTED β -D-IDOPYRANOSIDES BRINGS STRUCTURAL INSIGHTS INTO IDOSE CONFORMATIONAL FLEXIBILITY

(2-Adamantyl) 3-*O*-Benzyl-(*S*)-4,6-*O*-benzylidene-2-*O*-*tert*-butyldimethylsilyl- β -D-idopyranoside (**29**) and (2-Adamantyl) 3-*O*-Benzyl-(*S*)-4,6-*O*-benzylidene- β -D-idopyranoside (**31**).

Donor **24** (11.4 mg, 0.0197 mmol, 1.2 equiv), 2-adamantanol **11** (2.5 mg, 0.016 mmol, 1.0 equiv), and NIS (5.5 mg, 0.025 mg, 1.5 equiv) were dried together under high vacuum for 1 h. Then, activated 4 Å MS (46 mg) and dry DCE (330 μ L) were added. The suspension was stirred at rt under Ar for 1 h, cooled to -10 °C, and AgOTf (0.8 mg, 0.003 mmol, 0.2 equiv) was added. The reaction flask was protected from light with the help of aluminum foil. The mixture was stirred for 2 h under Ar at -10 °C to 0 °C, after which it was quenched with Et₃N, filtered over Celite, and concentrated under reduced pressure. The residue was purified by silica gel flash chromatography (Tol/EtOAc 995:5 to 9:1) to give compound **29** (4.4 mg, 41%) as a colorless oil along with desilylated analogue **31** (3.5 mg, 40%) as a white amorphous solid.

Data for compound 29: R_f 0.40 (Tol/EtOAc 96:4); $[\alpha]_D^{20}$ -14 (c 0.55, CHCl₃); ¹H NMR (600 MHz, CDCl₃): δ (ppm) 7.55–7.53 (m, 2H, 2 \times CH_{Ar}), 7.37–7.29 (m, 8H, 8 \times CH_{Ar}), 5.46 (s, 1H, CHPh), 4.78 (d, J = 1.2 Hz, 1H, H-1), 4.68 (d, J = 12.0 Hz, 1H, CHH_{Bn}), 4.61 (d, J = 12.0 Hz, 1H, CHH_{Bn}), 4.34 (d, J = 12.4 Hz, 1H, H-6a), 4.05 (dd, J = 12.5 Hz, J = 2.1 Hz, 1H, H-6b), 3.96 (br s, 1H, H-2_{ad}), 3.90 (br s, 1H, H-4), 3.75–3.74 (m, 1H, H-2), 3.72–3.71 (m, 1H, H-3), 3.63 (m, 1H, H-5), 2.22–1.42 (m, 14H, 5 \times CH_{2ad}, 4 \times CH_{ad}), 0.82 (s, 9H, C(CH₃)₃TBS), 0.10 (s, 3H, CH₃TBS), 0.01 (s, 3H, CH₃TBS); ¹³C{¹H} NMR (150 MHz, CDCl₃): δ (ppm) 138.3 (C_{Ar}), 138.1 (C_{Ar}), 128.9 (CH_{Ar}), 128.7 (2C, 2 \times CH_{Ar}), 128.1 (CH_{Ar}), 128.0 (2, 2 \times CH_{Ar}), 127.8 (2C, 2 \times CH_{Ar}), 127.0 (2C, 2 \times CH_{Ar}), 101.6 (CHPh), 96.7 (C-1, ¹J_{C1,H1} = 157 Hz), 79.6, (C-3), 79.4 (C-2_{ad}), 73.7 (C-4), 72.6 (CH_{2Bn}), 70.1 (C-6), 69.0 (C-2), 66.9 (C-5), 37.9–27.6 (9C, 5 \times CH_{2ad}, 4 \times CH_{ad}), 26.0 (3C, C(CH₃)₃TBS), 18.5 (C(CH₃)₃TBS), -4.3 (CH₃TBS), -5.1 (CH₃TBS); HRMS (ESI-TOF) m/z [M + NH₄]⁺ calcd for C₃₆H₅₄NO₆Si 624.3715; found 624.3733.

Data for desilylated glycoside 31: R_f 0.26 (Tol/EtOAc 96:4); $[\alpha]_D^{20}$ -36 (c 0.26, CHCl₃); ¹H NMR (600 MHz, CDCl₃): δ (ppm) 7.48–7.47 (m, 2H, 2 \times CH_{Ar}), 7.38–7.32 (m, 8H, 8 \times CH_{Ar}), 5.48 (s, 1H, CHPh), 4.91 (br s, 1H, H-1), 4.67 (d, J = 12.5 Hz, 1H, CHH_{Bn}), 4.65 (d, J = 12.6 Hz, 1H,

CHAPITRE 7 – C7 EPIMERIZATION OF BENZYLIDENE-PROTECTED β -D-IDOPYRANOSIDES BRINGS STRUCTURAL INSIGHTS INTO IDOSE CONFORMATIONAL FLEXIBILITY

CHH_{Bn}), 4.36 (dd, $J = 12.4$ Hz, $J = 1.0$ Hz, 1H, H-6a), 4.06 (dd, $J = 12.5$ Hz, $J = 1.8$ Hz, 1H, H-6b), 3.99 (t, $J = 1.3$ Hz, 1H, H-4*), 3.94 (br s, 1H, H-2_{ad}), 3.90 (t, $J = 2.8$ Hz, 1H, H-3*), 3.75–3.73 (m, 2H, H-5, H-2), 3.14 (d, $J = 11.2$ Hz, 1H, OH-2), 2.22–1.47 (m, 14H, 5 × CH_{2ad}, 4 × CH_{ad}); ¹³C{¹H} NMR (150 MHz, CDCl₃): δ (ppm) 137.7 (C_{Ar}), 137.6 (C_{Ar}), 129.3 (CH_{Ar}), 128.7 (2C, 2 × CH_{Ar}), 128.4 (2C, 2 × CH_{Ar}), 128.3 (CH_{Ar}), 127.8 (2C, 2 × CH_{Ar}), 126.3 (2C, 2 × CH_{Ar}), 101.6 (CHPh), 96.3 (C-1, ¹J_{C1,H1} = 155 Hz), 80.1 (C-2_{ad}), 77.2 (C-3*), 73.9 (C-4*), 72.7 (CH_{2Bn}), 70.0 (C-6), 68.1, 67.0 (2C, C-2, C-5), 37.7–27.5 (9C, 5 × CH_{2ad}, 4 × CH_{ad}); HRMS (ESI-TOF) m/z [M + NH₄]⁺ calcd for C₃₀H₄₀NO₆ 510.2850; found 510.2842.

(2-Adamantyl) 3-*O*-Acetyl-(*S*)-4,6-*O*-benzylidene-2-*O*-*tert*-butyldimethylsilyl- α -D-talopyranoside (**30 α**), (2-Adamantyl) 3-*O*-Acetyl-(*S*)-4,6-*O*-benzylidene-2-*O*-*tert*-butyldimethylsilyl- β -D-talopyranoside (**30 β**) and (2-Adamantyl) 3-*O*-Acetyl-(*S*)-4,6-*O*-benzylidene- α -D-talopyranoside (**32**).

Donor **28** (12.2 mg, 0.026 mmol, 1.2 equiv) and 2-adamantanol (3.3 mg, 0.022 mmol, 1.0 equiv) were reacted according to the general procedure for NIS/TMSOTf-promoted glycosylation. Purification by silica gel flash chromatography (Hex/EtOAc 95:5 to 85:15) gave compounds **30 α** (5.1 mg, 42%, colorless oil), and **32** and **30 β** (2.3 mg, 23%, colorless oil, inseparable mixture **32/30 β** 1.0:0.3).

Data for α -glycoside 30 α : R_f 0.37 (Hex/EtOAc 8:2); $[\alpha]_D^{20} +28$ (c 0.59, CHCl₃); ¹H NMR (600 MHz, CDCl₃): δ (ppm) 7.55–7.54 (m, 2H, 2 × CH_{Ar}), 7.32–7.31 (m, 3H, 3 × CH_{Ar}), 5.42 (s, 1H, CHPh), 5.08 (t, $J = 3.6$ Hz, 1H, H-3), 5.05 (br s, 1H, H-1), 4.31–4.29 (m, 2H, H-6a, H-4), 4.04 (dd, $J = 12.5$ Hz, $J = 1.6$ Hz, 1H, H-6b), 3.89 (br d, $J = 3.0$ Hz, 1H, H-2), 3.80 (br s, 1H, H-2_{ad}), 3.76 (br s, 1H, H-5), 2.10 (s, 3H, CH_{3Ac}), 2.06–1.49 (m, 14H, 4 × CH_{ad}, 5 × CH_{2ad}), 0.86 (s, 9H, C(CH₃)₃TBS), 0.05 (CH₃TBS), 0.02 (CH₃TBS); ¹³C{¹H} NMR (150 MHz, CDCl₃): δ (ppm) 170.9 (COOR_{Ac}), 138.4 (C_{Ar}), 128.9 (CH_{Ar}), 127.9 (2C, 2 × CH_{Ar}), 127.0 (2C, 2 × CH_{Ar}), 101.4 (CHPh), 99.5 (C-1, ¹J_{C1,H1} = 172 Hz), 78.9 (C-2_{ad}), 72.4 (C-4), 69.85, 69.83 (2C, C-3, C-6), 68.8 (C-2), 62.5 (C-5), 37.6–27.4 (9C, 4 × CH_{ad}, 5 × CH_{2ad}), 25.9 (3C, C(CH₃)₃TBS), 21.4 (CH_{3Ac}), 18.4

CHAPITRE 7 – C7 EPIMERIZATION OF BENZYLIDENE-PROTECTED β-D-IDOPYRANOSIDES BRINGS STRUCTURAL INSIGHTS INTO IDOSE CONFORMATIONAL FLEXIBILITY

(C(CH₃)₃TBS), -4.75 (CH₃TBS), -4.84 (CH₃TBS); HRMS (ESI-TOF) *m/z* [M + NH₄]⁺ calcd for C₃₆H₅₄NO₆Si 624.3715; found 624.3733.

Data for desilylated α-glycoside 32: *R_f* 0.16 (Hex/EtOAc 8:2); ¹H NMR (600 MHz, CDCl₃): δ (ppm) 7.49–7.47 (m, 2H, 2 × CH_{Ar}), 7.39–7.37 (m, 3H, 3 × CH_{Ar}), 5.48 (s, 1H, CHPh), 5.21 (t, *J* = 3.2 Hz, 1H, H-3), 5.18 (d, *J* = 1.6 Hz, 1H, H-1), 4.49–4.48 (m, 1H, H-4), 4.33 (dd, *J* = 12.5 Hz, *J* = 1.5 Hz, 1H, H-6a), 4.08 (dd, *J* = 12.5 Hz, *J* = 1.6 Hz, 1H, H-6b), 3.85–3.82 (m, 3H, H-2_{ad}, H-2, H-5), 3.78 (d, *J* = 11.6 Hz, OH-2), 2.18 (s, 3H, CH₃Ac), 2.05–1.48 (m, 14H, 5 × CH_{2ad}, 4 × CH_{ad}); ¹³C{¹H} NMR (150 MHz, CDCl₃): δ (ppm) 171.0 (COOR_{Ac}), 137.4 (C_{Ar}), 129.4 (CH_{Ar}), 128.5 (2C, 2 × CH_{Ar}), 126.2 (2C, 2 × CH_{Ar}), 101.6 (CHPh), 99.4 (C-1, ¹*J*_{C1,H1} = 175 Hz), 79.7 (C-2_{ad}), 74.9 (C-4), 69.9 (C-6), 69.2 (C-2), 68.7 (C-3), 62.8 (C-5), 37.5–27.3 (9C, 5 × CH_{2ad}, 4 × CH_{ad}), 21.4 (CH₃Ac); HRMS (ESI-TOF) *m/z* [M + NH₄]⁺ calcd for C₂₅H₃₆NO₇ 462.2486; found 462.2482.

Data for β-glycoside 30β: *R_f* 0.16 (Hex/EtOAc 8:2); ¹H NMR (600 MHz, CDCl₃): δ (ppm) 7.56–7.55 (m, 0.6H, 2 × CH_{Ar}), 7.32–7.30 (m, 0.9H, 3 × CH_{Ar}), 5.42 (s, 0.3H, CHPh), 4.79 (t, *J* = 3.6 Hz, 0.3H, H-3), 4.49–4.48 (m, 0.3H, H-1), 4.38 (dd, *J* = 12.4 Hz, *J* = 1.0 Hz, 0.3H, H-6a), 4.20 (br d, *J* = 3.9 Hz, 0.3H, H-4), 4.07 (dd, *J* = 12.5 Hz, *J* = 2.1 Hz, 0.3H, H-6b), 4.00–3.99 (m, 0.6H, H-2_{ad}, H-2), 3.31 (br s, 0.3H, H-5), 2.12 (s, 0.9H, CH₃Ac), 2.05–1.48 (m, 4.2H, 5 × CH_{2ad}, 4 × CH_{ad}), 0.87 (s, 3H, C(CH₃)₃TBS), 0.13 (s, 0.9H, CH₃TBS), 0.06 (s, 0.9H, CH₃TBS); ¹³C{¹H} NMR (150 MHz, CDCl₃): δ (ppm) 171.0 (COOR_{Ac}), 138.2 (C_{Ar}), 128.8 (CH_{Ar}), 127.9 (2C, 2 × CH_{Ar}), 127.0 (2C, 2 × CH_{Ar}), 101.5 (CHPh), 97.9 (C-1, ¹*J*_{C1,H1} = 155 Hz), 79.7 (C-2_{ad}), 72.4 (C-3), 72.2 (C-4), 69.6 (C-6), 69.3 (C-2), 67.1 (C-5), 37.7–27.6 (9C, 5 × CH_{2ad}, 4 × CH_{ad}), 26.0 (3C, C(CH₃)₃TBS), 21.4 (CH₃Ac), 18.7 (C(CH₃)₃TBS), -4.1 (CH₃TBS), -4.9 (CH₃TBS); HRMS (ESI-TOF) *m/z* [M + NH₄]⁺ calcd for C₃₁H₅₀NO₇Si 576.3351; found 576.3338.

CHAPITRE 7 – C7 EPIMERIZATION OF BENZYLIDENE-PROTECTED β -D-IDOPYRANOSIDES BRINGS STRUCTURAL INSIGHTS INTO IDOSE CONFORMATIONAL FLEXIBILITY

Allyl 3-*O*-Acetyl-(*S*)-4,6-*O*-benzylidene-2-*O*-*tert*-butyldimethylsilyl- α -D-idopyranosyl-(1 \rightarrow 4)-2-*O*-acetyl-3,6-di-*O*-*para*-methoxybenzyl- α -D-glucopyranoside (37 α) and Allyl 3-*O*-Acetyl-(*S*)-4,6-*O*-benzylidene-2-*O*-*tert*-butyldimethylsilyl- β -D-idopyranosyl-(1 \rightarrow 4)-2-*O*-acetyl-3,6-di-*O*-*para*-methoxybenzyl- α -D-glucopyranoside (37 β).

Donor **6a** (10.1 mg, 0.0215 mmol, 1.2 equiv), acceptor **33**⁵⁷⁸ (9.0 mg, 0.018 mmol, 1.0 equiv), and tri-*tert*-butylpyridine (13.3 mg, 0.0537 mmol, 3.0 equiv) were dried together under high vacuum for 1 h. Then, activated 4 Å MS (40 mg) and dry DCE (320 μ L) were added. The suspension was stirred at rt under Ar atmosphere for 1 h, after which Me₂S₂ (4.8 μ L, 0.054 mmol, 3.0 equiv) and MeOTf (5.9 μ L, 0.054 mmol, 3.0 equiv) were successively added. The mixture was stirred at rt for 2 h and was then quenched by adding Et₃N, filtered over Celite, and concentrated under reduced pressure. The residue was purified by silica gel flash chromatography (Hex/EtOAc 9:1 to 6:4) to give α -glycoside **37 α** (8.3 mg, 51%) and β -glycoside **37 β** (6.3 mg, 37%) as colorless oils.

Data for α -glycoside 37 α : *R*_f 0.36 (Hex/EtOAc 6:4); [α]_D²⁰ +16 (*c* 0.12, CHCl₃); ¹H NMR (600 MHz, CDCl₃): δ (ppm) 7.48–7.46 (m, 2H, 2 \times CH_{Ar}), 7.30–7.28 (m, 5H, 5 \times CH_{Ar}), 7.18–7.17 (m, 2H, 2 \times CH_{Ar}), 6.90–6.88 (m, 2H, 2 \times CH_{Ar}), 6.83–6.82 (m, 2H, 2 \times CH_{Ar}), 5.90 (ddd, *J* = 17.0 Hz, *J* = 10.8 Hz, *J* = 5.6 Hz, 1H, CH_{Allyl}), 5.41 (s, 1H, CH_{Ph}), 5.37 (d, *J* = 3.1 Hz, 1H, H-1B), 5.31 (ddd, *J* = 17.1 Hz, *J* = 3.2 Hz, *J* = 1.6 Hz, 1H, =CHH_{Allyl}), 5.21 (ddd, *J* = 10.5 Hz, *J* = 3.2 Hz, *J* = 1.2 Hz, 1H, =CHH_{Allyl}), 5.07 (d, *J* = 3.7 Hz, 1H, H-1A), 4.95 (dd, *J* = 5.1 Hz, *J* = 2.9 Hz, 1H, H-3B), 4.84 (dd, *J* = 9.8 Hz, *J* = 3.7 Hz, 1H, H-2A), 4.71 (d, *J* = 11.0 Hz, 1H, CHH_{PMB}), 4.65 (d, *J* = 11.0 Hz, 1H, CHH_{PMB}), 4.56 (d, *J* = 11.7 Hz, 1H, CHH_{PMB}), 4.53 (d, *J* = 11.7 Hz, 1H, CHH_{PMB}), 4.21 (ddt, *J* = 13.3 Hz, *J* = 5.0 Hz, *J* = 1.5 Hz, 1H, CHH_{Allyl}), 4.10 (dd, *J* = 12.8 Hz, *J* = 0.9 Hz, 1H, H-6Ba*), 4.04–4.01 (m, 2H, CHH_{Allyl}, H-3A), 3.97 (t, *J* = 9.3 Hz, 1H, H-4A), 3.89 (t, *J* = 2.3 Hz, 1H, H-4B), 3.84 (dd, *J* = 12.8 Hz, *J* = 2.1 Hz, 1H, H-6Bb*), 3.81–3.80 (m, 4H, H-5A, CH_{3PMB}), 3.77 (s, 3H, CH_{3PMB}), 3.73–3.70 (m, 3H, H-2B, H-6Aa*, H-6Ab*), 3.69 (br d, *J* = 1.4 Hz, 1H, H-5B), 2.10 (s, 3H, CH_{3Ac}), 1.94 (s, 3H, CH_{3Ac}), 0.78 (s, 9H, C(CH₃)₃TBS), 0.03 (s, 3H, CH₃TBS), 0.02 (s, 3H, CH₃TBS); ¹³C{¹H} NMR (150 MHz, CDCl₃): δ (ppm) 169.5 (2C, 2 \times COOR_{Ac}), 159.4 (C_{Ar}), 159.1 (C_{Ar}), 137.9 (C_{Ar}), 133.8 (CH_{Allyl}), 130.7–126.7 (11C, 9 \times CH_{Ar}, 2 \times C_{Ar}), 117.7 (=CH₂Allyl), 113.9 (4C, 4 \times CH_{Ar}), 101.4 (C-1B, ¹J_{C1,H1} = 175 Hz), 101.1 (CH_{Ph}), 95.0 (C-1A,

CHAPITRE 7 – C7 EPIMERIZATION OF BENZYLIDENE-PROTECTED β-D-IDOPYRANOSIDES BRINGS STRUCTURAL INSIGHTS INTO IDOSE CONFORMATIONAL FLEXIBILITY

$^1J_{C1,H1} = 176$ Hz), 80.3 (C-3A), 74.5 (C-4B), 74.0 (CH_{2PMB}), 73.8 (C-2A), 73.3 (CH_{2PMB}), 73.2 (C-4A), 72.6 (C-3B), 70.8 (C-5A), 69.4 (C-6B*), 68.9 (C-6A*), 68.5, 68.4 (2C, CH_{2Allyl} , C-2B), 60.8 (C-5B), 55.4 (2C, 2 x CH_{3PMB}), 25.8 (3C, $C(CH_3)_3TBS$), 21.4 (CH_3Ac), 21.0 (CH_3Ac), 18.0 ($C(CH_3)_3TBS$), -4.3 (CH_3TBS), -4.7 (CH_3TBS); HRMS (ESI-TOF) m/z $[M + NH_4]^+$ calcd for $C_{48}H_{68}NO_{15}Si$ 926.4353; found 926.4367.

Data for β-glycoside 37β: R_f 0.20 (Hex/EtOAc 6:4); $[\alpha]_D^{20} +16$ (c 0.66, $CHCl_3$); 1H NMR (600 MHz, $CDCl_3$): δ (ppm) 7.56–7.54 (m, 2H, 2 x CH_{Ar}), 7.43–7.42 (m, 2H, 2 x CH_{Ar}), 7.30–7.29 (m, 3H, 3 x CH_{Ar}), 7.24–7.23 (m, 2H, 2 x CH_{Ar}), 6.87–6.84 (m, 2H, 2 x CH_{Ar}), 6.72–6.70 (m, 2H, 2 x CH_{Ar}), 5.92–5.86 (m, 1H, CH_{Allyl}), 5.47 (s, 1H, $CHPh$), 5.32–5.29 (m, 1H, $=CHH_{Allyl}$), 5.26 (d, $J = 9.7$ Hz, 1H, CHH_{PMB}), 5.21 (dd, $J = 10.4$ Hz, $J = 1.4$ Hz, 1H, CHH_{Allyl}), 5.10 (d, $J = 3.9$ Hz, 1H, H-1A), 5.01 (t, $J = 2.4$ Hz, 1H, H-3B), 4.82 (dd, $J = 10.1$ Hz, $J = 3.9$ Hz, 1H, H-2A), 4.76 (d, $J = 0.9$ Hz, 1H, H-1B), 4.53–4.48 (m, 3H, CHH_{PMB} , CH_{2PMB}), 4.30 (br d, $J = 12.2$ Hz, 1H, H-6Ba), 4.19 (ddt, $J = 13.2$ Hz, $J = 5.1$ Hz, $J = 1.5$ Hz, 1H, CHH_{Allyl}), 4.08 (t, $J = 9.3$ Hz, 1H, H-4A), 4.03 (ddt, $J = 13.3$ Hz, $J = 6.2$ Hz, $J = 1.2$ Hz, 1H, CHH_{Allyl}), 3.98–3.93 (m, 2H, H-3A, H-6Bb), 3.82–3.80 (m, 4H, CH_{3PMB} , H-5A), 3.77 (br s, 1H, H-4B), 3.72 (dd, $J = 11.2$ Hz, $J = 1.7$ Hz, 1H, H-6Aa), 3.65–3.62 (m, 5H, CH_{3PMB} , H-2B, H-6Ab), 3.48 (br d, $J = 1.0$ Hz, 1H, H-5B), 2.12 (s, 3H, CH_3Ac), 1.96 (s, 3H, CH_3Ac), 0.81 (s, 9H, $C(CH_3)_3TBS$), 0.10 (s, 3H, CH_3TBS), 0.05 (s, 3H, CH_3TBS); $^{13}C\{^1H\}$ NMR (150 MHz, $CDCl_3$): δ (ppm) 170.4 ($COOR_{Ac}$), 169.0 ($COOR_{Ac}$), 159.3 (C_{Ar}), 159.2 (C_{Ar}), 138.3 (C_{Ar}), 133.7 (CH_{Allyl}), 131.4–127.0 (11C, 2 x C_{Ar} , 9 x CH_{Ar}), 117.9 ($=CH_{2Allyl}$), 113.9 (2C, 2 x CH_{Ar}), 113.8 (2C, 2 x CH_{Ar}), 101.7 ($CHPh$), 99.8 (C-1B, $^1J_{C1,H1} = 160.0$ Hz), 95.1 (C-1A, $^1J_{C1,H1} = 174.4$ Hz), 78.2, 78.1 (2C, C-4A, C-3A), 75.9 (CH_{2PMB}), 73.2, 73.1, 73.0 (3C, CH_{2PMB} , C-2A, C-3B), 72.2 (C-4B), 70.7 (C-5A), 69.3 (C-6B), 68.6 (C-6A), 68.4 (CH_{2Allyl}), 67.8, 67.4 (2C, C-2B, C-5B), 55.4 (CH_{3PMB}), 55.3 (CH_{3PMB}), 25.8 (3C, $C(CH_3)_3TBS$), 21.1 (CH_3Ac), 21.0 (CH_3Ac), 18.3 ($C(CH_3)_3TBS$), -4.3 (CH_3TBS), -5.0 (CH_3TBS); HRMS (ESI-TOF) m/z $[M + NH_4]^+$ calcd for $C_{48}H_{68}NO_{15}Si$ 926.4353; found 926.4359.

CHAPITRE 7 – C7 EPIMERIZATION OF BENZYLIDENE-PROTECTED β -D-IDOPYRANOSIDES BRINGS STRUCTURAL INSIGHTS INTO IDOSE CONFORMATIONAL FLEXIBILITY

Allyl 3-O-Acetyl-(S)-4,6-O-benzylidene-2-O-tert-butyltrimethylsilyl- α -D-idopyranosyl-(1 \rightarrow 2)-3-O-para-methoxybenzyl-4,6-O-para-methoxybenzylidene- α -D-glucopyranoside (38).

Donor **6a** (10.6 mg, 0.0227 mmol, 1.2 equiv), acceptor **34**⁵⁷⁸ (8.0 mg, 0.017 mmol, 1.0 equiv), and tri-*tert*-butylpyridine (13.0 mg, 0.0523 mmol, 3.0 equiv) were dried together under high vacuum for 1 h. Then, activated 4 Å MS (43 mg) and dry DCE (310 μ L) were added. The suspension was stirred at rt under Ar atmosphere for 1 h, after which Me₂S₂ (4.7 μ L, 0.052 mmol, 3.0 equiv) and MeOTf (5.7 μ L, 0.052 mmol, 3.0 equiv) were successively added. The mixture was stirred at rt for 2 h and was then quenched by adding Et₃N, filtered over Celite, and concentrated under reduced pressure. The residue was purified by silica gel flash chromatography (Hex/EtOAc 9:1 to 6:4) to give α -glycoside **38** (8.6 mg, 57%) as a colorless oil: *R*_f 0.48 (Hex/EtOAc 6:4); [α]_D²⁰ +49 (*c* 0.87, CHCl₃); ¹H NMR (600 MHz, CDCl₃): δ (ppm) 7.51–7.50 (m, 2H, 2 \times CH_{Ar}), 7.40–7.39 (m, 2H, 2 \times CH_{Ar}), 7.31–7.30 (m, 3H, 3 \times CH_{Ar}), 7.27–7.26 (m, 2H, 2 \times CH_{Ar}), 6.90–6.89 (m, 2H, 2 \times CH_{Ar}), 6.87–6.85 (m, 2H, 2 \times CH_{Ar}), 5.91 (dddd, *J* = 17.0 Hz, *J* = 10.4 Hz, *J* = 6.5 Hz, *J* = 5.2 Hz, 1H, CH_{Allyl}), 5.53 (s, 1H, CHPh_{OMe}*), 5.43 (s, 1H, CHPh*), 5.32 (dq, *J* = 17.2 Hz, *J* = 1.5 Hz, 1H, =CHH_{Allyl}), 5.23 (dq, *J* = 10.4 Hz, *J* = 1.2 Hz, =CHH_{Allyl}), 5.05 (d, *J* = 2.6 Hz, 1H, H-1A), 4.96 (t, *J* = 2.7 Hz, 1H, H-3B), 4.93 (br s, 1H, H-1B), 4.83 (d, *J* = 10.4 Hz, 1H, CHH_{PMB}), 4.69 (d, *J* = 10.4 Hz, 1H, CHH_{PMB}), 4.26 (dd, *J* = 10.2 Hz, *J* = 4.9 Hz, 1H, H-6Aa), 4.22 (ddt, *J* = 12.9 Hz, *J* = 5.2 Hz, *J* = 1.3 Hz, 1H, CHH_{Allyl}), 4.14 (dd, *J* = 12.7 Hz, *J* = 1.1 Hz, 1H, H-6Ba), 4.09 (br d, *J* = 1.3 Hz, 1H, H-5B), 4.01 (ddt, *J* = 13.0 Hz, *J* = 6.6 Hz, *J* = 1.2 Hz, 1H, CHH_{Allyl}), 3.96–3.95 (m, 2H, H-2A, H-3A), 3.89–3.85 (m, 2H, H-5A, H-4B), 3.81 (s, 6H, CH_{3PMB}, CH_{3PhOMe}), 3.75–3.76 (m, 2H, H-6Ab, H-2B), 3.69 (dd, *J* = 12.7 Hz, *J* = 1.7 Hz, 1H, H-6Bb), 3.65–3.62 (m, 1H, H-4A), 2.08 (s, 3H, CH_{3Ac}), 0.86 (s, 9H, C(CH₃)₃TBS), 0.11 (s, 3H, CH₃TBS), 0.11 (s, 3H, CH₃TBS); ¹³C{¹H} NMR (150 MHz, CDCl₃): δ (ppm) 169.6 (COOR_{Ac}), 160.1 (C_{Ar}), 159.5 (C_{Ar}), 138.0 (C_{Ar}), 133.5–126.7 (11C, 2 \times C_{Ar}, 9 \times CH_{Ar}), 118.5 (=CH₂Allyl), 113.9 (2C, 2 \times CH_{Ar}), 113.7 (2C, 2 \times CH_{Ar}), 101.4 (CHPh_{OMe}*), 101.3 (CHPh*), 98.2 (C-1B, ¹J_{C1,H1} = 171 Hz), 95.2 (C-1A, ¹J_{C1,H1} = 172 Hz), 82.3 (C-4A), 77.4 (C-3A*), 75.1 (CH₂PMB), 73.6 (C-2A*), 73.0 (C-4B), 71.7 (C-3B), 69.4 (C-6B), 69.1 (C-6A), 68.6 (CH₂Allyl), 67.2 (C-2B), 62.6 (C-5A), 59.4 (C-5B), 55.5 (CH₃OMe), 55.4

CHAPITRE 7 – C7 EPIMERIZATION OF BENZYLIDENE-PROTECTED β -D-IDOPYRANOSIDES BRINGS STRUCTURAL INSIGHTS INTO IDOSE CONFORMATIONAL FLEXIBILITY

(CH₃OMe), 25.8 (3C, C(CH₃)₃TBS), 21.4 (CH₃Ac), 18.1 (C(CH₃)₃TBS), -4.7 (CH₃TBS), -4.9 (CH₃TBS); HRMS (ESI-TOF) m/z [M + NH₄]⁺ calcd for C₄₆H₆₄NO₁₄Si 882.4093; found 882.4091.

Allyl 3-O-Acetyl-(S)-4,6-O-benzylidene-2-O-tert-butyltrimethylsilyl- α -D-idopyranosyl-(1 \rightarrow 4)-3-O-tert-butyltrimethylsilyl-2-deoxy-2-trichloroacetamido- β -D-glucopyranoside (39a) and Allyl 3-O-Acetyl-(S)-4,6-O-benzylidene-2-O-tert-butyltrimethylsilyl- α -D-idopyranosyl-(1 \rightarrow 3)-3-O-tert-butyltrimethylsilyl-2-deoxy-2-trichloroacetamido- β -D-glucopyranoside (39b).

Donor **6a** (10.2 mg, 0.0217 mmol, 1.2 equiv), acceptor **35**⁵⁷⁶ (8.0 mg, 0.017 mmol, 1.0 equiv), and tri-*tert*-butylpyridine (12.4 mg, 0.0501 mmol, 3.0 equiv) were dried together under high vacuum for 1 h. Then, activated 4 Å MS (41 mg) and dry DCE (300 μ L) were added. The suspension was stirred at rt under Ar atmosphere for 1 h, after which Me₂S₂ (4.5 μ L, 0.050 mmol, 3.0 equiv) and MeOTf (5.5 μ L, 0.050 mmol, 3.0 equiv) were successively added. The mixture was stirred at rt for 2 h and was then quenched by adding Et₃N, filtered over Celite, and concentrated under reduced pressure. The residue was purified by silica gel flash chromatography (Tol/EtOAc 95:5 to 8:2) to give (1 \rightarrow 4)-linked α -glycoside **39a** (1.2 mg, 8%) and (1 \rightarrow 3)-linked α -glycoside **39b** (4.4 mg, 30%) as colorless oils.

Data for (1 \rightarrow 4)-linked α -glycoside 39a: R_f 0.57 (Tol/EtOAc 8:2); $[\alpha]_D^{20}$ -5.6 (c 0.25, CHCl₃); ¹H NMR (600 MHz, CDCl₃) : δ (ppm) 7.52–7.51 (m, 2H, 2 \times CH_{Ar}), 7.33–7.32 (m, 3H, 3 \times CH_{Ar}), 6.96 (d, J = 6.1 Hz, 1H, NH), 5.87 (ddd, J = 22.3 Hz, J = 11.0 Hz, J = 5.8 Hz, 1H, CH_{Allyl}), 5.49 (s, 1H, CHPh), 5.43 (d, J = 2.8 Hz, 1H, H-1B), 5.28 (dd, J = 17.3 Hz, J = 1.6 Hz, 1H, =CHH_{Allyl}), 5.22 (dd, J = 10.4 Hz, J = 1.3 Hz, 1H, =CHH_{Allyl}), 4.97 (t, J = 3.6 Hz, 1H, H-3B), 4.72 (d, J = 7.9 Hz, 1H, H-1A), 4.36–4.31 (m, 2H, H-6Ba, CHH_{Allyl}), 4.17 (td, J = 9.7 Hz, J = 4.2 Hz, 1H, H-3A), 4.11–4.08 (m, 2H, H-6Bb, CHH_{Allyl}), 3.98–3.95 (m, 2H, H-4B, H-6Aa), 3.89 (br d, J = 1.4 Hz, 1H, H-5B), 3.84 (dd, J = 11.3 Hz, J = 5.5 Hz, 1H, H-6Ab), 3.79 (dd, J = 4.3 Hz, J = 2.9 Hz, 1H, H-2B), 3.72 (t, J = 8.7 Hz, 1H, H-4A), 3.44 (ddd, J = 9.9 Hz, J = 7.9 Hz, J = 6.2 Hz, 1H, H-2A), 3.40 (ddd, J = 8.0 Hz, J = 4.8 Hz, J = 2.0 Hz, 1H, H-5A), 3.20 (d, J = 4.6 Hz, 1H, OH-3), 2.09 (s, 3H, CH₃Ac), 0.91 (s, 9H, C(CH₃)₃TBS), 0.84 (s, 9H, C(CH₃)₃TBS), 0.11 (s, 3H, CH₃TBS), 0.09 (s, 6H,

CHAPITRE 7 – C7 EPIMERIZATION OF BENZYLIDENE-PROTECTED β-D-IDOPYRANOSIDES BRINGS STRUCTURAL INSIGHTS INTO IDOSE CONFORMATIONAL FLEXIBILITY

$2 \times \text{CH}_3\text{TBS}$), 0.08 (s, 3H, CH_3TBS); $^{13}\text{C}\{^1\text{H}\}$ NMR (150 MHz, CDCl_3) : δ (ppm) 169.5 (COOR_{Ac}), 162.6 (CONH), 137.8 (C_{Ar}), 133.4 (CH_{Allyl}), 129.1 (CH_{Ar}), 128.2 (2C, $2 \times \text{CH}_{\text{Ar}}$), 126.7 (2C, $2 \times \text{CH}_{\text{Ar}}$), 118.5 ($=\text{CH}_2\text{Allyl}$), 101.8 (C-1B, $^1J_{\text{C1,H1}} = 175$ Hz), 101.2 (CHPh), 98.1 (C-1A, $^1J_{\text{C1,H1}} = 164$ Hz), 76.1 (C-5A), 75.1 (C-4A), 73.9 (C-4B), 73.3 (C-3A), 72.3 (C-3B), 70.0, 69.7 (2C, CH_2Allyl , C-6B), 68.0 (C-2B), 62.9 (C-6A), 61.0 (C-5B), 59.6 (C-2A), 26.1 (3C, $\text{C}(\text{CH}_3)_3\text{TBS}$), 25.8 (3C, $\text{C}(\text{CH}_3)_3\text{TBS}$), 21.3 (CH_3Ac), 18.6 ($\text{C}(\text{CH}_3)_3\text{TBS}$), 18.1 ($\text{C}(\text{CH}_3)_3\text{TBS}$), -4.6 (CH_3TBS), -4.7 (CH_3TBS), -4.9 (CH_3TBS), -5.0 (CH_3TBS); HRMS (ESI-TOF) m/z $[\text{M} + \text{NH}_4]^+$ calcd for $\text{C}_{38}\text{H}_{64}\text{Cl}_2[^{37}\text{Cl}]\text{N}_2\text{O}_{12}\text{Si}_2$ 903.3039; found 903.3040.

Data for (1→3)-linked α-glycoside 39b: R_f 0.48 (Tol/EtOAc 8:2); $[\alpha]_{\text{D}}^{20} +8.2$ (c 0.44, CHCl_3); ^1H NMR (600 MHz, CDCl_3) : δ (ppm) 7.51–7.50 (m, 2H, $2 \times \text{CH}_{\text{Ar}}$), 7.32–7.31 (m, 3H, $3 \times \text{CH}_{\text{Ar}}$), 6.69 (d, $J = 8.9$ Hz, 1H, NH), 5.83 (ddd, $J = 16.9$ Hz, $J = 10.8$ Hz, $J = 5.6$ Hz, 1H, CH_{Allyl}), 5.53 (d, $J = 2.7$ Hz, 1H, H-1B), 5.47 (s, 1H, CHPh), 5.27 (dd, $J = 17.2$ Hz, $J = 1.5$ Hz, 1H, $=\text{CHH}_{\text{Allyl}}$), 5.17 (dd, $J = 10.4$ Hz, $J = 1.3$ Hz, 1H, $=\text{CHH}_{\text{Allyl}}$), 4.90 (t, $J = 3.4$ Hz, 1H, H-3B), 4.57 (d, $J = 8.3$ Hz, 1H, H-1A), 4.32 (dd, $J = 12.9$ Hz, $J = 5.0$ Hz, 1H, $\text{CHH}_{\text{Allyl}}$), 4.29 (d, $J = 12.8$ Hz, 1H, H-6Ba), 4.05–3.98 (m, 3H, $\text{CHH}_{\text{Allyl}}$, H-6Bb, H-6Aa), 3.92–3.91 (m, 3H, H-4A, H-4B, H-5B), 3.83 (t, $J = 3.4$ Hz, 1H, H-2B), 3.82–3.75 (m, 3H, H-2A, H-3A, H-6Ab), 3.59 (d, $J = 1.2$ Hz, 1H, OH-4), 3.40 (ddd, $J = 9.1$ Hz, $J = 7.7$ Hz, $J = 4.8$ Hz, 1H, H-5A), 2.10 (s, 3H, CH_3Ac), 0.90 (s, 9H, $\text{C}(\text{CH}_3)_3\text{TBS}$), 0.84 (s, 9H, $\text{C}(\text{CH}_3)_3\text{TBS}$), 0.12 (s, 3H, CH_3TBS), 0.11 (s, 3H, CH_3TBS), 0.11 (s, 3H, CH_3TBS), 0.08 (s, 3H, CH_3TBS); $^{13}\text{C}\{^1\text{H}\}$ NMR (150 MHz, CDCl_3) : δ (ppm) 170.0 (COOR_{Ac}), 161.8 (CONH), 137.9 (C_{Ar}), 133.5 (CH_{Allyl}), 129.1 (CH_{Ar}), 128.1 (2C, $2 \times \text{CH}_{\text{Ar}}$), 126.7 (2C, $2 \times \text{CH}_{\text{Ar}}$), 118.0 ($=\text{CH}_2\text{Allyl}$), 101.8 (C-1B, $^1J_{\text{C1,H1}} = 175$ Hz), 101.3 (CHPh), 99.9 (C-1A, $^1J_{\text{C1,H1}} = 164$ Hz), 77.9 (C-4A*), 76.4 (C-3A), 73.7 (C-4B*), 72.9 (C-5A), 72.0 (C-3B), 70.12, 70.08 (2C, CH_2Allyl , C-6B), 67.9 (C-2B), 65.6 (C-6A), 60.6 (C-5B), 56.1 (C-2A), 25.9 (3C, $\text{C}(\text{CH}_3)_3\text{TBS}$), 25.8 (3C, $\text{C}(\text{CH}_3)_3\text{TBS}$), 21.3 (CH_3Ac), 18.2 ($\text{C}(\text{CH}_3)_3\text{TBS}$), 18.1 ($\text{C}(\text{CH}_3)_3\text{TBS}$), -4.7 (CH_3TBS), -4.8 (CH_3TBS), -5.47 (CH_3TBS), -5.51 (CH_3TBS); HRMS (ESI-TOF) m/z $[\text{M} + \text{NH}_4]^+$ calcd for $\text{C}_{38}\text{H}_{64}\text{Cl}_2[^{37}\text{Cl}]\text{N}_2\text{O}_{12}\text{Si}_2$ 903.3039; found 903.3067.

CHAPITRE 7 – C7 EPIMERIZATION OF BENZYLIDENE-PROTECTED β -D-IDOPYRANOSIDES BRINGS STRUCTURAL INSIGHTS INTO IDOSE CONFORMATIONAL FLEXIBILITY

***tert*-Butyldimethylsilyl 3-*O*-Acetyl-(*S*)-4,6-*O*-benzylidene-2-*O*-*tert*-butyldimethylsilyl- α -D-idopyranosyl-(1 \rightarrow 4)-3,6-di-*O*-benzyl-2-deoxy-2-trichloroacetamido- β -D-glucopyranoside (40).**

Donor **6b** (14.6 mg, 0.0275 mmol, 1.2 equiv), acceptor **36**⁵⁷⁷ (14.2 mg, 0.0229 mmol, 1.0 equiv), and tri-*tert*-butylpyridine (17.1 mg, 0.0688 mmol, 3.0 equiv) were dried together under high vacuum for 1 h. Then, activated 4 Å MS (58 mg) and dry DCE (410 μ L) were added. The suspension was stirred at rt under Ar atmosphere for 1 h, after which Me₂S₂ (6.1 μ L, 0.069 mmol, 3.0 equiv) and MeOTf (7.5 μ L, 0.069 mmol, 3.0 equiv) were successively added. The mixture was stirred at rt for 2 h and was then quenched by adding Et₃N, filtered over Celite, and concentrated under reduced pressure. The residue was purified by silica gel flash chromatography (Hex/EtOAc 95:5 to 8:2) to give α -glycoside **40** (6.9 mg, 29%) as a colorless oil: *R*_f 0.52 (Hex/EtOAc 7:3); [α]_D²⁰ +29 (*c* 0.68, CHCl₃); ¹H NMR (600 MHz, CDCl₃): δ (ppm) 7.48–7.47 (m, 2H, 2 \times CH_{Ar}), 7.37–7.33 (m, 5H, 5 \times CH_{Ar}), 7.30–7.28 (m, 7H, 7 \times CH_{Ar}), 7.24–7.23 (m, 1H, CH_{Ar}), 7.03 (d, *J* = 7.8 Hz, 1H, NH), 5.43 (s, 1H, CHPh), 5.34 (d, *J* = 2.4 Hz, 1H, H-1B), 5.12 (d, *J* = 7.0 Hz, 1H, H-1A), 4.94 (t, *J* = 3.7 Hz, 1H, H-3B), 4.73 (d, *J* = 10.9 Hz, 1H, CHH_{Bn}), 4.63 (d, *J* = 11.0 Hz, 1H, CHH_{Bn}), 4.60 (s, 2H, CH_{2Bn}), 4.18 (t, *J* = 8.4 Hz, 1H, H-3A), 4.13–4.10 (m, 2H, H-6Aa, H-4A), 3.91 (br s, 1H, H-4B), 3.87 (br d, *J* = 12.3 Hz, 1H, H-6Ab), 3.83 (dd, *J* = 10.8 Hz, *J* = 2.7 Hz, 1H, H-6Ba), 3.77–3.75 (m, 2H, H-6Bb, H-5B), 3.69 (t, *J* = 3.5 Hz, 1H, H-2B), 3.63–3.58 (m, 2H, H-2A, H-5A), 2.09 (s, 3H, CH_{3Ac}), 0.89 (s, 9H, C(CH₃)₃TBS), 0.74 (s, 9H, C(CH₃)₃TBS), 0.15 (s, 3H, CH₃TBS), 0.12 (s, 3H, CH₃TBS), 0.02 (s, 3H, CH₃TBS), -0.02 (s, 3H, CH₃TBS); ¹³C{¹H} NMR (150 MHz, CDCl₃): δ (ppm) 169.5 (COOR_{Ac}), 161.9 (CONH), 138.3 (C_{Ar}), 137.8 (C_{Ar}), 137.6 (C_{Ar}), 129.9–126.6 (15C, 15 \times CH_{Ar}), 101.2 (CHPh), 100.7 (C-1B, ¹J_{C1,H1} = 175 Hz), 94.1 (C-1A, ¹J_{C1,H1} = 163 Hz), 79.4 (C-3A), 75.2 (C-5A), 74.1 (C-4B), 73.9 (CH_{2Bn}), 72.5 (CH_{2Bn}), 72.2 (C-3B), 71.6 (C-4A), 69.6 (C-6B), 69.3 (C-6A), 68.2 (C-2B), 60.7 (C-5B), 59.5 (C-2A), 25.8 (3C, C(CH₃)₃TBS), 25.7 (3C, C(CH₃)₃TBS), 21.4 (CH_{3Ac}), 18.0 (C(CH₃)₃TBS), 17.9 (C(CH₃)₃TBS), -4.1 (CH₃TBS), -4.5 (CH₃TBS), -4.7 (CH₃TBS), -5.0 (CH₃TBS); HRMS (ESI-TOF) *m/z* [M + NH₄]⁺ calcd for C₄₉H₇₂Cl₃N₂O₁₂Si₂ 1041.3684; found 1041.3683.

CHAPITRE 7 – C7 EPIMERIZATION OF BENZYLIDENE-PROTECTED β -D-IDOPYRANOSIDES BRINGS STRUCTURAL INSIGHTS INTO IDOSE CONFORMATIONAL FLEXIBILITY

***tert*-Butyldimethylsilyl 3-*O*-Benzyl-(*S*)-4,6-*O*-benzylidene-2-*O*-*tert*-butyldimethylsilyl- α -D-idopyranosyl-(1 \rightarrow 4)-3,6-di-*O*-benzyl-2-deoxy-2-trichloroacetamido- β -D-glucopyranoside (41 α) and *tert*-Butyldimethylsilyl 3-*O*-Benzyl-(*S*)-4,6-*O*-benzylidene-2-*O*-*tert*-butyldimethylsilyl- β -D-idopyranosyl-(1 \rightarrow 4)-3,6-di-*O*-benzyl-2-deoxy-2-trichloroacetamido- β -D-glucopyranoside (41 β).**

Donor **24** (11.2 mg, 0.0194 mmol, 1.2 equiv), acceptor **36**⁵⁷⁷ (10.0 mg, 0.0162 mmol, 1.0 equiv), and tri-*tert*-butylpyridine (12.0 mg, 0.0485 mmol, 3.0 equiv) were dried together under high vacuum for 1 h. Then, activated 4 Å MS (45 mg) and dry DCE (290 μ L) were added. The suspension was stirred at rt under Ar atmosphere for 1 h, after which Me₂S₂ (4.3 μ L, 0.049 mmol, 3.0 equiv) and MeOTf (5.3 μ L, 0.049 mmol, 3.0 equiv) were successively added. The mixture was stirred at rt for 2 h and was then quenched by adding Et₃N, filtered over Celite, and concentrated under reduced pressure. The residue was purified by silica gel flash chromatography (Hex/EtOAc 95:5 to 75:25) to give α -glycoside **41 α** (10.1 mg, 58%) as a colorless oil along with β -glycoside **41 β** (1.4 mg, 8%) as a white amorphous solid.

Data for α -glycoside 41 α : R_f 0.41 (Hex/EtOAc 8:2); $[\alpha]_D^{20}$ +27 (c 0.84, CHCl₃); ¹H NMR (600 MHz, CDCl₃): δ (ppm) 7.45–7.44 (m, 2H, 2 \times CH_{Ar}), 7.35–7.25 (m, 18H, 18 \times CH_{Ar}), 6.97 (d, J = 7.8 Hz, 1H, NH), 5.43 (s, 1H, CHPh), 5.30 (d, J = 4.6 Hz, 1H, H-1B), 5.13 (d, J = 7.4 Hz, 1H, H-1A), 4.82 (d, J = 10.8 Hz, 1H, CHH_{Bn}), 4.71 (d, J = 11.8 Hz, 1H, CHH_{Bn}), 4.63 (d, J = 11.8 Hz, 1H, CHH_{Bn}), 4.61–4.59 (m, 2H, CHH_{Bn}, CHH_{Bn}), 4.55 (d, J = 12.2 Hz, 1H, CHH_{Bn}), 4.21 (dd, J = 9.7 Hz, J = 8.2 Hz, 1H, H-3A), 4.09–4.06 (m, 2H, H-4A, H-6Aa*), 4.04 (t, J = 2.5 Hz, 1H, H-4B), 3.87 (dd, J = 12.8 Hz, J = 2.2 Hz, 1H, H-6Ab*), 3.74–3.70 (m, 2H, H-2B, H-6Ba*), 3.67–3.59 (m, 4H, H-6Bb*, H-5B, H-5A, H-3B), 3.54 (dt, J = 10.4 Hz, J = 7.6 Hz, 1H, H-2A), 0.89 (s, 9H, C(CH₃)₃TBS), 0.80 (s, 9H, C(CH₃)₃TBS), 0.15 (s, 3H, CH₃TBS), 0.12 (s, 3H, CH₃TBS), 0.05 (s, 3H, CH₃TBS), –0.01 (s, 3H, CH₃TBS); ¹³C{¹H} NMR (150 MHz, CDCl₃): δ (ppm) 161.8 (CONH), 138.5 (C_{Ar}), 138.3 (C_{Ar}), 138.0 (C_{Ar}), 137.9 (C_{Ar}), 129.0–126.5 (20C, 20 \times CH_{Ar}), 101.1 (C-1B, ¹J_{C1,H1} = 175 Hz), 100.5 (CHPh), 94.2 (C-1A, ¹J_{C1,H1} = 162 Hz), 80.4 (C-5A*), 80.0 (C-3A), 77.7 (C-4B), 75.0 (C-3B*), 73.6 (CH₂Bn), 72.8 (CH₂Bn), 72.6 (CH₂Bn), 71.6 (C-4A), 71.1 (C-2B), 69.5 (C-6B*), 69.3 (C-6A*), 61.9 (C-5B), 60.2 (C-2A), 26.0 (3C, C(CH₃)₃TBS), 25.8 (3C, C(CH₃)₃TBS), 18.2

CHAPITRE 7 – C7 EPIMERIZATION OF BENZYLIDENE-PROTECTED β-D-IDOPYRANOSIDES BRINGS STRUCTURAL INSIGHTS INTO IDOSE CONFORMATIONAL FLEXIBILITY

(C(CH₃)₃TBS), 18.0 (C(CH₃)₃TBS), -3.8 (CH₃TBS), -4.0 (CH₃TBS), -4.4 (CH₃TBS), -5.1 (CH₃TBS); HRMS (ESI-TOF) *m/z* [M + NH₄]⁺ calcd for C₅₄H₇₆Cl₂[³⁷Cl]N₂O₁₁Si₂ 1091.4035; found 1091.3980.

Data for β-glycoside 41β: *R_f* 0.31 (Hex/EtOAc 8:2); [α]_D²⁰ -7.5 (*c* 0.20, CHCl₃); ¹H NMR (600 MHz, CDCl₃) : δ (ppm) 7.53–7.51 (m, 4H, 4 × CH_{Ar}), 7.33–7.28 (m, 11H, 11 × CH_{Ar}), 7.26–7.23 (m, 3H, 3 × CH_{Ar}), 7.13–7.12 (m, 2H, 2 × CH_{Ar}), 6.98 (d, *J* = 7.4 Hz, 1H, NH), 5.46 (s, 1H, CHPh), 5.39 (d, *J* = 9.5 Hz, 1H, CHH_{Bn}), 5.20 (d, *J* = 7.8 Hz, 1H, H-1A), 4.88 (br s, 1H, H-1B), 4.66 (d, *J* = 11.9 Hz, 1H, CHH_{Bn}), 4.58 (d, *J* = 11.8 Hz, CHH_{Bn}), 4.54 (d, *J* = 12.3 Hz, 1H, CHH_{Bn}), 4.45 (d, *J* = 12.3 Hz, 1H, CHH_{Bn}), 4.43 (d, *J* = 9.5 Hz, 1H, CHH_{Bn}), 4.24 (d, *J* = 12.6 Hz, 1H, H-6Ba), 4.14–4.07 (m, 2H, H-3A, H-4A), 3.97 (dd, *J* = 12.6 Hz, *J* = 2.1 Hz, 1H, H-6Bb), 3.89 (br s, 1H, H-4B*), 3.76–3.74 (m, 2H, H-6Aa, H-2B), 3.69 (t, *J* = 2.4 Hz, 1H, H-3B*), 3.63 (dd, *J* = 11.0 Hz, *J* = 3.6 Hz, 1H, H-6Ab), 3.54 (s, 1H, H-5B), 3.52–3.51 (m, 1H, H-5A), 3.36 (td, *J* = 9.9 Hz, *J* = 7.6 Hz, 1H, H-2A), 0.89 (s, 9H, C(CH₃)₃TBS), 0.76 (s, 9H, C(CH₃)₃TBS), 0.13 (s, 3H, CH₃TBS), 0.10 (s, 3H, CH₃TBS), 0.05 (s, 3H, CH₃TBS), -0.05 (s, 3H, CH₃TBS); ¹³C{¹H} NMR (150 MHz, CDCl₃) : δ (ppm) 161.7 (CONH), 138.4 (2C, 2 × C_{Ar}), 138.3 (C_{Ar}), 137.9 (C_{Ar}), 129.6–127.1 (20C, 20 × CH_{Ar}), 101.8 (CHPh), 99.7 (C-1B, ¹*J*_{Cl,H1} = 158 Hz), 94.5 (C-1A, ¹*J*_{Cl,H1} = 162 Hz), 79.2 (C-3B*), 78.2, 77.8 (2C, C-3A, C-4A), 75.9 (CH₂Bn), 75.3 (C-5A), 73.1 (CH₂Bn), 72.7, 72.6 (2C, CH₂Bn, C-4B*), 69.7 (C-6B), 68.8 (C-6A), 68.5 (C-2B), 67.5 (C-5B), 60.9 (C-2A), 25.8 (18C, 2 × C(CH₃)₃TBS), 18.3 (C(CH₃)₃TBS), 18.1 (C(CH₃)₃TBS), -4.0 (CH₃TBS), -4.1 (CH₃TBS), -4.9 (CH₃TBS), -5.1 (CH₃TBS); HRMS (ESI-TOF) *m/z* [M + NH₄]⁺ calcd for C₅₄H₇₆Cl₂[³⁷Cl]N₂O₁₁Si₂ 1091.4035; found 1091.4047.

DFT Calculations.

3D models of simplified compounds **22a–22c** were generated on Spartan Student v8 and a conformer search was done with these models using MMFF force field. The conformers were then subjected to a geometrical optimization with the help of Gaussian⁵⁸¹ using the functional and basis set B3LYP/6-31G+(d,p). All DFT calculation were done using an ultrafine grid. Interaction with the solvent (dichloroethane) was taken into account with the polarizable continuum model (IEF-

CHAPITRE 7 – C7 EPIMERIZATION OF BENZYLIDENE-PROTECTED β-D-IDOPYRANOSIDES BRINGS STRUCTURAL INSIGHTS INTO IDOSE CONFORMATIONAL FLEXIBILITY

PCM). The thermochemical parameters were derived from the calculation of the frequencies, which was also used to confirm that true minima were obtained. The values of free energies were extracted to compute the Boltzmann distribution, which was used to select the conformers that would be used for further calculations (>1%). Thermochemical parameters of the selected conformers were again determined using the level of theory B3LYP/6-311++G(2d,2p) and the Boltzmann distribution was computed with the extracted values. ¹H and ¹³C chemical shifts of the selected conformers were predicted in chloroform through the calculation of the shielding tensors at the level of theory mPW1PW91/6-311+G(2d,p). The shielding tensors were averaged based on the respective Boltzmann weight of each conformer determined for both levels of theory (B3LYP/6-31G+(d,p) and B3LYP/6-311G++(2d,2p), and the chemical shifts were derived by scaling the shielding tensors against the experimental values. Theoretical ¹H-¹H coupling constants were determined by NMR single-point calculation and were again averaged based on the respective Boltzmann weight of each conformer determined for both levels of theory. Interproton distances were extracted from the optimized geometries on Spartan.

CHAPITRE 8 : TOWARDS THE SYNTHESIS OF AN IDOSE-CONTAINING DISACCHARIDE MIMIC OF *CAMPYLOBACTER JEJUNI* HS:4C CAPSULAR POLYSACCHARIDE

Maude Cloutier,^a Nitish Verma,^a and Charles Gauthier^{a*}

^a*Centre Armand-Frappier Santé Biotechnologie, Institut National de la Recherche Scientifique (INRS), 531, boulevard des Prairies, Laval (Québec), Canada, H7V 1B7.*

Article en préparation

Titre français : Vers la synthèse d'un disaccharide doté d'une unité idose mimant le polysaccharide capsulaire de *Campylobacter jejuni* HS:4c.

Contribution auteurs : Maude Cloutier (60%) et Nitish Verma (40%) ont réalisé la synthèse des composés et les études de glycosylation. Maude Cloutier a procédé à la caractérisation des molécules. Maude Cloutier a rédigé le brouillon d'article et Charles Gauthier l'a révisé.

8.1 Résumé

Campylobacter jejuni est l'agent causal de la campylobactériose, considérée comme l'une des principales causes de maladies diarrhéiques dans le monde. En raison du fardeau de santé publique que représente cette bactérie à Gram négatif, il existe un besoin urgent de développer des mesures prophylactiques pour prévenir des infections à *C. jejuni*. Des études récentes ont mis en évidence que son polysaccharide capsulaire (CPS), qui consiste en une unité répétitive disaccharidique de structure $[\rightarrow 3)\text{-6-désoxy-}\beta\text{-D-ido-heptopyranoside-(1}\rightarrow 4)\text{-2-désoxy-2-acétamido-}\beta\text{-D-glucopyranoside-(1}\rightarrow]$ non-stœchiométriquement substituée de groupements méthyl phosphoramidate (MeOPN), constitue un antigène potentiel pour le développement de vaccins. Bien que certaines approches synthétiques aient été récemment rapportées, elles présentent l'inconvénient de nécessiter de nombreuses étapes de fonctionnalisation et reposent sur des méthodes indirectes pour accéder à l'unité 1,2-*cis*- β -idoside. Pour pallier ces problèmes, nous présentons ici nos travaux vers le développement d'une approche rapide pour accéder à des mimes disaccharidiques du CPS de *C. jejuni* HS:4c. Nos travaux reposent sur l'accès à un stade précoce à la configuration *ido* via le réarrangement de Paulsen suivi par une homologation C6 \rightarrow C7 en quatre étapes médiées par une réaction de type MOM-Wittig. À l'aide d'une étude approfondie de glycosylation d'une variété de donneurs d'idose, nous montrons que les idosylations β -stéréosélectives directes sont à portée de main à l'aide d'approches intra- ou intermoléculaires. Une fois complétés, ces travaux ont le potentiel d'ouvrir la voie au développement de vaccins synthétiques contre *C. jejuni* HS:4c.

8.2 Abstract

Campylobacter jejuni is the causative agent of campylobacteriosis, considered one of the leading causes of diarrheal diseases worldwide. Due to the public health burden that this Gram-negative bacterium represents, there is an urgent need to develop prophylactic measures to prevent *C. jejuni* infections. Recent studies have highlighted that its capsular polysaccharide (CPS), which consists in a disaccharide repeating unit of structure $[\rightarrow 3)\text{-6-deoxy-}\beta\text{-D-ido-heptopyranoside-(1}\rightarrow 4)\text{-2-deoxy-2-acetamido-}\beta\text{-D-glucopyranoside-(1}\rightarrow]$ non-stoichiometrically modified with methyl phosphoramidate (MeOPN) moieties, could be a potent antigen for the development of vaccines.

Although some synthetic approaches have recently been reported, they present the drawback of requiring extensive building block modification and relies on indirect methods to access the 1,2-*cis*- β -idoside moiety. To address this, we herein present our work towards the development of an expeditious approach to access disaccharide mimics of *C. jejuni* HS:4c CPS. Our work relies on the early-stage access to the *ido*-configuration *via* the Paulsen rearrangement followed by a four-step MOM-Wittig-mediated C6→C7 homologation. Through an extensive glycosylation study involving a variety of idosyl donors, we show that direct β -stereoselective idosylations are within reach through either intra- or intermolecular approaches. This work has the potential to pave the way for the development of synthetic vaccines against *C. jejuni* HS:4c.

8.3 Introduction

Campylobacter spp. is a major diarrheal pathogen that has been classified as a serious threat by the Centers for Disease Control and Prevention (CDC) in their 2019 Antibiotic Resistance Threats Report⁴²⁴ and as a high priority pathogen by the World Health Organization (WHO).⁵⁸² It is estimated that *Campylobacter* spp. cause up to 400 million cases of campylobacteriosis each year, of which up to 90% are linked to the encapsulated Gram negative bacterium *C. jejuni*.⁴¹⁵⁻⁴¹⁷ Although campylobacteriosis—typically characterized by bloody diarrhea, abdominal pain, headaches, nausea and fever⁴¹⁸—is generally considered to be self-limiting, severe cases may require hospitalization and administration of antibiotics, and may sometimes be deadly. Moreover, the growing antibiotic resistance of *C. jejuni* makes the fight against this bacterium particularly complex.⁴²⁰⁻⁴²² *C. jejuni* infections additionally form the predominant risk factor associated with Guillain-Barré syndrome.⁴²⁵ Indeed, lipooligosaccharides (LOS) anchored in the outer membrane of this bacterium contain β -D-galactoside and α -N-acetyl-D-neuraminic acid units mimicking human gangliosides,^{426, 427} such that antibodies directed against these LOS can induce an autoimmune response resulting in Guillain-Barré syndrome.

The burden of *C. jejuni*-associated illnesses highlights the need for the development of prophylactic measures against this bacterium.⁴⁴ In that regard, *C. jejuni* CPS have been shown to stand as exquisite targets for the development of synthetic oligosaccharide-based vaccines because of their key roles as virulence factors and in the mediation of host-pathogen interactions.⁴³⁹⁻⁴⁴²

CHAPITRE 8 – TOWARDS THE SYNTHESIS OF AN IDOSE-CONTAINING DISACCHARIDE MIMIC OF *CAMPYLOBACTER JEJUNI* HS:4C CAPSULAR POLYSACCHARIDE

More significantly, conjugates of *C. jejuni* HS:4c and HS:23/36 CPS have been shown to be effective vaccines in animal models.^{493, 494}

Because *C. jejuni* HS:4c is among the 10 serotypes accounting for up to 70% of all *C. jejuni* infections in Africa, Middle East, Southeast Asia, and South America,^{121, 464, 583, 584} there is an increased interest in the preparation of synthetic mimics of its CPS, which possesses distinctive structural characteristics. Its repeating unit consists in a disaccharide containing a rare 6-deoxy-D-*ido*-heptopyranoside unit linked to a GlcNAc moiety through a 1,2-*cis*- β glycosidic linkage (Fig. 1).^{120, 121} The hydroxyl groups at C2 and C7 of the *ido* unit are additionally non-stoichiometrically decorated with methyl phosphoramidate (MeOPN) moieties. Remarkably, these latter have been found in about 70% of isolates of *C. jejuni*, whereas to date they have never been observed in other living organisms.⁴⁷³ It has been suggested that these MeOPN moieties could be involved in the process of host colonization and serum resistance.^{443, 474}

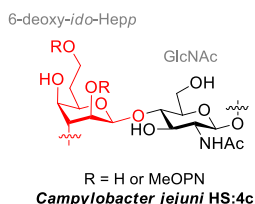


Figure 8.1. Structure of *C. jejuni* HS:4c CPS repeating unit

In that context, synthesis of *C. jejuni* HS:4c CPS mimics has been given more and more attention in recent years. Challenges related to their synthesis, *i.e.*, the need to synthetically achieve the rare *ido* configuration and the presence of a 1,2-*cis*- β glycosidic linkage, have lately been addressed via indirect approaches. Reported methods involved the formation of 1,2-*trans*- β -linked galactosides (Fig. 2A)^{504, 512} or gulosides (Fig. 2B)⁵⁴⁰ through anchimeric assistance of esters at C2. This was then followed by a double (C2/C3, from *galacto*) or mono (C2, from *gulo*) epimerization step to access the *ido* configuration as well as the 1,2-*cis*- β glycosidic linkage. In both cases, the 6-deoxy-hepto configuration was achieved prior to the glycosylation reaction, either via homologation of the galactoside precursor or via conversion of an allyl α -D-C-galactoside into the corresponding 6-deoxy-D-*gulo*-heptoside through a C1-to-C5 switch protocol.

CHAPITRE 8 – TOWARDS THE SYNTHESIS OF AN IDOSE-CONTAINING DISACCHARIDE MIMIC OF CAMPYLOBACTER JEJUNI HS:4C CAPSULAR POLYSACCHARIDE

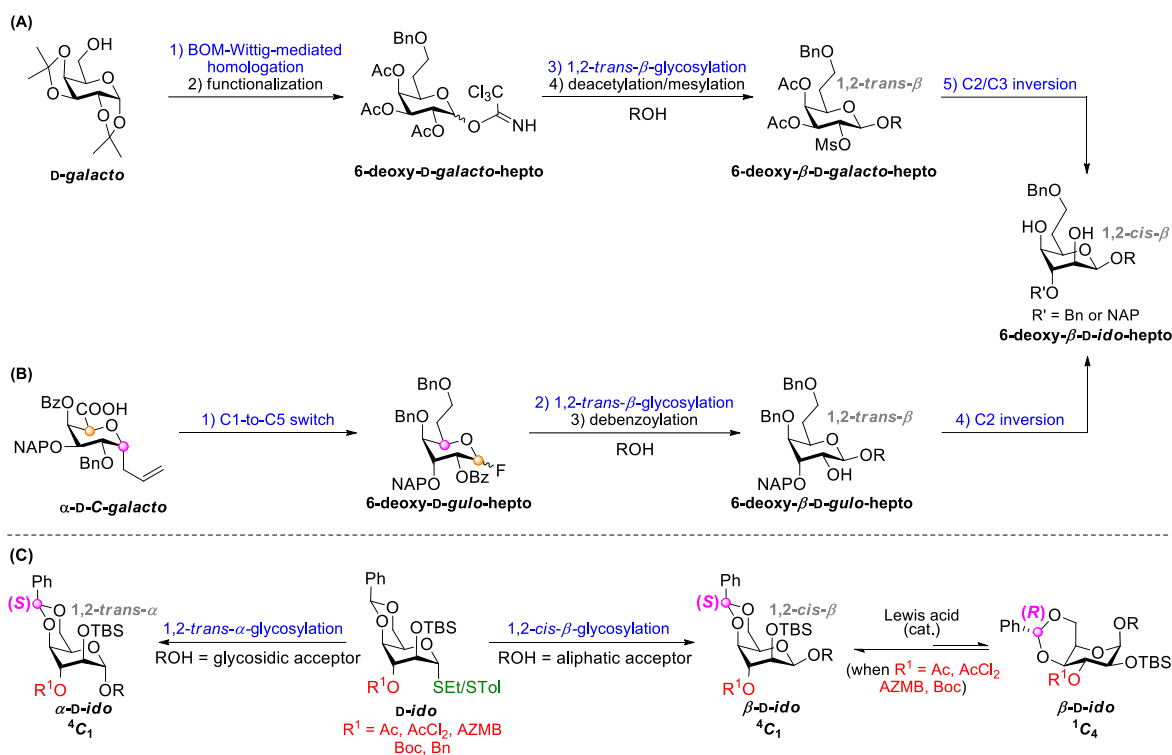


Figure 8.2. Ling's (A), Li's (B) and our (C) approaches to access 1,2-*cis*-β-linked idosides

Because both approaches involved extensive protecting groups manipulation and because an efficient direct β-glycosylation approach of D-*ido*-configured sugars had yet to be disclosed, we recently reported a β-stereoselective glycosylation method using benzylidene-protected thioidosyl donors (Fig. 2C).⁵⁸⁵ Unfortunately, this β-stereoselectivity was specific to aliphatic acceptors, as almost complete α-stereoselectivity was observed when the glycosylation was performed using glycosidic acceptors of diminished nucleophilicity. In this regard, we have been interested in pursuing our work towards the development of a β-idosylation method enabling direct access to the disaccharidic repeating unit of *C. jejuni* HS:4c CPS, which would be highly beneficial to the development of prophylactic tools against this bacterium. We herein report our progress towards this goal through the investigation of idosylation reactions *via* intramolecular aglycon delivery (IAD) and intermolecular approaches.

8.4 Results and Discussion

8.4.1 Intramolecular aglycon delivery approach

As previously mentioned, one of the challenges related to the synthesis of *C. jejuni* HS:4c CPS mimics is the presence of a 1,2-*cis*- β glycosidic bond linking the idoside to the GlcNAc moiety. While 1,2-*trans*- β linkages can readily be accessed through anchimeric assistance of an ester at C2, formation of 1,2-*cis*- β glycosidic bonds is nontrivial. Although a variety of methods have been developed for the formation of such linkages, IAD remains one of the most promising approaches.^{133, 553} Initially introduced by Hindsgaul,¹³⁴ this approach has been widely employed for the stereoselective preparation of challenging β -mannosides. IAD has since been used for the synthesis of a large variety of 1,2-*cis*-linked sugars including α -glucosides, α -arabinofuranosides and β -rhamnosides¹³³ and has been significantly improved by Ito and Ogawa through the development of the *p*-methoxybenzyl (PMB)-⁵⁸⁶⁻⁵⁸⁸ and 2-naphthylmethyl (NAP)-mediated⁵⁸⁹ IAD procedure.⁵⁹⁰ This strategy, which takes advantage of the stereochemistry at C2, involves a two-step tethering-glycosylation procedure. As depicted in Figure 3, NAP-mediated IAD (or PMB-mediated IAD) entails the oxidative activation of the NAP (or PMB) group in presence of the aglycon, resulting in the formation of mixed acetals. Subsequent activation of the leaving group sets in motion the rearrangement leading to the 1,2-*cis*-glycoside. Having had success with NAP-mediated IAD for the synthesis of *Burkholderia pseudomallei* and *Burkholderia mallei* CPS mimics bearing 1,2-*cis*- β -linked 6-deoxy-D-manno-heptosides moieties,²⁹³ we envisioned that this approach could be taken advantage of for the preparation of β -disaccharides related to *C. jejuni* HS:4c CPS.

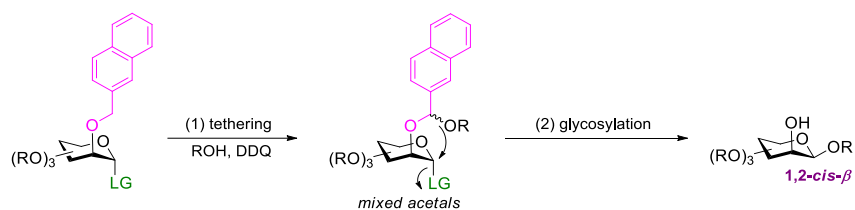


Figure 8.3. NAP-mediated IAD procedure

CHAPITRE 8 – TOWARDS THE SYNTHESIS OF AN IDOSE-CONTAINING DISACCHARIDE MIMIC OF CAMPYLOBACTER JEJUNI HS:4C CAPSULAR POLYSACCHARIDE

As shown in Figure 4A, disaccharides **1** and **2**, representing the repeating unit of *C. jejuni* HS:4c CPS, were chosen as synthetic targets. We aimed to synthesize two different disaccharides differing only in the substitution pattern of position C7 of the *ido* unit. Whereas this position would remain unprotected in compound **1**, disaccharide **2** would instead bear a 7-*O*-MeOPN group. Considering that the MeOPN modification is non-stoichiometric in *C. jejuni* CPS, we envisioned that synthesizing both disaccharides could help shed light on the antigenic potential of this unique group. These disaccharides would additionally carry an aminolinker at the reducing end to enable their conjugation to carrier proteins for future antigenicity and immunogenicity assays. We imagined that these target disaccharides could be accessed through NAP- or PMB-mediated IAD using 6-deoxy-D-*ido*-heptoside **A** and GlcNAc derivative **3**.⁵⁷⁷ Donor **A** would be orthogonally protected with a 7-*O*-levulinoyl (Lev) group which would later allow selective introduction of the MeOPN moiety at this position. In addition to the nature of the protecting group at C2 (PMB and NAP), we also planned on investigating different leaving groups. Considering the instability of the mixed acetals and the poor reactivity of thiotolyl donors in IAD, combined with the fact that IAD reactions are sometimes less reliable than standard intermolecular reactions, we envisioned that changing the nature of the leaving group (SEt, STol, S(O)Tol, and *o*-alkynylbenzoyl [*o*ABz]) might increase the mixed acetals stability and the reaction kinetics, overall resulting in better reaction yields. We expected that donor **A** could be accessed via homologation of 6-OH idoside **B** bearing either an SEt or STol group at the anomeric position, which could readily be converted into the corresponding *o*ABz and S(O)Tol donors subsequently to the homologation reaction.

CHAPITRE 8 – TOWARDS THE SYNTHESIS OF AN IDOSE-CONTAINING DISACCHARIDE MIMIC OF CAMPYLOBACTER JEJUNI HS:4C CAPSULAR POLYSACCHARIDE

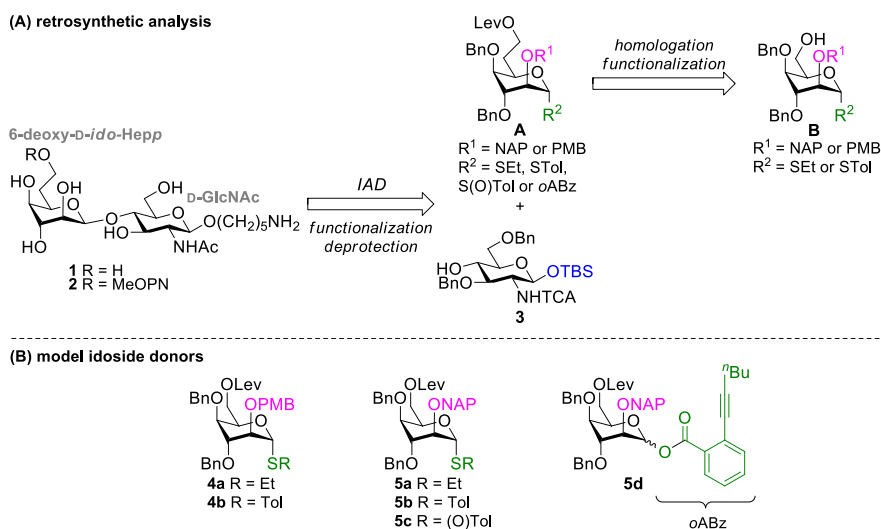


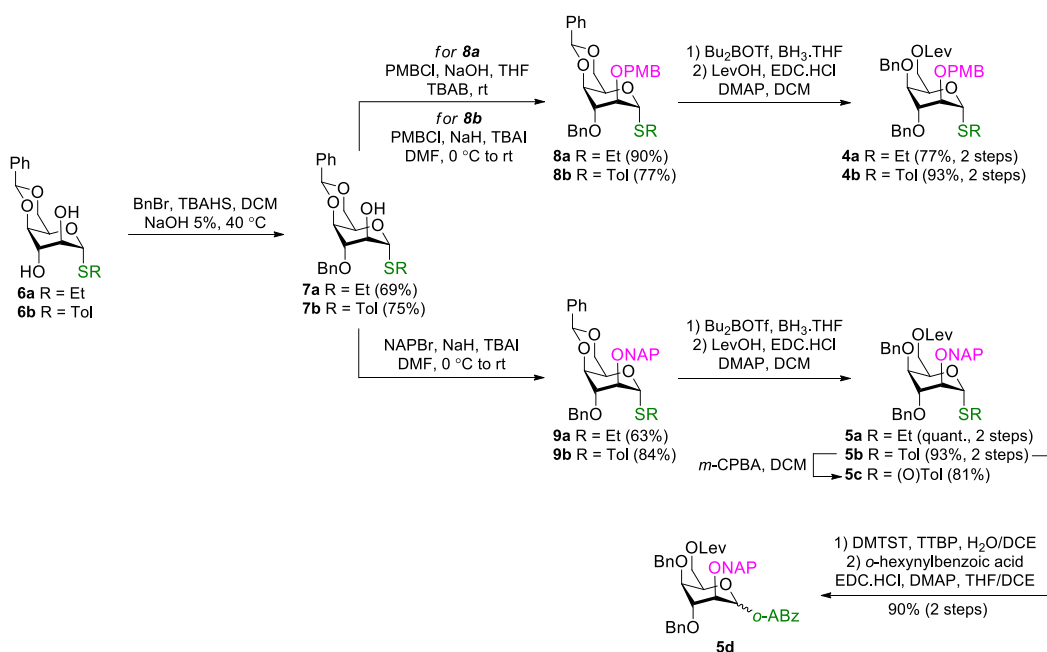
Figure 8.4. (A) Retrosynthetic analysis of disaccharides **1** and **2**; (B) Target model idoside donors

Anticipating that 6-deoxy-D-ido-heptoside **A** would be tedious and expensive to prepare, we designed a series of *ido*-configured hexose donors (**4a**, **4b**, **5a–5d**) that would be used as model compounds for the investigation of the IAD approach (Fig. 4B). We envisioned that reactivity of these hexosides would be similar to that of the corresponding heptosides. Coherently with our retrosynthetic analysis, our series of model compounds would either bear a NAP or PMB group at C2 as well as a variety of leaving groups at the anomeric position. Results with these model compounds would then guide the synthesis of donor **A** bearing the optimal functionalities at C1 and C2.

Synthesis of these model donors is described in Scheme 1. Our synthetic scheme took advantage of our previously reported *ido*-configured diols **6a** and **6b**,⁵⁸⁵ both synthesized in three-steps from peracetylated α -D-idopyranoside accessed *via* the Paulsen acetoxonium rearrangement of peracetylated β -D-glucopyranoside.⁵³⁹ Benzylolation of these diols was performed under phase transfer conditions⁵⁶⁵ and successfully afforded 3-*O*-Bn intermediates **7a** and **7b** with good regioselectivity. These latter were then *para*-methoxybenzylated at C2. Interestingly, when thioethyl intermediate **7a** was employed, incomplete conversion was observed under the action of NaH. Fortunately, when using powdered NaOH in THF,⁵⁹¹ the reaction was performed with an excellent yield. Then, the benzylidene acetal was regioselectively opened under reductive

CHAPITRE 8 – TOWARDS THE SYNTHESIS OF AN IDOSE-CONTAINING DISACCHARIDE MIMIC OF CAMPYLOBACTER JEJUNI HS:4C CAPSULAR POLYSACCHARIDE

conditions,⁵⁹² and the resulting free 6-OH was levulinoylated to yield model compounds **4a** and **4b**. In parallel, alcohols **7a** and **7b** were converted into the corresponding NAP ethers **9a** and **9b** under the action of NaH and NAPBr. Regioselective opening of the benzylidene ring and subsequent levulinoylation afforded compounds **5a** and **5b** in excellent yields. The latter was either oxidized using *m*-CPBA to access target sulfoxide **5c** or hydrolyzed under the action of dimethyl(methylthio)sulfonium trifluoromethanesulfonate (DMTST) and esterified with *o*-hexynylbenzoic acid⁵⁹³ to form *o*ABz donor **5d**.



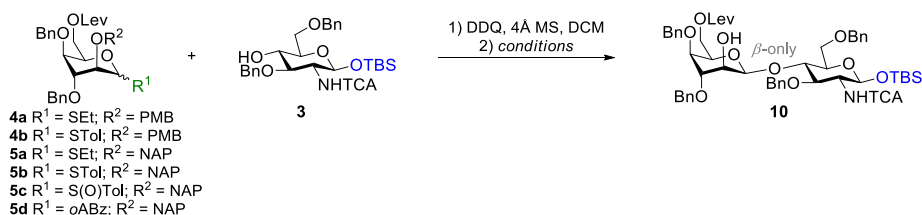
Scheme 8.1. Synthesis of idoside donors **4a**, **4b**, and **5a–5d**

With these model compounds in hand, we set out to investigate the IAD reaction (Table 1). For all entries, the tethering step between the donors and GlcNAc acceptor **3** was performed through the oxidative action of 2,3-dichloro-5,6-dicyano-1,4-benzoquinone (DDQ) in DCM under anhydrous conditions to yield the corresponding mixed acetals, which were used for the glycosylation step without further purification. Additionally, tri-*tert*-butylpyridine (TTBP) was used as an acid scavenger⁵⁵³ during the glycosylation step in the presence of 4 Å molecular sieves (MS). Our study demonstrated that when the glycosylation was performed using thioethyl donor **4a** bearing a PMB

CHAPITRE 8 – TOWARDS THE SYNTHESIS OF AN IDOSE-CONTAINING DISACCHARIDE MIMIC OF CAMPYLOBACTER JEJUNI HS:4C CAPSULAR POLYSACCHARIDE

group at C2 under the action of DMTST in DCE at 40 °C, β -disaccharide **10** could be isolated in 30% yield as the sole anomer (entry 1), as confirmed by NMR analysis ($^1J_{C1-H1} = 163$ Hz).⁵⁶⁰ Similar results were obtained when the same reaction was performed using MeOTf as the promoter (entry 2) or when thiotolyl donor **4b** was activated with DMTST (entry 3). On the other hand, performing the reaction in toluene was essentially unsuccessful (entry 4). We were then interested in performing the reaction using NAP-protected donors **5a-5d**, hoping the IAD yield could be improved. We however quickly observed that thioethyl donor **5a** was unstable under the employed conditions (entry 5). Switching to thiotolyl donor **5b** fortunately enabled access to β -disaccharide **10** in 28% yield (entry 6), but changing the acceptor equivalents (entry 7) or increasing the temperature (entry 8) did not improve the overall yield. Disappointedly, contrary to what we had hoped, performing the reaction with sulfoxide and *o*ABz idosyl donors **5c** and **5d**, respectively, proved unsuccessful (entries 9-12).

Table 8.1. Intramolecular aglycon delivery using idoside donors **4a**, **4b**, and **5a-5d**



entry	R ¹	R ²	promoter	solvent	T (°C)	time (h)	yield (%) ^a
1	SEt	PMB	DMTST	DCE	40	0.5	30
2	SEt	PMB	MeOTf	DCE	40	19	28
3	STol	PMB	DMTST	DCE	40	18	27
4	STol	PMB	DMTST	tol	40	18	traces
5	SEt	NAP	DMTST	DCE	40	17	N/A ^c
6	STol	NAP	DMTST	DCE	40	18	28
7^b	STol	NAP	DMTST	DCE	40	18	24
8	STol	NAP	DMTST	DCE	70	18	26
9	S(O)Tol	NAP	Tf ₂ O	DCM	-78 to rt	17	N/A ^c
10	S(O)Tol	NAP	Tf ₂ O	DCM	-78 to -58	1	traces
11	<i>o</i> ABz	NAP	NIS/TMSOTf	DCE	0 to rt	4	N/A ^c
12	<i>o</i> ABz	NAP	PPh ₃ AuCl/AgOTf	DCM	-40 to rt	2	N/A ^c

^aisolated yield; ^b1.0 equiv. of acceptor instead of the usual 1.2 equiv.; ^cdecomposition.

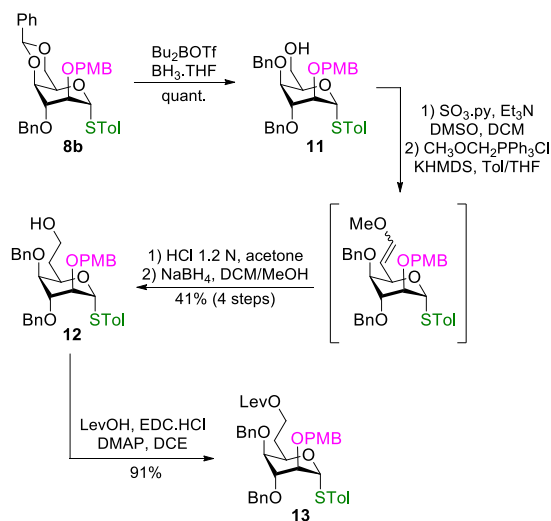
Although the yields were somewhat low, these results nonetheless established that the IAD procedure was successful and completely β -stereoselective when donors **4a**, **4b** and **5b** were employed. We thus decided to move on to the homologation step to access the three corresponding heptosides, which would then be used to further screen and optimize the IAD reaction.

Recently, Ling and co-workers reported the attempted homologation of an *ido*-configured β -hexopyranoside through a three-step sequence involving (1) oxidation of the 6-OH; (2) Wittig olefination; and (3) hydroboration-oxidation of the resulting terminal alkene.⁵¹¹ However, they observed that when the one-carbon elongation was performed with methyltriphenylphosphorane as the ylide, the resulting compound predominantly existed in the ¹C₄ conformation instead of the native ⁴C₁ chair. This change, which was attributed to the loss of intramolecular H-bonds that otherwise stabilized the ⁴C₁ conformation,⁵¹¹ oriented the C5 alkene axially, thus increasing its steric hindrance and causing the hydroboration step to be unsuccessful. Following the oxidation step, we thus envisioned that introducing the seventh carbon through a methoxymethyl (MOM)-Wittig reaction could prevent this conformational switch to occur. The formed enol ether could then readily undergo a two-step sequence entailing acid hydrolysis followed by reduction of the resulting C7 aldehyde.

This strategy was first attempted using the corresponding 6-OH thiotolyl idoside bearing a NAP group at C2. However, we soon observed that while the oxidation under Parikh-Doering conditions⁵⁹⁴ could be cleanly performed, the MOM-Wittig reaction predominantly led to formation of the corresponding α,β -unsaturated aldehyde via the base-mediated elimination of 1,2-*trans*-oriented H5 and 4-*O*-Bn. Even when using a less hindered ylide, *i.e.*, methyltriphenylphosphorane, the same phenomenon was observed. Although better results were achieved when toluene was used as solvent instead of THF and when the reaction was performed at higher temperatures (0 °C vs -78 °C), formation of the α,β -unsaturated aldehyde was systematically observed. We hypothesized that this could be attributed to the steric hindrance caused by the axial 2-*O*-NAP combined to its significant rigidity. We therefore decided to abandon this compound and focus on the idosides bearing a PMB group at C2. Unfortunately, the corresponding 6-OH thioethyl idoside was rapidly put aside as it was found to be highly unstable

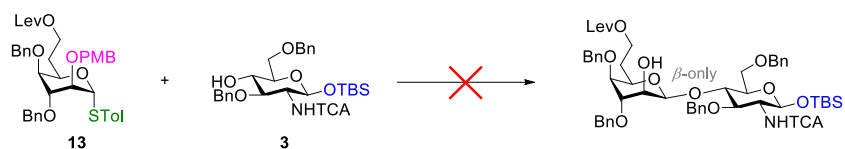
CHAPITRE 8 – TOWARDS THE SYNTHESIS OF AN IDOSE-CONTAINING DISACCHARIDE MIMIC OF CAMPYLOBACTER JEJUNI HS:4C CAPSULAR POLYSACCHARIDE

during the oxidation step. Our last potential thiotolyl idoside was thus employed for the optimization of the four-step homologation sequence. As depicted in Scheme 2, Bu₂BOTf-mediated regioselective opening of benzylidene **8b** afforded 6-OH **11**, which was then oxidized under Parikh-Doering conditions. The resulting aldehyde was then olefinated via a MOM-Wittig reaction using KHMDS in a mixture of toluene and THF at room temperature. Of note, we observed that other bases (*n*BuLi, *t*BuOK) and solvents (THF, DMF) and performing the reaction at lower temperatures (0 °C, -40 °C, -78 °C) tended to favor the elimination reaction resulting in the corresponding α,β -unsaturated aldehyde, as previously observed with the 2-*O*-NAP derivative. The resulting enol ether was hydrolyzed under acidic conditions to afford the corresponding C7-aldehyde, which was readily reduced to 7-OH **12**. Noteworthy, this four-step homologation sequence was optimized in such a way that no chromatographic purification of the intermediates was necessary. The 6-deoxy-hepto functionality was confirmed by ¹H and COSY NMR analyses through the observation of two sets of shielded signals corresponding to protons H-6a and H-6b (2.10 ppm and 1.64 ppm, respectively) coupling with signals at 3.64 ppm, which correspond to H-7a and H-7b. 6-Deoxy-D-*ido*-heptoside **12** was ultimately levulinoylated to afford target compound **13**.



Scheme 8.2. Homologation of alcohol **11**

After having established a reproducible and efficient protocol for the homologation step, we tested the previously established IAD conditions for the coupling of heptosyl donor **13** and GlcNAc acceptor **3** (Scheme 3). However, despite several trials, the reaction did not proceed successfully, as significant degradation systematically occurred, and no disaccharide was detected.



Scheme 8.3. Unsuccessful intramolecular aglycon delivery using heptoside **13**

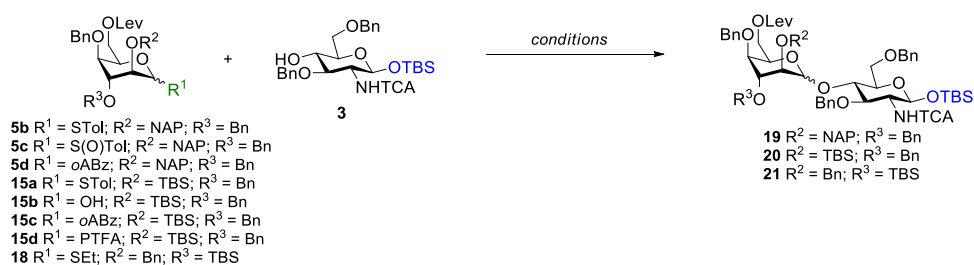
8.4.2 Intermolecular glycosylation approach

Having anticipated that such challenges may occur, various intermolecular glycosylation procedures were investigated in parallel to the IAD approach. Since we already had 2-*O*-NAP model donors **5b**, **5c** and **5d** in large quantities, we decided to valorize these compounds and screen different activation protocols with the hope that they would exhibit some β -stereoselectivities (Table 2). Glycosylation between thiotolyl **5b** and GlcNAc **3** under the promotion of DMTST unfortunately did not work (entry 1), but when α -sulfoxide donor **5c** was activated under the promotion of Tf_2O at low temperature, disaccharide **19** was achieved in good yield as a 1/1.2 α/β inseparable mixture (entry 2). Alternatively, Yu^{595, 596} and Li's^{597, 598} recent work highlighted that upon gold(I)-induced activation of α -configured *o*ABz glycosyl donors, the resulting glycosyloxy isocoumenylium intermediate preferably undergoes an $\text{S}_{\text{N}}2$ -type displacement by the incoming acceptor, resulting in the corresponding β -linked glycoside. In coherence with their work, we were interested in the use of our previously synthesized *o*ABz donor **5d** for its β -stereoselective coupling with acceptor **3**. Although we were not able to access this donor in pure α -form, the resulting anomeric mixture was nonetheless activated under the promotion of NIS/TMSOTf, leading to an α/β mixture of disaccharide **19** with a slight preference for the α -anomer (entry 3). A similar result was achieved when $\text{PPh}_3\text{AuCl}/\text{AgOTf}$ was used as the promoter system in DCM (entry 4), whereas switching the solvent to a mixture of DCM/ CH_3CN led to complete donor decomposition (entry

CHAPITRE 8 – TOWARDS THE SYNTHESIS OF AN IDOSE-CONTAINING DISACCHARIDE MIMIC OF CAMPYLOBACTER JEJUNI HS:4C CAPSULAR POLYSACCHARIDE

5). Not only good β -stereoselectivity could not be achieved when using the 2-*O*-NAP idosyl donors, but it is worth noting that the resulting disaccharides were additionally contaminated with an inseparable impurity, independently of the leaving group (STol, S(O)Tol, *o*ABz). Although determination of the α/β ratio could be achieved on the basis of undecoupled HSQC NMR analyses and formation of the compounds was confirmed by high resolution mass spectrometry (m/z 1215.4370, $[M + NH_4]^+$), complete characterization could not be done due to this inseparable impurity. This therefore led us to investigate other types of idosyl donors.

Table 8.2. Intermolecular glycosylation with model compounds

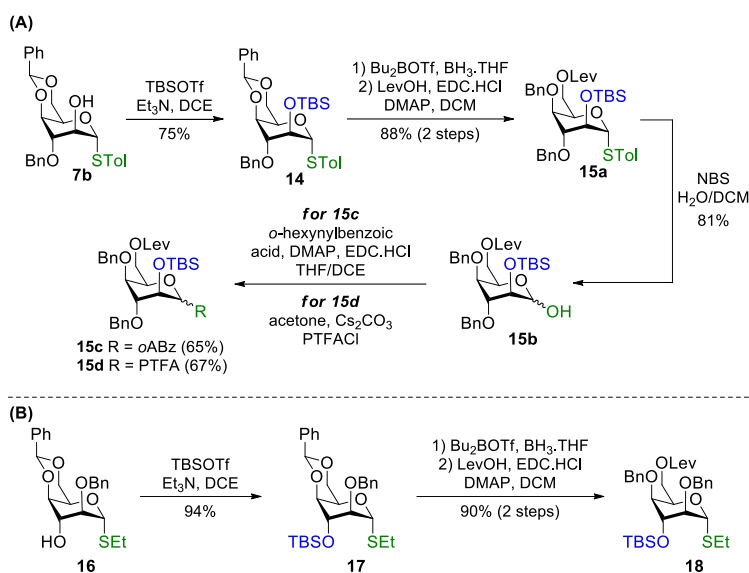


entry	R ¹	R ²	R ³	promoter	solvent	T (°C)	time (h)	yield, % ^a (product, α/β)
1	α -STol	NAP	Bn	DMTST	DCE	rt	1	N/A
2	α -S(O)Tol	NAP	Bn	Tf ₂ O	DCM	-78 to -60	1.5	70 ^b (19 , 1/1.2)
3	α,β - <i>o</i> ABz	NAP	Bn	NIS/TMSOTf	DCE	0 to rt	2	71 ^b (19 , 2.2/1)
4	α,β - <i>o</i> ABz	NAP	Bn	PPh ₃ AuCl/AgOTf	DCM	-40	1	83 ^b (19 , 1.5/1)
5	α,β - <i>o</i> ABz	NAP	Bn	PPh ₃ AuCl/AgOTf	DCM/CH ₃ CN	-40 to rt	3	N/A ^c
6	α,β - <i>o</i> ABz	TBS	Bn	NIS/TMSOTf	DCE	-10 to rt	1	N/A ^d
7	α,β - <i>o</i> ABz	TBS	Bn	PPh ₃ AuCl/AgOTf	DCM	-40 to rt	21	N/A ^e
8	α -STol	TBS	Bn	NIS/TMSOTf	DCE	-10 to rt	1	55 (20 , 3.7/1)
9	α -STol	TBS	Bn	NIS/TMSOTf	DCM/CH ₃ CN	-40	1	59 (20 , 1.7/1)
10	α,β -OH	TBS	Bn	Ph ₃ PO, (COCl) ₂ LiI, <i>i</i> Pr ₂ NEt	CHCl ₃	rt to 45	24	N/A ^c
11	α,β -OH	TBS	Bn	KHMDS/Ts ₂ O	THF	-78 to rt	21	N/A ^c
12	α,β -PTFA	TBS	Bn	TMSOTf	DCM/CH ₃ CN	-60 to rt	1	20 (20 , 1/0)
13	α,β -PTFA	TBS	Bn	FeCl ₃	DCM/CH ₃ CN	-60 to rt	1	9 (20 , 2/1) ^b
14	α -SEt	Bn	TBS	NIS/TMSOTf	DCM/CH ₃ CN	-40	1	12 (21 , 1/0)

^aisolated yield; ^bcontaminated with unseparable impurity; ^cdonor decomposed; ^ddonor hydrolysis; ^eno reaction

In their work on the development of a β -mannosylation procedure, Li and colleagues observed that equipping a 4,6-*O*-benzylidene-protected mannosyl *o*ABz donor with a 2-*O*-silyl group led to increased β -stereoselectivity.⁵⁹⁹ This observation acted as a premise for their recently reported synthetic approach for the assembly of β -1,6-oligomannosides.⁵⁹⁸ Similarly, Yu *et al.* showed that 2-*O*-TBS protected mannosyl donors exhibited good β -stereoselectivities in glycosylation reactions.⁵⁹⁶ Therefore, we envisioned that an idosyl *o*ABz donor bearing a 2-*O*-TBS group could help improve the β -stereoselectivity of the glycosylation. Moreover, although the 2-*O*-TBS may cause steric hindrance on the top face of the sugar, we hypothesized that the electron-donating nature of this group may arm the sugar, thus favoring the kinetically controlled β -glycoside. We also hoped that performing the glycosylation reactions at low temperature would also preferentially lead to the β -anomer. As depicted in Scheme 4A, synthesis of this target compound was performed using previously synthesized alcohol **7b** as starting material, which was 2-*O*-silylated. This was followed by regioselective opening of the benzylidene and levulinoylation, yielding thiotolyl donor **15a**. The latter was then hydrolyzed under the action of NBS and esterified with *o*-hexynylbenzoic acid to give 2-*O*-TBS idosyl *o*ABz donor **15c** as an α/β anomeric mixture. Unfortunately, when this compound was tested for its coupling with GlcNAc **3** under the promotion of either NIS/TMSOTf or PPh₃AuCl/AgOTf (Table 2, entries 6 and 7 respectively), the corresponding disaccharide was not formed.

CHAPITRE 8 – TOWARDS THE SYNTHESIS OF AN IDOSE-CONTAINING DISACCHARIDE MIMIC OF CAMPYLOBACTER JEJUNI HS:4C CAPSULAR POLYSACCHARIDE



Scheme 8.4. Synthesis of 2-O-TBS (A) and 3-O-TBS (B) donors 15a–15d and 18

In light of these unsuccessful results, we were then interested in investigating other types of idosyl donors, *i.e.*, thiotolyl **15a**, hemiacetal **15b**, and *N*-phenyltrifluoroacetimidate (PTFA) **15d** (Scheme 4A). In parallel, we undertook the synthesis of 3-O-silylated thioethyl donor **18** (Scheme 4B) using alcohol **16** as starting material, which was formed as a subproduct during the 3-O-regioselective benzylation of the corresponding diol (refer to Scheme 1). We reasoned that the bulkiness of the TBS group could favor formation of the β -glycosidic linkage by sterically hindering the bottom face of the sugar.

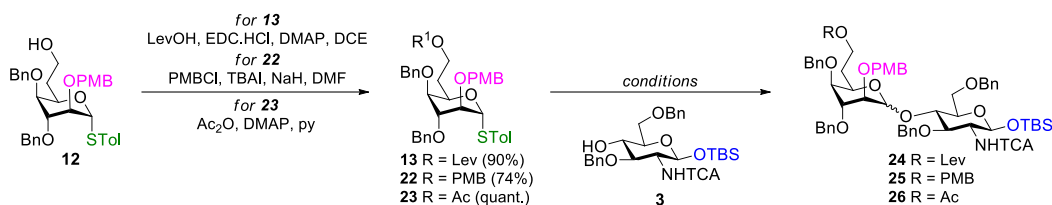
With this collection of donors in hand, we pursued our intermolecular glycosylation study (Table 2). When thioiodoside **15a** was activated under the promotion of NIS/TMSOTf in DCE, the glycosylation reaction proceeded with slight α -stereoselectivity (entry 8). Although using a mixture of DCM/CH₃CN as solvents improved the anomeric ratio, the corresponding α -disaccharide remained the predominantly formed compound (entry 9). Then, encouraged by the work of McGarrigle and co-workers who developed a β -stereoselective manno- and rhamnosylation procedure relying on the use of hemiacetal donors through a one-pot three-step sequence involving (1) chlorination; (2) iodination; and (3) glycosylation,⁶⁰⁰ we tested their optimized conditions for the activation of hemiacetal **15b**, but the reaction proved unsuccessful

(entry 10). Similarly, our attempt to perform an S_N2-type glycosylation through the formation of an intermediate α -glycosyl tosylate, as developed by Bennett's group for the preparation of β -linked 2-deoxy sugars,⁶⁰¹ was ineffective (entry 11). TMSOTf-mediated activation of PTFA donor **15d** proceeded poorly and with complete α -stereoselectivity (entry 12) although a mixture of DCM and CH₃CN was used as solvent, while switching to FeCl₃ as the promoter improved the α/β ratio but the glycosylation yield remained poor (entry 13). Finally, as opposed to what we had expected, the use of 3-O-silylated donor **18** solely led to α -disaccharide **21** (entry 14).

Although our different attempts at performing the intermolecular glycosylation in satisfying yields and with good β -stereoselectivity were not particularly successful, we were nonetheless interested in performing some trials with protected derivatives of 6-deoxy-D-*ido*-heptosyl donor **12** which we had already prepared in sufficient quantities. Results are reported in Table 3. We envisioned that the conditions employed in entry 8 of Table 2 (NIS/TMSOTf, DCM/CH₃CN, -40 °C) would be a good starting point in our investigation. 7-O-Levulinoylated heptosyl donor **13** was thus coupled with GlcNAc acceptor **3** under these conditions (entry 1). While completion of the reaction led to an anomeric mixture favoring the corresponding α -disaccharide (α/β 2:1), we were pleased to observe that disaccharides **25 α** and **25 β** could be readily separated chromatographically. Our attempt at improving the anomeric ratio towards the β -disaccharide using propionitrile as solvent and performing the reaction at a lower temperature was unfruitful (entry 2). Unfortunately, although both anomers could be separated, we observed that the β -disaccharide co-eluted with an important impurity. Despite our attempts, we were unable to access this compound in pure form, but its formation was confirmed with the help of high-resolution mass spectrometry (HRMS (ESI-TOF) m/z [M + NH₄]⁺ calcd for C₆₂H₈₀[³⁵Cl]₃N₂O₁₄Si 1209.4439; found 1209.4399).

CHAPITRE 8 – TOWARDS THE SYNTHESIS OF AN IDOSE-CONTAINING DISACCHARIDE MIMIC OF CAMPYLOBACTER JEJUNI HS:4C CAPSULAR POLYSACCHARIDE

Table 8.3 Intermolecular glycosylation with 6-deoxy-ido-heptopyranosyl donors 13 and 22–23



entry	R ¹	R ²	promoter	solvent	T (°C)	time (h)	yield, % ^a (product, α/β)
1	Lev	Tol	NIS/TMSOTf	DCM/CH ₃ CN	-40	1	85 ^b (24 , 2:1)
2	Lev	Tol	NIS/TMSOTf	propionitrile	-60 to -40	1	20 ^b (24 , 2.5:1)
3	PMB	Tol	NIS/TMSOTf	DCM/CH ₃ CN	-40	1	traces
4	Ac	Tol	NIS/TMSOTf	DCM/CH ₃ CN	-40	1	87 (26 , 1.7:1)

^aisolated yields; ^bβ-anomer contaminated with unknown impurity.

The poor stereoselectivity of this reaction combined with the difficulties related to the purification of β-disaccharide **24** led us to investigate alternative idoheptopyranosyl donors. We hypothesized that the preference towards the α-anomer when the glycosylation reaction was performed with heptosyl donor **13** could be attributed to the long distance anchimeric assistance in which could be involved the 7-*O*-levulinoyl group. To avoid this potential participation, we synthesized derivative **22** bearing a non-participating PMB group at C7. However, the glycosylation proceeded poorly (entry 3). Although traces of the compounds were detected, as confirmed by HRMS analysis through the observation of a molecular ion m/z 1231.4600 ($[M + NH_4]^+$), complete characterization could not be done. In light of this unsuccessful result, we decided to switch to 7-*O*-acetyl heptosyl donor **23**, hoping it might be less participating than the levulinoyl group. To our delight, performing the reaction in a mixture of DCM and CH₃CN at -40 °C led to disaccharide **26** in a slightly improved α/β ratio of 1.7:1 and in good yield (entry 4). Importantly, the resulting disaccharides could be readily isolated in pure anomeric form.

Because of the axial orientation of the substituent at C2, NMR determination of the anomeric configuration of idosides can typically not be achieved on the basis of the ³*J* between H-1 and H-

2, as both α - and β -anomers would be characterized by a small coupling constant when in the 4C_1 conformation. This problem can be solved with the help of the ${}^1J_{C1-H1}$: a glycoside bearing an equatorially-oriented anomeric proton is usually characterized by a coupling constant of approximately 170 Hz, whereas it is around 160 Hz for an axial anomeric proton.⁵⁶⁰ For compound **26**, we therefore expected that the *ido* unit would be characterized by a ${}^1J_{C1-H1}$ of 160 Hz in the β -disaccharide and of 170 Hz in the α -disaccharide. While the β -disaccharide was successfully distinguished using this approach (${}^1J_{C1-H1} = 162$ Hz), analysis of the second disaccharide was somewhat inconclusive (${}^1J_{C1-H1} = 165$ Hz). Upon further NMR analysis, we observed that protons H-1, H-2 and H-3 of the idoheptopyranoside unit in this disaccharide were characterized by unexpectedly large coupling constants, indicative of a 1C_4 conformation (Fig. 5). Based on the large 3J (7.1 Hz) between H-1 and H-2, which correlates with a 1,2-*trans*-diaxial, the α -configuration of the idoside could be confirmed. The same observation was also made for disaccharide **24a**. Conversely, the *ido* unit in disaccharide **26 β** exhibited small coupling constants between its protons, coherent with small dihedral angles between adjacent protons typical of idopyranosides in a 4C_1 conformation. Although this result was fairly surprising, as it was highlighted that α -idosides are usually stabilized in the 4C_1 conformation by the anomeric effect,⁵⁸⁵ this is yet another proof that idosides are uniquely flexible sugars with unexpected physicochemical behavior.

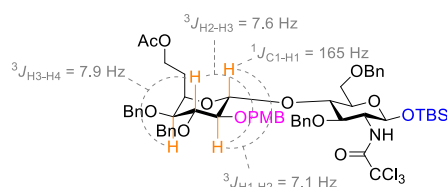


Figure 8.5. Significant NMR coupling constants of disaccharide **26 α**

8.5 Next steps

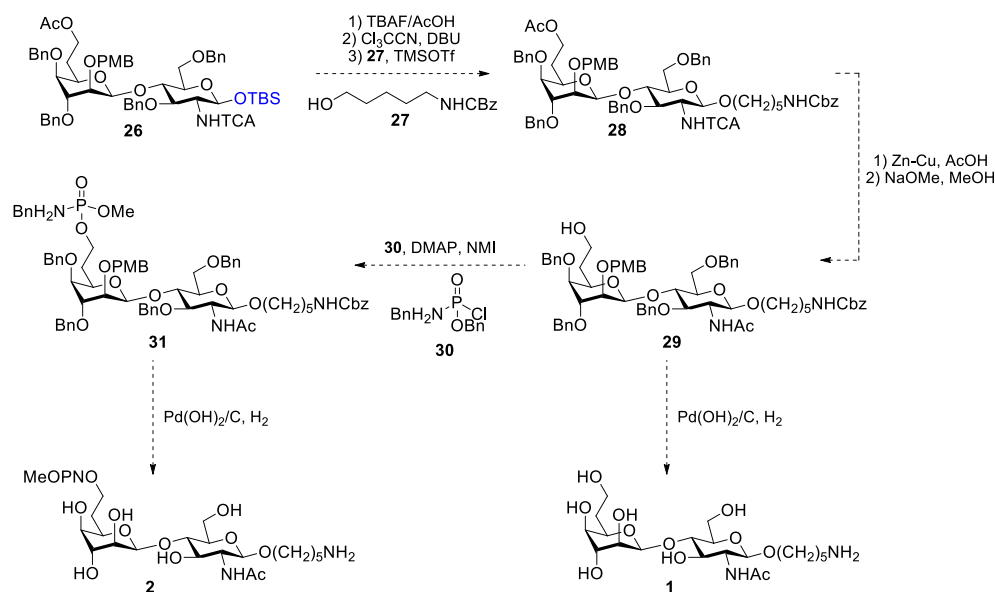
Following the previously performed study involving either an intra- or an intermolecular glycosylation step, we have highlighted that the best results were achieved under intermolecular conditions using 6-deoxy-*ido*-heptopyranosyl donor **24** bearing a 7-*O*-acetyl group. Although the yield for the β -disaccharide **26** remains modest (32%), we expect that it could be improved by

CHAPITRE 8 – TOWARDS THE SYNTHESIS OF AN IDOSE-CONTAINING DISACCHARIDE MIMIC OF CAMPYLOBACTER JEJUNI HS:4C CAPSULAR POLYSACCHARIDE

performing the reaction at lower temperature and by screening different solvents and promoter systems.

Upon optimization of the glycosylation conditions, we plan on accessing disaccharides **1** and **2** through the synthetic route described in Scheme 5. First, the anomeric TBS group will be cleaved to introduce a trichloroacetimidate group, which would allow glycosylation with linker **27**⁶⁰² with complete β -stereoselectivity through anchimeric assistance of C2-NHTCA. We anticipate that problems may arise if we were to perform the dehalogenation of the *N*-trichloroacetyl group under hydrogenolysis conditions during the last deprotection step of our constructs, as reviewed by Mulard *et al.*⁶⁰³ As such, we plan on performing this dehalogenation step earlier in our deprotection sequence with the help of Zn-Cu couple.⁶⁰⁴ This would be followed by cleavage of the C7 acetyl group, yielding intermediate **29**. The latter would then be hydrogenolyzed to concomitantly cleave the Bn, PMB, and CBz groups, enabling access target unprotected disaccharide **1**. In parallel, an *N*-benzylated MeOPN group would be introduced at position C7 of intermediate **29** using methyl benzylphosphoramidochloridate **30** in the presence of bases.⁴⁹⁷ The resulting compound would then undergo an hydrogenolysis step to yield target disaccharide **2** mimicking the C7 MeOPN modification of native *C. jejuni* HS:4c CPS.

CHAPITRE 8 – TOWARDS THE SYNTHESIS OF AN IDOSE-CONTAINING DISACCHARIDE MIMIC OF CAMPYLOBACTER JEJUNI HS:4C CAPSULAR POLYSACCHARIDE



Scheme 8.5. Planned synthetic route to access target disaccharides 1 and 2

These potential synthetic antigens would then be conjugated to a carrier protein to assess their immunogenicity. This would be performed by first introducing an adipate linker at the reducing end of the constructs by taking advantage of NHS ester chemistry.⁶⁰⁵ Then, the free *N*-succinimidyl extremity would allow conjugation of the disaccharides to CRM₁₉₇⁶⁰⁶ on its lysine residues. Finally, the last step of this project would consist in the *in vivo* immunogenicity assessment of our synthetic compounds in a chicken model, as chickens are the predominant reservoir of *C. jejuni*.

8.6 Conclusions

In summary, we have herein reported our progress towards the synthesis of disaccharide mimics of *C. jejuni* HS:4c CPS, one of the predominant serotypes at the origin of campylobacteriosis cases worldwide. We have developed a synthetic pathway to access orthogonally protected *ido*-hexopyranosyl and 6-deoxy-*ido*-heptopyranosyl donors bearing different leaving groups at the anomeric position. Noteworthy and to the best of our knowledge, it is the first time a synthetic approach enabling direct access to 6-deoxy-*ido*-heptopyranosides from *ido*-configured precursors is reported. These donors were employed in an extensive glycosylation study involving intra- and intermolecular reactions. Although we have highlighted that IAD with *ido*-hexopyranosyl donors

exhibits complete β -stereoselectivity, the yields remain modest, and the reaction was unsuccessful using a 6-deoxy-*ido*-heptopyranosyl donor. Alternatively, although we were not able to perform intermolecular glycosylations with both a good yield and a satisfying β -stereoselectivity, we have showed that performing the reaction with 7-*O*-acetyl donor **23** gave a good yield and that the resulting α - and β -disaccharides were chromatographically separable. We additionally expect that upon optimization of the glycosylation conditions, a better β -stereoselectivity could be achieved. Upon optimization, we plan on performing the large-scale synthesis of β -disaccharide **26**, which could then be functionalized and deprotected into target compounds **1** and **2**. These latter would ultimately be conjugated to CRM₁₉₇, which would allow immunogenicity assays to be performed in a chicken model. Altogether and once completed, our study will provide a straightforward and synthetically advantageous approach to access disaccharides related to the CPS of *C. jejuni* HS:4c and could pave the way towards the development of synthetic glyconjugate vaccines against this pathogen.

8.7 Acknowledgments

This work was supported by Discovery grants from the Natural Sciences and Engineering Research Council of Canada (NSERC) under award number RGPIN-2016-04950 (to C. G.) and RGPIN-2022-04515 (to C. G.). This work was also supported by a PTR (Programmes Transversaux de Recherche) grant (PTR 380-20) from Institut Pasteur Paris. M. C. thanks NSERC Vanier and Fonds de recherche du Québec – Nature et technologies (FRQNT) for Ph.D. scholarships. N. V. thanks the Centre de recherche en infectiologie porcine et avicole (CRIPA) for a postdoc fellowship.

8.8 Experimental section

General methods.

All starting materials and reagents were purchased from commercial sources and used as received without further purification. Air and water sensitive reactions were performed in oven-dried glassware under an Ar atmosphere. Anhydrous solvents were either prepared from commercial

CHAPITRE 8 – TOWARDS THE SYNTHESIS OF AN IDOSE-CONTAINING DISACCHARIDE MIMIC OF CAMPYLOBACTER JEJUNI HS:4C CAPSULAR POLYSACCHARIDE

solvents and dried over heat-gun activated 4 Å molecular sieves (MS) or supplied over MS and used as received. Powdered 4 Å MS were activated before use by heating with a heat gun for approx. 15 min under vacuum. Room temperature reactions were performed at 23 °C. Reactions were monitored by thin-layer chromatography (TLC) with silica gel 60 F₂₅₄ 0.25 mm pre-coated aluminum foil plates. Compounds were visualized by using UV₂₅₄ and/or orcinol (1 mg/mL) in 10% aqueous H₂SO₄ solution with heating. Normal-phase flash column chromatographies were performed on silica gel 60 Å (15-40 μm). NMR spectra were recorded at 297 K in CDCl₃ with 600 MHz, 500 MHz, or 400 MHz instruments, employing standard softwares given by the manufacturer. ¹H spectra were referenced to tetramethylsilane (TMS, δ_H = 0.00 ppm) as an internal reference while ¹³C spectra were referenced to the residual CHCl₃ peak (δ_C = 77.16 ppm). Assignments were based on ¹H, ¹³C, COSY, HSQC, and undecoupled HSQC experiments. Reducing sugars disaccharides are designated B, whereas sugars at the non-reducing end are designated A. Interchangeable NMR signals are marked with an asterisk (*). High-resolution mass spectra (HRMS) were recorded on an ESI-Q-TOF mass spectrometer. Optical rotations [α]_D²⁰ were measured on an Anton Paar polarimeter.

Ethyl 3-*O*-Benzyl-4,6-*O*-benzylidene-1-thio-α-D-idopyranoside (7a) and ethyl 2-*O*-benzyl-4,6-*O*-benzylidene-1-thio-α-D-idopyranoside (16).

To a solution of diol **6a**⁵⁸⁵ (500 mg, 1.60 mmol, 1.0 equiv) in DCM (19 mL) were successively added 5% aq. NaOH (6.4 mL), TBAHS (109 mg, 0.320 mmol, 0.2 equiv) and BnBr (0.29 mL, 2.4 mmol, 1.5 equiv). The mixture was stirred at 40 °C for 18 h, after which the organic and aqueous layers were separated. The aqueous layer was extracted with DCM (×3) and the combined organic layers were dried over MgSO₄, filtered, and concentrated under reduced pressure. The residue was purified by silica gel flash chromatography (Hex/EtOAc 9:1 to 6:4) to give 3-*O*-benzylated idoside **7a** (441 mg, 69%) as a colorless oil and 2-*O*-benzylated idoside **16** (64 mg, 10%) as a white amorphous solid: Data for 3-*O*-benzylated idoside **7a**: R_f 0.52 (Hex/EtOAc 7:3); [α]_D²⁰ +163 (*c* 1.2, CHCl₃); ¹H NMR (600 MHz, CDCl₃) : δ (ppm) 7.48–7.31 (m, 10H, 10 × CH_{Ar}), 5.53 (s, 1H, CHPh), 5.39 (br s, 1H, H-1), 4.77 (d, *J* = 11.8 Hz, 1H, CHH_{Bn}), 4.55 (d, *J* = 11.8 Hz, 1H, CHH_{Bn}), 4.34 (d, *J* = 1.0 Hz, 1H, H-5), 4.30 (dd, *J* = 12.6 Hz, *J* = 1.5 Hz, 1H, H-6a), 4.13–4.08 (m, 2H, H-

CHAPITRE 8 – TOWARDS THE SYNTHESIS OF AN IDOSE-CONTAINING DISACCHARIDE MIMIC OF CAMPYLOBACTER JEJUNI HS:4C CAPSULAR POLYSACCHARIDE

6b, H-4), 3.97–3.93 (m, 1H, H-2), 3.78–3.75 (m, 2H, H-3, OH), 2.74–2.60 (m, 2H, CH_{2SEt}), 1.32 (t, *J* = 7.4 Hz, 3H, CH_{3SEt}); ¹³C{¹H} NMR (150 MHz, CDCl₃): δ (ppm) 137.5 (C_{Ar}), 137.4 (C_{Ar}), 129.4 (CH_{Ar}), 128.6 (2C, 2 × CH_{Ar}), 128.5 (2C, 2 × CH_{Ar}), 128.1 (C_{Ar}), 127.9 (2C, 2 × CH_{Ar}), 126.1 (2C, 2 × CH_{Ar}), 101.7 (CHPh), 86.3 (C-1), 74.7 (C-4), 74.1 (C-3), 72.4 (CH_{2Bn}), 70.3 (C-6), 67.7 (C-2), 60.2 (C-5), 27.2 (CH_{2SEt}), 15.3 (CH_{3SEt}); HRMS (ESI-TOF) *m/z* [M + H]⁺ calcd for C₂₂H₂₇O₅S 403.1574; found 403.1576; Data for 2-*O*-benzylated idoside 16: *R_f* 0.29 (Hex/EtOAc 7:3); [α]_D²⁰ +93 (*c* 0.9, CHCl₃); ¹H NMR (400 MHz, CDCl₃): δ (ppm) 7.52–7.50 (m, 2H, 2 × CH_{Ar}), 7.37–7.26 (m, 8H, 8 × CH_{Ar}), 5.54 (s, 1H, CHPh), 5.46 (d, *J* = 3.8 Hz, 1H, H-1), 4.78 (d, *J* = 11.4 Hz, 1H, CHH_{Bn}), 4.65 (d, *J* = 11.4 Hz, 1H, CHH_{Bn}), 4.28 (dd, *J* = 12.8 Hz, *J* = 1.2 Hz, 1H, H-6a), 4.17 (dd, *J* = 12.8 Hz, *J* = 2.3 Hz, 1H, H-6b), 4.13–4.09 (m, 1H, H-3), 4.07–4.06 (m, 1H, H-4), 4.05–4.04 (m, 1H, H-5), 3.47 (dd, *J* = 5.7 Hz, *J* = 3.9 Hz, 1H, H-2), 2.78–2.70 (m, 1H, CHH_{SEt}), 2.66–2.58 (m, 1H, CHH_{SEt}), 2.52 (d, *J* = 5.9 Hz, 1H, OH); ¹³C{¹H} NMR (100 MHz, CDCl₃): δ (ppm) 138.01 (C_{Ar}), 137.97 (C_{Ar}), 129.1 (CH_{Ar}), 128.5 (2C, 2 × CH_{Ar}), 128.3 (2C, 2 × CH_{Ar}), 127.94 (2C, 2 × CH_{Ar}), 127.89 (CH_{Ar}), 126.6 (2C, 2 × CH_{Ar}), 100.9 (CHPh), 82.7 (C-1), 78.1 (C-2), 76.5 (C-4), 73.1 (CH_{2Bn}), 70.9 (C-3), 69.6 (C-6), 60.6 (C-5), 25.4 (CH_{2SEt}), 14.9 (CH_{3SEt}); HRMS (ESI-TOF) *m/z* [M + Na]⁺ calcd for C₂₂H₂₆NaO₅S 420.1839; found 420.1830.

***para*-Methylphenyl 3-*O*-Benzyl-4,6-*O*-benzylidene-1-thio- α -D-idopyranoside (7b).**

To a solution of diol **6b**⁵⁸⁵ (165 mg, 0.441 mmol, 1.0 equiv) in DCM (5.3 mL) were successively added NaOH 5% (1.8 mL), TBAHS (30 mg, 0.088 mmol, 0.2 equiv) and BnBr (79 μ L, 0.66 mmol, 1.0 equiv). The mixture was heated at 40 °C with an oil bath and stirred at this temperature for 18 h. The mixture was then extracted with DCM (×3), dried over MgSO₄, filtered, and concentrated under reduced pressure. The residue was purified by silica gel flash chromatography to give benzylated compound **7b** (154 mg, 75%) as a white foam: *R_f* 0.5 (Hex/EtOAc 6:4); [α]_D²⁰ +132 (*c* 1.00, CHCl₃); ¹H NMR (600 MHz, CDCl₃): δ (ppm) 7.47–7.31 (m, 12H, 12 × CH_{Ar}), 7.11–7.10 (m, 2H, 2 × CH_{STol}), 5.60 (br s, 1H, H-1), 5.54 (s, 1H, CHPh), 4.85 (d, *J* = 11.8 Hz, 1H, CHH_{Bn}), 4.60 (d, *J* = 11.8 Hz, 1H, CHH_{Bn}), 4.46 (br s, 1H, H-5), 4.33 (dd, *J* = 12.6 Hz, *J* = 1.4 Hz, 1H, H-6a), 4.14–4.10 (m, 3H, H-6b, H-2, H-4), 3.83–3.81 (m, 2H, H-3, OH), 2.32 (s, 3H, CH_{3STol}); ¹³C{¹H} NMR (150 MHz, CDCl₃): δ (ppm) 137.5 (C_{Ar}), 137.4 (C_{Ar}), 137.0 (C_{Ar}), 133.6 (C_{Ar}),

CHAPITRE 8 – TOWARDS THE SYNTHESIS OF AN IDOSE-CONTAINING DISACCHARIDE MIMIC OF CAMPYLOBACTER JEJUNI HS:4C CAPSULAR POLYSACCHARIDE

130.9 (2C, 2 × CH_{Ar}), 129.8 (2C, 2 × CH_{Ar}), 129.4 (CH_{Ar}), 128.7 (2C, 2 × CH_{Ar}), 128.5 (2C, 2 × CH_{Ar}), 128.2 (CH_{Ar}), 127.9 (2C, 2 × CH_{Ar}), 126.1 (2C, 2 × CH_{Ar}), 101.7 (CHPh), 89.6 (C-1), 74.6 (C-4*), 73.9 (C-3), 72.5 (CH_{2Bn}), 70.2 (C-6), 67.8 (C-2*), 60.7 (C-5), 21.2 (CH_{3STol}); HRMS (ESI-TOF) *m/z* [M + NH₄]⁺ calcd for C₂₇H₃₂NO₅S 482.1996; found 482.2004.

Ethyl 3-O-Benzyl-4,6-O-benzylidene-2-O-*para*-methoxybenzyl-1-thio- α -D-idopyranoside (8a).

To a solution of alcohol **7a** (100 mg, 0.248 mmol, 1.0 equiv) in dry THF (1.3 mL) were successively added TBAB (40 mg, 0.12 mmol, 0.5 equiv), PMBCl (61 μ L, 0.45 mmol, 1.8 equiv) and powdered NaOH (30 mg, 0.75 mmol, 3.0 equiv). The suspension was stirred at rt for 22 h, after which it was diluted with DCM and washed with H₂O and brine. The organic layer was dried over MgSO₄, filtered, and concentrated under reduced pressure. The residue was purified by silica gel flash chromatography (Hex/EtOAc 95:5 to 8:2) to give compound **8a** (117 mg, 90%) as a white amorphous solid: *R_f* 0.45 (Hex/EtOAc 8:2 *ran twice*); [α]_D²⁰ +119 (*c* 1.1, CHCl₃); ¹H NMR (400 MHz, CDCl₃): δ (ppm) 7.50–7.48 (m, 2H, 2 × CH_{Ar}), 7.35–7.23 (m, 10H, 10 × CH_{Ar}), 6.81–6.79 (m, 2H, 2 × CH_{Ar}), 5.53 (s, 1H, CHPh), 5.45 (d, *J* = 3.0 Hz, 1H, H-1), 4.68 (d, *J* = 12.0 Hz, 1H, CHH_{Bn}), 4.62 (d, *J* = 12.0 Hz, 1H, CHH_{Bn}), 4.57 (d, *J* = 11.1 Hz, 1H, CHH_{PMB}), 4.54 (d, *J* = 11.1 Hz, 1H, CHH_{PMB}), 4.26 (d, *J* = 12.0 Hz, 1H, H-6a), 4.15–4.12 (m, 2H, H-6b, H-5), 4.07 (t, *J* = 2.1 Hz, 1H, H-4), 3.83 (t, *J* = 3.6 Hz, 1H, H-3), 3.79 (s, 3H, CH_{3PMB}), 3.60 (dd, *J* = 4.4 Hz, *J* = 3.3 Hz, 1H, H-2), 2.76–2.58 (m, 2H, CH_{2SEt}), 1.31 (t, *J* = 7.4 Hz, 3H, CH_{3SEt}); ¹³C{¹H} NMR (100 MHz, CDCl₃): δ (ppm) 159.3 (C_{Ar}), 138.2 (C_{Ar}), 137.9 (C_{Ar}), 130.2 (C_{Ar}), 129.5 (2C, 2 × CH_{Ar}), 129.0 (CH_{Ar}), 128.6 (2C, 2 × CH_{Ar}), 128.2 (2C, 2 × CH_{Ar}), 128.0 (CH_{Ar}), 127.9 (2C, 2 × CH_{Ar}), 126.6 (2C, 2 × CH_{Ar}), 113.8 (2C, 2 × CH_{Ar}), 101.0 (CHPh), 83.7 (C-1), 76.4 (C-3), 75.6 (C-2), 75.2 (C-4), 72.7 (CH_{2Bn}*), 72.4 (CH_{2PMB}*), 69.9 (C-6), 60.8 (C-5), 55.4 (CH_{3PMB}), 26.2 (CH_{2SEt}), 15.3 (CH_{3SEt}); HRMS (ESI-TOF) *m/z* [M + NH₄]⁺ calcd for C₃₀H₃₈NO₆S 540.2414; found 540.2407.

***para*-Methylphenyl 3-*O*-Benzyl-4,6-*O*-benzylidene-2-*O*-*para*-methoxybenzyl-1-thio- α -D-idopyranoside (8b).**

To a solution of compound **7b** (964 mg, 2.08 mmol, 1.0 equiv) in dry DMF (25 mL) at 0 °C were added TBAI (383 mg, 1.04 mmol, 0.5 equiv) and NaH (60% dispersion in oil, 166 mg, 4.15 mmol, 2.0 equiv). The mixture was stirred at 0 °C for 10 min, after which PMBCl (0.56 mL, 4.2 mmol, 2.0 equiv) was added. The solution was stirred at 0 °C for 2.5 h and quenched by the slow addition of MeOH. The solution was then diluted with EtOAc and washed with H₂O. The aqueous layer was extracted with EtOAc ($\times 3$) and the combined organic phases were washed with H₂O ($\times 2$) and brine. The organic layer was dried over MgSO₄, filtered, and concentrated under reduced pressure. The residue was purified by silica gel flash chromatography (Hex/EtOAc 95:5 to 85:15) to give compound **8b** (935 mg, 77%) as a white amorphous solid: R_f 0.25 (Hex/EtOAc 8:2); $[\alpha]_D^{20} +71$ (c 0.3, CHCl₃); ¹H NMR (400 MHz, CDCl₃): δ (ppm) 7.49–7.47 (m, 2H, 2 \times CH_{Ar}), 7.42–7.29 (m, 10H, 10 \times CH_{Ar}), 7.26–7.22 (m, 2H, 2 \times CH_{Ar}), 7.11–7.09 (m, 2H, 2 \times CH_{Ar}), 6.81–6.79 (m, 2H, 2 \times CH_{Ar}), 5.69 (d, J = 2.5 Hz, 1H, H-1), 5.54 (s, 1H, CHPh), 4.74 (d, J = 12.0 Hz, 1H, CHH_{Bn}), 4.64 (d, J = 12.0 Hz, 1H, CHH_{Bn}), 4.60 (d, J = 11.2 Hz, 1H, CHH_{PMB}), 4.54 (d, J = 11.1 Hz, 1H, CHH_{PMB}), 4.31–4.28 (m, 2H, H-5, H-6a), 4.15 (dd, J = 12.9 Hz, J = 2.2 Hz, 1H, H-6b), 4.10–4.09 (m, 1H, H-4), 3.87 (t, J = 3.3 Hz, 1H, H-3), 3.80–3.78 (m, 4H, H-2, CH_{3PMB}), 2.32 (s, 3H, CH_{3STol}); ¹³C{¹H} NMR (100 MHz, CDCl₃): δ (ppm) 159.3 (C_{Ar}), 138.2 (C_{Ar}), 137.8 (C_{Ar}), 136.9 (C_{Ar}), 133.0 (C_{Ar}), 130.8–126.7 (17C, C_{Ar}, 16 \times CH_{Ar}), 113.8 (2C, 2 \times CH_{Ar}), 101.1 (CHPh), 87.0 (C-1), 75.8 (C-3), 75.1 (C-2), 74.6 (C-4), 72.7 (CH_{2Bn}), 72.2 (CH_{2PMB}), 69.9 (C-6), 61.2 (C-5), 55.4 (CH_{3PMB}), 21.2 (CH_{3STol}); HRMS (ESI-TOF) m/z [M + NH₄]⁺ calcd for C₃₅H₄₀NO₆S 602.2571; found 602.2570.

Ethyl 3,4-di-*O*-Benzyl-6-*O*-levulinoyl-2-*O*-*para*-methoxybenzyl-1-thio- α -D-idopyranoside (4a).

Compound **8a** (55 mg, 0.11 mmol, 1.0 equiv) was solubilized in BH₃.THF (1M in THF, 1.1 mL, 1.1 mmol, 10 equiv) at –10 °C under Ar. The solution was stirred at that temperature for 10 min, after which Bu₂BOTf (1M in DCM, 105 μ L, 0.105 mmol, 1.0 equiv) was added dropwise. The mixture was stirred for 40 min while being allowed to gradually warm to 0 °C, after which Et₃N

CHAPITRE 8 – TOWARDS THE SYNTHESIS OF AN IDOSE-CONTAINING DISACCHARIDE MIMIC OF CAMPYLOBACTER JEJUNI HS:4C CAPSULAR POLYSACCHARIDE

and MeOH were added to quench the reaction. The solution was diluted with DCM and washed with saturated aq. NaHCO₃. The organic layer was dried over MgSO₄, filtered, and concentrated under reduced pressure. The residue was roughly filtered over a pad of silica to remove most impurities. To a solution of the latter alcohol in dry DCE (0.9 mL) were successively added LevOH (14 μL, 0.14 mmol, 1.3 equiv), DMAP (6 mg, 0.05 mmol, 0.5 equiv) and EDC.HCl (30 mg, 0.16 mmol, 1.5 equiv). The mixture was stirred for 20 h at rt, after which it was diluted with DCM and washed with saturated aq. NaHCO₃. The organic layer was dried over MgSO₄, filtered, and concentrated under reduced pressure. The residue was purified by silica gel flash chromatography (Hex/EtOAc 3:1 to 2:1) to give compound **4a** (53 mg, 77% over two steps) as a colorless oil: R_f 0.25 (Hex/EtOAc 2:1); [α]_D²⁰ +42 (c 0.6, CHCl₃); ¹H NMR (400 MHz, CDCl₃) : δ (ppm) 7.36–7.22 (m, 12H, 12 × CH_{Ar}), 6.86–6.84 (m, 2H, 2 × CH_{Ar}), 5.19 (d, *J* = 4.0 Hz, 1H, H-1), 4.66–4.60 (m, 3H, CHH_{PMB}, CHH_{Bn}, CHH_{Bn}), 4.51–4.34 (m, 5H, CHH_{PMB}, CHH_{Bn}, CHH_{Bn}, H-5, H-6a), 4.25 (dd, *J* = 11.7 Hz, *J* = 4.5 Hz, 1H, H-6b), 3.81 (s, 3H, CH_{3PMB}), 3.67 (t, *J* = 4.9 Hz, 1H, H-3), 3.49 (dd, *J* = 4.8 Hz, *J* = 3.6 Hz, 1H, H-4), 3.46 (t, *J* = 4.5 Hz, 1H, H-2), 2.73–2.51 (m, 6H, CH_{2SEt}, 2 × CH_{2Lev}), 2.17 (s, 3H, CH_{3Lev}), 1.30 (t, *J* = 7.4 Hz, 3H, CH_{3SEt}); ¹³C{¹H} NMR (100 MHz, CDCl₃) : δ (ppm) 206.5 (CO_{Lev}), 172.5 (COOR_{Lev}), 159.5 (C_{Ar}), 138.0 (C_{Ar}), 137.9 (C_{Ar}), 130.1–128.0 (13C, C_{Ar}, 12 × CH_{Ar}), 114.0 (2C, 2 × CH_{Ar}), 82.2 (C-1), 77.0 (C-2), 75.2 (C-3*), 75.1 (C-4*), 73.3 (CH_{2PMB}*), 73.1 (CH_{2Bn}*), 72.6 (CH_{2Bn}*), 67.9 (C-5), 62.9 (C-6), 55.4 (CH_{3PMB}), 38.0 (CH_{2Lev}), 30.0 (CH_{3Lev}), 28.0 (CH_{2Lev}), 25.9 (CH_{2SEt}), 15.2 (CH_{3SEt}); HRMS (ESI-TOF) *m/z* [M + NH₄]⁺ calcd for C₃₅H₄₆NO₈S 640.2939; found 640.2948.

***para*-Methylphenyl 3,4-di-*O*-Benzyl-2-*O*-*para*-methoxybenzyl-1-thio- α -D-idopyranoside (11).**

Compound **8b** (200 mg, 0.342 mmol, 1.0 equiv) was solubilized in BH₃.THF (3.4 mL, 3.4 mmol, 10 equiv) at –10 °C under Ar. The solution was stirred at –10 °C for 4 min, after which Bu₂BOTf (342 μL, 0.342 mmol, 1.0 equiv) was added dropwise. The solution was allowed to stir for 30 min at –10 °C to 0 °C under Ar. The reaction was then quenched by the addition of Et₃N and MeOH, diluted with EtOAc, and washed with saturated aq. NaHCO₃ and brine. The organic layer was dried over MgSO₄, filtered, and concentrated under reduced pressure. The residue was purified by

CHAPITRE 8 – TOWARDS THE SYNTHESIS OF AN IDOSE-CONTAINING DISACCHARIDE MIMIC OF CAMPYLOBACTER JEJUNI HS:4C CAPSULAR POLYSACCHARIDE

silica gel flash chromatography (Hex/EtOAc 9:1 to 6:4) to give alcohol **11** (200 mg, quant.) as a colorless oil: R_f 0.38 (Hex/EtOAc 6:4); $[\alpha]_D^{20} +28$ (c 1.3, CHCl_3); ^1H NMR (400 MHz, CDCl_3): δ (ppm) 7.40–7.22 (m, 14H, $14 \times \text{CH}_{\text{Ar}}$), 7.12–7.10 (m, 2H, $2 \times \text{CH}_{\text{Ar}}$), 6.87–6.85 (m, 2H, $2 \times \text{CH}_{\text{Ar}}$), 5.39 (d, $J = 3.8$ Hz, 1H, H-1), 4.69–4.64 (m, 3H, $\text{CHH}_{\text{PMB}}^*$, CHH_{Bn}^* , CHH_{Bn}^*), 4.53 (d, $J = 11.4$ Hz, 1H, $\text{CHH}_{\text{PMB}}^*$), 4.49 (d, $J = 11.9$ Hz, 1H, CHH_{Bn}^*), 4.46–4.43 (m, 1H, H-5), 4.41 (d, $J = 11.9$ Hz, 1H, CHH_{Bn}^*), 3.90 (ddd, $J = 11.1$ Hz, $J = 7.5$ Hz, $J = 3.3$ Hz, 1H, H-6a), 3.81 (s, 3H, CH_3_{PMB}), 3.74 (t, $J = 4.9$ Hz, 1H, H-3), 3.69–3.62 (m, 2H, H-6b, H-2), 3.55 (dd, $J = 4.9$ Hz, $J = 3.7$ Hz, 1H, H-4), 2.32 (s, 3H, $\text{CH}_3_{\text{STol}}$), 1.77 (dd, $J = 9.4$ Hz, $J = 3.3$ Hz, 1H, OH); $^{13}\text{C}\{^1\text{H}\}$ NMR (100 MHz, CDCl_3): δ (ppm) 159.6 (C_{Ar}), 138.0 (C_{Ar}), 137.8 (C_{Ar}), 137.6 (C_{Ar}), 132.0–128.0 (18C, $2 \times \text{C}_{\text{Ar}}$, $16 \times \text{CH}_{\text{Ar}}$), 114.0 (2C, $2 \times \text{CH}_{\text{Ar}}$), 86.2 (C-1), 76.8 (C-2), 75.6 (C-4), 75.3 (C-3), 73.3 ($\text{CH}_2_{\text{PMB}}^*$), 73.2 ($\text{CH}_2_{\text{Bn}}^*$), 72.6 ($\text{CH}_2_{\text{Bn}}^*$), 70.3 (C-5), 61.9 (C-6), 55.4 (CH_3_{PMB}), 21.2 ($\text{CH}_3_{\text{STol}}$); HRMS (ESI-TOF) m/z $[\text{M} + \text{NH}_4]^+$ calcd for $\text{C}_{35}\text{H}_{42}\text{NO}_6\text{S}$ 604.2727; found 604.2732.

***para*-Methylphenyl 3,4-di-*O*-Benzyl-6-*O*-levulinoyl-2-*O*-*para*-methoxybenzyl-1-thio- α -D-idopyranoside (4b).**

To a solution of alcohol **11** (39 mg, 0.067 mmol, 1.0 equiv) in dry DCE (670 μL) were successively added LevOH (9 μL , 0.09 mmol, 1.3 equiv), EDC.HCl (19 mg, 0.10 mmol, 1.5 equiv) and DMAP (4 mg, 0.03 mmol, 0.5 equiv). The mixture was stirred at rt for 20h, after which it was diluted in EtOAc and washed with saturated aq. NH_4Cl and saturated aq. NaHCO_3 . The organic layer was dried over MgSO_4 , filtered, and concentrated under reduced pressure. The residue was purified by silica gel flash chromatography (Hex/EtOAc 9:1 to 6:4) to give compound **4b** (43 mg, 93%) as a colorless oil: R_f 0.33 (Hex/EtOAc 6:4); $[\alpha]_D^{20} +52$ (c 0.6, CHCl_3); ^1H NMR (400 MHz, CDCl_3): δ (ppm) 7.42–7.40 (m, 2H, $2 \times \text{CH}_{\text{Ar}}$), 7.37–7.27 (m, 7H, $7 \times \text{CH}_{\text{Ar}}$), 7.25–7.22 (m, 5H, $5 \times \text{CH}_{\text{Ar}}$), 7.11–7.09 (m, 2H, $2 \times \text{CH}_{\text{Ar}}$), 6.86–6.84 (m, 2H, $2 \times \text{CH}_{\text{Ar}}$), 5.42 (d, $J = 3.2$ Hz, 1H, H-1), 4.67–4.61 (m, 4H, H-5, $\text{CHH}_{\text{PMB}}^*$, CHH_{Bn}^* , CHH_{Bn}^*), 4.49 (d, $J = 11.6$ Hz, 1H, $\text{CHH}_{\text{PMB}}^*$), 4.44 (d, $J = 11.8$, 1H, CHH_{Bn}^*), 4.42 (d, $J = 12.1$ Hz, 1H, CHH_{Bn}^*), 4.35 (dd, $J = 11.7$ Hz, $J = 8.1$ Hz, 1H, H-6a), 4.26 (dd, $J = 11.7$ Hz, $J = 4.4$ Hz, 1H, H-6b), 3.81 (s, 3H, CH_3_{PMB}), 3.70 (t, $J = 4.3$ Hz, 1H, H-3), 3.64 (t, $J = 3.7$ Hz, 1H, H-2), 3.49 (t, $J = 3.5$ Hz, 1H, H-4), 2.66–2.62 (m, 2H, CH_2_{Lev}), 2.48–2.45 (m, 2H, CH_2_{Lev}), 2.32 (s, 3H, $\text{CH}_3_{\text{STol}}$); $^{13}\text{C}\{^1\text{H}\}$ NMR (100 MHz, CDCl_3): δ (ppm)

CHAPITRE 8 – TOWARDS THE SYNTHESIS OF AN IDOSE-CONTAINING DISACCHARIDE MIMIC OF CAMPYLOBACTER JEJUNI HS:4C CAPSULAR POLYSACCHARIDE

206.6 (CO_{Lev}), 172.5 (COOR_{Lev}), 159.5 (C_{Ar}), 137.9 (C_{Ar}), 137.8 (C_{Ar}), 137.2 (C_{Ar}), 132.5 (C_{Ar}), 131.3–126.3 (17C, C_{Ar} , $16 \times \text{CH}_{\text{Ar}}$), 114.0 (2C, $2 \times \text{CH}_{\text{Ar}}$), 86.0 (C-1), 76.1 (C-2), 74.4 (C-4), 74.0 (C-3), 73.0 ($\text{CH}_{2\text{PMB}}^*$), 72.9 ($\text{CH}_{2\text{Bn}}^*$), 72.4 ($\text{CH}_{2\text{Bn}}^*$), 67.7 (C-5), 63.3 (C-6), 55.4 ($\text{CH}_{3\text{PMB}}$), 38.1 ($\text{CH}_{2\text{Lev}}$), 29.9 ($\text{CH}_{3\text{Lev}}$), 28.0 ($\text{CH}_{2\text{Lev}}$), 21.2 ($\text{CH}_{3\text{STol}}$); HRMS (ESI-TOF) m/z [$\text{M} + \text{NH}_4$] $^+$ calcd for $\text{C}_{40}\text{H}_{48}\text{NO}_8\text{S}$ 702.3095; found 702.3105.

Ethyl 3-*O*-Benzyl-4,6-*O*-benzylidene-2-*O*-naphthylmethyl-1-thio- α -D-idopyranoside (9a).

To a solution of alcohol **7a** (357 mg, 0.888 mmol, 1.0 equiv) in dry DMF (11 mL) at 0 °C were successively added TBAI (164 mg, 0.444 mmol, 0.5 equiv) and NaH (60% dispersion in oil, 71 mg, 1.8 mmol, 2.0 equiv). The mixture was stirred at 0 °C for 10 min, after which NAPBr (393 mg, 1.78 mmol, 2.0 equiv) was added. The reaction was stirred for 4.5 h while being allowed to gradually warm to rt. The mixture was diluted with DCM and quenched by adding saturated aq. NaHCO_3 at 0 °C. The organic and aqueous layers were separated, and the organic layer was washed with saturated aq. NaHCO_3 ($\times 2$) and H_2O . The organic layer was dried over MgSO_4 , filtered, and concentrated under reduced pressure. The residue was purified by silica gel flash chromatography (Tol/EtOAc 98:2 to 96:4) to give compound **9a** (304 mg, 63%) as a white amorphous solid: R_f 0.55 (Hex/EtOAc 6:4); $[\alpha]_{\text{D}}^{20} +90$ (c 1.1, CHCl_3); ^1H NMR (400 MHz, CDCl_3): δ (ppm) 7.83–7.70 (m, 4H, $4 \times \text{CH}_{\text{Ar}}$), 7.51–7.44 (m, 5H, $5 \times \text{CH}_{\text{Ar}}$), 7.32–7.22 (m, 8H, $8 \times \text{CH}_{\text{Ar}}$), 5.55 (s, 1H, CHPh), 5.53 (d, $J = 3.0$ Hz, 1H, H-1), 4.80 (d, $J = 11.7$ Hz, 1H, $\text{CHH}_{\text{NAP}}^*$), 4.76 (d, $J = 11.7$ Hz, 1H, $\text{CHH}_{\text{NAP}}^*$), 4.69 (d, $J = 12.0$ Hz, 1H, CHH_{Bn}^*), 4.62 (d, $J = 12.0$ Hz, 1H, CHH_{Bn}^*), 4.28 (d, $J = 12.5$ Hz, 1H, H-6a), 4.19 (br s, 1H, H-5), 4.15 (dd, $J = 12.6$ Hz, $J = 2.1$ Hz, 1H, H-6b), 4.09 (t, $J = 2.3$ Hz, 1H, H-4), 3.89 (t, $J = 3.6$ Hz, H-3), 3.68 (dd, $J = 4.2$ Hz, $J = 3.2$ Hz, 1H, H-2), 2.77–2.59 (m, 2H, $\text{CH}_{2\text{SEt}}$), 1.32 (t, $J = 7.4$ Hz, 3H, $\text{CH}_{3\text{SEt}}$); $^{13}\text{C}\{^1\text{H}\}$ NMR (100 MHz, CDCl_3): δ (ppm) 138.2 (C_{Ar}), 137.9 (C_{Ar}), 135.7 (C_{Ar}), 133.4 (C_{Ar}), 133.1 (C_{Ar}), 129.0–125.9 (17C, $17 \times \text{CH}_{\text{Ar}}$), 101.1 (CHPh), 83.7 (C-1), 76.3 (C-3), 76.0 (C-2), 75.1 (C-4), 72.8 ($\text{CH}_{2\text{NAP}}^*$), 72.7 ($\text{CH}_{2\text{Bn}}^*$), 70.0 (C-6), 60.8 (C-5), 26.3 ($\text{CH}_{2\text{SEt}}$), 15.3 ($\text{CH}_{3\text{SEt}}$); HRMS (ESI-TOF) m/z [$\text{M} + \text{NH}_4$] $^+$ calcd for $\text{C}_{33}\text{H}_{38}\text{NO}_5\text{S}$ 560.2465; found 560.2463.

***para*-Methylphenyl 3-*O*-Benzyl-4,6-*O*-benzylidene-2-*O*-naphthylmethyl-1-thio- α -D-idopyranoside (9b).**

To a solution of alcohol **7b** (933 mg, 2.01 mmol, 1.0 equiv) in dry DMF (24 mL) at 0 °C were added TBAI (371 mg, 1.00 mmol, 0.5 equiv) and NaH (60% dispersion in oil, 161 mg, 4.02 mmol, 2.0 equiv). The mixture was stirred 20 min at 0 °C under Ar atmosphere, after which NAPBr (888 mg, 4.02 mmol, 2.0 equiv) was added. The mixture was stirred at 100 °C for 18 h, after which it was cooled to rt, quenched with MeOH, and co-evaporated with toluene. Then, EtOAc was added and the solution was washed with NaHCO₃ and brine. The organic layer was dried over MgSO₄, filtered, and concentrated under reduced pressure. The residue was purified by silica gel flash chromatography (Hex/EtOAc 9:1 to 85:15) to give compound **9b** (1022 mg, 84%) as a white amorphous solid: *R_f* 0.54 (Hex/EtOAc 8:2); [α]_D²⁰ +58 (*c* 1.4, CHCl₃); ¹H NMR (600 MHz, CDCl₃): δ (ppm) 7.82–7.80 (m, 1H, CH_{Ar}), 7.76–7.73 (m, 2H, 2 \times CH_{Ar}), 7.71–7.69 (m, 1H, CH_{Ar}), 7.50–7.48 (m, 2H, 2 \times CH_{Ar}), 7.46–7.44 (m, 3H, 3 \times CH_{Ar}), 7.42–7.40 (m, 2H, 2 \times CH_{Ar}), 7.37–7.26 (m, 6H, 6 \times CH_{Ar}), 7.23–7.20 (m, 2H, 2 \times CH_{Ar}), 7.09–7.08 (m, 2H, 2 \times CH_{Ar}), 5.76 (d, *J* = 2.3 Hz, 1H, H-1), 5.54 (s, 1H, CHPh), 4.82 (d, *J* = 11.7 Hz, 1H, CHH_{NAP}), 4.76 (d, *J* = 11.7 Hz, 1H, CHH_{NAP}), 4.73 (d, *J* = 12.0 Hz, 1H, CHH_{Bn}), 4.63 (d, *J* = 12.0 Hz, 1H, CHH_{Bn}), 4.32–4.30 (m, 2H, H-5, H-6a), 4.15 (dd, *J*_{6b-6a} = 13.0 Hz, *J*_{6b-5} = 2.3 Hz, 1H, H-6b), 4.11 (br s, 1H, H-4), 3.93 (t, *J* = 3.2 Hz, 1H, H-3), 3.86 (dd, *J*₂₋₃ = 4.1 Hz, *J*₂₋₁ = 2.8 Hz, 1H, H-2), 2.31 (s, 3H, CH_{3STol}); ¹³C{¹H} NMR (150 MHz, CDCl₃): δ (ppm) 138.1–125.9 (28C, 7 \times C_{Ar}, 21 \times CH_{Ar}), 101.2 (CHPh), 86.9 (C-1), 75.6, 75.5 (2C, C-2, C-3), 74.4 (C-4), 72.7, 72.6 (2C, CH_{2NAP}, CH_{2Bn}), 70.0 (C-6), 61.2 (C-5), 21.2 (CH_{3STol}); HRMS (ESI-TOF) *m/z* [M + NH₄]⁺ calcd for C₃₈H₄₀NO₅S 622.26217; found 622.25997.

Ethyl 3,4-di-*O*-Benzyl-6-*O*-levulinoyl-2-*O*-naphthylmethyl-1-thio- α -D-idopyranoside (5a).

Compound **9a** (100 mg, 0.184 mmol, 1.0 equiv) was cooled at –10 °C and BH₃.THF (1M in THF, 1.8 mL, 1.8 mmol, 10.0 equiv) was added. The solution was stirred at –10 °C under Ar atmosphere for 10 min, then Bu₂BOTf (1M in DCM, 0.18 mL, 0.18 mmol, 1.0 equiv) was added dropwise. The reaction mixture was stirred for 30 min under Ar atmosphere while being allowed to gradually warm to 0 °C. The mixture was quenched with Et₃N and MeOH and the solvents were evaporated

CHAPITRE 8 – TOWARDS THE SYNTHESIS OF AN IDOSE-CONTAINING DISACCHARIDE MIMIC OF CAMPYLOBACTER JEJUNI HS:4C CAPSULAR POLYSACCHARIDE

under reduced pressure and co-evaporated three times with MeOH. The residue was roughly filtered through a pad of silica gel to remove the main impurities. To a solution of the resulting alcohol in dry DCE (1.8 mL) were successively added LevOH (24 μ L, 0.24 mmol, 1.3 equiv), EDC.HCl (53 mg, 0.28 mmol, 1.5 equiv), and DMAP (11 mg, 0.09 mmol, 0.5 equiv). The solution was stirred at rt under Ar atmosphere for 18 h. The solvents were then evaporated under reduced pressure and the residue was purified by silica gel flash chromatography (Hex/EtOAc 8:2 to 6:4) to give compound **5a** (118 mg, quant. over two steps) as a colorless oil: R_f 0.43 (Hex/EtOAc 6:4); $[\alpha]_D^{20} +44$ (c 0.7, CHCl₃); ¹H NMR (400 MHz, CDCl₃): δ (ppm) 7.85–7.73 (m, 4H, 4 \times CH_{Ar}), 7.50–7.44 (m, 3H, 3 \times CH_{Ar}), 7.32–7.28 (m, 6H, 6 \times CH_{Ar}), 7.27–7.26 (m, 2H, 2 \times CH_{Ar}), 7.17–7.15 (m, 2H, 2 \times CH_{Ar}), 5.27 (d, J = 3.8 Hz, 1H, H-1), 4.87 (d, J = 11.9 Hz, 1H, CHH_{NAP}*), 4.71 (d, J = 11.9 Hz, 1H, CHH_{NAP}*), 4.65 (d, J = 11.9 Hz, 1H, CHH_{Bn}*), 4.59 (d, J = 11.8 Hz, 1H, CHH_{Bn}*), 4.52–4.48 (m, 1H, H-5), 4.45 (d, J = 11.8 Hz, 1H, CHH_{Bn}*), 4.42 (d, J = 12.1 Hz, 1H, CHH_{Bn}*), 4.41–4.36 (m, 1H, H-6a), 4.27 (dd, J = 11.7 Hz, J = 4.5 Hz, 1H, H-6b), 3.71 (t, J = 4.8 Hz, 1H, H-3), 3.53 (t, J = 4.3 Hz, 1H, H-2), 3.50 (dd, J = 4.9 Hz, J = 3.6 Hz, 1H, H-4), 2.73–2.59 (m, 4H, CH_{2SEt}, CH_{2Lev}), 2.55–2.51 (m, 2H, CH_{2Lev}), 2.17 (s, 3H, CH_{3Lev}), 1.30 (t, J = 7.4 Hz, 3H, CH_{3SEt}); ¹³C{¹H} NMR (100 MHz, CDCl₃): δ (ppm) 206.5 (CO_{Lev}), 172.5 (COOR_{Lev}), 137.9 (C_{Ar}), 137.9 (C_{Ar}), 135.5 (C_{Ar}), 133.4 (C_{Ar}), 133.2 (C_{Ar}), 128.5–126.1 (17C, 17 \times CH_{Ar}), 82.3 (C-1), 77.3 (C-2), 75.0 (2C, C-3, C-4), 73.6 (CH_{2NAP}*), 73.3 (CH_{2Bn}*), 72.7 (CH_{2Bn}*), 67.8 (C-5), 63.0 (C-6), 38.1 (CH_{2Lev}), 30.0 (CH_{3Lev}), 28.0 (CH_{2Lev}), 25.9 (CH_{2SEt}), 15.2 (CH_{3SEt}); HRMS (ESI-TOF) m/z [M + NH₄]⁺ calcd for C₃₈H₄₆NO₇S 660.2989; found 660.2995.

***para*-Methylphenyl 3,4-di-*O*-Benzyl-6-*O*-levulinoyl-2-*O*-naphthylmethyl-1-thio- α -D-idopyranoside (5b).**

Compound **9b** (560 mg, 0.926 mmol, 1.0 equiv) was cooled at –10 °C and BH₃.THF (1M in THF, 9.3 mL, 9.3 mmol, 10.0 equiv) was added. The solution was stirred at –10 °C under Ar atmosphere for 10 min, then Bu₂BOTf (1M in DCM, 0.93 mL, 0.93 mmol, 1.0 equiv) was added dropwise. The reaction mixture was stirred for 30 min under Ar atmosphere while being allowed to gradually warm to 0 °C. The mixture was quenched with Et₃N and MeOH and the solvents were evaporated under reduced pressure and co-evaporated three times with MeOH. The residue was roughly

CHAPITRE 8 – TOWARDS THE SYNTHESIS OF AN IDOSE-CONTAINING DISACCHARIDE MIMIC OF CAMPYLOBACTER JEJUNI HS:4C CAPSULAR POLYSACCHARIDE

filtered over a pad of silica to remove most impurities. To a solution of the latter alcohol (82 mg, 0.14 mmol, 1.0 equiv) in dry DCE (1.4 mL) were successively added EDC.HCl (39 mg, 0.20 mmol, 1.5 equiv), LevOH (18 μ L, 0.18 mmol, 1.3 equiv), and DMAP (8 mg, 0.07 mmol, 0.5 equiv). The solution was stirred at rt under Ar atmosphere for 3 h. The solvents were then evaporated under reduced pressure and the residue was purified by silica gel flash chromatography (Hex/EtOAc 8:2 to 7:3) to give compound **5b** (89 mg, 93% over two steps) as a colorless oil: R_f 0.35 (Hex/EtOAc 6:4); $[\alpha]_D^{20} +35$ (c 0.5, CHCl₃); ¹H NMR (600 MHz, CDCl₃): δ (ppm) 7.86–7.83 (m, 1H, CH_{Ar}), 7.80–7.79 (m, 1H, CH_{Ar}), 7.79–7.76 (m, 1H, CH_{Ar}), 7.72 (br s, 1H, CH_{Ar}), 7.51–7.48 (m, 2H, 2 \times CH_{Ar}), 7.45–7.44 (m, 1H, CH_{Ar}), 7.42–7.39 (m, 2H, 2 \times CH_{Ar}), 7.29–7.27 (m, 6H, 6 \times CH_{Ar}), 7.25–7.24 (m, 2H, 2 \times CH_{Ar}), 7.17–7.16 (m, 2H, 2 \times CH_{Ar}), 7.17–7.16 (m, 2H, 2 \times CH_{Ar}), 5.49 (d, J = 3.0 Hz, 1H, H-1), 4.88 (d, J = 12.1 Hz, 1H, CHH_{NAP}), 4.70 (d, J = 12.1 Hz, 1H, CHH_{NAP}), 4.67–4.65 (m, 1H, H-5), 4.65 (d, J = 11.9 Hz, 1H, CHH_{Bn}), 4.59 (d, J = 11.9 Hz, 1H, CHH_{Bn}), 4.44 (d, J = 11.9 Hz, 1H, CHH_{Bn}), 4.39 (d, J = 11.9 Hz, 1H, CHH_{Bn}), 4.38 (dd, J_{6a-6b} = 11.7 Hz, J_{6a-5} = 8.2 Hz, 1H, H-6a), 4.27 (dd, J_{6b-6a} = 11.7 Hz, J_{6b-5} = 4.3 Hz, 1H, H-6b), 3.74 (t, J = 4.1 Hz, 1H, H-3), 3.71 (t, J = 3.5 Hz, 1H, H-2), 3.50 (t, J = 3.5 Hz, 1H, H-4), 2.65 (t, J = 6.8 Hz, 2H, CH_{2Lev}), 2.48 (td, J = 6.8 Hz, J = 1.8 Hz, 2H, CH_{2Lev}), 2.32 (s, 3H, CH_{3STol}), 2.12 (s, 3H, CH_{3Lev}); ¹³C{¹H} NMR (150 MHz, CDCl₃): δ (ppm) 206.6 (CO_{Lev}), 172.5 (COOR_{Lev}), 137.8–126.1 (28C, 7 \times C_{Ar}, 21 \times CH_{Ar}), 86.1 (C-1), 76.4 (C-2), 74.3 (C-4), 73.8 (C-3), 73.3 (CH_{2NAP}), 73.0 (CH_{2Bn}), 72.5 (CH_{2Bn}), 67.7 (C-5), 63.3 (C-6), 38.0 (CH_{2Lev}), 29.9 (CH_{3Lev}), 28.0 (CH_{2Lev}), 21.2 (CH_{3STol}); HRMS (ESI-TOF) m/z [M + NH₄]⁺ calcd for C₄₃H₄₈NO₇S 722.31460; found 722.31376.

***para*-Methylphenylsulfenyl 3,4-di-*O*-Benzyl-6-*O*-levulinoyl-2-*O*-naphthylmethyl- α -D-idopyranoside (5c).**

To a solution of compound **5b** (20 mg, 0.028 mmol, 1.0 equiv) in dry DCM (142 μ L) at -78 °C was added *m*-CPBA (6 mg, 0.03 mmol, 1.2 equiv). The mixture was stirred at -10 °C for 2.5 h, after which it was diluted with DCM and quenched with saturated aq. NaHCO₃. The organic layer was then washed with saturated aq. NaHCO₃, dried over MgSO₄, filtered and concentrated under reduced pressure. The residue was purified by silica gel flash chromatography (Hex/EtOAc 3:1 to

CHAPITRE 8 – TOWARDS THE SYNTHESIS OF AN IDOSE-CONTAINING DISACCHARIDE MIMIC OF CAMPYLOBACTER JEJUNI HS:4C CAPSULAR POLYSACCHARIDE

2:1) to give sulfoxide **5c** (17 mg, 81%) as a white amorphous solid: R_f 0.28 (Hex/EtOAc 2:1); $[\alpha]_D^{20}$ -39 (c 0.7, CHCl_3); $^1\text{H NMR}$ (600 MHz, CDCl_3): δ (ppm) 7.85–7.75 (m, 4H, $4 \times \text{CH}_{\text{Ar}}$), 7.61–7.60 (m, 2H, $2 \times \text{CH}_{\text{Ar}}$), 7.50–7.48 (m, 2H, $2 \times \text{CH}_{\text{Ar}}$), 7.41–7.39 (m, 1H, CH_{Ar}), 7.29–7.7.24 (m, 8H, $8 \times \text{CH}_{\text{Ar}}$), 7.18–7.16 (m, 2H, $2 \times \text{CH}_{\text{Ar}}$), 7.11–7.10 (m, 2H, $2 \times \text{CH}_{\text{Ar}}$), 4.68 (d, $J = 12.1$ Hz, 1H, CHH_{NAP}), 4.71–4.65 (m, 3H, CHH_{NAP} , CHH_{Bn} , CHH_{Bn}), 4.63 (br s, 1H, H-1), 4.46–4.44 (m, 1H, H-5), 4.41 (br s, 1H, H-4), 4.34 (d, $J = 11.9$ Hz, 1H, CHH_{Bn}), 4.31–4.28 (m, 2H, CHH_{Bn} , H-6a), 4.12 (dd, $J = 11.7$ Hz, $J = 4.2$ Hz, 1H, H-6b), 3.84 (t, $J = 3.0$ Hz, 1H, H-3), 3.46 (br s, 1H, H-2), 2.79–2.69 (m, 2H, $\text{CH}_{2\text{Lev}}$), 2.61–2.55 (m, 2H, $\text{CH}_{2\text{Lev}}$), 2.38 (s, 3H, $\text{CH}_{3\text{S(O)Tol}}$), 2.18 (s, 3H, $\text{CH}_{3\text{Lev}}$); $^{13}\text{C}\{^1\text{H}\}$ NMR (150 MHz, CDCl_3): δ (ppm) 206.5 (CO_{Lev}), 172.5 (COOR_{Lev}), 141.7 (C_{Ar}), 140.3 (C_{Ar}), 137.4 (C_{Ar}), 137.2 (C_{Ar}), 135.1 (C_{Ar}), 133.3 (C_{Ar}), 133.2 (C_{Ar}), 129.8–124.7 (21C, $21 \times \text{CH}_{\text{Ar}}$), 95.7 (C-1), 72.9 ($\text{CH}_{2\text{NAP}}$), 72.6 ($\text{CH}_{2\text{Bn}}$), 72.2 ($\text{CH}_{2\text{Bn}}$), 72.0 (C-2), 70.84 (C-5*), 70.79 (C-3*), 69.1 (C-4), 64.1 (C-6), 38.0 ($\text{CH}_{2\text{Lev}}$), 30.0 ($\text{CH}_{3\text{Lev}}$), 27.9 ($\text{CH}_{2\text{Lev}}$), 21.6 ($\text{CH}_{3\text{S(O)Tol}}$); HRMS (ESI-TOF) m/z $[\text{M} + \text{Na}]^+$ calcd for $\text{C}_{43}\text{H}_{44}\text{NaO}_8\text{S}$ 743.2649; found 743.2656.

3,4-di-*O*-Benzyl-6-*O*-levulinoyl-2-*O*-naphthylmethyl-1-thio- α -D-idopyranosyl *ortho*-hexynylbenzoate (5d**).**

To a solution of thioglycoside **5b** (101 mg, 0.143 mmol, 1.0 equiv) in DCE (14 mL) were successively added tri-*tert*-butylpyridine (53 mg, 0.21 mmol, 1.5 equiv), Me_2S_2 (38 μL , 0.43 mmol, 3.0 equiv), MeOTf (47 μL , 0.43 mmol, 3.0 equiv) and H_2O (103 μL , 5.71 mmol, 40 equiv). The mixture was stirred at rt for 24 h, after which Me_2S_2 (38 μL , 0.43 mmol, 3.0 equiv), MeOTf (47 μL , 0.43 mmol, 3.0 equiv) and H_2O (103 μL , 5.71 mmol, 40 equiv) were added. The mixture was allowed to stir for an additional 24 h and was then diluted with DCM and washed with saturated aq. NaHCO_3 . The organic layer was dried over MgSO_4 , filtered, and concentrated under reduced pressure. The residue was purified by silica gel flash chromatography (Hex/EtOAc 2:1 to 1:1) to give 3,4-di-*O*-benzyl-6-*O*-levulinoyl-2-*O*-naphthylmethyl-D-idopyranoside (77 mg, 90%, α/β 0.5:1) as a colorless oil: R_f 0.26 (Hex/EtOAc 1:1); NMR data for β -anomer: $^1\text{H NMR}$ (600 MHz, CDCl_3): δ (ppm) 7.87–7.77 (m, 3H, $3 \times \text{CH}_{\text{Ar}}$), 7.68 (br s, 1H, CH_{Ar}), 7.53–7.44 (m, 3H, $3 \times \text{CH}_{\text{Ar}}$), 7.35–7.21 (m, 8H, $8 \times \text{CH}_{\text{Ar}}$), 7.04–7.03 (m, 2H, $2 \times \text{CH}_{\text{Ar}}$), 4.94 (dd, $J = 12.0$ Hz, $J = 2.1$ Hz, 1H, H-1), 4.77 (d, $J = 12.2$ Hz, 1H, CHH_{NAP}), 4.71 (d, $J = 12.2$ Hz, 1H, $\text{CHH}_{\text{NAP}}^*$), 4.59

CHAPITRE 8 – TOWARDS THE SYNTHESIS OF AN IDOSE-CONTAINING DISACCHARIDE MIMIC OF CAMPYLOBACTER JEJUNI HS:4C CAPSULAR POLYSACCHARIDE

(d, $J = 12.1$ Hz, 1H, CHH_{Bn}^*), 4.36–4.32 (m, 3H, CHH_{Bn}^* , CHH_{Bn}^* , H-6a), 4.28 (d, $J = 12.1$ Hz, 1H, CHH_{Bn}^*), 4.22 (dd, $J = 11.4$ Hz, $J = 5.4$ Hz, 1H, H-6b), 4.03 (ddd, $J = 7.3$ Hz, $J = 5.4$ Hz, $J = 2.1$ Hz, 1H, H-5), 3.91 (d, $J = 12.0$ Hz, 1H, OH), 3.69 (t, $J = 3.1$ Hz, 1H, H-3), 3.48–3.47 (m, 1H, H-2), 3.30 (t, $J = 2.0$ Hz, 1H, H-4), 2.77–2.70 (m, 2H, CH_{2Lev}), 2.61–2.48 (m, 2H, CH_{2Lev}), 2.17 (s, 3H, CH_{3Lev}); $^{13}C\{^1H\}$ NMR (150 MHz, $CDCl_3$): δ (ppm) 206.8 (CO_{Lev}), 172.6 ($COOR_{Lev}$), 137.6 (C_{Ar}), 137.4 (C_{Ar}), 134.7 (C_{Ar}), 133.4 (C_{Ar}), 133.3 (C_{Ar}), 128.8–126.2 (17C, $17 \times CH_{Ar}$), 92.6 (C-1, $^1J_{C1-H1} = 164$ Hz), 74.7 (C-2), 73.7 (CH_{2NAP}^*), 72.6 (CH_{2Bn}^*), 72.6 (CH_{2Bn}^*), 72.3 (C-5), 72.2 (C-4), 71.7 (C-3), 63.9 (C-6), 38.1 (CH_{2Lev}), 30.0 (CH_{3Lev}), 28.0 (CH_{2Lev}); NMR data for α -anomer: 1H NMR (600 MHz, $CDCl_3$): δ (ppm) 7.87–7.77 (m, 1.5H, $3 \times CH_{Ar}$), 7.72 (br s, 0.5 H, CH_{Ar}), 7.53–7.44 (m, 1.5H, $3 \times CH_{Ar}$), 7.35–7.21 (m, 4H, $8 \times CH_{Ar}$), 7.12–7.11 (m, 1H, $2 \times CH_{Ar}$), 5.18 (dd, $J = 7.3$ Hz, $J = 3.2$ Hz, 0.5H, H-1), 4.86 (d, $J = 12.2$ Hz, 0.5 H, CHH_{NAP}^*), 4.74 (d, $J = 12.3$ Hz, 0.5 H, CHH_{NAP}^*), 4.64 (d, $J = 11.9$ Hz, 0.5H, CHH_{Bn}^*), 4.55 (d, $J = 11.7$ Hz, 0.5H, CHH_{Bn}^*), 4.49–4.44 (m, 1.5H, CHH_{Bn}^* , CHH_{Bn}^* , H-6a), 4.36–4.32 (m, 0.5H, H-5), 4.25 (dd, $J = 12.0$ Hz, $J = 5.0$ Hz, 0.5H, H-6b), 4.14 (d, $J = 7.4$ Hz, 0.5H, OH), 3.74 (t, $J = 4.8$ Hz, 0.5H, H-3), 3.54 (t, $J = 4.0$ Hz, 0.5H, H-4), 3.48–3.47 (m, 0.5H, H-2), 2.77–2.70 (m, 1H, CH_{2Lev}), 2.61–2.48 (m, 1H, CH_{2Lev}), 2.19 (s, 1.5H, CH_{3Lev}); $^{13}C\{^1H\}$ NMR (150 MHz, $CDCl_3$): δ (ppm) 206.8 (CO_{Lev}), 172.6 ($COOR_{Lev}$), 137.6 (C_{Ar}), δ 137.3 (C_{Ar}), 135.5 (C_{Ar}), 133.4 (C_{Ar}), 133.3 (C_{Ar}), 128.8–126.2 (17C, $17 \times CH_{Ar}$), 93.9 (C-1, $^1J_{C1-H1} = 171$), 75.9 (C-2), 74.5 (C-3), 74.1 (C-4), 73.7 (CH_{2Bn}^*), 73.2 (CH_{2NAP}^*), 72.8 (CH_{2Bn}), 66.5 (C-5), 63.1 (C-6), 38.2 (CH_{2Lev}), 30.1 (CH_{3Lev}), 28.2 (CH_{2Lev}); HRMS (ESI-TOF) m/z $[M + NH_4]^+$ calcd for $C_{36}H_{42}NO_8$ 616.2905; found 616.2912. To a solution of the hemiacetal (5 mg, 0.008 mmol, 1.0 equiv) and *o*-hexynylbenzoic acid⁵⁹³ (3.4 mg, 0.017 mmol, 2.0 equiv) in dry DCE (120 μ L) and dry THF (120 μ L) were successively added DMAP (1.7 mg, 0.014 mmol, 1.7 equiv) and EDC.HCl (5 mg, 0.03 mmol, 3.0 equiv), The mixture was stirred at rt for 20 h, after which it was diluted with DCM and washed with saturated aq. $NaHCO_3$. The organic layer was dried over $MgSO_4$, filtered, and concentrated under reduced pressure. The residue was purified by silica gel flash chromatography (Hex/EtOAc 3:1 to 2:1) to give *o*-hexynylbenzoate **5d** (6.4 mg, quant., α/β 1:0.2) as a white amorphous solid: R_f 0.54 (Hex/EtOAc 1:1); NMR data for major α -anomer: 1H NMR (600 MHz, $CDCl_3$): δ (ppm) 7.82–7.07 (m, 21H, $21 \times CH_{Ar}$), 6.47 (d, $J = 2.1$ Hz, 1H, H-1), 4.97 (d, $J = 12.3$ Hz, 1H, CHH_{NAP}^*),

CHAPITRE 8 – TOWARDS THE SYNTHESIS OF AN IDOSE-CONTAINING DISACCHARIDE MIMIC OF CAMPYLOBACTER JEJUNI HS:4C CAPSULAR POLYSACCHARIDE

4.79 (d, $J = 12.4$ Hz, 1H, $\text{CHH}_{\text{NAP}}^*$), 4.71 (d, $J = 12.0$ Hz, 1H, CHH_{Bn}^*), 4.51–4.48 (m, 2H, CHH_{Bn}^* , CHH_{Bn}^*), 4.45–4.43 (m, 1H, H-5), 4.37 (d, $J = 11.4$ Hz, 1H, CHH_{Bn}^*), 4.35–4.30 (m, 2H, H-6a, H-6b), 3.82 (t, $J = 4.1$ Hz, 1H, H-3), 3.77 (t, $J = 3.1$ Hz, 1H, H-2), 3.60 (t, $J = 3.3$ Hz, 1H, H-4), 2.69–2.59 (m, 2H, $\text{CH}_{2\text{Lev}}$), 2.49–2.44 (4H, $\text{CH}_{2\text{Lev}}$, $\text{CH}_{2\text{oABz}}$), 2.09 (s, 3H, $\text{CH}_{3\text{Lev}}$), 1.63–1.58 (m, 2H, $\text{CH}_{2\text{oABz}}$), 1.51–1.46 (m, 2H, $\text{CH}_{2\text{oABz}}$), 0.94 (t, $J = 7.3$ Hz, 3H, $\text{CH}_{2\text{oABz}}$); $^{13}\text{C}\{^1\text{H}\}$ NMR (150 MHz, CDCl_3) : δ (ppm) 206.7 (CO_{Lev}), 172.5 (COOR_{Lev}), 164.1 ($\text{COOR}_{\text{oABz}}$), 137.7–125.4 (28C, $7 \times \text{C}_{\text{Ar}}$, $21 \times \text{CH}_{\text{Ar}}$), 96.9 (C_{alkyne}), 93.6 (C-1, $^1J_{\text{C1-H1}} = 174$ Hz), 79.3 (C_{alkyne}), 74.2 (C-3*), 74.1 (C-2*), 73.7 (C-4), 73.3 ($\text{CH}_{2\text{NAP}}^*$), 73.0 ($\text{CH}_{2\text{Bn}}^*$), 72.5 ($\text{CH}_{2\text{Bn}}^*$), 68.8 (C-5), 63.4 (C-6), 38.0 ($\text{CH}_{2\text{Lev}}$), 30.9 ($\text{CH}_{2\text{oABz}}$), 29.9 ($\text{CH}_{3\text{Lev}}$), 28.1 ($\text{CH}_{2\text{Lev}}$), 22.2 ($\text{CH}_{2\text{oABz}}$), 19.7 ($\text{CH}_{2\text{oABz}}$), 13.8 ($\text{CH}_{3\text{oABz}}$); HRMS (ESI-TOF) m/z $[\text{M} + \text{NH}_4]^+$ calcd for $\text{C}_{49}\text{H}_{54}\text{NO}_9$ 800.3793; found 800.3795.

***tert*-Butyldimethylsilyl 2,4-di-*O*-Benzyl-6-*O*-levulinoyl- β -D-idopyranosyl-(1 \rightarrow 4)-3,6-di-*O*-benzyl-2-deoxy-2-trichloroacetamido- β -D-glucopyranoside (10).**

Thioglycoside **5b** (10 mg, 0.014 mmol, 1.0 equiv) and acceptor **3**⁵⁷⁷ (11 mg, 0.017 mmol, 1.2 equiv) were dried in a round bottom flask under high vacuum for 1 h. Then, activated 4Å MS (40 mg) and dry DCM (284 μL) were added. The suspension was stirred at rt under Ar atmosphere for 1 h, after which DDQ (4 mg, 0.02 mmol, 1.2 equiv) was added. The mixture was stirred at rt for 2.5 h and was quenched by the addition of saturated aq. NaHCO_3 at 0 °C. The suspension was diluted with DCM and washed with saturated aq. NaHCO_3 ($\times 2$). The organic layer was dried over MgSO_4 , filtered, and concentrated under reduced pressure. The resulting mixed acetal was dried under high vacuum for 1 h, after which activated 4Å MS (80 mg) and dry DCE (1.4 mL) were added. The suspension was stirred at rt under Ar atmosphere for 1 h. Then, tri-*tert*-butylpyridine (10 mg, 0.04 mmol, 3.0 equiv), Me_2S_2 (3.8 μL , 0.043 mmol, 3.0 equiv) and MeOTf (4.7 μL , 0.043 mmol, 3.0 equiv) were successively added, and the mixture was stirred at 40 °C for 18.5 h. The reaction was brought back to rt, quenched with Et_3N , and concentrated under reduced pressure. The residue was purified by silica gel flash chromatography (Hex/EtOAc 8:2 to 6:4) to give β -disaccharide **10** (4 mg, 28%) as a white amorphous solid: R_f 0.41 (Hex/EtOAc 2:1 *ran twice*); $[\alpha]_{\text{D}}^{20} +6$ (c 0.4, CHCl_3); ^1H NMR (600 MHz, CDCl_3) : δ (ppm) 7.33–7.28 (m, 15H, $15 \times \text{CH}_{\text{Ar}}$),

CHAPITRE 8 – TOWARDS THE SYNTHESIS OF AN IDOSE-CONTAINING DISACCHARIDE MIMIC OF CAMPYLOBACTER JEJUNI HS:4C CAPSULAR POLYSACCHARIDE

7.25–7.22 (m, 5H, 5 x CH_{Ar}), 7.08 (d, $J = 7.3$ Hz, 1H, NHTCA), 5.04 (br s, 1H, H-1A), 4.99–4.97 (m, 2H, H-1B, CHH_{Bn}), 4.64 (d, $J = 10.7$ Hz, 1H, CHH_{Bn}), 4.62 (d, $J = 11.5$ Hz, 1H, CHH_{Bn}), 4.57–4.54 (m, 2H, CHH_{Bn} , CHH_{Bn}), 4.52–4.48 (m, 2H, CHH_{Bn} , CHH_{Bn}), 4.40 (d, $J = 11.5$ Hz, CHH_{Bn}), 4.24–4.21 (m, H-6Ba), 4.10–4.05 (m, 4H, H-6Bb, H-3B, H-5A, H-4B), 3.91 (t, $J = 3.7$ Hz, 1H, H-3A), 3.76–3.74 (m, 2H, H-6Aa, H-2A), 3.70 (dd, $J = 11.0$ Hz, $J = 3.7$ Hz, 1H, H-6Ab), 3.67–3.63 (m, 1H, H-2B), 3.60–3.58 (m, 1H, H-5B), 3.42 (br s, 1H, H-4A), 3.40 (d, $J = 11.1$ Hz, 1H, OH); $^{13}C\{^1H\}$ NMR (150 MHz, $CDCl_3$) δ 207.3 (CO_{Lev}), 172.5 ($COOR_{Lev}$), 161.7 (CO_{NHTCA}), 138.5 (C_{Ar}), 138.2 (C_{Ar}), 137.6 (C_{Ar}), 136.8 (C_{Ar}), 128.8–127.5 (20C, 20 x CH_{Ar}), 99.5 (C-1A, $^1J_{C1-H1} = 163$ Hz), 95.1 (C-1B, $^1J_{C1-H1} = 163$ Hz), 78.0 (C-4B*), 77.0 (C-3B*), 74.8 (C-5B), 74.1 (CH_{2Bn}), 74.0 (C-3A), 73.3 (2C, CH_{2Bn} , C-4A), 72.9 (CH_{2Bn}), 72.7 (CH_{2Bn}), 72.7 (C-5A), 69.0 (C-2A*), 68.9 (C-6A*), 63.4 (C-6B), 59.7 (C-2B), 38.0 (CH_{2Lev}), 30.0 (CH_{3Lev}), 27.9 (CH_{2Lev}), 25.8 (3C, $C(CH_3)_3TBS$), 18.0 ($C(CH_3)_3TBS$), -4.1 (CH_3TBS), -5.0 (CH_3TBS); HRMS (ESI-TOF) m/z [M + NH_4] $^+$ calcd for $C_{53}H_{70}[^{35}Cl]_3N_2O_{13}Si$ 1075.3707; found 1075.3703.

***para*-Methylphenyl 3,4-di-*O*-Benzyl-6-deoxy-2-*O*-*para*-methoxybenzyl-1-thio- α -D-ido-heptopyranoside (12).**

Oxidation. To a solution of alcohol **11** (405 mg, 0.690 mmol, 1.0 equiv) in dry DCM (4.1 mL) and DMSO (4.1 mL) at 0 °C were successively added Et_3N (404 μ L, 2.90 mmol, 4.2 equiv) and $SO_3 \cdot py$ (340 mg, 2.14 mmol, 3.1 equiv). The solution was stirred at 0 °C under Ar atmosphere for 30 min after which another portion of Et_3N (404 μ L, 2.90 mmol, 4.2 equiv) and $SO_3 \cdot py$ (340 mg, 2.14 mmol, 3.1 equiv) was added. After an additional stirring time of 30 min at 0 °C, the reaction mixture was diluted with EtOAc and washed with saturated NH_4Cl . The aqueous layer was extracted with EtOAc ($\times 2$) and the combined organic layers were washed with $NaHCO_3$ and brine. The organic layers were dried over $MgSO_4$, filtered, concentrated under reduced pressure, co-evaporated with toluene ($\times 3$), and the resulting residue was dried 1 h under high vacuum.

Homologation. $KHMDS$ (1M in THF, 0.9 mL, 0.9 mmol, 1.3 equiv) was added dropwise to a suspension of $CH_3OCH_2PPh_3Cl$ (378 mg, 1.10 mmol, 1.6 equiv) in dry toluene (6.2 mL) at rt under Ar. To the resulting orange mixture, a solution of the previously prepared crude aldehyde in dry toluene (4.1 mL + 3 mL for rinsing) was added. The reaction was allowed to stir at rt for 25 min,

CHAPITRE 8 – TOWARDS THE SYNTHESIS OF AN IDOSE-CONTAINING DISACCHARIDE MIMIC OF CAMPYLOBACTER JEJUNI HS:4C CAPSULAR POLYSACCHARIDE

after which it was diluted with EtOAc and washed with H₂O, saturated aq. NH₄Cl and saturated aq. NaHCO₃. The organic layer was dried over MgSO₄, filtered, and concentrated under reduced pressure. **Hydrolysis.** The resulting crude enol ether was solubilized in acetone (6.9 mL) and aq. 1.2 N HCl (380 μL) was added. The mixture was stirred at rt for 2 h, after which it was diluted with DCM and washed with saturated aq. NaHCO₃. The aqueous phase was extracted with DCM (2x) and the combined organic layers were dried over MgSO₄, filtered, concentrated under reduced pressure, and the resulting crude aldehyde was dried 1 h under high vacuum. **Reduction.** The crude C7-aldehyde was solubilized in dry DCE (3.1 mL) and MeOH (9.3 mL) and cooled to -10 °C. NaBH₄ (104 mg, 2.76 mmol, 4.0 equiv) was then slowly added and the reaction was allowed to stir from -10 °C to 0 °C for 45 min, after which it was diluted with DCM and washed with H₂O. The aqueous phase was extracted with DCM (×3) and the combined organic layers were dried over MgSO₄, filtered, and concentrated under reduced pressure. The residue was purified by silica gel flash chromatography (Hex/EtOAc 9:1 to 6:4) to give alcohol **12** (171 mg, 41%) as a white amorphous solid along with some starting material **11** (50 mg): R_f 0.19 (Hex/EtOAc 7:3); [α]_D²⁰ +46 (c 1.2, CHCl₃); ¹H NMR (400 MHz, CDCl₃): δ (ppm) 7.38–7.24 (m, 14H, 14 × CH_{Ar}), 7.12–7.10 (m, 2H, 2 × CH_{Ar}), 6.87–6.85 (m, 2H, 2 × CH_{Ar}), 5.38 (d, J = 3.9 Hz, 1H, H-1), 4.69–4.63 (m, 3H, CHH_{PMB}*, CHH_{Bn}*, CHH_{Bn}*), 4.55–4.47 (m, 3H, H-5, CHH_{PMB}*, CHH_{Bn}*), 4.45 (d, J = 11.9 Hz, 1H, CHH_{Bn}*), 3.81 (s, 3H, CH_{3PMB}), 3.72 (t, J = 4.9 Hz, 1H, H-3), 3.65–3.63 (m, 3H, H-7a, H-7b, H-2), 3.39 (dd, J = 4.7 Hz, J = 3.2 Hz, 1H, H-4), 2.32 (s, 3H, CH_{3STol}), 2.14–2.05 (m, 1H, H-6a), 1.68–1.60 (m, 2H, H-6b, OH); ¹³C{¹H} NMR (100 MHz, CDCl₃): δ (ppm) 159.5 (C_{Ar}), 138.0 (C_{Ar}), 137.4 (C_{Ar}), 131.9–128.0 (19C, 3 × C_{Ar}, 16 × CH_{Ar}), 114.0 (2C, 2 × CH_{Ar}), 86.0 (C-1), 76.72 (C-4*), 76.68 (C-2*), 75.3 (C-3), 73.3 (CH_{2PMB}*), 73.2 (CH_{2Bn}*), 72.7 (CH_{2Bn}*), 68.7 (C-5), 60.4 (C-7), 55.4 (CH_{3PMB}), 31.9 (C-6), 21.2 (CH_{3STol}); HRMS (ESI-TOF) m/z [M + NH₄]⁺ calcd for C₃₆H₄₄NO₆S 618.2884; found 618.2899.

***para*-Methylphenyl 3,4-di-*O*-Benzyl-6-deoxy-7-*O*-levulinoyl-2-*O*-*para*-methoxybenzyl-1-thio- α -D-ido-heptopyranoside (**13**).**

To a solution of alcohol **12** (64 mg, 0.11 mmol, 1.0 equiv) in dry DCE (1.1 mL) were successively added LevOH (14 μL, 0.14 mmol, 1.3 equiv), EDC.HCl (31 mg, 0.16 mmol, 1.5 equiv) and DMAP

CHAPITRE 8 – TOWARDS THE SYNTHESIS OF AN IDOSE-CONTAINING DISACCHARIDE MIMIC OF CAMPYLOBACTER JEJUNI HS:4C CAPSULAR POLYSACCHARIDE

(6 mg, 0.05 mmol, 0.5 equiv). The mixture was stirred at rt for 1.5 h, after which it was diluted with EtOAc and washed with saturated aq. NH₄Cl and saturated aq. NaHCO₃. The organic layer was dried over MgSO₄, filtered, and concentrated under reduced pressure. The residue was purified by silica gel flash chromatography (Hex/EtOAc 9:1 to 6:4) to give levulinoylated heptoside **13** (68 mg, 91%) as a colorless oil: *R_f* 0.37 (Hex/EtOAc 6:4); [α]_D²⁰ +46 (*c* 0.9, CHCl₃); ¹H NMR (400 MHz, CDCl₃) : δ (ppm) 7.35–7.31 (m, 11H, 11 \times CH_{Ar}), 7.24–7.22 (m, 3H, 3 \times CH_{Ar}), 7.10–7.08 (m, 2H, 2 \times CH_{Ar}), 6.86–6.84 (m, 2H, 2 \times CH_{Ar}), 5.39 (d, *J* = 3.2 Hz, 1H, H-1), 4.66–4.61 (m, 3H, CHH_{PMB}*, CHH_{Bn}*, CHH_{Bn}*), 4.50–4.41 (m, 4H, CHH_{PMB}*, CHH_{Bn}*, CHH_{Bn}*, H-5), 4.11–3.99 (m, 2H, H-7a, H-7b), 3.81 (s, 3H, CH_{3PMB}), 3.70 (t, *J* = 4.3 Hz, 1H, H-3), 3.64 (t, *J* = 3.8 Hz, 1H, H-2), 3.35 (t, *J* = 3.5 Hz, 1H, H-4), 2.62–2.58 (m, 2H, CH_{2Lev}), 2.51–2.37 (m, 2H, 2 \times CH_{Lev}), 2.32 (s, 3H, CH_{3STol}), 2.20–2.13 (m, 1H, H-6a), 2.11 (s, 3H, CH_{3Lev}), 1.80–1.71 (m, 1H, H-6b); ¹³C{¹H} NMR (100 MHz, CDCl₃) : δ (ppm) 206.8 (CO_{Lev}), 172.7 (COOR_{Lev}), 159.5 (C_{Ar}), 138.0 (C_{Ar}), 138.0 (C_{Ar}), 136.9 (C_{Ar}), 132.7 (C_{Ar}), 130.7–128.0 (17C, C_{Ar}, 16 \times CH_{Ar}), 114.0 (2C, 2 \times CH_{Ar}), 85.9 (C-1), 76.2 (C-2), 76.1 (C-4), 74.2 (C-3), 73.0 (CH_{2PMB}*), 72.9 (CH_{2Bn}*), 72.5 (CH_{2Bn}*), 66.2 (C-5), 61.4 (C-7), 55.4 (CH_{3PMB}), 38.1 (CH_{2Lev}), 30.0 (CH_{3Lev}), 28.5 (C-6), 28.1 (CH_{2Lev}), 21.2 (CH_{3STol}); HRMS (ESI-TOF) *m/z* [M + NH₄]⁺ calcd for C₄₁H₅₀NO₈S 716.3252; found 716.3270.

***para*-Methylphenyl 3-*O*-Benzyl-4,6-*O*-benzylidene-2-*O*-*tert*-butyldimethylsilyl-1-thio- α -D-idopyranoside (**14**).**

A solution of alcohol **7b** (124 mg, 0.267 mmol, 1.0 equiv) in dry DCE (4 mL) was cooled to 0 °C, and Et₃N (67 μ L, 0.48 mmol, 1.8 equiv) and TBSOTf (93 μ L, 0.40 mmol, 1.5 equiv) were successively added dropwise. The mixture was stirred at 0 °C under Ar atmosphere for 10 min, then quenched with Et₃N. The solvents were co-evaporated with toluene and the residue was purified by silica gel flash chromatography (Hex/EtOAc 95:5) to give silylated compound **14** (116 mg, 75%) as a white amorphous solid: *R_f* 0.6 (Hex/EtOAc 7:3); [α]_D²⁰ +89 (*c* 0.88, CHCl₃); ¹H NMR (600 MHz, CDCl₃): δ (ppm) 7.54–7.52 (m, 2H, 2 \times CH_{Ar}), 7.44–7.42 (m, 4H, 4 \times CH_{Ar}), 7.39–7.36 (m, 2H, 2 \times CH_{Ar}), 7.33–7.30 (m, 4H, 4 \times CH_{Ar}), 7.12–7.10 (m, 2H, 2 \times CH_{STol}), 5.53 (s, 1H, CHPh), 5.50 (d, *J* = 1.6 Hz, 1H, H-1), 4.75 (d, *J* = 12.0 Hz, 1H, CHH_{Bn}), 4.70 (d, *J* = 12.0

CHAPITRE 8 – TOWARDS THE SYNTHESIS OF AN IDOSE-CONTAINING DISACCHARIDE MIMIC OF CAMPYLOBACTER JEJUNI HS:4C CAPSULAR POLYSACCHARIDE

Hz, 1H, CHH_{Bn}), 4.33–4.31 (m, 2H, H-6a, H-5), 4.15 (dd, $J = 13.1$ Hz, $J = 2.5$ Hz, 1H, H-6b), 4.07 (br s, 1, H-4), 4.04 (dd, $J = 3.3$ Hz, $J = 2.5$ Hz, 1H, H-2), 3.66 (t, $J = 2.9$ Hz, 1H, H-3), 2.33 (s, 3H, CH_{3STol}), 0.84 (s, 9H, $C(CH_3)_3TBS$), 0.07 (s, 3H, CH_3TBS), -0.01 (s, 3H, CH_3TBS); $^{13}C\{^1H\}$ NMR (150 MHz, $CDCl_3$): δ (ppm) 138.1 (C_{Ar}), 137.9 (C_{Ar}), 136.9 (C_{Ar}), 133.1 (C_{Ar}), 130.9 (2C, $2 \times CH_{Ar}$), 129.8 (2C, $2 \times CH_{Ar}$), 129.0 (CH_{Ar}), 128.6 (2C, $2 \times CH_{Ar}$), 128.1 (2C, $2 \times CH_{Ar}$), 128.0 (CH_{Ar}), 127.9 (2C, $2 \times CH_{Ar}$), 126.8 (2C, $2 \times CH_{Ar}$), 101.3 ($CHPh$), 90.0 (C-1), 77.5 (C-3), 74.2 (C-4), 72.5 (CH_{2Bn}), 70.0 (C-6), 69.5 (C-2), 60.8 (C-5), 25.9 (3C, $C(CH_3)_3TBS$), 21.2 (CH_{3STol}), 18.2 ($C(CH_3)_3TBS$), -4.7 (2C, $2 \times CH_3TBS$); HRMS (ESI-TOF) m/z $[M + NH_4]^+$ calcd for $C_{33}H_{46}NO_5SSi$ 596.2861; found 596.2885.

Ethyl 3,4-di-*O*-Benzyl-2-*O*-*tert*-butyldimethylsilyl-6-*O*-levulinoyl-1-thio- α -D-idopyranoside (15a).

Compound **14** (41 mg, 0.070 mmol, 1.0 equiv) was solubilized in $BH_3.THF$ (1M in THF, 0.7 mL, 0.7 mmol, 10 equiv) at -10 °C under Ar. The solution was stirred at that temperature for 10 min, after which Bu_2BOTf (1M in DCM, 70 μ L, 0.070 mmol, 1.0 equiv) was added dropwise. The mixture was stirred for 40 min while being allowed to gradually warm to 0 °C, after which Et_3N and MeOH were added to quench the reaction. The solution was diluted with DCM and washed with saturated aq. $NaHCO_3$. The organic layer was dried over $MgSO_4$, filtered, and concentrated under reduced pressure. The residue was roughly filtered over a pad of silica gel to remove most impurities. To a solution of the resulting alcohol in dry DCE (0.7 mL) were successively added LevOH (9.4 μ L, 0.092 mmol, 1.3 equiv), DMAP (4 mg, 0.04 mmol, 0.5 equiv) and EDC.HCl (20 mg, 0.011 mmol, 1.5 equiv). The mixture was stirred for 23 h at rt, after which it was diluted with DCM and washed with saturated aq. $NaHCO_3$. The organic layer was dried over $MgSO_4$, filtered, and concentrated under reduced pressure. The residue was purified by silica gel flash chromatography (Hex/EtOAc 4:1 to 2:1) to give compound **15a** (42 mg, 88% over two steps) as a colorless oil: R_f 0.31 (Hex/EtOAc 4:1); $[\alpha]_D^{20} +89$ (c 1.1, $CHCl_3$); 1H NMR (600 MHz, $CDCl_3$): δ (ppm) 7.45–7.44 (m, 2H, $2 \times CH_{Ar}$), 7.38–7.37 (m, 4H, $4 \times CH_{Ar}$), 7.33–7.24 (m, 6H, $6 \times CH_{Ar}$), 7.11–7.10 (m, 2H, $2 \times CH_{Ar}$), 5.29 (d, $J = 2.5$ Hz, 1H, H-1), 4.72–4.70 (m, 1H, H-5), 4.69 (d, $J = 11.9$ Hz, 1H, CHH_{Bn}), 4.64–4.61 (m, 2H, CHH_{Bn} , CHH_{Bn}), 4.39–4.36 (m, 2H, CHH_{Bn} , H-6a), 4.29

CHAPITRE 8 – TOWARDS THE SYNTHESIS OF AN IDOSE-CONTAINING DISACCHARIDE MIMIC OF CAMPYLOBACTER JEJUNI HS:4C CAPSULAR POLYSACCHARIDE

(dd, $J = 11.7$ Hz, $J = 4.3$ Hz, 1H, H-6b), 3.97 (t, $J = 3.1$ Hz, 1H, H-2), 3.70 (t, $J = 3.8$ Hz, 1H, H-3), 3.51 (t, $J = 3.2$ Hz, 1H, H-4), 2.65 (t, $J = 6.8$ Hz, 2H, CH_{2Lev}), 2.50–2.48 (m, 2H, CH_{2Lev}), 2.32 (s, 3H, CH_{3STol}), 2.13 (s, 3H, CH_{3Lev}), 0.87 (s, 9H, $C(CH_3)_3TBS$), 0.09 (s, 3H, CH_3TBS), 0.04 (s, 3H, CH_3TBS); $^{13}C\{^1H\}$ NMR (150 MHz, $CDCl_3$): δ (ppm) 206.5 (CO_{Lev}), 172.5 ($COOR_{Lev}$), 137.9 (C_{Ar}), 137.8 (C_{Ar}), 137.1 (C_{Ar}), 132.6 (C_{Ar}), 131.6 (2C, $2 \times CH_{Ar}$), 129.7 (2C, $2 \times CH_{Ar}$), 128.6 (2C, $2 \times CH_{Ar}$), 128.4 (2C, $2 \times CH_{Ar}$), 128.0 (2C, $2 \times CH_{Ar}$), 127.9 (CH_{Ar}), 127.8 (CH_{Ar}), 127.7 (2C, $2 \times CH_{Ar}$), 89.2 (C-1), 74.9 (C-3), 75.0 (C-4), 72.8 (CH_{2Bn}), 71.8 (CH_{2Bn}), 70.7 (C-2), 67.0 (C-5), 63.7 (C-6), 38.0 (CH_{2Lev}), 29.9 (CH_{3Lev}), 27.9 (CH_{2Lev}), 26.0 (3C, $C(CH_3)_3TBS$), 21.2 (CH_{3STol}), 18.3 ($C(CH_3)_3TBS$), -4.5 (CH_3TBS), -4.6 (CH_3TBS); HRMS (ESI-TOF) m/z $[M + NH_4]^+$ calcd for $C_{38}H_{54}NO_7SSi$ 696.3385; found 696.3393.

3,4-di-*O*-Benzyl-2-*O*-*tert*-butyldimethylsilyl-6-*O*-levulinoyl-D-idopyranoside (15b).

To a solution of thioglycoside **15a** (10 mg, 0.014 mmol, 1.0 equiv) in DCM (157 μ L) at 0 °C were successively added H_2O (16 μ L) and NBS (4 mg, 0.02 mmol, 1.4 equiv). The mixture was stirred at 0 °C for 25 min, after which it was diluted with DCM and quenched by slowly adding saturated aq. $NaHCO_3$. The organic layer was washed with saturated aq. $NaHCO_3$, dried over $MgSO_4$, filtered, and concentrated under reduced pressure. The residue was purified by silica gel flash chromatography (Hex/EtOAc 5:1 to 4:1) to give hemiacetal **15b** (7 mg, 81%, α/β 0.7:1) as a white amorphous solid: R_f 0.19 (Hex/EtOAc 2:1); NMR data for β -anomer: 1H NMR (400 MHz, $CDCl_3$): δ (ppm) 7.38–7.24 (m, 10H, $10 \times CH_{Ar}$), 4.94–4.93 (m, 1H, H-1), 4.63–4.58 (m, 2H, CHH_{Bn} , CHH_{Bn}), 4.54 (d, $J = 12.0$ Hz, 1H, CHH_{Bn}), 4.43–4.36 (m, 2H, CHH_{Bn} , H-6a), 4.27–4.23 (m, 1H, H-6b), 4.09 (ddd, $J = 7.6$ Hz, $J = 5.2$ Hz, $J = 2.5$ Hz, 1H, H-5), 3.78 (t, $J = 3.6$ Hz, 1H, H-3), 3.70–3.67 (m, 1H, H-2), 3.39 (t, $J = 3.0$ Hz, 1H, H-4), 2.76–2.70 (m, 2H, CH_{2Lev}), 2.62–2.51 (m, 2H, CH_{2Lev}), 2.17 (s, 3H, CH_{3Lev}), 0.87 (s, 9H, $C(CH_3)_3TBS$), 0.05 (s, 3H, CH_3TBS), 0.00 (s, 3H, CH_3TBS); $^{13}C\{^1H\}$ NMR (100 MHz, $CDCl_3$): δ (ppm) 206.8 (CO_{Lev}), 172.7 ($COOR_{Lev}$), 137.8 (C_{Ar}), 137.7 (C_{Ar}), 128.7–127.9 (10C, $10 \times CH_{Ar}$), 93.1 (C-1, $^1J_{C1-H1} = 164$ Hz), 74.9 (C-3), 72.9 (CH_{2Bn}^*), 72.7 (C-4), 72.3 (CH_{2Bn}), 72.1 (C-5), 70.3 (C-2), 64.2 (C-6), 38.1 (CH_{2Lev}), 30.0 (CH_{3Lev}), 28.1 (CH_{2Lev}), 25.9 (3C, $C(CH_3)_3TBS$), 18.4 ($C(CH_3)_3TBS$), -4.3 (CH_3TBS), -5.0 (CH_3TBS); NMR data for α -anomer: 1H NMR (400 MHz, $CDCl_3$): δ (ppm) 7.38–7.24 (m, 7H, $10 \times CH_{Ar}$),

CHAPITRE 8 – TOWARDS THE SYNTHESIS OF AN IDOSE-CONTAINING DISACCHARIDE MIMIC OF CAMPYLOBACTER JEJUNI HS:4C CAPSULAR POLYSACCHARIDE

4.94–4.93 (m, 0.7H, H-1), 4.69 (d, $J = 11.7$ Hz, 0.7H, CHH_{Bn}), 4.65 (d, $J = 11.7$ Hz, 0.7H, CHH_{Bn}), 4.63–4.58 (m, 0.7H, CHH_{Bn}), 4.46 (dd, $J = 11.6$ Hz, $J = 8.6$ Hz, 0.7H, H-6a), 4.43–4.36 (m, 0.7H, CHH_{Bn}), 4.31 (dt, $J = 8.3$ Hz, $J = 4.0$ Hz, 0.7H, H-5), 4.27–4.23 (m, 0.7H, H-6b), 3.70–3.67 (m, 0.7H, H-3), 3.65–3.64 (m, 0.7H, H-2), 3.56 (t, $J = 4.4$ Hz, 1H, H-4), 2.76–2.70 (m, 1.4H, CH_{2Lev}), 2.62–2.51 (m, 1.4H, CH_{2Lev}), 2.18 (s, 2.1H, CH_{3Lev}), 0.86 (s, 6.3H, $C(CH_3)_{3TBS}$), 0.06 (s, 2.1H, CH_{3TBS}), 0.03 (s, 2.1H, CH_{3TBS}); $^{13}C\{^1H\}$ NMR (100 MHz, $CDCl_3$) : δ (ppm) 207.4 (CO_{Lev}), 172.6 ($COOR_{Lev}$), 137.9 (C_{Ar}) 137.7 (C_{Ar}), 128.7–127.9 (10C, $10 \times CH_{Ar}$), 95.2 (C-1, $^1J_{C1-H1} = 172$ Hz), 77.0 (C-3), 74.7 (C-4), 73.9 (CH_{2Bn}), 72.4 (CH_{2Bn}), 71.5 (C-2), 66.9 (C-5), 62.9 (C-6), 38.2 (CH_{2Lev}), 30.0 (CH_{3Lev}), 28.2 (CH_{2Lev}), 26.0 (3C, $C(CH_3)_{3TBS}$), 18.4 ($C(CH_3)_{3TBS}$), -4.5 (CH_{3TBS}), -4.5 (CH_{3TBS}); HRMS (ESI-TOF) m/z $[M + NH_4]^+$ calcd for $C_{31}H_{48}NO_8Si$ 590.3144; found 590.3139.

3,4-di-*O*-Benzyl-2-*O*-*tert*-butyldimethylsilyl-6-*O*-levulinoyl-D-idopyranosyl *ortho*-hexynylbenzoate (15c).

To a solution of hemiacetal **15b** (8 mg, 0.014 mmol, 1.0 equiv) and *o*-hexynylbenzoic acid⁵⁹³ (6 mg, 0.03 mmol, 2.0 equiv) in dry DCE (207 μ L) and dry THF (207 μ L) were successively added DMAP (3 mg, 0.02 mmol, 1.7 equiv) and EDC.HCl (8 mg, 0.04 mmol, 3.0 equiv). The mixture was stirred at rt under Ar atmosphere for 20 h, after which it was diluted with DCM and washed with saturated aq. $NaHCO_3$. The organic layer was dried over $MgSO_4$, filtered, and concentrated under reduced pressure. The residue was purified by silica gel flash chromatography (Hex/EtOAc 5:1 to 4:1) to give *o*-hexynylbenzoate **15c** (7 mg, 65%, α/β 1:0.2) as a white amorphous solid: R_f 0.32 (Hex/EtOAc 2:1); NMR data for major α -anomer: 1H NMR (600 MHz, $CDCl_3$) : δ (ppm) 7.96–7.94 (m, 1H, CH_{Ar}), 7.54–7.53 (m, 1H, CH_{Ar}), 7.46–7.44 (m, 1H, CH_{Ar}), 7.35–7.27 (m, 11H, $11 \times CH_{Ar}$), 6.29 (d, $J = 3.4$ Hz, 1H, H-1), 4.85 (d, $J = 11.2$ Hz, 1H, CHH_{Bn}), 4.82 (d, $J = 11.2$ Hz, 1H, CHH_{Bn}), 4.67 (d, $J = 11.5$ Hz, 1H, CHH_{Bn}), 4.60 (d, $J = 11.5$ Hz, 1H, CHH_{Bn}), 4.49 (dd, $J = 11.2$ Hz, $J = 4.6$ Hz, 1H, H-6a), 4.40–4.37 (m, 1H, H-5), 4.36–4.31 (m, 1H, H-6b), 3.95–3.90 (m, 2H, H-2, H-3), 3.77 (dd, $J = 7.5$ Hz, $J = 5.7$ Hz, 1H, H-4), 2.67–2.43 (m, 6H, $2 \times CH_{2Lev}$, CH_{2oABz}), 2.12 (s, 3H, CH_{3Lev}), 1.65–1.60 (m, 2H, CH_{2oABz}), 1.52–1.45 (m, 2H, CH_{2oABz}), 0.94 (t, $J = 7.4$ Hz, 3H, CH_{3oABz}), 0.81 (s, 9H, $C(CH_3)_{3TBS}$), 0.05 (s, 6H, $2 \times CH_{3TBS}$); $^{13}C\{^1H\}$ NMR (150 MHz,

CHAPITRE 8 – TOWARDS THE SYNTHESIS OF AN IDOSE-CONTAINING DISACCHARIDE MIMIC OF CAMPYLOBACTER JEJUNI HS:4C CAPSULAR POLYSACCHARIDE

CDCl₃) : δ (ppm) 206.7 (CO_{Lev}), 172.5 (COOR_{Lev}), 164.2 (COOR_{oABz}), 138.5 (C_{Ar}), 137.8 (C_{Ar}), 135.9–125.5 (16C, 2 \times C_{Ar}, 14 \times CH_{Ar}), 97.0 (C_{alkyne}), 92.9 (C-1, ¹J_{C1-H1} = 176 Hz), 79.4 (C_{alkyne}), 77.8 (C-3), 77.5 (C-4), 75.1 (CH_{2Bn}), 73.3 (CH_{2Bn}), 72.3 (C-5), 71.6 (C-2), 64.1 (C-6), 38.0 (CH_{2Lev}), 30.9 (CH_{2oABz}), 29.9 (CH_{3Lev}), 28.0 (CH_{2Lev}), 25.8 (3C, C(CH₃)_{3TBS}), 22.3 (CH_{2oABz}), 19.8 (CH_{2oABz}), 18.0 (C(CH₃)_{3TBS}), 13.8 (CH_{3oABz}), -4.61 (CH_{3TBS}), -4.63 (CH_{3TBS}); HRMS (ESI-TOF) *m/z* [M + NH₄]⁺ calcd for C₄₄H₆₀NO₉Si 774.4032; found 774.4043.

***N*-Phenyltrifluoroacetimidate 3,4-di-*O*-Benzyl-2-*O*-*tert*-butyldimethylsilyl-6-*O*-levulinoyl-*D*-idopyranoside (15d).**

To a solution of hemiacetal **15b** (22 mg, 0.038 mmol, 1.0 equiv) in acetone (192 μ L) were successively added PTFACl (12 μ L, 0.077 mmol, 2.0 equiv) and Cs₂CO₃ (14 mg, 0.042 mmol, 1.1 equiv). The mixture was stirred at rt under Ar atmosphere for 2 h, after which it was diluted with DCM, filtered over Celite, and quenched with Et₃N. The solvents were evaporated under reduced pressure and the resulting residue was purified by silica gel flash chromatography (Hex/EtOAc 2:1 + 1% Et₃N) to give compound **15d** (19 mg, 67%) as a white amorphous solid: R_f 0.51 (Hex/EtOAc 2:1); NMR data for major anomer: ¹H NMR (400 MHz, CDCl₃) : δ (ppm) 7.35–7.24 (m, 12H, 12 \times CH_{Ar}), 7.11–7.08 (m, 1H, CH_{Ar}), 6.83–6.82 (m, 2H, 2 \times CH_{Ar}), 6.24 (br s, 1H, H-1), 4.81 (d, *J* = 11.2 Hz, 1H, CHH_{Bn}), 4.77 (d, *J* = 11.2 Hz, 1H, CHH_{Bn}), 4.67 (m, 3H, CH_{2Bn}, H-6a), 4.34–4.31 (m, 2H, H-6b, H-5), 3.90–3.88 (m, 1H, H-3), 3.85 (br s, 1H, H-2), 3.71 (br s, 1H, H-4), 2.71 (t, *J* = 6.7 Hz, 2H, CH_{2Lev}), 2.56 (t, *J* = 6.9 Hz, 2H, CH_{2Lev}), 2.15 (s, 3H, CH_{3Lev}), 0.90 (s, 9H, C(CH₃)_{3TBS}), 0.08 (s, 3H, CH_{3TBS}), 0.06 (s, 3H, CH_{3TBS}); ¹³C{¹H} NMR (100 MHz, CDCl₃) : δ (ppm) 206.6 (CO_{Lev}), 172.6 (COOR_{Lev}), 143.9 (C=NPh), 138.4 (C_{Ar}), 137.8 (C_{Ar}), 128.9–119.5 (16C, C_{Ar}, 15 \times CH_{Ar}), 115.2 (CF₃), 95.2 (C-1), 77.3 (2C, C-3, C-4), 75.1 (CH_{2Bn}), 73.2 (CH_{2Bn}), 73.1 (C-5), 71.3 (C-2), 64.1 (C-6), 38.0 (CH_{2Lev}), 29.9 (CH_{3Lev}), 28.0 (CH_{2Lev}), 25.8 (3C, C(CH₃)_{3TBS}), 18.1 (C(CH₃)_{3TBS}), -4.65 (CH_{3TBS}), -4.7 (CH_{3TBS}); HRMS (ESI-TOF) *m/z* [M + Na]⁺ calcd for C₃₉H₄₈F₃NNaO₈Si 766.2994; found 766.2995.

***tert*-Butyldimethylsilyl 3,4-di-*O*-Benzyl-2-*O*-*tert*-butyldimethylsilyl-6-*O*-levulinoyl-D-idopyranosyl-(1→4)-3,6-di-*O*-benzyl-2-deoxy-2-trichloroacetamido-β-D-glucopyranoside (20).**

Acceptor **3**⁵⁷⁷ (12 mg, 0.018 mmol, 1.0 equiv) and donor **15a** (9 mg, 0.02 mmol, 1.2 equiv) were dried in a round bottom flask for 1 h under high vacuum. Then, activated 4Å MS (37 mg) and dry DCE (451 μL) were added and the resulting suspension was stirred at rt under Ar atmosphere for 1 h. NIS (5 mg, 0.02 mmol, 1.5 equiv) was added and the mixture was cooled to -10 °C, after which TMSOTf (0.5 μL, 0.003 mmol, 0.2 equiv) was added. The reaction was stirred for 1 h while being allowed to gradually warm to 0 °C. Then, the reaction was quenched with Et₃N, diluted with DCM, and filtered over Celite. The filtrate was washed with 10% aq. Na₂S₂O₃ and the organic layer was dried over MgSO₄, filtered, and concentrated under reduced pressure. The residue was purified by silica gel flash chromatography (Tol/EtOAc 9:1) to give disaccharide **20** (10 mg, 55%, α/β 1:0.3) as a white amorphous solid: R_f 0.73 (Tol/EtOAc 8:2); NMR data for major α-anomer: ¹H NMR (600 MHz, CDCl₃) : δ (ppm) 7.37–7.21 (m, 20H, 20 × CH_{Ar}), 7.11 (d, *J* = 8.0 Hz, 1H, NHTCA), 5.10 (d, *J* = 7.7 Hz, 1H, H-1B), 5.07 (d, *J* = 5.9 Hz, 1H, H-1A), 4.80 (d, *J* = 10.4 Hz, 1H, CHH_{Bn}), 4.74 (d, *J* = 11.5 Hz, 1H, CHH_{Bn}), 4.70 (d, *J* = 11.5 Hz, 1H, CHH_{Bn}), 4.64 (d, *J* = 10.4 Hz, 1H, CHH_{Bn}), 4.59–4.53 (m, 3H, CH₂Bn, CHH_{Bn}), 4.48 (d, *J* = 11.7 Hz, 1H, CHH_{Bn}), 4.21–4.15 (m, 2H, H-5A, H-6Aa), 4.13 (dd, *J* = 9.9 Hz, *J* = 8.4 Hz, 1H, H-3B), 3.95 (dd, *J* = 12.2 Hz, *J* = 9.7 Hz, 1H, H-6Ab), 3.92 (t, *J* = 8.8 Hz, 1H, H-4B), 3.89–3.87 (d, *J* = 8.9 Hz, 1H, H-6Ba), 3.66–3.60 (m, 3H, H-6Bb, H-5B, H-4A), 3.54 (dt, *J* = 10.1 Hz, *J* = 7.8 Hz, 1H, H-2B), 3.50–3.47 (m, 2H, H-2A, H-3A), 2.65–2.62 (m, 2H, CH₂Lev), 2.59–2.51 (m, 2H, CH₂Lev), 2.15 (s, 3H, CH₃Lev), 0.89 (s, 9H, C(CH₃)₃TBS), 0.88 (s, 9H, C(CH₃)₃TBS), 0.15 (s, 3H, CH₃TBS), 0.12 (s, 3H, CH₃TBS), 0.10 (s, 3H, CH₃TBS), 0.04 (s, 3H, CH₃TBS); ¹³C{¹H} NMR (150 MHz, CDCl₃) δ (ppm) 206.9 (CO_{Lev}), 172.4 (COOR_{Lev}), 161.8 (CONHTCA), 138.7 (C_{Ar}), 138.5 (C_{Ar}), 137.9 (C_{Ar}), 137.8 (C_{Ar}), 128.6–127.5 (20C, 20 × CH_{Ar}), 97.8 (C-1A, ¹J_{C1-H1} = 170 Hz), 94.4 (C-1B, ¹J_{C1-H1} = 162 Hz), 92.7 (CCl₃), 80.42 (C-3B*), 80.39 (C-2A*), 77.7 (C-4A*), 74.8 (C-5B*), 74.5 (CH₂Bn), 74.1 (C-3*), 73.9 (CH₂Bn), 73.4 (CH₂Bn), 73.3 (C-4B), 72.9 (CH₂Bn), 70.1 (C-6B), 68.9 (C-5A), 61.4 (C-6A), 60.6 (C-2B), 37.9 (CH₂Bn), 30.1 (CH₃Lev), 27.9 (CH₂Lev), 26.2 (3C, C(CH₃)₃TBS), 25.8 (3C, C(CH₃)₃TBS), 18.3 (C(CH₃)₃TBS), 18.0 (C(CH₃)₃TBS), -3.5 (CH₃TBS), -4.0 (CH₃TBS), -4.4 (CH₃TBS),

CHAPITRE 8 – TOWARDS THE SYNTHESIS OF AN IDOSE-CONTAINING DISACCHARIDE MIMIC OF CAMPYLOBACTER JEJUNI HS:4C CAPSULAR POLYSACCHARIDE

–5.1 (CH₃TBS); HRMS (ESI-TOF) m/z [M + NH₄]⁺ calcd for C₅₉H₈₄[³⁵Cl]₃N₂O₁₃Si₂ 1189.4572; found 1189.4590.

Ethyl 2-*O*-Benzyl-4,6-*O*-benzylidene-3-*O*-*tert*-butyldimethylsilyl-1-thio- α -D-idopyranoside (17).

To a solution of alcohol **16** (59 mg, 0.15 mmol, 1.0 equiv) in dry DCE (2.2 mL) at 0 °C were successively added Et₃N (37 μ L, 0.26 mmol, 1.8 equiv) and TBSOTf (51 μ L, 0.22 mmol, 1.5 equiv) dropwise. The mixture was stirred at 0 °C for 30 min, after which it was diluted with DCM and washed with saturated aq. NaHCO₃ and brine. The organic layer was dried over MgSO₄, filtered, and concentrated under reduced pressure. The residue was purified by silica gel flash chromatography (Hex/EtOAc 9:1) to give compound **17** (71 mg, 94%) as a colorless oil: R_f 0.67 (Hex/EtOAc 6:4); $[\alpha]_D^{20}$ +84 (c 1.3, CHCl₃); ¹H NMR (400 MHz, CDCl₃) : δ (ppm) 7.53–7.51 (m, 2H, 2 \times CH_{Ar}), 7.38–7.36 (m, 2H, 2 \times CH_{Ar}), 7.31–7.26 (m, 6H, 6 \times CH_{Ar}), 5.53 (s, 1H, CHPh), 5.51 (br s, 1H, H-1), 4.70 (d, J = 11.6 Hz, 1H, CHH_{Bn}), 4.62 (d, J = 11.6 Hz, 1H, CHH_{Bn}), 4.28–4.24 (m, 2H, H-6a, H-5), 4.13 (dd, J = 12.2 Hz, J = 1.5 Hz, 1H, H-6b), 4.06 (t, J = 2.8 Hz, 1H, H-3), 3.80 (br s, 1H, H-4), 3.46 (dd, J = 2.7 Hz, J = 1.9 Hz, H-2), 2.72–2.55 (m, 2H, CH₂SEt), 1.30 (t, J = 7.4 Hz, 3H, CH₃SEt), 0.92 (s, 9H, C(CH₃)₃TBS), 0.08 (s, 3H, CH₃TBS), 0.05 (s, 3H, CH₃TBS); ¹³C{¹H} NMR (100 MHz, CDCl₃) : δ (ppm) 138.2 (2C, 2 \times C_{Ar}), 129.0 (CH_{Ar}), 128.4 (2C, 2 \times CH_{Ar}), 128.3 (2C, 2 \times CH_{Ar}), 127.8 (2C, 2 \times CH_{Ar}), 127.6 (CH_{Ar}), 126.8 (2C, 2 \times CH_{Ar}), 101.4 (CHPh), 83.1 (C-1), 77.9 (C-2), 76.1 (C-4), 72.2 (CH₂Bn), 70.3 (C-6), 68.8 (C-3), 59.7 (C-5), 26.8 (CH₂SEt), 25.9 (3C, C(CH₃)₃TBS), 18.2 (C(CH₃)₃TBS), 15.3 (CH₃SEt), –4.8 (CH₃TBS), –4.90 (CH₃TBS); HRMS (ESI-TOF) m/z [M + NH₄]⁺ calcd for C₂₈H₄₄NO₅SSi 534.2704; found 534.2693.

Ethyl 2,4-di-*O*-Benzyl-3-*O*-*tert*-butyldimethylsilyl-6-*O*-levulinoyl-1-thio- α -D-idopyranoside (18).

Compound **17** (58 mg, 0.11 mmol, 1.0 equiv) was cooled to –10 °C and solubilized in BH₃.THF (1M in THF, 1.1 mL, 1.1 mmol, 10 equiv). The solution was stirred at –10 °C for 4 min, after which Bu₂BOTf (1M in DCM, 110 μ L, 0.112 mmol, 1.0 equiv) was added dropwise. The mixture was stirred for 35 min while being allowed to gradually warm to 0 °C. Then, the reaction was

CHAPITRE 8 – TOWARDS THE SYNTHESIS OF AN IDOSE-CONTAINING DISACCHARIDE MIMIC OF CAMPYLOBACTER JEJUNI HS:4C CAPSULAR POLYSACCHARIDE

quenched by adding Et₃N and MeOH. The solution was diluted with EtOAc and washed with saturated NaHCO₃ and brine. The organic layer was dried over MgSO₄, filtered, and concentrated under reduced pressure, and the residue was roughly filtered over a pad of silica to remove most impurities. To a solution of the resulting alcohol in dry DCE (1.1 mL) were successively added LevOH (15 μL, 0.14 mmol, 1.3 equiv), EDC.HCl (32 mg, 0.16 mmol, 1.5 equiv), and DMAP (7 mg, 0.05 mmol, 0.5 equiv). The mixture was stirred at rt for 3h, after which it was diluted with EtOAc and washed consecutively with saturated aq. NH₄Cl and saturated aq. NaHCO₃. The organic layer was dried over MgSO₄, filtered, and concentrated under reduced pressure. The residue was purified by silica gel flash chromatography (Tol/EtOAc 9:1 to 85:15) to give compound **18** (61 mg, 90% over two steps) as a colorless oil: R_f 0.31 (Tol/EtOAc 85:15); [α]_D²⁰ +34 (c 1.2, CHCl₃); ¹H NMR (400 MHz, CDCl₃): δ (ppm) 7.37–7.26 (m, 10H, 10 × CH_{Ar}), 5.34 (br s, 1H, H-1), 4.76 (d, *J* = 12.4 Hz, 1H, CHH_{Bn}), 4.69 (d, *J* = 12.1 Hz, 1H, CHH_{Bn}), 4.60 (ddd, *J* = 7.2 Hz, *J* = 5.2 Hz, *J* = 1.7 Hz, 1H, H-5), 4.55–4.48 (m, 2H, CHH_{Bn}, CHH_{Bn}), 4.33 (dd, *J* = 11.3 Hz, *J* = 7.5 Hz, 1H, H-6a), 4.23 (dd, *J* = 11.4 Hz, *J* = 5.2 Hz, 1H, H-6b), 3.94 (t, *J* = 2.8 Hz, 1H, H-3), 3.34–3.33 (m, 1H, H-2), 3.20 (br s, 1H, H-4), 2.73–2.50 (m, 6H, CH₂SEt, 2 × CH₂Lev), 2.17 (s, 3H, CH₃Lev), 1.28 (t, *J* = 7.4 Hz, 3H, CH₃SEt), 0.83 (s, 9H, C(CH₃)₃TBS), –0.13 (s, 3H, CH₃TBS), –0.15 (s, 3H, CH₃TBS); ¹³C{¹H} NMR (100 MHz, CDCl₃): δ (ppm) 206.6 (CO_{Lev}), 172.5 (COOR_{Lev}), 138.1 (2C, 2 × C_{Ar}), 128.6–128.0 (10C, 10 × CH_{Ar}), 82.5 (C-1), 78.0 (C-2), 75.1 (C-4), 72.5 (CH₂Bn), 72.3 (CH₂Bn), 66.0 (C-3), 65.1 (C-5), 64.1 (C-6), 38.0 (CH₂Lev), 30.0 (CH₃Lev), 28.0 (CH₂Lev), 26.6 (CH₂SEt), 25.8 (3C, C(CH₃)₃TBS), 18.0 (C(CH₃)₃TBS), 15.2 (CH₃SEt), –5.0 (CH₃TBS), –5.10 (CH₃TBS); HRMS (ESI-TOF) *m/z* [M + NH₄]⁺ calcd for C₃₃H₅₂NO₇SSi 634.3228; found 634.3237.

***tert*-Butyldimethylsilyl 2,4-di-*O*-Benzyl-3-*O*-*tert*-butyldimethylsilyl-6-*O*-levulinoyl- α -D-idopyranosyl-(1→4)-3,6-di-*O*-benzyl-2-deoxy-2-trichloroacetamido- β -D-glucopyranoside (21).**

Acceptor **3**⁵⁷⁷ (10 mg, 0.017 mmol, 1.0 equiv) and donor **18** (12 mg, 0.020 mmol, 1.2 equiv) were dried in a round bottom flask for 1 h under high vacuum. Then, activated 4Å MS (41 mg) and dry DCM (371 μL) and dry CH₃CN (123 μL) were added and the resulting suspension was stirred at

CHAPITRE 8 – TOWARDS THE SYNTHESIS OF AN IDOSE-CONTAINING DISACCHARIDE MIMIC OF CAMPYLOBACTER JEJUNI HS:4C CAPSULAR POLYSACCHARIDE

rt under Ar atmosphere for 1 h. NIS (6 mg, 0.02 mmol, 1.5 equiv) was added and the mixture was cooled to $-40\text{ }^{\circ}\text{C}$, after which TMSOTf (0.6 μL , 0.003 mmol, 0.2 equiv) was added. The reaction was stirred for 1 h at $-40\text{ }^{\circ}\text{C}$, after which it was quenched with Et_3N , diluted with DCM, and filtered over Celite. The filtrate was washed with 10% aq. $\text{Na}_2\text{S}_2\text{O}_3$ and the organic layer was dried over MgSO_4 , filtered, and concentrated under reduced pressure. The residue was purified by silica gel flash chromatography (Hex/EtOAc 4:1 to 2:1) to give α -disaccharide **21** (2 mg, 12%) as a white amorphous solid: R_f 0.43 (Hex/EtOAc 2:1); $[\alpha]_D^{20}$ -8.3 (c 0.2, CHCl_3); ^1H NMR (500 MHz, CDCl_3) : δ (ppm) 7.33–7.21 (m, 20H, $20 \times \text{CH}_{\text{Ar}}$), 6.96 (d, $J = 7.8$ Hz, 1H, NHTCA), 5.26 (d, $J = 4.3$ Hz, 1H, H-1A), 5.10 (d, $J = 7.7$ Hz, 1H, H-1B), 4.64–4.50 (m, 7H, $3 \times \text{CH}_{2\text{Bn}}$, CHH_{Bn}), 4.46 (d, $J = 11.8$ Hz, 1H, CHH_{Bn}), 4.23–4.20 (m, 1H, H-5A), 4.19–4.16 (H-6aA), 4.11 (dd, $J = 11.5$ Hz, $J = 8.2$ Hz, 1H, H-6bA), 4.06 (dd, $J = 10.2$ Hz, $J = 8.6$ Hz, 1H, H-3B), 3.88 (dg, $J = 10.7$ Hz, $J = 1.8$ Hz, 1H, H-6aB), 3.86–3.81 (m, 2H, H-3A, H-4B), 3.66 (dd, $J = 10.7$ Hz, $J = 6.7$ Hz, H-6bB), 3.58–3.55 (m, 1H, H-5B), 3.50 (dt, $J = 10.3$ Hz, $J = 7.8$ Hz, H-2B), 3.38 (dd, $J = 5.5$ Hz, $J = 3.9$ Hz, 1H, H-4A), 3.22 (t, $J = 4.9$ Hz, 1H, H-2A), 2.66–2.56 (m, 2H, $\text{CH}_{2\text{Lev}}$), 2.48–2.37 (m, 2H, $\text{CH}_{2\text{Lev}}$), 2.13 (s, 3H, $\text{CH}_{3\text{Lev}}$), 0.88 (s, 9H, $\text{C}(\text{CH}_3)_3\text{TBS}$), 0.86 (s, 9H, $\text{C}(\text{CH}_3)_3\text{TBS}$), 0.14 (s, 3H, CH_3TBS), 0.11 (s, 3H, CH_3TBS), -0.03 (s, 3H, CH_3TBS), -0.05 (s, 3H, CH_3TBS); $^{13}\text{C}\{^1\text{H}\}$ NMR (125 MHz, CDCl_3) δ 206.6 (CO_{Lev}), 172.4 (COOR_{Lev}), 161.7 (CONHTCA), 138.8 (C_{Ar}), 138.3 (C_{Ar}), 137.9 (C_{Ar}), 128.7–127.4 (21C, C_{Ar} , $20 \times \text{CH}_{\text{Ar}}$), 98.7 (C-1A), 94.3 (C-1B), 92.7 (CCl_3), 80.7 (C-3B), 80.2 (C-2A), 74.8 (C-4A), 74.1 (C-4B*), 73.9 ($\text{CH}_{2\text{Bn}}$ *), 73.43 ($\text{CH}_{2\text{Bn}}$), 73.39 ($\text{CH}_{2\text{Bn}}$), 72.9 ($\text{CH}_{2\text{Bn}}$), 70.1 (C-6B), 69.2 (C-3A), 67.3 (C-5A), 62.4 (C-6A), 60.8 (C-2B), 38.0 ($\text{CH}_{2\text{Lev}}$), 30.0 (CH_3Lev), 27.9 (CH_2Lev), 25.9 (3C, $\text{C}(\text{CH}_3)_3\text{TBS}$), 25.8 (3C, $\text{C}(\text{CH}_3)_3\text{TBS}$), 18.2 ($\text{C}(\text{CH}_3)_3\text{TBS}$), 18.0 ($\text{C}(\text{CH}_3)_3\text{TBS}$), -3.9 (CH_3TBS), -4.4 (CH_3TBS), -4.6 (CH_3TBS), -5.1 (CH_3TBS); HRMS (ESI-TOF) m/z $[\text{M} + \text{NH}_4]^+$ calcd for $\text{C}_{59}\text{H}_{84}[^{35}\text{Cl}]_3\text{N}_2\text{O}_{13}\text{Si}_2$ 1189.4572; found 1189.4544.

***para*-Methylphenyl 3,4-di-*O*-Benzyl-6-deoxy-2,7-di-*O*-*para*-methoxybenzyl-1-thio- α -D-ido-heptopyranoside (22).**

To a solution of alcohol **12** (20 mg, 0.033 mmol, 1.0 equiv) in dry DMF (400 μL) at $0\text{ }^{\circ}\text{C}$ were successively added TBAI (6 mg, 0.02 mmol, 0.5 equiv) and NaH (60% dispersion in oil, 3 mg, 0.07 mmol, 2.0 equiv). The mixture was stirred at $0\text{ }^{\circ}\text{C}$ for 10 min, after which PMBCl (9 μL , 0.07

CHAPITRE 8 – TOWARDS THE SYNTHESIS OF AN IDOSE-CONTAINING DISACCHARIDE MIMIC OF CAMPYLOBACTER JEJUNI HS:4C CAPSULAR POLYSACCHARIDE

mmol, 2.0 equiv) was added. The reaction was allowed to stir at rt for 4 h and was then quenched with MeOH, diluted with EtOAc and washed with H₂O. The aqueous phase was washed with DCM (×3) and the combined organic layers were washed with H₂O and brine, dried over MgSO₄, filtered, and concentrated under reduced pressure. The residue was purified by silica gel flash chromatography (Hex/EtOAc 9:1 to 6:4) to give compound **22** (18 mg, 74%) as a white amorphous solid: R_f 0.56 (Hex/EtOAc 6:4); [α]_D²⁰ +38 (c 0.3, CHCl₃); ¹H NMR (400 MHz, CDCl₃) : δ (ppm) 7.39–7.37 (m, 2H, 2 × CH_{Ar}), 7.34–7.27 (m, 8H, 8 × CH_{Ar}), 7.25–7.23 (m, 4H, 4 × CH_{Ar}), 7.18–7.15 (m, 2H, 2 × CH_{Ar}), 7.08–7.06 (m, 2H, 2 × CH_{Ar}), 6.86–6.81 (m, 4H, 4 × CH_{Ar}), 5.34 (d, *J* = 4.3 Hz, 1H, H-1), 4.69–4.63 (m, 2H, CHH_{PMB}*, CHH_{PMB}*), 4.60 (d, *J* = 12.0 Hz, 1H, CHH_{PMB}*), 4.54–4.49 (m, 3H, H-5, CH_{2Bn}*), 4.44 (d, *J* = 11.9 Hz, CHH_{PMB}*), 4.27 (d, *J* = 11.4 Hz, 1H, CHH_{Bn}*), 4.22 (d, *J* = 11.4 Hz, 1H, CHH_{Bn}*), 3.81 (s, 3H, CH_{3PMB}), 3.78 (s, 3H, CH_{3PMB}), 3.70 (t, *J* = 5.1 Hz, 1H, H-3), 3.60 (t, *J* = 4.7 Hz, 1H, H-2), 3.41 (dd, *J* = 4.8 Hz, *J* = 3.5 Hz, 1H, H-4), 3.38–3.34 (m, 2H, H-7a, H-7b), 2.32 (s, 3H, CH_{3STol}), 2.10–2.02 (m, 1H, H-6a), 1.84–1.75 (m, 1H, H-6b); ¹³C{¹H} NMR (100 MHz, CDCl₃) : δ (ppm) 159.5 (C_{Ar}), 159.2 (C_{Ar}), 138.3 (C_{Ar}), 138.2 (C_{Ar}), 136.9 (C_{Ar}), 132.6–127.8 (21C, 3 × C_{Ar}, 18 × CH_{Ar}), 114.0 (2C, 2 × CH_{Ar}), 113.9 (2C, 2 × CH_{Ar}), 85.6 (C-1), 77.4 (C-2), 76.8 (C-4), 75.8 (C-3), 73.4 (CH_{2PMB}*), 73.3 (CH_{2PMB}*), 72.8 (CH_{2Bn}*), 72.6 (CH_{2Bn}*), 67.6 (C-5), 66.7 (C-7), 55.44 (CH_{3PMB}), 55.41 (CH_{3PMB}), 29.4 (C-6), 21.2 (CH_{3STol}); HRMS (ESI-TOF) *m/z* [M + NH₄]⁺ calcd for C₄₄H₅₂NO₇S 738.3459; found 738.3474.

***para*-Methylphenyl 7-*O*-Acetyl-3,4-di-*O*-benzyl-6-deoxy-2-*O*-*para*-methoxybenzyl-1-thio-*α*-D-ido-heptopyranoside (23).**

To a solution of alcohol **12** (16 mg, 0.026 mmol, 1.0 equiv) in dry pyridine (130 μL) and Ac₂O (130 μL) was added DMAP (1 mg, 0.008 mmol, 0.3 equiv). The mixture was stirred at rt for 21 h, after which it was concentrated under reduced pressure and co-evaporated with toluene (×3). The residue was purified by silica gel flash chromatography (Hex/EtOAc 3:1) to give compound **23** (16 mg, quant.) as a white amorphous solid: R_f 0.51 (Hex/EtOAc 2:1); [α]_D²⁰ +42 (c 0.3, CHCl₃); ¹H NMR (400 MHz, CDCl₃) : δ (ppm) 7.36–7.22 (m, 14H, 14 × CH_{Ar}), 7.10–7.08 (m, 2H, 2 × CH_{Ar}), 6.86–6.84 (m, 2H, 2 × CH_{Ar}), 5.38 (d, *J* = 3.5 Hz, 1H, H-1), 4.67–4.61 (m, 3H, CHH_{Bn}, CHH_{Bn}, CHH_{PMB}), 4.51–4.41 (m, 4H, CHH_{Bn}, CHH_{Bn}, CHH_{PMB}, H-5), 4.08–3.96 (m, 2H, H-7a,

CHAPITRE 8 – TOWARDS THE SYNTHESIS OF AN IDOSE-CONTAINING DISACCHARIDE MIMIC OF CAMPYLOBACTER JEJUNI HS:4C CAPSULAR POLYSACCHARIDE

H-7b), 3.81 (s, 3H, CH_{3PMB}), 3.71 (t, $J = 4.5$ Hz, 1H, H-3), 3.64 (t, $J = 3.9$ Hz, 1H, H-2), 3.36 (dd, $J = 4.6$, $J = 3.3$ Hz, 1H, H-4), 2.32 (s, 3H, CH_{3STol}), 2.20–2.11 (m, 1H, H-6a), 1.92 (s, 3H, CH_{3AC}), 1.80–1.72 (m, 1H, H-6b); $^{13}C\{^1H\}$ NMR (100 MHz, $CDCl_3$): δ (ppm) 171.2 ($COOR_{Ac}$), 159.5 (C_{Ar}), 138.1 (C_{Ar}), 138.0 (C_{Ar}), 137.1 (C_{Ar}), 132.5 (C_{Ar}), 131.0–114.0 (19C, C_{Ar} , $18 \times CH_{Ar}$), 85.9 (C-1), 76.3 (C-2*), 76.2 (C-4*), 74.4 (C-3), 73.1 (CH_{2Bn}^*), 73.0 (CH_{2Bn}^*), 72.5 (CH_{2PMB}^*), 66.5 (C-5), 61.3 (C-7), 55.4 (CH_{3PMB}), 28.4 (C-6), 21.2 (CH_{3STol}), 21.0 (CH_{3Ac}); HRMS (ESI-TOF) m/z $[M + NH_4]^+$ calcd for $C_{38}H_{544}NO_7S$ 660.2989; found 660.3018.

***tert*-Butyldimethylsilyl 3,4-di-*O*-Benzyl-6-deoxy-7-*O*-levulinoyl-2-*O*-*para*-methoxybenzyl- α -D-ido-heptopyranosyl-(1 \rightarrow 4)-3,6-di-*O*-benzyl-2-deoxy-2-trichloroacetamido- β -D-glucopyranoside (24 α) and *tert*-butyldimethylsilyl 3,4-di-*O*-benzyl-6-deoxy-7-*O*-levulinoyl-2-*O*-*para*-methoxybenzyl- β -D-ido-heptopyranosyl-(1 \rightarrow 4)-3,6-di-*O*-benzyl-2-deoxy-2-trichloroacetamido- β -D-glucopyranoside (24 β).**

Acceptor **3**⁵⁷⁷ (7 mg, 0.012 mmol, 1.0 equiv) and donor **13** (10 mg, 0.014 mmol, 1.2 equiv) were dried in a round bottom flask for 1 h under high vacuum. Then, activated 4Å MS (29 mg) and dry DCM (260 μ L) and dry CH_3CN (87 μ L) were added and the resulting suspension was stirred at rt under Ar atmosphere for 1 h. NIS (4 mg, 0.02 mmol, 1.5 equiv) was added and the mixture was cooled to -40 °C, after which TMSOTf (0.4 μ L, 0.002 mmol, 0.2 equiv) was added. The reaction was stirred for 45 min at -40 °C, after which it was quenched with Et_3N , diluted with DCM, and filtered over Celite. The filtrate was washed with 10% aq. $Na_2S_2O_3$ and the organic layer was dried over $MgSO_4$, filtered, and concentrated under reduced pressure. The residue was purified by silica gel flash chromatography (Tol/EtOAc 94:6 to 92:8) to give disaccharide **24 α** (6 mg, 34%) as a white amorphous solid and disaccharide **24 β** (approx. 2 mg, 12%): Data for **24 α** : R_f 0.63 (Hex/EtOAc 2:1 *ran twice*); $[\alpha]_D^{20} +2.9$ (c 0.5, $CHCl_3$); 1H NMR (400 MHz, $CDCl_3$): δ (ppm) 7.32–7.19 (m, 23H, $22 \times CH_{Ar}$, $NHTCA$), 6.84–6.82 (m, 2H, $2 \times CH_{Ar}$), 5.20 (d, $J = 7.8$ Hz, 1H, H-1B), 5.07 (d, $J = 6.9$ Hz, 1H, H-1A), 4.78 (d, $J = 11.3$ Hz, 1H, CHH_{PMB}^*), 4.73–4.50 (m, 9H, CHH_{PMB}^* , $4 \times CH_{2Bn}^*$), 4.20 (dd, $J = 10.2$ Hz, $J = 8.3$ Hz, 1H, H-3B), 4.05–3.93 (m, 3H, H-7Aa, H-7Ab, H-5A), 3.89 (d, $J = 8.9$ Hz, 1H, H-6Ba), 3.78 (s, 3H, CH_{3PMB}), 3.75–3.70 (m, 1H, H-4B), 3.62–3.56 (m, 3H, H-6Bb, H-5B, H-4A), 3.49 (t, $J = 8.1$ Hz, 1H, H-3A), 3.39 (dt, $J = 10.2$ Hz, J

CHAPITRE 8 – TOWARDS THE SYNTHESIS OF AN IDOSE-CONTAINING DISACCHARIDE MIMIC OF CAMPYLOBACTER JEJUNI HS:4C CAPSULAR POLYSACCHARIDE

= 7.7 Hz, 1H, H-2B), 3.31 (t, $J = 7.5$ Hz, 1H, H-2A), 2.76–2.59 (m, 2H, CH_{2Lev}), 2.53–2.50 (m, 2H, CH_{2Lev}), 2.15 (s, 3H, CH_{3Lev}), 1.82–1.74 (m, 1H, H-6Aa), 1.52–1.47 (m, 1H, H-6Ab), 0.89 (s, 9H, $C(CH_3)_3TBS$), 0.15 (s, 3H, CH_3TBS), 0.12 (s, 3H, CH_3TBS); $^{13}C\{^1H\}$ NMR (100 MHz, $CDCl_3$): δ (ppm) 207.0 (CO_{Lev}), 172.8 ($COOR_{Lev}$), 161.7 (CO_{NHTCA}), 159.3 (C_{Ar}), 138.8 (C_{Ar}), 138.6 (C_{Ar}), 138.2 (2C, $2 \times C_{Ar}$), 130.7 (C_{Ar}), 130.0–127.5 (22C, $22 \times CH_{Ar}$), 113.9 (2C, $2 \times CH_{Ar}$), 97.6 (C-1A, $^1J_{C1-H1} = 166$ Hz), 93.9 (C-1B, $^1J_{C1-H1} = 162$ Hz), 92.7 (CCl_3), 81.5 (C-2A), 80.5 (C-3B), 79.7 (C-3A), 78.8 (C-4A), 75.0 (C-5B), 74.9–73.1 (6C, $4 \times CH_{2Bn}$, CH_{2PMB} , C-4B), 70.2 (C-6B), 69.2 (C-5A), 61.4 (2C, C-2B, C-7A), 55.4 (CH_{3PMB}), 38.0 (CH_{2Lev}), 29.9 (CH_{3Lev}), 28.1 (CH_{2Lev}), 25.8 (4C, $C(CH_3)_3TBS$, C-6A), 18.0 ($C(CH_3)_3TBS$), -4.0 (CH_3TBS), -5.1 (CH_3TBS); HRMS (ESI-TOF) m/z $[M + NH_4]^+$ calcd for $C_{62}H_{80}[^{35}Cl]_3N_2O_{14}Si$ 1209.4439; found 1209.4461; Partial data for **24 β** (contaminated with unknown impurity): R_f 0.53 (Hex/EtOAc 2:1 *ran twice*); HRMS (ESI-TOF) m/z $[M + NH_4]^+$ calcd for $C_{62}H_{80}[^{35}Cl]_3N_2O_{14}Si$ 1209.4439; found 1209.4399.

***tert*-Butyldimethylsilyl 7-*O*-Acetyl-3,4-di-*O*-benzyl-6-deoxy-2-*O*-*para*-methoxybenzyl- α -*D*-ido-heptopyranosyl-(1 \rightarrow 4)-3,6-di-*O*-benzyl-2-deoxy-2-trichloroacetamido- β -*D*-glucopyranoside (26 α) and *tert*-butyldimethylsilyl 7-*O*-acetyl-3,4-di-*O*-benzyl-6-deoxy-2-*O*-*para*-methoxybenzyl- β -*D*-ido-heptopyranosyl-(1 \rightarrow 4)-3,6-di-*O*-benzyl-2-deoxy-2-trichloroacetamido- β -*D*-glucopyranoside (26 β).**

Acceptor **3**⁵⁷⁷ (9 mg, 0.02 mmol, 1.0 equiv) and donor **23** (12 mg, 0.018 mmol, 1.2 equiv) were dried in a round bottom flask for 1 h under high vacuum. Then, activated 4Å MS (38 mg) and dry DCM (341 μ L) and dry CH_3CN (114 μ L) were added and the resulting suspension was stirred at rt under Ar atmosphere for 1 h. NIS (5 mg, 0.02 mmol, 1.5 equiv) was added and the mixture was cooled to -40 °C, after which TMSOTf (0.6 μ L, 0.003 mmol, 0.2 equiv) was added. The reaction was stirred for 1 h at -40 °C, after which it was quenched with Et_3N , diluted with DCM, and filtered over Celite. The filtrate was washed with 10% aq. $Na_2S_2O_3$ and the organic layer was dried over $MgSO_4$, filtered, and concentrated under reduced pressure. The residue was purified by silica gel flash chromatography (Tol/EtOAc 92:8) to give disaccharide **26 α** (9.5 mg, 51%) as a white amorphous solid and disaccharide **26 β** (5.4 mg, 32%) as a white amorphous solid: Data for **26 α** : R_f 0.51 (Tol/EtOAc 91:9); $[\alpha]_D^{20} +4.9$ (c 0.6, $CHCl_3$); 1H NMR (400 MHz, $CDCl_3$): δ (ppm)

CHAPITRE 8 – TOWARDS THE SYNTHESIS OF AN IDOSE-CONTAINING DISACCHARIDE MIMIC OF CAMPYLOBACTER JEJUNI HS:4C CAPSULAR POLYSACCHARIDE

7.32–7.19 (m, 22H, $22 \times \text{CH}_{\text{Ar}}$), 6.99 (d, $J = 7.6$ Hz, 1H, NHTCA), 6.83 (m, 2H, $2 \times \text{CH}_{\text{Ar}}$), 5.18 (d, $J = 7.7$ Hz, 1H, H-1B), 5.07 (d, $J = 6.8$ Hz, 1H, H-1A), 4.77 (d, $J = 11.2$ Hz, 1H, CHH_{Bn}), 4.72–4.63 (m, 5H, CHH_{Bn} , $\text{CH}_{2\text{PMB}}^*$, CHH_{Bn}^* , CHH_{Bn}), 4.57–4.49 (m, 4H, $\text{CH}_{2\text{Bn}}^*$, CHH_{Bn}^* , CHH_{Bn}^*), 4.20 (dd, $J = 10.1$ Hz, $J = 8.1$ Hz, 1H, H-3B), 4.02–3.96 (m, 3H, H-7Aa, H-7Ab, H-5A), 3.89 (d, $J = 8.9$ Hz, 1H, H-6Ba), 3.78 (s, 3H, $\text{CH}_{3\text{PMB}}$), 3.72 (t, $J = 8.7$ Hz, 1H, H-4B), 3.65–3.55 (m, 3H, H-5B, H-4A, H-6Bb), 3.49 (t, $J = 7.9$ Hz, 1H, H-3A), 3.40 (dt, $J = 10.1$ Hz, $J = 7.7$ Hz, 1H, H-2B), 3.31 (t, $J = 7.3$ Hz, 1H, H-2A), 1.98 (s, 3H, $\text{CH}_{3\text{Ac}}$), 1.82–1.73 (m, 1H, H-6Aa), 1.54–1.48 (m, 1H, H-6Ab), 0.89 (s, 9H, $\text{C}(\text{CH}_3)_{3\text{TBS}}$), 0.15 (s, 3H, $\text{CH}_{3\text{TBS}}$), 0.12 (s, 3H, $\text{CH}_{3\text{TBS}}$); $^{13}\text{C}\{^1\text{H}\}$ NMR (100 MHz, CDCl_3) δ (ppm) 171.0 (COOR_{Ac}), 161.7 (C_{Ar}), 159.4 (CONHTCA), 138.8 (C_{Ar}), 138.6 (C_{Ar}), 138.2 (C_{Ar}), 130.6 (C_{Ar}), 130.0–113.9 (25C, C_{Ar} , $24 \times \text{CH}_{\text{Ar}}$), 97.6 (C-1A, $^1J_{\text{C1-H1}} = 165$ Hz), 93.9 (C-1B, $^1J_{\text{C1-H1}} = 162$ Hz), 92.7 (CCl_3), 81.3 (C-2A), 80.6 (C-3B), 79.5 (C-3A), 78.7 (C-4A), 74.9 (2C, C-5B, $\text{CH}_{2\text{PMB}}^*$), 74.7 ($\text{CH}_{2\text{Bn}}^*$), 74.1 (2C, $\text{CH}_{2\text{Bn}}^*$, C-4B), 73.5 ($\text{CH}_{2\text{Bn}}^*$), 73.1 ($\text{CH}_{2\text{Bn}}^*$), 70.1 (C-6B), 68.9 (C-5A), 61.4 (C-2B), 61.1 (C-7A), 55.4 ($\text{CH}_{3\text{PMB}}$), 26.2 (C-6A), 25.8 (3C, $\text{C}(\text{CH}_3)_{3\text{TBS}}$), 21.1 ($\text{CH}_{3\text{Ac}}$), 18.0 ($\text{C}(\text{CH}_3)_{3\text{TBS}}$), –4.0 ($\text{CH}_{3\text{TBS}}$), –5.1 ($\text{CH}_{3\text{TBS}}$); HRMS (ESI-TOF) m/z $[\text{M} + \text{NH}_4]^+$ calcd for $\text{C}_{59}\text{H}_{76}[\text{Cl}]_3\text{N}_2\text{O}_{13}\text{Si}$ 1153.4177; found 1153.4177; Data for **26 β** : R_f 0.36 (Tol/EtOAc 91:9); $[\alpha]_{\text{D}}^{20}$ –4.4 (c 0.2, CHCl_3); ^1H NMR (400 MHz, CDCl_3) : δ (ppm) 7.34–7.14 (m, 23H, $22 \times \text{CH}_{\text{Ar}}$, NHTCA), 6.80–6.78 (m, 2H, $2 \times \text{CH}_{\text{Ar}}$), 5.10 (d, $J = 7.4$ Hz, 1H, H-1B), 4.96 (d, $J = 10.4$ Hz, 1H, CHH_{Bn}), 4.94 (br s, 1H, H-1A), 4.69 (d, $J = 11.9$ Hz, 1H, CHH_{Bn}^*), 4.60–4.52 (m, 4H, CHH_{Bn}^* , $\text{CH}_{2\text{PMB}}^*$, CHH_{Bn}^*), 4.48 (d, $J = 12.3$ Hz, 1H, CHH_{Bn}^*), 4.38 (d, $J = 12.0$ Hz, 1H, CHH_{Bn}^*), 4.32 (d, $J = 11.9$ Hz, 1H, CHH_{Bn}^*), 4.31 (d, $J = 12.0$ Hz, 1H, CHH_{Bn}^*), 4.20–4.16 (m, 1H, H-7Aa), 4.12 (t, $J = 8.8$ Hz, 1H, H-3B), 4.00 (t, $J = 8.5$ Hz, 1H, H-4B), 3.97–3.93 (m, 1H, H-7Ab), 3.80–3.75 (m, 6H, $\text{CH}_{3\text{PMB}}$, H-6Ba, H-5A, H-3A), 3.70–3.66 (m, 2H, H-2B, H-5B), 3.63 (dd, $J = 10.5$ Hz, $J = 4.5$ Hz, 1H, H-6Bb), 3.48 (br s, 1H, H-2A), 3.12 (br s, 1H, H-4A), 2.11–2.04 (m, 1H, H-6Aa), 1.95 (s, 3H, $\text{CH}_{3\text{Ac}}$), 1.69–1.64 (m, 1H, H-6Ab), 0.88 (s, 9H, $\text{C}(\text{CH}_3)_{3\text{TBS}}$), 0.13 (s, 3H, $\text{CH}_{3\text{TBS}}$), 0.10 (s, 3H, $\text{CH}_{3\text{TBS}}$); $^{13}\text{C}\{^1\text{H}\}$ NMR (100 MHz, CDCl_3) δ (ppm) 171.5 (COOR_{Ac}), 161.8 (CONHTCA), 159.2 (C_{Ar}), 138.53 (C_{Ar}), 138.5 (C_{Ar}), 138.2 (C_{Ar}), 137.8 (C_{Ar}), 130.9 (C_{Ar}) 129.5–127.5 (22C, $22 \times \text{CH}_{\text{Ar}}$), 113.8 (2C, $2 \times \text{CH}_{\text{Ar}}$), 99.3 (C-1A, $^1J_{\text{C1-H1}} = 162$ Hz), 94.9 (C-1B, $^1J_{\text{C1-H1}} = 163$ Hz), 92.8 (CCl_3), 77.4 (C-3B), 77.0 (C-4B), 75.2 (C-5B), 74.7 (C-4A), 74.1 (C-2A), 73.9 (C-3A), 73.5–72.0 (5C, $4 \times \text{CH}_{2\text{Bn}}$,

CHAPITRE 8 – TOWARDS THE SYNTHESIS OF AN IDOSE-CONTAINING DISACCHARIDE MIMIC OF CAMPYLOBACTER JEJUNI HS:4C CAPSULAR POLYSACCHARIDE

CH₂PMB), 71.5 (C-5A), 69.6 (C-6B), 61.3 (C-7A) 59.4 (C-2B), 55.4 (CH₃PMB), 29.9 (C-6), 25.8 (3C, C(CH₃)₃TBS), 21.2 (CH₃Ac), 18.1 (C(CH₃)₃TBS), -4.1 (CH₃TBS), -5.0 (CH₃TBS); HRMS (ESI-TOF) m/z [M + NH₄]⁺ calcd for C₅₉H₇₆[³⁵Cl]₃N₂O₁₃Si 1153.4177; found 1153.4194.

CHAPITRE 9 : CONCLUSIONS ET PERSPECTIVES

Dans la présente thèse, nous nous sommes ainsi intéressés au développement de voies de synthèse donnant accès à des composés mono- et oligosaccharidiques afin d'en évaluer leur potentiel comme agents thérapeutiques et prophylactiques. Plus spécifiquement, ce travail s'est inscrit dans trois thèmes différents, *i.e.*, (A) la synthèse totale et l'évaluation biologique et physicochimique des ananatosides et d'analogues macrolactonisés non-naturels; (B) la synthèse de potentiels vaccins tétrasaccharidiques contre *B. pseudomallei* et *B. mallei*; et (C) la synthèse de potentiels vaccins contre *C. jejuni* HS:4c.

Synthèse totale et évaluation biologique et physicochimique des ananatosides et d'analogues macrolactonisés non-naturels (Chapitre 2)⁹⁷

Tel que présenté au chapitre 2, les glycolipides sont d'un intérêt particulier pour le développement de nouveaux agents thérapeutiques ainsi que pour la mise au point de nouvelles biotechnologies. Les glycolipides d'origine naturelle les plus étudiés actuellement sont les rhamnolipides, mais leur exploitation à grande échelle est entravée par le fait qu'ils sont principalement produits par les pathogènes humains du genre *Pseudomonas* et *Burkholderia*. Dans ce contexte, la bactérie *P. ananatis* a été identifiée comme producteur alternatif de tels biosurfactants, et l'analyse de métabolites secondaires produits par cette bactérie a notamment permis d'identifier les ananatosides A et B (Fig. 1A). Notre projet visait donc à réaliser la synthèse des ananatosides A et B ainsi que de dérivés rhamnolipides (1→2)-, (1→3), et (1→4)-macrolactonisés non-naturels dans l'objectif d'étudier leur potentiel bioactif et tensioactif (Fig. 1A).

CHAPITRE 9 – CONCLUSIONS ET PERSPECTIVES

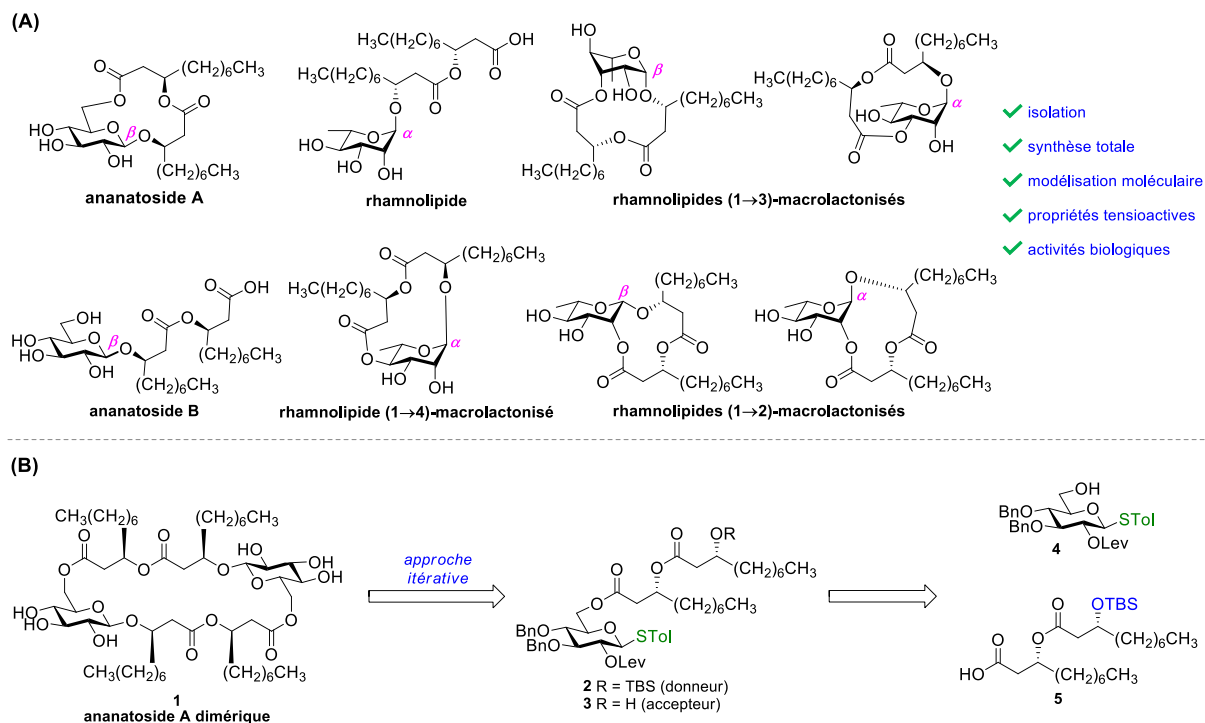


Figure 9.1. (A) Structure des ananatosides A et B, du rhamnolipide, et d’analogues rhamnolipidiques macrolactonisés; (B) Analyse rétrosynthétique de l’ananatoside A dimérique

Dans un premier temps, nous avons réalisé la synthèse de l’ananatoside A *via* trois différentes voies, *i.e.*, (1) une glycosylation intramoléculaire; (2) une macrolactonisation chimique; et (3) une macrolactonisation enzymatique à partir de l’ananatoside B. Les analogues rhamnolipidiques macrolactonisés ont quant à eux été préparés en prenant avantage de notre méthode de glycosylation intramoléculaire optimisée, et leur structure et conformation ont été confirmées et étudiées par modélisation moléculaire. Nous avons démontré que les propriétés tensioactives de l’ananatoside B sont similaires à celles de son congénère rhamnolipidique, alors que l’ananatoside A ne présentait pas de telles propriétés. L’étude des activités cytotoxiques et hémolytiques de nos composés synthétiques ont montré que ces activités sont exacerbées par la macrolactonisation, suggérant un mécanisme impliquant la formation de pores dans la membrane cellulaire. Enfin, nos travaux ont mis en évidence que ces composés synthétiques sont reconnus par le système immunitaire de plantes, et que cette reconnaissance semblerait être influencée par la conformation du squelette saccharidique.

À la suite de ces travaux, nous envisageons qu'il serait intéressant de réaliser la synthèse de l'ananatoside A dimérique (Fig. 1B). Inspirés des structures macrolactoniques de la glucolipsine⁶⁰⁷ A et des cycloviracines,¹⁸³ tous les deux démontrant des activités antibiotiques intéressantes,⁶⁰⁸ nous hypothétisons qu'une structure dimérique pourrait améliorer les propriétés biologiques de l'ananatoside A. Ce dimère de l'ananatoside A (**1**), tel qu'illustré à la figure 1B, pourrait être synthétisé *via* une approche itérative à partir de dérivés glucolipidiques. Plus spécifiquement, le donneur de glycosyle **2** et l'accepteur **3** seraient glycosylés afin de former un dimère glucolipidique qui, suivant le clivage du groupement TBS, pourrait être sujet à une glycosylation intramoléculaire et une séquence de déprotection. Les composés **2** et **3** pourraient quant à eux être préparés à partir du glucoside **4** et du dilipide **5**, déjà synthétisés dans le cadre de notre projet présenté au chapitre 2. La synthèse de dérivés lactames par l'introduction d'un groupement azoture en position C6 du composé **4** serait une autre avenue intéressante à investiguer, les liens lactames étant plus stables que les liens esters.

Synthèse de mimes du LPS de *B. pseudomallei* et *B. mallei* (Chapitres 3–4)¹⁶⁹

Dû au spectre clinique très large de la mélioïdose et de la morve, combiné à leur difficulté à être diagnostiquées, à leur résistance intrinsèque aux antibiotiques ainsi qu'à leur habileté à infecter par voie aérienne, les bactéries causatrices de ces maladies, *i.e.*, *B. pseudomallei* et *B. mallei* respectivement, sont considérées comme de potentielles armes bioterroristes. Pour ces raisons, beaucoup d'efforts sont actuellement investis dans la préparation de vaccins contre ces pathogènes bactériens. C'est donc dans ce contexte que nous avons réalisé la synthèse de mimes de l'antigène-O du LPS de *B. pseudomallei* et *B. mallei* en tant que potentiels agents prophylactiques. Plus spécifiquement, nous avons réalisé la synthèse de tétrasaccharides mimant les épitopes terminal et intra-chaîne majoritaires de cet antigène-O (Fig. 2A). Ces tétrasaccharides ont été synthétisés à l'échelle de quelques milligrammes à l'aide d'une approche de glycosylations itératives et impliquant une étape tardive d'épimérisation du résidu rhamnose intra-chaîne pour accéder à la configuration 6-désoxy-L-*talo*. L'étude de leur antigénicité a mis en évidence que ces composés synthétiques mimaient étroitement l'antigénicité de l'antigène-O du LPS de *B. pseudomallei*, suggérant qu'ils constitueraient des candidats potentiels pour le développement de vaccins et/ou d'outils diagnostiques contre la mélioïdose et la morve.

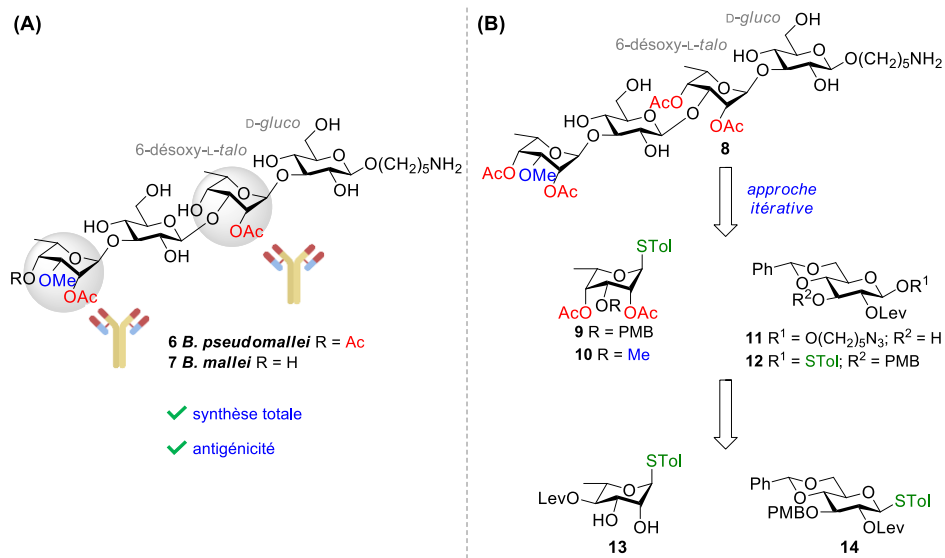


Figure 9.2. (A) Structure des tétrasaccharides synthétiques mimant l'antigène-O du LPS de *B. pseudomallei* et *B. mallei*; (B) Rétrosynthèse du nouveau tétrasaccharide cible

Dans l'optique de simplifier la voie de synthèse et de faciliter l'accès à ces mimes oligosaccharidiques, notre groupe investigate actuellement un nouveau tétrasaccharide (**8**, Fig. 2B) incorporant l'épitope terminal et l'épitope intrachaîne 2,4-di-*O*-acétylés de *B. pseudomallei*. Nous envisageons que ce changement structurel minimal ne devrait pas altérer la reconnaissance du composé par les anticorps polyclonaux spécifiques au LPS de *B. pseudomallei* et *B. mallei*. L'avantage principal de cette nouvelle cible de synthèse est qu'elle pourrait être accédée directement à partir de donneur de glycosyles de configuration 6-désoxy-*L*-talo, tel que démontré dans des travaux précédemment publiés.²⁴¹ Ceux-ci ont en effet montré que l'insertion du résidu *gluco* intrachaîne en position C3 du résidu *talo* peut être réalisée lorsque la position C4 de ce dernier est protégé par un groupement acétyle. À l'inverse, lorsque cette position est protégée par un autre groupement orthogonal (*e.g.*, Lev), l'insertion du résidu *gluco* ne peut pas être réalisée et nécessite une séquence impliquant l'insertion d'un résidu *rhamno* et, à la fin de l'assemblage du tétrasaccharide, son épimérisation en C4 pour accéder à la configuration 6-désoxy-*L*-talo, tel qu'effectué pour préparer nos tétrasaccharides **6** et **7**.¹⁶⁹ Ce faisant, le tétrasaccharide **8** pourrait être accédé par une approche de glycosylations itératives à partir des glucosides **11** et **12** et des 6-désoxy-*L*-talosides **9** et **10**. Ces composés pourraient quant à eux être synthétisés par méthode

convergente à partir du glucoside **14** et du rhamnoside **13**, dont la synthèse est déjà rapportée au chapitre 4.

Synthèse de vaccins potentiels contre *C. jejuni* HS:4c (Chapitres 5–8)

Considérant le fardeau socio-économique et de santé publique que représente la campylobactériose, de sa grandissante résistance aux antibiotiques et de son association au syndrome de Guillain-Barré, il existe un besoin pressant de développer un vaccin contre cette maladie causée par *C. jejuni*. Le CPS de cette bactérie étant un antigène prometteur pour le développement d'agents prophylactiques, une partie de notre programme de recherche s'est concentrée sur la synthèse de mimes de celui-ci, et plus spécifiquement du sérotype HS:4c à l'origine de la majorité des infections.

Optimisation du réarrangement de Paulsen⁶⁰⁹

Le CPS du prédominant sérotype HS:4c de *C. jejuni* est doté d'unités [\rightarrow 3)-6-désoxy- β -D-ido-heptopyranosyl-(1 \rightarrow) non-stœchiométriquement substituées avec des groupements MeOPN en C2 et C7 et liées à des résidus [\rightarrow 4)-2-acétamido-2-désoxy- β -D-glucopyranosyl-(1 \rightarrow) (Fig. 3A). Or, la synthèse de 6-désoxy- β -D-ido-heptopyranosides se veut particulièrement complexe, notamment dû au besoin d'accéder à la configuration *ido* par voie synthétique ainsi que par la présence de liens 1,2-*cis*- β . Ainsi, notre premier objectif visait à optimiser le réarrangement de Paulsen afin d'accéder à un α -D-idopyranoside peracétylé à partir de β -D-glucose peracétylé (Fig. 3B). Nous avons observé que le protocole proposé par Paulsen⁵⁰² n'était pas reproductible lorsque les conditions en laboratoire étaient particulièrement humides. Nous avons ainsi développé un protocole basé sur une étape de filtration en conditions anhydres à l'aide d'une technique de filtration par canule adaptée et davantage d'étapes de traitements pour éviter toute décomposition. Notre protocole optimisé a permis la synthèse d'un α -D-idopyranoside peracétylé à l'échelle du gramme avec un rendement de 38% en quatre étapes. Ce protocole a pu être employé dans la suite de nos travaux sur la synthèse de mimes du CPS de *C. jejuni* HS:4c.

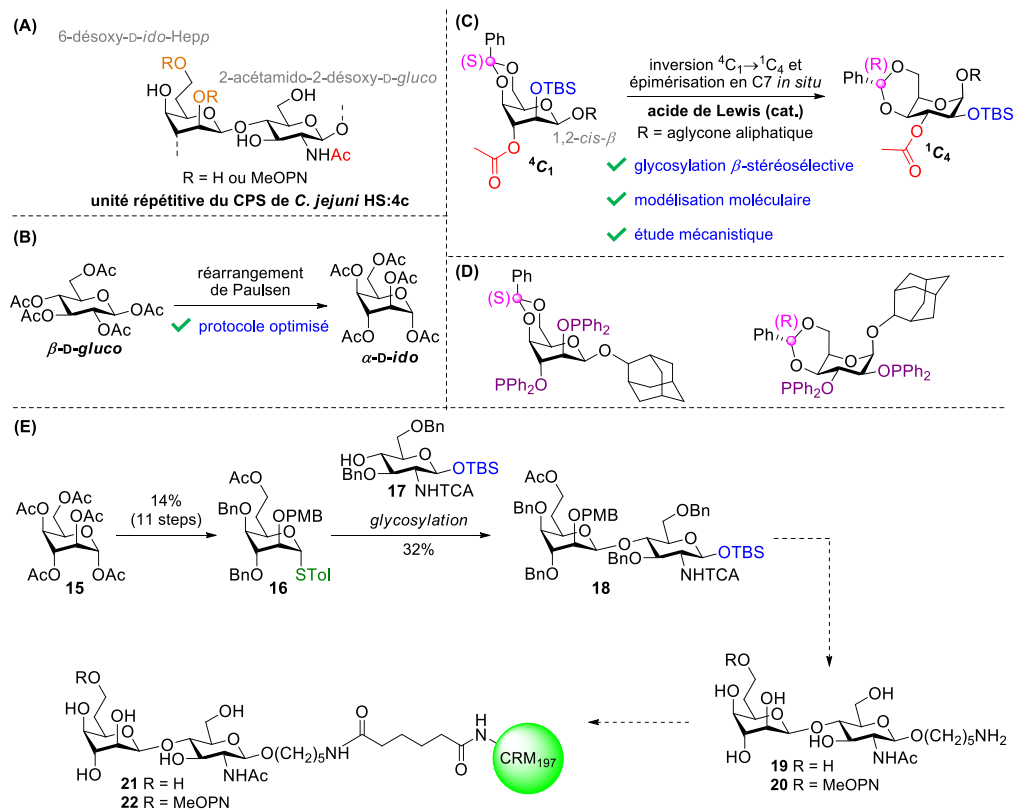


Figure 9.3. (A) Structure de l'unité répétitive du CPS de *C. jejuni* HS:4c; (B) Optimisation du réarrangement de Paulsen; (C) Étude de flexibilité conformationnelle de β-D-idopyranosides; (D) Potentiels ligands diphosphonate pour catalyse asymétrique; (E) Synthèse de mimes du CPS de *C. jejuni* HS:4c et conjugaison à CRM₁₉₇

Flexibilité conformationnelle des β-D-idopyranosides⁵⁸⁵

Tel que mentionné, un défi associé à la synthèse de mimes du CPS de *C. jejuni* HS:4c est la présence de liens 1,2-*cis*-β. Ainsi, au cours de nos travaux visant à développer une méthode de 1,2-*cis*-β-idosylation, nous avons découvert un phénomène d'épimérisation d'acétals de benzyldène concomitant à un changement conformationnel ${}^4C_1 \rightarrow {}^1C_4$ spécifique aux β-D-idopyranosides 3-O-acylés (Fig. 3C). L'existence d'interactions 1,3-*syn*-diaxiales déstabilisantes chez les composés à configuration *D-ido* réduit significativement la barrière énergétique entre les conformations 4C_1 et 1C_4 , faisant de ces composés des substances particulièrement flexibles. À l'aide d'une étude de glycosylation combinée à des expériences de résonance magnétique nucléaire, nous avons proposé que la configuration β diminue la stabilité du conformère 4C_1 . Nous posons l'hypothèse qu'à la suite de la réaction de β-glycosylation, l'acétal de benzyldène subirait

une ouverture de cycle catalysée par un acide de Lewis *in situ*, conduisant à un système labile permettant une isomérisation ${}^4C_1 \rightarrow {}^1C_4$ avec épimérisation concomitante (*S*) \rightarrow (*R*) du centre benzyldénique afin de réduire l'encombrement stérique causé par le groupe phényle. Nous avons postulé que la force motrice de cette séquence d'isomérisation/épimérisation serait l'effet anomérique présent chez les β -D-idosides dans leur conformation 1C_4 . Enfin, nous avons montré que des thioglycosides dotés d'un groupement 4,6-*O*-benzyldène pouvait être sujet à une glycosylation β -stéréosélective en présence d'accepteurs aliphatiques de forte nucléophilicité, mais que cette glycosylation se voulait plutôt α -stéréosélective lorsque des accepteurs glycosidiques étaient employés.

Afin de prendre avantage des isomères (*S*)- 4C_1 et (*R*)- 1C_4 obtenus, de futurs travaux pourraient porter sur l'investigation du potentiel de ces composés pour la préparation de ligands chiraux pouvant être employés en catalyse asymétrique.⁶¹⁰ En effet, grâce à leurs multiples centres stéréogènes, les glucides sont de plus en plus étudiés pour la préparation de tels ligands. Ainsi, suivant le clivage des groupements Ac et TBS des isomères obtenus à la suite de la séquence d'isomérisation/épimérisation, les diols obtenus pourraient être convertis en ligands diphosphane (Fig. 3D). Ceux-ci pourraient être investigués dans différents types de réactions, notamment dans des réactions d'hydrogénation asymétrique.⁶¹¹

Synthèse d'un disaccharide mimant le CPS de *C. jejuni* HS:4c

Suivant ces travaux, nous nous sommes enfin consacrés entièrement à la synthèse des disaccharides **19** et **20** mimant le CPS de *C. jejuni* HS:4c. Après avoir investigué de nombreux donneurs d'idosyles (SEt, STol, S(O)Tol, OH, *o*ABz, PTFA) différemment protégés (NAP, PMB, TBS) ainsi que de nombreuses approches de glycosylation intramoléculaire et intermoléculaire), nous avons mis en évidence que l'utilisation du donneur 6-désoxy-*ido*-heptopyranosyle **16** et l'accepteur **17** permettait d'accéder au disaccharide **18** avec un rendement de 32% sous des conditions intermoléculaires (Fig. 3E). Bien que ce rendement demeure modeste, cette réaction de glycosylation est avantageuse car les disaccharides α et β résultant peuvent être séparés par chromatographie sur gel de silice. Nous envisageons que ce rendement pourrait être amélioré en optimisant les conditions réactionnelles (solvants, température, promoteurs, additifs, *etc.*). Les

prochaines étapes du projet consisteront ainsi en la réalisation de cette optimisation suivie de la fonctionnalisation et déprotection du β -disaccharide résultant afin d'accéder aux composés cibles **19** et **20**, qui pourront être conjugués à la protéine de transport CRM₁₉₇. Les glycoconjugués résultants pourront enfin faire l'objet de tests d'antigénicité et d'immunogénicité chez un modèle de poulet (réalisés par le groupe du Prof. Charles Dozois à l'INRS).

Par ailleurs, nous avons développé une voie de synthèse optimisée pour accéder au donneur de glycosyle **16** de configuration 6-désoxy-*ido*-heptopyranoside. Après avoir réalisé différentes étapes de protection/déprotection régiosélectives en s'appuyant sur nos travaux précédents,⁵⁸⁵ nous avons mis au point une méthode d'homologation en C6. Celle-ci est basée sur une séquence en quatre étapes impliquant (1) l'oxydation de la position C6 sous les conditions de Parikh-Doering; (2) l'insertion du carbone C7 *via* une réaction MOM-Wittig; (3) l'hydrolyse de l'éther d'énol formé et (4) la réduction du C7-aldéhyde résultant. Non seulement cette approche adresse de nombreux problèmes récemment évoqués quant à l'homologation des idopyranosides,⁵¹¹ mais celle-ci pourrait également être utilisée comme source d'inspiration pour la synthèse de mimes du CPS de *C. jejuni* HS:3. Celui-ci est effectivement doté d'unité L-glycéro-D-*ido*-heptopyranosides (*cf* Chapitre 5) et fait partie des huit sérotypes à l'origine de la majorité des infections à *C. jejuni* rapportées mondialement.⁴⁷⁵ Cette synthèse se voudrait être particulièrement pertinente dans le cadre de développement de vaccins multivalents contre différentes souches de *C. jejuni*.

Conclusion

Pour conclure, la présente thèse a présenté nos réalisations et progrès quant au développement de méthodes de synthèses régio- et stéréosélectives permettant l'accès à des composés naturels ou à des mimes de ceux-ci et possédant des propriétés biologiques intéressantes dans un contexte thérapeutique ou prophylactique. Ces travaux pavent non seulement la voie à de futurs travaux sur le développement d'agents thérapeutiques à base de sucres et de vaccins glycoconjugués, mais mettent également en lumière les avantages que possèdent la synthèse de glucides comparativement à l'isolation de produits naturels. Dans le même ordre d'idées, l'ensemble des travaux présentés contribue à l'avancée des connaissances en glycochimie, notamment en ce qui a

CHAPITRE 9 – CONCLUSIONS ET PERSPECTIVES

trait aux glycosylations intramoléculaires, à la chimie enzymatique, à la flexibilité des glucides, aux réactions régiosélectives, ainsi qu'aux glycosylations stéréosélectives.

LISTE DES RÉALISATIONS

Articles et chapitres de livres

1. Verma, N., **Cloutier, M.**, Gauthier, C. “Thioglycoside-based glycosylations in oligosaccharide synthesis.” In: *Synthetic Strategies in Carbohydrate Chemistry*, 1st edition, Ed.: Tiwari, V. K., **2023**, Elsevier, Chapitre accepté (contribution invitée).
2. **Cloutier, M.**, Lavoie, S., Gauthier, C. “C7 epimerization of benzylidene-protected β -D-idopyranosides brings structural insights into idose conformational flexibility.” *J. Org. Chem.* **2022**, *87*, 12932-12953.
3. Verma, N., **Cloutier, M.**, Gauthier, C. “Synthesis of α -D-idose pentaacetate from β -D-glucose pentaacetate via Paulsen acetoxonium rearrangement.” In: *Carbohydrate Chemistry: Proven Synthetic Methods*, Volume 6, Ed.: Giguère, D., Vincent, S. P. **2023**, CRC Press, Chapitre accepté.
4. Muru, K., **Cloutier, M.**, Provost-Savard, A., Di Cintio, S., Burton, O., Cordeil, J., Groleau, M.-C., Legault, J., Déziel, E., Gauthier, C. “Total synthesis of a chimeric glycolipid bearing the partially acetylated backbone of sponge-derived agminoside E.” *J. Org. Chem.* **2021**, *21*, 15357-15375.
5. Schellenberger, R., Crouzet, J., Nickzad, A., Shu, L.-J., Kutschera, A., Gerster, T., Borie, N., Dawid, C., **Cloutier, M.**, Villaume, S., Dhondt-Cordelier, S., Hubert, J., Cordelier, S., Mazeyrat-Gourbeyre, F., Schmid, C., Ongena, M., Renault, J. H., Haudrechy, A., Hofmann, T., Baillieul, F., Clément, C., Zipfel, C., Gauthier, C., Déziel, E., Ranf, S., Dorey, S. “Bacterial rhamnolipids and their 3-hydroxyalkanoate precursors activate *Arabidopsis* innate immunity through two independent mechanisms.” *Proc. Natl. Acad. Sci. USA* **2021**, *118*, e210136118.
6. **Cloutier, M.**, Prévost, M.-J., Lavoie, S., Feroldi, T., Piochon, M., Groleau, M.-C., Legault, J., Villaume, S., Crouzet, J., Dorey, S., De Rienzo, M. A. D., Déziel, E., Gauthier, C. “Total synthesis, isolation, surfactant properties, and biological evaluation of ananatosides and related macrolactone-containing rhamnolipids.” *Chem. Sci.* **2021**, *12*, 7533-7546.
7. **Cloutier, M.**, Gauthier, C. “Progress towards the development of glycan-based vaccines against campylobacteriosis.” *ACS Infect. Dis.* **2021**, *7*, 969-986.

8. **Cloutier, M.**, Gauthier, C. “3-Deoxy-D-manno-oct-2-ulosonic acid (Kdo) derivatives in antibacterial drug discovery.” In: *Carbohydrates in Drug Discovery and Development*, 1st edition, Ed.: Tiwari, V. K.; **2020**, Elsevier, 700 pp.
9. **Cloutier, M.**, Muru, K., Gauthier, C. “Synthesis of oligosaccharides related to potential bioterrorist pathogens.” In: *Recent Trends in Carbohydrate Chemistry*, 1st edition, Ed.: Rauter, A. P., Christensen, B., Somsak, L., Kosma, P., Adamo, R. **2020**, Elsevier, 532 pp.
10. **Cloutier, M.**, Delar, E., Muru, K., Ndong, S., Hoyeck, R. R., Kaewarpai, T., Chantratita, N., Burtnick, M. N., Brett, P. J., Gauthier, C. “Melioidosis patient serum-reactive synthetic tetrasaccharides bearing the predominant epitopes of *Burkholderia pseudomallei* and *Burkholderia mallei* O-antigens.” *Org. Biomol. Chem.* **2019**, *17*, 8878-8901.
11. **Cloutier, M.**, Muru, K., Ravicoularamin, G., Gauthier, C. “Polysaccharides from *Burkholderia* species as targets for vaccine development, immunomodulation and chemical synthesis.” *Nat. Prod. Rep.* **2018**, *35*, 1251-1293.

Brevet

1. Gauthier, C., **Cloutier, M.** “Tetrasaccharides for diagnosis, prevention, and treatment of melioidosis and glanders.” *PCT* application, **2019**, 62/857,346, 71 pp.

Présentations orales et par affiches

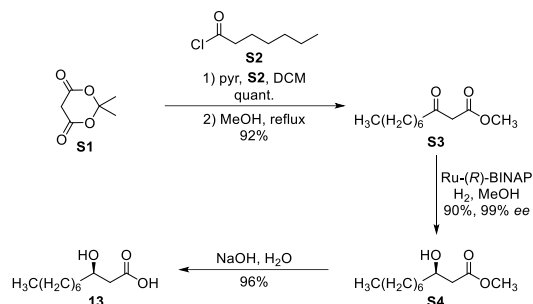
1. **Cloutier, M.**, Lavoie, S., Gauthier, C. “C7 epimerization of benzylidene-protected β -D-idopyranosides brings structural insights into idose conformational flexibility” 105th Canadian Chemistry Conference and Exhibition, Calgary, Canada, **2022**, (présentation orale).
2. **Cloutier, M.**, Gauthier, C. “Total synthesis and biological evaluation of ananatosides and related macrolactone-containing rhamnolipids” 104th Canadian Chemistry Conference and Exhibition, en ligne **2021**, (présentation orale).
3. **Cloutier, M.**, Gauthier, C. “*Burkholderia pseudomallei* and *B. mallei* synthetic lipopolysaccharides as potential vaccine candidates” EuroCarb2019, Leiden, Pays-Bas, **2019** (présentation orale).

4. **Cloutier, M.**, Gauthier, C. “*Burkholderia pseudomallei* and *B. mallei* synthetic lipopolysaccharides as potential vaccine candidates.” 102nd Canadian Chemistry Conference and Exhibition, Québec, Canada, **2019** (présentation orale).
5. **Cloutier, M.**, Prévost, M.-J., Gauthier, C. “Total synthesis of ananatosides as a novel class of biosurfactants” 22nd annual Chemistry and Biochemistry Graduate Research Conference (CBGRC), Montréal, Canada, **2019** (présentation orale).
6. **Cloutier, M.**, Prévost, M.-J., Gauthier, C. “Synthèse totale de dérivés de l’ananatoside A comme nouvelle classe de biosurfactants.” 9^e colloque scientifique annuel du Réseau québécois de la recherche sur les médicaments (RQRM), Orford, Canada, **2019** (présentation par affiche).
7. **Cloutier, M.**, Prévost, M.-J., Gauthier, C. “Synthèse totale de dérivés de l’ananatoside A comme nouvelle classe de biosurfactants.” Congrès Armand-Frappier, Saint-Sauveur, Canada, **2019** (présentation par affiche).
8. **Cloutier, M.**, Gauthier, C. “*Burkholderia pseudomallei* and *B. mallei* synthetic lipopolysaccharide mimics as potential vaccine candidates” 21st annual Chemistry and Biochemistry Graduate Research Conference (CBGRC), Montréal, Canada, **2018** (présentation orale).
9. **Cloutier, M.**, Gauthier, C. “Synthesis of *Burkholderia pseudomallei* lipopolysaccharide mimics as potential vaccines against melioidosis.” 29th annual Quebec-Ontario Mini-Symposium for Synthetic and Bioorganic Chemistry (QOMSSOC), Toronto, Canada, **2018** (présentation par affiche).
10. **Cloutier, M.**, Gauthier, C. “Synthesis of *Burkholderia pseudomallei* lipopolysaccharide mimics as potential vaccines against melioidosis” 8^e colloque scientifique annuel du Réseau québécois de la recherche sur les médicaments (RQRM), Montréal, Canada, **2018** (présentation par affiche).

ANNEXE DU CHAPITRE 2

1. Supplementary Schemes, Figures, and Tables

Scheme S1. Synthesis of Monolipid 13 from Meldrum's Acid (S1).



Scheme S2. Alternative Synthesis of Rhamnolipid 3.

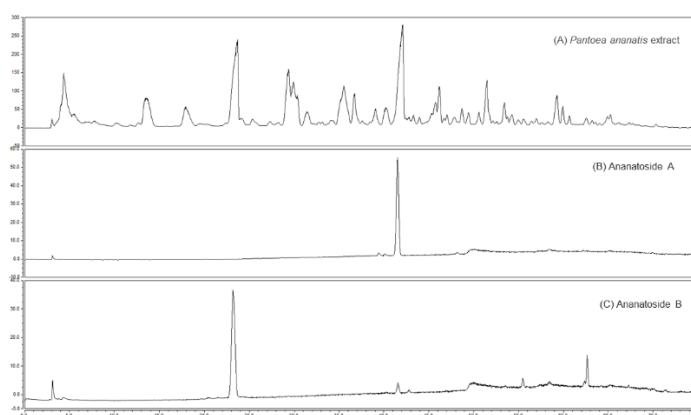
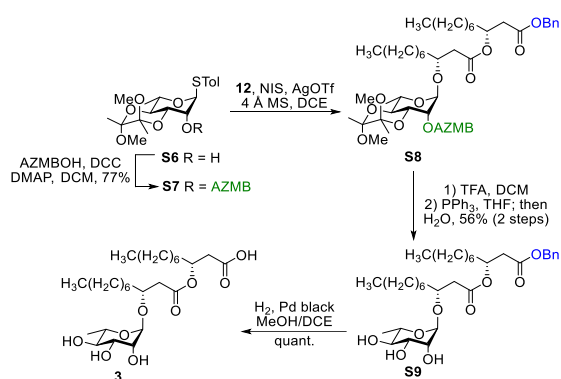


Figure S1. HPLC-CAD chromatograms comparison of (A) crude ethyl acetate *Pantoea Ananatis* extract, (B) synthetic ananatoside A (1) and (C) synthetic ananatoside B (2).

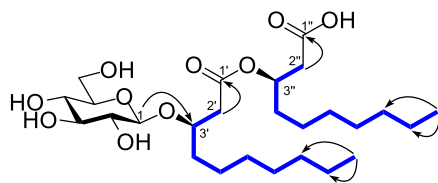


Figure S2. Proposed structure of anatoside B (**2**) along with key 2D NMR COSY (—) and HMBC (→) correlations.

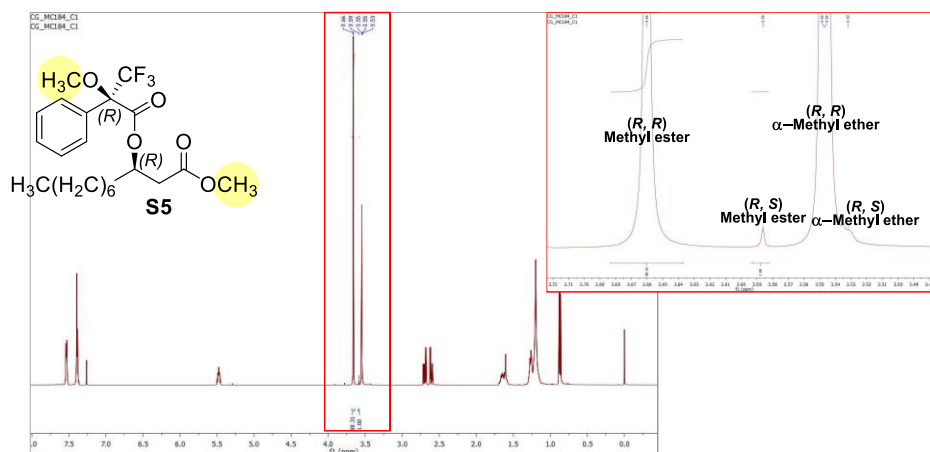


Figure S3. Enlargement of the ^1H NMR spectrum of Mosher's ester **S5**.

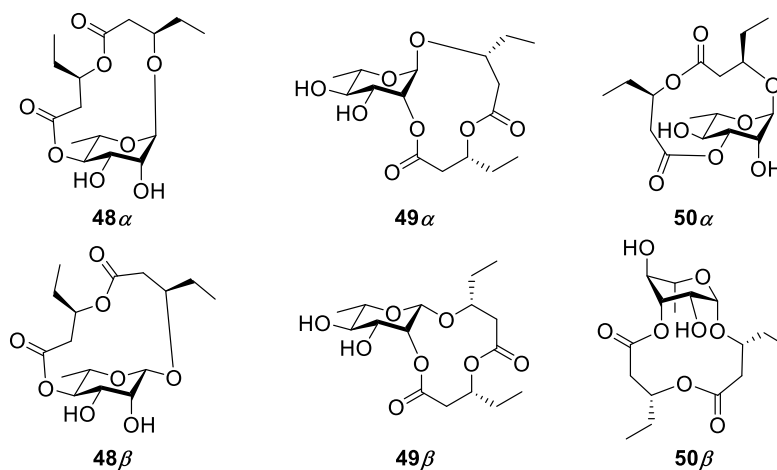


Figure S4. Structures of the *in silico* modeled compounds.

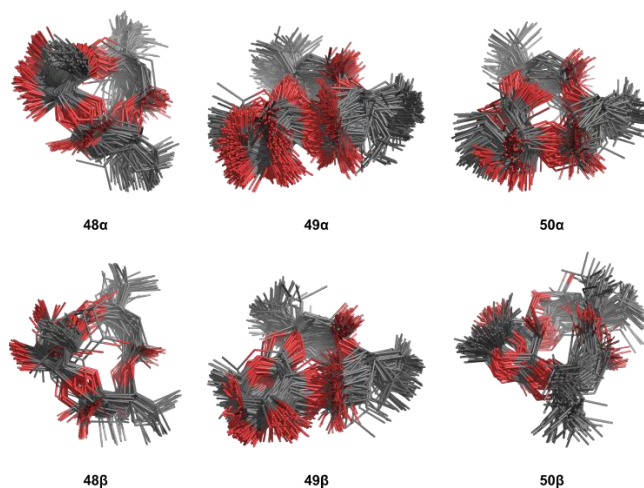


Figure S5. MMFF94 conformer populations for the macrolactonized rhamnolipid models **48–50**. Only carbon (grey) and oxygen (red) are displayed for simplicity.

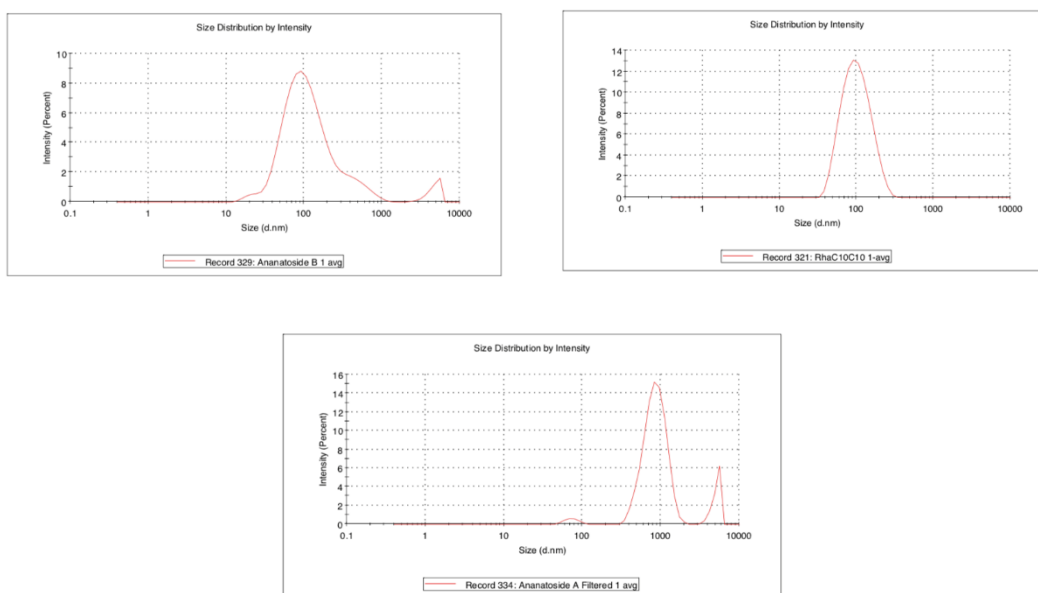


Figure S6. Size distribution of (A) ananatoside B (**2**), (B) RhaC₁₀C₁₀ (**3**), and (C) ananatoside A (**1**) measured by DLS.

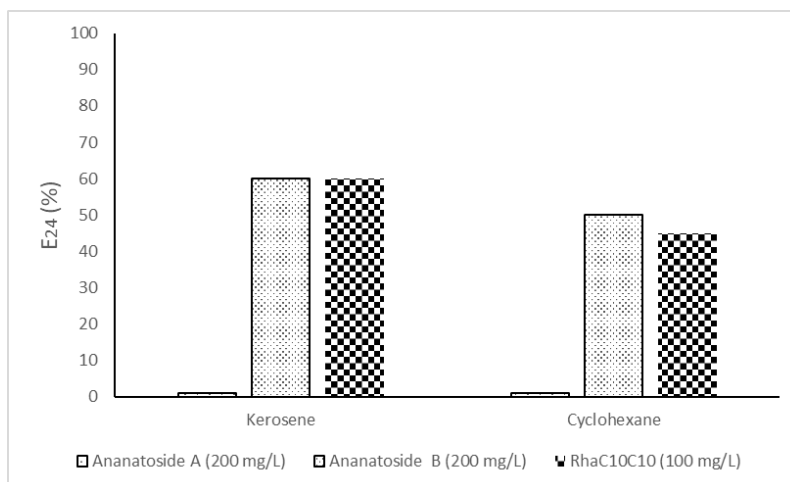


Figure S7. Emulsification activity (E₂₄) of kerosene and cyclohexane by anatanoside A (1), anatanoside B (2), and RhaC₁₀C₁₀ (3).

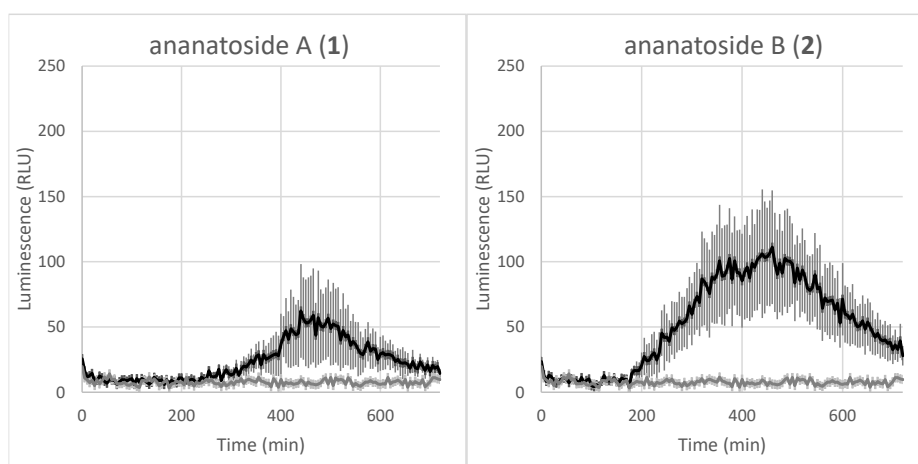


Figure S8. Extracellular ROS production following treatment of *Arabidopsis* petiole with anatanoside A (1) or anatanoside B (2). Production of reactive oxygen species (ROS) was measured in *Arabidopsis* petiole following treatment at 100 μ M with anatanoside A (1) and anatanoside B (2). Methanol (0.5%) was used as a control. ROS production was measured using the chemiluminescence of luminol and photon counts were expressed as relative luminescence units (RLUs). Data are mean \pm SEM ($n = 6$). Experiments were realized three times with similar results.

Table S1. ^{13}C and ^1H NMR MAE Values Related to Comparison of Experimental and Predicted Chemical Shifts.

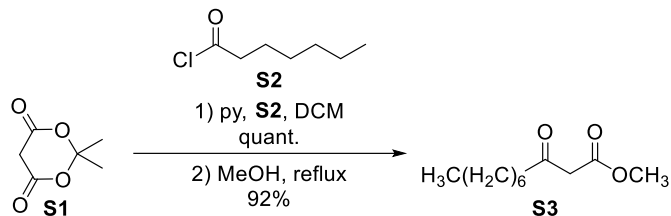
Comparison pair	mPW1PW91/6-31g(d,p)		mPW1PW91/6-311+g(d,p)		B97-2/cc-pVTZ			
	^{13}C MAE	^1H MAE	^{13}C MAE	^1H MAE	^{13}C MAE	^1H MAE		
Classic comparison	4 \rightarrow 48 α \rightarrow 48 β	0.90	0.17	3.13	0.08	3.01	0.09	
		1.62	0.24	3.60	0.15	3.05	0.18	
	5 α \rightarrow 49 α \rightarrow 49 β	0.89	0.08	2.77	0.08	2.75	0.09	
		3.06	0.28	3.87	0.30	4.54	0.26	
	5 β \rightarrow 49 α \rightarrow 49 β	1.74	0.23	3.45	0.14	3.04	0.19	
		1.39	0.12	2.86	0.12	3.43	0.10	
	6 α \rightarrow 50 α \rightarrow 50 β	2.58	0.24	4.05	0.17	3.73	0.19	
		3.49	0.25	4.30	0.25	4.69	0.23	
	6 β \rightarrow 50 α \rightarrow 50 β	3.02	0.31	3.74	0.23	3.08	0.23	
		1.08	0.12	2.91	0.10	2.96	0.09	
	Comparison alignment	5 α \rightarrow 49 α	1.43	0.12	1.25	0.09	1.36	0.08
		5 β \rightarrow 49 β						
5 α \rightarrow 49 β		4.67	0.47	5.01	0.42	5.10	0.41	
5 β \rightarrow 49 α								
6 α \rightarrow 50 α		2.32	0.24	2.12	0.21	2.14	0.19	
6 β \rightarrow 50 β								
6 α \rightarrow 50 β	6.38	0.50	6.02	0.45	5.71	0.44		
6 β \rightarrow 50 α								

Table S2. Number of Conformers Retained after Each Step of Modeling.

Filter	Number of Conformers					
	48 α	48 β	49 α	49 β	50 α	50 β
ETKDGv2	100 000	100 000	100 000	100 000	100 000	100 000
1 st RMSD (0.5 Å)	420	255	831	710	363	497
MMFF94s energy window (80 kJ•mol ⁻¹)	262	133	523	306	238	216
2 nd RMSD (0.25 Å)	137	73	367	229	135	114
mPW1PW91/6-31G(d,p) energy window (10 kJ•mol ⁻¹)	10	10	15	9	12	5

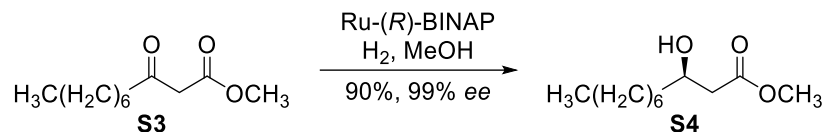
2. Additional Experimental Procedures for Synthesis

Methyl 3-Oxodecanoate (**S3**).



To a solution of Meldrum's acid (**S1**, 7.44 g, 51.64 mmol, 1.05 equiv) in anhydrous DCM (22 mL) at 0 °C under Ar was slowly added anhydrous pyridine (8.0 mL, 98 mmol, 2.0 equiv). A solution of octanoyl chloride (**S2**, 8.00 g, 49.18 mmol, 1.0 equiv) in anhydrous DCM (15 mL) was then added dropwise, and the mixture was stirred for 1 h at rt under Ar. The solution was washed with aqueous 2 M HCl (2 × 40 mL), the aqueous layer was extracted with DCM (2 × 15 mL), and the combined organic phases were washed with aqueous 2 M HCl (2 × 15 mL) and brine (40 mL). The organic phase was dried over MgSO₄, filtered, and evaporated under reduced pressure to give the corresponding enol as a brown-red oil (13.3 g, quant.). The latter compound (12.8 g, 47.4 mmol, 1.0 equiv) was solubilized in anhydrous MeOH and the solution was refluxed for 3 h under Ar. The solution was evaporated under reduced pressure and the residue was purified by silica gel flash chromatography (Hex/EtOAc 10:0 to 95:5) to give keto-ester **S3** as a colorless oil (8.77 g, 92%). Physical and analytical data of compound **S3** agreed with those published.¹⁸⁹

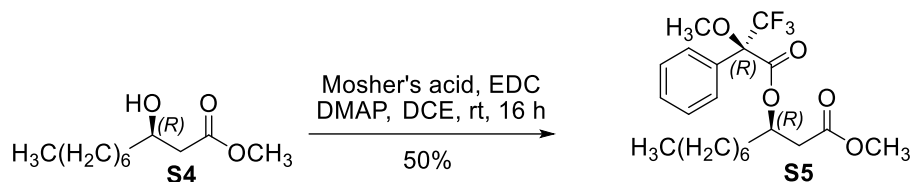
(R)-Methyl 3-Hydroxydecanoate (S4).



Preparation of the catalyst: In a heat gun-dried reaction flask under an Ar atmosphere were added (R)-BINAP (379 mg, 0.608 mmol, 0.024 equiv) and (COD)Ru(2-methylallyl)₂ (162 mg, 0.507 mmol, 0.020 equiv). The reactants were then solubilized in anhydrous acetone (25 mL), which was previously degassed with Ar. A solution of 48% aqueous HBr (0.13 mL) in degassed anhydrous MeOH (6.3 mL) was added to the reaction flask, and the mixture was stirred at rt for 30 min under an Ar atmosphere. The solvents were then evaporated under nitrogen flux.

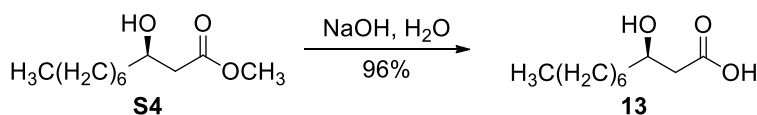
Preparation of hydroxy-ester: To the previously prepared catalyst was cannulated a solution of keto-ester **S3** (5.07 g, 25.33 mmol, 1.0 equiv) in anhydrous degassed MeOH (51 mL). The solution was stirred at 55 °C for 18 h under an H₂ atmosphere. The solution was then cooled at 0 °C, filtered over Celite, and evaporated under reduced pressure. The residue was purified by silica gel flash chromatography (Hex/EtOAc 9:1 to 8:2) to give hydroxy-ester **S4** (4.61 g, 90%) as a colorless oil. Physical and analytical data of compound **S4** agreed with those published.¹⁸⁹ The enantiomeric purity of compound **S4** was determined through the synthesis of Mosher's ester **S5**.¹⁸⁸

(R)-Methyl α -Methoxy- α -trifluoromethylphenylacetyl-(R)-3-hydroxydecanoate (S5).



Methyl ester **S4** (15 mg, 0.074 mmol, 1.0 equiv) was solubilized in anhydrous DCE (0.4 mL). Mosher's acid (26 mg, 0.11 mmol, 1.5 equiv), EDC (28 mg, 0.15 mmol, 2.0 equiv), and DMAP (2 mg, 0.02 mmol, 0.2 equiv) were successively added to the solution, which was then stirred at rt for 16 h under an Ar atmosphere. The solution was evaporated under reduced pressure and the residue was purified by silica gel flash chromatography (DCM) to give Mosher's ester **S5** (15 mg, 50%) as a colorless oil. Physical and analytical data of compound **S5** agreed with those published.¹⁸⁸ Analysis of this spectrum allowed to determine the enantiomeric purity of methyl ester **S4** (99% *ee*, see Fig. S3) as previously reported.¹⁸⁸

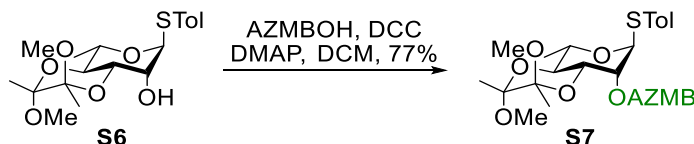
(R)-3-Hydroxydecanoic Acid (13).



Alcohol **S4** (4.31 g, 21.3 mmol, 1.0 equiv) was solubilized in aqueous 1 M NaOH (43 mL) at 0 °C. The mixture was stirred at 0 °C for 1 h, then at rt for an additional 1.5 h. The solution was acidified with aqueous 2 M HCl until a pH of ~2–3 was reached and the aqueous phase was extracted with EtOAc (3×). The combined organic layers were washed with brine, dried over anhydrous MgSO₄, filtered, and evaporated under reduced pressure to give acid **13** (3.84 g, 96%) as a white amorphous

solid without further purification. Physical and analytical data of compound **13** agreed with those published.¹⁸⁹

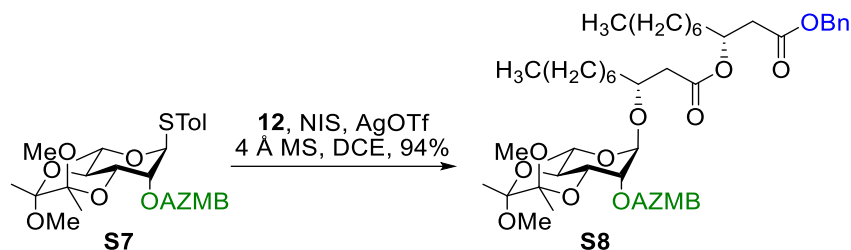
***para*-Methylphenyl 2-*O*-*ortho*-(Azidomethyl)benzoyl-3,4-*O*-(2,3-dimethoxybutan-2,3-diyl)-1-thio- α -L-rhamnopyranoside (**S7**).**



To a solution of compound **S6**²⁰⁰ (129 mg, 0.33 mmol, 1.0 equiv) in anhydrous DCM (3.3 mL) were successively added DMAP (78 mg, 0.050 mmol, 1.0 equiv), EDC (129 mg, 1.00 mmol, 3.0 equiv), and AZMBOH (89 mg, 0.37 mmol, 1.5 equiv). The mixture was refluxed for 4 h under an Ar atmosphere, then cooled at rt and the solvents were evaporated under reduced pressure. The residue was purified by silica gel flash chromatography (Hex/EtOAc 98:2 to 95:5) to give compound **S7** (141 mg, 77%) as a white amorphous solid: R_f 0.67 (Hex/EtOAc 8:2); $[\alpha]_D^{20}$ -164 (c 0.5, CHCl_3); $^1\text{H NMR}$ (600 MHz, CDCl_3) δ (ppm) 8.04-8.02 (m, 1H, CH_{AZMB}), 7.58-7.53 (m, 2H, $2 \times \text{CH}_{\text{AZMB}}$), 7.41-7.38 (m, 3H, CH_{AZMB} , $2 \times \text{CH}_{\text{STol}}$), 7.12-7.11 (m, 2H, $2 \times \text{CH}_{\text{STol}}$), 5.53-5.52 (m, 2H, H-1, H-2), 4.87 (d, $J = 15.2$ Hz, 1H, CHH_{AZMB}), 4.81 (d, $J = 15.2$ Hz, 1H, CHH_{AZMB}), 4.37 (dq, $J_{5-4} = 9.6$ Hz, $J_{5-6} = 6.1$ Hz, 1H, H-5), 4.19 (dd, $J_{3-4} = 10.2$ Hz, $J_{3-2} = 3.1$ Hz, 1H, H-3), 3.90 (t, $J = 10.0$ Hz, 1H, H-4), 3.33 (s, 3H, $\text{CH}_{3\text{OMe}}$), 3.31 (s, 3H, CH_{OMe}), 2.32 (s, 3H, $\text{CH}_{3\text{STol}}$), 1.35 (s, 3H, CH_3), 1.31-1.30 (m, 6H, H-6, CH_3); $^{13}\text{C NMR}$ (150 MHz, CDCl_3) δ (ppm) 166.7 ($\text{COOR}_{\text{AZMB}}$), 138.1-128.0 (12C, $4 \times \text{C}_{\text{Ar}}$, $8 \times \text{CH}_{\text{Ar}}$), 100.4 (2C, $2 \times \text{C}(\text{O})_2\text{CH}_3$), 86.7 (C-1), 73.9 (C-2), 69.4 (C-4), 67.9 (C-5), 66.9 (C-3), 53.2 ($\text{CH}_{2\text{AZMB}}$), 48.3 ($\text{CH}_{3\text{OMe}}$), 47.9 ($\text{CH}_{3\text{OMe}}$), 21.2 ($\text{CH}_{3\text{STol}}$), 17.9 (CH_3), 17.7 (CH_3), 16.7 (C-6); HRMS (ESI-TOF) m/z $[\text{M} + \text{Na}]^+$ calcd for

C₂₇H₃₃NaN₃O₇S 566.1931; found 566.1953; *m/z* [M + K]⁺ calcd for C₂₇H₃₃KN₃O₇S 582.1671; found 582.1687.

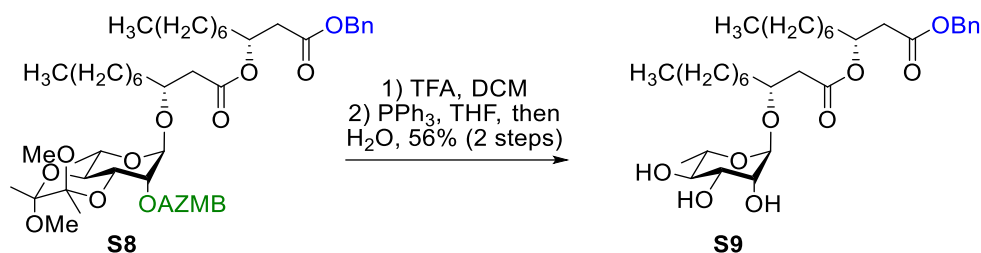
1-*O*-{Benzyl (R)-3-*O*-[(R)-(3'-*O*-Decyl)-2-*O*-*ortho*-(azidomethyl)benzoyl]-[3,4-*O*-(2,3-dimethoxybutan-2,3-diyl)]- α -L-rhamnopyranosyl} Decanoate (S8).



Donor **S7** (85 mg, 0.16 mmol, 1.2 equiv), acceptor **12** (59 mg, 0.13 mmol, 1.0 equiv), and NIS (47 mg, 0.21 mmol, 1.6 equiv) were dried under high vacuum for 1 h. Activated 4 Å MS (234 mg, 4 mg•mg⁻¹ of acceptor **12**) and anhydrous DCE (2.6 mL) were added and the suspension was stirred under an Ar atmosphere for 1 h. The mixture was cooled to -10 °C and AgOTf (7 mg, 0.03 mmol, 0.2 equiv) was added while the reaction flask was protected from light with aluminum foil. The suspension was stirred from -10 to 0 °C for 1.5 h, quenched with Et₃N, and filtered over Celite. The solvents were evaporated under reduced pressure and the residue was purified by silica gel flash chromatography (Tol/EtOAc 99:1 to 985:15) to give compound **S8** (106 mg, 94%) as a colorless oil: *R_f* 0.56 (Tol/EtOAc 95:5); [α]_D²⁰ -74 (*c* 0.6, CHCl₃); ¹H NMR (600 MHz, CDCl₃) δ (ppm) 8.05-8.04 (m, 1H, CH_{AZMB}), 7.59-7.55 (m, 2H, 2 × CH_{AZMB}), 7.42-7.39 (m, 1H, CH_{AZMB}), 7.35-7.31 (m, 5H, 5 × CH_{AZMB}), 5.25-5.21 (m, 1H, H-3''), 5.18 (dd, *J*₂₋₃ = 3.2 Hz, *J*₂₋₁ = 1.5 Hz, 1H, H-2), 5.11 (s, 2H, CH₂COOBn), 4.99 (d, *J* = 1.1 Hz, 1H, H-1), 4.89 (d, *J* = 15.2 Hz, 1H, CHH_{AZMB}), 4.82 (d, *J* = 15.3 Hz, 1H, CHH_{AZMB}), 4.14 (dd, *J*₃₋₄ = 10.2 Hz, *J*₃₋₂ = 3.3 Hz, 1H, H-3), 4.08-4.04 (m, 1H, H-3'), 3.94-3.90 (m, 1H, H-5), 3.79 (t, *J* = 10.0 Hz, 1H, H-4), 3.28 (s, 3H,

CH_{3OMe}), 3.27 (s, 3H, CH_{3OMe}), 2.69 (dd, $J = 15.5$ Hz, $J = 7.0$ Hz, 1H, H-2a''), 2.64-2.56 (m, 2H, H-2b'', H-2a'), 2.42 (dd, $J = 15.3$ Hz, $J = 6.9$ Hz, 1H, H-2b'), 1.59-1.23 (m, 33H, $12 \times CH_2$, $2 \times CH_3$, H-6), 0.89-0.85 (m, 6H, $2 \times CH_3$); ^{13}C NMR (150 MHz, $CDCl_3$) δ (ppm) 170.5, 170.3 (2C, C-1', C-1''), 166.9 ($COOR_{AZMB}$), 137.3-128.0 (12C, $3 \times C_{Ar}$, $9 \times CH_{Ar}$), 100.3 ($C(O)_2CH_3$), 99.9 ($C(O)_2CH_3$), 97.3 (C-1), 75.7 (C-3'), 72.7 (C-2), 70.9 (C-3''), 69.2 (C-4), 67.1 (C-5), 66.6, 66.2 (2C, CH_2COOBn , C-3), 53.3 (CH_2AZMB), 48.2 (CH_3OMe), 47.8 (CH_3OMe), 40.6 (C-2'), 39.2 (C-2''), 34.0-22.8 (12C, $12 \times CH_2$), 17.9, 17.8 (2C, $2 \times CH_3$), 16.7 (C-6), 14.2 (2C, $2 \times CH_3$); HRMS (ESI-TOF) m/z $[M + NH_4]^+$ calcd for $C_{47}H_{77}N_4O_{12}$ 885.5220 found 885.5225; m/z $[M + Na]^+$ calcd for $C_{47}H_{69}NaN_3O_{12}$ 890.4774; found 890.4779.

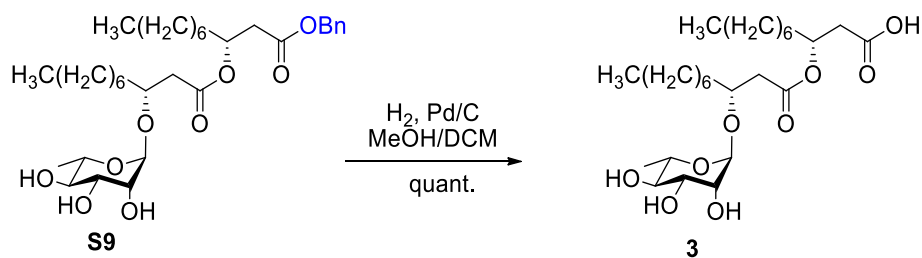
Benzyl (*R*)-3-*O*-[(*R*)-(3'-*O*-Decyl)- α -L-rhamnopyranosyl]decanoate (S9**).**



TFA (223 μ L) and H_2O (12 μ L) were added to a solution of compound **S8** (20 mg, 23 μ mol, 1.0 equiv) in DCM (230 μ L). The mixture was stirred at rt for 1 h and quenched with saturated aqueous $NaHCO_3$. The organic layer was washed with brine, dried over $MgSO_4$, filtered, and the solvents were evaporated under reduced pressure. The residue was filtered over silica gel, then solubilized in anhydrous THF (0.7 mL). PPh_3 (9 mg, 40 μ mol, 1.6 equiv) was added and the mixture was stirred under an Ar atmosphere at 60 $^\circ$ C for 2 h. H_2O (90 μ L) was then added and the solution was stirred at 60 $^\circ$ C for 4 h. The solution was co-evaporated with toluene and the residue was purified

by silica gel flash chromatography (DCM/MeOH 99:1 to 97:3) to give triol **S9** (8 mg, 56%) as a colorless oil: R_f 0.38 (DCM/MeOH 95:5); $[\alpha]_D^{20}$ -60 (c 0.1, CHCl_3); $^1\text{H NMR}$ (600 MHz, CDCl_3) δ (ppm) 7.38-7.32 (m, 5H, $5 \times \text{CHCOOBn}$), 5.28-5.22 (m, 1H, H-3''), 5.11 (s, 2H, CH_2COOBn), 4.88 (d, $J = 1.4$ Hz, 1H, H-1), 4.21-4.15 (m, 1H, H-3'), 3.86-3.80 (m, 1H, H-2), 3.76-3.68 (m, 2H, H-3, H-5), 3.38-3.32 (m, 1H, H-4), 2.66 (dd, $J_{2a''-2b''} = 16.1$ Hz, $J_{2a''-3''} = 8.4$ Hz, 1H, H-2a''), 2.59 (dd, $J_{2b''-2a''} = 16.1$ Hz, $J_{2b''-3''} = 4.2$ Hz, 1H, H-2b''), 2.47 (dd, $J_{2a'-2b'} = 15.4$ Hz, $J_{2a'-3'} = 8.5$ Hz, 1H, H-2a'), 2.40 (dd, $J_{2b'-2a'} = 15.4$ Hz, $J_{2b'-3'} = 4.2$ Hz, 1H, H-2b'), 1.52-1.45 (m, 2H, CH_2), 1.31 (d, $J = 6.2$ Hz, 3H, H-6), 1.26-1.21 (m, 22H, $11 \times \text{CH}_2$), 0.89-0.84 (m, 6H, $2 \times \text{CH}_3$); $^{13}\text{C NMR}$ (150 MHz, CDCl_3) δ (ppm) 171.2 (2C, C-1', C-1''), 135.5 (C_{COOBn}), 128.8-128.3 (5C, $5 \times \text{CHCOOBn}$), 96.9 (C-1), 74.0 (C-4), 72.9 (C-3''), 72.0 (C-3'), 71.3 (C-2), 70.9 (C-3'), 68.2 (C-5), 67.0 (CH_2COOBn), 40.0 (C-2'), 39.2 (C-2''), 34.2-22.8 (12C, $12 \times \text{CH}_2$), 17.4 (C-6), 14.2 (2C, $2 \times \text{CH}_3$); HRMS (ESI-TOF) m/z $[\text{M} + \text{NH}_4]^+$ calcd for $\text{C}_{33}\text{H}_{58}\text{NO}_9$ 612.4106; found 612.4100; m/z $[\text{M} + \text{Na}]^+$ calcd for $\text{C}_{33}\text{H}_{54}\text{NaO}_9$ 617.3660; found 617.3657.

Rhamnolipid 3 from compound S9.



Pd black (11 mg, $1 \text{ mg} \cdot \text{mg}^{-1}$ of triol **S9**) was added to a solution of triol **S9** (11 mg, $19 \mu\text{mol}$, 1.0 equiv) in MeOH (0.38 mL) and DCE (0.19 mL). The suspension was stirred under an H_2 atmosphere at 40°C for 16 h. The mixture was then filtered over Celite and the solvents were evaporated under reduced pressure. The residue was purified by silica gel flash chromatography

(DCM/MeOH 95:5 to 8:2) to give C₁₀-C₁₀ rhamnolipid **3** (9.5 mg, quant.) as a colorless oil. Physical and analytical data of C₁₀-C₁₀ rhamnolipid (**3**) agreed with those published.¹⁹¹

3. Traces of NMR Spectra for New Compounds

Figure S9 | ^1H NMR spectrum (CDCl_3 , 600 MHz) of (*R*)-benzyl 3-hydroxydecanoate (14).

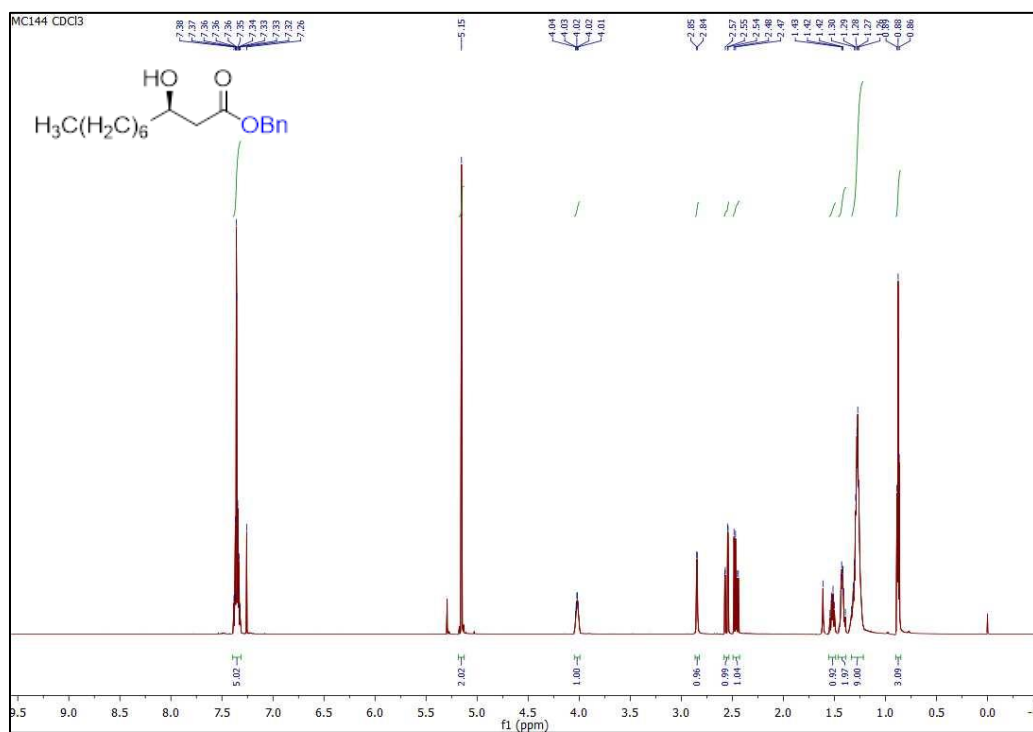


Figure S10 | ^{13}C NMR spectrum (CDCl_3 , 150 MHz) of (*R*)-benzyl 3-hydroxydecanoate (14).

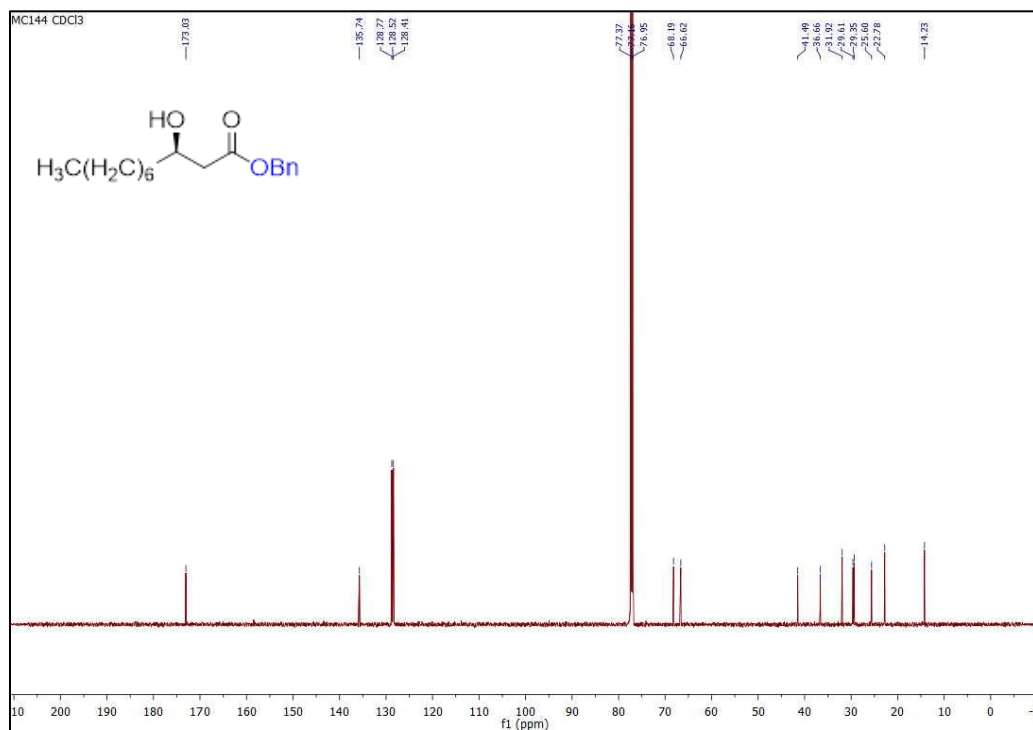


Figure S11 | ^1H NMR spectrum (CDCl_3 , 600 MHz) of (*R*)-benzyl 3-(((*R*)-(*tert*-butyldimethylsilyl)oxy)decanoyl)oxy)decanoate (16).

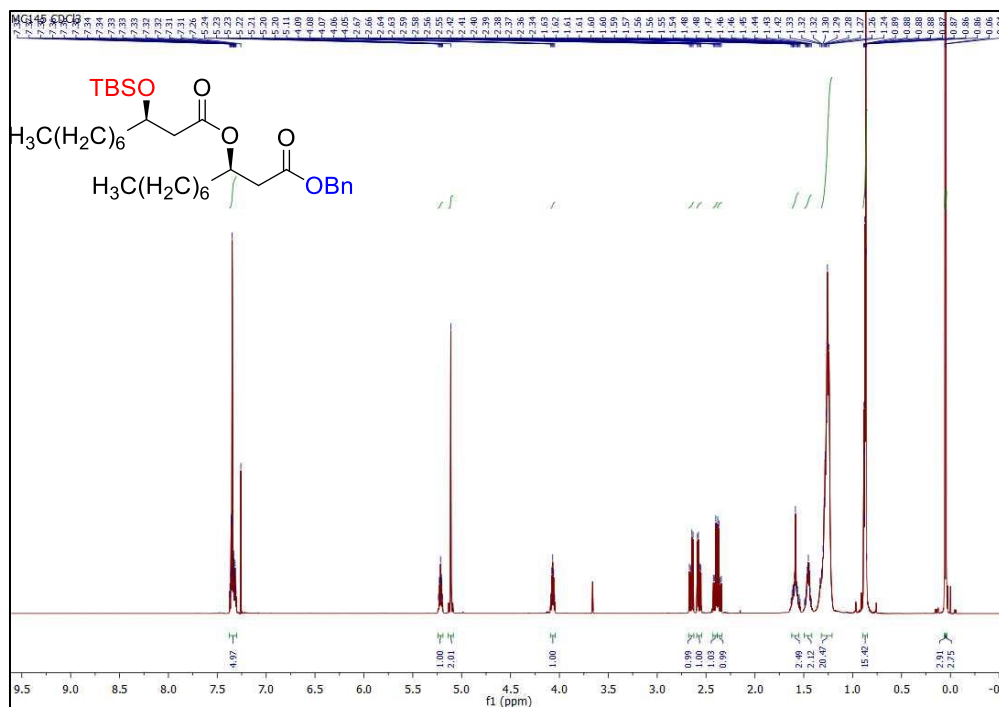


Figure S12 | ^{13}C NMR spectrum (CDCl_3 , 150 MHz) of (*R*)-benzyl 3-(((*R*)-(*tert*-butyldimethylsilyl)oxy)decanoyl)oxy)decanoate (16).

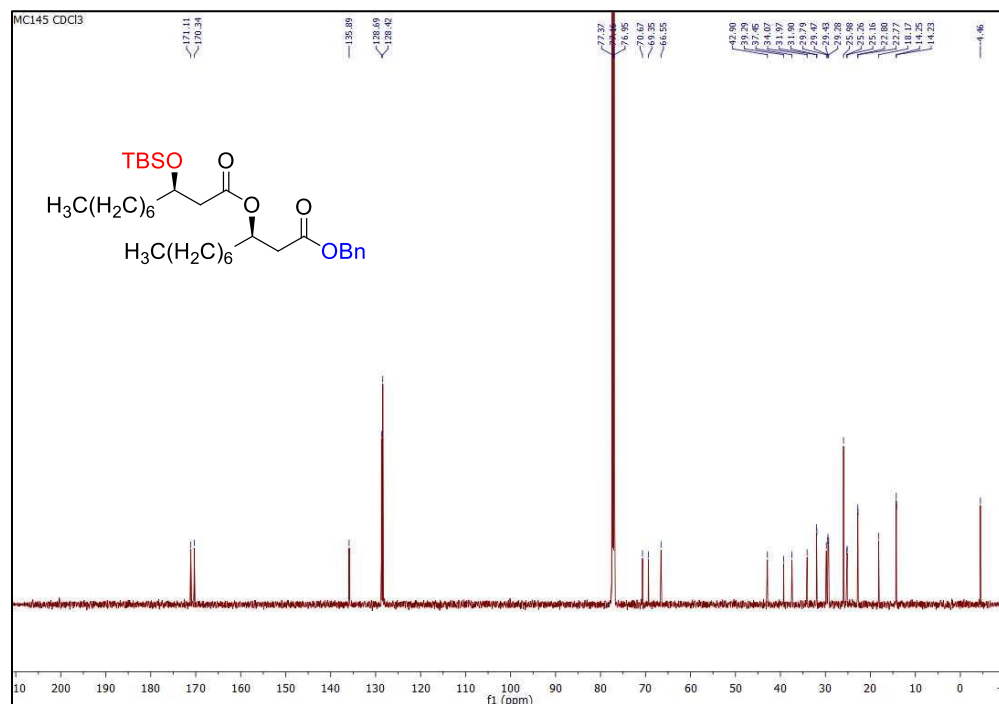


Figure S13 | ^1H NMR spectrum (CDCl_3 , 600 MHz) of (*R*)-3-(((*R*)-3-((*tert*-butyldimethylsilyl)oxy)decanoyl)oxy)decanoic acid (**10**).

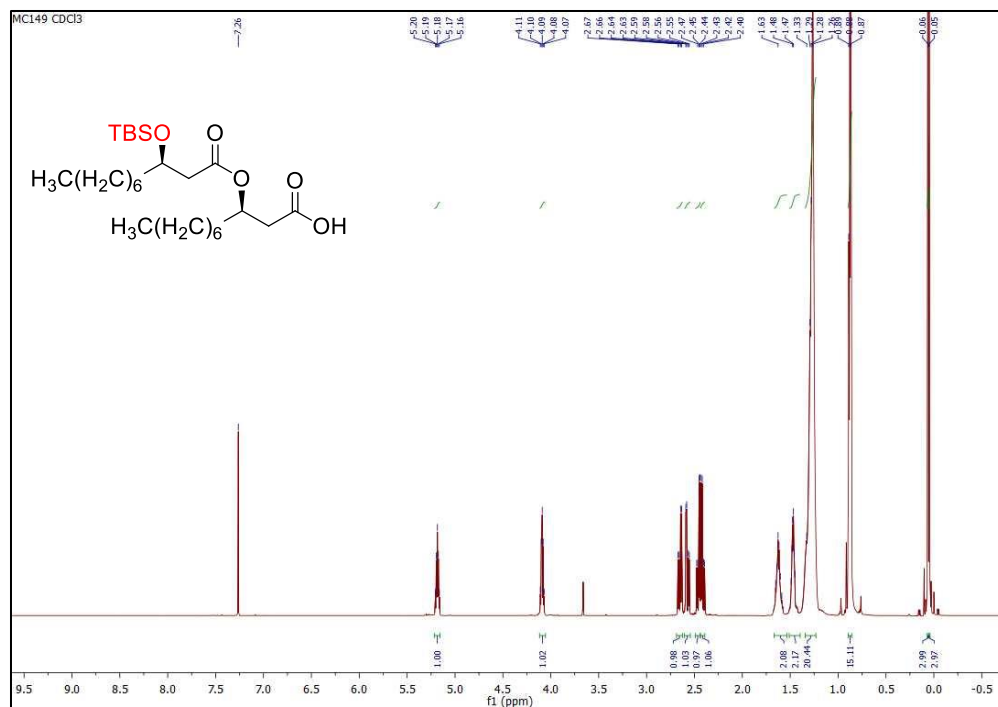


Figure S14 | ^{13}C NMR spectrum (CDCl_3 , 600 MHz) of (*R*)-3-(((*R*)-3-((*tert*-butyldimethylsilyl)oxy)decanoyl)oxy)decanoic acid (**10**).

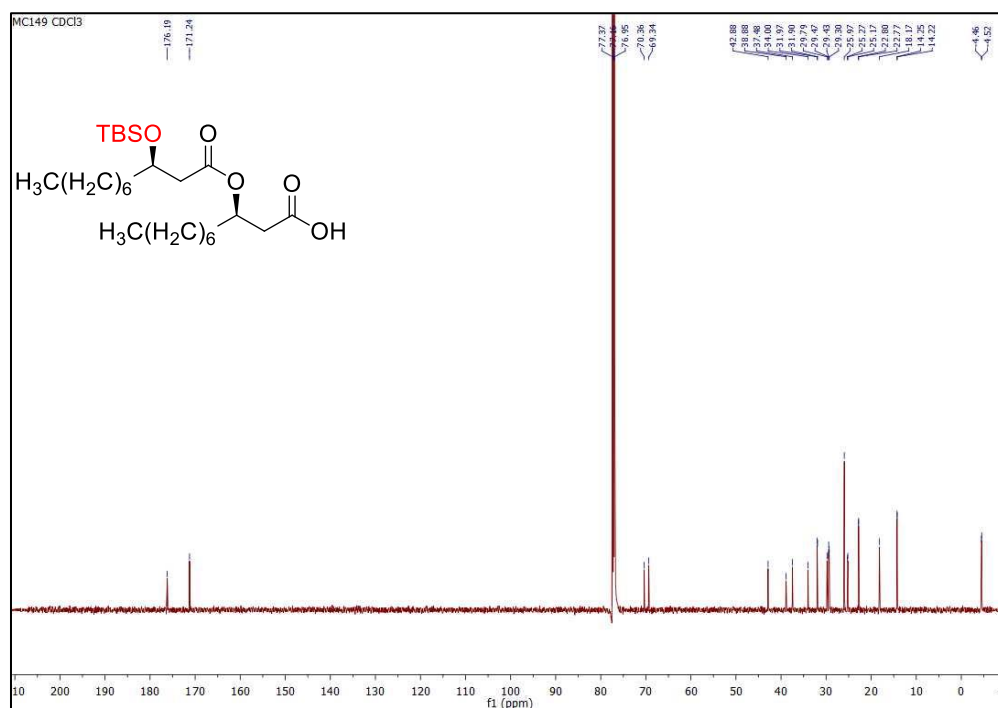


Figure S15 | ^1H NMR spectrum (CDCl_3 , 600 MHz) of (*R*)-benzyl 3-(((*R*)-3-hydroxydecanoyl)oxy)decanoate (**12**).

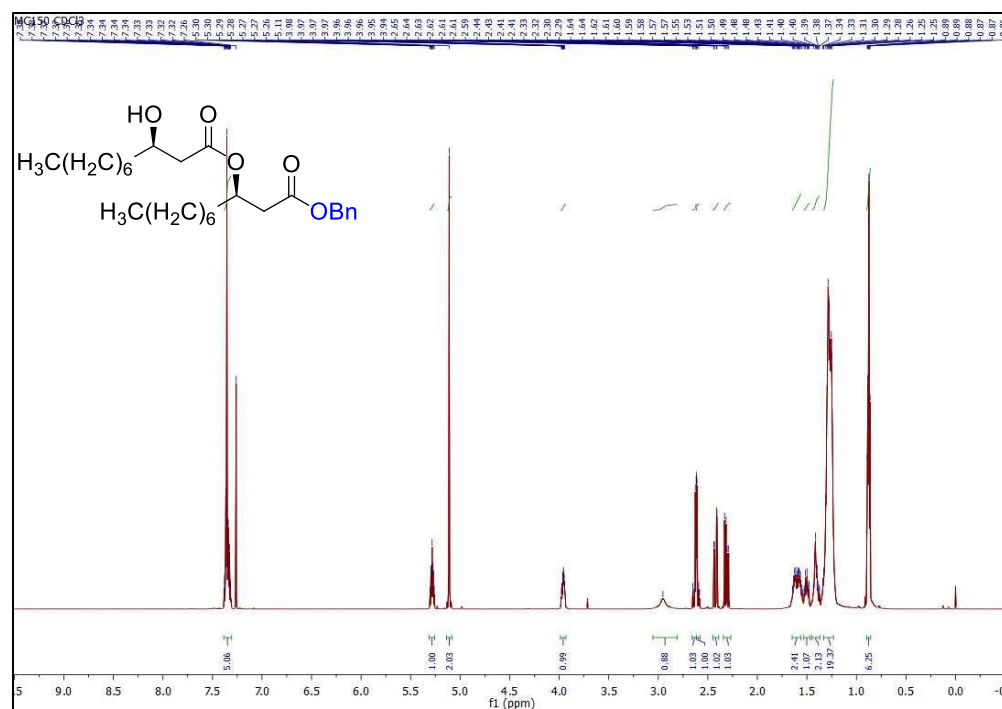


Figure S16 | ^{13}C NMR spectrum (CDCl_3 , 150 MHz) of (*R*)-benzyl 3-(((*R*)-3-hydroxydecanoyl)oxy)decanoate (**12**).

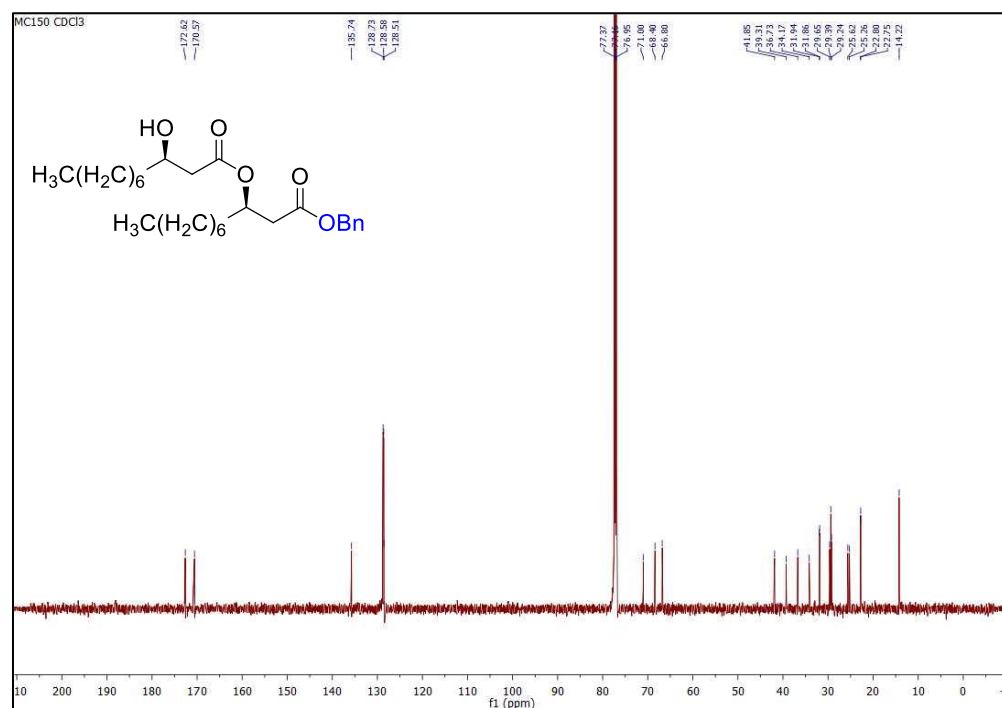


Figure S17 | ^1H NMR spectrum (CDCl_3 , 600 MHz) of *para*-methylphenyl 3,4-di-*O*-benzyl-6-*O*-*tert*-butyldimethylsilyl-1-thio- β -D-glucopyranoside (18).

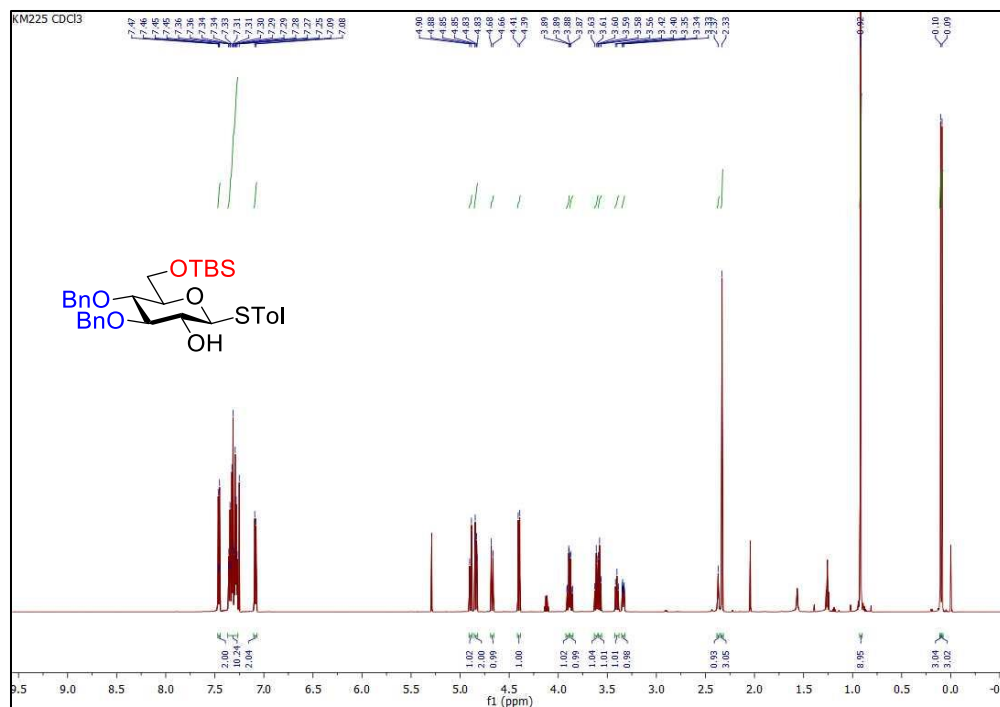


Figure S18 | ^{13}C NMR spectrum (CDCl_3 , 600 MHz) of *para*-methylphenyl 3,4-di-*O*-benzyl-6-*O*-*tert*-butyldimethylsilyl-1-thio- β -D-glucopyranoside (18).

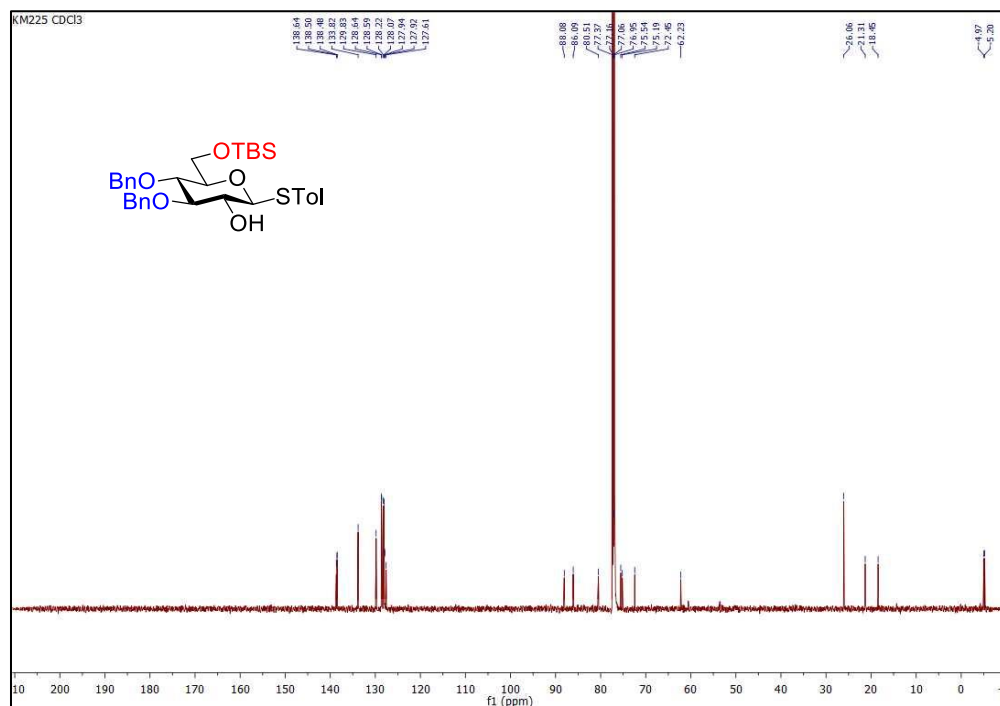


Figure S19 | ^1H NMR spectrum (CDCl_3 , 600 MHz) of *para*-methylphenyl 3,4-di-*O*-benzyl-6-*O*-*tert*-butyldimethylsilyl-2-*O*-levulinoyl-1-thio- β -D-glucopyranoside (11).

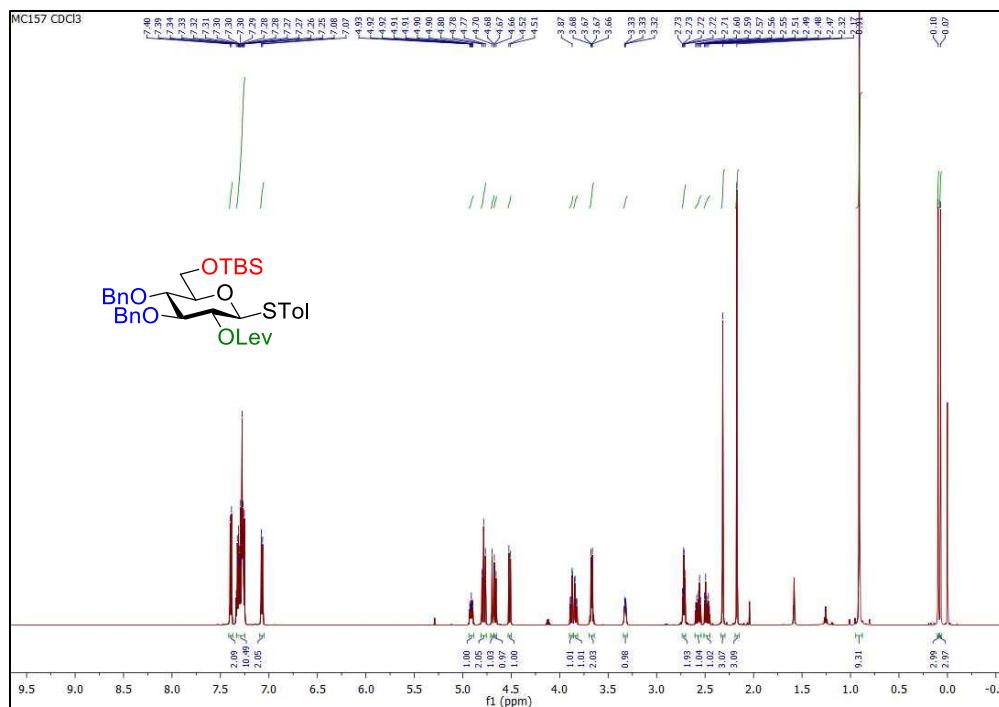


Figure S20 | ^{13}C NMR spectrum (CDCl_3 , 600 MHz) of *para*-methylphenyl 3,4-di-*O*-benzyl-6-*O*-*tert*-butyldimethylsilyl-2-*O*-levulinoyl-1-thio- β -D-glucopyranoside (11).

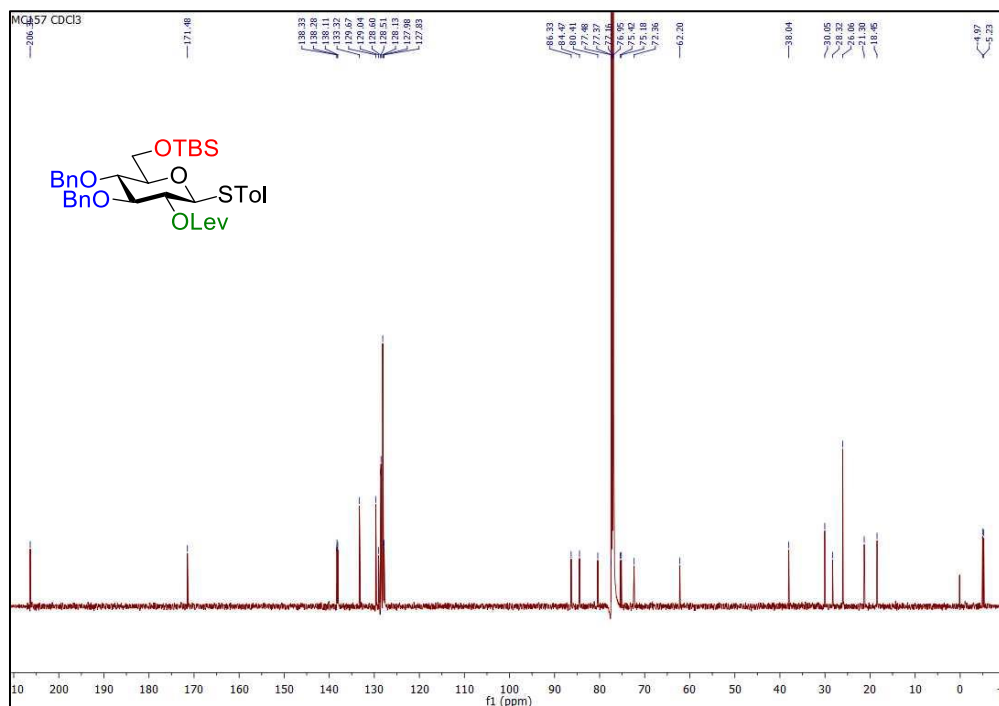


Figure S21 | ^1H NMR spectrum (CDCl_3 , 600 MHz) of benzyl (*R*)-3-*O*-[(*R*)-(3'-*O*-decyl)-3,4-di-*O*-benzyl-6-*O*-*tert*-butyldimethylsilyl-2-*O*-levulinoyl- β -D-glucopyranosyl]decanoate (8).

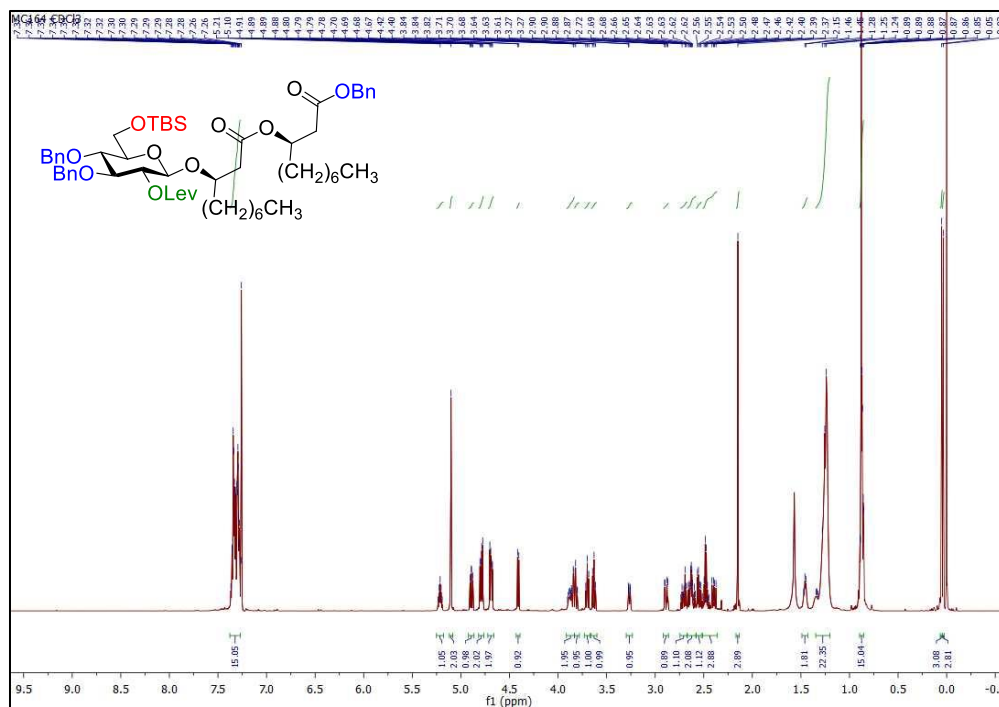


Figure S22 | ^{13}C NMR spectrum (CDCl_3 , 600 MHz) of benzyl (*R*)-3-*O*-[(*R*)-(3'-*O*-decyl)-3,4-di-*O*-benzyl-6-*O*-*tert*-butyldimethylsilyl-2-*O*-levulinoyl- β -D-glucopyranosyl]decanoate (8).

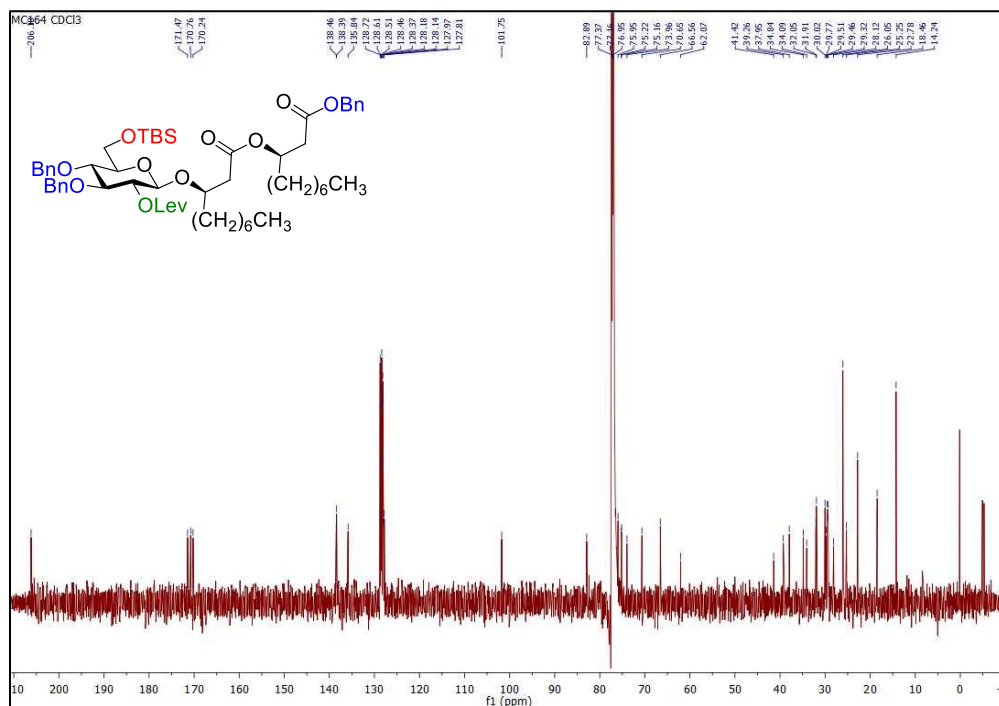


Figure S23 | ¹H NMR spectrum (CDCl₃, 600 MHz) of benzyl (*R*)-3-*O*-[*R*]-(*3'*-*O*-decyl)-3,4-di-*O*-benzyl-2-*O*-levulinoyl-β-*D*-glucopyranosyl]decanoate (20).

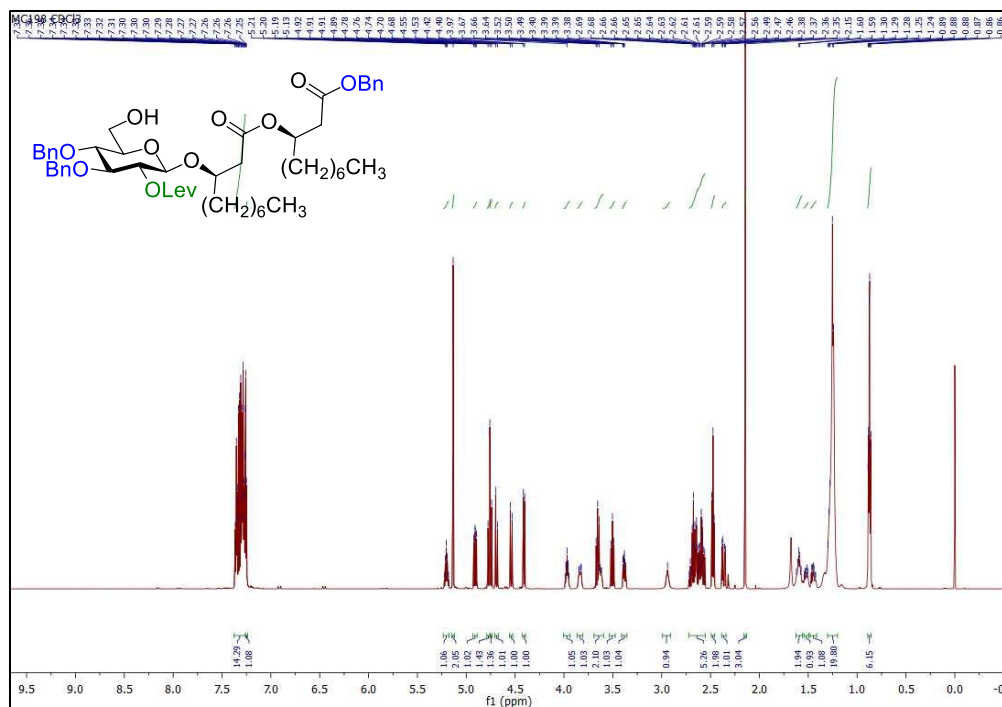


Figure S24 | ¹³C NMR spectrum (CDCl₃, 600 MHz) of benzyl (*R*)-3-*O*-[*R*]-(*3'*-*O*-decyl)-3,4-di-*O*-benzyl-2-*O*-levulinoyl-β-*D*-glucopyranosyl]decanoate (20).

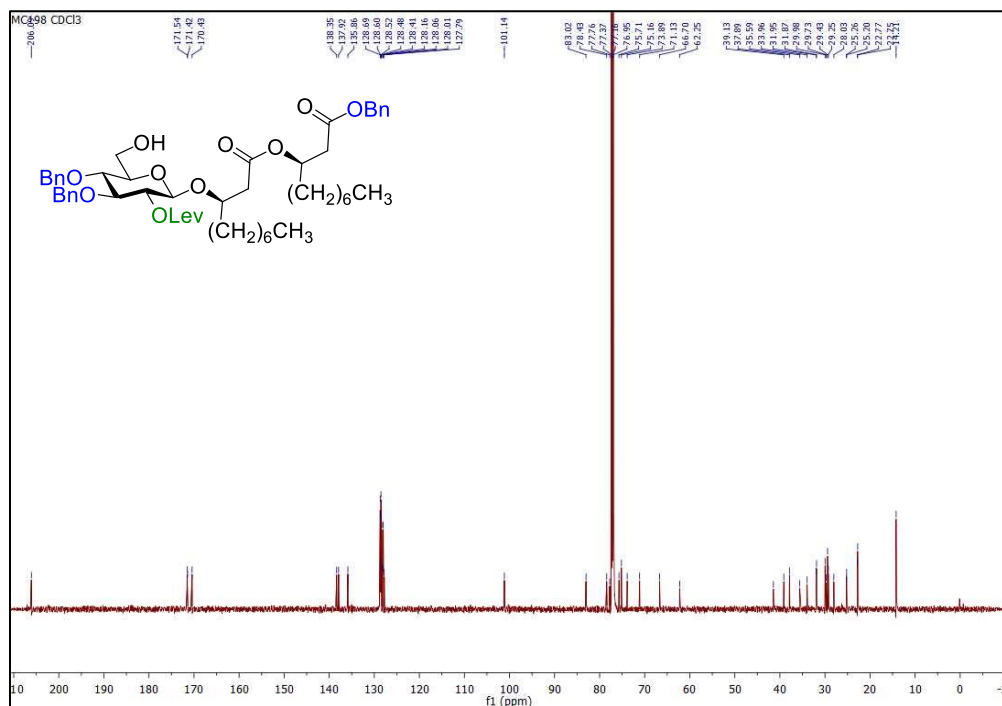


Figure S25 | ¹H NMR spectrum (CDCl₃, 600 MHz) of benzyl (R)-3-O-[(R)-(3'-O-decyl)-3,4-di-O-benzyl-β-D-glucopyranosyl]decanoate (21).

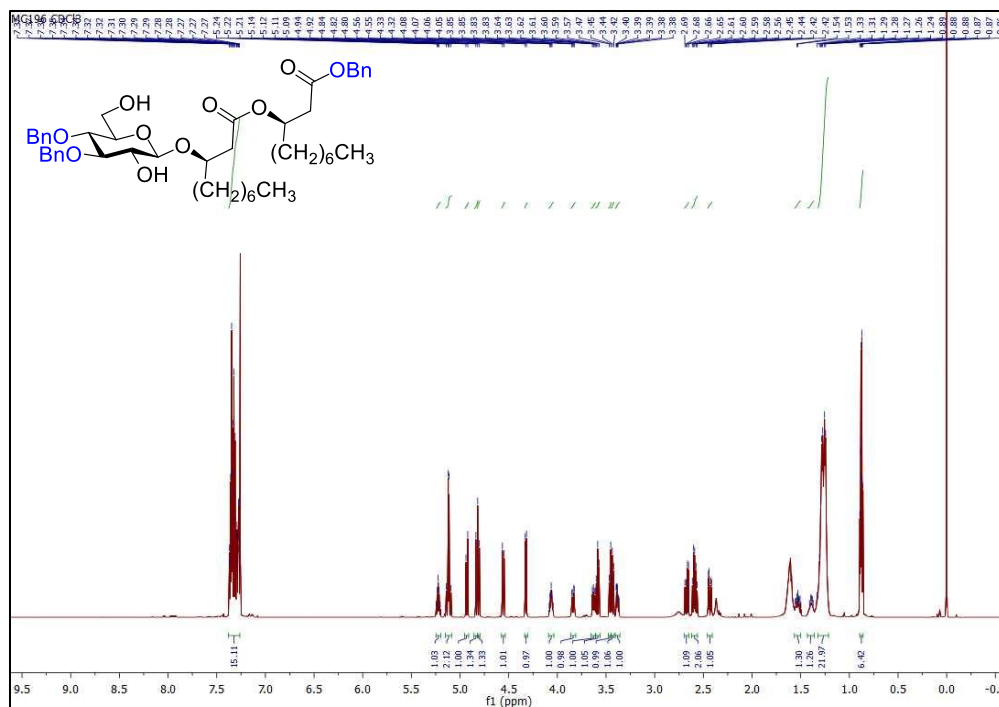


Figure S26 | ¹³C NMR spectrum (CDCl₃, 600 MHz) of benzyl (R)-3-O-[(R)-(3'-O-decyl)-3,4-di-O-benzyl-β-D-glucopyranosyl]decanoate (21).

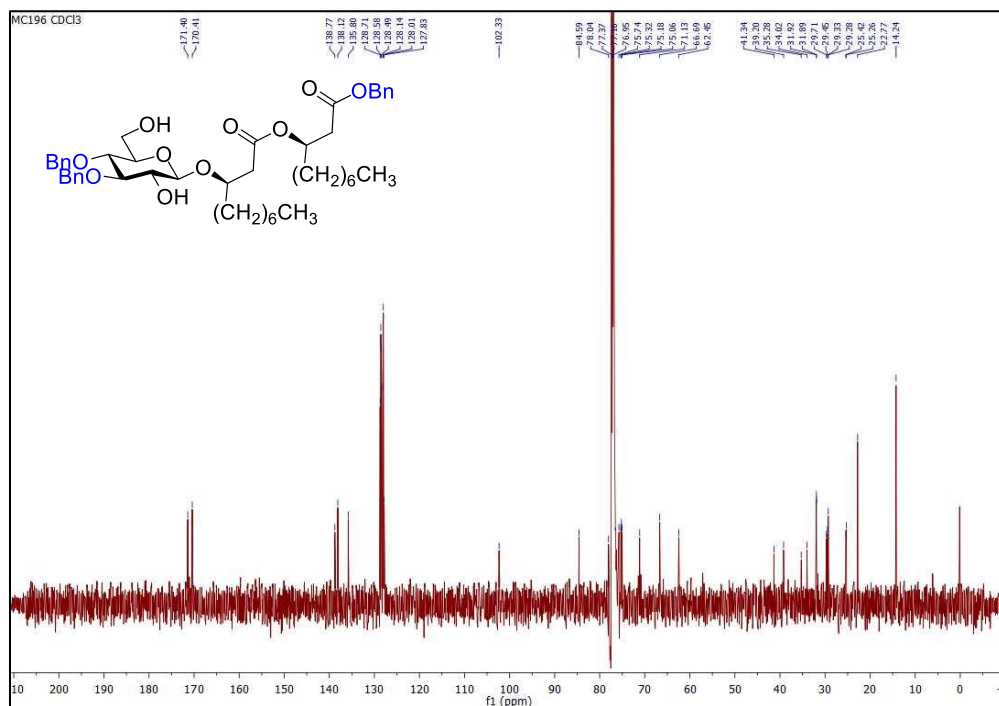


Figure S27 | ¹H NMR spectrum (pyr-d₅, 600 MHz) of synthetic ananatoside B (2).

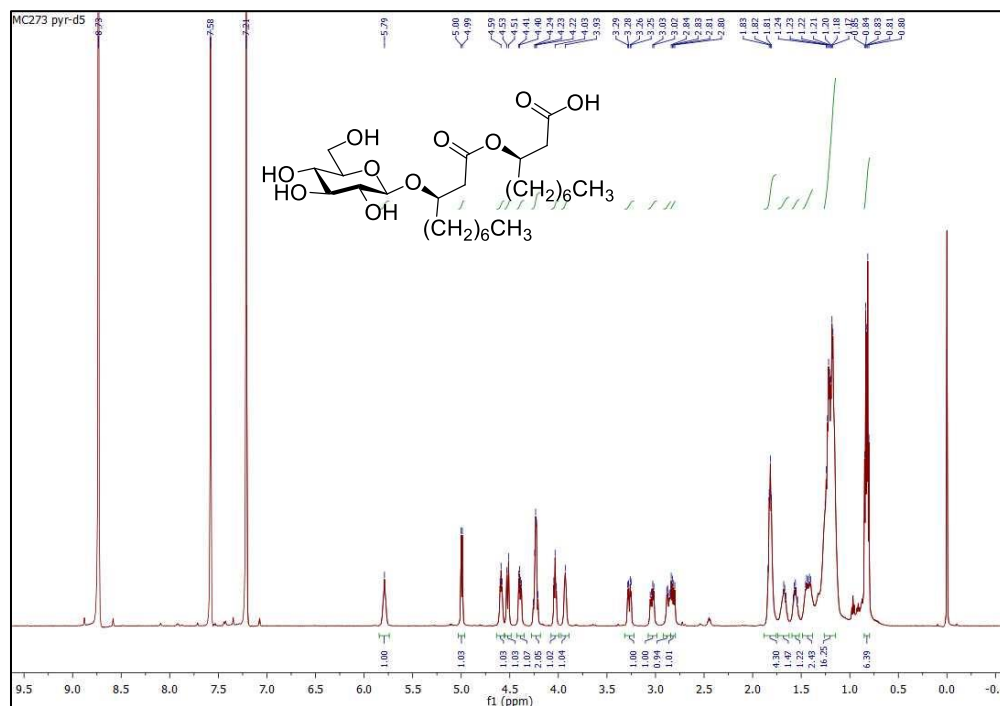


Figure S28 | ¹³C NMR spectrum (pyr-d₅, 600 MHz) of synthetic ananatoside B (2).

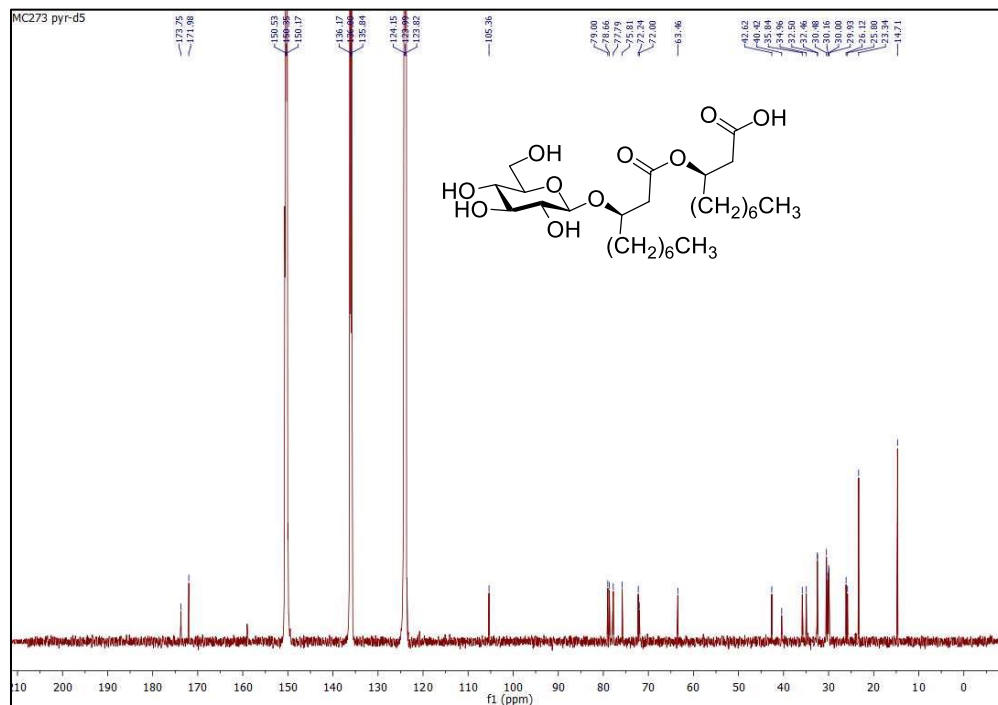


Figure S29 | ¹H NMR spectrum (pyr-d₅, 600 MHz) of natural ananatoside B (2).

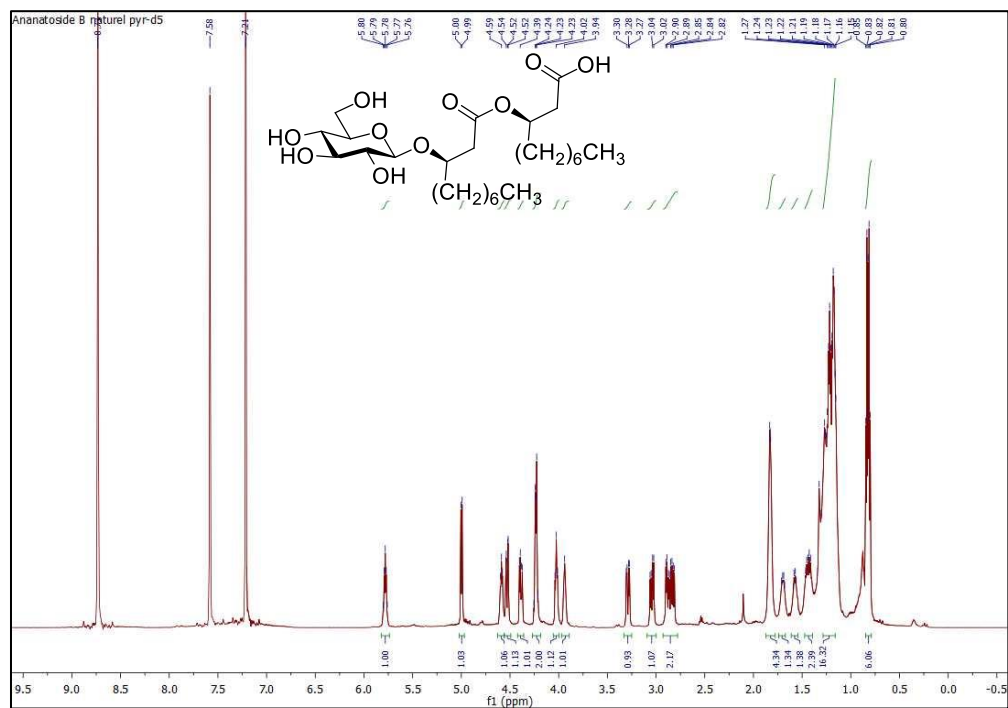


Figure S32 | ^1H NMR spectrum (CDCl_3 , 600 MHz) of *para*-methylphenyl 2-*O*-ortho-(azidomethyl)benzoyl-3,4-di-*O*-benzyl-1-thio- β -D-glucopyranoside (9).

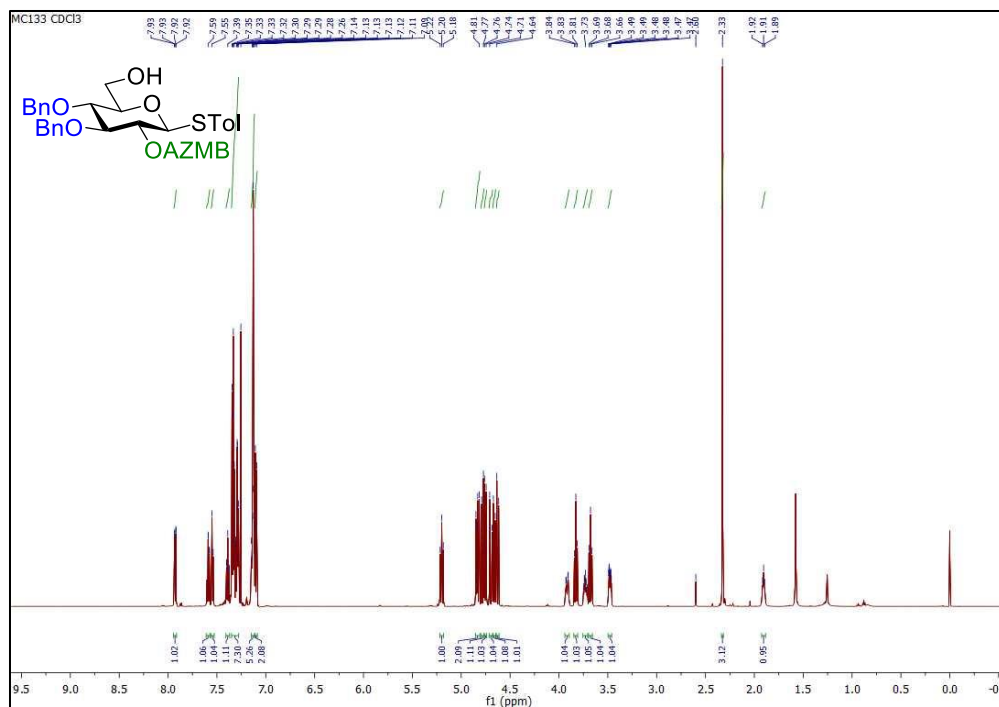


Figure S33 | ^{13}C NMR spectrum (CDCl_3 , 600 MHz) of *para*-methylphenyl 2-*O*-ortho-(azidomethyl)benzoyl-3,4-di-*O*-benzyl-1-thio- β -D-glucopyranoside (9).

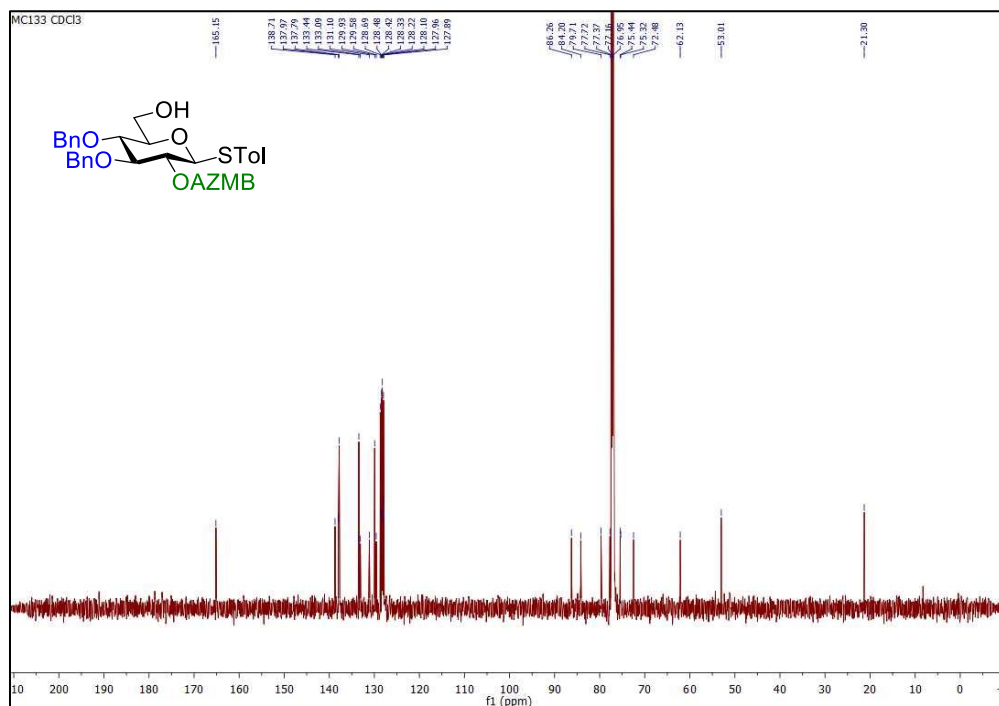


Figure S34 | ¹H NMR spectrum (CDCl₃, 600 MHz) of *para*-methylphenyl 2-*O*-*ortho*-(azidomethyl)benzoyl-3,4-di-*O*-benzyl-6-*O*-(*R*)-3-((*R*)-3-(((*tert*-butyldimethylsilyl)oxy)decanoyl)oxy)decanoyl-1-thio-β-D-glucopyranoside (7).

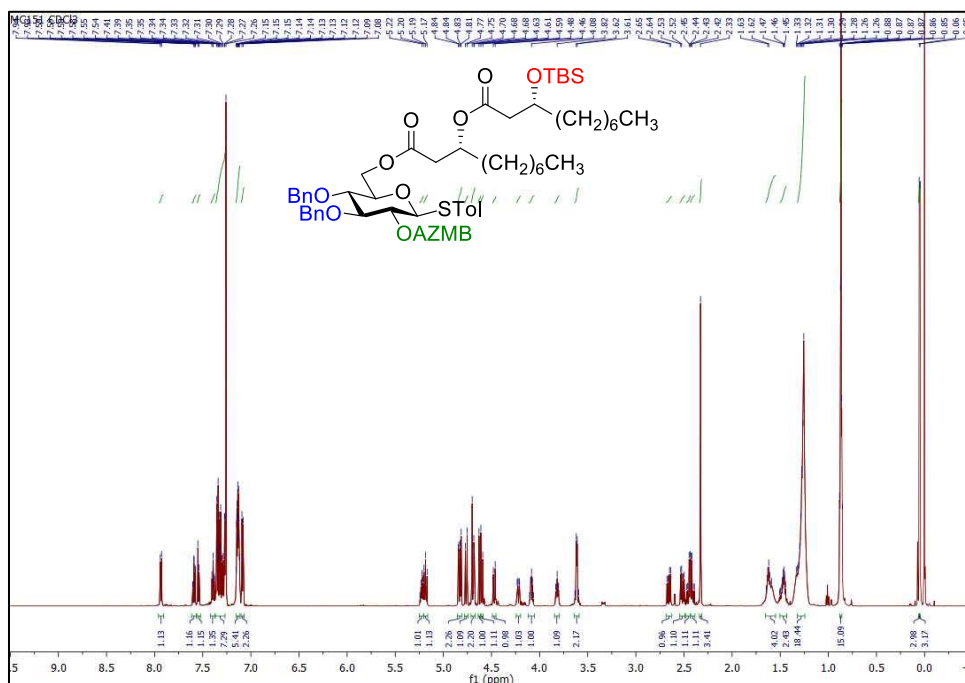


Figure S35 | ¹³C NMR spectrum (CDCl₃, 600 MHz) of *para*-methylphenyl 2-*O*-*ortho*-(azidomethyl)benzoyl-3,4-di-*O*-benzyl-6-*O*-(*R*)-3-((*R*)-3-(((*tert*-butyldimethylsilyl)oxy)decanoyl)oxy)decanoyl-1-thio-β-D-glucopyranoside (7).

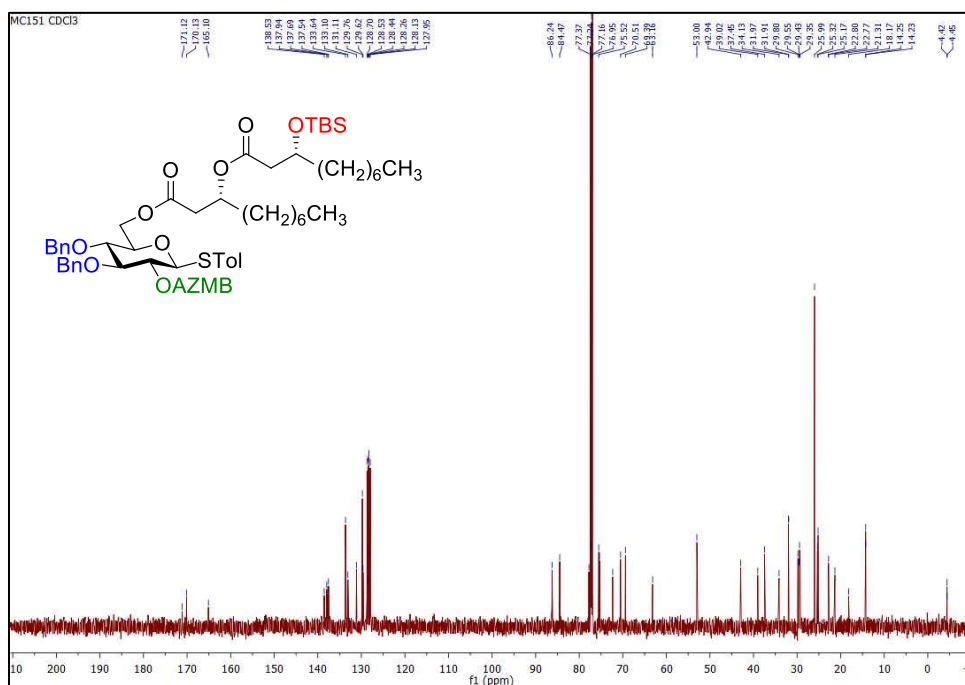


Figure S38 | ^1H NMR spectrum (CDCl_3 , 600 MHz) of macrolide 23.

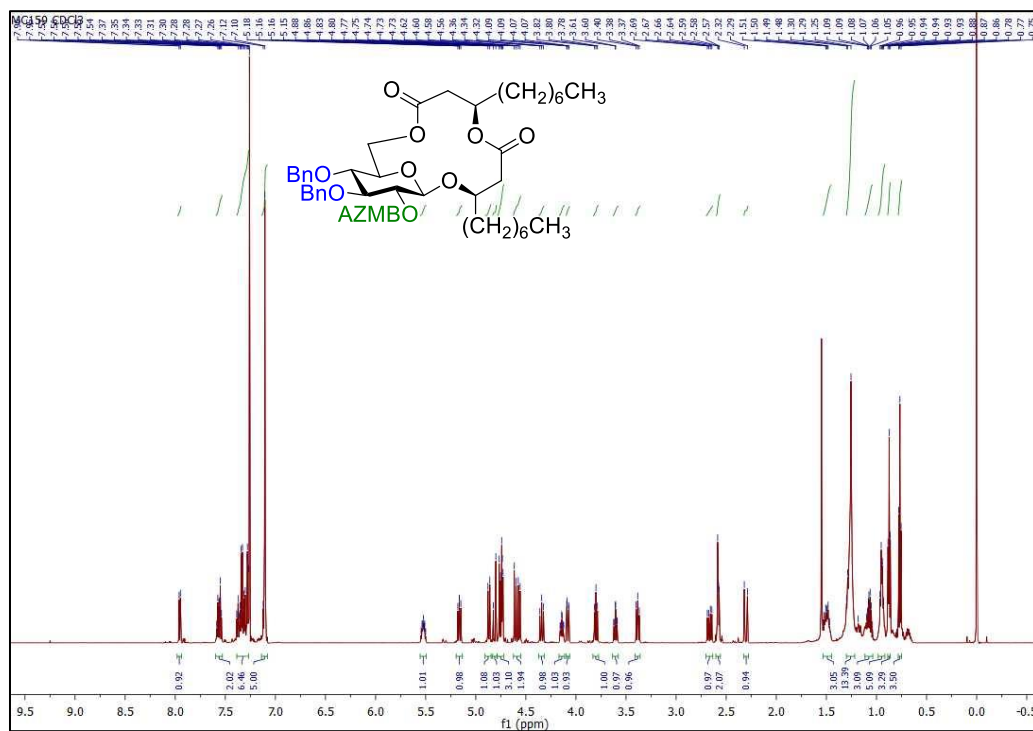


Figure S39 | ^{13}C NMR spectrum (CDCl_3 , 600 MHz) of macrolide 23.

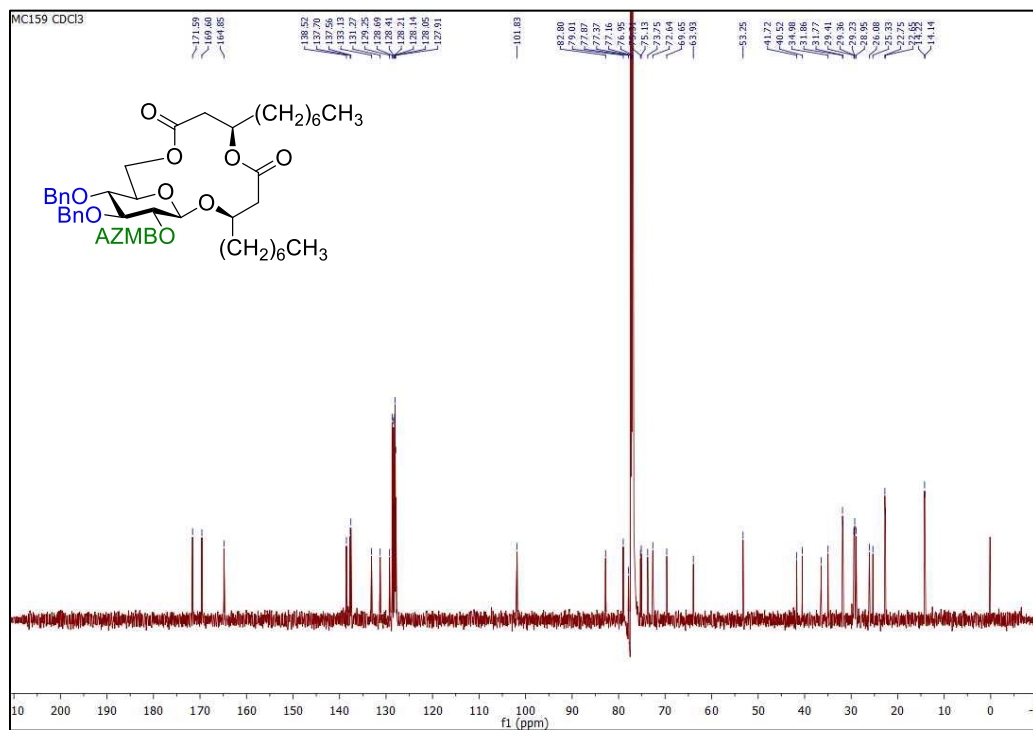


Figure S40 | ^1H NMR spectrum (CDCl_3 , 600 MHz) of (*R*)-3-*O*-[(*R*)-(3'-*O*-decyl)-3,4-di-*O*-benzyl-2-*O*-levulinoyl- β -D-glucopyranosyl] decanoic acid (**25**).

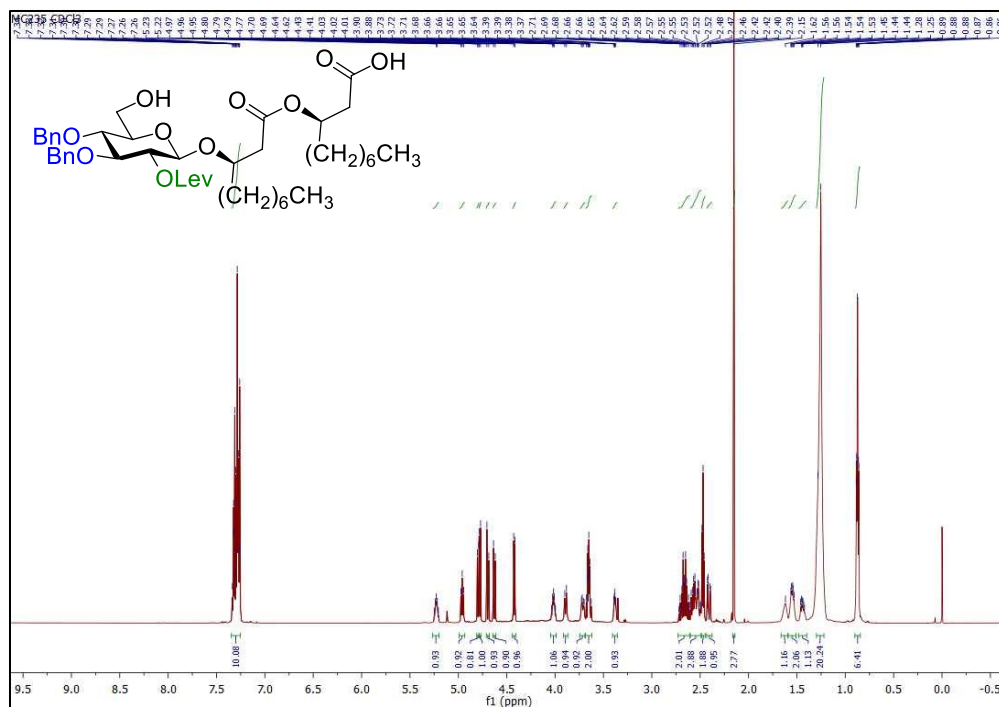


Figure S41 | ^{13}C NMR spectrum (CDCl_3 , 600 MHz) of (*R*)-3-*O*-[(*R*)-(3'-*O*-decyl)-3,4-di-*O*-benzyl-2-*O*-levulinoyl- β -D-glucopyranosyl] decanoic acid (**25**).

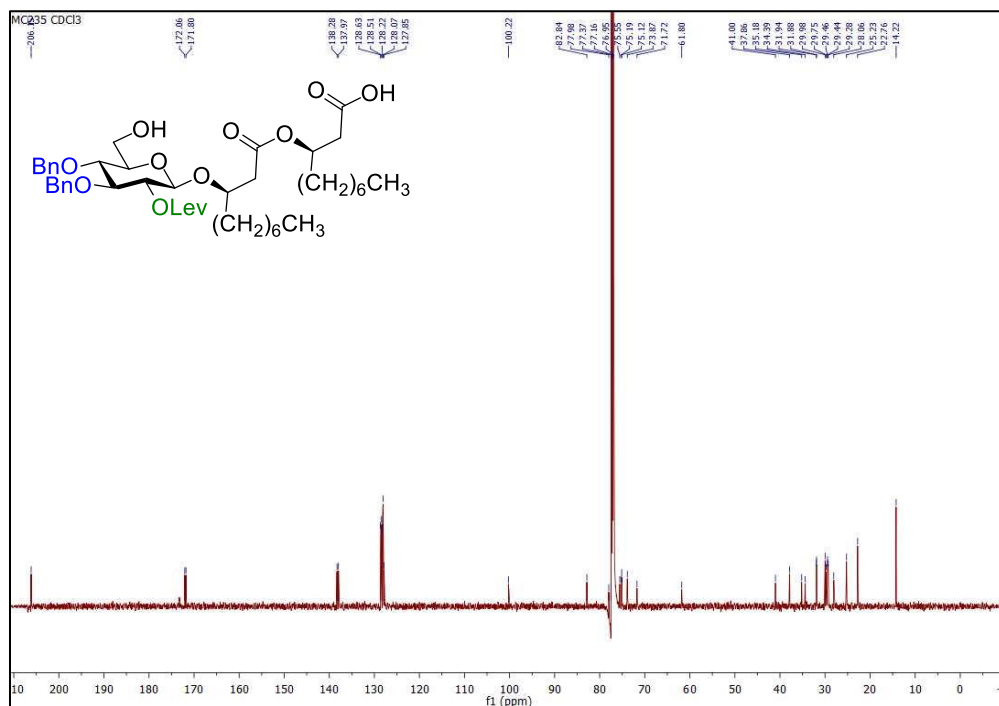


Figure S42 | ^1H NMR spectrum (CDCl_3 , 600 MHz) of macrolide 26.

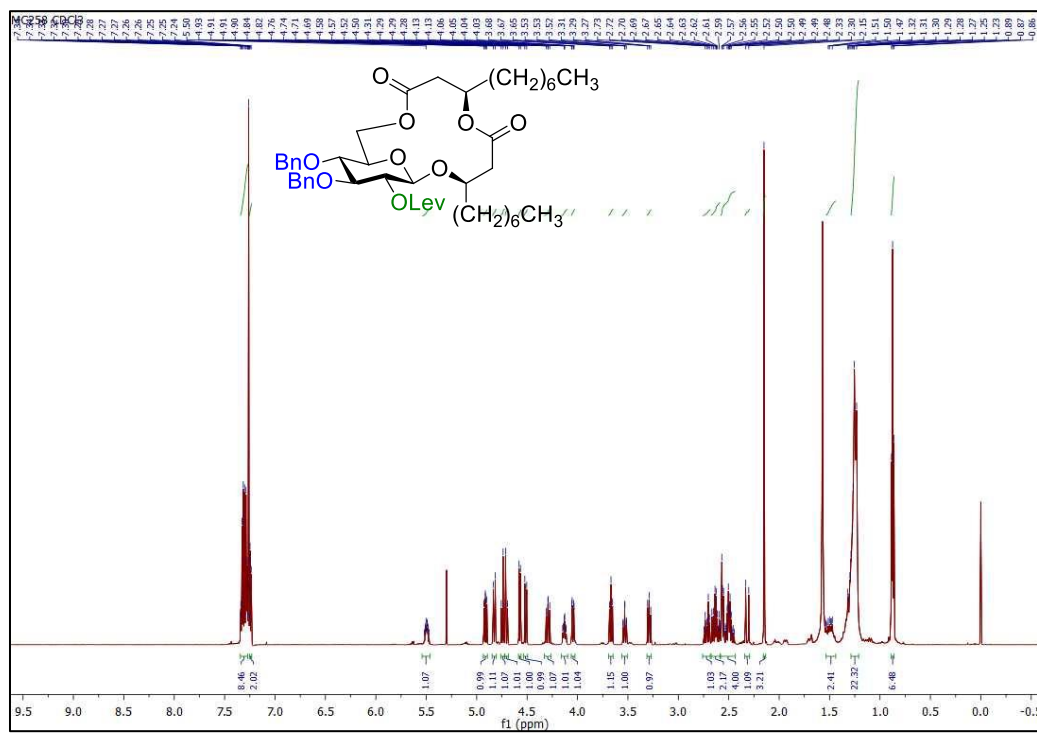


Figure S43 | ^{13}C NMR spectrum (CDCl_3 , 600 MHz) of macrolide 26.

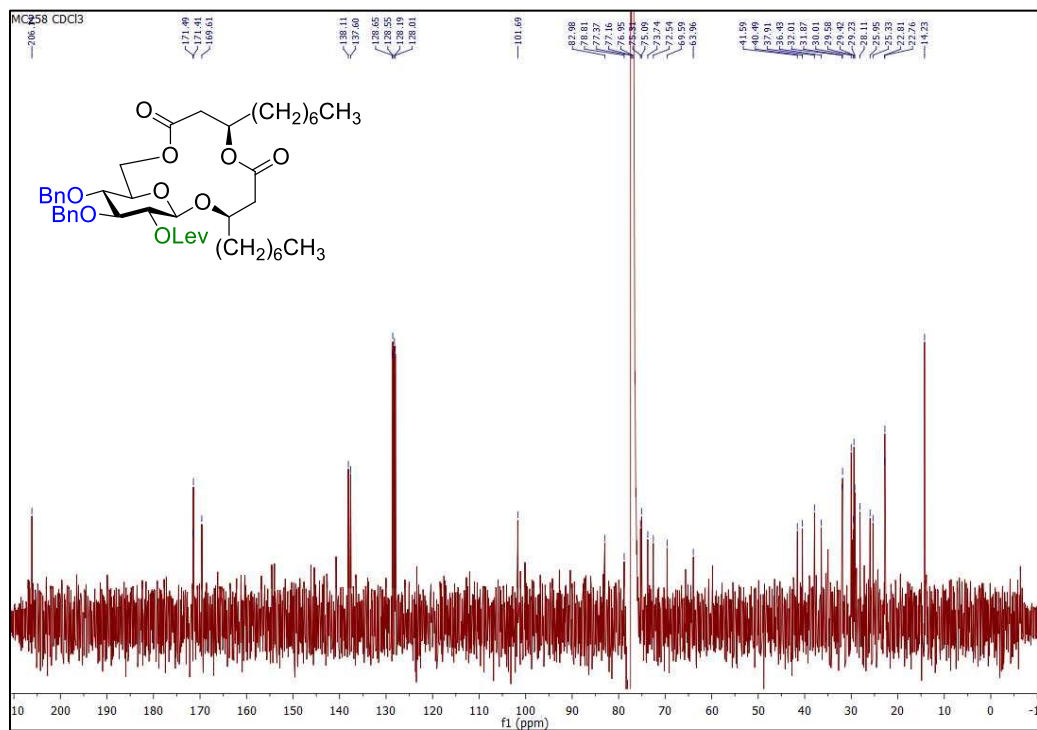


Figure S44 | ^1H NMR spectrum (CDCl_3 , 600 MHz) of macrolide 24.

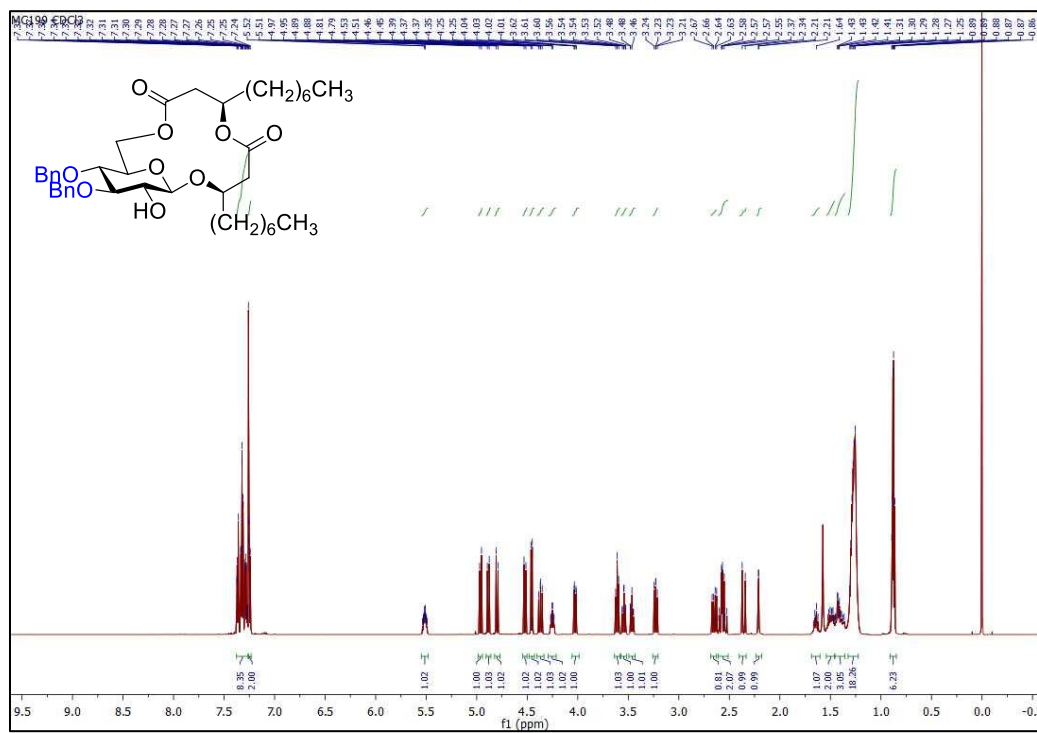


Figure S45 | ^{13}C NMR spectrum (CDCl_3 , 600 MHz) of macrolide 24.

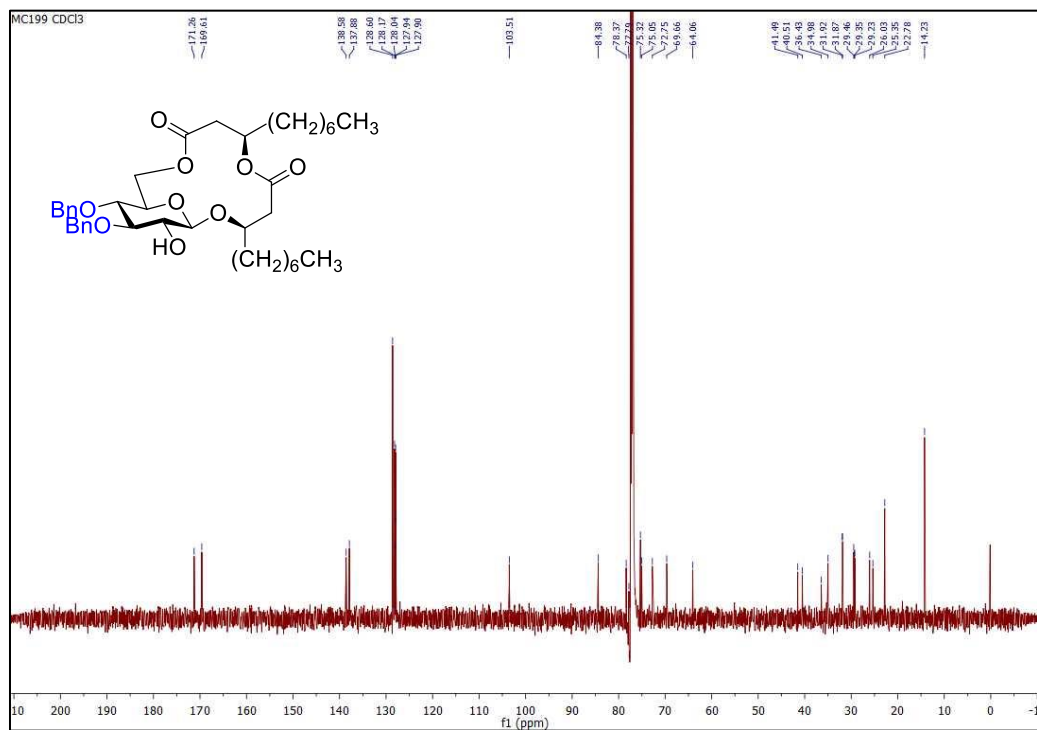


Figure S46 | ^1H NMR spectrum (pyr- d_5 , 600 MHz) of anatoside A (1).

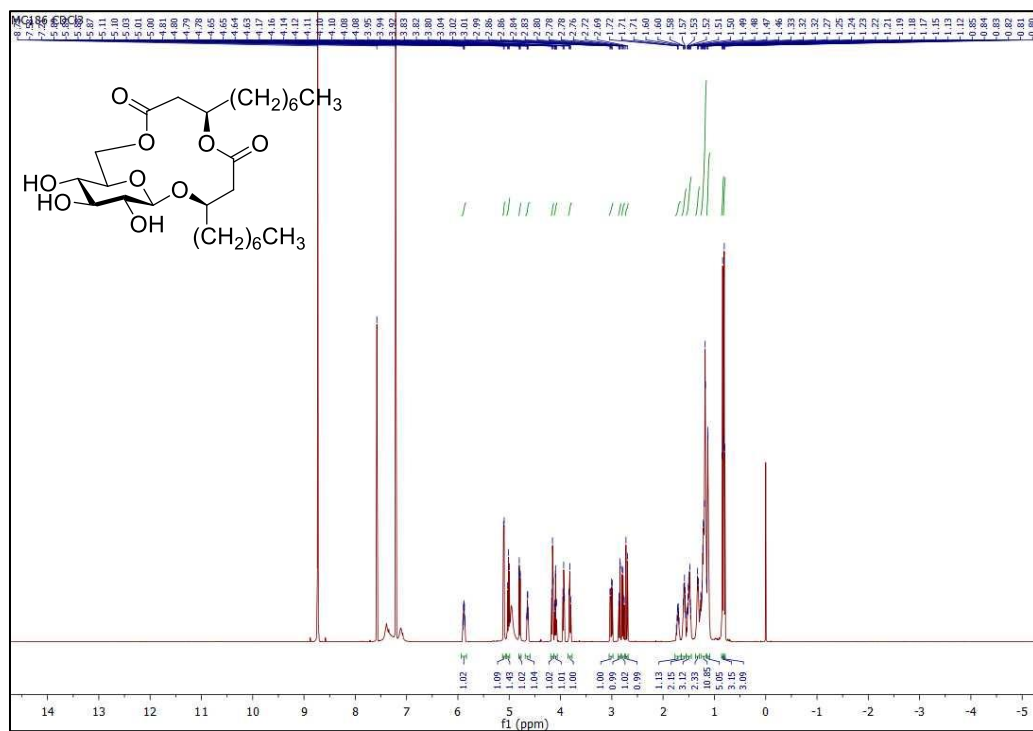


Figure S47 | ^1H NMR spectrum (CDCl_3 , 600 MHz) of *para*-methylphenyl 4-*O*-levulinoyl-3-*O*-*para*-methoxybenzyl-1-thio- α -L-rhamnopyranoside (32).

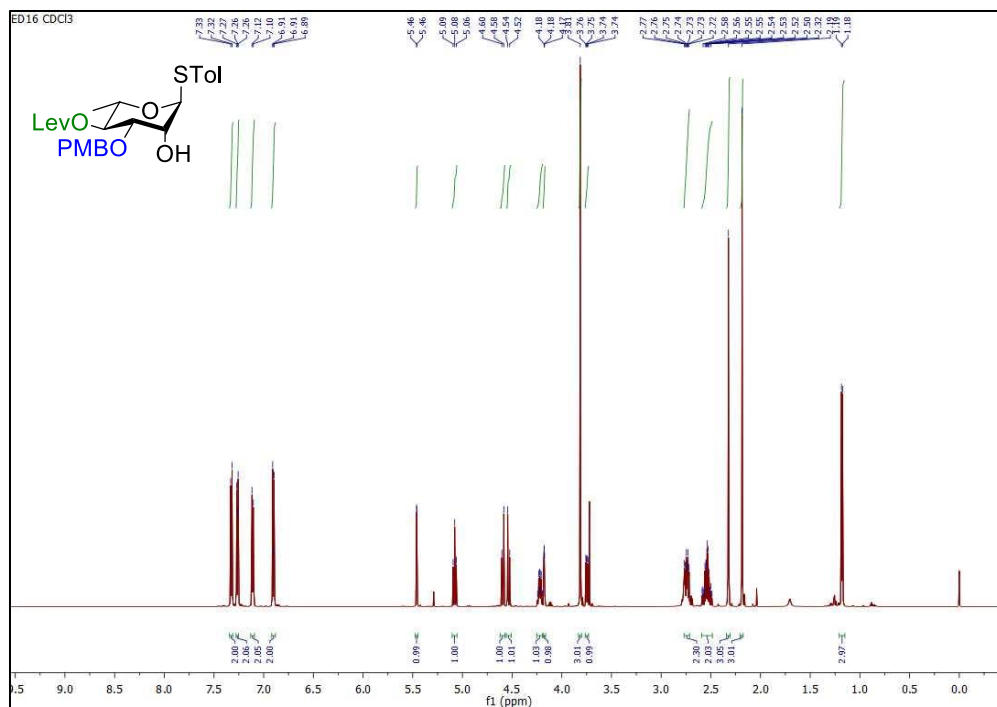


Figure S48 | ^{13}C NMR spectrum (CDCl_3 , 600 MHz) of *para*-methylphenyl 4-*O*-levulinoyl-3-*O*-*para*-methoxybenzyl-1-thio- α -L-rhamnopyranoside (32).

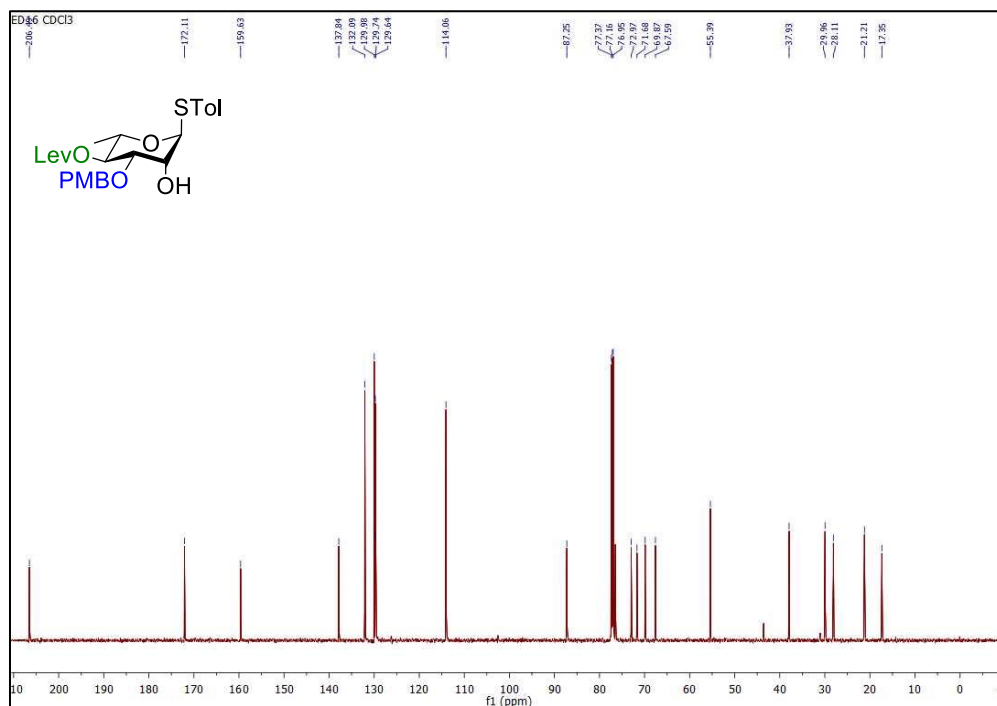


Figure S49 | ^1H NMR spectrum (CDCl_3 , 600 MHz) of *para*-methylphenyl 2-*O*-*ortho*-(azidomethyl)benzoyl-4-*O*-levulinoyl-3-*O*-*para*-methoxybenzyl-1-thio- α -L-rhamnopyranoside (33).

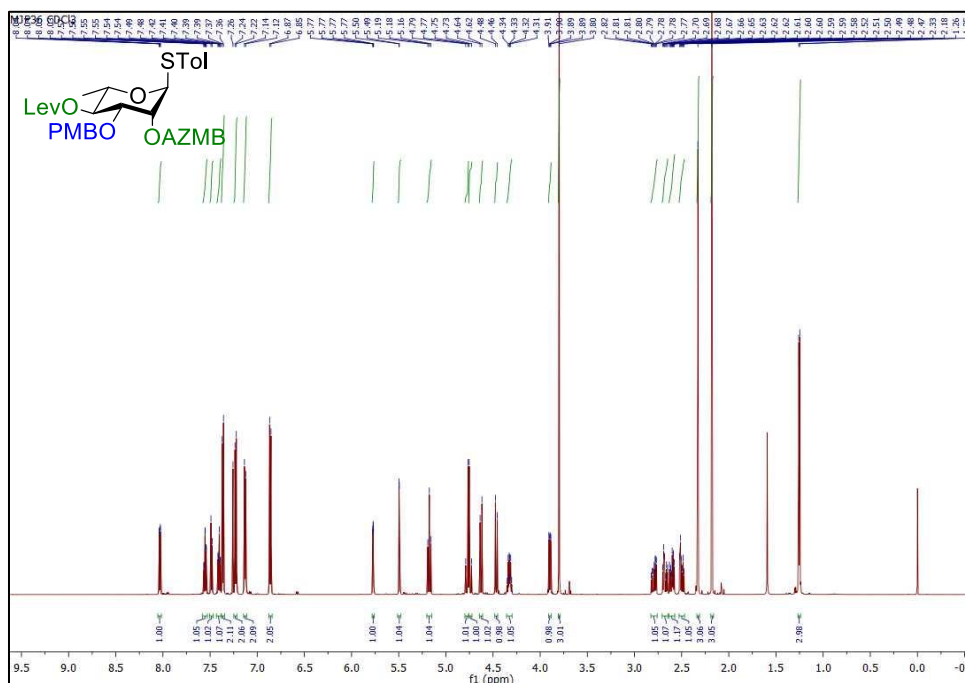


Figure S50 | ^{13}C NMR spectrum (CDCl_3 , 600 MHz) of *para*-methylphenyl 2-*O*-*ortho*-(azidomethyl)benzoyl-4-*O*-levulinoyl-3-*O*-*para*-methoxybenzyl-1-thio- α -L-rhamnopyranoside (33).

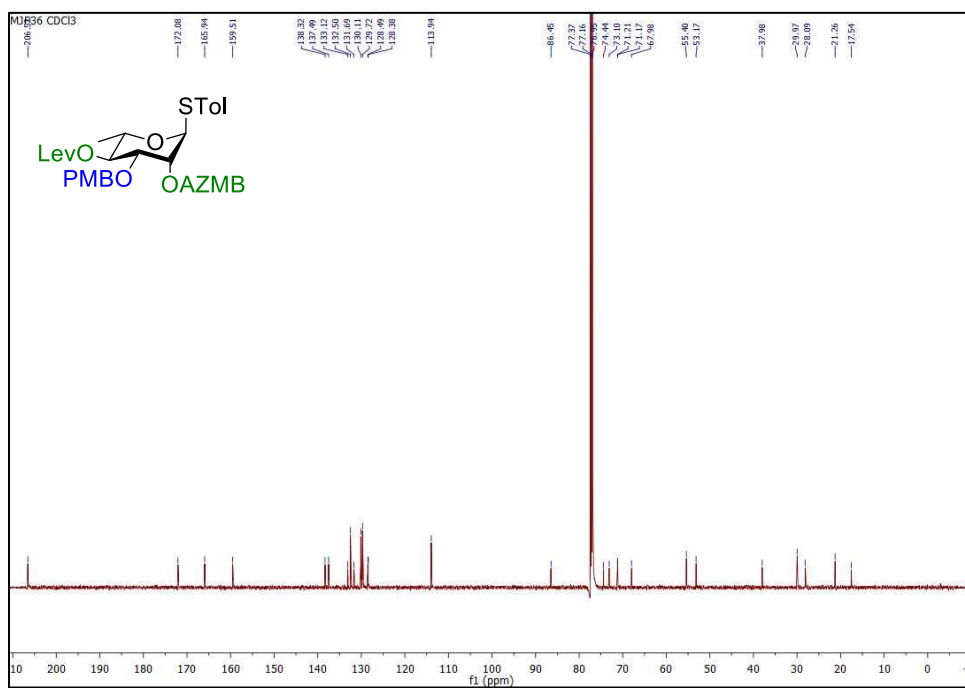


Figure S51 | ^1H NMR spectrum (CDCl_3 , 600 MHz) of benzyl (*R*)-3-*O*-[(*R*)-(3'-*O*-decyl)-2-*O*-*ortho*-(azidomethyl)benzoyl-4-*O*-levulinoyl-3-*O*-*para*-methoxybenzyl- α -L-rhamnopyranosyl]decanoate (27).

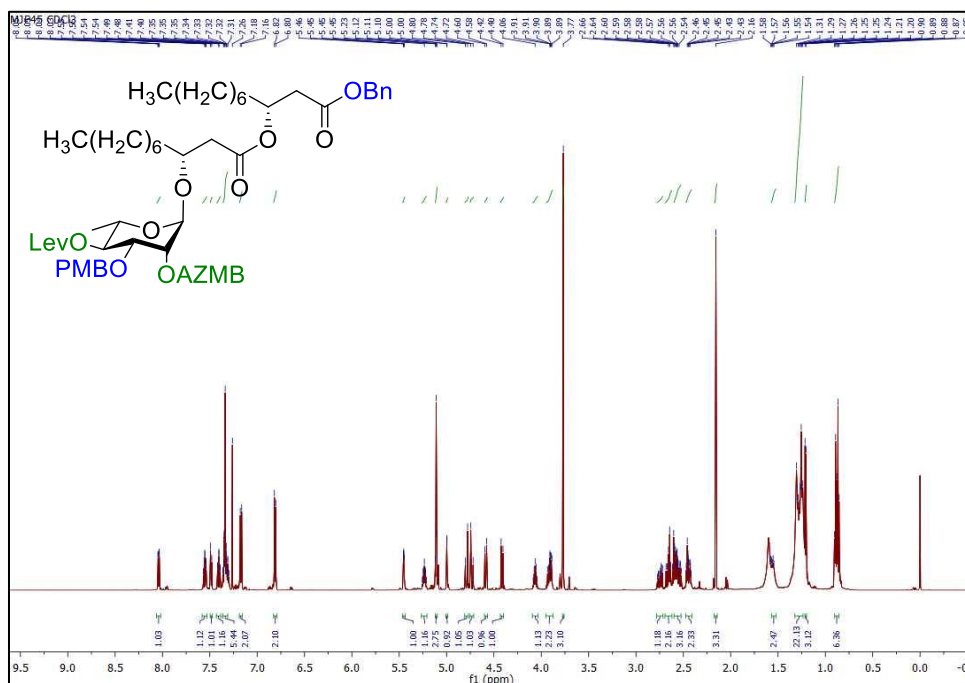


Figure S52 | ^{13}C NMR spectrum (CDCl_3 , 600 MHz) of benzyl (*R*)-3-*O*-[(*R*)-(3'-*O*-decyl)-2-*O*-*ortho*-(azidomethyl)benzoyl-4-*O*-levulinoyl-3-*O*-*para*-methoxybenzyl- α -L-rhamnopyranosyl]decanoate (27).

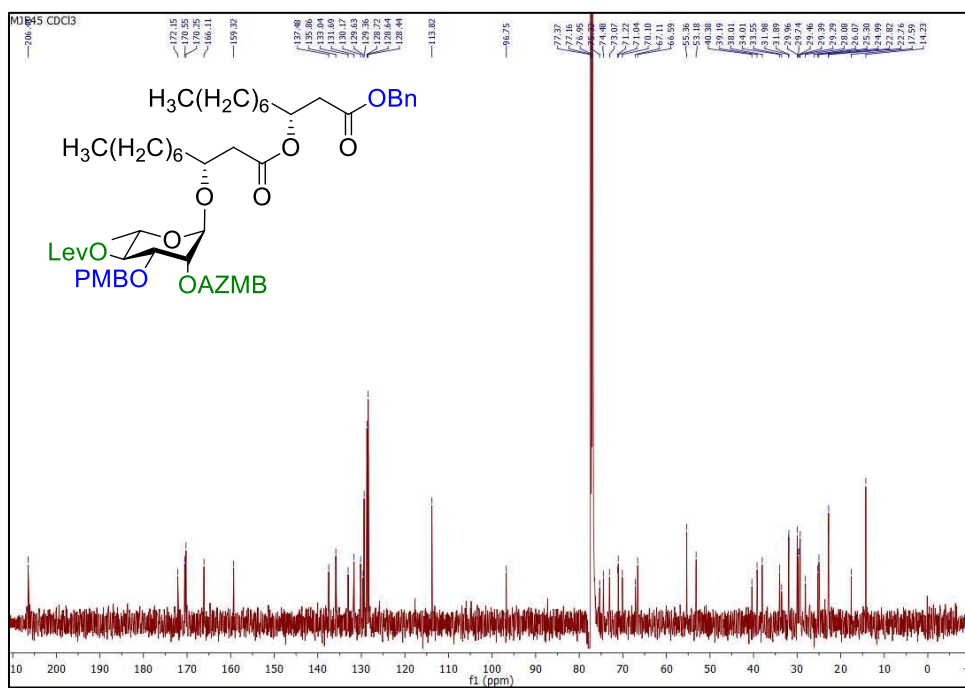


Figure S53 | ^1H NMR spectrum (CDCl_3 , 600 MHz) of benzyl (*R*)-3-*O*-[(*R*)-(3'-*O*-decyl)-4-*O*-levulinoyl-3-*O*-*para*-methoxybenzyl- α -L-rhamnopyranosyl]decanoate (34).

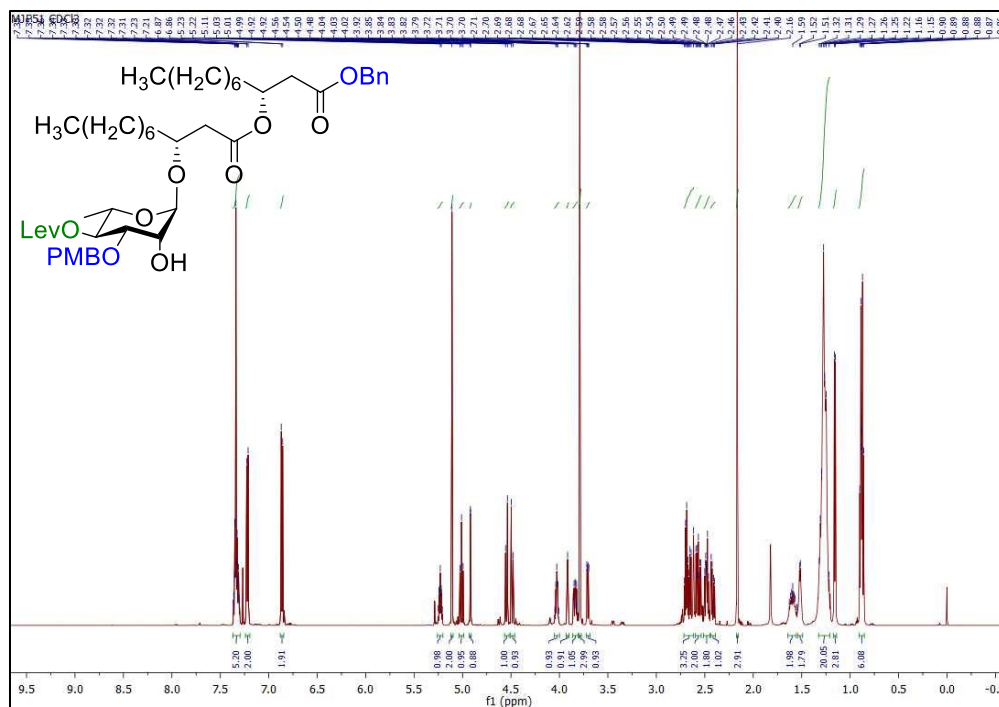


Figure S54 | ^{13}C NMR spectrum (CDCl_3 , 600 MHz) of benzyl (*R*)-3-*O*-[(*R*)-(3'-*O*-decyl)-4-*O*-levulinoyl-3-*O*-*para*-methoxybenzyl- α -L-rhamnopyranosyl]decanoate (34).

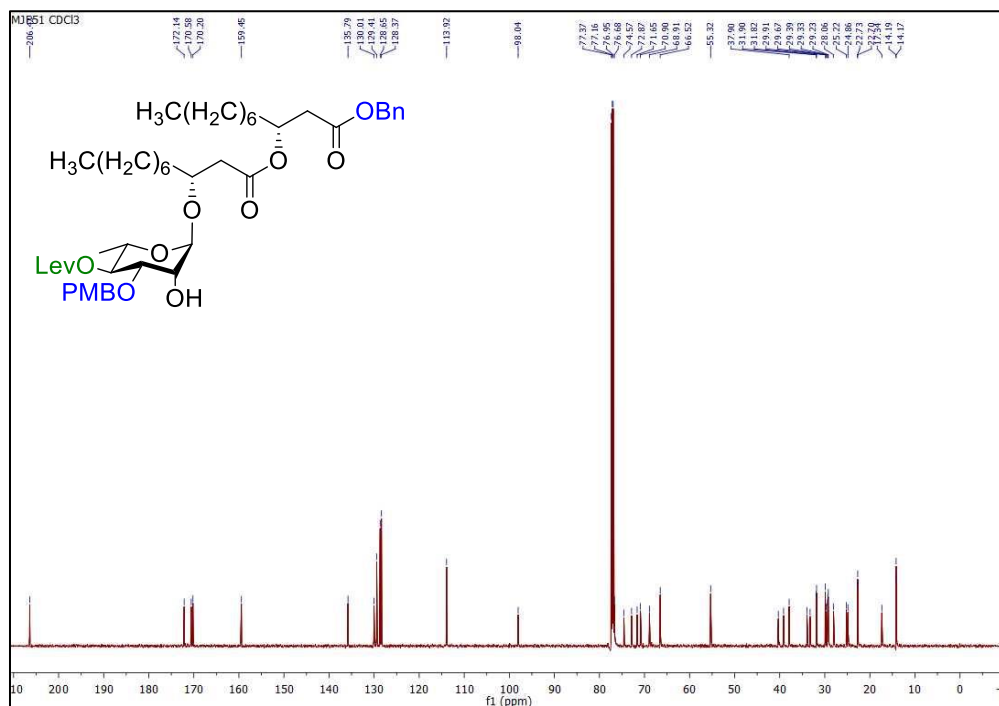


Figure S55 | ¹H NMR spectrum (CDCl₃, 600 MHz) of benzyl (R)-3-O-[(R)-(3'-O-decyl)-3-O-para-methoxybenzyl-α-L-rhamnopyranosyl]decanoate (35).

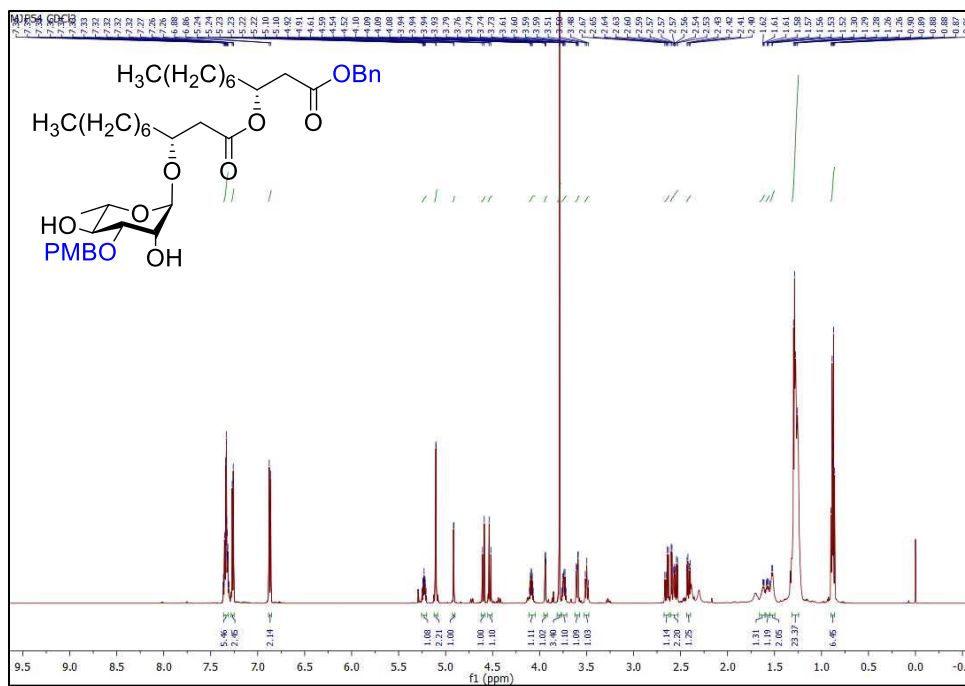


Figure S56 | ¹³C NMR spectrum (CDCl₃, 600 MHz) of benzyl (R)-3-O-[(R)-(3'-O-decyl)-3-O-para-methoxybenzyl-α-L-rhamnopyranosyl]decanoate (35).

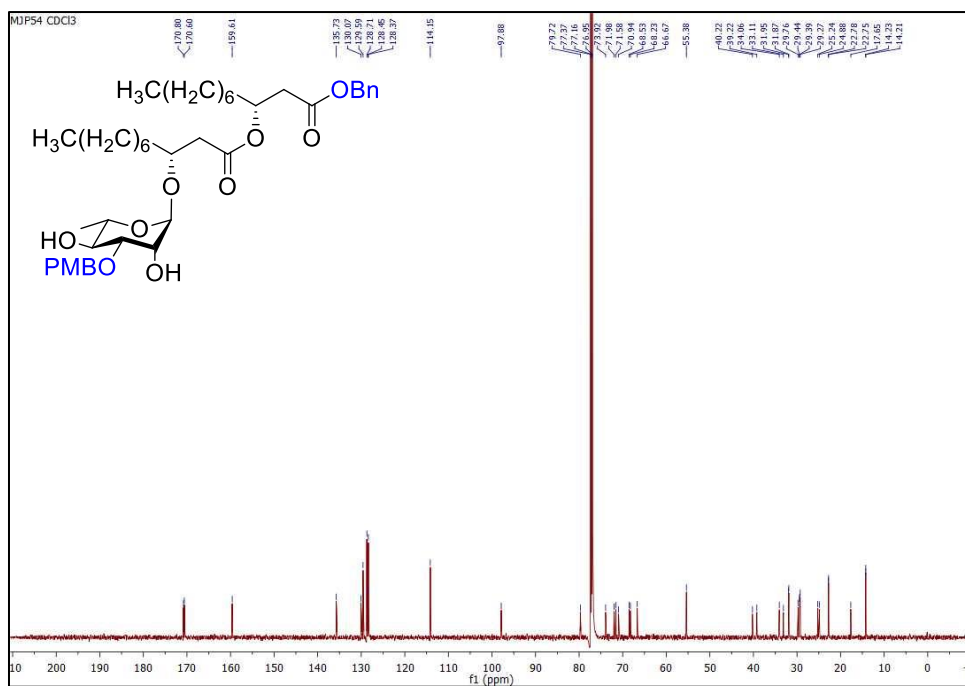


Figure S57 | ¹H NMR spectrum (CDCl₃/CD₃OD, 600 MHz) of (R)-3-O-[(R)-(3'-O-decyl)-α-L-rhamnopyranosyl]decanoic acid (3).

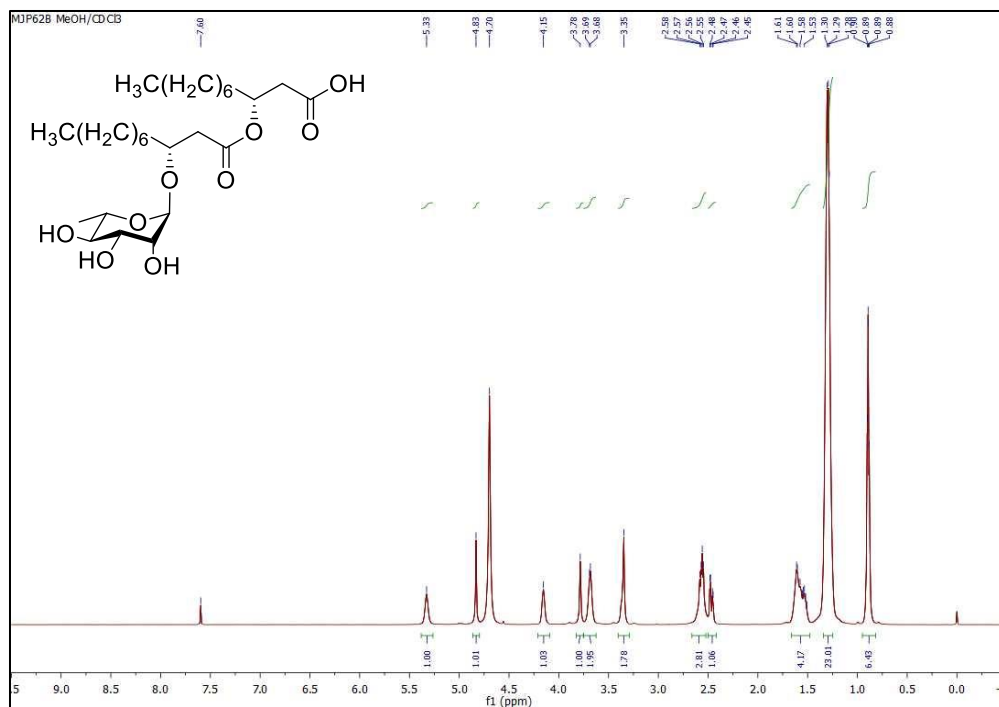


Figure S58 | ^1H NMR spectrum (CDCl_3 , 600 MHz) of *para*-methylphenyl 2-*O*-*ortho*-(azidomethyl)benzoyl-3,4-*O*-(2,3-dimethoxybutan-2,3-diyl)-1-thio- α -L-rhamnopyranoside (S7).

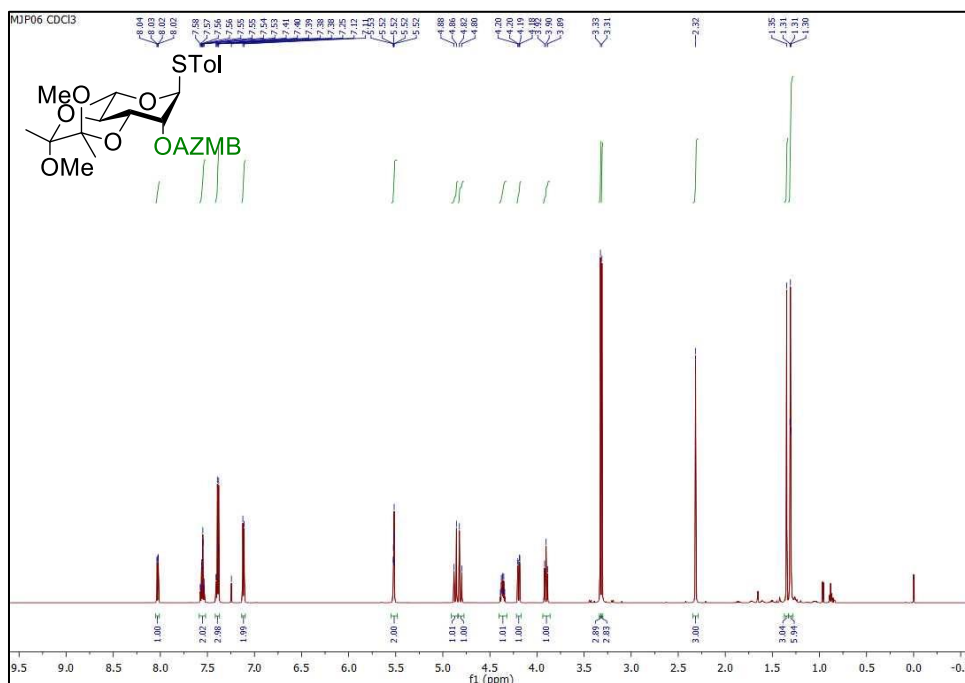


Figure S59 | ^{13}C NMR spectrum (CDCl_3 , 600 MHz) of *para*-methylphenyl 2-*O*-*ortho*-(azidomethyl)benzoyl-3,4-*O*-(2,3-dimethoxybutan-2,3-diyl)-1-thio- α -L-rhamnopyranoside (S7).

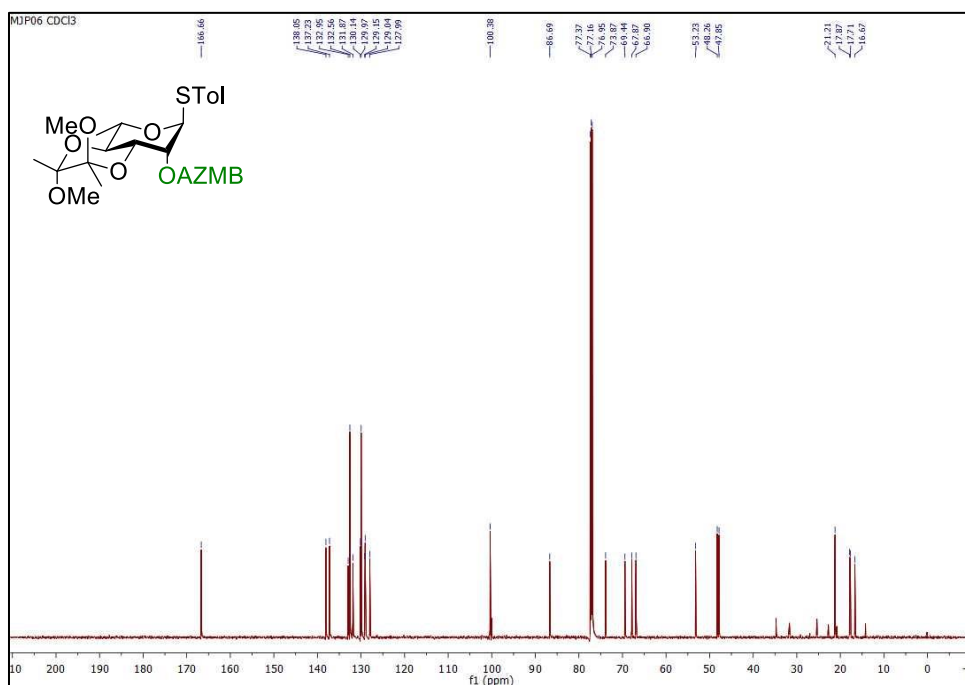


Figure S60 | ^1H NMR spectrum (CDCl_3 , 600 MHz) of benzyl (*R*)-3-*O*-[(*R*)-(3'-*O*-decyl)-2-*O*-*ortho*-(azidomethyl)benzoyl-[3,4-*O*-(2,3-dimethoxybutan-2,3-diyl)]- α -L-rhamnopyranosyl]decanoate (S8).

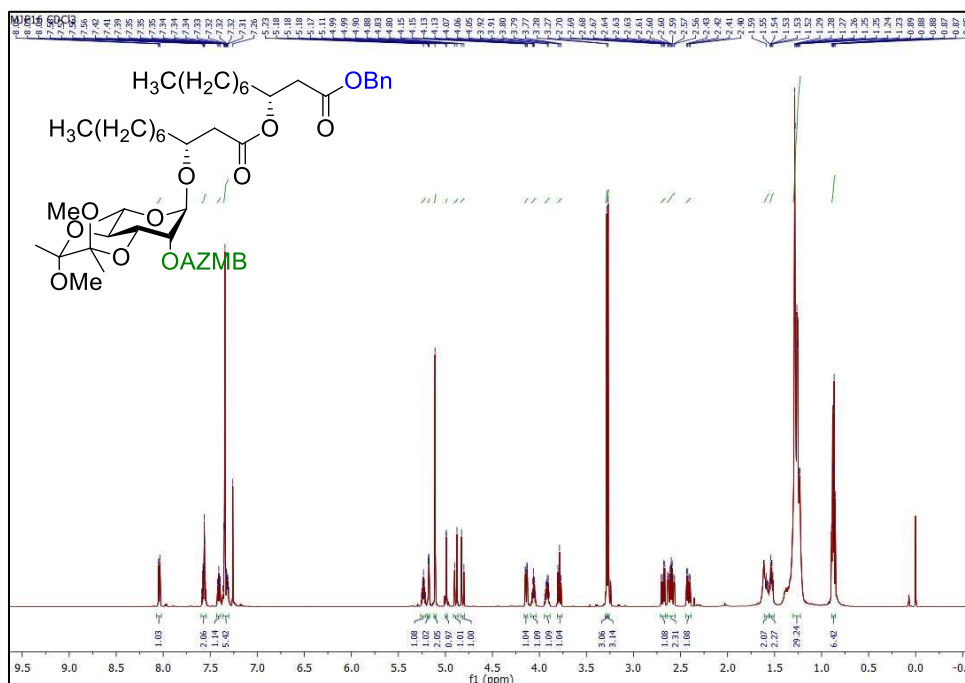


Figure S61 | ^{13}C NMR spectrum (CDCl_3 , 600 MHz) of benzyl (*R*)-3-*O*-[(*R*)-(3'-*O*-decyl)-2-*O*-*ortho*-(azidomethyl)benzoyl-[3,4-*O*-(2,3-dimethoxybutan-2,3-diyl)]- α -L-rhamnopyranosyl]decanoate (S8).

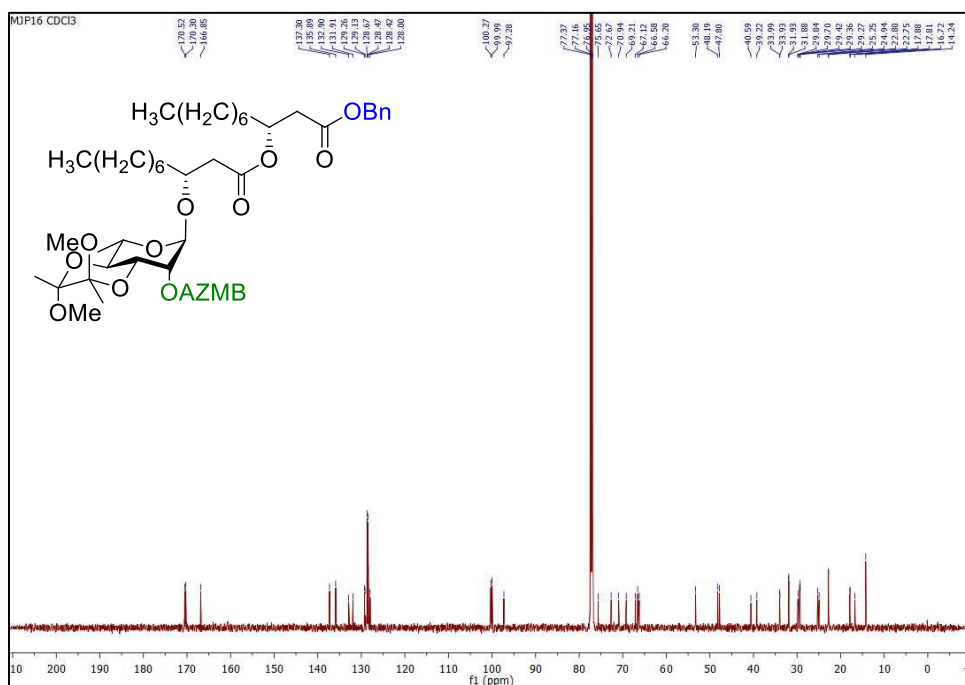


Figure S62 | ^1H NMR spectrum (CDCl_3 , 600 MHz) of benzyl (*R*)-3-*O*-[(*R*)-(3'-*O*-decyl)- α -L-rhamnopyranosyl]decanoate (S9).

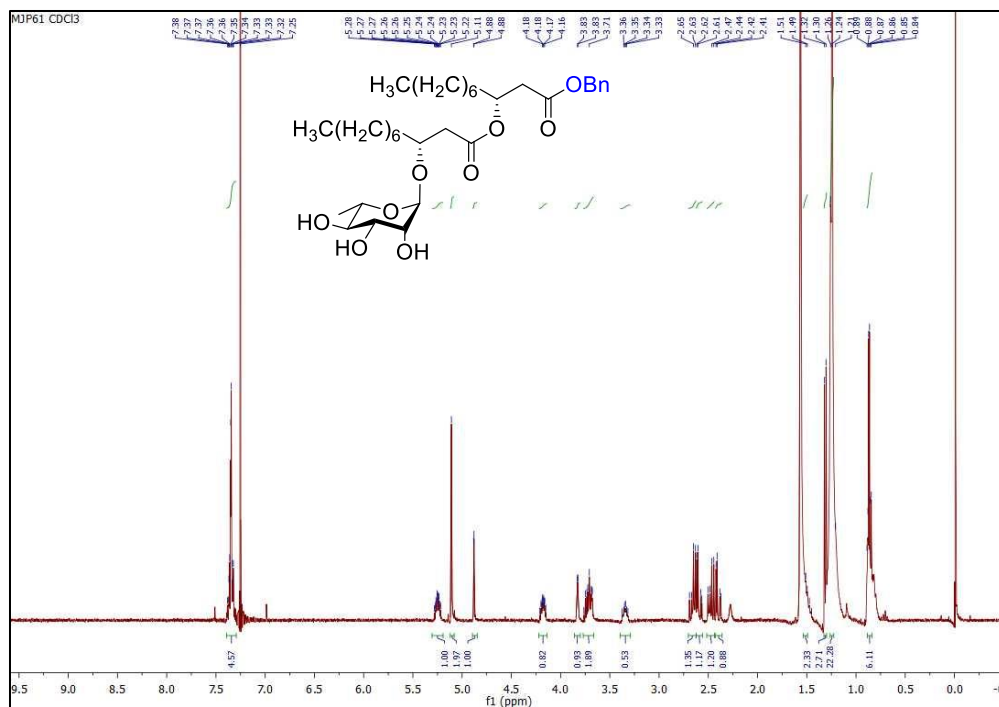


Figure S63 | ^{13}C NMR spectrum (CDCl_3 , 600 MHz) of benzyl (*R*)-3-*O*-[(*R*)-(3'-*O*-decyl)- α -L-rhamnopyranosyl]decanoate (S9)

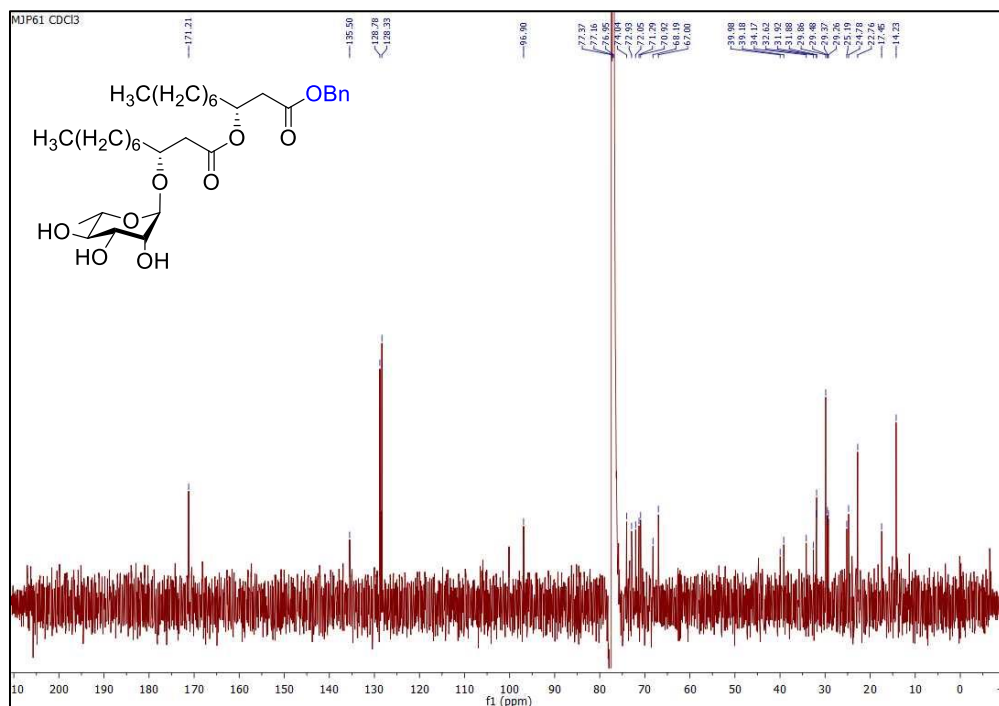


Figure S64 | ^1H NMR spectrum (CDCl_3 , 600 MHz) of *para*-methylphenyl 3-*O*-benzyl-4-*O*-levulinoyl-1-thio- α -L-rhamnopyranoside (36).

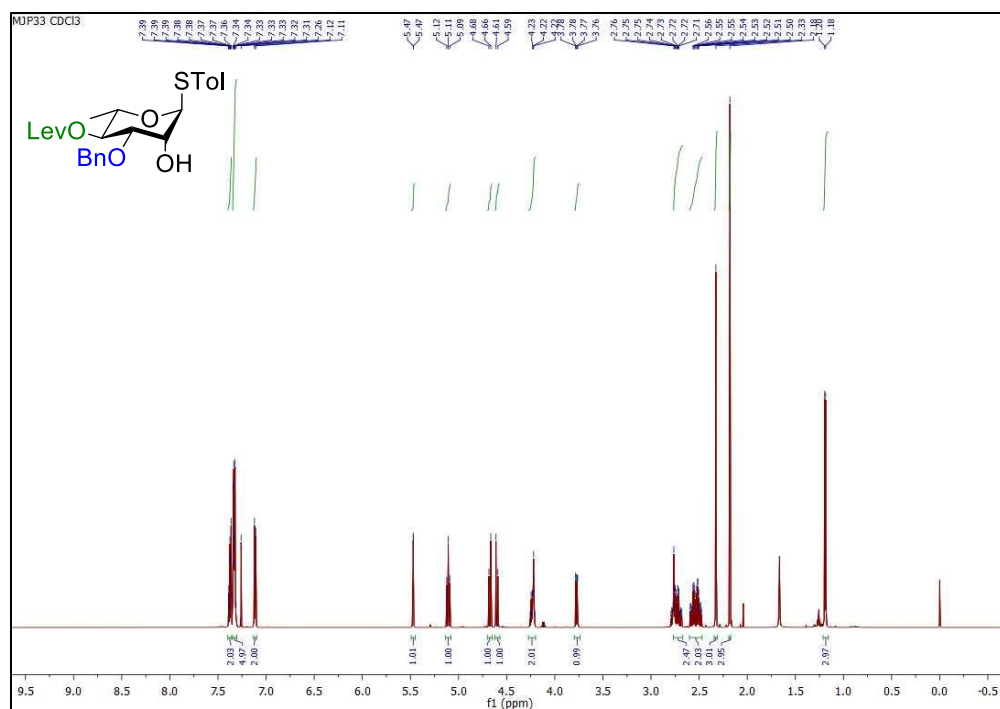


Figure S65 | ^{13}C NMR spectrum (CDCl_3 , 600 MHz) of *para*-methylphenyl 3-*O*-benzyl-4-*O*-levulinoyl-1-thio- α -L-rhamnopyranoside (36).

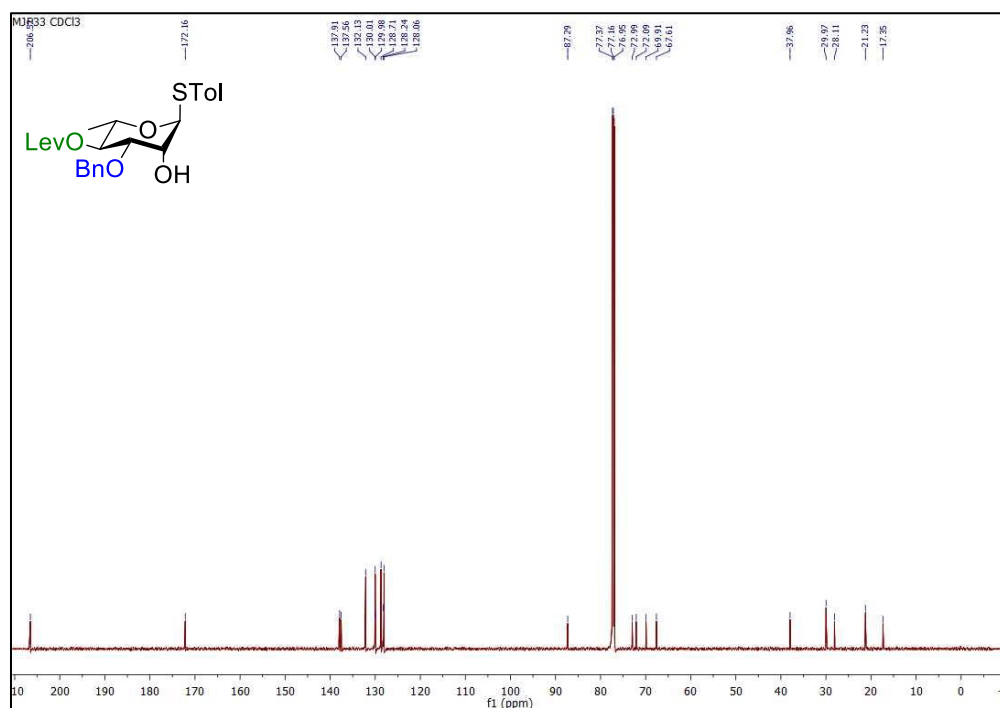


Figure S66 | ^1H NMR spectrum (CDCl_3 , 600 MHz) of *para*-methylphenyl 2-*O*-*ortho*-(azidomethyl)benzoyl-3-*O*-benzyl-4-*O*-levulinoyl-1-thio- α -L-rhamnopyranoside (37).

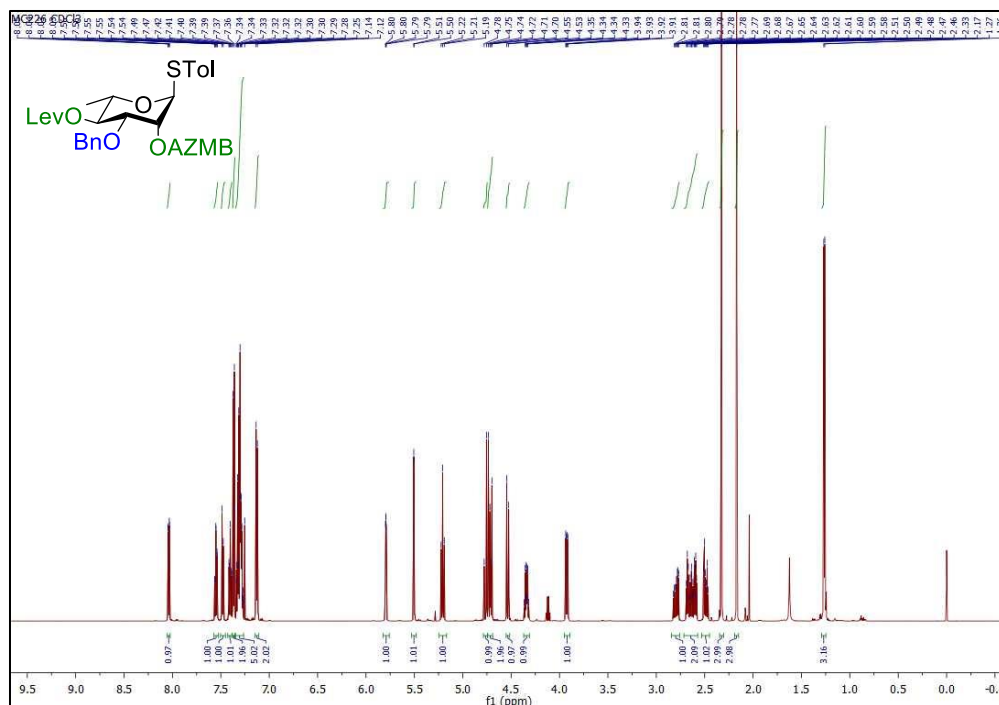


Figure S67 | ^{13}C NMR spectrum (CDCl_3 , 600 MHz) of *para*-methylphenyl 2-*O*-*ortho*-(azidomethyl)benzoyl-3-*O*-benzyl-4-*O*-levulinoyl-1-thio- α -L-rhamnopyranoside (37).

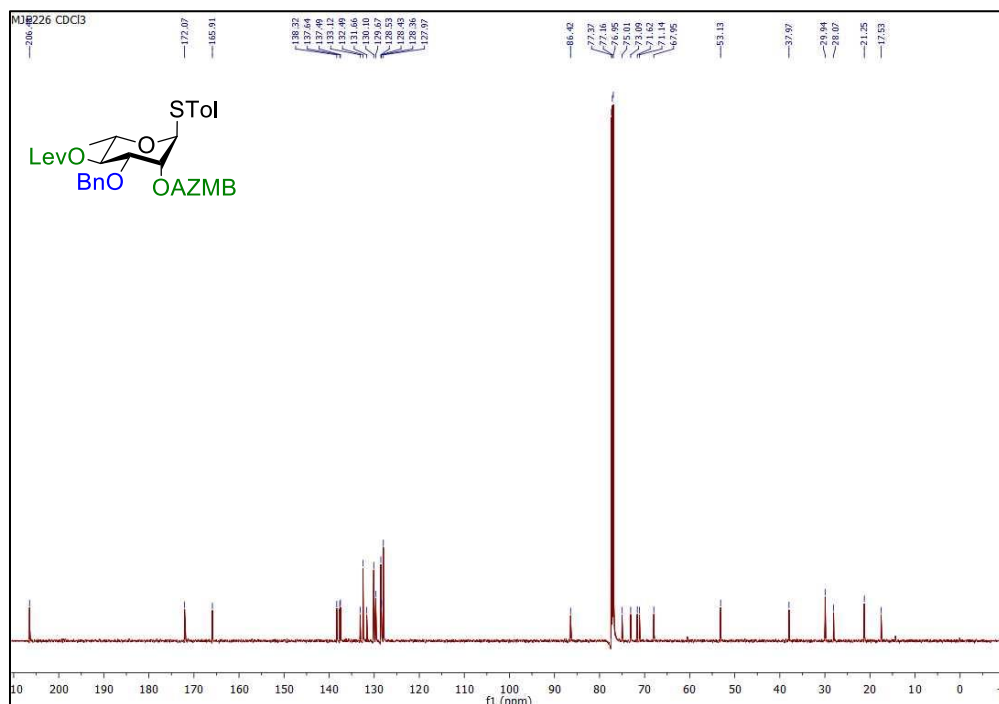


Figure S68 | ^1H NMR spectrum (CDCl_3 , 600 MHz) of *para*-methylphenyl 2-*O*-ortho-(azidomethyl)benzoyl-3-*O*-benzyl-1-thio- α -L-rhamnopyranoside (38).

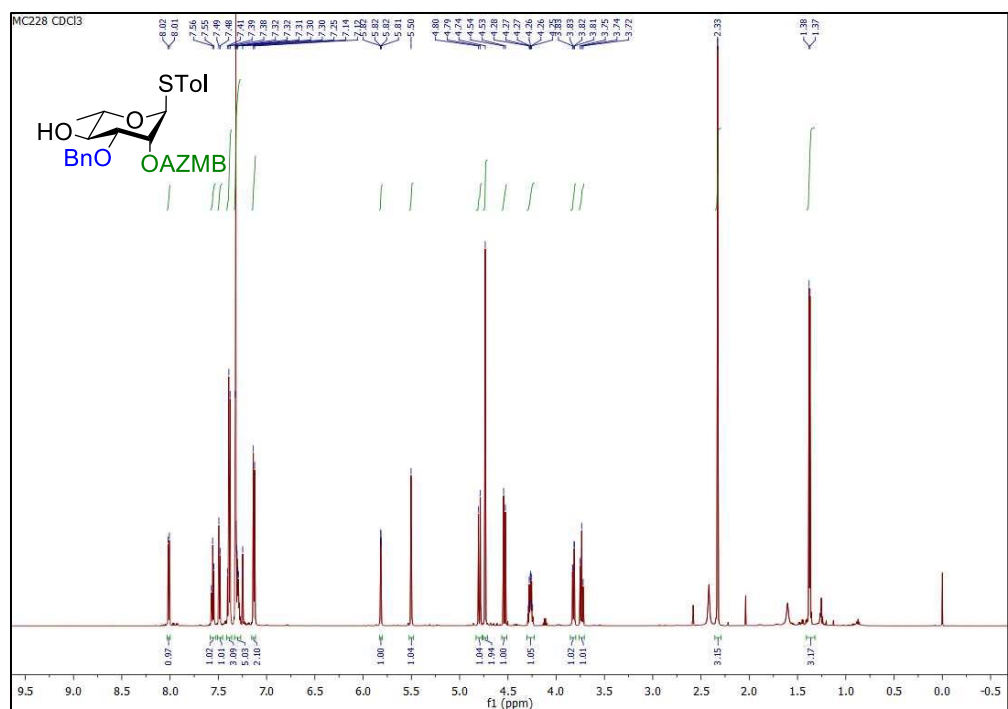


Figure S69 | ^{13}C NMR spectrum (CDCl_3 , 600 MHz) of *para*-methylphenyl 2-*O*-ortho-(azidomethyl)benzoyl-3-*O*-benzyl-1-thio- α -L-rhamnopyranoside (38).

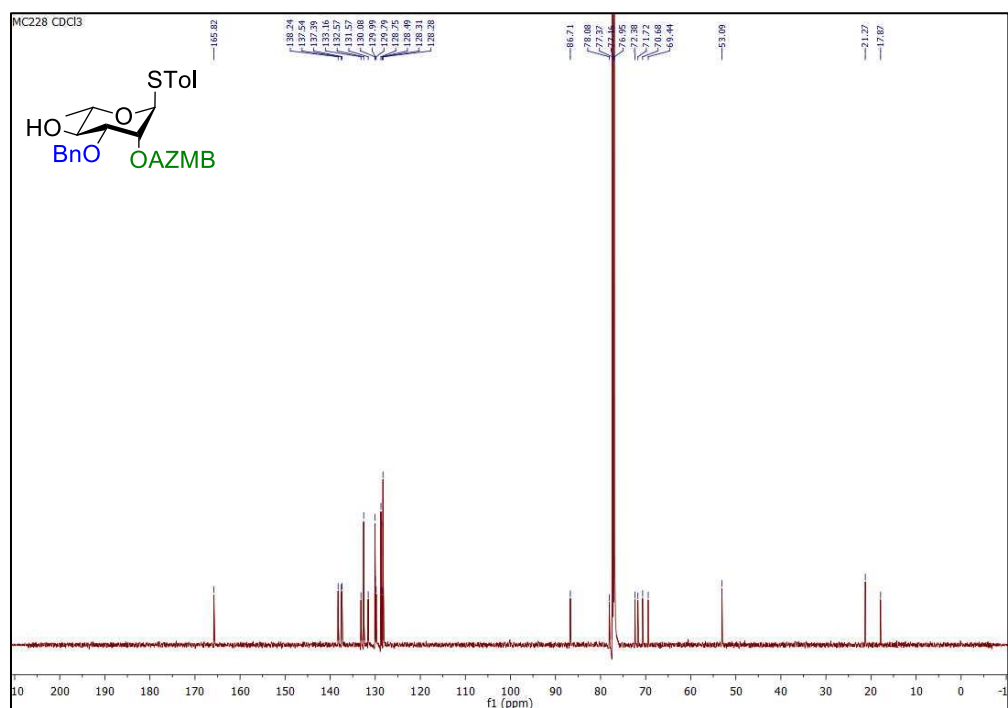


Figure S70 | ^1H NMR spectrum (CDCl_3 , 600 MHz) of *para*-methylphenyl 2-*O*-*ortho*-(azidomethyl)benzoyl-3-*O*-benzyl-4-*O*-(*R*)-3-(((*R*)-3-hydroxydecanoyl)oxy)decanoyl-1-thio- α -L-rhamnopyranoside (39).

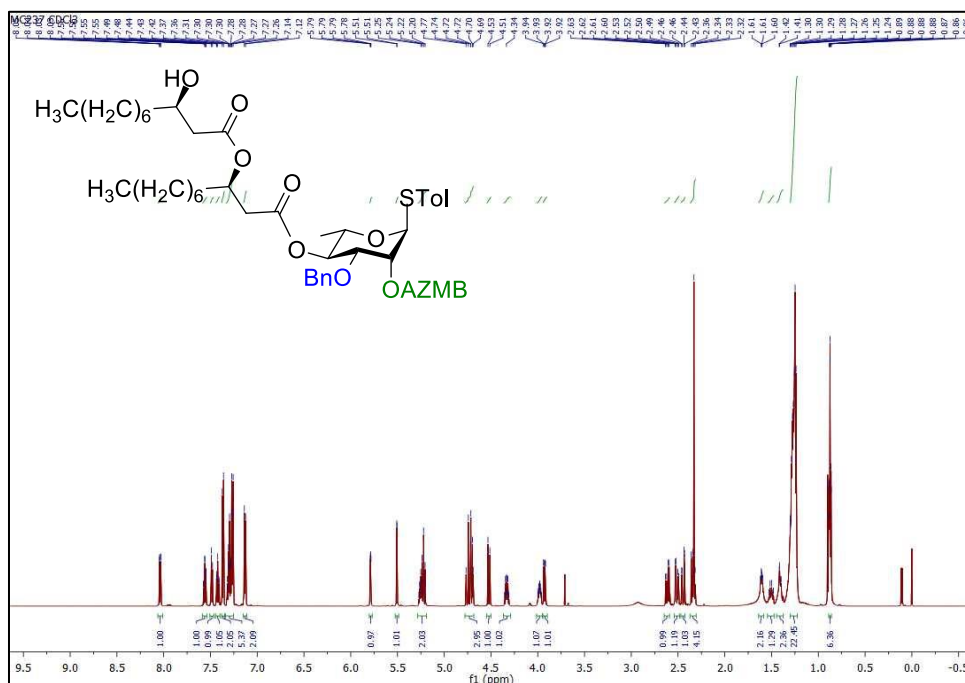


Figure S71 | ^{13}C NMR spectrum (CDCl_3 , 600 MHz) of *para*-methylphenyl 2-*O*-*ortho*-(azidomethyl)benzoyl-3-*O*-benzyl-4-*O*-(*R*)-3-(((*R*)-3-hydroxydecanoyl)oxy)decanoyl-1-thio- α -L-rhamnopyranoside (39).

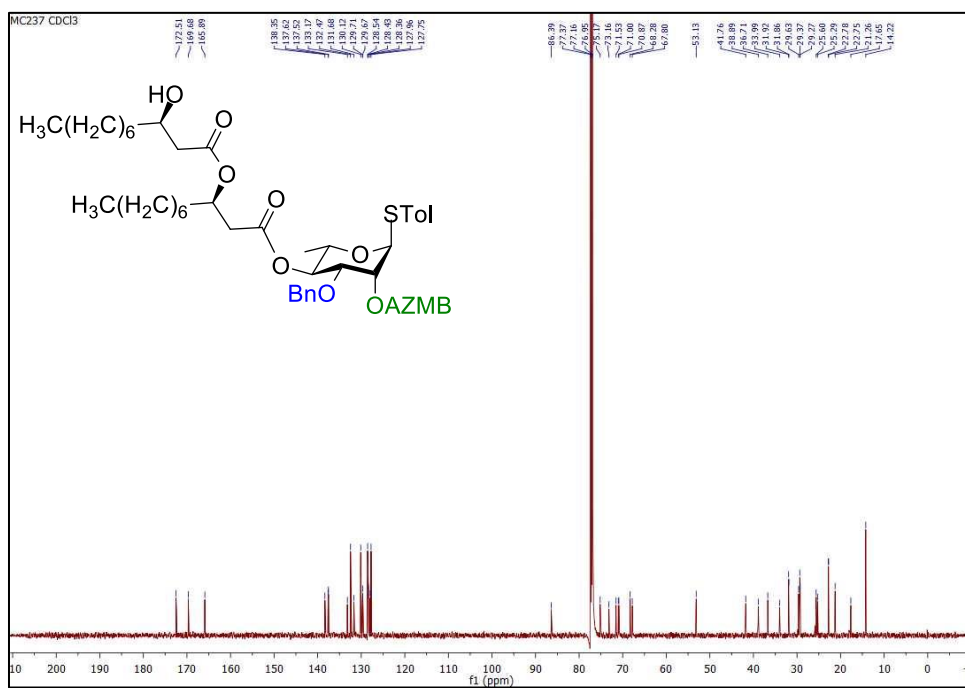


Figure S72 | ¹H NMR spectrum (CDCl₃, 600 MHz) of macrolide 40.

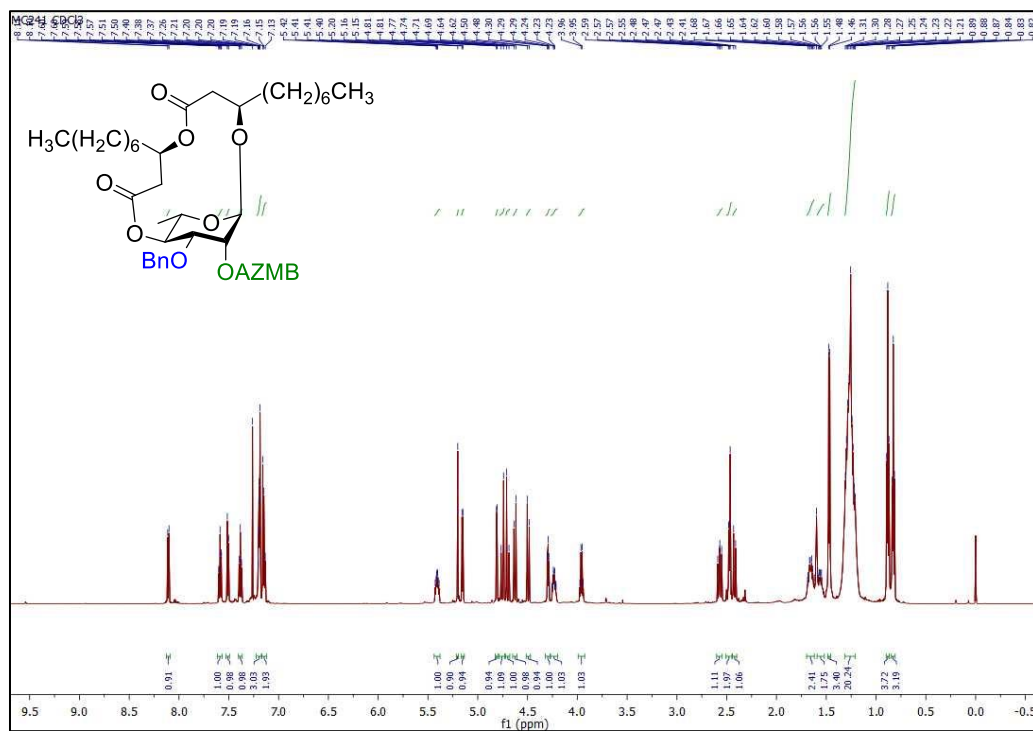


Figure S73 | ¹³C NMR spectrum (CDCl₃, 600 MHz) of macrolide 40.

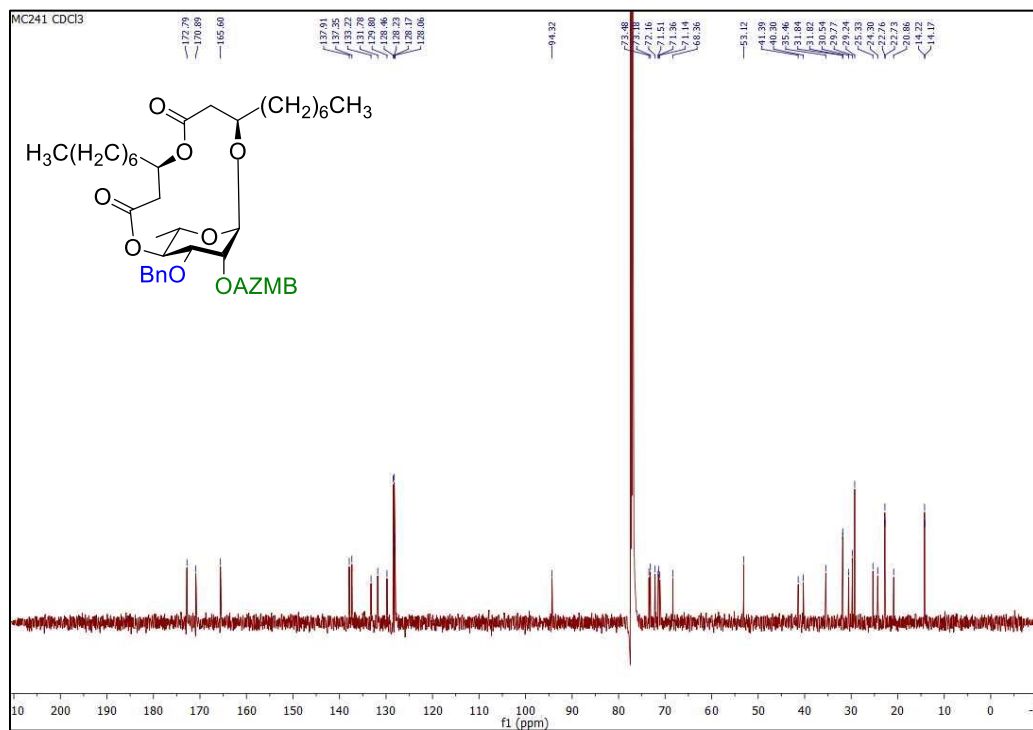


Figure S74 | ^1H NMR spectrum (CDCl_3 , 600 MHz) of macrolide S10.

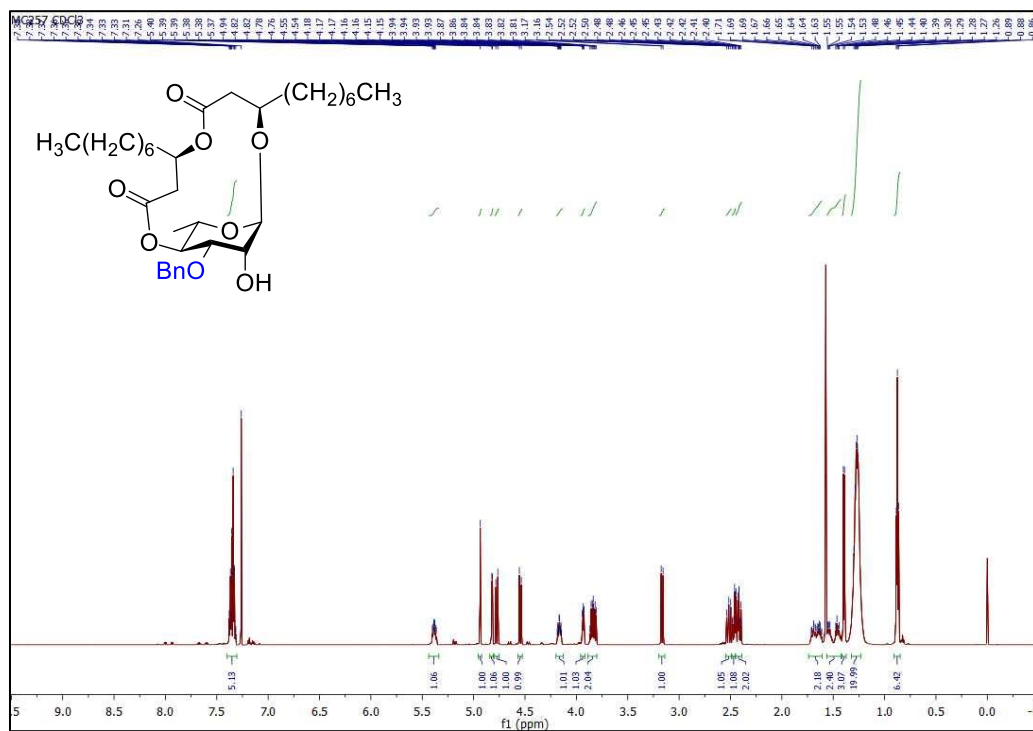


Figure S75 | ^{13}C NMR spectrum (CDCl_3 , 600 MHz) of macrolide S10.

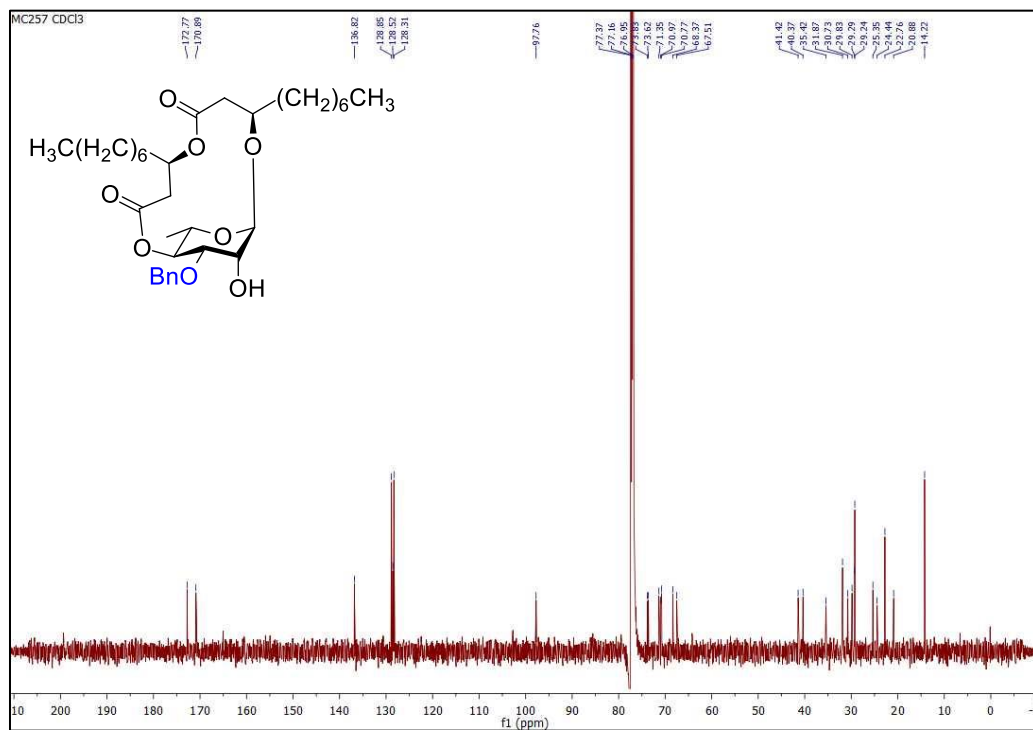


Figure S76 | ^1H NMR spectrum (CDCl_3 , 600 MHz) of (1 \rightarrow 4)-macrolactonized rhamnolipid 4.

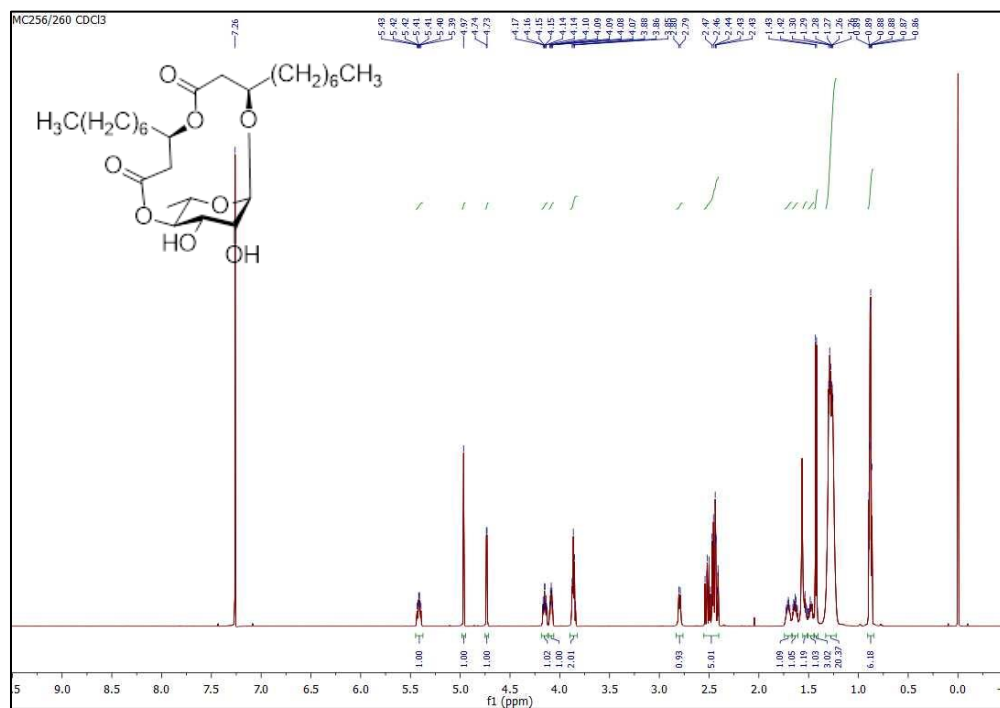


Figure S77 | ^{13}C NMR spectrum (CDCl_3 , 600 MHz) of (1 \rightarrow 4)-macrolactonized rhamnolipid 4.

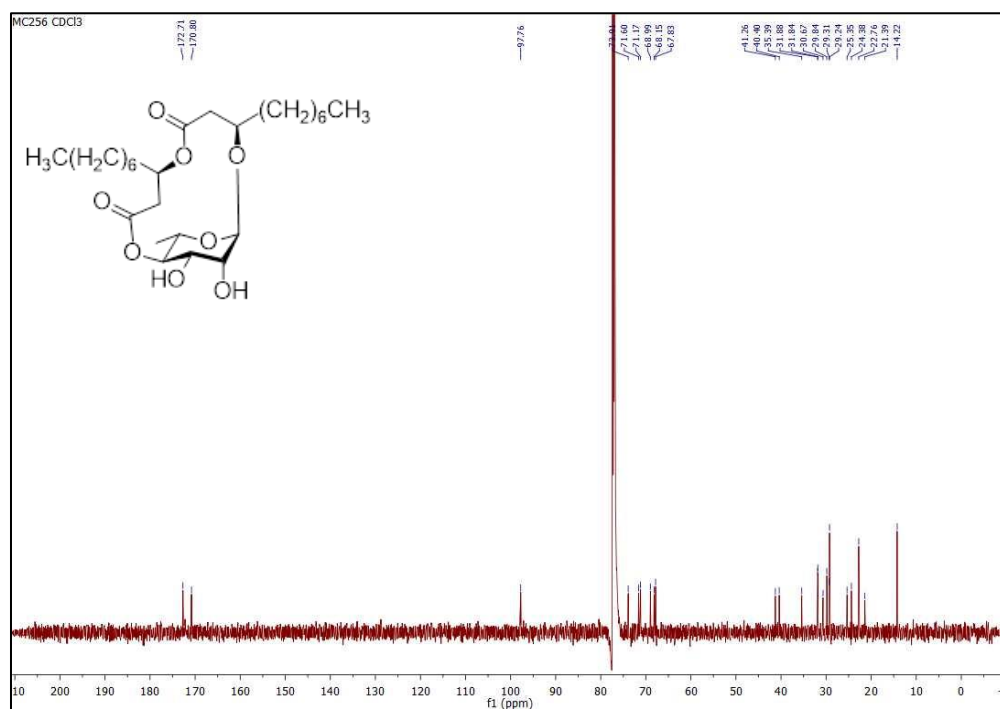


Figure S78 | ^1H NMR spectrum (CDCl_3 , 600 MHz) of *para*-methylphenyl 3-*O*-benzyl-2-*O*-(*R*)-3-(((*R*)-3-(*tert*-butyldimethylsilyl)oxy)decanoyl)oxy)decanoyl-4-*O*-levulinoyl-1-thio- α -L-rhamnopyranoside (29).

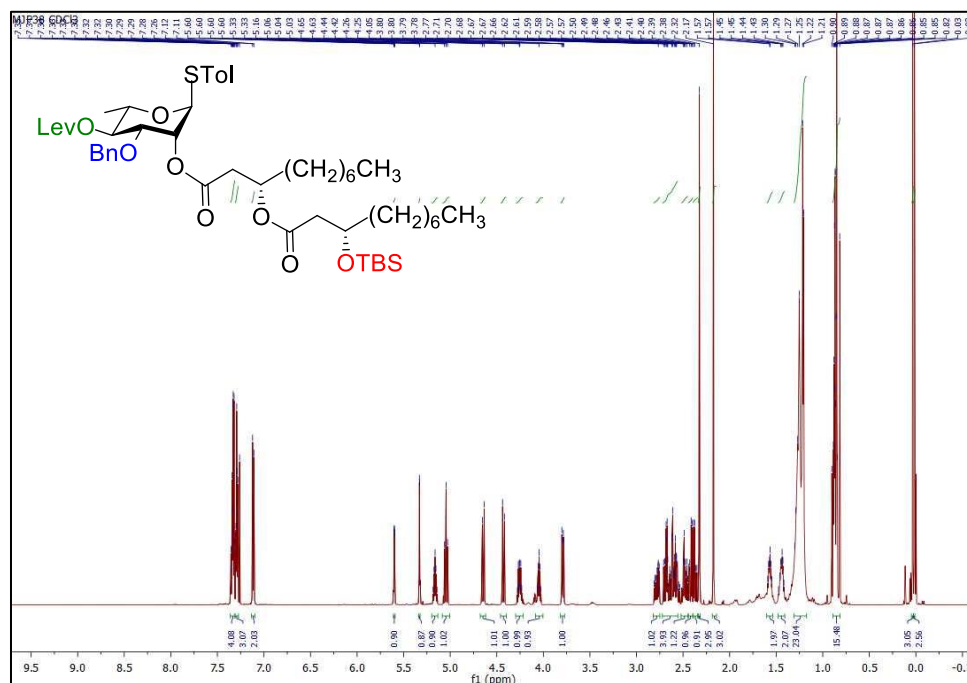


Figure S79 | ^{13}C NMR spectrum (CDCl_3 , 600 MHz) of *para*-methylphenyl 3-*O*-benzyl-2-*O*-(*R*)-3-(((*R*)-3-(*tert*-butyldimethylsilyl)oxy)decanoyl)oxy)decanoyl-4-*O*-levulinoyl-1-thio- α -L-rhamnopyranoside (29).

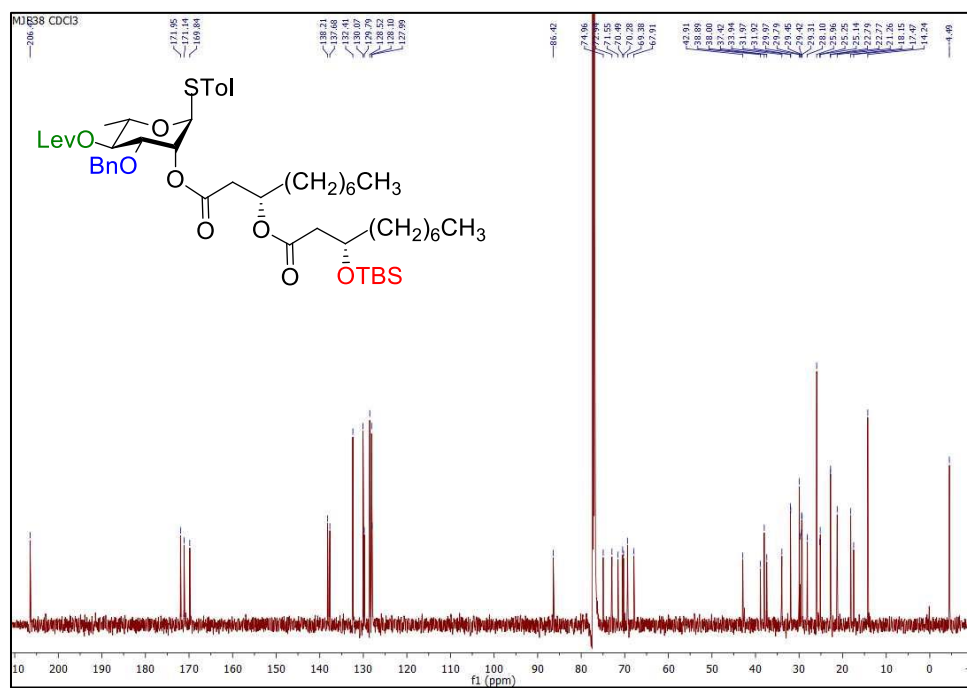


Figure S80 | ^1H NMR spectrum (CDCl_3 , 600 MHz) of *para*-methylphenyl 3-*O*-benzyl-2-*O*-(*R*)-3-(((*R*)-3-(hydroxydecanoyl)oxy)decanoyl-4-*O*-levulinoyl-1-thio- α -L-rhamnopyranoside (42).

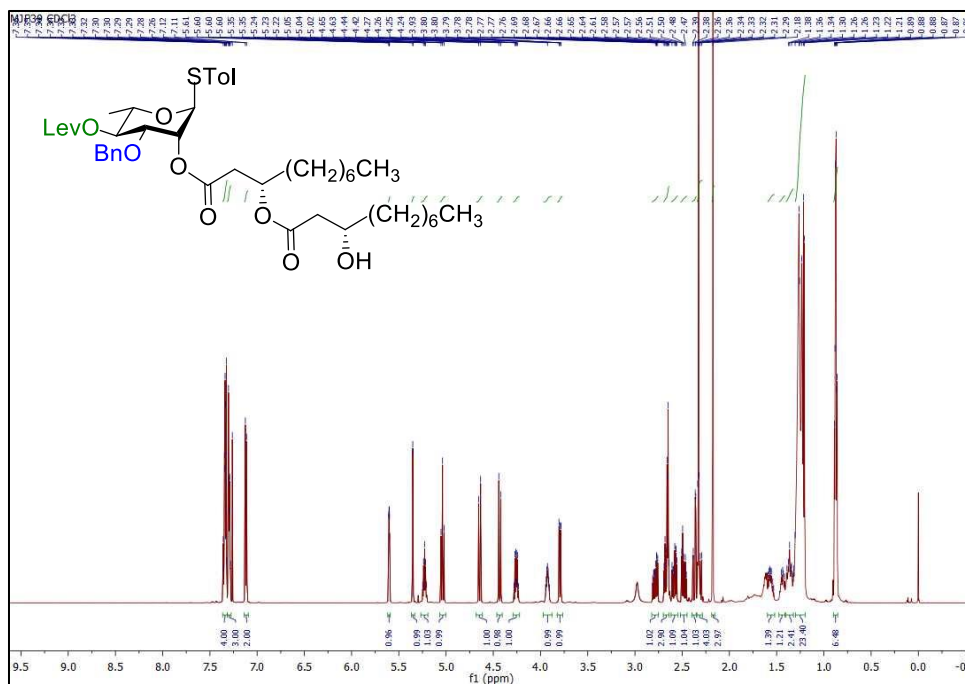


Figure S81 | ^{13}C NMR spectrum (CDCl_3 , 600 MHz) of *para*-methylphenyl 3-*O*-benzyl-2-*O*-(*R*)-3-(((*R*)-3-(hydroxydecanoyl)oxy)decanoyl-4-*O*-levulinoyl-1-thio- α -L-rhamnopyranoside (42).

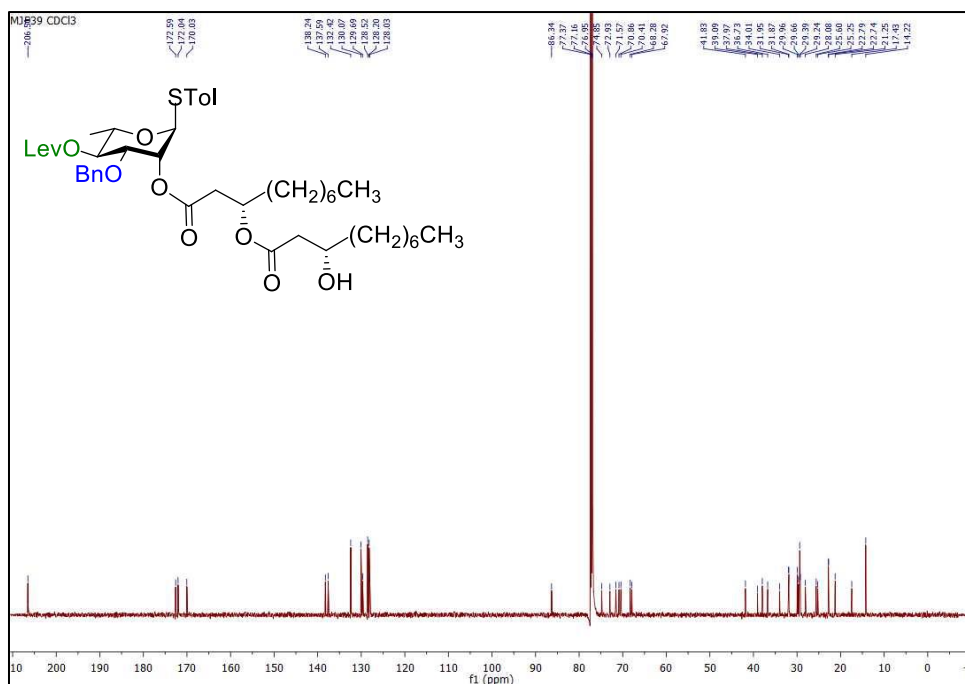


Figure S82 | ^1H NMR spectrum (CDCl_3 , 600 MHz) of macrolide 43.

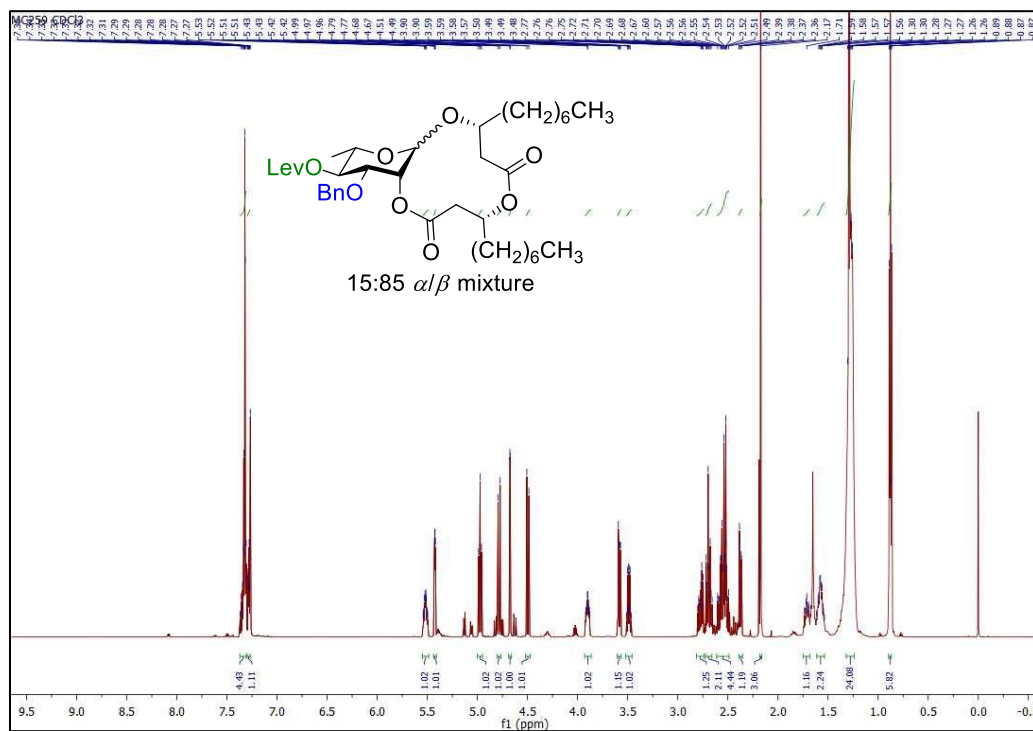


Figure S83 | ^{13}C NMR spectrum (CDCl_3 , 600 MHz) of macrolide 43.

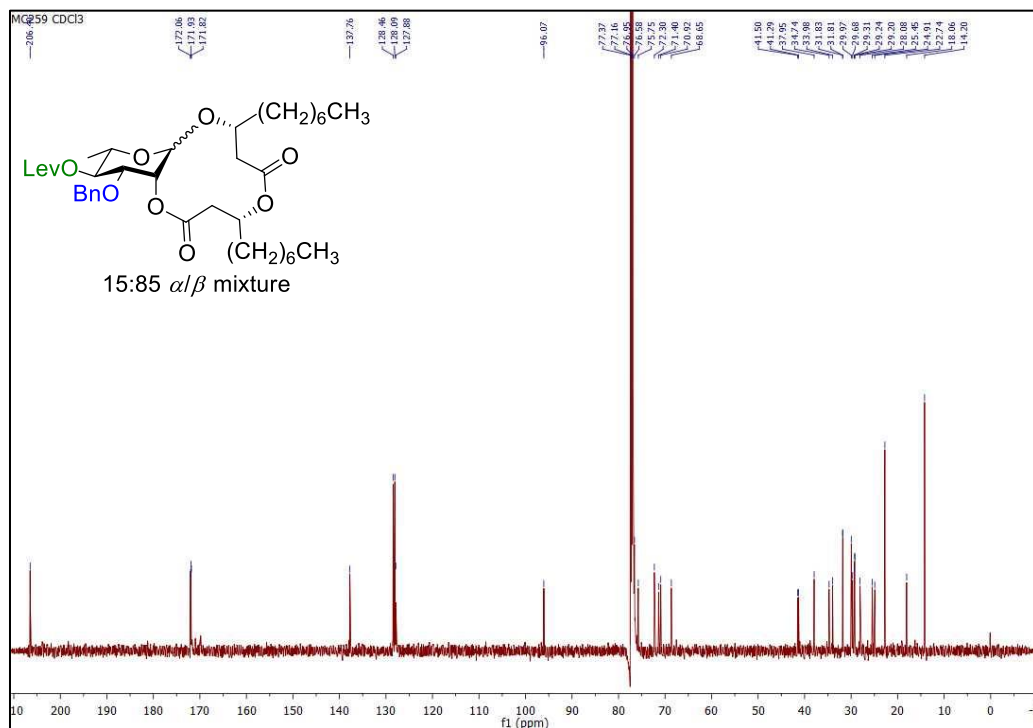


Figure S84 | ^1H NMR spectrum (CDCl_3 , 600 MHz) of macrolide S11 β .

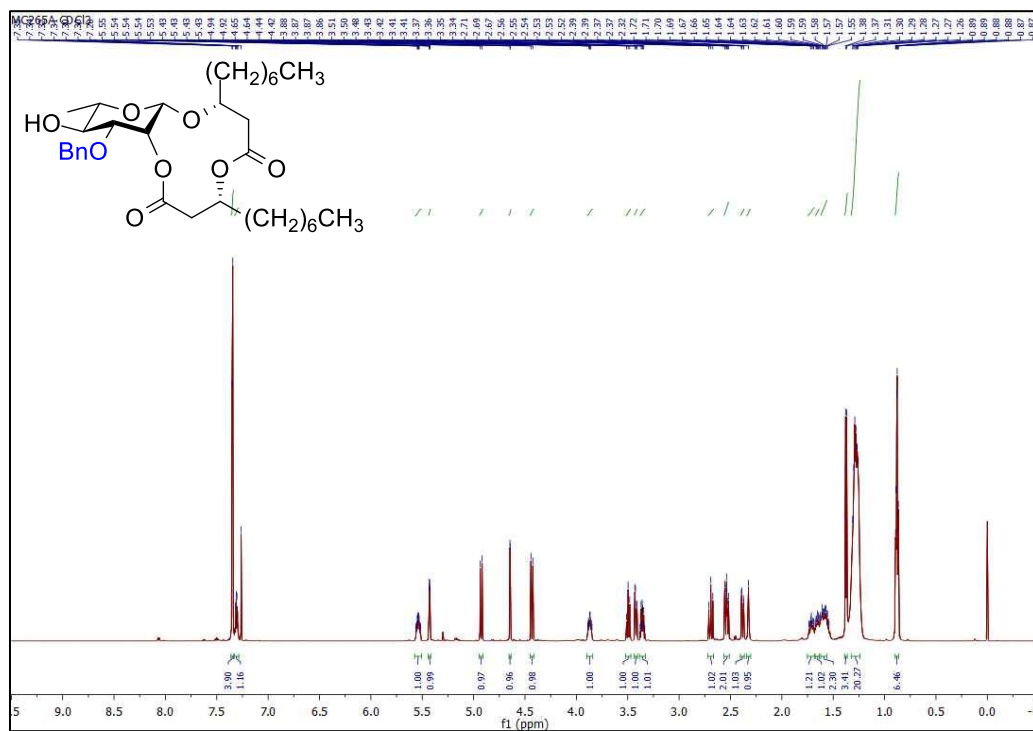


Figure S85 | ^{13}C NMR spectrum (CDCl_3 , 600 MHz) of macrolide S11 β .

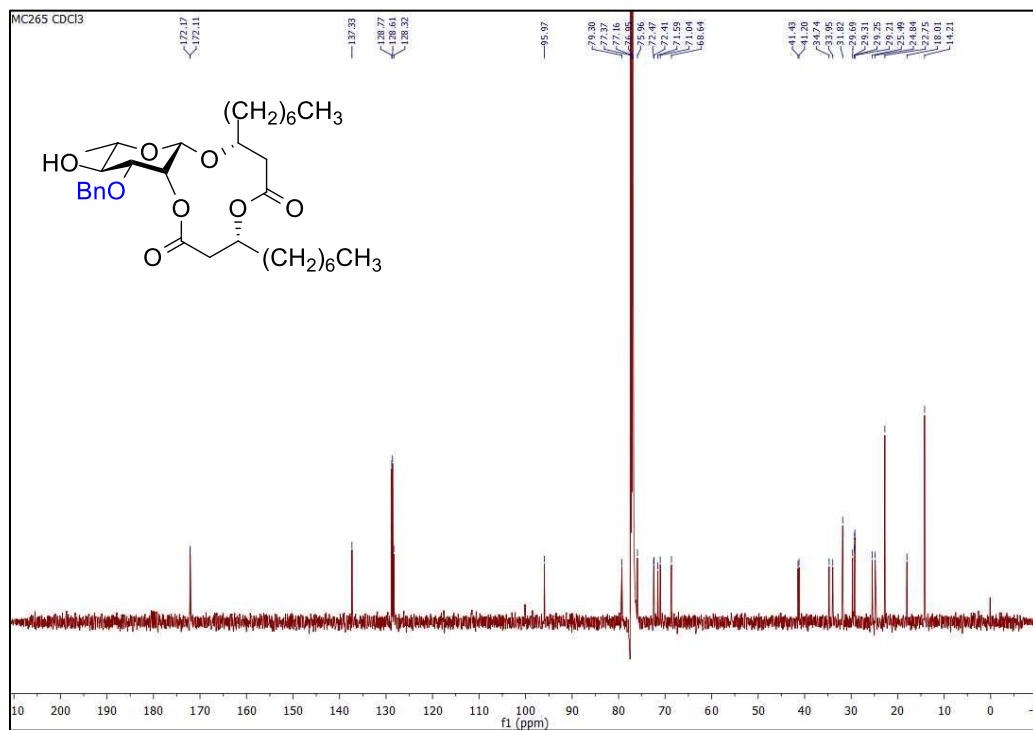


Figure S86 | ^1H NMR spectrum (CDCl_3 , 600 MHz) of (1 \rightarrow 2)-macrolactonized rhamnolipid 5β .

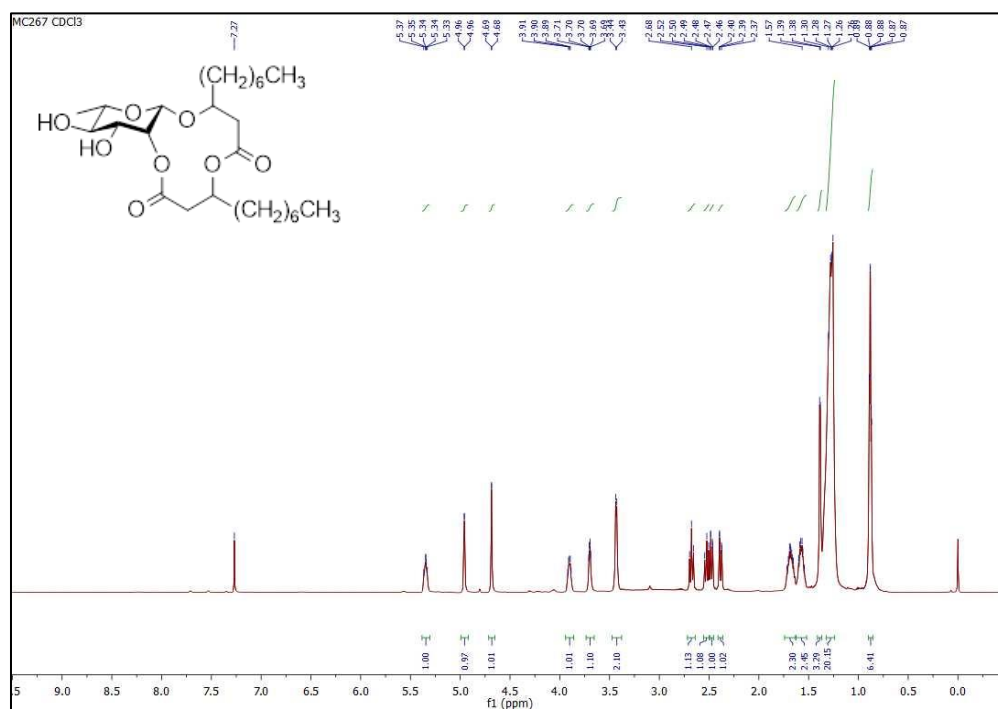


Figure S87 | ^{13}C NMR spectrum (CDCl_3 , 600 MHz) of (1 \rightarrow 2)-macrolactonized rhamnolipid 5β .

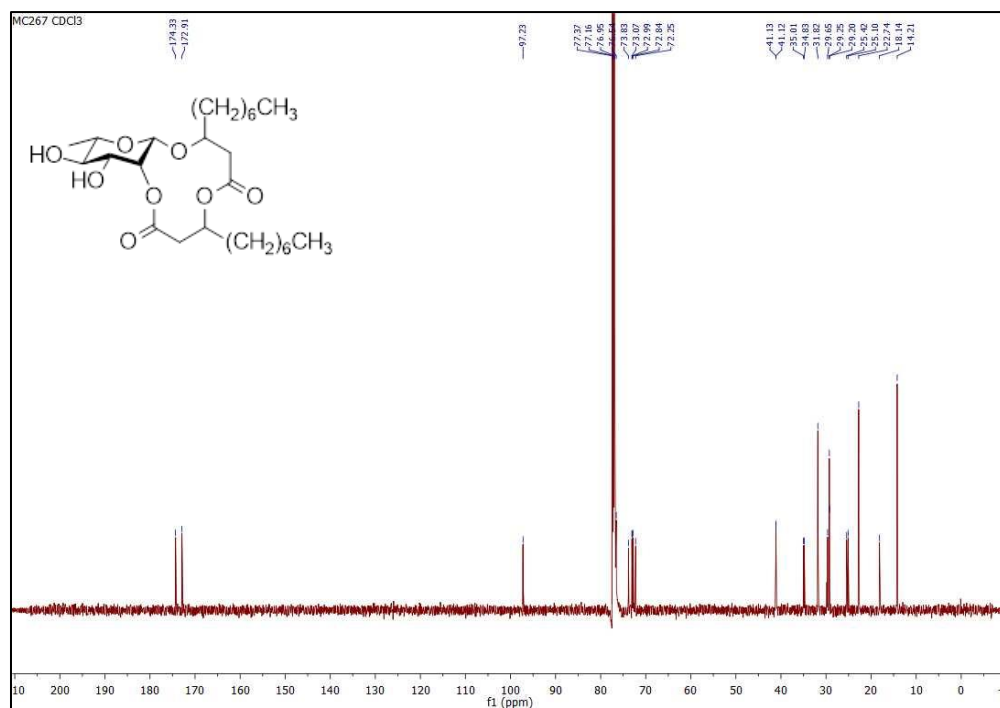


Figure S88 | ^1H NMR spectrum (CDCl_3 , 600 MHz) of (1 \rightarrow 2)-macrolactonized rhamnolipid **5a**.

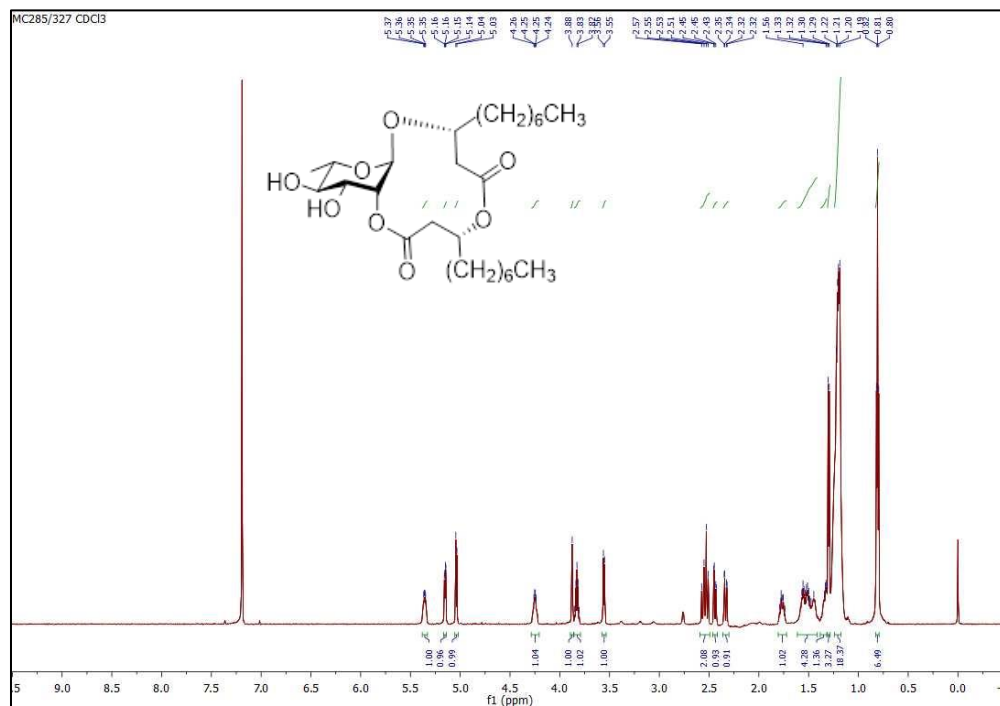


Figure S89 | ^{13}C NMR spectrum (CDCl_3 , 600 MHz) of (1 \rightarrow 2)-macrolactonized rhamnolipid **5a**.

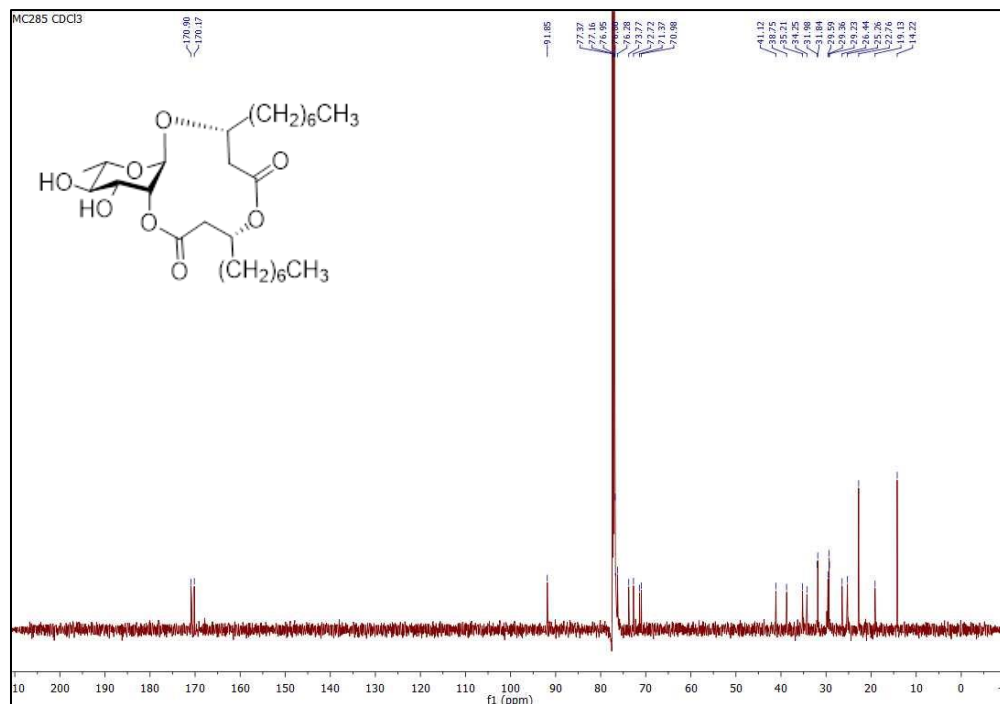


Figure S90 | ^1H NMR spectrum (CDCl_3 , 600 MHz) of *para*-methylphenyl 2-*O*-ortho-(azidomethyl)benzoyl-4-*O*-levulinoyl-1-thio- α -L-rhamnopyranoside (45).

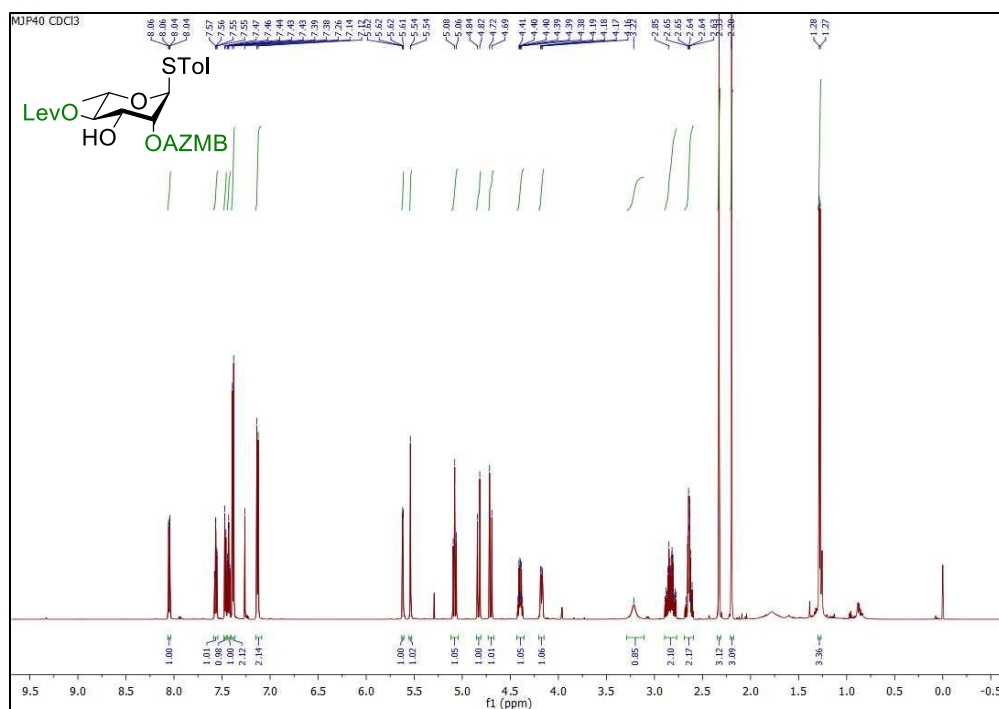


Figure S91 | ^{13}C NMR spectrum (CDCl_3 , 600 MHz) of *para*-methylphenyl 2-*O*-ortho-(azidomethyl)benzoyl-4-*O*-levulinoyl-1-thio- α -L-rhamnopyranoside (45).

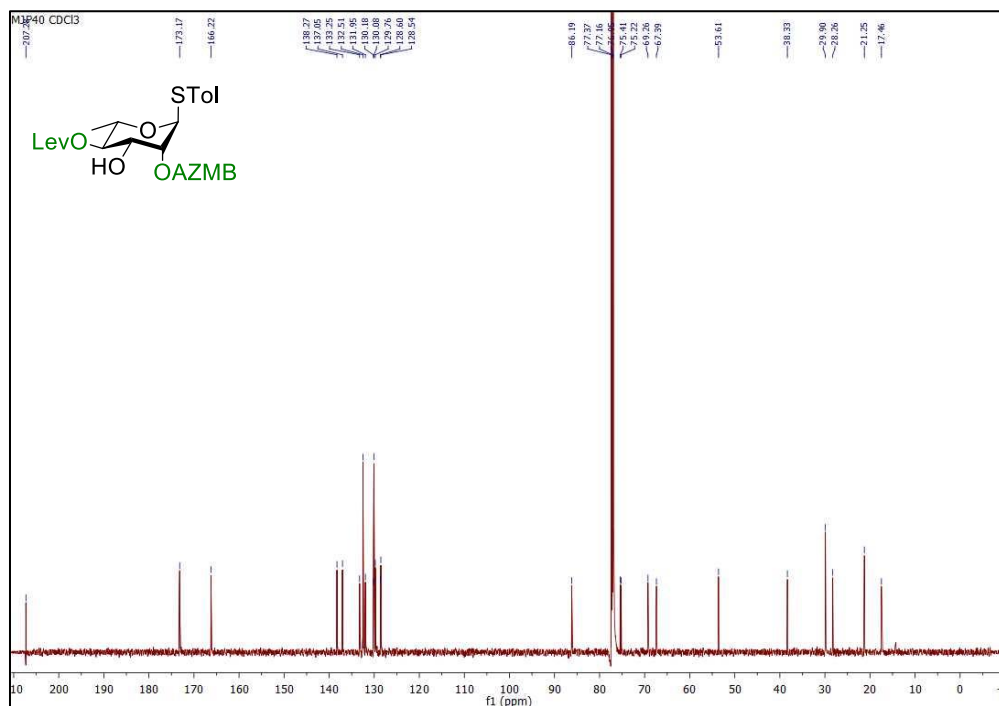


Figure S92 | ^1H NMR spectrum (CDCl_3 , 600 MHz) of *para*-methylphenyl 2-*O*-ortho-(azidomethyl)benzoyl-3-*O*-(*R*)-3-(((*R*)-3-((*tert*-butyldimethylsilyl)oxy)decanoyl)oxy)decanoyl-4-*O*-levulinoyl-1-thio- α -L-rhamnopyranoside (30).

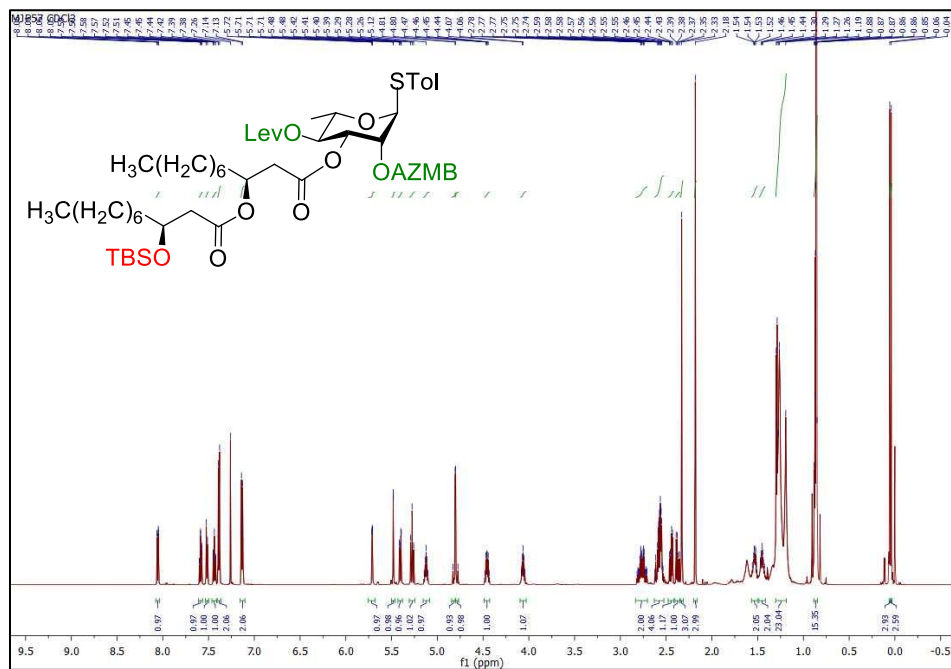


Figure S93 | ^{13}C NMR spectrum (CDCl_3 , 600 MHz) of *para*-methylphenyl 2-*O*-ortho-(azidomethyl)benzoyl-3-*O*-(*R*)-3-(((*R*)-3-((*tert*-butyldimethylsilyl)oxy)decanoyl)oxy)decanoyl-4-*O*-levulinoyl-1-thio- α -L-rhamnopyranoside (30).

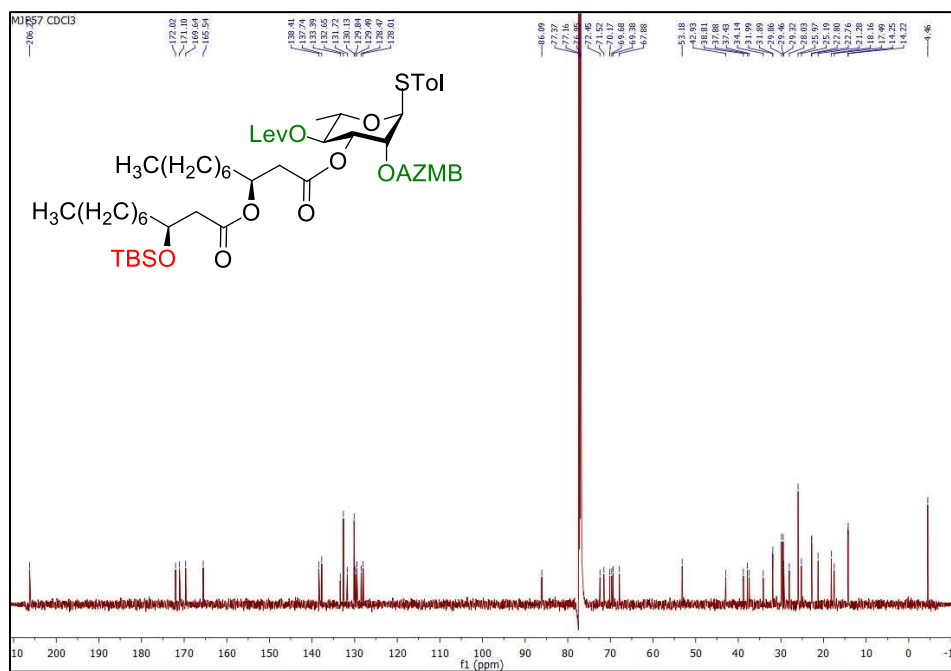


Figure S94 | ^1H NMR spectrum (CDCl_3 , 600 MHz) of *para*-methylphenyl 2-*O*-*ortho*-(azidomethyl)benzoyl-3-*O*-(*R*)-3-(((*R*)-3-(hydroxydecanoyl)oxy)decanoyl-4-*O*-levulinoyl-1-thio- α -L-rhamnopyranoside (46).

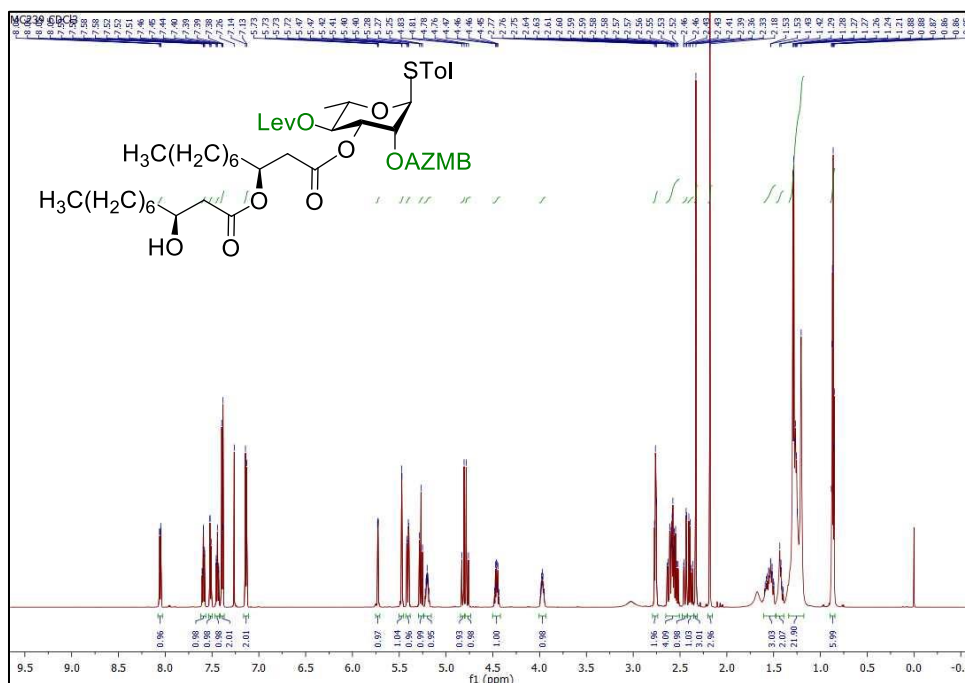


Figure S95 | ^{13}C NMR spectrum (CDCl_3 , 600 MHz) of *para*-methylphenyl 2-*O*-*ortho*-(azidomethyl)benzoyl-3-*O*-(*R*)-3-(((*R*)-3-(hydroxydecanoyl)oxy)decanoyl-4-*O*-levulinoyl-1-thio- α -L-rhamnopyranoside (46).

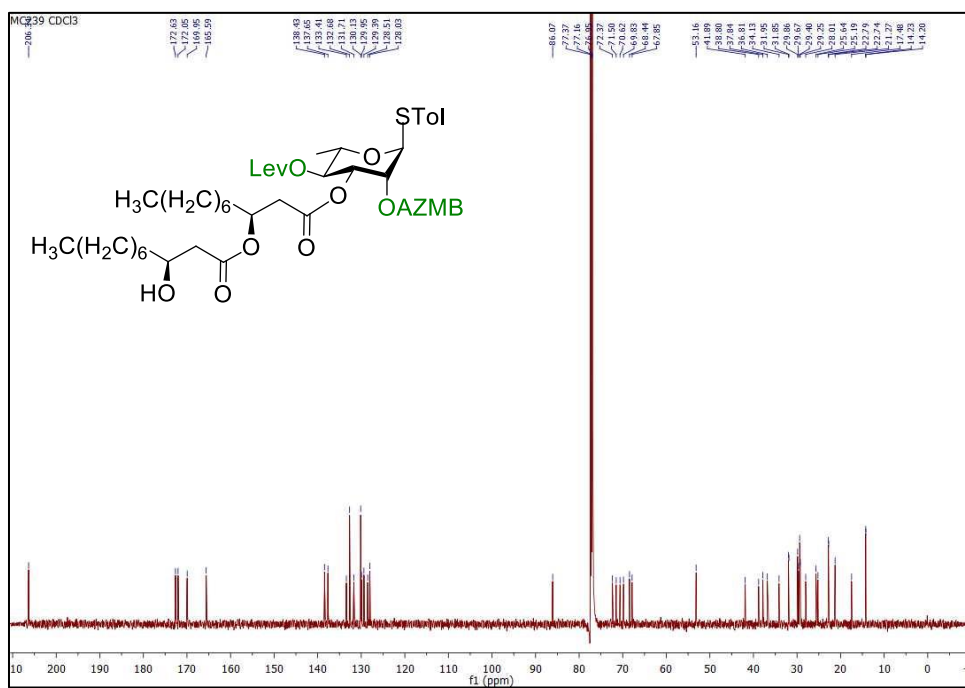


Figure S96 | ^1H NMR spectrum (CDCl_3 , 600 MHz) of macrolide 47β .

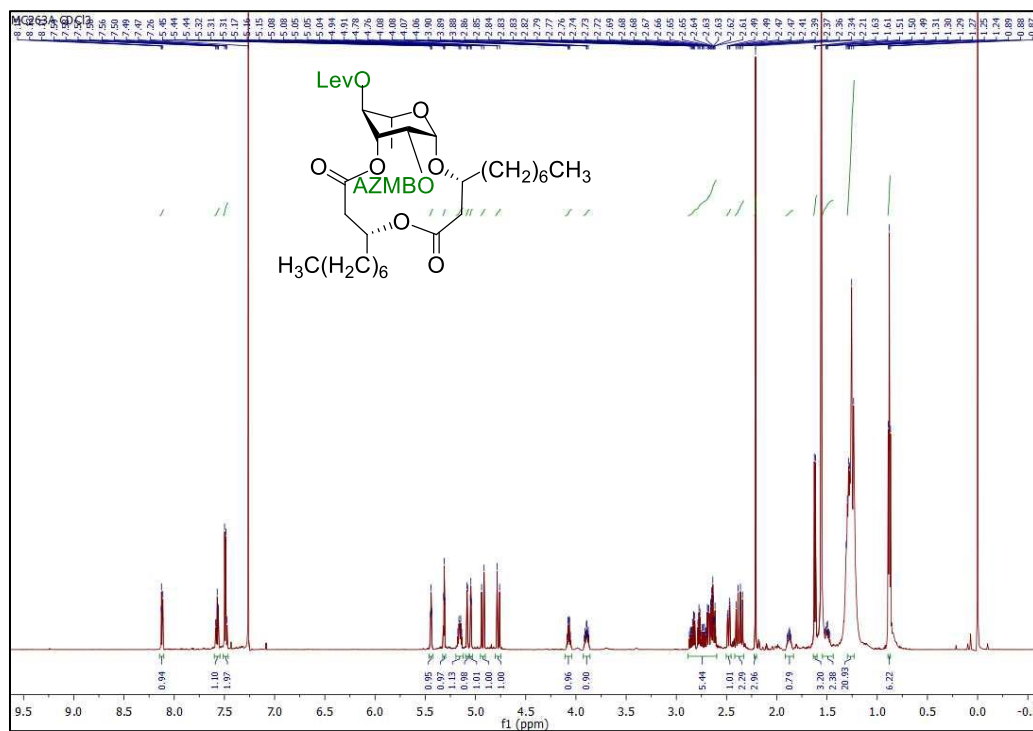


Figure S97 | ^{13}C NMR spectrum (CDCl_3 , 600 MHz) of macrolide 47β .

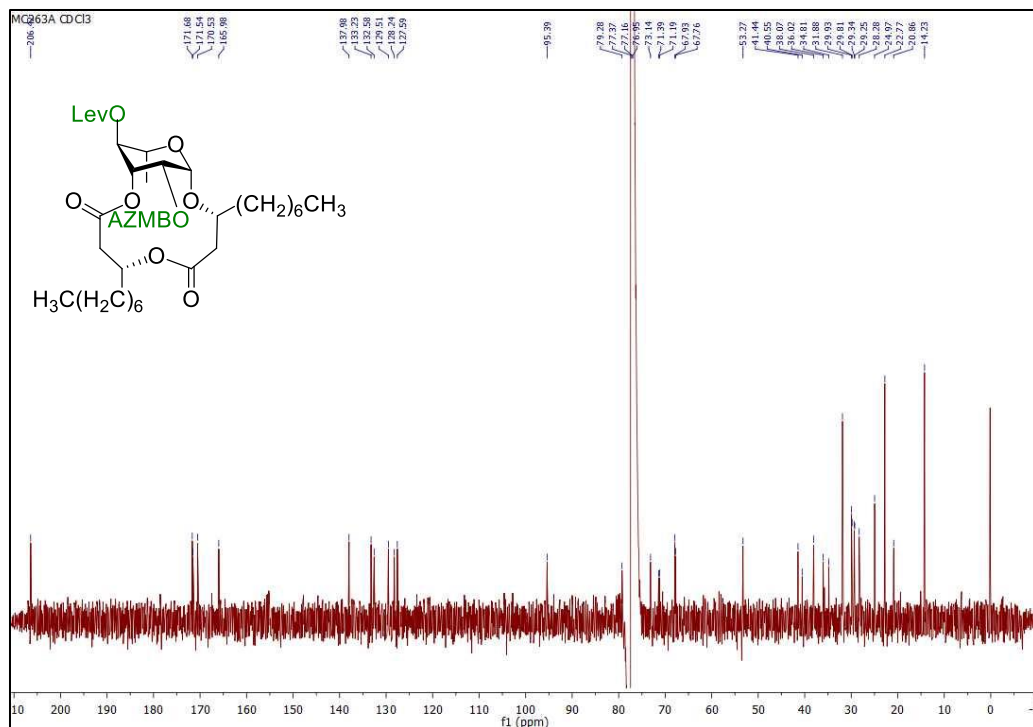


Figure S98 | ¹H NMR spectrum (CDCl₃, 600 MHz) of macrolide **47a**.

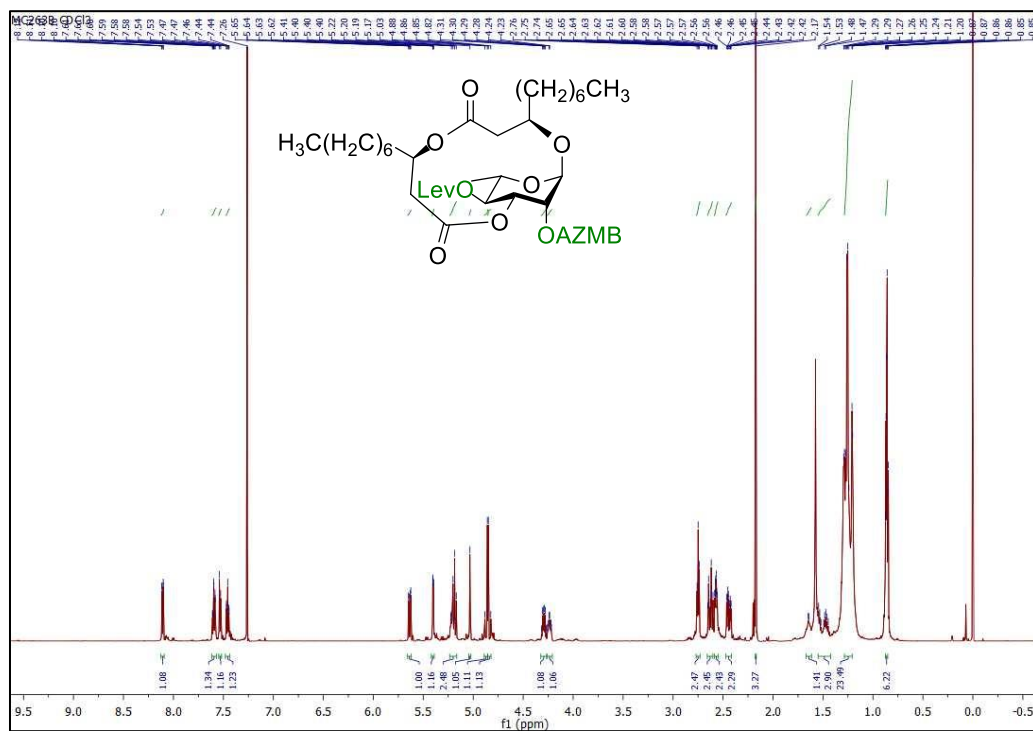


Figure S99 | ¹³C NMR spectrum (CDCl₃, 600 MHz) of macrolide **47a**.

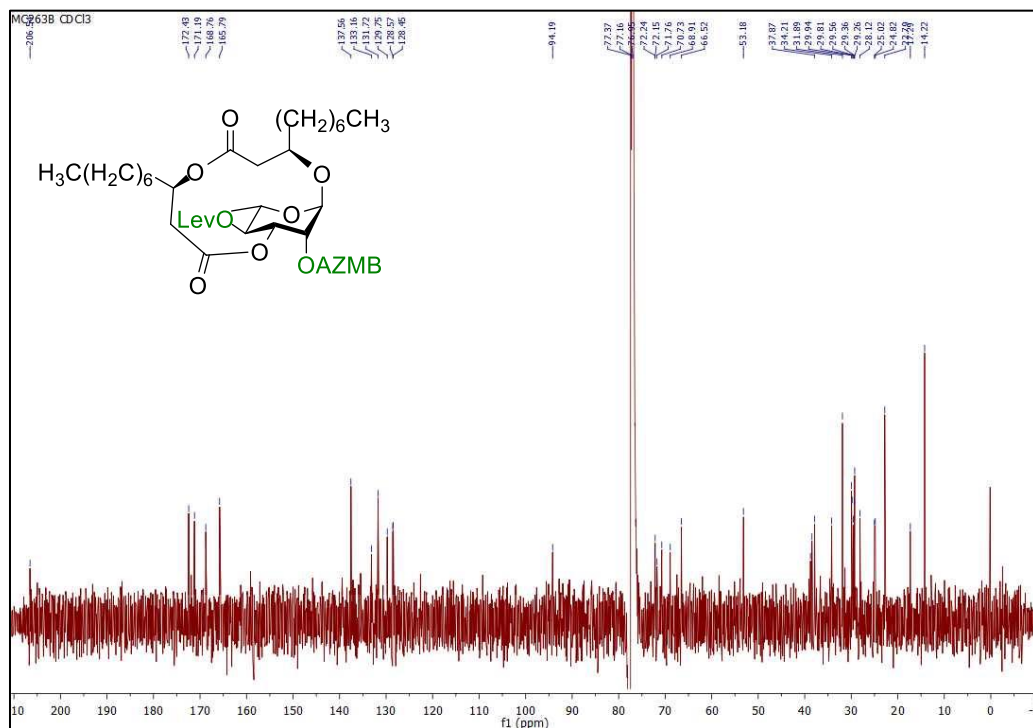


Figure S100 | ^1H NMR spectrum (CDCl_3 , 600 MHz) of macrolide S12 β .

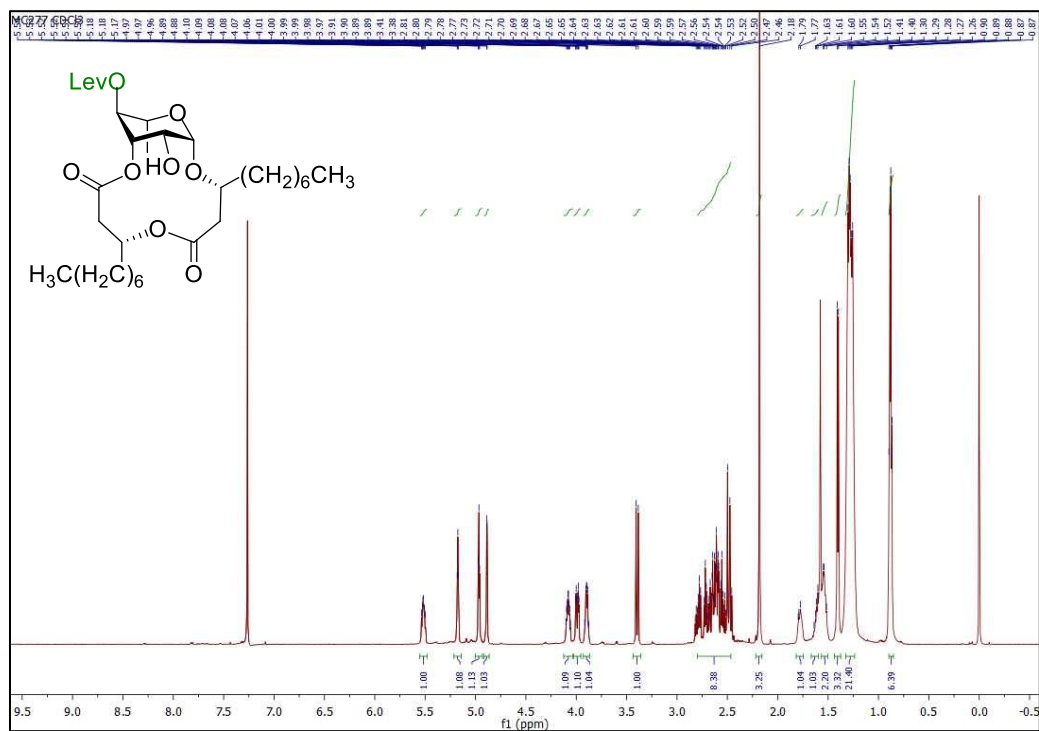


Figure S101 | ^{13}C NMR spectrum (CDCl_3 , 600 MHz) of macrolide S12 β .

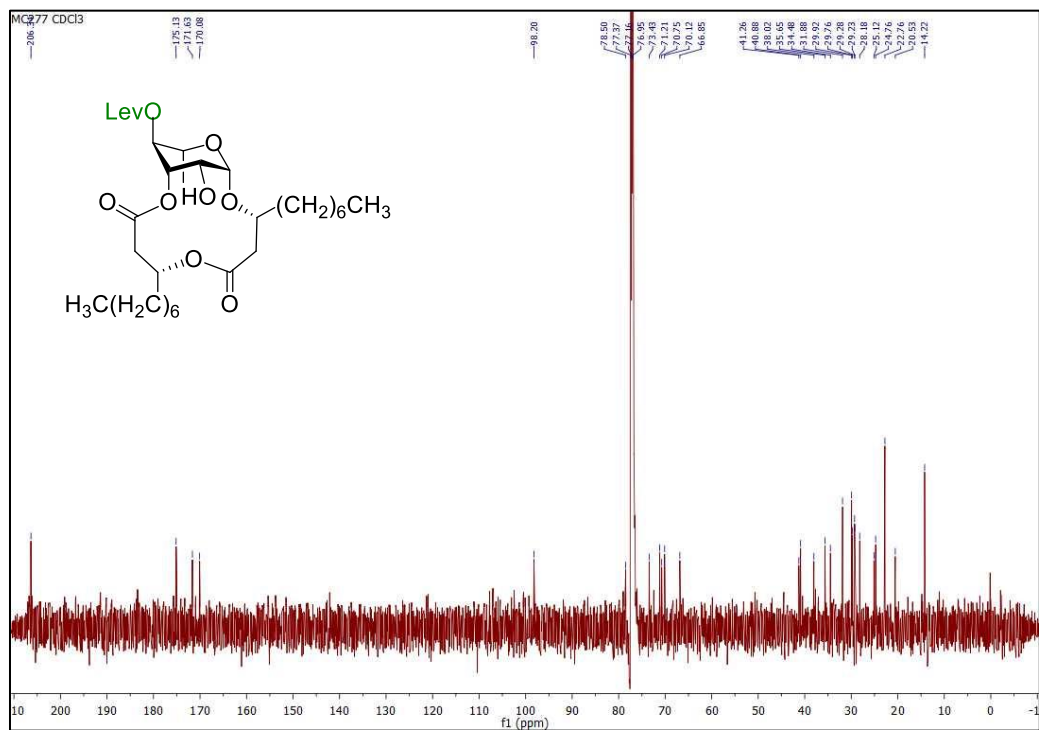


Figure S102 | ^1H NMR spectrum (CDCl_3 , 600 MHz) of (1 \rightarrow 3)-macrolactonized rhamnolipid 6β .

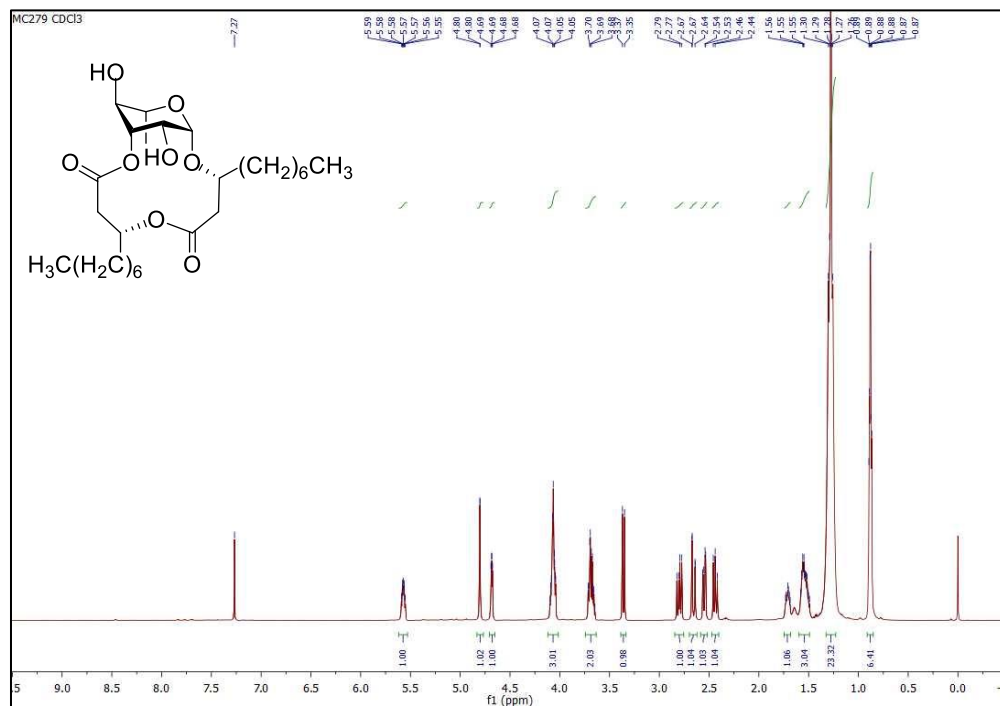


Figure S103 | ^{13}C NMR spectrum (CDCl_3 , 600 MHz) of (1 \rightarrow 3)-macrolactonized rhamnolipid 6β .

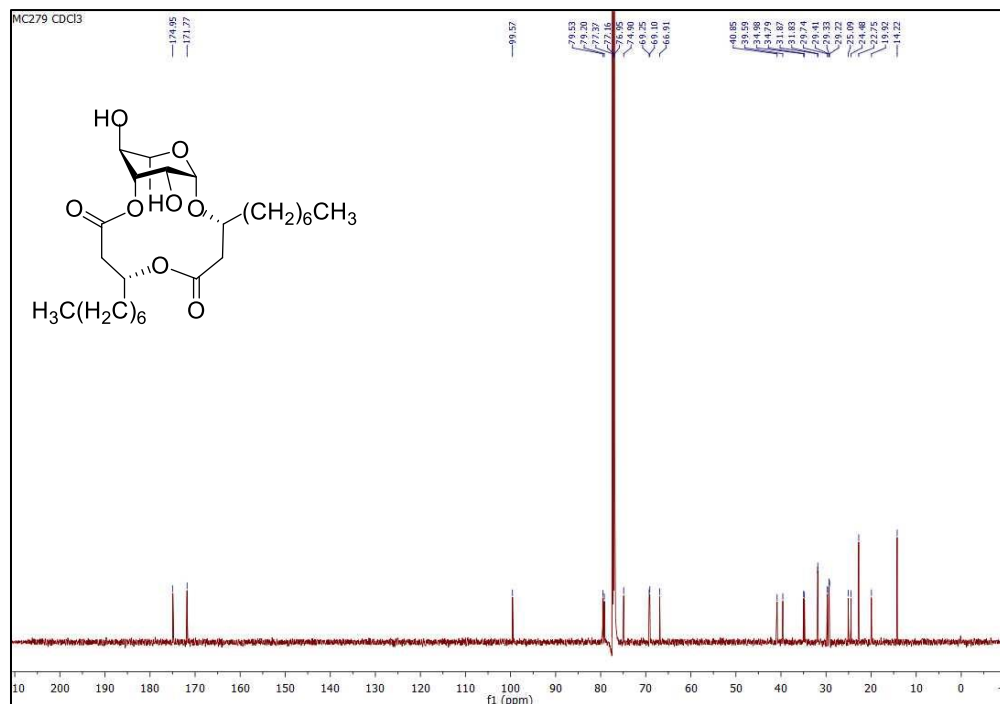


Figure S104 | ^1H NMR spectrum (CDCl_3 , 600 MHz) of macrolide S12a.

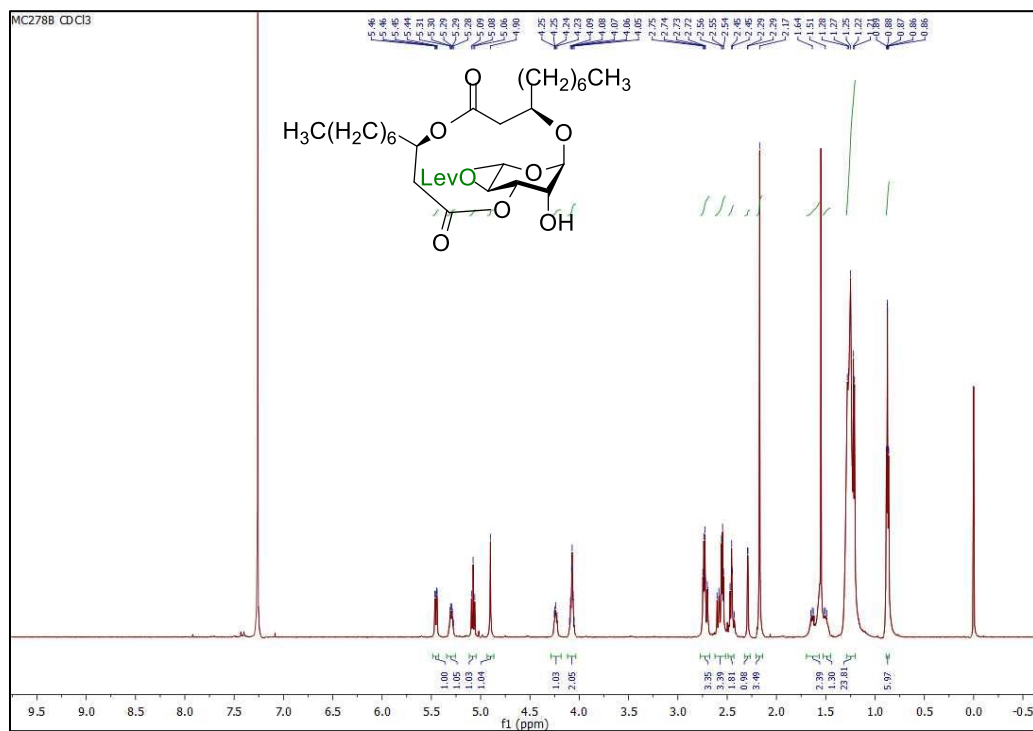


Figure S105 | ^{13}C NMR spectrum (CDCl_3 , 600 MHz) of macrolide S12a.

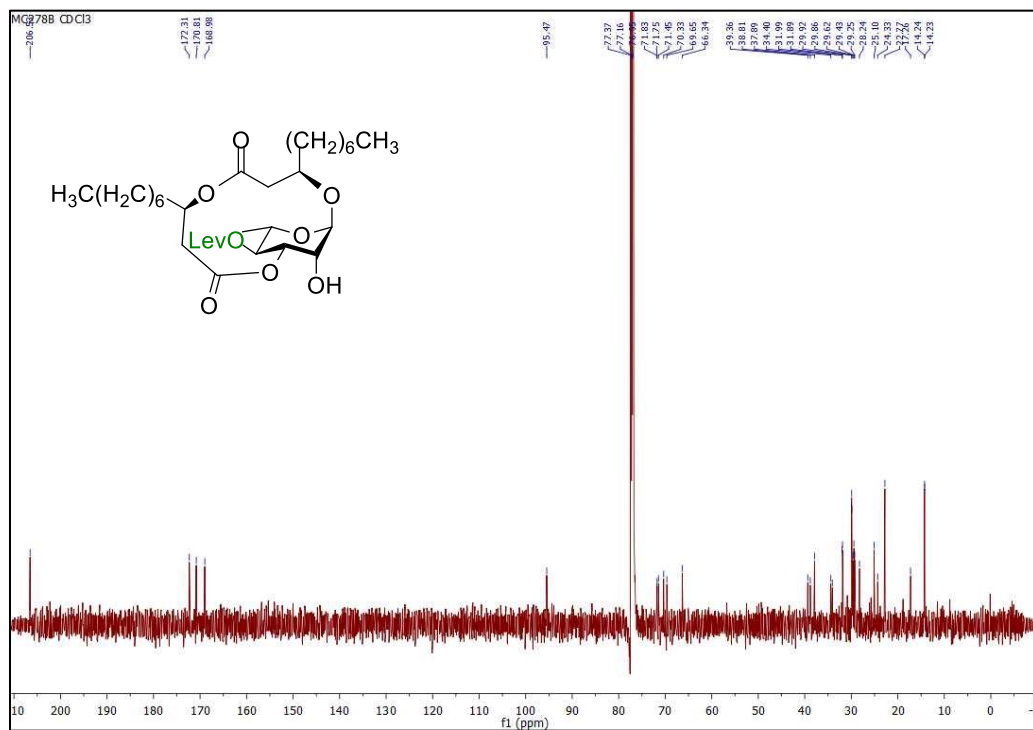


Figure S106 | ^1H NMR spectrum (CDCl_3 , 600 MHz) of (1 \rightarrow 3)-macrolactonized rhamnolipid **6a**.

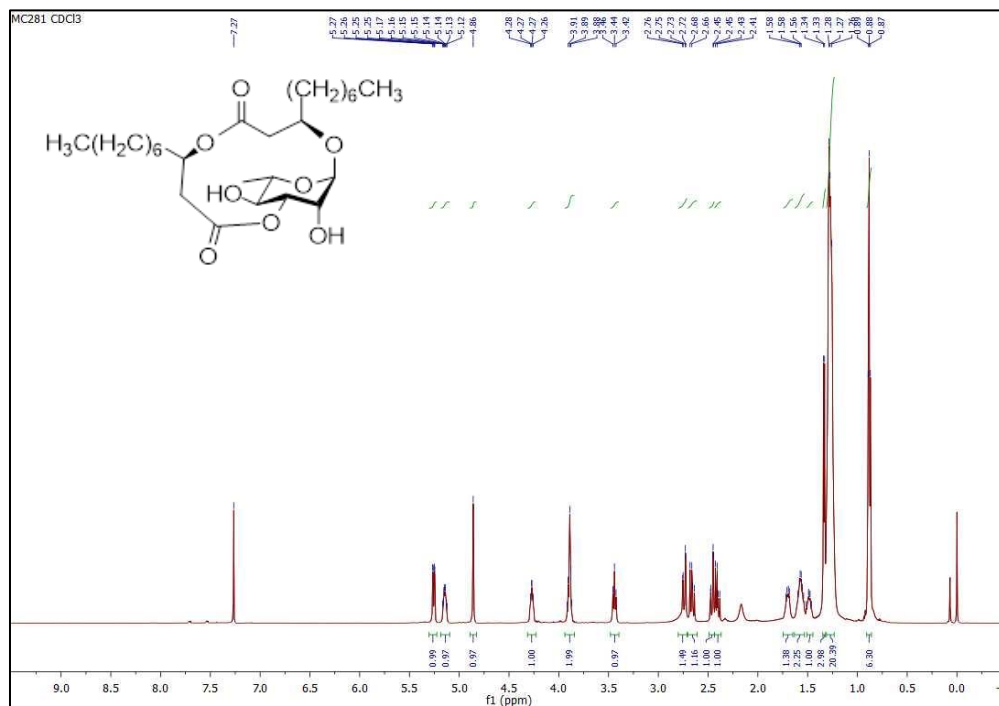
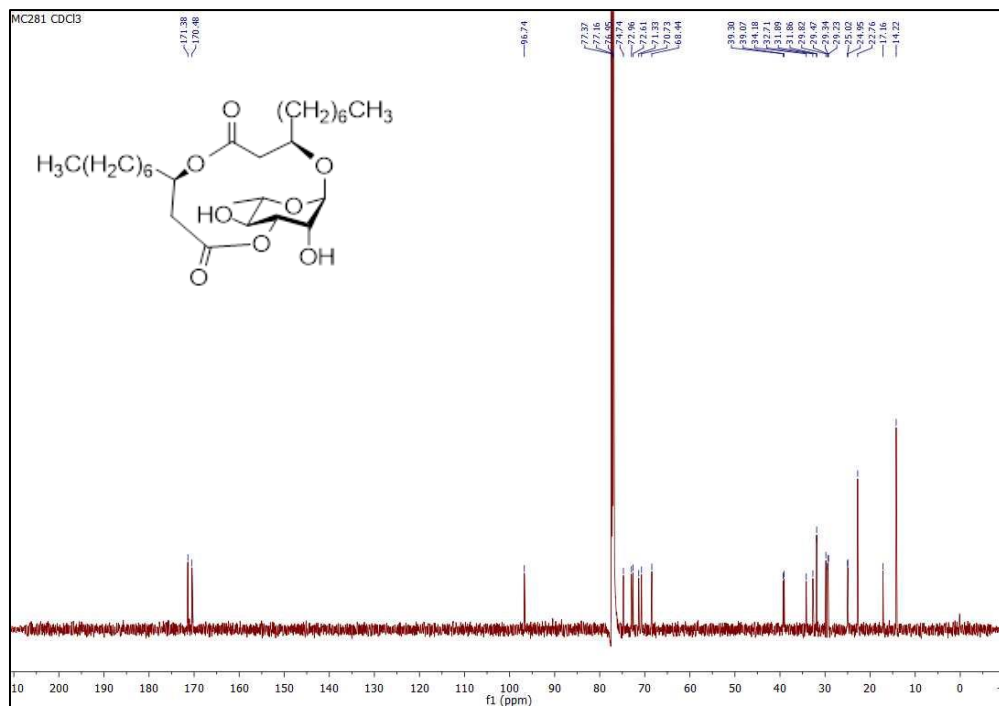


Figure S107 | ^{13}C NMR spectrum (CDCl_3 , 600 MHz) of (1 \rightarrow 3)-macrolactonized rhamnolipid **6a**.



7. HPLC Traces of Synthetic and Natural Surfactants

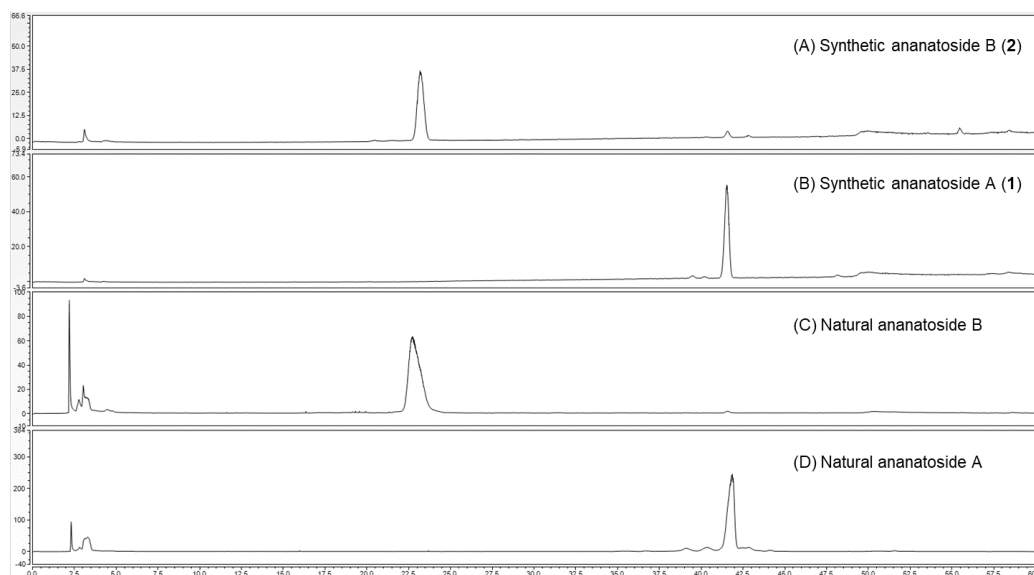


Figure S108. HPLC-CAD chromatograms of (A) synthetic ananatoside B (**2**); (B) synthetic ananatoside A (**1**); (C) natural ananatoside B (**2**); and (D) natural ananatoside A (**1**).

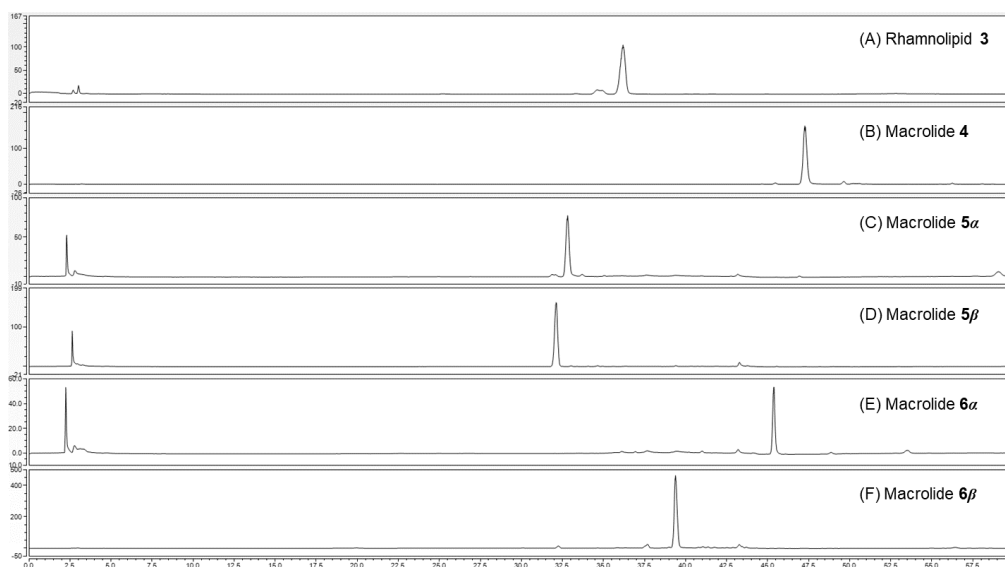


Figure S109. HPLC-CAD chromatograms of synthetic compounds (A) **3**; (B) **4**; (C) **5 α** ; (D) **5 β** ; (E) **6 α** and (F) **6 β** .

ANNEXE DU CHAPITRE 4

1. Supplementary Results

Table S1. Unsuccessful attempts to epimerize tetrasaccharide **23**.

entry	oxidation reagents	solvent	temperature (°C)	yield (%)
1	DMSO, PDCP, Et ₃ N	DCM	-10 to rt	nd ^a
2	DMSO, PDCP, Et ₃ N	DCM	-78 to rt	nd ^b
3	oxalyl chloride, DMSO, Et ₃ N	DCM	-78	nd ^b
4	DMSO, Ac ₂ O	-	rt	nd ^b
5	Dess-Martin periodinane	DCE	reflux	nd ^a

^aDegradation of starting material; ^bNo reaction.

2. Traces of NMR Spectra for New Compounds

Figure S1 | ^1H NMR spectrum (CDCl_3 , 600 MHz) of *para*-methylphenyl 2-*O*-*ortho*-(azidomethyl)benzoyl-4,6-*O*-benzylidene-3-*O*-*para*-methoxybenzyl-1-thio- β -D-glucopyranoside (18).

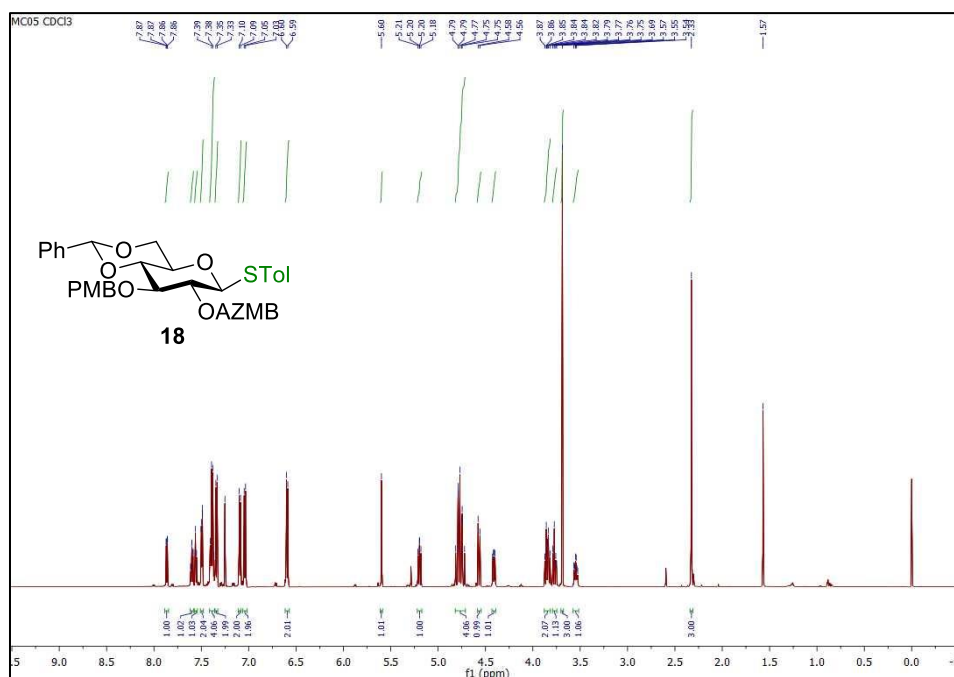


Figure S2 | $^{13}\text{C}\{^1\text{H}\}$ NMR spectrum (CDCl_3 , 150 MHz) of *para*-methylphenyl 2-*O*-*ortho*-(azidomethyl)benzoyl-4,6-*O*-benzylidene-3-*O*-*para*-methoxybenzyl-1-thio- β -D-glucopyranoside (18).

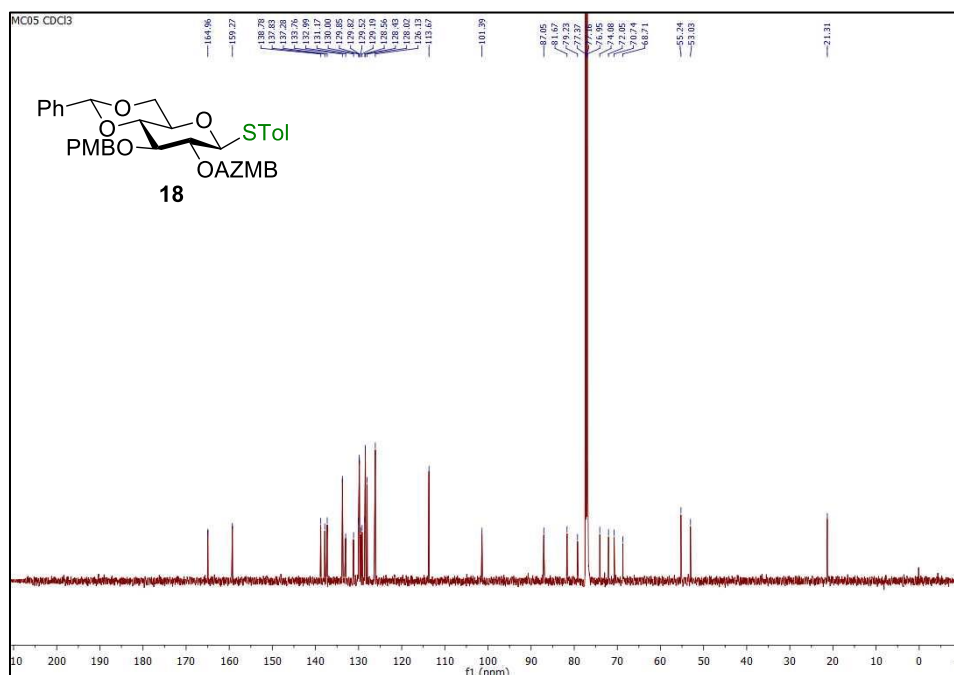


Figure S3 | ^1H NMR spectrum (CDCl_3 , 600 MHz) of *para*-methylphenyl 2-*O*-*ortho*-(azidomethyl)benzoyl-4,6-*O*-benzylidene-1-thio- β -D-glucopyranoside (15).

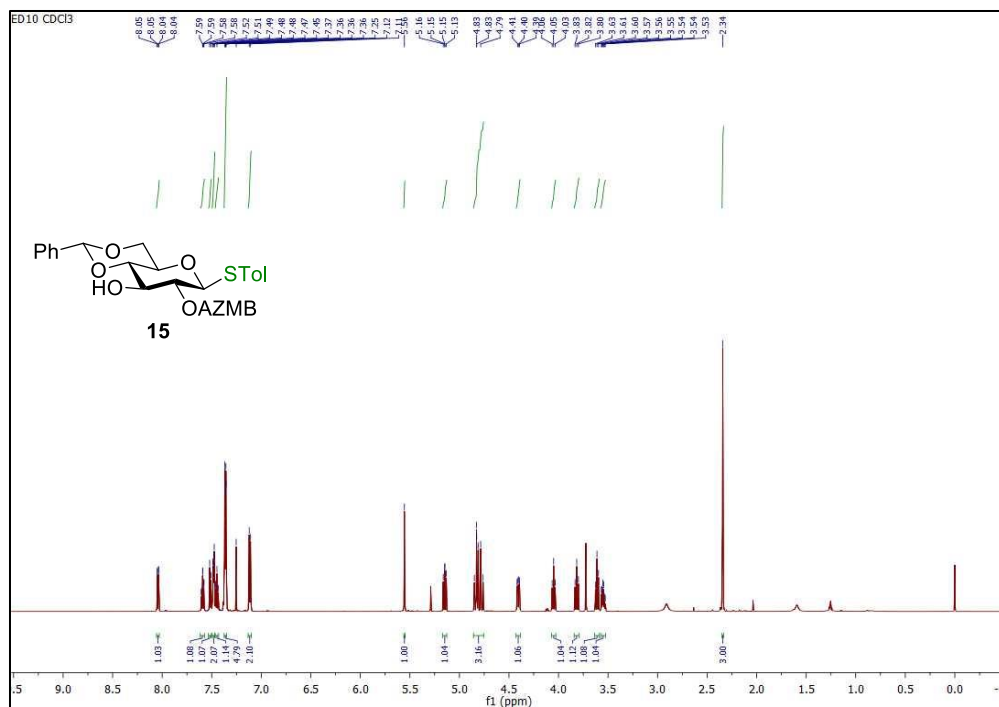


Figure S4 | $^{13}\text{C}\{^1\text{H}\}$ NMR spectrum (CDCl_3 , 150 MHz) of *para*-methylphenyl 2-*O*-*ortho*-(azidomethyl)benzoyl-4,6-*O*-benzylidene-1-thio- β -D-glucopyranoside (15).

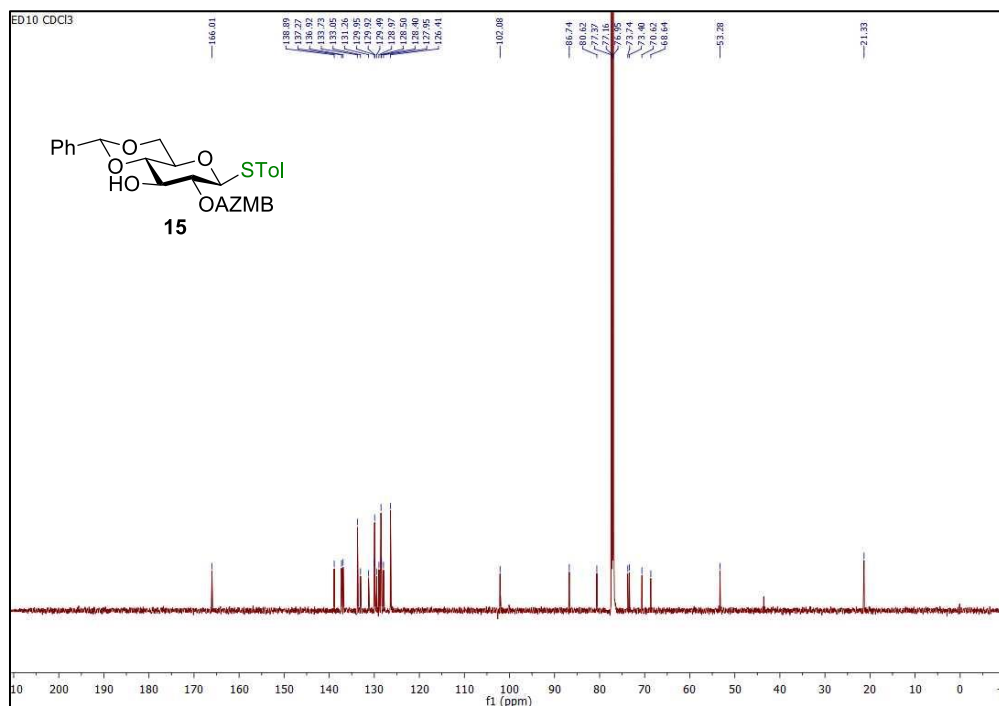


Figure S5 | ^1H NMR spectrum (CDCl_3 , 400 MHz) of allyl 3-*tert*-butyldimethylsilyl-4-*O*-levulinoyl- α -L-rhamnopyranoside.

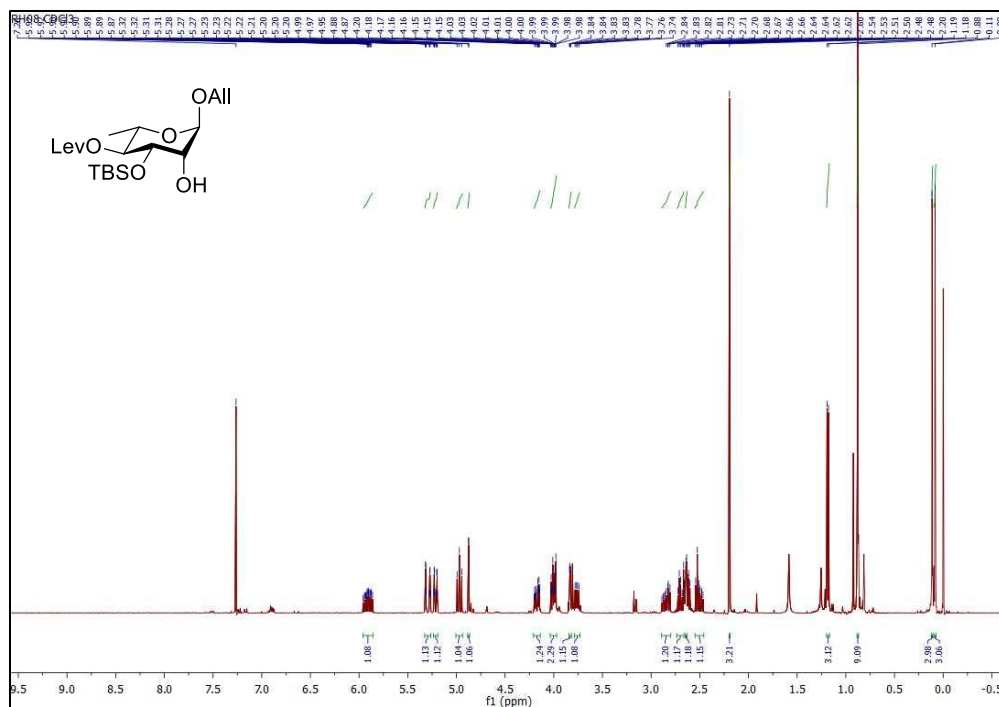


Figure S6 | $^{13}\text{C}\{^1\text{H}\}$ NMR spectrum (CDCl_3 , 100 MHz) of allyl 3-*tert*-butyldimethylsilyl-4-*O*-levulinoyl- α -L-rhamnopyranoside.

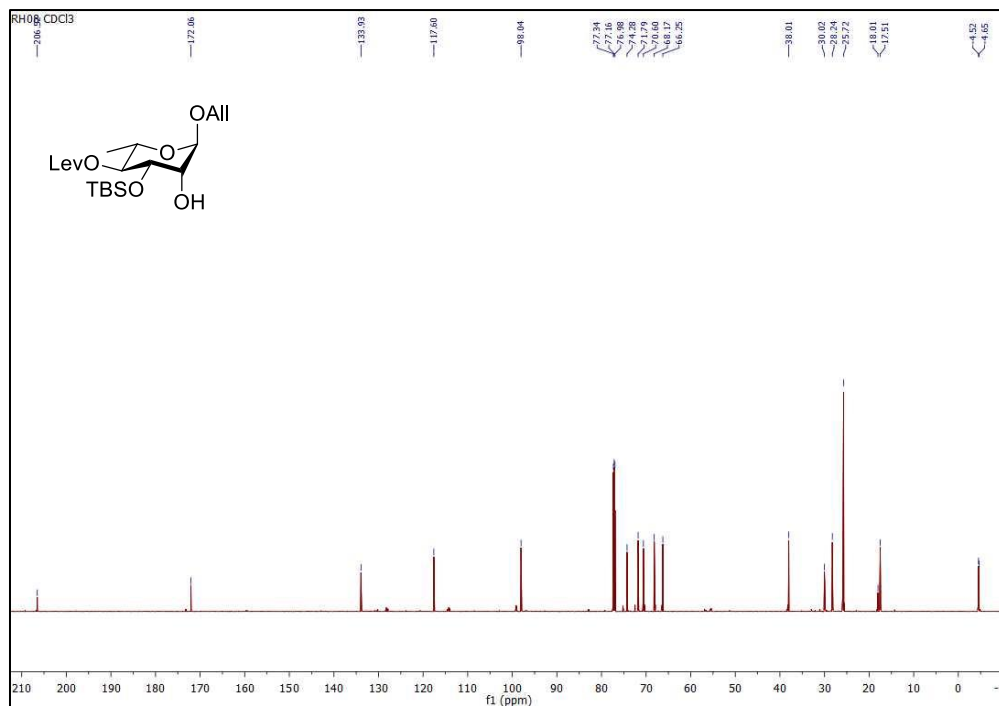


Figure S7 | ^1H NMR spectrum (CDCl_3 , 600 MHz) of allyl 2-O-acetyl-3-O-tert-butylidimethylsilyl-4-O-levulinoyl- α -L-rhamnopyranoside (20).

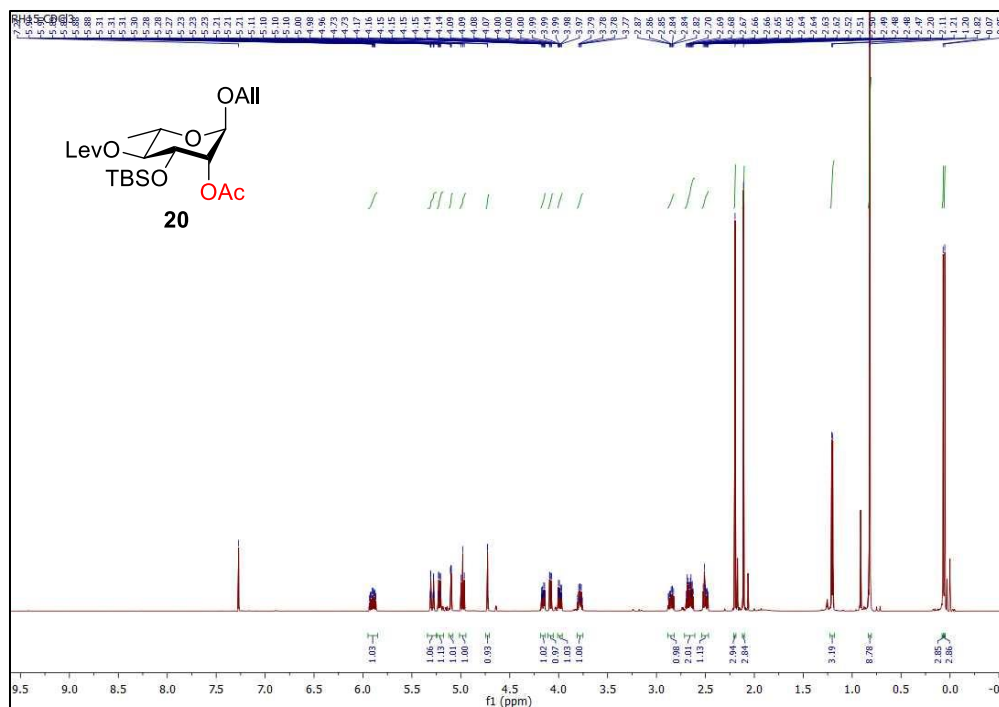


Figure S8 | $^{13}\text{C}\{^1\text{H}\}$ NMR spectrum (CDCl_3 , 150 MHz) of allyl 2-O-acetyl-3-O-tert-butylidimethylsilyl-4-O-levulinoyl- α -L-rhamnopyranoside (20).

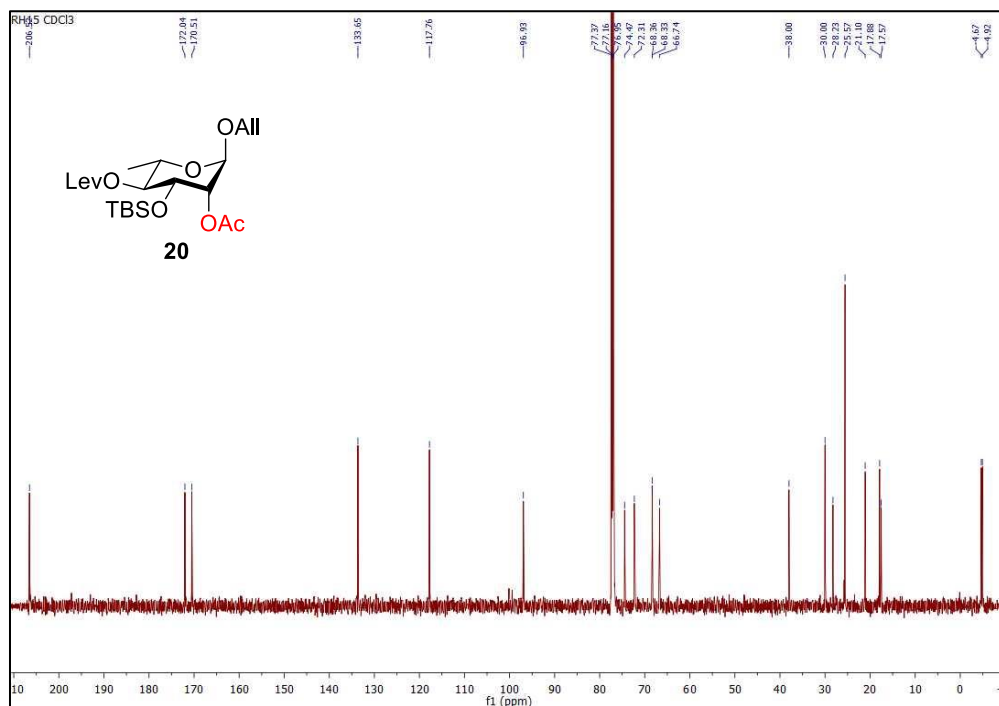


Figure S9 | ^1H NMR spectrum (CDCl_3 , 600 MHz) of 2-*O*-acetyl-3-*O*-*tert*-butyldimethylsilyl-4-*O*-levulinoyl-L-rhamnopyranose (21).

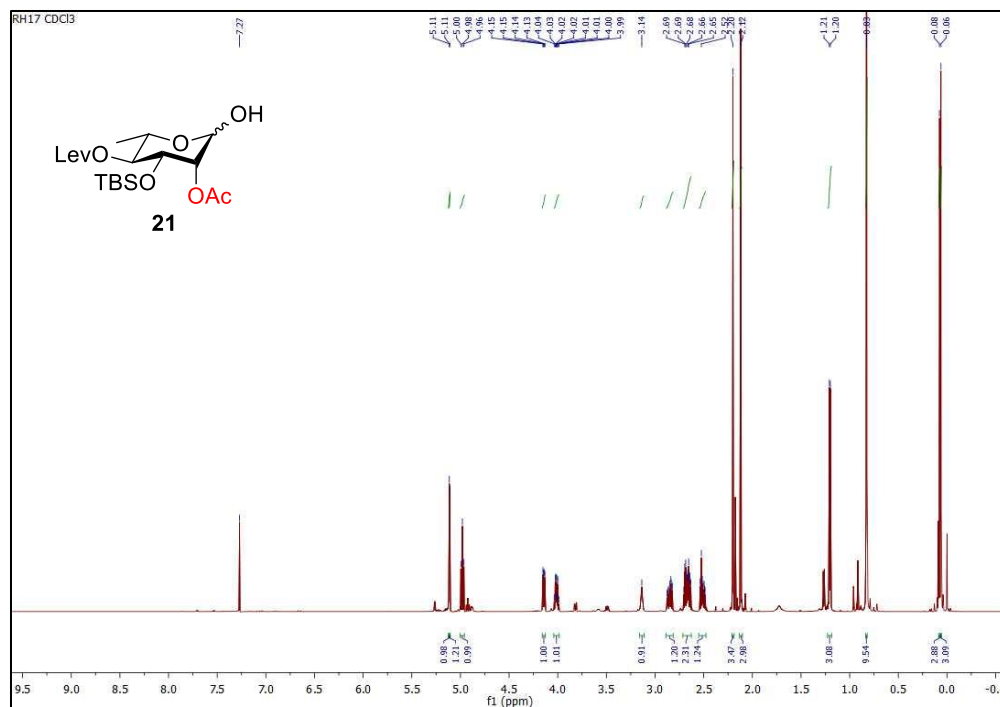


Figure S10 | $^{13}\text{C}\{^1\text{H}\}$ NMR spectrum (CDCl_3 , 150 MHz) of 2-*O*-acetyl-3-*O*-*tert*-butyldimethylsilyl-4-*O*-levulinoyl-L-rhamnopyranose (21).

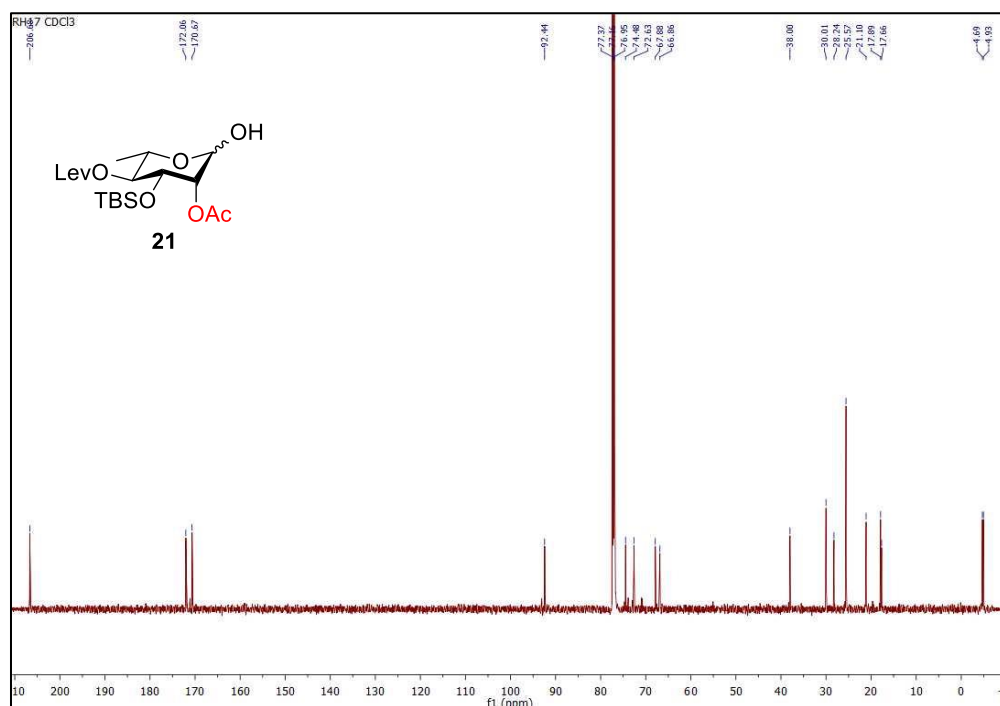


Figure S11 | ^1H NMR spectrum (pyridine- d_5 , 600 MHz) of 2-*O*-acetyl-3-*O*-*tert*-butyldimethylsilyl-4-*O*-levulinoyl- α -L-rhamnopyranosyl 2,2,2-trichloroacetimidate (13).

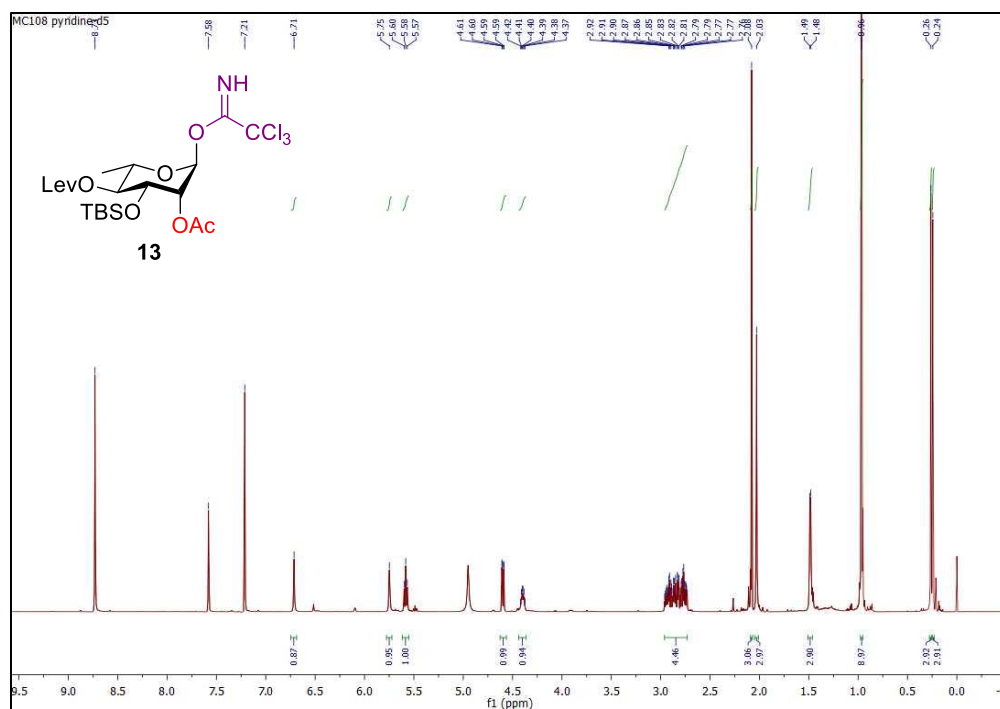


Figure S12 | $^{13}\text{C}\{^1\text{H}\}$ NMR spectrum (pyridine- d_5 , 150 MHz) of 2-*O*-acetyl-3-*O*-*tert*-butyldimethylsilyl-4-*O*-levulinoyl- α -L-rhamnopyranosyl 2,2,2-trichloroacetimidate (13).

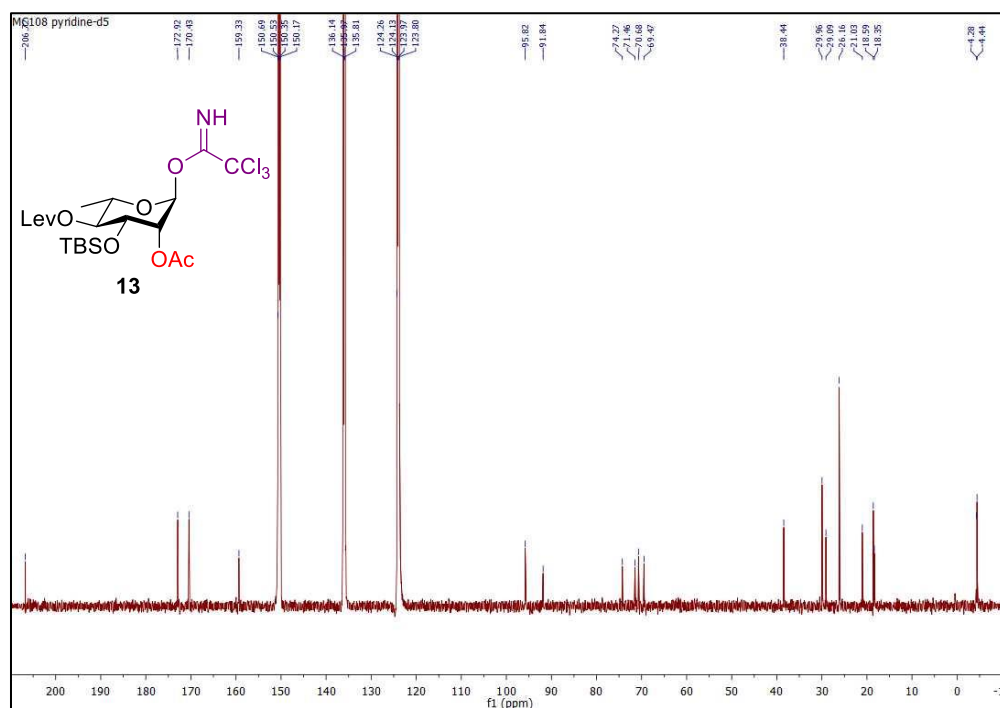


Figure S13 | ^1H NMR spectrum (CDCl_3 , 600 MHz) of (5-azido-1-pentyl) 2-O-acetyl-3-O-tert-butylidimethylsilyl-4-O-levulinoyl- α -L-rhamnopyranosyl-(1 \rightarrow 3)-2-O-benzyl-4,6-O-benzylidene- β -D-glucopyranoside (22).

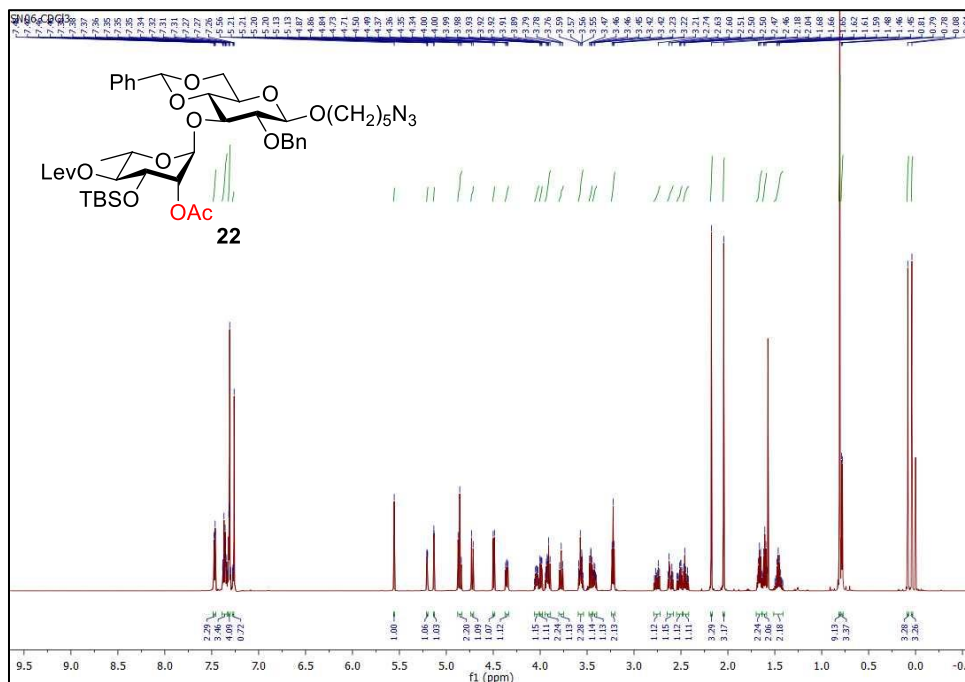


Figure S14 | $^{13}\text{C}\{^1\text{H}\}$ NMR spectrum (CDCl_3 , 150 MHz) of (5-azido-1-pentyl) 2-O-acetyl-3-O-tert-butylidimethylsilyl-4-O-levulinoyl- α -L-rhamnopyranosyl-(1 \rightarrow 3)-2-O-benzyl-4,6-O-benzylidene- β -D-glucopyranoside (22).

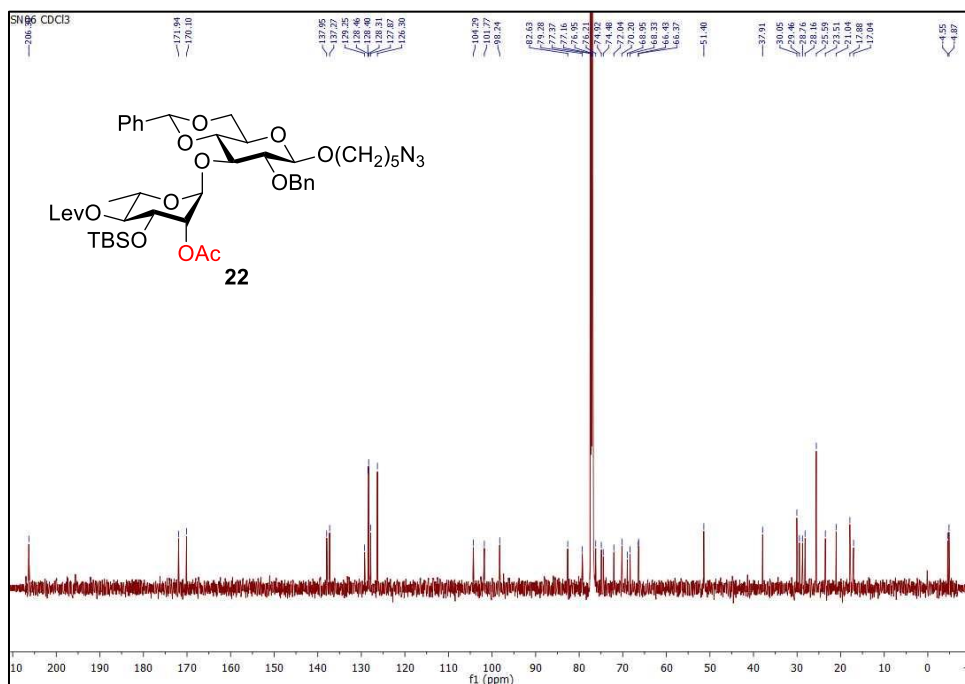


Figure S15 | ^1H NMR spectrum (CDCl_3 , 600 MHz) of *para*-methylphenyl 4-*O*-levulinoyl-2,3-*O*-isopropylidene-1-thio- α -L-rhamnopyranoside.

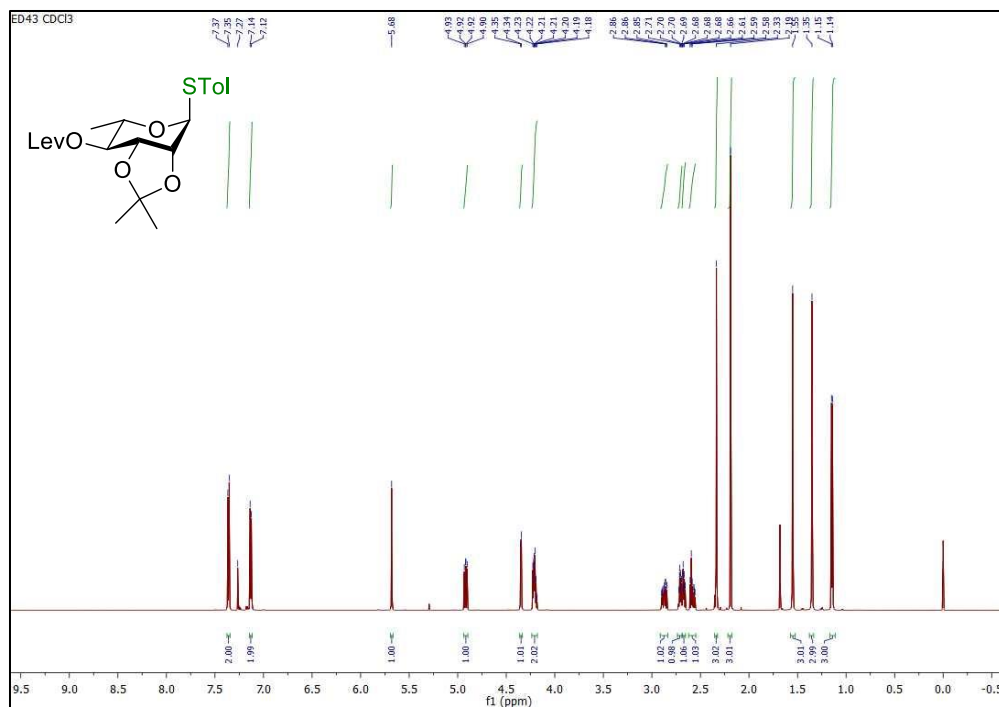


Figure S16 | $^{13}\text{C}\{^1\text{H}\}$ NMR spectrum (CDCl_3 , 150 MHz) of *para*-methylphenyl 4-*O*-levulinoyl-2,3-*O*-isopropylidene-1-thio- α -L-rhamnopyranoside.

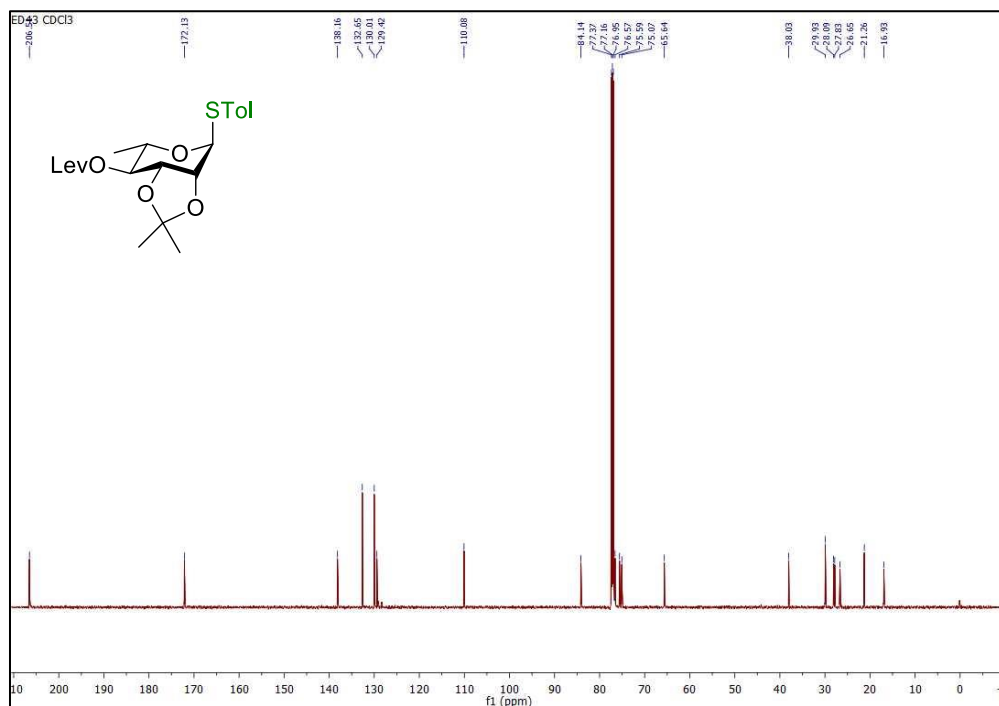


Figure S19 | ^1H NMR spectrum (CDCl_3 , 600 MHz) of *para*-methylphenyl 4-*O*-levulinoyl-3-*O*-*para*-methoxybenzyl-1-thio- α -L-rhamnopyranoside.

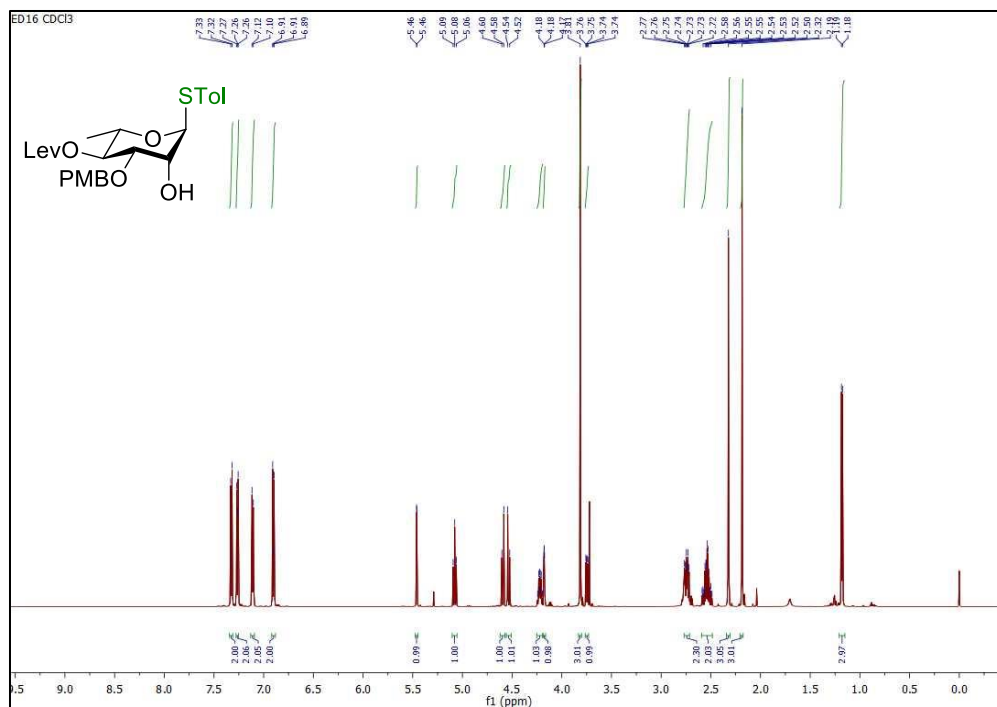


Figure S20 | $^{13}\text{C}\{^1\text{H}\}$ NMR spectrum (CDCl_3 , 150 MHz) of *para*-methylphenyl 4-*O*-levulinoyl-3-*O*-*para*-methoxybenzyl-1-thio- α -L-rhamnopyranoside.

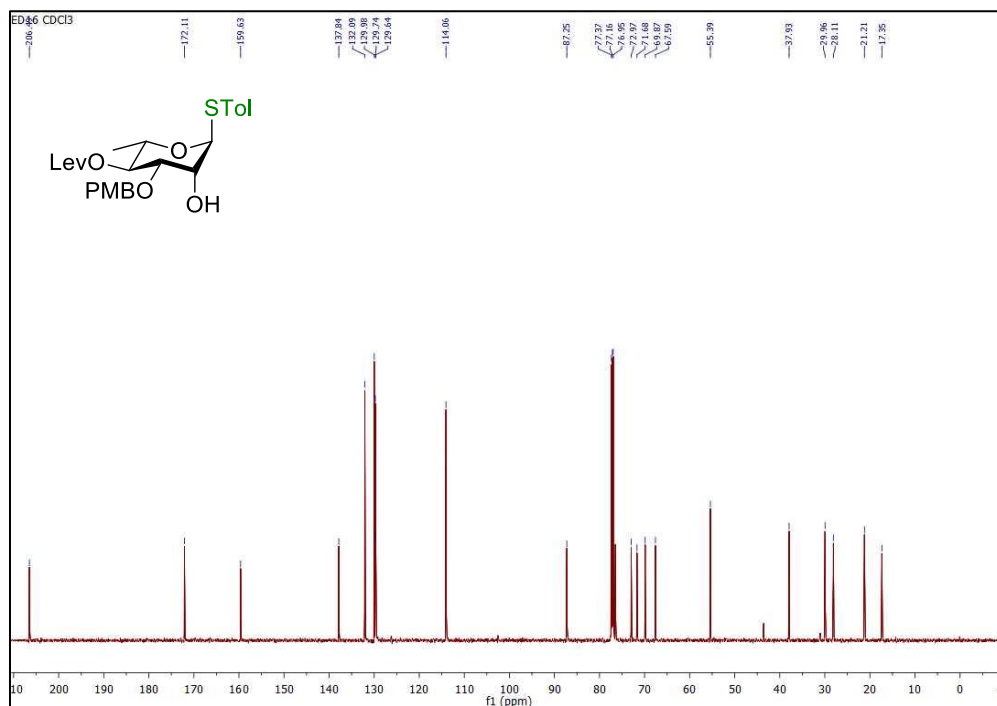


Figure S21 | ^1H NMR spectrum (CDCl_3 , 600 MHz) of *para*-methylphenyl 2-*O*-acetyl-4-*O*-levulinoyl-3-*O*-*para*-methoxybenzyl-1-thio- α -L-rhamnopyranoside (25).

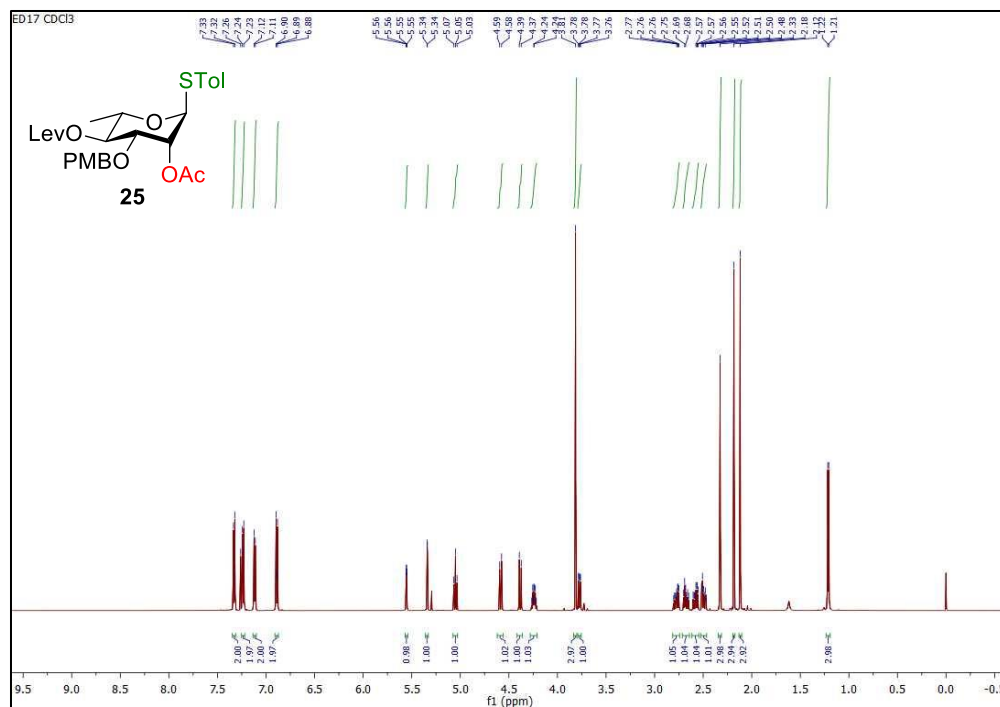


Figure S22 | $^{13}\text{C}\{^1\text{H}\}$ NMR spectrum (CDCl_3 , 150 MHz) of *para*-methylphenyl 2-*O*-acetyl-4-*O*-levulinoyl-3-*O*-*para*-methoxybenzyl-1-thio- α -L-rhamnopyranoside (25).

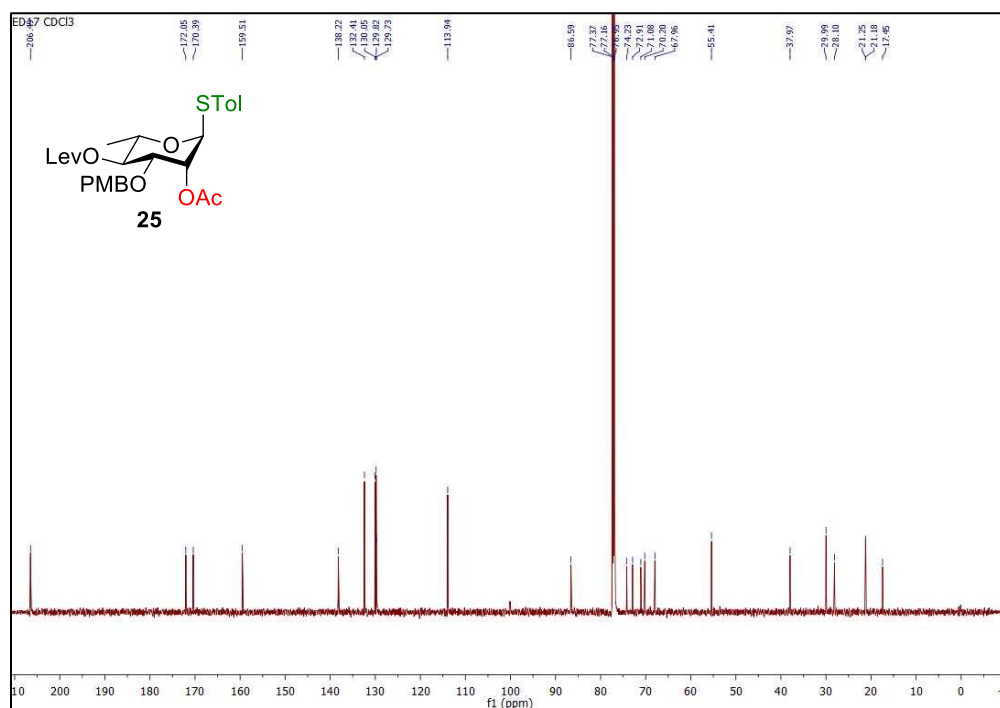


Figure S23 | ^1H NMR spectrum (CDCl_3 , 600 MHz) of (5-azido-1-pentyl) 2-*O*-acetyl-4-*O*-levulinoyl-3-*O*-*para*-methoxybenzyl- α -L-rhamnopyranosyl-(1 \rightarrow 3)-2-*O*-benzyl-4,6-*O*-benzylidene- β -D-glucopyranoside (26).

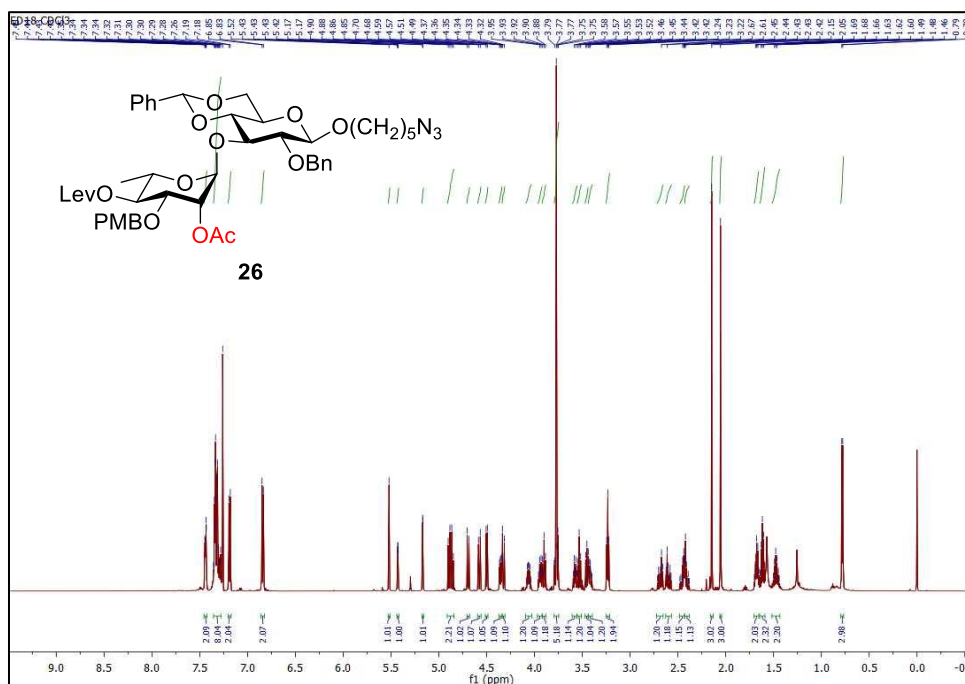


Figure S24 | $^{13}\text{C}\{^1\text{H}\}$ NMR spectrum (CDCl_3 , 150 MHz) of (5-azido-1-pentyl) 2-*O*-acetyl-4-*O*-levulinoyl-3-*O*-*para*-methoxybenzyl- α -L-rhamnopyranosyl-(1 \rightarrow 3)-2-*O*-benzyl-4,6-*O*-benzylidene- β -D-glucopyranoside (26).

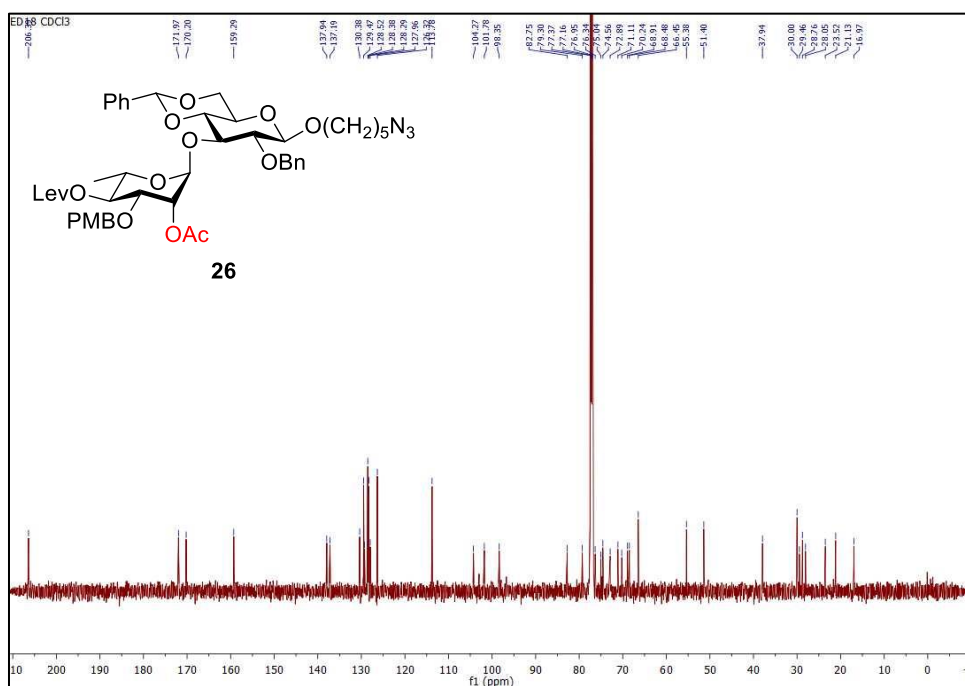


Figure S25 | ^1H NMR spectrum (CDCl_3 , 600 MHz) of (5-azido-1-pentyl) 2-*O*-acetyl-4-*O*-levulinoyl- α -L-rhamnopyranosyl-(1 \rightarrow 3)-2-*O*-benzyl-4,6-*O*-benzylidene- β -D-glucopyranoside (12).

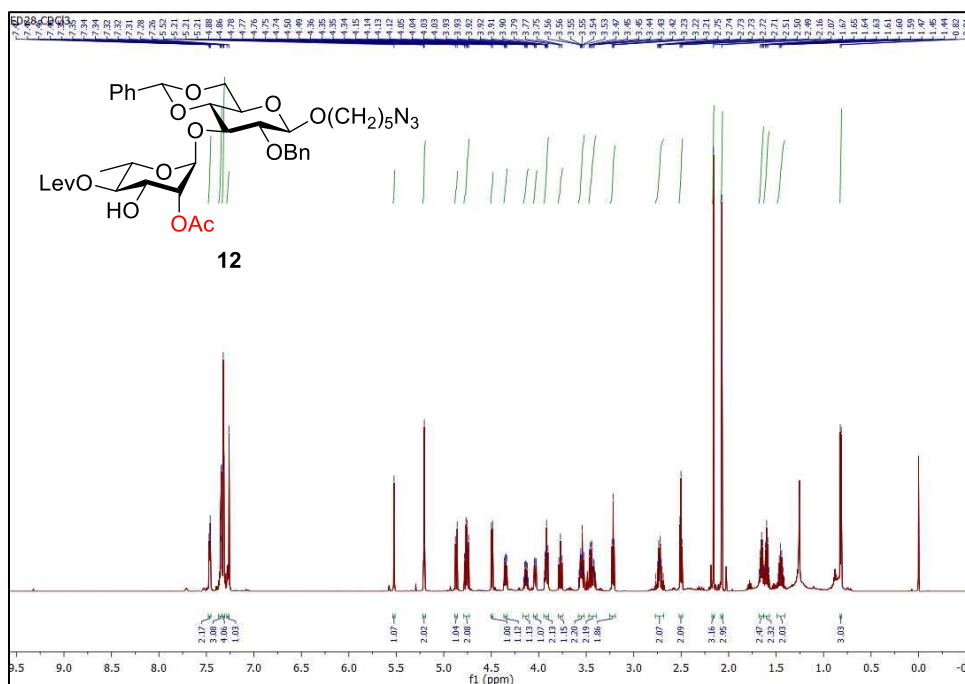


Figure S26 | $^{13}\text{C}\{^1\text{H}\}$ NMR spectrum (CDCl_3 , 150 MHz) of (5-azido-1-pentyl) 2-*O*-acetyl-4-*O*-levulinoyl- α -L-rhamnopyranosyl-(1 \rightarrow 3)-2-*O*-benzyl-4,6-*O*-benzylidene- β -D-glucopyranoside (12).

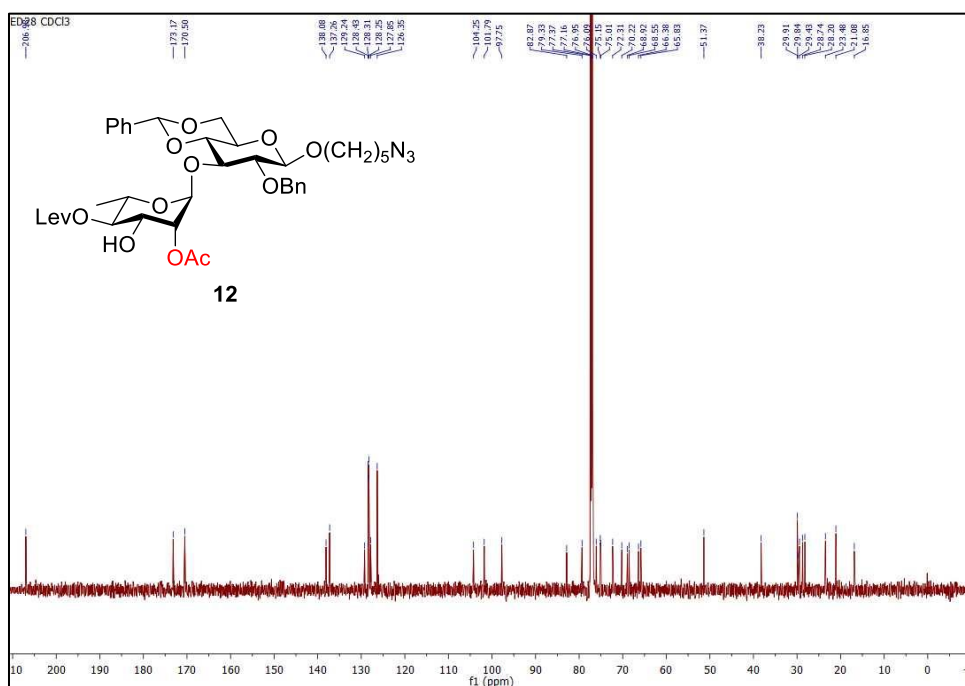


Figure S27 | ^1H NMR spectrum (CDCl_3 , 600 MHz) of (5-azido-1-pentyl) 2-*O*-ortho-(azidomethyl)benzoyl-4,6-*O*-benzylidene-3-*O*-*para*-methoxybenzyl- β -D-glucopyranosyl-(1 \rightarrow 3)-2-*O*-acetyl-4-*O*-levulinoyl- α -L-rhamnopyranosyl-(1 \rightarrow 3)-2-*O*-benzyl-4,6-*O*-benzylidene- β -D-glucopyranoside (27) (+ 10% of unknown inseparable impurity).

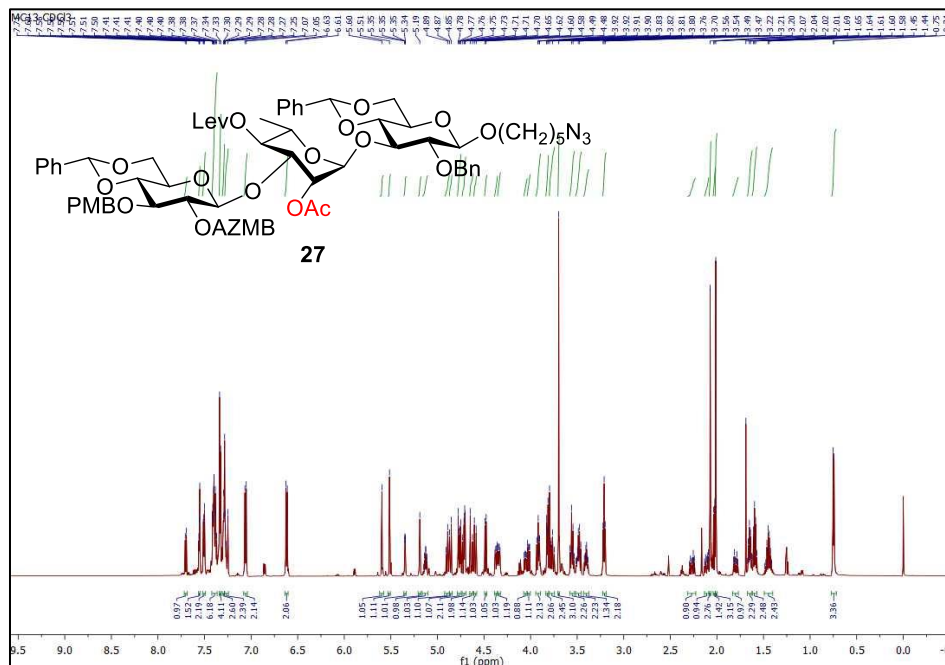


Figure S28 | $^{13}\text{C}\{^1\text{H}\}$ NMR spectrum (CDCl_3 , 150 MHz) of (5-azido-1-pentyl) 2-*O*-ortho-(azidomethyl)benzoyl-4,6-*O*-benzylidene-3-*O*-*para*-methoxybenzyl- β -D-glucopyranosyl-(1 \rightarrow 3)-2-*O*-acetyl-4-*O*-levulinoyl- α -L-rhamnopyranosyl-(1 \rightarrow 3)-2-*O*-benzyl-4,6-*O*-benzylidene- β -D-glucopyranoside (27) (+ 10% of unknown inseparable impurity).

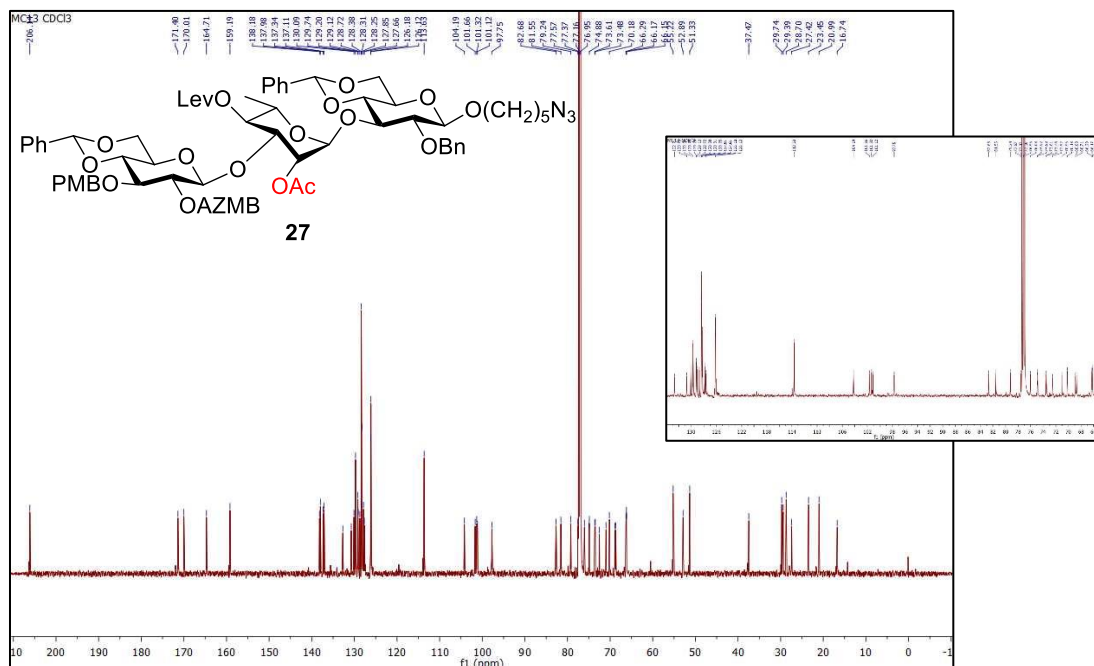


Figure S29 | ^1H NMR spectrum (CDCl_3 , 600 MHz) of (5-azido-1-pentyl) 2-*O*-ortho-(azidomethyl)benzoyl-4,6-*O*-benzylidene- β -D-glucopyranosyl-(1 \rightarrow 3)-2-*O*-acetyl-4-*O*-levulinoyl- α -L-rhamnopyranosyl-(1 \rightarrow 3)-2-*O*-benzyl-4,6-*O*-benzylidene- β -D-glucopyranoside (28).

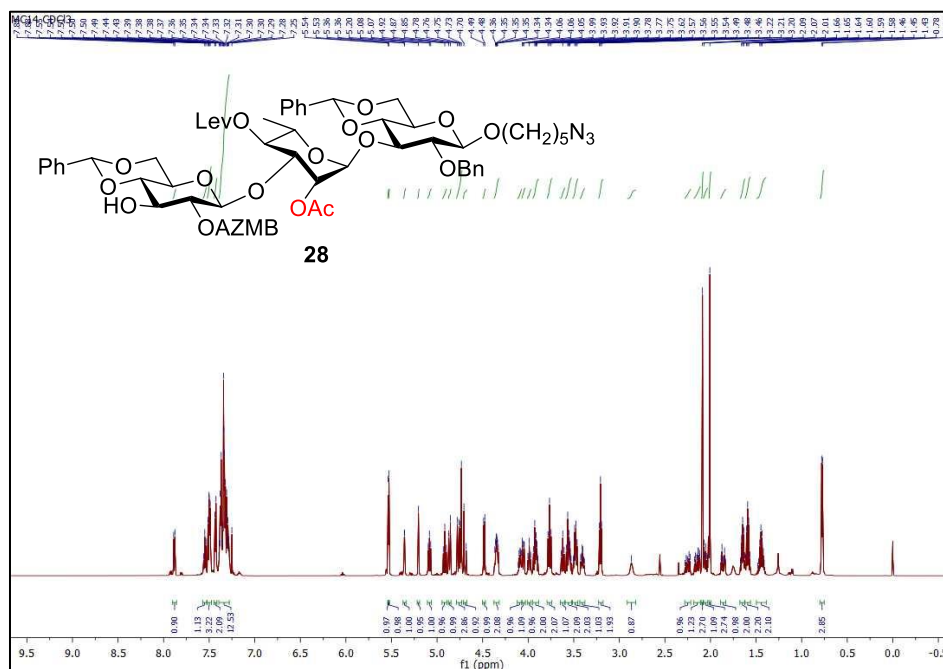


Figure S30 | $^{13}\text{C}\{^1\text{H}\}$ NMR spectrum (CDCl_3 , 150 MHz) of (5-azido-1-pentyl) 2-*O*-ortho-(azidomethyl)benzoyl-4,6-*O*-benzylidene- β -D-glucopyranosyl-(1 \rightarrow 3)-2-*O*-acetyl-4-*O*-levulinoyl- α -L-rhamnopyranosyl-(1 \rightarrow 3)-2-*O*-benzyl-4,6-*O*-benzylidene- β -D-glucopyranoside (28).

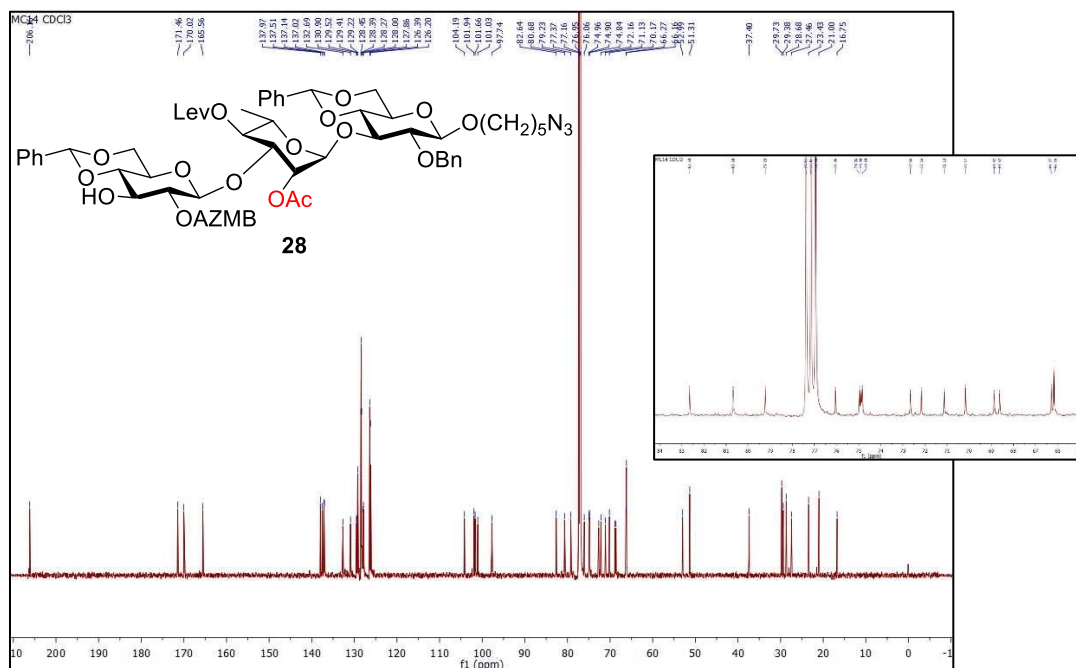


Figure S31 | ^1H NMR spectrum (CDCl_3 , 600 MHz) of *para*-methylphenyl 4-*O*-levulinoyl-3-*O*-methyl-1-thio- α -L-rhamnopyranoside.

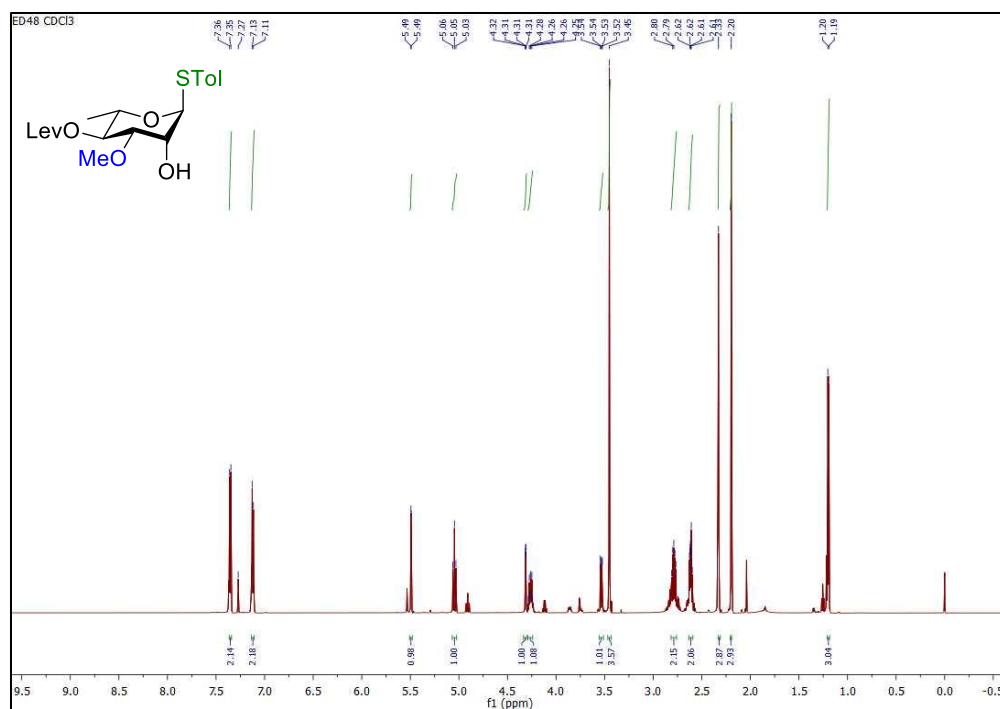


Figure S32 | $^{13}\text{C}\{^1\text{H}\}$ NMR spectrum (CDCl_3 , 150 MHz) of *para*-methylphenyl 4-*O*-levulinoyl-3-*O*-methyl-1-thio- α -L-rhamnopyranoside.

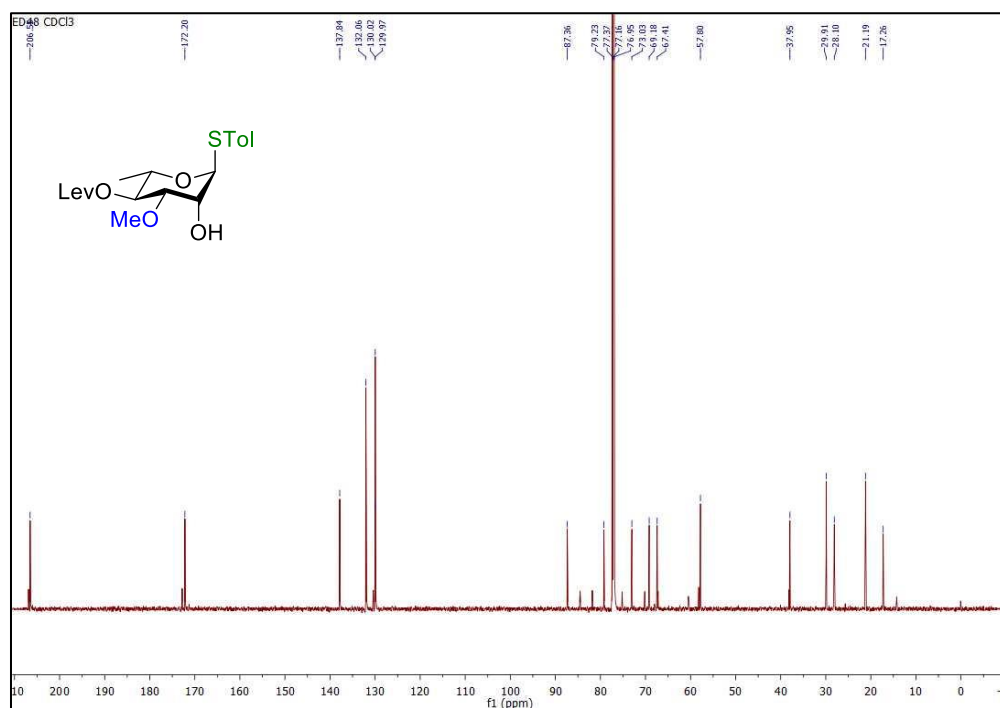


Figure S33 | ^1H NMR spectrum (CDCl_3 , 600 MHz) of *para*-methylphenyl 2-*O*-acetyl-4-*O*-levulinoyl-3-*O*-methyl-1-thio- α -L-rhamnopyranoside (29).

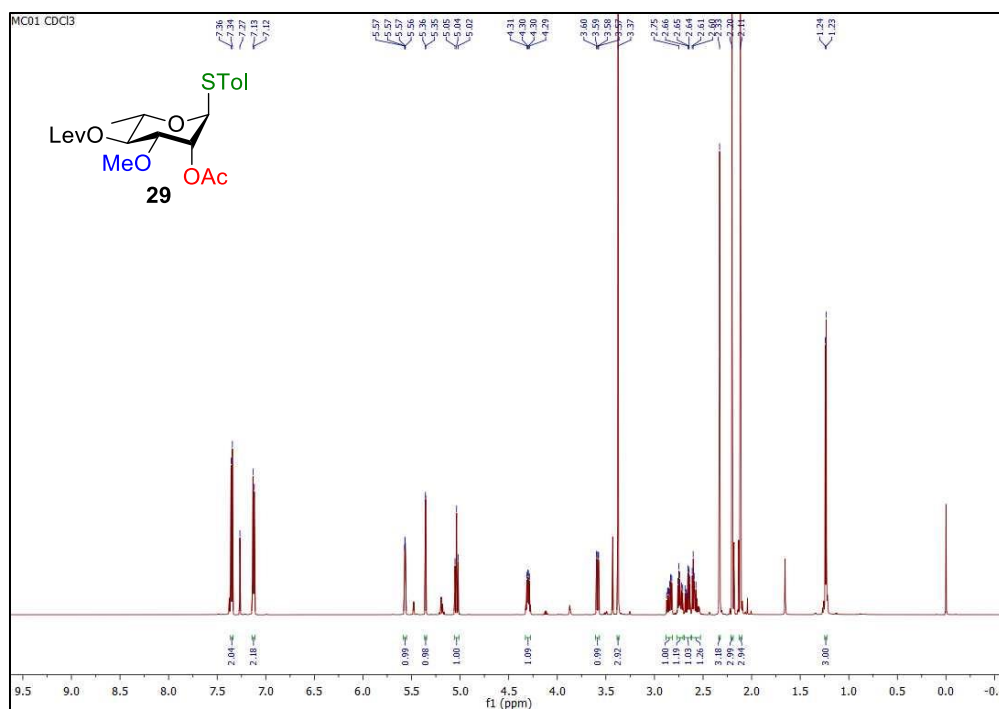


Figure S34 | $^{13}\text{C}\{^1\text{H}\}$ NMR spectrum (CDCl_3 , 150 MHz) of *para*-methylphenyl 2-*O*-acetyl-4-*O*-levulinoyl-3-*O*-methyl-1-thio- α -L-rhamnopyranoside (29).

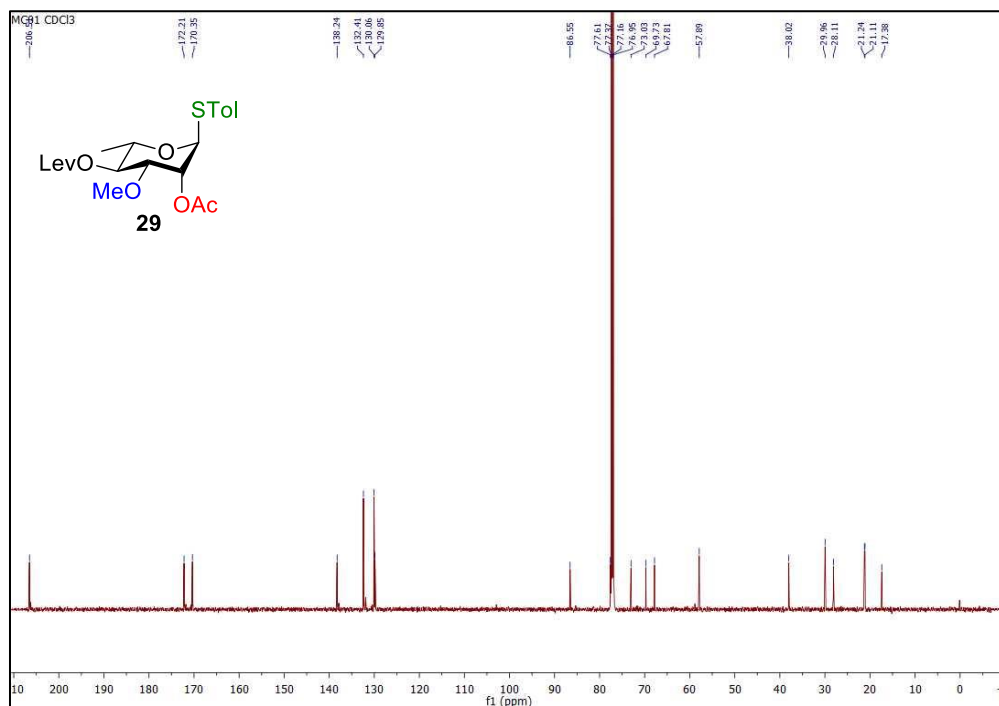


Figure S35 | ^1H NMR spectrum (CDCl_3 , 600 MHz) of (5-azido-1-pentyl) 2-*O*-acetyl-4-*O*-levulinoyl-3-*O*-methyl- α -L-rhamnopyranosyl-(1 \rightarrow 3)-2-*O*-ortho-(azidomethyl)benzoyl-4,6-*O*-benzylidene- β -D-glucopyranosyl-(1 \rightarrow 3)-2-*O*-acetyl-4-*O*-levulinoyl- α -L-rhamnopyranosyl-(1 \rightarrow 3)-2-*O*-benzyl-4,6-*O*-benzylidene- β -D-glucopyranoside (10) (+ 12% of unknown inseparable impurity).

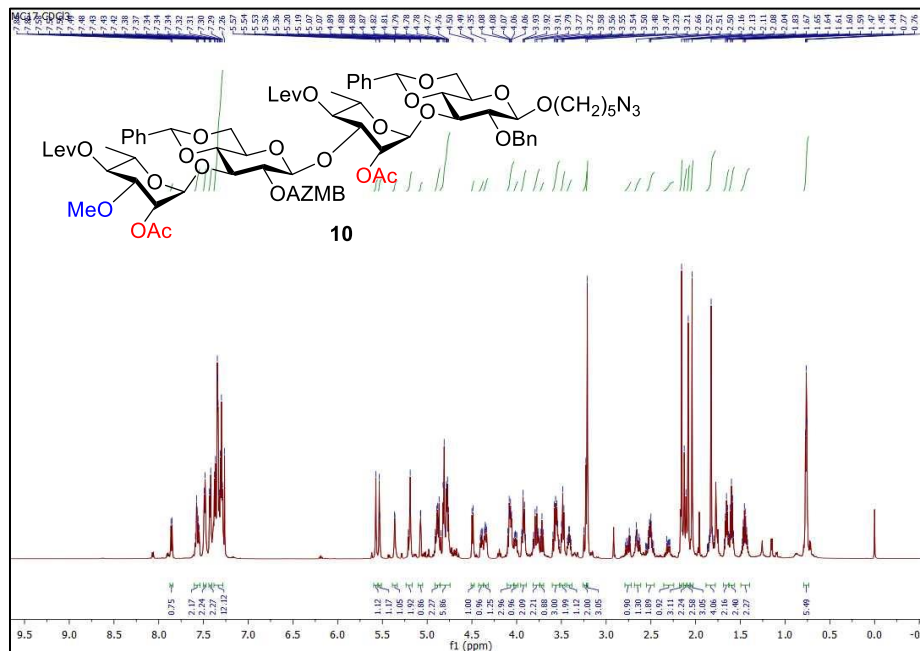


Figure S36 | $^{13}\text{C}\{^1\text{H}\}$ NMR spectrum (CDCl_3 , 150 MHz) of (5-azido-1-pentyl) 2-*O*-acetyl-4-*O*-levulinoyl-3-*O*-methyl- α -L-rhamnopyranosyl-(1 \rightarrow 3)-2-*O*-ortho-(azidomethyl)benzoyl-4,6-*O*-benzylidene- β -D-glucopyranosyl-(1 \rightarrow 3)-2-*O*-acetyl-4-*O*-levulinoyl- α -L-rhamnopyranosyl-(1 \rightarrow 3)-2-*O*-benzyl-4,6-*O*-benzylidene- β -D-glucopyranoside (10) (+ 12% of unknown inseparable impurity).

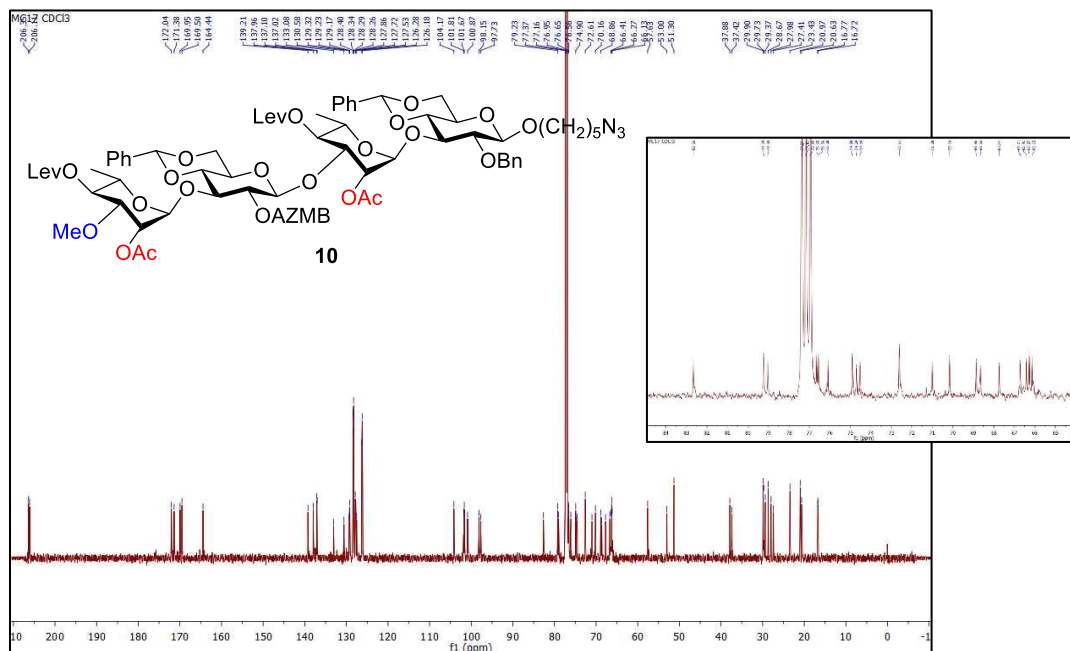


Figure S37 | ^1H NMR spectrum (CDCl_3 , 600 MHz) of (5-azido-1-pentyl) 2-*O*-acetyl-3-*O*-methyl- α -L-rhamnopyranosyl-(1 \rightarrow 3)-2-*O*-ortho-(azidomethyl)benzoyl-4,6-*O*-benzylidene- β -D-glucopyranosyl-(1 \rightarrow 3)-2-*O*-acetyl- α -L-rhamnopyranosyl-(1 \rightarrow 3)-2-*O*-benzyl-4,6-*O*-benzylidene- β -D-glucopyranoside (**30**).

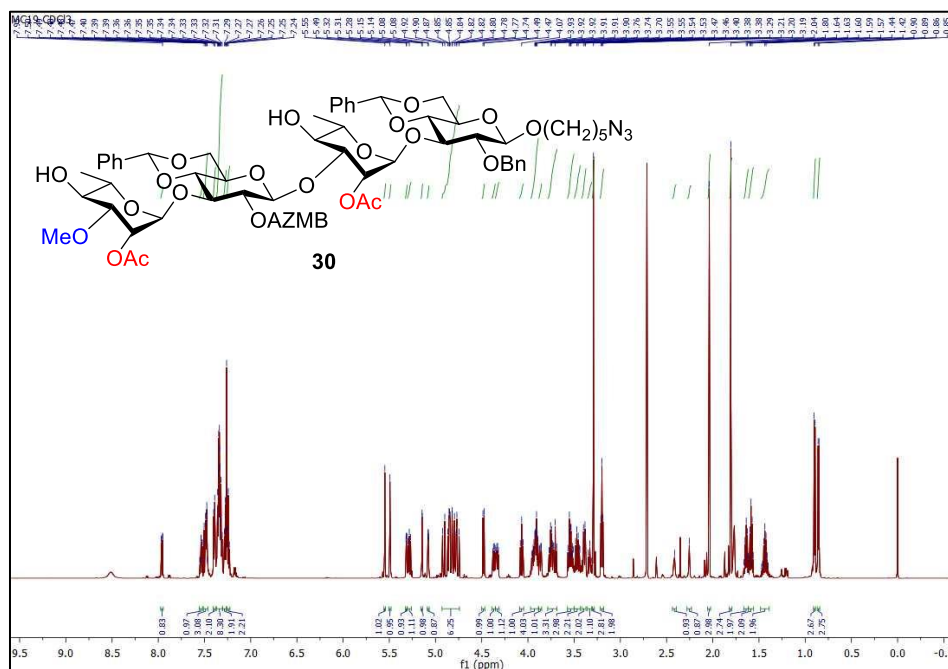


Figure S38 | $^{13}\text{C}\{^1\text{H}\}$ NMR spectrum (CDCl_3 , 150 MHz) of (5-azido-1-pentyl) 2-*O*-acetyl-3-*O*-methyl- α -L-rhamnopyranosyl-(1 \rightarrow 3)-2-*O*-ortho-(azidomethyl)benzoyl-4,6-*O*-benzylidene- β -D-glucopyranosyl-(1 \rightarrow 3)-2-*O*-acetyl- α -L-rhamnopyranosyl-(1 \rightarrow 3)-2-*O*-benzyl-4,6-*O*-benzylidene- β -D-glucopyranoside (**30**).

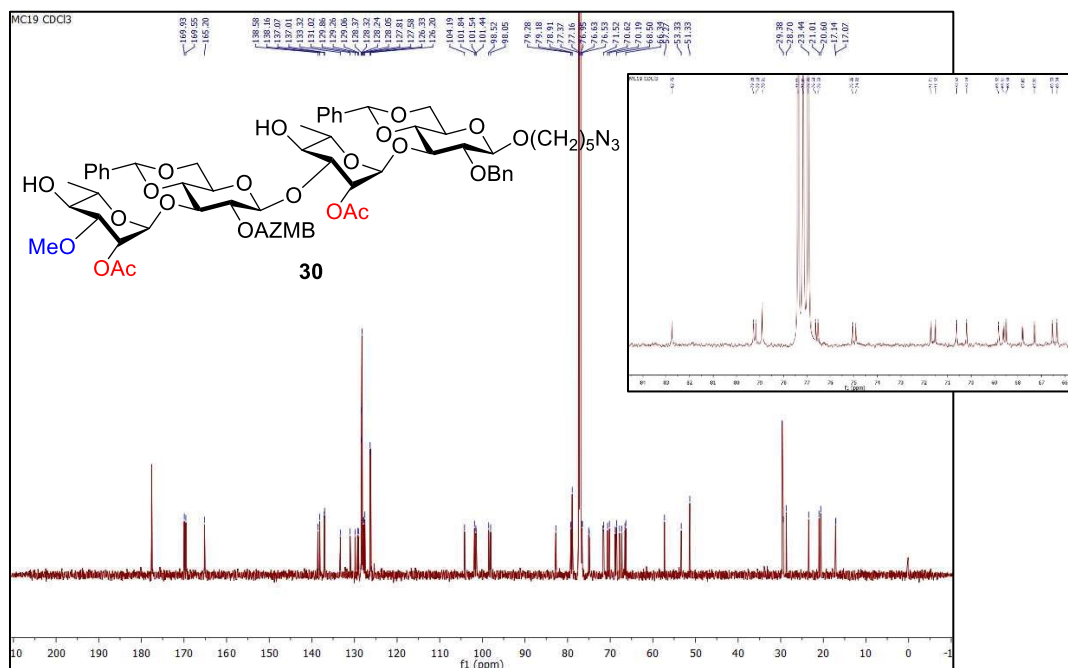


Figure S39 | ^1H NMR spectrum (CDCl_3 , 600 MHz) of *para*-methylphenyl 2-*O*-acetyl-3-*O*-methyl-1-thio- α -L-rhamnopyranoside (32).

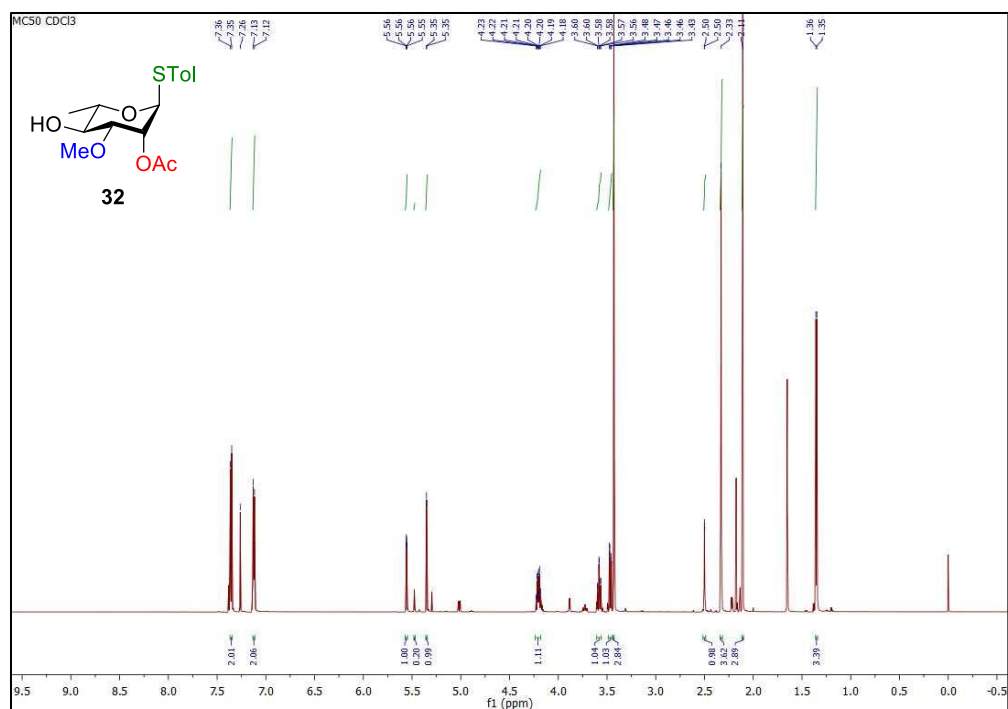


Figure S40 | $^{13}\text{C}\{^1\text{H}\}$ NMR spectrum (CDCl_3 , 150 MHz) of *para*-methylphenyl 2-*O*-acetyl-3-*O*-methyl-1-thio- α -L-rhamnopyranoside (32).

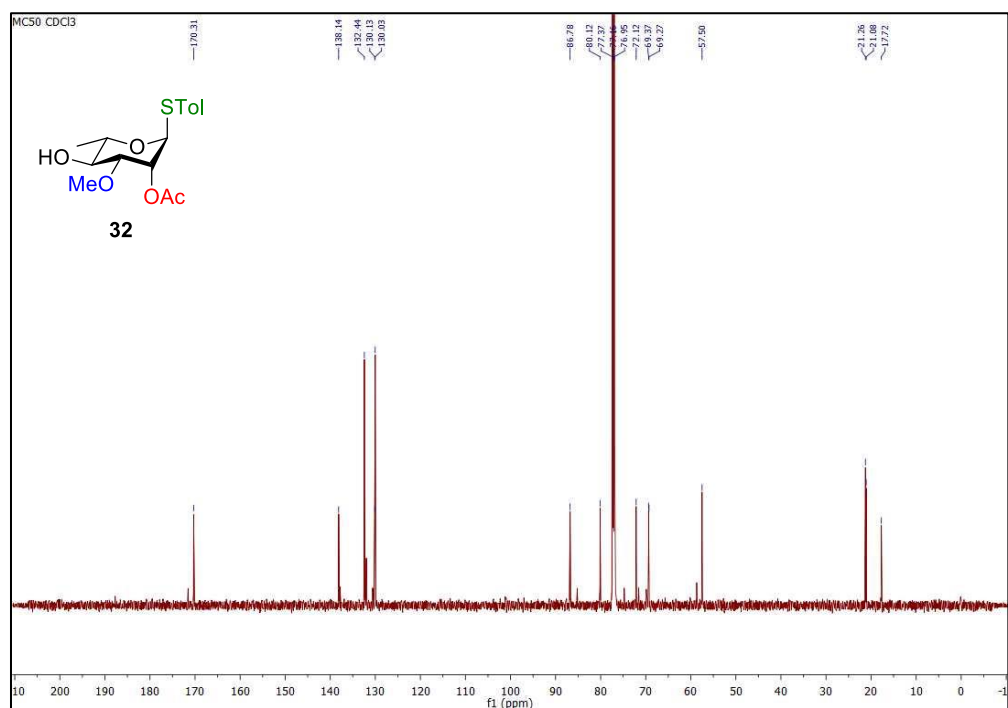


Figure S41 | ^1H NMR spectrum (CDCl_3 , 600 MHz) of *para*-methylphenyl 2-*O*-acetyl-6-deoxy-3-*O*-methyl-1-thio- α -L-talopyranoside (33).

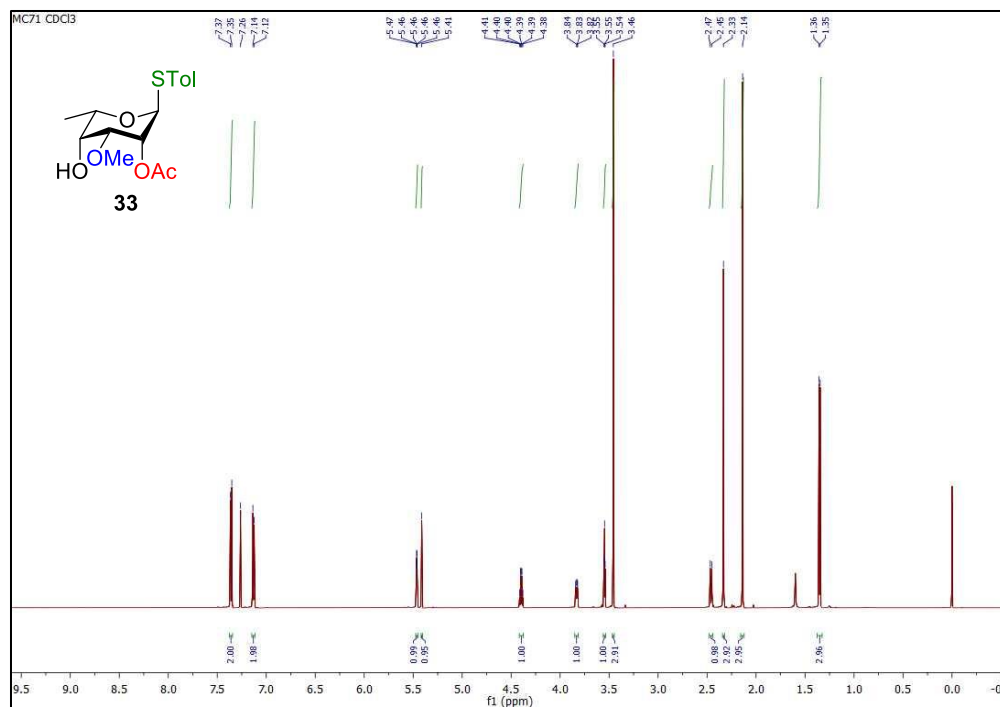


Figure S42 | $^{13}\text{C}\{^1\text{H}\}$ NMR spectrum (CDCl_3 , 150 MHz) of *para*-methylphenyl 2-*O*-acetyl-6-deoxy-3-*O*-methyl-1-thio- α -L-talopyranoside (33).

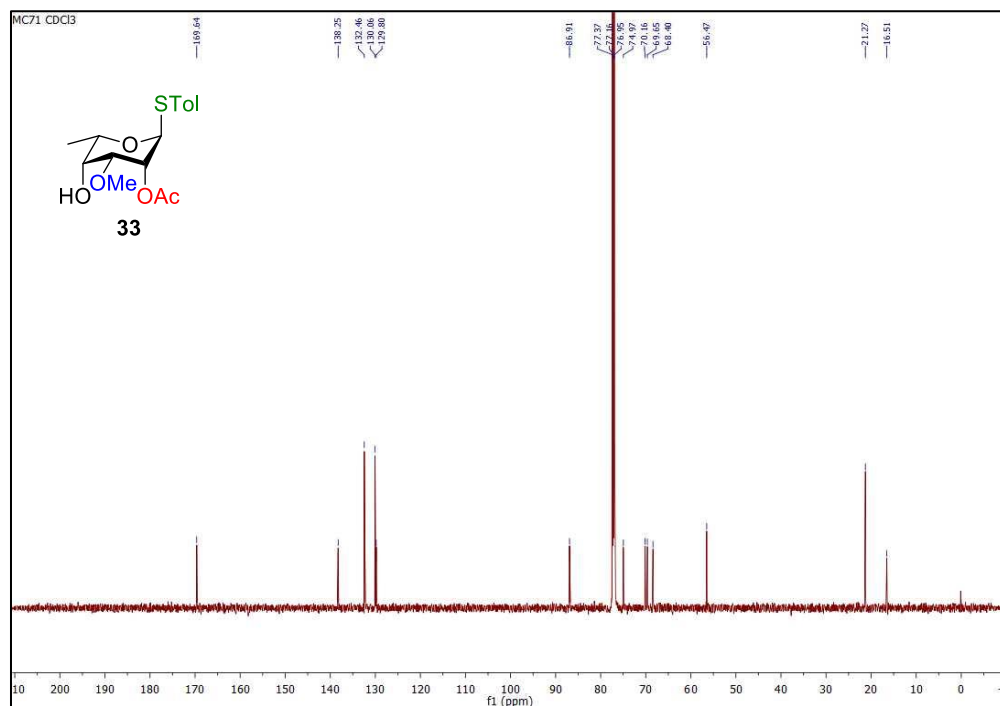


Figure S43 | ^1H NMR spectrum (CDCl_3 , 600 MHz) of *para*-methylphenyl 2,4-di-*O*-acetyl-6-deoxy-3-*O*-methyl-1-thio- α -L-talopyranoside (**34**).

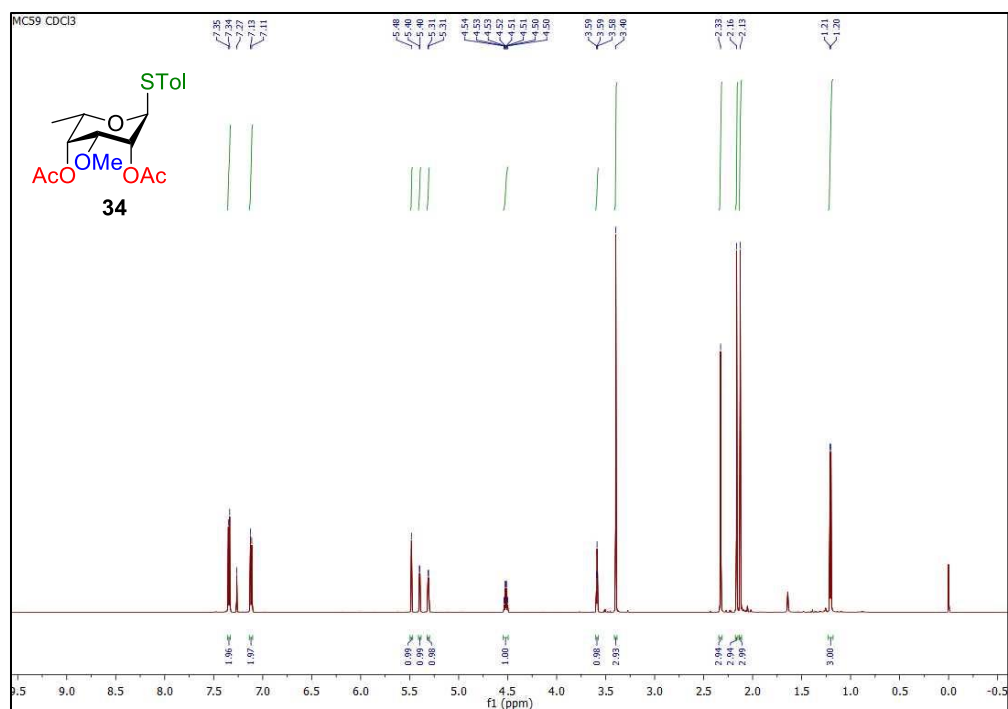


Figure S44 | $^{13}\text{C}\{^1\text{H}\}$ NMR spectrum (CDCl_3 , 150 MHz) of *para*-methylphenyl 2,4-di-*O*-acetyl-6-deoxy-3-*O*-methyl-1-thio- α -L-talopyranoside (**34**).

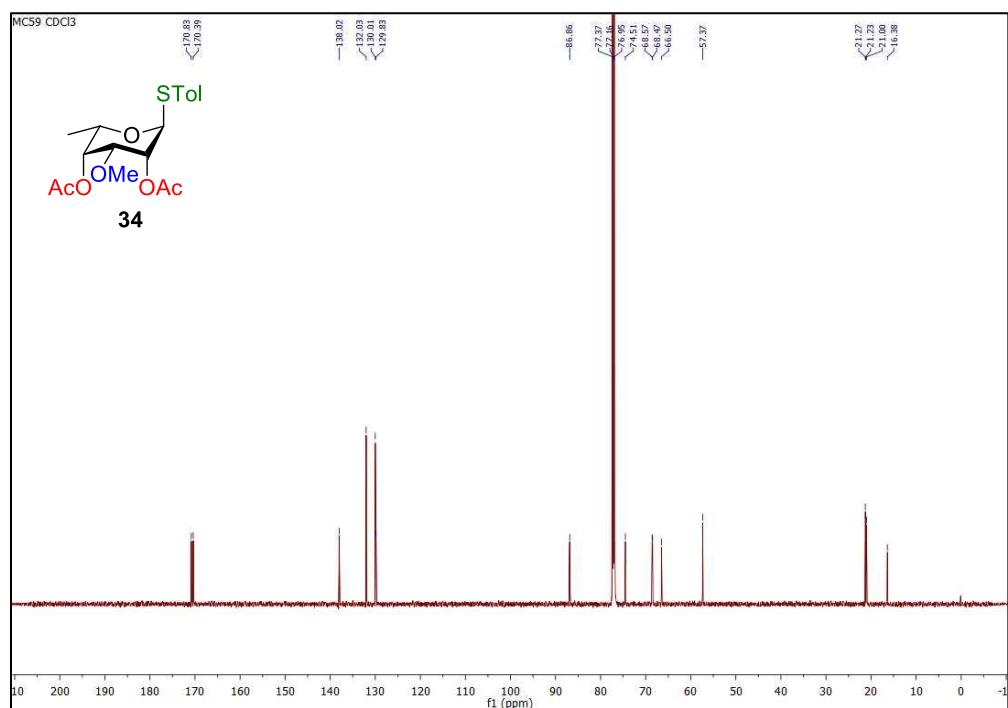


Figure S45 | ^1H NMR spectrum (CDCl_3 , 600 MHz) of *para*-methylphenyl 2-*O*-acetyl-4-*O*-chloroacetyl-6-deoxy-3-*O*-methyl-1-thio- α -L-talopyranoside (35).

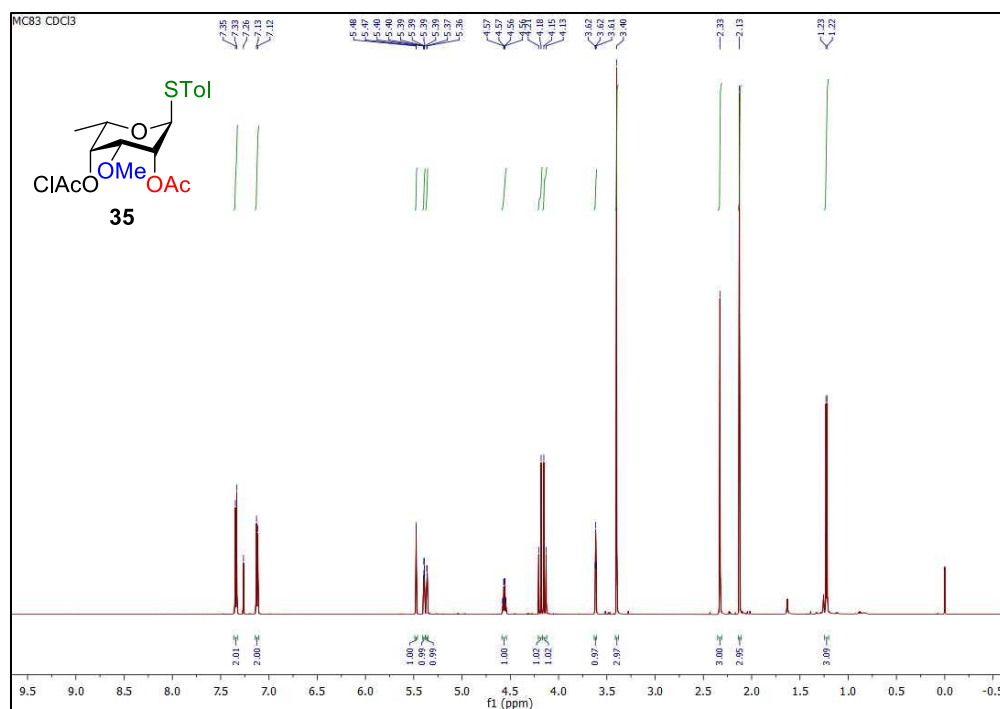


Figure S46 | $^{13}\text{C}\{^1\text{H}\}$ NMR spectrum (CDCl_3 , 150 MHz) of *para*-methylphenyl 2-*O*-acetyl-4-*O*-chloroacetyl-6-deoxy-3-*O*-methyl-1-thio- α -L-talopyranoside (35).

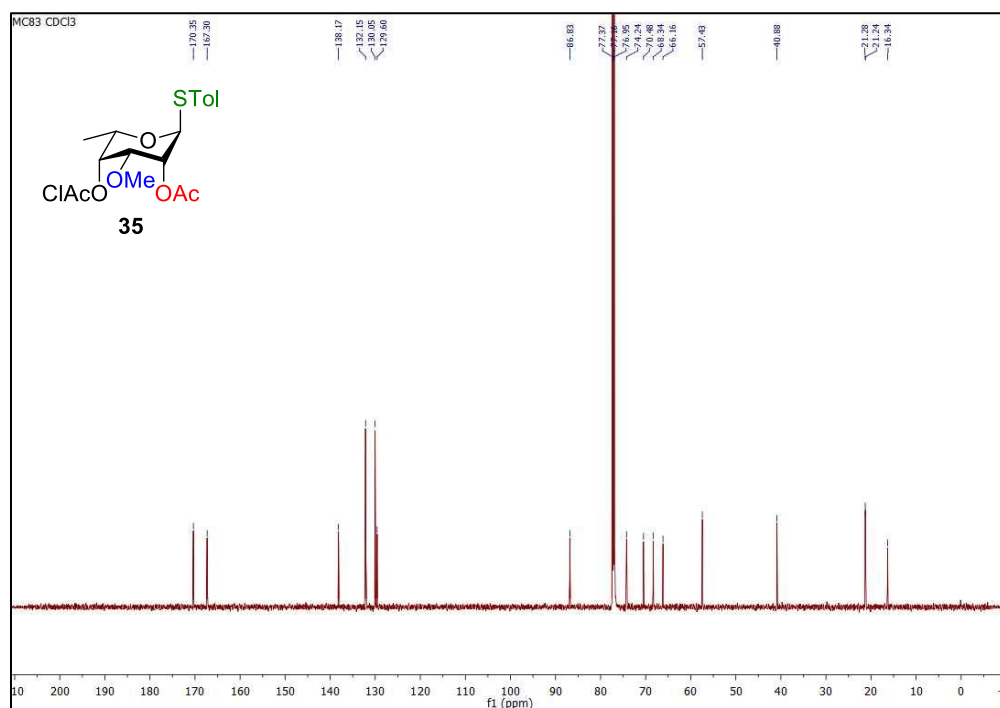


Figure S47 | ^1H NMR spectrum (CDCl_3 , 600 MHz) of (5-azido-1-pentyl) 2,4-di-*O*-acetyl-6-deoxy-3-*O*-methyl- α -L-talopyranosyl-(1 \rightarrow 3)-2-*O*-ortho-(azidomethyl)benzoyl-4,6-*O*-benzylidene- β -D-glucopyranosyl-(1 \rightarrow 3)-2-*O*-acetyl-4-*O*-levulinoyl- α -L-rhamnopyranosyl-(1 \rightarrow 3)-2-*O*-benzyl-4,6-*O*-benzylidene- β -D-glucopyranoside (36).

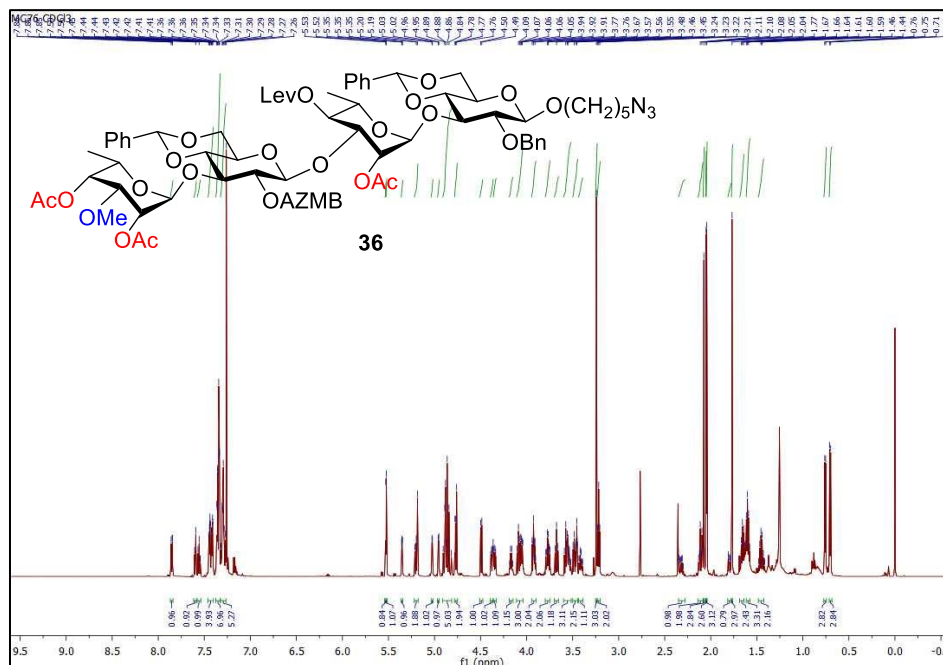


Figure S48 | $^{13}\text{C}\{^1\text{H}\}$ NMR spectrum (CDCl_3 , 150 MHz) of (5-azido-1-pentyl) 2,4-di-*O*-acetyl-6-deoxy-3-*O*-methyl- α -L-talopyranosyl-(1 \rightarrow 3)-2-*O*-ortho-(azidomethyl)benzoyl-4,6-*O*-benzylidene- β -D-glucopyranosyl-(1 \rightarrow 3)-2-*O*-acetyl-4-*O*-levulinoyl- α -L-rhamnopyranosyl-(1 \rightarrow 3)-2-*O*-benzyl-4,6-*O*-benzylidene- β -D-glucopyranoside (36).

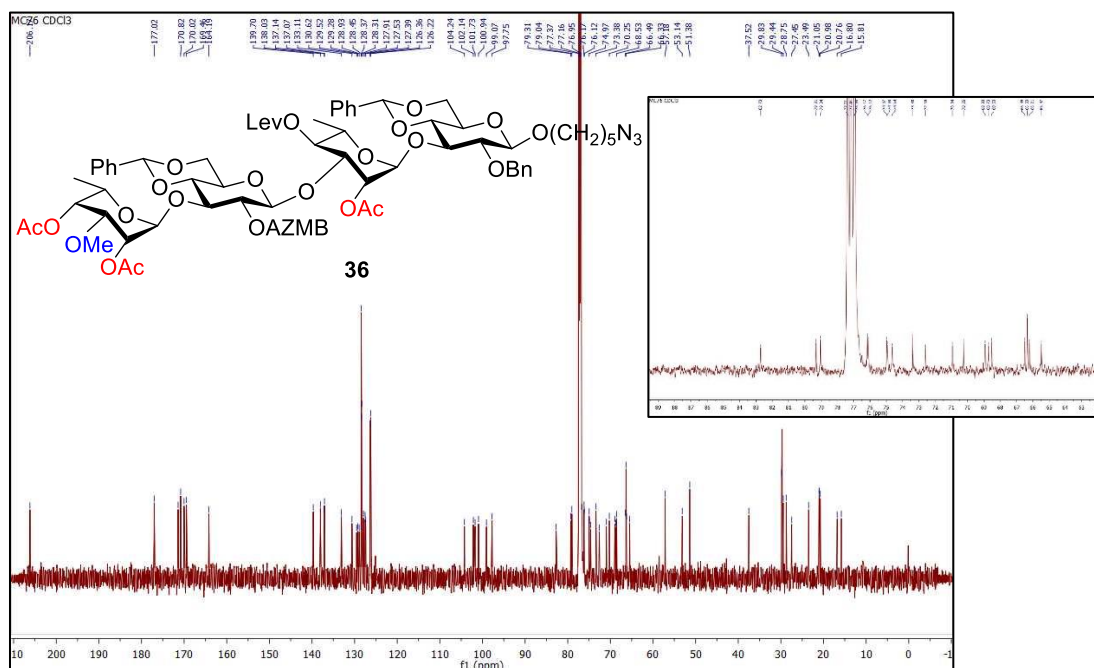


Figure S49 | ^1H NMR spectrum (CDCl_3 , 600 MHz) of (5-azido-1-pentyl) 2-*O*-acetyl-4-*O*-chloroacetyl-6-deoxy-3-*O*-methyl- α -L-talopyranosyl-(1 \rightarrow 3)-2-*O*-ortho-(azidomethyl)benzoyl-4,6-*O*-benzylidene- β -D-glucopyranosyl-(1 \rightarrow 3)-2-*O*-acetyl-4-*O*-levulinoyl- α -L-rhamnopyranosyl-(1 \rightarrow 3)-2-*O*-benzyl-4,6-*O*-benzylidene- β -D-glucopyranoside (37).

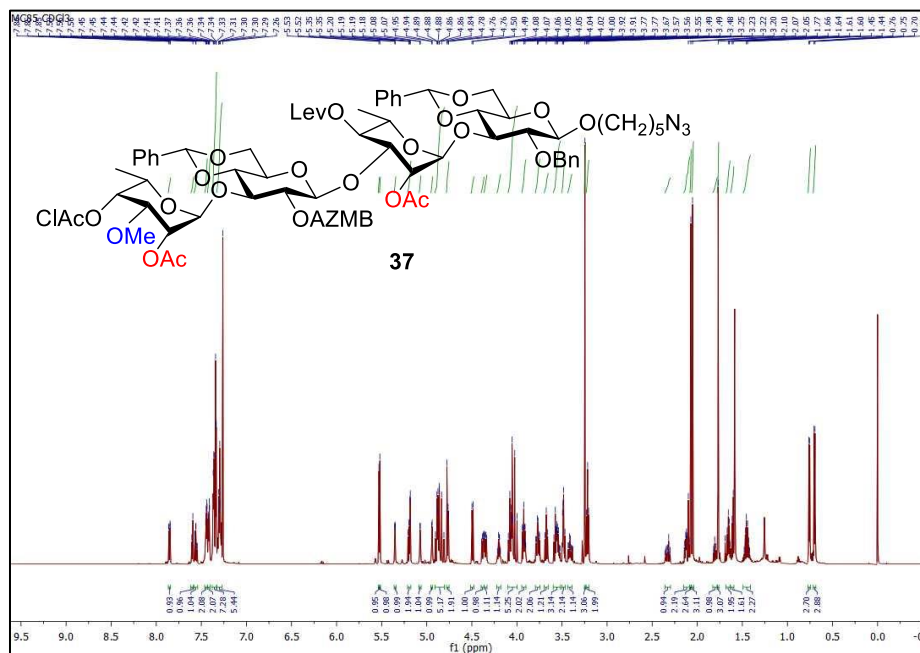


Figure S50 | $^{13}\text{C}\{^1\text{H}\}$ NMR spectrum (CDCl_3 , 150 MHz) of (5-azido-1-pentyl) 2-*O*-acetyl-4-*O*-chloroacetyl-6-deoxy-3-*O*-methyl- α -L-talopyranosyl-(1 \rightarrow 3)-2-*O*-ortho-(azidomethyl)benzoyl-4,6-*O*-benzylidene- β -D-glucopyranosyl-(1 \rightarrow 3)-2-*O*-acetyl-4-*O*-levulinoyl- α -L-rhamnopyranosyl-(1 \rightarrow 3)-2-*O*-benzyl-4,6-*O*-benzylidene- β -D-glucopyranoside (37).

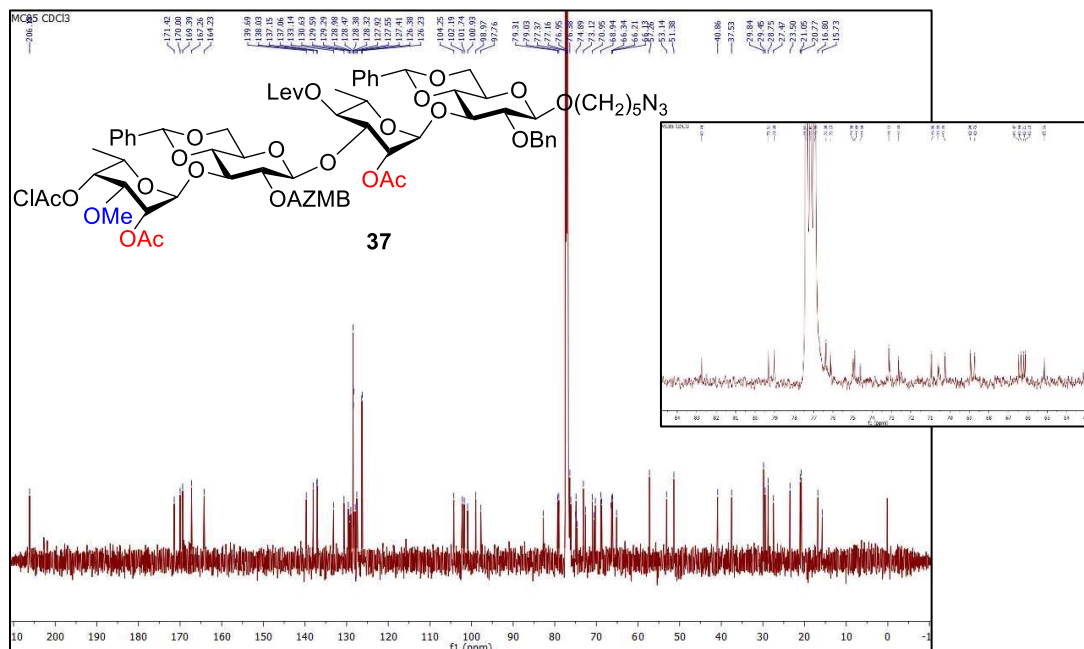


Figure S51 | ^1H NMR spectrum (CDCl_3 , 600 MHz) of (5-azido-1-pentyl) 2,4-di-*O*-acetyl-6-deoxy-3-*O*-methyl- α -L-talopyranosyl-(1 \rightarrow 3)-2-*O*-ortho-(azidomethyl)benzoyl-4,6-*O*-benzylidene- β -D-glucopyranosyl-(1 \rightarrow 3)-2-*O*-acetyl- α -L-rhamnopyranosyl-(1 \rightarrow 3)-2-*O*-benzyl-4,6-*O*-benzylidene- β -D-glucopyranoside (38).

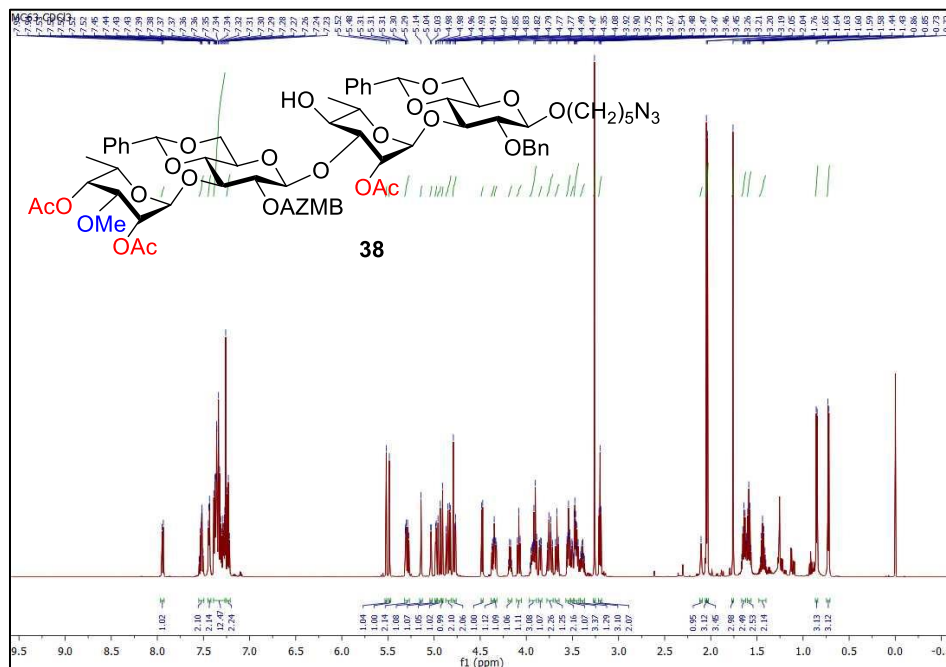


Figure S52 | $^{13}\text{C}\{^1\text{H}\}$ NMR spectrum (CDCl_3 , 150 MHz) of (5-azido-1-pentyl) 2,4-di-*O*-acetyl-6-deoxy-3-*O*-methyl- α -L-talopyranosyl-(1 \rightarrow 3)-2-*O*-ortho-(azidomethyl)benzoyl-4,6-*O*-benzylidene- β -D-glucopyranosyl-(1 \rightarrow 3)-2-*O*-acetyl- α -L-rhamnopyranosyl-(1 \rightarrow 3)-2-*O*-benzyl-4,6-*O*-benzylidene- β -D-glucopyranoside (38).

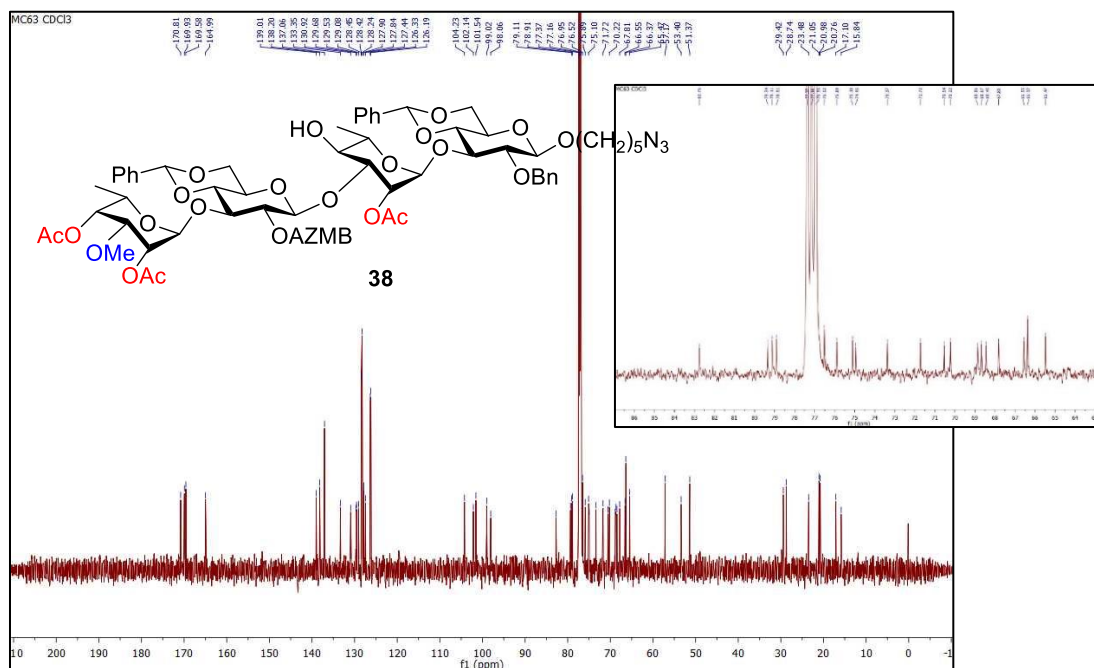


Figure S53 | ^1H NMR spectrum (CDCl_3 , 600 MHz) of (5-azido-1-pentyl) 2-*O*-acetyl-4-*O*-chloroacetyl-6-deoxy-3-*O*-methyl- α -L-talopyranosyl-(1 \rightarrow 3)-2-*O*-ortho-(azidomethyl)benzoyl-4,6-*O*-benzylidene- β -D-glucopyranosyl-(1 \rightarrow 3)-2-*O*-acetyl- α -L-rhamnopyranosyl-(1 \rightarrow 3)-2-*O*-benzyl-4,6-*O*-benzylidene- β -D-glucopyranoside (39).

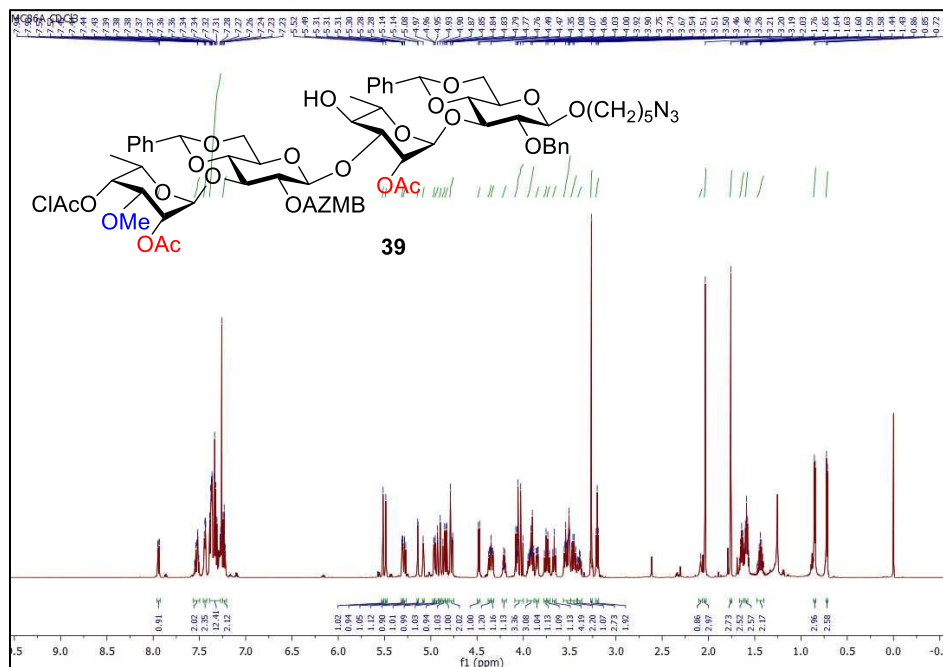


Figure S54 | $^{13}\text{C}\{^1\text{H}\}$ NMR spectrum (CDCl_3 , 150 MHz) of (5-azido-1-pentyl) 2-*O*-acetyl-4-*O*-chloroacetyl-6-deoxy-3-*O*-methyl- α -L-talopyranosyl-(1 \rightarrow 3)-2-*O*-ortho-(azidomethyl)benzoyl-4,6-*O*-benzylidene- β -D-glucopyranosyl-(1 \rightarrow 3)-2-*O*-acetyl- α -L-rhamnopyranosyl-(1 \rightarrow 3)-2-*O*-benzyl-4,6-*O*-benzylidene- β -D-glucopyranoside (39).

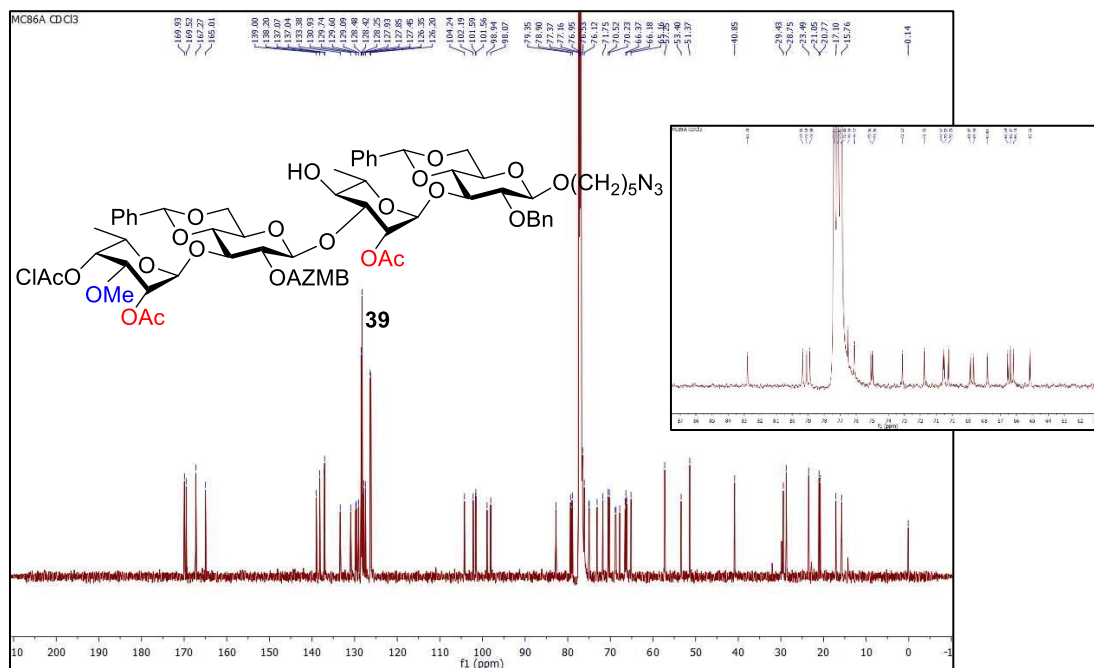


Figure S55 | ^1H NMR spectrum (CDCl_3 , 600 MHz) of (5-azido-1-pentyl) 2,4-di-*O*-acetyl-6-deoxy-3-*O*-methyl- α -L-talopyranosyl-(1 \rightarrow 3)-2-*O*-ortho-(azidomethyl)benzoyl-4,6-*O*-benzylidene- β -D-glucopyranosyl-(1 \rightarrow 3)-2-*O*-acetyl-6-deoxy- α -L-talopyranosyl-(1 \rightarrow 3)-2-*O*-benzyl-4,6-*O*-benzylidene- β -D-glucopyranoside (40).

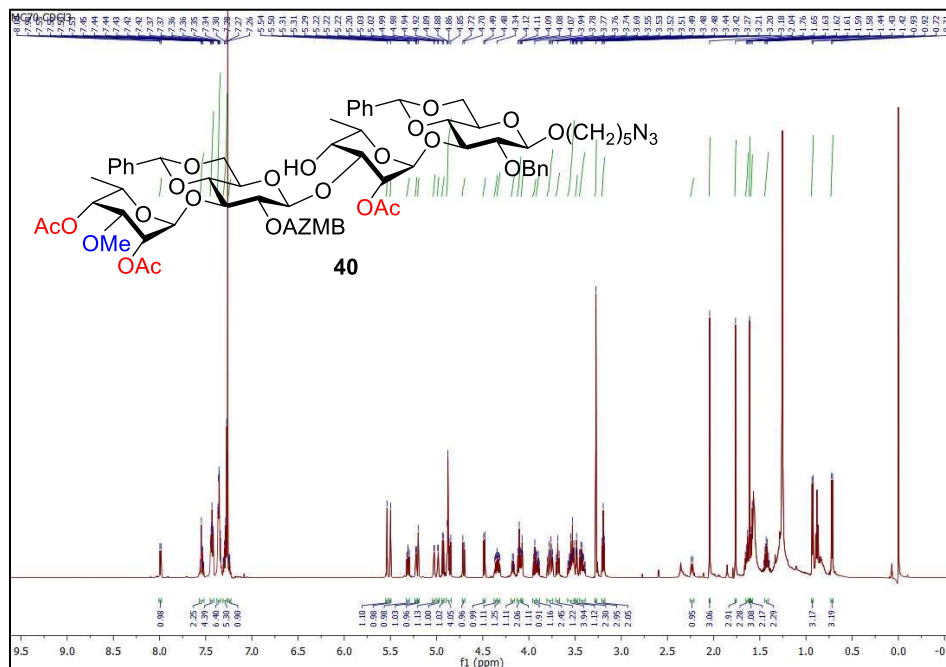


Figure S56 | ^{13}C NMR spectrum (CDCl_3 , 150 MHz) of (5-azido-1-pentyl) 2,4-di-*O*-acetyl-6-deoxy-3-*O*-methyl- α -L-talopyranosyl-(1 \rightarrow 3)-2-*O*-ortho-(azidomethyl)benzoyl-4,6-*O*-benzylidene- β -D-glucopyranosyl-(1 \rightarrow 3)-2-*O*-acetyl-6-deoxy- α -L-talopyranosyl-(1 \rightarrow 3)-2-*O*-benzyl-4,6-*O*-benzylidene- β -D-glucopyranoside (40).

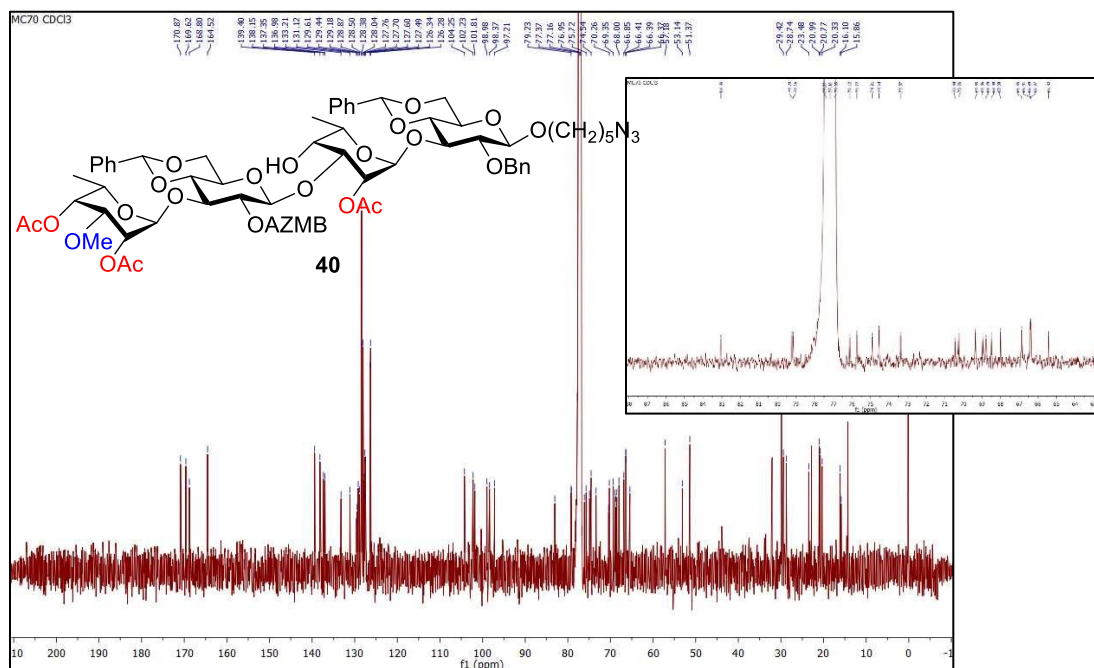


Figure S57 | ^1H NMR spectrum (CDCl_3 , 600 MHz) of (5-azido-1-pentyl) 2-*O*-acetyl-4-*O*-chloroacetyl-6-deoxy-3-*O*-methyl- α -L-talopyranosyl-(1 \rightarrow 3)-2-*O*-ortho-(azidomethyl)benzoyl-4,6-*O*-benzylidene- β -D-glucopyranosyl-(1 \rightarrow 3)-2-*O*-acetyl-6-deoxy- α -L-talopyranosyl-(1 \rightarrow 3)-2-*O*-benzyl-4,6-*O*-benzylidene- β -D-glucopyranoside (31).

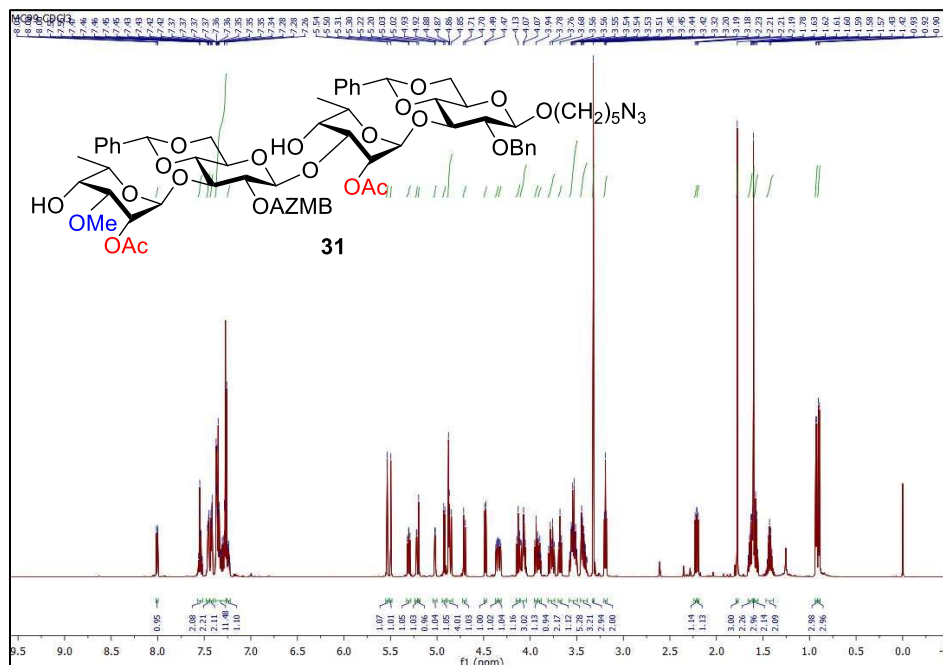


Figure S58 | $^{13}\text{C}\{^1\text{H}\}$ NMR spectrum (CDCl_3 , 150 MHz) of (5-azido-1-pentyl) 2-*O*-acetyl-4-*O*-chloroacetyl-6-deoxy-3-*O*-methyl- α -L-talopyranosyl-(1 \rightarrow 3)-2-*O*-ortho-(azidomethyl)benzoyl-4,6-*O*-benzylidene- β -D-glucopyranosyl-(1 \rightarrow 3)-2-*O*-acetyl-6-deoxy- α -L-talopyranosyl-(1 \rightarrow 3)-2-*O*-benzyl-4,6-*O*-benzylidene- β -D-glucopyranoside (31).

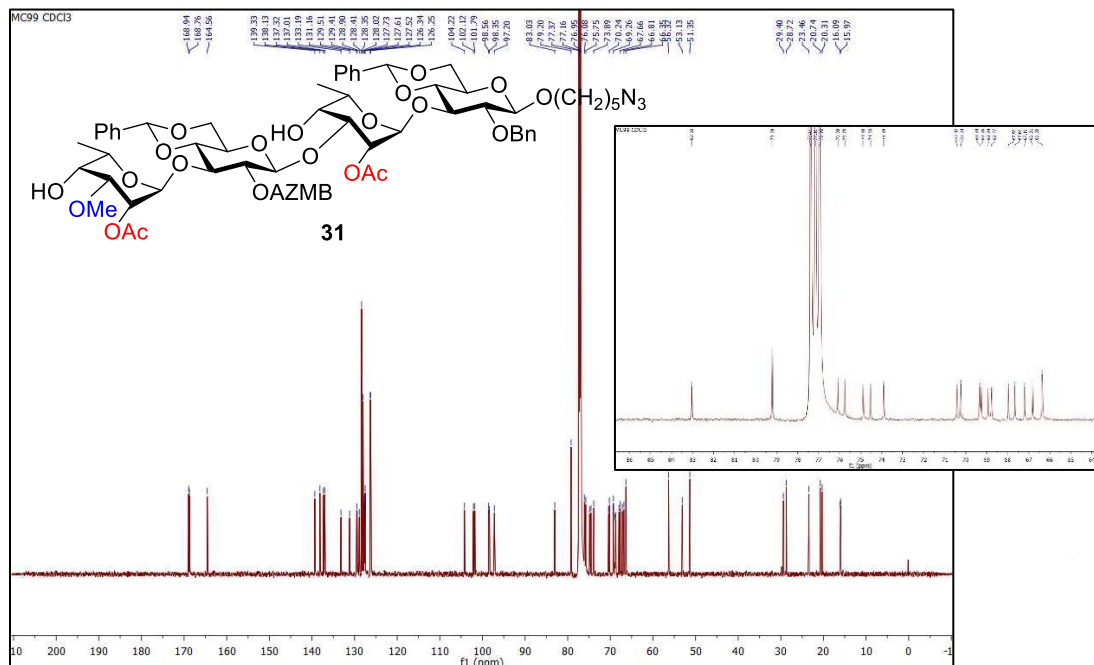


Figure S59 | ^1H NMR spectrum (CDCl_3 , 600 MHz) of (5-amino-1-pentyl) 2-*O*-acetyl-4-*O*-levulinoyl-3-*O*-*para*-methoxybenzyl- α -L-rhamnopyranosyl-(1 \rightarrow 3)-2-*O*-benzyl-4,6-*O*-benzylidene- β -D-glucopyranoside (41).

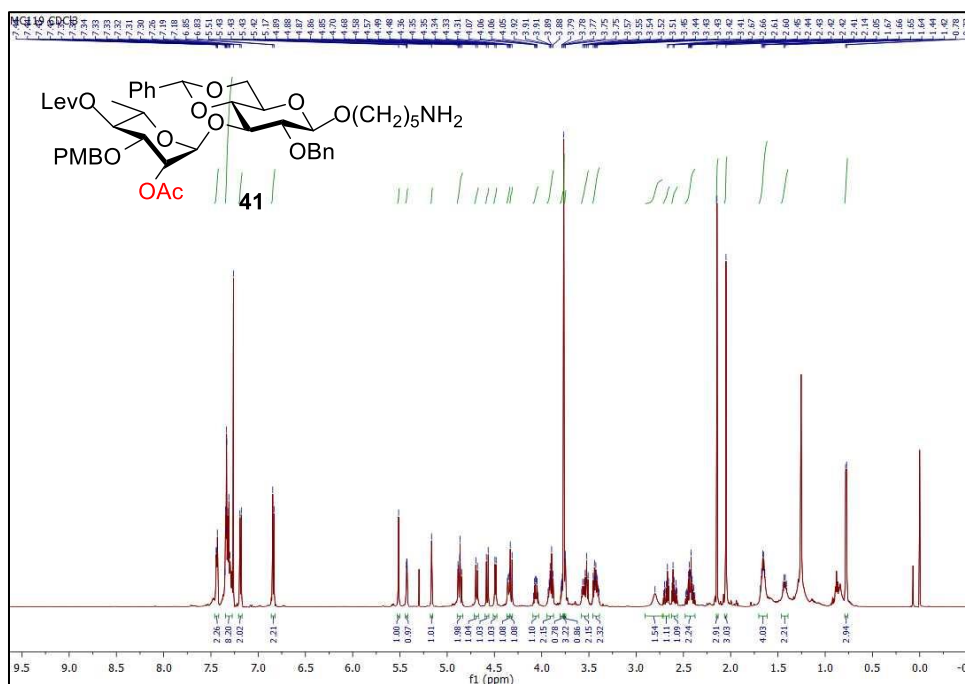


Figure S60 | $^{13}\text{C}\{^1\text{H}\}$ NMR spectrum (CDCl_3 , 150 MHz) of (5-amino-1-pentyl) 2-*O*-acetyl-4-*O*-levulinoyl-3-*O*-*para*-methoxybenzyl- α -L-rhamnopyranosyl-(1 \rightarrow 3)-2-*O*-benzyl-4,6-*O*-benzylidene- β -D-glucopyranoside (41).

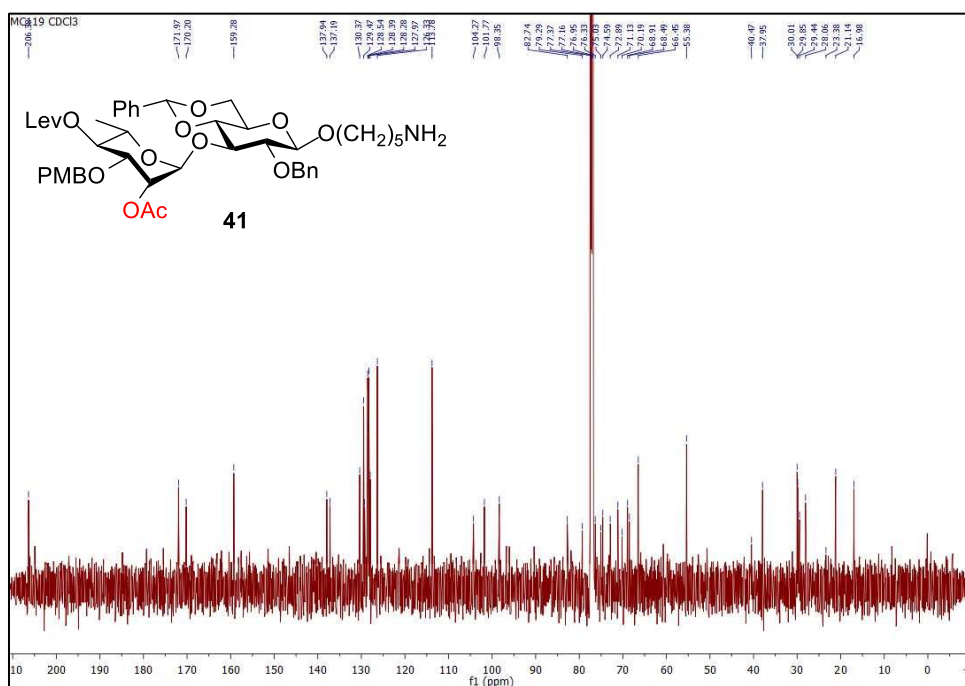


Figure S61 | ^1H NMR spectrum (CDCl_3 , 600 MHz) of (5-amino-1-pentyl) 4,6-*O*-benzylidene-3-*O*-*para*-methoxybenzyl- β -D-glucopyranosyl-(1 \rightarrow 3)-2-*O*-acetyl-4-*O*-levulinoyl- α -L-rhamnopyranosyl-(1 \rightarrow 3)-2-*O*-benzyl-4,6-*O*-benzylidene- β -D-glucopyranoside (42).

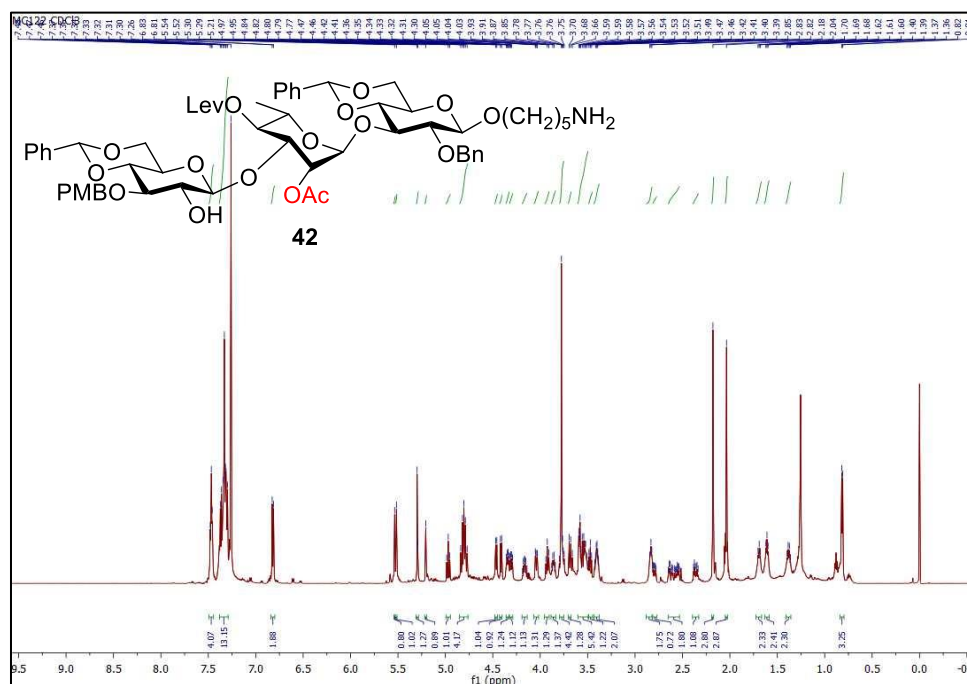


Figure S62 | $^{13}\text{C}\{^1\text{H}\}$ NMR spectrum (CDCl_3 , 150 MHz) of (5-amino-1-pentyl) 4,6-*O*-benzylidene-3-*O*-*para*-methoxybenzyl- β -D-glucopyranosyl-(1 \rightarrow 3)-2-*O*-acetyl-4-*O*-levulinoyl- α -L-rhamnopyranosyl-(1 \rightarrow 3)-2-*O*-benzyl-4,6-*O*-benzylidene- β -D-glucopyranoside (42).

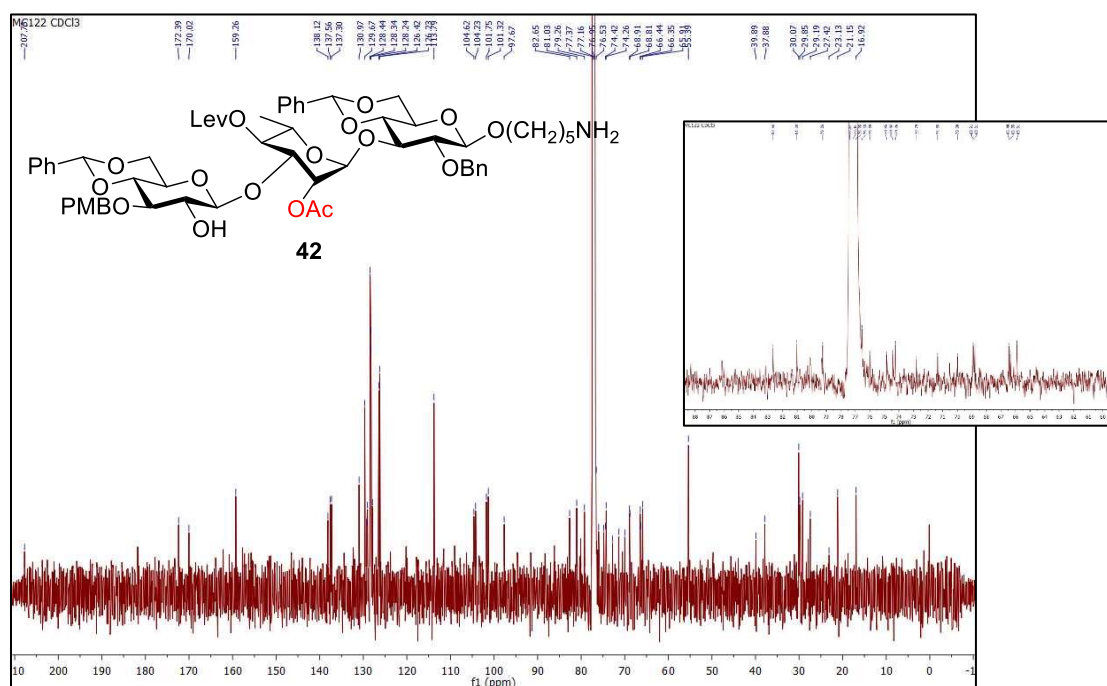


Figure S63 | ^1H NMR spectrum (CDCl_3 , 600 MHz) of (5-amino-1-pentyl) 2-*O*-acetyl-4-*O*-chloroacetyl-6-deoxy-3-*O*-methyl- α -L-talopyranosyl-(1 \rightarrow 3)-4,6-*O*-benzylidene- β -D-glucopyranosyl-(1 \rightarrow 3)-2-*O*-acetyl-6-deoxy- α -L-talopyranosyl-(1 \rightarrow 3)-2-*O*-benzyl-4,6-*O*-benzylidene- β -D-glucopyranoside (43).

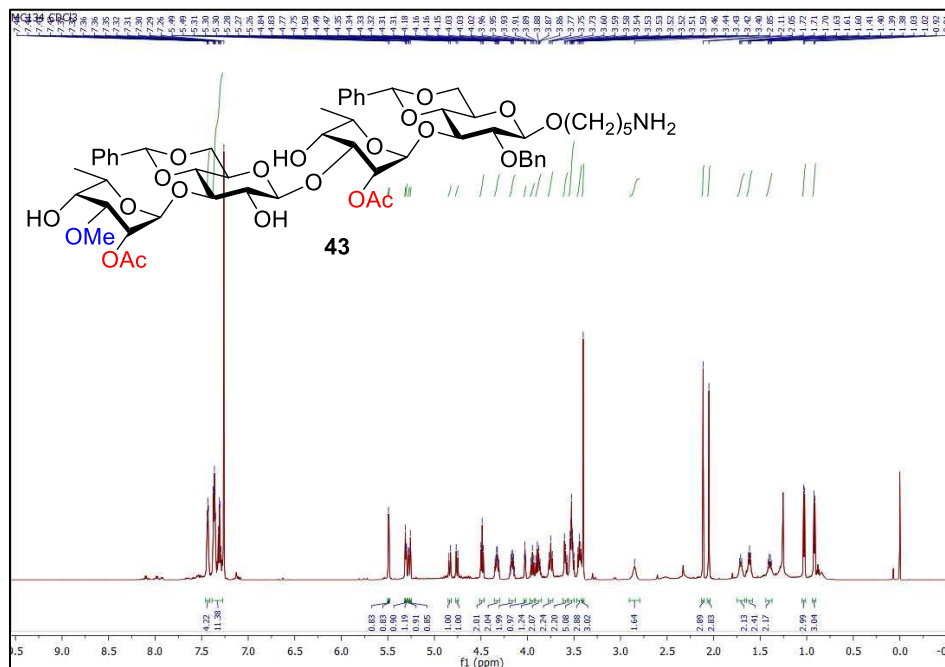


Figure S64 | $^{13}\text{C}\{^1\text{H}\}$ NMR spectrum (CDCl_3 , 150 MHz) of (5-amino-1-pentyl) 2-*O*-acetyl-4-*O*-chloroacetyl-6-deoxy-3-*O*-methyl- α -L-talopyranosyl-(1 \rightarrow 3)-4,6-*O*-benzylidene- β -D-glucopyranosyl-(1 \rightarrow 3)-2-*O*-acetyl-6-deoxy- α -L-talopyranosyl-(1 \rightarrow 3)-2-*O*-benzyl-4,6-*O*-benzylidene- β -D-glucopyranoside (43).

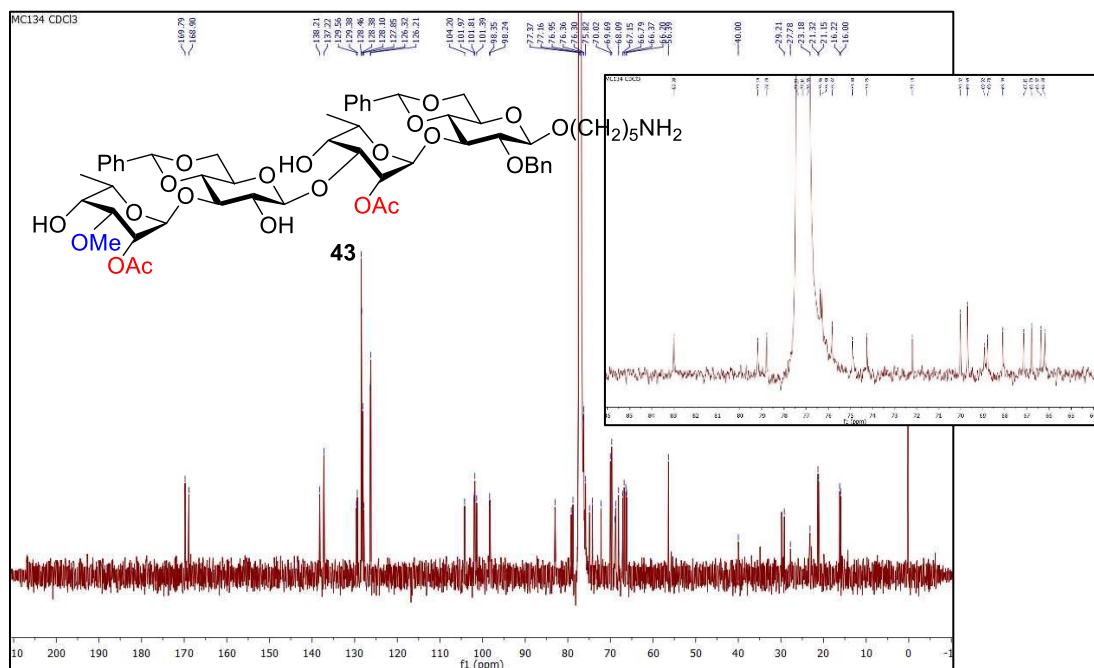


Figure S65 | ^1H NMR spectrum (D_2O , 600 MHz) of (5-amino-1-pentyl) 2,4-di-*O*-acetyl-6-deoxy-3-*O*-methyl- α -L-talopyranosyl-(1 \rightarrow 3)- β -D-glucopyranosyl-(1 \rightarrow 3)-2-*O*-acetyl-6-deoxy- α -L-talopyranosyl-(1 \rightarrow 3)- β -D-glucopyranoside hydrochloride (8).

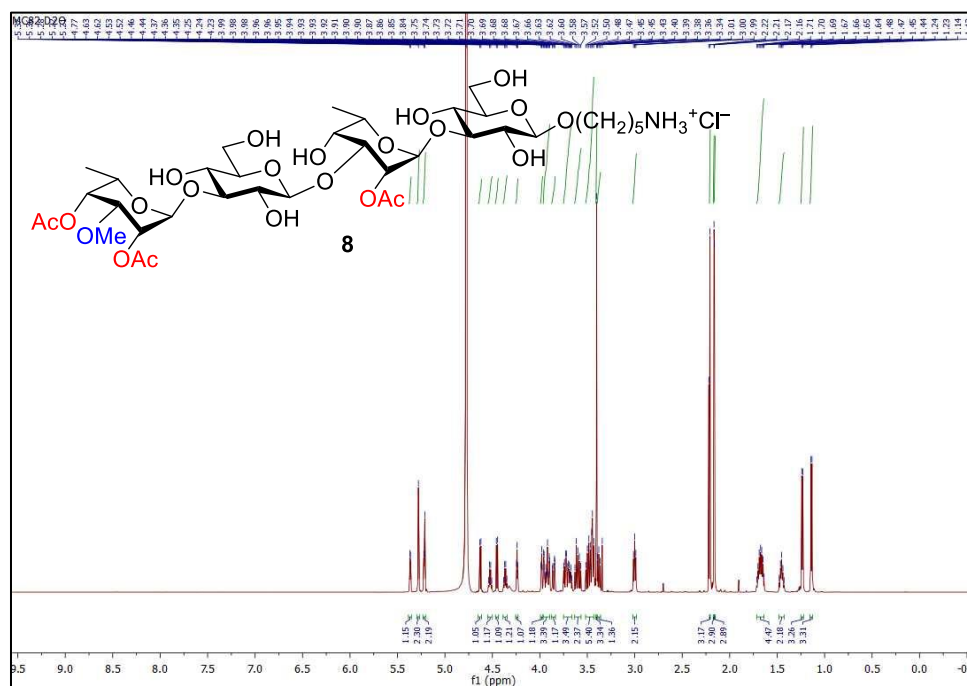


Figure S66 | $^{13}\text{C}\{^1\text{H}\}$ NMR spectrum (D_2O , 150 MHz) of compound (5-amino-1-pentyl) 2,4-di-*O*-acetyl-6-deoxy-3-*O*-methyl- α -L-talopyranosyl-(1 \rightarrow 3)- β -D-glucopyranosyl-(1 \rightarrow 3)-2-*O*-acetyl-6-deoxy- α -L-talopyranosyl-(1 \rightarrow 3)- β -D-glucopyranoside hydrochloride (8).

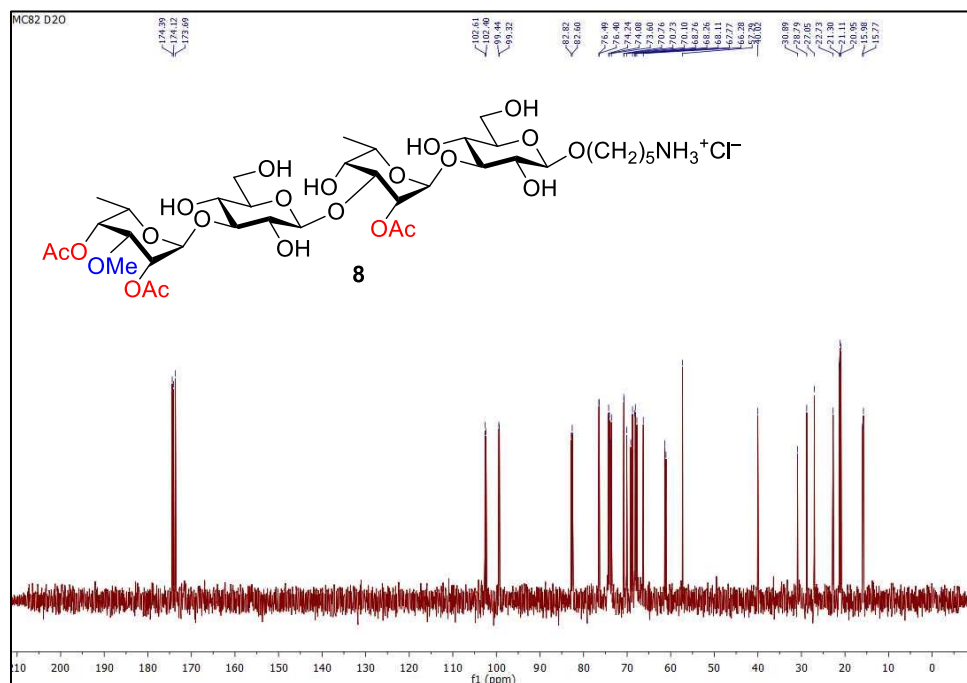


Figure S67 | ^1H NMR spectrum (D_2O , 600 MHz) of (5-amino-1-pentyl) 2-*O*-acetyl-6-deoxy-3-*O*-methyl- α -L-talopyranosyl-(1 \rightarrow 3)- β -D-glucopyranosyl-(1 \rightarrow 3)-2-*O*-acetyl-6-deoxy- α -L-talopyranosyl-(1 \rightarrow 3)- β -D-glucopyranoside hydrochloride (9).

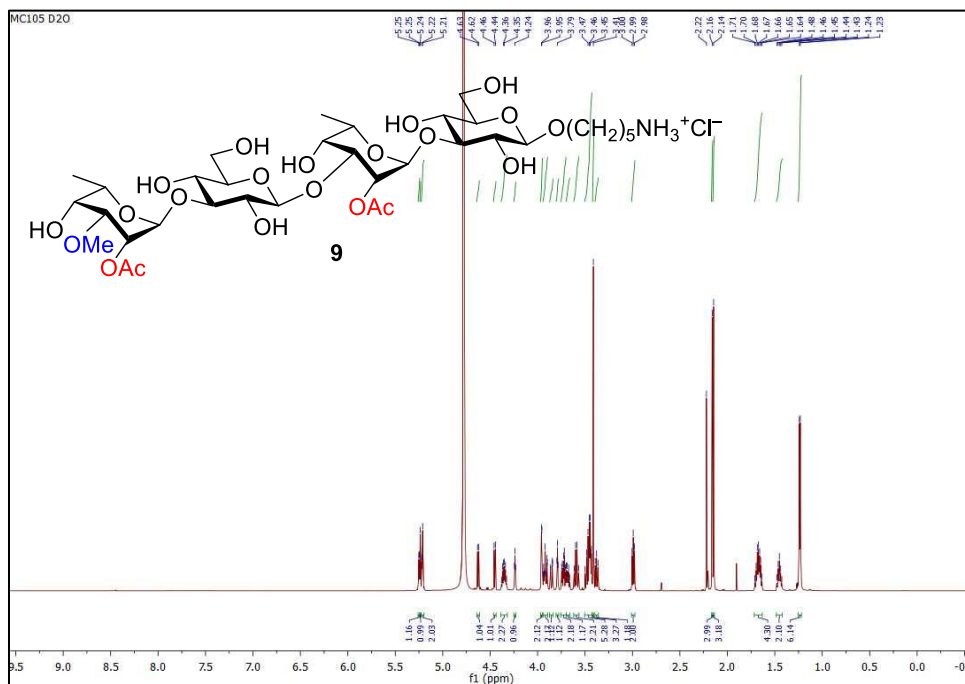
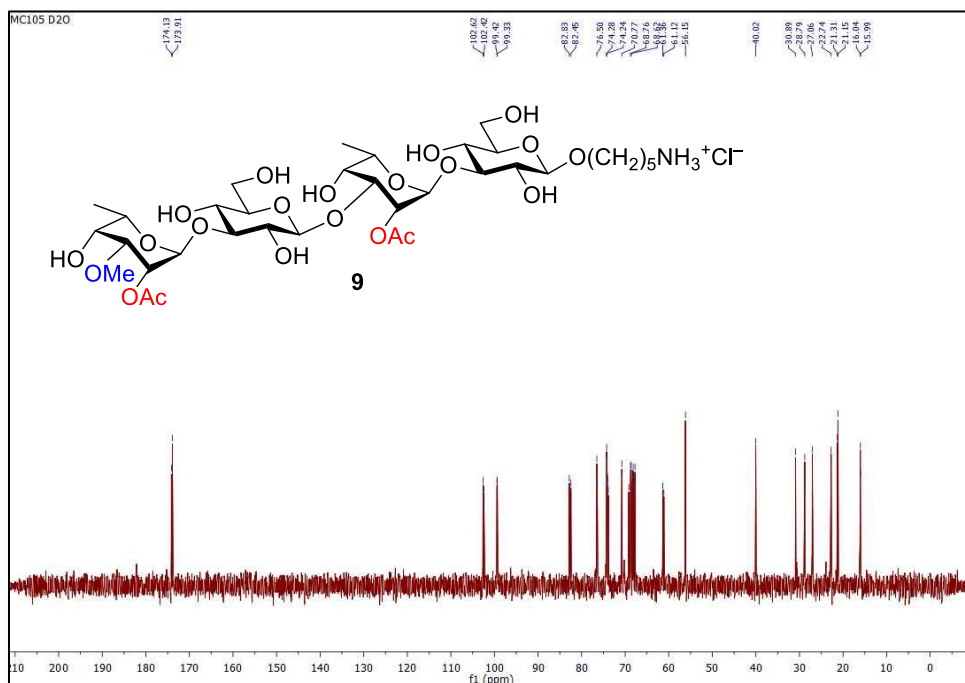


Figure S68 | $^{13}\text{C}\{^1\text{H}\}$ NMR spectrum (D_2O , 150 MHz) of (5-amino-1-pentyl) 2-*O*-acetyl-6-deoxy-3-*O*-methyl- α -L-talopyranosyl-(1 \rightarrow 3)- β -D-glucopyranosyl-(1 \rightarrow 3)-2-*O*-acetyl-6-deoxy- α -L-talopyranosyl-(1 \rightarrow 3)- β -D-glucopyranoside hydrochloride (9).



ANNEXE DU CHAPITRE 7

1. X-ray Diffraction.

The data for **20a**, crystallised from $\text{CHCl}_3/\text{hexanes}$, were collected from a shock-cooled single crystal at 150 K on a Bruker Venture Metaljet k-geometry diffractometer with a Metal Jet using Helios MX Mirror Optics as monochromator and a Bruker CMOS Photon III detector. The diffractometer was equipped with an Oxford Cryostream 700 low temperature device and used Ga K_α radiation ($\lambda = 1.34139 \text{ \AA}$). All data were integrated with *SAINT* (2020) and a multi-scan absorption correction using *SADABS* 2016/2 was applied.⁶¹² The structure was solved by dual methods with *XT* and refined by full-matrix least-squares methods against F^2 using *XL*.^{613, 614} Structure solution and refinement cycles were performed within the graphical user interface of *OLEX2*.⁶¹⁵ All non-hydrogen atoms were refined with anisotropic displacement parameters. The hydrogen atoms were refined isotropically on calculated positions using a riding model with their U_{iso} values constrained to 1.5 times the U_{eq} of their pivot atoms for terminal sp^3 carbon atoms and oxygen atoms, and 1.2 times for all other carbon atoms. This report and the CIF file were generated using FinalCif.

Table S1. Crystal Data and Structure Refinement for Compound 20a.

Parameter	Data	Parameter	Data
Empirical formula	$\text{C}_{23}\text{H}_{30}\text{O}_6$	Crystal size [mm^3]	0.03×0.04×0.19
Formula weight	402.47	Crystal colour	clear light colourless
Temperature [K]	150	Crystal shape	needle
Crystal system	orthorhombic	Radiation	Ga K_α ($\lambda=1.34139 \text{ \AA}$)
Space group (number)	$P2_12_12_1$ (19)	2θ range [$^\circ$]	8.20 to 121.22 (0.77 \AA)
a [\AA]	10.6168(4)	Index ranges	$-13 \leq h \leq 11$ $-14 \leq k \leq 14$ $-21 \leq l \leq 20$
b [\AA]	11.4428(4)	Reflections collected	41569
c [\AA]	16.4108(6)	Independent reflections	4567 $R_{\text{int}} = 0.0696$ $R_{\text{sigma}} = 0.0447$
α [$^\circ$]	90	Completeness to $\theta = 53.594^\circ$	100.0 %
β [$^\circ$]	90	Data / Restraints / Parameters	4567 / 0 / 266
γ [$^\circ$]	90	Goodness-of-fit on F^2	1.053
Volume [\AA^3]	1993.68(13)	Final R indexes [$I \geq 2\sigma(I)$]	$R_1 = 0.0440$ $wR_2 = 0.0705$
Z	4	Final R indexes [all data]	$R_1 = 0.0658$ $wR_2 = 0.0752$
ρ_{calc} [gcm^{-3}]	1.341	Largest peak/hole [e \AA^{-3}]	0.20/−0.21
μ [mm^{-1}]	0.500	Extinction coefficient	0.00127(19)
$F(000)$	864	Flack X parameter	0.0(3)

Table S2. Atomic Coordinates and U_{eq} [\AA^2] for Compound 20a.

Atom	x	y	z	U_{eq}
O1	0.67251(13)	0.30565(13)	0.57814(9)	0.0230(3)
O2	0.59438(14)	0.08841(14)	0.50669(10)	0.0301(4)
H2	0.595538	0.143107	0.472561	0.045
O3	0.92042(15)	0.10810(18)	0.56885(10)	0.0426(5)
H3	0.988920	0.098564	0.544113	0.064
O4	0.58084(14)	0.18093(13)	0.66940(9)	0.0241(4)
O5	0.68079(15)	0.44042(14)	0.42991(9)	0.0293(4)
O6	0.73368(13)	0.24487(15)	0.40923(9)	0.0270(4)
C1	0.6865(2)	0.19653(19)	0.62063(13)	0.0232(5)
H1	0.763418	0.199646	0.655709	0.028
C2	0.6999(2)	0.0984(2)	0.55923(14)	0.0257(5)
H2A	0.709424	0.023283	0.589705	0.031
C3	0.8213(2)	0.1206(2)	0.51135(14)	0.0284(5)
H3A	0.830482	0.061215	0.467037	0.034
C4	0.8237(2)	0.2431(2)	0.47543(13)	0.0261(5)
H4	0.909741	0.260036	0.453675	0.031
C5	0.7876(2)	0.3364(2)	0.53800(14)	0.0246(5)
H5	0.856366	0.343999	0.579305	0.030
C6	0.7674(2)	0.4523(2)	0.49688(15)	0.0292(5)
H6A	0.733533	0.509098	0.536748	0.035
H6B	0.848939	0.482492	0.476575	0.035
C7	0.7285(2)	0.3575(2)	0.37359(14)	0.0292(6)
H7	0.815588	0.381264	0.357414	0.035
C8	0.6467(2)	0.3548(2)	0.29850(15)	0.0326(6)
C9	0.5984(2)	0.4584(3)	0.26765(16)	0.0409(7)
H9	0.610721	0.529478	0.296418	0.049
C10	0.5318(3)	0.4582(3)	0.19460(17)	0.0520(8)
H10	0.498342	0.529232	0.173816	0.062
C11	0.5142(3)	0.3558(4)	0.15242(17)	0.0542(9)
H11	0.469298	0.356258	0.102342	0.065
C12	0.5614(3)	0.2525(3)	0.18257(16)	0.0500(8)
H12	0.548844	0.181714	0.153431	0.060
C13	0.6280(2)	0.2517(3)	0.25621(15)	0.0401(7)
H13	0.660374	0.180362	0.277121	0.048
C14	0.5823(2)	0.2522(2)	0.74250(13)	0.0257(5)
H14	0.599318	0.335337	0.727242	0.031
C15	0.6810(2)	0.2118(2)	0.80391(14)	0.0308(6)
H15	0.766583	0.216578	0.778697	0.037
C16	0.6547(2)	0.0862(2)	0.83017(15)	0.0305(6)
H16A	0.719745	0.060429	0.869482	0.037
H16B	0.658185	0.033957	0.782155	0.037
C17	0.5239(2)	0.0788(2)	0.86986(14)	0.0257(5)
H17	0.506658	-0.003413	0.887162	0.031
C18	0.5184(2)	0.1598(2)	0.94396(14)	0.0340(6)
H18A	0.582439	0.135674	0.984427	0.041
H18B	0.434384	0.154354	0.969900	0.041
C19	0.5432(3)	0.2863(2)	0.91695(16)	0.0409(7)
H19	0.539215	0.339176	0.965369	0.049
C20	0.4449(3)	0.3238(2)	0.85461(16)	0.0390(7)
H20A	0.460595	0.405568	0.837800	0.047
H20B	0.359838	0.319588	0.879171	0.047
C21	0.4516(2)	0.2432(2)	0.78004(14)	0.0281(5)

H21	0.386937	0.267780	0.739143	0.034
C22	0.4257(2)	0.11731(19)	0.80705(14)	0.0251(5)
H22A	0.340383	0.112120	0.831186	0.030
H22B	0.428808	0.064706	0.759204	0.030
C24	0.6747(3)	0.2938(2)	0.87821(16)	0.0432(7)
H24A	0.739363	0.270802	0.918595	0.052
H24B	0.691861	0.375122	0.860970	0.052

U_{eq} is defined as 1/3 of the trace of the orthogonalized U_{ij} tensor.

Table S3. Bond Lengths and Angles for Compound 20a.

Atom-Atom	Length [Å]	Atom-Atom-Atom	Angle [°]	Atom-Atom-Atom	Angle [°]
O1-C1	1.438(3)	C5-O1-C1	110.42(16)	C9-C10-H10	119.9
O1-C5	1.432(3)	C2-O2-H2	109.5	C11-C10-C9	120.3(3)
O2-H2	0.8400	C3-O3-H3	109.5	C11-C10-H10	119.9
O2-C2	1.419(3)	C1-O4-C14	113.29(16)	C10-C11-H11	119.9
O3-H3	0.8400	C7-O5-C6	109.43(17)	C10-C11-C12	120.1(3)
O3-C3	1.420(3)	C7-O6-C4	110.42(17)	C12-C11-H11	119.9
O4-C1	1.389(3)	O1-C1-H1	109.4	C11-C12-H12	120.0
O4-C14	1.451(3)	O1-C1-C2	109.30(17)	C11-C12-C13	120.0(3)
O5-C6	1.439(3)	O4-C1-O1	107.92(17)	C13-C12-H12	120.0
O5-C7	1.418(3)	O4-C1-H1	109.4	C8-C13-C12	120.0(3)
O6-C4	1.447(3)	O4-C1-C2	111.35(18)	C8-C13-H13	120.0
O6-C7	1.416(3)	C2-C1-H1	109.4	C12-C13-H13	120.0
C1-H1	1.0000	O2-C2-C1	112.95(18)	O4-C14-H14	109.3
C1-C2	1.515(3)	O2-C2-H2A	108.3	O4-C14-C15	112.56(18)
C2-H2A	1.0000	O2-C2-C3	111.50(18)	O4-C14-C21	106.66(18)
C2-C3	1.531(3)	C1-C2-H2A	108.3	C15-C14-H14	109.3
C3-H3A	1.0000	C1-C2-C3	107.34(18)	C21-C14-H14	109.3
C3-C4	1.520(3)	C3-C2-H2A	108.3	C21-C14-C15	109.78(18)
C4-H4	1.0000	O3-C3-C2	105.43(18)	C14-C15-H15	109.5
C4-C5	1.531(3)	O3-C3-H3A	110.0	C14-C15-C16	110.27(19)
C5-H5	1.0000	O3-C3-C4	109.76(19)	C14-C15-C24	108.0(2)
C5-C6	1.503(3)	C2-C3-H3A	110.0	C16-C15-H15	109.5
C6-H6A	0.9900	C4-C3-C2	111.44(18)	C16-C15-C24	110.0(2)
C6-H6B	0.9900	C4-C3-H3A	110.0	C24-C15-H15	109.5
C7-H7	1.0000	O6-C4-C3	107.06(17)	C15-C16-H16A	109.7
C7-C8	1.508(3)	O6-C4-H4	109.4	C15-C16-H16B	109.7
C8-C9	1.387(4)	O6-C4-C5	109.17(17)	C15-C16-C17	109.7(2)
C8-C13	1.383(4)	C3-C4-H4	109.4	H16A-C16-H16B	108.2
C9-H9	0.9500	C3-C4-C5	112.29(18)	C17-C16-H16A	109.7
C9-C10	1.392(4)	C5-C4-H4	109.4	C17-C16-H16B	109.7
C10-H10	0.9500	O1-C5-C4	110.51(17)	C16-C17-H17	109.7
C10-C11	1.374(5)	O1-C5-H5	109.4	C18-C17-C16	109.76(19)
C11-H11	0.9500	O1-C5-C6	107.57(18)	C18-C17-H17	109.7
C11-C12	1.376(4)	C4-C5-H5	109.4	C18-C17-C22	109.58(19)
C12-H12	0.9500	C6-C5-C4	110.51(18)	C22-C17-C16	108.33(18)
C12-C13	1.400(4)	C6-C5-H5	109.4	C22-C17-H17	109.7
C13-H13	0.9500	O5-C6-C5	110.54(18)	C17-C18-H18A	109.8
C14-H14	1.0000	O5-C6-H6A	109.5	C17-C18-H18B	109.8
C14-C15	1.525(3)	O5-C6-H6B	109.5	C17-C18-C19	109.54(19)
C14-C21	1.522(3)	C5-C6-H6A	109.5	H18A-C18-H18B	108.2
C15-H15	1.0000	C5-C6-H6B	109.5	C19-C18-H18A	109.8
C15-C16	1.526(3)	H6A-C6-H6B	108.1	C19-C18-H18B	109.8
C15-C24	1.540(3)	O5-C7-H7	108.7	C18-C19-H19	109.5
C16-H16A	0.9900	O5-C7-C8	109.92(19)	C20-C19-C18	110.0(2)
C16-H16B	0.9900	O6-C7-O5	110.71(18)	C20-C19-H19	109.5
C16-C17	1.537(3)	C3-C4-H4	109.4	C20-C19-C24	109.2(2)
C17-H17	1.0000	C3-C4-C5	112.29(18)	C24-C19-C18	109.2(2)
C17-C18	1.530(3)	C5-C4-H4	109.4	C24-C19-H19	109.5
C17-C22	1.531(3)	O1-C5-C4	110.51(17)	C19-C20-H20A	109.8
C18-H18A	0.9900	O1-C5-H5	109.4	C19-C20-H20B	109.8
C18-H18B	0.9900	O1-C5-C6	107.57(18)	C19-C20-C21	109.6(2)
C18-C19	1.536(4)	C4-C5-H5	109.4	H20A-C20-H20B	108.2
C19-H19	1.0000	C6-C5-C4	110.51(18)	C21-C20-H20A	109.8

C19-C20	1.523(4)	C6-C5-H5	109.4	C21-C20-H20B	109.8
C19-C24	1.536(4)	O5-C6-C5	110.54(18)	C14-C21-C20	108.9(2)
C20-H20A	0.9900	O5-C6-H6A	109.5	C14-C21-H21	109.6
C20-H20B	0.9900	O5-C6-H6B	109.5	C14-C21-C22	110.13(19)
C20-C21	1.533(3)	C5-C6-H6A	109.5	C20-C21-H21	109.6
C21-H21	1.0000	C5-C6-H6B	109.5	C22-C21-C20	109.02(19)
C21-C22	1.532(3)	H6A-C6-H6B	108.1	C22-C21-H21	109.6
C22-H22A	0.9900	O5-C7-H7	108.7	C17-C22-C21	110.06(19)
C22-H22B	0.9900	O5-C7-C8	109.92(19)	C17-C22-H22A	109.6
C24-H24A	0.9900	O6-C7-O5	110.71(18)	C17-C22-H22B	109.6
C24-H24B	0.9900	O6-C7-H7	108.7	C21-C22-H22A	109.6
		O6-C7-C8	110.0(2)	C21-C22-H22B	109.6
		C8-C7-H7	108.7	H22A-C22-H22B	108.2
		C9-C8-C7	119.6(2)	C15-C24-H24A	109.8
		C13-C8-C7	120.7(2)	C15-C24-H24B	109.8
		C13-C8-C9	119.5(2)	C19-C24-C15	109.5(2)
		C8-C9-H9	120.0	C19-C24-H24A	109.8
		C8-C9-C10	120.1(3)	C19-C24-H24B	109.8
		C10-C9-H9	120.0	H24A-C24-H24B	108.2

Table S4. Torsion Angles for Compound 20a.

Atom-Atom-Atom-Atom	Torsion Angle [°]	Atom-Atom-Atom-Atom	Torsion Angle [°]
O1-C1-C2-O2	-60.0(2)	C7-O6-C4-C3	178.75(17)
O1-C1-C2-C3	63.3(2)	C7-O6-C4-C5	57.0(2)
O1-C5-C6-O5	-68.8(2)	C7-C8-C9-C10	174.5(2)
O2-C2-C3-O3	-169.98(18)	C7-C8-C13-C12	-174.2(2)
O2-C2-C3-C4	71.0(2)	C8-C9-C10-C11	-0.4(4)
O3-C3-C4-O6	171.63(16)	C9-C8-C13-C12	0.4(4)
O3-C3-C4-C5	-68.6(2)	C9-C10-C11-C12	0.6(4)
O4-C1-C2-O2	59.2(2)	C10-C11-C12-C13	-0.3(4)
O4-C1-C2-C3	-177.53(17)	C11-C12-C13-C8	-0.2(4)
O4-C14-C15-C16	-60.2(2)	C13-C8-C9-C10	-0.1(4)
O4-C14-C15-C24	179.62(18)	C14-O4-C1-O1	-76.2(2)
O4-C14-C21-C20	-176.19(18)	C14-O4-C1-C2	163.80(17)
O4-C14-C21-C22	64.3(2)	C14-C15-C16-C17	-60.1(2)
O5-C7-C8-C9	39.1(3)	C14-C15-C24-C19	60.9(3)
O5-C7-C8-C13	-146.3(2)	C14-C21-C22-C17	59.5(2)
O6-C4-C5-O1	68.1(2)	C15-C14-C21-C20	61.6(2)
O6-C4-C5-C6	-50.8(2)	C15-C14-C21-C22	-57.9(2)
O6-C7-C8-C9	161.3(2)	C15-C16-C17-C18	-59.3(2)
O6-C7-C8-C13	-24.2(3)	C15-C16-C17-C22	60.3(2)
C1-O1-C5-C4	60.7(2)	C16-C15-C24-C19	-59.5(3)
C1-O1-C5-C6	-178.54(17)	C16-C17-C18-C19	60.1(3)
C1-O4-C14-C15	-70.3(2)	C16-C17-C22-C21	-60.1(2)
C1-O4-C14-C21	169.28(17)	C17-C18-C19-C20	59.4(3)
C1-C2-C3-O3	65.8(2)	C17-C18-C19-C24	-60.4(3)
C1-C2-C3-C4	-53.2(2)	C18-C17-C22-C21	59.6(2)
C2-C3-C4-O6	-72.0(2)	C18-C19-C20-C21	-60.1(3)
C2-C3-C4-C5	47.8(2)	C18-C19-C24-C15	59.9(3)
C3-C4-C5-O1	-50.4(2)	C19-C20-C21-C14	-60.2(2)
C3-C4-C5-C6	-169.38(18)	C19-C20-C21-C22	60.0(3)
C4-O6-C7-O5	-65.2(2)	C20-C19-C24-C15	-60.4(3)
C4-O6-C7-C8	173.11(17)	C20-C21-C22-C17	-59.9(2)
C4-C5-C6-O5	51.9(2)	C21-C14-C15-C16	58.5(2)
C5-O1-C1-O4	169.92(16)	C21-C14-C15-C24	-61.7(2)
C5-O1-C1-C2	-68.8(2)	C22-C17-C18-C19	-58.8(3)
C6-O5-C7-O6	65.0(2)	C24-C15-C16-C17	58.9(3)
C6-O5-C7-C8	-173.27(18)	C24-C19-C20-C21	59.7(3)
C7-O5-C6-C5	-58.2(2)		

Table S5. Hydrogen Bonds for Compound 20a.

D-H...A [Å]	d(D-H) [Å]	d(H...A) [Å]	d(D...A) [Å]	<(DHA) [°]
O2-H2...O6	0.84	2.14	2.820(2)	137.6
O3-H3...O5 ^{#1}	0.84	2.13	2.820(2)	139.4

Symmetry transformations used to generate equivalent atoms: #1: 0.5+X, 0.5-Y, 1-Z.

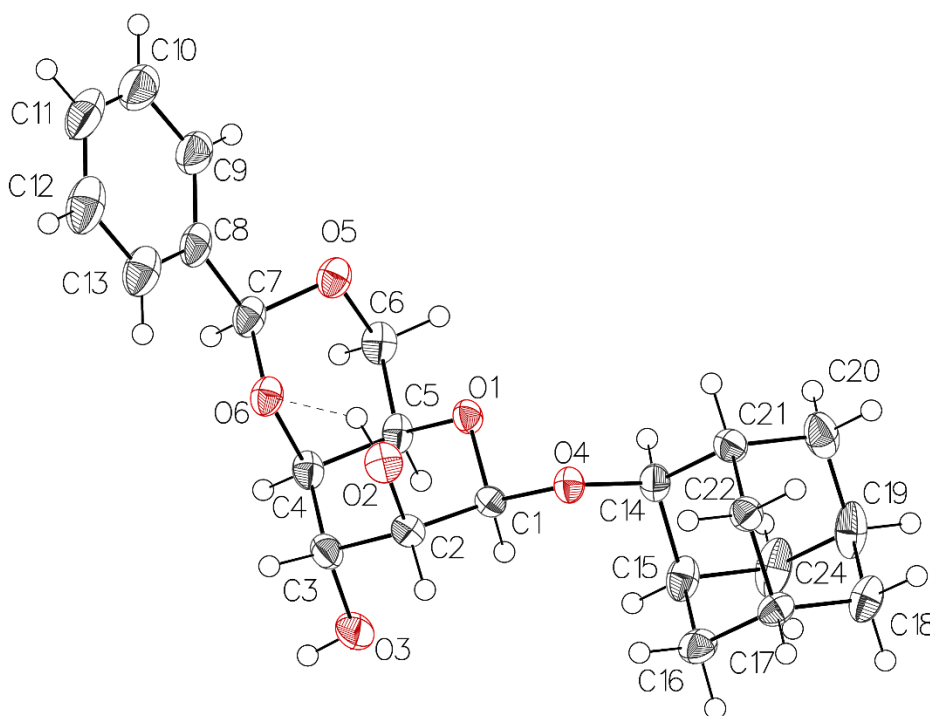


Figure S1. Thermal atomic displacement ellipsoid plot for compound 20a with the atomic numbering scheme. Ellipsoids are drawn at the 50% probability level and hydrogen atoms are shown as sphere of arbitrary size.

2. Molecular Modeling.

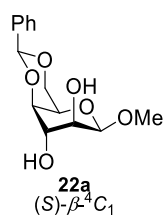


Table S6. 3D Coordinates of B3LYP/6-31+G(d,p) Optimized Geometries of 22aA-22aD.

ID	atom	22aA coordinates			22aB coordinates			22aC coordinates		
		X	Y	Z	X	Y	Z	X	Y	Z
1	C	1.3784	-0.8246	-1.2160	-1.3058	-0.8651	1.1874	-1.3085	-0.8651	1.1862
2	C	2.8360	0.4922	0.1446	-2.9193	0.4065	-0.0010	-2.9193	0.4087	-0.0055
3	C	1.6705	-1.4358	1.2474	-1.6471	-1.3638	-1.2984	-1.6543	-1.3632	-1.3015
4	C	2.2167	-0.0038	1.4590	-2.4257	-0.0354	-1.3856	-2.4265	-0.0366	-1.3895
5	C	0.7548	-1.4999	0.0171	-0.6946	-1.4510	-0.0964	-0.6962	-1.4506	-0.0974
6	O	1.8483	0.4891	-0.8946	-1.8580	0.4336	0.9504	-1.8592	0.4337	0.9479
7	O	1.1957	0.8593	1.9455	-1.5873	0.9469	-1.9808	-1.5829	0.9428	-1.9829
8	O	2.7248	-2.3679	1.0010	-2.5601	-2.4544	-1.1333	-2.6553	-2.3810	-1.1925
9	O	-0.4687	-0.8260	0.3695	0.5213	-0.7730	-0.4359	0.5210	-0.7746	-0.4358
10	C	0.3275	-0.6933	-2.3117	-0.2345	-0.7429	2.2645	-0.2379	-0.7431	2.2639
11	O	-0.8780	-0.0959	-1.8140	0.9520	-0.1152	1.7629	0.9493	-0.1158	1.7632
12	C	-1.4071	-0.8060	-0.7143	1.4638	-0.7989	0.6288	1.4630	-0.7990	0.6301
13	H	2.2096	-1.4426	-1.5857	-2.0952	-1.5423	1.5475	-2.0987	-1.5418	1.5452
14	H	1.0888	-1.7246	2.1312	-1.0567	-1.4809	-2.2153	-1.0699	-1.4826	-2.2219
15	H	2.9991	-0.0225	2.2250	-3.3134	-0.2012	-2.0146	-3.3096	-0.2116	-2.0191
16	H	0.5420	-2.5533	-0.2115	-0.4787	-2.5161	0.0745	-0.4720	-2.5145	0.0824
17	H	0.4050	0.7193	1.3964	-2.0057	1.8088	-1.8310	-1.9999	1.8053	-1.8332
18	H	3.2369	-2.4864	1.8130	-3.1105	-2.5285	-1.9254	-2.2402	-3.2481	-1.3000
19	H	0.6853	-0.0449	-3.1132	-0.5899	-0.1247	3.0909	-0.5935	-0.1244	3.0899
20	H	0.1074	-1.6874	-2.7262	0.0084	-1.7448	2.6472	0.0044	-1.7449	2.6472
21	H	-1.5976	-1.8506	-1.0101	1.6546	-1.8501	0.9051	1.6547	-1.8501	0.9063
22	C	-2.6719	-0.1380	-0.2404	2.7339	-0.1250	0.1771	2.7327	-0.1238	0.1793
23	C	-5.0209	1.0832	0.6812	5.1051	1.1207	-0.6528	5.1030	1.1237	-0.6500
24	C	-2.7000	1.2428	0.0022	3.9414	-0.8316	0.1824	3.9393	-0.8320	0.1771
25	C	-3.8240	-0.9012	-0.0209	2.7174	1.2118	-0.2463	2.7166	1.2154	-0.2365
26	C	-4.9967	-0.2931	0.4392	3.8983	1.8313	-0.6596	3.8971	1.8358	-0.6494
27	C	-3.8706	1.8502	0.4609	5.1255	-0.2114	-0.2312	5.1230	-0.2108	-0.2362
28	H	-1.8105	1.8388	-0.1751	3.9588	-1.8679	0.5096	3.9564	-1.8701	0.4986
29	H	-3.8073	-1.9712	-0.2105	1.7818	1.7618	-0.2524	1.7816	1.7665	-0.2367
30	H	-5.8867	-0.8927	0.6054	3.8790	2.8667	-0.9871	3.8782	2.8731	-0.9708
31	H	-3.8866	2.9203	0.6457	6.0580	-0.7680	-0.2238	6.0549	-0.7685	-0.2346
32	H	-5.9308	1.5574	1.0373	6.0228	1.6042	-0.9748	6.0205	1.6080	-0.9717
33	H	3.6549	-0.1862	-0.1499	-3.6994	-0.2878	0.3559	-3.7026	-0.2820	0.3513
34	O	3.3086	1.7886	0.3041	-3.4277	1.6971	-0.1358	-3.4228	1.7010	-0.1421
35	C	4.1481	2.2469	-0.7635	-4.1469	2.1900	1.0035	-4.1435	2.1965	0.9950
36	H	5.0024	1.5716	-0.9009	-4.9744	1.5151	1.2544	-4.9744	1.5247	1.2432
37	H	4.5089	3.2337	-0.4701	-4.5445	3.1644	0.7172	-4.5365	3.1725	0.7079
38	H	3.5888	2.3248	-1.7008	-3.4856	2.3001	1.8675	-3.4845	2.3039	1.8611

Table S7. 3D Coordinates of B3LYP/6-31+G(d,p) Optimized Geometries of 22aA-22aD (continued).

ID	atom	22aD <i>coordinates</i>		
		X	Y	Z
1	C	-1.3784	-0.8246	1.2160
2	C	-2.8360	0.4922	-0.1446
3	C	-1.6705	-1.4358	-1.2474
4	C	-2.2167	-0.0038	-1.4590
5	C	-0.7548	-1.4999	-0.0171
6	O	-1.8484	0.4891	0.8946
7	O	-1.1957	0.8593	-1.9455
8	O	-2.7248	-2.3679	-1.0010
9	O	0.4687	-0.8260	-0.3695
10	C	-0.3275	-0.6933	2.3117
11	O	0.8780	-0.0959	1.8140
12	C	1.4071	-0.8060	0.7143
13	H	-2.2096	-1.4426	1.5857
14	H	-1.0888	-1.7247	-2.1312
15	H	-2.9991	-0.0226	-2.2250
16	H	-0.5420	-2.5533	0.2115
17	H	-0.4050	0.7193	-1.3964
18	H	-3.2369	-2.4864	-1.8130
19	H	-0.6853	-0.0448	3.1132
20	H	-0.1074	-1.6874	2.7262
21	H	1.5976	-1.8506	1.0102
22	C	2.6719	-0.1380	0.2404
23	C	5.0209	1.0832	-0.6812
24	C	2.7000	1.2428	-0.0022
25	C	3.8240	-0.9012	0.0209
26	C	4.9967	-0.2931	-0.4392
27	C	3.8706	1.8502	-0.4609
28	H	1.8105	1.8388	0.1751
29	H	3.8073	-1.9712	0.2105
30	H	5.8867	-0.8927	-0.6054
31	H	3.8866	2.9203	-0.6457
32	H	5.9308	1.5574	-1.0373
33	H	-3.6549	-0.1862	0.1498
34	O	-3.3086	1.7886	-0.3041
35	C	-4.1481	2.2469	0.7635
36	H	-5.0024	1.5716	0.9009
37	H	-4.5090	3.2337	0.4700
38	H	-3.5888	2.3248	1.7008

Table S8. Energy and Abundance of Conformers 22aA-22aD.

conformer	B3LYP/6-31+G(d,p)				B3LYP/6-311++G(2d,2p)			
	ΔE (Ha)	ΔG (Ha)	abundance (%)	imaginary frequencies	ΔE (Ha)	ΔG (Ha)	abundance (%)	imaginary frequencies
22aA	-995.70163	-995.43434	45.0	0	-995.95748	-995.68914	44.4	0
22aB	-995.69900	-995.43242	5.91	0	-995.95503	-995.68731	6.40	0
22aC	-995.69876	-995.43211	4.25	0	-995.95480	-995.68705	4.85	0
22aD	-995.70163	-995.43434	44.9	0	-995.95748	-995.68914	44.3	0

Table S9. Comparison Between Experimental (20a) and Calculated (22aA-22aD) NMR 3J Coupling Constants.

protons	experimental 3J (Hz)	B3LYP/6-31+G(d,p)		B3LYP/6-311++G(2d,2p)	
		calculated 3J (Hz)	Δ	calculated 3J (Hz)	Δ
1-2	N/A	1.05	N/A	1.05	N/A
2-3	2.50	2.84	+0.34	2.83	+0.23
3-4	2.50	2.59	+0.09	2.58	-0.02
4-5	N/A	1.27	N/A	1.27	N/A
5-6a	1.10	1.55	+0.45	1.55	+0.45
5-6b	1.90	1.87	-0.03	1.87	-0.03
6a-6b	12.45	11.82	-0.63	11.82	-0.63
		<i>Rmsd : 0.32</i>		<i>Rmsd : 0.32</i>	

Table S10. Comparison Between Experimental (20a) and Calculated (22aA-22aD) NMR 1H and ^{13}C Chemical Shifts.

atom	experimental δ (ppm)	B3LYP/6-31+G(d,p)		B3LYP/6-311++G(2d,2p)	
		calculated δ (ppm)	Δ	calculated δ (ppm)	Δ
H-1	4.94	4.84	-0.10	4.84	-0.10
H-2	3.62	3.48	-0.14	3.48	-0.14
H-3	4.21	4.18	-0.03	4.18	-0.03
H-4	3.93	4.09	+0.16	4.09	+0.16
H-5	3.75	3.78	+0.03	3.78	+0.03
H-6a	4.37	4.35	-0.02	4.35	-0.02
H-6b	4.06	4.16	+0.10	4.16	+0.10
		<i>Rmsd : 0.10</i>		<i>Rmsd : 0.10</i>	
C-1	95.9	97.3	+1.4	97.3	+1.4
C-2	70.4	70.7	+0.3	70.7	+0.3
C-3	70.4	71.2	+0.8	71.2	+0.8
C-4	75.6	74.7	-0.9	74.7	-0.9
C-5	66.6	67.1	+0.5	67.1	+0.5
C-6	70.0	69.1	-0.9	69.1	-0.9
C-7	101.5	100.4	-1.1	100.4	-1.1
		<i>Rmsd : 0.93</i>		<i>Rmsd : 0.93</i>	

Table S11. Comparison Between Experimental (20a) and Calculated (22aA-22aD) H-H Distances by Quantitative NOESY NMR.

protons	experimental distance (Å)	B3LYP/6-31+G(d,p)		B3LYP/6-311++G(2d,2p)		
		calculated distance (Å)	Δ	calculated distance (Å)	Δ	
6ax-7''	2.337	2.422	+0.085	2.422	+0.085	
5-1	2.253	2.390	+0.137	2.390	+0.137	
4-7''	2.254	2.388	+0.134	2.388	+0.134	
2-1	2.430	2.462	+0.032	2.461	+0.031	
2-3	2.431	2.563	+0.132	2.563	+0.132	
4-3	2.547	2.569	+0.022	2.569	+0.022	
5-6eq	2.691	2.572	-0.119	2.572	-0.119	
5-6ax	2.453	2.402	-0.051	2.412	-0.041	
			<i>Rmsd : 0.30</i>	<i>Rmsd : 0.30</i>		

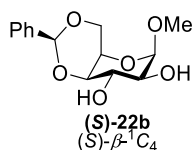


Table S12. 3D Coordinates of B3LYP/6-31+G(d,p) Optimized Geometries of (S)-22bA-(S)-22bF.

ID	atom	(S)-22bA coordinates			(S)-22bB coordinates			(S)-22bC coordinates		
		X	Y	Z	X	Y	Z	X	Y	Z
1	C	-1.3796	-1.3512	-0.9595	-1.4400	-1.2841	-1.0029	-1.4400	1.2841	1.0029
2	C	-2.7831	0.1122	0.4285	-2.7768	0.2460	0.3839	-2.7769	-0.2460	-0.3839
3	C	-0.7837	1.1195	-0.7605	-0.6777	1.1250	-0.7001	-0.6777	-1.1250	0.7001
4	C	-2.2297	1.3443	-0.2953	-2.1227	1.4449	-0.3119	-2.1226	-1.4448	0.3120
5	C	-0.7323	-0.1297	-1.6434	-0.6921	-0.0948	-1.6326	-0.6921	0.0949	1.6326
6	O	-2.6565	-1.0540	-0.3700	-2.7160	-0.9027	-0.4617	-2.7160	0.9027	0.4617
7	O	-2.3231	2.5114	0.5182	-2.2047	2.5839	0.5329	-2.2047	-2.5839	-0.5328
8	O	-0.3419	2.2346	-1.5327	-0.1720	2.2900	-1.3580	-0.1719	-2.2900	1.3581
9	O	0.5843	-0.4721	-2.1189	0.6087	-0.5119	-2.0905	0.6087	0.5120	2.0905
10	C	-0.4001	-2.0016	0.0219	-0.5377	-2.0001	0.0079	-0.5377	2.0001	-0.0079
11	O	0.7804	-2.3582	-0.7145	0.6667	-2.3993	-0.6705	0.6667	2.3993	0.6704
12	C	1.4441	-1.2446	-1.2819	1.4037	-1.3319	-1.2297	1.4037	1.3319	1.2297
13	H	-1.6058	-2.0889	-1.7339	-1.6827	-1.9952	-1.7972	-1.6827	1.9953	1.7972
14	H	-0.1405	1.0005	0.1196	-0.0978	0.9339	0.2080	-0.0978	-0.9339	-0.2080
15	H	-2.8554	1.5362	-1.1726	-2.6948	1.6245	-1.2341	-2.6947	-1.6245	1.2342
16	H	-1.2854	0.1028	-2.5593	-1.2037	0.2094	-2.5512	-1.2037	-0.2093	2.5512
17	H	-2.0062	2.2684	1.4037	-1.6856	3.2834	0.1071	-1.6856	-3.2834	-0.1070
18	H	-0.5064	3.0293	-1.0025	0.7948	2.2587	-1.3452	0.7948	-2.2587	1.3452
19	H	-0.1558	-1.3404	0.8589	-0.3125	-1.3673	0.8701	-0.3125	1.3673	-0.8702
20	H	-0.8114	-2.9333	0.4153	-1.0056	-2.9216	0.3595	-1.0056	2.9216	-0.3596
21	H	2.1592	-1.6813	-1.9861	2.1082	-1.8131	-1.9148	2.1082	1.8132	1.9147
22	C	2.2210	-0.4194	-0.2515	2.2005	-0.5199	-0.2050	2.2005	0.5199	0.2050
23	C	3.8475	1.0196	1.5361	3.8151	0.9385	1.5790	3.8151	-0.9386	-1.5790
24	C	2.6723	-1.0136	0.9355	2.4219	-0.9876	1.0960	2.4219	0.9876	-1.0961
25	C	2.6076	0.8957	-0.5442	2.8264	0.6678	-0.6156	2.8264	-0.6678	0.6156
26	C	3.4131	1.6119	0.3457	3.6241	1.3958	0.2705	3.6241	-1.3958	-0.2705
27	C	3.4748	-0.2960	1.8279	3.2173	-0.2572	1.9858	3.2173	0.2571	-1.9859
28	H	2.3941	-2.0381	1.1608	1.9767	-1.9243	1.4143	1.9767	1.9242	-1.4144
29	H	2.2613	1.3623	-1.4596	2.7056	1.0104	-1.6400	2.7056	-1.0103	1.6400
30	H	3.7000	2.6326	0.1089	4.0998	2.3138	-0.0621	4.0998	-2.3138	0.0622
31	H	3.8095	-0.7665	2.7480	3.3708	-0.6269	2.9955	3.3708	0.6268	-2.9956
32	H	4.4728	1.5769	2.2277	4.4328	1.5040	2.2704	4.4328	-1.5041	-2.2703
33	H	-3.8627	0.2100	0.5934	-3.8518	0.4209	0.5138	-3.8518	-0.4210	-0.5137
34	O	-2.1139	0.0292	1.6662	-2.1653	0.0457	1.6288	-2.1653	-0.0458	-1.6288
35	C	-2.7531	-0.8070	2.6402	-2.9033	-0.7982	2.5204	-2.9033	0.7981	-2.5205
36	H	-3.7768	-0.4616	2.8295	-3.9062	-0.3889	2.6957	-3.9062	0.3887	-2.6958
37	H	-2.1648	-0.7249	3.5548	-2.3496	-0.8169	3.4601	-2.3496	0.8168	-3.4601
38	H	-2.7734	-1.8503	2.3098	-2.9895	-1.8164	2.1268	-2.9897	1.8163	-2.1269

Table S13. 3D Coordinates of B3LYP/6-31+G(d,p) Optimized Geometries of (S)-22bA-(S)-22bF (continued).

ID	atom	(S)-22bD coordinates			(S)-22bE coordinates			(S)-22bF coordinates		
		X	Y	X	X	X	Z	X	Y	Z
1	C	-1.4118	-1.1721	-1.2117	-1.4225	-1.4094	-0.8480	1.3795	1.2336	-1.0933
2	C	-3.1857	-0.0163	0.0510	-2.7973	0.2723	0.2904	2.7486	-0.0077	0.5262
3	C	-1.0068	1.2021	-0.3618	-0.6832	1.0419	-0.8650	0.8281	-1.2119	-0.5963
4	C	-2.5291	1.3372	-0.2418	-2.1239	1.4121	-0.4945	2.2677	-1.3302	-0.0900
5	C	-0.6793	0.1703	-1.4455	-0.6925	-0.2990	-1.6177	0.7641	-0.0781	-1.6240
6	O	-2.8092	-0.9930	-0.9078	-2.7078	-0.9771	-0.3754	2.6453	1.0357	-0.4427
7	O	-2.8783	2.3080	0.7428	-2.2104	2.6265	0.2393	2.3007	-2.4202	0.8293
8	O	-0.4312	2.4528	-0.7441	-0.1675	2.0790	-1.6976	0.4340	-2.4214	-1.2420
9	O	0.7268	-0.0444	-1.6202	0.6240	-0.7416	-2.0090	-0.5519	0.1681	-2.1569
10	C	-0.6533	-2.0329	-0.1706	-0.5211	-1.9753	0.2522	0.3668	1.9949	-0.2320
11	O	0.5070	-1.3459	0.3238	0.6870	-2.4471	-0.3704	-0.7998	2.2290	-1.0371
12	C	1.3655	-0.9769	-0.7345	1.4210	-1.4527	-1.0532	-1.4374	1.0358	-1.4511
13	H	-1.4342	-1.7066	-2.1639	-1.6473	-2.2210	-1.5453	1.6143	1.8649	-1.9547
14	H	-0.5929	0.8816	0.6009	-0.0858	0.9715	0.0517	0.1674	-1.0131	0.2552
15	H	-2.9259	1.7129	-1.1902	-2.6897	1.5733	-1.4177	2.9210	-1.5426	-0.9458
16	H	-1.0080	0.5903	-2.4014	-1.2024	-0.1270	-2.5712	1.3357	-0.4119	-2.4962
17	H	-2.7776	1.8821	1.6101	-1.9473	2.4257	1.1520	3.1934	-2.7900	0.8594
18	H	-0.7770	3.1209	-0.1325	0.7481	1.8544	-1.9172	0.6455	-3.1442	-0.6312
19	H	-1.2789	-2.2340	0.6964	-0.3042	-1.2319	1.0239	0.1090	1.4486	0.6798
20	H	-0.3405	-2.9858	-0.6178	-0.9803	-2.8476	0.7213	0.7559	2.9779	0.0406
21	H	1.6034	-1.8758	-1.3262	2.1262	-2.0102	-1.6770	-2.1471	1.3563	-2.2204
22	C	2.6332	-0.3852	-0.1586	2.2167	-0.5260	-0.1299	-2.2189	0.3507	-0.3257
23	C	4.9784	0.6372	0.9903	3.8309	1.1261	1.4771	-3.8530	-0.8493	1.6240
24	C	3.7234	-1.2280	0.0925	2.4224	-0.8318	1.2212	-2.7211	1.1052	0.7440
25	C	2.7243	0.9760	0.1599	2.8593	0.5954	-0.6769	-2.5577	-1.0060	-0.4202
26	C	3.8938	1.4832	0.7337	3.6560	1.4201	0.1205	-3.3671	-1.6031	0.5506
27	C	4.8922	-0.7209	0.6674	3.2174	-0.0049	2.0223	-3.5275	0.5073	1.7173
28	H	3.6594	-2.2827	-0.1636	1.9659	-1.7183	1.6482	-2.4786	2.1606	0.8150
29	H	1.8882	1.6337	-0.0556	2.7530	0.8120	-1.7365	-2.1711	-1.5965	-1.2436
30	H	3.9601	2.5399	0.9766	4.1433	2.2859	-0.3181	-3.6162	-2.6573	0.4686
31	H	5.7331	-1.3818	0.8566	3.3587	-0.2492	3.0711	-3.9019	1.1024	2.5454
32	H	5.8871	1.0351	1.4327	4.4484	1.7669	2.0996	-4.4809	-1.3140	2.3786
33	H	-4.2755	0.0521	-0.0492	-3.8748	0.4563	0.3741	3.8228	-0.0523	0.7479
34	O	-2.8480	-0.3566	1.3776	-2.2111	0.2652	1.5734	2.0235	0.2482	1.6975
35	C	-3.6997	-1.3392	1.9807	-2.9645	-0.4315	2.5748	2.5970	1.2550	2.5396
36	H	-4.7428	-1.0007	1.9727	-3.9707	-0.0043	2.6641	3.6226	0.9833	2.8202
37	H	-3.3609	-1.4551	3.0109	-2.4275	-0.3011	3.5150	1.9759	1.3025	3.4351
38	H	-3.6244	-2.3000	1.4604	-3.0387	-1.4981	2.3400	2.6021	2.2326	2.0464

Table S14. Energy and Abundance of Conformers (S)-22bA-(S)-22bF.

conformer	B3LYP/6-31+G(d,p)				B3LYP/6-311++G(2d,2p)			
	ΔE (Ha)	ΔG (Ha)	abundance (%)	imaginary frequencies	ΔE (Ha)	ΔG (Ha)	abundance (%)	imaginary frequencies
(S)-22bA	-995.69310	-995.42434	32.9	0	-995.94854	-995.67915	45.7	0
(S)-22bB	-995.69053	-995.42188	2.43	0	-995.94598	-995.67689	4.14	0
(S)-22bC	-995.69053	-995.42188	2.43	0	-995.94598	-995.67689	4.16	0
(S)-22bD	-995.69161	-995.42486	57.0	0	-995.94724	-995.67896	37.2	0
(S)-22bE	-995.69105	-995.42248	4.60	0	-995.94661	-995.67750	7.90	0
(S)-22bF	-995.68894	-995.42052	0.58	0	-995.94462	-995.67552	0.98	0

Table S15. Comparison Between Experimental (20b) and Calculated [(S)-22bA-(S)-22bF] NMR 3J Coupling Constants.

protons	experimental 3J (Hz)	B3LYP/6-31+G(d,p)		B3LYP/6-311++G(2d,2p)	
		calculated 3J (Hz)	Δ	calculated 3J (Hz)	Δ
1-2	4.30	3.97	-0.33	3.94	-0.36
2-3	8.60	9.44	+0.84	9.42	+0.82
3-4	8.70	9.86	+1.16	9.92	+1.22
4-5	5.20	7.11	+1.91	6.89	+1.69
5-6a	9.90	7.33	-2.57	8.82	-1.08
5-6b	5.20	6.98	+1.78	6.33	+1.13
6a-6b	11.10	11.14	+0.05	10.88	-0.22
			<i>Rmsd : 1.49</i>	<i>Rmsd : 1.04</i>	

Table S16. Comparison Between Experimental (20b) and Calculated [(S)-22bA-(S)-22bF] NMR 1H and ^{13}C Chemical Shifts.

atom	experimental δ (ppm)	B3LYP/6-31+G(d,p)		B3LYP/6-311++G(2d,2p)	
		calculated δ (ppm)	Δ	calculated δ (ppm)	Δ
H-1	4.96	4.78	-0.18	4.73	-0.23
H-2	3.57	3.53	-0.04	3.63	+0.06
H-3	4.55	4.22	-0.33	4.09	-0.46
H-4	4.06	4.20	+0.14	4.25	+0.19
H-5	4.20	4.48	+0.28	4.48	+0.28
H-6a	4.30	4.36	+0.06	4.40	+0.10
H-6b	4.06	4.12	+0.06	4.12	+0.06
		<i>Rmsd : 0.19</i>		<i>Rmsd : 0.24</i>	
C-1	96.1	96.7	+0.6	96.9	+0.8
C-2	72.4	71.8	-0.6	72.2	-0.2
C-3	65.7	69.2	+3.5	69.1	+3.4
C-4	74.4	72.1	-2.3	73.2	-1.2
C-5	66.9	68.4	+1.5	68.8	+1.9
C-6	67.2	65.1	-2.1	63.9	-3.3
C-7	95.6	95.0	-0.6	94.3	-1.3
		<i>Rmsd : 1.91</i>		<i>Rmsd : 2.06</i>	

Table S17. Comparison between Experimental (20b) and Calculated [(S)-22bA-(S)-22bF] H-H Distances by Quantitative NOESY NMR.

protons	experimental distance (Å)	B3LYP/6-31+G(d,p)		B3LYP/6-311++G(2d,2p)	
		calculated distance (Å)	Δ	calculated distance (Å)	Δ
3-7''	2.244	4.056	+1.812	4.075	+1.831
6a-7''	2.362	3.599	+1.237	3.630	+1.268
6a-3	2.656	2.706	+0.050	2.591	-0.065
5-7''	3.552	3.339	-0.213	3.456	-0.096
5-1	2.807	3.963	+1.156	3.968	+1.161
4-7''	3.516	3.817	+0.310	3.852	+0.336
2-1	2.319	2.425	+0.106	2.425	+0.106
2-4	2.392	2.528	+0.136	2.528	+0.136
2-3	2.894	3.055	+0.161	3.054	+0.160
		<i>Rmsd : 0.76</i>		<i>Rmsd : 0.76</i>	

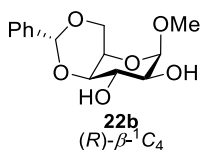


Table S18. 3D Coordinates of B3LYP/6-31+G(d,p) Optimized Geometries of (*R*)-22bA-(*R*)-22bE.

ID	atom	<i>(R)</i> -22bA coordinates			<i>(R)</i> -22bB coordinates			<i>(R)</i> -22bC coordinates		
		X	Y	Z	X	Y	Z	X	Y	Z
1	C	-1.4356	1.3552	-0.0109	1.3991	1.3464	-0.1394	-1.4104	1.3691	-0.0528
2	C	-3.3299	-0.2812	-0.2561	3.3321	-0.2299	0.3216	-3.3254	-0.2537	-0.3159
3	C	-1.1226	-0.9222	-1.1369	1.1221	-0.7752	1.2480	-1.1107	-0.9514	-1.1117
4	O	-2.5555	-1.0277	-1.1955	2.5547	-0.8822	1.3126	-2.5419	-1.0494	-1.1911
5	C	-0.6534	0.5447	-1.0498	0.6392	0.6717	1.0048	-0.6435	0.5134	-1.0707
6	C	-2.9276	1.1981	-0.2953	2.9050	1.2318	0.1378	-2.9113	1.2301	-0.3222
7	H	-0.8064	1.0277	-2.0199	0.8116	1.2666	1.9071	-0.7961	0.9663	-2.0557
8	H	-4.3609	-0.4022	-0.6104	4.3586	-0.2882	0.7029	-4.3474	-0.3607	-0.6982
9	H	-0.7816	-1.3271	-2.0936	0.7830	-1.0741	2.2433	-0.7556	-1.3936	-2.0464
10	O	-3.2097	-0.7551	1.0569	3.2589	-0.8373	-0.9495	-3.2691	-0.6810	1.0279
11	C	-3.8916	-1.9897	1.3034	3.9749	-2.0739	-1.0655	-3.9990	-1.8827	1.3064
12	H	-3.7705	-2.2049	2.3659	3.8878	-2.3876	-2.1064	-3.9149	-2.0564	2.3799
13	H	-3.4641	-2.8074	0.7134	3.5438	-2.8405	-0.4138	-3.5775	-2.7344	0.7630
14	H	-4.9596	-1.8922	1.0705	5.0324	-1.9300	-0.8124	-5.0551	-1.7617	1.0358
15	O	0.7693	0.6170	-0.8373	-0.7887	0.6780	0.8435	0.7807	0.5870	-0.8608
16	C	-0.4908	-1.7733	-0.0259	0.4965	-1.7469	0.2350	-0.5000	-1.7599	0.0413
17	H	-0.8721	-1.5019	0.9648	0.8753	-1.5776	-0.7798	-0.8906	-1.4453	1.0159
18	H	-0.6786	-2.8346	-0.2002	0.7019	-2.7803	0.5213	-0.6926	-2.8265	-0.0901
19	O	0.9328	-1.5884	-0.0733	-0.9277	-1.5823	0.2649	0.9252	-1.5856	0.0000
20	C	1.2782	-0.2395	0.1870	-1.2889	-0.2635	-0.0961	1.2816	-0.2294	0.2014
21	H	0.8475	0.0521	1.1574	-0.8536	-0.0486	-1.0869	0.8526	0.1087	1.1572
22	C	2.7795	-0.1032	0.2153	-2.7971	-0.1378	-0.1518	2.7838	-0.1039	0.2251
23	C	5.5716	0.1368	0.2868	-5.5860	0.1245	-0.3539	5.5771	0.1215	0.2878
24	C	3.5417	-0.3995	-0.9236	-3.5989	-1.2650	-0.3732	3.5451	-0.4646	-0.8956
25	C	3.4219	0.3124	1.3863	-3.3995	1.1230	-0.0391	3.4275	0.3689	1.3734
26	C	4.8153	0.4328	1.4236	-4.7874	1.2522	-0.1382	4.8216	0.4820	1.4063
27	C	4.9319	-0.2799	-0.8871	-4.9876	-1.1334	-0.4710	4.9360	-0.3525	-0.8634
28	H	3.0448	-0.7211	-1.8332	-3.1366	-2.2417	-0.4613	3.0474	-0.8303	-1.7880
29	H	2.8350	0.5420	2.2719	-2.7824	1.9981	0.1336	2.8412	0.6492	2.2447
30	H	5.3053	0.7565	2.3370	-5.2436	2.2336	-0.0449	5.3128	0.8506	2.3019
31	H	5.5171	-0.5109	-1.7724	-5.6001	-2.0149	-0.6371	5.5206	-0.6335	-1.7346
32	H	6.6534	0.2297	0.3131	-6.6648	0.2255	-0.4298	6.6595	0.2087	0.3106
33	H	-1.2303	1.0107	1.0098	1.1828	0.8588	-1.0994	-1.2058	1.0360	0.9736
34	H	-3.1197	1.5509	-1.3190	3.1324	1.7753	1.0603	-3.1262	1.6432	-1.3128
35	O	-3.7314	1.9245	0.6235	3.6594	1.8679	-0.8903	-3.7119	1.9641	0.5934
36	H	-3.4184	2.8413	0.6144	3.6990	1.2501	-1.6388	-3.7239	1.4640	1.4252
37	O	-1.1402	2.7503	-0.1148	1.0077	2.7151	-0.2011	-1.0459	2.7408	-0.1910
38	H	-0.1954	2.8774	0.0536	1.6161	3.1568	-0.8133	-0.0784	2.7884	-0.1651

Table S19. 3D Coordinates of B3LYP/6-31+G(d,p) Optimized Geometries of (R)-22bA-(R)-22bE (continued).

ID	atom	<i>(R)-22bD</i> coordinates			<i>(R)-22bE</i> coordinates		
		X	Y	Z	X	Y	Z
1	C	-1.2323	1.7858	-0.2841	-1.4275	1.3720	-0.0025
2	C	-2.9992	0.0033	-0.2802	-3.3219	-0.2676	-0.2584
3	C	-0.7920	-0.6506	-0.9068	-1.1260	-0.9208	-1.1372
4	O	-1.9793	-0.9996	-0.1886	-2.5576	-1.0159	-1.2039
5	C	-0.1919	0.6603	-0.3749	-0.6605	0.5430	-1.0438
6	C	-2.5285	1.2951	0.4041	-2.9212	1.2241	-0.2736
7	H	0.6200	0.9834	-1.0382	-0.8151	1.0274	-2.0133
8	H	-3.1919	0.2073	-1.3480	-4.3548	-0.3825	-0.6129
9	H	-1.0197	-0.5336	-1.9767	-0.7810	-1.3227	-2.0939
10	O	-4.1468	-0.4691	0.3419	-3.2040	-0.7555	1.0499
11	C	-4.8155	-1.5160	-0.3709	-3.8840	-1.9933	1.2829
12	H	-5.7289	-1.7327	0.1849	-3.7651	-2.2189	2.3436
13	H	-4.1960	-2.4164	-0.4241	-3.4544	-2.8049	0.6860
14	H	-5.0752	-1.1887	-1.3864	-4.9518	-1.8958	1.0484
15	O	0.3067	0.4572	0.9617	0.7631	0.6178	-0.8334
16	C	0.2198	-1.7748	-0.7322	-0.4969	-1.7756	-0.0274
17	H	-0.2456	-2.7441	-0.9196	-0.8778	-1.5060	0.9638
18	H	1.0443	-1.6309	-1.4425	-0.6837	-2.8366	-0.2043
19	O	0.7147	-1.8307	0.6133	0.9270	-1.5896	-0.0751
20	C	1.2480	-0.6097	1.0841	1.2730	-0.2418	0.1893
21	H	1.3579	-0.7487	2.1633	0.8425	0.0482	1.1600
22	C	2.6055	-0.2624	0.4696	2.7742	-0.1054	0.2165
23	C	5.1752	0.3525	-0.4910	5.5663	0.1348	0.2866
24	C	3.4622	-1.2810	0.0303	3.5353	-0.3955	-0.9247
25	C	3.0528	1.0657	0.4371	3.4176	0.3043	1.3891
26	C	4.3291	1.3720	-0.0437	4.8110	0.4247	1.4256
27	C	4.7386	-0.9751	-0.4508	4.9255	-0.2759	-0.8889
28	H	3.1282	-2.3131	0.0667	3.0376	-0.7123	-1.8356
29	H	2.4012	1.8593	0.7888	2.8314	0.5296	2.2763
30	H	4.6614	2.4058	-0.0672	5.3018	0.7439	2.3402
31	H	5.3906	-1.7741	-0.7918	5.5099	-0.5019	-1.7761
32	H	6.1671	0.5903	-0.8642	6.6481	0.2279	0.3123
33	H	-0.8096	2.6057	0.3095	-1.2214	1.0245	1.0179
34	H	-3.3103	2.0531	0.2861	-3.1256	1.6039	-1.2833
35	O	-2.3299	1.1364	1.8022	-3.6484	1.9746	0.6899
36	H	-1.5147	0.6210	1.9267	-4.5210	2.1873	0.3331
37	O	-1.4776	2.2006	-1.6297	-1.0686	2.7476	-0.1228
38	H	-2.0119	3.0068	-1.6181	-0.1009	2.7955	-0.1012

Table S20. Energy and Abundance of Conformers (R)-22bA-(R)-22bE.

conformer	B3LYP/6-31+G(d,p)				B3LYP/6-311++G(2d,2p)			
	ΔE (Ha)	ΔG (Ha)	abundance (%)	imaginary frequencies	ΔE (Ha)	ΔG (Ha)	abundance (%)	imaginary frequencies
(R)-22bA	-995.70054	-995.43419	27.0	0	-995.95595	-995.68804	19.6	0
(R)-22bB	-995.70163	-995.43448	36.5	0	-995.95715	-995.68853	33.0	0
(R)-22bC	-995.70175	-995.43433	31.1	0	-995.95721	-995.68870	39.4	0
(R)-22bD	-995.70023	-995.43230	3.62	0	-995.95575	-995.68701	6.57	0
(R)-22bE	-995.69773	-995.43160	1.73	0	-995.95344	-995.68551	1.35	0

Table S21. Comparison Between Experimental (20b) and Calculated [(R)-22bA-(R)-22bE] NMR 3J Coupling Constants.

protons	experimental 3J (Hz)	B3LYP/6-31+G(d,p)		B3LYP/6-311++G(2d,2p)	
		calculated 3J (Hz)	Δ	calculated 3J (Hz)	Δ
1-2	4.30	3.76	-0.54	3.70	-0.60
2-3	8.60	9.04	+0.44	8.85	+0.25
3-4	8.70	9.71	+1.01	9.49	+0.79
4-5	5.20	6.35	+1.15	6.18	+0.98
5-6a	9.90	11.15	+1.25	10.85	+0.95
5-6b	5.20	5.41	+0.21	5.30	+0.10
6a-6b	11.10	10.44	+0.66	10.48	+0.62
			<i>Rmsd : 0.83</i>	<i>Rmsd : 0.69</i>	

Table S22. Comparison Between Experimental (20b) and Calculated [(R)-22bA-(R)-22bE] NMR 1H and ^{13}C Chemical Shifts.

atom	experimental δ (ppm)	B3LYP/6-31+G(d,p)		B3LYP/6-311++G(2d,2p)	
		calculated δ (ppm)	Δ	calculated δ (ppm)	Δ
H-1	4.96	4.79	-0.17	4.80	-0.16
H-2	3.57	3.49	-0.08	3.47	-0.10
H-3	4.55	4.61	+0.06	4.59	+0.04
H-4	4.06	4.10	+0.04	4.08	+0.02
H-5	4.20	4.31	+0.11	4.28	+0.08
H-6a	4.30	4.35	+0.05	4.33	+0.03
H-6b	4.06	4.04	-0.02	4.04	-0.02
			<i>Rmsd : 0.09</i>	<i>Rmsd : 0.08</i>	
C-1	96.1	97.6	+1.5	97.6	+1.5
C-2	72.4	72.2	+0.2	72.1	-0.3
C-3	65.7	65.2	-0.5	65.5	-0.2
C-4	74.4	75.5	+1.1	75.3	+0.9
C-5	66.9	67.6	+0.7	67.6	+0.7
C-6	67.2	66.7	-0.5	66.6	-0.6
C-7	95.6	93.7	-2.1	93.5	-2.1
			<i>Rmsd : 1.15</i>	<i>Rmsd : 1.10</i>	

Table S23. Comparison Between Experimental (20b) and Calculated [(R)-22bA-(R)-22bE] H-H Distances by Quantitative NOESY NMR.

protons	experimental distance (Å)	B3LYP/6-31+G(d,p)		B3LYP/6-311++G(2d,2p)	
		calculated distance (Å)	Δ	calculated distance (Å)	Δ
3-7''	2.244	2.272	+0.028	2.282	+0.038
6a-7''	2.362	2.345	-0.017	2.358	-0.004
6a-3	2.656	2.518	-0.138	2.529	-0.127
5-7''	3.552	3.890	+0.338	3.905	+0.353
5-1	2.807	3.621	+0.814	3.445	+0.638
4-7''	3.516	3.696	+0.180	3.698	+0.182
2-1	2.319	2.426	+0.107	2.428	+0.109
2-4	2.392	2.527	+0.135	2.545	+0.153
2-3	2.894	3.015	+0.121	2.991	+0.097
		<i>Rmsd : 0.46</i>		<i>Rmsd : 0.43</i>	

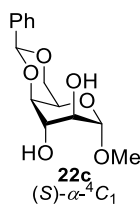


Table S24. 3D Coordinates of B3LYP/6-31+G(d,p) Optimized Geometries of 22cA-22cC.

ID	atom	22cA coordinates			22cB coordinates			22cC coordinates		
		X	Y	Z	X	Y	Z	X	Y	Z
1	C	-1.4076	1.1978	0.2835	-1.1849	0.6928	0.9913	1.1957	-0.7806	0.9004
2	C	-2.6235	-0.4714	-0.9691	-2.9108	0.3705	-0.6337	2.9285	-0.3379	-0.6881
3	C	-1.6863	-1.1399	1.2836	-1.4829	-1.6152	-0.0074	1.4982	1.5962	0.0792
4	C	-2.0373	-1.6276	-0.1372	-2.9079	-1.0654	-0.0793	2.9234	1.0527	-0.0282
5	C	-0.8178	0.1305	1.2165	-0.5915	-0.7232	0.8653	0.6035	0.6423	0.8800
6	O	-1.7532	0.6471	-1.0016	-1.7399	1.0948	-0.2707	1.7548	-1.0855	-0.3867
7	O	-3.8836	-0.1564	-0.4046	-4.0853	0.9839	-0.1588	4.0995	-0.9863	-0.2529
8	O	-0.9042	-2.1817	-0.7971	-3.6496	-1.9458	-0.9234	3.6683	1.9939	-0.8006
9	O	-2.8542	-0.9006	2.0663	-1.4724	-2.9396	0.5208	1.4863	2.8774	0.7052
10	O	0.4826	-0.2712	0.7367	0.7054	-0.6990	0.2440	-0.6909	0.6645	0.2545
11	C	-0.3822	2.2992	0.0446	-0.1286	1.7003	1.4289	0.1377	-1.8195	1.2558
12	O	0.8896	1.7610	-0.3421	1.1051	1.5428	0.7200	-1.0937	-1.6043	0.5594
13	C	1.3820	0.8382	0.6056	1.6033	0.2204	0.8507	-1.5811	-0.2988	0.7937
14	C	-4.6701	0.7744	-1.1634	-4.4134	2.2169	-0.8107	4.4278	-2.1711	-0.9886
15	H	-2.2969	1.6393	0.7510	-1.9739	0.6888	1.7551	1.9822	-0.8355	1.6648
16	H	-2.7339	-0.7674	-2.0185	-2.9110	0.3529	-1.7312	2.9351	-0.2390	-1.7812
17	H	-1.1149	-1.9206	1.7944	-1.0628	-1.6153	-1.0226	1.0817	1.6724	-0.9346
18	H	-2.7860	-2.4217	-0.0711	-3.3488	-1.0598	0.9257	3.3600	0.9714	0.9755
19	H	-0.7213	0.5487	2.2279	-0.5066	-1.1680	1.8673	0.5156	1.0111	1.9122
20	H	-0.1460	-1.5948	-0.6274	-4.5943	-1.8175	-0.7614	4.6124	1.8552	-0.6435
21	H	-3.5249	-0.4924	1.4898	-2.1003	-3.4601	-0.0034	2.1188	3.4341	0.2254
22	H	-0.7017	2.9527	-0.7690	-0.4745	2.7181	1.2394	0.4832	-2.8186	0.9849
23	H	-0.2717	2.8961	0.9611	0.0502	1.5813	2.5074	-0.0430	-1.7874	2.3400
24	H	-4.8285	0.3942	-2.1794	-4.5273	2.0643	-1.8915	4.5452	-1.9433	-2.0558
25	H	-5.6283	0.8600	-0.6501	-5.3630	2.5489	-0.3886	5.3757	-2.5333	-0.5882
26	H	-4.1860	1.7545	-1.2100	-3.6464	2.9762	-0.6278	3.6590	-2.9399	-0.8616
27	H	1.4531	1.3268	1.5907	1.6962	-0.0212	1.9228	-1.6448	-0.1417	1.8863
28	C	2.7250	0.3189	0.1623	2.9408	0.1222	0.1632	-2.9424	-0.1292	0.1534
29	C	5.2199	-0.6842	-0.6296	5.4353	-0.0595	-1.1045	-5.5082	0.2164	-0.9361
30	C	2.9148	-0.1439	-1.1476	3.0573	0.3973	-1.2070	-3.7454	-1.2412	-0.1304
31	C	3.7890	0.2778	1.0703	4.0777	-0.2433	0.8921	-3.4344	1.1578	-0.1061
32	C	5.0343	-0.2229	0.6766	5.3231	-0.3345	0.2610	-4.7103	1.3291	-0.6495
33	C	4.1582	-0.6428	-1.5412	4.2996	0.3068	-1.8375	-5.0221	-1.0679	-0.6748
34	H	2.0940	-0.1050	-1.8567	2.1769	0.6811	-1.7748	-3.3701	-2.2382	0.0710
35	H	3.6466	0.6384	2.0857	3.9921	-0.4572	1.9543	-2.8166	2.0224	0.1124
36	H	5.8550	-0.2495	1.3872	6.2000	-0.6190	0.8350	-5.0797	2.3308	-0.8492
37	H	4.2998	-0.9981	-2.5576	4.3835	0.5213	-2.8989	-5.6345	-1.9376	-0.8948
38	H	6.1865	-1.0719	-0.9378	6.4010	-0.1295	-1.5965	-6.4999	0.3498	-1.3586

Table S25. Energy and Abundance of Conformers 22cA-22cC.

conformer	B3LYP/6-31+G(d,p)				B3LYP/6-311++G(2d,2p)			
	ΔE (Ha)	ΔG (Ha)	abundance (%)	imaginary frequencies	ΔE (Ha)	ΔG (Ha)	abundance (%)	imaginary frequencies
22cA	-995.70793	-995.43926	97.1	0	-995.96321	-995.69375	97.5	0
22cB	-995.70123	-995.43569	2.22	0	-995.95704	-995.68997	1.77	0
22cC	-995.70046	-995.43456	0.67	0	-995.95639	-995.68908	0.69	0

Table S26. Comparison between experimental (20c) and calculated (22cA-22cC) NMR 3J coupling constants.

protons	experimental 3J (Hz)	B3LYP/6-31+G(d,p)		B3LYP/6-311++G(2d,2p)	
		calculated 3J (Hz)	Δ	calculated 3J (Hz)	Δ
1-2	N/A	1.70	N/A	1.68	N/A
2-3	1.20	2.98	-1.78	2.95	-1.75
3-4	2.70	3.12	-0.42	3.11	-0.41
4-5	N/A	1.38	N/A	1.38	N/A
5-6a	1.30	1.56	-0.26	1.56	+0.26
5-6b	1.70	1.90	+0.20	1.90	+0.20
6a-6b	12.60	11.92	-0.68	11.92	-0.68
			<i>Rmsd : 0.75</i>	<i>Rmsd : 0.74</i>	

Table S27. Comparison Between Experimental (20c) and Calculated (22cA-22cC) NMR 1H and ^{13}C Chemical Shifts.

atom	experimental δ (ppm)	B3LYP/6-31+G(d,p)		B3LYP/6-311++G(2d,2p)	
		calculated δ (ppm)	Δ	calculated δ (ppm)	Δ
H-1	5.20	5.12	-0.08	5.12	-0.08
H-2	3.71	3.66	-0.05	3.66	-0.05
H-3	4.00	3.91	-0.09	3.91	-0.09
H-4	4.14	4.24	+0.10	4.24	+0.10
H-5	4.00	3.97	-0.03	3.97	-0.03
H-6a	4.36	4.42	+0.06	4.42	+0.06
H-6b	4.13	4.22	+0.09	4.22	+0.09
		<i>Rmsd : 0.08</i>		<i>Rmsd : 0.08</i>	
C-1	99.2	100.6	+1.4	100.6	+1.4
C-2	67.2	67.3	+0.1	67.2	+0.0
C-3	68.0	68.4	+0.4	68.4	+0.4
C-4	76.0	75.7	-0.3	75.7	-0.3
C-5	59.5	60.4	+0.9	60.4	+0.9
C-6	70.2	68.9	-1.3	68.9	-1.3
C-7	101.6	100.5	-1.1	100.5	-1.1
		<i>Rmsd : 0.93</i>		<i>Rmsd : 0.93</i>	

3. Traces of NMR Spectra for New Compounds.

Figure S2 | ^1H NMR spectrum (CDCl_3 , 600 MHz) of 1,2,3,4,6-penta-*O*-acetyl α -D-idopyranose (2)

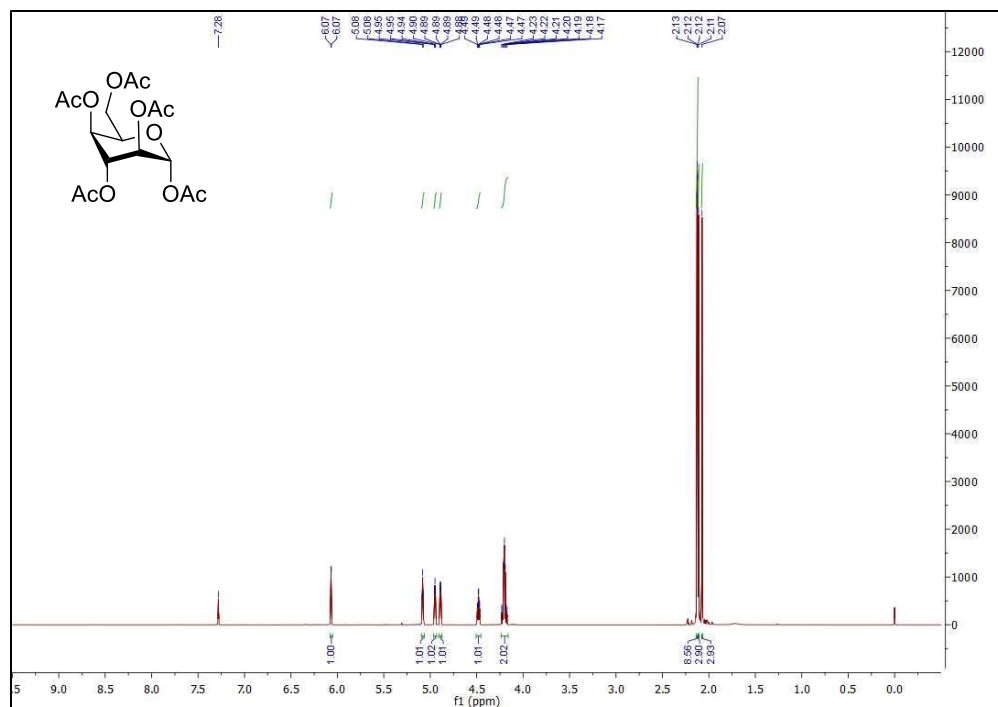


Figure S3 | ^1H NMR spectrum (CDCl_3 , 600 MHz) of ethyl 2,3,4,6-tetra-*O*-acetyl-1-thio- α -D-idopyranoside (3a)

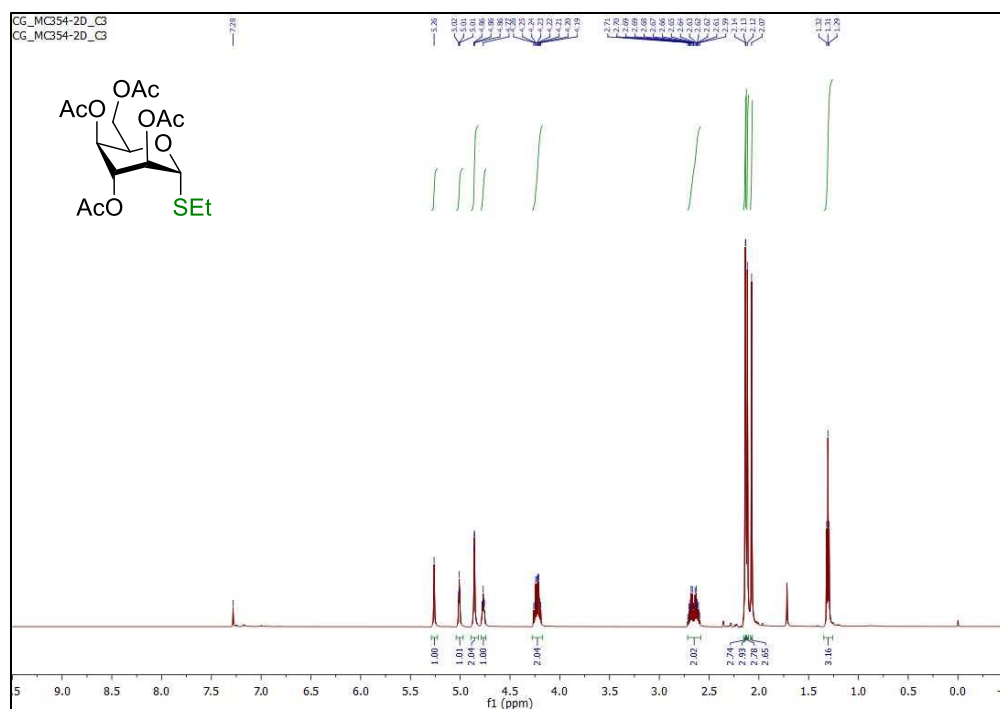


Figure S4 | $^{13}\text{C}\{^1\text{H}\}$ NMR spectrum (CDCl_3 , 150 MHz) of ethyl 2,3,4,6-tetra-*O*-acetyl-1-thio- α -D-idopyranoside (3a)

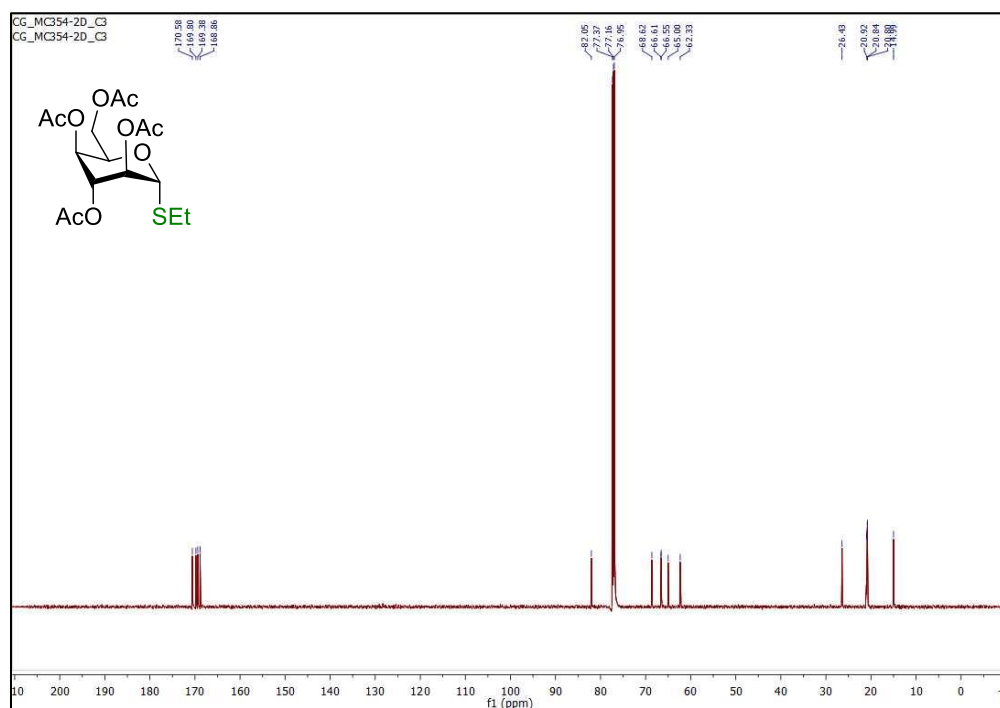


Figure S5 | ^1H NMR spectrum (CDCl_3 , 600 MHz) of *para*-methylphenyl 2,3,4,6-tetra-*O*-acetyl-1-thio- α -D-idopyranoside (3b)

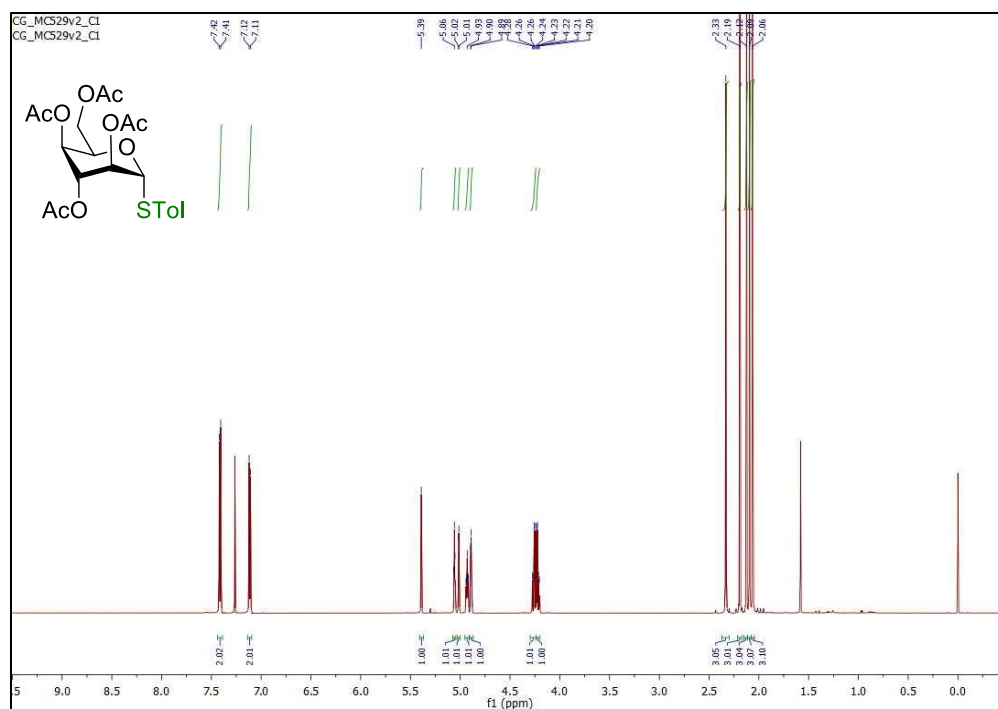


Figure S6 | $^{13}\text{C}\{^1\text{H}\}$ NMR spectrum (CDCl_3 , 150 MHz) of *para*-methylphenyl 2,3,4,6-tetra-*O*-acetyl-1-thio- α -D-idopyranoside (3b)

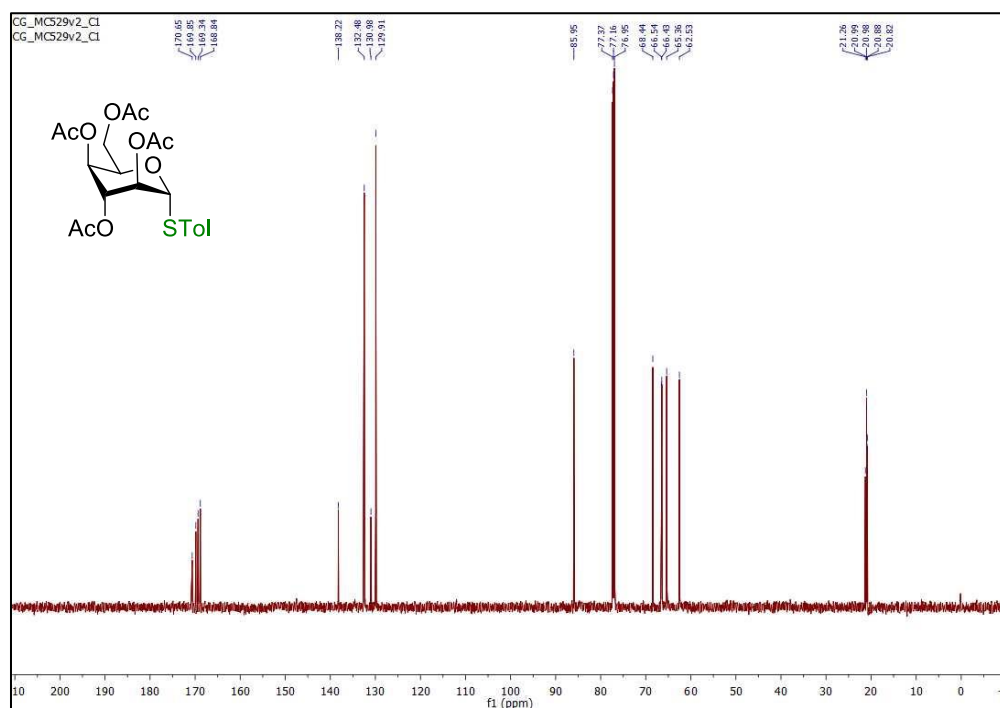


Figure S7 | ^1H NMR spectrum (CDCl_3 , 600 MHz) of ethyl 4,6-*O*-benzylidene-1-thio- α -D-idopyranoside (4a)

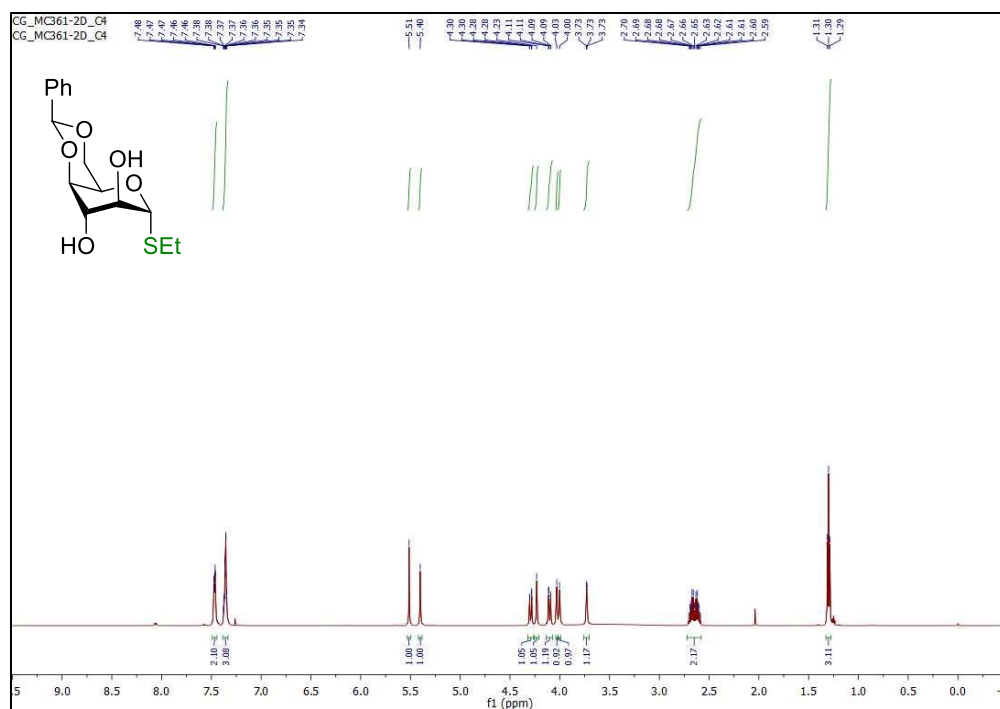


Figure S8 | $^{13}\text{C}\{^1\text{H}\}$ NMR spectrum (CDCl_3 , 150 MHz) of ethyl 4,6-*O*-benzylidene-1-thio- α -D-idopyranoside (4a)

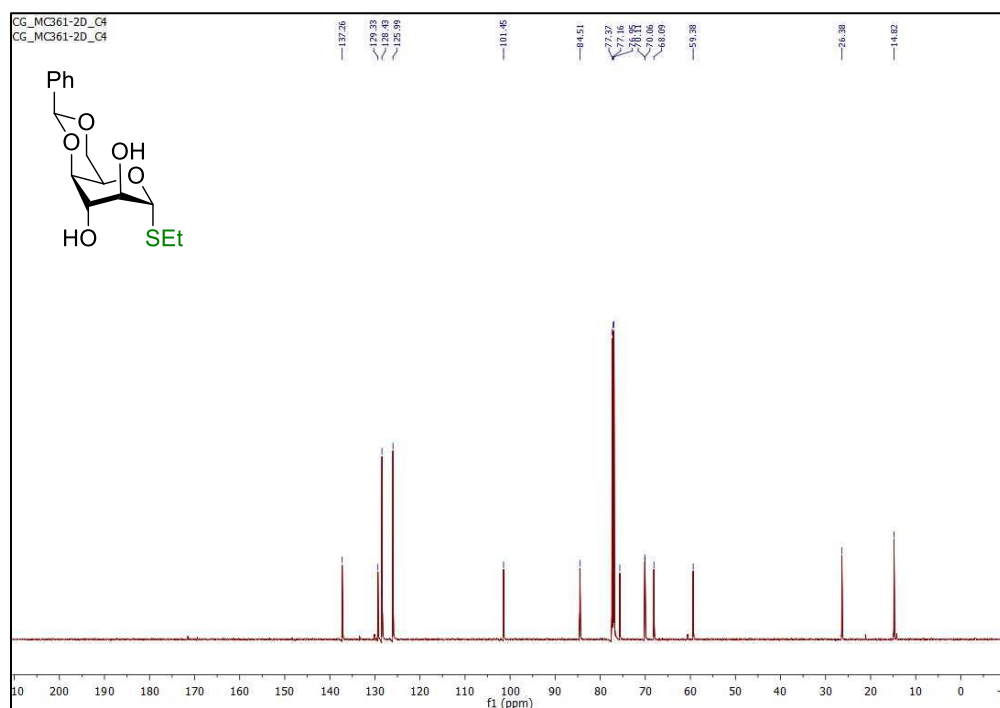


Figure S9 | ^1H NMR spectrum (CDCl_3 , 600 MHz) of *para*-methylphenyl 4,6-*O*-benzylidene-1-thio- α -D-idopyranoside (4b)

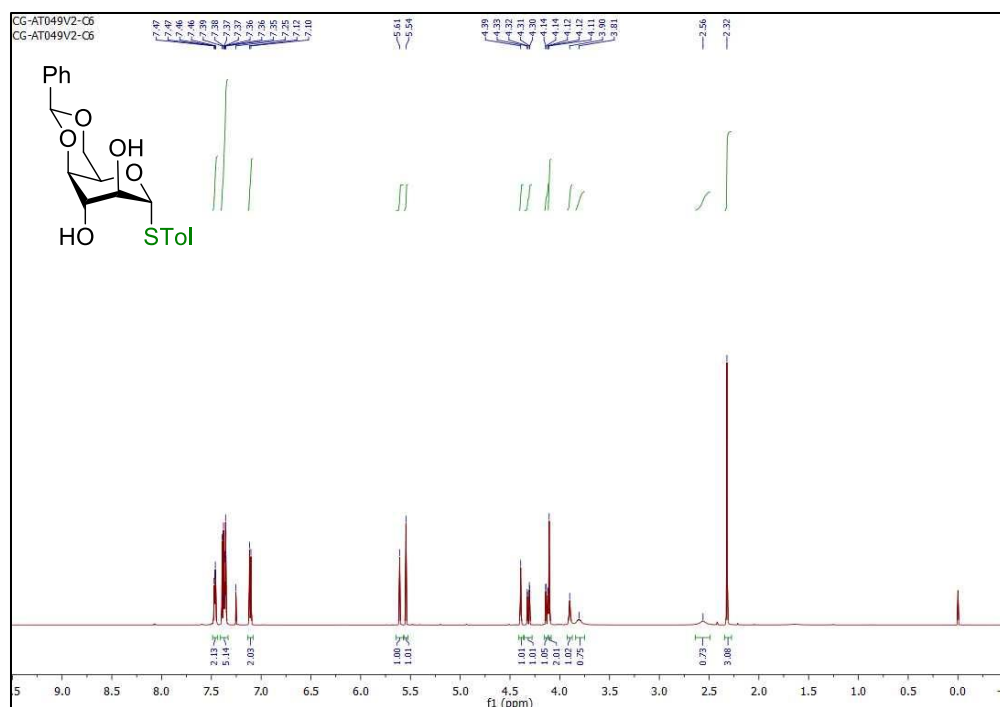


Figure S10 | $^{13}\text{C}\{^1\text{H}\}$ NMR spectrum (CDCl_3 , 150 MHz) of *para*-methylphenyl 4,6-*O*-benzylidene-1-thio- α -D-idopyranoside (4b)

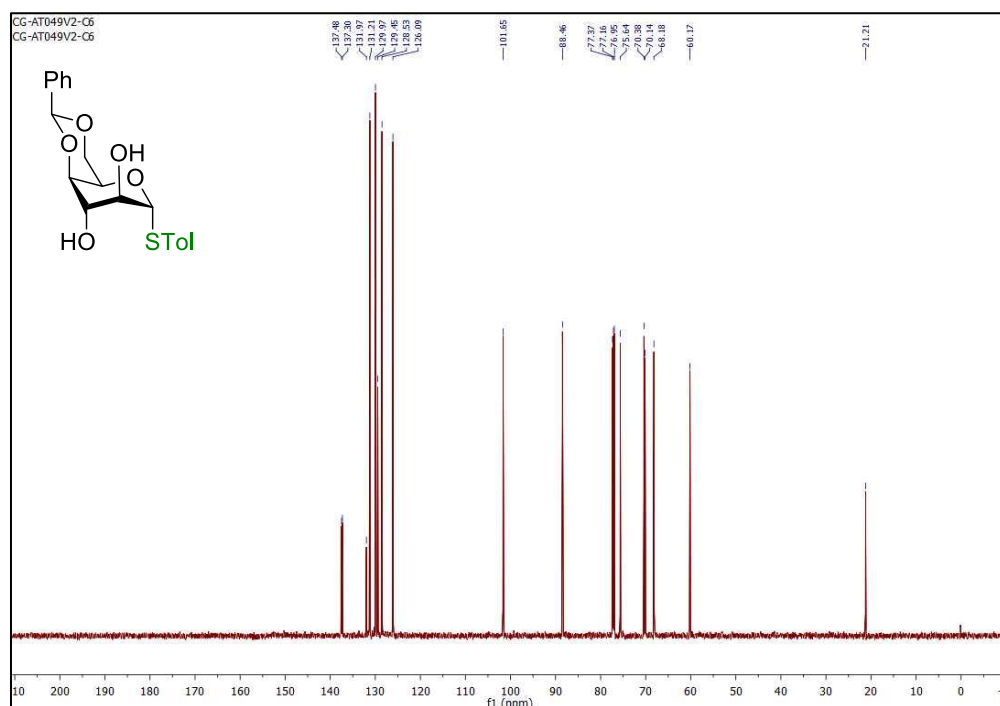


Figure S11 | ^1H NMR spectrum (CDCl_3 , 600 MHz) of ethyl 4,6-*O*-benzylidene-2-*O*-*tert*-butyldimethylsilyl-1-thio- α -D-idopyranoside (5a)

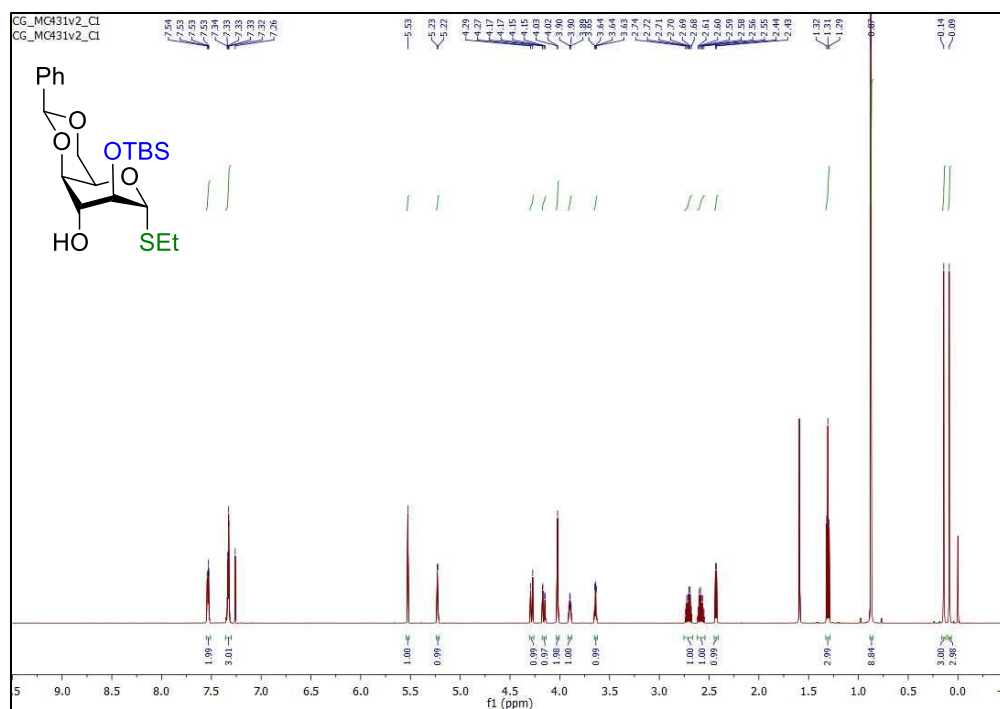


Figure S12 | $^{13}\text{C}\{^1\text{H}\}$ NMR spectrum (CDCl_3 , 150 MHz) of ethyl 4,6-*O*-benzylidene-2-*O*-*tert*-butyldimethylsilyl-1-thio- α -D-idopyranoside (5a)

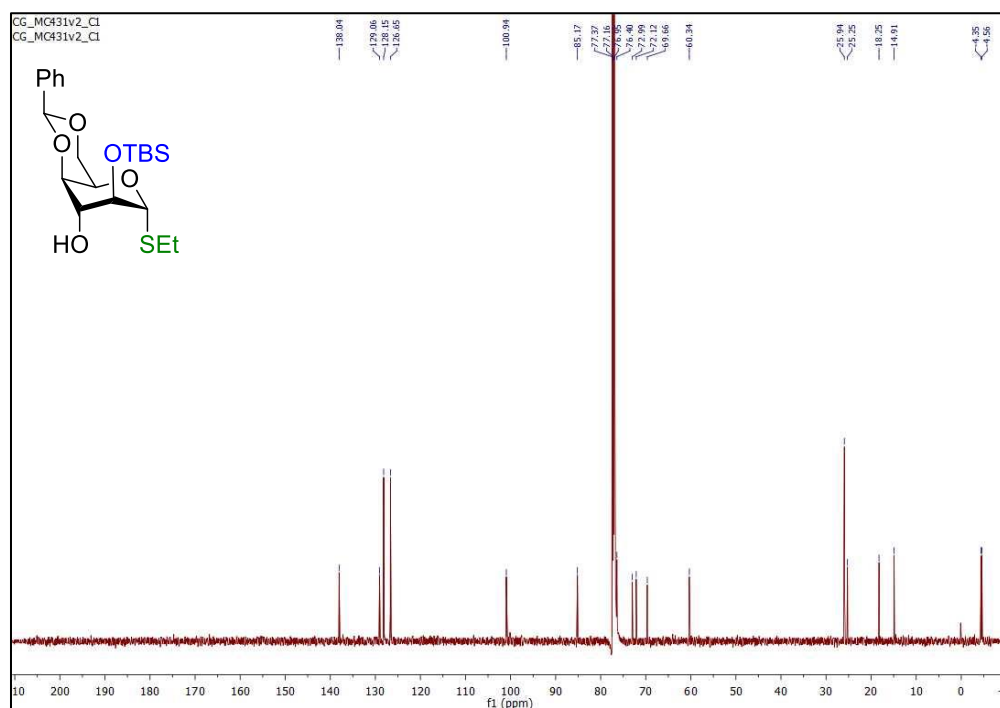


Figure S13 | ^1H NMR spectrum (CDCl_3 , 600 MHz) of ethyl 4,6-*O*-benzylidene-3-*O*-*tert*-butyldimethylsilyl-1-thio- α -D-idopyranoside (10)

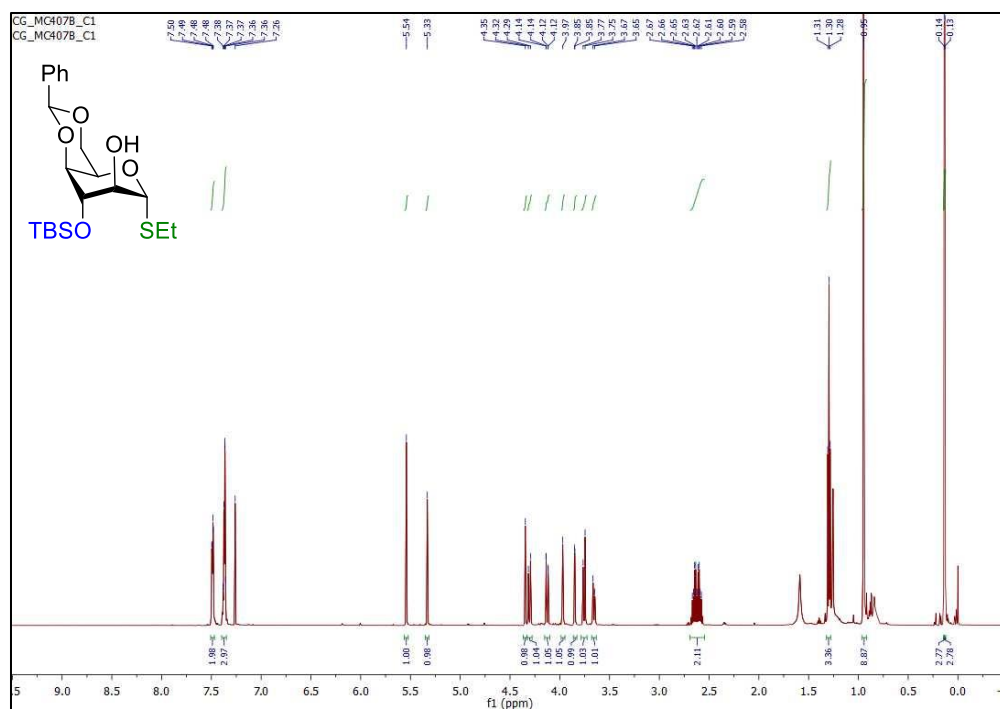


Figure S14 | $^{13}\text{C}\{^1\text{H}\}$ NMR spectrum (CDCl_3 , 150 MHz) of ethyl 4,6-*O*-benzylidene-3-*O*-*tert*-butyldimethylsilyl-1-thio- α -D-idopyranoside (10)

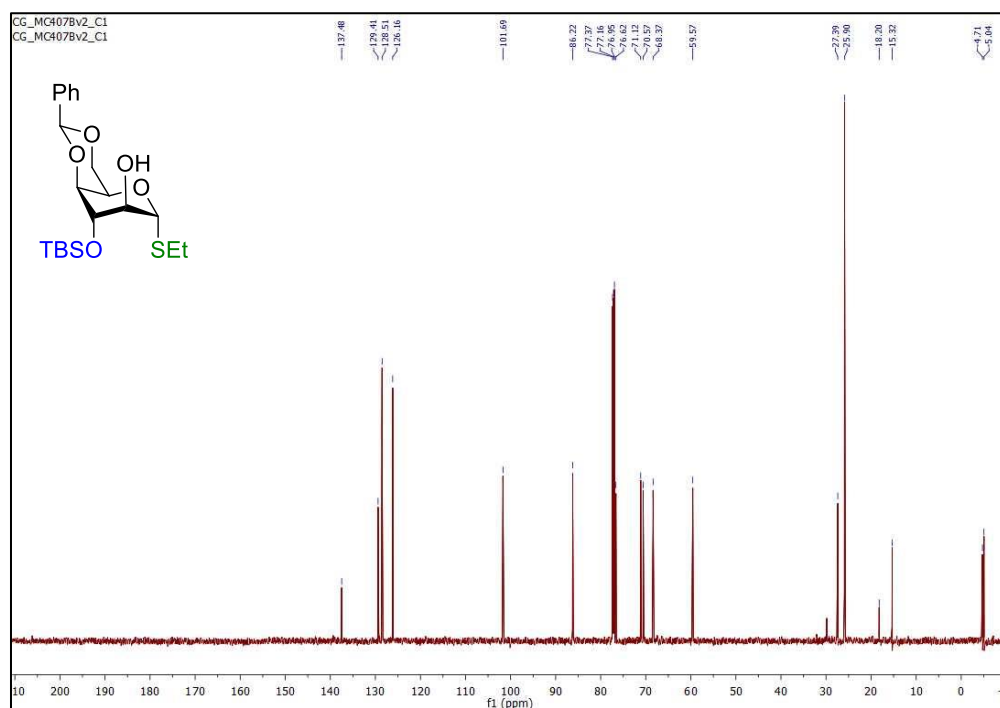


Figure S15 | ^1H NMR spectrum (CDCl_3 , 600 MHz) of *para*-methylphenyl 4,6-*O*-benzylidene-2-*O*-*tert*-butyldimethylsilyl-1-thio- α -D-idopyranoside (**5b**)

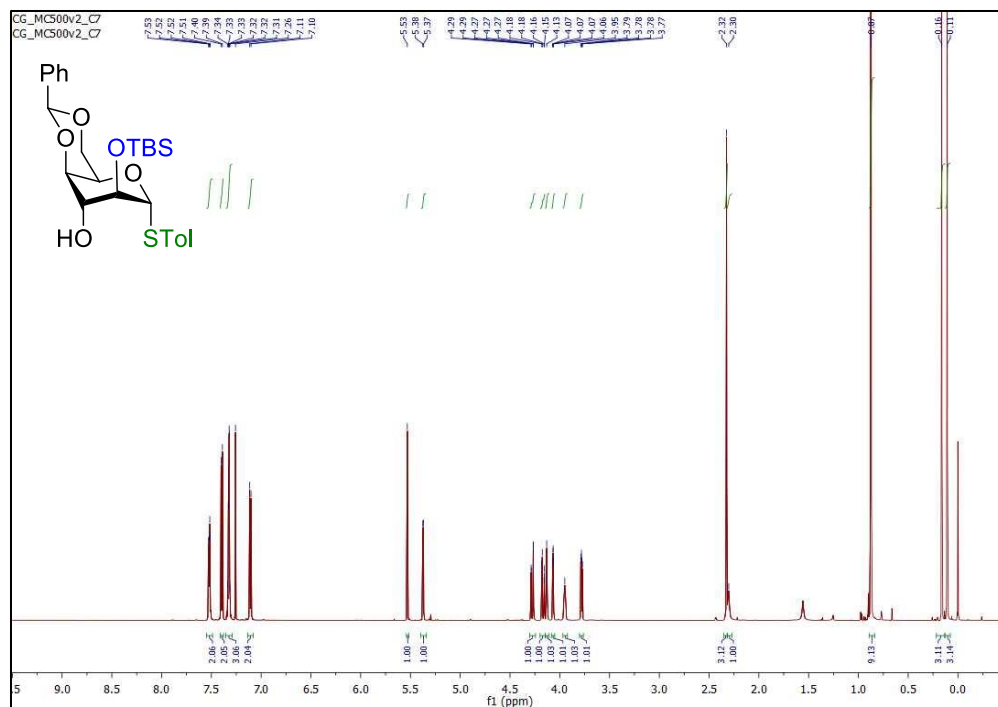


Figure S16 | $^{13}\text{C}\{^1\text{H}\}$ NMR spectrum (CDCl_3 , 150 MHz) of *para*-methylphenyl 4,6-*O*-benzylidene-2-*O*-*tert*-butyldimethylsilyl-1-thio- α -D-idopyranoside (**5b**)

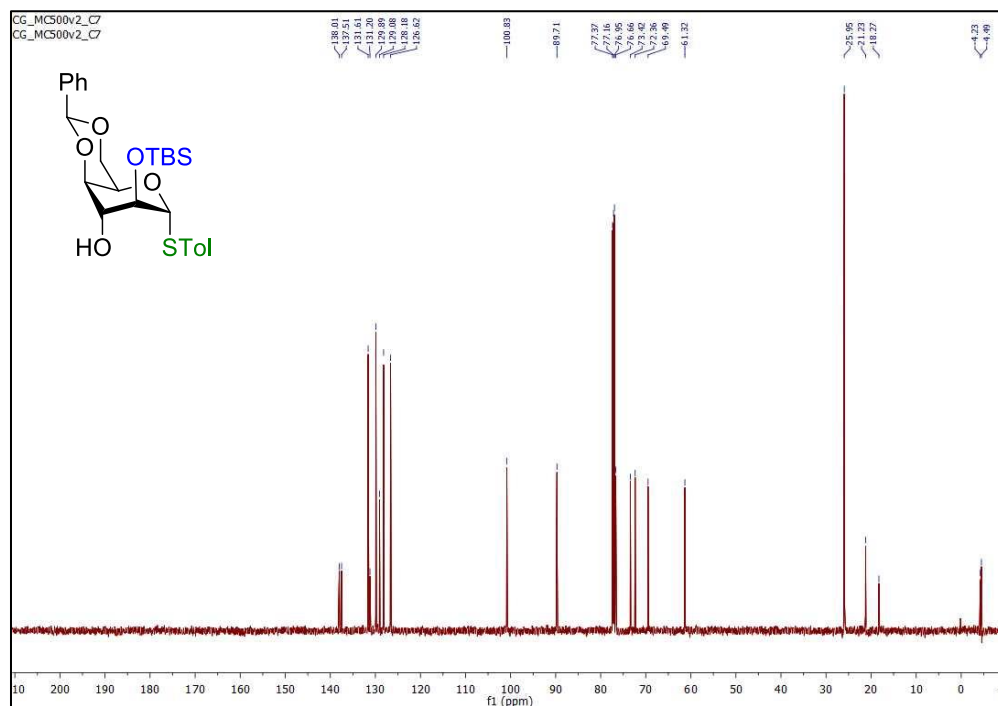


Figure S19 | ^1H NMR spectrum (CDCl_3 , 600 MHz) of *para*-methylphenyl 3-*O*-acetyl-4,6-*O*-benzylidene-2-*O*-*tert*-butyldimethylsilyl-1-thio- α -D-idopyranoside (6b)

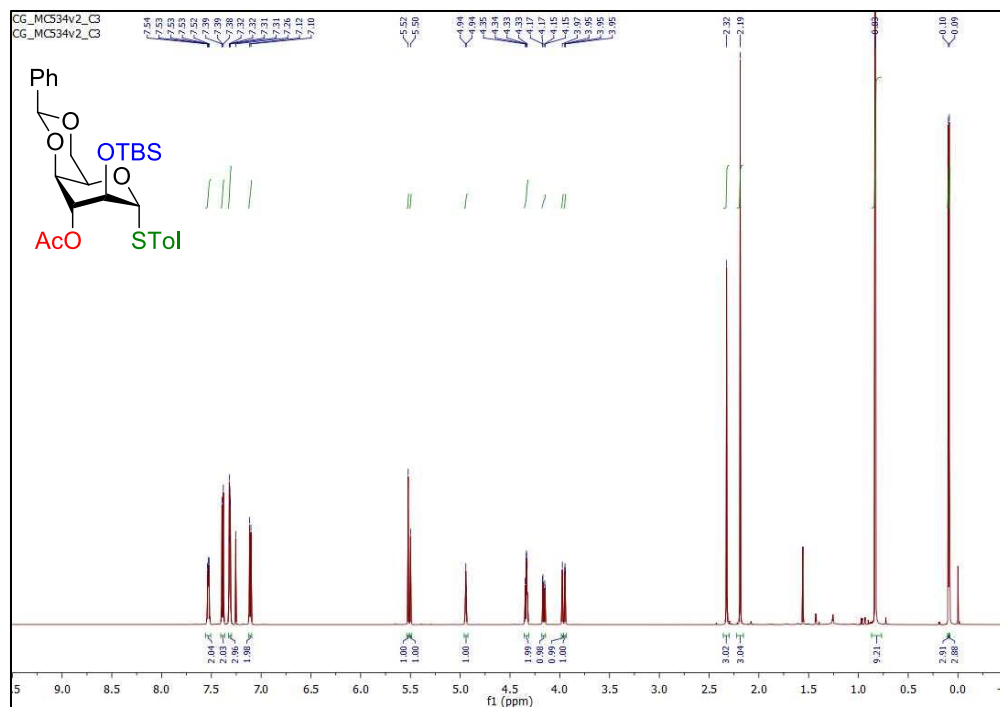


Figure S20 | $^{13}\text{C}\{^1\text{H}\}$ NMR spectrum (CDCl_3 , 150 MHz) of *para*-methylphenyl 3-*O*-acetyl-4,6-*O*-benzylidene-2-*O*-*tert*-butyldimethylsilyl-1-thio- α -D-idopyranoside (6b)

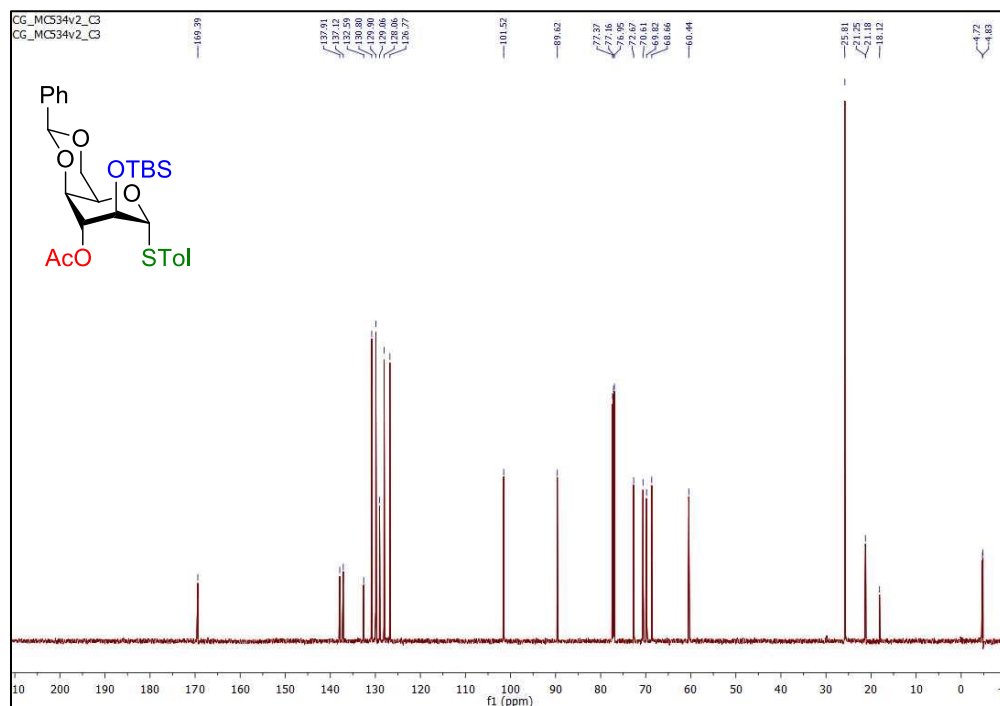


Figure S21 | ^1H NMR spectrum (CDCl_3 , 600 MHz) of *para*-methylphenyl 4,6-*O*-benzylidene-2-*O*-*tert*-butyldimethylsilyl-3-*O*-dichloroacetyl-1-thio- α -D-idopyranoside (7)

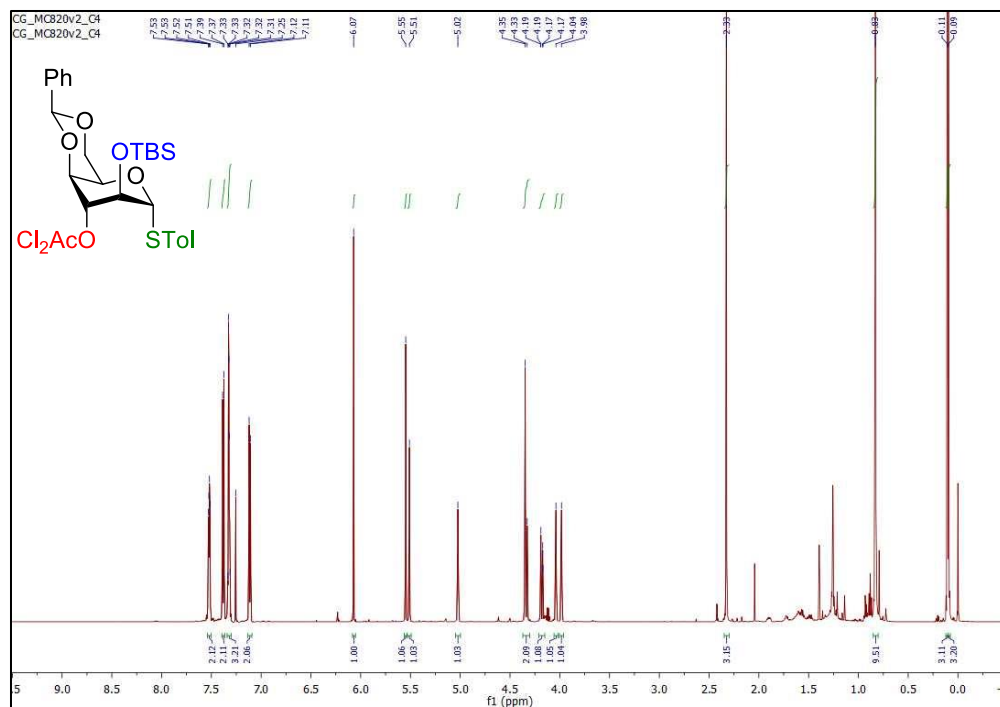


Figure S22 | $^{13}\text{C}\{^1\text{H}\}$ NMR spectrum (CDCl_3 , 150 MHz) of *para*-methylphenyl 4,6-*O*-benzylidene-2-*O*-*tert*-butyldimethylsilyl-3-*O*-dichloroacetyl-1-thio- α -D-idopyranoside (7)

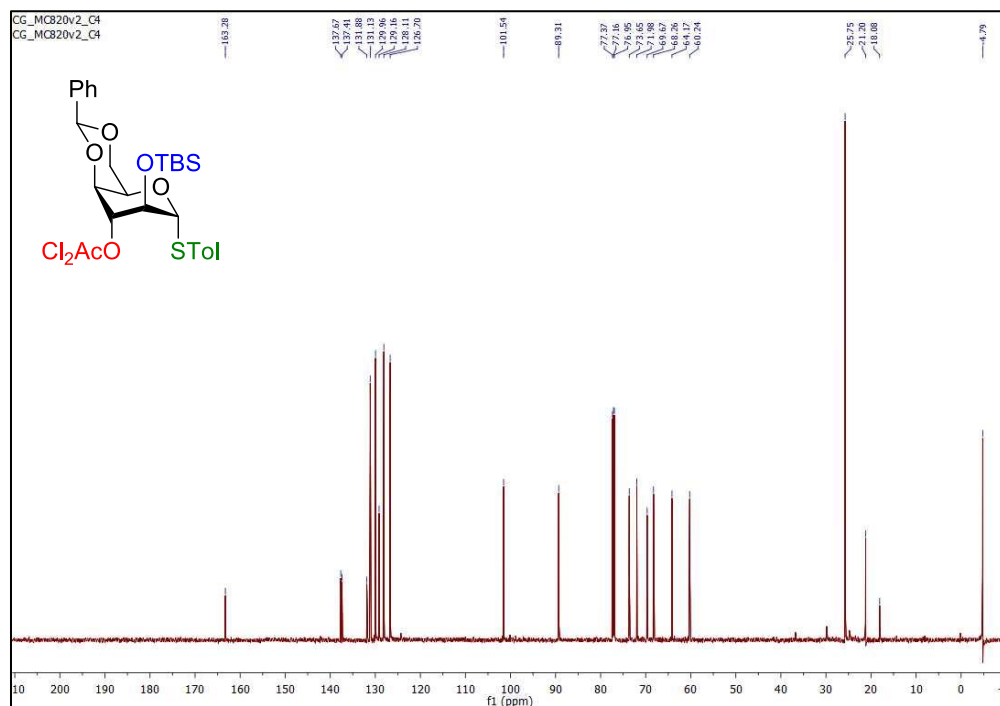


Figure S23 | ^1H NMR spectrum (CDCl_3 , 600 MHz) of *para*-methylphenyl 3-*O*-(2-azidomethyl)benzoyl-4,6-*O*-benzylidene-2-*O*-*tert*-butyldimethylsilyl-1-thio- α -D-idopyranoside (8)

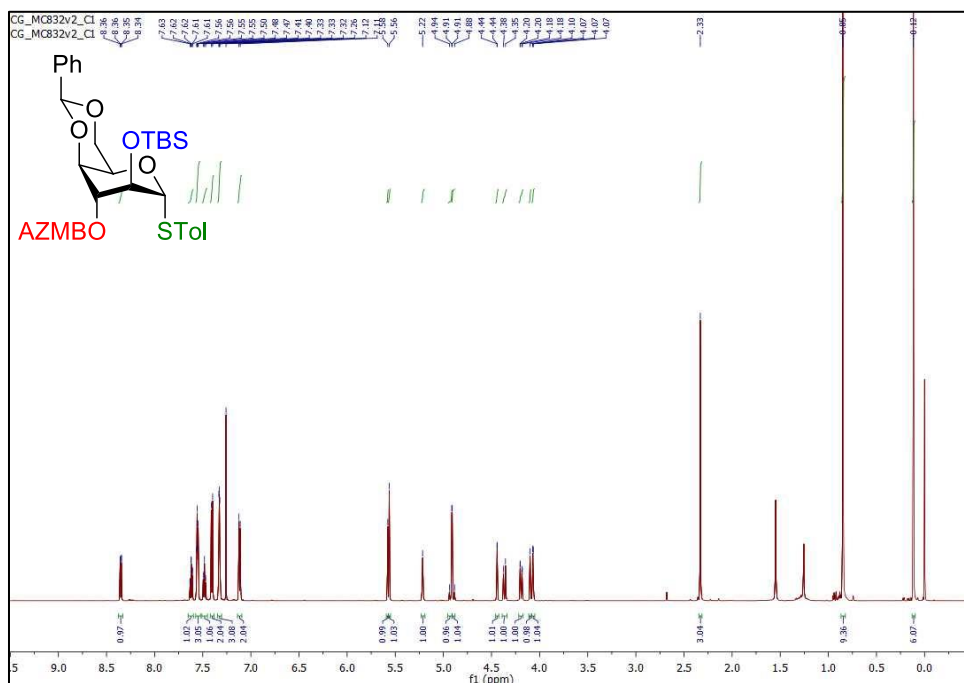


Figure S24 | $^{13}\text{C}\{^1\text{H}\}$ NMR spectrum (CDCl_3 , 150 MHz) of *para*-methylphenyl 3-*O*-(2-azidomethyl)benzoyl-4,6-*O*-benzylidene-2-*O*-*tert*-butyldimethylsilyl-1-thio- α -D-idopyranoside (8)

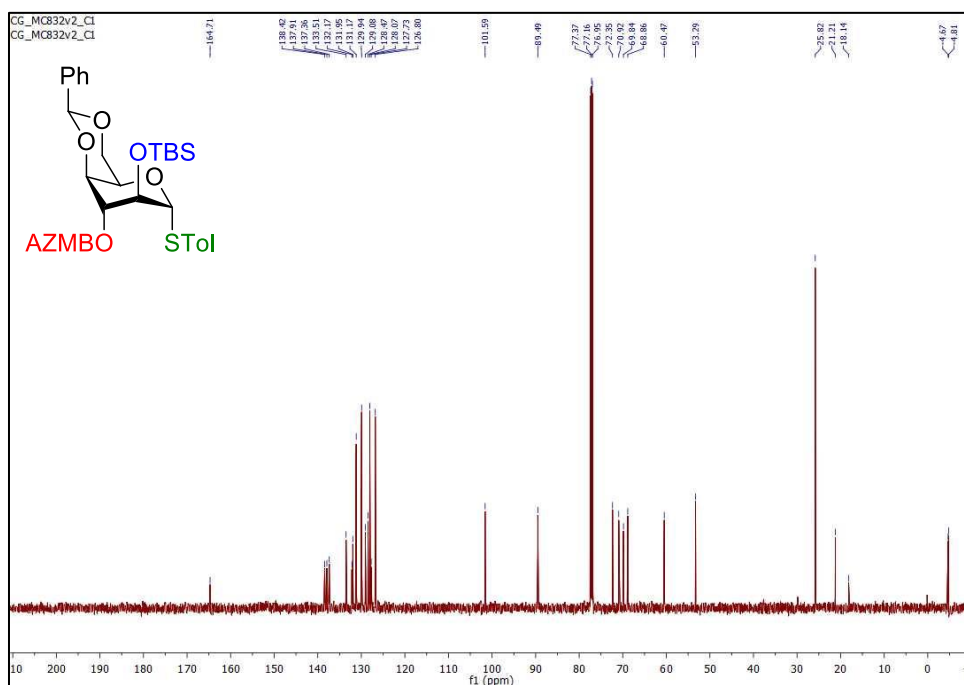


Figure S25 | ^1H NMR spectrum (CDCl_3 , 600 MHz) of *para*-methylphenyl 4,6-*O*-benzylidene-2-*O*-*tert*-butyldimethylsilyl-3-*O*-*tert*-butoxycarbonyl-1-thio- α -D-idopyranoside (9)

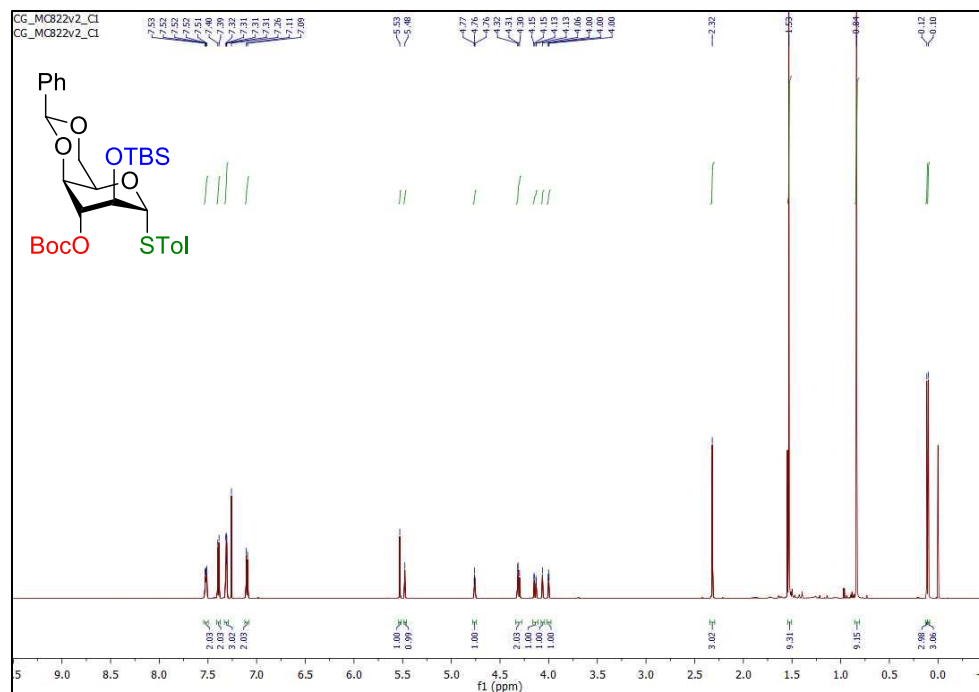


Figure S26 | $^{13}\text{C}\{^1\text{H}\}$ NMR spectrum (CDCl_3 , 150 MHz) of *para*-methylphenyl 4,6-*O*-benzylidene-2-*O*-*tert*-butyldimethylsilyl-3-*O*-*tert*-butoxycarbonyl-1-thio- α -D-idopyranoside (9)

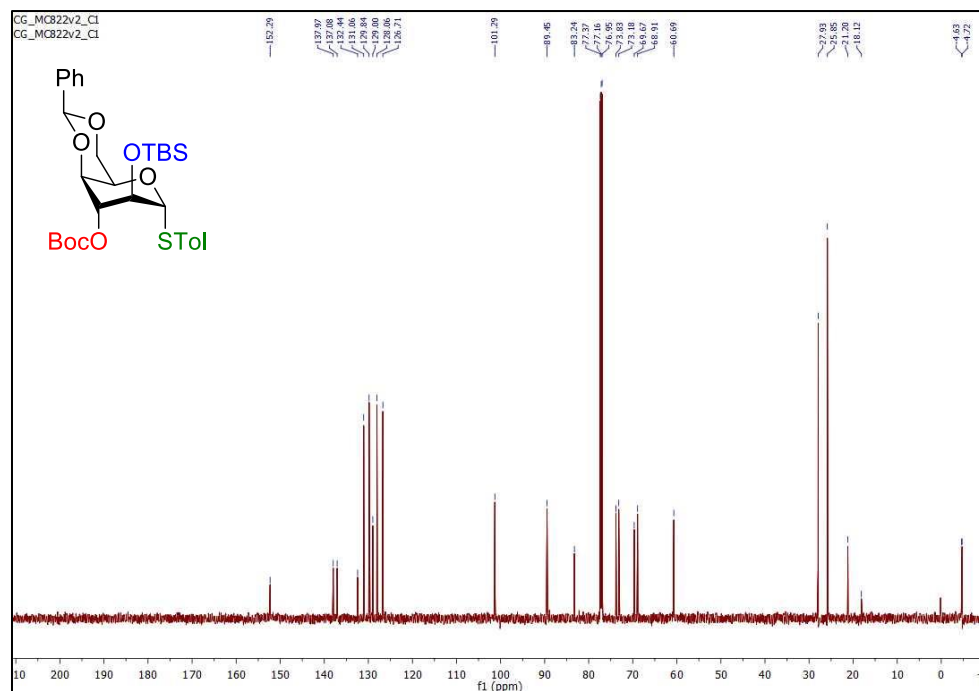


Figure S27 | ^1H NMR spectrum (CDCl_3 , 600 MHz) of (2-adamantyl) 3-*O*-acetyl-(*S*)-4,6-*O*-benzylidene-2-*O*-*tert*-butyldimethylsilyl- β -D-idopyranoside (14a)

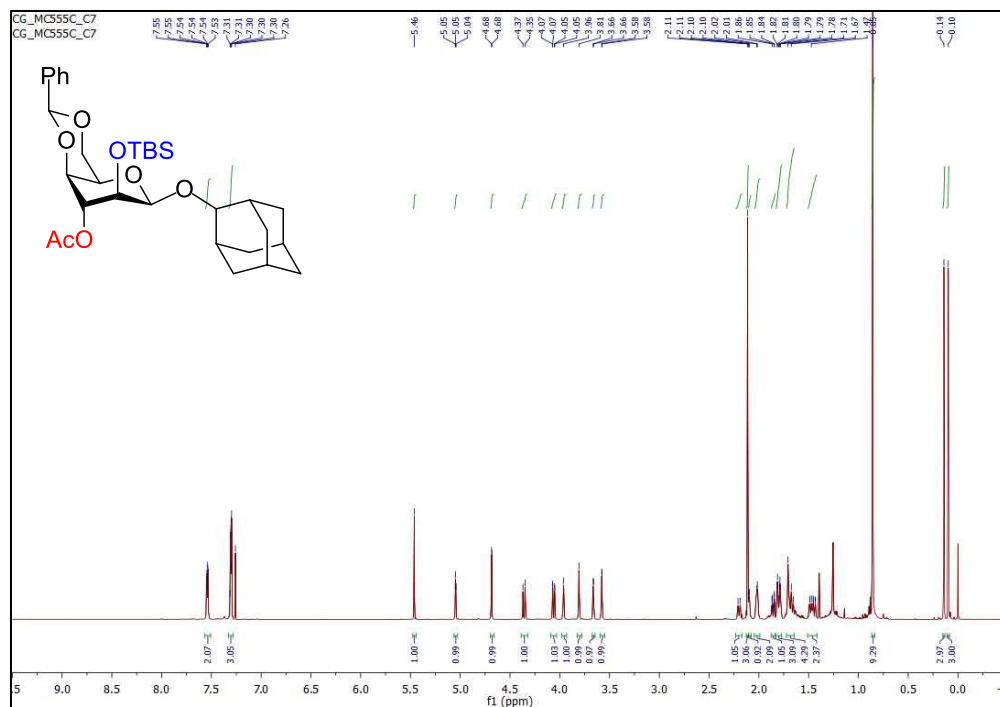


Figure S28 | $^{13}\text{C}\{^1\text{H}\}$ NMR spectrum (CDCl_3 , 150 MHz) of (2-adamantyl) 3-*O*-acetyl-(*S*)-4,6-*O*-benzylidene-2-*O*-*tert*-butyldimethylsilyl- β -D-idopyranoside (14a)

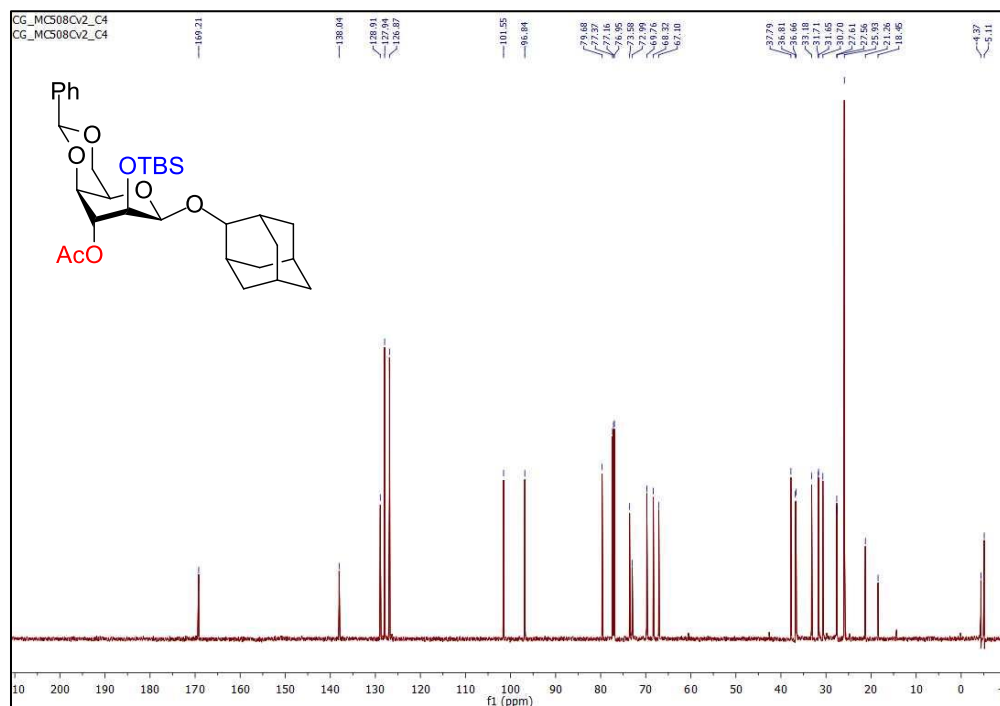


Figure S29 | ^1H NMR spectrum (CDCl_3 , 600 MHz) of (2-adamantyl) 3-*O*-acetyl-(*R*)-4,6-*O*-benzylidene-2-*O*-*tert*-butyldimethylsilyl- β -D-idopyranoside (14b)

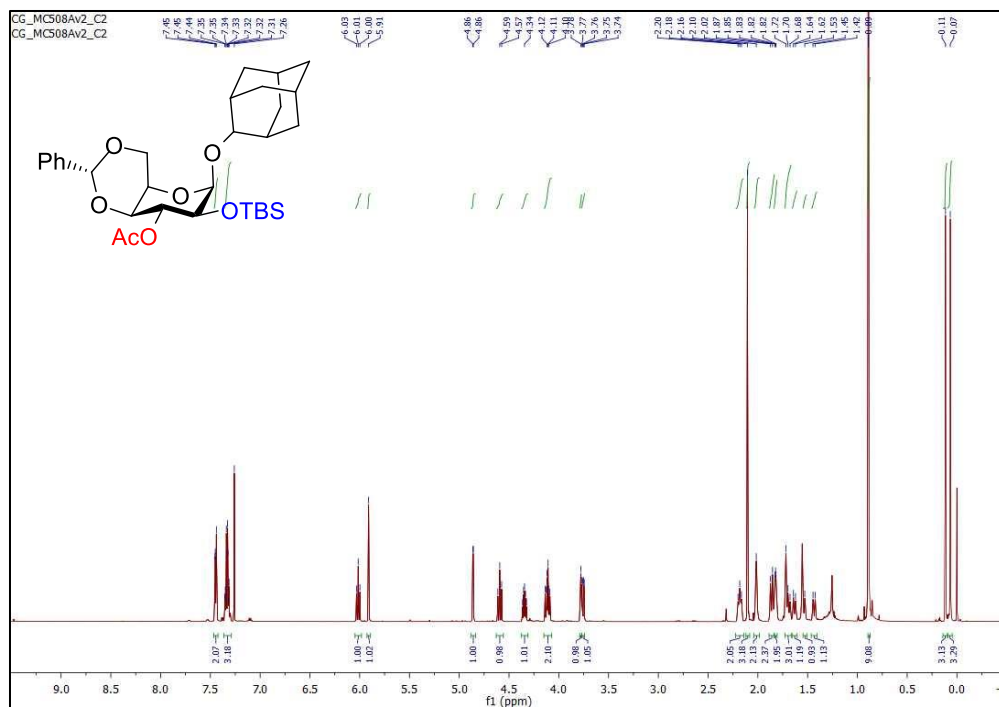


Figure S30 | $^{13}\text{C}\{^1\text{H}\}$ NMR spectrum (CDCl_3 , 150 MHz) of (2-adamantyl) 3-*O*-acetyl-(*R*)-4,6-*O*-benzylidene-2-*O*-*tert*-butyldimethylsilyl- β -D-idopyranoside (14b)

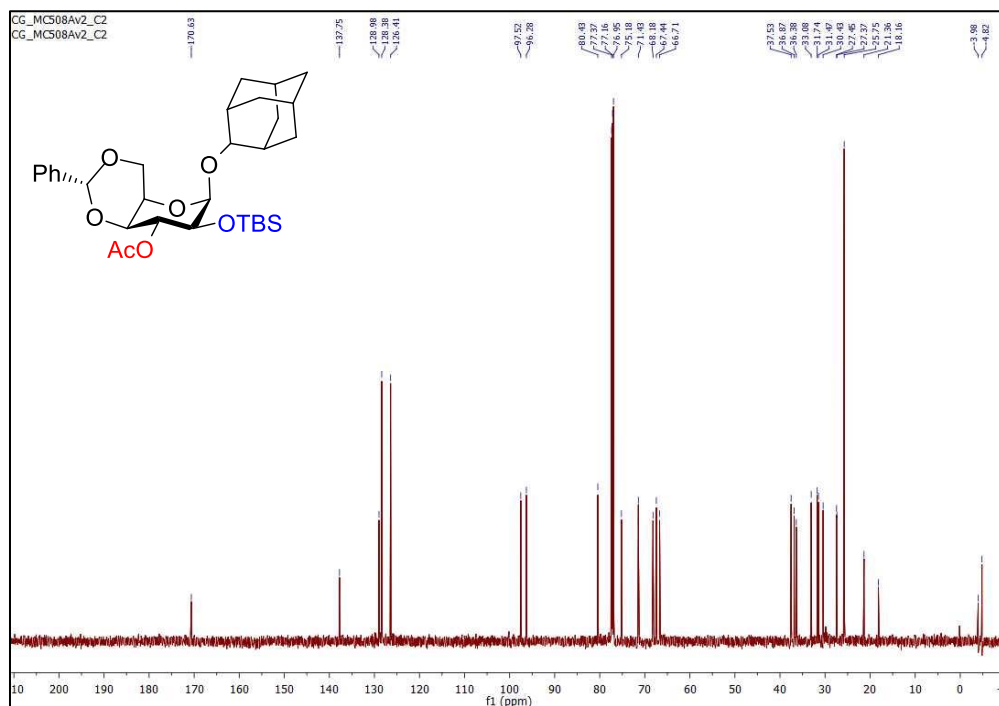


Figure S31 | ^1H NMR spectrum (CDCl_3 , 600 MHz) of (2-adamantyl) 3-*O*-acetyl-(*S*)-4,6-*O*-benzylidene-2-*O*-*tert*-butyldimethylsilyl- α -D-idopyranoside (14c)

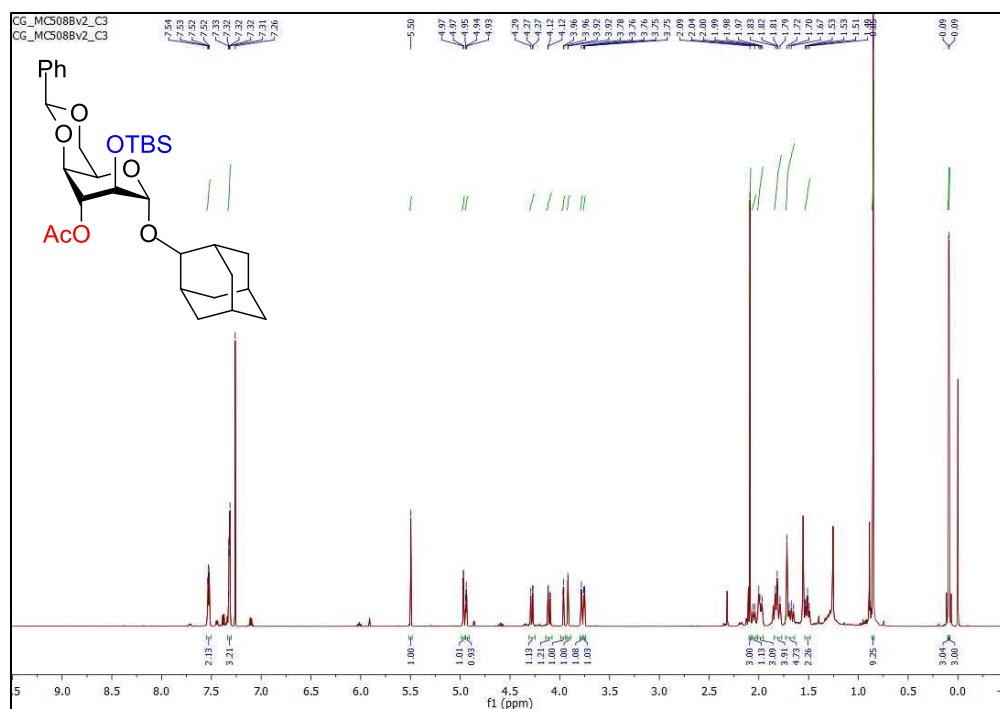


Figure S32 | $^{13}\text{C}\{^1\text{H}\}$ NMR spectrum (CDCl_3 , 150 MHz) of (2-adamantyl) 3-*O*-acetyl-(*S*)-4,6-*O*-benzylidene-2-*O*-*tert*-butyldimethylsilyl- α -D-idopyranoside (14c)

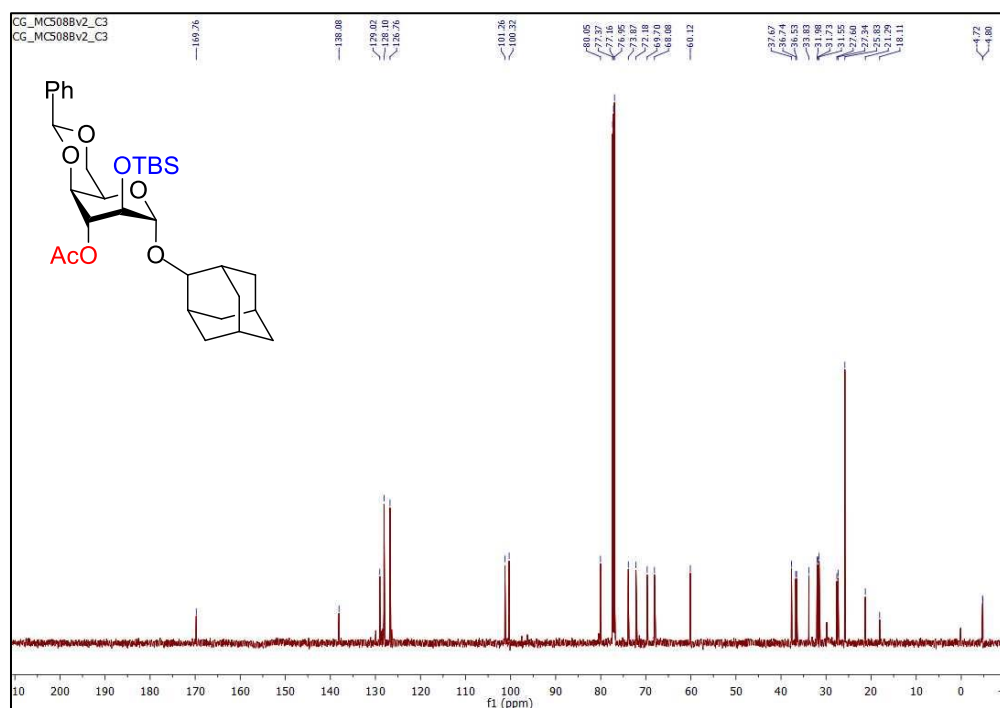


Figure S33 | ^1H NMR spectrum (CDCl_3 , 600 MHz) of (1-adamantyl) 3-*O*-acetyl-(*S*)-4,6-*O*-benzylidene-2-*O*-*tert*-butyldimethylsilyl- β -D-idopyranoside (15a)

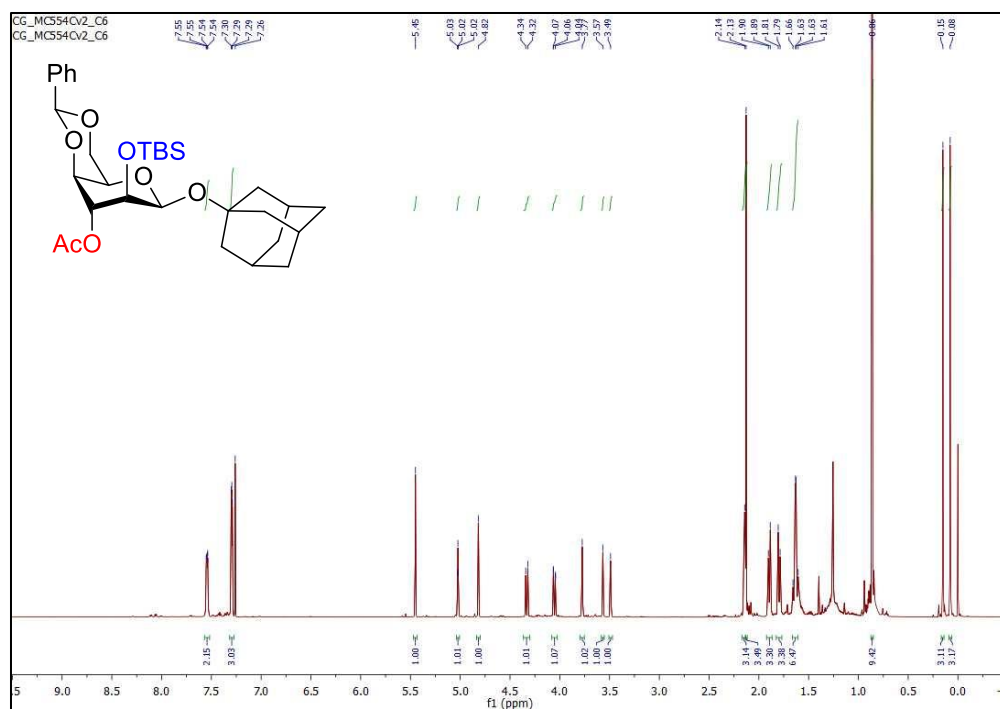


Figure S34 | $^{13}\text{C}\{^1\text{H}\}$ NMR spectrum (CDCl_3 , 150 MHz) of (1-adamantyl) 3-*O*-acetyl-(*S*)-4,6-*O*-benzylidene-2-*O*-*tert*-butyldimethylsilyl- β -D-idopyranoside (15a)

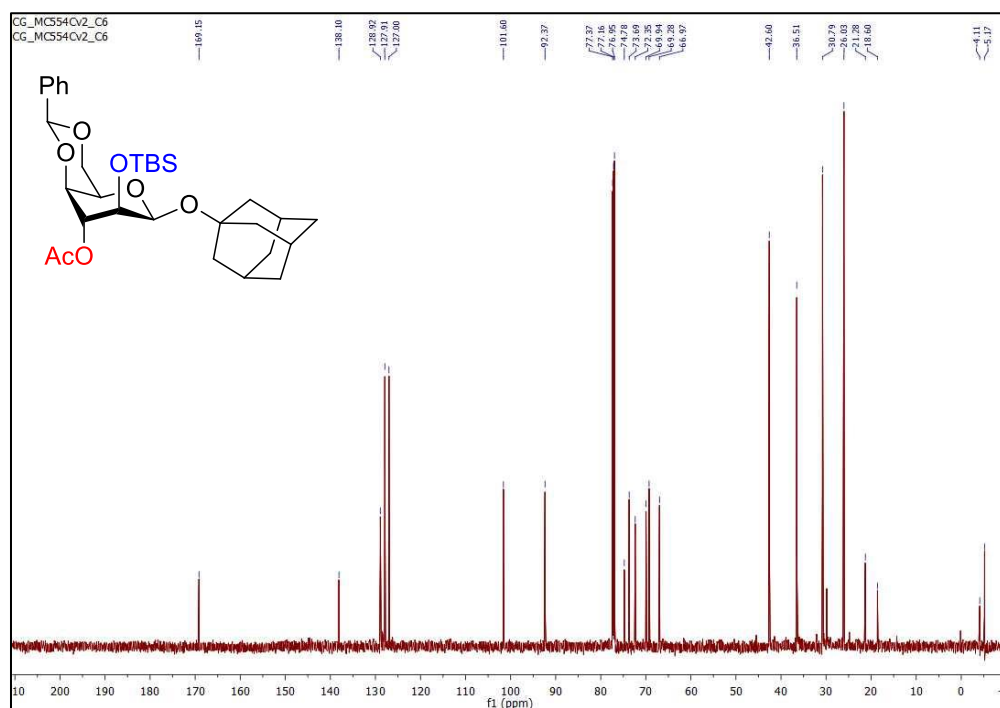


Figure S35 | ^1H NMR spectrum (CDCl_3 , 600 MHz) of (1-adamantyl) 3-*O*-acetyl-(*R*)-4,6-*O*-benzylidene-2-*O*-*tert*-butyldimethylsilyl- β -D-idopyranoside (15b)

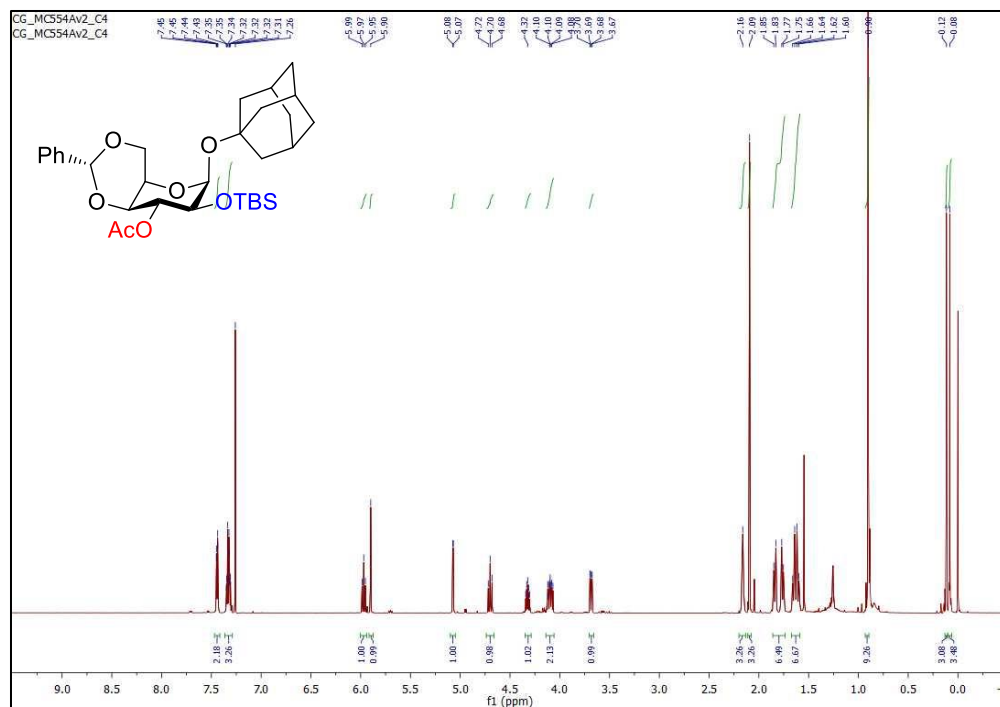


Figure S36 | $^{13}\text{C}\{^1\text{H}\}$ NMR spectrum (CDCl_3 , 150 MHz) of (1-adamantyl) 3-*O*-acetyl-(*R*)-4,6-*O*-benzylidene-2-*O*-*tert*-butyldimethylsilyl- β -D-idopyranoside (15b)

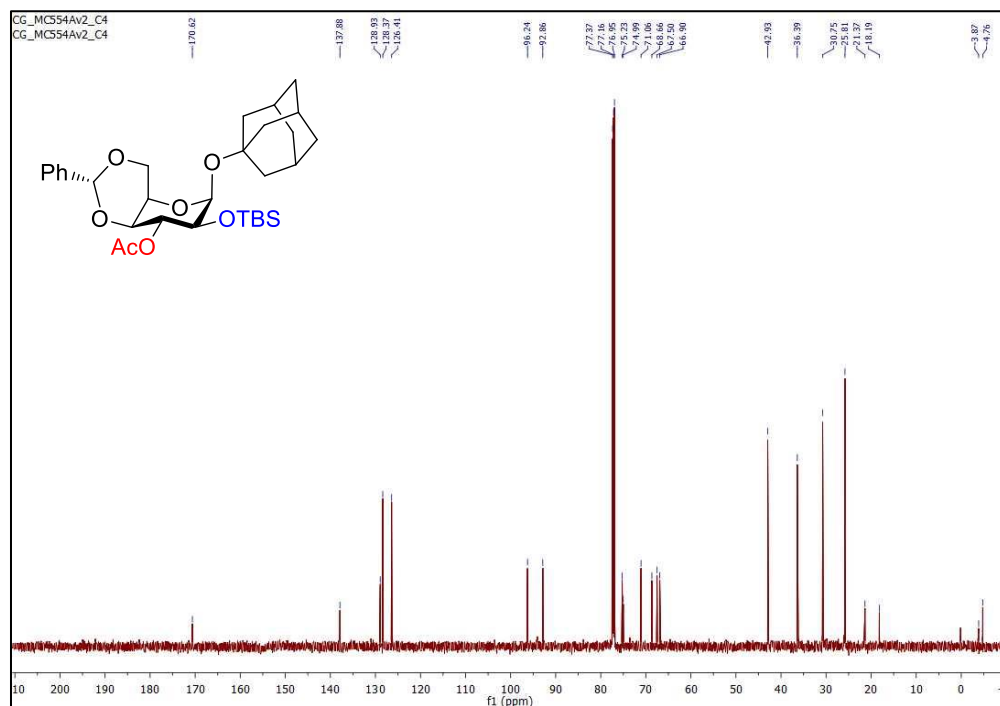


Figure S37 | ^1H NMR spectrum (CDCl_3 , 600 MHz) of (1-adamantyl) 3-*O*-acetyl-(*S*)-4,6-*O*-benzylidene-2-*O*-*tert*-butyldimethylsilyl- α -D-idopyranoside (15c)

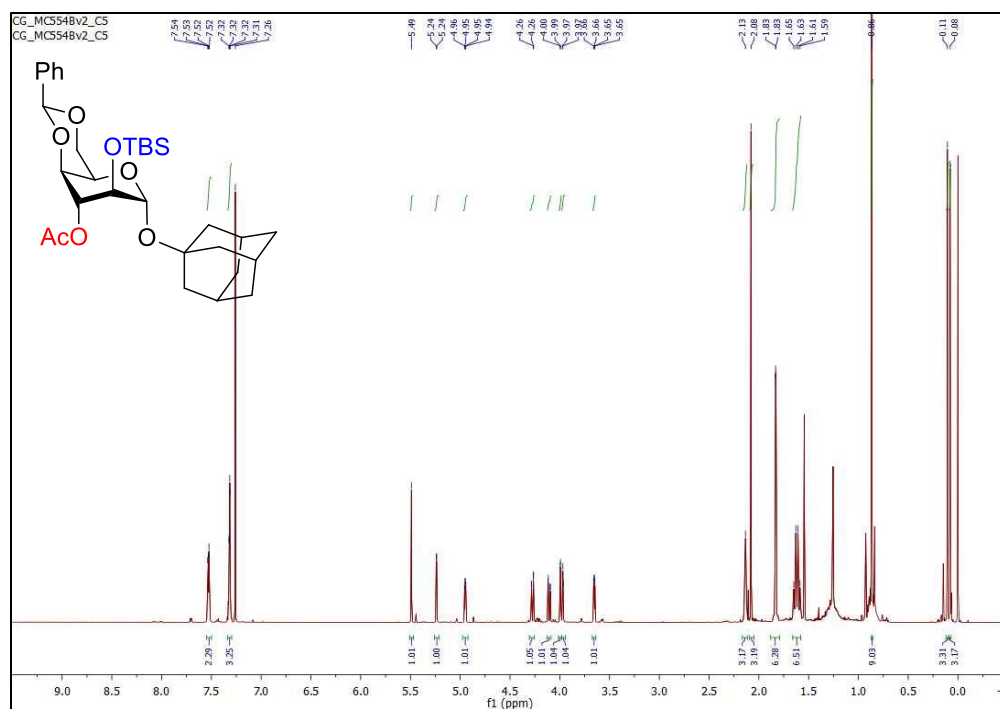


Figure S38 | $^{13}\text{C}\{^1\text{H}\}$ NMR spectrum (CDCl_3 , 150 MHz) of (1-adamantyl) 3-*O*-acetyl-(*S*)-4,6-*O*-benzylidene-2-*O*-*tert*-butyldimethylsilyl- α -D-idopyranoside (15c)

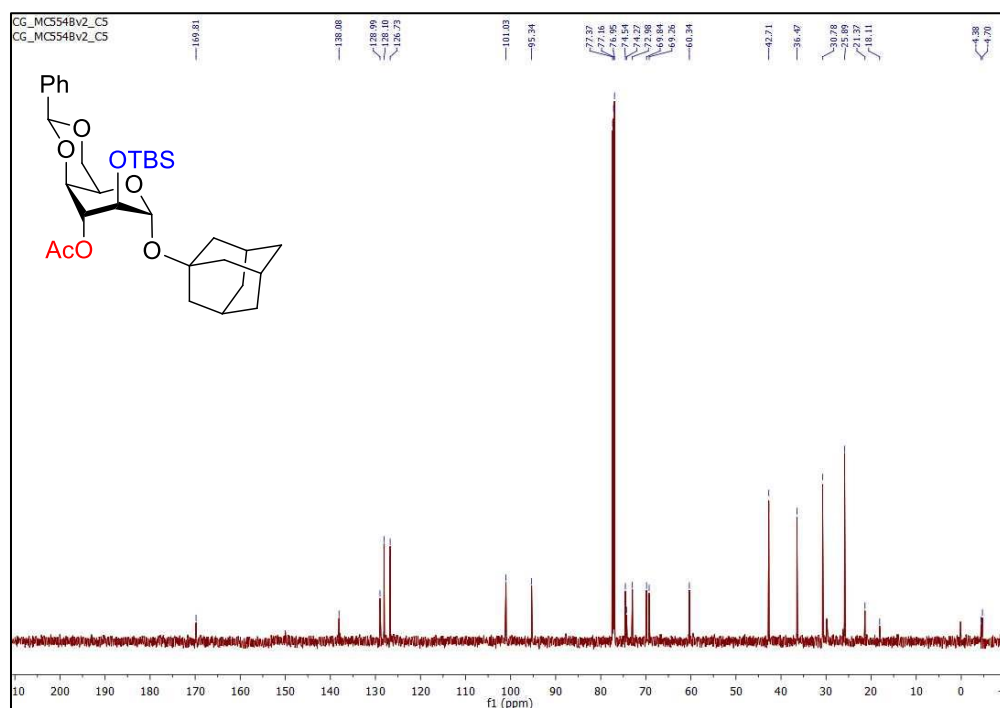


Figure S39 | ^1H NMR spectrum (CDCl_3 , 600 MHz) of (3-stigmastanyl) 3-*O*-acetyl-(*S*)-4,6-*O*-benzylidene-2-*O*-*tert*-butyldimethylsilyl- β -D-idopyranoside (16a)

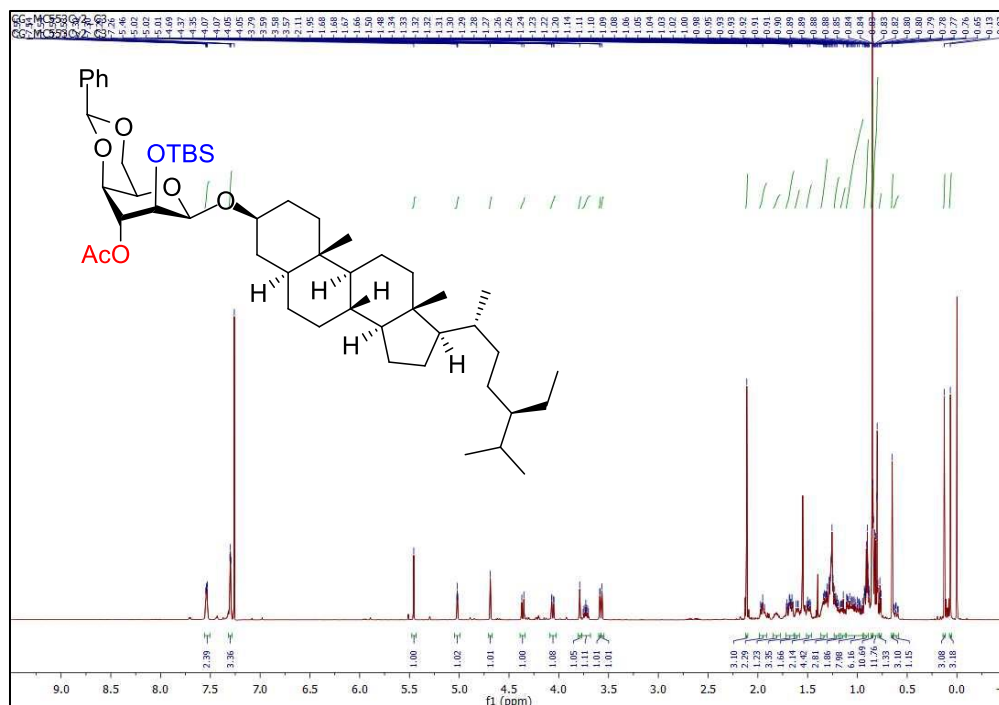


Figure S40 | $^{13}\text{C}\{^1\text{H}\}$ NMR spectrum (CDCl_3 , 150 MHz) of (3-stigmastanyl) 3-*O*-acetyl-(*S*)-4,6-*O*-benzylidene-2-*O*-*tert*-butyldimethylsilyl- β -D-idopyranoside (16a)

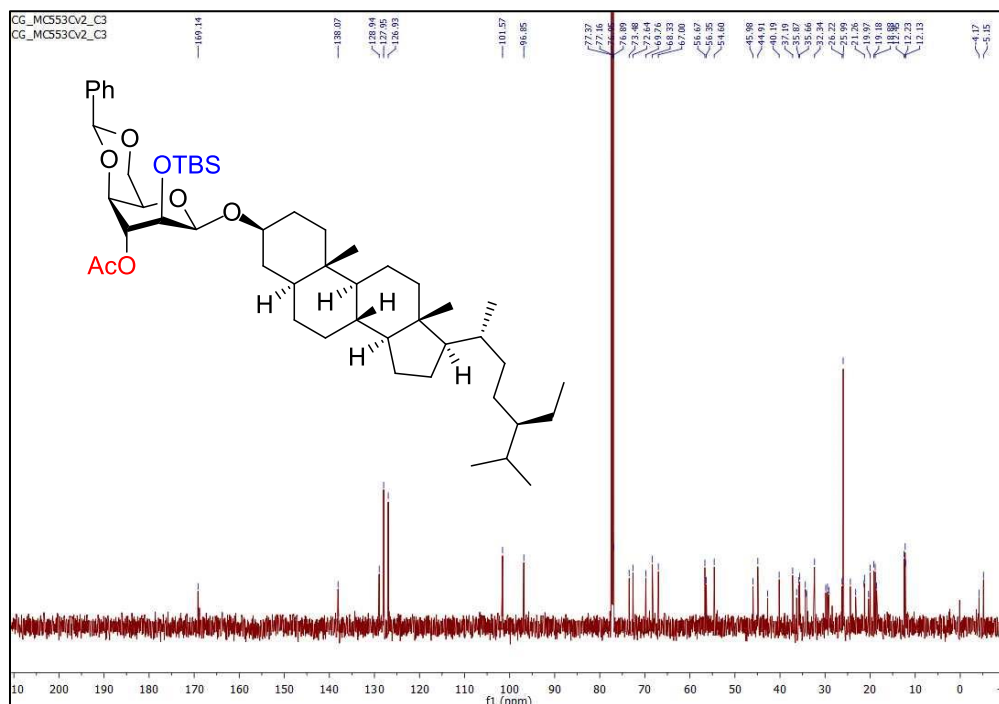


Figure S41 | ^1H NMR spectrum (CDCl_3 , 600 MHz) of (3-stigmastanyl) 3-*O*-acetyl-(*R*)-4,6-*O*-benzylidene-2-*O*-*tert*-butyldimethylsilyl- β -D-idopyranoside (16b)

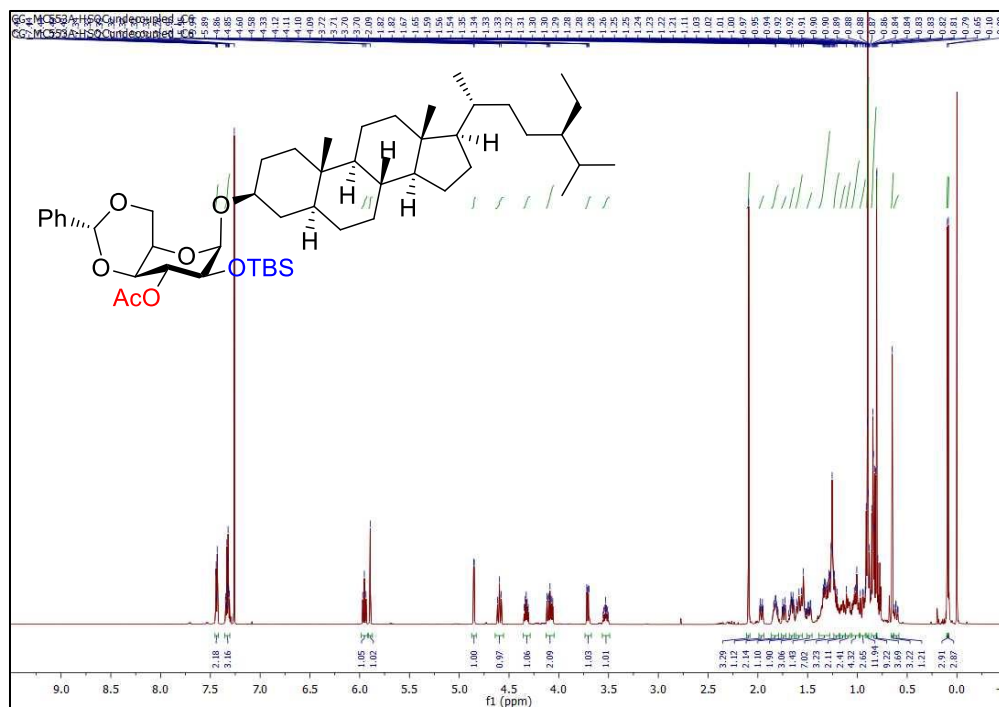


Figure S42 | $^{13}\text{C}\{^1\text{H}\}$ NMR spectrum (CDCl_3 , 150 MHz) of (3-stigmastanyl) 3-*O*-acetyl-(*R*)-4,6-*O*-benzylidene-2-*O*-*tert*-butyldimethylsilyl- β -D-idopyranoside (16b)

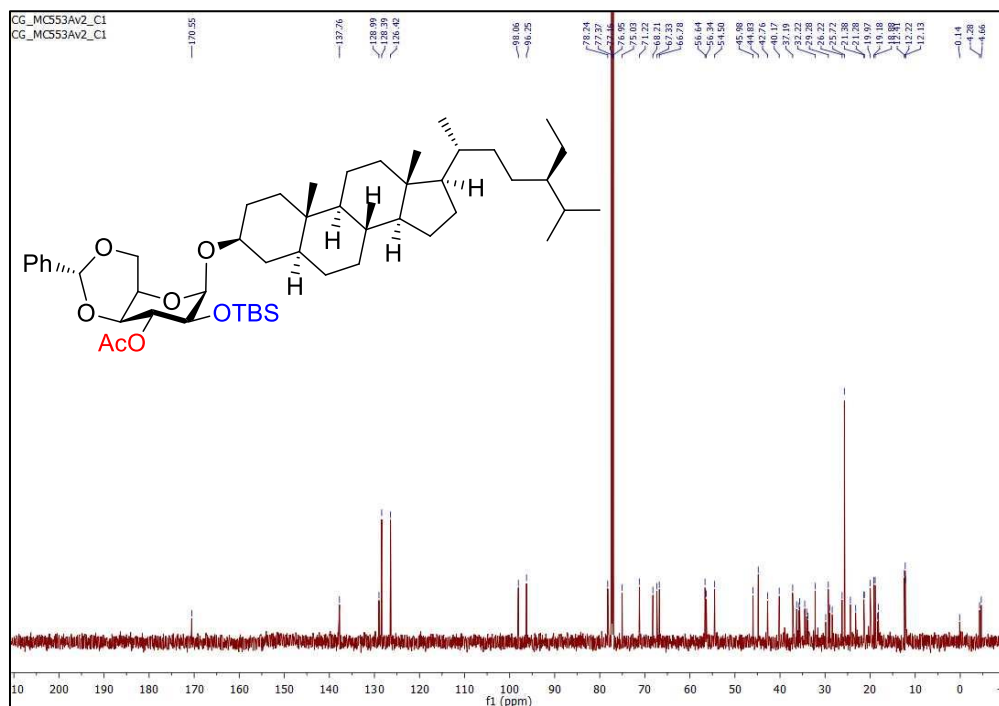


Figure S43 | ^1H NMR spectrum (CDCl_3 , 600 MHz) of (3-stigmastanyl) 3-*O*-acetyl-(*S*)-4,6-*O*-benzylidene-2-*O*-*tert*-butyldimethylsilyl- α -D-idopyranoside (16c)

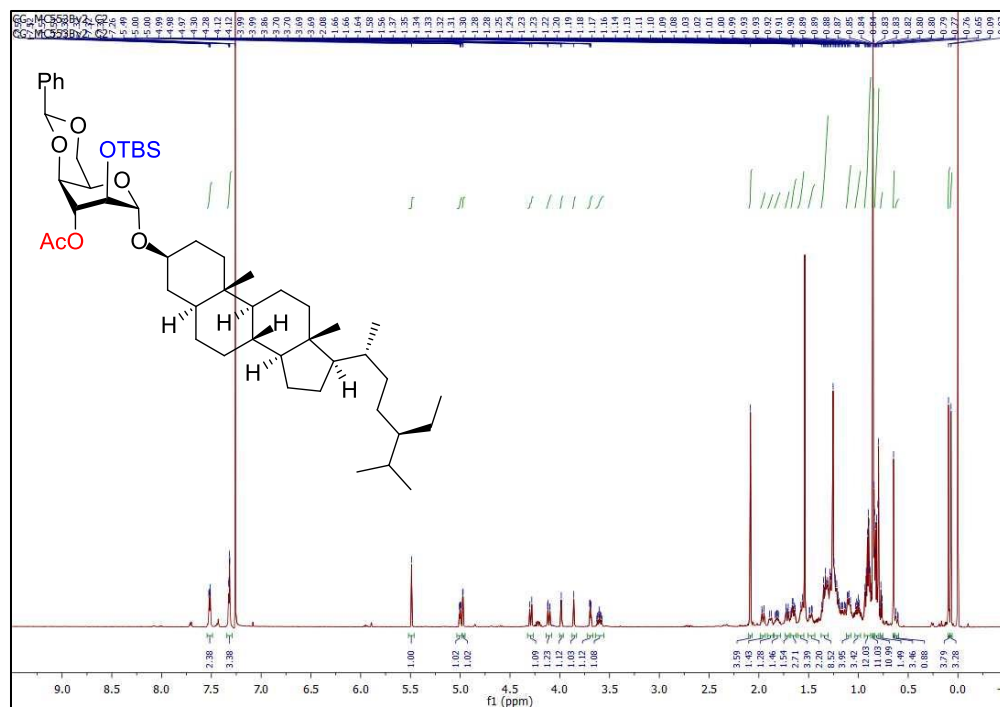


Figure S44 | $^{13}\text{C}\{^1\text{H}\}$ NMR spectrum (CDCl_3 , 150 MHz) of (3-stigmastanyl) 3-*O*-acetyl-(*S*)-4,6-*O*-benzylidene-2-*O*-*tert*-butyldimethylsilyl- α -D-idopyranoside (16c)

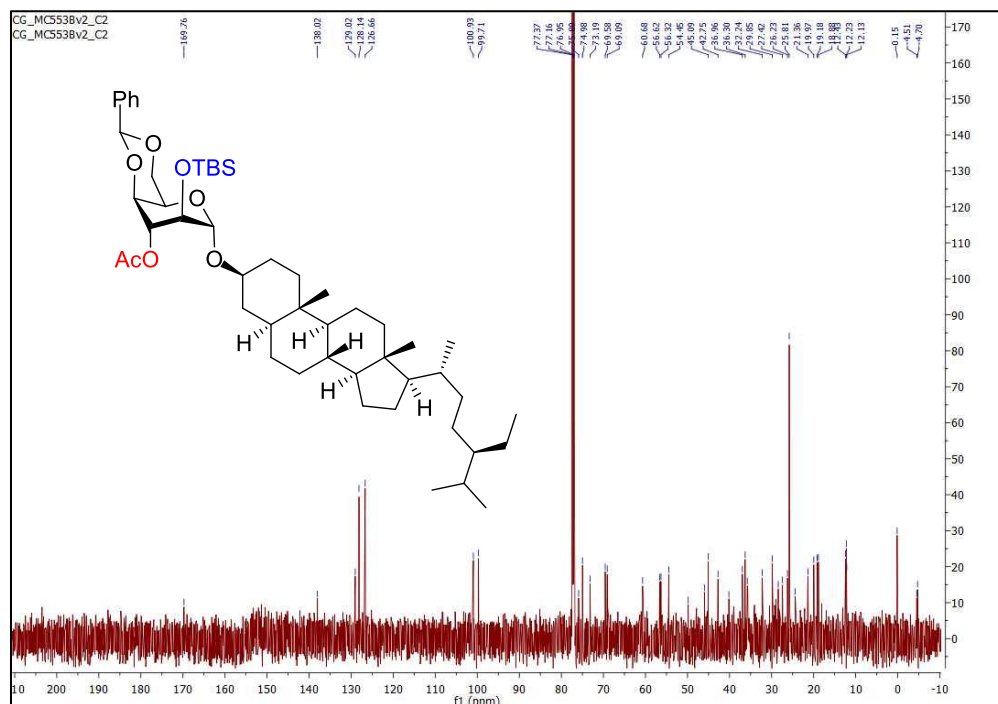


Figure S45 | ^1H NMR spectrum (CDCl_3 , 600 MHz) of (2-adamantyl) (*S*)-4,6-*O*-benzylidene-2-*O*-*tert*-butyldimethylsilyl-3-*O*-dichloroacetyl- β -D-idopyranoside (17a)

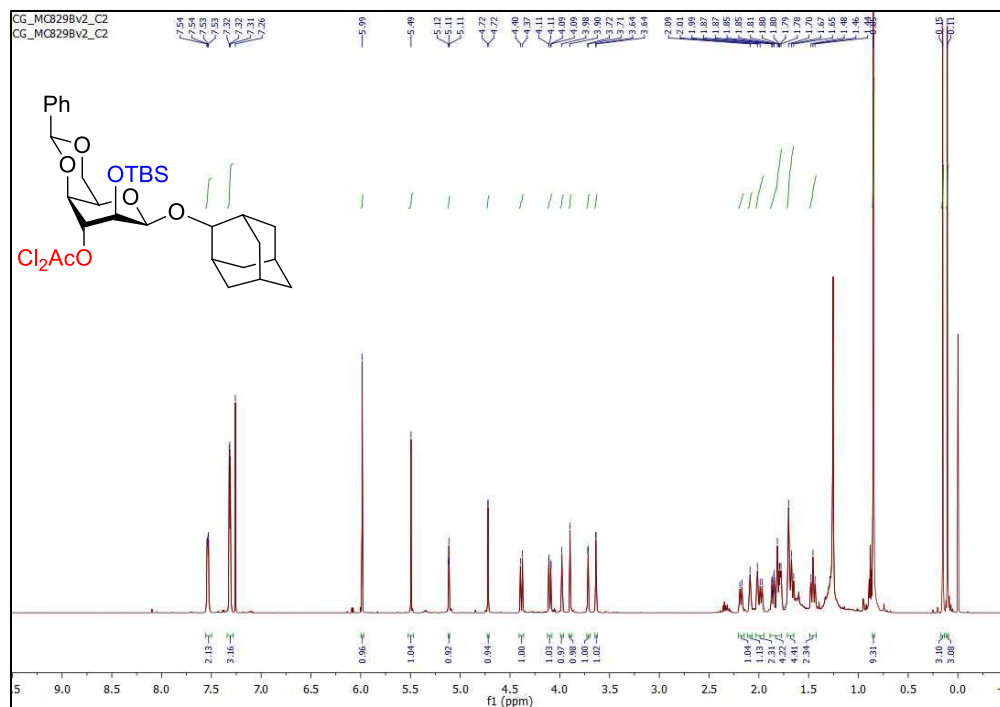


Figure S46 | $^{13}\text{C}\{^1\text{H}\}$ NMR spectrum (CDCl_3 , 150 MHz) of (2-adamantyl) (*S*)-4,6-*O*-benzylidene-2-*O*-*tert*-butyldimethylsilyl-3-*O*-dichloroacetyl- β -D-idopyranoside (17a)

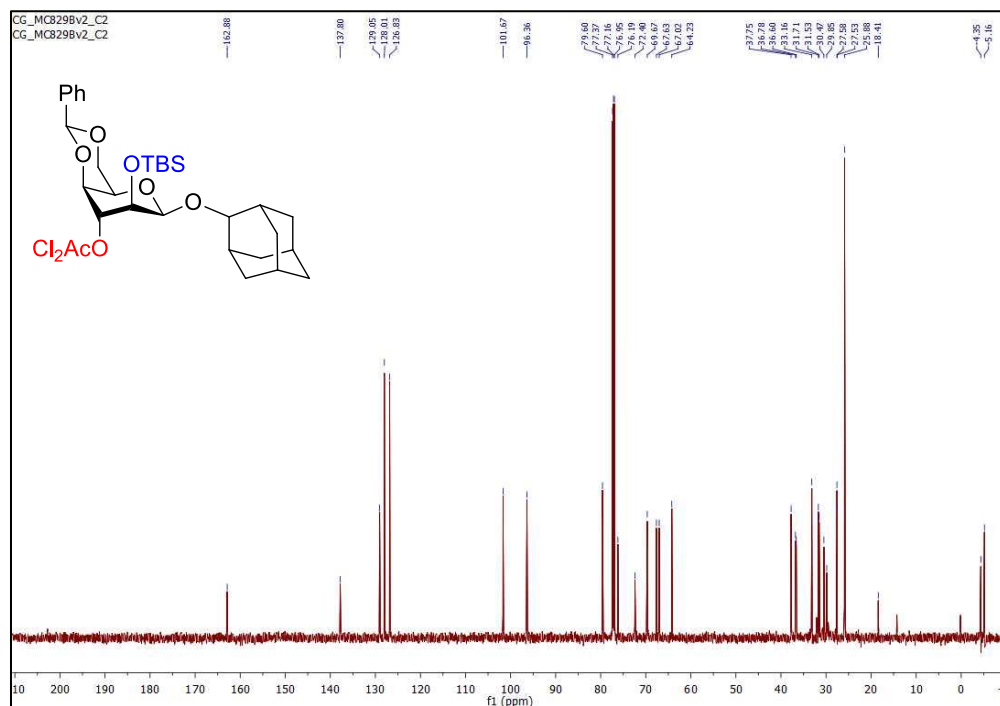


Figure S47 | ^1H NMR spectrum (CDCl_3 , 600 MHz) of (2-adamantyl) (*R*)-4,6-*O*-benzylidene-2-*O*-*tert*-butyldimethylsilyl-3-*O*-dichloroacetyl- β -D-idopyranoside (17b) and (2-adamantyl) (*S*)-4,6-*O*-benzylidene-2-*O*-*tert*-butyldimethylsilyl-3-*O*-dichloroacetyl- α -D-idopyranoside (17c)

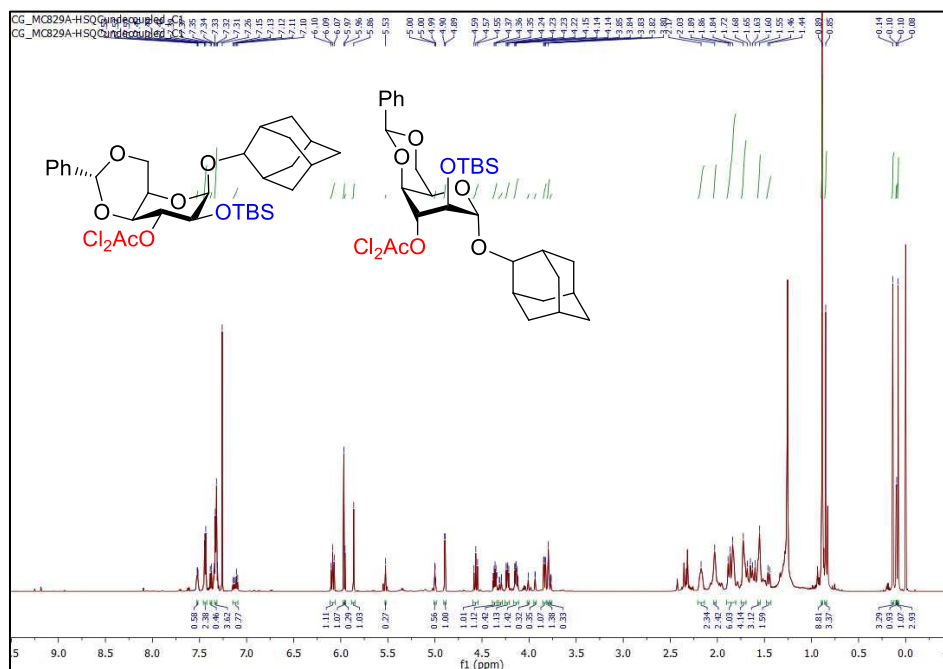


Figure S48 | $^{13}\text{C}\{^1\text{H}\}$ NMR spectrum (CDCl_3 , 150 MHz) of (2-adamantyl) (*R*)-4,6-*O*-benzylidene-2-*O*-*tert*-butyldimethylsilyl-3-*O*-dichloroacetyl- β -D-idopyranoside (17b) and (2-adamantyl) (*S*)-4,6-*O*-benzylidene-2-*O*-*tert*-butyldimethylsilyl-3-*O*-dichloroacetyl- α -D-idopyranoside (17c)

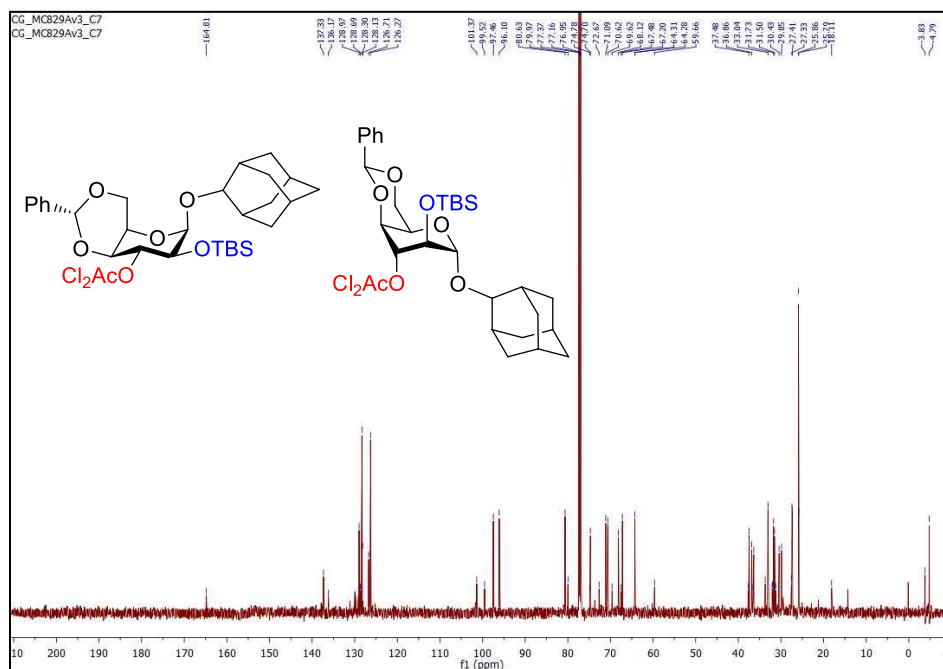


Figure S51 | ^1H NMR spectrum (CDCl_3 , 600 MHz) of (2-adamantyl) 3-*O*-(2-azidomethyl)benzoyl-*R*-4,6-*O*-benzylidene-2-*O*-*tert*-butyldimethylsilyl- β -D-idopyranoside (18b) and (2-adamantyl) 3-*O*-(2-azidomethyl)benzoyl-*S*-4,6-*O*-benzylidene-2-*O*-*tert*-butyldimethylsilyl- α -D-idopyranoside (18c)

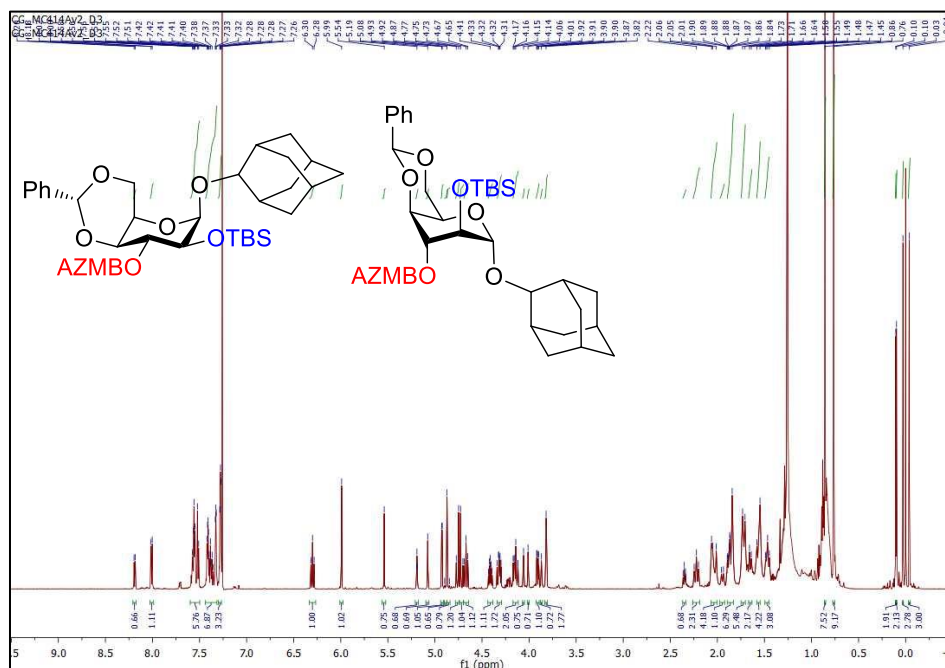


Figure S52 | $^{13}\text{C}\{^1\text{H}\}$ NMR spectrum (CDCl_3 , 150 MHz) of (2-adamantyl) 3-*O*-(2-azidomethyl)benzoyl-*R*-4,6-*O*-benzylidene-2-*O*-*tert*-butyldimethylsilyl- β -D-idopyranoside (18b) and (2-adamantyl) 3-*O*-(2-azidomethyl)benzoyl-*S*-4,6-*O*-benzylidene-2-*O*-*tert*-butyldimethylsilyl- α -D-idopyranoside (18c)

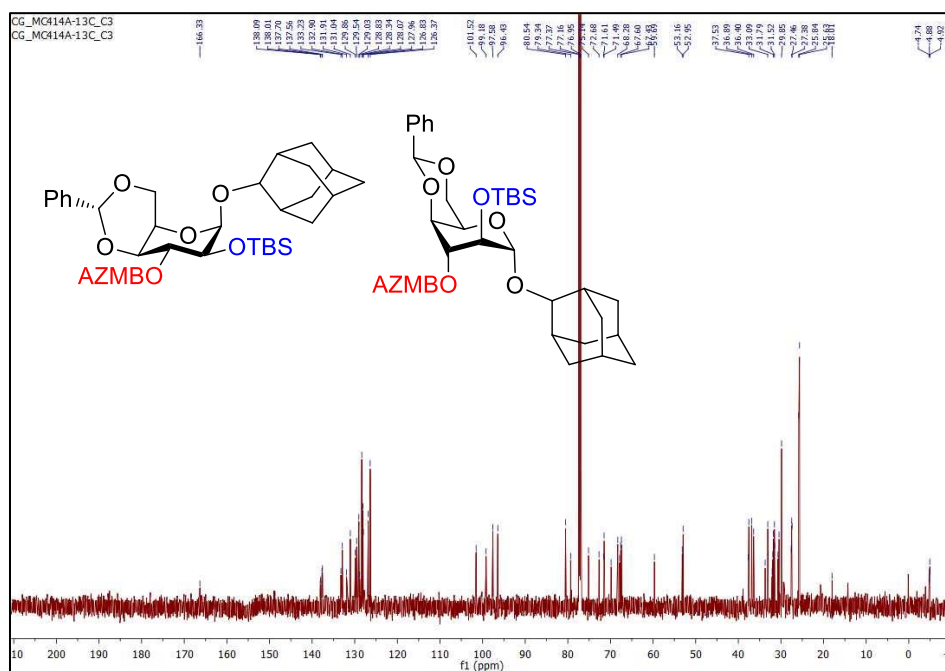


Figure S53 | ^1H NMR spectrum (CDCl_3 , 600 MHz) of (2-adamantyl) (*S*)-4,6-*O*-benzylidene-2-*O*-*tert*-butyldimethylsilyl-3-*O*-*tert*-butoxycarbonyl- β -D-idopyranoside (19a)

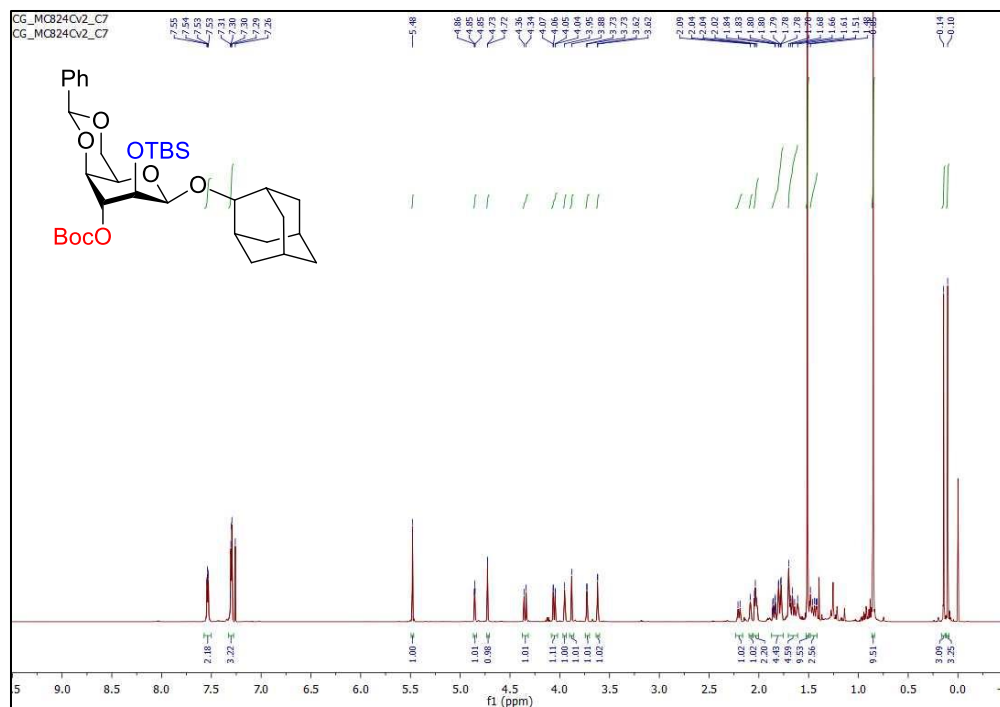


Figure S54 | $^{13}\text{C}\{^1\text{H}\}$ NMR spectrum (CDCl_3 , 150 MHz) of (2-adamantyl) (*S*)-4,6-*O*-benzylidene-2-*O*-*tert*-butyldimethylsilyl-3-*O*-*tert*-butoxycarbonyl- β -D-idopyranoside (19a)

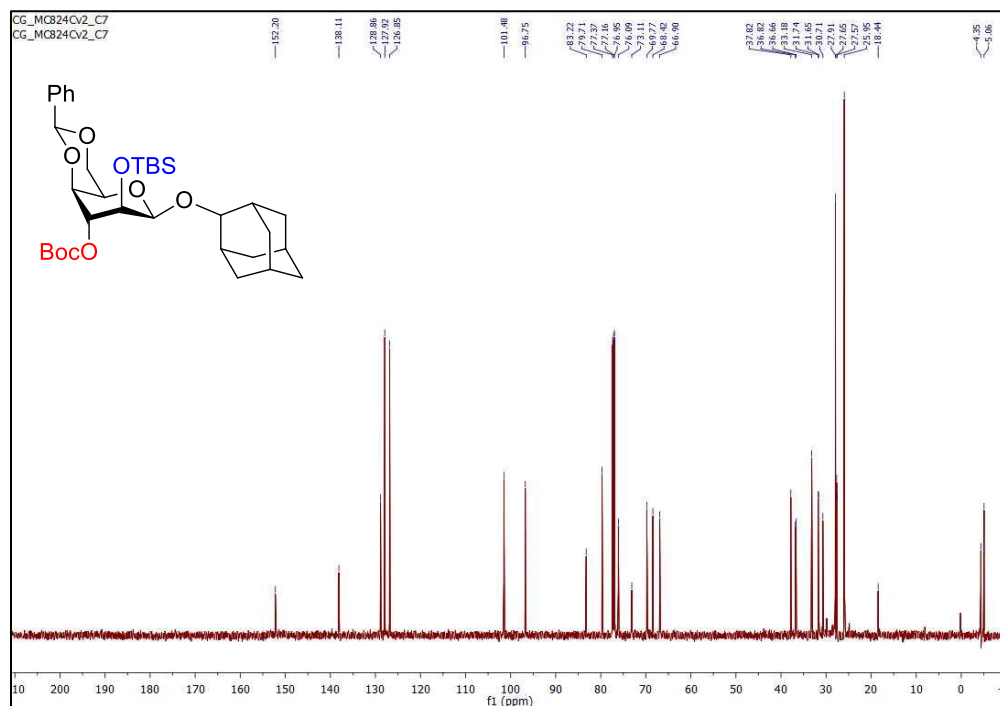


Figure S55 | ^1H NMR spectrum (CDCl_3 , 600 MHz) of (2-adamantyl) (*R*)-4,6-*O*-benzylidene-2-*O*-*tert*-butyldimethylsilyl-3-*O*-*tert*-butoxycarbonyl- β -D-idopyranoside (19b) and (2-adamantyl) (*S*)-4,6-*O*-benzylidene-2-*O*-*tert*-butyldimethylsilyl-3-*O*-*tert*-butoxycarbonyl- α -D-idopyranoside (19c)

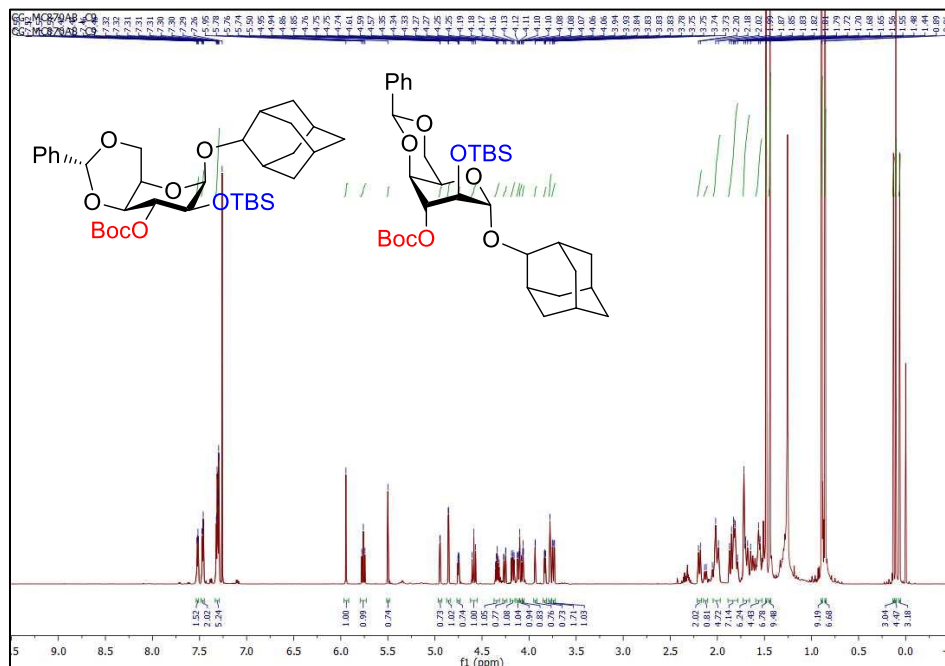


Figure S56 | $^{13}\text{C}\{^1\text{H}\}$ NMR spectrum (CDCl_3 , 150 MHz) of (2-adamantyl) (*R*)-4,6-*O*-benzylidene-2-*O*-*tert*-butyldimethylsilyl-3-*O*-*tert*-butoxycarbonyl- β -D-idopyranoside (19b) and (2-adamantyl) (*S*)-4,6-*O*-benzylidene-2-*O*-*tert*-butyldimethylsilyl-3-*O*-*tert*-butoxycarbonyl- α -D-idopyranoside (19c)

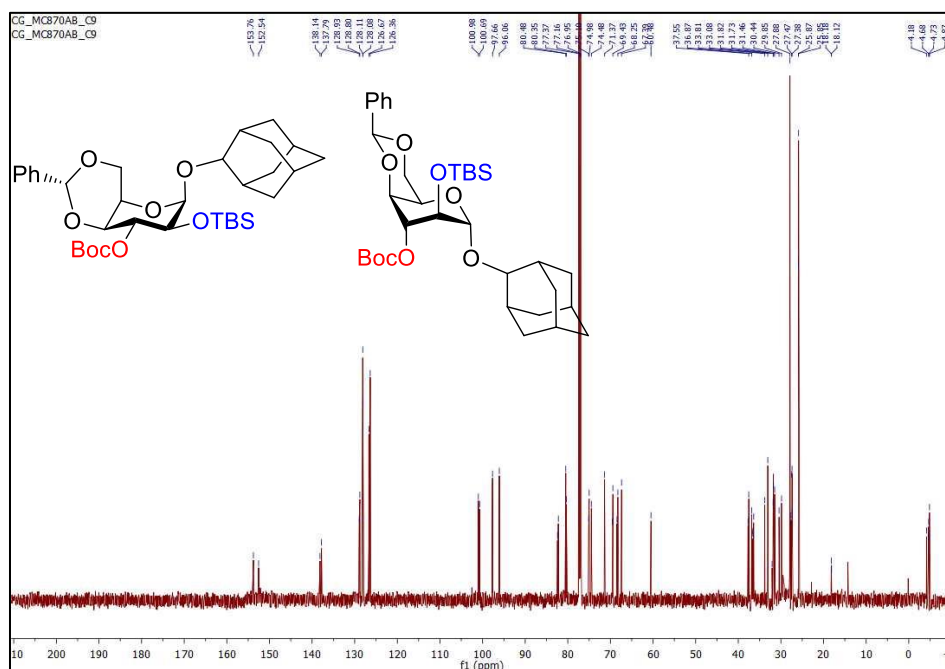


Figure S57 | ^1H NMR spectrum (CDCl_3 , 500 MHz) of (2-adamantyl) (S)-4,6-O-benzylidene- β -D-idopyranoside (20a)

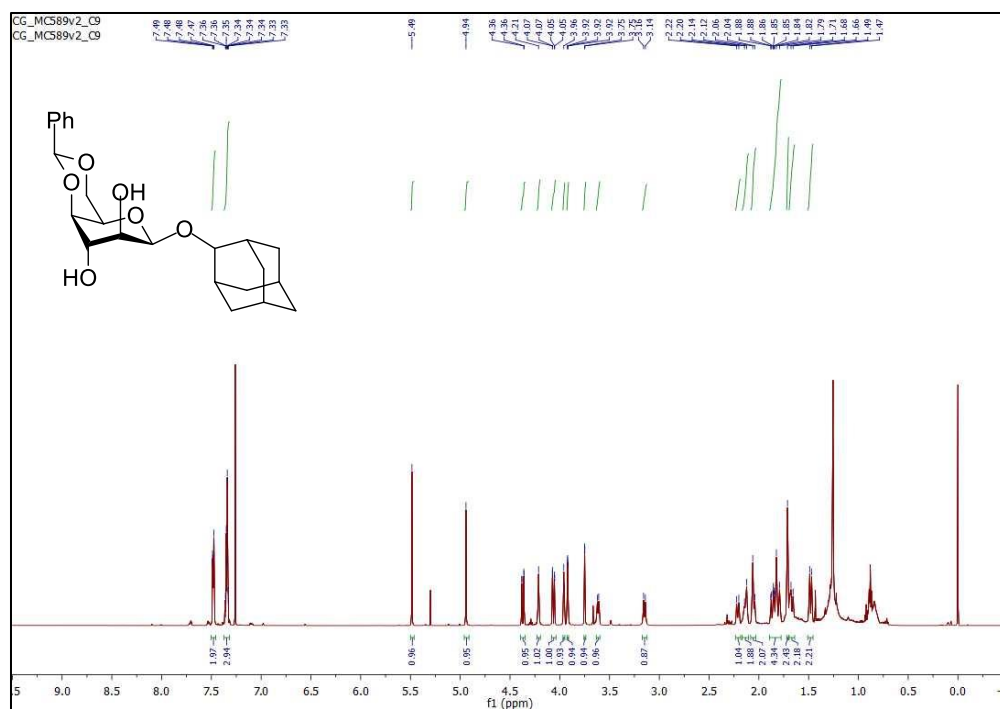


Figure S58 | $^{13}\text{C}\{^1\text{H}\}$ NMR spectrum (CDCl_3 , 125 MHz) of (2-adamantyl) (S)-4,6-O-benzylidene- β -D-idopyranoside (20a)

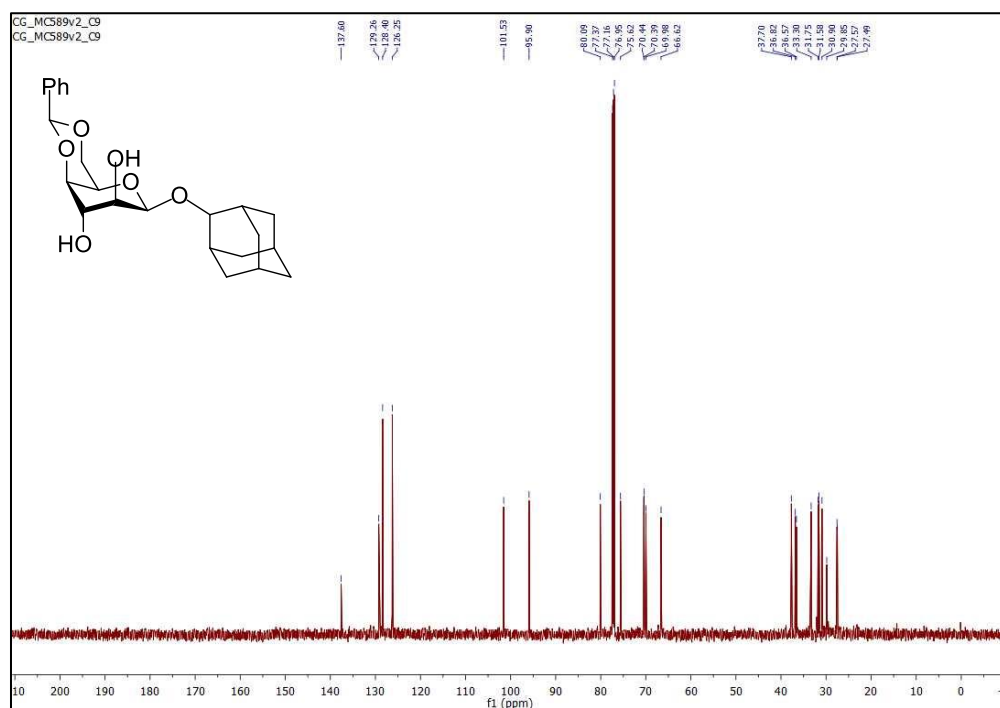


Figure S63 | ^1H NMR spectrum (CDCl_3 , 600 MHz) of (2-adamantyl) 3-*O*-acetyl-2-*O*-*tert*-butyldimethylsilyl- β -D-idopyranoside (21)

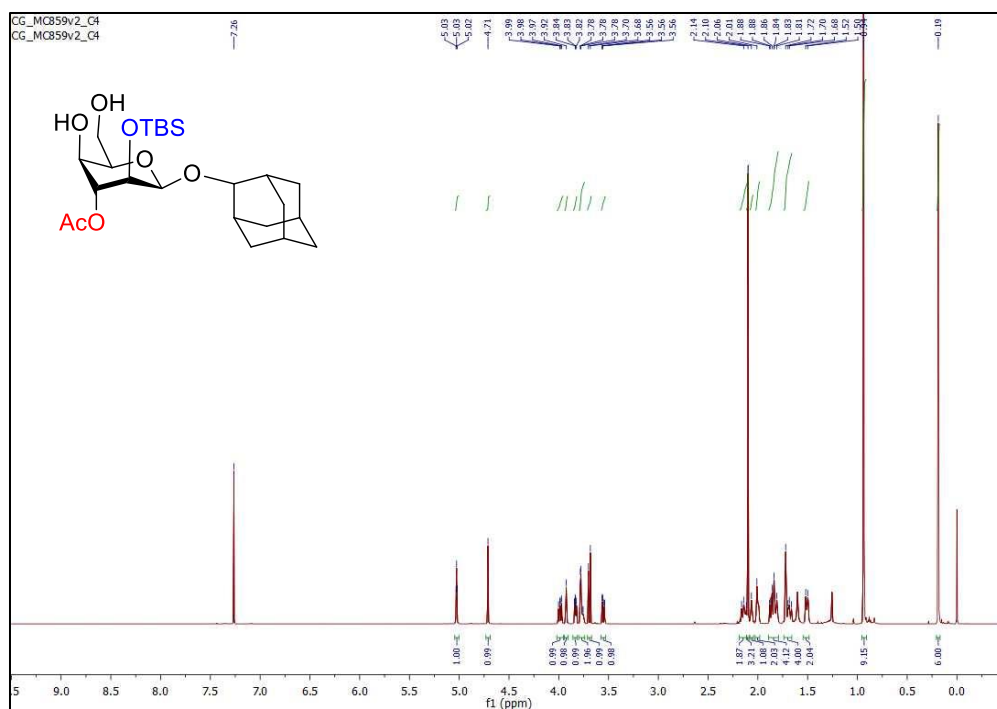


Figure S64 | $^{13}\text{C}\{^1\text{H}\}$ NMR spectrum (CDCl_3 , 150 MHz) of (2-adamantyl) 3-*O*-acetyl-2-*O*-*tert*-butyldimethylsilyl- β -D-idopyranoside (21)

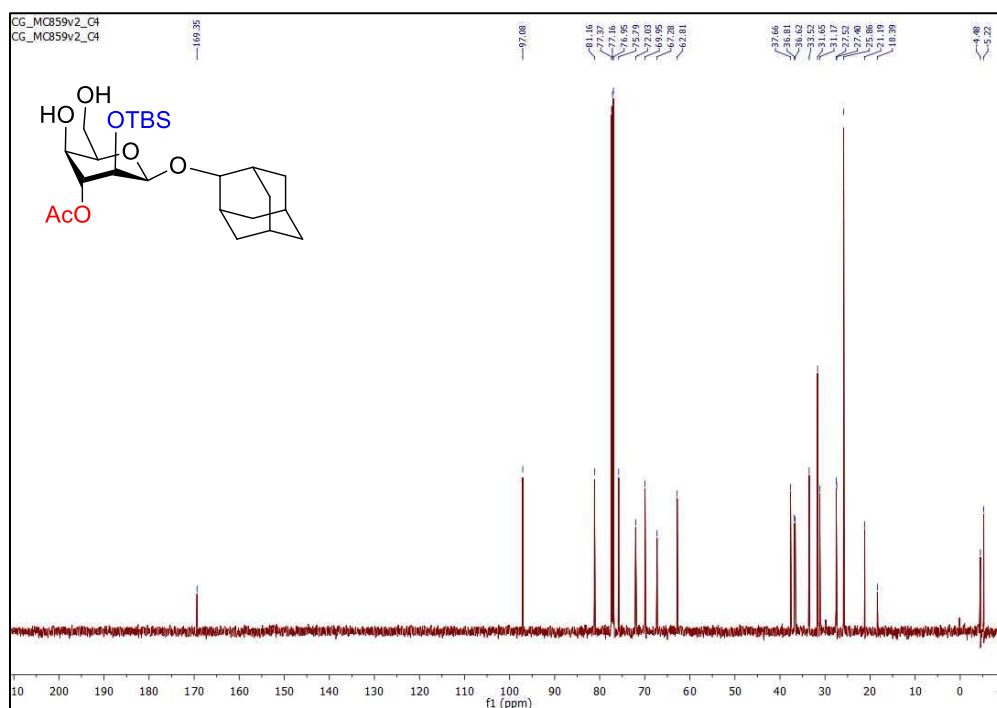


Figure S65 | ^1H NMR spectrum (CDCl_3 , 600 MHz) of *para*-methylphenyl 3-*O*-benzyl-4,6-*O*-benzylidene-1-thio- α -D-idopyranoside (23)

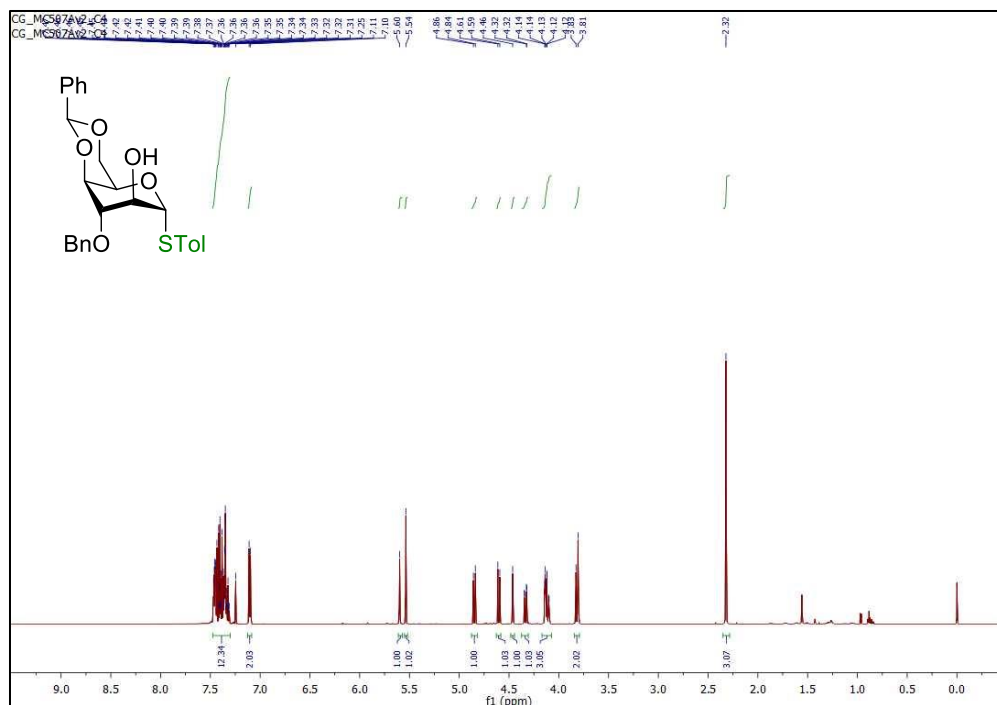


Figure S66 | $^{13}\text{C}\{^1\text{H}\}$ NMR spectrum (CDCl_3 , 150 MHz) of *para*-methylphenyl 3-*O*-benzyl-4,6-*O*-benzylidene-1-thio- α -D-idopyranoside (23)

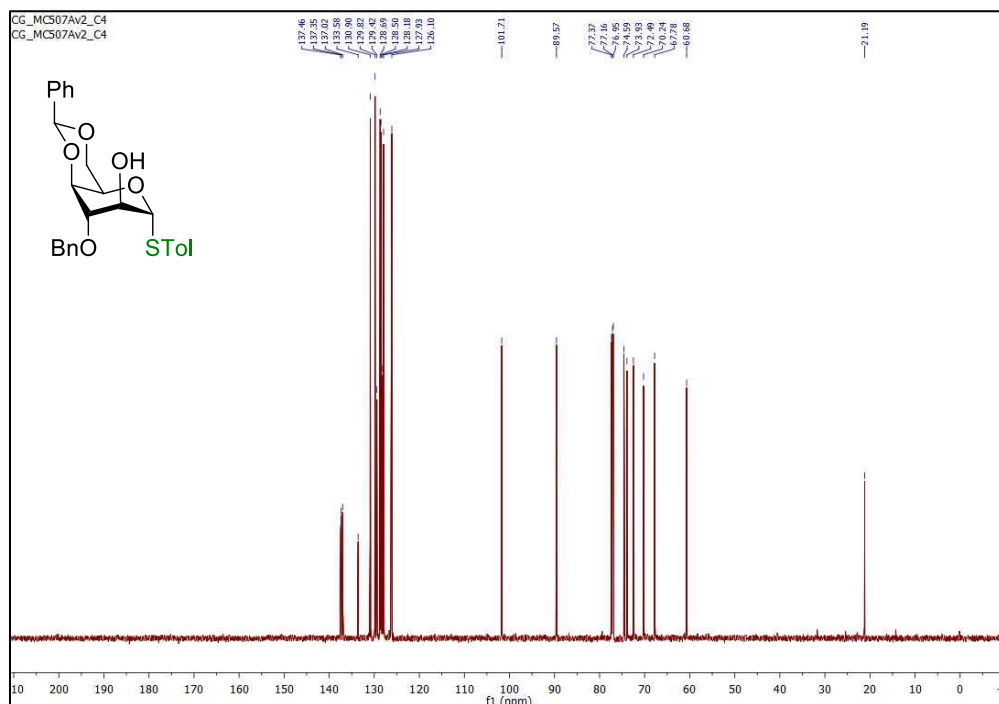


Figure S67 | ^1H NMR spectrum (CDCl_3 , 600 MHz) of *para*-methylphenyl 3-*O*-benzyl-4,6-*O*-benzylidene-2-*O*-*tert*-butyldimethylsilyl-1-thio- α -D-idopyranoside (24)

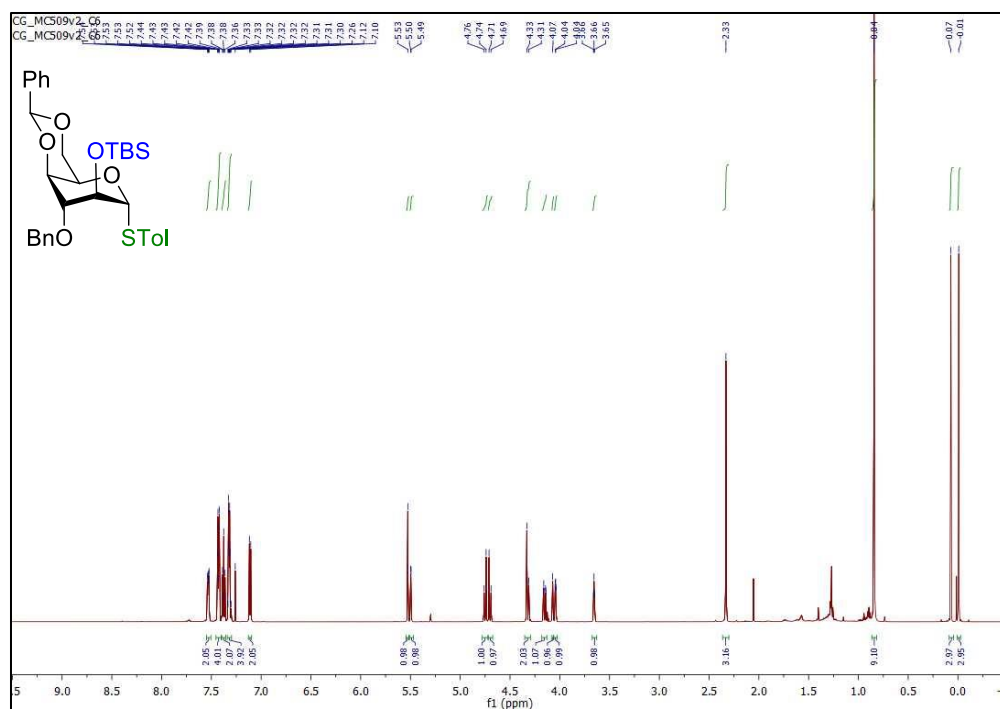


Figure S68 | $^{13}\text{C}\{^1\text{H}\}$ NMR spectrum (CDCl_3 , 150 MHz) of *para*-methylphenyl 3-*O*-benzyl-4,6-*O*-benzylidene-2-*O*-*tert*-butyldimethylsilyl-1-thio- α -D-idopyranoside (24)

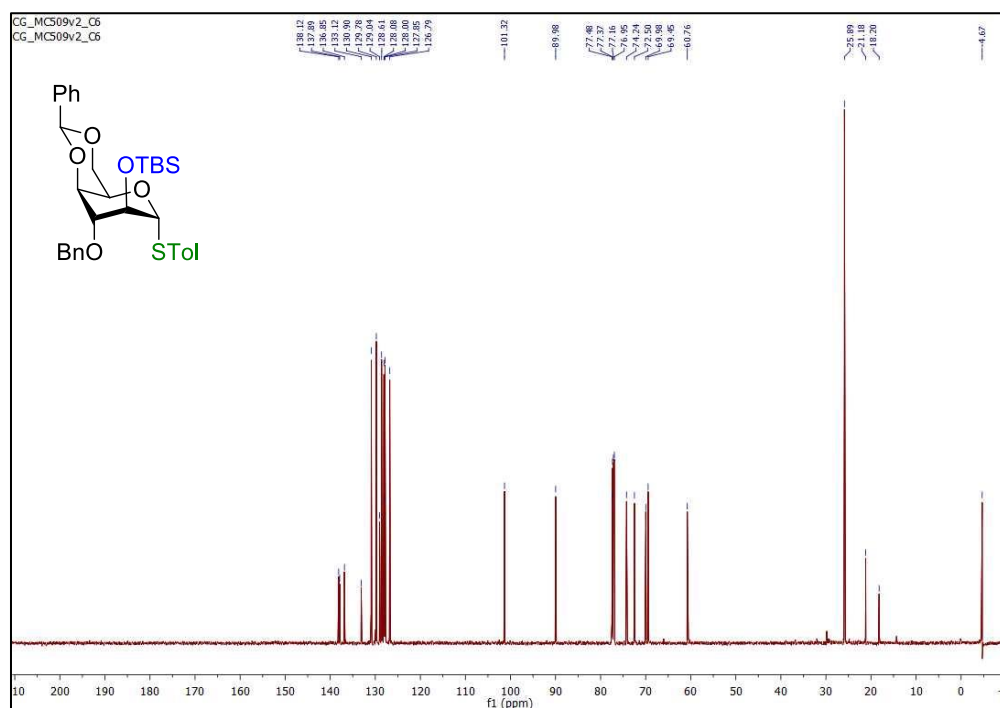


Figure S69 | ^1H NMR spectrum (CDCl_3 , 600 MHz) of 1,2,3,4,6-penta-*O*-acetyl α -D-talopyranose (26)

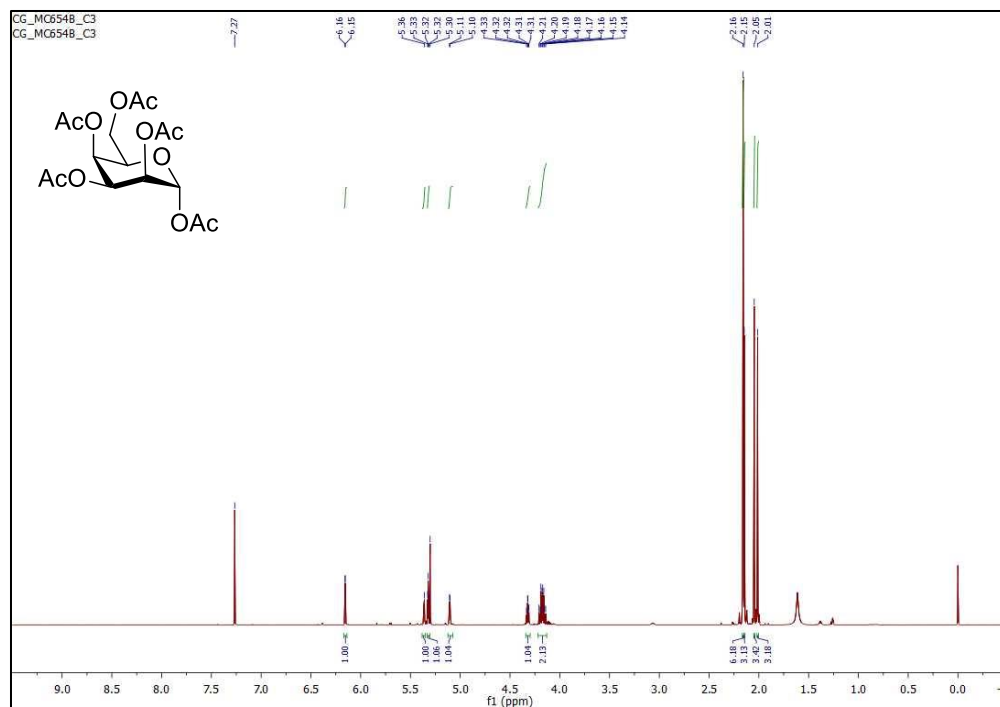


Figure S70 | ^1H NMR spectrum (CDCl_3 , 600 MHz) of ethyl 2,3,4,6-tetra-*O*-acetyl-1-thio- α -D-talopyranoside

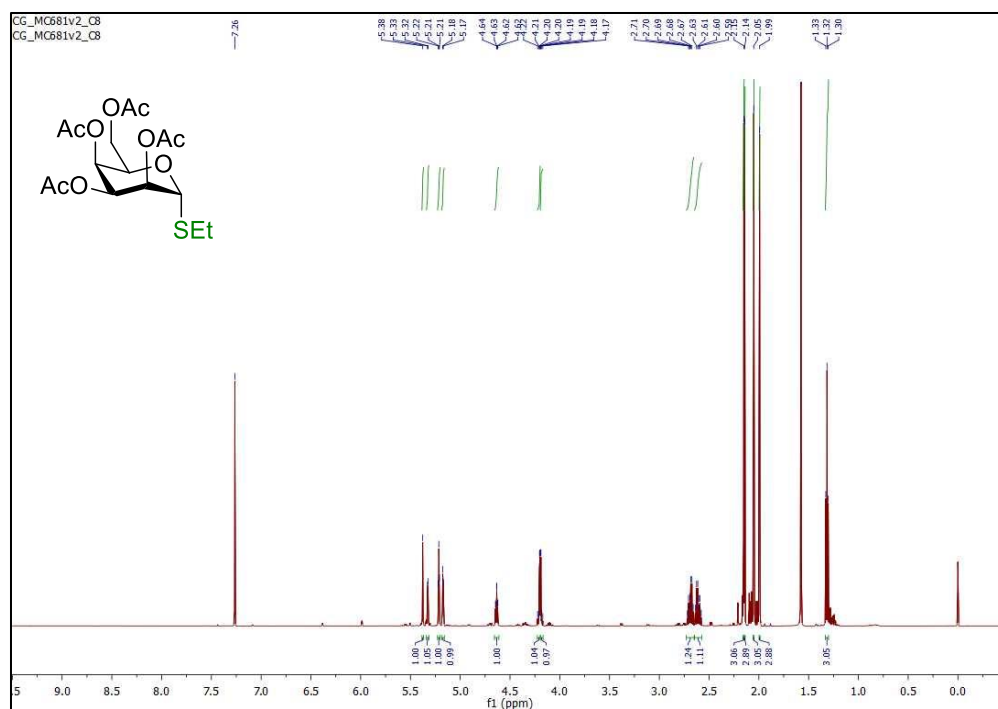


Figure S71 | $^{13}\text{C}\{^1\text{H}\}$ NMR spectrum (CDCl_3 , 150 MHz) of ethyl 2,3,4,6-tetra-*O*-acetyl-1-thio- α -D-talopyranoside

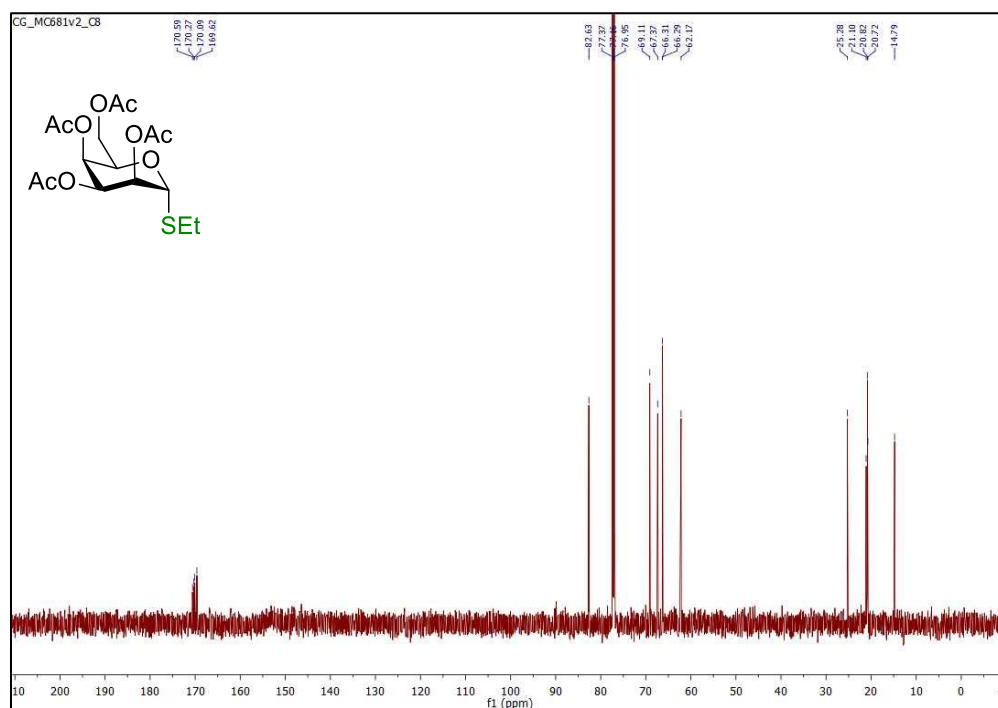


Figure S72 | ^1H NMR spectrum (CDCl_3 , 600 MHz) of ethyl 4,6-*O*-benzylidene-1-thio- α -D-talopyranoside (27)

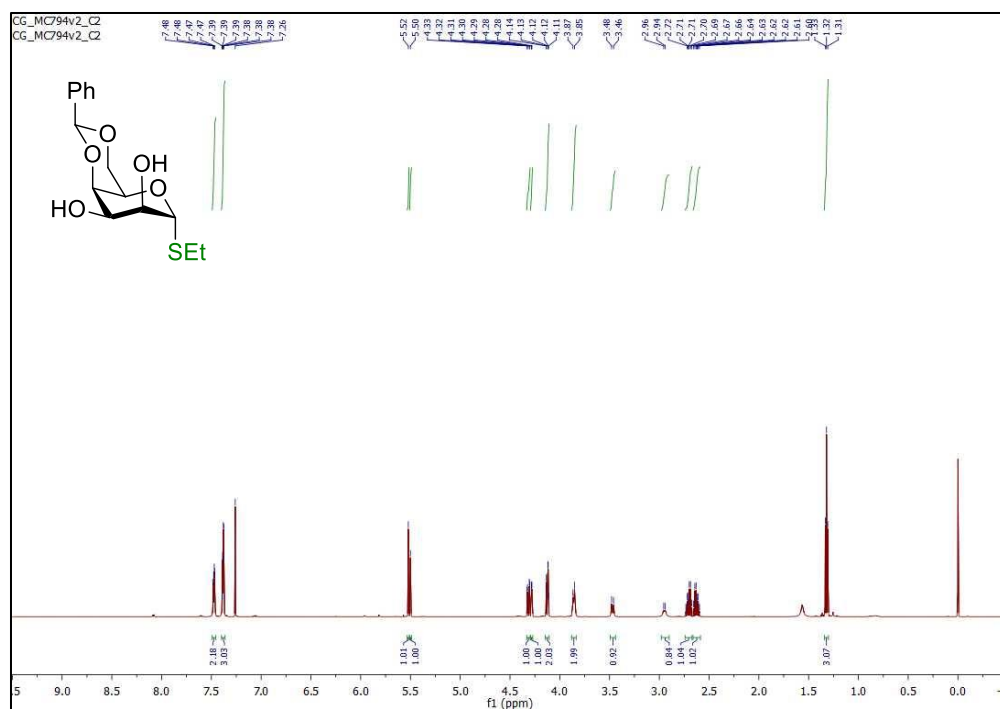


Figure S73 | $^{13}\text{C}\{^1\text{H}\}$ NMR spectrum (CDCl_3 , 150 MHz) of ethyl 4,6-*O*-benzylidene-1-thio- α -D-talopyranoside (27)

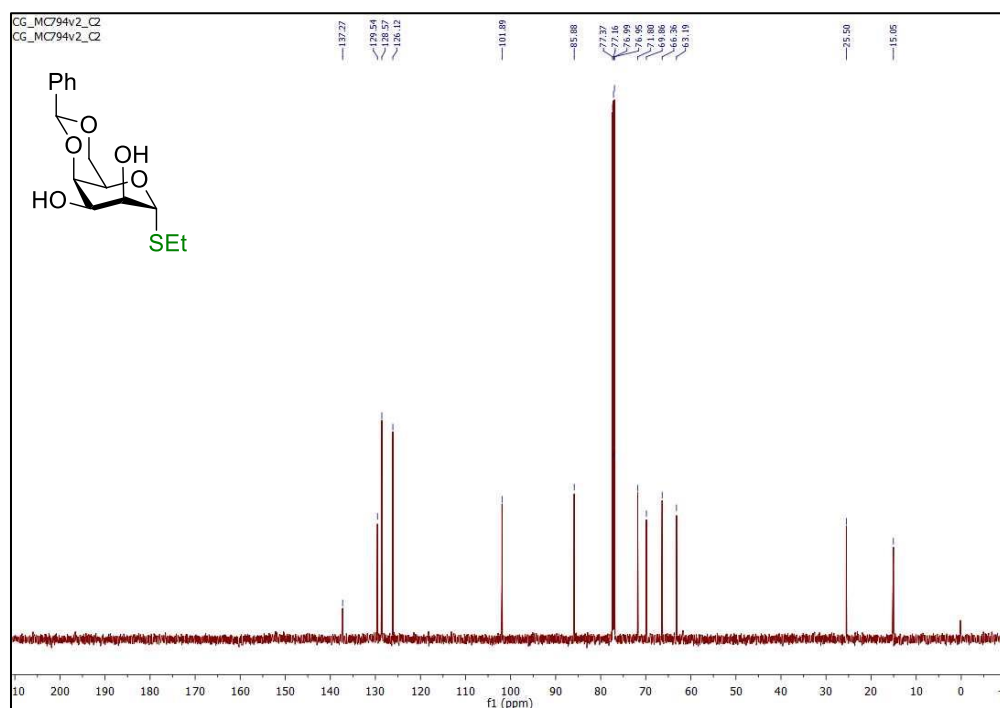


Figure S74 | ^1H NMR spectrum (CDCl_3 , 600 MHz) of ethyl 3-*O*-acetyl-4,6-*O*-benzylidene-1-thio- α -D-talopyranoside

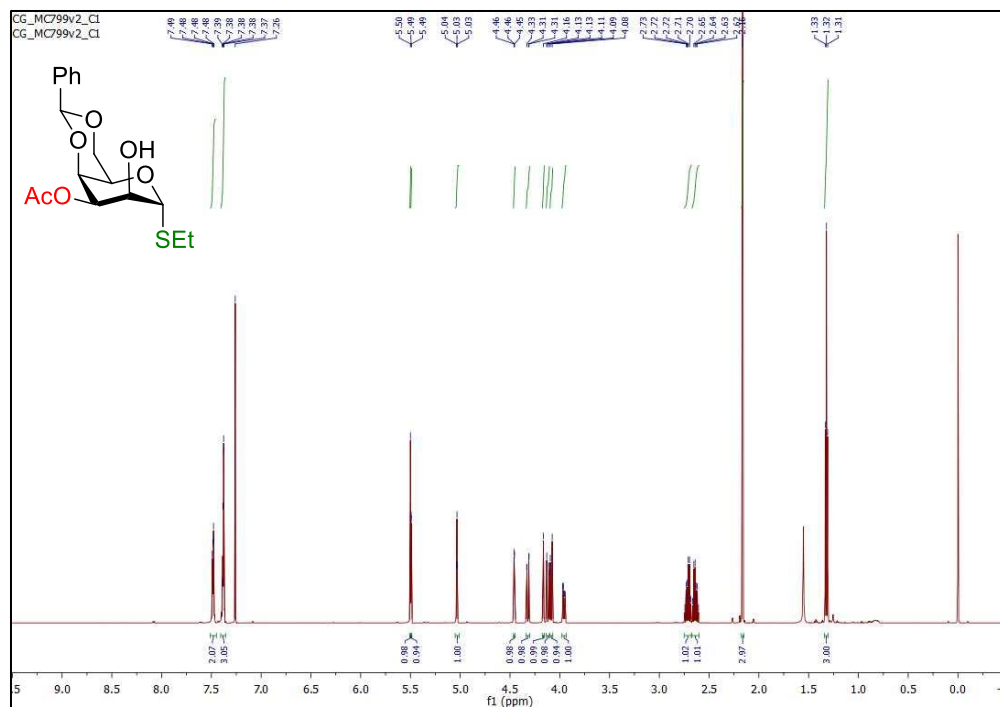


Figure S75 | $^{13}\text{C}\{^1\text{H}\}$ NMR spectrum (CDCl_3 , 150 MHz) of ethyl 3-*O*-acetyl-4,6-*O*-benzylidene-1-thio- α -D-talopyranoside

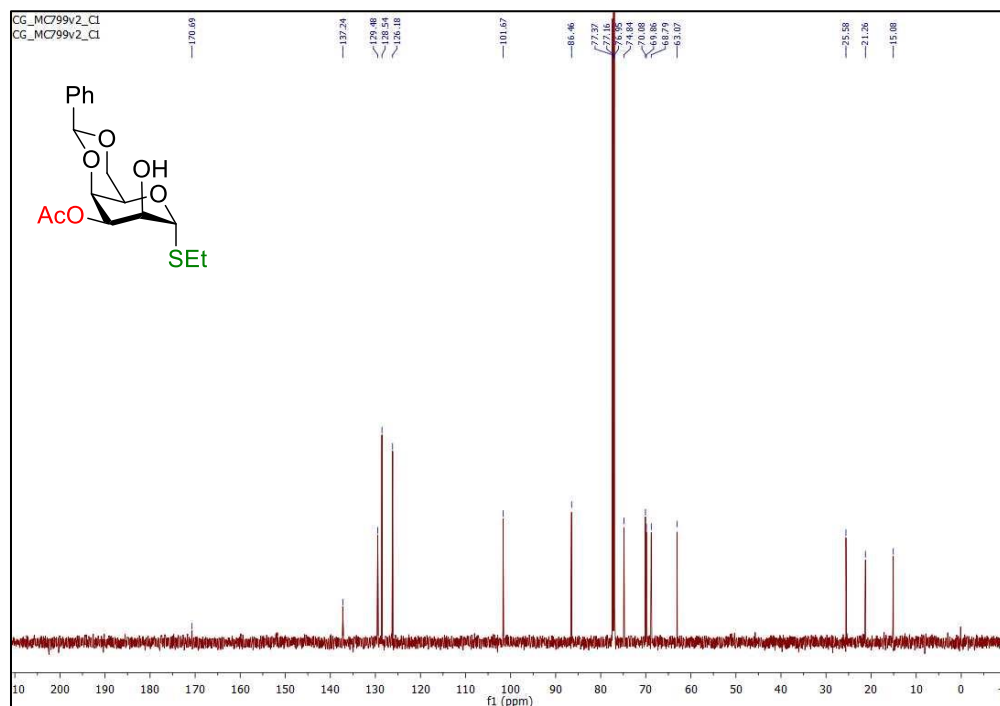


Figure S76 | ¹H NMR spectrum (CDCl₃, 600 MHz) of ethyl 3-*O*-acetyl-4,6-*O*-benzylidene-2-*O*-*tert*-butyldimethylsilyl-1-thio- α -D-talopyranoside (28)

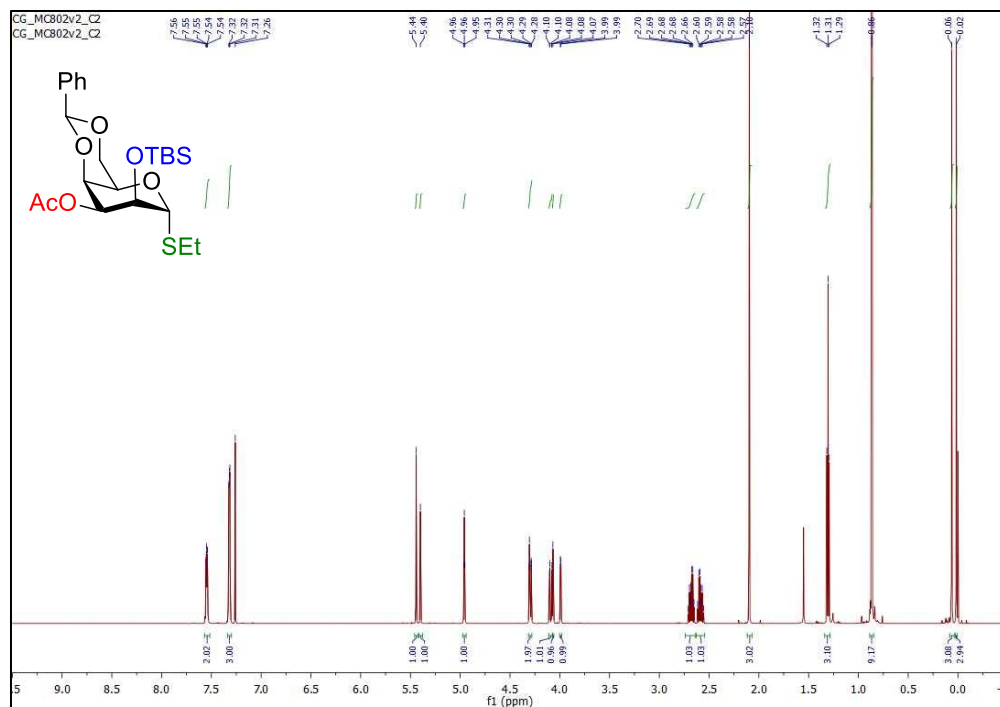


Figure S77 | ¹³C{¹H} NMR spectrum (CDCl₃, 150 MHz) of ethyl 3-*O*-acetyl-4,6-*O*-benzylidene-2-*O*-*tert*-butyldimethylsilyl-1-thio- α -D-talopyranoside (28)

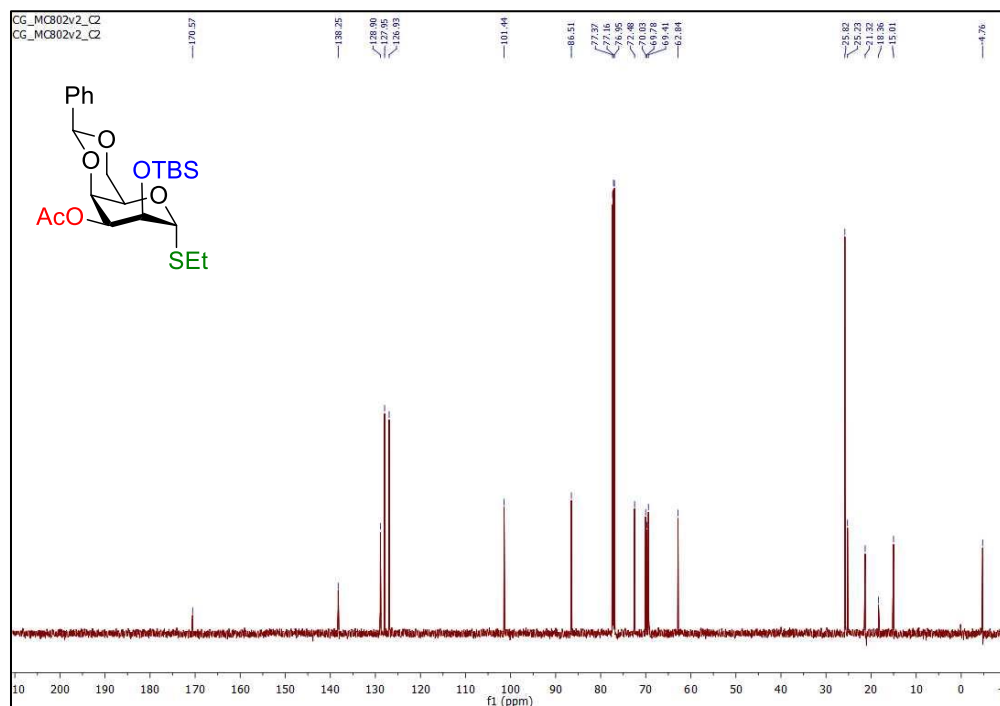


Figure S78 | ^1H NMR spectrum (CDCl_3 , 600 MHz) of (2-adamantyl) 3-*O*-benzyl-(*S*)-4,6-*O*-benzylidene-2-*O*-*tert*-butyldimethylsilyl- β -D-idopyranoside (29)

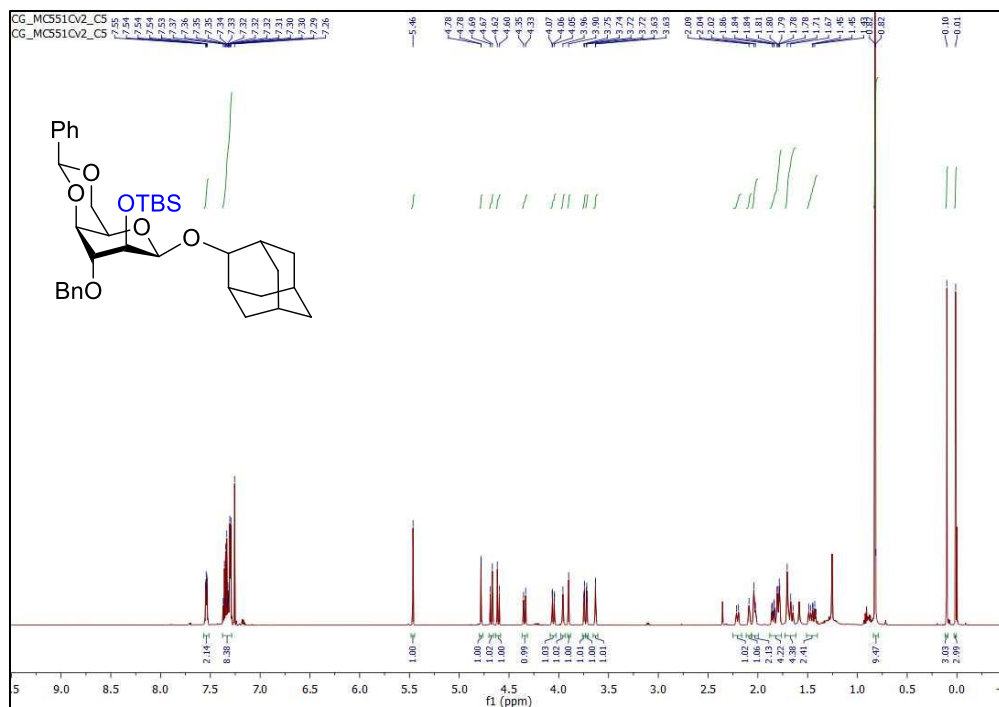


Figure S79 | $^{13}\text{C}\{^1\text{H}\}$ NMR spectrum (CDCl_3 , 150 MHz) of (2-adamantyl) 3-*O*-benzyl-(*S*)-4,6-*O*-benzylidene-2-*O*-*tert*-butyldimethylsilyl- β -D-idopyranoside (29)

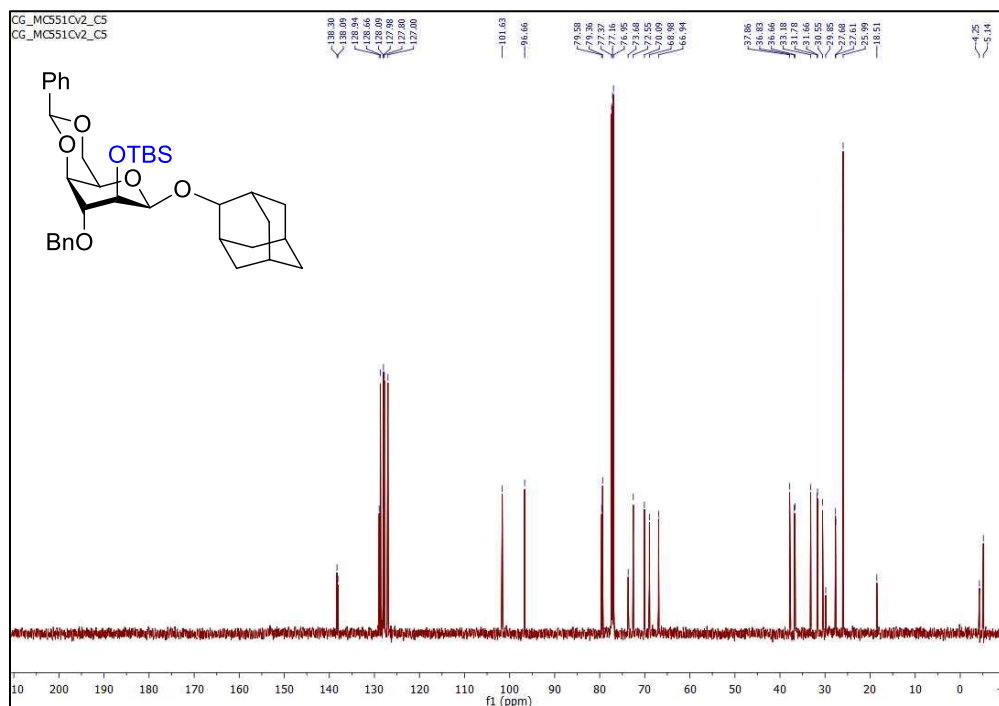


Figure S80 | ^1H NMR spectrum (CDCl_3 , 600 MHz) of (2-adamantyl) 3-*O*-benzyl-(*S*)-4,6-*O*-benzylidene- β -D-idopyranoside (31)

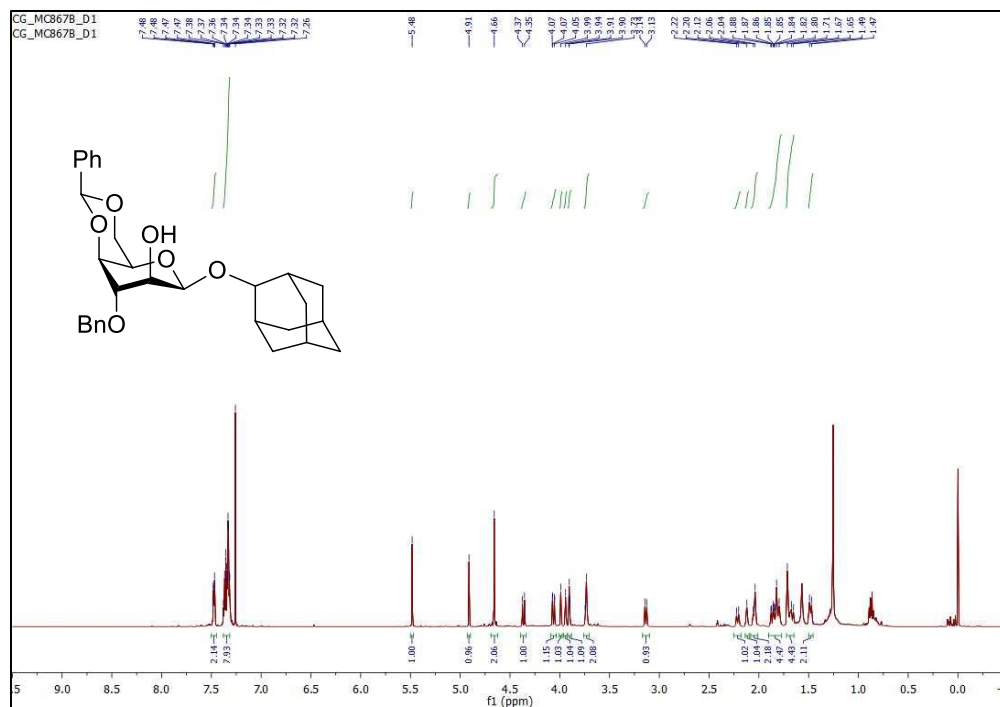


Figure S81 | $^{13}\text{C}\{^1\text{H}\}$ NMR spectrum (CDCl_3 , 150 MHz) of (2-adamantyl) 3-*O*-benzyl-(*S*)-4,6-*O*-benzylidene- β -D-idopyranoside (31)

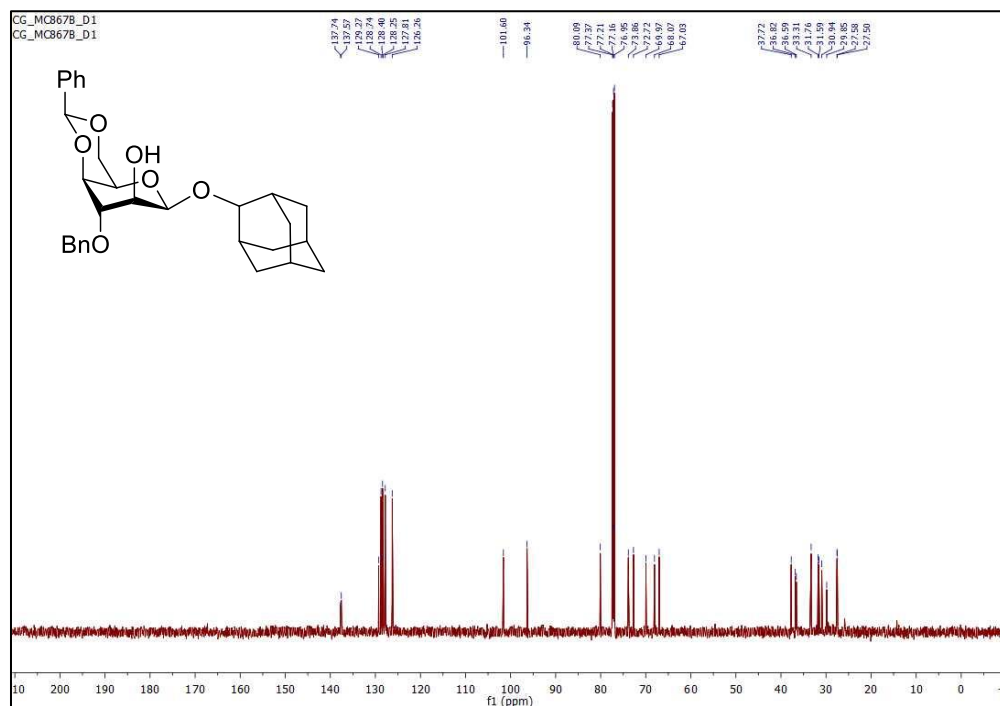


Figure S84 | ^1H NMR spectrum (CDCl_3 , 600 MHz) of (2-adamantyl) 3-*O*-acetyl-(*S*)-4,6-*O*-benzylidene-2-*O*-*tert*-butyldimethylsilyl- β -D-talopyranoside (30β) and (2-adamantyl) 3-*O*-acetyl-(*S*)-4,6-*O*-benzylidene- α -D-talopyranoside (32)

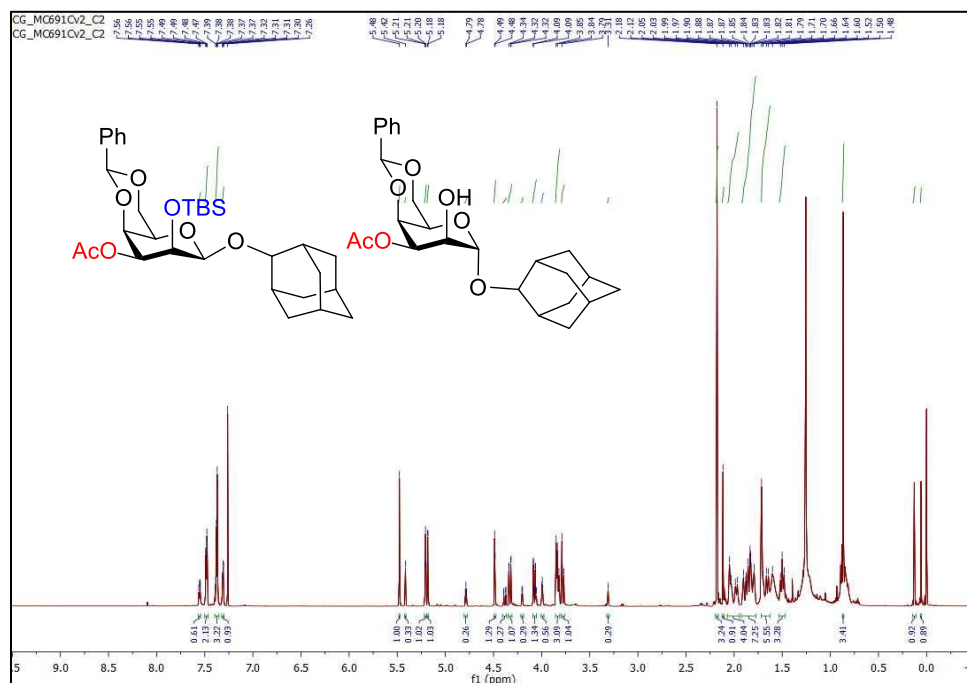


Figure S86 | ^1H NMR spectrum (CDCl_3 , 600 MHz) of allyl 3-*O*-acetyl-(*S*)-4,6-*O*-benzylidene-2-*O*-*tert*-butyldimethylsilyl- α -D-idopyranosyl-(1 \rightarrow 4)-2-*O*-acetyl-3,6-di-*O*-*para*-methoxybenzyl- α -D-glucopyranoside (**37a**)

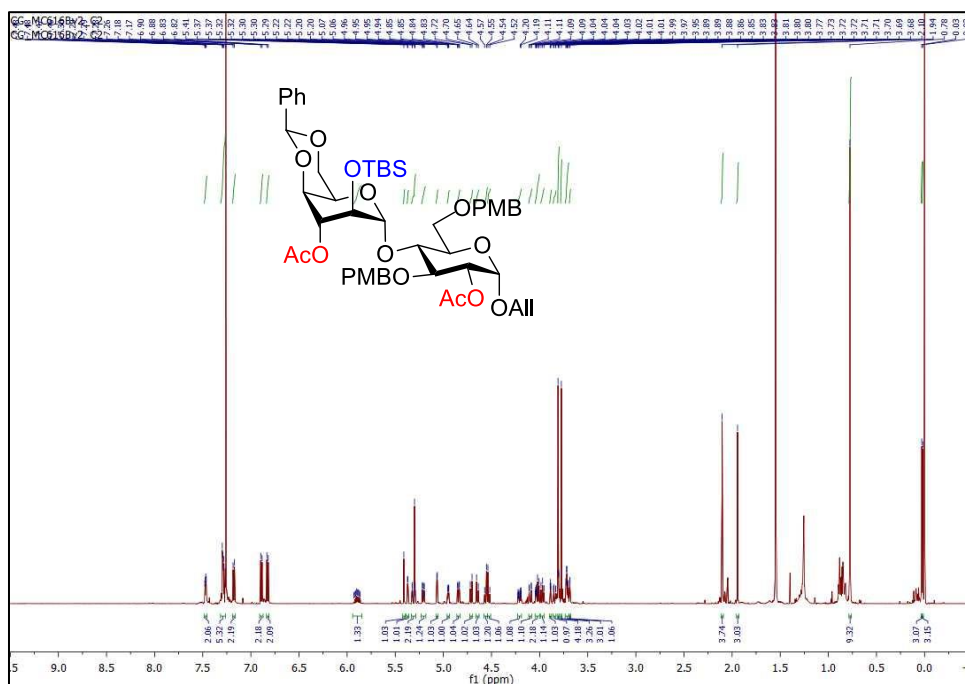


Figure S92 | ^1H NMR spectrum (CDCl_3 , 600 MHz) of allyl 3-*O*-acetyl-(*S*)-4,6-*O*-benzylidene-2-*O*-*tert*-butyldimethylsilyl- α -D-idopyranosyl-(1 \rightarrow 4)-3-*O*-*tert*-butyldimethylsilyl-2-deoxy-2-trichloroacetamido- β -D-glucopyranoside (39a)

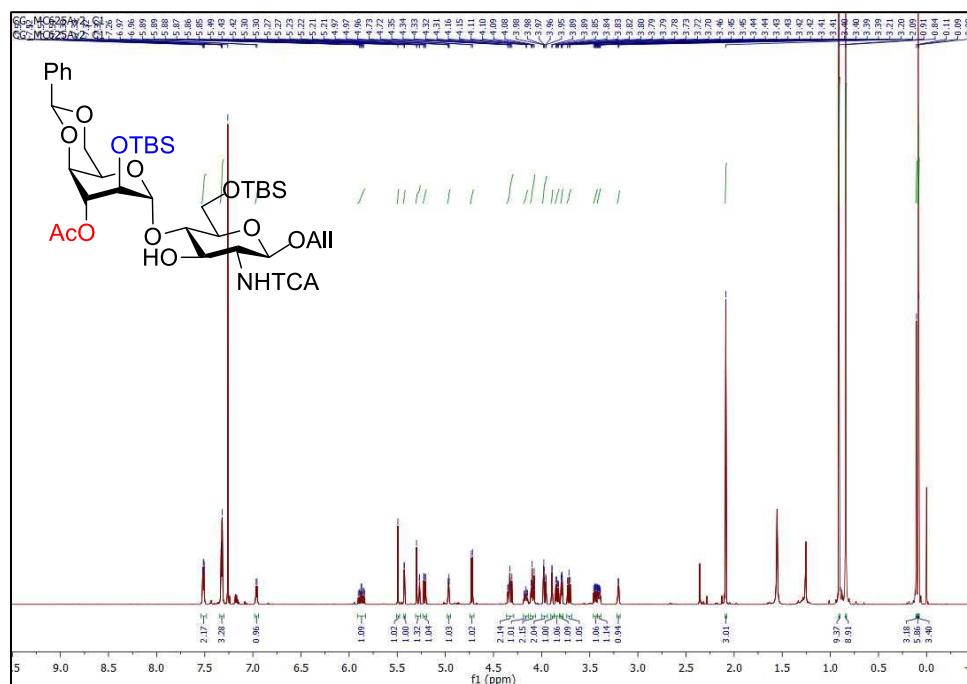


Figure S93 | $^{13}\text{C}\{^1\text{H}\}$ NMR spectrum (CDCl_3 , 150 MHz) of allyl 3-*O*-acetyl-(*S*)-4,6-*O*-benzylidene-2-*O*-*tert*-butyldimethylsilyl- α -D-idopyranosyl-(1 \rightarrow 4)-3-*O*-*tert*-butyldimethylsilyl-2-deoxy-2-trichloroacetamido- β -D-glucopyranoside (39a)

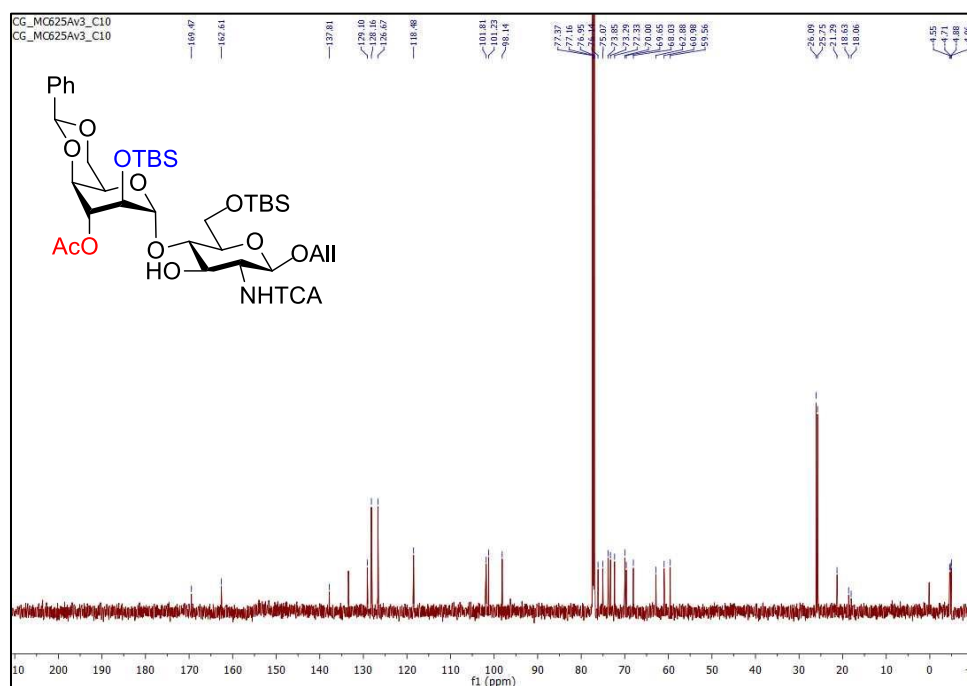


Figure S94 | ^1H NMR spectrum (CDCl_3 , 600 MHz) of allyl 3-*O*-acetyl-(*S*)-4,6-*O*-benzylidene-2-*O*-*tert*-butyldimethylsilyl- α -D-idopyranosyl-(1 \rightarrow 3)-3-*O*-*tert*-butyldimethylsilyl-2-deoxy-2-trichloroacetamido- β -D-glucopyranoside (39b)

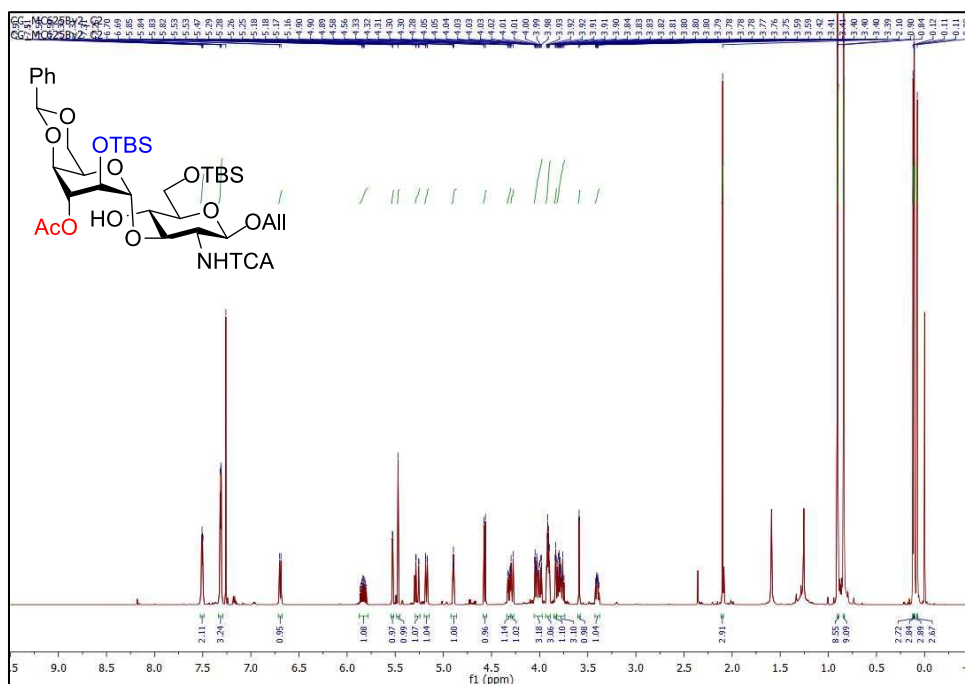


Figure S95 | $^{13}\text{C}\{^1\text{H}\}$ NMR spectrum (CDCl_3 , 150 MHz) of allyl 3-*O*-acetyl-(*S*)-4,6-*O*-benzylidene-2-*O*-*tert*-butyldimethylsilyl- α -D-idopyranosyl-(1 \rightarrow 3)-3-*O*-*tert*-butyldimethylsilyl-2-deoxy-2-trichloroacetamido- β -D-glucopyranoside (39b)

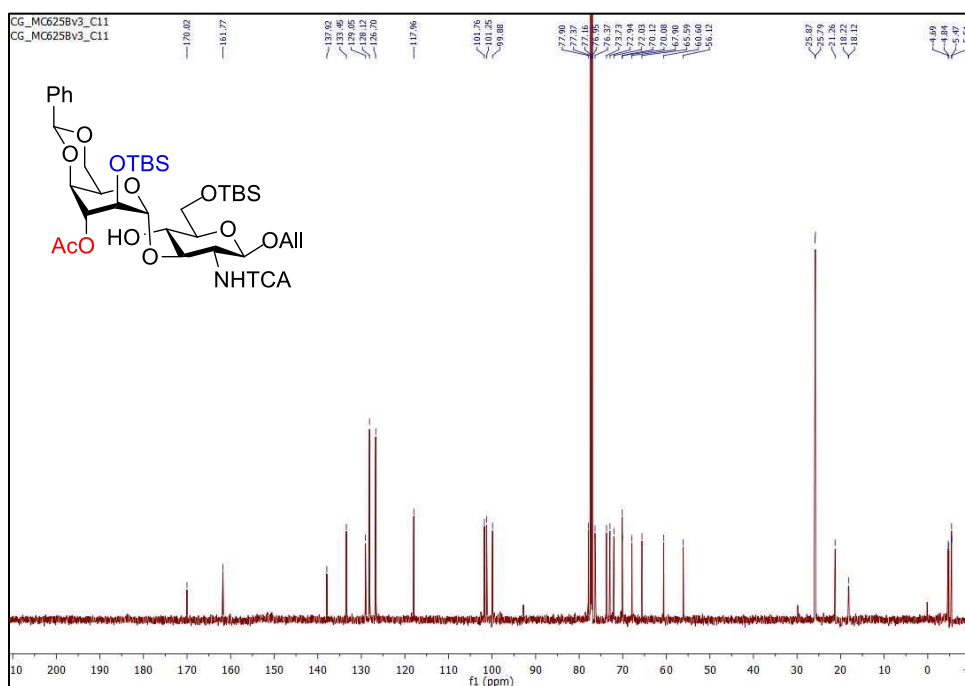


Figure S96 | ^1H NMR spectrum (CDCl_3 , 600 MHz) of *tert*-butyldimethylsilyl 3-*O*-acetyl-(*S*)-4,6-*O*-benzylidene-2-*O*-*tert*-butyldimethylsilyl- α -D-idopyranosyl-(1 \rightarrow 4)-3,6-di-*O*-benzyl-2-deoxy-2-trichloroacetamido- β -D-glucopyranoside (40)

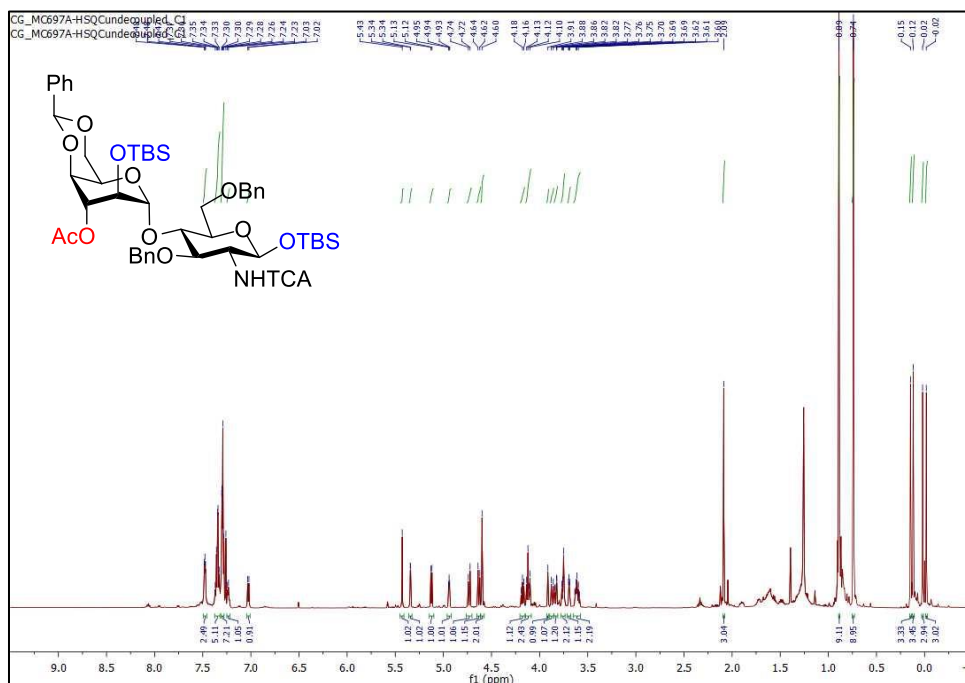


Figure S97 | $^{13}\text{C}\{^1\text{H}\}$ NMR spectrum (CDCl_3 , 150 MHz) of *tert*-butyldimethylsilyl 3-*O*-acetyl-(*S*)-4,6-*O*-benzylidene-2-*O*-*tert*-butyldimethylsilyl- α -D-idopyranosyl-(1 \rightarrow 4)-3,6-di-*O*-benzyl-2-deoxy-2-trichloroacetamido- β -D-glucopyranoside (40)

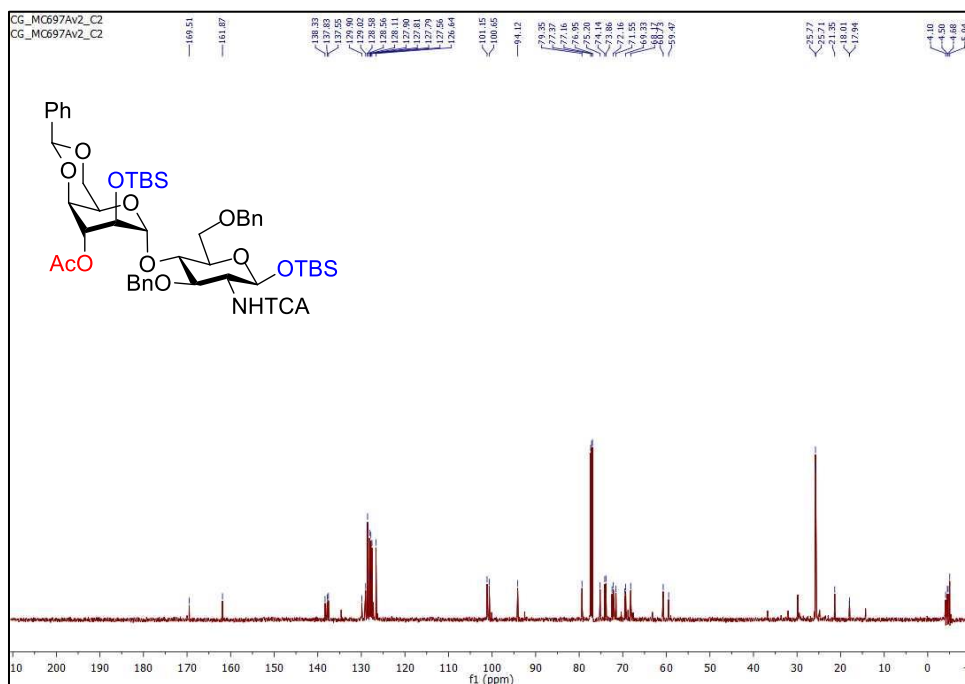


Figure S98 | ^1H NMR spectrum (CDCl_3 , 600 MHz) of *tert*-butyldimethylsilyl 3-*O*-benzyl-(*S*)-4,6-*O*-benzylidene-2-*O*-*tert*-butyldimethylsilyl- α -D-idopyranosyl-(1 \rightarrow 4)-3,6-di-*O*-benzyl-2-deoxy-2-trichloroacetamido- β -D-glucopyranoside (**41a**)

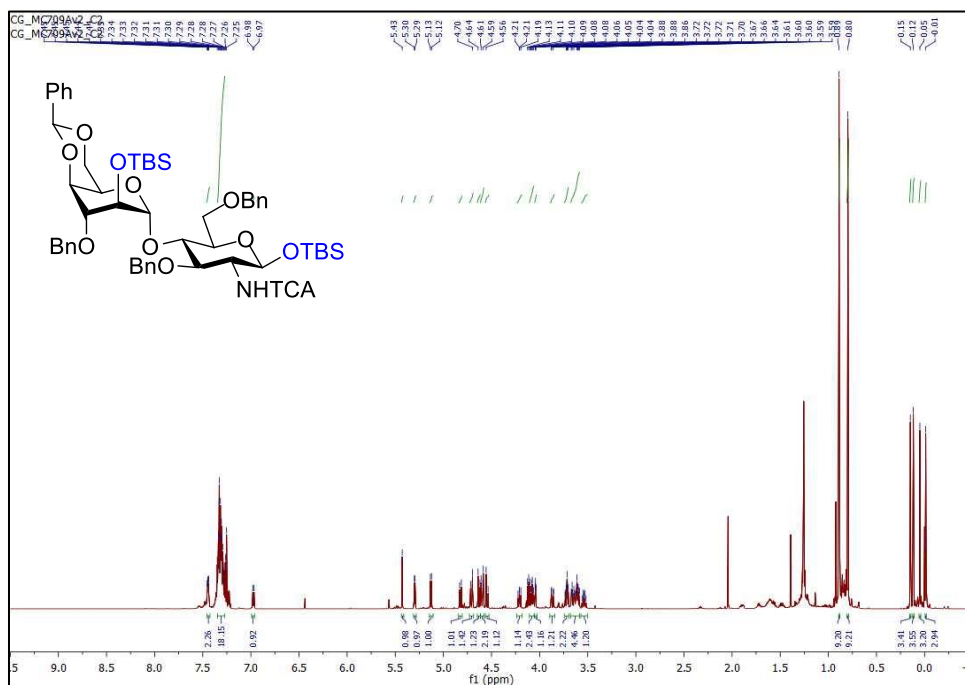
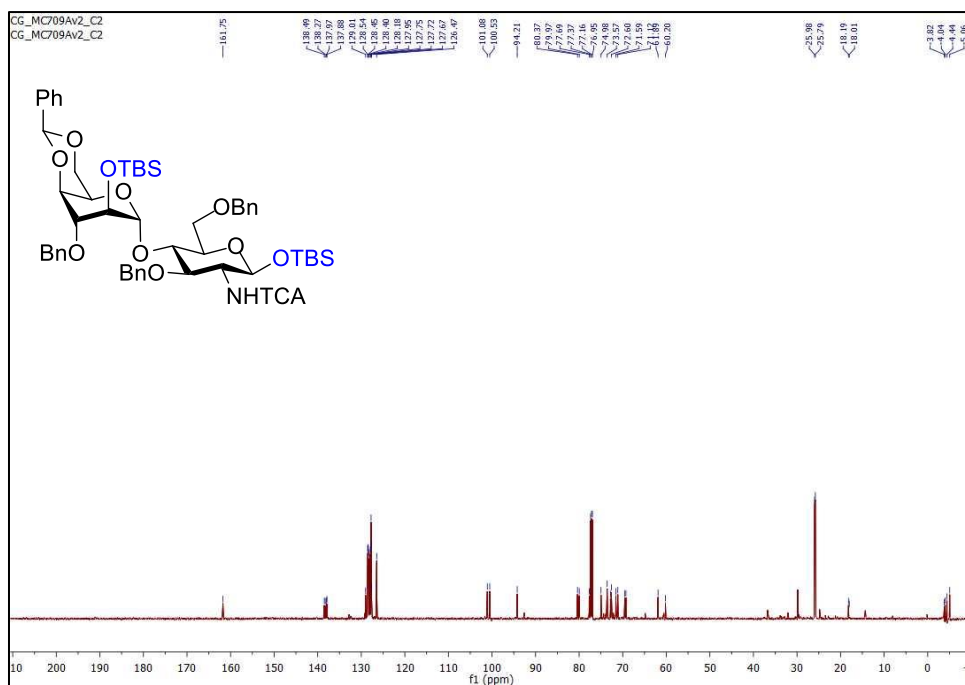


Figure S99 | $^{13}\text{C}\{^1\text{H}\}$ NMR spectrum (CDCl_3 , 150 MHz) of *tert*-butyldimethylsilyl 3-*O*-benzyl-(*S*)-4,6-*O*-benzylidene-2-*O*-*tert*-butyldimethylsilyl- α -D-idopyranosyl-(1 \rightarrow 4)-3,6-di-*O*-benzyl-2-deoxy-2-trichloroacetamido- β -D-glucopyranoside (**41a**)



ANNEXE DU CHAPITRE 8

1. Traces of NMR Spectra for New Compounds

Figure S1 | ^1H NMR spectrum (CDCl_3 , 600 MHz) of ethyl 3-*O*-benzyl-4,6-*O*-benzylidene-1-thio- α -D-idopyranoside (**7a**)

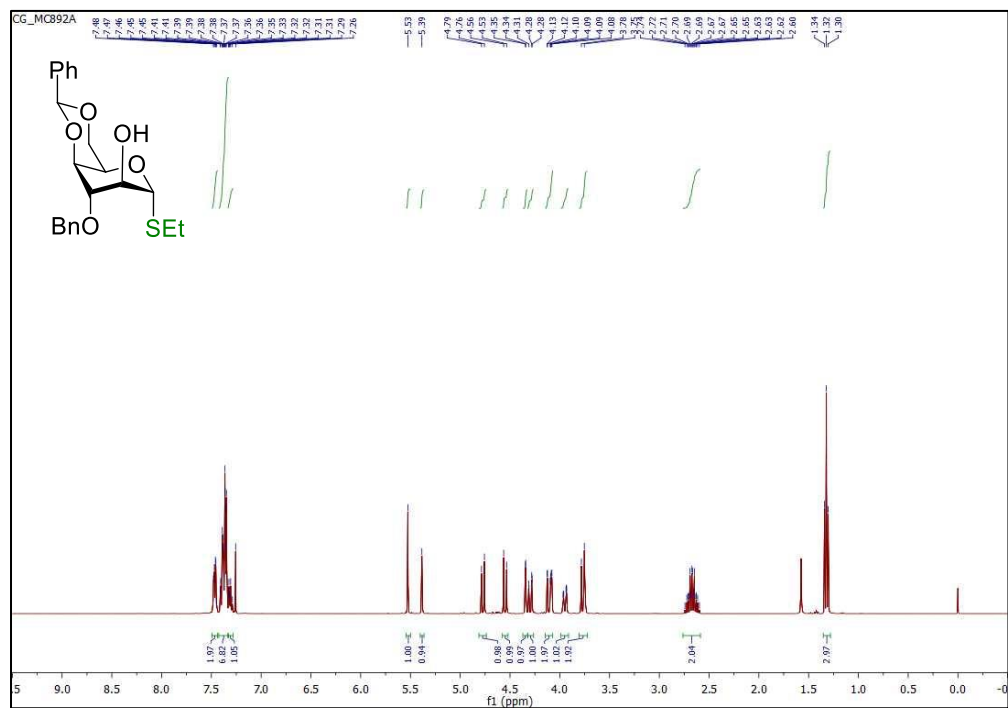


Figure S2 | $^{13}\text{C}\{^1\text{H}\}$ NMR spectrum (CDCl_3 , 150 MHz) of ethyl 3-*O*-benzyl-4,6-*O*-benzylidene-1-thio- α -D-idopyranoside (**7a**)

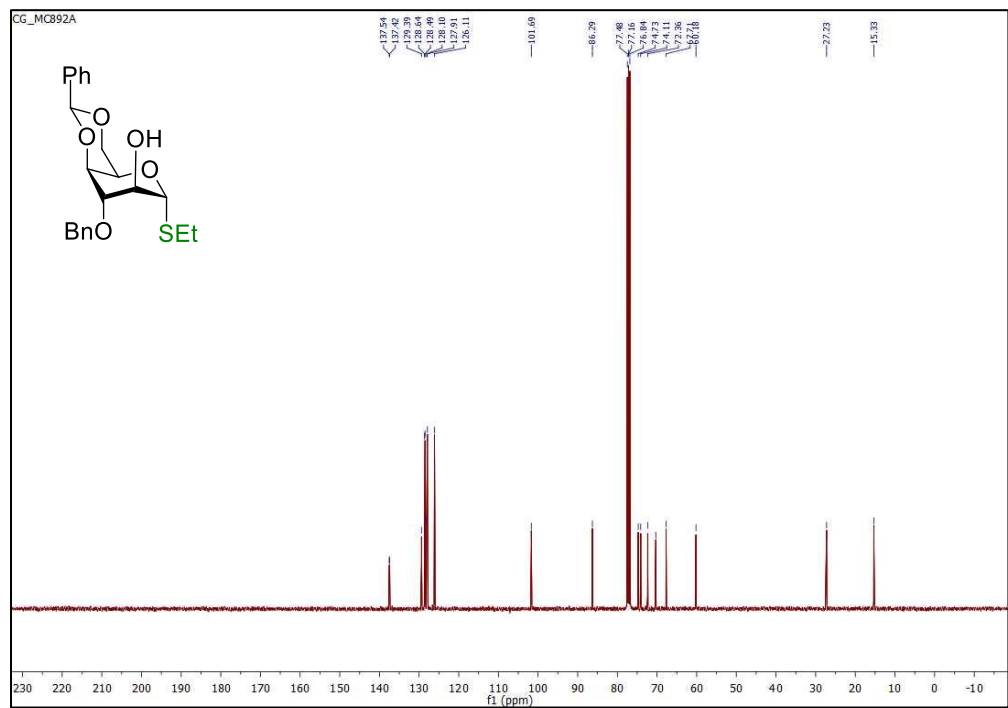


Figure S5 | ^1H NMR spectrum (CDCl_3 , 600 MHz) of *para*-methylphenyl 3-*O*-benzyl-4,6-*O*-benzylidene-1-thio- α -D-idopyranoside (7b)

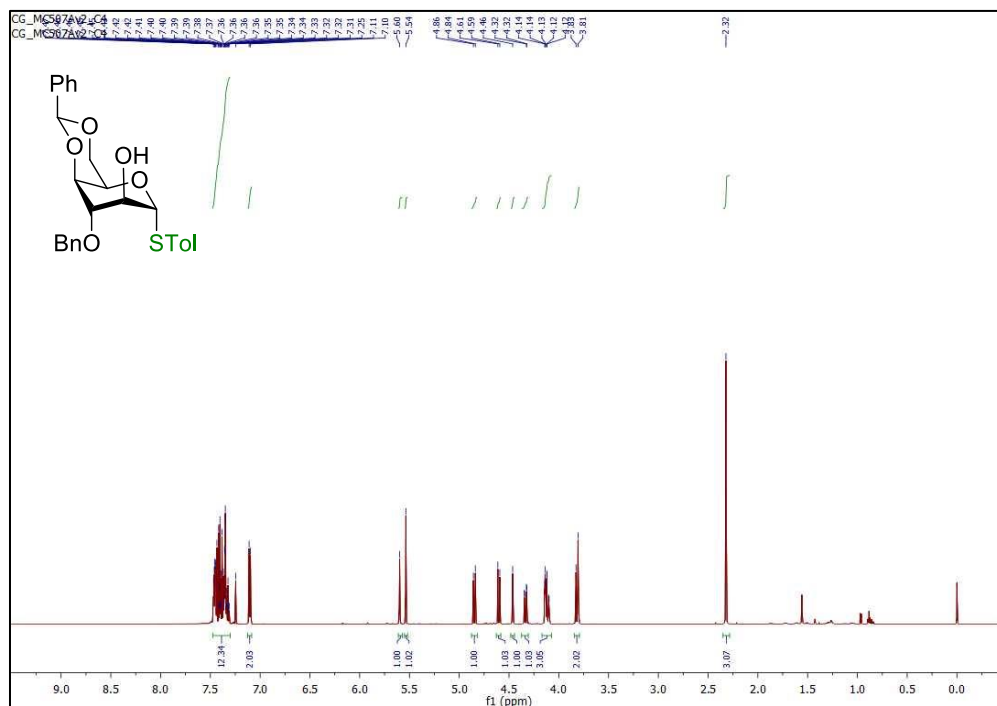


Figure S6 | $^{13}\text{C}\{^1\text{H}\}$ NMR spectrum (CDCl_3 , 150 MHz) of *para*-methylphenyl 3-*O*-benzyl-4,6-*O*-benzylidene-1-thio- α -D-idopyranoside (7b)

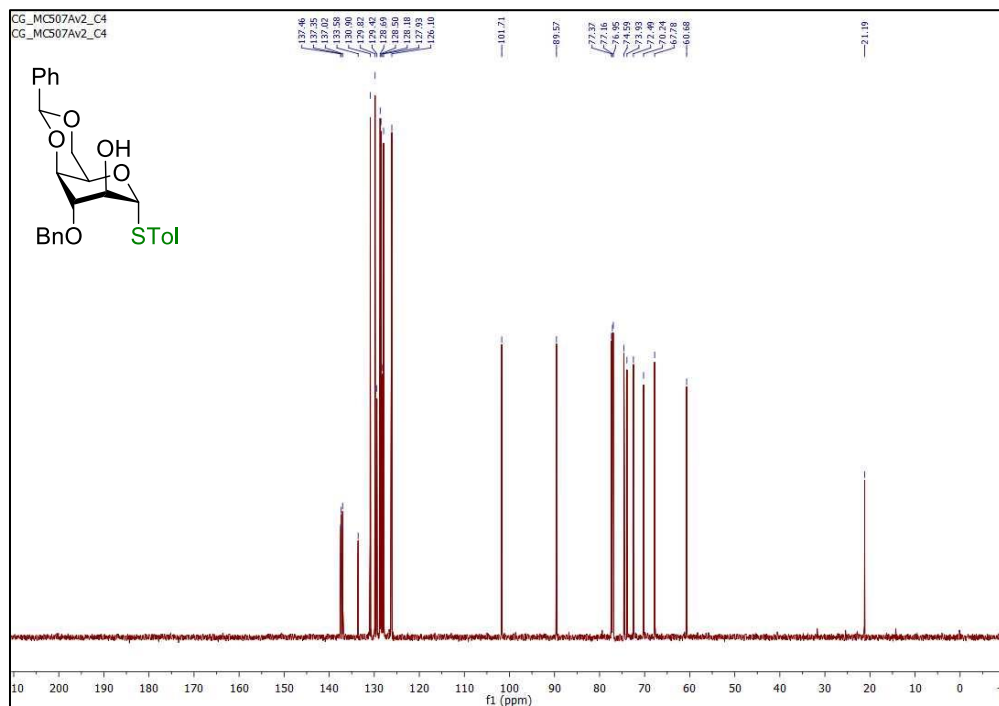


Figure S7 | ^1H NMR spectrum (CDCl₃, 400 MHz) of ethyl 3-*O*-benzyl-4,6-*O*-benzylidene-2-*O*-*para*-methoxybenzyl-1-thio- α -D-idopyranoside (8a)

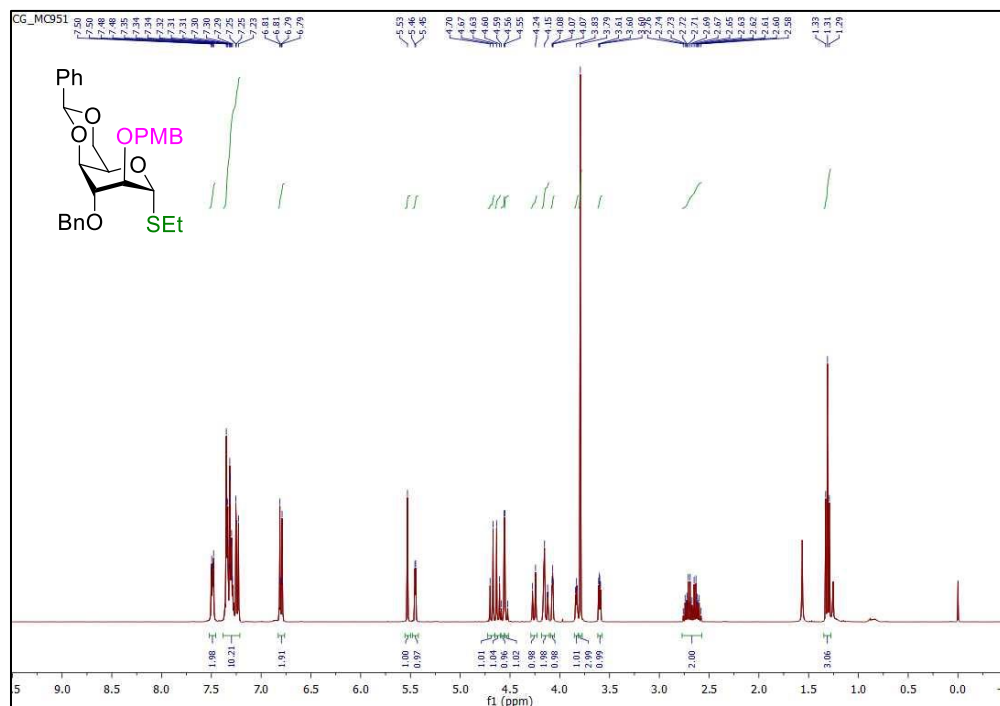


Figure S8 | $^{13}\text{C}\{^1\text{H}\}$ NMR spectrum (CDCl₃, 100 MHz) of ethyl 3-*O*-benzyl-4,6-*O*-benzylidene-2-*O*-*para*-methoxybenzyl-1-thio- α -D-idopyranoside (8a)

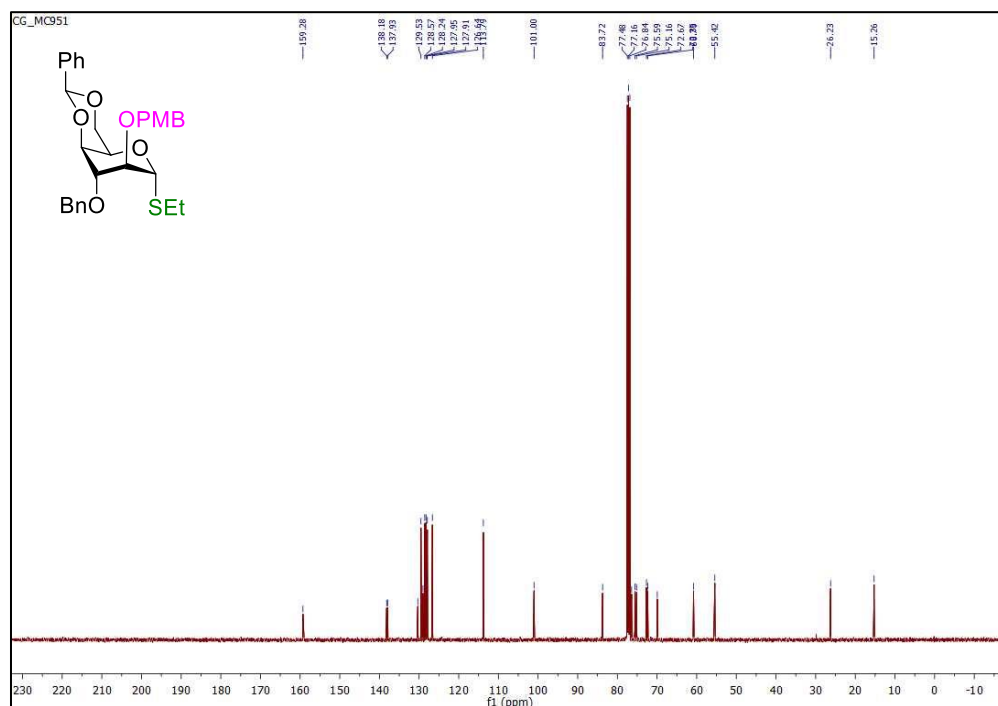


Figure S11 | ^1H NMR spectrum (CDCl_3 , 400 MHz) of ethyl 3,4-di-*O*-benzyl-6-*O*-levulinoyl-2-*O*-*para*-methoxybenzyl-1-thio- α -D-idopyranoside (4a)

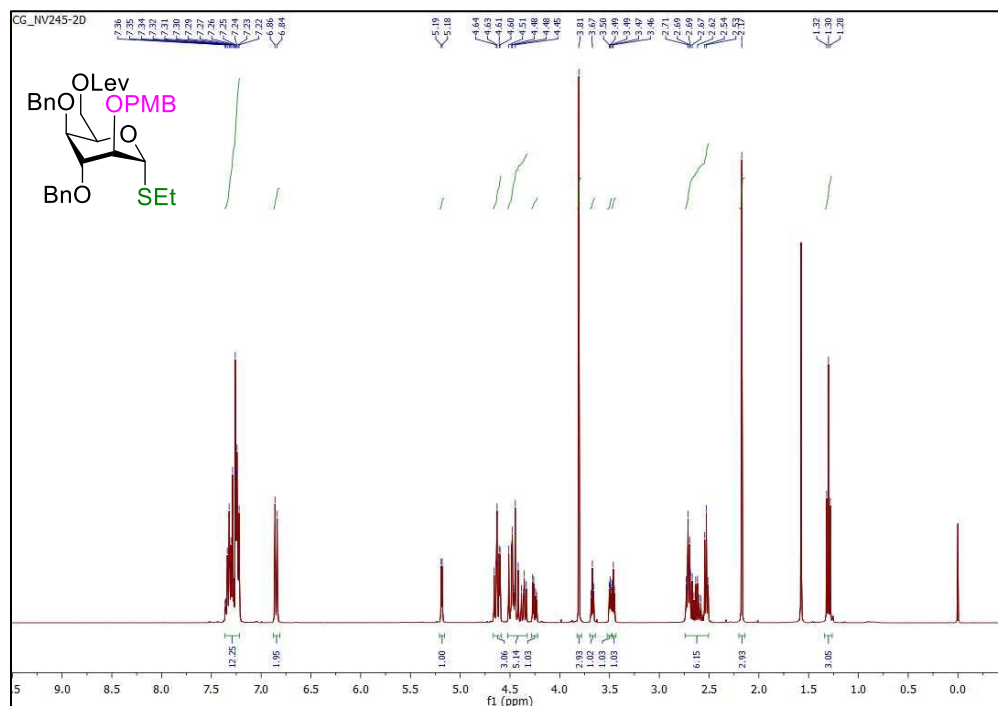


Figure S12 | $^{13}\text{C}\{^1\text{H}\}$ NMR spectrum (CDCl_3 , 100 MHz) of ethyl 3,4-di-*O*-benzyl-6-*O*-levulinoyl-2-*O*-*para*-methoxybenzyl-1-thio- α -D-idopyranoside (4a)

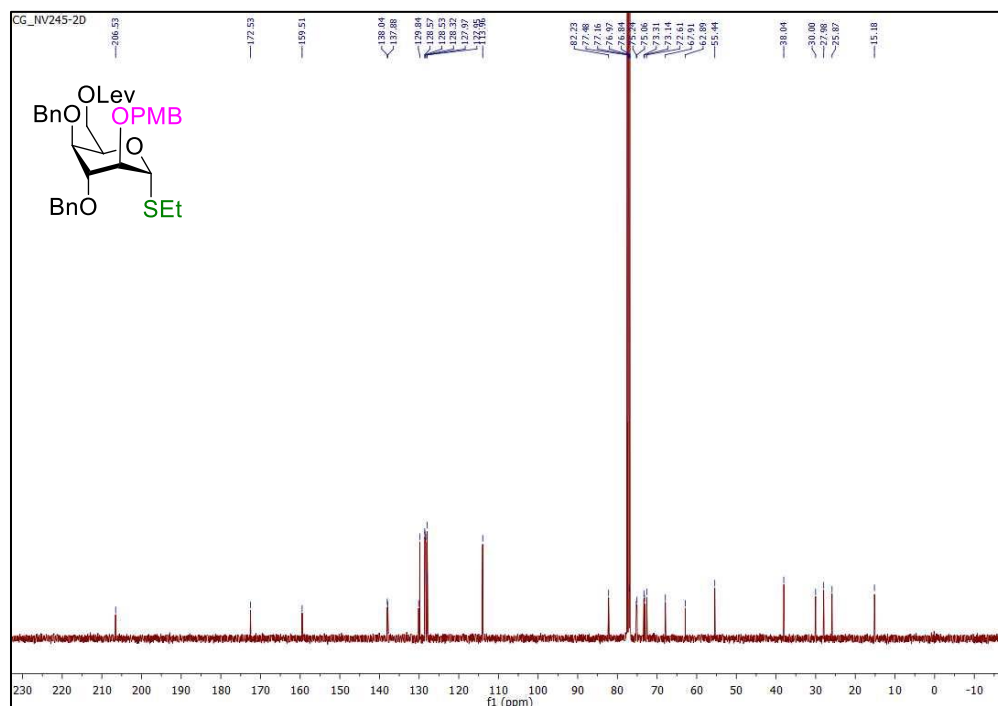


Figure S13 | ^1H NMR spectrum (CDCl_3 , 400 MHz) of *para*-methylphenyl 3,4-di-*O*-benzyl-2-*O*-*para*-methoxybenzyl-1-thio- α -D-idopyranoside (11)

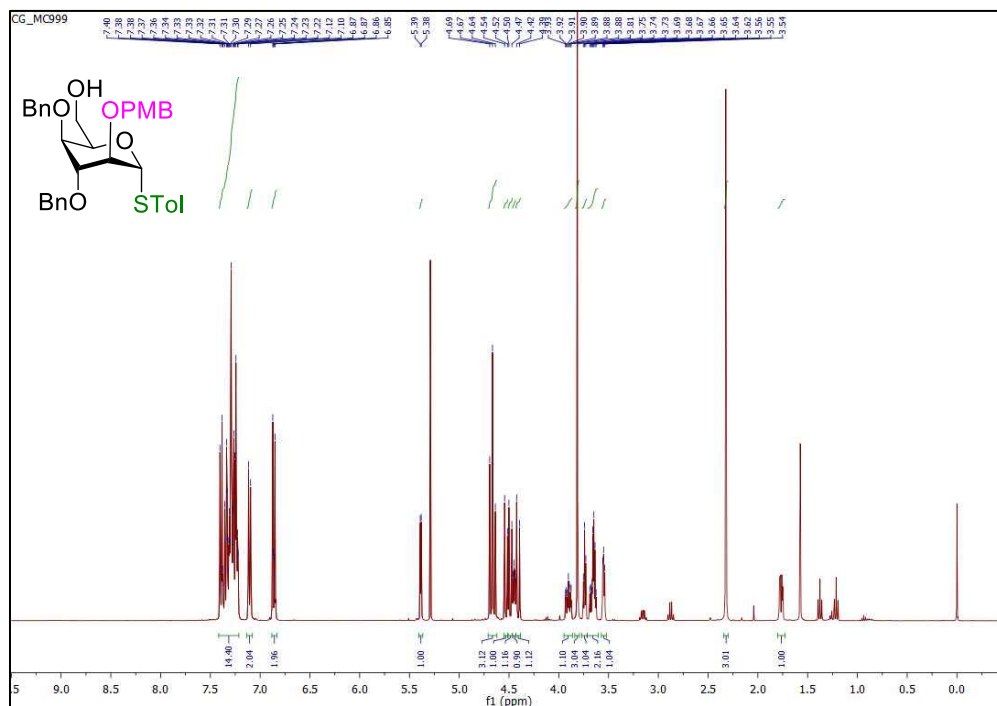


Figure S14 | $^{13}\text{C}\{^1\text{H}\}$ NMR spectrum (CDCl_3 , 100 MHz) of *para*-methylphenyl 3,4-di-*O*-benzyl-2-*O*-*para*-methoxybenzyl-1-thio- α -D-idopyranoside (11)

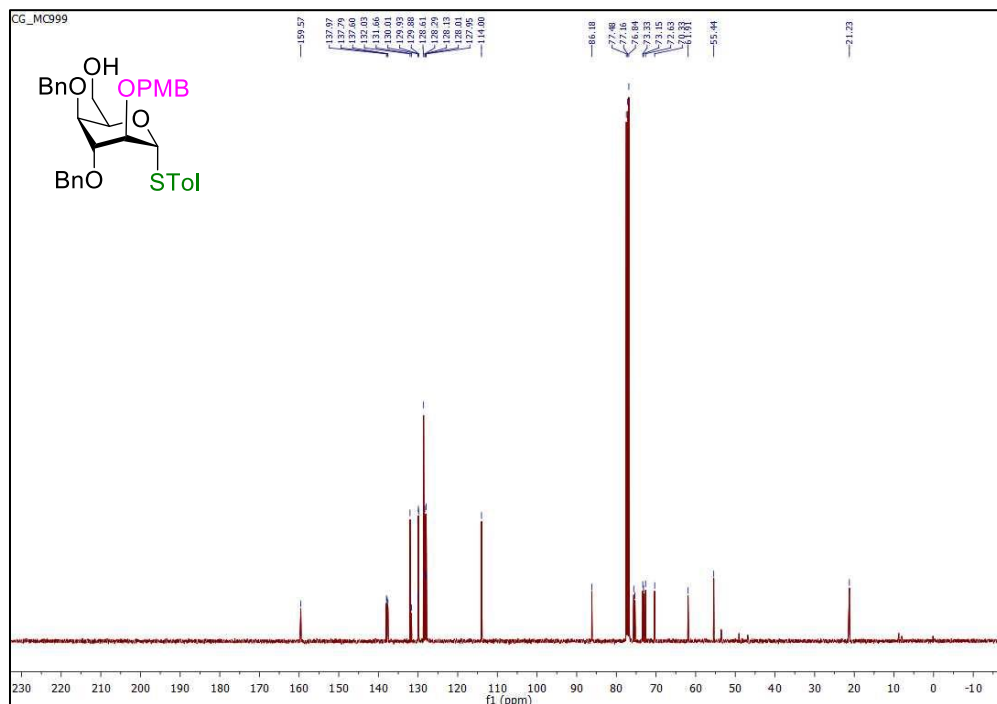


Figure S15 | ^1H NMR spectrum (CDCl_3 , 400 MHz) of *para*-methylphenyl 3,4-di-*O*-benzyl-6-*O*-levulinoyl-2-*O*-*para*-methoxybenzyl-1-thio- α -D-idopyranoside (4b)

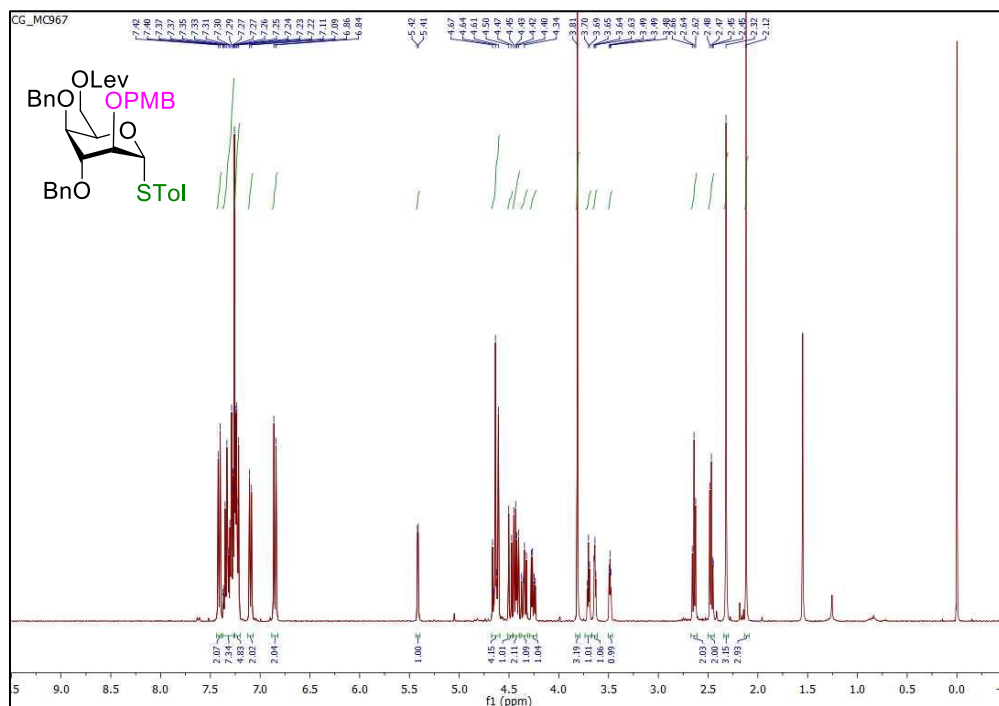


Figure S16 | $^{13}\text{C}\{^1\text{H}\}$ NMR spectrum (CDCl_3 , 100 MHz) of *para*-methylphenyl 3,4-di-*O*-benzyl-6-*O*-levulinoyl-2-*O*-*para*-methoxybenzyl-1-thio- α -D-idopyranoside (4b)

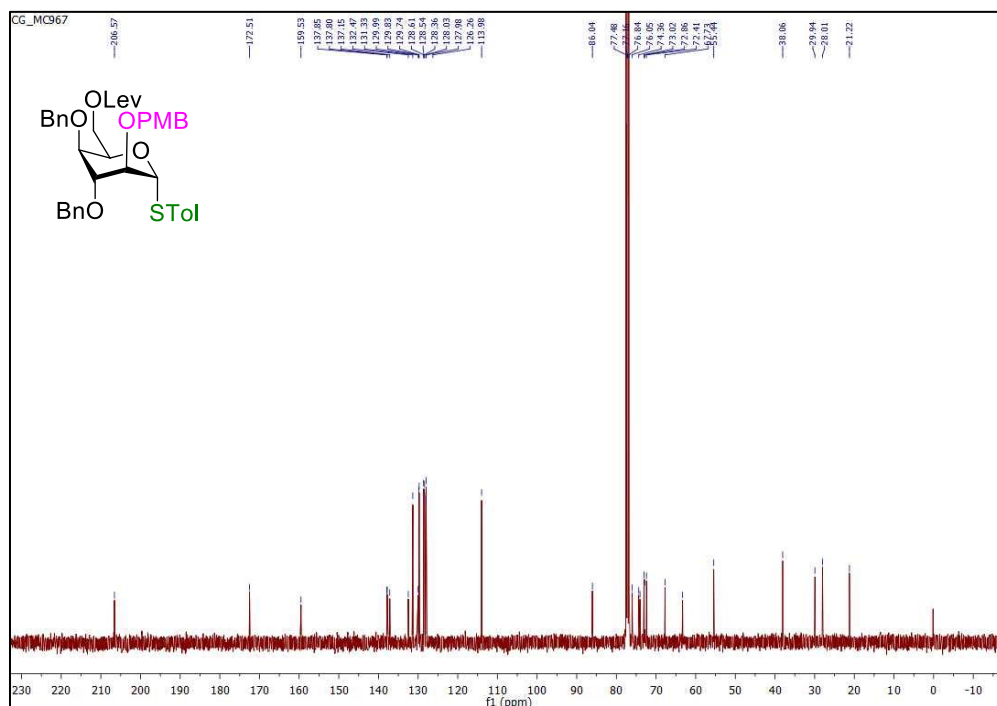


Figure S17 | ¹H NMR spectrum (CDCl₃, 400 MHz) of ethyl 3-*O*-benzyl-4,6-*O*-benzylidene-2-*O*-naphthylmethyl-1-thio- α -D-idopyranoside (9a)

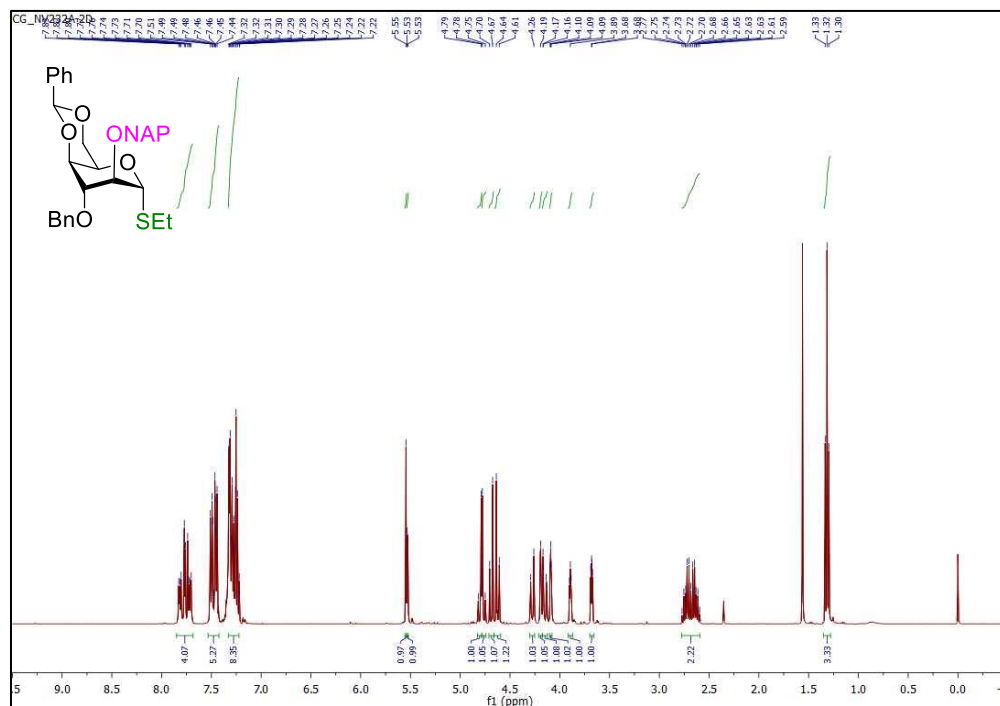


Figure S18 | ¹³C{¹H} NMR spectrum (CDCl₃, 100 MHz) of ethyl 3-*O*-benzyl-4,6-*O*-benzylidene-2-*O*-naphthylmethyl-1-thio- α -D-idopyranoside (9a)

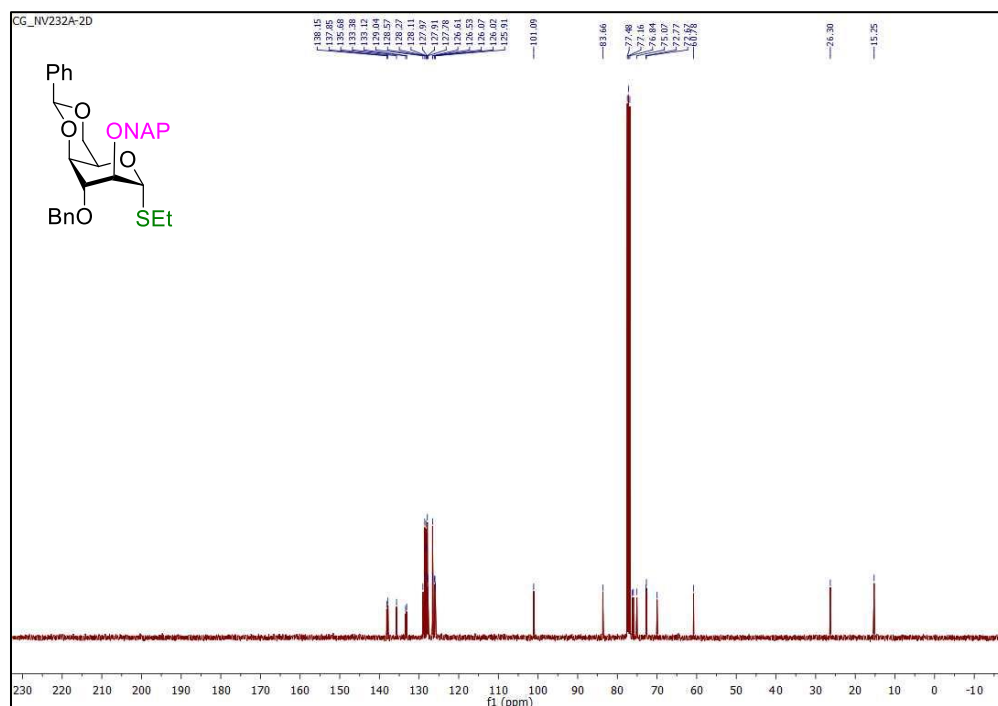


Figure S19 | ^1H NMR spectrum (CDCl_3 , 600 MHz) of *para*-methylphenyl 3-*O*-benzyl-4,6-*O*-benzylidene-2-*O*-naphthylmethyl-1-thio- α -D-idopyranoside (**9b**)

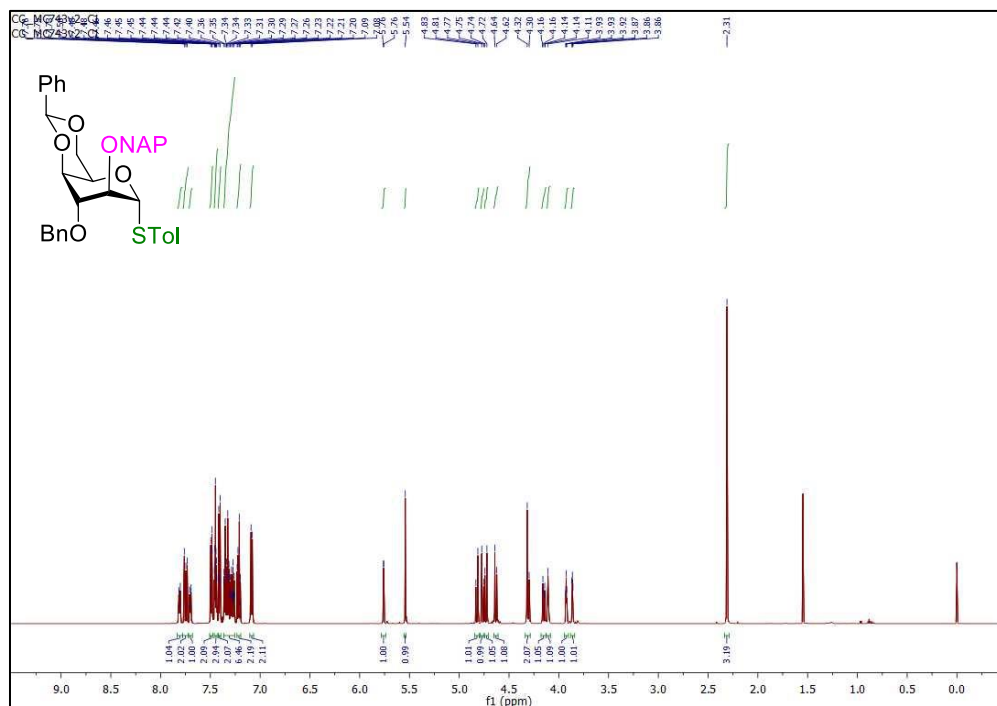


Figure S20 | $^{13}\text{C}\{^1\text{H}\}$ NMR spectrum (CDCl_3 , 150 MHz) of *para*-methylphenyl 3-*O*-benzyl-4,6-*O*-benzylidene-2-*O*-naphthylmethyl-1-thio- α -D-idopyranoside (**9b**)

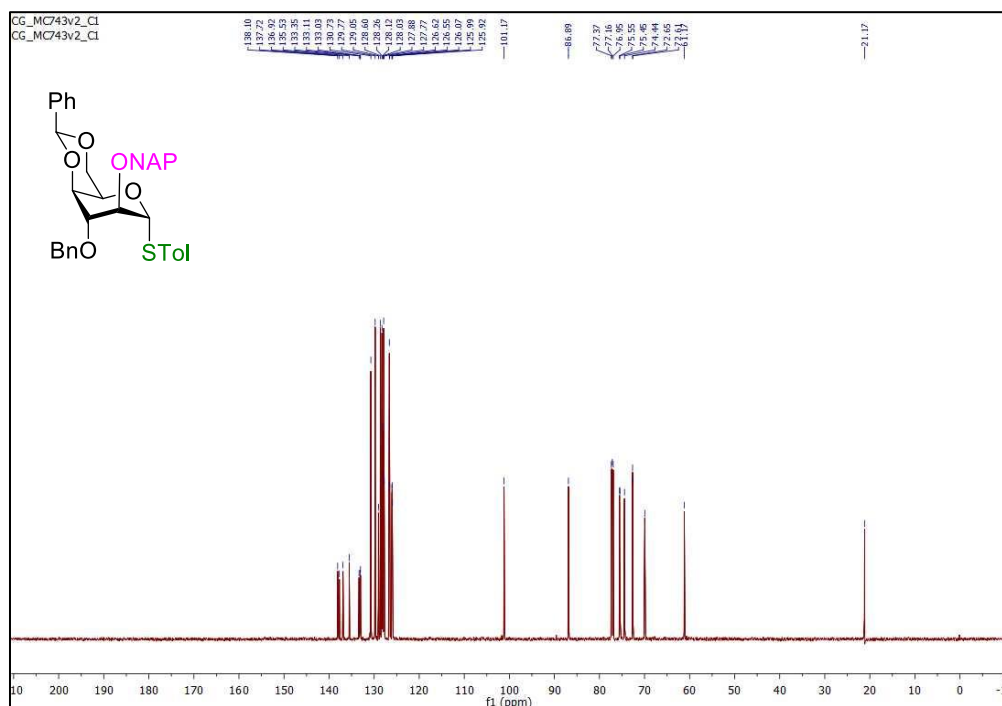


Figure S25 | ^1H NMR spectrum (CDCl_3 , 600 MHz) of *para*-methylphenylsulfenyl 3,4-di-*O*-benzyl-6-*O*-levulinoyl-2-*O*-naphthylmethyl- α -D-idopyranoside (5c)

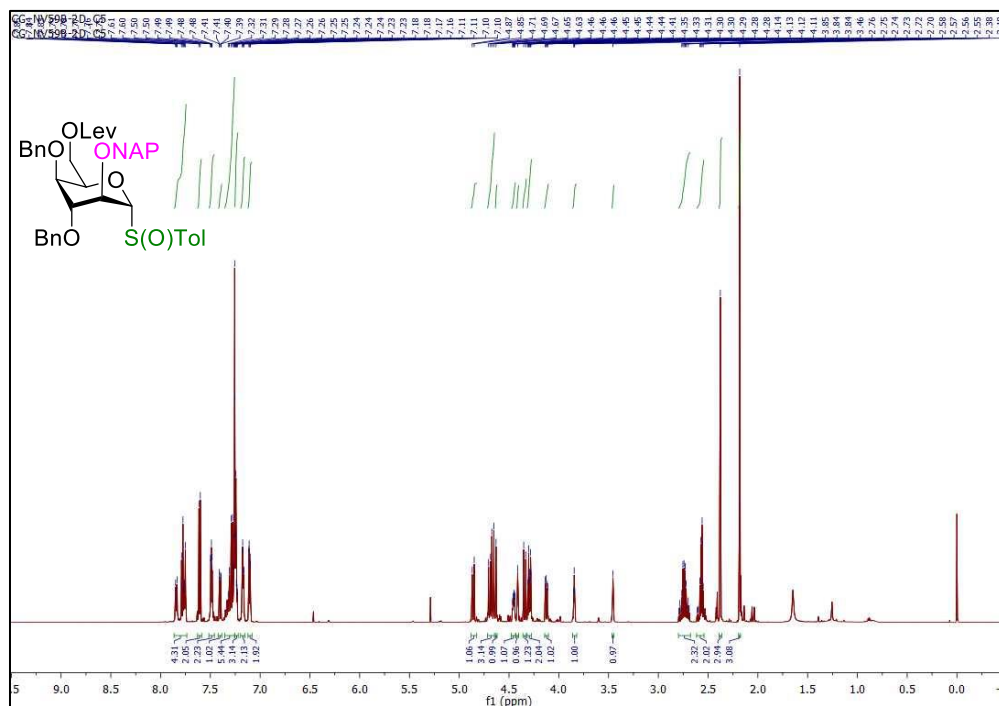


Figure S26 | $^{13}\text{C}\{^1\text{H}\}$ NMR spectrum (CDCl_3 , 150 MHz) of *para*-methylphenylsulfenyl 3,4-di-*O*-benzyl-6-*O*-levulinoyl-2-*O*-naphthylmethyl- α -D-idopyranoside (5c)

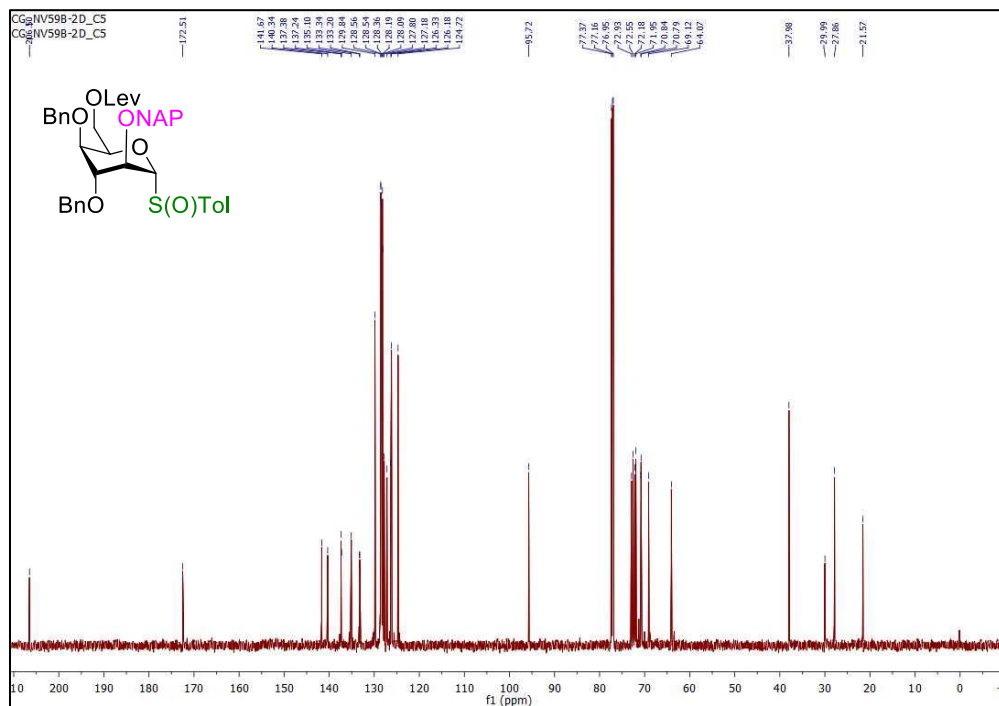


Figure S29 | ^1H NMR spectrum (CDCl_3 , 600 MHz) of 3,4-di-*O*-benzyl-6-*O*-levulinoyl-2-*O*-naphthylmethyl-1-thio- α -D-idopyranosyl *ortho*-hexynylbenzoate (5d)

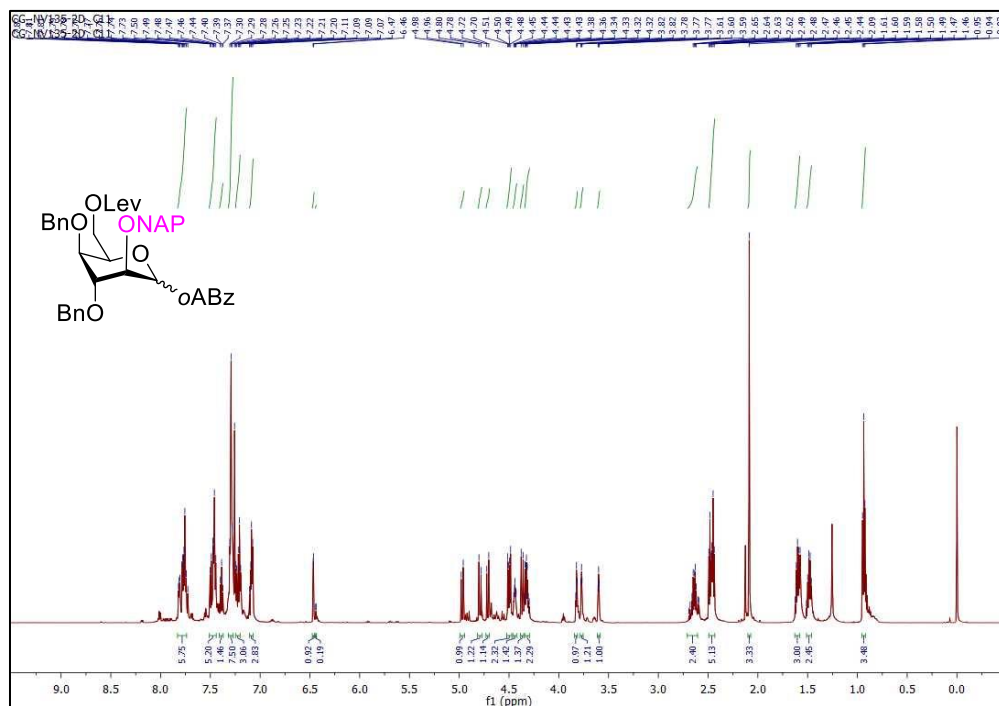


Figure S30 | $^{13}\text{C}\{^1\text{H}\}$ NMR spectrum (CDCl_3 , 150 MHz) of 3,4-di-*O*-benzyl-6-*O*-levulinoyl-2-*O*-naphthylmethyl-1-thio- α -D-idopyranosyl *ortho*-hexynylbenzoate (5d)

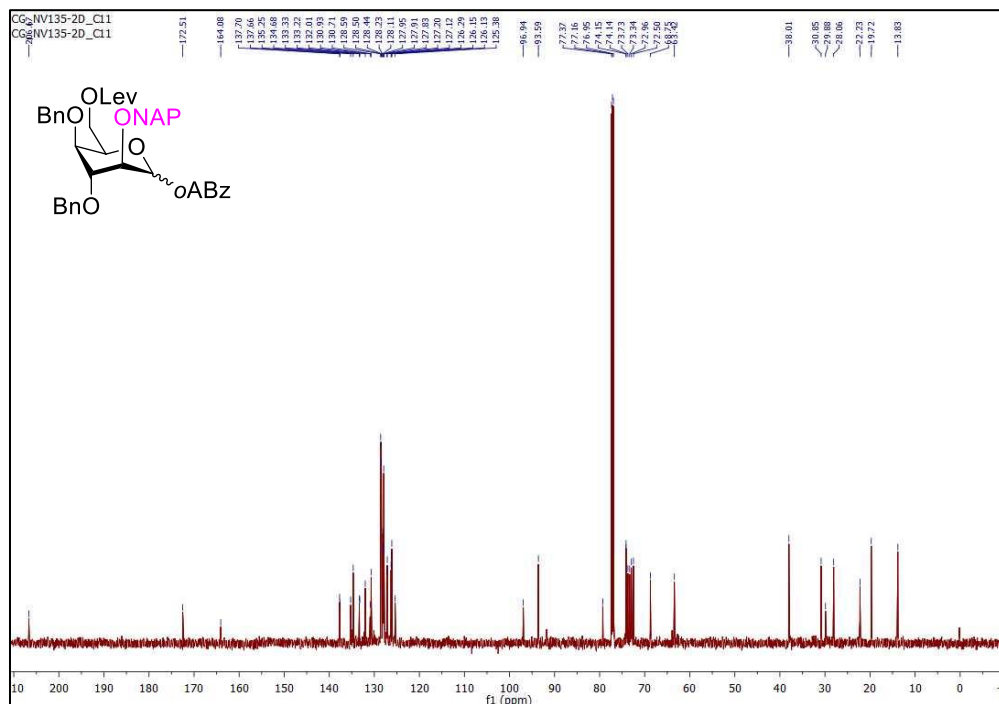


Figure S31 | ^1H NMR spectrum (CDCl_3 , 600 MHz) of *tert*-butyldimethylsilyl 2,4-di-*O*-benzyl-6-*O*-levulinoyl- β -D-idopyranosyl-(1 \rightarrow 4)-3,6-di-*O*-benzyl-2-deoxy-2-trichloroacetamido- β -D-glucopyranoside (10)

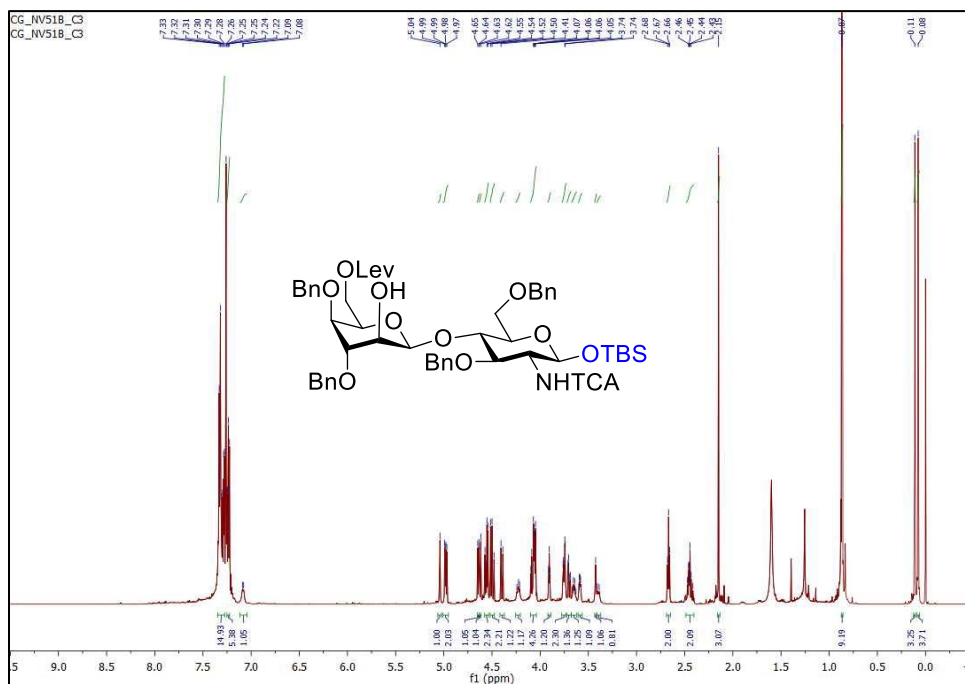


Figure S32 | $^{13}\text{C}\{^1\text{H}\}$ NMR spectrum (CDCl_3 , 150 MHz) of *tert*-butyldimethylsilyl 2,4-di-*O*-benzyl-6-*O*-levulinoyl- β -D-idopyranosyl-(1 \rightarrow 4)-3,6-di-*O*-benzyl-2-deoxy-2-trichloroacetamido- β -D-glucopyranoside (10)

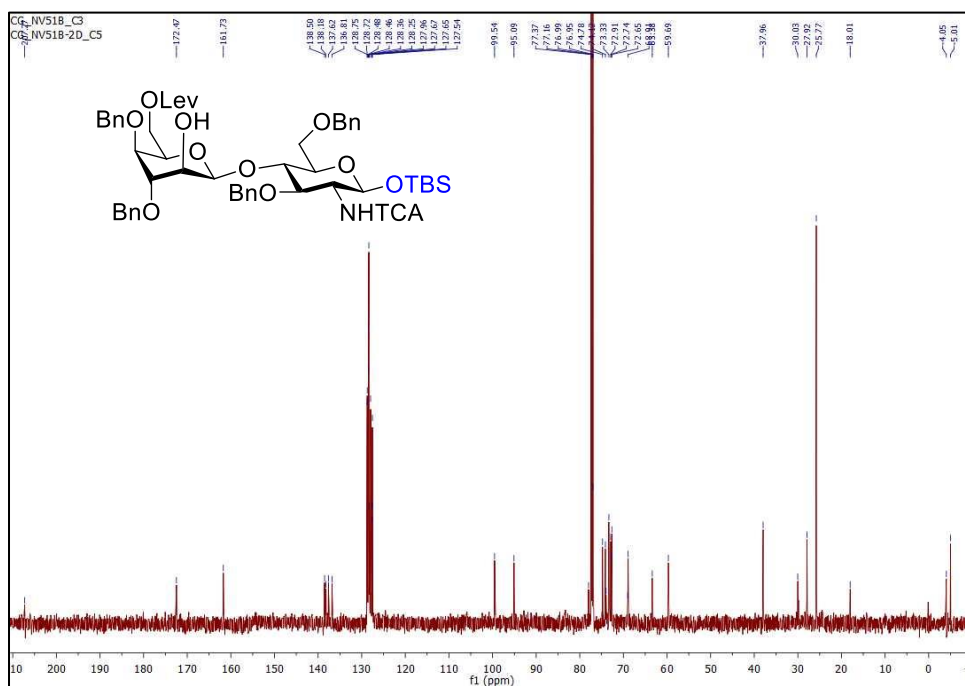


Figure S33 | ^1H NMR spectrum (CDCl_3 , 400 MHz) of *para*-methylphenyl 3,4-di-*O*-benzyl-6-deoxy-2-*O*-*para*-methoxybenzyl-1-thio- α -D-ido-heptopyranoside (12)

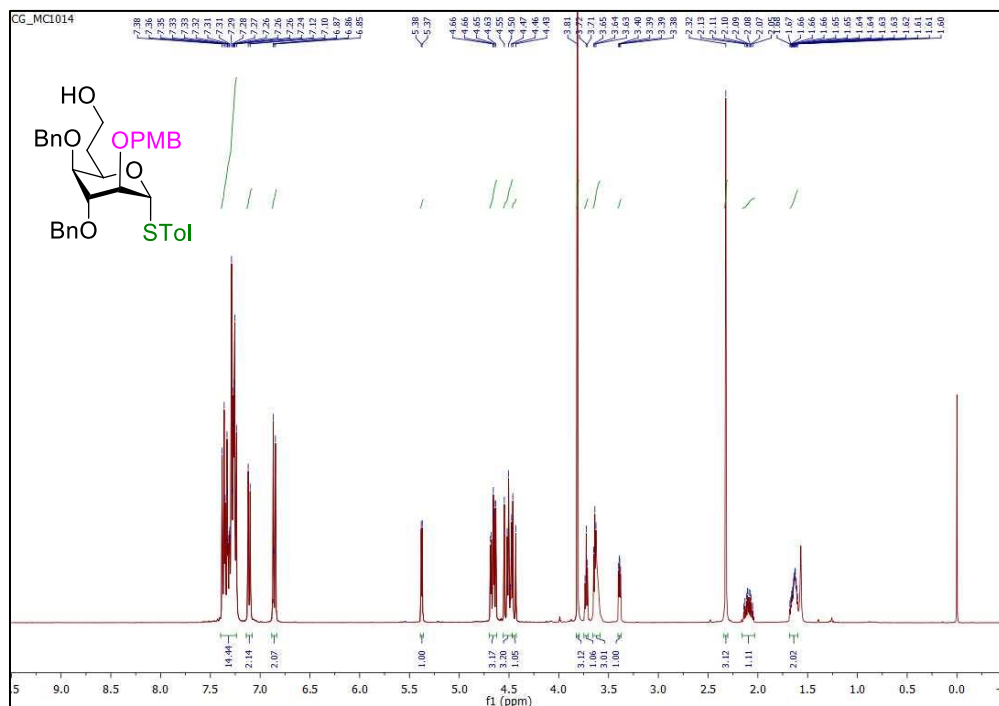


Figure S34 | $^{13}\text{C}\{^1\text{H}\}$ NMR spectrum (CDCl_3 , 100 MHz) of *para*-methylphenyl 3,4-di-*O*-benzyl-6-deoxy-2-*O*-*para*-methoxybenzyl-1-thio- α -D-ido-heptopyranoside (12)

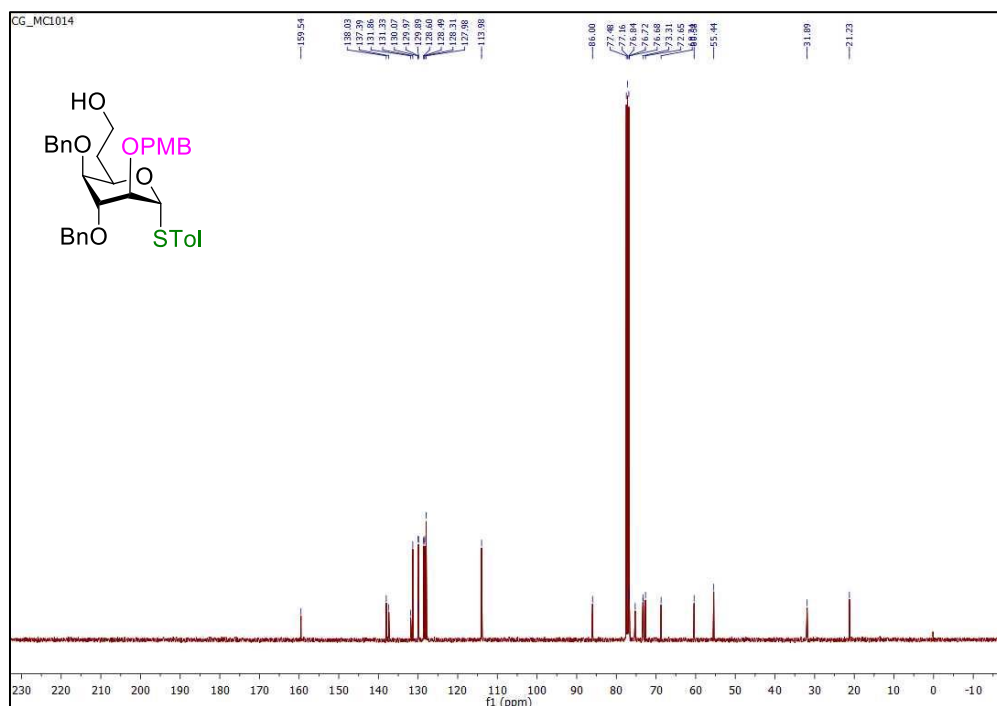


Figure S35 | ^1H NMR spectrum (CDCl_3 , 400 MHz) of *para*-methylphenyl 3,4-di-*O*-benzyl-6-deoxy-7-*O*-levulinoyl-2-*O*-*para*-methoxybenzyl-1-thio- α -D-ido-heptopyranoside (13)

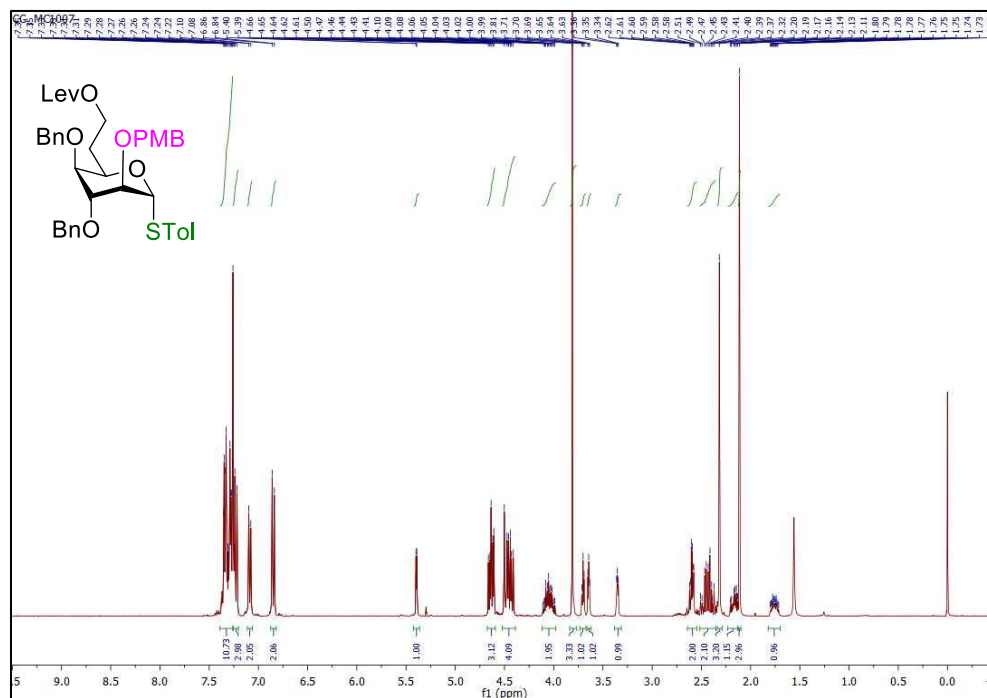


Figure S36 | $^{13}\text{C}\{^1\text{H}\}$ NMR spectrum (CDCl_3 , 100 MHz) of *para*-methylphenyl 3,4-di-*O*-benzyl-6-deoxy-7-*O*-levulinoyl-2-*O*-*para*-methoxybenzyl-1-thio- α -D-ido-heptopyranoside (13)

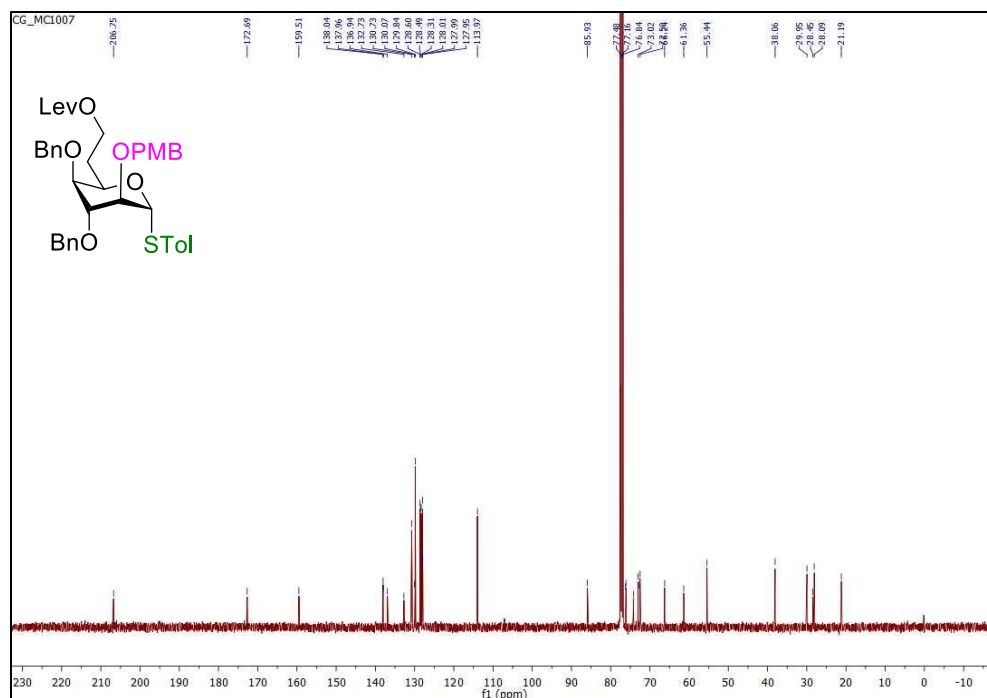


Figure S41 | ^1H NMR spectrum (CDCl_3 , 400 MHz) of 3,4-di-*O*-benzyl-2-*O*-*tert*-butyldimethylsilyl-6-*O*-levulinoyl-D-idopyranoside (15b)

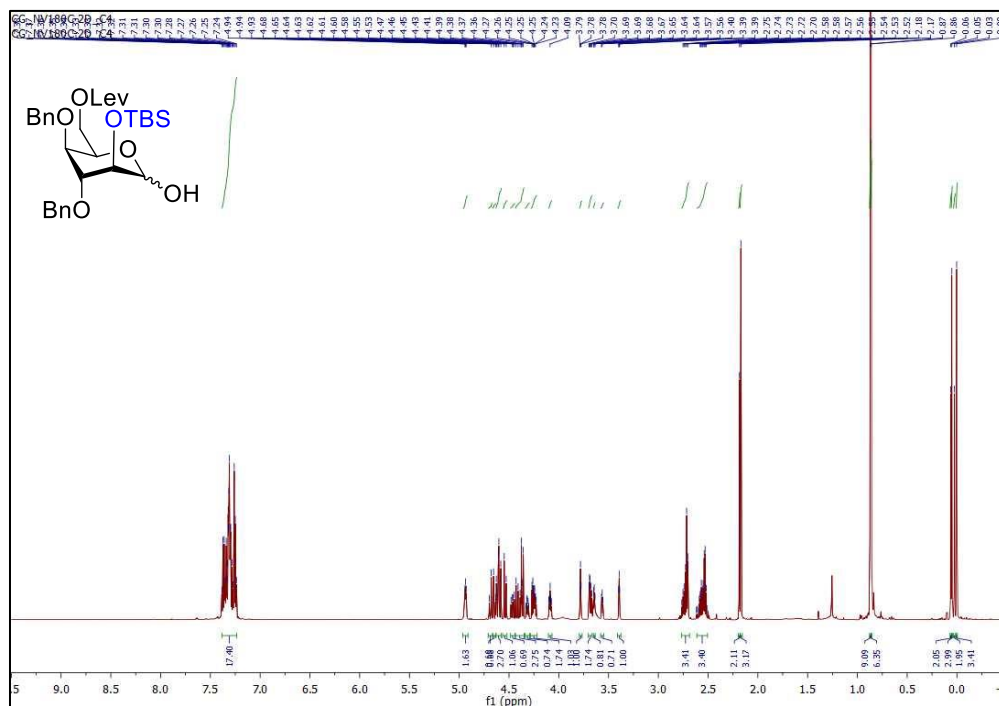


Figure S43 | ^1H NMR spectrum (CDCl_3 , 600 MHz) of 3,4-di-*O*-benzyl-2-*O*-*tert*-butyldimethylsilyl-6-*O*-levulinoyl-*D*-idopyranosyl *ortho*-hexynylbenzoate (15c)

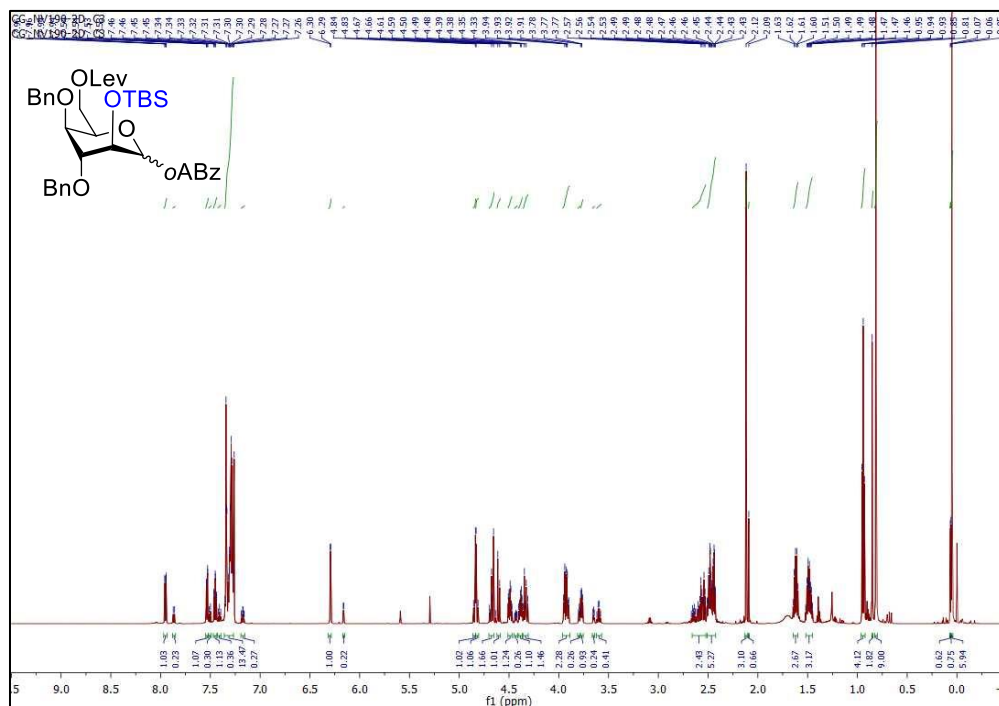


Figure S44 | $^{13}\text{C}\{^1\text{H}\}$ NMR spectrum (CDCl_3 , 150 MHz) of 3,4-di-*O*-benzyl-2-*O*-*tert*-butyldimethylsilyl-6-*O*-levulinoyl-*D*-idopyranosyl *ortho*-hexynylbenzoate (15c)

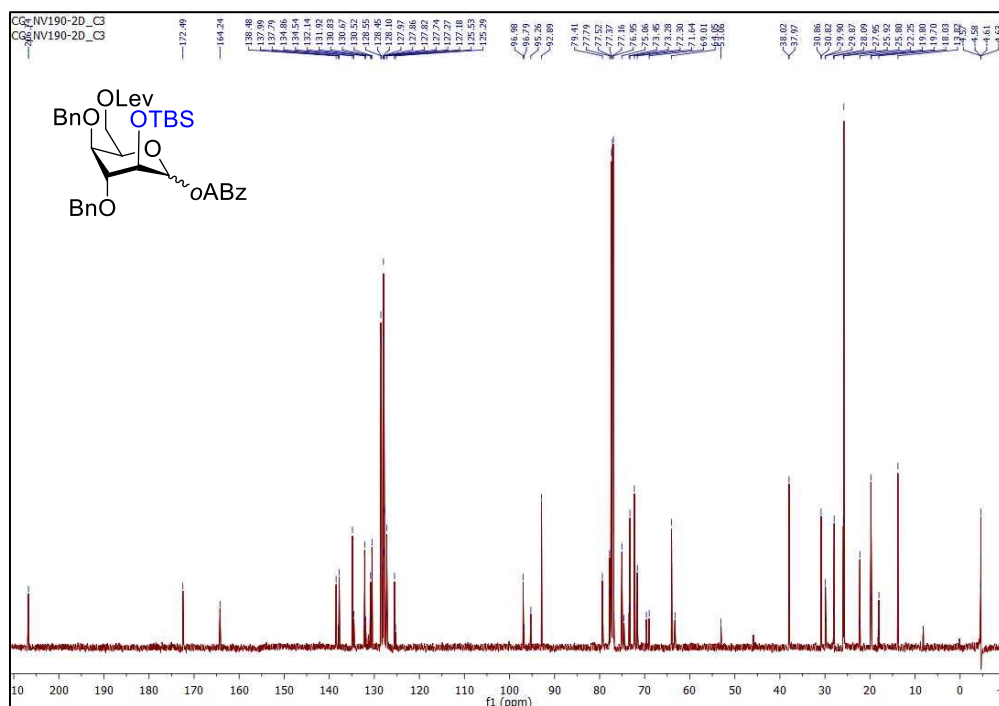


Figure S45 | ^1H NMR spectrum (CDCl_3 , 400 MHz) of *N*-phenyltrifluoroacetimidate 3,4-di-*O*-benzyl-2-*O*-*tert*-butyldimethylsilyl-6-*O*-levulinoyl-*D*-idopyranoside (15d)

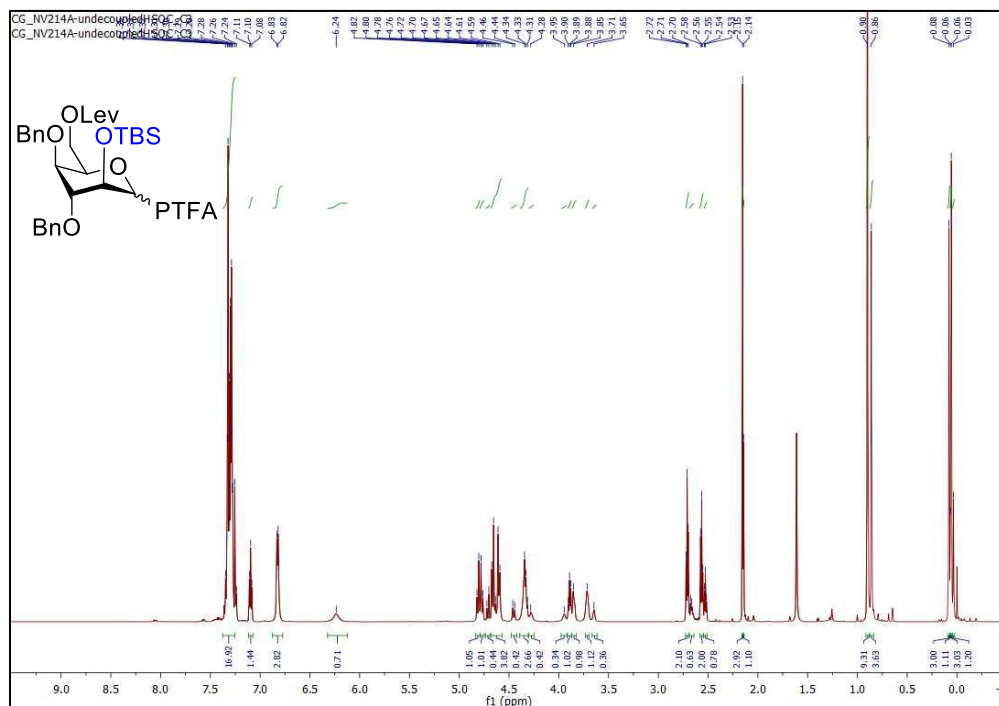


Figure S46 | $^{13}\text{C}\{^1\text{H}\}$ NMR spectrum (CDCl_3 , 100 MHz) of *N*-phenyltrifluoroacetimidate 3,4-di-*O*-benzyl-2-*O*-*tert*-butyldimethylsilyl-6-*O*-levulinoyl-*D*-idopyranoside (15d)

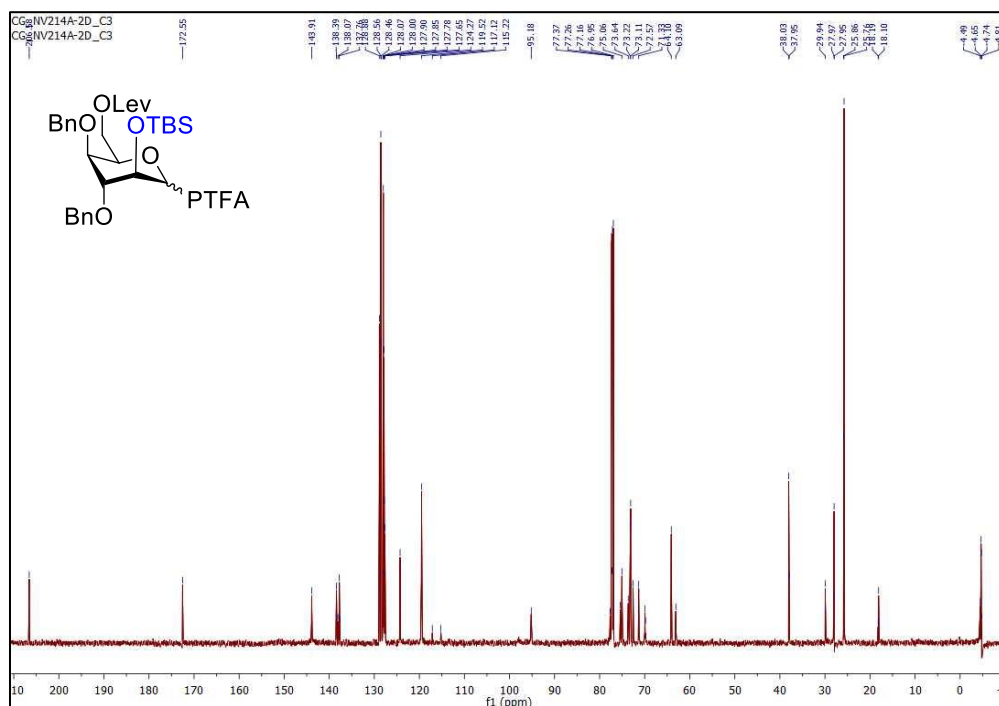


Figure S47 | ^1H NMR spectrum (CDCl_3 , 600 MHz) of *tert*-butyldimethylsilyl 3,4-di-*O*-benzyl-2-*O*-*tert*-butyldimethylsilyl-6-*O*-levulinoyl-D-idopyranosyl-(1 \rightarrow 4)-3,6-di-*O*-benzyl-2-deoxy-2-trichloroacetamido- β -D-glucopyranoside (20)

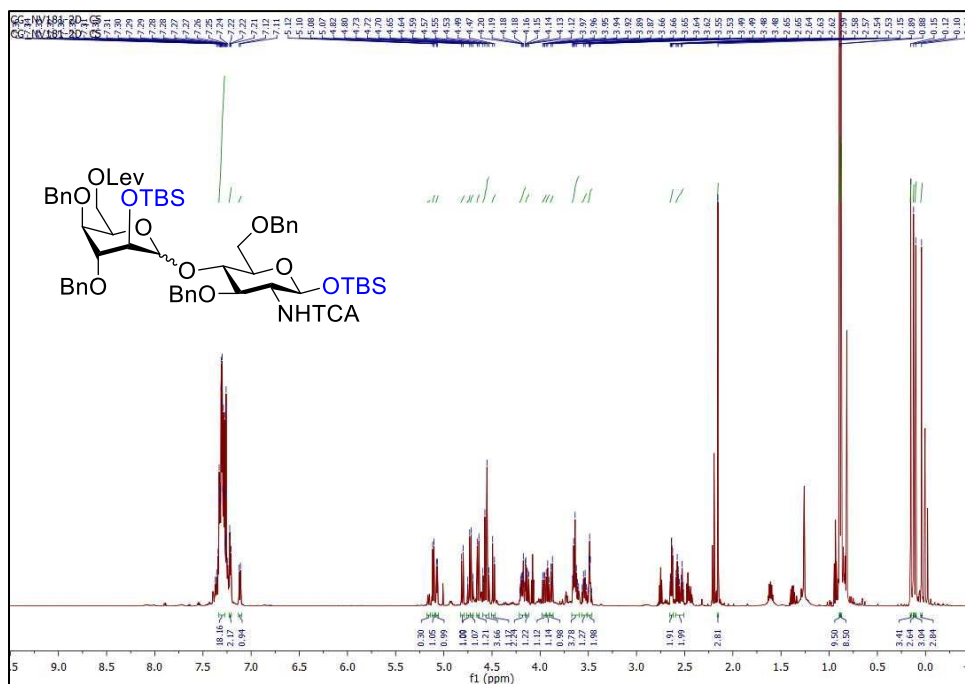


Figure S48 | $^{13}\text{C}\{^1\text{H}\}$ NMR spectrum (CDCl_3 , 150 MHz) of *tert*-butyldimethylsilyl 3,4-di-*O*-benzyl-2-*O*-*tert*-butyldimethylsilyl-6-*O*-levulinoyl-D-idopyranosyl-(1 \rightarrow 4)-3,6-di-*O*-benzyl-2-deoxy-2-trichloroacetamido- β -D-glucopyranoside (20)

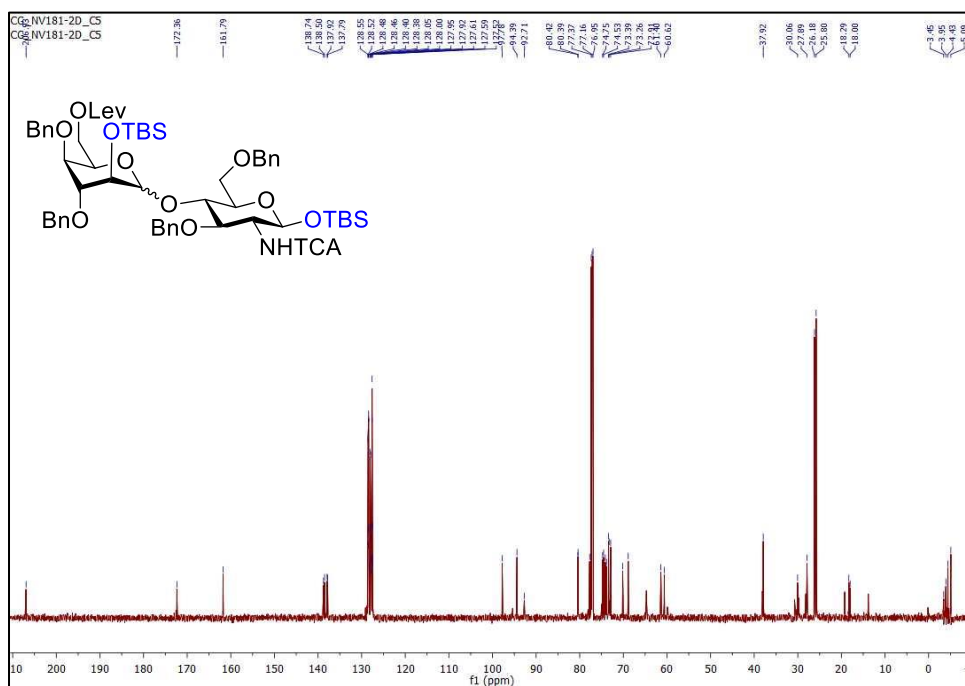


Figure S49 | ^1H NMR spectrum (CDCl_3 , 400 MHz) of ethyl 2-*O*-benzyl-4,6-*O*-benzylidene-3-*O*-*tert*-butyldimethylsilyl-1-thio- α -D-idopyranoside (17)

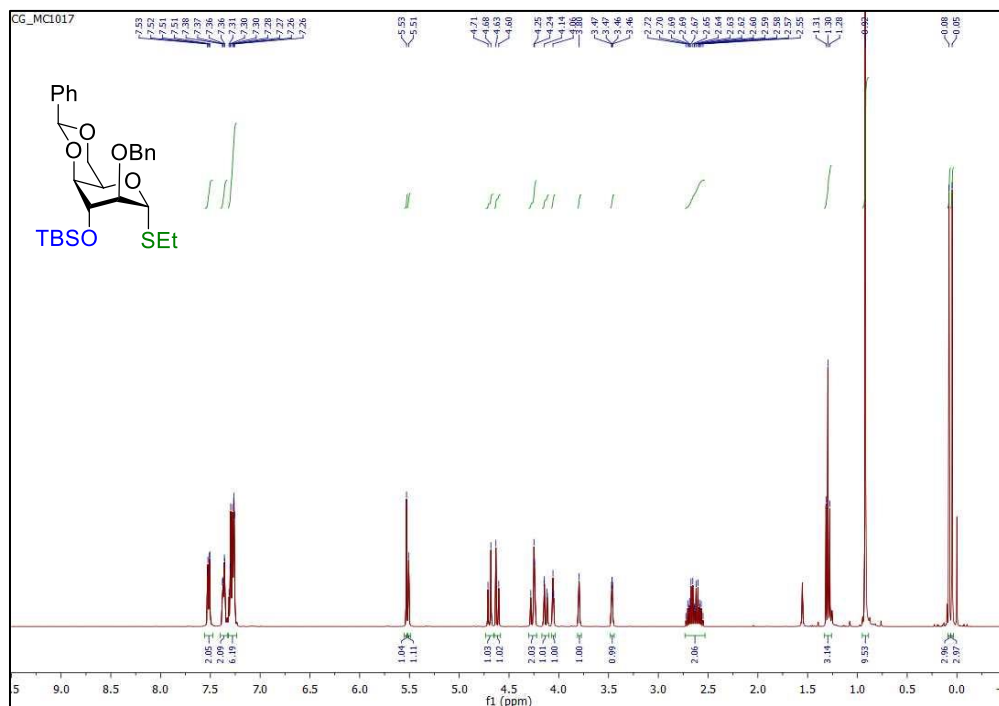


Figure S50 | $^{13}\text{C}\{^1\text{H}\}$ NMR spectrum (CDCl_3 , 100 MHz) of ethyl 2-*O*-benzyl-4,6-*O*-benzylidene-3-*O*-*tert*-butyldimethylsilyl-1-thio- α -D-idopyranoside (17)

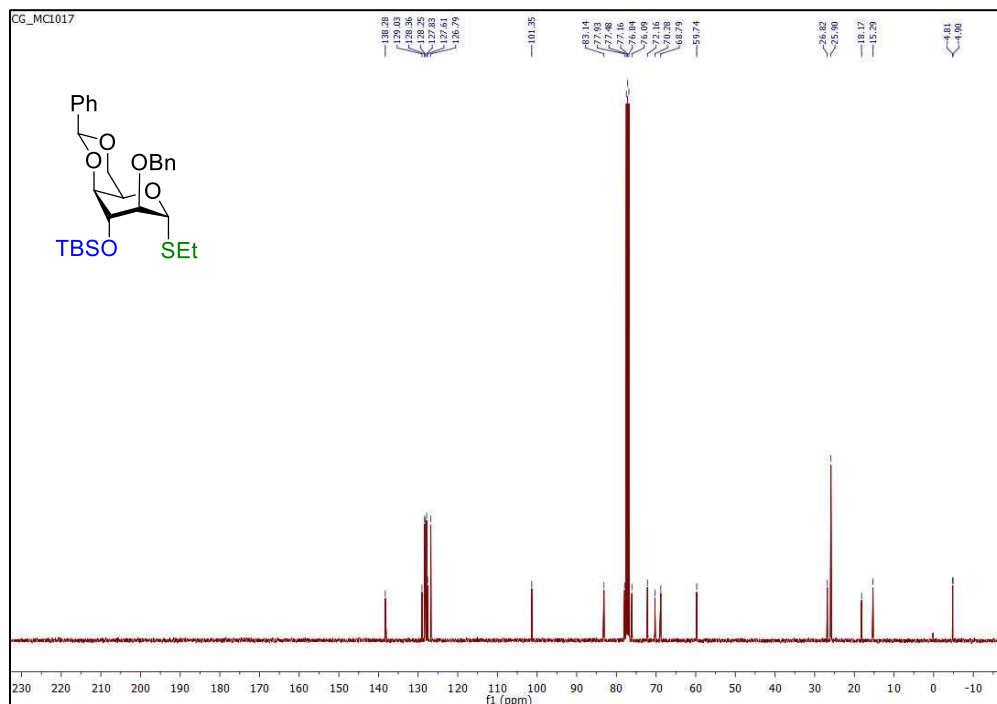


Figure S51 | ^1H NMR spectrum (CDCl_3 , 400 MHz) of ethyl 2,4-di-*O*-benzyl-3-*O*-*tert*-butyldimethylsilyl-6-*O*-levulinoyl-1-thio- α -D-idopyranoside (18)

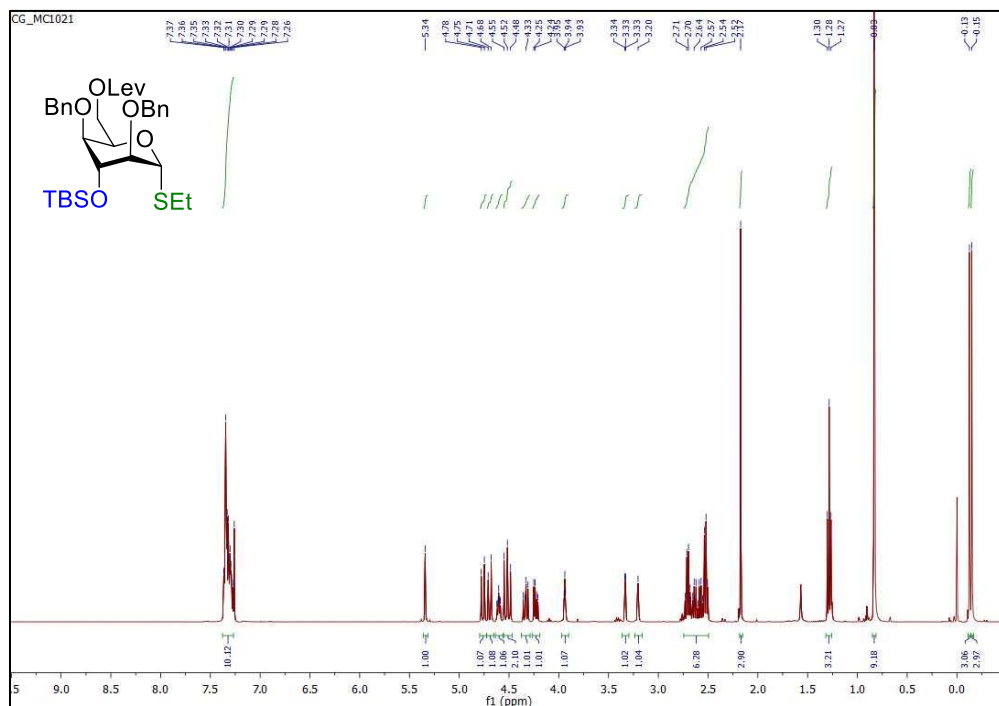


Figure S52 | $^{13}\text{C}\{^1\text{H}\}$ NMR spectrum (CDCl_3 , 100 MHz) of ethyl 2,4-di-*O*-benzyl-3-*O*-*tert*-butyldimethylsilyl-6-*O*-levulinoyl-1-thio- α -D-idopyranoside (18)

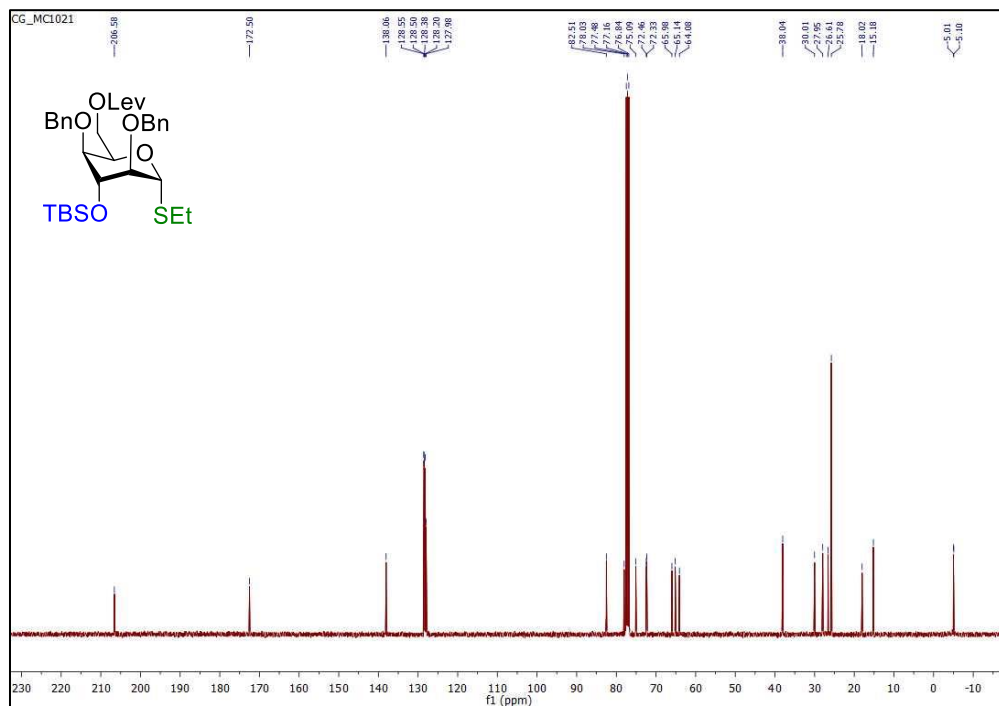


Figure S55 | ^1H NMR spectrum (CDCl_3 , 400 MHz) of *para*-methylphenyl 3,4-di-*O*-benzyl-6-deoxy-2,7-di-*O*-*para*-methoxybenzyl-1-thio- α -D-*ido*-heptopyranoside (22)

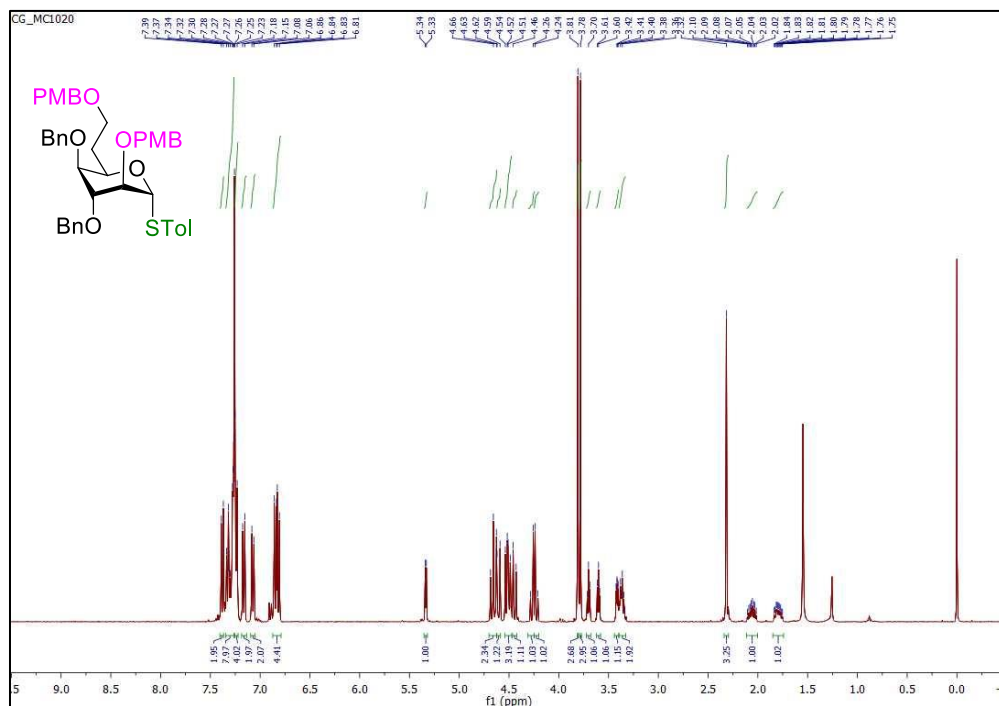


Figure S56 | $^{13}\text{C}\{^1\text{H}\}$ NMR spectrum (CDCl_3 , 100 MHz) of *para*-methylphenyl 3,4-di-*O*-benzyl-6-deoxy-2,7-di-*O*-*para*-methoxybenzyl-1-thio- α -D-*ido*-heptopyranoside (22)

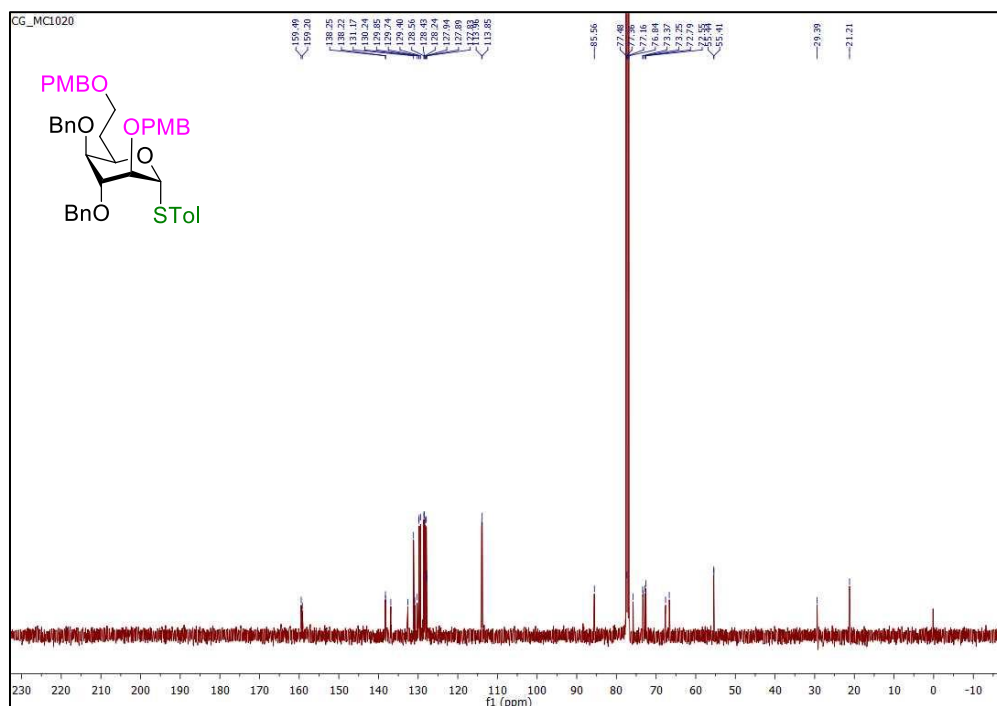


Figure S57 | ^1H NMR spectrum (CDCl_3 , 400 MHz) of *para*-methylphenyl 7-*O*-acetyl-3,4-di-*O*-benzyl-6-deoxy-2-*O*-*para*-methoxybenzyl-1-thio- α -D-ido-heptopyranoside (23)

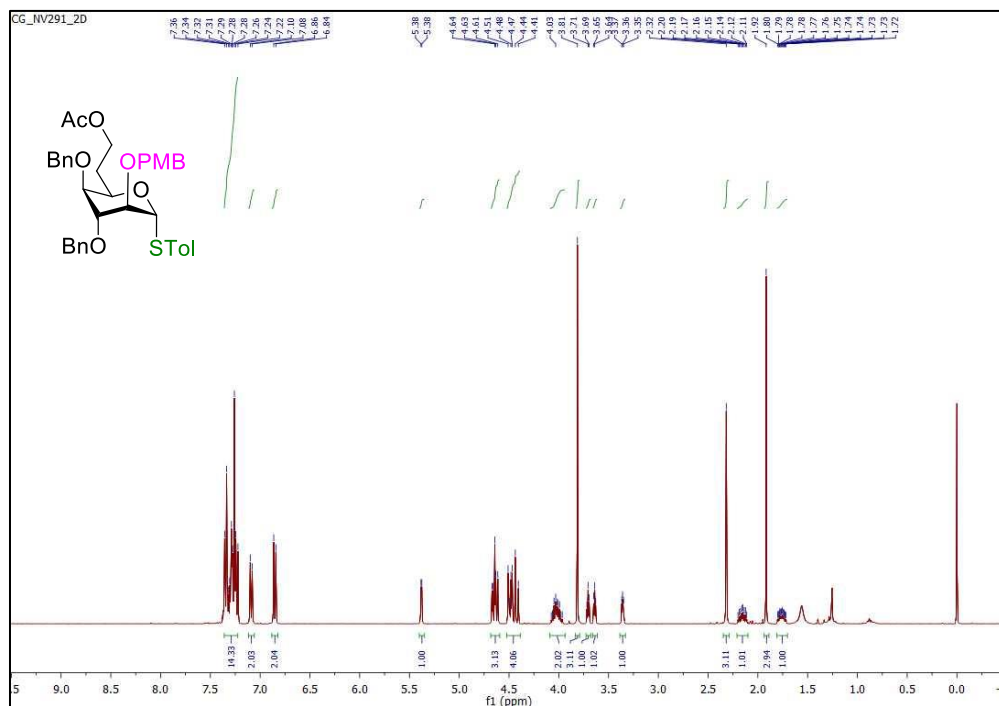


Figure S58 | $^{13}\text{C}\{^1\text{H}\}$ NMR spectrum (CDCl_3 , 100 MHz) of *para*-methylphenyl 7-*O*-acetyl-3,4-di-*O*-benzyl-6-deoxy-2-*O*-*para*-methoxybenzyl-1-thio- α -D-ido-heptopyranoside (23)

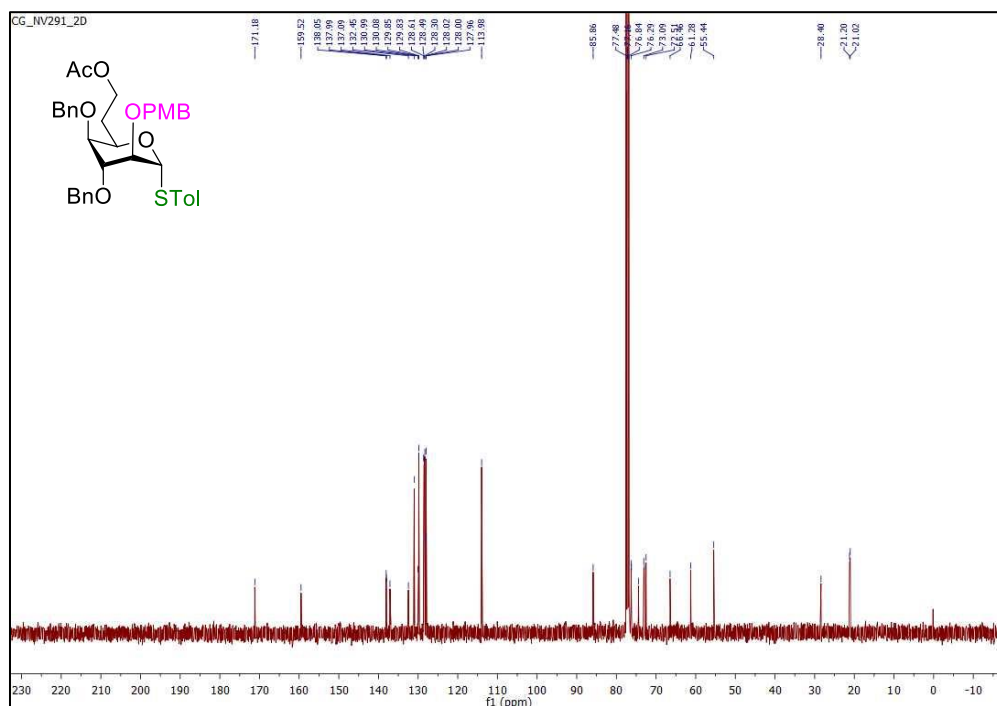


Figure S61 | ^1H NMR spectrum (CDCl_3 , 400 MHz) of *tert*-butyldimethylsilyl 7-*O*-acetyl-3,4-di-*O*-benzyl-6-deoxy-2-*O*-*para*-methoxybenzyl- α -D-ido-heptopyranosyl-(1 \rightarrow 4)-3,6-di-*O*-benzyl-2-deoxy-2-trichloroacetamido- β -D-glucopyranoside (26α)

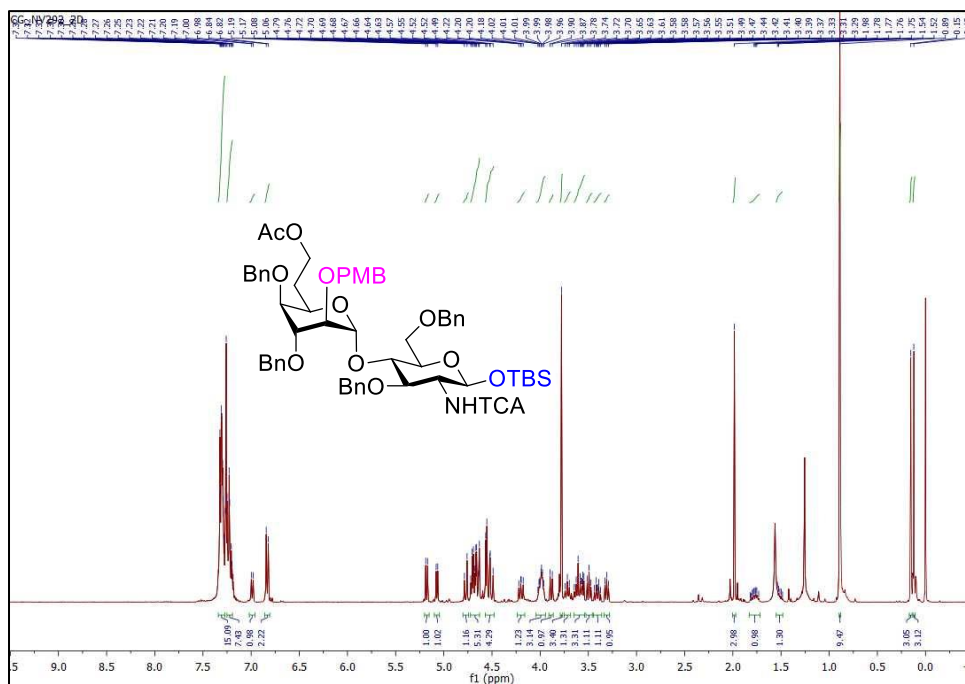


Figure S62 | $^{13}\text{C}\{^1\text{H}\}$ NMR spectrum (CDCl_3 , 100 MHz) of *tert*-butyldimethylsilyl 7-*O*-acetyl-3,4-di-*O*-benzyl-6-deoxy-2-*O*-*para*-methoxybenzyl- α -D-ido-heptopyranosyl-(1 \rightarrow 4)-3,6-di-*O*-benzyl-2-deoxy-2-trichloroacetamido- β -D-glucopyranoside (26α)

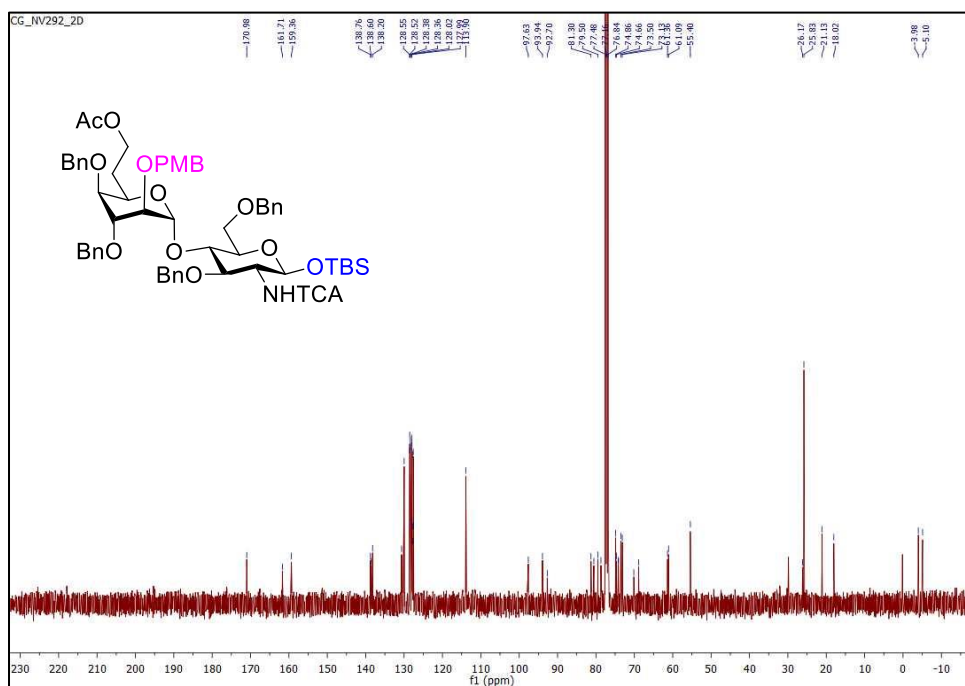


Figure S63 | ^1H NMR spectrum (CDCl_3 , 400 MHz) of *tert*-butyldimethylsilyl 7-*O*-acetyl-3,4-di-*O*-benzyl-6-deoxy-2-*O*-*para*-methoxybenzyl- β -D-ido-heptopyranosyl-(1 \rightarrow 4)-3,6-di-*O*-benzyl-2-deoxy-2-trichloroacetamido- β -D-glucopyranoside (26β)

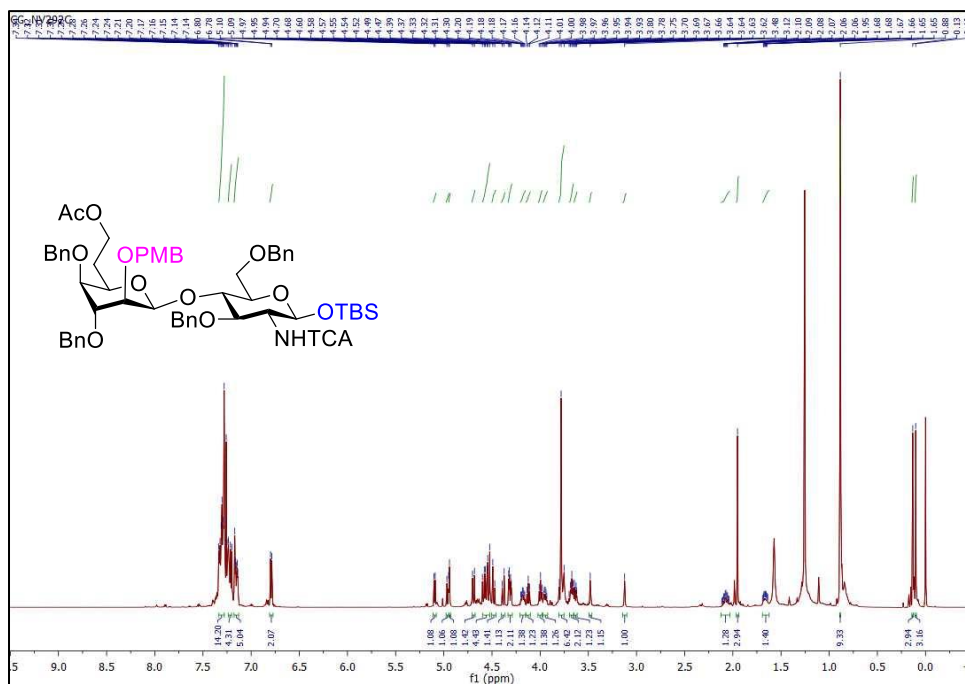
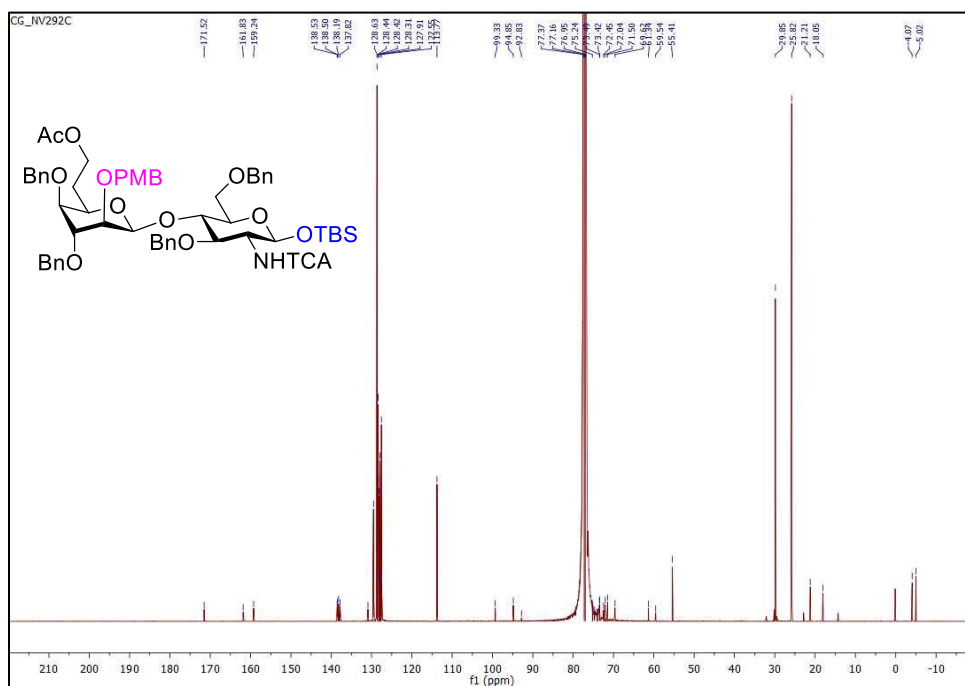


Figure S64 | $^{13}\text{C}\{^1\text{H}\}$ NMR spectrum (CDCl_3 , 100 MHz) of *tert*-butyldimethylsilyl 7-*O*-acetyl-3,4-di-*O*-benzyl-6-deoxy-2-*O*-*para*-methoxybenzyl- β -D-ido-heptopyranosyl-(1 \rightarrow 4)-3,6-di-*O*-benzyl-2-deoxy-2-trichloroacetamido- β -D-glucopyranoside (26β)



Bibliographie

1. Liu, F.-T.; Patterson, R. J.; Wang, J. L., Intracellular functions of galectins. *Biochim. Biophys. Acta Gen. Subj.* **2002**, *1572*, 263-273.
2. Fernández-Tejada, A.; Cañada, F. J.; Jiménez-Barbero, J., Recent developments in synthetic carbohydrate-based diagnostics, vaccines, and therapeutics. *Chem. Eur. J.* **2015**, *21*, 10616-10628.
3. Imberty, A.; Varrot, A., Microbial recognition of human cell surface glycoconjugates. *Curr. Opin. Struct. Biol.* **2008**, *18*, 567-576.
4. Hakomori, S.I., Aberrant glycosylation in tumors and tumor-associated carbohydrate antigens. *Adv. Cancer Res.* **1989**, *52*, 257-331.
5. Kappler, K.; Hennet, T., Emergence and significance of carbohydrate-specific antibodies. *Genes Imm.* **2020**, *21*, 224-239.
6. Jiang, H.; Qin, X.; Wang, Q.; Xu, Q.; Wang, J.; Wu, Y.; Chen, W.; Wang, C.; Zhang, T.; Xing, D., Application of carbohydrates in approved small molecule drugs: A review. *Eur. J. Med. Chem.* **2021**, *223*, 113633.
7. Schatz, A.; Waksman, S. A., Effect of streptomycin and other antibiotic substances upon *Mycobacterium tuberculosis* and related organisms. *Proc. Soc. Exp. Biol. Med.* **1944**, *57*, 244-248.
8. Varma, R.; Kaushal, R.; Junnarkar, A.; Thomas, G.; Naidu, M.; Singh, P.; Tripathi, R.; Shridhar, D., Polysorbate 80: a pharmacological study. *Arzneimittel forschung* **1985**, *35*, 804-808.
9. van der Meer, J.-Y.; Kellenbach, E.; Van den Bos, L. J., From farm to pharma: an overview of industrial heparin manufacturing methods. *Molecules* **2017**, *22*, 1025.
10. Johnson, D. J.; Li, W.; Adams, T. E.; Huntington, J. A., Antithrombin–S195A factor Xa-heparin structure reveals the allosteric mechanism of antithrombin activation. *EMBO J.* **2006**, *25*, 2029-2037.
11. Eriksson, B. I.; Bauer, K. A.; Lassen, M. R.; Turpie, A. G., Fondaparinux compared with enoxaparin for the prevention of venous thromboembolism after hip-fracture surgery. *N. Engl. J. Med.* **2001**, *345*, 1298-1304.
12. Weitz, D. S.; Weitz, J. I., Update on heparin: what do we need to know? *J. Thromb. Thrombolysis* **2010**, *29*, 199-207.
13. Blossom, D. B.; Kallen, A. J.; Patel, P. R.; Elward, A.; Robinson, L.; Gao, G.; Langer, R.; Perkins, K. M.; Jaeger, J. L.; Kurkjian, K. M., Outbreak of adverse reactions associated with contaminated heparin. *N. Engl. J. Med.* **2008**, *359*, 2674-2684.

14. Yang, L. P.; Keam, S. J., Sugammadex. *Drugs* **2009**, *69*, 919-942.
15. Nag, K.; Singh, D. R.; Shetti, A. N.; Kumar, H.; Sivashanmugam, T.; Parthasarathy, S., Sugammadex: A revolutionary drug in neuromuscular pharmacology. *Anesth. Essays Res.* **2013**, *7*, 302.
16. Hawkins, J.; Khanna, S.; Argaliou, M., Sugammadex for reversal of neuromuscular blockade: uses and limitations. *Curr. Pharm. Des.* **2019**, *25*, 2140-2148.
17. de Boer, H. D.; van Esmond, J.; Booij, L. H.; Driessen, J. J., Reversal of rocuronium-induced profound neuromuscular block by sugammadex in Duchenne muscular dystrophy. *Pediatr. Anesth.* **2009**, *19*, 1226-1228.
18. Shields, M.; Giovannelli, M.; Mirakhur, R.; Moppett, I.; Adams, J.; Hermens, Y., Org 25969 (sugammadex), a selective relaxant binding agent for antagonism of prolonged rocuronium-induced neuromuscular block. *Br. J. Anaesth.* **2006**, *96*, 36-43.
19. Buie, L. W.; Epstein, S. S.; Lindley, C. M., Nelarabine: a novel purine antimetabolite antineoplastic agent. *Clin. Ther.* **2007**, *29*, 1887-1899.
20. Gordon, C. J.; Tchesnokov, E. P.; Woolner, E.; Perry, J. K.; Feng, J. Y.; Porter, D. P.; Götte, M., Remdesivir is a direct-acting antiviral that inhibits RNA-dependent RNA polymerase from severe acute respiratory syndrome coronavirus 2 with high potency. *J. Biol. Chem.* **2020**, *295*, 6785-6797.
21. Eastman, R. T.; Roth, J. S.; Brimacombe, K. R.; Simeonov, A.; Shen, M.; Patnaik, S.; Hall, M. D., Remdesivir: a review of its discovery and development leading to emergency use authorization for treatment of COVID-19. *ACS Cent. Sci.* **2020**, *6*, 672-683.
22. Undheim, K., Scaffold modifications in erythromycin macrolide antibiotics: A chemical minireview. *Molecules* **2020**, *25*, 3941.
23. Qin, Y.; Ma, S., Recent advances in the development of macrolide antibiotics as antimicrobial agents. *Mini Rev. Med. Chem.* **2020**, *20*, 601-625.
24. Chen, C.; Lu, L.; Yan, S.; Yi, H.; Yao, H.; Wu, D.; He, G.; Tao, X.; Deng, X., Autophagy and doxorubicin resistance in cancer. *Anticancer Drugs* **2018**, *29*, 1-9.
25. Binaschi, M.; Bigioni, M.; Cipollone, A.; Rossi, C.; Goso, C.; Maggi, C.; Capranico, G.; Animati, F., Anthracyclines: selected new developments. *Curr. Med. Chem. Anticancer Agents* **2001**, *1*, 113-130.
26. Cheng, J.; Tennilä, J.; Stenman, L.; Ibarra, A.; Kumar, M.; Gupta, K. K.; Sharma, S. S.; Sen, D.; Garg, S.; Penurkar, M., Influence of lactitol and psyllium on bowel function in constipated Indian volunteers: a randomized, controlled trial. *Nutrients* **2019**, *11*, 1130.
27. Galan, M. C.; Benito-Alifonso, D.; Watt, G. M., Carbohydrate chemistry in drug discovery. *Org. Biomol. Chem.* **2011**, *9*, 3598-3610.

28. Weintraub, A., Immunology of bacterial polysaccharide antigens. *Carbohydr. Res.* **2003**, *338*, 2539-2547.
29. Astronomo, R. D.; Burton, D. R., Carbohydrate vaccines: developing sweet solutions to sticky situations? *Nat. Rev. Drug Discov.* **2010**, *9*, 308-324.
30. Poolman, J.; Borrow, R., Hyporesponsiveness and its clinical implications after vaccination with polysaccharide or glycoconjugate vaccines. *Expert Rev. Vaccines* **2011**, *10*, 307-322.
31. Rijkers, G.; Sanders, E.; Breukels, M.; Zegers, B., Infant B cell responses to polysaccharide determinants. *Vaccine* **1998**, *16*, 1396-1400.
32. Mitchison, N., The carrier effect in the secondary response to hapten-protein conjugates. II. Cellular cooperation. *Eur. J. Immunol.* **1971**, *1*, 18-27.
33. Avci, F. Y.; Li, X.; Tsuji, M.; Kasper, D. L., A mechanism for glycoconjugate vaccine activation of the adaptive immune system and its implications for vaccine design. *Nat. Med.* **2011**, *17*, 1602-1609.
34. Anish, C.; Beurret, M.; Poolman, J., Combined effects of glycan chain length and linkage type on the immunogenicity of glycoconjugate vaccines. *NPJ Vaccines* **2021**, *6*, 1-13.
35. Micoli, F.; Adamo, R.; Costantino, P., Protein carriers for glycoconjugate vaccines: history, selection criteria, characterization and new trends. *Molecules* **2018**, *23*, 1451.
36. Pichichero, M. E., Protein carriers of conjugate vaccines: characteristics, development, and clinical trials. *Hum. Vaccines Immunother.* **2013**, *9*, 2505-2523.
37. Zhu, H.; Rollier, C. S.; Pollard, A. J., Recent advances in lipopolysaccharide-based glycoconjugate vaccines. *Expert Rev. Vaccines* **2021**, *20*, 1515-1538.
38. Avery, O. T.; Goebel, W. F., Chemo-immunological studies on conjugated carbohydrate-proteins: II. Immunological specificity of synthetic sugar-protein antigens. *J. Exp. Med.* **1929**, *50*, 533.
39. Grabenstein, J.; Klugman, K., A century of pneumococcal vaccination research in humans. *Clin. Microbiol. Infect.* **2012**, *18*, 15-24.
40. Knuf, M.; Kowalzik, F.; Kieninger, D., Comparative effects of carrier proteins on vaccine-induced immune response. *Vaccine* **2011**, *29*, 4881-4890.
41. Lesinski, G. B.; Westerink, J., Vaccines against polysaccharide antigens. *Curr. Drug Targets Infect. Disord.* **2001**, *1*, 325-334.
42. Zasłona, M. E.; Downey, A. M.; Seeberger, P. H.; Moscovitz, O., Semi- and fully synthetic carbohydrate vaccines against pathogenic bacteria: recent developments. *Biochem. Soc. Trans.* **2021**, *49*, 2411-2429.
43. Pozsgay, V., Recent developments in synthetic oligosaccharide-based bacterial vaccines. *Curr. Top. Med. Chem.* **2008**, *8*, 126-140.

44. Cloutier, M.; Gauthier, C., Progress toward the development of glycan-based vaccines against campylobacteriosis. *ACS Infect. Dis.* **2020**, *7*, 969-986.
45. Cloutier, M.; Muru, K.; Gauthier, C., Synthesis of oligosaccharides related to potential bioterrorist pathogens. In *Recent Trends in Carbohydrate Chemistry*, Elsevier: 2020; pp 143-206.
46. Verez-Bencomo, V.; Fernandez-Santana, V.; Hardy, E.; Toledo, M. E.; Rodríguez, M. C.; Heynngnezz, L.; Rodriguez, A.; Baly, A.; Herrera, L.; Izquierdo, M., A synthetic conjugate polysaccharide vaccine against *Haemophilus influenzae* type b. *Science* **2004**, *305*, 522-525.
47. van der Put, R. M.; Smitsman, C.; de Haan, A.; Hamzink, M.; Timmermans, H.; Uittenbogaard, J.; Westdijk, J.; Stork, M.; Ophorst, O.; Thouron, F. O., The first-in-human synthetic glycan-based conjugate vaccine candidate against *Shigella*. *ACS Cent. Sci.* **2022**, *8*, 449-460.
48. Bélot, F.; Wright, K.; Costachel, C.; Phalipon, A.; Mulard, L. A., Blockwise Approach to fragments of the O-specific polysaccharide of *Shigella flexneri* serotype 2a: convergent synthesis of a decasaccharide representative of a dimer of the branched repeating unit. *J. Org. Chem.* **2004**, *69*, 1060-1074.
49. Phalipon, A.; Costachel, C.; Grandjean, C.; Thuizat, A.; Guerreiro, C.; Tanguy, M.; Nato, F.; Normand, V.-L.; Bélot, F.; Wright, K., Characterization of functional oligosaccharide mimics of the *Shigella flexneri* serotype 2a O-antigen: implications for the development of a chemically defined glycoconjugate vaccine. *J. Immunol.* **2006**, *176*, 1686-1694.
50. Cohen, D.; Atsmon, J.; Artaud, C.; Meron-Sudai, S.; Gougeon, M.-L.; Bialik, A.; Goren, S.; Asato, V.; Ariel-Cohen, O.; Reizis, A., Safety and immunogenicity of a synthetic carbohydrate conjugate vaccine against *Shigella flexneri* 2a in healthy adult volunteers: a phase 1, dose-escalating, single-blind, randomised, placebo-controlled study. *Lancet Infect. Dis.* **2021**, *21*, 546-558.
51. Costantino, P.; Rappuoli, R.; Berti, F., The design of semi-synthetic and synthetic glycoconjugate vaccines. *Expert Opin. Drug Discov.* **2011**, *6*, 1045-1066.
52. Trkola, A.; Purtscher, M.; Muster, T.; Ballaun, C.; Buchacher, A.; Sullivan, N.; Srinivasan, K.; Sodroski, J.; Moore, J. P.; Katinger, H., Human monoclonal antibody 2G12 defines a distinctive neutralization epitope on the gp120 glycoprotein of human immunodeficiency virus type 1. *J. Virol.* **1996**, *70*, 1100-1108.
53. Saphire, E. O.; Stanfield, R. L.; Crispin, M.; Morris, G.; Zwick, M. B.; Pantophlet, R. A.; Parren, P. W.; Rudd, P. M.; Dwek, R. A.; Burton, D. R., Crystal structure of an intact human IgG: antibody asymmetry, flexibility, and a guide for HIV-1 vaccine design. *Glycobiol. Med.* **2003**, 55-66.
54. Haynes, B. F.; Fleming, J.; St. Clair, E. W.; Katinger, H.; Stiegler, G.; Kunert, R.; Robinson, J.; Scarce, R. M.; Plonk, K.; Staats, H. F., Cardiophilic polyspecific autoreactivity in two broadly neutralizing HIV-1 antibodies. *Science* **2005**, *308*, 1906-1908.

55. Cardoso, R. M.; Zwick, M. B.; Stanfield, R. L.; Kunert, R.; Binley, J. M.; Katinger, H.; Burton, D. R.; Wilson, I. A., Broadly neutralizing anti-HIV antibody 4E10 recognizes a helical conformation of a highly conserved fusion-associated motif in gp41. *Immunity* **2005**, *22*, 163-173.
56. Zwick, M. B.; Komori, H. K.; Stanfield, R. L.; Church, S.; Wang, M.; Parren, P. W.; Kunert, R.; Katinger, H.; Wilson, I. A.; Burton, D. R., The long third complementarity-determining region of the heavy chain is important in the activity of the broadly neutralizing anti-human immunodeficiency virus type 1 antibody 2F5. *J. Virol.* **2004**, *78*, 3155-3161.
57. Scanlan, C. N.; Pantophlet, R.; Wormald, M. R.; Ollmann Saphire, E.; Stanfield, R.; Wilson, I. A.; Katinger, H.; Dwek, R. A.; Rudd, P. M.; Burton, D. R., The broadly neutralizing anti-human immunodeficiency virus type 1 antibody 2G12 recognizes a cluster of $\alpha 1 \rightarrow 2$ mannose residues on the outer face of gp120. *J. Virol.* **2002**, *76*, 7306-7321.
58. Hessel, A. J.; Rakasz, E. G.; Poignard, P.; Hangartner, L.; Landucci, G.; Forthal, D. N.; Koff, W. C.; Watkins, D. I.; Burton, D. R., Broadly neutralizing human anti-HIV antibody 2G12 is effective in protection against mucosal SHIV challenge even at low serum neutralizing titers. *PLoS Pathog.* **2009**, *5*, e1000433.
59. Doores, K. J.; Fulton, Z.; Hong, V.; Patel, M. K.; Scanlan, C. N.; Wormald, M. R.; Finn, M.; Burton, D. R.; Wilson, I. A.; Davis, B. G., A nonself sugar mimic of the HIV glycan shield shows enhanced antigenicity. *Proc. Natl. Acad. Sci. USA.* **2010**, *107*, 17107-17112.
60. Mascola, J. R.; Stiegler, G.; VanCott, T. C.; Katinger, H.; Carpenter, C. B.; Hanson, C. E.; Beary, H.; Hayes, D.; Frankel, S. S.; Birx, D. L., Protection of macaques against vaginal transmission of a pathogenic HIV-1/SIV chimeric virus by passive infusion of neutralizing antibodies. *Nat. Med.* **2000**, *6*, 207-210.
61. Calarese, D. A.; Lee, H.-K.; Huang, C.-Y.; Best, M. D.; Astronomo, R. D.; Stanfield, R. L.; Katinger, H.; Burton, D. R.; Wong, C.-H.; Wilson, I. A., Dissection of the carbohydrate specificity of the broadly neutralizing anti-HIV-1 antibody 2G12. *Proc. Natl. Acad. Sci. USA.* **2005**, *102*, 13372-13377.
62. Binley, J. M.; Wrin, T.; Korber, B.; Zwick, M. B.; Wang, M.; Chappay, C.; Stiegler, G.; Kunert, R.; Zolla-Pazner, S.; Katinger, H., Comprehensive cross-clade neutralization analysis of a panel of anti-human immunodeficiency virus type 1 monoclonal antibodies. *J. Virol.* **2004**, *78*, 13232-13252.
63. Mogus, A. T.; Liu, L.; Jia, M.; Ajayi, D. T.; Xu, K.; Kong, R.; Huang, J.; Yu, J.; Kwong, P. D.; Mascola, J. R., Virus-like particle based vaccines elicit neutralizing antibodies against the HIV-1 fusion peptide. *Vaccines* **2020**, *8*, 765.
64. Hudak, J. E.; Bertozzi, C. R., Glycotherapy: new advances inspire a reemergence of glycans in medicine. *Chem. Biol.* **2014**, *21*, 16-37.
65. Ragupathi, G., Carbohydrate antigens as targets for active specific immunotherapy. *Cancer Immunol. Immunother.* **1996**, *43*, 152-157.

66. Chang, W.-W.; Lee, C. H.; Lee, P.; Lin, J.; Hsu, C.-W.; Hung, J.-T.; Lin, J.-J.; Yu, J.-C.; Shao, L.-e.; Yu, J., Expression of Globo H and SSEA3 in breast cancer stem cells and the involvement of fucosyl transferases 1 and 2 in Globo H synthesis. *Proc. Natl. Acad. Sci. USA*. **2008**, *105*, 11667-11672.
67. Slovin, S.; Ragupathi, G.; Adluri, S.; Ungers, G.; Terry, K.; Kim, S.; Spassova, M.; Bornmann, W.; Fazzari, M.; Dantis, L., Carbohydrate vaccines in cancer: immunogenicity of a fully synthetic Globo H hexasaccharide conjugate in man. *Proc. Natl. Acad. Sci. USA*. **1999**, *96*, 5710-5715.
68. Bilodeau, M. T.; Park, T. K.; Hu, S.; Randolph, J. T.; Danishefsky, S. J.; Livingston, P. O.; Zhang, S., Total synthesis of a human breast tumor associated antigen. *J. Am. Chem. Soc.* **1995**, *117*, 7840-7841.
69. Park, T. K.; Kim, I. J.; Hu, S.; Bilodeau, M. T.; Randolph, J. T.; Kwon, O.; Danishefsky, S. J., Total synthesis and proof of structure of a human breast tumor (Globo-H) antigen. *J. Am. Chem. Soc.* **1996**, *118*, 11488-11500.
70. Allen, J. R.; Allen, J. G.; Zhang, X. F.; Williams, L. J.; Zatorski, A.; Ragupathi, G.; Livingston, P. O.; Danishefsky, S. J., A second generation synthesis of the MBr1 (Globo-H) breast tumor antigen: new application of the *n*-pentenyl glycoside method for achieving complex carbohydrate protein linkages. *Chem. Eur. J.* **2000**, *6*, 1366-1375.
71. Danishefsky, S. J.; Shue, Y.-K.; Chang, M. N.; Wong, C.-H., Development of Globo-H cancer vaccine. *Acc. Chem. Res.* **2015**, *48*, 643-652.
72. Tsai, T.-I.; Lee, H.-Y.; Chang, S.-H.; Wang, C.-H.; Tu, Y.-C.; Lin, Y.-C.; Hwang, D.-R.; Wu, C.-Y.; Wong, C.-H., Effective sugar nucleotide regeneration for the large-scale enzymatic synthesis of Globo H and SSEA4. *J. Am. Chem. Soc.* **2013**, *135*, 14831-14839.
73. Ragupathi, G.; Park, T. K.; Zhang, S.; Kim, I. J.; Graber, L.; Adluri, S.; Lloyd, K. O.; Danishefsky, S. J.; Livingston, P. O., Immunization of mice with a fully synthetic Globo H antigen results in antibodies against human cancer cells: A combined chemical—immunological approach to the fashioning of an anticancer vaccine. *Angew. Chem. Int. Ed. Engl.* **1997**, *36*, 125-128.
74. Gilewski, T.; Ragupathi, G.; Bhuta, S.; Williams, L. J.; Musselli, C.; Zhang, X.-F.; Bencsath, K. P.; Panageas, K. S.; Chin, J.; Hudis, C. A., Immunization of metastatic breast cancer patients with a fully synthetic Globo H conjugate: a phase I trial. *Proc. Natl. Acad. Sci. USA* **2001**, *98*, 3270-3275.
75. Huang, C.-S.; Alice, L. Y.; Tseng, L.-M.; Chow, L. W.; Hou, M.-F.; Hurvitz, S. A.; Schwab, R. B.; Murray, J. L.; Chang, H.-K.; Chang, H.-T., Globo H-KLH vaccine adagloxad simolenin (OBI-822)/OBI-821 in patients with metastatic breast cancer: phase II randomized, placebo-controlled study. *J. Immunother. Cancer* **2020**, *8* (2).
76. Huang, C.-S.; Yu, A. L.; Tseng, L.-M.; Chow, L. W.; Hou, M.-F.; Hurvitz, S. A.; Schwab, R. B.; Wong, C.-H.; Murray, J. L.; Chang, H.-K., Randomized phase II/III trial of active

- immunotherapy with OPT-822/OPT-821 in patients with metastatic breast cancer. *J. Clin. Onc.* **2016**, *34*, 1003.
77. Lacaille-Dubois, M.-A., Updated insights into the mechanism of action and clinical profile of the immunoadjuvant QS-21: A review. *Phytomedicine* **2019**, *60*, 152905.
 78. Kensil, C. R.; Patel, U.; Lennick, M.; Marciani, D., Separation and characterization of saponins with adjuvant activity from *Quillaja saponaria* Molina cortex. *J. Immunol.* **1991**, *146*, 431-437.
 79. Sun, H.-X.; Xie, Y.; Ye, Y.-P., Advances in saponin-based adjuvants. *Vaccine* **2009**, *27*, 1787-1796.
 80. Fernández-Tejada, A.; Tan, D. S.; Gin, D. Y., Development of improved vaccine adjuvants based on the saponin natural product QS-21 through chemical synthesis. *Acc. Chem. Res.* **2016**, *49*, 1741-1756.
 81. Pifferi, C.; Fuentes, R.; Fernández-Tejada, A., Natural and synthetic carbohydrate-based vaccine adjuvants and their mechanisms of action. *Nature Rev. Chem.* **2021**, *5*, 197-216.
 82. Horlacher, T.; Seeberger, P. H., Carbohydrate arrays as tools for research and diagnostics. *Chem. Soc. Rev.* **2008**, *37*, 1414-1422.
 83. Blixt, O.; Hoffmann, J.; Svenson, S.; Norberg, T., Pathogen specific carbohydrate antigen microarrays: a chip for detection of *Salmonella* O-antigen specific antibodies. *Glycoconj. J.* **2008**, *25*, 27-36.
 84. Kamena, F.; Tamborrini, M.; Liu, X.; Kwon, Y.-U.; Thompson, F.; Pluschke, G.; Seeberger, P. H., Synthetic GPI array to study antitoxic malaria response. *Nat. Chem. Biol.* **2008**, *4*, 238-240.
 85. Wang, C.-C.; Huang, Y.-L.; Ren, C.-T.; Lin, C.-W.; Hung, J.-T.; Yu, J.-C.; Yu, A. L.; Wu, C.-Y.; Wong, C.-H., Glycan microarray of Globo H and related structures for quantitative analysis of breast cancer. *Proc. Natl. Acad. Sci. USA* **2008**, *105*, 11661-11666.
 86. Adams, E. W.; Ratner, D. M.; Bokesch, H. R.; McMahon, J. B.; O'Keefe, B. R.; Seeberger, P. H., Oligosaccharide and glycoprotein microarrays as tools in HIV glycobiology: glycan-dependent gp120/protein interactions. *Chem. Biol.* **2004**, *11*, 875-881.
 87. Muthana, S. M.; Gildersleeve, J. C., Glycan microarrays: powerful tools for biomarker discovery. *Cancer Biomarkers* **2014**, *14*, 29-41.
 88. Sekhon Randhawa, K. K.; Rahman, P. K., Rhamnolipid biosurfactants—past, present, and future scenario of global market. *Front. Microbiol.* **2014**, *5*, 454.
 89. Santos, D. K. F.; Rufino, R. D.; Luna, J. M.; Santos, V. A.; Sarubbo, L. A., Biosurfactants: multifunctional biomolecules of the 21st century. *Int. J. Mol. Sci.* **2016**, *17*, 401.

90. Mnif, I.; Ellouz-Chaabouni, S.; Ghribi, D., Glycolipid biosurfactants, main classes, functional properties and related potential applications in environmental biotechnology. *J. Polym. Environ.* **2018**, *26*, 2192-2206.
91. Lourith, N.; Kanlayavattanakul, M., Natural surfactants used in cosmetics: glycolipids. *Int. J. Cosmet. Sci.* **2009**, *31*, 255-261.
92. Nalini, S.; Parthasarathi, R.; Inbakanadan, D., Biosurfactant in food and agricultural application. *Environ. Biotechn.* **2020**, *2*, 75-94.
93. Henkel, M.; Müller, M. M.; Kügler, J. H.; Lovaglio, R. B.; Contiero, J.; Syldatk, C.; Hausmann, R., Rhamnolipids as biosurfactants from renewable resources: concepts for next-generation rhamnolipid production. *Process Biochem.* **2012**, *47*, 1207-1219.
94. Chong, H.; Li, Q., Microbial production of rhamnolipids: opportunities, challenges and strategies. *Microb. Cell Factories* **2017**, *16*, 1-12.
95. Compton, A. A.; Deodhar, B. S.; Fathi, A.; Pemberton, J. E., Optimization of a chemical synthesis for single-chain rhamnolipids. *ACS Sustain. Chem. Eng.* **2020**, *8*, 8918-8927.
96. Duynstee, H. I.; van Vliet, M. J.; van der Marel, G. A.; van Boom, J. H., An efficient synthesis of (R)-3-[(R)-3-[2-O-(α -L-rhamnopyranosyl)- α -L-rhamnopyranosyl]oxydecanoyl]oxydecanoic acid, a rhamnolipid from *Pseudomonas aeruginosa*. *Eur. J. Org. Chem.* **1998**, 303-307.
97. Cloutier, M.; Prévost, M.-J.; Lavoie, S.; Feroldi, T.; Piochon, M.; Groleau, M.-C.; Legault, J.; Villaume, S.; Crouzet, J.; Dorey, S., Total synthesis, isolation, surfactant properties, and biological evaluation of anatosides and related macrodilactone-containing rhamnolipids. *Chem. Sci.* **2021**, *12*, 7533-7546.
98. de Jesús Cortés-Sánchez, A.; Hernández-Sánchez, H.; Jaramillo-Flores, M. E., Biological activity of glycolipids produced by microorganisms: new trends and possible therapeutic alternatives. *Microbiol. Res.* **2013**, *168*, 22-32.
99. Abdel-Megeed, A.; Al-Rahma, A.; Mostafa, A.; Baser, K. H. C., Biochemical characterization of anti-microbial activity of glycolipids produced by *Rhodococcus erythropolis*. *Pak. J. Bot.* **2011**, *43*, 1323-1334.
100. Haba, E.; Pinazo, A.; Jauregui, O.; Espuny, M.; Infante, M. R.; Manresa, A., Physicochemical characterization and antimicrobial properties of rhamnolipids produced by *Pseudomonas aeruginosa* 47T2 NCBIM 40044. *Biotechnol. Bioeng.* **2003**, *81*, 316-322.
101. Williams, J.; Richardson, A., Selective acylation of pyranoside—i.: Benzoylation of methyl α -D-glycopyranosides of mannose, glucose and galactose. *Tetrahedron* **1967**, *23*, 1369-1378.
102. Wang, T.; Demchenko, A. V., Synthesis of carbohydrate building blocks via regioselective uniform protection/deprotection strategies. *Org. Biomol. Chem.* **2019**, *17*, 4934-4950.

103. Shivatare, S. S.; Wong, C.-H., Synthetic carbohydrate chemistry and translational medicine. *J. Org. Chem.* **2020**, *85*, 15780-15800.
104. Adero, P. O.; Amarasekara, H.; Wen, P.; Bohé, L.; Crich, D., The experimental evidence in support of glycosylation mechanisms at the S_N1–S_N2 interface. *Chem. Rev.* **2018**, *118*, 8242-8284.
105. Elferink, H.; Pedersen, C. M., L-Rhamnosylation: the solvent is the solution. *Eur. J. Org. Chem.* **2017**, *2017*, 53-59.
106. Stalford, S. A.; Kilner, C. A.; Leach, A. G.; Turnbull, W. B., Neighbouring group participation vs. addition to oxacarbenium ions: studies on the synthesis of mycobacterial oligosaccharides. *Org. Biomol. Chem.* **2009**, *7*, 4842-4852.
107. Crich, D.; Sun, S., Are glycosyl triflates intermediates in the sulfoxide glycosylation method? A chemical and ¹H, ¹³C, and ¹⁹F NMR spectroscopic investigation. *J. Am. Chem. Soc.* **1997**, *119*, 11217-11223.
108. Walvoort, M. T.; van der Marel, G. A.; Overkleeft, H. S.; Codée, J. D., On the reactivity and selectivity of donor glycosides in glycochemistry and glycobiology: trapped covalent intermediates. *Chem. Sci.* **2013**, *4*, 897-906.
109. Santana, A. G.; Montalvillo-Jimenez, L.; Diaz-Casado, L.; Corzana, F.; Merino, P.; Cañada, F. J.; Jimenez-Oses, G.; Jimenez-Barbero, J.; Gomez, A. M.; Asensio, J. L., Dissecting the essential role of anomeric β-triflates in glycosylation reactions. *J. Am. Chem. Soc.* **2020**, *142*, 12501-12514.
110. Kendale, J. C.; Valentín, E. M.; Woerpel, K., Solvent effects in the nucleophilic substitutions of tetrahydropyran acetals promoted by trimethylsilyl trifluoromethanesulfonate: trichloroethylene as solvent for stereoselective C- and O-glycosylations. *Org. Lett.* **2014**, *16*, 3684-3687.
111. Boltje, T. J.; Kim, J.-H.; Park, J.; Boons, G.-J., Stereoelectronic effects determine oxacarbenium vs β-sulfonium ion mediated glycosylations. *Org. Lett.* **2011**, *13*, 284-287.
112. Van der Vorm, S.; Hansen, T.; Overkleeft, H.; Van der Marel, G.; Codée, J., The influence of acceptor nucleophilicity on the glycosylation reaction mechanism. *Chem. Sci.* **2017**, *8*, 1867-1875.
113. Chatterjee, S.; Moon, S.; Hentschel, F.; Gilmore, K.; Seeberger, P. H., An empirical understanding of the glycosylation reaction. *J. Am. Chem. Soc.* **2018**, *140*, 11942-11953.
114. Mensink, R. A.; Boltje, T. J., Advances in stereoselective 1,2-*cis* glycosylation using C-2 auxiliaries. *Chem. Eur. J.* **2017**, *23*, 17637-17653.
115. Masoud, H.; Ho, M.; Schollaardt, T.; Perry, M. B., Characterization of the capsular polysaccharide of *Burkholderia (Pseudomonas) pseudomallei* 304b. *J. Bacteriol.* **1997**, *179*, 5663-5669.

116. Nimitz, M.; Wray, V.; Domke, T.; Brenneke, B.; Häussler, S.; Steinmetz, I., Structure of an acidic exopolysaccharide of *Burkholderia pseudomallei*. *Eur. J. Biochem.* **1997**, *250*, 608-616.
117. Knirel, Y. A.; Paramonov, N. A.; Shashkov, A. S.; Kochetkov, N. K.; Yarullin, R. G.; Farber, S. M.; Efremenko, V. I., Structure of the polysaccharide chains of *Pseudomonas pseudomallei* lipopolysaccharides. *Carbohydr. Res.* **1992**, *233*, 185-193.
118. Perry, M. B.; MacLean, L. L.; Schollaardt, T.; Bryan, L. E.; Ho, M., Structural characterization of the lipopolysaccharide O-antigens of *Burkholderia pseudomallei*. *Infect. Immun.* **1995**, *63*, 3348-3352.
119. Heiss, C.; Burtnick, M. N.; Wang, Z.; Azadi, P.; Brett, P. J., Structural analysis of capsular polysaccharides expressed by *Burkholderia mallei* and *Burkholderia pseudomallei*. *Carbohydr. Res.* **2012**, *349*, 90-94.
120. Chen, Y.-H.; Poly, F.; Pakulski, Z.; Guerry, P.; Monteiro, M. A., The chemical structure and genetic locus of *Campylobacter jejuni* CG8486 (serotype HS: 4) capsular polysaccharide: the identification of 6-deoxy-D-ido-heptopyranose. *Carbohydr. Res.* **2008**, *343*, 1034-1040.
121. Poly, F.; Serichantalergs, O.; Kuroiwa, J.; Pootong, P.; Mason, C.; Guerry, P.; Parker, C. T., Updated *Campylobacter jejuni* capsule PCR multiplex typing system and its application to clinical isolates from South and Southeast Asia. *PLoS ONE* **2015**, *10*, e0144349.
122. Yasomane, J. P.; Demchenko, A. V., Effect of remote picolinyl and picoloyl substituents on the stereoselectivity of chemical glycosylation. *J. Am. Chem. Soc.* **2012**, *134*, 20097-20102.
123. Pistorio, S. G.; Yasomane, J. P.; Demchenko, A. V., Hydrogen-bond-mediated aglycone delivery: focus on β -mannosylation. *Org. Lett.* **2014**, *16*, 716-719.
124. Eby, R.; Schuerch, C., The use of 1-O-tosyl-D-glucopyranose derivatives in α -D-glucoside synthesis. *Carbohydr. Res.* **1974**, *34*, 79-90.
125. Crich, D.; Smith, M., S-(4-Methoxyphenyl) benzenethiosulfinate (MPBT)/trifluoromethanesulfonic anhydride: a convenient system for the generation of glycosyl triflates from thioglycosides. *Org. Lett.* **2000**, *2*, 4067-4069.
126. Crich, D.; Banerjee, A.; Yao, Q., Direct chemical synthesis of the β -D-mannans: the β -(1 \rightarrow 2) and β -(1 \rightarrow 4) series. *J. Am. Chem. Soc.* **2004**, *126*, 14930-14934.
127. Crich, D.; Pedersen, C. M.; Bowers, A. A.; Wink, D. J., On the use of 3,5-O-benzylidene and 3,5-O-(di-*tert*-butylsilylene)-2-O-benzylarabinothiofuranosides and their sulfoxides as glycosyl donors for the synthesis of β -arabinofuranosides: importance of the activation method. *J. Org. Chem.* **2007**, *72*, 1553-1565.
128. Walvoort, M. T.; Lodder, G.; Mazurek, J.; Overkleeft, H. S.; Codee, J. D.; van der Marel, G. A., Equatorial anomeric triflates from mannuronic acid esters. *J. Am. Chem. Soc.* **2009**, *131*, 12080-12081.

129. Walvoort, M. T.; Lodder, G.; Overkleeft, H. S.; Codee, J. D.; van der Marel, G. A., Mannosazide methyl uronate donors. Glycosylating properties and use in the construction of β -ManNAcA-containing oligosaccharides. *J. Org. Chem.* **2010**, *75*, 7990-8002.
130. Elferink, H.; Mensink, R. A.; White, P. B.; Boltje, T. J., Stereoselective β -mannosylation by neighboring-group participation. *Angew. Chem. Int. Ed. Engl.* **2016**, *128*, 11383-11386.
131. Hashimoto, Y.; Tanikawa, S.; Saito, R.; Sasaki, K., β -Stereoselective mannosylation using 2,6-lactones. *J. Am. Chem. Soc.* **2016**, *138*, 14840-14843.
132. Sasaki, K.; Hashimoto, Y., 2,6-Lactones as a new entry in stereoselective glycosylations. *Synlett* **2017**, *28*, 1121-1126.
133. Cumpstey, I., Intramolecular aglycon delivery. *Carbohydr. Res.* **2008**, *343*, 1553-1573.
134. Barresi, F.; Hindsgaul, O., Synthesis of β -mannopyranosides by intramolecular aglycon delivery. *J. Am. Chem. Soc.* **1991**, *113*, 9376-9377.
135. Elshahawi, S. I.; Shaaban, K. A.; Kharel, M. K.; Thorson, J. S., A comprehensive review of glycosylated bacterial natural products. *Chem. Soc. Rev.* **2015**, *44*, 7591-7697.
136. Mnif, I.; Ghribi, D., Glycolipid biosurfactants: main properties and potential applications in agriculture and food industry. *J. Sci. Food Agric.* **2016**, *96*, 4310-4320.
137. Inès, M.; Dhouha, G., Glycolipid biosurfactants: potential related biomedical and biotechnological applications. *Carbohydr. Res.* **2015**, *416*, 59-69.
138. Saravanakumari, P.; Mani, K., Structural characterization of a novel xylolipid biosurfactant from *Lactococcus lactis* and analysis of antibacterial activity against multi-drug resistant pathogens. *Bioresour. Technol.* **2010**, *101*, 8851-8854.
139. Sha, R.; Jiang, L.; Meng, Q.; Zhang, G.; Song, Z., Producing cell-free culture broth of rhamnolipids as a cost-effective fungicide against plant pathogens. *J. Basic Microbiol.* **2012**, *52*, 458-466.
140. Shah, V.; Doncel, G. F.; Seyoum, T.; Eaton, K. M.; Zalenskaya, I.; Hagver, R.; Azim, A.; Gross, R., Sophorolipids, microbial glycolipids with anti-human immunodeficiency virus and sperm-immobilizing activities. *Antimicrob. Agents Chemother.* **2005**, *49*, 4093-4100.
141. Hewald, S.; Josephs, K.; Bölker, M., Genetic analysis of biosurfactant production in *Ustilago maydis*. *Appl. Environ. Microbiol.* **2005**, *71*, 3033-3040.
142. Chen, J.; Song, X.; Zhang, H.; Qu, Y., Production, structure elucidation and anticancer properties of sophorolipid from *Wickerhamiella domercqiae*. *Enzyme Microb. Technol.* **2006**, *39*, 501-506.
143. Lima, V. M. F.; Bonato, V. L. D.; Lima, K. M.; Dos Santos, S. A.; Dos Santos, R. R.; Gonçalves, E. D. C.; Faccioli, L. H.; Brandao, I. T.; Rodrigues-Junior, J. M.; Silva, C. L., Role of trehalose dimycolate in recruitment of cells and modulation of production of cytokines and NO in tuberculosis. *Infect. Immun.* **2001**, *69*, 5305-5312.

144. Abdel-Mawgoud, A.; Lépine, F.; Déziel, E., Rhamnolipids: diversity of structures, microbial origins and roles. *Appl. Microbiol. Biotechnol.* **2010**, *86*, 1323-1336.
145. Chen, J.; Wu, Q.; Hua, Y.; Chen, J.; Zhang, H.; Wang, H., Potential applications of biosurfactant rhamnolipids in agriculture and biomedicine. *Appl. Microbiol. Biotechnol.* **2017**, *101*, 8309-8319.
146. Zheng, H.; Singh, N.; Shetye, G. S.; Jin, Y.; Li, D.; Luk, Y.-Y., Synthetic analogs of rhamnolipids modulate structured biofilms formed by rhamnolipid-nonproducing mutant of *Pseudomonas aeruginosa*. *Bioorg. Med. Chem.* **2017**, *25*, 1830-1838.
147. Aleksic, I.; Petkovic, M.; Jovanovic, M.; Milivojevic, D.; Vasiljevic, B.; Nikodinovic-Runic, J.; Senerovic, L., Anti-biofilm properties of bacterial di-rhamnolipids and their semi-synthetic amide derivatives. *Front. Microbiol.* **2017**, *8*, 2454.
148. Nickzad, A.; Déziel, É., The involvement of rhamnolipids in microbial cell adhesion and biofilm development—an approach for control? *Lett. Appl. Microbiol.* **2014**, *58*, 447-453.
149. Jiang, L.; Shen, C.; Long, X.; Zhang, G.; Meng, Q., Rhamnolipids elicit the same cytotoxic sensitivity between cancer cell and normal cell by reducing surface tension of culture medium. *Appl. Microbiol. Biotechnol.* **2014**, *98*, 10187-10196.
150. Leite, G. G. F.; Figueirôa, J. V.; Almeida, T. C. M.; Valões, J. L.; Marques, W. F.; Duarte, M. D. D. C.; Górlach-Lira, K., Production of rhamnolipids an diesel oil degradation by bacteria isolated from soil contaminated by petroleum. *Biotechnol. Prog.* **2016**, *32*, 262-270.
151. Manaargadoo-Catin, M.; Ali-Cherif, A.; Pougna, J.-L.; Perrin, C., Hemolysis by surfactants - A review. *Adv. Colloid Interface Sci.* **2016**, *228*, 1-16.
152. Zhou, M.; Wang, W., Recent advances in synthetic chemical inducers of plant immunity. *Front. Plant Sci.* **2018**, *9*, 1613.
153. Luzuriaga-Loaiza, W. P.; Schellenberger, R.; De Gaetano, Y.; Akong, F. O.; Villaume, S. A.; Crouzet, J.; Haudrechy, A.; Baillieux, F.; Clément, C.; Lins, L.; Allais, F.; Ongena, M.; Bouquillon, S.; Deleu, M.; Dorey, S., Synthetic rhamnolipid bolaforms trigger an innate immune response in *Arabidopsis thaliana*. *Sci. Rep.* **2018**, *8*, 8534.
154. Kutschera, A.; Dawid, C.; Gisch, N.; Schmid, C.; Raasch, L.; Gerster, T.; Schäffer, M.; Smakowska-Luzan, E.; Belkhadir, Y.; Vlot, A. C.; Chandler, C. E.; Schellenberger, R.; Schwudke, D.; Ernst, R. K.; Dorey, S.; Hückelhoven, R.; Hofmann, T.; Ranf, S., Bacterial medium-chain 3-hydroxy fatty acid metabolites trigger immunity in *Arabidopsis* plants. *Science* **2019**, *364*, 178-181.
155. Robineau, M.; Le Guenic, S.; Sanchez, L.; Chaveriat, L.; Lequart, V.; Joly, N.; Calonne, M.; Jacquard, C.; Declerck, S.; Martin, P.; Dorey, S.; Barka, E. A., Synthetic mono-rhamnolipids display direct antifungal effects and trigger an innate immune response in tomato against *Botrytis cinerea*. *Molecules* **2020**, *25*, 3108.

156. Crouzet, J.; Arguelles-Arias, A.; Dhondt-Cordelier, S.; Cordelier, S.; Pršic, J.; Hoff, G.; Mazeyrat-Gourbeyre, F.; Baillieul, F.; Clément, C.; Ongena, M.; Dorey, S., Biosurfactants in plant protection against diseases: rhamnolipids and lipopeptides case study. *Front. Bioeng. Biotechnol.* **2020**, *8*, 1014.
157. Soberon-Chavez, G.; Lépine, F.; Déziel, E., Production of rhamnolipids by *Pseudomonas aeruginosa*. *Appl. Microbiol. Biotechnol.* **2005**, *68*, 718-725.
158. Smith, D. D. N.; Nickzad, A.; Déziel, E.; Stavrinides, J., A novel glycolipid biosurfactant confers grazing resistance upon *Pantoea ananatis* BRT175 against the social amoeba *Dictyostelium discoideum*. *mSphere* **2016**, *1*, e00075-15.
159. Gauthier, C.; Lavoie, S.; Piochon, M.; Martinez, S.; Milot, S.; Déziel, E., Structural determination of anatoside A: an unprecedented 15-membered macrodilactone-containing glycolipid from *Pantoea ananatis*. *Carbohydr. Res.* **2019**, *471*, 13-18.
160. Ochsner, U. A.; Fiechter, A.; Reiser, J., Isolation, characterization, and expression in *Escherichia coli* of the *Pseudomonas aeruginosa* rhlAB genes encoding a rhamnosyltransferase involved in rhamnolipid biosurfactant synthesis. *J. Biol. Chem.* **1994**, *269*, 19787-19795.
161. Rahim, R.; Ochsner, U. A.; Olvera, C.; Graninger, M.; Messner, P.; Lam, J. S.; Soberon-Chavez, G., Cloning and functional characterization of the *Pseudomonas aeruginosa* rhlC gene that encodes rhamnosyltransferase 2, an enzyme responsible for di-rhamnolipid biosynthesis. *Mol. Microbiol.* **2001**, *40*, 708-718.
162. Xie, J.; Bogliotti, N., Synthesis and applications of carbohydrate-derived macrocyclic compounds. *Chem. Rev.* **2014**, *114*, 7678-7739.
163. Rodriguez, J.; O'Neill, S.; Walczak, M. A., Constrained saccharides: a review of structure, biology, and synthesis. *Nat. Prod. Rep.* **2018**, *35*, 220-229.
164. Abdel-Mawgoud, A. M.; Stephanopoulos, G., Simple glycolipids of microbes: Chemistry, biological activity and metabolic engineering. *Synth. Syst. Biotechnol.* **2018**, *3*, 3-19.
165. Pereda-Miranda, R.; Bah, M., Biodynamic constituents in the Mexican morning glories: purgative remedies transcending boundaries. *Curr. Top. Med. Chem.* **2003**, *3*, 111-131.
166. Tamigney Kenfack, M.; Blériot, Y.; Gauthier, C., Intramolecular aglycon delivery enables the synthesis of 6-deoxy- β -D-manno-heptosides as fragments of *Burkholderia pseudomallei* and *Burkholderia mallei* capsular polysaccharide. *J. Org. Chem.* **2014**, *79*, 4615-4634.
167. Laroussarie, A.; Barycza, B.; Andriamboavonjy, H.; Tamigney Kenfack, M.; Blériot, Y.; Gauthier, C., Synthesis of the tetrasaccharide repeating unit of the β -Kdo-containing exopolysaccharide from *Burkholderia pseudomallei* and *B. cepacia* complex. *J. Org. Chem.* **2015**, *80*, 10386-10396.
168. Tamigney Kenfack, M.; Mazur, M.; Nualnoi, T.; Shaffer, T. L.; Ngassimou, A.; Blériot, Y.; Marrot, J.; Marchetti, R.; Sintiprungrat, K.; Chantratita, N.; Silipo, A.; Molinaro, A.;

- AuCoin, D. P.; Burtnick, M. N.; Brett, P. J.; Gauthier, C., Deciphering minimal antigenic epitopes associated with *Burkholderia pseudomallei* and *Burkholderia mallei* lipopolysaccharide O-antigens. *Nat. Commun.* **2017**, *8*, 115.
169. Cloutier, M.; Delar, E.; Muru, K.; Ndong, S.; Hoyeck, R. R.; Kaewarpai, T.; Chantratita, N.; Burtnick, M. N.; Brett, P. J.; Gauthier, C., Melioidosis patient serum-reactive synthetic tetrasaccharides bearing the predominant epitopes of *Burkholderia pseudomallei* and *Burkholderia mallei* O-antigens. *Org. Biomol. Chem.* **2019**, *17*, 8878-8901.
170. Vehovec, T.; Obreza, A., Review of operating principle and applications of the charged aerosol detector. *J. Chromatogr. A* **2010**, *1217*, 1549-1556.
171. Fürstner, A., Total syntheses and biological assessment of macrocyclic glycolipids. *Eur. J. Org. Chem.* **2004**, 943-958.
172. Bisht, K. S.; Bhatt, S.; Muppalla, K., Synthesis of glycolipid analogs via highly regioselective macrolactonization catalyzed by lipase. *Tetrahedron Lett.* **2006**, *47*, 8645-8649.
173. Gagnon, C.; Godin, É.; Minozzi, C.; Sosoe, J.; Pochet, C.; Collins, S. K., Biocatalysis synthesis of planar chiral macrocycles. *Science* **2020**, *367*, 917-921.
174. Ortiz, C.; Ferreira, M. L.; Barbosa, O.; dos Santos, J. C. S.; Rodrigues, R. C.; Berenguer-Murcia, A.; Briand, L. E.; Fernandez-Lafuente, R., Novozym 435: the "perfect" lipase immobilized biocatalyst? *Catal. Sci. Technol.* **2019**, *9*, 2380-2420.
175. Das, R.; Mukhopadhyay, B., Chemical O-glycosylations: an overview. *ChemistryOpen* **2016**, *5*, 401-433.
176. Yang, Y.; Zhang, X.; Yu, B., O-Glycosylation methods in the total synthesis of complex natural glycosides. *Nat. Prod. Rep.* **2015**, *32*, 1331-1355.
177. Jia, X. G.; Demchenko, A. V., Intramolecular glycosylation. *Beilstein J. Org. Chem.* **2017**, *13*, 2028-2048.
178. Lian, G.; Zhang, X.; Yu, B., Thioglycosides in Carbohydrate Research. *Carbohydr. Res.* **2014**, *403* (11), 13-22.
179. Wada, T.; Ohkubo, A.; Mochizuki, A.; Sekine, M., 2-(Azidomethyl)benzoyl as a new protecting group in nucleosides. *Tetrahedr. Lett.* **2001**, *42*, 1069-1072.
180. Gauthier, C.; Chassagne, P.; Theillet, F.-X.; Guerreiro, C.; Thouron, F.; Nato, F.; Delepierre, M.; Sansonetti, P. J.; Phalipon, A.; Mulard, L. A., Non-stoichiometric O-acetylation of *Shigella flexneri* 2a O-specific polysaccharide: synthesis and antigenicity. *Org. Biomol. Chem.* **2014**, *12*, 4218-4232.
181. Neises, B.; Steglich, W., Simple method for the esterification of carboxylic acids. *Angew. Chem. Int. Ed. Engl.* **1978**, *17*, 522-524.
182. Parenty, A.; Moreau, X.; Campagne, J. M., Macrolactonizations in the total synthesis of natural products. *Chem. Rev.* **2006**, *106*, 911-939.

183. Fürstner, A.; Albert, M.; Mlynarski, J.; Matheu, M.; DeClercq, E., Structure assignment, total synthesis, and antiviral evaluation of cycloviracin B1. *J. Am. Chem. Soc.* **2003**, *125*, 13132-13142.
184. Zhu, S.-Y.; Huang, J.-S.; Zheng, S.-S.; Zhu, K.; Yang, J.-S., First total synthesis of the proposed structure of batatin VI. *Org. Lett.* **2013**, *15*, 4154-4157.
185. Mateus-Ruiz, J. R.; Cordero-Vargas, A., Stereoselective total synthesis of aspergillide A: a visible light-mediated photoredox access to the trisubstituted tetrahydropyran core. *J. Org. Chem.* **2019**, *84*, 11848-11855.
186. Hassner, A.; Strand, G.; Rubinstein, M.; Patchornik, A., Levulinic esters - Alcohol protecting group applicable to some nucleosides. *J. Am. Chem. Soc.* **1975**, *97*, 1614-1615.
187. Menhour, B.; Mayon, P.; Plé, K.; Bouquillon, S.; Dorey, S.; Clément, C.; Deleu, M.; Haudrechy, A., A stereocontrolled synthesis of the hydrophobic moiety of rhamnolipids. *Tetrahedr. Lett.* **2015**, *56*, 1159-1161.
188. Bauer, J.; Brandenburg, K.; Zähringer, U.; Rademann, J., Chemical synthesis of a glycolipid library by a solid-phase strategy allows elucidation of the structural specificity of immunostimulation by rhamnolipids. *Chem. Eur. J.* **2006**, *12*, 7116-7124.
189. De Vleeschouwer, M.; Sinnaeve, D.; Van den Begin, J.; Coenye, T.; Martins, J. C.; Madder, A., Rapid total synthesis of cyclic lipodepsipeptides as a premise to investigate their self-assembly and biological activity. *Chem. Eur. J.* **2014**, *20*, 7766-7775.
190. Coss, C.; Carrocci, T.; Maier, R. M.; Pemberton, J. E.; Polt, R., Minimally competent Lewis acid catalysts: indium(III) and bismuth(III) salts produce rhamnosides (=6-deoxymannosides) in high yield and purity. *Helv. Chim. Acta* **2012**, *95*, 2652-2659.
191. Pacheco, R. P.; Eismin, R. J.; Coss, C. S.; Wang, H.; Maier, R. M.; Polt, R.; Pemberton, J. E., Synthesis and characterization of four diastereomers of monorhamnolipids. *J. Am. Chem. Soc.* **2017**, *139*, 5125-5132.
192. Hu, Y.-P.; Lin, S.-Y.; Huang, C.-Y.; Zulueta, M.; Liu, J.-Y.; Chang, W.; Hung, S.-C., Synthesis of 3-O-sulfonated heparan sulfate octasaccharides that inhibit the herpes simplex virus type 1 host-cell interaction. *Nat. Chem.* **2011**, *3*, 557-563.
193. Konradsson, P.; Udodong, U. E.; Fraser-Reid, B., Iodonium promoted reactions of disarmed thioglycosides. *Tetrahedr. Lett.* **1990**, *31*, 4313-4316.
194. Felix, A. M.; Heimer, E. P.; Lambros, T. J.; Tzougraki, C.; Meienhofer, J., Rapid removal of protecting groups from peptides by catalytic transfer hydrogenation with 1,4-cyclohexadiene. *J. Org. Chem.* **1978**, *43*, 4194-4196.
195. Bajwa, J. S., Chemoselective deprotection of benzyl esters in the presence of benzyl ethers, benzyloxymethyl ethers and N-benzyl groups by catalytic transfer hydrogenation. *Tetrahedr. Lett.* **1992**, *33*, 2299-2302.

196. Boden, E. P.; Keck, G. E., Proton-transfer steps in Steglich esterification: a very practical new method for macrolactonization. *J. Org. Chem.* **1985**, *50*, 2394-2395.
197. Fujisawa, T.; Mori, T.; Fukumoto, K.; Sato, T., *N,N,N',N'*-Tetramethylchloroformamidinium chloride as an efficient condensation reagent for a novel esterification applicable to the macrolide synthesis. *Chem. Lett.* **1982**, *11*, 1891-1894.
198. Westerduin, P.; De Haan, P. E.; Dees, M. J.; van Boom, J. H., Synthesis of methyl 3-[2-*O*- α -L-rhamnopyranosyl- α -L-rhamnopyranosyloxy]decanoyloxy]decanoate, a rhamnolipid from *Pseudomonas aeruginosa*. *Carbohydr. Res.* **1988**, *180*, 195-205.
199. David, S.; Hanessian, S., Regioselective manipulation of hydroxyl groups via organotin derivatives. *Tetrahedron* **1985**, *41*, 643-663.
200. Cumpstey, I.; Fairbanks, A. J.; Redgrave, A. J., Allyl protecting group mediated intramolecular aglycon delivery (IAD): synthesis of α -glucofuranosides and β -rhamnopyranosides. *Tetrahedron* **2004**, *60*, 9061-9074.
201. Duus, J. Ø.; Gotfredsen, C. H.; Bock, K., Carbohydrate structural determination by NMR spectroscopy: modern methods and limitations. *Chem. Rev.* **2000**, *100*, 4589-4614.
202. Feng, L.; Senchenkova, S. N.; Wang, W.; Shashkov, A. S.; Liu, B.; Shevelev, S. D.; Liu, D.; Knirel, Y. A.; Wang, L., Structural and genetic characterization of the *Shigella boydii* type 18 O antigen. *Gene* **2005**, *355* (1-2), 79-86.
203. Bock, K.; Pedersen, C., A study of ^{13}C coupling constants in hexopyranoses. *J. Chem. Soc., Perkin Trans* **1974**, *2*, 293-297.
204. Wang, S.; Witek, J.; Landrum, G. A.; Riniker, S., Improving conformer generation for small rings and macrocycles based on distance geometry and experimental torsional-angle preferences. *J. Chem. Inf. Model.* **2020**, *60*, 2044-2058.
205. Sarotti, A. M.; Pellegrinet, S. C., A multi-standard approach for GIAO ^{13}C NMR calculations. *J. Org. Chem.* **2009**, *74*, 7254-7260.
206. Sarotti, A. M.; Pellegrinet, S. C., Application of the multi-standard methodology for calculating ^1H NMR chemical shifts. *J. Org. Chem.* **2012**, *77*, 6059-6065.
207. Lauro, G.; Das, P.; Riccio, R.; Reddy, D. S.; Bifulco, G., DFT/NMR approach for the configuration assignment of groups of stereoisomers by the combination and comparison of experimental and predicted sets of data. *J. Org. Chem.* **2020**, *85*, 3297-3306.
208. Bércecs, A.; Whitfield, D. M.; Nukada, T., Quantitative description of six-membered ring conformations following the IUPAC conformational nomenclature. *Tetrahedron* **2001**, *57*, 477-491.
209. Daverey, A.; Pakshirajan, K., Recent advances in bioremediation of contaminated soil and water using microbial surfactants. In: Ahmad, I.; Ahmad, F.; Pichtel, J. (eds) *Microbes and Microbial Technology*, Springer: New York, NY, **2011**.

210. Lebrón-Paler, A.; Pemberton, J. E.; Becker, B. A.; Otto, W. H.; Larive, C. K.; Maier, R. M., Determination of the acid dissociation constant of the biosurfactant monorhamnolipid in aqueous solution by potentiometric and spectroscopic methods. *Anal. Chem.* **2006**, *78*, 7649-7658.
211. Zhong, H.; Yang, L.; Yang, X.; Zeng, G.; Liu, Z.; Liu, Y.; Yuan, X., Aggregation of low-concentration dirhamnolipid biosurfactant in electrolyte solution. *RSC Adv.* **2015**, *5*, 88578-88582.
212. Gauthier, C.; Legault, J.; Lavoie, S.; Rondeau, S.; Tremblay, S.; Pichette, A., Synthesis and cytotoxicity of bidesmosidic betulin and betulinic acid saponins. *J. Nat. Prod.* **2009**, *72*, 72-81.
213. Coutinho, T. A.; Venter, S. N., *Pantoea ananatis*: an unconventional plant pathogen. *Mol. Plant Pathol.* **2009**, *10*, 325-335.
214. Qi, J.; Wang, J.; Gong, Z.; Zhou, J. M., Apoplastic ROS signaling in plant immunity. *Curr. Opin. Plant Biol.* **2017**, *38*, 92-100.
215. Orhan, G.; Bayram, A.; Zer, Y.; Balci, I., Synergy tests by E test and checkerboard methods of antimicrobial combinations against *Brucella melitensis*. *J. Clin. Microbiol.* **2005**, *43*, 140-143.
216. O'Brien, J.; Wilson, I.; Orton, T.; Pognan, F., Investigation of the Alamar Blue (resazurin) fluorescent dye for the assessment of mammalian cell cytotoxicity. *Eur. J. Biochem.* **2000**, *267*, 5421-5426.
217. Gauthier, C.; Legault, J.; Girard-Lalancette, K.; Mshvildadze, V.; Pichette, A., Haemolytic activity, cytotoxicity and membrane cell permeabilization of semi-synthetic and natural lupane- and oleanane-type saponins. *Bioorg. Med. Chem.* **2009**, *17*, 2002-2008.
218. Díaz De Rienzo, M. A.; Kamalanathan, I. D.; Martin, P. J., Comparative study of the production of rhamnolipid biosurfactants by *B. thailandensis* E264 and *P. aeruginosa* ATCC 9027 using foam fractionation. *Process Biochem.* **2016**, *5*, 820-827.
219. Lu, P. J.; Fu, W. E.; Huang, S. C.; Lin, C. Y.; Ho, M. L.; Chen, Y. P.; Cheng, H. F., Methodology for sample preparation and size measurement of commercial ZnO nanoparticles. *J. Food Drug Anal.* **2017**, *26*, 628-636.
220. Hanwell, M. D.; Curtis, D. E.; Lonie, D. C.; Vandermeersch, T.; Zurek, E.; Hutchison, G. R., Avogadro: An advanced semantic chemical editor, visualization, and analysis platform. *J. Cheminformatics* **2012**, *4*, 1-17.
221. Dalby, A.; Nourse, J. G.; Hounshell, W. D.; Gushurst, A. K. I.; Grier, D. L.; Leland, B. A.; Laufer, J., Description of several chemical structure file formats used by computer programs developed at molecular design limited. *J. Chem. Inf. Comp. Sci.* **1992**, *32*, 244-255.
222. Riniker, S.; Landrum, G. A., Better informed distance geometry: using what we know to improve conformation generation. *J. Chem. Inf. Model.* **2015**, *55*, 2562-2574.

223. Adamo, C.; Barone, V., Exchange functionals with improved long-range behavior and adiabatic connection methods without adjustable parameters: The mPW and mPW1PW models. *J. Chem. Phys.* **1998**, *108*, 664-675.
224. Frisch, M. J.; Trucks, G. W.; Schlegel, H. B.; Scuseria, G. E.; Robb, M. A.; Cheeseman, J. R.; Scalmani, G.; Barone, V.; Petersson, G. A.; Nakatsuji, H.; Li, X.; Caricato, M.; Marenich, A. V.; Bloino, J.; Janesko, B. G.; Gomperts, R.; Mennucci, B.; Hratchian, H. P.; Ortiz, J. V.; Izmaylov, A. F.; Sonnenberg, J. L.; Williams-Young, D.; Ding, F.; Lipparini, F.; Egidi, F.; Goings, J.; Peng, B.; Petrone, A.; Henderson, T.; Ranasinghe, D.; Zakrzewski, V. G.; Gao, J.; Rega, N.; Zheng, G.; Liang, W.; Hada, M.; Ehara, M.; Toyota, K.; Fukuda, R.; Hasegawa, J.; Ishida, M.; Nakajima, T.; Honda, Y.; Kitao, O.; Nakai, H.; Vreven, T.; Throssell, K.; Jr., J. A. M.; Peralta, J. E.; Ogliaro, F.; Bearpark, M. J.; Heyd, J. J.; Brothers, E. N.; Kudin, K. N.; Staroverov, V. N.; Keith, T. A.; Kobayashi, R.; Normand, J.; Raghavachari, K.; Rendell, A. P.; Burant, J. C.; Iyengar, S. S.; Tomasi, J.; Cossi, M.; Millam, J. M.; Klene, M.; Adamo, C.; Cammi, R.; Ochterski, J. W.; Martin, R. L.; Morokuma, K.; Farkas, O.; Foresman, J. B.; Fox, D. J. *Gaussian 16, Revision C.01*, Wallingford, CT, **2019**.
225. Wilson, P. J.; Bradley, T. J.; Tozer, D. J., Hybrid exchange-correlation functional determined from thermochemical data and ab initio potentials. *J. Chem. Phys.* **2001**, *115*, 9233-9242.
226. Kendall, R. A.; Dunning Jr, T. H.; Harrison, R. J., Electron affinities of the first-row atoms revisited. Systematic basis sets and wave functions. *J. Chem. Phys.* **1992**, *96*, 6796-6806.
227. Wolinski, K.; Hinton, J. F.; Pulay, P., Efficient implementation of the gauge-independent atomic orbital method for NMR chemical shift calculations. *J. Am. Chem. Soc.* **1990**, *112* (23), 8251-8260.
228. Willoughby, P. H.; Jansma, M. J.; Hoye, T. R., A guide to small-molecule structure assignment through computation of (¹H and ¹³C) NMR chemical shifts. *Nat. Protoc.* **2014**, *9*, 643-660.
229. Danzig, R.; Berkowsky, P. B., Why should we be concerned about biological warfare? *J. Amer. Med. Assoc.* **1997**, *278*, 431-432.
230. Pearson, G. S., The threat of deliberate disease in the 21st century. *Biological Weapons Proliferation: Reasons for Concern, Courses of Action* **1998**, 31.
231. Kaplan, D. E., Aum Shinrikyo. In Tucker, J. B. (Ed) *Toxic terror: Assessing terrorist use of chemical and biological weapons*. Boston, MIT Press, **2000**, 207-226.
232. Olson, K. B., Aum Shinrikyo: once and future threat? *Emerg. Infect. Dis.* **1999**, *5*, 513.
233. Török, T. J.; Tauxe, R. V.; Wise, R. P.; Livengood, J. R.; Sokolow, R.; Mauvais, S.; Birkness, K. A.; Skeels, M. R.; Horan, J. M.; Foster, L. R., A large community outbreak of salmonellosis caused by intentional contamination of restaurant salad bars. *J. Amer. Med. Assoc.* **1997**, *278* (5), 389-395.

234. Schupp, J. M.; Klevytska, A. M.; Zinser, G.; Price, L. B.; Keim, P., vrrB, a hypervariable open reading frame in *Bacillus anthracis*. *J. Bacteriol.* **2000**, *182*, 3989-3997.
235. Weintraub, A., Immunology of bacterial polysaccharide antigens. *Carbohydr. Res.* **2003**, *338*, 2539-2547.
236. Wuorimaa, T.; Käyhty, H.; Eskola, J.; Bloigu, A.; Leroy, O.; Surcel, H., Activation of cell-mediated immunity following immunization with pneumococcal conjugate or polysaccharide vaccine. *Scand. J. Immunol.* **2001**, *53*, 422-428.
237. Micoli, F.; Costantino, P.; Adamo, R., Potential targets for next generation antimicrobial glycoconjugate vaccines. *FEMS Microbiol. Rev.* **2018**, *42*, 388-423.
238. Boltje, T. J.; Buskas, T.; Boons, G.-J., Opportunities and challenges in synthetic oligosaccharide and glycoconjugate research. *Nat. Chem.* **2009**, *1*, 611.
239. Vliegenthart, J. F., Carbohydrate based vaccines. *FEBS Lett.* **2006**, *580*, 2945-2950.
240. Colombo, C.; Pitirollo, O.; Lay, L., Recent advances in the synthesis of glycoconjugates for vaccine development. *Molecules* **2018**, *23*, 1712.
241. Tamigney Kenfack, M.; Mazur, M.; Nualnoi, T.; Shaffer, T. L.; Ngassimou, A.; Bleriot, Y.; Marrot, J.; Marchetti, R.; Sintiprungrat, K.; Chantratita, N.; Silipo, A.; Molinaro, A.; AuCoin, D. P.; Burtnick, M. N.; Brett, P. J.; Gauthier, C., Deciphering minimal antigenic epitopes associated with *Burkholderia pseudomallei* and *Burkholderia mallei* lipopolysaccharide O-antigens. *Nat. Commun.* **2017**, *8*, 115.
242. Mock, M.; Fouet, A., Anthrax. *Annu. Rev. Microbiol.* **2001**, *55*, 647-671.
243. Priest, F. G., Systematics and ecology of *Bacillus*, In Sonenshein, A. L.; Hoch, J. A.; Losick, R. (Eds) *Bacillus subtilis and other gram-positive bacteria: biochemistry, physiology and molecular genetics*. Washington, D. C., **1993**, 3-16.
244. Steichen, C.; Chen, P.; Kearney, J. F.; Turnbough Jr, C. L., Identification of the immunodominant protein and other proteins of the *Bacillus anthracis* exosporium. *J. Bacteriol.* **2003**, *185*, 1903-1910.
245. Daubenspeck, J. M.; Zeng, H.; Chen, P.; Dong, S.; Steichen, C. T.; Krishna, N. R.; Pritchard, D. G.; Turnbough, C. L., Novel oligosaccharide side chains of the collagen-like region of BclA, the major glycoprotein of the *Bacillus anthracis* exosporium. *J. Biol. Chem.* **2004**, *279*, 30945-30953.
246. Milhomme, O.; Grandjean, C., Synthetic efforts towards glycoconjugate-based vaccines active against anthrax. *Curr. Org. Chem.* **2014**, *18*, 291-311.
247. Werz, D. B.; Seeberger, P. H., Total synthesis of antigen *Bacillus anthracis* tetrasaccharide--creation of an anthrax vaccine candidate. *Angew. Chem. Int. Ed. Engl.* **2005**, *44*, 6315-8.

248. Tamborrini, M.; Werz, D. B.; Frey, J.; Pluschke, G.; Seeberger, P. H., Anti-carbohydrate antibodies for the detection of anthrax spores. *Angew. Chem. Int. Ed. Engl.* **2006**, *45*, 6581-6582.
249. Werz, D. B.; Adibekian, A.; Seeberger, P. H., Synthesis of a spore surface pentasaccharide of *Bacillus anthracis*. *Eur. J. Org. Chem.* **2007**, *2007*, 1976-1982.
250. Tamborrini, M.; Oberli, M. A.; Werz, D. B.; Schürch, N.; Frey, J.; Seeberger, P. H.; Pluschke, G., Immuno-detection of anthrose containing tetrasaccharide in the exosporium of *Bacillus anthracis* and *Bacillus cereus* strains. *J. Appl. Microbiol.* **2009**, *106*, 1618-1628.
251. Tamborrini, M.; Holzer, M.; Seeberger, P. H.; Schürch, N.; Pluschke, G., Anthrax spore detection by a luminex assay based on monoclonal antibodies that recognize anthrose-containing oligosaccharides. *Clin. Vaccine. Immunol.* **2010**, *17*, 1446-1451.
252. Oberli, M. A.; Tamborrini, M.; Tsai, Y.-H.; Werz, D. B.; Horlacher, T.; Adibekian, A.; Gauss, D.; Möller, H. M.; Pluschke, G.; Seeberger, P. H., Molecular analysis of carbohydrate-antibody interactions: case study using a *Bacillus anthracis* tetrasaccharide. *J. Am. Chem. Soc.* **2010**, *132*, 10239-10241.
253. Adamo, R.; Saksena, R.; Kováč, P., Synthesis of the β -anomer of the spacer-equipped tetrasaccharide side chain of the major glycoprotein of the *Bacillus anthracis* exosporium. *Carbohydr. Res.* **2005**, *340*, 2579-2582.
254. Adamo, R.; Saksena, R.; Kováč, P., Studies towards a conjugate vaccine for Anthrax: synthesis of the tetrasaccharide side chain of the *Bacillus anthracis* exosporium. *Helv. Chim. Acta* **2006**, *89*, 1075-1089.
255. Saksena, R.; Adamo, R.; Kováč, P., Synthesis of the tetrasaccharide side chain of the major glycoprotein of the *Bacillus anthracis* exosporium. *Bioorg. Med. Chem. Lett.* **2006**, *16* (3), 615-617.
256. Saksena, R.; Adamo, R.; Kováč, P., Immunogens related to the synthetic tetrasaccharide side chain of the *Bacillus anthracis* exosporium. *Bioorg. Med. Chem.* **2007**, *15*, 4283-4310.
257. Saksena, R.; Adamo, R.; Kováč, P., Studies toward a conjugate vaccine for anthrax. Synthesis and characterization of anthrose [4,6-dideoxy-4-(3-hydroxy-3-methylbutanamido)-2-O-methyl-D-glucopyranose] and its methyl glycosides. *Carbohydr. Res.* **2005**, *340*, 1591-1600.
258. Parthasarathy, N.; Saksena, R.; Kováč, P.; DeShazer, D.; Peacock, S.; Wuthiekanun, V.; Heine, H.; Friedlander, A.; Cote, C.; Welkos, S., Application of carbohydrate microarray technology for the detection of *Burkholderia pseudomallei*, *Bacillus anthracis* and *Francisella tularensis* antibodies. *Carbohydr. Res.* **2008**, *343*, 2783-2788.
259. Wang, D.; Carroll, G. T.; Turro, N. J.; Koberstein, J. T.; Kováč, P.; Saksena, R.; Adamo, R.; Herzenberg, L. A.; Herzenberg, L. A.; Steinman, L., Photogenerated glycan arrays identify immunogenic sugar moieties of *Bacillus anthracis* exosporium. *Proteomics* **2007**, *7*, 180-184.

260. Kováč, P.; Hou, S., Conjugation-amenable tetrasaccharide of the side chain of the major glycoprotein of the *Bacillus anthracis* exosporium: A large-scale preparation. *Synthesis* **2009**, *2009*, 545-550.
261. Hou, S.; Kováč, P., A Convenient synthesis of furanose-free D-fucose per-*O*-acetates and a precursor for anthrose. *Eur. J. Org. Chem.* **2008**, *2008*, 1947-1952.
262. Kuehn, A.; Kováč, P.; Saksena, R.; Bannert, N.; Klee, S. R.; Ranisch, H.; Grunow, R., Development of antibodies against anthrose tetrasaccharide for specific detection of *Bacillus anthracis* spores. *Clin. Vaccine. Immunol.* **2009**, *16*, 1728-1737.
263. Mehta, A. S.; Saile, E.; Zhong, W.; Buskas, T.; Carlson, R.; Kannenberg, E.; Reed, Y.; Quinn, C. P.; Boons, G. J., Synthesis and antigenic analysis of the BclA glycoprotein oligosaccharide from the *Bacillus anthracis* exosporium. *Chem. Eur. J.* **2006**, *12*, 9136-49.
264. Saile, E.; Boons, G.-J.; Buskas, T.; Carlson, R. W.; Kannenberg, E. L.; Barr, J. R.; Boyer, A. E.; Gallegos-Candela, M.; Quinn, C. P., Antibody responses to a spore carbohydrate antigen as a marker of nonfatal inhalation anthrax in rhesus macaques. *Clin. Vaccine. Immunol.* **2011**, *18*, 743-748.
265. Crich, D.; Vinogradova, O., Synthesis of the antigenic tetrasaccharide side chain from the major glycoprotein of *Bacillus anthracis* exosporium. *J. Org. Chem.* **2007**, *72*, 6513-6520.
266. Dhénin, S. G.; Moreau, V.; Morel, N.; Nevers, M.-C.; Volland, H.; Créminon, C.; Djedäini-Pilard, F., Synthesis of an anthrose derivative and production of polyclonal antibodies for the detection of anthrax spores. *Carbohydr. Res.* **2008**, *343*, 2101-2110.
267. Dhénin, S. G.; Moreau, V.; Nevers, M.-C.; Créminon, C.; Djedäini-Pilard, F., Sensitive and specific enzyme immunoassays for antigenic trisaccharide from *Bacillus anthracis* spores. *Org. Biomol. Chem.* **2009**, *7*, 5184-5199.
268. Milhomme, O.; John, C.; Djedaini-Pilard, F.; Grandjean, C., Access to antigens related to anthrose using pivotal cyclic sulfite/sulfate intermediates. *J. Org. Chem.* **2011**, *76*, 5985-98.
269. Carlsen, P. H.; Katsuki, T.; Martin, V. S.; Sharpless, K. B., A greatly improved procedure for ruthenium tetroxide catalyzed oxidations of organic compounds. *J. Org. Chem.* **1981**, *46*, 3936-3938.
270. Kim, B. M.; Sharpless, K. B., Cyclic sulfates containing acid-sensitive groups and chemoselective hydrolysis of sulfate esters. *Tetrahedr. Lett.* **1989**, *30*, 655-658.
271. Vinogradov, E.; Nossova, L.; Korenevsky, A.; Beveridge, T. J., The structure of the capsular polysaccharide of *Shewanella oneidensis* strain MR-4. *Carbohydr. Res.* **2005**, *340*, 1750-1753.
272. Kubler-Kielb, J.; Vinogradov, E.; Hu, H.; Leppla, S. H.; Robbins, J. B.; Schneerson, R., Saccharides cross-reactive with *Bacillus anthracis* spore glycoprotein as an anthrax vaccine component. *Proc. Natl. Acad. Sci. USA.* **2008**, *105*, 8709-8712.

273. Milhomme, O.; Kohler, S. M.; Ropartz, D.; Lesur, D.; Pilard, S.; Djedaini-Pilard, F.; Beyer, W.; Grandjean, C., Synthesis and immunochemical evaluation of a non-methylated disaccharide analogue of the anthrax tetrasaccharide. *Org. Biomol. Chem.* **2012**, *10*, 8524-32.
274. Milhomme, O.; Dhenin, S. G.; Djedaini-Pilard, F.; Moreau, V.; Grandjean, C., Synthetic studies toward the anthrax tetrasaccharide: alternative synthesis of this antigen. *Carbohydr. Res.* **2012**, *356*, 115-31.
275. Wang, Y.; Liang, X.; Wang, P., Concise synthesis of *Bacillus anthracis* exosporium tetrasaccharide via two-stage activation of allyl glycosyl donor strategy. *Tetrahedr. Lett.* **2011**, *52*, 3912-3915.
276. Guo, H.; O'Doherty, G. A., De novo asymmetric synthesis of the anthrax tetrasaccharide by a palladium-catalyzed glycosylation reaction. *Angew. Chem. Int. Ed. Engl.* **2007**, *46*, 5206-8.
277. Guo, H.; O'Doherty, G. A., De novo asymmetric synthesis of anthrax tetrasaccharide and related tetrasaccharide. *J. Org. Chem.* **2008**, *73*, 5211-5220.
278. Babu, R. S.; O'Doherty, G. A., A palladium-catalyzed glycosylation reaction: the de novo synthesis of natural and unnatural glycosides. *J. Am. Chem. Soc.* **2003**, *125*, 12406-12407.
279. Wang, H. Y.; Guo, H.; O'Doherty, G. A., De novo asymmetric synthesis of oligo-rhamno di- and tri-saccharides related to the anthrax tetrasaccharide. *Tetrahedron* **2013**, *69*, 3432-3436.
280. De Ricco, R.; Ventura, C.; Carboni, F.; Saksena, R.; Kováč, P.; Adamo, R., Structure-immunogenicity relationship of α - and β -tetrasaccharide glycoforms from *Bacillus anthracis* exosporium and fragments thereof. *Molecules* **2018**, *23*, 2079.
281. Takeuchi, K.; Ono, H.; Yoshida, M.; Ishii, T.; Katoh, E.; Taguchi, F.; Miki, R.; Murata, K.; Kaku, H.; Ichinose, Y., Flagellin glycans from two pathovars of *Pseudomonas syringae* contain rhamnose in D and L configurations in different ratios and modified 4-amino-4, 6-dideoxyglucose. *J. Bacteriol.* **2007**, *189*, 6945-6956.
282. Choudhury, B.; Leoff, C.; Saile, E.; Wilkins, P.; Quinn, C. P.; Kannenberg, E. L.; Carlson, R. W., The structure of the major cell wall polysaccharide of *Bacillus anthracis* is species-specific. *J. Biol. Chem.* **2006**, *281*, 27932-27941.
283. Oberli, M. A.; Bindschädler, P.; Werz, D. B.; Seeberger, P. H., Synthesis of a hexasaccharide repeating unit from *Bacillus anthracis* vegetative cell walls. *Org. Lett.* **2008**, *10*, 905-908.
284. Vasan, M.; Rauvolfova, J.; Wolfert, M. A.; Leoff, C.; Kannenberg, E. L.; Quinn, C. P.; Carlson, R. W.; Boons, G. J., Chemical synthesis and immunological properties of oligosaccharides derived from the vegetative cell wall of *Bacillus anthracis*. *ChemBioChem* **2008**, *9*, 1716-20.
285. Leoff, C.; Saile, E.; Rauvolfova, J.; Quinn, C. P.; Hoffmaster, A. R.; Zhong, W.; Mehta, A. S.; Boons, G.-J.; Carlson, R. W.; Kannenberg, E. L., Secondary cell wall polysaccharides of *Bacillus anthracis* are antigens that contain specific epitopes which cross-react with three

- pathogenic *Bacillus cereus* strains that caused severe disease, and other epitopes common to all the *Bacillus cereus* strains tested. *Glycobiology* **2009**, *19*, 665-673.
286. Smartt, A. E.; Ripp, S., Bacteriophage reporter technology for sensing and detecting microbial targets. *Anal. Bioanal. Chem.* **2011**, *400*, 991-1007.
287. Loessner, M. J., Bacteriophage endolysins—current state of research and applications. *Curr. Opin. Microbiol.* **2005**, *8*, 480-487.
288. Mo, K. F.; Li, X.; Li, H.; Low, L. Y.; Quinn, C. P.; Boons, G. J., Endolysins of *Bacillus anthracis* bacteriophages recognize unique carbohydrate epitopes of vegetative cell wall polysaccharides with high affinity and selectivity. *J. Am. Chem. Soc.* **2012**, *134*, 15556-15562.
289. Gilad, J.; Harary, I.; Dushnitsky, T.; Schwartz, D.; Amsalem, Y., *Burkholderia mallei* and *Burkholderia pseudomallei* as bioterrorism agents: national aspects of emergency preparedness. *Isr. Med. Assoc. J.* **2007**, *9*, 499.
290. Wheelis, M., First shots fired in biological warfare. *Nature* **1998**, *395*, 213.
291. Choh, L.-C. C.; Ong, G.-H. O.; Vellasamy, K. M. K.; Kalaiselvam, K. K.; Kang, W.-T. K.; Al-Maleki, A. R. A.; Mariappan, V. V.; Vadivelu, J. J., *Burkholderia* vaccines: are we moving forward? *Front. Cell. Infect. Mi.* **2013**, *3*, 5.
292. Knirel, Y. A.; Paramonov, N. A.; Shashkov, A. S.; Kochetkov, N. K.; Yarullin, R. G.; Farber, S. M.; Efremenko, V. I., Structure of the polysaccharide chains of *Pseudomonas pseudomallei* lipopolysaccharides. *Carbohydr. Res.* **1992**, *233*, 185-193.
293. Tamigney Kenfack, M.; Bleriot, Y.; Gauthier, C., Intramolecular aglycon delivery enables the synthesis of 6-deoxy- β -D-manno-heptosides as fragments of *Burkholderia pseudomallei* and *Burkholderia mallei* capsular polysaccharide. *J. Org. Chem.* **2014**, *79*, 4615-34.
294. Ishiwata, A.; Lee, Y. J.; Ito, Y., Recent advances in stereoselective glycosylation through intramolecular aglycon delivery. *Org. Biomol. Chem.* **2010**, *8*, 3596-3608.
295. Marchetti, R.; Dillon, M. J.; Burtnick, M. N.; Hubbard, M. A.; Kenfack, M. T.; Blériot, Y.; Gauthier, C.; Brett, P. J.; AuCoin, D. P.; Lanzetta, R., *Burkholderia pseudomallei* capsular polysaccharide recognition by a monoclonal antibody reveals key details toward a biodefense vaccine and diagnostics against melioidosis. *ACS Chem. Biol.* **2015**, *10*, 2295-2302.
296. Scott, A. E.; Christ, W. J.; George, A. J.; Stokes, M. G.; Lohman, G. J.; Guo, Y.; Jones, M.; Titball, R. W.; Atkins, T. P.; Campbell, A. S.; Prior, J. L., Protection against experimental melioidosis with a synthetic *manno*-heptopyranose hexasaccharide glycoconjugate. *Bioconjugate Chem.* **2016**, *27*, 1435-1446.
297. Bayliss, M.; Donaldson, M. I.; Nepogodiev, S. A.; Pergolizzi, G.; Scott, A. E.; Harmer, N. J.; Field, R. A.; Prior, J. L., Structural characterisation of the capsular polysaccharide expressed by *Burkholderia thailandensis* strain E555:: *wbiI* (pKnock-KmR) and assessment of the significance of the 2-*O*-acetyl group in immune protection. *Carbohydr. Res.* **2017**, *452*, 17-24.

298. Heiss, C.; Burtnick, M. N.; Roberts, R. A.; Black, I.; Azadi, P.; Brett, P. J., Revised structures for the predominant O-polysaccharides expressed by *Burkholderia pseudomallei* and *Burkholderia mallei*. *Carbohydr. Res.* **2013**, *381*, 6-11.
299. Heiss, C.; Burtnick, M. N.; Black, I.; Azadi, P.; Brett, P. J., Detailed structural analysis of the O-polysaccharide expressed by *Burkholderia thailandensis* E264. *Carbohydr. Res.* **2012**, *363*, 23-28.
300. Yan, S. Q.; Wu, X. M.; Liang, X. M.; Zhang, J. J.; Wang, D. Q., Synthesis of di- and tetrasaccharide containing 6-deoxytalose from the O-antigenic polysaccharide of *B. pseudomallei* strain 304b. *Chin. Chem. Lett.* **2009**, *20*, 582-585.
301. Zong, G.; Cai, X.; Liang, X.; Zhang, J.; Wang, D., Facile syntheses of the disaccharide repeating unit of the O-antigenic polysaccharide of *Burkholderia pseudomallei* strain 304b and its dimer and trimer. *Carbohydr. Res.* **2011**, *346*, 2533-9.
302. Nimtz, M.; Wray, V.; Domke, T.; Brenneke, B.; Häussler, S.; Steinmetz, I., Structure of an acidic exopolysaccharide of *Burkholderia pseudomallei*. *Eur. J. Biochem.* **1997**, *250*, 608-616.
303. Masoud, H.; Ho, M.; Schollaardt, T.; Perry, M. B., Characterization of the capsular polysaccharide of *Burkholderia (Pseudomonas) pseudomallei* 304b. *J. Bacteriol.* **1997**, *179*, 5663-5669.
304. Steinmetz, I.; Rohde, M.; Brenneke, B., Purification and characterization of an exopolysaccharide of *Burkholderia (Pseudomonas) pseudomallei*. *Infect. Immun.* **1995**, *63*, 3959-3965.
305. Laroussarie, A.; Barycza, B.; Andriamboavonjy, H.; Tamigney Kenfack, M.; Bleriot, Y.; Gauthier, C., Synthesis of the tetrasaccharide repeating unit of the β -Kdo-containing exopolysaccharide from *Burkholderia pseudomallei* and *B. cepacia* complex. *J. Org. Chem.* **2015**, *80*, 10386-10396.
306. Elkins, K. L.; Cowley, S. C.; Collazo, C. M., Francisella: a little bug hits the big time. *Expert Rev. Vacc.* **2003**, *2*, 735-738.
307. Ellis, J.; Oyston, P. C.; Green, M.; Titball, R. W., Tularemia. *Clin. Microbiol. Rev.* **2002**, *15*, 631-46.
308. Tigertt, W., Soviet viable *Pasteurella tularensis* vaccines - a review of selected articles. *Bacteriol. Rev.* **1962**, *26*, 354.
309. Conlan, J. W.; Shen, H.; Webb, A.; Perry, M. B., Mice vaccinated with the O-antigen of *Francisella tularensis* LVS lipopolysaccharide conjugated to bovine serum albumin develop varying degrees of protective immunity against systemic or aerosol challenge with virulent type A and type B strains of the pathogen. *Vaccine* **2002**, *20*, 3465-3471.
310. Conlan, J. W.; Vinogradov, E.; Monteiro, M. A.; Perry, M. B., Mice intradermally-inoculated with the intact lipopolysaccharide, but not the lipid A or O-chain, from *Francisella tularensis*

- LVS rapidly acquire varying degrees of enhanced resistance against systemic or aerogenic challenge with virulent strains of the pathogen. *Microb. Pathog.* **2003**, *34*, 39-45.
311. Gregory, S. H.; Chen, W. H.; Mott, S.; Palardy, J. E.; Parejo, N. A.; Heninger, S.; Anderson, C. A.; Artenstein, A. W.; Opal, S. M.; Cross, A. S., Detoxified endotoxin vaccine (J5dLPS/OMP) protects mice against lethal respiratory challenge with *Francisella tularensis* SchuS4. *Vaccine* **2010**, *28*, 2908-2915.
312. Boltje, T. J.; Zhong, W.; Park, J.; Wolfert, M. A.; Chen, W.; Boons, G. J., Chemical synthesis and immunological evaluation of the inner core oligosaccharide of *Francisella tularensis*. *J. Am. Chem. Soc.* **2012**, *134*, 14255-62.
313. Boltje, T. J.; Li, C.; Boons, G.-J., Versatile set of orthogonal protecting groups for the preparation of highly branched oligosaccharides. *Org. Lett.* **2010**, *12*, 4636-4639.
314. Vinogradov, E.; Perry, M. B.; Conlan, J. W., Structural analysis of *Francisella tularensis* lipopolysaccharide. *Eur. J. Biochem.* **2002**, *269*, 6112-6118.
315. Jensen, H. H.; Nordstrøm, L. U.; Bols, M., The disarming effect of the 4,6-acetal group on glycoside reactivity: torsional or electronic? *J. Am. Chem. Soc.* **2004**, *126*, 9205-9213.
316. Georgiev, V. S., Defense against biological weapons (biodefense). In Georgiev, V. S. (Ed.) *Impact on Global Health*, National Institute of Allergy and Infectious Diseases, NIH, Humana Press, **2009**, 221-305.
317. Inglesby, T. V.; Dennis, D. T.; Henderson, D. A.; Bartlett, J. G.; Ascher, M. S.; Eitzen, E.; Fine, A. D.; Friedlander, A. M.; Hauer, J.; Koerner, J. F., Plague as a biological weapon: medical and public health management. *J. Amer. Med. Assoc.* **2000**, *283*, 2281-2290.
318. Atlas, R. M., Bioterrorism: from threat to reality. *Ann. Rev. Microbiol.* **2002**, *56*, 167-185.
319. Gilligan, P. H., Therapeutic challenges posed by bacterial bioterrorism threats. *Curr. Opin. Microbiol.* **2002**, *5*, 489-495.
320. Raetz, C. R.; Whitfield, C., Lipopolysaccharide endotoxins. *Ann. Rev. Biochem.* **2002**, *71*, 635-700.
321. Raetz, C. R.; Reynolds, C. M.; Trent, M. S.; Bishop, R. E., Lipid A modification systems in gram-negative bacteria. *Ann. Rev. Biochem.* **2007**, *76*, 295-329.
322. Holst, O.; Brade, H., Chemical structure of the core region of lipopolysaccharides. In Brade, H.; Opal, S. M.; Vogel, S. N.; Morrison, D. C. (Eds) *Endotoxin in Health and Disease*, New York, **1999**, 115-154.
323. Ohara, T.; Adibekian, A.; Esposito, D.; Stallforth, P.; Seeberger, P. H., Towards the synthesis of a *Yersinia pestis* cell wall polysaccharide: enantioselective synthesis of an L-glycero-D-manno-heptose building block. *Chem. Commun.* **2010**, *46*, 4106-4108.
324. Anish, C.; Guo, X.; Wahlbrink, A.; Seeberger, P. H., Plague detection by anti-carbohydrate antibodies. *Angew. Chem. Int. Ed. Engl.* **2013**, *52*, 9524-9528.

325. Yang, Y.; Oishi, S.; Martin, C. E.; Seeberger, P. H., Diversity-oriented synthesis of inner core oligosaccharides of the lipopolysaccharide of pathogenic Gram-negative bacteria. *J. Am. Chem. Soc.* **2013**, *135*, 6262-6271.
326. Itoh, Y.; Wang, X.; Hinnebusch, B. J.; Preston, J. F.; Romeo, T., Depolymerization of β -1,6-*N*-acetyl-D-glucosamine disrupts the integrity of diverse bacterial biofilms. *J. Bacteriol.* **2005**, *187*, 382-387.
327. Rohde, H.; Frankenberger, S.; Zähringer, U.; Mack, D., Structure, function and contribution of polysaccharide intercellular adhesin (PIA) to *Staphylococcus epidermidis* biofilm formation and pathogenesis of biomaterial-associated infections. *Eur. J. Cell Biol.* **2010**, *89*, 103-111.
328. Leung, C.; Chibba, A.; Gomez-Biagi, R. F.; Nitz, M., Efficient synthesis and protein conjugation of β -(1 \rightarrow 6)-D-*N*-acetylglucosamine oligosaccharides from the polysaccharide intercellular adhesin. *Carbohydr. Res.* **2009**, *344*, 570-575.
329. Boschioli, M.-L.; Foulongne, V.; O'Callaghan, D., Brucellosis: a worldwide zoonosis. *Curr. Opin. Microbiol.* **2001**, *4*, 58-64.
330. Young, E. J., An overview of human brucellosis. *Clin. Infect. Dis.* **1995**, *21*, 283-289.
331. Nielsen, K., Diagnosis of brucellosis by serology. *Vet. Microbiol.* **2002**, *90*, 447-459.
332. Mandal, S. S.; Duncombe, L.; Ganesh, N. V.; Sarkar, S.; Howells, L.; Hogarth, P. J.; Bundle, D. R.; McGiven, J., Novel solutions for vaccines and diagnostics to combat brucellosis. *ACS Cent. Sci.* **2017**, *3*, 224-231.
333. Wilson, G.; Miles, A., The serological differentiation of smooth strains of the *Brucella* group. *Brit. J. Exp. Pathol.* **1932**, *13*, 1.
334. Caroff, M.; Bundle, D.; Perry, M.; Cherwonogrodzky, J.; Duncan, J., Antigenic S-type lipopolysaccharide of *Brucella abortus* 1119-3. *Infect. Immun.* **1984**, *46*, 384-388.
335. Bundle, D. R.; Cherwonogrodzky, J.; Perry, M. B., Structural elucidation of the *Brucella melitensis* M antigen by high-resolution NMR at 500 MHz. *Biochemistry* **1987**, *26*, 8717-8726.
336. Meikle, P. J.; Perry, M.; Cherwonogrodzky, J.; Bundle, D., Fine structure of A and M antigens from *Brucella biovars*. *Infect. Immun.* **1989**, *57*, 2820-2828.
337. Bundle, D.; Cherwonogrodzky, J.; Gidney, M.; Meikle, P.; Perry, M.; Peters, T., Definition of *Brucella* A and M epitopes by monoclonal typing reagents and synthetic oligosaccharides. *Infect. Immun.* **1989**, *57*, 2829-2836.
338. Zaccheus, M. V.; Ali, T.; Cloeckert, A.; Zygmunt, M. S.; Weintraub, A.; Iriarte, M.; Moriyón, I.; Widmalm, G., The epitopic and structural characterization of *Brucella suis* biovar 2 O-polysaccharide demonstrates the existence of a new M-negative C-negative smooth *Brucella* serovar. *PLoS ONE* **2013**, *8*, e53941.

339. Kubler-Kielb, J.; Vinogradov, E., Reinvestigation of the structure of *Brucella* O-antigens. *Carbohydr. Res.* **2013**, *378*, 144-147.
340. Bundle, D. R.; Gerken, M.; Peters, T., Synthesis of antigenic determinants of the *Brucella* A antigen, utilizing methyl 4-azido-4,6-dideoxy- α -D-mannopyranoside efficiently derived from D-mannose. *Carbohydr. Res.* **1988**, *174*, 239-251.
341. Peters, T.; Bundle, D. R., Synthetic antigenic determinants of the *Brucella* A polysaccharide: A disaccharide thioglycoside for block synthesis of pentasaccharide and lower homologues of α 1,2-linked 4,6-dideoxy-4-formamido- α -D-mannose. *Can. J. Chem.* **1989**, *67*, 491-496.
342. Peters, T.; Bundle, D. R., Block synthesis of two pentasaccharide determinants of the *Brucella* M antigen using thioglycoside methodologies. *Can. J. Chem.* **1989**, *67*, 497-502.
343. Eichler, E.; Kihlberg, J.; Bundle, D. R., Access to fluorescent probes via allyl glycosides: the synthesis of a *Brucella* trisaccharide epitope linked to a coumarin. *Glycoconj. J.* **1991**, *8*, 69-74.
344. Kihlberg, J.; Eichler, E.; Bundle, D. R., The design and synthesis of antibody binding site probes: three pentasaccharide analogues of the *Brucella* A antigen prepared by activation in situ of thioglycosides with bromine. *Carbohydr. Res.* **1991**, *211*, 59-75.
345. Kihlberg, J.; Bundle, D. R., The synthesis of antibody binding-site probes: a hexasaccharide and two pentasaccharides related to the *Brucella* A antigen and prepared by in situ activation of thioglycosides with bromine. *Carbohydr. Res.* **1992**, *216*, 67-78.
346. Bundle, D. R.; McGiven, J., Brucellosis: improved diagnostics and vaccine insights from synthetic glycans. *Acc. Chem. Res.* **2017**, *50*, 2958-2967.
347. Guiard, J.; Paszkiewicz, E.; Sadowska, J.; Bundle, D. R., Design and synthesis of a universal antigen to detect brucellosis. *Angew. Chem. Int. Ed. Engl.* **2013**, *52*, 7181-5.
348. Ganesh, N. V.; Sadowska, J. M.; Sarkar, S.; Howells, L.; McGiven, J.; Bundle, D. R., Molecular recognition of *Brucella* A and M antigens dissected by synthetic oligosaccharide glycoconjugates leads to a disaccharide diagnostic for brucellosis. *J. Am. Chem. Soc.* **2014**, *136*, 16260-16269.
349. McGiven, J.; Howells, L.; Duncombe, L.; Stack, J.; Ganesh, N. V.; Guiard, J.; Bundle, D. R., Improved serodiagnosis of bovine brucellosis by novel synthetic oligosaccharide antigens representing the capping M epitope elements of *Brucella* O-polysaccharide. *J. Clin. Microbiol.* **2015**, *53*, 1204-1210.
350. Mandal, S. S.; Ganesh, N. V.; Sadowska, J. M.; Bundle, D. R., Synthetic glycoconjugates characterize the fine specificity of *Brucella* A and M monoclonal antibodies. *Org. Biomol. Chem.* **2017**, *15*, 3874-3883.
351. Dance, D., Melioidosis: the tip of the iceberg? *Clin. Microbiol. Rev.* **1991**, *4*, 52-60.

352. Cheng, A. C.; Currie, B. J., Melioidosis: epidemiology, pathophysiology, and management. *Clin. Microbiol. Rev.* **2005**, *18*, 383-416.
353. Keluangkhot, V.; Pethsouvanh, R.; Strobel, M., Mélioiidose. *Med. Maladies Infect.* **2005**, *35*, 469-475.
354. Currie, B. J. Melioidosis: evolving concepts in epidemiology, pathogenesis, and treatment, In *Seminars in respiratory and critical care medicine*, Thieme Medical Publishers, **2015**, 111-125.
355. Khan, I.; Wieler, L.; Melzer, F.; Elschner, M.; Muhammad, G.; Ali, S.; Sprague, L.; Neubauer, H.; Saqib, M., Glanders in animals: a review on epidemiology, clinical presentation, diagnosis and countermeasures. *Transbound. Emerg. Dis.* **2013**, *60*, 204-221.
356. Limmathurotsakul, D.; Wongratanacheewin, S.; Teerawattanasook, N.; Wongsuvan, G.; Chaisuksant, S.; Chetchotisakd, P.; Chaowagul, W.; Day, N. P.; Peacock, S. J., Increasing incidence of human melioidosis in Northeast Thailand. *Am. J. Trop. Med. Hyg.* **2010**, *82*, 1113-1117.
357. Wiersinga, W. J.; Currie, B. J.; Peacock, S. J., Melioidosis. *N. Engl. J. Med.* **2012**, *367*, 1035-1044.
358. U.S. Department of Health and Human Services; Centers for Disease Control and Prevention and US Department of Agriculture, Animal and Plant Health Inspection Services. *2017 Annual Report of the Federal Select Agent Program*, **2018**.
359. Titball, R. W.; Burtnick, M. N.; Bancroft, G. J.; Brett, P., *Burkholderia pseudomallei* and *Burkholderia mallei* vaccines: are we close to clinical trials? *Vaccine* **2017**, *35*, 5981-5989.
360. Muruato, L. A.; Tapia, D.; Hatcher, C. L.; Kalita, M.; Brett, P. J.; Gregory, A. E.; Samuel, J. E.; Titball, R. W.; Torres, A. G., Use of reverse vaccinology in the design and construction of nanoglycoconjugate vaccines against *Burkholderia pseudomallei*. *Clin. Vaccine Immunol.* **2017**, *24*, e00206-17.
361. Cloutier, M.; Muru, K.; Ravicoularamin, G.; Gauthier, C., Polysaccharides from *Burkholderia* species as targets for vaccine development, immunomodulation and chemical synthesis. *Nat. Prod. Rep.* **2018**, *35*, 1251-1293.
362. Bryan, L. E.; Wong, S.; Woods, D. E.; Dance, D. A.; Chaowagul, W., Passive protection of diabetic rats with antisera specific for the polysaccharide portion of the lipopolysaccharide isolated from *Pseudomonas pseudomallei*. *Can. J. Infect. Dis. Med.* **1994**, *5*, 170-178.
363. Ho, M.; Schollaardt, T.; Smith, M. D.; Perry, M. B.; Brett, P. J.; Chaowagul, W.; Bryan, L. E., Specificity and functional activity of anti-*Burkholderia pseudomallei* polysaccharide antibodies. *Infect. Immun.* **1997**, *65*, 3648-3653.
364. Jones, S.; Ellis, J.; Russell, P.; Griffin, K.; Oyston, P., Passive protection against *Burkholderia pseudomallei* infection in mice by monoclonal antibodies against capsular polysaccharide, lipopolysaccharide or proteins. *J. Med. Microbiol.* **2002**, *51*, 1055-1062.

365. Treviño, S. R.; Permenter, A. R.; England, M. J.; Parthasarathy, N.; Gibbs, P. H.; Waag, D. M.; Chanh, T. C., Monoclonal antibodies passively protect BALB/c mice against *Burkholderia mallei* aerosol challenge. *Infect. Immun.* **2006**, *74*, 1958-1961.
366. Zhang, S.; Feng, S.-H.; Li, B.; Kim, H.-Y.; Rodriguez, J.; Tsai, S.; Lo, S.-C., In vitro and in vivo studies on monoclonal antibodies with prominent bactericidal activity against *Burkholderia pseudomallei* and *Burkholderia mallei*. *Clin. Vaccine Immunol.* **2011**, *18*, 825-834.
367. AuCoin, D. P.; Reed, D. E.; Marlenee, N. L.; Bowen, R. A.; Thorkildson, P.; Judy, B. M.; Torres, A. G.; Kozel, T. R., Polysaccharide specific monoclonal antibodies provide passive protection against intranasal challenge with *Burkholderia pseudomallei*. *PLoS ONE* **2012**, *7*, e35386.
368. Scott, A. E.; Ngugi, S. A.; Laws, T. R.; Corser, D.; Lonsdale, C. L.; D'Elia, R. V.; Titball, R. W.; Williamson, E. D.; Atkins, T. P.; Prior, J. L., Protection against experimental melioidosis following immunisation with a lipopolysaccharide-protein conjugate. *J. Immunol. Res.* **2014**, *2014*, 392170.
369. Anuntagool, N.; Wuthiekanun, V.; White, N. J.; Currie, B. J.; Sermswan, R. W.; Wongratanacheewin, S.; Taweechaisupapong, S.; Chaiyaroj, S. C.; Sirisinha, S., Lipopolysaccharide heterogeneity among *Burkholderia pseudomallei* from different geographic and clinical origins. *Am. J. Trop. Med. Hyg.* **2006**, *74*, 348-352.
370. Knirel, Y. A.; Paramonov, N. A.; Shashkov, A. S.; Kochetkov, N. K.; Yarullin, R. G.; Farber, S. M.; Efremenko, V. I., Structure of the polysaccharide chains of *Pseudomonas pseudomallei* lipopolysaccharides. *Carbohydr. Res.* **1992**, *233*, 185-193.
371. Perry, M. B.; MacLean, L. L.; Schollaardt, T.; Bryan, L. E.; Ho, M., Structural characterization of the lipopolysaccharide O antigens of *Burkholderia pseudomallei*. *Infect. Immun.* **1995**, *63*, 3348-3352.
372. Burtnick, M. N.; Brett, P. J.; Woods, D. E., Molecular and physical characterization of *Burkholderia mallei* O antigens. *J. Bacteriol.* **2002**, *184*, 849-852.
373. Brett, P. J.; Burtnick, M. N.; Woods, D. E., The *wbiA* locus is required for the 2-O-acetylation of lipopolysaccharides expressed by *Burkholderia pseudomallei* and *Burkholderia thailandensis*. *FEMS Microbiol. Lett.* **2003**, *218*, 323-328.
374. Heiss, C.; Burtnick, M. N.; Roberts, R. A.; Black, I.; Azadi, P.; Brett, P. J., Revised structures for the predominant O-polysaccharides expressed by *Burkholderia pseudomallei* and *Burkholderia mallei*. *Carbohydr. Res.* **2013**, *381*, 6-11.
375. Heiss, C.; Burtnick, M. N.; Black, I.; Azadi, P.; Brett, P. J., Detailed structural analysis of the O-polysaccharide expressed by *Burkholderia thailandensis* E264. *Carbohydr. Res.* **2012**, *363*, 23-28.
376. Wada, T.; Ohkubo, A.; Mochizuki, A.; Sekine, M., 2-(Azidomethyl) benzoyl as a new protecting group in nucleosides. *Tetrahedr. Lett.* **2001**, *42*, 1069-1072.

377. Love, K. R.; Andrade, R. B.; Seeberger, P. H., Linear synthesis of a protected H-type II pentasaccharide using glycosyl phosphate building blocks. *J. Org. Chem.* **2001**, *66*, 8165-8176.
378. Arasappan, A.; Fuchs, P., Regiospecific 4,6-functionalization of pyranosides via dimethylboron bromide-mediated cleavage of phthalide orthoesters. *J. Am. Chem. Soc.* **1995**, *117*, 177-183.
379. Gauthier, C.; Chassagne, P.; Theillet, F.-X.; Guerreiro, C.; Thouron, F.; Nato, F.; Delepierre, M.; Sansonetti, P. J.; Phalipon, A.; Mulard, L. A., Non-stoichiometric O-acetylation of *Shigella flexneri* 2a O-specific polysaccharide: synthesis and antigenicity. *Org. Biomol. Chem.* **2014**, *12*, 4218-4232.
380. Lian, G.; Zhang, X.; Yu, B., Thioglycosides in carbohydrate research. *Carbohydr. Res.* **2015**, *403*, 13-22.
381. Frihed, T. G.; Pedersen, C. M.; Bols, M., Synthesis of all eight stereoisomeric 6-deoxy-L-hexopyranosyl donors—trends in using stereoselective reductions or Mitsunobu epimerizations. *Eur. J. Org. Chem.* **2014**, *2014*, 7924-7939.
382. Ellervik, U.; Grundberg, H.; Magnusson, G., Synthesis of lactam and acetamido analogues of sialyl Lewis X tetrasaccharide and Lewis X trisaccharide. *J. Org. Chem.* **1998**, *63*, 9323-9338.
383. Wang, C.-C.; Lee, J.-C.; Luo, S.-Y.; Kulkarni, S. S.; Huang, Y.-W.; Lee, C.-C.; Chang, K.-L.; Hung, S.-C., Regioselective one-pot protection of carbohydrates. *Nature* **2007**, *446*, 896-899.
384. Neises, B.; Steglich, W., Simple method for the esterification of carboxylic acids. *Angew. Chem. Int. Ed. Engl.* **1978**, *17*, 522-524.
385. Baudry, D.; Ephritikhine, M.; Felkin, H., Isomerisation of allyl ethers catalysed by the cationic iridium complex [Ir(cyclo-octa-1,5-diene)(PMePh₂)₂]PF₆. A highly stereoselective route to *trans*-propenyl ethers. *J. Chem. Soc. Chem. Commun.* **1978**, 694-695.
386. Oltvoort, J.; Van Boeckel, C.; De Koning, J.; Van Boom, J., Use of the cationic iridium complex 1,5-cyclooctadiene-bis[methyldiphenylphosphine]-iridium hexafluorophosphate in carbohydrate chemistry: Smooth isomerization of allyl ethers to 1-propenyl ethers. *Synthesis* **1981**, *1981*, 305-308.
387. Nashed, M. A.; Anderson, L., Iodine as a reagent for the ready hydrolysis of prop-1-enyl glycosides, or their conversion into oxazolines. *J. Chem. Soc. Chem. Commun.* **1982**, 1274-1276.
388. Baker, D. C., Preparative carbohydrate chemistry, *J. Am. Chem. Soc.* **1997**, *119*, 12028-12029.
389. Schmidt, R. R.; Michel, J., Facile synthesis of α - and β -O-glycosyl imidates; preparation of glycosides and disaccharides. *Angew. Chem. Int. Ed. Engl.* **1980**, *19*, 731-732.

390. Schmidt, R. R., New methods for the synthesis of glycosides and oligosaccharides—are there alternatives to the Koenigs-Knorr method? *Angew. Chem. Int. Ed. Engl.* **1986**, *25*, 212-235.
391. Schmidt, R. R.; Kinzy, W., Anomeric-oxygen activation for glycoside synthesis: the trichloroacetimidate method. In *Adv. Carbohydr. Chem. Biochem.*, Academic Press, **1994**, *50*, 21-123.
392. Schmidt, R. R.; Jung, K.-H., Oligosaccharide synthesis with trichloroacetimidates. *Prep. Carbohydr. Chem.* **1997**, *1*, 283-312.
393. Mukhopadhyay, B.; Field, R. A., Convergent synthesis of a trisaccharide as its 2-(trimethylsilyl)ethyl glycoside related to the flavonoid triglycoside from *Gymnema sylvestre*. *Carbohydr. Res.* **2006**, *341*, 1697-1701.
394. Konradsson, P.; Mootoo, D. R.; McDevitt, R. E.; Fraser-Reid, B., Iodonium ion generated in situ from *N*-iodosuccinimide and trifluoromethanesulphonic acid promotes direct linkage of 'disarmed' pent-4-enyl glycosides. *J. Chem. Soc. Chem. Commun.* **1990**, *1990*, 270-272.
395. Konradsson, P.; Udodong, U. E.; Fraser-Reid, B., Iodonium promoted reactions of disarmed thioglycosides. *Tetrahedr. Lett.* **1990**, *31*, 4313-4316.
396. Hodosi, G.; Kováč, P., Epimerization of carbohydrates via stannylene acetals. A practical synthesis of D-talose. *J. Carbohydr. Chem.* **1998**, *17*, 557-565.
397. Miethchen, R., Epimerization by non-classical acetalization—a new three component reaction for carbohydrates and inositols. *J. Carbohydr. Chem.* **2003**, *22*, 801-825.
398. Mitsunobu, O., The use of diethyl azodicarboxylate and triphenylphosphine in synthesis and transformation of natural products. *Synthesis* **1981**, *1981*, 1-28.
399. Banaszek, A., Synthesis of isomeric benzyl 6-deoxy- α -L-talo- and α -L-gulopyranosides. *J. Carbohydr. Chem.* **1994**, *13*, 285-291.
400. Sanapala, S. R.; Kulkarni, S. S., From L-rhamnose to rare 6-deoxy-L-hexoses. *Org. Lett.* **2016**, *18*, 3790-3793.
401. Muskat, I. E., The mechanism of walden inversion in sugars: the inversion of *p*-toluenesulfonyl esters of rhamnose. *J. Am. Chem. Soc.* **1934**, *56*, 2653-2656.
402. Song, W.; Cai, J.; Zou, X.; Wang, X.; Hu, J.; Yin, J., Applications of controlled inversion strategies in carbohydrate synthesis. *Chin. Chem. Lett.* **2018**, *29*, 27-34.
403. Aspinall, G. O., Derivatives of 6-deoxy-L-talose and the synthesis of 6-deoxy-2-O-(α -L-rhamnopyranosyl)-L-talose. *Carbohydr. Res.* **1983**, *121*, 61-77.
404. Zsoldos-Mády, V.; Zbiral, E., A new approach to 6-deoxy-D-allofuranose- and 6-deoxy-L-talofuranose derivatives from 1,2:5,6-di-O-isopropylidene α -D-glucofuranose. *Monatsh. Chem.* **1986**, *117*, 1325-1338.

405. Cai, X.; Zong, G.; Xu, Y.; Zhang, J.; Liang, X.; Wang, D., Efficient synthesis of a 6-deoxytalose tetrasaccharide related to the antigenic O-polysaccharide produced by *Aggregatibacter actinomycetemcomitans* serotype c. *Carbohydr. Res.* **2010**, *345*, 1230-1234.
406. Ohara, K.; Lin, C.-C.; Yang, P.-J.; Hung, W.-T.; Yang, W.-B.; Cheng, T.-J. R.; Fang, J.-M.; Wong, C.-H., Synthesis and bioactivity of β -(1 \rightarrow 4)-linked oligomannoses and partially acetylated derivatives. *J. Org. Chem.* **2013**, *78*, 6390-6411.
407. Suttisunhakul, V.; Wuthiekanun, V.; Brett, P. J.; Khusmith, S.; Day, N. P.; Burtnick, M. N.; Limmathurotsakul, D.; Chantratita, N., Development of rapid enzyme-linked immunosorbent assays for detection of antibodies to *Burkholderia pseudomallei*. *J. Clin. Microbiol.* **2016**, *54*, 1259-1268.
408. Burtnick, M. N.; Heiss, C.; Schuler, A.; Azadi, P.; Brett, P. J., Development of novel O-polysaccharide based glycoconjugates for immunization against glanders. *Front. Cell. Infect. Microbiol.* **2012**, *2*, 148.
409. Murray, C. J.; Barber, R. M.; Foreman, K. J.; Ozgoren, A. A.; Abd-Allah, F.; Abera, S. F.; Aboyans, V.; Abraham, J. P.; Abubakar, I.; Abu-Raddad, L. J., Global, regional, and national disability-adjusted life years (DALYs) for 306 diseases and injuries and healthy life expectancy (HALE) for 188 countries, 1990–2013: quantifying the epidemiological transition. *Lancet* **2015**, *386*, 2145-2191.
410. Abubakar, I.; Tillmann, T.; Banerjee, A., Global, regional, and national age-sex specific all-cause and cause-specific mortality for 240 causes of death, 1990-2013: a systematic analysis for the Global Burden of Disease Study 2013. *Lancet* **2015**, *385*, 117-171.
411. Kotloff, K. L.; Nataro, J. P.; Blackwelder, W. C.; Nasrin, D.; Farag, T. H.; Panchalingam, S.; Wu, Y.; Sow, S. O.; Sur, D.; Breiman, R. F., Burden and aetiology of diarrhoeal disease in infants and young children in developing countries (the Global Enteric Multicenter Study, GEMS): a prospective, case-control study. *Lancet* **2013**, *382*, 209-222.
412. Liu, J.; Platts-Mills, J. A.; Juma, J.; Kabir, F.; Nkeze, J.; Okoi, C.; Operario, D. J.; Uddin, J.; Ahmed, S.; Alonso, P. L., Use of quantitative molecular diagnostic methods to identify causes of diarrhoea in children: a reanalysis of the GEMS case-control study. *Lancet* **2016**, *388*, 1291-1301.
413. Platts-Mills, J. A.; Babji, S.; Bodhidatta, L.; Gratz, J.; Haque, R.; Havt, A.; McCormick, B. J.; McGrath, M.; Olortegui, M. P.; Samie, A., Pathogen-specific burdens of community diarrhoea in developing countries: a multisite birth cohort study (MAL-ED). *Lancet Glob. Health* **2015**, *3*, e564-e575.
414. Murray, C. J.; Vos, T.; Lozano, R.; Naghavi, M.; Flaxman, A. D.; Michaud, C.; Ezzati, M.; Shibuya, K.; Salomon, J. A.; Abdalla, S., Disability-adjusted life years (DALYs) for 291 diseases and injuries in 21 regions, 1990–2010: a systematic analysis for the Global Burden of Disease Study 2010. *Lancet* **2012**, *380*, 2197-2223.

415. Batz, M. B.; Hoffmann, S.; Morris Jr, J. G., Ranking the disease burden of 14 pathogens in food sources in the United States using attribution data from outbreak investigations and expert elicitation. *J. Food Prot.* **2012**, *75*, 1278-1291.
416. Jagusztyn-Krynicka, E. K.; Łaniewski, P.; Wyszynska, A., Update on *Campylobacter jejuni* vaccine development for preventing human campylobacteriosis. *Exp. Rev. Vacc.* **2009**, *8*, 625-645.
417. O’Ryan, M.; Vidal, R.; del Canto, F.; Carlos Salazar, J.; Montero, D., Vaccines for viral and bacterial pathogens causing acute gastroenteritis: Part II: Vaccines for *Shigella*, *Salmonella*, enterotoxigenic *E. coli* (ETEC), enterohemorrhagic *E. coli* (EHEC) and *Campylobacter jejuni*. *Hum. Vacc. Immunother.* **2015**, *11*, 601-619.
418. Hansson, I.; Sandberg, M.; Habib, I.; Lowman, R.; Engvall, E., Knowledge gaps in control of *Campylobacter* for prevention of campylobacteriosis. *Transbound. Emerg. Dis.* **2018**, *65*, 30-48.
419. Kaakoush, N. O.; Castaño-Rodríguez, N.; Mitchell, H. M.; Man, S. M., Global epidemiology of *Campylobacter* infection. *Clin. Microbiol. Rev.* **2015**, *28*, 687-720.
420. Lindow, J.; Poly, F.; Tribble, D.; Guerry, P.; Carmolli, M.; Baqar, S.; Porter, C.; Pierce, K.; Darsley, M.; Sadigh, K., Caught in the act: in vivo development of macrolide resistance to *Campylobacter jejuni* infection. *J. Clin. Microbiol.* **2010**, *48*, 3012-3015.
421. Kittl, S.; Kuhnert, P.; Hächler, H.; Korczak, B., Comparison of genotypes and antibiotic resistance of *Campylobacter jejuni* isolated from humans and slaughtered chickens in Switzerland. *J. Appl. Microbiol.* **2011**, *110*, 513-520.
422. Zhao, S.; Young, S.; Tong, E.; Abbott, J.; Womack, N.; Friedman, S.; McDermott, P., Antimicrobial resistance of *Campylobacter* isolates from retail meat in the United States between 2002 and 2007. *Appl. Environ. Microbiol.* **2010**, *76*, 7949-7956.
423. Crich, D.; Banerjee, A., Stereocontrolled synthesis of the D- and L-glycero- β -D-manno-heptopyranosides and their 6-deoxy analogues. Synthesis of methyl α -L-rhamno-pyranosyl-(1 \rightarrow 3)-D-glycero- β -D-manno-heptopyranosyl-(1 \rightarrow 3)-6-deoxy-glycero- β -D-manno-heptopyranosyl-(1 \rightarrow 4)- α -L-rhamno-pyranoside, a tetrasaccharide subunit of the lipopolysaccharide from *Plesimonas shigelloides*. *J. Am. Chem. Soc.* **2006**, *128*, 8078-8086.
424. Centers for Disease Control and Prevention (US). *Antibiotic resistance threats in the United States, 2019*. US Department of Health and Human Services, CDC, **2019**.
425. Kuwabara, S.; Yuki, N., Axonal Guillain-Barré syndrome: concepts and controversies. *Lancet Neurol.* **2013**, *12*, 1180-1188.
426. Moran, A.; Appelmelk, B.; Aspinall, G., Molecular mimicry of host structures by lipopolysaccharides of *Campylobacter* and *Helicobacter* spp.: implications in pathogenesis. *J. Endotoxin Res.* **1996**, *3*, 521-531.

427. Moran, A.; O'Malley, D., Potential role of lipopolysaccharides of *Campylobacter jejuni* in the development of Guillain-Barré syndrome. *J. Endotoxin Res.* **1995**, *2*, 233-235.
428. Aspinall, G. O.; McDonald, A. G.; Pang, H.; Kurjanczyk, L. A.; Penner, J. L., Lipopolysaccharides of *Campylobacter jejuni* serotype O: 19: structures of core oligosaccharide regions from the serostrain and two bacterial isolates from patients with the Guillain-Barré syndrome. *Biochemistry* **1994**, *33*, 241-249.
429. Yuki, N.; Taki, T.; Inagaki, F.; Kasama, T.; Takahashi, M.; Saito, K.; Handa, S.; Miyatake, T., A bacterium lipopolysaccharide that elicits Guillain-Barré syndrome has a GM1 ganglioside-like structure. *J. Exp. Med.* **1993**, *178*, 1771-1775.
430. Aspinall, G. O.; McDonald, A. G.; Raju, T. S.; Pang, H.; Moran, A. P.; Penner, J. L., Chemical structures of the core regions of *Campylobacter jejuni* serotypes O:1, O:4, O:23, and O:36 lipopolysaccharides. *Eur. J. Biochem.* **1993**, *213*, 1017-1027.
431. Gilbert, M.; Parker, C. T.; Moran, A. P., *Campylobacter jejuni* lipooligosaccharides: structures and biosynthesis. In Nachamkin, I.; Szymanski, C. M.; Blaser, M. (Eds) *Campylobacter*, 3rd ed., ASM Press, Washington DC, **2008**, 483-504.
432. Blaser, M. J.; Engberg, J., Clinical aspects of *Campylobacter jejuni* and *Campylobacter coli* infections. In Nachamkin, I.; Szymanski, C. M.; Blaser, M. (Eds) *Campylobacter*, 3rd ed., ASM Press, Washington DC, **2008**, 99-121.
433. Havelaar, A. H.; Mangen, M. J. J.; De Koeijer, A. A.; Bogaardt, M. J.; Evers, E. G.; Jacobs-Reitsma, W. F.; Van Pelt, W.; Wagenaar, J. A.; De Wit, G. A.; Van Der Zee, H., Effectiveness and efficiency of controlling *Campylobacter* on broiler chicken meat. *Risk Anal.* **2007**, *27*, 831-844.
434. Mangen, M. J. J.; Havelaar, A. H.; Poppe, K. P.; De Wit, G. A.; Team, C. P., Cost-utility analysis to control campylobacter on chicken meat—dealing with data limitations. *Risk Anal.* **2007**, *27*, 815-830.
435. de Zoete, M. R.; van Putten, J. P.; Wagenaar, J. A., Vaccination of chickens against *Campylobacter*. *Vaccine* **2007**, *25*, 5548-5557.
436. Guerry, P.; Poly, F.; Riddle, M.; Maue, A. C.; Chen, Y.-H.; Monteiro, M. A., *Campylobacter* polysaccharide capsules: virulence and vaccines. *Front. Cell. Infect. Microbiol.* **2012**, *2*, 7.
437. Miller, G.; Dunn, G. M.; Reid, T. M.; Ogden, I. D.; Strachan, N. J., Does age acquired immunity confer selective protection to common serotypes of *Campylobacter jejuni*? *BMC Infect. Dis.* **2005**, *5*, 66.
438. Tribble, D. R.; Baqar, S.; Scott, D. A.; Oplinger, M. L.; Trespalacios, F.; Rollins, D.; Walker, R. I.; Clements, J. D.; Walz, S.; Gibbs, P., Assessment of the duration of protection in *Campylobacter jejuni* experimental infection in humans. *Infect. Immun.* **2010**, *78*, 1750-1759.

439. Bacon, D. J.; Szymanski, C. M.; Burr, D. H.; Silver, R. P.; Alm, R. A.; Guerry, P., A phase-variable capsule is involved in virulence of *Campylobacter jejuni* 81-176. *Mol. Microbiol.* **2001**, *40*, 769-777.
440. Bachtiar, B. M.; Coloe, P. J.; Fry, B. N., Knockout mutagenesis of the kpsE gene of *Campylobacter jejuni* 81116 and its involvement in bacterium–host interactions. *FEMS Immunol. Med. Microbiol.* **2007**, *49*, 149-154.
441. Corcionivoschi, N.; Clyne, M.; Lyons, A.; Elmi, A.; Gundogdu, O.; Wren, B.; Dorrell, N.; Karlyshev, A.; Bourke, B., *Campylobacter jejuni* cocultured with epithelial cells reduces surface capsular polysaccharide expression. *Infect. Immun.* **2009**, *77*, 1959-1967.
442. Guerry, P.; Szymanski, C. M., *Campylobacter* sugars sticking out. *Trends Microbiol.* **2008**, *16*, 428-435.
443. Maue, A. C.; Mohawk, K. L.; Giles, D. K.; Poly, F.; Ewing, C. P.; Jiao, Y.; Lee, G.; Ma, Z.; Monteiro, M. A.; Hill, C. L., The polysaccharide capsule of *Campylobacter jejuni* modulates the host immune response. *Infect. Immun.* **2013**, *81*, 665-672.
444. Adamo, R.; Nilo, A.; Castagner, B.; Boutureira, O.; Berti, F.; Bernardes, G. J., Synthetically defined glycoprotein vaccines: current status and future directions. *Chem. Sci.* **2013**, *4*, 2995-3008.
445. Maue, A. C.; Poly, F.; Guerry, P., A capsule conjugate vaccine approach to prevent diarrheal disease caused by *Campylobacter jejuni*. *Hum. Vaccines Immunother.* **2014**, *10*, 1499-1504.
446. Riddle, M. S.; Guerry, P., Status of vaccine research and development for *Campylobacter jejuni*. *Vaccine* **2016**, *34*, 2903-2906.
447. Poly, F.; Noll, A. J.; Riddle, M. S.; Porter, C. K., Update on *Campylobacter* vaccine development. *Hum. Vaccines Immunother.* **2019**, *15*, 1389-1400.
448. Aspinall, G. O.; McDonald, A. G.; Pang, H., Structures of the O chains from lipopolysaccharides of *Campylobacter jejuni* serotypes O:23 and O:36. *Carbohydr. Res.* **1992**, *231*, 13-30.
449. Aspinall, G.; McDonald, A.; Pang, H.; Kurjanczyk, L.; Penner, J., An antigenic polysaccharide from *Campylobacter coli* serotype O:30. Structure of a teichoic acid-like antigenic polysaccharide associated with the lipopolysaccharide. *J. Biol. Chem.* **1993**, *268*, 18321-18329.
450. Aspinall, G., Lipopolysaccharides and associated carbohydrate polymers from *Campylobacter jejuni* and *Helicobacter pylori*. *Carbohydr. Polym.* **1998**, *21*, 24-29.
451. Aspinall, G. O.; Monteiro, M. A.; Pang, H., Lipo-oligosaccharide of the *Campylobacter lari* type strain ATCC 35221. Structure of the liberated oligosaccharide and an associated extracellular polysaccharide. *Carbohydr. Res.* **1995**, *279*, 245-264.

452. Aspinall, G. O.; Monteiro, M. A.; Pang, H.; Kurjanczyk, L. A.; Penner, J. L., Lipooligosaccharide of *Campylobacter lari* strain PC 637. Structure of the liberated oligosaccharide and an associated extracellular polysaccharide. *Carbohydr. Res.* **1995**, *279*, 227-244.
453. Parkhill, J.; Wren, B.; Mungall, K.; Ketley, J.; Churcher, C.; Basham, D.; Chillingworth, T.; Davies, R.; Feltwell, T.; Holroyd, S., The genome sequence of the food-borne pathogen *Campylobacter jejuni* reveals hypervariable sequences. *Nature* **2000**, *403*, 665-668.
454. Penner, J.; Hennessy, J., Passive hemagglutination technique for serotyping *Campylobacter fetus* subsp. *jejuni* on the basis of soluble heat-stable antigens. *J. Clin. Microbiol.* **1980**, *12*, 732-737.
455. Preston, M. A.; Penner, J., Characterization of cross-reacting serotypes of *Campylobacter jejuni*. *Can. J. Microbiol.* **1989**, *35*, 265-273.
456. Michael, F. S.; Szymanski, C. M.; Li, J.; Chan, K. H.; Khieu, N. H.; Larocque, S.; Wakarchuk, W. W.; Brisson, J. R.; Monteiro, M. A., The structures of the lipooligosaccharide and capsule polysaccharide of *Campylobacter jejuni* genome sequenced strain NCTC 11168. *Eur. J. Biochem.* **2002**, *269*, 5119-5136.
457. Næss, V.; Hofstad, T., Chemical studies of partially hydrolysed lipopolysaccharides from four strains of *Campylobacter jejuni* and two strains of *Campylobacter coli*. *Microbiology* **1984**, *130*, 2783-2789.
458. Szymanski, C. M.; Michael, F. S.; Jarrell, H. C.; Li, J.; Gilbert, M.; Larocque, S.; Vinogradov, E.; Brisson, J.-R., Detection of conserved *N*-linked glycans and phase-variable lipooligosaccharides and capsules from *Campylobacter* cells by mass spectrometry and high resolution magic angle spinning NMR spectroscopy. *J. Biol. Chem.* **2003**, *278*, 24509-24520.
459. Karlyshev, A. V.; Champion, O. L.; Churcher, C.; Brisson, J. R.; Jarrell, H. C.; Gilbert, M.; Brochu, D.; St Michael, F.; Li, J.; Wakarchuk, W. W., Analysis of *Campylobacter jejuni* capsular loci reveals multiple mechanisms for the generation of structural diversity and the ability to form complex heptoses. *Mol. Microbiol.* **2005**, *55*, 90-103.
460. Poly, F.; Serichantalergs, O.; Kuroiwa, J.; Pootong, P.; Mason, C.; Guerry, P.; Parker, C. T., Updated *Campylobacter jejuni* capsule PCR multiplex typing system and its application to clinical isolates from South and Southeast Asia. *PLoS ONE* **2015**, *10*, e0144349.
461. Pequegnat, B.; Laird, R. M.; Ewing, C. P.; Hill, C. L.; Omari, E.; Poly, F.; Monteiro, M. A.; Guerry, P., Phase-variable changes in the position of *O*-methyl phosphoramidate modifications on the polysaccharide capsule of *Campylobacter jejuni* modulate serum resistance. *J. Bacteriol.* **2017**, *199*, e00027-17.
462. Kanipes, M. I.; Papp-Szabo, E.; Guerry, P.; Monteiro, M. A., Mutation of *waaC*, encoding heptosyltransferase I in *Campylobacter jejuni* 81-176, affects the structure of both lipooligosaccharide and capsular carbohydrate. *J. Bacteriol.* **2006**, *188*, 3273-3279.

463. Aspinall, G. O.; Lynch, C. M.; Pang, H.; Shaver, R. T.; Moran, A. P., Chemical structures of the core region of *Campylobacter jejuni* O:3 lipopolysaccharide and an associated polysaccharide. *Eur. J. Biochem.* **1995**, *231*, 570-578.
464. Monteiro, M. A.; Noll, A.; Laird, R. M.; Pequegnat, B.; Ma, Z.; Bertolo, L.; DePass, C.; Omari, E.; Gabryelski, P.; Redkyna, O., *Campylobacter jejuni* capsule polysaccharide conjugate vaccine. In Prasad, K. A. (Ed) *Carbohydrate-Based Vaccines: From Concept to Clinic*, ACS Symposium Series 1290, Washington DC, **2018**, 249-271.
465. Hanniffy, O. M.; Shashkov, A. S.; Moran, A. P.; Prendergast, M. M.; Sof'ya, N. S.; Knirel, Y. A.; Savage, A. V., Chemical structure of a polysaccharide from *Campylobacter jejuni* 176.83 (serotype O:41) containing only furanose sugars. *Carbohydr. Res.* **1999**, *319*, 124-132.
466. Gilbert, M.; Mandrell, R. E.; Parker, C. T.; Li, J.; Vinogradov, E., Structural analysis of the capsular polysaccharide from *Campylobacter jejuni* RM1221. *ChemBioChem* **2007**, *8*, 625-631.
467. Bertolo, L.; Ewing, C. P.; Maue, A.; Poly, F.; Guerry, P.; Monteiro, M. A., The design of a capsule polysaccharide conjugate vaccine against *Campylobacter jejuni* serotype HS15. *Carbohydr. Res.* **2013**, *366*, 45-49.
468. Aspinall, G. O.; McDonald, A. G.; Pang, H., Lipopolysaccharides of *Campylobacter jejuni* serotype O:19: structures of O antigen chains from the serostrain and two bacterial isolates from patients with the Guillain-Barré syndrome. *Biochemistry* **1994**, *33*, 250-255.
469. McNally, D. J.; Jarrell, H. C.; Khieu, N. H.; Li, J.; Vinogradov, E.; Whitfield, D. M.; Szymanski, C. M.; Brisson, J. R., The HS:19 serostrain of *Campylobacter jejuni* has a hyaluronic acid-type capsular polysaccharide with a nonstoichiometric sorbose branch and *O*-methyl phosphoramidate group. *FEBS J.* **2006**, *273*, 3975-3989.
470. McNally, D. J.; Jarrell, H. C.; Li, J.; Khieu, N. H.; Vinogradov, E.; Szymanski, C. M.; Brisson, J. R., The HS:1 serostrain of *Campylobacter jejuni* has a complex teichoic acid-like capsular polysaccharide with nonstoichiometric fructofuranose branches and *O*-methyl phosphoramidate groups. *FEBS J.* **2005**, *272*, 4407-4422.
471. McDonald, A. G. Lipopolysaccharides from *Campylobacter*. Ph.D. Thesis, York University, **1993**.
472. Shin, J. E. N.; Ackloo, S.; Mainkar, A. S.; Monteiro, M. A.; Pang, H.; Penner, J. L.; Aspinall, G. O., Lipo-oligosaccharides of *Campylobacter jejuni* serotype O:10. Structures of core oligosaccharide regions from a bacterial isolate from a patient with the Miller-Fisher syndrome and from the serotype reference strain. *Carbohydr. Res.* **1997**, *305*, 223-232.
473. McNally, D. J.; Lamoureux, M. P.; Karlyshev, A. V.; Fiori, L. M.; Li, J.; Thacker, G.; Coleman, R. A.; Khieu, N. H.; Wren, B. W.; Brisson, J.-R., Commonality and biosynthesis of the *O*-methyl phosphoramidate capsule modification in *Campylobacter jejuni*. *J. Biol. Chem.* **2007**, *282*, 28566-28576.

474. van Alphen, L. B.; Wenzel, C. Q.; Richards, M. R.; Fodor, C.; Ashmus, R. A.; Stahl, M.; Karlyshev, A. V.; Wren, B. W.; Stintzi, A.; Miller, W. G., Biological roles of the O-methyl phosphoramidate capsule modification in *Campylobacter jejuni*. *PloS ONE* **2014**, *9*, e87051.
475. Pike, B. L.; Guerry, P.; Poly, F., Global distribution of *Campylobacter jejuni* Penner serotypes: a systematic review. *PloS ONE* **2013**, *8*, e67375.
476. Sainato, R.; ElGendy, A.; Poly, F.; Kuroiwa, J.; Guerry, P.; Riddle, M. S.; Porter, C. K., Epidemiology of *Campylobacter* infections among children in Egypt. *Am. J. Trop. Med. Hyg.* **2018**, *98*, 581-585.
477. Rojas, J. D.; Reynolds, N. D.; Pike, B. L.; Espinoza, N. M.; Kuroiwa, J.; Jani, V.; Ríos, P. A.; Nunez, R. G.; Yori, P. P.; Bernal, M., Distribution of capsular types of *Campylobacter jejuni* isolates from symptomatic and asymptomatic children in Peru. *Am. J. Trop. Med. Hyg.* **2019**, *101*, 541-548.
478. Gruber, W. C.; Scott, D. A.; Emini, E. A., Development and clinical evaluation of Prevnar 13, a 13-valent pneumococcal CRM197 conjugate vaccine. *Ann. N. Y. Acad. Sci.* **2012**, *1263*, 15-26.
479. Huang, Y.-L.; Wu, C.-Y., Carbohydrate-based vaccines: challenges and opportunities. *Exp. Res. Vaccines* **2010**, *9*, 1257-1274.
480. Astronomo, R. D.; Burton, D. R., Carbohydrate vaccines: developing sweet solutions to sticky situations? *Nat. Rev. Drug Discov.* **2010**, *9*, 308.
481. Mond, J. J.; Vos, Q.; Lees, A.; Snapper, C. M., T cell independent antigens. *Curr. Opin. Immunol.* **1995**, *7*, 349-354.
482. Mond, J. J.; Lees, A.; Snapper, C. M., T cell-independent antigens type 2. *Ann. Rev. Immunol.* **1995**, *13*, 655-692.
483. Avci, F. Y.; Li, X.; Tsuji, M.; Kasper, D. L., A mechanism for glycoconjugate vaccine activation of the adaptive immune system and its implications for vaccine design. *Nat. Med.* **2011**, *17*, 1602.
484. Czerkinsky, C.; Holmgren, J., Vaccines against enteric infections for the developing world. *Philos. Trans. R. Soc. B* **2015**, *370*, 20150142.
485. Dougan, G.; Huett, A.; Clare, S., Vaccines against human enteric bacterial pathogens. *Br. Med. Bull.* **2002**, *62*, 113-123.
486. Passwell, J. H.; Harlev, E.; Ashkenazi, S.; Chu, C.; Miron, D.; Ramon, R.; Farzan, N.; Shiloach, J.; Bryla, D. A.; Majadly, F., Safety and immunogenicity of improved *Shigella* O-specific polysaccharide-protein conjugate vaccines in adults in Israel. *Infect. Immun.* **2001**, *69*, 1351-1357.
487. Cohen, D.; Ashkenazi, S.; Green, M. S.; Gdalevich, M.; Robin, G.; Slepon, R.; Yavzori, M.; Orr, N.; Block, C.; Ashkenazi, I., Double-blind vaccine-controlled randomised efficacy

- trial of an investigational *Shigella sonnei* conjugate vaccine in young adults. *Lancet* **1997**, *349*, 155-159.
488. Barel, L.-A.; Mulard, L. A., Classical and novel strategies to develop a *Shigella* glycoconjugate vaccine: from concept to efficacy in human. *Hum. Vaccines Immunother.* **2019**, *15*, 1338-1356.
489. Phalipon, A.; Costachel, C.; Grandjean, C.; Thuizat, A.; Guerreiro, C.; Tanguy, M.; Nato, F.; Vulliez-Le Normand, B.; Bélot, F.; Wright, K., Characterization of functional oligosaccharide mimics of the *Shigella flexneri* serotype 2a O-antigen: implications for the development of a chemically defined glycoconjugate vaccine. *J. Immunol.* **2006**, *176*, 1686-1694.
490. Phalipon, A.; Tanguy, M.; Grandjean, C.; Guerreiro, C.; Bélot, F.; Cohen, D.; Sansonetti, P. J.; Mulard, L. A., A synthetic carbohydrate-protein conjugate vaccine candidate against *Shigella flexneri* 2a infection. *J. Immunol.* **2009**, *182*, 2241-2247.
491. Pozsgay, V.; Chu, C.; Pannell, L.; Wolfe, J.; Robbins, J. B.; Schneerson, R., Protein conjugates of synthetic saccharides elicit higher levels of serum IgG lipopolysaccharide antibodies in mice than do those of the O-specific polysaccharide from *Shigella dysenteriae* type 1. *Proc. Natl. Acad. Sci. USA.* **1999**, *96*, 5194-5197.
492. Robbins, J. B.; Kubler-Kielb, J.; Vinogradov, E.; Mocca, C.; Pozsgay, V.; Shiloach, J.; Schneerson, R., Synthesis, characterization, and immunogenicity in mice of *Shigella sonnei* O-specific oligosaccharide-core-protein conjugates. *Proc. Natl. Acad. Sci. USA.* **2009**, *106*, 7974-7978.
493. Monteiro, M. A.; Baqar, S.; Hall, E. R.; Chen, Y.-H.; Porter, C. K.; Bentzel, D. E.; Applebee, L.; Guerry, P., Capsule polysaccharide conjugate vaccine against diarrheal disease caused by *Campylobacter jejuni*. *Infect. Immun.* **2009**, *77*, 1128-1136.
494. Jones, F. R.; Baqar, S.; Gozalo, A.; Nunez, G.; Espinoza, N.; Reyes, S. M.; Salazar, M.; Meza, R.; Porter, C. K.; Walz, S. E., New World monkey *Aotus nancymae* as a model for *Campylobacter jejuni* infection and immunity. *Infect. Immun.* **2006**, *74*, 790-793.
495. Monteiro, M. A., Personal communication, **2020**.
496. Ashmus, R. A.; Lowary, T. L., Synthesis of carbohydrate methyl phosphoramidates. *Org. Lett.* **2014**, *16*, 2518-2521.
497. Dhurandhare, V. M.; Mishra, G. P.; Lam, S.; Wang, C.-C., Direct synthesis of methyl phosphoramidates in carbohydrates. *Org. Biomol. Chem.* **2015**, *13*, 9457-9461.
498. Jiao, Y. Syntheses of carbohydrate antigens expressed by gastric-intestinal bacteria and conjugates thereof. Ph.D. Thesis, University of Guelph, **2017**.
499. Jiao, Y.; Ma, Z.; Ewing, C. P.; Guerry, P.; Monteiro, M. A., Synthesis and immunodetection of 6-O-methyl-phosphoramidyl- α -D-galactose: a *Campylobacter jejuni* antigenic determinant. *Carbohydr. Res.* **2015**, *418*, 9-12.

500. Szekrenyi, A.; Garrabou, X.; Parella, T.; Joglar, J.; Bujons, J.; Clapés, P., Asymmetric assembly of aldose carbohydrates from formaldehyde and glycolaldehyde by tandem biocatalytic aldol reactions. *Nat. Chem.* **2015**, *7*, 724.
501. Dromowicz, M.; Köll, P., A convenient synthesis of D-idose. *Carbohydr. Res.* **1998**, *308*, 169-171.
502. Paulsen, H.; Trautwein, W. P.; Espinosa, F. G.; Heyns, K., Carboxoniumverbindungen in der kohlenhydratchemie, III. Einfache synthese von D-idose aus D-glucose durch mehrfache acetoxonium-ion-umlagerungen. Darstellung eines stabilen acetoxonium-salzes der tetraacetyl-idose. *Chem. Ber.* **1967**, *100*, 2822-2836.
503. Wiggins, L., 143. The conversion of galactose into derivatives of D-idose. *J. Chem. Soc.* **1944**, 522-526.
504. Hevey, R.; Morland, A.; Ling, C.-C., A scalable approach to obtaining orthogonally protected β -D-idopyranosides. *J. Org. Chem.* **2012**, *77*, 6760-6772.
505. Hevey, R.; Ling, C.-C., Evidence of cation-coordination involvement in directing the regioselective di-inversion reaction of vicinal di-sulfonate esters. *Org. Biomol. Chem.* **2013**, *11*, 1887-1895.
506. Hevey, R.; Chen, X.; Ling, C.-C., Role of the 4,6-O-acetal in the regio- and stereoselective conversion of 2,3-di-O-sulfonyl- β -D-galactopyranosides to D-idopyranosides. *Carbohydr. Res.* **2013**, *376*, 37-48.
507. Lee, Y. C.; Lee, R. T. (Eds), Recognition of carbohydrates in biological systems, part B: specific applications, *Methods in Enzymology*, Academic Press, New York, **2003**, 363.
508. Borén, H. B.; Eklind, K.; Garegg, P.; Lindberg, B.; Pilotti, A., Synthesis of 6-deoxy-D-manno-heptose. *Acta Chem. Scand.* **1972**, *26*, 4143-4146.
509. Aspinall, G. O.; McDonald, A. G.; Sood, R. K., Syntheses of methyl glycosides of 6-deoxyheptoses. *Can. J. Chem.* **1994**, *72*, 247-251.
510. 신영숙; 천근호, Preparation of α -linked 6-deoxy-D-altro-heptopyranosidic residues. *Bull. Korean Chem. Soc.* **1995**, *16*, 625-630.
511. Hevey, R.; Ling, C.-C., Studies on the 6-homologation of β -D-idopyranosides. *Carbohydr. Res.* **2017**, *445*, 65-74.
512. Zhang, P.; Hevey, R.; Ling, C.-C., Total synthesis of β -D-ido-heptopyranosides related to capsular polysaccharides of *Campylobacter jejuni* HS:4. *J. Org. Chem.* **2017**, *82*, 9662-9674.
513. Zhang, P. Total synthesis of 6-deoxy- β -D-ido-heptopyranosides. M.Sc. Thesis, University of Calgary, **2017**.

514. Yun, M.-K.; Shin, J. E. N., Synthesis of the 2'-azidoethyl trisaccharide, 6d-altroHepp-GlcNAc-Gal hapten, an O-antigenic repeating unit of *Campylobacter jejuni* serotypes O:23 and O:36. *Bull. Korean Chem. Soc.* **2008**, *29*, 1315-1319.
515. Yoon, S.-S.; Shin, Y.-S.; Chun, K.-H.; Nam Shin, J. E., Synthesis of GlcNAcp- β -(1 \rightarrow 3)-Galp- α -(1 \rightarrow 2)-6-deoxy-altroHepp- α -(1 \rightarrow O-propyl, an O-antigenic repeating unit from *C. jejuni* O:23 and O:36. *Bull. Korean Chem. Soc.* **2004**, *25*, 289-292.
516. Yun, M.; Yoon, S.; Shin, Y.; Chun, K. H.; Shin, J. E. N., Synthesis of 2'-Azidoethyl Trisaccharide, α -D-Gal-(1 \rightarrow 2)-6d- α -D-Altro-Hepp-(1 \rightarrow 3)- β -D-GlcNAc, an O-antigenic repeating unit of *C. jejuni* O:23 and O:36. *Arch. Pharmacol Res.* **2004**, *27*, 143-150.
517. Thota, V. N.; Ferguson, M. J.; Sweeney, R. P.; Lowary, T. L., Synthesis of the *Campylobacter jejuni* 81-176 strain capsular polysaccharide repeating unit reveals the absolute configuration of its O-methyl phosphoramidate motif. *Angew. Chem. Int. Ed. Engl.* **2018**, *57*, 15592-15596.
518. van der Klein, P. A.; van Boom, J. H., Application of cyclic sulfates in the synthesis of 6-deoxy-D-manno-heptopyranose derivatives. *Carbohydr. Res.* **1992**, *224*, 193-200.
519. Peng, W.; Jayasuriya, A. B.; Imamura, A.; Lowary, T. L., Synthesis of the 6-O-methyl-D-glycero- α -L-gluco-heptopyranose moiety present in the capsular polysaccharide from *Campylobacter jejuni* NCTC 11168. *Org. Lett.* **2011**, *13*, 5290-5293.
520. Takeuchi, M.; Taniguchi, T.; Ogasawara, K., Back to the Sugars: a new enantio and diastereocontrolled route to hexoses from furfural. *Synthesis* **1999**, *1999*, 341-354.
521. Harris, J. M.; Keranen, M. D.; O'Doherty, G. A., Syntheses of D- and L-mannose, gulose, and talose via diastereoselective and enantioselective dihydroxylation reactions. *J. Org. Chem.* **1999**, *64*, 2982-2983.
522. Ahmed, M. M.; Berry, B. P.; Hunter, T. J.; Tomcik, D. J.; O'Doherty, G. A., *De novo* enantioselective syntheses of galacto-sugars and deoxy sugars via the iterative dihydroxylation of dienolate. *Org. Lett.* **2005**, *7*, 745-748.
523. Shan, M.; Xing, Y.; O'Doherty, G. A., *De novo* asymmetric synthesis of an α -6-deoxyaltropyranoside as well as its 2-/3-deoxy and 2,3-dideoxy congeners. *J. Org. Chem.* **2009**, *74*, 5961-5966.
524. Ashmus, R. A.; Jayasuriya, A. B.; Lim, Y.-J.; O'Doherty, G. A.; Lowary, T. L., *De novo* asymmetric synthesis of a 6-O-methyl-D-glycero-L-gluco-heptopyranose-derived thioglycoside for the preparation of *Campylobacter jejuni* NCTC11168 capsular polysaccharide fragments. *J. Org. Chem.* **2016**, *81*, 3058-3063.
525. Crich, D.; Picard, S., Highly stereoselective synthesis of α -D-mannopyranosyl phosphosugars. *J. Org. Chem.* **2009**, *74*, 9576-9579.

526. Crich, D.; Hu, T.; Cai, F., Does neighboring group participation by non-vicinal esters play a role in glycosylation reactions? Effective probes for the detection of bridging intermediates. *J. Org. Chem.* **2008**, *73*, 8942-8953.
527. Picard, S.; Crich, D., Improved methods for the stereoselective synthesis of mannoheptosyl donors and their glycosides: toward the synthesis of the trisaccharide repeating unit of the *Campylobacter jejuni* RM1221 capsular polysaccharide. *Tetrahedron* **2013**, *69*, 5501-5510.
528. Wang, X.; Chen, Y.; Wang, J.; Yang, Y., Total synthesis of the trisaccharide antigen of the *Campylobacter jejuni* RM1221 capsular polysaccharide via *de novo* synthesis of the 6-deoxy-D-manno-heptose building blocks. *J. Org. Chem.* **2019**, *84*, 2393-2403.
529. Safari, D.; Dekker, H. A.; Joosten, J. A.; Michalik, D.; de Souza, A. C.; Adamo, R.; Lahmann, M.; Sundgren, A.; Oscarson, S.; Kamerling, J. P., Identification of the smallest structure capable of evoking opsonophagocytic antibodies against *Streptococcus pneumoniae* type 14. *Infect. Immun.* **2008**, *76*, 4615-4623.
530. Jansen, W.; Snippe, H., Short-chain oligosaccharide protein conjugates as experimental pneumococcal vaccines. *Indian J. Med. Res.* **2004**, *119*, 7-12.
531. Benaissa-Trouw, B.; Lefeber, D. J.; Kamerling, J. P.; Vliegthart, J. F.; Kraaijeveld, K.; Snippe, H., Synthetic polysaccharide type 3-related di-, tri-, and tetrasaccharide-CRM197 conjugates induce protection against *Streptococcus pneumoniae* type 3 in mice. *Infect. Immun.* **2001**, *69*, 4698-4701.
532. Parameswarappa, S. G.; Reppe, K.; Geissner, A.; Ménová, P.; Govindan, S.; Calow, A. D.; Wahlbrink, A.; Weishaupt, M. W.; Monnanda, B. P.; Bell, R. L., A semi-synthetic oligosaccharide conjugate vaccine candidate confers protection against *Streptococcus pneumoniae* serotype 3 infection. *Cell Chem. Biol.* **2016**, *23*, 1407-1416.
533. Mawas, F.; Niggemann, J.; Jones, C.; Corbel, M. J.; Kamerling, J. P.; Vliegthart, J. F., Immunogenicity in a mouse model of a conjugate vaccine made with a synthetic single repeating unit of type 14 pneumococcal polysaccharide coupled to CRM197. *Infect. Immun.* **2002**, *70*, 5107-5114.
534. Jansen, W. T.; Hogenboom, S.; Thijssen, M. J.; Kamerling, J. P.; Vliegthart, J. F.; Verhoef, J.; Snippe, H.; Verheul, A. F., Synthetic 6B di-, tri-, and tetrasaccharide-protein conjugates contain pneumococcal type 6A and 6B common and 6B-specific epitopes that elicit protective antibodies in mice. *Infect. Immun.* **2001**, *69*, 787-793.
535. Adamo, R.; Hu, Q.-Y.; Torosantucci, A.; Crotti, S.; Brogioni, G.; Allan, M.; Chiani, P.; Bromuro, C.; Quinn, D.; Tontini, M., Deciphering the structure-immunogenicity relationship of anti-*Candida* glycoconjugate vaccines. *Chem. Sci.* **2014**, *5*, 4302-4311.
536. Spiekermann, G. M.; Finn, P. W.; Ward, E. S.; Dumont, J.; Dickinson, B. L.; Blumberg, R. S.; Lencer, W. I., Receptor-mediated immunoglobulin G transport across mucosal barriers in adult life: functional expression of FcRn in the mammalian lung. *J. Exp. Med.* **2002**, *196*, 303-310.

537. Robert-Guroff, M., IgG surfaces as an important component in mucosal protection. *Nat. Med.* **2000**, *6*, 129-130.
538. Cmoch, P.; Korda, A.; Rárová, L.; Okleštková, J.; Strnad, M.; Gwardiak, K.; Karczewski, R.; Pakulski, Z., Synthesis of lupane-type saponins containing an unusual α -D-idopyranoside fragment as potent cytotoxic agents. *Eur. J. Org. Chem.* **2014**, *2014*, 4089-4098.
539. Kopitzki, S.; Thiem, J., Short synthetic route to benzaldehyde-functionalized idose and talose derivatives by acetoxonium ion rearrangements. *Eur. J. Org. Chem.* **2013**, *2013*, 4008-4016.
540. Li, T.; Wang, J.; Zhu, X.; Zhou, X.; Sun, S.; Wang, P.; Cao, H.; Yu, G.; Li, M., Synthesis of rare 6-deoxy-D-/L-heptopyranosyl fluorides: assembly of a hexasaccharide corresponding to *Campylobacter jejuni* strain CG8486 capsular polysaccharide. *J. Am. Chem. Soc.* **2021**, *143*, 11171-11179.
541. Liu, Z.; Jenkinson, S. F.; Yoshihara, A.; Wormald, M. R.; Izumori, K.; Fleet, G. W., D-Idose, D-iduronic acid, and D-idonic acid from D-glucose via seven-carbon sugars. *Molecules* **2019**, *24*, 3758.
542. Szekrenyi, A.; Garrabou, X.; Parella, T.; Joglar, J.; Bujons, J.; Clapés, P., Asymmetric assembly of aldose carbohydrates from formaldehyde and glycolaldehyde by tandem biocatalytic aldol reactions. *Nat. Chem.* **2015**, *7*, 724-729.
543. Vibhute, A. M.; Muvvala, V.; Sureshan, K. M., A sugar-based gelator for marine oil-spill recovery. *Angew. Chem. Int. Ed. Engl.* **2016**, *128*, 7913-7916.
544. Augé, J.; David, S., Hexopyranose sugars conformation revised. *Tetrahedron* **1984**, *40*, 2101-2106.
545. Angyal, S. J., Conformational analysis in carbohydrate chemistry. I. Conformational free energies. The conformations and α : β ratios of aldopyranoses in aqueous solution. *Aust. J. Chem.* **1968**, *21*, 2737-2746.
546. Paulsen, H.; Friedmann, M., Konformationsanalyse, I. Abhängigkeit der *syn*-1.3-diaxialen Wechselwirkung von der Art des Substituenten und vom Lösungsmittel. Untersuchungen der Konformationsgleichgewichte von D-Idopyranose-derivaten. *Chem. Ber.* **1972**, *105*, 705-717.
547. Angyal, S. J.; Kondo, Y., The 4,6-benzylidene acetals, and the conformation, of methyl α -D-idopyranoside. *Carbohydr. Res.* **1980**, *81*, 35-48.
548. Komarova, B. S.; Gerbst, A. G.; Finogenova, A. M.; Dmitrenok, A. S.; Tsvetkov, Y. E.; Nifantiev, N. E., 1,3-*syn*-Diaxial repulsion of typical protecting groups used in carbohydrate chemistry in 3-O-substituted derivatives of isopropyl D-idopyranosides. *J. Org. Chem.* **2017**, *82*, 8897-8908.
549. Thelin, M. A.; Bartolini, B.; Axelsson, J.; Gustafsson, R.; Tykesson, E.; Pera, E.; Oldberg, Å.; Maccarana, M.; Malmstrom, A., Biological functions of iduronic acid in chondroitin/dermatan sulfate. *FEBS J.* **2013**, *280*, 2431-2446.

550. Uchio, Y.; Nagasaki, M.; Eguchi, S.; Matsuo, A.; Nakayama, M.; Hayashi, S., Labdane diterpene glycosides with 6-deoxy-L-idose from *Aster spathulifolius Maxim.* *Tetrahedr. Lett.* **1980**, *21*, 3775-3778.
551. Sakoguchi, H.; Yoshihara, A.; Izumori, K.; Sato, M., Screening of biologically active monosaccharides: growth inhibitory effects of D-allose, D-talose, and L-idose against the nematode *Caenorhabditis elegans*. *Biosci. Biotechnol. Biochem.* **2016**, *80*, 1058-1061.
552. Ishiyama, H.; Yanagita, R. C.; Takemoto, K.; Kitaguchi, N.; Uezato, Y.; Sugiyama, Y.; Sato, M.; Kawanami, Y., Evaluation of the anti-proliferative activity of rare aldohexoses against MOLT-4F and DU-145 human cancer cell line and structure-activity relationship of D-idose. *J. Appl. Glycosci.* **2020**, *67*, 95-101.
553. Ishiwata, A.; Lee, Y. J.; Ito, Y., Recent advances in stereoselective glycosylation through intramolecular aglycon delivery. *Org. Biomol. Chem.* **2010**, *8*, 3596-3608.
554. Khanam, A.; Tiwari, A.; Mandal, P. K., Chiral auxiliaries: Usefulness in stereoselective glycosylation reactions and their synthetic applications. *Carbohydr. Res.* **2020**, *495*, 108045.
555. Kafle, A.; Liu, J.; Cui, L., Controlling the stereoselectivity of glycosylation via solvent effects. *Can. J. Chem.* **2016**, *94*, 894-901.
556. Hettikankanamalage, A. A.; Lassfolk, R.; Ekholm, F. S.; Leino, R.; Crich, D., Mechanisms of stereodirecting participation and ester migration from near and far in glycosylation and related reactions. *Chem. Rev.* **2020**, *120*, 7104-7151.
557. Jin, H.; Tsai, T. Y.; Wiesner, K., On the synthesis of cardioactive steroid glycosides. On cardioactive steroids. XI. *Can. J. Chem.* **1983**, *61*, 2442-2444.
558. Vucko, T.; Moïse, N. P.; Lamandé-Langle, S., Value-added carbohydrate building blocks by regioselective O-alkylation of C-glucosyl compounds. *Carbohydr. Res.* **2019**, *477*, 1-10.
559. Bols, M.; Pedersen, C. M., Silyl-protective groups influencing the reactivity and selectivity in glycosylations. *Beilstein J. Org. Chem.* **2017**, *13*, 93-105.
560. Bubb, W. A., NMR spectroscopy in the study of carbohydrates: Characterizing the structural complexity. *Concepts Magn. Reson. Part A Bridg. Educ. Res.* **2003**, *19*, 1-19.
561. Sarotti, A. M.; Pellegrinet, S. C., Application of the multi-standard methodology for calculating ¹H NMR chemical shifts. *J. Org. Chem.* **2012**, *77*, 6059-6065.
562. Sarotti, A. M.; Pellegrinet, S. C., A multi-standard approach for GIAO ¹³C NMR calculations. *J. Org. Chem.* **2009**, *74*, 7254-7260.
563. Janssens, J.; Risseeuw, M. D.; Van der Eycken, J.; Van Calenbergh, S., Regioselective Ring opening of 1,3-dioxane-type acetals in carbohydrates. *Eur. J. Org. Chem.* **2018**, *2018*, 6405-6431.
564. Wang, C. C.; Lee, J. C.; Luo, S. Y.; Fan, H. F.; Pai, C. L.; Yang, W. C.; Lu, L. D.; Hung, S. C., Synthesis of biologically potent α 1 \rightarrow 2-linked disaccharide derivatives via

- regioselective one-pot protection–glycosylation. *Angew. Chem. Int. Ed. Engl.* **2002**, *41*, 2360-2362.
565. Garegg, P. J.; Iversen, T.; Oscarson, S., Monobenylation of diols using phase-transfer catalysis. *Carbohydr. Res.* **1976**, *50*, C12-C14.
566. Paulsen, H.; Espinosa, F. G.; Trautwein, W. P., Carboxoniumverbindungen in der Kohlenhydratchemie, V. eine einfache Synthese von D-Talose durch Acetoxonium-Umlagerung von D-Galaktose. *Chem. Ber.* **1968**, *101*, 186-190.
567. Percec, V.; Leowanawat, P.; Sun, H.-J.; Kulikov, O.; Nusbaum, C. D.; Tran, T. M.; Bertin, A.; Wilson, D. A.; Peterca, M.; Zhang, S., Modular synthesis of amphiphilic Janus glycodendrimers and their self-assembly into glycodendrimersomes and other complex architectures with bioactivity to biomedically relevant lectins. *J. Am. Chem. Soc.* **2013**, *135*, 9055-9077.
568. Bum-Erdene, K.; Gagarinov, I. A.; Collins, P. M.; Winger, M.; Pearson, A. G.; Wilson, J. C.; Leffler, H.; Nilsson, U. J.; Grice, I. D.; Blanchard, H., Investigation into the feasibility of thioditaloside as a novel scaffold for galectin-3-specific inhibitors. *ChemBioChem* **2013**, *14*, 1331-1342.
569. Cao, S.; Meunier, S. J.; Andersson, F. O.; Letellier, M.; Roy, R., Mild stereoselective syntheses of thioglycosides under PTC conditions and their use as active and latent glycosyl donors. *Tetrahedron Asymm.* **1994**, *5*, 2303-2312.
570. Lowary, T.; Eichler, E.; Bundle, D., Oligosaccharide recognition by antibodies: Synthesis and evaluation of talose oligosaccharide analogues. *Can. J. Chem.* **2002**, *80*, 1112-1130.
571. Escopy, S.; Singh, Y.; Demchenko, A. V., Triflic acid-mediated synthesis of thioglycosides. *Org. Biomol. Chem.* **2019**, *17*, 8379-8383.
572. Ren, B.; Rahm, M.; Zhang, X.; Zhou, Y.; Dong, H., Regioselective acetylation of diols and polyols by acetate catalysis: mechanism and application. *J. Org. Chem.* **2014**, *79*, 8134-8142.
573. Van Boeckel, C.; Beetz, T., Substituent effects in carbohydrate chemistry, Part II. Coupling reactions involving *gluco*- and *galacto*-pyranosyl bromides promoted by insoluble silver salts. *Recl. Trav. Chim.* **1985**, *104*, 171-173.
574. Nigudkar, S. S.; Demchenko, A. V., Stereocontrolled 1,2-*cis* glycosylation as the driving force of progress in synthetic carbohydrate chemistry. *Chem. Sci.* **2015**, *6*, 2687-2704.
575. Montalvillo-Jimenez, L.; Santana, A. S. G.; Corzana, F.; Jiménez-Osés, G.; Jiménez-Barbero, J. S.; Gomez, A. M.; Asensio, J. L., Impact of aromatic stacking on glycoside reactivity: balancing CH/π and cation/π interactions for the stabilization of glycosyl-oxocarbenium ions. *J. Am. Chem. Soc.* **2019**, *141*, 13372-13384.
576. Ehret, M. S.; Virlovet, M.; Biskup, M. B., Regioselective acylation of 3,4-OH free D-glucosamines: a rapid access to orthogonally functionalized building blocks. *Synthesis* **2010**, *2010*, 3481-3485.

577. Ratner, D. M.; Swanson, E. R.; Seeberger, P. H., Automated synthesis of a protected *N*-linked glycoprotein core pentasaccharide. *Org. Lett.* **2003**, *5*, 4717-4720.
578. Muru, K.; Cloutier, M.; Provost-Savard, A.; Di Cintio, S.; Burton, O.; Cordeil, J.; Groleau, M.-C.; Legault, J.; Déziel, E.; Gauthier, C., Total synthesis of a chimeric glycolipid bearing the partially acetylated backbone of sponge-derived agminoside E. *J. Org. Chem.* **2021**, *86*, 15357-15375.
579. Chen, L.; Kong, F., Unusual α -glycosylation with galactosyl donors with a C2 ester capable of neighboring group participation. *Tetrahedr. Lett.* **2003**, *44*, 3691-3695.
580. Daragics, K.; Szabó, P.; Fügedi, P., Some observations on the reductive ring opening of 4,6-*O*-benzylidene acetals of hexopyranosides with the borane trimethylamine–aluminium chloride reagent. *Carbohydr. Res.* **2011**, *346*, 1633-1637.
581. Gaussian 09, Revision A.02, M. J. Frisch, G. W. Trucks, H. B. Schlegel, G. E. Scuseria, M. A. Robb, J. R. Cheeseman, G. Scalmani, V. Barone, G. A. Petersson, H. Nakatsuji, X. Li, M. Caricato, A. Marenich, J. Bloino, B. G. Janesko, R. Gomperts, B. Mennucci, H. P. Hratchian, J. V. Ortiz, A. F. Izmaylov, J. L. Sonnenberg, D. Williams-Young, F. Ding, F. Lipparini, F. Egidi, J. Goings, B. Peng, A. Petrone, T. Henderson, D. Ranasinghe, V. G. Zakrzewski, J. Gao, N. Rega, G. Zheng, W. Liang, M. Hada, M. Ehara, K. Toyota, R. Fukuda, J. Hasegawa, M. Ishida, T. Nakajima, Y. Honda, O. Kitao, H. Nakai, T. Vreven, K. Throssell, J. A. Montgomery, Jr., J. E. Peralta, F. Ogliaro, M. Bearpark, J. J. Heyd, E. Brothers, K. N. Kudin, V. N. Staroverov, T. Keith, R. Kobayashi, J. Normand, K. Raghavachari, A. Rendell, J. C. Burant, S. S. Iyengar, J. Tomasi, M. Cossi, J. M. Millam, M. Klene, C. Adamo, R. Cammi, J. W. Ochterski, R. L. Martin, K. Morokuma, O. Farkas, J. B. Foresman, and D. J. Fox, Gaussian, Inc., Wallingford CT, 2016.
582. Tacconelli, E., Global priority list of antibiotic-resistant bacteria to guide research, discovery, and development of new antibiotics. World Health Organization, **2017**.
583. Sainato, R.; ElGendy, A.; Poly, F.; Kuroiwa, J.; Guerry, P.; Riddle, M. S.; Porter, C. K., Epidemiology of *Campylobacter* infections among children in Egypt. *Am. J. Trop. Med. Hyg.* **2018**, *98*, 581.
584. Rojas, J. D.; Reynolds, N. D.; Pike, B. L.; Espinoza, N. M.; Kuroiwa, J.; Jani, V.; Ríos, P. A.; Nunez, R. G.; Yori, P. P.; Bernal, M., Distribution of capsular types of *Campylobacter jejuni* isolates from symptomatic and asymptomatic children in Peru. *Am. J. Trop. Med. Hyg.* **2019**, *101*, 541.
585. Cloutier, M.; Lavoie, S.; Gauthier, C., C7 epimerization of benzylidene-protected β -D-idopyranosides brings structural insights into idose conformational flexibility. *J. Org. Chem.* **2022**, *87*, 12932-12953.
586. Ito, Y.; Ohnishi, Y.; Ogawa, T.; Nakahara, Y., Highly optimized β -mannosylation via *p*-methoxybenzyl assisted intramolecular aglycon delivery. *Synlett* **1998**, *1998*, 1102-1104.

587. Lergenmüller, M.; Nukada, T.; Kuramochi, K.; Dan, A.; Ogawa, T.; Ito, Y., On the stereochemistry of tethered intermediates in *p*-methoxybenzyl-assisted β -mannosylation. *Eur. J. Org. Chem.* **1999**, 1999, 1367-1376.
588. Ito, Y.; Ando, H.; Wada, M.; Kawai, T.; Ohnishi, Y.; Nakahara, Y., On the mechanism of *p*-methoxybenzylidene assisted intramolecular aglycon delivery. *Tetrahedron* **2001**, 57, 4123-4132.
589. Ishiwata, A.; Munemura, Y.; Ito, Y., NAP ether mediated intramolecular aglycon delivery: A unified strategy for 1,2-*cis*-glycosylation. *Eur. J. Org. Chem.* **2008**, 2008, 4219-4219.
590. Ito, Y.; Ogawa, T., A novel approach to the stereoselective synthesis of β -mannosides. *Angew. Chem. Int. Ed. Engl.* **1994**, 33, 1765-1767.
591. Mandal, P. K.; Misra, A. K., Synthesis of oligosaccharides corresponding to the polysaccharides of *Lactobacillus* and *Thermophilus* strains. *Synthesis* **2007**, 2007, 2660-2666.
592. Jiang, L.; Chan, T.-H., Borane-Bu₂BOTf: A mild reagent for the regioselective reductive ring opening of benzylidene acetals in carbohydrates. *Tetrahedr. Lett.* **1998**, 39, 355-358.
593. Li, Y.; Yang, X.; Liu, Y.; Zhu, C.; Yang, Y.; Yu, B., Gold (I)-catalyzed glycosylation with glycosyl *ortho*-alkynylbenzoates as donors: General scope and application in the synthesis of a cyclic triterpene saponin. *Chem.-Eur. J.* **2010**, 16, 1871-1882.
594. Parikh, J. R.; Doering, W. v. E., Sulfur trioxide in the oxidation of alcohols by dimethyl sulfoxide. *J. Am. Chem. Soc.* **1967**, 89, 5505-5507.
595. Tang, Y.; Li, J.; Zhu, Y.; Li, Y.; Yu, B., Mechanistic insights into the gold (I)-catalyzed activation of glycosyl *ortho*-alkynylbenzoates for glycosidation. *J. Am. Chem. Soc.* **2013**, 135, 18396-18405.
596. Zhu, Y.; Yu, B., Highly stereoselective β -mannopyranosylation via the 1- α -glycosyloxy-isochromenylium-4-gold(I) intermediates. *Chem.-Eur. J.* **2015**, 21, 8771-8780.
597. Wang, X.; Wang, P.; Li, D.; Li, M., 2, 4-Dinitrobenzenesulfonamide-directed S_N2-type displacement reaction enables synthesis of β -D-glycosaminosides. *Org. Lett.* **2019**, 21, 2402-2407.
598. Wang, P.; Wang, J.; Yin, W.; Wang, X.; Song, N.; Ren, S.; Li, M., Direct β -mannosylation of primary alcohol acceptors: trisaccharide iteration assembly of β -1,6-oligomannosides corresponding to kakelokelose. *Org. Lett.* **2022**, 24, 971-976.
599. Sun, P.; Wang, P.; Zhang, Y.; Zhang, X.; Wang, C.; Liu, S.; Lu, J.; Li, M., Construction of β -mannosidic bonds via gold(I)-catalyzed glycosylations with mannopyranosyl *ortho*-hexynylbenzoates and its application in synthesis of cremomannolipin A. *J. Org. Chem.* **2015**, 80, 4164-4175.

600. Pongener, I.; Pepe, D. A.; Ruddy, J. J.; McGarrigle, E. M., Stereoselective β -mannosylations and β -rhamnosylations from glycosyl hemiacetals mediated by lithium iodide. *Chem. Sci.* **2021**, *12*, 10070-10075.
601. Issa, J. P.; Bennett, C. S., A reagent-controlled S_N2 -glycosylation for the direct synthesis of β -linked 2-deoxy-sugars. *J. Am. Chem. Soc.* **2014**, *136*, 5740-5744.
602. Okitsu, O.; Suzuki, R.; Kobayashi, S., Efficient synthesis of piperidine derivatives. Development of metal triflate-catalyzed diastereoselective nucleophilic substitution reactions of 2-methoxy- and 2-acyloxy-piperidines. *J. Org. Chem.* **2001**, *66*, 809-823.
603. Dhara, D.; Dhara, A.; Murphy, P. V.; Mulard, L. A., Protecting group principles suited to late stage functionalization and global deprotection in oligosaccharide synthesis. *Carbohydr. Res.* **2022**, *521*, 108644.
604. Vibert, A.; Lopin-Bon, C.; Jacquinet, J.-C., Efficient alternative for the reduction of *N*-trichloroacetyl groups in synthetic chondroitin oligosaccharide intermediates. *Tetrahedr. Lett.* **2010**, *51*, 1867-1869.
605. Martin, C. E.; Broecker, F.; Oberli, M. A.; Komor, J.; Mattner, J.; Anish, C.; Seeberger, P. H., Immunological evaluation of a synthetic *Clostridium difficile* oligosaccharide conjugate vaccine candidate and identification of a minimal epitope. *J. Am. Chem. Soc.* **2013**, *135*, 9713-9722.
606. Bröker, M.; Costantino, P.; DeTora, L.; McIntosh, E. D.; Rappuoli, R., Biochemical and biological characteristics of cross-reacting material 197 (CRM197), a non-toxic mutant of diphtheria toxin: use as a conjugation protein in vaccines and other potential clinical applications. *Biologicals* **2011**, *39*, 195-204.
607. Fürstner, A.; Ruiz-Caro, J.; Prinz, H.; Waldmann, H., Structure assignment, total synthesis, and evaluation of the phosphatase modulating activity of glucolipin A. *J. Org. Chem.* **2004**, *69*, 459-467.
608. Fürstner, A., Total syntheses and biological assessment of macrocyclic glycolipids. *Eur. J. Org. Chem.* **2004**, *2004*, 943-958.
609. Verma, N.; Cloutier, M.; Clément, C.; Gauthier, C. Synthesis of α -D-idose pentaacetate from β -D-glucose pentaacetate via Paulsen acetoxonium rearrangement. In: *Carbohydrate Chemistry: Proven Synthetic Methods*, Volume 6, Ed.: Giguère, D., Vincent, S. P. **2023**, CRC Press, accepted.
610. Diéguez, M.; Claver, C.; Pàmies, O., Recent progress in asymmetric catalysis using chiral carbohydrate-based ligands. *Eur. J. Org. Chem.* **2007**, *2007*, 4621-4634.
611. Tang, W.; Zhang, X., New chiral phosphorus ligands for enantioselective hydrogenation. *Chem. Rev.* **2003**, *103*, 3029-3070.

612. Bruker, S., L. Krause, R. Herbst-Irmer, G. M. Sheldrick, D. Stalke. Comparison of silver and molybdenum microfocus X-ray sources for single-crystal structure determination. *J. Appl. Crystallogr.* **2015**, *48*, 3-10.
613. Sheldrick, G., SHELXT-Integrated space-group and crystals-structure determination. *Acta Crystallogr., Sect. A Found. Adv* **2015**, *71*.
614. Sheldrick, G. M., SHELXL-97: Program for structure refinement. University of Göttingen, Germany, **1997**.
615. Sheldrick, G., SHELXS-97: Program for crystal structure resolution. University of Göttingen: Göttingen, Germany, **1997**.

